8.06x Physical Review

Edited by Jolyon K. Blooomfield

June 2019

Contents

21 cm Line of Atomic Hydrogen and its Use in Astrophysics

MikeS1

(Dated: June 10, 2019)

The 21 cm line has its origin in the hyperfine splitting of the 1S state of Hydrogen whereby the magnetic dipole moment of the nuclear proton couples to the spin magnetic moment of the orbiting electron. The present paper will give a brief history of the discovery of this splitting ΔE and its overriding importance to astrophysics before moving on to the derivation of the expression using perturbation theory for the energy splitting (time-independent theory) and the expression for the magnetic dipole transition rate (time-dependent theory) between the relevant states. Comparison of the magnitude of ΔE to that of the fine structure will be made as well as discussion of the significance of the small magnitude of the transition rate.

I. INTRODUCTION

The advent of radio astronomy in the late 1930s and throughout the 1940s opened the first major window on the electromagnetic spectrum beyond the visible range. H.C. van de Hulst [1] predicted that a hyperfine transition in the ground state of Hydrogen should be detectable in the cold interstellar gas clouds within the Milky Way Galaxy. This was finally detected in 1951 by H. Ewen and E. Purcell [2][3].

Hydrogen accounts for $\approx 75\%$ of the baryonic mass of the universe. Because of its ubiquity it is a major tracer of the universe's observed structure. In environments where hydrogen is in its atomic form, i.e. un-ionized, the 21cm line can be observed. The precise shape and relative strength of the spectral line ("line profile") as well as its Doppler shift away from 21cm gives detailed information about the radiating source and its line-of-site motion. Soon after its initial discovery the line was observed in the Magellanic Clouds and other extragalactic sources [3].

This transition continues to be a powerful tool in the studies of astrophysical radiation sources from helping to determine the nature of the interstellar medium to mapping out the Galaxy's spiral structure. In the present century it remains an important tool in modern precision cosmology[4][5].

Using non-relativistic quantum mechanics both the energy splitting and the transition rate between the two relevant ground state sublevels will be calculated in the present paper. The perturbation to the exact Hydrogen proton-electron Hamiltonian H_0 is the coupling between the spin states of the proton and electron

$$\delta H = -\vec{m_e} \cdot \vec{B} \tag{1}$$

where $\vec{m_e}$ is the magnetic moment of the electron and $\vec{B}$ is the magnetic field of the proton resulting from its magnetic moment. (We ignore any internal structure of the proton and treat it as a point charge).This is a magnetic dipole transition and will be fully developed in SecII and III.

In the classical electromagnetic multipole expansion of the vector potential[6] for the radiation field, there is also an electric dipole moment contributing to a possible transition. Schematically, the expansion goes as $\exp(ikr) = 1 + ikr + ...$ where r is the characteristic size of the source and k is the wavenumber of the radiation. In the regime where $kr \ll 1$ which corresponds to $r \ll \lambda = \frac{2\pi}{k}$, the size of the expansion terms falls off rapidly. We also assume that the observation point, $r_{obs} \gg \lambda$. These approximations (collectively known as "the far zone") are trivially satisfied for astronomical objects at almost all wavelengths where observed. The first term of the expansion corresponds to electric dipole radiation. In the present case of interest (electron-proton system) this term would be governed by the electric dipole moment which we can write as

$$\vec{d} = e\vec{r} \tag{2}$$

where quantum mechanically $\vec{r}$ is the position operator representing the classical vector from proton to electron and e is the electronic charge. ($\vec{d}$ is the electric counterpart of $\vec{m_e}$ above). Since $\vec{r}$ is an odd parity operator ($\vec{r} \rightarrow -\vec{r}$) and the ground state $|\psi\rangle$ is a parity eigenstate it follows that under the parity transformation

$$\langle\psi|\,\vec{r}\,|\psi\rangle = \langle\psi|\,P\left(P\vec{r}P\right)P\,|\psi\rangle = -\langle\psi|\,\vec{r}\,|\psi\rangle = 0 \tag{3}$$

where P is the usual parity operator, $P^2 = 1$, and has eigenvalues ± 1. In an incoherent radiation field with frequencies ω_k, and with the electric field given by

$$\vec{E_k}(t) = E_0(k)\cos(\omega_k t)\,\hat{n_k}, \tag{4}$$

the square of the matrix element of the electric dipole Hamiltonian $\left|\langle\psi|\,e\vec{r}\cdot\vec{E}(t)\,|\psi\rangle\right|^2$, is averaged over all space [7] with the result

$$\left|\langle\psi|\,e\vec{r}\cdot\vec{E}(t)\,|\psi\rangle\right|^2 = \frac{E_0^2}{3}\left|\langle\psi|\,\vec{d}\,|\psi\rangle\right|^2 = 0 \tag{5}$$

and so electric dipole transitions are ruled out for the present system.

The next term in the multipole expansion ($\sim kr$) gives the magnetic dipole radiation term (and an electric quadrupole term which won't be relevant for the present paper). This term will be much smaller than the typical electric dipole radiation term and we will see the effect that this has on quantum mechanical transition rates and lifetimes.

II. DERIVATION OF THE 1S HYPERFINE SPLITTING

We can rewrite the Hamiltonian Eq.(1) in terms of magnetic moments only as [8]

$$\delta H = -\frac{1}{r^3}\left[3(\vec{m_e}\cdot\hat{r})(\vec{m_p}\cdot\hat{r}) - \vec{m_e}\cdot\vec{m_p}\right] \\ -\frac{8\pi}{3}\vec{m_e}\cdot\vec{m_p}\delta^3(\vec{r}) \qquad (6)$$

where $\vec{m_p}$ is the proton magnetic moment, $\delta^3(\vec{r})$ is the 3 dimensional δ function and r is the proton-electron separation. We can get an order of magnitude estimate of the splitting by taking

$$\frac{|m_e||m_p|}{a_0^3} \approx 10^{-6}\text{eV}$$

where a_0 is the Bohr radius. We already anticipate that the result of our calculation will be a very small fraction of the ground state energy of 13.6eV

Both particles are spin $\frac{1}{2}$ so that the state of the electron-proton system is given by

$$|\Psi\rangle = |\psi\rangle \otimes |m_s\rangle_e \otimes |m_s\rangle_p \qquad (7)$$

where $m_s = \pm\frac{1}{2}$ are the up/down components of the two $s = \frac{1}{2}$ spin states and ψ is the usual hydrogen ground state given in position space by

$$\psi(r) = \frac{1}{\sqrt{\pi a_0^3}}e^{-r/a_0} \qquad (8)$$

The $s = \frac{1}{2}$ index has been suppressed in the spin kets. (Technical note- Eq.(7) emphasizes that we are working with a space that is a tensor product of 3 spaces: 1) that of the hydrogen atom without spin, 2) the electron spin, and 3) the proton spin. To avoid cumbersome notation the tensor product symbols will be suppressed for the corresponding operators.)

Let's consider the expectation value of the square bracketed term in Eq.(6) in the state $|\Psi\rangle$. When integrating over solid angle $d\Omega$ the first bracketed term must evaluate to an expression linear in both $\vec{m_e}$ and $\vec{m_p}$ and must also be a scalar. The only suitable scalar in the problem is $\vec{m_e}\cdot\vec{m_p}$. Therefore,

$$< (\vec{m_e}\cdot\hat{r})(\vec{m_p}\hat{r}) >_{d\Omega} = \eta(\vec{m_e}\cdot\vec{m_p}) \qquad (9)$$

where η is a constant independent of $\vec{m_e}$ and $\vec{m_p}$. To evaluate η we can take any two constant vectors and the calculation is best performed using two identical unit vectors parallel to the z direction. The scalar products are each equal to $\cos(\theta)$ in this case so that

$$\eta = \int \cos^2(\theta)d\Omega = 2\pi\int_0^\pi \cos^2(\theta)\sin(\theta)d\theta = 4\pi/3. \qquad (10)$$

The second bracketed term integrated over solid angle simply evaluates to $4\pi(\vec{m_e}\cdot\vec{m_p})$ so the entire bracketed term vanishes. Therefore, for the position space part of the electron-proton state we have

$$\langle\Psi|\,\delta H\,|\Psi\rangle = -\frac{8\pi}{3} < (\vec{m_e}\cdot\vec{m_p}) > \psi(0)^2 \\ = -\frac{8}{3a_0^3} < (\vec{m_e}\cdot\vec{m_p}) > \qquad (11)$$

where the full three dimensional position space integral has been done leaving the spin contribution still to be evaluated.

Considering the full state $|\Psi\rangle$ we have a fourfold degeneracy whose source is exclusively from the spin contribution. We must use degenerate pertubation theory to determine the first order energy shift. Rather than diagonalizing a 4x4 matrix in the uncoupled $|m_s\rangle_e |m_s\rangle_p$ basis we can proceed by analogy with the treatment of the spin-orbit coupling in the fine structure of the hydrogen atom. In the present spin-spin coupling we first note that

$$-\frac{8}{3a_0^3}(\vec{m_e}\cdot\vec{m_p}) = \frac{8}{3a_0^3}\left(\frac{eg_e}{2M_ec}\vec{S_e}\right)\cdot\left(\frac{eg_p}{2M_pc}\vec{S_p}\right) \qquad (12)$$

where we have expressed the magnetic moments in terms of their spin operators. M_e, M_p are the electron, proton masses respectively and g_e, g_p their respective g-factors. e is the electronic charge ($-e$ for the electron). We form the total angular momentum $\vec{S} = \vec{S_e} + \vec{S_p}$ so that the interaction term becomes

$$\vec{S_e}\cdot\vec{S_p} = \frac{1}{2}\left(\vec{S}^2 - \vec{S_e}^{\,2} - \vec{S_p}^{\,2}\right) \qquad (13)$$

The sum of two spin $\frac{1}{2}$ angular momenta gives one spin-0 state and three spin-1 states which can be written as $|00\rangle$, (the singlet state) and $|1-1\rangle, |10\rangle, |11\rangle$, (the triplet states). In terms of the uncoupled basis:

$$|00\rangle = \frac{1}{\sqrt{2}}\left(|1/2\rangle_e \otimes |-1/2\rangle_p - |(-1/2)\rangle_e \otimes |(1/2)\rangle_p\right) \qquad (14)$$

$$|10\rangle = \frac{1}{\sqrt{2}}\left(|1/2\rangle_e \otimes |-1/2\rangle_p + |(-1/2)\rangle_e \otimes |(1/2)\rangle_p\right) \qquad (15)$$

$$|11\rangle = |1/2\rangle_e \otimes |1/2\rangle_p \qquad (16)$$

$$|1-1\rangle = |-1/2\rangle_e \otimes |-1/2\rangle_p \qquad (17)$$

where the notation for the uncoupled basis follows Eq.(7). It's clear that the coupled basis states are eigenstates of the interaction term and independent of S_z. The eigenvalues themselves are easily evaluated:

$$\vec{S_e}\cdot\vec{S_p}\,|\rangle_{triplet} = \frac{\hbar^2}{4} \qquad (18)$$

$$\vec{S_e}\cdot\vec{S_p}\,|\rangle_{singlet} = \frac{-3\hbar^2}{4} \qquad (19)$$

Since the coupled basis vectors are orthonormal the perturbation is diagonal and we can immediately calculate the energy corrections from Eqs.(11),(12),(18),(19).

$$E_+ = \frac{1}{4}\left(\frac{2}{3}\left(M_e c^2\right)\alpha^4\left(\frac{M_e}{M_p}\right)g_e g_p\right) \tag{20}$$

$$E_- = \frac{-3}{4}\left(\frac{2}{3}\left(M_e c^2\right)\alpha^4\left(\frac{M_e}{M_p}\right)g_e g_p\right) \tag{21}$$

where E_+ is the shift for the triplet states and E_- for the singlet state. We've expressed the physical constants in terms of the fine structure constant α and the electron rest energy to facilitate comparison to the fine structure shifts. These latter are of the order of $(M_e c^2)\alpha^4$ so the hyperfine split of the ground state is about 1800 times smaller or a factor of $\left(\frac{M_e}{M_p}\right)$. The full energy shift is $\Delta E = E_+ - E_-$.

$$\boxed{\Delta E = \frac{2}{3}\left(M_e c^2\right)\alpha^4\left(\frac{M_e}{M_p}\right)g_e g_p} \tag{22}$$

Putting in the values[9] (including $g_e = 2.00$ and $g_p = 5.59$) we find that $\Delta E = 5.89 \times 10^{-6}\text{eV} = 4.33 \times 10^{-7}\text{Ry}$. This shift corresponds to frequency $\nu = 1420\text{MHz}$ and wavelength $\lambda = 21.1\text{cm}$. The shifts from the unperturbed level are shown schematically in Figure1

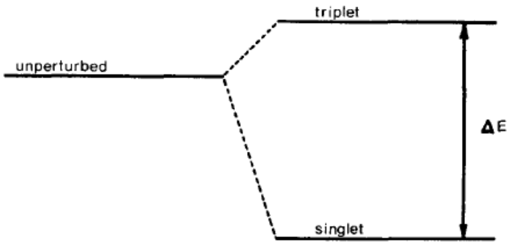

Figure 1. Energy shift due to spin-spin coupling of the proton and electron in the ground state of the Hydrogen atom (adapted from [8]).

It is interesting to note that the singlet state, with anti-parallel spins, is the state of lower energy despite the fact that the magnetic dipoles of the two particles are parallel. This contrasts with the case of two macroscopic bar magnets where the moments will line up antiparallel on closest approach. This traces directly back to the existence of the delta function term in Eq.(6) which gives us a contact interaction. (Indeed, without this term there would be no hyperfine splitting.) If we look at two small current loops, moments that line up parallel while at a finite distance will remain that way as the distance tends to zero since the currents are parallel and attract. Therefore parallel magnetic moments are the energetically favorable configuration, all the way down to point of contact. See Figure2.

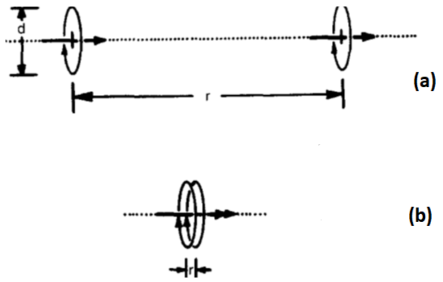

Figure 2. Two magnetic current loops (a) a finite distance apart; (b) at contact adapted from [8]).

This is in contrast to two small electric dipoles that if initially parallel will flip to anti-parallel as the distance tends to zero at contact. See Figure3. On the other hand, two macroscopic bar magnets, having finite extent, can never merge to a $r = 0$ limit. Therefore there is no effective contact. The energetically favorable configuration will be for the moments to be anti-parallel at closest possible approach.

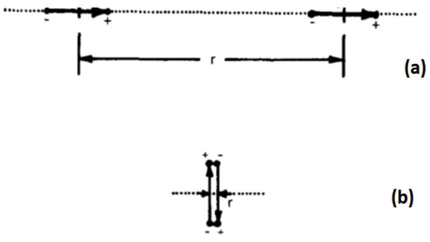

Figure 3. Two electric dipoles (a) at a finite distance apart; (b) at contact (adapted from [8]).

III. DERIVATION OF THE SPONTANEOUS TRANSITION RATE

To get the spontaneous transition rate A and associated lifetime we use time dependent perturbation theory to calculate the rate of stimulated emission, and then use the relation between the Einstein A coefficient for spontaneous emission and B coefficient for stimulated emission.

$$A = \frac{\hbar\omega_{10}^3}{\pi^2 c^3}B \tag{23}$$

where

$$\omega_{10} = \frac{\Delta E}{\hbar} = \frac{2}{3\hbar}\left(M_e c^2\right)\alpha^4\left(\frac{M_e}{M_p}\right)g_e g_p \tag{24}$$

is the emission frequency from one of the triplet states (S=1) to the singlet state (S=0). It will turn out that the relevant matrix elements from each triplet → singlet are identical.

We assume electromagnetic radiation impinging on the hydrogen atom in its ground state. The magnetic field component is given by

$$\vec{B(t)}_{ext} = 2B_0\cos(\omega t)\,\hat{n} \tag{25}$$

(This is similar in approach to the electric dipole case treated in [7]. Also, see [10]). The radiation interacts with the magnetic moments of both the electron and proton but since $|m_p| \ll |m_e|$ we can neglect the proton magnetic moment in what follows([10]). The perturbing Hamiltonian is then

$$\begin{aligned}\delta H &= -\vec{m}_e \cdot \vec{B(t)}_{ext}\\ &= 2H'\cos(\omega t)\end{aligned} \tag{26}$$

where

$$H' = \frac{e g_e B_0}{2M_e c}\left(\hat{n}\cdot\vec{S}_e\right) \tag{27}$$

We recognize the radiation is not coherent and will be a superposition of many modes $\omega(k)$ with $B_0(k)$ and $\hat{n}_k$. The general expression for the transition probability from one of the triplet states to the singlet will then be

$$\begin{aligned}P^k_{0\leftarrow 1}(t) &= \frac{|H'(k)_{10}|^2}{\hbar^2}\frac{\sin^2\left(\frac{\omega_{10}-\omega_k}{2}t\right)}{\left(\frac{\omega_{10}-\omega_k}{2}\right)^2}\\ &= \frac{e^2 g_e^2 B_0^2(k)}{4M_e^2c^2\hbar^2}\left|\left(\hat{n}_k\cdot(\vec{S}_e)_{10}\right)\right|^2\frac{\sin^2\left(\frac{\omega_{10}-\omega_k}{2}t\right)}{\left(\frac{\omega_{10}-\omega_k}{2}\right)^2}\end{aligned} \tag{28}$$

where $(\vec{S}_e)_{10}$ is the relevant matrix element between the hyperfine states. In exact analogy with the treatment of electric dipole radiation (see discussion following Eq.(4); also [7]), we average the term $\left|(\hat{n}_k\cdot(\vec{S}_e)_{10})\right|^2$ over all space so that the transition probability per unit time becomes

$$P^k_{0\leftarrow 1}(t) = \frac{e^2 g_e^2 B_0^2(k)}{4M_e^2c^2\hbar^2}\frac{1}{3}\left|(\vec{S}_e)_{10}\right|^2\frac{\sin^2\left(\frac{\omega_{10}-\omega_k}{2}t\right)}{\left(\frac{\omega_{10}-\omega_k}{2}\right)^2} \tag{29}$$

Now the energy density of the external magnetic field is given by

$$u_B = \frac{(2B_0(k))^2}{8\pi}\cos^2(\omega_k t) \tag{30}$$

which we can replace by its time average $\frac{B_0(k)^2}{4\pi}$. Since the energy density of the magnetic and electric fields in the waves are equal, the total energy density in each mode is given by

$$u(\omega_k) = \frac{B_0(k)^2}{2\pi} \tag{31}$$

We can now express the transition probability in terms of the energy density

$$P^k_{0\leftarrow 1}(t) = \frac{\pi e^2 g_e^2 u(\omega_k)}{6M_e^2c^2\hbar^2}\left|(\vec{S}_e)_{10}\right|^2\frac{\sin^2\left(\frac{\omega_{10}-\omega_k}{2}t\right)}{\left(\frac{\omega_{10}-\omega_k}{2}\right)^2} \tag{32}$$

To get the total transition probability we need to sum over all modes k. Similar to the argument in [7] this is equivalent to replacing the right side of Eq.(32) by an integral over $d\omega$

$$P_{0\leftarrow 1}(t) = \frac{\pi e^2 g_e^2}{6M_e^2c^2\hbar^2}\left|(\vec{S}_e)_{10}\right|^2\int u(\omega)\frac{\sin^2\left(\frac{\omega_{10}-\omega_k}{2}t\right)}{\left(\frac{\omega_{10}-\omega_k}{2}\right)^2}d\omega. \tag{33}$$

Over long times we can take the energy density out of the integral and evaluate it at ω_{10}. The remaining integral evaluates to $2\pi t$ so that

$$P_{0\leftarrow 1}(t) = \frac{\pi^2 e^2 g_e^2 u(\omega_{10})}{3M_e^2c^2\hbar^2}\left|(\vec{S}_e)_{10}\right|^2 t \tag{34}$$

The matrix elements to be computed are with the states given in Eqs.(14) to (17). The three possible initial states $|1\rangle$ are the triplets and the state $|0\rangle$ is the singlet. (Implicit in these calculations is the fact that the electron spin operator is in a tensor product with the identity operator in the proton spin space). Writing the matrix elements explicitly in component form gives

$$\langle 11|\,\vec{S}_e\,|00\rangle = \left(\frac{-\hbar}{2\sqrt{2}},\frac{i\hbar}{2\sqrt{2}},0\right) \tag{35}$$

$$\langle 10|\,\vec{S}_e\,|00\rangle = \left(0,0,\frac{\hbar}{2}\right) \tag{36}$$

$$\langle 1-1|\,\vec{S}_e\,|00\rangle = \left(\frac{\hbar}{2\sqrt{2}},\frac{i\hbar}{2\sqrt{2}},0\right) \tag{37}$$

At a glance it is seen that the squared norms of these vectors are the same and equal to $\frac{\hbar^2}{4}$. Putting this result into Eq.(34) yields

$$P_{0\leftarrow 1}(t) = \frac{\pi^2 e^2 g_e^2 u(\omega_{10})}{12M_e^2c^2}t \tag{38}$$

Identifying the transition rate

$$R_{0\leftarrow 1}(t) = \frac{P_{0\leftarrow 1}(t)}{t} \tag{39}$$

with $Bu(\omega_{10})$ gives

$$B = \frac{\pi^2 e^2 g_e^2}{12M_e^2c^2} \tag{40}$$

Finally, putting this into Eq.(23), substituting our previous result for ω_{10} from Eq.(24), and simplifying, we get the spontaneous emission rate

$$\boxed{A = \frac{2}{81}\alpha^{13}\left(\frac{M_e}{M_p}\right)^3 g_e^5 g_p^3\frac{(M_e c^2)}{\hbar}} \tag{41}$$

This is the rate for transition from any one of the triplet states. Substituting numerical values[9] gives $A = 2.89\times 10^{-15}\text{sec}^{-1}$ which implies a lifetime $\tau = \frac{1}{A} = 3.45\times 10^{14}\text{sec} = 1.09\times 10^{7}\text{yr}$. These values agree to those quoted in the literature, e.g., see [11],[12]

IV. DISCUSSION

The extremely long lifetime of the triplet state is characteristic of many magnetic dipole transitions and is expected based on the discussion of the radiation multipole expansion given earlier. From [10] typical ratios of magnetic dipole radiation rates to those of electric dipole radiation are of the order of

$$\frac{R_{\text{magnetic dipole}}}{R_{\text{electric dipole}}} \approx \alpha^8 \tag{42}$$

in the hydrogen atom. The 21cm transitions actually observed are mainly the result of stimulated emission. One of these processes is collisional excitation and de-excitation. In the typical interstellar environments where atomic hydrogen is found this rate[12] is on the order of $\approx 400\text{yr}^{-1}$ which is very fast compared to the spontaneous transition rate.

The ground state of the atom is also overwhelmingly likely to find itself in the higher triplet state. Assuming thermodynamic equilibrium the number of atoms, n_1, in the higher energy state, is related to the number, n_0, in the lower energy state by

$$\frac{n_1}{n_0} = 3\exp\left(\frac{-\hbar\omega_{10}}{k_B T_k}\right) \tag{43}$$

where T_k is the kinetic temperature of the gas with the factor of 3 owing to the degeneracy of the higher energy state. Note that the typical energy of CMB photons at $T_{CMB} = 3\text{K}$ is $\approx 2.6 \times 10^{-4}\text{eV}$. The interstellar medium will be at a temperature T_k higher than this, typically[13] $T_k \approx 10$ to 100K, so that

$$\hbar\omega_{10} \approx 5.9 \times 10^{-6}\text{eV} \ll k_B T_k \tag{44}$$

will hold implying $\frac{n_1}{n_0} \approx 3$, even at the $T = 10\text{K}$ end of the scale. The process of collisional emission rapidly followed by collisional absorption is one of the ways that ensures that the spectral line will likely be observed.

The second major process involving stimulated emission relates to Lyman-α radiation[14][15]. The atom is pumped to the first excited state ($n = 2$) from one of the hyperfine levels and then transitions to the ground state's other hyperfine level. See Figure4. Each of the fine structure n=2 levels is split into hyperfine levels ($S = J \pm \frac{1}{2}$). Only allowed transitions that couple both ground state levels are shown.

This process is known as the Wouthuysen–Field coupling and is particularly important in the intergalactic medium where the gas densities may be too small for thermodynamic equilibrium (Eq.(43)) to hold. It is also of great importance in modern studies of cosmology in the reionization era[5]

To cope with the differing temperatures (including that of the background CMB) a convenient parameter known as the spin temperature [15][5] has been defined:

$$\frac{n_1}{n_0} = 3\exp\left(\frac{-T_*}{T_{\text{spin}}}\right) \tag{45}$$

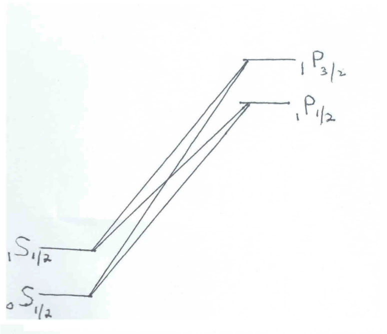

Figure 4. Allowed transitions from n=2 to n=1 hyperfine levels. Notation: $_SL_J$.

where

$$T_* = \frac{\hbar\omega_{10}}{k_B} \approx 0.0681\text{K} \tag{46}$$

is the effective temperature of the ground state hyperfine transition. It's a parameter that determines the occupation ratio of the two states and encodes the effects of CMB, kinetic and Lyman-α contributions:

$$T_{\text{spin}} = \frac{T_{CMB} + y_k T_k + y_\alpha T_k}{1 + y_k + y_\alpha} \tag{47}$$

where y_k and y_α are kinetic and Lyman-α coupling terms respectively whose values will depend on the specific environment of the hydrogen gas. Predictions and comparison to observations often involve estimating these coupling terms. In Field's original (pre-CMB) formulation there was also a background Lyman-α temperature T_α which in modern applications is simply set equal to T_k [5].

21CM physics is a vast subject and the current paper only covers the basic physics and immediate implications. Doing justice to its applications is far beyond this paper's scope. Current research is heavily focused on cosmological applications particularly in the onset of reionization and the first generation of stars and galaxies [4][5]. Both of these references, particularly[5] give detailed accounts (and extensive references) and are good starting points for interested persons. We also recommend [16] as a good starting point for YouTube presentations/ lectures.

……

Additional Note following from [17]. In this paper we have adhered to standard treatments of the hyperfine structure of hydrogen which use the nonrelativistic hydrogen ground state wavefunction. As is well known [18], the relativistic hydrogen atom ground state wavefunction that follows from the Dirac Equation contains a singularity at the origin. At small distances $r \ll a_0/2$ the Dirac wavefuncion behaves as

$$\backsim \psi(0) \exp\left(\frac{1}{2}\alpha^2 \ln\left(\frac{a_0}{2r}\right)\right)$$

which becomes infinite at the origin. This is a very mild singularity. To get the factor multiplying our $\psi(0)$ to be as large as 1.001 would require $r \backsim 10^{-27}\,\text{m}$. This would be deep inside the proton (radius $\backsim 10^{-15}\,\text{m}$). The underlying issue here is the assumption, in both our nonrelativistic calculation and the calculation using the Dirac wavefunction [19], that the proton is a point particle. This is clearly not the case and the point charge approximation breaks down at the order of the proton radius irrespective of the wavefunction (nonrelativistic versus relativistic) used in the computation. One must take into account relativistic corrections as well as corrections from QED and proton-structure contributions [20], particularly in the regime where r is of the order of the proton radius or less. So we are justified in making a cutoff at the lower limit in the radial integral of the Dirac wavefunction at the level of the point charge approximation. A calculation, to lowest order in α, using the Dirac wavefunction gives an identical result as our Eq.(22) [19].

[1] L. H. Aller, *Atoms, Stars and Nebulae.* Cambridge University Press, 3rd ed., 1991.

[2] R. I. Ewen and Purcell, *Observation of a Line in the Galactic Radio Spectrum.* Nature168, (1951)356. reprinted in Woodruff,Turner,SullivanIII, Classics in Radio Astronomy,Reidel(1982)328.

[3] H. I. Ewen, *Radio Waves from Interstellar Hydrogen.* Scientific American, (Dec.1953)42.

[4] R.Barkana, A.Loeb,, *Detecting the Earliest Galaxies Through Two New Sources of 21CM Fluctuations.* ApJ626, (2005)1.

[5] S.Zaroubi, *The Epoch of Reionization.* arXiv:1206.0267v1 [astro-ph.CO] 1 Jun 2012.

[6] J. D. Jackson, *Classical Electrodynamics.* John Wiley and Sons, (1999)Ch9.

[7] B. Zwiebach, *Light and Atoms.* 8.06x Notes, 2019(Ch6.3).

[8] D. J. Griffiths, *Hyperfine splitting in the ground state of hydrogen.* AJP50, (1982)698.

[9] P.J.Mohr, D.B.Newell, B.N.Taylor, *CODATA recommended values of the fundamental physical constants: 2014.* RMP88, (2016)035009.

[10] R. Fitzpatrick, *Quantum Mechanics.* World Scientific, (2015). Ch8.

[11] T.Padmanabhan, *Theoretical Astrophysics, Vol.1.* Cambridge University Press, (2000). Ch7.

[12] J.Binney, M.Merrifield, *Galactic Astronomy.* Princeton University Press, (1998). Sec8.1.4.

[13] F.H.Shu, *The Physical Universe.* University Science Books, (1982). Ch11.

[14] S.A.Wouthuysen, *On the excitation mechanism of the 21-cm (radio-frequency) interstellar hydrogen emission line.* AJ57, (1952)31.

[15] G.B.Field, *The Spin Temperature of Intergalactic Neutral Hydrogen.* ApJ129, (1959)536.

[16] A.Lidz(University of Pennsylvania, *Cosmic Reionization from the Lyman-alpha Forest, 21 cm, and Line-Intensity Mapping.* https://www.youtube.com/watch?v=5NaF8rPnU40, 2018-12-10.

[17] Jim Freericks, forum posting.

[18] H.A.Bethe, E.E.Salpeter, *Quantum Mechanics of One- and Two-Electron Atoms.* Springer-Verlag, (1957). p.70.

[19] E.D.Commins, *Quantum Mechanics, A Experimentalist's Approach.* Cambridge University Press, (2014). Sec21.8 and Prob21.5.

[20] A.V.Volotka, *High-Precision QED Calculations of the Hyperfine Structure in Hydrogen and Transition Rates in Multicharged Ions.* Institut für Theoretische Physik, Fakultät Mathematik und Naturwissenschaften, Technische Universität Dresden, (2006).

The 21-cm Line of Hydrogen and its Role in Astrophysics

Kiwirobot

June 19, 2019

Abstract The neutral hydrogen atom has a hyperfine transition of the 1S state due to the energy difference between the nucleus spin (proton) and the electron spin being either parallel or antiparallel. The radiation associated with this transition is at 21-cm (1.42 GHz). The transition is forbidden and so has a very narrow spectral line. On Earth, hydrogen normally exists as a diatomic molecule and so this radiation is not easily seen but in the very tenuous interstellar medium, single neutral hydrogen atoms can exist. The existence and detection of this 21-cm line has been very important in astrophysics. This article will explain the quantum mechanics of the transition in the 1S neutral atom and discuss its uses in astrophysics and cosmology.

1 Introduction

Astrophysics is the application of physics to the structure and evolution of our universe. Astrophysical theories developed from the physics cannot be tested in the usual way by performing scientific experiments on the subject in a controlled environment. Instead, astrophysics and astronomy have to rely on making observations that infer the theory being tested. Historically, these observations have been based on what can be seen with our eyes and so have been of the optical light arriving at the Earth. More recently, say the last 80 years, observations have extended to the full range of the electromagnetic spectrum. Further, observations have now been made of subatomic particles arriving at Earth from astronomical events and, most recently, gravitational waves from merging black holes.

Interpretation of these observations requires a thorough understanding of the physics, both of the processes that created the radiation and the way in which the radiation propagates through the intervening space. This paper discusses one such source of radiation; the 21-cm radio waves that originate from a hyperfine transition in atomic, neutral hydrogen. Finally, two important examples of the role of the 21-cm line in astrophysics are discussed. A knowledge of the contents of the course MITx 8.06[1] is assumed – and it is referenced at several points in the text – but all the astrophysics is presented at an introductory level. The units used throughout are cgs.

2 Hyperfine Splitting

Any undergraduate textbook on quantum mechanics will develop the theory that describe the behaviour of an electron in the simplest of atoms, i.e hydrogen.[2] The starting model for this atom is a single electron in a $\frac{1}{r}$ Coulomb potential. The result of this gives a complete set of eigenstates for the electron which are enumerated by n (principal quantum number), l (total angular momentum), m_l (z component of angular momentum) and m_s (electron spin). The electron spin does not form part of the model but is tacked on to give the required number of states. The eigenenergies of the electron are dependent only on n and are distributed thus

$$E_n = -\frac{13.6}{n^2}\, eV \tag{1}$$

Each energy level has degenerate states labelled by l, m_l and m_s.

This simple model can be refined using the Dirac equation which is relativistically correct and incorporates electron spin. The Dirac equation adds terms to the Hamiltonian of the hydrogen atom which represent a relativistic correction, the coupling between the orbital angular momentum of the electron L and its spin S (L-S coupling), and a term called the Darwin correction. These terms are all of the order α^2 smaller than the binding energy of the atom, where α is the fine structure constant (1/137). These perturbations are therefore about 10^{-4} smaller than the base energy levels Eq.(1) and represent small shifts in the energy levels of the hydrogen atom. These shifts break some, but not all, of the degeneracies noted above and are called the fine structure of the hydrogen atom.

There is yet another element missing from this model of the hydrogen atom. The atomic nucleus of hydrogen, a single proton, has a spin and therefore a magnetic moment. Adding this to the model of the hydrogen atom results in the hyperfine splitting of the energy spectrum.

The magnetic moment of a proton is given by

$$\boldsymbol{\mu}_p = \frac{g_p e}{2m_p c}\boldsymbol{I} \tag{2}$$

where g_p is the gyromagnetic ratio and $\boldsymbol{I}$ is the proton spin. Because the proton is made from 3 quarks and has structure, the value of g_p is 5.59 instead of ∼2, as for the electron. The magnetic field produced by the proton couples to the electron spin in a similar way to the L-S coupling of the fine structure, but note that $\boldsymbol{\mu}_p$ has the proton mass m_p in the denominator. This makes the magnetic field due to the proton $\frac{m_e}{m_p}$ smaller and so the energies in hyperfine splitting are ∼1/1800 times smaller than the already small fine structure.

The magnetic field due to the proton is given by [3]

$$\boldsymbol{B} = \frac{1}{r^3}(3(\boldsymbol{\mu}_p \cdot \boldsymbol{r})\boldsymbol{r} - \boldsymbol{\mu}_p) + \frac{8\pi}{3}\boldsymbol{\mu}_p \delta^3(r) \tag{3}$$

This equation has two parts. The first part is what would be expected from classical electromagnetism. It is correct but it has an issue of a singularity at $r = 0$. By considering an infinitesimal sphere with a magnetic dipole, it is possible to show that the field has a constant value inside the sphere which then gives the value at $r = 0$ [3]. This value appears as the second term with the δ function. Given this $\boldsymbol{B}$ field, the Hamiltonian for the electron is

$$\begin{aligned} H_{hf} &= -\boldsymbol{\mu}_e \cdot \boldsymbol{B} \\ &= -\frac{1}{r^3}(3(\boldsymbol{\mu}_p \cdot \boldsymbol{r})(\boldsymbol{\mu_e} \cdot \boldsymbol{r}) - \boldsymbol{\mu}_e \cdot \boldsymbol{\mu}_p) \qquad (4) \\ &\quad - \frac{8\pi}{3}\boldsymbol{\mu}_e \cdot \boldsymbol{\mu}_p \delta^3(r) \end{aligned}$$

This Hamiltonian represents a small perturbation of the main Hamiltonian. The first order energy shift due to H_{hf} can be obtained from perturbation theory [1] and to first order is

$$\Delta E = \langle \psi | H_{hf} | \psi \rangle. \tag{5}$$

3 Application to the 1S Hydrogen Atom

The 1S ground state of an hydrogen atom is

$$\psi_0 = \frac{1}{\sqrt{(\pi a_o^3)}} e^{-r/a_0} \otimes |s\rangle \tag{6}$$

where the spin states have been included through a tensor product. This state has no θ or ϕ dependence and is spherically symmetric; as are all $l = 0$ states. Consider the first term in Eq.(4). Assuming the spins are aligned with the z-axis – without loss of generality – the integral for this term becomes, after expanding the dot products

$$\int_V -\frac{1}{\pi a_o^3} e^{-2r/a_0} \frac{\mu_e \mu_p}{r^3}(3cos^2\theta - 1)r^2 sin\theta dr d\theta d\phi \tag{7}$$

where θ is the spherical polar coordinate between $\boldsymbol{r}$ and the z-axis, i.e $z = rcos\theta$. Because of the lack of angular dependence of the ground state Eq.(6), the θ part of this integral evaluates to zero making the whole integral zero Now consider the second term of Eq.(4). The ground state Eq.(6) is non-zero at $r = 0$ and so integration with the δ function of Eq.(4) returns a non-zero result.

$$\begin{aligned} \Delta E &= \langle \psi_0 | H_{hf} | \psi_0 \rangle \\ &= -\langle \psi_0 | \frac{8\pi}{3}\boldsymbol{\mu}_e \cdot \boldsymbol{\mu}_p \delta^3(r) | \psi_0 \rangle \\ &= -\frac{8\pi}{3}(\langle \psi_0 | \delta(r) | \psi_0 \rangle \otimes \langle s | \boldsymbol{\mu}_e \cdot \boldsymbol{\mu}_p | s \rangle) \qquad (8) \\ &= -\frac{8\pi}{3}|\psi_0(r=0)|^2 \langle s | \boldsymbol{\mu}_e \cdot \boldsymbol{\mu}_p | s \rangle \\ &= \frac{8\pi}{3}\frac{1}{\pi a_0^3}\frac{e^2 g_p g_e}{4 m_p m_e c^2}\langle s | \boldsymbol{S} \cdot \boldsymbol{I} | s \rangle \end{aligned}$$

The minus is removed from the last equation because $\boldsymbol{\mu}_e = -\frac{eg_e}{2m_e c}\boldsymbol{S}$. This then leaves the expectation value for $\boldsymbol{S} \cdot \boldsymbol{I}$. This is another spin-spin coupling and so it can be treated the same as L-S coupling. The z components of $\boldsymbol{S}$ and $\boldsymbol{I}$ do not commute; it is the sum of the spins $\boldsymbol{F} = \boldsymbol{S} + \boldsymbol{I}$ that are diagonalisable and $\boldsymbol{S} \cdot \boldsymbol{I}$ can be obtained in the usual way [1].

$$\begin{aligned} F^2 &= I^2 + S^2 + 2\boldsymbol{S} \cdot \boldsymbol{I} \\ \boldsymbol{S} \cdot \boldsymbol{I} &= \frac{1}{2}(F^2 - S^2 - I^2) \qquad (9) \end{aligned}$$

The basis states that diagonalise F^2, F_z, S^2 and I^2 are given by [4]

$$\begin{aligned} &\frac{1}{\sqrt{2}}(|\downarrow\uparrow\rangle - |\uparrow\downarrow\rangle) \quad (f = 0) \\ &\frac{1}{\sqrt{2}}(|\downarrow\uparrow\rangle + |\uparrow\downarrow\rangle) \quad (f = 1) \qquad (10) \\ &|\uparrow\uparrow\rangle \quad (f = 1) \\ &|\downarrow\downarrow\rangle \quad (f = 1) \end{aligned}$$

The eigenvalues f from F^2 are in brackets. The matrix elements for $\boldsymbol{S} \cdot \boldsymbol{I}$ in this basis can be evaluated using Eq.(9).

$$\begin{aligned} \langle s | \boldsymbol{S}.\boldsymbol{I} | s \rangle &= \frac{1}{2}\hbar^2(f(f+1) \\ &\quad - s(s+1) - i(i+1)) \qquad (11) \\ &= -\frac{3}{4}\hbar^2 \\ &\quad \text{for } f = 0, s = \frac{1}{2}, i = \frac{1}{2} \text{ singlet state} \\ &= \frac{1}{4}\hbar^2 \\ &\quad \text{for } f = 1, s = \frac{1}{2}, i = \frac{1}{2} \text{ triplet state} \end{aligned}$$

The singlet state is shifted down and the triplet states are shifted up. The total shift is $\hbar^2$ and so the energy shift between the two levels is given by Eq.(8) as

$$\begin{aligned} \Delta E_{tot} &= \frac{8\pi}{3}\frac{\hbar^2}{\pi a_0^3}\frac{e^2 g_p g_e}{4 m_p m_e c^2} \qquad (12) \\ &= 5.884 \times 10^{-6}\text{eV} \end{aligned}$$

The corresponding photon for this energy difference has a frequency (using $\Delta E = h\nu$) of 1422.8 MHz and a wavelength of 21.07cm. It is this radiation that is referred to as the 21-cm line and which has such importance in astrophysics.

4 Transition Rate and Line Width

The hyperfine splitting of the 1S energy levels in hydrogen can be traced to the orientation of the spin of the proton and the electron. Changes to these spin states have no effect on the distribution of charge in the atom and so the dominant interaction with the electromagnetic field, i.e. through the electric field, does not affect these transitions. The 21-cm transition is therefore forbidden. Transitions can still happen through the magnetic field interaction (and the quadrupole interaction) but these are much less likely; the magnetic field for an electromagnetic wave is $1/c$ smaller. Derivations of the transition rate are sparse in the literature and textbooks but here are two [5][6].

The transition is mediated through the magnetic interaction. The Hamilton for the electron's interaction is

$$\begin{aligned} H_B &= -\boldsymbol{\mu}_e \cdot \boldsymbol{B} \\ &= \frac{g_e e}{2m_e c}\boldsymbol{S}\cdot\boldsymbol{B} \end{aligned} \tag{13}$$

The interaction between the nuclear spin and the magnetic field can be ignored because it will be m_e/m_p smaller. The B-field is taken as a sinusoidal oscillation.

$$\boldsymbol{B} = B_0\,\boldsymbol{p}\,cos\omega t \tag{14}$$

The quantity $\boldsymbol{p}$ is a unit vector specifying the polarisation of the electromagnetic wave. It is necessary to include this because the interaction with a dipole is polarization dependent. Applying time-dependent perturbation theory to the Hamilton gives the transition probability to go from initial state (i) to final state (f) as [1]

$$P_f = |\langle f|\boldsymbol{S}\cdot\boldsymbol{p}|i\rangle|^2 \left(\frac{g_e e B_0}{2m_e c\hbar}\right)^2 \frac{sin^2((\omega-\omega_{fi})t/2)}{(\omega-\omega_{fi})^2} \tag{15}$$

where $\omega_{fi} = (E_f - E_i)/\hbar$. This probability must be summed over all the final states. There is only a single final state for the electron, i.e. the singlet state of the ground state. Not so the photon. It is necessary to sum over all the final photons state. To achieve this we apply box regularisation[1]. This involves a summation over a large but finite sized volume with periodic boundary conditions. Before doing this, it is necessary to address two parts of Eq.(15), i.e. the matrix elements and the value of B_0.

The matrix element contains a reference to $\boldsymbol{p}$. Setting this up as a unit vector at an angle θ to the z-axis and in the z-x plane, without loss of generality, gives

$$\boldsymbol{S}\cdot\boldsymbol{p} = S_z cos\theta + S_x sin\theta \tag{16}$$

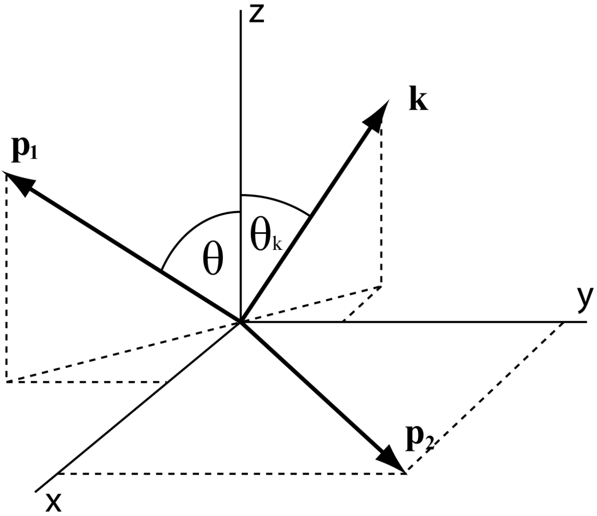

Figure 1: The arrangement of polarisation vectors and photon momentum vector.

The electron transitions from an initial triplet state to a final singlet, ground state, see Eq.(10). Choosing the actual initial state as $|\uparrow\uparrow\rangle$ gives

$$\langle f|\boldsymbol{S}\cdot\boldsymbol{p}|i\rangle = \langle \frac{1}{\sqrt{2}}(\langle\downarrow\uparrow| - \langle\uparrow\downarrow|)|S_z cos\theta + S_x sin\theta|\uparrow\uparrow\rangle \tag{17}$$

The initial and final states are eigenstates of S_z and are orthogonal. The S_z part is therefore zero. Noting that S_x only works on the first arrow in the bras and kets and applying S_x to the spins states leads to

$$\begin{aligned} \langle f|\boldsymbol{S}\cdot\boldsymbol{p}|i\rangle &= \frac{1}{\sqrt{2}}\langle\downarrow\uparrow|S_x sin\theta|\uparrow\uparrow\rangle \\ &= \frac{\hbar}{2\sqrt{2}} sin\theta \end{aligned} \tag{18}$$

The value of B_0 can be found from a semi-classical argument by asking what would the B-field be for a single photon. A proper handling of this would require quantisation of the electromagnetic field. The total B-field energy in a volume V is given by

$$\frac{B_0^2}{8\pi} \times \frac{1}{2} \times 2 \times V = n\hbar\omega \tag{19}$$

The first term is taken from classical electromagnetism. The second is because the field is oscillating and so we actually need the root-mean-square value. The final 2 is because there is the same amount of energy in the E-field. If we have a single photon ($n = 1$) this can be rearranged to give B_0^2. The probability of a transition, Eq(15), then becomes

$$P_f = \frac{\pi\hbar\omega}{4V}\left(\frac{g_e e}{m_e c}\right)^2 \frac{sin^2((\omega-\omega_{fi})t/2)}{(\omega-\omega_{fi})^2} sin^2\theta \tag{20}$$

To proceed from here requires the summation of P_f over all photon directions $\boldsymbol{k}$ and both polarisations, $\boldsymbol{p_1}$ and $\boldsymbol{p_2}$. The polarisations enter P_f through $sin^2\theta$.

Consider the arrangement of vectors in Fig 1. The $\boldsymbol{k}$ vector is at an angle θ_k to the z-axis. The new angle θ_k will be the variable used to sum the $\boldsymbol{k}$ vectors. $\boldsymbol{p_2}$ is then defined to lie in the x-y plane and, as it should be, is normal to $\boldsymbol{k}$. It's angle to the z-axis θ_2 is $\pi/2$. The third vector is normal to both $\boldsymbol{p_2}$ and $\boldsymbol{k}$ and is at an angle $\theta_1 = \pi/2 - \theta_k$ to the z axis. The summation of these polarisation can then be reduced to

$$\begin{aligned}\sum_{i=1,2} sin^2\theta_i &= sin^2(\pi/2-\theta_k) + sin^2(\pi/2) \\ &= cos^2\theta_k + 1 \qquad (21)\end{aligned}$$

We can now sum over all the photon vectors $\boldsymbol{k}$. The values of $\boldsymbol{k}$ are discrete in the large volume V used in box regularisation. As the volume goes to infinite, these become a continuum with the number of state per unit volume given by $\frac{Vd^3\boldsymbol{k}}{8\pi^3}$ [1]. The probability integral then becomes

$$P = \int_{V_k} \Gamma \frac{sin^2((\omega-\omega_{fi})t/2)}{(\omega-\omega_{fi})^2}(cos^2\theta_k + 1)\, dV_k \qquad (22)$$

where

$$\begin{aligned}\Gamma &= \frac{V}{8\pi^3}\frac{\pi\hbar\omega}{4V}\left(\frac{g_e e}{m_e c}\right)^2 \\ dV_k &= dk\, k^2 sin\theta_k d\theta_k d\phi_k \qquad (23)\end{aligned}$$

V_k is the volume in k-space. Note that the infinite volume V used for box regularisation cancels on the top and bottom. This integral can then be solved using the arguments from Fermi Golden Rule [1], i.e as t gets larger, the main contribution comes from the central lobe of the sin^2x/x^2 distibution and so $\omega \sim \omega_{fi}$. This makes k in Eq.(23) a constant equal to ω_{fi}/c. The integral of the sin^2x/x^2 part becomes

$$\int_0^\infty \frac{sin^2((\omega-\omega_{fi})t/2)}{(\omega-\omega_{fi})^2}\frac{d\omega}{c} = \frac{\pi t}{2c} \qquad (24)$$

Pulling all these results together gives the Einstein coefficient A for the transition rate as

$$\begin{aligned}A = P/t &= \frac{V}{8\pi^3}\frac{\omega_{fi}^2}{c^2}\frac{\pi\hbar\omega_{fi}}{4V}\left(\frac{g_e e}{m_e c}\right)^2\frac{\pi}{2c}\frac{16\pi}{3} \\ &= \frac{g_e^2\omega_{fi}^3\hbar e^2}{12m_e^2c^5} \qquad (25)\end{aligned}$$

where the last fraction comes from the integration of the θ_k terms. The transition rate can now be calculated as $2.85 \times 10^{-15}s^{-1}$ This is a very small transition rate and corresponds to a lifetime of the triplet state of $\tau = 1.1 \times 10^7$ years.

This very long lifetime has an effect on the natural line width of the radiation. A radiation process with a large uncertainty in the time that it will happen δt has a correspondingly small uncertainty in the energy δE of the transition. These are related through the Heisenberg uncertainty principle.

$$\delta E = \frac{\hbar}{\delta t} \qquad (26)$$

$$h\delta\nu = \frac{\hbar}{\tau} \qquad (27)$$

Using the value of τ from above gives a frequency uncertainty of $10^{-15}Hz$. This represents a very small line width resulting in a very precise frequency of the radiation from hydrogen. Astonishingly, the frequency of this radiation has been determined as 1420.4057517667 MHz. This is one of the most precisely known physical values.

5 Importance in Astrophysics

The 21-cm line radiation is rarely produced on Earth because of the slow transition rate and the fact that hydrogen normally exists as a diatomic molecule. An exception to this is the hydrogen maser [7]. In space, where gas densities can be measured as several atoms per cubic metre, it is possible for isolated, neutral hydrogen atoms to exist. The slow transition rate of these atoms is balanced by the amount of hydrogen; 75% of the normal matter in the universe is hydrogen. The 21-cm line was observed in the 1930s and was the first step out of the optical part of the electromagnetic spectrum for astronomers. The 21-cm line observations have an advantage over optical observations. Not only does it pass though the Earth's atmosphere (1.4 GHz is a frequency used in satellite communication) but it also passes through the dust and gas in the universe that obscure large parts of the sky, particularly for our galaxy.

Observations of the 21-cm line radiation from neutral hydrogen (usually referred to as HI) have made a huge contribution to astrophysics. It is the properties noted earlier, i.e. precise frequency and long life of the state, that make the transition so useful. We consider two important examples of this.

5.1 Mapping the Dynamics of Hydrogen Gas in Galaxies

Radiation from a source that is moving is Doppler shifted. This is very familiar when listening to the tone of a passing vehicle lowering as it drives by. A receding object has an observed lowering of its frequency and visa versa for an approaching object. The same thing happens to light but the velocities required to produce a measurable shift are much higher. The fre-

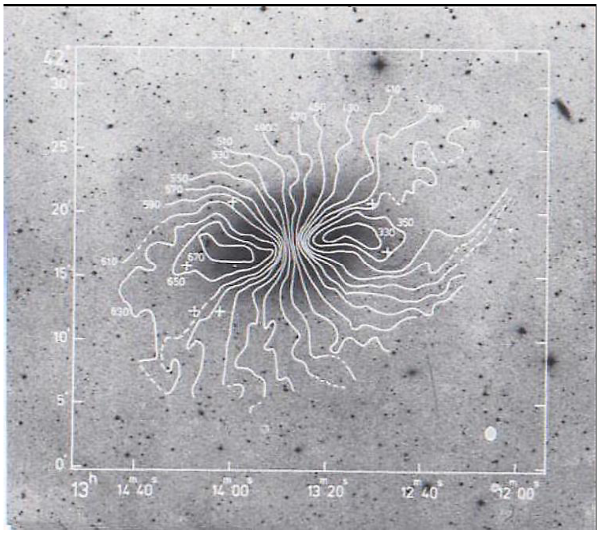

Figure 2: A contour map showing the line of sight velocities of the HI gas in the galaxy NGC5055. [9]

quency shift for light can be quantified using [8]

$$\nu' = \nu \left(\frac{1 - \frac{v}{c}}{1 + \frac{v}{c}} \right) \tag{28}$$

Galaxies have typical recession velocities of 100's km s^{-1}. A recession velocity of 100 km s^{-1} would produce a frequency shift of about 1 MHz on 21-cm radiation at 1.4GHz. The very precise frequency of the 21-cm line makes measuring the accurate Doppler shifts of the HI gas in galaxies a possibility.

Galaxies are broadly categorised as either spiral or elliptical. The elliptical galaxies are gas poor and so are not candidates for observation. On the other hand, spiral galaxies have large amounts of neutral hydrogen. Fig 2 shows a typical contour map of the observed line of sight velocities of HI gas for a spiral galaxy. The pattern of the contours is consistent with a flat, rotating, disc galaxy viewed at an angle.[9] The velocities in the central contours are about 510 km s^{-1} and this is the velocity at which the galaxy is receding. On one side of this there is an area where the velocities are smaller than the recessional velocity due to the motions in the rotating disc projected towards the observer. On the other side the reverse happens. These observations have provided an invaluable tool in studying the internal motion of spiral galaxies.

One of the most important discoveries from these observations of spiral galaxies was that the rotation curves – the variation of the rotation velocity of the disc with radius – showed that the speed of rotation was approx. constant out to very large radii. It was expected that the velocities would fall away based on the distribution of matter that could be seen. This was the first indication that there was a large amount of unseen, dark matter. At the time it was speculated that this was just cold, ordinary matter. It is now thought these rotation curves indicate the presence of exotic dark matter which forms a large part of the universe and has a central role in its evolution. The nature of dark matter is still unknown and its study links straight back to quantum physics.

5.2 21-cm Cosmology

Before discussing the 21-cm hyperfine transition in the context of cosmology [10], it is necessary to tell a part of the currently accepted story of the universe. The universe began with a big bang about 1.38×10^{10} years ago. Soon after the big bang, the universe was an expanding plasma of heavily interacting charged particles and photons. After about 380,000 years the expansion had cooled the universe to the point where electrons could combine with protons to form hydrogen atoms. This point is called recombination and is where matter becomes neutral allowing the photons to decouple from the atoms. These photons are visible today as the cosmic microwave background (CMB) which carries an imprint of the structure of the universe at this time period. The universe at this point was mainly flat and homogeneous but with some small variations in density. After recombination, the universe continues to cool and go dark. This is referred to as the cosmic dark ages and lasted about 1 billion years during which little was visible. The initial variations in the density of the universe started to grow, driven by gravity and assisted by dark matter. The universe then entered the re-ionisation phase. In this phase, gravity had pulled together enough matter, to high enough densities, to start star formation in early galaxies. The photons from these stars start to re-ionise the gas in the universe which becomes visible again. From here, the universe keeps expanding, stars and planets form, life begins onward to the present day. From our current position we look out into space and can see the history of the universe mapped out against distance from the Earth: the further away we observe, the longer the light has been travelling and the further back in time we see. Also, the light from further away experiences a cosmological redshift due to the light propagating in space that is expanding; the wavelength increases for light that has been travelling for longer.

The cosmic dark ages are a period of great importance because it is the missing link between the very early universe with small density enhancements and the modern universe with all its fully formed structure. We know very little about this period because the universe was dark and not emitting light. This is where the 21-cm line has become another tool for observation because of the long life of the HI state and its precise frequency. During the dark ages, the universe was largely made of neutral hydrogen. This hydrogen was illuminated by the photons from the big bang.

These photons are visible today, after being redshifted, as the cosmic microwave background. It is possible for the neutral hydrogen to absorb photons from the CMB at the very precise frequency of the 21-cm line leaving a small gap in the continuous, black body spectrum of the CMB. This small gap, called an absorption line, is then redshifted to lower frequencies. The amount of redshift depends on the time during the cosmic dark ages that the absorption happened. Current observational effort is therefore looking for a 'forest' of these absorption lines in the CMB. The frequency shifts in these forests then maps out the distribution of neutral hydrogen in time and space in the early universe and provide a window into the cosmic dark ages. Also, the amount of absorption is dependent on the proportion of hydrogen atoms sitting in the singlet state; only these unexcited atoms can absorb a photon at 21-cm. The hyperfine transition of hydrogen has a very low energy threshold and so the atoms can be excited to the triplet state as a result of atomic collisions. Once excited, the atoms can remain in this excited state for a significant proportion of the period of the dark ages. Therefore, the proportion of excited hydrogen atom is related to the environment around the neutral hydrogen and so observations of 21-cm absorption can provide information not only about the distribution of neutral hydrogen but also about the conditions in the cosmic dark ages.

6 Conclusion

This paper has shown how quantum physics has a central role in astrophysics not only in theorising about the particle physics of the big bang but also in allowing and interpreting astrophysical observations. Much of our understanding of the universe is grounded in the theory and predictions of quantum physics. Further, astrophysics provides opportunities to contribute to our knowledge of quantum physics through, for instance, the study of dark matter.

References

[1] B. Zwiebach, “Applications of quantum mechanics,” *MITx 8.06x, edx course*, 2019.

[2] D. Griffiths, *Introduction to Quantum Mechanics.* Prentice Hall, 1995.

[3] D. Griffiths, “Hyperfine splitting in the ground state of hydrogen,” *American Journal of Physics*, 1982.

[4] R. Feynman, *Feynman Lectures in Physics III ch 12.* AddisonWesley, 1964.

[5] P. J. E. Peebles, *Quantum Mechanics.* Princeton University Press, 1992.

[6] R. J. Gould, “Radiative hyperfine transitions,” *Astrophysical Journal vol 362, p 284*, 1990.

[7] D. Kleppner, H. M. Goldenberg, and N. F. Ramsey, “The atomic hydrogen maser,” *Physical Review. 126 603*, 1962.

[8] Wikipedia, “Doppler effect,” 2019.

[9] P. van der Kruit, “The kinematics of spiral and irregular galaxies,” *Annual Review of Astronomy and Astrophysics, vol 16, pp 103-139*, 1978.

[10] J. R. Pritchard and A. Loeb, “21-cm cosmology in the 21st century,” *Reports on Progress in Physics*, 2012.

A case of study: CP violation in the neutral kaons system

Antonio Mason

(Dated: June 19, 2019)

This work describes the neutral kaons system by choosing suitable bases, stressing how strangeness eigenstates, CP eigenstates and mass eigenstates differ. We'll see in particular that CP eigenstates are almost mass eigenstates in the vacuum, thus allowing only for a small CP violation.

I. INTRODUCTION

In high energy physics particles and their antiparticles are produced in equal amounts. The observable universe, instead, is almost entirely made up of matter, with only traces of antimatter: how can we reconcile these two facts?

The Russian physicist Andrei Sacharov in 1967 stated three necessary conditions for the universe to develop asymmetry between matter and antimatter. The first condition states that the universe be not in thermal equilibrium, the second requires the violation of the baryonic number and the third is concerned with the violation of CP symmetry. In our understanding of particle physics processes violating the baryonic numbers are beyond the standard model, while processes violating CP can be accommodated in the Cabibbo-Kobayashi-Maskawa matrix, which describes the mixing among the three generations of quarks [1]. Up to now, however, the observed violation of CP symmetry is too scarce to explain the asymmetry between matter and antimatter.

Processes where CP is violated were observed for the first time in the system of neutral kaons by Cronin and Fitch in 1964. In 1972 Kobayashi and Maskawa showed that the standard model of particles can allow for CP violation if there are at least three generations of quarks (only two were known at that time); the quark bottom was discovered in 1977 and the quark top in 1995. The search for CP violating processes is now well established: an interesting sector concerns neutral mesons involving the quark bottom, because of its higher masses and energies with respect to the kaons, allowing perturbative methods. Finally CP violating processes concerning leptons are under investigation because neutrinos, whose observed phenomenology is beyond the standard model of particles, can account for other sources of CP violation.

Quantum mechanics can describe the neutral kaons system as an abstract two-states system, regardless of the standard model of particles. CP violation shows a rich phenomenology (direct and indirect) and coherent and incoherent regeneration allows for comparison with light polarization (respectively birefringence and dichroism).

This work describes the neutral kaons system by choosing suitable bases, stressing how strangeness eigenstates, CP eigenstates and mass eigenstates differ. We'll see in particular that CP eigenstates are *almost* mass eigenstates, thus allowing only for a small CP violation.

II. DISCRETE TRANSFORMATIONS IN PHYSICS

There are three discrete transformations who play a fundamental role in the description of microscopic interactions, namely the parity P, the charge conjugation C and the time reversal T. The discussion of these symmetries will introduce us to the consequences of CP violation.

A. Parity

Parity transformation consists in exchanging left with right or, more precisely, consider what happen when you reverse the spatial coordinates, letting, with standard notation, $(x, y, z) \to (-x, -y, -z)$ or, in vector notation, $\vec{r} \to -\vec{r}$. This transformation, as well as charge conjugation and time reversal, is called discrete because it cannot be described in terms of a continuous parameter, like spatial translations or rotations. By applying parity transformation to a wave-function we have the equation $P\psi(\vec{r}) = \psi(-\vec{r})$. Let's apply two times the parity transformation:

$$P^2\psi(\vec{r}) = PP\psi(\vec{r}) = P\psi(-\vec{r}) = \psi(\vec{r}), \tag{1}$$

obtaining the important result that the $P^2 = 1$, where 1 means the identity operator. Equation (1) means that the eigenvalues of the parity transformation are ± 1 and its eigenfunctions are the familiar even (with eigenvalue 1) and odd (with eigenvalue -1) functions. From quantum mechanics we knows that an operator is conserved if it commutes with the Hamiltonian; for example a spherically symmetric potential is invariant under parity because $V(\vec{r}) = V(r) = V(-\vec{r})$. The relation $\vec{r} \to -\vec{r}$ in spherical coordinates provides the relations $\theta \to \pi - \theta, \phi \to \pi + \phi$. By applying these rules to the general formula of spherical harmonics it can be shown that

$$PY_{lm}(\theta, \phi) = (-1)^l Y_{lm}(\theta, \phi), \tag{2}$$

so even l states have positive parity and odd l states have negative parity.

It is an experimental fact that electromagnetic and strong interactions preserve parity. As a consequence, wave-functions describing particles have definite parity. Let's consider a electric dipole transition: the selection rule $\Delta L = 1$ holds, therefore atomic initial and final states have opposite parity. In order to ensure parity conservation the emitted dipole radiation, that is identified with a single photon, has value -1. In this sense we affirm that the intrinsic parity of the photon is -1. The reader should have guessed that parity is a *multiplicative* quantum number: the parity of a composite system is the product of the parities of each sub-system.

Weak interactions violates parity. Just consider an electronic neutrino, a spin 1/2 particle that do not have electromagnetic or strong interaction. If parity were preserved we should expect that the projection of the spin along the direction of motion may assume $\pm\frac{\hbar}{2}$ values, but only electronic neutrinos with $S_z = -\frac{\hbar}{2}$ have been observed. If we apply parity to such a particle we reverse its momentum, whilst its spin remains unchanged. The net result is a neutrino with $S_z = \frac{\hbar}{2}$ along the direction of motion, which simply does not exists, as far as we know.

B. Charge conjugation

Now we discuss the charge conjugation operator C: originally it was defined by its action onto an electric charge q, namely $Cq = -q$ and, thinking of the wavefunction of a particle with electric charge q we have, $C\psi(q) = \psi(-q)$. By repeating the same steps of Eq. (1) we conclude that the C operator has eigenvalues ± 1.

More generally now we consider the operator C as an operator transforming a particle into its antiparticle; according to this definition C can be applied also to electrically neutral particles and it reverse the sign of all the quantum numbers associated with a particle. As a consequence, it does not preserve leptonic and baryonic numbers, meaning that the charge conjugation is not associated with a real physical process.

Let's consider an example: by applying C to a proton we end up with an anti-proton, which has electrical charge, baryonic number and magnetic dipole moment opposite with respect to the proton, but it has the same spin. This fact is in agreement with experiments so we say that strong and electromagnetic interactions preserve C.

Weak interaction instead does not preserve C, as it can be shown by following the same argument used for parity violation. By applying C to an electronic neutrino we would obtain an electronic anti-neutrino with the same momentum and the same spin, namely an anti-neutrino with spin anti-aligned with respect to momentum, which does not exists. We conclude that weak interaction violates both parity and charge conjugation, but it could preserve CP symmetry because if we apply both C and P to a neutrino, whose spin is anti-aligned with respect to its momentum we end up with an anti-neutrino whose spin is aligned with momentum, and this is a physical state.

Up to the Cronin and Fitch experiment [2] the common opinion was that weak interaction, even if it strongly violates parity and charge conjugation, it would preserve the combined CP symmetry. The discovery of a small CP violation in the neutral kaons system was a real surprise.

C. CP, T and CPT symmetries

In the description on the physical world the CPT symmetry is a cornerstone. It means that if in a process we reverse the coordinates, we exchange particles with antiparticles and we reverse all momenta then, by applying CPT to a real process we should end up into another real process.

The violation of CP implies therefore a violation of T, in order for CPT to hold. The observed CP violation could account, at least partially, for the asymmetry between matter and antimatter that we observe in our universe. Another consequence of the CPT theorem is the equality of mass and average life of a particle and its antiparticle. If weak interaction preserved C, this symmetry would suffice to ensure this equality, but the violation of C requires the more general CPT symmetry.

III. A PRIMER OF THE QUARK MODEL

At a fundamental level strong interaction concerns quarks and gluons. There are six flavors of quark: up, down, charm, strange, top, bottom. Gluons transmit strong interaction and the charge associated with the interaction is called *color* (just a conventional name, without any reference to the ordinary colors). Each quark flavour can exists in three different colors and gluons are classified in eight types. Strong interaction affects the color of the quarks, but leaves unchanged their flavour: in order to change flavour, i.e. when a neutron decays into a proton a quark up changes into a quark down, weak interaction has to be taken into account.

Strong interaction produces states with definite flavor, described in the quark model in the following way:

$$\left|K^0\right\rangle = \left|d\bar{s}\right\rangle , \quad \left|\bar{K^0}\right\rangle = \left|\bar{d}s\right\rangle \tag{3}$$

$$\left|K^+\right\rangle = \left|u\bar{s}\right\rangle , \quad \left|\bar{K^-}\right\rangle = \left|\bar{u}s\right\rangle , \tag{4}$$

where the superscripts $0, +, -$ refer to the electric charge: in unit of the elementary charge, quark up has charge $2/3$ and quark down $-1/3$; anti-quarks, denoted by bars, have opposite electrical charges. In particular strong interaction preserve *strangeness*, a quantum number equal to 1 for the s quark and equal to -1 for the $\bar{s}$ quark.

Strong interaction distinguishes between $\left|K^0\right\rangle$ and $\left|\bar{K^0}\right\rangle$ because they are produced by different reactions:

$$K^+ + n \to K^0 + p \tag{5}$$

$$K^- + p \to \bar{K^0} + n, \tag{6}$$

where $n = \left|udd\right\rangle$ is the neutron and $p = \left|uud\right\rangle$ is the proton. Moreover the products in Eq. (5) and (6) interacts in different ways, for example

$$K^0 + p \to K^+ + n \quad \text{but} \qquad \bar{K^0} + p \nrightarrow K^+ + n \tag{7}$$

$$\bar{K^0} + p \to \pi^0 + \Sigma^+ \quad \text{but} \qquad K^0 + p \nrightarrow \pi^0 + \Sigma^+, \tag{8}$$

where the meson π^0 is a neutral combination of quark u and d and $\Sigma^+ = |suu\rangle$ is a baryon with strangeness equal to -1. As said before, strong interaction preserves strangeness, thus allowing the left reaction of Eq.(7) and Eq. (8) but forbidding the right reaction of Eq. (7) and Eq. (8).

IV. KAONS DECAY AND CP VIOLATION

Neutral kaons, produced by strong interaction with definite flavor, decay through weak interaction in states containing two or three pions. Pions are pseudoscalar particles, meaning that the quantum numbers describing their spin j and parity P are $j^P = 0^-$. As neutral mesons they are invariant under the charge conjugation symmetry C, hence the state composed of two pions is a CP eigenstate with eigenvalue $+1$ whilst the state composed of three pions is a CP eigenstate with eigenvalue -1. If weak interaction preserved CP symmetry only a $+1$ eigenstate would decay into two pions and only a -1 eigenstate would decay into three pions.

By remembering Eq. (3) it's clear that definite flavor states are not CP eigenstates:

$$CP\left|K^0\right\rangle = \left|\bar{K^0}\right\rangle \quad \text{and} \quad CP\left|\bar{K^0}\right\rangle = \left|K^0\right\rangle, \tag{9}$$

but we can express these states are linear combination of CP eigenstates, by defining the states $\left|K_1^0\right\rangle$ and $\left|K_2^0\right\rangle$ in the following way:

$$\begin{aligned} \left|K_1^0\right\rangle &= \frac{1}{\sqrt{2}}\left(\left|K^0\right\rangle + \left|\bar{K^0}\right\rangle\right) \\ \left|K_2^0\right\rangle &= \frac{1}{\sqrt{2}}\left(\left|K^0\right\rangle - \left|\bar{K^0}\right\rangle\right). \end{aligned} \tag{10}$$

With a straightforward calculation we can express the states $\left|K^0\right\rangle$ and $\left|\bar{K^0}\right\rangle$ as linear combination of the CP eigenstates:

$$\begin{aligned} \left|K^0\right\rangle &= \frac{1}{\sqrt{2}}\left(\left|K_1^0\right\rangle + \left|K_2^0\right\rangle\right) \\ \left|\bar{K^0}\right\rangle &= \frac{1}{\sqrt{2}}\left(\left|K_1^0\right\rangle - \left|K_2^0\right\rangle\right). \end{aligned} \tag{11}$$

Suppose we prepare, through nuclear reactions, a pure state of $\left|K^0\right\rangle$. If CP were not violated the eigenstates in the vacuum would be $\left|K_1^0\right\rangle$ and $\left|K_2^0\right\rangle$ defined in Eq. (10). Because of the narrow energy space, i.e. the mass of three pions in slightly lower than the mass of the kaon, the decay into three pions is suppressed with respect to the two pion decay. As a consequence the average life for the two pion decay is about 600 times shorter than the average life for the three pions decay.

In 1964 Christenson, Cronin, Fitch and Turlay discovered that also the long life kaons can decay into two pions, thus violating CP [2]. The states defined in Eq. (10) are not exactly states with definite mass and average life. Let's call these states $|K_S\rangle$ and $|K_L\rangle$, where S stand for short and L stands for long. We can follow the same steps that led us to define the CP eigenstates in Eq. (10) by expressing the definite flavor states $|K_0\rangle$ and $\left|\bar{K}_0\right\rangle$, which we consider, as far as the propagation in vacuum is concerned, as di-chromatic waves, superposition of the monochromatic waves $|K_S\rangle$ and $|K_L\rangle$.

Likewise we can express $|K_S\rangle$ and $|K_L\rangle$ as superposition of the definite CP states $\left|K_1^0\right\rangle$ and $\left|K_2^0\right\rangle$. From an abstract point of view we are dealing with a two states system, so any basis composed of two orthogonal states is legit: according to the relevant Hamiltonian one basis is more convenient that another one. By implementing this guideline we can write the following equations:

$$\begin{aligned} |K_S\rangle &= p\left|K^0\right\rangle + q\left|\bar{K^0}\right\rangle \\ |K_L\rangle &= q\left|K^0\right\rangle - p\left|\bar{K^0}\right\rangle. \end{aligned} \tag{12}$$

Ortho-normalization requires that $|p|^2 + \left|q^2\right| = 1$. In a similar manner we can express the definite mass states $|K_S\rangle$ and $|K_L\rangle$ as superposition of states $\left|K_1^0\right\rangle$ and $\left|K_2^0\right\rangle$ defined in Eq. (10):

$$\begin{aligned} |K_S\rangle &= \frac{\left|K_1^0\right\rangle + \epsilon\left|K_2^0\right\rangle}{\sqrt{1+|\epsilon|^2}} \\ |K_L\rangle &= \frac{\left|K_2^0\right\rangle - \epsilon\left|K_1^0\right\rangle}{\sqrt{1+|\epsilon|^2}} \quad . \end{aligned} \tag{13}$$

The idea behind Eq.(13) is straightforward: the observed *indirect* violation of CP symmetry is embodied in the complex parameter ϵ, who magnitude is about 2.3×10^{-3}. If CP were conserved $\epsilon = 0$ and $p = q$ therefore we could identify CP eigenstates with definite mass eigenstates. Note that, because of the small value of ϵ, at first order in epsilon Eq. (13) can be simplified as

$$\begin{aligned} |K_S\rangle &= \left|K_1^0\right\rangle + \epsilon\left|K_2^0\right\rangle \\ |K_L\rangle &= \left|K_2^0\right\rangle - \epsilon\left|K_1^0\right\rangle \quad . \end{aligned} \tag{14}$$

This kind of CP violation is called indirect because we ascribe it to the presence of a small contribution of the $CP = -1$ eigenstate $\left|K_2^0\right\rangle$ in the definite mass eigenstate $|K_S\rangle$ and of a small contribution of the $CP = 1$ eigenstate $\left|K_1^0\right\rangle$ in the definite mass eigenstate $|K_L\rangle$. This raise e question: what would be a *direct* violation of CP symmetry? It would involve for example the $CP = -1$ eigenstate $\left|K_2^0\right\rangle$ decaying into two pions. Experimentally this can be shown by comparing the amplitudes of charge conjugate mesons. Experiments have detect this kind of CP violation, with even smaller amplitude.

V. TIME EVOLUTION

In order to study the time evolution of the states we choose a basis in terms of energy eigenstates: the time evolution is relatively simple and, for stable states, it reduces to a phase. Kaons states are not stable and this phenomenon can be accounted for by including complex matrix eigenvalues.

In order to keep the algebra cleaner in this section we set $c = 1$ and $\hbar = 1$ in order to treat with the same footing masses and decay width, which have the units of energy.

Let's suppose for the sake of simplicity that CP is not violated by the weak interaction and analyze the following experimental situation: at time $t = 0$ we have produced, through strong interaction, a pure $\left|K^0\right\rangle$ state, that is a pure $s = 1$ state. We have already pointed out that this state, from the point of view of weak interaction, has to be thought as made of 50% of $\left|K_1^0\right\rangle$ and of 50% of $\left|K_2^0\right\rangle$, as shown in Eq. (11). After about 10^{-9} almost all the $\left|K_1^0\right\rangle$ have decayed leaving a beam of $\left|K_2^0\right\rangle$ with intensity half with respect to the initial one.

Consider again the strong interaction: our beam of $\left|K_2^0\right\rangle$ can be described as a superposition of $\left|K^0\right\rangle$ and $\left|\bar{K^0}\right\rangle$ so by starting with a pure $\left|K^0\right\rangle$ beam we can generate $\left|\bar{K^0}\right\rangle$. By interacting with a target the $\left|\bar{K^0}\right\rangle$ component will be absorbed more with respect to $\left|K^0\right\rangle$ (more reaction channels are open at low energies) enabling the regeneration of the $\left|K^0\right\rangle$. This chain of reactions is an oscillation of strangeness because we can swap back and forth from eigenstates with strangeness equal to 1 to eigenstates with strangeness equal to -1.

A key feature of the formalism is the different mass associated with different eigenstates: $\left|K^0\right\rangle$ and $\left|\bar{K^0}\right\rangle$ have the same mass because they are a particle antiparticle couple. The CP eigenstates $\left|K_1^0\right\rangle$ and $\left|K_2^0\right\rangle$ instead show a little mass difference because their weak interaction is slightly different. This phenomenon is similar to the different mass of proton and neutron due to the electromagnetic interaction (in the latter case the difference is much greater).

We know from quantum mechanics that an eigenstate wave-function contain the term $e^{-\frac{iEt}{\hbar}}$ [3]. In the reference frame where the particle is at rest the energy is the rest energy $E = mc^2 = m$. In natural units the phase factor is reduced to e^{-imt}. In addition we have to include a term describing the decay of the particle. A standard way consists in including a imaginary term to the mass, thus allowing us define a complex mass $M = m - i\Gamma/2$ where Γ is related to the average life of the particle by $\tau = \frac{\hbar}{\Gamma} = \frac{1}{\Gamma}$ in natural units. This approach reflects very closely the relation between the refraction index and the absorption index in classical electrodynamics [4].

Let's apply this formalism to the CP eigenstates supposing that we have produced a pure $S = -1$ eigenstate $\left|K^0\right\rangle$ at $t = 0$. By including the time dependence into Eq. (11) we start with

$$\begin{aligned}\left|K^0(0)\right\rangle &= \frac{1}{\sqrt{2}}\left(\left|K_1^0(0)\right\rangle + \left|K_2^0(0)\right\rangle\right) \\ \left|K^{\bar{0}}(0)\right\rangle &= 0,\end{aligned} \tag{15}$$

where we have included also $\left|\bar{K}^0(0)\right\rangle$ because we expect to generate it.

In our approximation $\left|K_1^0\right\rangle$ and $\left|K_2^0\right\rangle$ are energy eigenstates hence their time evolution is simple. By defining $M_1 = m_1 - i\frac{\Gamma_1}{2}$ as the complex masses of $\left|K_1^0\right\rangle$ and $M_2 = m_2 - i\frac{\Gamma_2}{2}$ the states $\left|K_1^0(t)\right\rangle$ and $\left|K_2^0(t)\right\rangle$ are

$$\begin{aligned}\left|K_1^0(t)\right\rangle &= \left|K_1^0(0)\right\rangle e^{-iM_1t} = \left|K_1^0(0)\right\rangle e^{-im_1t}e^{-\frac{\Gamma_1 t}{2}} \\ \left|K_2^0(t)\right\rangle &= \left|K_2^0(0)\right\rangle e^{-iM_2t} = \left|K_1^0(0)\right\rangle e^{-im_2t}e^{-\frac{\Gamma_2 t}{2}}.\end{aligned} \tag{16}$$

We can now express the time evolution of $\left|K^0\right\rangle$ as a superposition of CP eigenstates:

$$\left|K^0(t)\right\rangle = \frac{1}{\sqrt{2}}\left(\left|K_1^0(0)\right\rangle e^{-iM_1t} + \left|K_2^0(0)\right\rangle e^{-iM_2t}\right). \tag{17}$$

Equation (17) is a key one because it allows to express a series of interference effects, among which there are the strangeness oscillations. In order to put into evidence this oscillation let's evaluate the intensity of the particle beam, which is proportional to the absolute square of the wave function.

By defining $I_{K_0^1}(t) = \left\langle K_1^0(t)\middle|K_1^0(t)\right\rangle$ and inserting Eq. (16) we have

$$I_{K_0^1}(t) = \left\langle K_1^0(0)\middle|K_1^0(0)\right\rangle e^{-\Gamma_1 t}, \tag{18}$$

because the imaginary phases involving m_1 cancel out, whilst the real phases involving Γ_1 add up. Following the same line of reasoning

$$I_{K_0^2}(t) = \left\langle K_2^0(0)\middle|K_2^0(0)\right\rangle e^{-\Gamma_2 t}. \tag{19}$$

At this point we have all the tools to evaluate a very interesting quantity, that is the ratio $\frac{I_{K^0}(t)}{I_{K^0}(0)} = \left\langle K^0(t)\middle|K^0(t)\right\rangle$. This ratio does not depend on the initial intensity of the $\left|K^0\right\rangle$ beam so we can, without any loss of generality, put $I_{K^0}(0) = 1$; as a consequence $I_{K_1^0}(0) = I^0_{K_2}(0) = \frac{1}{2}$.

Inserting Eq. (16) we have

$$\begin{aligned}\frac{I_{K^0}(t)}{I_{K^0}(t)} &= \left\langle K^0(t)\middle|K^0(0)\right\rangle \\ &= \frac{\left\langle K_1^0(t)\right| + \left\langle K_2^0(t)\right|}{\sqrt{2}}\,\frac{\left|K_1^0(t)\right\rangle + \left|K_2^0(t)\right\rangle}{\sqrt{2}}\end{aligned} \tag{20}$$

Let's evaluate Eq. (20) product by product:

$$\begin{aligned}\left\langle K_1^0(t)\middle|K_1^0(t)\right\rangle &= \frac{1}{2}e^{-\Gamma_1 t} \\ \left\langle K_2^0(t)\middle|K_2^0(t)\right\rangle &= \frac{1}{2}e^{-\Gamma_2 t}\end{aligned} \tag{21}$$

The remaining products are complex conjugates and, by using the Euler identity $\cos(x) = \frac{e^{ix}+e^{-ix}}{2}$ they can be written as

$$\left\langle K_1^0(t)\middle|K_2^0(0)\right\rangle + \left\langle K_2^0(t)\middle|K_1^0(0)\right\rangle = e^{-\frac{\Gamma_1+\Gamma_2}{2}t}\cos((\Delta m)t), \tag{22}$$

where $\Delta m = m_2 - m_1$.

By putting all together we have the key result

$$\frac{I_{K^0}(t)}{I_{K^0}(0)} = \frac{1}{4}\left(e^{-\Gamma_1 t} + e^{-\Gamma_2 t} + 2e^{-\frac{\Gamma_1+\Gamma_2}{2}t}\cos((\Delta m)t)\right). \tag{23}$$

By following the same steps we evaluate also $\frac{I_{\bar{K}^0}(t)}{I_{K^0}(0)}$:

$$\frac{I_{\bar{K}^0}(t)}{I_{K^0}(0)} = \frac{1}{4}\left(e^{-\Gamma_1 t} + e^{-\Gamma_2 t} - 2e^{-\frac{\Gamma_1+\Gamma_2}{2}t}\cos((\Delta m)t)\right). \tag{24}$$

As we said in the previous section the half-life for decaying into two pions is 600 times shorter for the three pion decay; in terms of width decay therefore $\Gamma_1 \approx 600\Gamma_2$.

Let's study Eq. (23) and (24) when it has elapsed enough time that practically all $\left|K_1^0\right\rangle$ is decayed but basically no $\left|K_2^0\right\rangle$ has already decayed. Consider for example the time scale of the nanosecond: $\tau_1 \approx 90$ pc so the fraction of $\left|K_1^0\right\rangle$ surviving after 1 ns is about $e^{-11} \approx 0$ while all $\left|K_2^0\right\rangle$ are still there, as we can check by comparing this timescale with the average-life of $\left|K_2^0\right\rangle$, that is about 50 ns. Let's insert these approximation into Eq. (23) and (24) by substituting the first $e^{-\Gamma_1 t}$ with 0, $e^{-\Gamma_2 t}$ with one, and neglecting $e^{-\Gamma_2 t}$ in the decay width sum, obtaining the simpler equation for $\frac{I_{\bar{K}^0}(t)}{I_{K^0}(0)}$

$$\frac{I_{\bar{K}^0}(t)}{I_{K^0}(0)} \approx \frac{1}{4}\left(1 + 2e^{-\frac{\Gamma_1}{2}t}\cos((\Delta m)t)\right). \tag{25}$$

This equation states that in the time windows where $\left|K_1^0\right\rangle$ is almost all decayed and $\left|K_2^0\right\rangle$ is not yet decayed the ratio between the intensity of $\left|\bar{K}_0\right\rangle$ and $\left|K^0\right\rangle$ is a steady $\frac{1}{4}$; indeed the last term of Eq. (25) is suppresses by the exponential factor and the tiny value of Δm, amounting approximately to 3.5μeV makes the cosine modulation very hard to notice.

Likewise for the regeneration of $\left|\bar{K}_0\right\rangle$ we have

$$\frac{I_{\bar{K}^0}(t)}{I_{K^0}(0)} \approx \frac{1}{4}\left(1 - 2e^{-\frac{\Gamma_1}{2}t}\cos((\Delta m)t)\right). \tag{26}$$

We have obtained a interesting result: at $t = 0$ we produce a pure $\left|K^0\right\rangle$ beam by strong interaction, then we let evolve the system in vacuum and for the relatively long time of a few nanoseconds we have two beams of particles made of $\left|K^0\right\rangle$ and $\left|\bar{K}^0\right\rangle$, each one with intensity approximately $\frac{1}{4}$ of the original beam.

VI. DISCUSSION

The analysis carried out in the previous section in not entirely accurate because we have identified mass eigenstates with CP eigenstates even if we know that this is not true. In any case, the observed violation is small so this approximation does not make our conclusions invalid. Moreover it enables us to develop a relatively simple formalism that would become much cumbersome (and probably it would not allow us to grasp better this system) if we had included CP violation, thus working with the states of Eq. (12).

The kaons system shows interesting features allowing us a comparison with other physical systems, both in the classical and in the quantum level, both in quantum mechanics and in quantum field theory where CP violation can play a role in understanding fundamental interactions.

In fact other sources of CP violation processes are being investigated: a promising realm is provided by the charm and bottom quark physics. With respect to the kaons, the true stationary states have very short and almost equal mean lives. Experiments with such mesons are therefore challenging.

Finally I would mention the search for CP violation in the neutrino sector. Neutrinos are elementary particles and the observed flavour oscillations prove that they possess a tiny mass. A common feature with the kaons system is that the states produced by weak interaction are not mass eigenstates and the complete mixing concern three kinds of neutrinos, making the general expressions for the oscillations much more involved with respect to two states mixing.

ACKNOWLEDGMENTS

I thank the 8.06x staff for this amazing course. As professor Zwiebach described the book "Principle of Quantum Mechanics" by P.A.M. Dirac in the MIT open course ware, I describe this course: "deep, hard and rewarding".

---

[1] S. Braibant, G. Giacomelli, M. Spurio, *Particelle e interazoni fondamentali*. Springer, 2009.

[2] J.H. Christenson, J.W. Cronin, V.L. Fitch, R. Turlay", "Evidence for the 2π decay of the k_2^0 meson," *Phys. Rev. Lett.* **13** (1964) no. 4, 138–140.

[3] D. J. Griffiths, *Introduction to Quantum Mechanics*. Cambridge University Press, 2018.

[4] M. S. R.P. Feynman, R.B. Leighton, *Feynman Lectures on Physics*. Addison Wesley, 2006.

Bell's inequalities and Tsirelson's bound

Felix Antonio Junjiro Obando Molina

(Dated: June 18, 2019)

Bell's inequality draws a distinction between quantum mechanics and classical mechanics as a description of the world. It states a limit that bounds classical statistical correlations, but that is violated only by quantum mechanic correlations. It is natural to ask if quantum mechanic correlations also have limits. The answer to this question is given by the Tsirelson's bound, which gives an upper limit to quantum correlations that can not be violated. In this paper, we derive the original Bell's inequality and its generalization or Clauser-Horne-Shimony-Holt inequality. We will also discuss their importance for quantum mechanics. Finally, we derive and discuss the Tsirelson's bound. The derivations done in this paper are for the system of two entangled spin 1/2 particles.

I. OVERVIEW

This paper aims to derive and discuss 3 of the limits to which statistical and quantum correlations are bounded. The first limit is known as Bell's Inequality and is particularly biased for ideal systems. The second limit is the generalized Bell's inequality (also known as Clauser-Horne-Shimony-Holt, and in the rest of the paper named as CHSH inequality), and takes into account real experimental systems. Both of the mentioned limits describe a bound which cannot be violated by classical or statistical correlations, but which are in many cases violated by quantum correlations. The last bound is the Tsirelson's Bound. This bound puts a limit that cannot be surpassed even by quantum correlations.

This paper begins with a background to explain quantum predictions and EPR (Einstein–Podolsky–Rosen) arguments. EPR arguments are arguments that vow for the existence of hidden-variable theories that assume the incompleteness of quantum mechanics. Then, we begin the derivation of the first Bell's inequality aimed at ideal systems. This Bell's inequality proves the inconsistency of EPR arguments and therefore the supremacy of quantum mechanics. We then derive the Generalized Bell Inequality which takes into account real experimental systems. We begin its derivation by mentioning some of the problems with the first Bell's Inequality for real experimental systems. We then state solutions for these problems that will be used in the derivation of the Generalized Bell's inequality. After deriving the Generalized Bell's inequality, we proceed to state a particular case, in which it transforms to the first Bell's inequality

Then, we derive the Tsirelson's bound based on mathematical formalities of quantum algebra that are stated at the beginning of the corresponding chapter. We then present an example to give an overview of the three derived inequalities. We finish with a discussion.

II. BACKGROUND

The lack of determinism and the "spooky" action at a distance of the theory of quantum mechanics led Albert Einstein, Rosen and Podolsky ([1], hereafter referred to as EPR), to propose an argument which, by means of "hidden variables", seeked to restore the apparent lack of completeness, determinism and causality of quantum mechanics. One of the derivations of EPR was the *Gedankenexperiment* proposed by Bohm [2]. Eventhough the scope of this paper is not aimed to describe hidden variable theories (EPR and its variations), the experiment proposed initially as part of the *Gedankenexperiment* is of particular importance, as it was used as a set-up in which to develop Bell's theorem and its later generalization.

A. Bohm's set-up

Bohm considered an entangled pair of spin one-half particles produced somehow in a singlet state and moving in opposite directions. These spin particles are entangled, and are sufficiently far away from each other. The spin components of each of these particles could be measured independently by means of measurement devices, for example, Stern-Gerlach magnets. The decision of in which direction to measure, is up to the experimenter. Our general state can be expressed as [3]:

$$\Psi = \frac{1}{\sqrt{2}}\left(u_{\hat{n}}^{+}(1)\ \otimes\ u_{\hat{n}}^{-}(2)\ -\ u_{\hat{n}}^{-}(1)\otimes u_{\hat{n}}^{+}(2)\right) \qquad (1)$$

The experimenter use the operator σ to make a measurement to the state $u_{\hat{n}}^{\pm}(1)$ so that $\boldsymbol{\sigma \cdot u_{\hat{n}}^{\pm}(1) = \pm u_{\hat{n}}^{\pm}(1)}$. Here, $\hat{n}$ represents a unit vector in a particular direction along which the measurement is taken; in Eq.(1), numbers in parentheses "(1)" and "(2)" represent the label of the first and second measured particle respectively; and "±" represents the eigenvalue of $+1$ or -1 respectively. Since the singlet state Ψ is spherically symmetric, $\hat{n}$ can specify any measured direction.

B. Quantum Mechanic Prediction

According to quantum mechanics, in Eq.(1), if the measurement of the component of the first particle $u_{\hat{n}}(1)$ along $\hat{n}$ yields the eigenvalue $+1$, then, the measurement of the second particle $u_{\hat{n}}(2)$ along $\hat{n}$ will yield -1. To exemplify this, we can measure along the $\hat{z}$ axis without loss of generality (the state Ψ is spherically symmetric). We define:

$$\sigma_z = \begin{pmatrix} 1 & 0 \\ 0 & -1 \end{pmatrix}$$

$$|\uparrow\rangle = \begin{pmatrix} 1 \\ 0 \end{pmatrix} \qquad |\downarrow\rangle = \begin{pmatrix} 0 \\ 1 \end{pmatrix} \tag{2}$$

where $|\uparrow\rangle$ and $|\downarrow\rangle$ represent our basis states. We therefore represent Eq. (1) as:

$$\Psi = \frac{1}{\sqrt{2}} \left(|\uparrow\rangle \otimes |\downarrow\rangle - |\downarrow\rangle \otimes |\uparrow\rangle \right) \tag{3}$$

As an example, we suppose that our state collapses to $\Psi = |\uparrow\rangle \otimes |\downarrow\rangle$; then we could measure the spin of the first particle (measurement along the first Hilbert space) and obtain: $\langle\Psi| \, \sigma_z \otimes 1 \, |\Psi\rangle = (+1)$; when we measure the spin of the second particle, we would then get: $\langle\downarrow| \, 1 \otimes \sigma_z \, |\downarrow\rangle = (-1)$.

For a measurement along different directions [4], with the first particle being measured along the $\vec{a}$ direction and the second particle being measured along the $\vec{b}$ direction, we define $QM\left(\vec{a}, \vec{b}\right)$ as:

$$QM\left(\vec{a}, \vec{b}\right) = \langle\Psi| \, \vec{\sigma} \cdot \vec{a} \otimes \vec{\sigma} \cdot \vec{b} \, |\Psi\rangle = -\vec{a} \cdot \vec{b} = -\cos\theta \tag{4}$$

where θ is the angle between the directions of $\vec{a}$ and $\vec{b}$. If the measurement is done along the same direction, we get:

$$QM\left(\vec{a}, \vec{a}\right) = \langle\Psi| \, \vec{\sigma} \cdot \vec{a} \otimes \vec{\sigma} \cdot \vec{a} \, |\Psi\rangle = -1 \tag{5}$$

C. EPR premises

The EPR argument is based on three main premises [3]. These premises were of great importance for the development of Bell's inequality, which states a contradiction between them, and, subsequently, the impossibility of hidden-variable theories. The premises are:

1. The EPR argument takes for granted, that some of the quantum-mechanical predictions are correct.
2. "But on one supposition we should, in my opinion, absolutely hold fast: the real factual situation of the system S_2 is independent of what is done with the system S_1, which is spatially separated from the former." [5]
3. "If, without in any way disturbing a system, we can predict with certainty the value of a physical quantity (i.e. the spin of the particle), then there exists an element of physical reality corresponding to this physical quantity." [1]

The first premise states the validity of some quantum-mechanical predictions (namely, Eq.(5)). The second premise states the impossibility that the measurement of a system S_1 perturbs in any way another system S_2. This premise is known as locality, or, more colloquially, impossibility of spooky action at a distance. The third premise confirms the existence of hidden variable theories: since we can predict in advance the value of a physical quantity (i.e. the spin of a particle) by measuring the value of another physical quantity (i.e. the spin of the entangled particle), both physical systems are far away without possibly interfering the other, and our wave-function does not determine the result of any individual measurement (for example, in Eq. (3), the wave-function does not determine to which entangled pair our state will collapse after the measurement), then, there should be a more complete specification of the state (a hidden variable theory).

III. BELL'S INEQUALITY

A. Assumptions

Bell's inequality is based on the contradiction of the mentioned EPR premises. This contradiction is proved by showing that a hidden-variable theory satisfying both the EPR premise 3. and the condition of locality stated in the premise 2., can not at the same time satisfy the partial agreement with quantum mechanics stated in the premise 1. To begin with, Bell parametrises the existence of hidden-variable theories (premise 3.) by means of the parameter λ. He states that the observables A and B, which are the result of measuring the first particle by using the operator $\vec{\sigma} \cdot \vec{a}$ and the second particle by using the operator $\vec{\sigma} \cdot \vec{b}$ respectively, depend on $\vec{a}$, $\vec{b}$ and λ. He then states:

$$A\left(\vec{a}, \lambda\right) = \pm 1, \; B\left(\vec{b}, \lambda\right) = \pm 1. \tag{6}$$

Eq.(6) assumes not only the fact that the values of A and B depend on the parameter λ, but also the locality premise (premise 2.): A depends on $\vec{a}$ but not on $\vec{b}$, and B depends on $\vec{b}$ but not on $\vec{a}$. A and B can only take values +1 and -1, which represent the spin being up and down respectively. Bell then represents the probability distribution of λ as $\rho(\lambda)$, where $\rho(\lambda)$ is a normalized probability distribution:

$$\int d\lambda \rho(\lambda) = 1 \tag{7}$$

He then asserts that the assumptions of EPR stated here as part of (6) and (7) should agree with some quantum mechanical predictions (premise 1.) for the hidden variable theory to be true.

This partial agreement with quantum mechanics is enunciated as follows:

First, we define a classical expectation value of the product of two measurements of $\vec{\sigma} \cdot \vec{a}$ and $\vec{\sigma} \cdot \vec{b}$ acting on the first and second particle respectively by:

$$P\left(\vec{a},\vec{b}\right)=\int d\lambda\rho(\lambda)A\left(\vec{a},\lambda\right)B\left(\vec{b},\lambda\right)\tag{8}$$

Premise 1. expresses that our classical correlation should have a partial agreement with some quantum mechanical correlations, namely, with Eq. (5). Therefore, we should have:

$$QM\left(\vec{a},\vec{a}\right)=P\left(\vec{a},\vec{a}\right)=-1\tag{9}$$

By Eq. (6), P cannot be less than -1. For Eq. (9) to be true, we should therefore have:

$$A\left(\vec{a},\lambda\right)=-B\left(\vec{a},\lambda\right)\tag{10}$$

Eq. (10) represents the statement of partial agreement with quantum mechanics (Premise 1.).

B. Contradiction

The contradiction is stated by finding a hidden-variable correlation (Bell's limit) that assumes locality and the existence of a hidden variable theory (Eq.(6) and Eq.(7)), and is derived with help of a partial agreement with quantum mechanics (Eq.(10)), but that is in fact violated by quantum mechanical correlations.

By Eq.(10), we can rewrite Eq.(8) as:

$$P\left(\vec{a},\vec{b}\right)=-\int d\lambda\rho(\lambda)A\left(\vec{a},\lambda\right)A\left(\vec{b},\lambda\right)\tag{11}$$

We can now introduce a second vector $\vec{c}$ and do the following calculation:

$$\begin{aligned}P\left(\vec{a},\vec{b}\right)-P\left(\vec{a},\vec{c}\right)=&-\int d\lambda\rho(\lambda)A\left(\vec{a},\lambda\right)A\left(\vec{b},\lambda\right)\\&+\int d\lambda\rho(\lambda)A\left(\vec{a},\lambda\right)A\left(\vec{c},\lambda\right)\end{aligned}\tag{12}$$

Noticing that $A\left(\vec{b},\lambda\right)A\left(\vec{b},\lambda\right)=1$, we then say:

$$\begin{aligned}&P\left(\vec{a},\vec{b}\right)-P\left(\vec{a},\vec{c}\right)=\\&\int d\lambda\rho(\lambda)A\left(\vec{a},\lambda\right)A\left(\vec{b},\lambda\right)\left[A\left(\vec{b},\lambda\right)A\left(\vec{c},\lambda\right)-1\right]\end{aligned}\tag{13}$$

Then, by the theorem of the Triangle Inequality of Integrals (theorem 13.24 in [6]), we affirm:

$$\begin{aligned}&\left|P\left(\vec{a},\vec{b}\right)-P\left(\vec{a},\vec{c}\right)\right|\leq\\&\int d\lambda\rho(\lambda)\left|A\left(\vec{a},\lambda\right)A\left(\vec{b},\lambda\right)\left[A\left(\vec{b},\lambda\right)A\left(\vec{c},\lambda\right)-1\right]\right|\end{aligned}\tag{14}$$

By the multiplicativity property of the absolute value, we state:

$$\begin{aligned}&\left|A\left(\vec{a},\lambda\right)A\left(\vec{b},\lambda\right)\left[A\left(\vec{b},\lambda\right)A\left(\vec{c},\lambda\right)-1\right]\right|=\\&\left|A\left(\vec{a},\lambda\right)A\left(\vec{b},\lambda\right)\right|\left|\left[A\left(\vec{b},\lambda\right)A\left(\vec{c},\lambda\right)-1\right]\right|\end{aligned}\tag{15}$$

Then, by the triangle inequality:

$$\left|\left[A\left(\vec{b},\lambda\right)A\left(\vec{c},\lambda\right)-1\right]\right|\leq\left[\left|A\left(\vec{b},\lambda\right)A\left(\vec{c},\lambda\right)\right|+\left|-1\right|\right]\tag{16}$$

As a result, we have:

$$\begin{aligned}&\left|P\left(\vec{a},\vec{b}\right)-P\left(\vec{a},\vec{c}\right)\right|\leq\\&\int d\lambda\rho(\lambda)\left|A\left(\vec{a},\lambda\right)A\left(\vec{b},\lambda\right)\right|\left[\left|A\left(\vec{b},\lambda\right)A\left(\vec{c},\lambda\right)\right|+1\right]\end{aligned}\tag{17}$$

To progress, we use Eq. (10) to say:

$$\begin{aligned}\left|A\left(\vec{b},\lambda\right)A\left(\vec{c},\lambda\right)\right|&=\left|-A\left(\vec{b},\lambda\right)B\left(\vec{c},\lambda\right)\right|\\&=A\left(\vec{b},\lambda\right)B\left(\vec{c},\lambda\right)\\&=-A\left(\vec{b},\lambda\right)A\left(\vec{c},\lambda\right)\end{aligned}\tag{18}$$

We also notice that:

$$\left|A\left(\vec{a},\lambda\right)A\left(\vec{b},\lambda\right)\right|=\left|\pm1\right|=1\tag{19}$$

We use Eq. (18) and Eq. (19) in Eq. (17) to get:

$$\begin{aligned}\left|P\left(\vec{a},\vec{b}\right)-P\left(\vec{a},\vec{c}\right)\right|&\leq\int d\lambda\rho(\lambda)\left[1-A\left(\vec{b},\lambda\right)A\left(\vec{c},\lambda\right)\right]\\&\leq\int d\lambda\rho(\lambda)-\int d\lambda\rho(\lambda)A\left(\vec{b},\lambda\right)A\left(\vec{c},\lambda\right)\end{aligned}\tag{20}$$

and, by Eq. (7) and Eq. (10):

$$\begin{aligned}&\int d\lambda\rho(\lambda)-\int d\lambda\rho(\lambda)A\left(\vec{b},\lambda\right)A\left(\vec{c},\lambda\right)=\\&1+\int d\lambda\rho(\lambda)A\left(\vec{b},\lambda\right)B\left(\vec{c},\lambda\right)=\\&1+P\left(\vec{b},\vec{c}\right)\end{aligned}\tag{21}$$

so that we get:

$$\left|P\left(\vec{a},\vec{b}\right)-P\left(\vec{a},\vec{c}\right)\right|\leq1+P\left(\vec{b},\vec{c}\right)\tag{22}$$

which is the Bell's inequality (Eq. (22)).

As we see, Bell's inequality was calculated on the premises of existence of hidden variable theories (Premise 3.) and of locality (Premise 2.). We can prove that, for some quantum mechanical expectation value given by Eq. (4), this inequality is violated. As an example, we suppose that the angle between axis $\vec{a}$ and $\vec{c}$ is $2\pi/3$ and $\vec{b}$ makes an angle of $\pi/3$ with both $\vec{a}$ and $\vec{c}$. Then:

$$\begin{aligned}QM\left(\vec{a},\vec{b}\right)=QM\left(\vec{b},\vec{c}\right)=-\vec{a}\cdot\vec{b}=-\vec{b}\cdot\vec{c}=-\frac{1}{2}\\QM\left(\vec{a},\vec{c}\right)=-\vec{a}\cdot\vec{c}=\frac{1}{2}\end{aligned}\tag{23}$$

We evaluate these quantum mechanical expectation value on Bell's inequality Eq. (22):

$$\begin{aligned} \left|QM\left(\vec{a},\vec{b}\right) - QM\left(\vec{a},\vec{c}\right)\right| &\nleq 1 + QM\left(\vec{b},\vec{c}\right) \\ \left|-\frac{1}{2}-\frac{1}{2}\right| &\nleq 1 - \frac{1}{2} \\ 1 &\nleq \frac{1}{2} \end{aligned} \tag{24}$$

With Eq. (24), we prove that hidden variables theories that rely on premises 2. and 3. of EPR cannot agree with premise 1. at the same time, which is the main result of Bell's inequality.

IV. THE GENERALIZATION OF BELL'S INEQUALITY

A. The problem of the first Bell's inequality

Even though the first Bell's inequality [4] is an argument of great value as it provides a mathematical framework that could be used to test hidden-variable theories, it is strictly limited to ideal systems, what makes it of little value to real experiments. There are two main problems that arise from the first Bell's inequality:

First, for its derivation, the first Bell's inequality relies on that Eq. (9) hold exactly in order to state Eq. (10) (partial agreement with Quantum Mechanics or Premise 1.). Also, for the proof of its violation, Bell's inequality relies on that Eq. (4) holds exactly, what we will call as perfect quantum correlation.

Unfortunately, Eq. (9) and Eq. (4) cannot hold exactly in an actual experiment: the detector used to do the measurements will have an efficiency less than 100%, and any real analyzer will have some attenuation [3].

Second, the mathematical derivation of the first Bell's inequality also relies on the idealized situation, in which particle detectors will detect either +1 or −1 (Eq. (6)). However, in a real situation, there exists an additional possibility: that the particle detectors could also contain hidden variables that could influence the results [7]. This additional possibility is interpreted by some authors [3] as the detection of an additional 0 (which means no particle detection).

B. Solutions to problems

The first problem was first tackled by John F. Clauser, Michael A. Horne, Abner Shimony and Richard A. Holt (CHSH). In their work [8], they propose a new derivation of the Bell inequality independent of Eq. (9) and Eq. (10), so that it does not need a perfect statistical correlation to be valid. For this, CHSH uses another unitary vector $\vec{b'}$, apart of $\vec{a}$, $\vec{b}$, and $\vec{c}$, in which the measure is to be taken. The same derivation is used later by Bell [7], but with the vectors $\vec{a}$, $\vec{b}$, $\vec{a'}$ and $\vec{b'}$. For the derivation of the generalized Bell inequality in this paper, we will use the variables used by Bell in [7], as it pertains essentially the same derivation as that of CHSH, but with the addition that it also includes a solution to the second problem. Additionally, CHSH [3] uses a modification of Eq. (4) by including a coefficient C that bounds by one the QM prediction. This way, we avoid relying on a perfect quantum correlation. Eq. (4) is then modified to:

$$QM\left(\vec{a},\vec{b}\right) = -C\vec{a}\cdot\vec{b} \tag{25}$$

The second problem was tackled by Bell [7]. He assumed that, if particle detectors can possibly contain hidden variables, then, we should first average the corresponding distributions of instrument hidden variables, so that our derivation takes it into account. As a result, we modify Eq. (6) to:

$$\left|\bar{A}\left(\vec{a},\lambda\right)\right| \leq 1, \ \left|\bar{B}\left(\vec{b},\lambda\right)\right| \leq 1. \tag{26}$$

For the derivation of the generalization of Bell's theorem, we will use $\bar{A}$ and $\bar{B}$ to denote the averaged values.

C. Derivation of generalized Bell's inequality

We now proceed to derive Bell's inequality. We define:

$$P\left(\vec{a},\vec{b}\right) = \int d\lambda\rho(\lambda)\bar{A}\left(\vec{a},\lambda\right)\bar{B}\left(\vec{b},\lambda\right) \tag{27}$$

We then calculate:

$$\begin{aligned} &P\left(\vec{a},\vec{b}\right) - P\left(\vec{a},\vec{b'}\right) = \\ &\int d\lambda\rho(\lambda)\left[\bar{A}\left(\vec{a},\lambda\right)\bar{B}\left(\vec{b},\lambda\right) - \bar{A}\left(\vec{a},\lambda\right)\bar{B}\left(\vec{b'},\lambda\right)\right] = \\ &\int d\lambda\rho(\lambda)\left[\bar{A}\left(\vec{a},\lambda\right)\bar{B}\left(\vec{b},\lambda\right)\left(1 \pm \bar{A}\left(\vec{a'},\lambda\right)\bar{B}\left(\vec{b'},\lambda\right)\right)\right] \\ &-\int d\lambda\rho(\lambda)\left[\bar{A}\left(\vec{a},\lambda\right)\bar{B}\left(\vec{b'},\lambda\right)\left(1 \pm \bar{A}\left(\vec{a'},\lambda\right)\bar{B}\left(\vec{b},\lambda\right)\right)\right] \end{aligned} \tag{28}$$

As we did in the derivation of the first Bell's inequality, we use now the triangle inequality, the triangle inequality for integrals, and the property of multiplicativity of the absolute value to get:

$$\begin{aligned} &\left|P\left(\vec{a},\vec{b}\right) - P\left(\vec{a},\vec{b'}\right)\right| \leq \\ &\int d\lambda\rho(\lambda)\left[\left|\bar{A}\left(\vec{a},\lambda\right)\bar{B}\left(\vec{b},\lambda\right)\right|\left|\left(1 \pm \bar{A}\left(\vec{a'},\lambda\right)\bar{B}\left(\vec{b'},\lambda\right)\right|\right)\right] \\ &+\int d\lambda\rho(\lambda)\left[\left|\bar{A}\left(\vec{a},\lambda\right)\bar{B}\left(\vec{b'},\lambda\right)\right|\left|\left(1 \pm \bar{A}\left(\vec{a'},\lambda\right)\bar{B}\left(\vec{b},\lambda\right)\right)\right|\right] \end{aligned} \tag{29}$$

We know from Eq. (26) that:

$$\left|\bar{A}\left(\vec{a},\lambda\right)\bar{B}\left(\vec{b},\lambda\right)\right| \leq 1, \left|\bar{A}\left(\vec{a},\lambda\right)\bar{B}\left(\vec{b'},\lambda\right)\right| \leq 1 \tag{30}$$

Also, the minimum value of $\bar{A}\bar{B} = -1$, so that:

$$\left(1 \pm \bar{A}\left(\vec{a'},\lambda\right)\bar{B}\left(\vec{b'},\lambda\right)\right) \geq 0, \left(1 \pm \bar{A}\left(\vec{a'},\lambda\right)\bar{B}\left(\vec{b},\lambda\right)\right) \geq 0 \tag{31}$$

As a result:

$$\begin{aligned} \left|1 \pm \bar{A}\left(\vec{a'},\lambda\right)\bar{B}\left(\vec{b'},\lambda\right)\right| &= \left(1 \pm \bar{A}\left(\vec{a'},\lambda\right)\bar{B}\left(\vec{b'},\lambda\right)\right), \\ \left|1 \pm \bar{A}\left(\vec{a'},\lambda\right)\bar{B}\left(\vec{b},\lambda\right)\right| &= \left(1 \pm \bar{A}\left(\vec{a'},\lambda\right)\bar{B}\left(\vec{b},\lambda\right)\right), \end{aligned} \tag{32}$$

We now use Eq. (30) and Eq. (32) in Eq. (29) to get:

$$\begin{aligned} &\left|P\left(\vec{a},\vec{b}\right) - P\left(\vec{a},\vec{b'}\right)\right| \leq \\ &\int d\lambda\rho(\lambda)\left(1 \pm \bar{A}\left(\vec{a'},\lambda\right)\bar{B}\left(\vec{b'},\lambda\right)\right) \\ &+\int d\lambda\rho(\lambda)\left(1 \pm \bar{A}\left(\vec{a'},\lambda\right)\bar{B}\left(\vec{b},\lambda\right)\right) = \\ &\int 2d\lambda\rho(\lambda) \pm \int d\lambda\rho(\lambda)\bar{A}\left(\vec{a'},\lambda\right)\bar{B}\left(\vec{b'},\lambda\right) \\ &\pm \int d\lambda\rho(\lambda)\bar{A}\left(\vec{a'},\lambda\right)\bar{B}\left(\vec{b},\lambda\right) \end{aligned} \tag{33}$$

As a result, we get the generalized Bell's inequality (Eq. (34) and Eq. (35)):

$$\left|P\left(\vec{a},\vec{b}\right) - P\left(\vec{a},\vec{b'}\right)\right| \leq 2 \pm \left(P\left(\vec{a'},\vec{b'}\right) + P\left(\vec{a'},\vec{b}\right)\right) \tag{34}$$

or:

$$\left|P\left(\vec{a},\vec{b}\right) - P\left(\vec{a},\vec{b'}\right)\right| + \left|P\left(\vec{a'},\vec{b'}\right) + P\left(\vec{a'},\vec{b}\right)\right| \leq 2 \tag{35}$$

D. Particular case

We see that the first Bell's inequality (Eq. (22)) is in fact a particular case of Eq. (34). Assuming $\vec{a'} = \vec{b'} = \vec{c}$, and Eq. (9), we get:

$$\begin{aligned} \left|P\left(\vec{a},\vec{b}\right) - P\left(\vec{a},\vec{c}\right)\right| &\leq 2 \pm \left(P\left(\vec{c},\vec{c}\right) + P\left(\vec{c},\vec{b}\right)\right) \\ &\leq 2 + \left(-1 + P\left(\vec{c},\vec{b}\right)\right) \\ &\leq 1 + P\left(\vec{b},\vec{c}\right) \end{aligned} \tag{36}$$

V. TSIRELSON'S BOUND

Bell's inequality and its generalization described a bound that could be violated by a variety of quantum correlations, but not by statistical correlations or hidden-variable theories. It is natural to ask, whether quantum correlations also obey a certain limit, and which this limit is. Boris Tsirelson [9] was the first to answer these questions, initiating the study of the limitations of quantum correlations. Tsirelson's paper [9] contains 4 theorems, the first of which is only needed for our purposes on the derivation of the Tsirelson's bound (in fact, an elementary proof of the Tsirelson's bound is also given on his paper as part of the discussion of his first theorem). What makes Tsirelson's derivation and theorems different from the derivations of Bell's inequality, is that Tsirelson uses the mathematical formalism of linear algebra to provide a precise mathematical characterization of quantum systems that allows for the calculation of its bound; while Bell's inequalities relied on statistical correlations to be derived. In the first part of this chapter, we will introduce some of the mathematical formalities needed for the derivation of the bound. We will then state without derivation the elementary proof given in Tsirelson's paper, and derive the proof most commonly used in today's literature. At the end, we translate the generalized Bell's inequality (Eq. (35)) into the notation used for Tsirelson's Bound, so that we can compare both limits and bring the whole work into overview at the discussion.

A. Mathematical formalities

We list the mathematical formalities used for the derivation [9]:

- There is a complex-algebra $\mathcal{A}$ with identity.
- We let an operator A_k be given for $k = 1, ..., m$ and an operator B_l be given for $l = 1, ..., n$. Operators $A_k, B_l \in \mathcal{A}$ and are Hermitian operators.
- We then let two Hilbert spaces $\mathcal{H}_1$ and $\mathcal{H}_2$ so that $\mathcal{H} = \mathcal{H}_1 \otimes \mathcal{H}_2$.
- We now say that $A_k = A_k^{(1)} \otimes \mathbb{I}^{(2)}$ and $B_l = \mathbb{I}^{(1)} \otimes B_l^{(2)}$, where $A_k^{(1)}$ and $B_l^{(2)}$ are some operators in $\mathcal{H}_1$ and $\mathcal{H}_2$ respectively.
- We state that $[A_k, B_k] = 0$, and that $C = [A_k, A_{k'}] \neq 0$ and $D = [B_l, B_{l'}] \neq 0$ for different values of k, k' and l, l', and for which C and D are scalar.
- We say that A_k and B_l have an spectra consisting of two points included in the interval $[-1; 1]$.
- We state the expected value: $\langle\Psi| A_k B_l |\Psi\rangle = c_{kl}$
- We let $A_k^2 = \mathbb{I}$ and $B_k^2 = \mathbb{I}$.

Notice that the fact that A_k and B_k have an spectra in the interval $[-1; 1]$ assures the suitability of the said operators for their use on experimental set-ups. If we had chosen the spectra of A_k and B_k to be of two unique points $\{-1; 1\}$, we would have committed the same problem of the first Bell's inequality: reliance on perfect quantum correlations.

Also notice that the mentioned mathematical formalities consider a number $m+n$ of operators. For our particular case (of two spin one half particles), we choose $m=2$ and $n=2$; however, Tsirelson's bound is more general and it can allow for its derivation for a greater number of operators.

B. Derivation of Tsirelson's bound

We now write the elementary Tsirelson's bound stated in Tsirelson's paper [9]. No great detail is given about this derivation, but it is enough to solve it in order to prove its validity:

$$\begin{aligned} A_1B_1 + A_1B_2 + A_2B_1 - A_2B_2 = \\ \frac{1}{\sqrt{2}}\left(A_1^2 + A_2^2 + B_1^2 + B_2^2\right) \\ -\frac{1-\sqrt{2}}{8}\left(\left(\sqrt{2}+1\right)(A_1 - B_2) + A_2 - B_2\right)^2 \\ -\frac{1-\sqrt{2}}{8}\left(\left(\sqrt{2}+1\right)(A_1 - B_2) - A_2 - B_1\right)^2 \\ -\frac{1-\sqrt{2}}{8}\left(\left(\sqrt{2}+1\right)(A_2 - B_1) + A_1 - B_2\right)^2 \\ -\frac{1-\sqrt{2}}{8}\left(\left(\sqrt{2}+1\right)(A_2 - B_2) - A_1 - B_1\right)^2 \\ \leq \left(A_1^2 + A_2^2 + B_1^2 + B_2^2\right) \leq 2\sqrt{2}\cdot\mathbb{I} \end{aligned} \tag{37}$$

The derivation of the Tsirelson's bound mostly used in today's literature is due to L. J. Landau [10]. This derivation is presented in the next lines; however, it is important to mention that our derivation will keep the notation used in the chapter "Mathematical Formalities" of this paper. For its translation to the notation of Landau's paper [10] it is enough to state: $A_1 = a, B_1 = b, A_2 = a', B_2 = b'$.

We define:

$$C = A_1B_1 + A_2B_1 + A_1B_2 - A_2B_2 \tag{38}$$

We square C:

$$\begin{aligned} C^2 = &+A_1^2B_1^2 + A_1A_2B_1^2 + A_1^2B_1B_2 - A_1A_2B_1B_2 \\ &+A_2A_1B_1^2 + A_2^2B_2^2 + A_2A_1B_1B_2 - A_2^2B_1B_2 \\ &+A_1^2B_2B_1 + A_1A_2B_2B_1 + A_1^2B_2^2 - A_1A_2B_2^2 \\ &-A_2A_1B_2B_1 - A_2^2B_2B_1 - A_2A_1B_2^2 + A_2^2B_2^2 \end{aligned} \tag{39}$$

We recall that $A_k^2 = B_l^2 = \mathbb{I}$:

$$\begin{aligned} C^2 = &+\mathbb{I} + A_1A_2 + B_1B_2 - A_1A_2B_1B_2 \\ &+A_2A_1 + \mathbb{I} + A_2A_1B_1B_2 - B_1B_2 \\ &+B_2B_1 + A_1A_2B_2B_1 + \mathbb{I} - A_1A_2 \\ &-A_2A_1B_2B_1 - B_2B_1 - A_2A_1 + \mathbb{I} \end{aligned} \tag{40}$$

We notice that some terms cancel pairwise, so that we are left with:

$$\begin{aligned} C^2 &= +\mathbb{I} - A_1A_2B_1B_2 + \mathbb{I} + A_2A_1B_1B_2 \\ &\quad +A_1A_2B_2B_1 + \mathbb{I} - A_2A_1B_2B_1 + \mathbb{I} \\ &= +4\cdot\mathbb{I} - A_1A_2B_1B_2 + A_2A_1B_1B_2 \\ &\quad +A_1A_2B_2B_1 - A_2A_1B_2B_1 \end{aligned} \tag{41}$$

After applying the triangle inequality and the property of multiplicativity of absolute value, since $||A_1|| = ||A_2|| = ||B_1|| = ||B_2|| = 1$, we get:

$$\begin{aligned} &|| - A_1A_2B_1B_2 + A_2A_1B_1B_2 + A_1A_2B_2B_1 - A_2A_1B_2B_1|| \\ &\leq ||A_1A_2B_1B_2|| + ||A_2A_1B_1B_2|| \\ &+||A_1A_2B_2B_1|| + ||A_2A_1B_2B_1|| \\ &\leq ||A_1||||A_2||||B_1||||B_2|| + ||A_2||||A_1||||B_1||||B_2|| \\ &+||A_1||||A_2||||B_2||||B_1|| + ||A_2||||A_1||||B_2||||B_1|| \\ &\leq 1+1+1+1 = 4 \end{aligned} \tag{42}$$

So, we calculate:

$$||C^2|| \leq 4 + 4 = 8 \tag{43}$$

C is hermitian, so that $||C^2|| = ||C||^2$:

$$\begin{aligned} ||C||^2 &\leq 8 \\ \Rightarrow ||C|| &\leq 2\sqrt{2} \end{aligned} \tag{44}$$

Eq. (44) is Tsirelson's bound.

C. Overview

In order to get an overview of the two bounds (Generalized Bell's Inequality and Tsirelson's Bound), we first calculate the Generalized Bell's Inequality in terms of C, and compare it with the Tsirelson's Bound and a particular example by means of a diagram (Fig. 1). First, we can write Eq. (8) as:

$$P\left(\vec{a},\vec{b}\right) = \langle(\sigma\cdot\vec{a})(\sigma\cdot\vec{b})\rangle \tag{45}$$

and we define $A_1 = \sigma\cdot\vec{a'}$, $A_2 = \sigma\cdot\vec{a}$, $B_1 = \sigma\cdot\vec{b}$ and $B_2 = \sigma\cdot\vec{b'}$. For the Generalized Bell's Inequality (Eq. (35)) we have:

$$\begin{aligned} &|\langle A_2B_1\rangle - \langle A_2B_2\rangle + \langle A_1B_2\rangle + \langle A_1B_1\rangle| \leq 2 \\ &\Rightarrow |\langle A_2B_1 - A_2B_2 + A_1B_2 + A_1B_1\rangle| \leq 2 \end{aligned} \tag{46}$$

We notice the presence of Eq. (38), so we write:

$$|\langle C\rangle|_{Bell} \leq 2 \tag{47}$$

Following, we present a particular example. For this particular example, we suppose that $\vec{a}$, $\vec{b}$, $\vec{a'}$ and $\vec{b'}$ are co-planar vectors separated from each other by an angle θ. We calculate the expected value of C as follows:

$$\begin{aligned} |\langle C\rangle| &= \\ |\langle A_2B_1\rangle - \langle A_2B_2\rangle + \langle A_1B_2\rangle + \langle A_1B_1\rangle| &= \\ |\langle(\sigma\cdot\vec{a})(\sigma\cdot\vec{b})\rangle - \langle(\sigma\cdot\vec{a})(\sigma\cdot\vec{b'})\rangle \\ +\langle(\sigma\cdot\vec{a'})(\sigma\cdot\vec{b'})\rangle + \langle(\sigma\cdot\vec{a'})(\sigma\cdot\vec{b})\rangle| \end{aligned} \tag{48}$$

By using Eq. (4) to calculate the quantum mechanical expected value, we get:

$$|\langle C\rangle| = |-3\cos\theta + \cos 3\theta| \tag{49}$$

We now present Eq. (44) (Tsirelson's Bound - red dotted), Eq. (47) (Bell's Inequality - green dotted) and Eq. (49) (example - blue continuous) in Fig. 1:

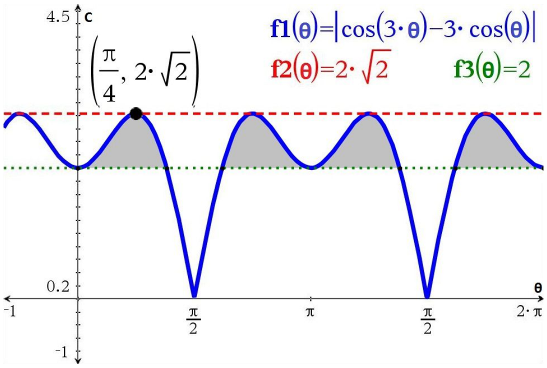

Figure 1. Comparison of Bell's Inequality ($f3(\theta)$ - green), Tsirelson's bound ($f2(\theta)$ - red) and example $\langle C\rangle$(f1(θ) - blue)

In the shadowed regions of Fig. 1, we can see that our quantum expected value $\langle C\rangle$ surpasses our Bell's Inequality(green). However, our graph of $\langle C\rangle$ is bounded by the Tsirelson's Bound (red). We can also appreciate that our graph for $\langle C\rangle$ is saturated, or, reaches its first peak of $2\sqrt{2}$ (Tsirelson's Bound), for $\theta = \pi/4$.

VI. DISCUSSION

We have derived two Bell's inequalities. Bell's inequalities are bounds that could be violated by quantum correlations, but not classical or statistical correlations. The generalized Bell's Inequality (Eq. (35)) takes into consideration problems that were part of the first Bell's Inequality (Eq. (22)) and that were part of ideal systems. Because the generalized Bell Inequality considers real systems, and not ideal systems, this inequality provides with an adequate framework for real life experiments. However, it is important to mention, that even for this inequality some loopholes can arise, which is in fact a matter of research of other papers.

On the other hand, the Tsirelson's bound was also calculated (Eq. (44)). This bound was derived from the formalism of quantum algebra and provides an additional limit that cannot be surpassed by quantum correlations. The importance of this bound, is that it helps determining the possible saturation for quantum correlations. This bound was calculated for our system of spin 1/2, which means it took into account a 2×2 dimensional set of operators ($m = n = 2$); however, the mathematical formalism mentioned also allows for the calculation of the bound for a higher dimension. The calculation of the bound for higher dimensions is part of other research papers.

To conclude, we put into perspective our two limits in Eq. (50):

$$|\langle C\rangle|_{Bell} \leq ||C|| \leq 2\sqrt{2} \tag{50}$$

ACKNOWLEDGMENTS

I would like to thank Jolyon Bloomfield for providing feedback that helped to improve the focus of this paper. I am also grateful for the feedback and writing suggestions provided by Jim Freericks, Zhang Rundong and Rene Galvan, that helped to improve the content of this paper.

[1] A. Einstein, B. Podolsky, and N. Rosen, "Can Quantum-Mechanical Description of Physical Reality Be Considered Complete?," *Physical Review* **47** (May, 1935) 777–780.

[2] D. Bohm, *Quantum theory*. Prentice-Hall, New York, 1951.

[3] J. Clauser and A. Shimony, "Bell's theorem. Experimental tests and implications," *Reports on Progress in Physics* **41** (Feb., 2001) 1881.

[4] J. S. Bell, "On the Einstein Podolsky Rosen paradox," *Physics Physique Fizika* **1** (Nov., 1964) 195–200.

[5] P. Schilpp and A. Einstein, *Albert Einstein, philosopher-scientist*. Library of Living Philosophers, 1949.

[6] K. Binmore, *Mathematical Analysis: A Straightforward Approach*. EBL-Schweitzer. Cambridge University Press, 1977.

[7] J. S. Bell, *Speakable and Unspeakable in Quantum Mechanics*. Cambridge University Press, July, 1988.

[8] J. Clauser, M. A Horne, A. Shimony, and R. Holt, "Proposed Experiment to Test Local Hidden-Variable Theories," *Phys. Rev. Lett.* **23** (Oct., 1969) 880–884.

[9] B. S. Cirel'son, "Quantum generalizations of Bell's inequality," *Letters in Mathematical Physics* **4** (Mar., 1980) 93–100.

[10] L. J. Landau, "On the violation of Bell's inequality in quantum theory," *Physics Letters A* **120** (Feb., 1987) 54–56.

BLOCH SPHERE AND PRESKILL'S BOXES: A WAY OF LEARNING QUANTUM PHYSICS FROM A QUBIT OR AN OAR

Pedro José Morillas Rosa

(Dated: June 19, 2019)

We live in a fundamentally quantum mechanical world, so it is imperative to learn quantum physics in high school. However, the teaching of quantum physics is usually very brief at school, and students basically memorize some formulas that they ponder without a correct conceptual understanding of what they represent. We know that the quantum world is not intuitive, so we present in this document a way to visualize the concepts of quantum physics through the Bloch sphere and Preskill's boxes. We consider that high school students can get a more practical idea of what is quantum physics by using pure mathematics and excellent illustrations inspired on a qubit (instead of only using a historical presentation from Planck to Schrödinger through Einstein and Bohr). Using this method, we show fundamental concepts and applications in various fields and we recommend physics teachers to consider using the qubit to illustrate the principles of non-relativistic quantum physics, rather than more difficult examples for the students to understand as the black body (whose relationship with quantum physics is much more subtle).

I. INTRODUCTION

Physics is a science in continuous transformation. From time to time, new experimental results force the theories that until that moment were considered valid to be modified. But no change has revolutionized in such an important way the physical conception of the world and matter as that introduced by quantum mechanics. Despite its great importance and the recent developments of quantum physics in many fields, its teaching in high school is quite brief, which, together with the difficulty of the subject, often means for students a dark part of physics. But before hearing about quantum physics, in high school students begin to learn notions of computers and bits. It is not until the courses closet to the university that they begin to learn their first notions of quantum physics. They learn very briefly the limitations of classical physics and some quantum mechanics (wave-particle duality, Heisenberg uncertainty principle, spin and some applications). All this, in spite of the many advances achieved in this matter and in the new developments of quantum computing. We believe that a new approach to quantum physics can help students understand in a much more visual way the great oddities involved in some of the facts and experiments of quantum physics. Such an approach is not intended to replace the way in which this subject is currently taught, but it does propose to complement it, introducing concepts such as the qubit, Bloch sphere, Preskill's boxes, or some of their own ideas inspired by them, so that the concepts can be better visualized and understood, thus subtracting difficulty from everything that we find unusual or not at all intuitive. Therefore, we briefly review what each one of these concepts is and how we can help young people to become interested in the fascinating and booming field of research. We end the document showing how to explain using this approach some concepts such as the photoelectric effect, the Heisenberg uncertainty principle and we make a brief reference to the importance of quantum in cryptography.

II. CLASSICAL AND QUANTUM BITS

Since the early years of high school, students have come into contact with the concept of the classical bit (binary digit). In technology subjects, they learn that information is composed of zeros and ones, and that the bit is the minimum unit of information used in computing. With it, they can represent any two values, such as true or false, open or closed, white or black, green or red, etc. They are generally given the example that a classic bit 0 could be represented as a light bulb off, while a bit 1 would be the bulb on.

On the other hand, the qubit is the minimum unit of quantum information theory and the concept is much more abstract than in the case of the classical bit. The qubit can be described as a vector of length unit in a complex two-dimensional vector space. The qubit presents two basic states $|0\rangle$ and $|1\rangle$, which would become the counterparts of the classical bit 0 and the classical bit 1 respectively. The worrying thing about the qubit is that it does not have to be only in one of these two states, but it can be in a quantum superposition of them, that is, it can be in both at the same time, something

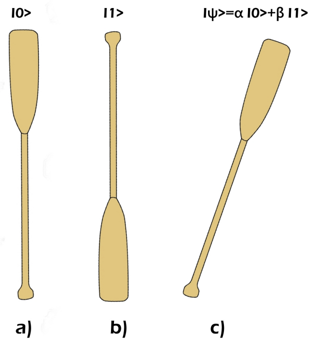

Figure 1: Classical and quantum bits. a) Representation of the classic bit 0 as an oar with the paddle upwards. b) Representation of the classic bit 1 as an oar with the paddle facing down. c) Representation of a qubit as an oar that can be in an overlap of the states $|0\rangle$ and $|1\rangle$, that is, it can be inclined in infinite different positions in space.

that mathematically is expressed like this:

$$|\Psi\rangle = \alpha\,|0\rangle + \beta\,|1\rangle \tag{1}$$

This would be equivalent to having a light bulb on, off or in a situation between the two, as if you had a potentiometer that controlled the intensity of the bulb. Things are no longer true or false, they can be half truth or half lie or be in infinite situations more or less close to the truth or the lie. The representation of a qubit is no longer as simple as the series of steps of 0 or 5 V that represent the series of classic ones and zeros, but we can try to visualize it in some way, for this the Bloch sphere is used, of which we will talk next; but let's start now with some revealing visualizations 1, if we represent the classic bit $0 = |0\rangle$ as an upward oar and the classic bit $1 = |1\rangle$, as a downward oar, a qubit could be represented as that same oar in infinite inclination possibilities.

III. BLOCH SPHERE

Bloch's sphere, named after the Swiss physicist Felix Bloch, is a generalization of the representation of a complex number z with $|z| = 1$ and, as we will see, it is a very appropriate way to represent a qubit. A complex number z has a real part x and an imaginary part y 2.

$$z = x + iy \quad x, y \in \mathbb{R} \tag{2}$$

and, as $|z| = 1 \Rightarrow \sqrt{x^2+y^2} = 1$. Every complex number can be represented in polar coordinates, where $\left\{ \begin{array}{l} x = |z|\,cos\theta \\ y = |z|\,sin\theta \end{array} \right. \Rightarrow z = |z|\,(cos\theta + isin\theta)$. Using Euler's identity: $e^{i\theta} = cos\theta + isin\theta$, we can write a complex number like this: $z = |z|\,e^{i\theta}$. In the case of our complex number of module 1: $z = e^{i\theta}$. Well, as we have seen, a qubit is a mathematical object that can be found in two possible states,$|0\rangle$ and $|1\rangle$, and also in any linear combination of them, that is, it can exist in a continuous of states between them.

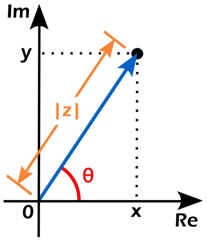

Figure 2: Representation of a complex number z in the complex plane. z can be defined in cartesian coordinates (x, y) or in polar coordinates $(|z|, \theta)$.

In equation (1) α and β are complex numbers such that $|\alpha|^2 + |\beta|^2 = 1$, since the quantum states must be normalized. Since $\alpha, \beta \in \mathbb{C}$, taking into account our previous development, we can do $\left\{ \begin{array}{l} \alpha = |\alpha|\,e^{i\phi_\alpha} \\ \beta = |\beta|\,e^{i\phi_\beta} \end{array} \right.$, so that by substituting in equation (1), we have:

$$|\Psi\rangle = |\alpha|\,e^{i\phi_\alpha}\,|0\rangle + |\beta|\,e^{i\phi_\beta}\,|1\rangle \tag{3}$$

where $|\alpha|, |\beta|, \phi_\alpha, \phi_\beta \in \mathbb{R}$. In quantum physics, the quantities that can be measured are $|\alpha|^2$and $|\beta|^2$, which are the respective probabilities that $|\Psi\rangle$ is in the state $|0\rangle$ or in the state $|1\rangle$. To free ourselves from parameters, we will show that if we multiply our state by an arbitrary factor that is a global phase $e^{i\gamma}$, this will not have consequences for the probabilities:

$$\left|e^{i\gamma}\alpha\right|^2 = (e^{i\gamma}\alpha)^*(e^{i\gamma}\alpha) = (e^{-i\gamma}\alpha^*)(e^{i\gamma}\alpha) = \alpha^*\alpha = |\alpha|^2 \tag{4}$$

And the same would happen with $|\beta|^2$. So, if we multiply our state $|\Psi\rangle$ by $e^{-i\phi_\alpha}$, in equation (3), we get

$$|\Psi'\rangle = |\alpha|\,|0\rangle + |\beta|\,e^{i(\phi_\beta-\phi_\alpha)}\,|1\rangle = |\alpha|\,|0\rangle + |\beta|\,e^{i\phi}\,|1\rangle \tag{5}$$

where we have called $\phi = \phi_\beta - \phi_\alpha$. At this point, we only have three parameters $|\alpha|, |\beta|, \phi \in \mathbb{R}$. And since our quantum state is normalized, that is: $\langle \Psi' |\, \Psi' \rangle = 1$, we can go further in our development, to express our state according to the smaller amount possible of parameters. Suppose we write β in Cartesian form: $\beta = x + iy$. Substituting in equation (1), we have:

$$|\Psi'\rangle = |\alpha|\,|0\rangle + (x+iy)\,|1\rangle \tag{6}$$

For the normalization condition: $|\alpha|^2 + |x+iy|^2 = |\alpha|^2 + (x+iy)^*\,(x+iy) = |\alpha|^2 + (x-iy)\,(x+iy) = |\alpha|^2 + x^2 + y^2 = 1$. And this is the equation of a sphere of unit radius with Cartesian coordinates $(x, y, |\alpha|)$.

Recalling the relationship between the Cartesian and spherical coordinates: $x = rcos\varphi sin\theta$, $y = rsin\varphi sin\theta$,

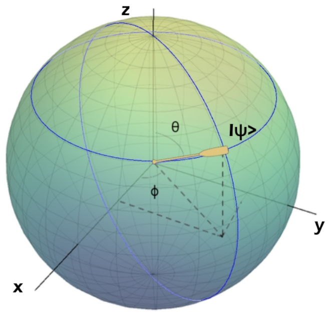

Figure 3: Representation of the Bloch sphere, in which we can represent any state $|\Psi\rangle$ as an oar of length unit that starts from the origin of the sphere and whose blade is defined by the angles θ and φ.

$z = rcos\theta$, if we make $|\alpha| = z$ and remember that the sphere's radius is one: $r = 1$:

$$\begin{aligned}|\Psi'\rangle = z\,|0\rangle + (x+iy)\,|1\rangle = cos\theta\,|0\rangle + sin\theta\,(cos\varphi + isin\varphi)\,|1\rangle \\ = cos\theta\,|0\rangle + sin\theta e^{i\varphi}\,|1\rangle \qquad (7)\end{aligned}$$

with which, suddenly, our state already depends only on two parameters θ and φ.

Suppose now a state $|\Psi\rangle = cos\theta'\,|0\rangle + sin\theta' e^{i\varphi}\,|1\rangle$. We see that $\begin{cases} if\,\theta' = 0 \quad \Rightarrow & |\Psi\rangle = |0\rangle \\ if\,\theta' = {}^{\pi}/2 \Rightarrow & |\Psi\rangle = e^{i\varphi}\,|1\rangle \end{cases}$ which suggests that making θ' to take the values $0 \leq \theta' \leq {}^{\pi}/2$, all points on the Bloch sphere could be generated. Now, let's consider a state $|\Psi'\rangle$ opposite to $|\Psi\rangle$, this means that if $|\Psi\rangle$ has spherical coordinates $(1, \theta', \varphi)$, $|\Psi'\rangle$ will have coordinates $(1, \pi - \theta', \varphi + \pi)$, as can be seen:

$$\begin{aligned}|\Psi'\rangle = cos(\pi - \theta')\,|0\rangle + sin(\pi - \theta')e^{i(\varphi+\pi)}\,|1\rangle = \\ cos\theta'\,|0\rangle - sin\theta' e^{i\varphi}\,|1\rangle = -\,|\Psi\rangle \qquad (8)\end{aligned}$$

Therefore, it is only necessary to consider the upper hemisphere of the sphere $0 \leq \theta' \leq {}^{\pi}/2$, since the lower hemisphere differs from the superior hemisphere by a factor of phase -1. We can, therefore, make the change $\theta = 2\theta' \Rightarrow \theta' = \theta/2$ and define θ as an angle with possible values $0 \leq \theta \leq \pi$. All in all, we finally come to:

$$|\Psi'\rangle = cos\frac{\theta}{2}\,|0\rangle + sin\frac{\theta}{2}e^{i\varphi} \qquad (9)$$

with $0 \leq \theta \leq \pi$ and $0 \leq \varphi \leq 2\pi$. Thi is the mathematical expression that allows expressing any state in Bloch sphere. If we continue with our example of the oar as a qubit represented in 1, the Bloch sphere could be considered as the result of the infinite positions that that the length of the oar 1 placed at its center can have. In 3 we can see the representation of the Bloch sphere and the Bloch vector as an oar representing our state$|\Psi\rangle$. Simply by changing the angles θ and φ, we can get oars in every conceivable positions. In 4 are shown those in which the oar points in the direction of the x, y and z coordinate axes. We will see in point V how we can manipulate our oar in Bloch sphere, read it and apply it in the explanation of some key concepts of quantum physics.

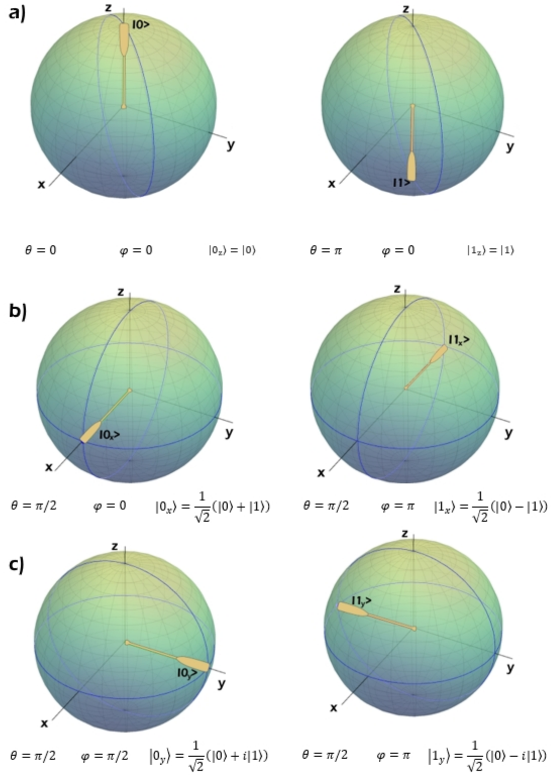

Figure 4: Different states in the Bloch sphere, under each of them it is indicated the angles θ and φ that define them. a) States along the z-axis. b) States along the x-axis. c) States along the y-axis.

IV. PRESKILL'S BOXES

Theoretical physicist John Prekill, a quantum computing expert and professor at Caltech, likes to visualize a bit as a ball that can be one of two colors, either red for 0 and green for 1. If the information is saved, that is, if we keep a ball in a box, and we want to read that information later, we only have to open the box and there will be the result of its color. In the case of the classic bits, the ball that comes out of the box will be the same color as the ball that we put in. We believe that, if the Bloch sphere is a good way to visualize a qubit, the simile of Preskill's boxes is very useful to understand the measurement process, our ultimate goal will be to mix both concepts to bring a new approach to quantum physics. For Preskill, a quantum bit could be, as we say, a box with a ball stored inside, but in this case, we have two doors, door 1 and door 2, which are like two orthogonal axes to each other. Our qubits will be two-colored spheres. Writing a qubit in a Preskill's box consists of choosing one of the two doors and inserting a red or green ball. Reading a qubit in a Preskill's box is to choose another door and take out the ball. That is the process in which the observer intervenes and looks at the ball and sees if it is red or green. In a classic bit, if I put a ball of any color through any door and take it out through any door, the ball always keeps the color, but that is not true in a quantum bit. In a qubit, if the door through which I put the ball and the door through which I take out the ball are the same, nothing happens, the ball maintains its color. But if I put the ball through one door and take it out through another one, it's like flipping a coin, I have a 50% chance of it coming out of one color or the other.

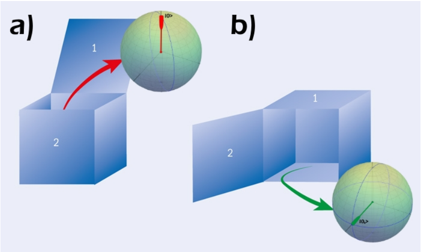

Figure 5: Preskill's boxes. a) If I insert a vertical oar through a vertical door and take it out through that door, the oar does not change. b) If I open a horizontal door when introducing a vertical oar, the oar changes its position with a certain probability.

Using our example of the oar, as we see in 5, if we put an oar in the direction of the z-axis through door 1 and open that door, the oar will continue as we left it. And this is because the door 1 is associated with the way of measuring on the z-axis. So if the qubit has been prepared on such an axis, we will see it as it is. But if we put our oar in that state, we open the door 2, which we can imagine associated with a measurement on the x-axis, the state will have changed and the paddle will now point in the direction of the x-axis, in one direction or another with certain probability.

V. A NEW WAY OF TEACHING QUANTUM PHYSICS

We have seen that a qubit is like an oar in Bloch sphere; it was not by chance that this object was chosen to be used in future developments. An oar resembles a vector, has an origin, a length and an end that points and we could place it in any position, besides it could travel as information that moves. We should not, therefore, think of our oar as something static, we can make operations on it and manipulate it. The operations with qubits, are equivalent to rotations of the state vector (of our oar) in the Bloch sphere. Pauli's matrices:

$$\sigma_x = \begin{pmatrix} 0 & 1 \\ 1 & 0 \end{pmatrix}, \sigma_y = \begin{pmatrix} 0 & -i \\ i & 0 \end{pmatrix}, \sigma_z = \begin{pmatrix} 1 & 0 \\ 0 & -1 \end{pmatrix} \tag{10}$$

when they are exponentiated, they form rotation vectors, that is, the oar rotates an angle α around the axes. A rotation operator $R_n(\alpha)$ is defined by an axis $\hat{n}$ and a rotation angle α. The action of a rotation operator on the quantum state is translated, in what refers to the point associated with the state on the Bloch sphere, in a rotation of the point with respect to the axis of rotation in the angle of rotation. The rotation around any axis $\hat{n}$, would be given by:

$$R_n(\alpha) = e^{-i\alpha\hat{n}\cdot\hat{\sigma}/2} = cos\frac{\alpha}{2}I - isin\frac{\alpha}{2}(n_x\sigma_x + n_y\sigma_y + n_z\sigma_z) \tag{11}$$

With successive rotations around the axes x, y and z we can express manipulations of our oar and, therefore, its evolution. Let's see now what happens when we want to read such a qubit. In quantum, depending on how we measure, the result can be random, that is, quantum mechanics can only provide statistical predictions. A very visual way of understanding the measurement process with Bloch sphere is to imagine our oar dragged by a current trying to pass through an opening made under a bridge, what it is equivalent to have an observable σ. In physics, an observable is all property of the state of a system that can be determined ("observed") by some sequence of physical operations.

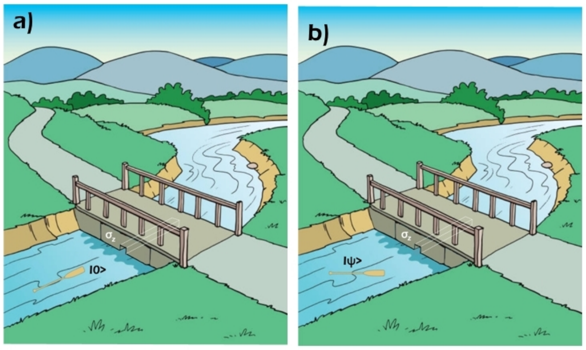

Figure 6: a) An oar travels in the direction of the$z$-axis, so an observable σ_z, will measure the oar as it travels. b) An oar is traveling with a certain inclination with respect to an observable σ_z, so there will be different possibilities for it to go under the bridge in one direction or another.

If the traveling state is $|0\rangle$, that is, an oar in the Bloch sphere oriented in the direction of the z-axis, and we look at it vertically (that is, we make it pass through a vertical opening under the bridge, which is equivalent to an observable σ_z), our measurement will correspond to the qubit itself, that is, we will see a qubit in the state $|0\rangle$ (6a)). The same will happen if, through said slot passes a $|1\rangle$. However, if the original qubit is in a superpositon state, it is not so clear how it will pass through the slot. There will be a probability that it crosses it vertically and another that it will cross it horizontally, with such probabilities being greater the closer the state of one of its superimposed states is (6b)). That is, if the oar was in the state $|\Psi\rangle = cos\frac{\theta}{2}|0\rangle + sin\frac{\theta}{2}|1\rangle$, once we measure it (once it goes under the bridge) , there will be a probability $p_0 = cos^2\frac{\theta}{2}$ that we find it in the state $|0\rangle$ and a probability $p_1 = sin^2\frac{\theta}{2}$ that we find it in the state $|1\rangle$. Now, if the slot is horizontal and crosses the same state $|\Psi\rangle$, Since: $\begin{cases} |0_x\rangle = \frac{1}{\sqrt{2}}(|0\rangle + |1\rangle) \\ |1_x\rangle = \frac{1}{\sqrt{2}}(|0\rangle - |1\rangle) \end{cases} \Rightarrow \begin{cases} |0\rangle = \frac{1}{\sqrt{2}}(|0_x\rangle + |1_x\rangle) \\ |1\rangle = \frac{1}{\sqrt{2}}(|0_x\rangle - |1_x\rangle) \end{cases} \Rightarrow$ $|\Psi\rangle = \frac{1}{\sqrt{2}}\left(cos\frac{\theta}{2} + sin\frac{\theta}{2}\right)|0_x\rangle + \frac{1}{\sqrt{2}}\left(cos\frac{\theta}{2} - sin\frac{\theta}{2}\right)|1_x\rangle$; the probability of finding it this time in the state $|0_x\rangle$will be $p_{0x} = \left[\frac{1}{\sqrt{2}}\left(cos\frac{\theta}{2} + sin\frac{\theta}{2}\right)\right]^2 = \frac{1}{2} + cos\frac{\theta}{2}sin\frac{\theta}{2}$, while the probability of finding it in the state $|1_x\rangle$ will be $p_{1x} = \left[\frac{1}{\sqrt{2}}\left(cos\frac{\theta}{2} - sin\frac{\theta}{2}\right)\right]^2 = \frac{1}{2} - cos\frac{\theta}{2}sin\frac{\theta}{2}$.

In summary, writing a qubit is to choose an axis in the Bloch sphere and make the vector on that axis point in one direction or the opposite. After the various operations that I can do on the qubit, later I will want to read it. So we choose another axis, which can be the same or different, and we project that vector onto it. Such a projection has a probability that I get the vector projected after the measurement in one direction or in the other. Thus, to understand the measurement of the state of a qubit, it is enough for a student to know the concept of the orthogonal projection of a vector. Let's see below the potential of this point of view to bring clarity to the key concepts of quantum physics.

VI. CONCEPTS AND APPLICATIONS

An important concept that can be explained by our approach is the quantum-mechanical property called spin, that is, the intrinsic angular momentum of a particle.

Stern and Gerlach designed an experiment with silver atoms in 1922 that led to this concept. They sent a bundle of silver atoms through a non-uniform magnetic field. If the atoms are small magnets, then they will deviate to one side or to the other. The peculiarity of the silver atom is that all its layers are closed, but a single electron remains in the last layer. In the closed layers, $L = 0$, so if it is discovered that there is angular momentum, it will be due to the electron of the last layer. What Stern and Gerlach expected from a classical point of view, is that, since each silver atom of the beam would have its own magnetic moment, when passing through the magnetic field, they would find a whole range of deviations. But they discovered that atoms only deviated into two spots. It turns out that, no matter how disordered the silver atoms were, when going through the magnetic field they were ordered, either in one area or in another. This was the experiment that revealed spin $\overrightarrow{S}$. And this is something that we can explain with our qubit, our oar or our Bloch sphere 7. When our qubit traverses a slot, which in the case of the Stern and Gerlach experiment would be equivalent to the magnetic field, it is forced to position itself in one of two options, this would also provide an idea of what spin is, although such an idea would not be exempt from loss of interpretation, since there is no classical analogy for spin; in fact, the spin is often mistakenly associated with a rotation of the particles.

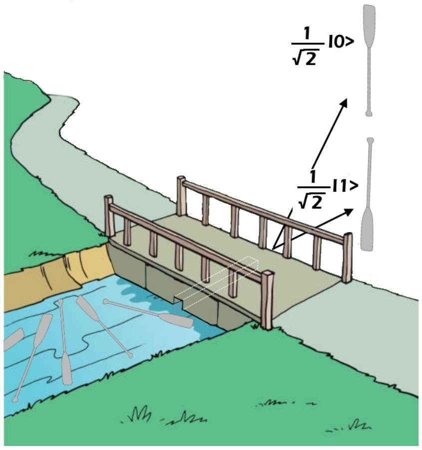

Figure 7: Stern-Gerlach experiment. The orientation of the inhomogeneous magnetic field determines the direction of measurement (opening under the bridge). The coupling of the spin to the magnetic field leads to a discrete displacement of the oar, corresponding to the two results of the measurement +1 (spin up) or -1 (spin down).

Another concept, perhaps the one that students of Baccalaureate know best, is the photoelectric effect. Theorized by Albert Einstein in 1905, it explains the relationship between the energy of the photons that illuminate a metal, the work of extracting said metal and the kinetic energy of the emitted electrons. This quantum theory which could be expressed in the following terms:

$$E = W_0 + E_k \tag{12}$$

where E is the energy of the photons: $E = hf = \frac{hc}{\lambda}$; $W_0 = hf_0 = \frac{hc}{\lambda_0}$ is the work function or extraction work, characteristic of the illuminated metal and $E_k = \frac{1}{2}mv^2 = qV$ is the kinetic energy of the electrons issued. No matter how many photons are cast against a metal, if they do not exceed the threshold frequency of the same f_0, there will be no photoelectric effect. Let's place our oar now in this context acting as a photon. And suppose that the bridge is the metal that we are going to illuminate. If our oar travels in a calm current, regardless of the number of oars that go down and hit the bridge, the stones or the wood that make up the bridge do not have to be damaged and to shoot out of the structure the make up; however, if the oars (the photons) have a sufficiently large energy E due to a storm that causes the flow of the river to grow and strike the bridge overcoming its structural capacity W_0, then the stones (the electrons) weakly linked to the bridge will escape with a maximum kinetic energy E_k, which gives us the expression of the photoelectric equation. We can see this effect illustrated in 8.

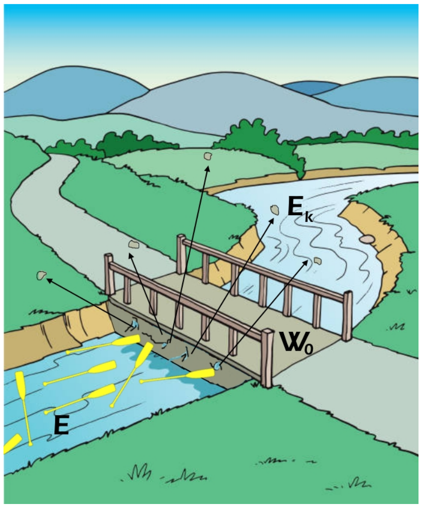

Figure 8: Photoelectric effect. If the oars strike the bridge with an energy $E > W_0$, the parts of the structure less bound to it will be fired at a maximum kinetic energy E_k.

Let's now apply this approach to the Heisenberg uncertainty principle. As we know, this principle of indeterminacy reveals a characteristic of nature at the quantum level and that there are pairs of magnitudes that are simply not simultaneously defined. If we try to measure one of them we lose the knowledge of the other and vice versa. Basically the principle says that it is not possible to simultaneously determine the exact value of the position x and the linear momentum p of a quantum object; or that it is not possible to simultaneously determine the measured value of the energy E of a quantum object and the interval of time necessary to effect the measurement. This is formulated as follows:

$$\Delta x \cdot \Delta p \geq \frac{h}{4\pi} \; \Delta E \cdot \Delta t \geq \frac{h}{4\pi} \tag{13}$$

This is very complex to understand by the students. Let's see it with our qubit-oar. Suppose a state in which our qubit is very close to the state $|0\rangle$. This means that if I execute a measurement in z it is very likely that I will end up obtaining $|0\rangle$. I mean, I'm pretty sure of what's going to happen. But if I measure it in x (which would be equivalent to a bridge whose opening the oar can only enter horizontally), the chances of obtaining $|0_x\rangle$ or $|1_x\rangle$ are almost equal, so I have an almost complete uncertainty of the result. The qubit, when it gains definition in z, loses it indeterminately in x, we can see this situation illustrated in 9.

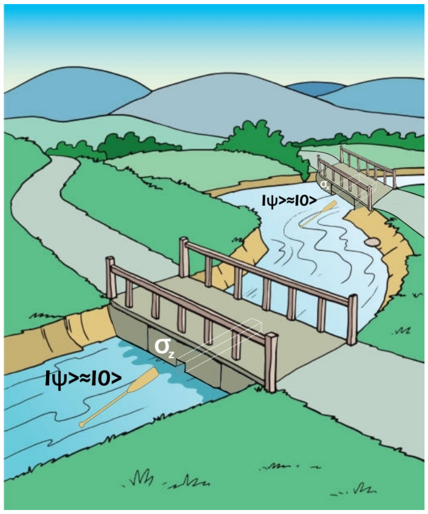

Figure 9: Heisenberg uncertainty principle. If an oar is very close to the state $|0\rangle$, there is a good chance that an observable σ_z (first bridge) will finish measuring $|0\rangle$. Now, if that state is measured with an observable σ_x (second bridge), we have a lot of uncertainty about whether I will get $|0_x\rangle$ or $|1_x\rangle$.

Another very interesting application is quantum cryptography and, in particular, the BB84 protocol. Suppose an emitter, Alice, wants to communicate with Bob by sending her oars down a river. Alice and Bob are each on a bridge. It is decided that if the oars are sent vertically (|) or forming 45º (/), that will be equivalent to sending a 1. Now, if they are sent horizontally ($-$) or forming -45^{o}(\), it would be like sending a 0. To send them in the position they want, Alice changes the openings under the bridge. When Alice sends a polarized oar to Bob, Bob does not know which polarizer (what bridge opening) Alice has used, so he has to randomly choose a + or other slot in the form of × to detect the oar. If Alice sends Bob a vertical (1) or horizontal (0) oar and Bob uses the + opening, he will detect a 1 or a 0 respectively. Now, if Bob uses the opening ×, then the oar will be detected \ setminus or /, with a 50 probability in each case. What is clear is that Bob has to use openings compatible with Alice's message if he wants to get the right message (the process can be seen in 10). Once Bob has received enough oars, both sender and receiver announce publicly through an insecure network, such as the internet, the sequence of openings they used; that is, when Bob used + and when he used ×; what they do not do is tell themselves the sequence of bits. Then they discard the qubits in which they did not use the same opening, and keep those in which they did coincide. Since Bob randomly chooses one opening for each oar, he will choose the wrong opening half the time, so they will end up discarding half of the qubits and the new random oar sequence will be half as long. This sequence is what is called a sifted key. From this key, Alice and Bob take a fraction of oars and compare them through a public channel to see if they match. If so, then they have achieved a secure quantum security key and know that no one has intercepted their message, that is, there is no Eve that has disturbed their signal. Then, the sifted key is safe to use from now on for encryption and decryption. Now, if there are discrepancies between Alice and Bob it is possible that someone has heard (that someone has built a bridge between them) or that the signal is deficient so we will have to order new shipments of oars until we confirm that their message is well safeguarded.

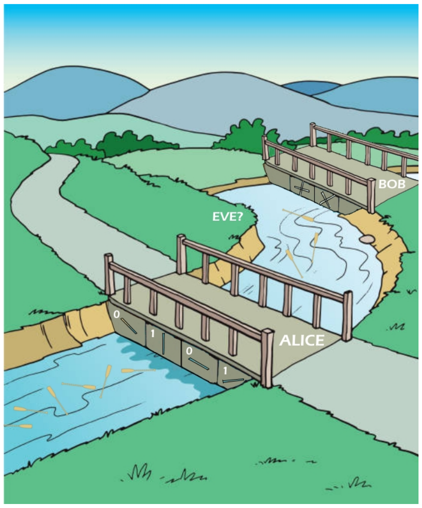

Figure 10: Quantum cryptography. An Alice transmitter sends oars in different positions using openings under a bridge. The receiver, Bob, will decode the message using openings under another bridge. They will know if the information is correct by telling the sequences of openings they used. If Eve intercepts the message, it will modify the sequence expected by Bob and he and Alice will have to start their communication again to make it secure.

Students will find in these examples and in many others, something fascinating that can be done with quantum mechanics and learn the implications, even political, that these new methods of communication and computation can have.

VII. SUMMARY AND CONCLUSIONS

Quantum mechanics is something complicated, yes, that's why it is necessary to search for a "quantum intuition" that permits the explanation of the phenomena that surrounds it and its unpredictability. To do this, we must study and reflect on the main concepts surrounding quantum mechanics to develop a new way of learning and subsequently understanding it. Quantum physics undoubtedly arouses special curiosity in students, so educational research must take steps in the direction of promoting the learning of this valuable discipline. In high school, there is almost no time to explain Modern Physics, students memorize some equations that sound like science fiction and then apply them to solve problems that they learn more or less by heart.

In this document we have seen how the qubit seen from the perspective of the Bloch sphere or the Preskill's box can be used to provide a more intuitive vision to a completely contraintuitive (quantum) world. With simple examples and graphics you can get students to acquire a much more revealing conception of quantum physics than just following a historical description of the phenomena. This can help new generations of students feel attached to this discipline, whose frequent obscurity many times in the way of teaching it, makes them quickly disengage from it. We hope that this approach will inspire teachers and students and bring some light to the many complicated mathematics and difficult concepts that surround quantum mechanics.

ACKNOWLEDGEMENTS

"It is my opinion, Mr. Jeorling," replied the boatswain, "that what we see there is neither a blower nor a wreck, but merely a lump of ice." **Jules Verne**, The Sphinx of the Ice.

I am especially grateful for the inspiring classes of Barton Zwiebach and the valuable advice from Jim Freericks without which this document would not have been possible. Also to all the classmates of the Applications of Quantum Mechanics course, whose hard work in their respective papers has been the source of motivation to work on mine. Finally, a mention that it would not have been possible to inspire the oar simile without the nocturnal readings before sleeping of The Sphinx of the Ice by Jules Verne.

REFERENCES

1. Wolfgang Dür, Stefan Heusler, "What we can learn about quantum physics from a single qubit", Decembre 6, 2013. https://arxiv.org/abs/1312.1463
2. John Preskill, "Making Weirdness Work: Quantum Information and Computation".
3. Francis Villatoro, "El timo del ordenador cuántico comercial", Naukas Quantum Conference, October 2013. https://www.youtube.com/watch?v=IactWXBA3Us
4. Anastasios Kyrillidis, "Introduction to quantum computing: Bloch sphere", http://akyrillidis.github.io/notes/quant_post_7
5. Javier García, "¿Qué es realmente el espín del electrón?" Conference, June 2017. https://www.youtube.com/watch?v=JaZwliv9isQ
6. Dag Roar Hjelme, Lars Lydersen, Vadim Makarov, "Quantum Cryptography". Chapter on quantum cryptography for the book "A Multidisciplinary Introduction to Information Security". August, 2011.

Bohm-Aharonov effect for a particle in a defective ring

Nikos Kipouros,
HAFA, Greece

(Dated: June 19, 2019)

Aharonov and Bohm [1] suggested a long time ago an interference two-slit experiment where a charged particle can go either way round a region where a magnetic field exists. Crucially the particle is excluded from the region where the magnetic field is non-vanishing. It is found that the fringe pattern depends on the magnetic flux enclosed by the possible particle trajectories. A well-known variant of the Aharonov-Bohm effect involves a charged particle constrained to move in a ring enclosing a magnetic field. The energy spectrum of the particle depends on the enclosed flux. In the present paper a defective ring is considered, the defect being defined by a potential depending on the azimuthal angle and the energy spectrum is studied as a function of the enclosed flux and of the potential strength.

I. INTRODUCTION

In classical physics the motion of a charged particle in an electromagnetic field is completely determined by Newton's law and the Lorentz expression for the force which of course vanishes at a point where the fields **E** and **B** vanish. The electromagnetic vector and scalar potentials **A** and φ (see e. g. Chapter 10 of Griffiths [2] for a discussion) are particularly convenient in deriving the invariance properties of the theory under Lorentz transformations (see e. g. paragraph 24 of Landau and Lifshitz [3]). Radiation by accelerating particles is beautifully described by retarded electromagnetic potentials (see e. g. Chapter 8 of Landau and Lifshitz [3] on Lienard-Wiechert potentials). At the interface between classical and quantum physics we must point at the adiabatic invariants for charges moving in electromagnetic fields (Jackson [4], Chapter 12, paragraph 5).

The status of the electromagnetic potentials is rather different when one incorporates electromagnetism in quantum mechanics. The latter is based on the Hamiltonian formalism and the Hamiltonian function features the kinetic energy term $\mathbf{p}^2/(2m)$. From the word go this term is modified to $(\mathbf{p} - q\mathbf{A}/c)^2/(2m)$ (the *minimal substitution*) to describe the quantum mechanics of a non-relativistic charged particle interacting with the electromagnetic field (for an account of minimal substitution see e. g. Chapter 4 of Griffiths [5] or Chapter 15 of Bohm [6]). This has been known since the 1920s. People at the time may have thought that gauge invariance would reinstate the electric and magnetic fields as somehow the real fields and fall back to the classical view that it is the latter only, and not the potentials, that have observable effects. To paraphrase Feynman [7] the Aharonov-Bohm effect has been waiting to be discovered for about thirty years.

The suggestion by Bohm and Aharonov [1] was to modify the well-known two-slit interference experiment by including a magnetic field as in Figure 1. The beam consists of charged particles that can go either way round the magnetic field. The field is confined in the cylindrical region shown in the Figure and the charged particles are forbidden to enter the field region. They point out that this can be achieved by erecting an impenetrable potential barrier round the field. Hence all possible trajectories (in the sense of a Feynman [7] path integral). Yet the Bohm-Aharonov analysis shows that the pattern of the interference fringes does depend on the enclosed magnetic flux.

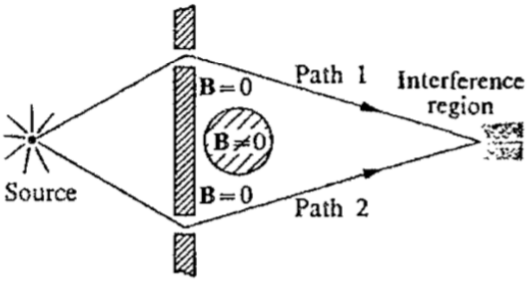

Figure 1. The two-slit experiment of Aharonov and Bohm (from Sakurai [8] p 17)

A well-known variant of the above situation consists of a charged particle constrained to move in a ring as in Figure 2 surrounding a cylindrical region where a magnetic field exists:

$$\begin{aligned} \mathbf{B} &= B\hat{\mathbf{z}}, \quad r < a \\ \mathbf{B} &= 0, \quad r > a. \end{aligned} \tag{1}$$

Then the energy spectrum of the particle depends on the enclosed magnetic flux; for details see Example 4.6 of Griffiths [5].

Clearly the interference pattern disappears if one slit in Figure 1 is shut. Similarly no dependence of the energy levels on the magnetic flux would be detected if an impenetrable obstacle is located at some point on the ring. In this paper we set out to do that in a controlled fashion as follows. Rather than having the constrained particle to move freely on the ring we dig a potential well V that depends on the azimuthal angle ϕ as in Figure 3. Clearly when the potential strength vanishes we go back to perfect interference as in Griffiths.

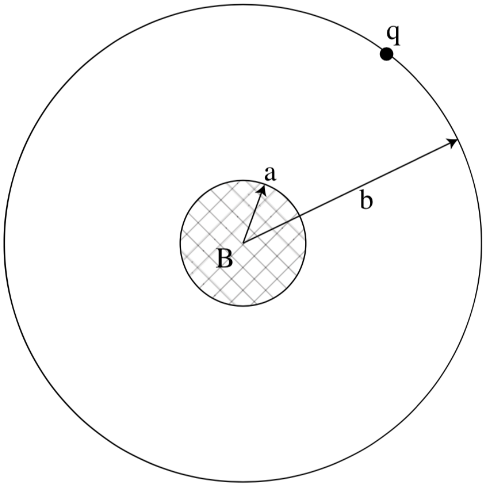

Figure 2. Motion of a particle on a ring of radius b. A solenoid of radius a runs perpendicular to the plane of the ring through its center (from Zwiebach [9], Problem 5, Problem Set 5).

The Hamiltonian reads

$$H = \frac{1}{2m}\left(\frac{\hbar}{i}\nabla - \frac{q}{c}\mathbf{A}(\mathbf{x},t)\right)^2 + q\varphi(\mathbf{x},t) + V(\mathbf{x}) \tag{2}$$

where m, q are the particle's mass and charge respectively and c is the speed of light.

II. CONSTRUCTION OF THE VECTOR POTENTIAL

Given the cylindrical symmetry of the problem we write the vector potential in cylindrical coordinates (see e. g. Weisstein [10]) in the form

$$\mathbf{A} = A_r\hat{\mathbf{r}} + A_\varphi\hat{\varphi} + A_z\hat{\mathbf{z}} \tag{3}$$

Having introduced the vector potential we have to choose a gauge. We choose the Coulomb gauge

$$\nabla\cdot\mathbf{A} = 0. \tag{4}$$

Then (see p. 440 of Griffiths [2]) the scalar potential obeys Poisson's equation and in the absence of external charges

$$\varphi = 0. \tag{5}$$

The magnetic field created by a solenoid is given in p. 237 of Griffiths [2]. We define the magnetic flux through the solenoid

$$\Phi = B\pi a^2, \tag{6}$$

and then

$$\mathbf{A} = \frac{\Phi}{2\pi a^2} r\hat{\phi}. \tag{7}$$

That the above equations are consistent can be shown by using the fundamental equation $\mathbf{B} = \nabla\times\mathbf{A}$ and use the expression of curl in cylindrical coordinates [10].

III. SCHRODINGER'S EQUATION FOR A PARTICLE IN A RING

A. The Hamiltonian

$$H = \frac{\hbar^2}{2mb^2}\left(\frac{1}{i}\frac{d}{d\phi} - \frac{q\Phi}{2\pi\hbar c}\right)^2 + \lambda V_0(\phi) \tag{8}$$

The time-independent Schrodinger's equation reads

$$H\psi = E\psi \tag{9}$$

We substitute equation (8) in (9), expand the square in the former, recall expression $\Phi_0 = 2\pi\hbar c/q$ for the elementary flux quantum and define

$$\beta = \frac{\Phi}{\Phi_0} \tag{10}$$

to obtain (from now on derivatives with respect to ϕ are denoted by primes)

$$\psi'' - 2i\beta\psi' - \frac{2Vmb^2}{\hbar^2}\psi + \left(\frac{2Emb^2}{\hbar^2} - \beta^2\right)\psi = 0, \tag{11}$$

where the angle ϕ varies in the range $[-\pi, \pi]$. We define dimensionless quantities

$$\varepsilon = \frac{2mb^2}{\hbar^2}E, \quad v(\phi) = \frac{2mb^2}{\hbar^2}V(\phi), \tag{12}$$

to rewrite (11) in the form

$$\psi'' - 2i\beta\psi' - v(\phi)\psi + \left(\varepsilon - \beta^2\right)\psi = 0. \tag{13}$$

The wavefunction must also satisfy the periodic boundary condition

$$\psi(-\pi) = \psi(\pi). \tag{14}$$

For simplicity we take the potential to be of finite range, have angular width 2α and be symmetric about $\phi = 0$ (see Figure 3).

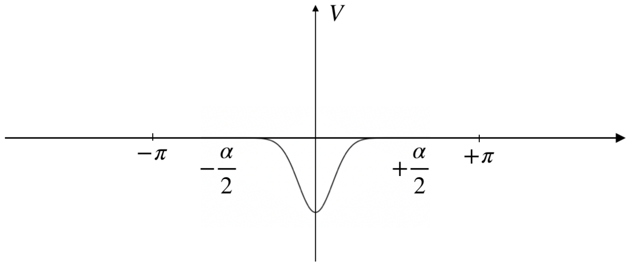

Figure 3. The potential $V_0(\phi)$ on the ring is characterized by an angular width α.

B. Relaxation of the Boundary Condition and Connection with the case of an Electron in a one-dimensional Lattice

We can certainly attack the problem defined by eqns (13) and (14) directly by writing ψ as a superposition of exponential wavefunctions inside and outside the potential and apply matching conditions at $\pm\pi$ and $\pm\alpha/2$. This procedure is straightforward but rather tedious. So we decide to temporarily abandon boundary condition (14) and consider the particle in a periodic potential as in Figure 4. Then, for $\beta = 0$, the Schrodinger equation (11) is familiar from the problem of an electron in a periodic lattice and for a square potential it defines the Kronig-Penney model (see pages 146-149 of Ashcroft and Mermin [11]). The presence of β makes of course a difference.

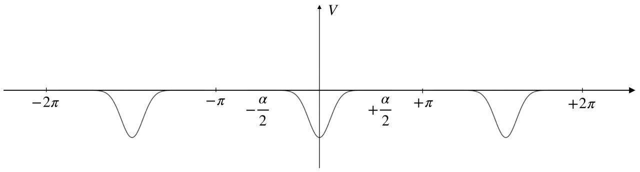

Figure 4. The potential with period 2π

Bloch's theorem provides an important tool in the construction of the wavefunction in a periodic potential. A general discussion is given in the book by Ashcroft and Mermin. For our purposes the short, mathematical treatment of the one-dimensional case in Problem 28 of Fluegge [12] based on Floquet's theorem suffices for our purposes (the theorem deals with a general second order linear differential equation and does cover the case of a first-derivative term as in (13)). According to the theorem the solution of (13) is of the form

$$\psi(\phi) = e^{ik\phi}u(\phi), \tag{15}$$

where k is a wavevector to be determined and u is any *periodic* solution of (13):

$$u(\phi) = u(\phi + 2\pi). \tag{16}$$

Then from the above two equations

$$\psi(\phi + 2\pi) = e^{ik2\pi}\psi(\phi). \tag{17}$$

Clearly for the derivatives

$$\psi'(\phi + 2\pi) = e^{ik2\pi}\psi'(\phi). \tag{18}$$

.

C. Solution of the Schrodinger Equation

Differential equation (13) features a first derivative and the standard technique to get rid of it (see p. 159 of Simmons [13]) is to introduce a new unknown function w by

$$u(\phi) = e^{i\beta\phi}w(\phi). \tag{19}$$

Then

$$\begin{aligned} u' &= i\beta e^{i\beta\phi}w + e^{i\beta\phi}w', \\ u'' &= -\beta^2 e^{i\beta\phi}w + e^{i\beta\phi}w'' + 2i\beta e^{i\beta\phi}w'. \end{aligned} \tag{20}$$

We substitute the above in (13) to deduce the differential equation obeyed by w

$$w'' - \lambda v_0(\phi)w + \varepsilon w = 0. \tag{21}$$

This is the standard equation of a particle in a potential.

For positive energy we define the (real) wavevector

$$p = \sqrt{\varepsilon} \tag{22}$$

and denote by w_L, w_R the usual waves incident from left and right respectively. Let R, T be the usual reflection and transmission coefficient of the potential λv_0. Then in accordance with (19) we can construct u_L, u_R (see Figure 4):

$$\begin{aligned} u_L &= e^{i(\beta+p)\phi} + Re^{i(\beta-p)\phi}, \quad -\pi < \phi < -\alpha/2, \\ &= Te^{i(\beta+p)\phi}, \quad \pi + \alpha/2 < \phi < \pi, \end{aligned} \tag{23}$$

$$\begin{aligned} u_R &= e^{i(\beta-p)\phi} + Re^{i(\beta+p)\phi}, \quad \pi + \alpha/2 < \phi < \pi, \\ &= Te^{i(\beta-p)\phi}, \quad -\pi < \phi < -\alpha/2. \end{aligned} \tag{24}$$

We also quote the first derivatives of the above that will be needed below:

$$\begin{aligned} u_L' &= i(\beta+p)e^{i(\beta+p)\phi} + i(\beta-p)Re^{i(\beta-p)\phi}, \quad -\pi < \phi < -\alpha/2, \\ &= i(\beta+p)Te^{i(\beta+p)\phi}, \quad \pi + \alpha/2 < \phi < \pi, \end{aligned} \tag{25}$$

$$\begin{aligned} u_R' &= i(\beta-p)e^{i(\beta-p)\phi} + i(\beta+p)Re^{i(\beta+p)\phi}, \quad \pi + \alpha/2 < \phi < \pi, \\ &= i(\beta-p)Te^{i(\beta-p)\phi}, \quad -\pi < \phi < -\alpha/2. \end{aligned} \tag{26}$$

The solution u that enters (15) is a linear combination of u_L, u_R. Thus (15) reads

$$\psi = e^{ik\phi}\left(Au_L + Bu_R\right), \tag{27}$$

where the coefficients A, B are to be determined. We apply properties (17), (18) to the wavefunction (27) and obtain

$$\begin{aligned} Au_L(\pi) + Bu_R(\pi) &= e^{ik2\pi}[Au_L(-\pi) + Bu_R(-\pi)], \\ Au_L'(\pi) + Bu_R'(\pi) &= e^{ik2\pi}[Au_L'(-\pi) + Bu_R'(-\pi)]. \end{aligned} \tag{28}$$

We rearrange the above

$$\begin{aligned} A[u_L(\pi) - e^{ik2\pi}u_L(-\pi)] &= B[e^{ik2\pi}u_R(-\pi) - u_R(\pi)], \\ A[u_L'(\pi) - e^{ik2\pi}u_L'(-\pi)] &= B[e^{ik2\pi}u_R'(-\pi) - u_R'(\pi)]. \end{aligned} \tag{29}$$

The set of equations (29) is a homogeneous linear systems for the unknowns A, B. Consistency requires

$$\begin{aligned}&[u_L(\pi) - e^{ik2\pi}u_L(-\pi)][e^{ik2\pi}u'_R(-\pi) - u'_R(\pi)]\\ &= [u'_L(\pi) - e^{ik2\pi}u'_L(-\pi)][e^{ik2\pi}u_R(-\pi) - u_R(\pi)].\end{aligned} \tag{30}$$

We substitute equations (23) to (26) in the above and multiply both sides by $e^{-i2k\pi}$ to deduce

$$e^{i2k\pi}K_1 + K_2 + e^{-i2k\pi}K_3 = 0, \tag{31}$$

where the constants K_i turn out to be

$$\begin{aligned}K_1 = K_3 &= 2ipe^{-i2\beta\pi}T,\\ K_2 &= 2ip\left((R^2 - T^2)e^{i2p\pi} - e^{-i2p\pi}\right).\end{aligned} \tag{32}$$

We use the above in (31) to deduce

$$\cos 2\pi(k - \beta) = \frac{e^{-i2p\pi}}{2T} - \frac{R^2 - T^2}{2T}e^{i2p\pi}. \tag{33}$$

It is known (see Barton [14]) that the reflection and transmission coefficients of a symmetric one-dimensional potential are parametrized by two angles Δ and θ that are functions of energy

$$T = \cos\theta e^{i\Delta}, \quad R = i\sin\theta e^{i\Delta}, \tag{34}$$

where Δ is the familiar phase shift. Then the two properties $|T|^2 + |R|^2 = 1$ (the unitarity condition) and $RT^\star + R^\star T = 0$, that can be proved by considering appropriate Wronskians, are satisfied. Substituting (34) in (33) we obtain

$$\cos 2\pi(k - \beta) = \frac{\cos(2p\pi + \Delta)}{\cos\theta}. \tag{35}$$

It is also shown in the previous reference that $-\pi/2 < \theta < \pi/2$ and then from the first of (34)

$$|T| = \cos\theta. \tag{36}$$

Hence equation (35) is equivalent to (8.76) of Ashcroft and Mermin [11].

For negative energy states we define

$$\hat{p} = \sqrt{|\varepsilon|}, \tag{37}$$

and define solutions that behave outside the well as follows

$$\begin{aligned}\hat{w}_L &= e^{\hat{p}\phi} + c_2e^{-\hat{p}\phi}, \quad -\pi < \phi < -\alpha/2,\\ &= c_1e^{-\hat{p}\phi}, \quad \alpha/2 < \phi < \pi,\end{aligned} \tag{38}$$

$$\begin{aligned}\hat{w}_R &= e^{-\hat{p}\phi} + c_2e^{\hat{p}\phi}, \quad \alpha/2 < \phi < \pi,\\ &= c_1e^{\hat{p}\phi}, -\pi < \phi < -\alpha/2,\end{aligned} \tag{39}$$

where the c_i coefficients in eqns (38, 39) are identical to the symmetry of then well. In accordance with (19) we define

$$\hat{u}_{L,R} = e^{i\beta\phi}\hat{w}_{L,R}. \tag{40}$$

Then eqns (27) to (31) read the same provided we use hats over the relevant quantities. The quantities $\hat{K}_i$ turn out to be

$$\begin{aligned}\hat{K}_1 &= -2c_1c_2\hat{p}e^{-i2\pi\beta},\\ \hat{K}_2 &= 2\hat{p}\left(e^{2p\pi}c_2^2 + e^{-2p\pi}c_1^2 - e^{-2p\pi}\right),\\ \hat{K}_3 &= -2c_1c_2\hat{p}e^{i2\pi\beta}.\end{aligned} \tag{41}$$

We substitute the above in the hatted analog of (31) to obtain the equation that determines the spectrum of the negative energy states:

$$\cos 2\pi(k - \beta) = \frac{e^{2p\pi}}{2}\frac{c_2}{c_1} + \frac{e^{-2p\pi}}{2}\frac{c_1}{c_2} - \frac{e^{-2p\pi}}{2}\frac{1}{c_1c_2}. \tag{42}$$

D. Reinstatement of the Boundary Condition and Calculation of the Energy Spectrum

In the previous two Subsections we solved the mathematical problem of a charge moving in infinite ϕ space in a periodic potential of period 2π. We now return to reality and require that after a full circle the wavefunction returns to its original value (eqn (14)). Then eqn (17) gives

$$k = n, \quad n : \text{integer}, \tag{43}$$

and eqns (35), (42 become

$$\cos 2\pi(n - \beta) = \frac{\cos(2p\pi + \Delta)}{|T|}, \tag{44}$$

$$\cos 2\pi(n - \beta) = \frac{e^{2p\pi}}{2}\frac{c_2}{c_1} + \frac{e^{-2p\pi}}{2}\frac{c_1}{c_2} - \frac{e^{-2p\pi}}{2}\frac{1}{c_1c_2}. \tag{45}$$

A given enclosed flux Φ determines β through (10) and a given potential determines the transmission amplitude $T(p)$ and the phase shift $\Delta(p)$. Then (44) determines the acceptable values of p given n and hence the spectrum through (22). One conclusion from the above equation is that the spectrum is unchanged when $\beta \to \beta + 1$ similarly to the case of a vanishing potential.

The main features of the model are sufficiently well illustrated by the choice of a square well (Figure 5). The transmission amplitude in this case is determined in e. g. paragraph 11.7 of Bohm [6]

$$T = \frac{4e^{-ip\alpha}}{(1 + \frac{p'}{p})(1 + \frac{p}{p'})e^{-i\alpha p'} + (1 - \frac{p'}{p})(1 - \frac{p}{p'})e^{i\alpha p'}}, \tag{46}$$

where p' is the wavevector inside the well

$$p' = \sqrt{\lambda + \varepsilon}. \tag{47}$$

The quantities c_i are calculated by continuity of either $\hat{w}$ (eqns (38), (39)) at $\phi = \alpha/2$:

$$\begin{aligned}c_1 &= \frac{2\hat{p}\hat{p}'}{(\hat{p}^2 + \hat{p}'^2)\sin\hat{p}'\alpha},\\ c_2 &= e^{-pa}\frac{2\hat{p}\hat{p}'\cos\hat{p}'\alpha + (\hat{p}^2 - \hat{p}'^2)^2\sin\hat{p}'\alpha}{(\hat{p}^2 + \hat{p}'^2)\sin\hat{p}'\alpha},\end{aligned} \tag{48}$$

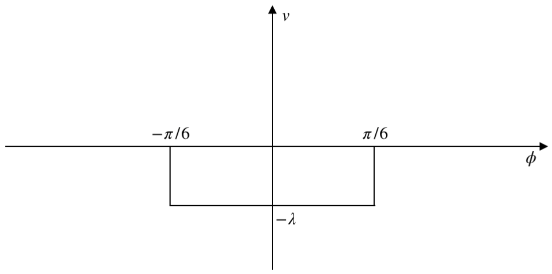

Figure 5. The square well of Subsection III.D

where $\hat{p}' \equiv \sqrt{\lambda - |\varepsilon|}$.

We first look at the negative energy states and plot in Figure 6 the right hand side of (45) as a function of $|\varepsilon|$ and the horizontal line $y = \cos 2\pi\beta$ for the relatively small strength $\lambda = 1$, and repeat this in 7 for $\lambda = 120$.

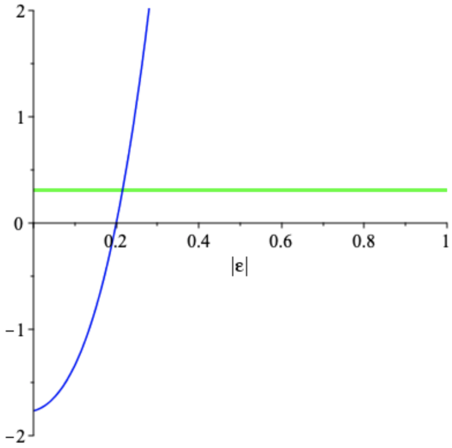

Figure 6. The green and blue curves respectively stand for $y = \cos 2\beta\pi$, $\beta = 0.2$ and the right hand side of eqn (45) for a potential with $\lambda = 1.0$.

Clearly in Figure 6 the intersection of the blue curve with the green line varies as β varies. On the other the hand for deep-lying bound states ($|\varepsilon|$ large) the exponentially large factor $e^{2\pi p}$ causes the right hand side of eqn (45) to oscillate wildly and as a result the blue curve in 7 is essentially vertical. Hence in that regime the spectrum is independent of β. This vindicates the assertion in question (f), Problem 5 of Problem Set 5 of Zwiebach's [9] notes.

We turn to positive-energy states. In the absence of a potential eqn (44) gives

$$\cos 2\pi(n - \beta) = \cos 2p\pi, \qquad (49)$$

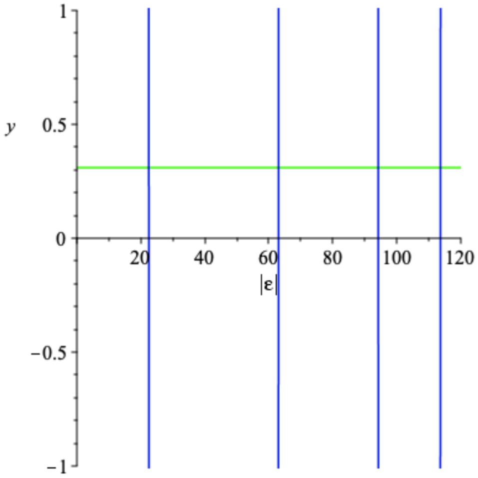

Figure 7. Same as Figure 6 for $\lambda = 120.0$.

where n is an integer and p by definition positive. Then the above equation gives

$$\varepsilon = (n - \beta)^2, \quad n = 0, \pm 1, \pm 2, .. \quad , \qquad (50)$$

in accordance with Griffiths [5]. To apply eqn (44) we need (apart from $|T|$ which is immediately calculable from (46) the phase shift Δ given by $\arg T$ (see the first of (34) and (36)). To choose the correct branch of the arg we use Levinson's theorem that determines the behaviour of the phase shift as $p \to 0$ through $\Delta(0) = (n_b - 1/2)\pi$. For the values $\beta = 0.2$, $\lambda = 1.0$ and $\lambda = 120.0$ examined previously the potential supports one and five bound states respectively (note that by bound states we refer to *one* well in *unlimited* ϕ space and that this is not directly related to the spectrum in the present). In Figures 8 to 11 the phase shift and the modulus of the transition amplitude are plotted as functions of p for the above λ values. In Figure 12 we estimate graphically the positive energy spectrum for $\lambda = 1$. Two conclusions are drawn. If we compare with the case of zero potential the state marked with a cross in Figure 12 is lost. This state corresponds to the state that appeared in Figure 6 as negative energy states, hence the total number of states is conserved as expected. We also observe that as p grows larger the spectrum is unaffected by the potential. The case $\lambda = 120.0$ is more intriguing. Clearly the first conclusion drawn from Figure 12 still holds: For large eigenvalues the percentage change $\delta E/E$ in the absence and presence of the potential is negligible for a given β value and as mentioned previously the spectrum is periodic in β. One question that remains has to do with variation of λ for a given β: Patiently counting the number of eigenstates up to, say, $p = 20$ in Figure 13 we note that the number of positive-energy eigenstates in the absence of the potential exceeds the number in the presence of the

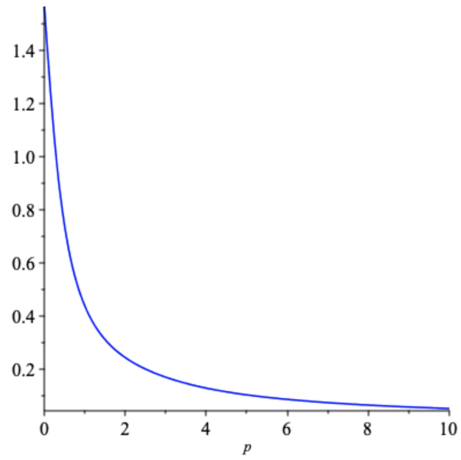

Figure 8. The phase shift as function of p for $\lambda = 1.0$

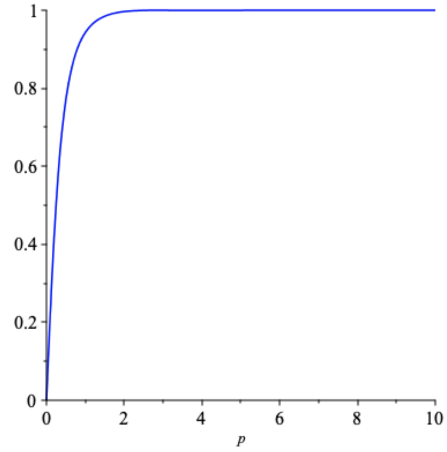

Figure 9. The modulus $|T|$ of the transmission amplitude as function of p for $\lambda = 1.0$

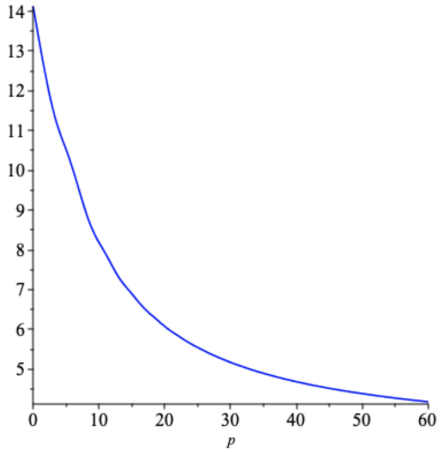

Figure 10. The phase shift $\Delta(p)$ for $\lambda = 120.0$

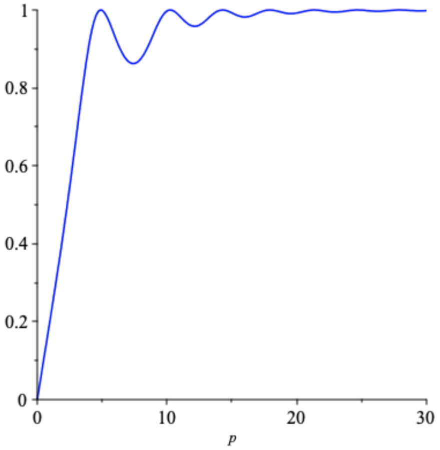

Figure 11. The modulus $|T|$ of the transition amplitude for $\lambda = 120.0$

potential by three whereas, according to Figure 7 there are four negative energy eigenstates. To check that the number of eigenstates is conserved one would have to look at the asymptotic distribution of eigenstates in the presence of the potential. I understand that this problem has been solved in its generality but there was no time to apply these results to the present problem.

IV. DISCUSSION

We considered the presence of a defect along the path of charge q in the interference experiment of Figure 2. The Bohm-Aharonov effect predicts that the energy spectrum is sensitive to the enclosed magnetic flux and that this is due to interference between waves going to the left and right of the enclosed magnetic field. Our findings confirm the expectation that the energy spectrum of states lying deep inside the defect are insensitive to the enclosed flux since no interference is there. On the other hand high energy states are impervious of the presence of the well, perfect interference takes place, and the Bohm-Aharonov spectrum is recovered.

ACKNOWLEDGMENTS

The idea behind this paper was motivated by a Problem in Professor Barton Zwiebach's edX course in Quantum Mechanics. The author also wishes to thank

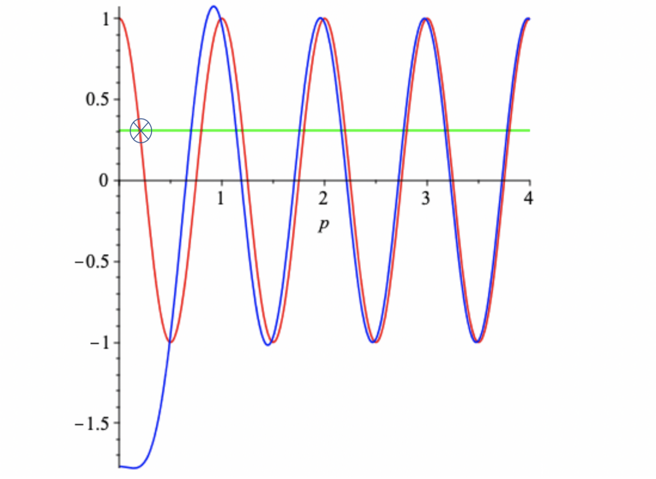

Figure 12. The green line stands for $y = \cos 2\beta\pi$, the red and blue curves depict the right hand side of eqn (44) in the absence of a potential and for a potential with $\lambda = 1.0$.

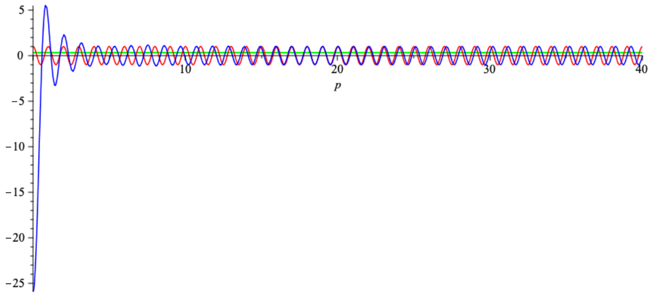

Figure 13. The green line stands for $y = \cos 2\beta\pi$, the red and blue curves depict the right hand side of eqn (44) in the absence of a potential and for a potential with $\lambda = 120.0$.

Dr Jolyon Bloomfield for comments and Dr Alex Calogeracos for a comment on the Kronig-Penney model and for advice on one-dimensional potentials.

---

[1] Y. Aharonov and D. Bohm, “Significance of electromagnetic potentials in the quantum theory,” *Physical Review* **115** (1959) 485–491.

[2] D. J. Griffiths, *Introduction to Electrodynamics, 4th ed.* Prentice Hall, 2012.

[3] L. D. Landau and E. M. Lifshitz, *The Classical Theory of Fields.* Pergamon Press, 1975.

[4] J. D. Jackson, *Classical Electrodynamics, 3rd ed.* John Wiley and Sons, 1999.

[5] D. J. Griffiths, *Introduction to Quantum Mechanics, 3rd ed.* Cambridge University Press, 2018.

[6] D. Bohm, *Quantum Theory.* Prentice-Hall, 1951.

[7] R. P. Feynman, R. B. Leighton, and M. Sands, *The Feynman Lectures on Physics, vol 2.* Addison-Wesley, 1964.

[8] J. J. Sakurai, *Advanced Quantum Mechanics.* Addison-Wesley, 1967.

[9] B. Zwiebach, *Quantum Mechanics III 8.06.* `http://www.edx.org`.

[10] E. W. Weisstein, *Cylindrical Coordinates. From MathWorld–A Wolfram Web Resource.* `http://mathworld.wolfram.com/CylindricalCoordinates.html`.

[11] N. W. Ashcroft and N. D. Mermin, *Solid State Physics.* Cengage Learning, 1976.

[12] S. Fluegge, *Practical Quantum Mechanics.* Springer, 1999.

[13] G. F. Simmons, *Differential Equations with Applications and Historical Notes, 2nd ed.* McGraw-Hill, 1991.

[14] G. Barton, “Levinson’s theorem in one dimension: heuristics,” *J. Phys. A: Math. Gen.* **115** (1985) 479–494.

Case Study of the Momentum Operator

Rohan Kulkarni
Term paper for MIT 8.06x : Applications of Quantum Mechanics

I. INTRODUCTION

In this review paper, I focus mainly on how to see if one can construct a *specific operator* for a *given domain.* This is a lost art as many books take the existence of meaningful physical operators on a Hilbert space for granted. If I had to categorize this paper it would go under *Mathematical quantum mechanics.* The modern mathematical toolkit explaining quantum mechanics is *Functional analysis.* Therefore before starting to read this paper, I would request the reader to familiarize themselves with the most important basic facts of Functional analysis needed for Quantum mechanics. One can read this in [Szekeres] or even better [Background read] (This is a link of some lecture notes I have uploaded online, they are password protected as they are not mine and I don't want to publicly post some notes that don't belong to me. The password can be found along with the link in the bibliography). The paper could be somewhat difficult to read for someone who is not familiar with basics of *Functional analysis.* If you feel this please leave a comment on the abstract post so we can take this matter to *Prof. Bloomfield*

II. OPERATORS

Hilbert spaces are what coordinate systems or phase space are to classical mechanics. In order to construct an entire physical system we needs the concept of *function* or *observable.*

Definition II.1 (***Operator***)**.** Let A and B be two normed spaces. An **operator** $\mathcal{T}$ is a linear map $\mathcal{T} : A \to B$.

Remark II.1. In most of the linear algebra courses it is assumed that the concept of *continuity* is well-defined. This is true in the case when A is assumed to be finite dimensional. The reason for this is that all norm's are equivalent in finite dimensional vector spaces. This is not true in infinite dimensional vector spaces.. In order to understand the concept of continuity in infinite dimensional vector spaces like $L^2\left(\mathbb{R}^N\right)$ which is one of the most fundamental Hilbert space in Quantum mechanics. We need to understand the idea of a *bounded operator* before we talk about continuity.

Definition II.2 (***Bounded Operator***)**.** Let $(V, \|.\|_V)$ be a normed space and $(W, \|.\|_W)$ be a Banach space. A linear operator $A : V \to W$ is called *bounded* if $\forall\, f \in V \setminus \{0\}$,

$$\sup_{f\in V} \frac{\|Af\|_W}{\|f\|_V} < \infty \tag{II.1}$$

another definition is,
If $\exists\, C \in \mathbb{R}$ with $\forall\, \boldsymbol{x} \in H$

$$\|A\boldsymbol{x}\|_W \leq C\, \|\boldsymbol{x}\|_V \tag{II.2}$$

Lemma II.1. *An operator $\mathcal{T} : A \to B$ is called **continuous** iff it is bounded.*

Definition II.3. We denote H' to be the set of continuous operators from $H \to \mathbb{C}$. Also, we denote $\mathcal{B}(H)$ to be the set of continuous operators from $H \to H$. Basically a map $\mathcal{T} \in H'$ is a continuous bounded map $T : H \to \mathbb{C}$. Also, a map $A \in \mathcal{B}(H)$ is a continuous bounded map $A : H \to H$.

Definition II.4 (***Unbounded operator***)**.** An operator which is not bounded is an unbounded operator.

The most frequently used in physics is the $L^2\left(\mathbb{R}^3\right)$ which is the space of square-integrable functions. The most important operators up-to a multiplicative constant are

1. The *position operat*or

$$\hat{\boldsymbol{x}} : L^2\left(\mathbb{R}^3\right) \to L^2\left(\mathbb{R}^3\right) \tag{II.3}$$

$$\hat{x}\psi \mapsto \boldsymbol{x}\psi \tag{II.4}$$

2. The momentum operator

$$\hat{\boldsymbol{p}} \boldsymbol{:} L^2\left(\mathbb{R}^3\right) \to L^2\left(\mathbb{R}^3\right) \tag{II.5}$$

$$\hat{\boldsymbol{p}}\psi \mapsto \frac{\hbar}{i}\nabla\psi \tag{II.6}$$

These operators are not well defined on the entire *Hilbert space* and even on the subspace where they are well defined, they are not bounded. As this paper focuses on the study of the momentum operator. The momentum operator is just the derivative operator with some finite multiplicative constant (we have an imaginary number so the concept of finite seems vague, what we mean is that the real and imaginary part of it is finite). The finite multiplicative constant will not matter if we have an unbounded operator. One can easily using basic analysis techniques prove that the derivative operator D is an unbounded operator. We know from basic real analysis that D is a *linear* operator.

Consider the following the derivative operator defined abstractly in the following way :

$$\begin{aligned} D : C^1_{\mathbb{C}}[0,1] &\to C^0_{\mathbb{C}}[0,1] \\ f &\mapsto f' \end{aligned} \tag{II.7}$$

We will now show that this operator is indeed unbounded. The momentum operator is defined on a subset of $C^1_{\mathbb{C}}$ with additional structure. If we prove that this operator is unbounded on such a big space, then we can later use this result claiming that the momentum operator is unbounded.

Proposition II.1. *The operator D defined in (II.7) is unbounded.*

Proof. Can be found in literature [Szekeres, Hall]. Not extremely necessary right now. ☐

III. SELF ADJOINT AND ESSENTIALLY SELF-ADJOINT OPERATORS

Definition III.1 (***Densely defined linear operator***)**.** A linear map or operator $\mathcal{T} : \mathcal{D}_{\mathcal{T}} \to \mathcal{H}$ is said to be **densely defined** if $\mathcal{D}_{\mathcal{T}}$ is a *dense set* in $\mathcal{H}$, i.e.

$$\forall \varepsilon > 0 : \forall \psi \in \mathcal{H} : \exists \varphi \in \mathcal{D}_{\mathcal{T}} : \|\varphi - \psi\| < \varepsilon \tag{III.1}$$

Remark III.1. Equivalently we can say, if $\overline{\mathcal{D}_{\mathcal{T}}} = \mathcal{H}$ then we have a densely defined operator. Essentially, $\forall \psi \in \mathcal{H} : \exists \{\varphi_n\}_{n\in\mathbb{N}} \in \mathcal{D}_{\mathcal{T}} : \{\varphi_n\} \longrightarrow_{n\to\infty} \psi$.

Definition III.2 (***Adjoint operator***)**.** Let $\mathcal{T} : \mathcal{D}_{\mathcal{T}} \to \mathcal{H}$ be a *densely* defined operator on $\mathcal{H}$. The **adjoint** of $\mathcal{T}$ is the operator $\mathcal{T}^* : \mathcal{D}_{\mathcal{T}^*} \to \mathcal{H}$ defined by $\mathcal{T}$ if

$\mathcal{D}_{\mathcal{T}^*} := \{\psi \in \mathcal{H} | \exists \eta \in \mathcal{H} : \forall \varphi \in \mathcal{D}_{\mathcal{T}} : \langle \psi \mid \mathcal{T}\varphi \rangle = \langle \eta \mid \varphi \rangle\}$ and $\mathcal{T}^*\psi := \eta$ is true.

Let us use the definition above to prove a trivial property of the *adjoint.*

Proposition III.1. *The adjoint operator $\mathcal{T}^* : \mathcal{D}_{\mathcal{T}^*} \to \mathcal{H}$ is well defined.*

Proof. Let $\psi \in \mathcal{H}$ and let $\eta, \tilde{\eta} \in \mathcal{H}$ be such that

$$\begin{gathered} \forall \varphi \in \mathcal{D}_{\mathcal{T}} \\ \langle \psi \mid \mathcal{T}\varphi \rangle = \langle \eta \mid \varphi \rangle \text{ and } \langle \psi \mid \mathcal{T}\varphi \rangle = \langle \tilde{\eta} \mid \varphi \rangle \end{gathered}$$

Then $\forall \varphi \in \mathcal{D}_{\mathcal{T}}$,

$$\begin{aligned} \langle \eta - \tilde{\eta} \mid \varphi \rangle &= \langle \eta \mid \varphi \rangle - \langle \tilde{\eta} \mid \varphi \rangle \\ &= \langle \psi \mid \mathcal{T}\varphi \rangle - \langle \psi \mid \mathcal{T}\varphi \rangle = 0 \qquad \text{(III.2)} \\ \langle \eta \mid \varphi \rangle &= \langle \tilde{\eta} \mid \varphi \rangle \\ \eta &= \tilde{\eta} \qquad \text{(III.3)} \end{aligned}$$

In the last step we use positive-definiteness. ☐

Definition III.3 (***Kernel and Range of a Linear operator***)**.** The definitions of *kernel and range* are the same that one knows from their elementary linear algebra course.

- $\ker(\mathcal{T}) := \{\varphi \in \mathcal{D}_{\mathcal{T}} | \mathcal{T}\varphi = 0\}$
- $\operatorname{ran}(\mathcal{T}) := \{\mathcal{T}\varphi | \varphi \in \mathcal{D}_{\mathcal{T}}\}$

The range is also known as the *image* and $\operatorname{im}(\mathcal{T})$ is an alternative notation.

Definition III.4 (***Invertible operator***)**.** An operator $\mathcal{T}$ is called **invertible** if,

$$\exists \text{ an operator } : \mathcal{O} \text{ such that } \mathcal{T} \circ \mathcal{O} = \mathrm{id}_{\mathcal{H}} \mathcal{O} \circ \mathcal{T} = \mathrm{id}_{\mathcal{D}_{\mathcal{T}}}$$

An operator is **invertible** iff

1. $\ker(\mathcal{T}) = \{0\}$
2. $\overline{\operatorname{ran}(\mathcal{T})} = \mathcal{H}$

Proposition III.2. *Let $\mathcal{T}$ be a densely defined operator. Then $\ker(\mathcal{T}^*) = ran(\mathcal{T})^{\perp}$.*

Proof. Let $\psi \in \ker(\mathcal{T}^*) \iff \mathcal{T}\psi = 0$, then

$$\forall \varphi \in \mathcal{D}_{\mathcal{T}} : \langle \psi \mid \mathcal{T}\varphi \rangle = \langle \mathcal{T}^*\psi \mid \varphi \rangle = 0 \Rightarrow \psi \in \operatorname{ran}(\mathcal{T})^{\perp}$$

☐

Definition III.5 (***Extension of an operator***)**.** Let $\mathcal{T}$ and $\widetilde{\mathcal{T}}$ be operators defined in the following way

$$\mathcal{T} : \mathcal{D}_{\mathcal{T}} \to \mathcal{H} \tag{III.4}$$

$$\widetilde{\mathcal{T}} : \mathcal{D}_{\widetilde{\mathcal{T}}} \to \mathcal{H} \tag{III.5}$$

We say that $\widetilde{\mathcal{T}}$ is an **extension** of $\mathcal{T}$ i.e. $\mathcal{T} \subseteq \widetilde{\mathcal{T}}$ if

1. $\mathcal{D}_{\mathcal{T}} \subseteq \mathcal{D}_{\widetilde{\mathcal{T}}}$
2. $\forall \varphi \in \mathcal{D}_{\mathcal{T}} \Rightarrow \mathcal{T}\varphi = \widetilde{\mathcal{T}}\varphi$

Proposition III.3. *Let $\mathcal{T}, \widetilde{\mathcal{T}}$ be densely defined operators. If $\mathcal{T} \subseteq \widetilde{\mathcal{T}}$ then $\widetilde{\mathcal{T}}^* \subseteq \mathcal{T}^*$*

Proof. Let $\psi \in \mathcal{D}_{\widetilde{\mathcal{T}}^*}$. Then $\exists \eta \in \mathcal{H}$ such that $\forall \beta \in \mathcal{D}_{\mathcal{T}}$: $\left\langle \psi | \widetilde{\mathcal{T}}\beta \right\rangle = \langle \eta | \beta \rangle$ where $\eta := \widetilde{\mathcal{T}}^*\psi$

In the above line we just redefined what we know. Now we will use some more facts to prove our proposition.

Particularly, as $\mathcal{T} \subseteq \widetilde{\mathcal{T}}$ we have $\mathcal{D}_{\mathcal{T}} \subseteq \mathcal{D}_{\widetilde{\mathcal{T}}}$ and then

$$\forall \alpha \in \mathcal{D}_{\mathcal{T}} \subseteq \mathcal{D}_{\widetilde{\mathcal{T}}} : \left\langle \psi | \widetilde{\mathcal{T}}\alpha \right\rangle = \langle \psi | \mathcal{T}\alpha \rangle = \langle \eta | \alpha \rangle \tag{III.6}$$

Therefore $\psi \in \mathcal{D}_{\mathcal{T}^*}$ and hence $\mathcal{D}_{\widetilde{\mathcal{T}}^*} \subseteq \mathcal{D}_{\mathcal{T}^*}$ ☐

A. Adjoint of a Symmetric operator

Definition III.6 (***Symmetric operator***)**.** A *densely defined operator* $\mathcal{T} : \mathcal{D}_{\mathcal{T}} \to \mathcal{H}$ is called **symmetric** if

$$\forall\, \alpha, \beta \in \mathcal{D}_{\mathcal{T}} \Rightarrow \langle \alpha | \mathcal{T} \beta \rangle$$

Remark III.2. Let us address the big elephant in the mathematical notions related to quantum mechanics. What are these *so called Hermitian operators and what do they have to do with symmetric or self-adjointness?* In a lot of Physics literature, these symmetric operators are referred to as *Hermitian operators.* However, many times the notion of *Hermitian* is associated with the notion of self-adjointness. Statements like *Observables in quantum mechanics correspond to Hermitian operators* are incorrect as *Hermitian* corresponds to symmetric operators and not self-adjointness. On the other hand, if one decides to use Hermitian as a synonym of self-adjoint, then it is not true that all symmetric operators are *Hermitian.* We can avoid this confusion by completely erasing the word Hermitian and instead just using *symmetric* and *self-adjoint* operator.

Lemma III.1. *If $\mathcal{T}$ is symmetric, then $\mathcal{T} \subseteq \mathcal{T}^*$.*

Proof. Let $\psi \in \mathcal{D}_{\mathcal{T}}$ and let $\eta \equiv \mathcal{T}\psi$. Then by symmetry we have

$$\forall\, \alpha \in \mathcal{D}_{\mathcal{T}} : \langle \psi | \mathcal{T} \alpha \rangle = \langle \mathcal{T} \psi | \alpha \rangle = \langle \eta | \alpha \rangle$$

This means $\psi \in \mathcal{D}_{\mathcal{T}^*}$. Hence, $\mathcal{D}_{\mathcal{T}} \subseteq \mathcal{D}_{\mathcal{T}^*}$ and $\mathcal{T}^*\psi \equiv \eta = \mathcal{T}\psi$. ☐

Definition III.7 (***Self adjoint operator***)**.** A *densely defined operator* $\mathcal{T} : \mathcal{D}_{\mathcal{T}} \to \mathcal{H}$ is called *self-adjoint* if $\mathcal{T} = \mathcal{T}^*$. We are comparing operators, so this means the following must be true if the equality must hold

1. $\mathcal{D}_{\mathcal{T}} = \mathcal{D}_{\mathcal{T}^*}$
2. $\forall\, \varphi \in \mathcal{D}_{\mathcal{T}} : \mathcal{T}\varphi = \mathcal{T}^*\varphi$

Corollary III.1. *A self-adjoint operator is maximal with respect to the self-adjoint extension.*

Proof. Let $\mathcal{T}, \widetilde{\mathcal{T}}$ be self-adjoint operators and suppose $\mathcal{T} \subseteq \widetilde{\mathcal{T}}$. Then we have

$$\mathcal{T} \subseteq \widetilde{\mathcal{T}} = \widetilde{\mathcal{T}}^* \subseteq \mathcal{T}^* = \mathcal{T}$$

and hence $\widetilde{\mathcal{T}} = \mathcal{T}$. ☐

Remark III.3. As a fact, self-adjoint operators are maximal even with respect to symmetric extension. The difference will be $\widetilde{\mathcal{T}} \subseteq \widetilde{\mathcal{T}}^*$ instead of $\widetilde{\mathcal{T}} \subseteq \widetilde{\mathcal{T}}^*$.

B. Closability, closure, closedness of an operator

Definition III.8 (***Closable operator***)**.** A *densely defined operator* $\mathcal{T}$ is called **closeable** if it's *adjoint* $\mathcal{T}^*$ is also *densely defined*

Definition III.9 (***Closure of an operator***)**.** The **closure** of a *closable operator* $\mathcal{T}$ is

$$\overline{\mathcal{T}} \equiv \mathcal{T}^{**} = (\mathcal{T}^*)^*$$

where the *over-line* denotes closure.

Definition III.10 (***Closed operator***)**.** An *operator* $\mathcal{T}$ is called **closed** if

$$\mathcal{T} = \overline{\mathcal{T}}$$

Proposition III.4. *A symmetric operator is necessarily closable.*

Proof. Let $\mathcal{T}$ be a symmetric operator. Then, $\mathcal{T} \subseteq \mathcal{T}^*$ and $\mathcal{D}_{\mathcal{T}} \subseteq \mathcal{D}_{\mathcal{T}^*}$. Symmetric operators by definition are densely defined. Hence

$$\mathcal{H} = \overline{\mathcal{D}_{\mathcal{T}}} \subseteq \overline{\mathcal{D}_{\mathcal{T}^*}} \subseteq \mathcal{H}$$

which concludes the fact that the adjoint of a symmetric operator is also densely defined. Hence, $\mathcal{T}$ is **closable** if it is symmetric. ☐

C. Essentially Self Adjoint operators

Definition III.11 (***Essentially self-adjoint operator***)**.** A *symmetric* operator $\mathcal{T}$ is called **essentially self-adjoint** if $\overline{\mathcal{T}}$ is self-adjoint.

Remark III.4. The condition for *essentially-self adjointness* is a weaker condition than self-adjointness i.e if an operator is self-adjoint it is implied that it is also essentially self adjoint. The other way is not true in general.

Proof. $\mathcal{T} = \mathcal{T}^* \Rightarrow \mathcal{T}^* = \mathcal{T}^{**} \Rightarrow \mathcal{T}^{**} = \mathcal{T}^{***} \Rightarrow \overline{\mathcal{T}} = \overline{\mathcal{T}}^*$ ☐

Theorem III.1. *If $\mathcal{T}$ is essentially self-adjoint, then there exists a unique self-adjoint extension of $\mathcal{T}$, namely $\overline{\mathcal{T}}$.*

Proof. This theorem is the essence of essentially self-adjoint operators. So we will go through the proof here, ☐

1. $\mathcal{T}$ is symmetric $\Rightarrow$ $\mathcal{T}$ is closable $\Rightarrow$ $\overline{\mathcal{T}}$ exists
2. $\mathcal{T} \subseteq \overline{\mathcal{T}} = \mathcal{T}^{**}$ is known. Hence, $\overline{\mathcal{T}}$ is an extension of $\mathcal{T}$.
3. The only thing that remains to be shown is that $\overline{\mathcal{T}}$ is the *unique* self-adjoint extension.

IV. CASE STUDY OF THE MOMENTUM OPERATOR

In this section we will exclusively talk about the momentum operator in quantum mechanics in the language we built in the previous sections. Let us define the momentum operator precisely.

Definition IV.1 (***Momentum operator***)**.** The momentum operator on the j'th coordinate (in the operator language described above) is defined as follows

$$\hat{\mathcal{P}}_j : \mathcal{D}_{\mathcal{P}} \to L^2(\mathbb{R}) \tag{IV.1}$$
$$\psi \mapsto -i\hbar\partial_j\psi \tag{IV.2}$$
$$\psi \mapsto -i\psi' \tag{IV.3}$$

We will use the last equation from above indefinite times. We use $\hbar = 1$.

Remark IV.1. This is one of the most commonly found definition of the momentum operator in quantum mechanics. In the previous sections whenever we are talking about operators which are self-adjoint or have some other property, we have assumed them to be densely defined. If an operator needs to be explicitly defined, along with the map we also need to define it's domain. This is something that is always exclusively skipped in most of the quantum mechanics texts.

A. Absolutely continuous functions and Sobolev spaces

In some of the calculations in this section we will be needing a few more definitions. Let us take a moment to define them before proceeding. More precisely we will be needing the following relation between *Continuous functions* $\mathcal{C}^1$*, absolutely continuous functions* $\mathcal{AC}$ *and Sobolev spaces* $\mathscr{H}^1$

$$\mathcal{C}^1([a,b]) \subseteq \mathscr{H}^1([a,b]) \subseteq \mathcal{AC}([a,b]) \tag{IV.4}$$

Definition IV.2 (***Absolutely continuous spaces*** ($\mathcal{AC}$))**.** Let us define a function $\psi : [a,b] \to \mathbb{C}$. ψ is *absolutely continuous i.e.* $\psi \in \mathcal{AC}$ *if* $\exists\, \rho \in [a,b] \to \mathbb{C}$ *integrable* (Lebesgue integrable) such that

$$\psi(x) = \psi(a) + \int_a^x \rho(y)\, y$$

where ρ is the derivative of ψ almost everywhere (a.e), i.e $\rho =_{\text{a.e}} \psi'$.

$$\mathcal{AC}([a,b]) \equiv \left\{\psi \in L^2(\mathbb{R}) \mid \psi \text{ is absolutely continuous}\right\} \tag{IV.5}$$

Definition IV.3 (***Sobolev space***)**.** The Sobolev space is defined by the following set

$$\mathscr{H}([a,b]) \equiv \left\{\psi \in \mathcal{AC}([a,b]) \mid \psi' \in L^2(\mathbb{R})\right\} \tag{IV.6}$$

Momentum operator on a Compact interval v/s on a Circle

In this section we will try defining our momentum operator precisely on a compact interval and on a circle. We do this so we can analyze the properties of this operator by looking at spaces that are one dimensional but not $\mathbb{R}$ itself. In both the cases we will define our Hilbert space to be $\mathcal{H} \equiv L^2([0,2\pi])$.

Let us try to define *reasonable* domains for the momentum operators on both these intervals by eyeballing the situation:

- On a *compact interval*

$$\mathcal{D}_{\mathcal{P}} \equiv \left\{\psi \in \mathcal{C}^1([0,2\pi]) \mid \psi(0) = 0 = \psi(2\pi)\right\} \tag{IV.7}$$

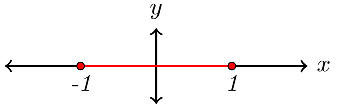

Figure IV.1. Compact interval from $x = -1$ to $x = 1$

- On a *circle*

$$\mathcal{D}_{\mathcal{P}} \equiv \left\{\psi \in \mathcal{C}^1([0,2\pi]) \mid \psi(0) = \psi(2\pi)\right\} \tag{IV.8}$$

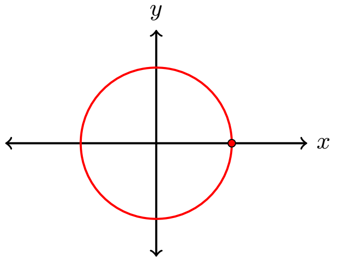

Figure IV.2. Unit circle

These look like reasonable guesses but we need to actually check if the $\hat{\mathcal{P}}_j$ defined on these domains are self-adjoint or not (It turns out that neither of them are self-adjoint). This is the main goal of this review paper - *understanding the procedure of formulating a momentum operator on some Hilbert space.*

B. Momentum operator on a *Compact interval*

We consider the interval $\mathcal{I} = [0,2\pi]$ with the operator defined as follows (we will take $\hbar = 1$ i.e. use Planck units for convenience). Let us rewrite the momentum operator

$$\hat{\mathcal{P}}_j : \mathcal{D}_{\mathcal{P}} \to L^2\left([0, 2\pi]\right) \tag{IV.9}$$

$$\psi \mapsto -i\psi' \tag{IV.10}$$

$$\psi' = \frac{\partial \psi}{\partial x_j} \tag{IV.11}$$

The main goal of this part is to check if $\hat{\mathcal{P}}_j$ defined as above is self adjoint with respect to our domain $\mathcal{I}$. Let us do this one step at a time and formulate an algorithm to do this eventually :

1. *Step I : Is $\hat{\mathcal{P}}_j$ symmetric?*

We need to check if our operator is symmetric because it is a necessary condition for self-adjointness. We check if the operator is self-adjoint by checking if, $\forall\, \psi, \varphi \in \mathcal{D}_{\mathcal{P}}$

$$\left\langle \psi | \hat{\mathcal{P}}_j \varphi \right\rangle = \left\langle \hat{\mathcal{P}}_j \psi | \varphi \right\rangle \tag{IV.12}$$

Let us explicitly compute this to check. We will be using integration by parts $\left(\int u\, dv = uv - \int v\, du\right)$ which is a common technique for such computations.

$$\begin{aligned} -i \int_0^{2\pi} dx_j\, \overline{\psi\left(x_j\right)}\, \varphi'\left(x_j\right) &= \int_0^{2\pi} dx_j \overline{\left(-i\right) \psi'\left(x_j\right)}\, \varphi\left(x_j\right) \\ &= i \int_0^{2\pi} dx_j \overline{\psi'\left(x_j\right)}\, \varphi\left(x_j\right) \\ &= i[\left(\overline{\psi\left(x_j\right)} \varphi\left(x_j\right)\right) \Big|_0^{2\pi} \\ &\quad - \int_0^{2\pi} dx_j\, \varphi'\left(x_j\right) \overline{\psi\left(x_j\right)}] \end{aligned} \tag{IV.13}$$

We need to be careful with the boundary term. We know that $\psi, \varphi \in \mathcal{D}_{\mathcal{P}}$ and hence $\psi\left(0\right) = \varphi\left(0\right) = \psi\left(2\pi\right) = \varphi\left(2\pi\right) = 0$. Using this in the above condition we get the following

$$\begin{aligned} \left\langle \psi | \hat{\mathcal{P}}_j \varphi \right\rangle &= 0 - i \int_0^{2\pi} \varphi'\left(x_j\right) \overline{\psi\left(x_j\right)}\, dx_j \\ &= \left\langle \hat{\mathcal{P}}_j \psi | \varphi \right\rangle \end{aligned} \tag{IV.14}$$

Hence, proving that $\hat{\mathcal{P}}_j$ is symmetric indeed.

2. *Step II : Is $\hat{\mathcal{P}}_j$ self adjoint?*

To check this, we need to calculate the adjoint of $\hat{\mathcal{P}}_j$ and see if it coincides with the original operator. As we recall, when we are comparing the equality between two *operators* we need to make sure that their domains match along with their actions on the elements of these domains.

Let us start with something that we know - $\hat{\mathcal{P}}_j$ is symmetric and by using lemma(III.1), we can say

$$\hat{\mathcal{P}}_j \subseteq \hat{\mathcal{P}}_j^* \to \hat{\mathcal{P}}_j^* \text{ is an extension of } \hat{\mathcal{P}}_j$$

Let $\psi \in \mathcal{D}_{\mathcal{P}^*}$ then we have to show that

$$\exists\, \eta \in L^2\left(R\right) : \forall\, \varphi \in \mathcal{D}_{\mathcal{P}} : \left\langle \psi | \hat{\mathcal{P}}_j \varphi \right\rangle = \left\langle \eta | \varphi \right\rangle \tag{IV.15}$$

The above condition is equivalent to showing

$$\int_0^{2\pi} dx_j\, \overline{\psi\left(x_j\right)} \left(-i\right) \varphi'\left(x_j\right) = \int_0^{2\pi} dx_j\, \overline{\eta\left(x_j\right)} \varphi\left(x_j\right) \tag{IV.16}$$

With a loose argument we can always find a function $N : [a, b] \to \mathbb{C}$ such that $\eta =_{\text{ae}} N'$. Using this we will rewrite the above equation as

$$\begin{aligned} \int_0^{2\pi} dx_j\, \overline{\psi\left(x_j\right)} \left(-i\right) \varphi'\left(x_j\right) &= \int_0^{2\pi} \overline{\eta\left(x_j\right)} \varphi\left(x_j\right) \\ &= \int_0^{2\pi} dx_j\, \overline{N'\left(x_j\right)} \varphi\left(x_j\right) \end{aligned}$$

$$\begin{aligned} \int_0^{2\pi} dx_j \left(\overline{\psi\left(x_j\right)} \left(-i\right) \varphi'\left(x_j\right)\right) &= -\int_0^{2\pi} \overline{N'\left(x\right)} \varphi'\left(x_j\right) dx_j \\ &\quad + \left[\overline{N\left(x_j\right)} \varphi\left(x_j\right)\right] \Big|_0^{2\pi} \end{aligned}$$

$$\int_0^{2\pi} dx_j \left[\overline{\psi\left(x_j\right)} \left(-i\right) \varphi'\left(x_j\right) + \overline{N'\left(x\right)} \varphi'\left(x_j\right)\right] = 0 \tag{IV.17}$$

$$-i \int_0^{2\pi} \left(\varphi'\left(x_j\right) \overline{\left(\psi\left(x_j\right) - iN\left(x_j\right)\right)}\right) dx_j = 0 \tag{IV.18}$$

$$\left\langle \psi\left(x_j\right) - iN\left(x_j\right) | \varphi'\left(x_j\right) \right\rangle = 0 \tag{IV.19}$$

From this last statement we can conclude that $\psi\left(x_j\right) - iN\left(x_j\right) \in \left\{\varphi' | \varphi \in \mathcal{D}_{\mathcal{P}}\right\}^{\perp}$ where $\perp$ means the orthogonal complement.

We can make two observations at this point :

1.

$$\left\{\varphi'\left(x_j\right) \mid \varphi \in \mathcal{D}_{\mathcal{P}}\right\} = \left\{\xi \in \mathcal{C}^0\left(\mathcal{I}\right) \mid \int_0^{2\pi} \xi\left(x_j\right) dx_j = 0\right\}$$

Proof. We will prove equality of the sets by proving LHS $\subseteq$ RHS and LHS $\supseteq$ RHS simultaneously :

$(\subseteq)$

Let $\varphi' \in \left\{\varphi'\left(x_j\right) \mid \varphi \in \mathcal{D}_{\mathcal{P}}\right\}$. Let $\varphi' = \xi$,

$$\begin{aligned} \int_0^{2\pi} \xi\, dx_j &= \int_0^{2\pi} \varphi'\, dx_j = \left[\varphi'\left(x_j\right)\right]\Big|_0^{2\pi} = 0 \\ &\Rightarrow \varphi'\left(x_j\right) \in \left\{\xi \in \mathcal{C}^0\left(\mathcal{I}\right) \mid \int_0^{2\pi} \xi\left(x_j\right) dx_j = 0\right\} \end{aligned}$$

$(\supseteq)$

Let $\xi \in \left\{\xi \in \mathcal{C}^0(\mathcal{I}) \mid \int_0^{2\pi} \xi(x_j)\, dx_j = 0\right\}$. This implies

$$\begin{aligned} \varphi_\xi(x_j) = \int_0^{\pi} \xi(y)\, dy &\Rightarrow \varphi_\xi \in \mathcal{C}^1 \\ &\Rightarrow \varphi_\xi(0) = 0 = \varphi_\xi(2\pi) \\ &\Rightarrow \varphi_\xi \in \{\varphi'(x_j) \mid \varphi \in \mathcal{D}_{\mathcal{P}}\} \end{aligned}$$

Together with $(\subseteq)$ and $(\supseteq)$ we can conclude the proof. □

2. $\overline{\{\varphi'(x_j) | \varphi(x_j) \in \mathcal{D}_{\mathcal{P}}\}} = \{1\}^{\perp}$ where 1 is the constant function.

Proof. We can write

$$\int_0^{2\pi} \xi(x)\, dx = 0 \Rightarrow \langle 1|\xi\rangle = 0$$

Using this and the proof from above we can effectively say

$$\left\{\xi \in \overline{\mathcal{C}^0(\mathcal{I})} \mid \langle 1|\xi\rangle = 0\right\} = \{1\}^{\perp}$$

□

We can now proceed the following way

$$\begin{aligned} \psi - iN \in \{\varphi'(x_j) \mid \varphi \in \mathcal{D}_{\mathcal{P}}\}^{\perp} &= \overline{\{\varphi'(x_j) \mid \varphi \in \mathcal{D}_{\mathcal{P}}\}^{\perp}} \\ \hookrightarrow \left(\{\varphi'(x_j) \mid \varphi \in \mathcal{D}_{\mathcal{P}}\}^{\perp}\right)^{\perp\perp} &= \left(\{\varphi'(x_j) \mid \varphi \in \mathcal{D}_{\mathcal{P}}\}^{\perp\perp}\right)^{\perp} \\ \hookrightarrow \overline{\{\varphi'(x_j) \mid \varphi \in \mathcal{D}_{\mathcal{P}}\}}^{\perp} &= \left(\{1\}^{\perp}\right)^{\perp} = \{1\}^{\perp\perp} \\ \hookrightarrow \overline{\{1\}} &= \{C : [a,b] \to \mathbb{C} \\ &\quad \mid x \mapsto \text{Constant}\} \end{aligned}$$

Hence we say $\psi(x_j) - iN(x_j) = \text{Constant} \Rightarrow \psi(x_j) = \text{Constant} + iN(x_j)$ and we use the fact that $N(x_j) \in \mathcal{AC}$ to say

$$\psi(x_j) \in \mathcal{AC}$$

Thus, $\psi \in \mathcal{D}_{\mathcal{P}^*} \Rightarrow \psi(x_j) \in \mathcal{AC}(\mathcal{I}) \Rightarrow \mathcal{D}_{\mathcal{P}^*} \subseteq \mathcal{AC}(\mathcal{I})$

What we need is $\hat{\mathcal{P}}_j^* : \mathcal{D}_{\mathcal{P}^*} \to L^2(\mathbb{R})$ which requires $-i\psi'(x_j) \in L^2(\mathbb{R})$

$$\begin{aligned} \psi(x_j) &\in \mathscr{H}^1(\mathcal{I}) \\ \Rightarrow \mathcal{D}_{\mathcal{P}^*} &\subseteq \mathscr{H}^1(\mathcal{I}) \end{aligned}$$

So, as expected we get

$$\begin{aligned} \hat{\mathcal{P}}_j &\subseteq \hat{\mathcal{P}}_j^* \\ \Rightarrow \mathcal{D}_{\mathcal{P}} &\subseteq \mathcal{D}_{\mathcal{P}^*} \end{aligned}$$

$\hat{\mathcal{P}}_j$ was defined on $\mathcal{C}^1$ with boundary conditions and $\hat{\mathcal{P}}_j^*$ was defined on $\mathscr{H}^1$

$$\Rightarrow \hat{\mathcal{P}}_j \subsetneq \hat{\mathcal{P}}_j^*$$

Hence, $\hat{\mathcal{P}}_j$ is not self adjoint. This *problem* can goes further ahead and can be dealt with the notion of Essentially self adjointness.

So, we showed that $\hat{\mathcal{P}}_j$ is not self-adjoint. It could be *essentially self-adjoint?* We recall that essentially self-adjoint means the *closure (double adjoint)* of $\hat{\mathcal{P}}_j$ is self-adjoint. If we could prove this then it works in our favor, Why? Because we have theorem saying, If the closure is self-adjoint, then the closure is the unique self-adjoint extension. In this case, we just take the closure instead of the original operator and we will have a self-adjoint operator.

3. Step III: Calculate the closure $\hat{\mathcal{P}_j^{**}}$ of $\hat{\mathcal{P}}_j$

We know that $\hat{\mathcal{P}}_j$ is symmetric and from one of the theorem we proved earlier : $\hat{\mathcal{P}}_j \subseteq \hat{\mathcal{P}_j^{**}} \subseteq \hat{\mathcal{P}_j^{*}}$. We also know from previous section that $\hat{\mathcal{P}_j^{**}}$ is also symmetric.

Let $\psi \in \mathcal{D}_{\mathcal{P}^{**}}$ then $\forall\ \varphi \in \mathcal{D}_{\mathcal{P}^*}$: $\left\langle \psi | \hat{\mathcal{P}}_j \varphi \right\rangle = \left\langle \hat{\mathcal{P}_j^{**}} \psi | \varphi \right\rangle$.

Now we use a standard trick from the book using the fact : $\hat{\mathcal{P}_j^{**}} \subseteq \hat{\mathcal{P}}_j$ which means $\mathcal{D}_{\mathcal{P}^{**}} \subseteq \mathcal{D}_{\mathcal{P}^*}$ and $\hat{\mathcal{P}_j^{**}}\psi = \hat{\mathcal{P}}_j^*\psi$. The above two lines give us the equality

$$\left\langle \psi | \hat{\mathcal{P}}_j \varphi \right\rangle = \left\langle \hat{\mathcal{P}_j^{**}} \psi | \varphi \right\rangle = \left\langle \hat{\mathcal{P}}_j^* \psi | \varphi \right\rangle \tag{IV.20}$$

Thus, $\forall\, \psi \in \mathcal{D}_{\mathcal{P}^{**}}$ and $\forall\, \varphi \in \mathcal{D}_{\mathcal{P}^*}$ we have

$$\begin{aligned} \left\langle \psi | \hat{\mathcal{P}}_j^* \varphi \right\rangle &= \int_0^{2\pi} \overline{\psi(x)}\, (-i)\, \varphi'(x)\, dx \\ \left\langle \hat{\mathcal{P}}_j^* \psi | \varphi \right\rangle &= \int_0^{2\pi} \overline{(-i)\psi'(x)}\varphi(x)\, dx \end{aligned}$$

The left hand side of both the equations are the same and hence we get

$$\begin{aligned} \int_0^{2\pi} \overline{\psi(x)}\, (-i)\, \varphi'(x)\, dx &= i \int_0^{2\pi} \overline{\psi(x)}\varphi(x)\, dx \\ -i \int_0^{2\pi} \overline{\psi(x)}\varphi'(x)\, dx &= i \left[\overline{\psi(x)}\varphi(x)|_0^{2\pi} - \int_0^{2\pi} \overline{\psi(x)}\varphi'(x)\, dx \right] \\ 0 &= i \left[\overline{\psi(x)}\varphi(x) \right]_0^{2\pi} \\ 0 &= \overline{\psi(2\pi)}\varphi(2\pi) - \overline{\psi(0)}\varphi(0) \end{aligned}$$

We know nothing about φ at the endpoints 0 and 2π as $\varphi \in \mathscr{H}^1(I)$ (Sobolev space). Hence, $\overline{\psi(2\pi)} = \overline{\psi(0)} = 0$ in order to satisfy the equation above. This condition precisely means that $\psi \in \mathcal{D}_{\mathcal{P}^{**}}$. This gives is

$$\begin{aligned} \psi &\in \{\theta \in \mathcal{D}_{\mathcal{P}^*} | \psi(2\pi) = 0 = \psi(0)\} \\ &= \left\{\theta \in \mathscr{H}^1(I) | \psi(2\pi) = 0 = \psi(0)\right\} \end{aligned}$$

Hence, we can conclude that

$$\mathcal{D}_{\mathcal{P}^{**}} = \left\{\theta \in \mathscr{H}^1(I) | \psi(2\pi) = 0 = \psi(0)\right\}$$

At this point if one summarizes the definitions of the operators $\hat{\mathcal{P}}_j, \hat{\mathcal{P}}_j^*, \hat{\mathcal{P}}_j^{**}$ (don't forget their domain) one will believe that $\hat{\mathcal{P}}_j$ is neither self-adjoint nor essentially self-adjoint. This in particular is not good as this means one cannot compute a meaningful momentum operator on an interval. This problem is solved by calculating the defect indices of the operators and is beyond the scope of this paper. In the next example, this problem does not arise and a much more meaningful result is concluded quite early.

C. Momentum operator on a *Circle*

Let us begin by first stating our operator and domain like always.

$$\begin{aligned} \hat{\mathcal{P}}_j &: \mathcal{D}_{\mathcal{P}} \to L^2(I) \\ &: \psi \mapsto (-i)\,\psi' \\ \mathcal{D}_{\mathcal{P}} &\equiv \left\{\psi \in \mathcal{C}^1 | \psi(0) = \psi(2\pi)\right\} \end{aligned}$$

We can note that $\left(\hat{\mathcal{P}}_j\right)_{\text{Interval}} \subsetneq \left(\hat{\mathcal{P}}_j\right)_{\text{Circle}}$ as $\psi(2\pi) = 0 = \psi(0)$ is a stronger condition than $\psi(2\pi) = \psi(0)$. Hence we say momentum on the circle is an extension of the momentum operator on a interval. In this section whenever we write $\hat{\mathcal{P}}_j$ without specifying whether it is on the circle or interval, we will assume that it is $\left(\hat{\mathcal{P}}_j\right)_{\text{Circle}}$. Same applies to similar notations like $\hat{\mathcal{P}}_j^*, \mathcal{D}_{\mathcal{P}}$,etc.

1. *Step I : Is $\hat{\mathcal{P}}_j$ symmetric?*

We won't go through the calculations again. Using the algorithm from momentum on an interval one can effectively check that this is true. One of the major differences being that $[\psi\varphi]_0^{2\pi} = 0$ because of different boundary conditions.

2. *Step II : Calculate the adjoint $\hat{\mathcal{P}}_j^*$*

We will use the fact $\left(\hat{\mathcal{P}}_j\right)_{\text{Interval}} \subsetneq \left(\hat{\mathcal{P}}_j\right)_{\text{Circle}}$. As $\hat{\mathcal{P}}_j$ is symmetric we can conclude $\hat{\mathcal{P}}_j \subseteq \hat{\mathcal{P}}_j^*$ and $\left(\hat{\mathcal{P}}_j^*\right)_{\text{Circle}} \subsetneq \left(\hat{\mathcal{P}}_j^*\right)_{\text{Interval}}$. Using these two facts we can write the following

$$(\mathcal{D}_{\mathcal{P}^*})_{\text{Circle}} \subseteq (\mathcal{D}_{\mathcal{P}^*})_{\text{Interval}} = \mathscr{H}^1(I) \qquad \text{(IV.21)}$$

Hence, we already know that $\mathcal{D}_{\mathcal{P}^*}$ lies in the $\mathscr{H}$ space. We proceed like we did in the previous example.

Let $\psi \in \mathcal{D}_{\mathcal{P}^*} \Rightarrow \forall\, \varphi \in \mathcal{D}_{\mathcal{P}} : \left\langle \psi | \hat{\mathcal{P}}_j \varphi \right\rangle = \left\langle \hat{\mathcal{P}}_j^* \psi | \varphi \right\rangle$. We already know that $\left(\hat{\mathcal{P}}_j^*\right)_{\text{Interval}}$ is an extension of the $\left(\hat{\mathcal{P}}_j^*\right)_{\text{Circle}}$ operator. Hence, we can replace $\hat{\mathcal{P}}_j^* \psi$ by $\left(\hat{\mathcal{P}}_j^*\right)_{\text{Interval}} \psi$ as we already know the properties of $\left(\hat{\mathcal{P}}_j^*\right)_{\text{Interval}}$.

$$\begin{aligned} \int_0^{2\pi} dx\, \overline{\psi(x)}\,(-i)\,\varphi'(x) &= \int dx\, \overline{(-i)\,\psi'(x)}\varphi(x) \\ &\vdots \\ 0 &= i\left[\overline{\psi(x)}\varphi(x)\right]_0^{2\pi} \end{aligned}$$

We do not know anything about the boundaries for $\varphi(x)$ or $\psi(x)$. Let us expand the above equation and see if we can reach somewhere

$$\begin{aligned} i\,\varphi(0)\left[\psi(2\pi) - \psi(0)\right] &= 0 \\ \Rightarrow \psi(2\pi) &= \psi(0) \end{aligned}$$

Which gives is the domain,

$$\mathcal{D}_{\mathcal{P}^*} = \left\{\psi \in \mathscr{H}^1(I) | \psi(2\pi) = \psi(0)\right\} \qquad \text{(IV.22)}$$

So now we see that the $\mathcal{D}_{\mathcal{P}^*}$ for $\hat{\mathcal{P}}_j^*$ on a circle is not just $\mathscr{H}^1$ but $\mathscr{H}^1$ with some boundary condition. As we see, every case is unique enough to work out this everytime. So our intermediate result for the operator is

$$\begin{aligned} \hat{\mathcal{P}}_j^* &: \left\{\mathscr{H}^1(I) | \psi(2\pi) = \psi(0) \to L^2(I)\right\} \\ &\psi \mapsto (-i)\,\psi' \end{aligned}$$

3. *Step III : Is $\hat{\mathcal{P}}_j$ self adjoint?*

Let us recall the following things :

1. $\mathcal{C}^1 \subsetneq \mathscr{H}^1$
2. These two equations

$$\begin{aligned} \mathcal{D}_{\mathcal{P}^*} &= \left\{\psi \in \mathscr{H}^1(I) | \psi(2\pi) = \psi(0)\right\} \\ \mathcal{D}_{\mathcal{P}} &= \left\{\psi \in \mathcal{C}^1 | \psi(2\pi) = \psi(0)\right\} \end{aligned}$$

Using these two facts we can effectively conclude, $\hat{\mathcal{P}}_j \subseteq \hat{\mathcal{P}}_j^* \Rightarrow \hat{\mathcal{P}}_j$ is **not** self-adjoint! Is it *essentially self adjoint?*

4. *Step IV : Is $\hat{\mathcal{P}}_j$ essentially self adjoint?*

We need to check $\hat{\mathcal{P}}_j^{**} = \hat{\mathcal{P}}_j^{***}$. To check that, we need to calculate the *closure.*

We know that $\hat{\mathcal{P}}_j$ is symmetric which gives us $\hat{\mathcal{P}}_j \subseteq \hat{\mathcal{P}}_j^{**} \subseteq \hat{\mathcal{P}}_j^*$. In this relation we know that $\mathcal{P} \in \mathcal{C}^1_{\text{Circle}}$ and $\mathcal{P} \in \mathscr{H}^1_{\text{Circle}}$.

Let $\psi \in \mathcal{D}_{\mathcal{P}^{**}}$, then $\forall \varphi \in \mathcal{D}_{\mathcal{P}^{*}}$: $\left\langle \psi | \hat{\mathcal{P}}_j^{*} \varphi \right\rangle = \left\langle \hat{\mathcal{P}}_j^{**} \psi | \varphi \right\rangle$. From the previous line we can say $\hat{\mathcal{P}}_j^{**}\psi = \hat{\mathcal{P}}_j^{*}\psi$ as $\hat{\mathcal{P}}_j^{**} \subseteq \hat{\mathcal{P}}_j^{*}$. So now we have

$$\begin{gathered}\left\langle \psi|\hat{\mathcal{P}}_j^{*}\varphi\right\rangle = \left\langle \hat{\mathcal{P}}_j^{*}\psi|\varphi\right\rangle \\ \vdots \\ 0 = i[\overline{\psi\left(x\right)}\varphi\left(x\right)]_0^{2\pi}\end{gathered}$$

We know $\varphi\left(2\pi\right) = \varphi\left(0\right)$ because $\varphi \in \mathcal{D}_{\mathcal{P}^{*}}$. So we get

$$0 = i\varphi\left(0\right)\left[\overline{\psi\left(2\pi\right)} - \overline{\psi\left(0\right)}\right]$$

This means $\psi\left(2\pi\right) = \psi\left(0\right)$. This conclusively means $\mathcal{D}_{\mathcal{P}^{**}} = \mathscr{H}^1 = \mathcal{D}_{\mathcal{P}^{*}} \Rightarrow \hat{\mathcal{P}}_j^{**} = \hat{\mathcal{P}}_j^{*}$. Hence, we have shown that it is essentially self-adjoint.

5. *Step V : Replace by the closure.*

We succeeded in constructing the unique momentum operator on a circle by taking the closure $\hat{\mathcal{P}}_j^{**}$ of our initial guess $\hat{\mathcal{P}}_j : \mathscr{H}^1\left(I\right) \to L^2\left(I\right)$ where $\forall \psi \in \mathscr{H}^1 : \psi \mapsto \left(-i\right)\psi'$.

V. CONCLUSION

The goal of this review paper was to show that defining operators in quantum mechanics mathematically precisely is not a trivial task. One needs to define the domain, check if it is self-adjoint, if it is not then check if it is essentially-self adjoint at least. We still did not discuss why we take the momentum operator as $\hat{\mathcal{P}}_j\psi \mapsto -i\psi'$. This is the goal of something known as the Stone-von Neumann theorem. After understand this review paper, a starting point would be to understand the Stone von-Neumann theorem which helps us construct observables like the momentum operator by taking analogues from Classical mechanics. Analogues like the Poisson bracket which in Quantum mechanics are *replaced* by commutator brackets, this is known as the quantization prescription.

[Schuller] *Lectures on Quantum theory, Fredric Schuller, University of Erlangen-Nuremberg*
Lecture 6 to 9 : `https://www.youtube.com/playlist?list=PLPH7f_7ZlzxQVx5jRjbfRGEzWY_upS5K6`

[Hall] *Quantum theory for Mathematicians, Brian C.Hall, Springer 2013*
Various topics from Chapter 7 to 10.
II.1

[R&S] *Methods of modern mathematical physics: Volume 1 - Functional Analysis, Michael Reed and Barry Simon, Academic Press 1980*
Various topics from chapter VI to VIII.

[QM Leipzig] Notes taken during the course 12-PHY-BIPTP4: Theoretical Physics IV - Quantum Mechanics at University of Leipzig, 2017. (Unpublished)

[Szekeres] *A course in Modern Mathematical Physics : Groups, Hilbert Space and Differential Geometry, Peter Szekeres, Cambridge University Press 2004.* (Chapter 13,14) (Recommended background reading).
I, II.1

[Background read] Link to transcript of a 10 page talk that might be sufficient as a quick background read. (Password : 806x)
`http://rohankulkarni.me/sdm_downloads/functional-analysis0-for-qm/`

Charge Quantization, Dirac String and Wu-Yang Monopole

Mert Kurttutan

(Dated: June 19, 2019)

Magnetic monopoles are particles that carry magnetic charge. They were proposed because of two reasons: Symmetry between electric and magnetic field, and quantization of electrical charge. The first example of magnetic monopole was proposed by Pauli M. Dirac, namely Dirac string. I will first discuss how Dirac string leads to charge quantization and properties of it. To better understand it, I will look at some interactions between an electron and a magnetic monopole in classical physics. However, Dirac string requires singularities in the vector potential $\mathbf{A}$. One monopole that doesn't require was proposed by Wu and Yang. I will derive charge quantization using gauge invariance and study topological properties of it.

I. INTRODUCTION

The idea of magnetic monopole can be motivated by the dual symmetry of classical electrodynamics. If we have a magnetic charge ρ_m, Maxwell's Equations become,

$$\nabla \cdot \mathbf{E} = 4\pi\rho_e, \nabla \cdot \mathbf{B} = 4\pi\rho_m$$

$$\nabla \times \mathbf{E} = -\frac{4\pi}{c}\mathbf{J}_m - \frac{1}{c}\frac{\partial \mathbf{B}}{\partial t}, \nabla \times \mathbf{B} = \frac{4\pi}{c}\mathbf{J}_e + \frac{1}{c}\frac{\partial \mathbf{E}}{\partial t}$$

where $\mathbf{J_m}$ and ρ_m are corresponding magnetic current and charge, respectively. Due to existence of magnetic charge, Maxwell's equations is invariant under transformation

$$\{\mathbf{E}, \rho_e, \mathbf{J}_e\} \rightarrow \{\mathbf{B}, \rho_m, \mathbf{J}_m\}$$

$$\{\mathbf{B}, \rho_m, \mathbf{J}_m\} \rightarrow \{-\mathbf{E}, -\rho_e, -\mathbf{J}_e\}$$

Another important reason why this idea is appealing to physicists is regarding charge quantization. The quantization of the quantities such as energy levels in atoms and spin of an electron was explained by quantum mechanics. However, physicist couldn't explain one of the fundamental quantization in nature, namely the quantization of electrical charge. But, one can demonstrate Dirac Quantization condition by requiring the existence of magnetic charges. In section II, I will list some of the important concepts of electromagnetism in quantum mechanics. In section III, I will explain one model of magnetic monopoles called Dirac String. Then, using this model, I will show the Dirac quantization condition given that magnetic charges exist. In section IV, I will study physical properties of Dirac string such as singularities of magnetic field and rotational invariance. To gain more insight into Dirac string, I will look at the classical interaction between electrically charged particle and magnetic monopoles. In section V, I will look another type of magnetic monopole called Wu-Yang monopole. This monopole doesn't include any singularity in the vector potential, which is the unpleasant property in Dirac String.

II. VECTOR POTENTIAL AND GAUGE INVARIANCE IN QUANTUM MECHANICS

Here, I summarize some necessary results from the electromagnetism in quantum physics, obtained from Ref. [1]. The time-dependent Schrödinger equation for a charged particle in a magnetic field $\mathbf{B}(\mathbf{r}) = \nabla \times \mathbf{A}(\mathbf{r})$ is given by

$$i\hbar\frac{\partial \Psi(\mathbf{r}, t)}{\partial t} = \left(\frac{1}{2m}(\mathbf{p} - \frac{q}{c}\mathbf{A})^2 + q\Phi\right)\Psi(\mathbf{r}, t)$$

If two different vector potential $(\mathbf{A}, \Phi)$ and $(\mathbf{A}', \Phi)$ are connected by a Gauge transformation,

$$\mathbf{A}' = \mathbf{A} + \nabla\Lambda, \Phi' = \Phi - \frac{1}{c}\frac{\partial \Lambda}{\partial t}$$

They describe the same system even though they are not equal. If we transform $\mathbf{A}$ into $\mathbf{A}'$, then the wavefunction transforms as follows,

$$\Psi' = \mathrm{U}(\Lambda)\Psi \qquad \text{with } \mathrm{U}(\Lambda) = \exp(i\frac{q\Lambda}{\hbar c})$$

satisfying the Schrödinger equation with $\mathbf{A}'$ and Φ'. The two wavefunctions describe the same physics since they differ by a pure phase.

III. MAGNETIC MONOPOLES AND CHARGE QUANTIZATION USING DIRAC STRING

Magnetic charges are hypothetical objects carrying quantized charges in units of $\frac{\hbar c}{2e}$, which was first derived by Dirac in 1931 [3]. But, how one can model such an object that is not allowed by Maxwell's equations? In his paper 1931, Dirac proposed a model called Dirac String. In 1938, Jordan found that Dirac String can be represented by a semi-infinite solenoid [6]. We first begin by studying this semi-infinite model. Imagine you have a semi-infinite solenoid that starts from $z = 0$ and extends to $z = -\infty$. Near the point $z = 0$, there are magnetic fields coming off from the point $z = 0$, just as solenoid. As we go down, we won't be able to see magnetic field going back into solenoid since the solenoid extends to $z = -\infty$. Hence, the magnetic fields are as if they come from magnetic charge. The system will be a magnetic monopole only if the solenoid is physically undetectable.

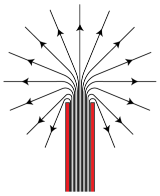

FIG. 1. Dirac string as a Semi-Infinite Solenoid.

To see how this leads to magnetic charge, we need to calculate vector potential **A** due to this semi-infinite solenoid. The vector potential of a magnetic is given by

$$\mathbf{A} = \frac{\mathbf{m}\times\mathbf{r}}{r^2},$$

where **m** is magnetic dipole moment and **r** is the point of interest. Hence,

$$d\mathbf{A} = \frac{d\mathbf{m}\times\mathbf{r}}{r^2}, d\mathbf{m} = \frac{DNIdz}{c}\hat{\mathbf{k}},$$

where D the area of cross section of solenoid, I is the current through the wire, and n is the number of turns per length. To calculate A of the entire solenoid, we integrate over all solenoid,

$$\begin{aligned}
\mathbf{A} &= \int_{\text{string}} \frac{d\mathbf{m}\times\mathbf{r}_m}{{r_m}^2} && (1)\\
&= \int_{-\infty}^{0} \frac{DNIdz_m\hat{\mathbf{k}}\times\mathbf{r}_m}{{r_m}^2} && (2)\\
&= \frac{IND}{c}\int_{-\infty}^{0} \frac{r_0\,dz_m}{((z_m-z_0)^2+r_0^2)^{3/2}}\hat{\phi} && (3)\\
&= \frac{InD}{c}\frac{1-\cos\theta}{r\sin\theta}\hat{\phi} && (4)\\
&= g\frac{1-\cos\theta}{r\sin\theta}\hat{\phi} && (5)
\end{aligned}$$

where c is the speed of light and g is the magnetic charge.

Indeed, one can show that

$$\mathbf{B} = \boldsymbol{\nabla}\times\mathbf{A} = g\frac{\hat{\mathbf{r}}}{r^2}$$

Now, we are ready to obtain charge quantization. To do this, let's imagine a usual experimental set-up for Aharonov-Bohm effect. We consider an electron trapped at the radius r_0.

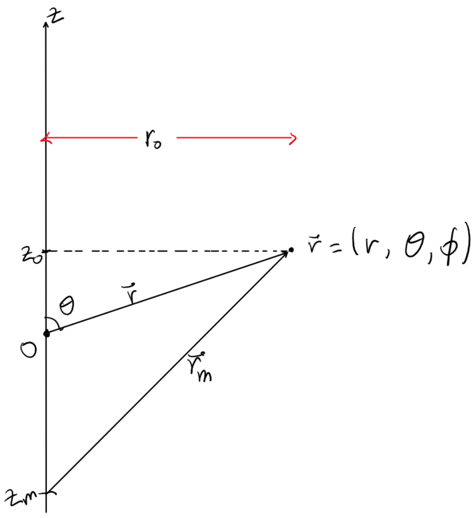

FIG. 2. The contribution to the magnetic field at the point (r, θ, ϕ) due to the magnetic moment at the point $z = z_m$.

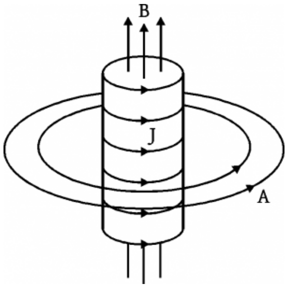

FIG. 3. An Electron Moving around Solenoid at radius r_0.

We know that there are 2 scenarios that can happen. First, the magnetic flux may not be integer multiple of ϕ_0, in which case the shift in energy spectrum can be realized. Hence, the solenoid is physically realizable. On the other hand, if the magnetic flux is integer multiple of $\phi_0 = \frac{\hbar c}{2e}$, the shift in energy spectrum is not realizable. For we want our system to be a magnetic charge, it is required that the solenoid is physically undetectable. The magnetic flux through solenoid is $\Phi = \frac{4\pi}{c}nID = 4\pi g$. Hence, it follows

$$\begin{aligned}
\Phi &= n\Phi_0 && (6)\\
4\pi g &= n\frac{2\pi\hbar c}{e} && (7)\\
g &= n\frac{\hbar c}{2e} && (8)
\end{aligned}$$

where n is an integer number. Hence, we obtained Dirac quantization condition.

IV. THE DIRAC STRING AND ITS CLASSICAL INTERACTION WITH A CHARGED PARTICLE

Even though the Dirac String leads to desired magnetic field, it contains singularities in magnetic field. We couldn't account for these singularities. To do this more delicately, we need to use the regularized version of the vector potential $\mathbf{A}$. Expressing $\mathbf{A}$ in cylindrical coordinates, it follows

$$\mathbf{A} = \frac{g}{\rho}\left(1 - \frac{z}{\sqrt{z^2+\rho^2}}\right) \tag{9}$$

Then, the regularized version is obtained by taking $\frac{1}{\rho} \to \frac{\Theta(\rho-\epsilon)}{\rho}$ and $\frac{z}{\sqrt{z^2+\rho^2}} \to \frac{z}{\sqrt{z^2+\rho^2+\epsilon^2}}$

$$\mathbf{A}_R(z,\rho,\epsilon) = \frac{g\Theta(\rho-\epsilon)}{\rho}\left(1 - \frac{z}{\sqrt{z^2+\rho^2+\epsilon^2}}\right) \tag{10}$$

One can show

$$\lim_{\epsilon\to 0} \boldsymbol{\nabla} \times \mathbf{A}_R(z,\rho,\epsilon) \tag{11}$$
$$= g\tfrac{\hat{\mathbf{r}}}{r^2} + 4\pi g\,\Theta(-z)\delta(x)\delta(y)\hat{\mathbf{z}} \tag{12}$$

Hence, we obtain

$$\mathbf{B} = g\frac{\hat{\mathbf{r}}}{r^2} + 4\pi g\,\Theta(-z)\delta(x)\delta(y)\hat{\mathbf{z}} = \mathbf{B}_{\text{mon}} + \mathbf{B}_{\text{str},1}$$

We can see that magnetic field from the Dirac String doesn't have only monopole component but also string component. In fact, it is this string component that reconciles the magnetic monopole with Maxwell's equations. But this additional magnetic field does not change the physics of the magnetic charge system by the Dirac quantization condition.

One can also study the rotational symmetry of this system. Indeed, T the magnetic field of magnetic charge is manifestly rotationally invariant even though its vector potential and Hamiltonian is not. How are these compatible with each other?

Say we have rotation operator $\hat{\mathbf{R}}(\theta_0)$ which rotates around x axis by θ_0. Then, it follows that the rotated Hamiltonian is given by

$$\hat{\mathbf{R}}^\dagger \hat{\mathbf{H}} \hat{\mathbf{R}} = \frac{1}{2m}\left(\mathbf{p} - \frac{q}{c}\mathbf{A}'\right)^2 \tag{13}$$

and

$$\mathbf{A}' = \hat{\mathbf{R}}^\dagger \mathbf{A} \hat{\mathbf{R}} \tag{14}$$
$$= -g\frac{1+\cos(\theta+\theta_0)}{r\sin(\theta+\theta_0)}\hat{\phi} \tag{15}$$

The magnetic field for the rotated system is

$$\mathbf{B}' = \boldsymbol{\nabla} \times \mathbf{A}' \tag{16}$$
$$= g\frac{\hat{\mathbf{r}}}{r^2} - 4\pi g\,\Theta(z)\delta(x)\delta(y - z\cos\theta_0)\hat{\mathbf{z}} \tag{17}$$
$$= \mathbf{B}'_{mon} + \mathbf{B}'_{\text{str},2} \tag{18}$$

From this, we can see that the string is also rotated, as expected. By Dirac quantization condition, the direction of the Dirac string doesn't change the physics of the system. Hence, the system is rotationally invariant.

To gain some intuition for the magnetic monopoles, we now study the classical interaction between a charged particle and magnetic monopole. The equation of motion for a particle with charge q in the field of magnetic monopole is given by

$$m\ddot{\mathbf{r}} = \frac{q}{c}(\mathbf{v} \times \mathbf{B}) = \frac{qg}{cr^3}\left(\dot{\mathbf{r}} \times \mathbf{r}\right) \tag{19}$$

We can find the constants of motions to calculate trajectory of the particle. By taking dot product of $\mathbf{v}$ and $\ddot{\mathbf{r}}$, we have

$$\dot{E} = \frac{d}{dt}\left(\frac{m}{2}v^2\right) = 0 \tag{20}$$

In addition to kinetic energy of the particle, the magnitude of the mechanical angular momentum is also conserved as in the case of central potentials. To show this, the mechanical angular momentum of the systems is given by

$$\mathbf{L} = \mathbf{r} \times m\mathbf{v} \tag{21}$$

The time derivative of mechanical angular momentum is

$$\dot{\mathbf{L}} = \mathbf{r} \times m\dot{\mathbf{v}} \tag{22}$$
$$= \frac{qg}{mr^3}\mathbf{r} \times \dot{\mathbf{r}} \times \mathbf{r} \tag{23}$$
$$= \frac{qg}{mr^3}\left(\mathbf{L} \times \mathbf{r}\right) \tag{24}$$

Then, we have

$$\frac{d}{dt}\left(\mathbf{L}\cdot\mathbf{L}\right) = 2\mathbf{L}\cdot\dot{\mathbf{L}} \tag{25}$$
$$= 0 \tag{26}$$

where the last step is obtained using (24). Hence $|\mathbf{L}|$ is a constant of the motion.

Different from central potential systems, the conserved angular momentum has the form,

$$\mathbf{J} = m\mathbf{r} \times \dot{\mathbf{r}} - qg\frac{\mathbf{r}}{r} \tag{27}$$

Now, we show that this is a constant of motion.

$$\dot{\mathbf{J}} = \dot{\mathbf{L}} - qg\dot{\hat{\mathbf{r}}} \tag{28}$$
$$= \frac{qg}{r^3}\left(\dot{\mathbf{r}}(\mathbf{r}\cdot\mathbf{r}) - \mathbf{r}(\dot{\mathbf{r}}\cdot\mathbf{r})\right) - qg\left(\frac{1}{r}\dot{\mathbf{r}} - \frac{\mathbf{r}}{r^2}\dot{r}\right) \tag{29}$$
$$= 0 \tag{30}$$

From (27), it follows

$$\mathbf{J}\cdot\hat{\mathbf{r}} = -qg \tag{31}$$

Hence, both $\mathbf{J}$ and $\hat{\mathbf{r}}$ are constants of motion. We also found that the angle between $\mathbf{J}$ and $\hat{\mathbf{r}}$ is constant. To find the equation for r, it follows from (19),

$$\begin{aligned} 0 &= \mathbf{r}\cdot\ddot{\mathbf{r}} && (32)\\ &= \frac{1}{2}\ddot{r^2} - (r^2(\dot{\hat{r}})^2 - (\dot{r})^2) && (33)\\ &= \frac{1}{2}\ddot{r^2} - v^2 && (34) \end{aligned}$$

Due to conservation of energy, we can write

$$r = \sqrt{v^2\,t^2 + C} \tag{35}$$

with initial conditions $\mathbf{r}(t=0) = C$ and $\dot{\mathbf{r}}(t=0) = 0$.

Using (30), (31) and (35), one can conclude that the motion of cone with the vertex at the magnetic monopole.

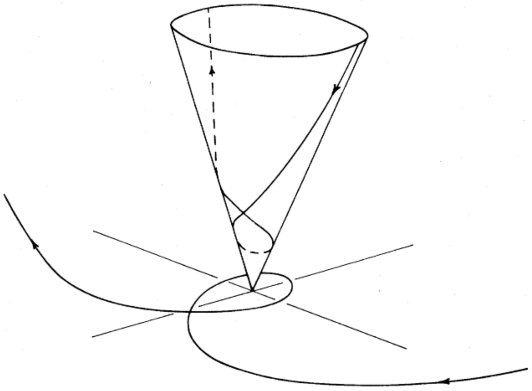

FIG. 4. The Motion of an Electron Being Scattered by a Magnetic Monopole at the Origin.

V. WU-YANG MONOPOLE

In the vector potential of Dirac string, there are singularities. These singularities exist even at points that are not the origin. Hence, the phase that charged particles take $\exp(i\frac{e}{\hbar c}\oint \mathbf{A}\cdot d\mathbf{l})$ becomes ill-defined when the particle goes through a singularity. But it is true that every vector potential for a magnetic monopole possesses such singularities. We now prove this.

Let's assume that there exists a vector potential for magnetic monopole, which does not include singularity. Consider a loop integral at fixed radius r_0 and polar angle θ_0.

$$\begin{aligned} \oint \mathbf{A}\cdot d\mathbf{r} &= \iint \mathbf{B}\cdot d\mathbf{S} && (36)\\ &= \int_0^{2\pi} r^2\frac{g}{r^2}(\hat{\mathbf{r}}\cdot\hat{\mathbf{r}})d\phi\int_0^{\theta_0}\sin\theta d\theta && (37)\\ \Phi_m &= 2\pi g(1-\cos\theta_0) && (38) \end{aligned}$$

As $\theta_0 \to \pi$, $\Phi_m \to 4\pi g$. However, when $\theta_0 = \pi$, the boundary of the loop integral shrinks into a point. Since $\mathbf{A}$ does not contain any singularity, $\Phi_m = 0$ when $\theta_0 = \pi$, which is a contradiction. Hence, $\mathbf{A}$ must have a singularity.

However, the problem of singularity can be resolved in the following way, as suggested by Wu and Yang in their 1975 paper [9]. Instead of having one vector potential, we can have two vector potentials that are defined in different regions. As long as they are connected by a gauge transformation in the overlapping region, this formulation is physically valid. The vector potentials are given as follows

$$\mathbf{A}_1 = g\frac{1-\cos\theta}{r\sin\theta}\hat{\phi} \quad \text{for } S^1 : 0 \leqslant \theta < \pi + \frac{\epsilon}{2} \tag{39}$$

$$\mathbf{A}_2 = -g\frac{1+\cos\theta}{r\sin\theta}\hat{\phi} \quad \text{for } S^2 : \pi - \frac{\epsilon}{2} < \theta \leqslant \pi \tag{40}$$

In the region they overlap, they must be connected by a gauge transformation. Therefore, we obtain

$$\begin{aligned} \boldsymbol{\nabla}\Lambda &= \mathbf{A}_1 - \mathbf{A}_2 && (41)\\ &= \frac{2g}{r\sin\theta}\hat{\phi} && (42)\\ \Lambda &= 2g\phi\hat{\phi} && (43) \end{aligned}$$

One can see that $\mathbf{A}_1$ and $\mathbf{A}_2$ do not have singularities on the region where they are defined. By using two single-valuedness of $\psi(\phi)$ and $\psi'(\phi)$, it follows

$$\begin{aligned} \psi'(\phi) &= \exp(i\frac{e2g\phi}{\hbar c})\psi'(\phi) && (44)\\ &= \exp(i\frac{e2g\phi}{\hbar c})\psi'(\phi+2\pi) && (45)\\ &= \exp(i\frac{e2g(\phi+2\pi)}{\hbar c})\psi'(\phi+2\pi) && (46) \end{aligned}$$

where we used the fact that they are connnected by a gauge transformation. Therefore,

$$\begin{aligned} \exp(i\frac{2ge}{\hbar c}2\pi) &= 1 && (47)\\ g &= n\frac{\hbar c}{2e}, n\in\mathbb{Z} && (48) \end{aligned}$$

Therefore, the magnetic charge g is quantized in units of $\frac{\hbar c}{2e}$. Note that this method works for any magnetic monopole model.

One can discover the link between charge quantization and topology using Wu-Yang Monopole. We know that the gauge transformation is single-valued function. If we choose $U(\phi)$ such that $U(0) = 1$, it follows

$$\begin{aligned} U(2\pi) &= U(0) = 1 && (49) \\ &= \exp(i\frac{e}{\hbar c}\oint(\mathbf{A}_1 - \mathbf{A}_2)\cdot d\mathbf{l}) && (50) \\ &= \exp(i\frac{e}{\hbar c}(\phi_N + \phi_S)) && (51) \\ &= \exp(i\frac{4\pi eg}{\hbar c}) && (52) \end{aligned}$$

We found that the winding number has the form $n = \frac{2eg}{\hbar c}$. This quantity tells us how many times the vector potential encircles the magnetic monopole as $\phi : 0 \to 2\pi$. Indeed, the magnetic charge is quantized since the winding number is quantized. This gives us the topological aspect of Dirac quantization condition.

DISCUSSION

1. In the Wu-Yang Monopole, we used 2 different vector potentials $\mathbf{A}_1$ and $\mathbf{A}_2$, which are connected by a gauge transformation. The magnetic fields of these vector potentials give insight about the gauge transformation of Dirac string.

By using the method we used, one can obtain the magnetic field for this vector potential,

$$\begin{aligned} \mathbf{B} &= \boldsymbol{\nabla}\times\mathbf{A}_2 && (53) \\ &= g\frac{\hat{\mathbf{r}}}{r^2} - 4\pi g\,\Theta(z)\delta(x)\delta(y)\hat{\mathbf{z}} && (54) \\ &= \mathbf{B}_{\text{mon}} + \mathbf{B}_{\text{str},2} && (55) \end{aligned}$$

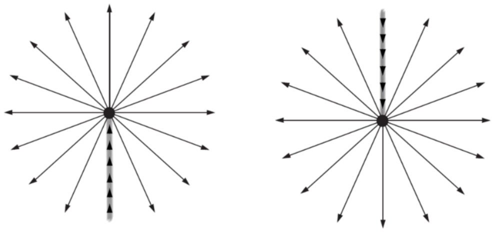

FIG. 5. The picture of Dirac Strings with the vector potential $\mathbf{A}_1$ and $\mathbf{A}_2$, respectively.

In the first system, the string extends down to infinity while in the second it extends up to infinity. The effect of the gauge transformation is to rotate the string by an angle π. More generally, this implies that magnetic monopole is defined up to the direction of Dirac string.

2. We can gain insight into the force between magnetic charges by comparing it to electrical charges. The force between electrical charges is proportional to e^2, which has the value

$$e^2 = \frac{\hbar c}{137} \qquad (56)$$

However, the value of g^2 is

$$g^2 = \frac{137}{4}\hbar c \qquad (57)$$

which is approximately 4700 times higher than e^2. It requires much more energy to separate two opposite magnetic charges as compared to electrical charges. This explains why it is much harder to obtain magnetic charge alone.

ACKNOWLEDGEMENT

This paper is prepared for the course 8.06x on edX/MITx. I would like to thank Prof. Barton Zwiebach, Prof. Jolyon Bloomfield, all the TA's of 8.06x, and edX/MITx for giving this amazing experience and helping the students on the way.

---

[1] J. J. Sakurai, J. Napolitano, *et al.*, *Modern quantum mechanics.* Pearson Harlow, 2014.

[2] Y. Aharonov and D. Bohm, "Significance of electromagnetic potentials in the quantum theory," *Phys. Rev.*, vol. 115, pp. 485–491, Aug 1959.

[3] P. A. M. Dirac, "Quantised singularities in the electromagnetic field," *Proceedings of the Royal Society of London. Series A, Containing Papers of a Mathematical and Physical Character*, vol. 133, no. 821, pp. 60–72, 1931.

[4] P. A. M. Dirac, "The theory of magnetic poles," *Physical Review*, vol. 74, no. 7, p. 817, 1948.

[5] R. Heras, "Dirac quantisation condition: a comprehensive review," *Contemporary Physics*, vol. 59, no. 4, pp. 331–355, 2018.

[6] P. Jordan, "Über die diracschen magnetpole," *Annalen der Physik*, vol. 424, no. 1-2, pp. 66–70, 1938.

[7] J. Preskill, "Magnetic monopoles," *Annual Review of Nuclear and Particle Science*, vol. 34, no. 1, pp. 461–530, 1984.

[8] Y. M. Shnir, *Magnetic monopoles.* Springer Science & Business Media, 2006.

[9] T. T. Wu and C. N. Yang, "Concept of nonintegrable phase factors and global formulation of gauge fields,"

Physical Review D, vol. 12, no. 12, p. 3845, 1975.

Constructing Dirac spinors using representations of Lorentz group

Fedor Indutnyy

(Dated: June 9, 2019)

Spin-$\frac{1}{2}$ particles are governed by Dirac equation and are described by 4-component objects named spinors. Given the influence of Special Relativity on the derivation of Dirac equation it is inevitable that the physical processes involving spin-$\frac{1}{2}$ particles have to be independent of observer and their inertial frame. Measurements made in one frame should agree with the measurements made in another, and thus the components of spinor have to transform between frames. In this paper we introduce the generators of Lorentz transformations that form a Lie algebra, find the decomposition of Lorentz algebra into a sum of two sub-algebras $\mathfrak{su}(2) \oplus \mathfrak{su}(2)$, build left- and right- handed representations of spin-$\frac{1}{2}$ particles and combine them to form a full Dirac spinor.

I. OVERVIEW

A. Conventions

Through the rest of the paper it is assumed that:

$$\hbar = c = 1 \tag{1}$$

and thus all quantities are expressed in *Natural Units*.

The energy and momentum of the particle are combined into 4-momentum:

$$p_\mu = (E, p_x, p_y, p_z)\,; \mu = 0, 1, 2, 3 \tag{2}$$

and dot product of two 4-momenta is defined as:

$$p \cdot q = p_\mu \, \eta^{\mu\nu} \, q_\nu \tag{3}$$

with the metric:

$$\eta^{\mu\nu} = \eta_{\mu\nu} = \begin{pmatrix} 1 & 0 & 0 & 0 \\ 0 & -1 & 0 & 0 \\ 0 & 0 & -1 & 0 \\ 0 & 0 & 0 & -1 \end{pmatrix}. \tag{4}$$

The dot product of 4-momentum with itself is:

$$p^2 = p \cdot p = E^2 - p_x^2 - p_y^2 - p_z^2 = E^2 - \vec{\mathbf{p}}^2. \tag{5}$$

Einstein summation is used for every repeating index:

$$A^\mu B_{\mu\nu} \equiv \sum_{\mu=0}^{4} A^\mu B_{\mu\nu}. \tag{6}$$

B. Dirac Equation

Scrödinger equation is famously non-relativistic. Special relativity makes no distinction between space and time and thus they should appear on an equal footing. However, the powers of derivatives $\frac{d}{dt}$ and $\frac{d}{dx}$ in

$$i\frac{d}{dt}\psi = E\psi = \left(\frac{1}{2m}\left(\frac{1}{i}\frac{d}{dx}\right)^2 + V(x)\right)\psi \tag{7}$$

are not the same.

In order to account for relativistic effects the equation of motion should use the relativistic energy formula

$$E = \sqrt{\vec{\mathbf{p}}^2 + m^2}, \tag{8}$$

which could be rewritten differently as

$$\sqrt{E^2 - \vec{\mathbf{p}}^2} = m. \tag{9}$$

Dirac's ingenious coup is finding such γ^μ that:

$$\left(\gamma^0 E + \gamma^1 p_x + \gamma^2 p_y + \gamma^3 p_z\right)^2 = E^2 - \vec{\mathbf{p}}^2. \tag{10}$$

Then the square root in (9) could be taken exactly:

$$\sqrt{E^2 - \vec{\mathbf{p}}^2} = \gamma^0 E + \gamma^1 p_x + \gamma^2 p_y + \gamma^3 p_z. \tag{11}$$

In terms of operators $E = i\partial_t$ and $p_i = -i\partial_i$ equation (10) takes following form:

$$\left(i\gamma^0\partial_t - i\sum_i \gamma^i \partial_i\right)^2 \psi = \left(-\partial_t^2 + \sum_i \partial_i^2\right)\psi \tag{12}$$

Simple calculation shows that in order to satisfy (12), γ^μ have to be matrices with following anti-commutation relations:

$$\{\gamma^\mu, \gamma^\nu\} = \gamma^\mu\gamma^\nu + \gamma^\nu\gamma^\mu = 2\eta^{\mu\nu} \tag{13}$$

Substituting differential version of Dirac's coup (12) back into the square root (9) and redefining $\gamma^i \equiv -\gamma^i$ results in famous Dirac equation:

$$\left(i\gamma^\mu\partial_\mu - m\right)\psi = 0 \tag{14}$$

There are different ways to select γ^μ satisfying anti-commutation relations (13). In this paper we use *Weyl basis*:

$$\gamma^0 = \begin{pmatrix} 0 & \mathbb{1} \\ \mathbb{1} & 0 \end{pmatrix}, \; \gamma^i = \begin{pmatrix} 0 & \sigma^i \\ -\sigma^i & 0 \end{pmatrix}; \tag{15}$$

where σ^i are usual Pauli matrices. Each γ^μ is a complex 4×4 matrix and ψ^a is a complex vector (not a 4-vector!) with $a = 0, 1, 2, 3$. Fully expanded Dirac equation reads as:

$$\left(i(\gamma^\mu)^a_{\;b}\partial_\mu - m\delta^a_{\;b}\right)\psi^b = 0. \tag{16}$$

Note that greek letters (μ, ν, ...) are used for coordinates, and the first letters of latin alphabet (a, b, ...) are used for spinor components.

C. 4-vector representations

The defining idea of Special Relativity is invariance under Lorentz transformations $X'^{\mu} = \Lambda^{\mu}{}_{\nu} X^{\nu}$:

$$\mathbf{X} \cdot \mathbf{Y} = X^{\mu} \eta_{\mu\nu} X^{\nu} = X'^{\mu} \eta_{\mu\nu} X'^{\nu}. \tag{17}$$

In turn the Lorentz transformations Λ have to leave the metric invariant:

$$\eta^{\sigma\rho} = \ \Lambda^{\sigma}{}_{\mu} \Lambda^{\rho}{}_{\nu} \eta^{\mu\nu}. \tag{18}$$

Skipping the parity change and time reversal transformations we are left with are 6 "basic" operations: boosts

$$K_x(\beta) = \begin{pmatrix} \cosh(\beta) & \sinh(\beta) & 0 & 0 \\ \sinh(\beta) & \cosh(\beta) & 0 & 0 \\ 0 & 0 & 1 & 0 \\ 0 & 0 & 0 & 1 \end{pmatrix}, \tag{19}$$

$$K_y(\beta) = \begin{pmatrix} \cosh(\beta) & 0 & \sinh(\beta) & 1 \\ 0 & 1 & 0 & 0 \\ \sinh(\beta) & 0 & \cosh(\beta) & 0 \\ 1 & 0 & 0 & 1 \end{pmatrix}, \tag{20}$$

$$K_z(\beta) = \begin{pmatrix} \cosh(\beta) & 0 & 0 & \sinh(\beta) \\ 0 & 1 & 0 & 0 \\ 0 & 0 & 1 & 0 \\ \sinh(\beta) & 0 & 0 & \cosh(\beta) \end{pmatrix} \tag{21}$$

and rotations

$$J_x(\theta) = \begin{pmatrix} 1 & 0 & 0 & 0 \\ 0 & 1 & 0 & 0 \\ 0 & 0 & \cos(\theta) & \sin(\theta) \\ 0 & 0 & -\sin(\theta) & \cos(\theta) \end{pmatrix}, \tag{22}$$

$$J_y(\theta) = \begin{pmatrix} 1 & 0 & 0 & 0 \\ 0 & \cos(\theta) & 0 & -\sin(\theta) \\ 0 & 0 & 1 & 0 \\ 0 & \sin(\theta) & 0 & \cos(\theta) \end{pmatrix}, \tag{23}$$

$$J_z(\theta) = \begin{pmatrix} 1 & 0 & 0 & 0 \\ 0 & \cos(\theta) & \sin(\theta) & 0 \\ 0 & -\sin(\theta) & \cos(\theta) & 0 \\ 0 & 0 & 0 & 1 \end{pmatrix}. \tag{24}$$

The subset formed by $K_x, K_y, K_z, J_x, J_y, J_z$ and their combinations is called *proper ortochronous* Lorentz group $\mathcal{L}$ which we'll just call *Lorentz group* from now on.

Suppose now that two observers see the particle governed by Dirac equation from two different frames related by Λ. The laws of physics should be the same in both frames, and thus both observers should find that the particle's wave function satisfy the same Dirac equation.

Each $\psi(x) = \psi(t, \vec{\mathbf{x}})$ is a function of space and time and therefore has to abide to coordinate transformation:

$$\psi'(x) = \psi(\Lambda x) \tag{25}$$

Putting (25) into Dirac equation (14):

$$\begin{aligned} &(i\gamma^{\mu}\partial_{\mu} - m)\,\psi'(x^{\nu}) = 0 \\ &= (i\gamma^{\mu}\partial_{\mu} - m)\,\psi(\Lambda^{\nu}{}_{\rho} x^{\rho}) \\ &= \big(i\gamma^{\mu}\Lambda^{\nu}{}_{\mu}\,(\partial_{\nu}\psi)\,(\Lambda x) - m\psi\,(\Lambda x)\big) \\ &= (i\gamma'^{\nu}\partial_{\nu} - m)\,\psi = 0 \end{aligned} \tag{26}$$

with $\gamma'^{\nu} \equiv \Lambda^{\nu}{}_{\mu}\gamma^{\mu}$. Simple application of the main property of Lorentz transformations (18) shows that

$$\{\gamma'^{\mu}, \gamma'^{\nu}\} = \{\gamma^{\mu}, \gamma^{\nu}\} = \eta^{\mu\nu}. \tag{27}$$

γ'^{μ} is a **different** set of matrices satisfying the same anti-commutation relations as γ.

Apparently naïve wave function transformation is not enough to make physics observer-independent! This should not be surprising: ψ has 4 components and we assumed that they do not mix under Lorentz transformation. We have to introduce "mixing" to compensate for the coordinate transformation. As we shall see in the next sections, finding the right way of "mixing" the components of the Dirac spinor is crucial for Lorentz invariance of the Dirac equation.

D. Representations of Lorentz group

Components of ψ can't mix arbitrarily. Lorentz transformations form a group (i.e. there is an identity transformation, inverse for every Λ, matrix multiplication is a group action), and thus two successive "mixings" of the spinor components have to act as a single "mixing" using combined Lorentz transformations:

$$T(\Lambda_2)^{a}{}_{b} T(\Lambda_1)^{b}{}_{c} \psi^{c} = e^{i\phi_{12}} T(\Lambda_2\Lambda_1)^{a}{}_{b} \psi^{c} \tag{28}$$

up to a phase ϕ_{12}.

Such map $T : \mathcal{L} \to SL(N, \mathbb{C})$ is a *representation* of the group $\mathcal{L}$, where $SL(N, \mathbb{C})$ is a group of complex $N \times N$ matrices. In case of Dirac spinors the target group has to be a subgroup of $SU(4)$ (unitary 4×4 matrices) because spinors have to remain normalized under transformations:

$$\psi^{\dagger}\psi \to \psi^{\dagger} T^{\dagger}(\Lambda) T(\Lambda) \psi = \psi^{\dagger}\psi. \tag{29}$$

E. Lie Algebra of Lorentz group

Although it is convenient to define the Lorentz group $\mathcal{L}$ in terms of matrices $\Lambda^{\mu}{}_{\nu}$, the group $\mathcal{L}$ itself is independent of particular matrix representation. $\mathcal{L}$ has mathematical structure that is best seen on infinitesimal transformations of K_x (19):

$$K_1 = \frac{1}{i} \partial_{\beta} K_x(\beta)\big|_{\beta=0} = i \begin{pmatrix} 0 & -1 & 0 & 0 \\ -1 & 0 & 0 & 0 \\ 0 & 0 & 0 & 0 \\ 0 & 0 & 0 & 0 \end{pmatrix} \tag{30}$$

and similarly of other operations (20) – (24):

$$K_2 = i\begin{pmatrix} 0 & 0 & -1 & 0 \\ 0 & 0 & 0 & 0 \\ -1 & 0 & 0 & 0 \\ 0 & 0 & 0 & 0 \end{pmatrix}, K_3 = i\begin{pmatrix} 0 & 0 & 0 & -1 \\ 0 & 0 & 0 & 0 \\ 0 & 0 & 0 & 0 \\ -1 & 0 & 0 & 0 \end{pmatrix}, \tag{31}$$

$$J_1 = i\begin{pmatrix} 0 & 0 & 0 & 0 \\ 0 & 0 & 0 & 0 \\ 0 & 0 & 0 & -1 \\ 0 & 0 & 1 & 0 \end{pmatrix}, J_2 = i\begin{pmatrix} 0 & 0 & 0 & 0 \\ 0 & 0 & 0 & 1 \\ 0 & 0 & 0 & 0 \\ 0 & -1 & 0 & 0 \end{pmatrix}, \tag{32}$$

$$J_3 = i\begin{pmatrix} 0 & 0 & 0 & 0 \\ 0 & 0 & -1 & 0 \\ 0 & 1 & 0 & 0 \\ 0 & 0 & 0 & 0 \end{pmatrix}. \tag{33}$$

The matrices (30), (31), (32), (33) are called *generators* of *Lie algebra* $\mathfrak{so}(1,3)$. Any Lorentz transformation could be put into an exponential form

$$\Lambda(\theta,\beta) = \exp\left[i\theta^i J_i + i\beta^i K_i\right] \tag{34}$$

by combining several generators together.

Note that neither of J_i or K_i commute with each other, e.g. rotating by 90° around z-axis and then rotating by 90° around x-axis is not the same as doing 90° x-axis rotation first and applying 90° z-axis rotation afterwards:

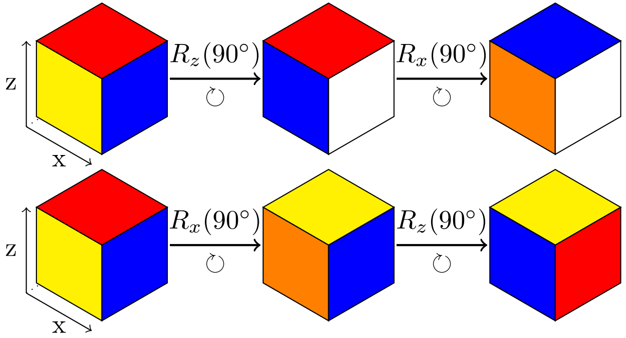

After few steps of derivation the commutators of infinitesimal rotations J_i familiarly are:

$$[J_i, J_k] = i\epsilon_{ijk}J_k. \tag{35}$$

The rest of the commutators are:

$$\begin{aligned} [J_i, K_j] &= i\epsilon_{ijk}K_k, \\ [K_i, K_j] &= -i\epsilon_{ijk}J_k. \end{aligned} \tag{36}$$

Neither (35) nor (36) make any reference to a particular matrix form (representation) of $\mathcal{L}$. In fact these commutators **define** Lie algebra of $\mathcal{L}$. Exponentiating different set of matrices J_i', K_i', that have the same commutation relations (35), (36) will yield a different valid representation of Lorentz group! Therefore we set ourselves on a quest to find J_i and K_i that have an appropriate action on Dirac spinors.

II. DECOMPOSITION OF LORENTZ ALGEBRA

The spin of a quantum particle is defined by its transformation properties under rotations. In non-relativistic Quantum Mechanics we found that spinors transform through an application of the exponential unitary operator

$$\psi^a \to \left(\exp\left[i\theta^i S_i\right]\right)^a_{\ b}\psi^b, \tag{37}$$

where $S_i \equiv \frac{\sigma_i}{2}$ are spin operators for spin-$\frac{1}{2}$ particles constructed from Pauli matrices σ_i.

The commutators

$$[S_i, S_j] = i\epsilon_{ijk}S_k \tag{38}$$

define the Lie algebra $\mathfrak{su}(2)$ of the group of unitary matrices with $\det M = 1$ $SU(2)$. The $\mathfrak{su}(2)$ (38) is the same as $\mathfrak{so}(3)$ (35). Thus, because these Lie algebras are the same, each 3-dimensional rotation in $SO(3)$ (orthogonal matrices with $\det M = 1$) can be mapped to an element of $SU(2)$. The only difference between these groups is that for every $SO(3)$ element there are two elements in $SU(2)$, and thus single full rotation in $SU(2)$ is not equal to identity transformation. Peculiarly spinors change the sign of their wave function under a single 360° rotation. This is very easy to see by putting $\theta^i = (0, 0, 2\pi)$ into the transformation (37).

We wish to find such representation of $\mathcal{L}$ that the relativistic spinor would transform under rotations using unitary matrices, i.e. using $SU(2)$ representations. Even though the S_i's commutation relations (38) are exactly the same as (35), the boosts K_i commutators (36) make the $\mathfrak{so}(1,3)$ different from $\mathfrak{su}(2)$.

The trick [1, ch. 10.1.2] is to study combinations of J_i and K_i:

$$J_i^+ = \frac{1}{2}\left(J_i + iK_i\right), \ J_i^- = \frac{1}{2}\left(J_i - iK_i\right). \tag{39}$$

Their commutators

$$\left[J_i^+, J_i^-\right] = 0, \tag{40}$$

$$\left[J_i^+, J_j^+\right] = i\epsilon_{ijk}J_k^+, \tag{41}$$

$$\left[J_i^-, J_j^-\right] = i\epsilon_{ijk}J_k^-, \tag{42}$$

indicate that $\mathfrak{so}(3,1)$ is a direct sum of two commuting sub-albegras:

$$\mathfrak{so}(3,1) = \mathfrak{su}(2) \oplus \mathfrak{su}(2). \tag{43}$$

Instead of looking for representations of full $\mathcal{L}$ we can combine two representations of $SU(2)$ into a tensor product $SU(2)\otimes SU(2)$. Each epresentation of $SU(2)$ acts on a $(2j+1)$-dimensional vector space, where j is a half-integer characterizing the representation. The combination of two $SU(2)$ representations therefore can be labeled by a pair of half-integers (A, B) with the total number of basis states equal to $(2A+1)(2B+1)$.

The rotation and boost operators J, K can be reconstructed from J^+ and J^-:

$$J_i = J_i^+ + J_i^-, \tag{44}$$

$$K_i = i\left(J_i^- - J_i^+\right). \tag{45}$$

Despite unfamiliar context, (44) is practically the same as total angular momentum operator in non-relativistic quantum mechanics:

$$J_i = L_i + S_i. \tag{46}$$

Just as in Clebsch-Gordan tables, the tensor product of spin-A and spin-B spinors decomposes into a sum of representations of $SO(3)$ with spins:

$$A+B,\ A+B-1,\ \ldots,\ |A-B|. \tag{47}$$

III. LEFT- AND RIGHT- HANDED WEYL SPINORS

Since we are looking for spin-$\frac{1}{2}$ particles the relevant pairs of A and B are left- and right-handed Weyl spinors: $(\frac{1}{2},0)$ and $(0,\frac{1}{2})$, respectively. It is easy to check that these values of A and B combined generate spin-$\frac{1}{2}$ representation using the summation formula (47). For the left-handed spinor we set:

$$\psi_L : J_i^- = \frac{\sigma_i}{2},\ J_i^+ = 0,\ J_i = \frac{\sigma_i}{2},\ K_i = i\frac{\sigma_i}{2}; \tag{48}$$

and for right-handed:

$$\psi_R : J_i^- = 0,\ J_i^+ = \frac{\sigma_i}{2},\ J_i = \frac{\sigma_i}{2},\ K_i = -i\frac{\sigma_i}{2}. \tag{49}$$

Substituting matrices (48) and (49) into the exponential form of Lorentz transformation (34) we find that ψ_L and ψ_R transform according to:

$$\psi_L \to \exp\left[\frac{1}{2}\left(i\theta^i - \beta^i\right)\sigma_i\right]\psi_L, \tag{50}$$

$$\psi_R \to \exp\left[\frac{1}{2}\left(i\theta^i + \beta^i\right)\sigma_i\right]\psi_R. \tag{51}$$

Note that both ψ_L and ψ_R have two components, just as usual non-relativistic spinors.

IV. DIRAC SPINORS AND LORENTZ INVARIANCE

Starting from (30) there was a trouble following us through all derivations. The boosts K_i are not Hermitian, and therefore very evidently transformations of left- and right-handed Weyl spinors (50) and (51) are not unitary for $\beta^i \neq 0$! The reality is that there are no non-trivial finite-dimensional unitary representations of Lorentz group $\mathcal{L}$, because it is non-compact [2]. Proper solution is attainable only in fully-relativistic Quantum Field Theory with the use of representations of Poincaré group (Lorentz group with addition of time- and space-translations), which we will not discuss here.

A. Scalar quantities

Despite this flaw we can still study the transformations of Weyl and Dirac spinors. To get more insights into this it would be suggestive to build several Lorentz-invariant quantities out of ψ_L and ψ_R. The infinitesimal versions of transformations (50) and (51)

$$\delta\psi_L = \frac{1}{2}\left(i\theta^i - \beta^i\right)\sigma_i\psi_L, \tag{52}$$

$$\delta\psi_R = \frac{1}{2}\left(i\theta^i + \beta^i\right)\sigma_i\psi_R \tag{53}$$

and similarly of their conjugates

$$\delta\psi_L^\dagger = \frac{1}{2}\left(-i\theta^i - \beta^i\right)\psi_L^\dagger\sigma_i, \tag{54}$$

$$\delta\psi_R^\dagger = \frac{1}{2}\left(-i\theta^i + \beta^i\right)\psi_R^\dagger\sigma_i \tag{55}$$

will be useful in this process.

The norm of ψ_R:

$$\begin{aligned}\delta\left(\psi_R^\dagger\psi_R\right) &= \delta\psi_R^\dagger\psi_R + \psi_R^\dagger\delta\psi_R\\ &= \frac{1}{2}\left(-i\theta^i + \beta^i + i\theta^i + \beta^i\right)\psi_R^\dagger\sigma_i\psi_R\\ &= \beta^i\psi_R^\dagger\sigma_i\psi_R\end{aligned} \tag{56}$$

is non Lorentz invariant for $\beta^i \neq 0$, just as the norm of ψ_L:

$$\delta\left(\psi_L^\dagger\psi_L\right) = -\beta^i\psi_L^\dagger\sigma_i\psi_L. \tag{57}$$

The $\psi_L^\dagger\psi_R$ combination however

$$\begin{aligned}&\delta\left(\psi_L^\dagger\psi_R\right)\\ &= \frac{1}{2}\left(-i\theta^i - \beta^i + i\theta^i + \beta^i\right)\psi_L^\dagger\sigma_i\psi_R = 0\end{aligned} \tag{58}$$

and therefore its complex conjugate $\psi_R^\dagger\psi_L$ are Lorentz invariant **scalar** quantities.

B. Vector quantities

Since every complex matrix could be decomposed into a combination of identity and σ_i, it would be sufficient to study the transformation properties of $\psi_R^\dagger \sigma_i \psi_R$

$$\begin{aligned}\delta\left(\psi_R^\dagger \sigma_i \psi_R\right) =& \frac{1}{2}\left(-i\theta^j + \beta^j\right)\psi_R^\dagger \sigma_j \sigma_i \psi_R + \\ & \frac{1}{2}\left(i\theta^j + \beta^j\right)\psi_R^\dagger \sigma_i \sigma_j \psi_R + \\ =& \frac{1}{2} i\theta^j \psi_R^\dagger \left[\sigma_i, \sigma_j\right]\psi_R + \\ & \frac{1}{2}\beta^j \psi_R^\dagger \left\{\sigma_i, \sigma_j\right\}\psi_R + \\ =& \ \beta^j \psi_R^\dagger \psi_R - \epsilon_{ijk}\theta^j \psi_R^\dagger \sigma_k \psi_R\end{aligned} \tag{59}$$

using $[\sigma_i, \sigma_j] = 2i\epsilon_{ijk}\sigma_k$ and $\{\sigma_i, \sigma_j\} = 2\delta_{ij}$. Similarly $\psi_L^\dagger \sigma_i \psi_L$ transforms as:

$$\delta\left(\psi_L^\dagger \sigma_i \psi_L\right) = -\beta^j \psi_L^\dagger \psi_L - \epsilon_{ijk}\theta^j \psi_L^\dagger \sigma_k \psi_L. \tag{60}$$

It could be checked that infinitesimal action of the exponential Lorentz transformation (34) on a 4-vector X^μ is:

$$\begin{aligned}\delta X^0 &= \beta^i X^i, \\ \delta X^i &= \beta^i X^0 - \epsilon_{ijk}\theta^j X^k.\end{aligned} \tag{61}$$

Comparing it to change of the non-invariant quantities (56) and (59):

$$\begin{aligned}\delta\left(\psi_R^\dagger \psi_R\right) &= \beta^i \psi_R^\dagger \sigma_i \psi_R, \\ \delta\left(\psi_R^\dagger \sigma_i \psi_R\right) &= \beta^j \psi_R^\dagger \psi_R - \epsilon_{ijk}\theta^j \psi_R^\dagger \sigma_k \psi_R,\end{aligned} \tag{62}$$

we see that 4-component combinations

$$\left(\psi_R^\dagger \psi_R, \psi_R^\dagger \sigma_i \psi_R\right), \ \left(\psi_L^\dagger \psi_L, -\psi_L^\dagger \sigma_i \psi_L\right) \tag{63}$$

behave like **vectors** under Lorentz transformations!

We therefore define:

$$\begin{aligned}\sigma^\mu &\equiv (1, \sigma_1, \sigma_2, \sigma_3) \\ \overline{\sigma}^\mu &\equiv (1, -\sigma_1, -\sigma_2, -\sigma_3)\end{aligned} \tag{64}$$

and conveniently the combinations (63) become:

$$\psi_R^\dagger \sigma^\mu \psi_R, \ \psi_L^\dagger \overline{\sigma}^\mu \psi_L. \tag{65}$$

C. Back to Dirac equation

In previous sections we have derived several Lorentz invariant quantities:

$$\begin{aligned}&\psi_R^\dagger \psi_L, \ \psi_L^\dagger \psi_R, \\ &\psi_R^\dagger \sigma^\mu \psi_R, \ \psi_L^\dagger \overline{\sigma}^\mu \psi_L.\end{aligned} \tag{66}$$

It is time now to combine them into the Lorentz-invariant Dirac equation. Since quantities (65) act as 4-vectors, they could be paired with a derivative

$$\psi_R^\dagger \sigma^\mu \partial_\mu \psi_R, \ \psi_L^\dagger \overline{\sigma}^\mu \partial_\mu \psi_L \tag{67}$$

to become scalars.

Combining ψ_L and ψ_R into a 4-component Dirac spinor

$$\psi \equiv \begin{pmatrix}\psi_L \\ \psi_R\end{pmatrix} \tag{68}$$

and restating Weyl-basis (15) in terms of (64)

$$\gamma^\mu = \begin{pmatrix}0 & \sigma^\mu \\ \overline{\sigma}^\mu & 0\end{pmatrix}, \tag{69}$$

we see that derivative terms (67) are nothing else, but

$$\psi^\dagger \gamma^0 \gamma^\mu \partial_\mu \psi. \tag{70}$$

The scalars from (66) could be built similarly:

$$\psi^\dagger \gamma^0 \psi. \tag{71}$$

Defining $\overline{\psi} \equiv \psi^\dagger \gamma^0$ It is easy to see from (70) and (71) that

$$\overline{\psi}\left(i\gamma^\mu \partial_\mu - m\right)\psi \tag{72}$$

is a Lorentz invariant quantity. What we have found is that (72) is nothing else, but Dirac equation (14) multiplied on the left by $\overline{\psi}$!

Given the definition of ψ in (68) and properties of left- and right- handed Weyl spinors (50) and (51) we see that it transforms under rotations as:

$$\psi' = \exp\left[i\theta^i \frac{1}{2}\begin{pmatrix}\sigma_i & 0 \\ 0 & \sigma_i\end{pmatrix}\right]\psi. \tag{73}$$

D. Weyl spinors

Quite interestingly setting mass to zero $m = 0$ in Dirac's equation (14)

$$\begin{pmatrix}0 & i\partial_0 + i\partial_i \sigma^i \\ i\partial_0 - i\partial_i \sigma^i & 0\end{pmatrix} \times \begin{pmatrix}\psi_L \\ \psi_R\end{pmatrix} = 0 \tag{74}$$

decouples ψ_L and ψ_R parts of ψ:

$$\left(i\partial_0 - i\vec{\partial}\cdot\vec{\sigma}\right)\psi_L = 0, \tag{75}$$

$$\left(i\partial_0 + i\vec{\partial}\cdot\vec{\sigma}\right)\psi_R = 0. \tag{76}$$

If we would replace partial derivatives with momenta $\vec{p} = i\vec{\partial}$ and energy $E = i\partial_0$ the equations (75) and (76) become:

$$\vec{p}\cdot\vec{\sigma}\psi_L = E\psi_L, \tag{77}$$

$$\vec{p}\cdot\vec{\sigma}\psi_R = -E\psi_R. \tag{78}$$

When the particle is massless its energy is equal to the magnitude of its momentum $E = \sqrt{\vec{p}^2 + m^2} = \sqrt{\vec{p}^2} = |p|$ and so equations (77) and (78) simplify even further:

$$\frac{\vec{p}}{|p|} \cdot \vec{\sigma}\psi_L = +\psi_L \tag{79}$$

$$\frac{\vec{p}}{|p|} \cdot \vec{\sigma}\psi_R = -\psi_R. \tag{80}$$

The expression $\frac{\vec{p}}{|p|} \cdot \vec{\sigma}$ is called *Helicity* operator, and is a projection of spin along the particle's momentum. Thus in **massless limit** left- and right- handed Weyl spinors are helicity eigenstates with opposite eigenvalues.

Demanding certain helicity (79) of a particle might seem restrictive, but due to Special Relativity massless objects always move with the speed of light in all reference frames. Such objects cannot be slowed down, and their direction of motion cannot be reversed. Therefore they must have fixed helicity.

V. DISCUSSION

We have seen that Lorentz invariance and representations of Lorentz group play key role in defining the properties of Dirac spinor. The scalar quantity (72) that we have derived plays central role in both Quantum Electrodynamics and Quantum Chromodynamics, where it is included as a part of Lagrangian describing the behavior and mass of spin-$\frac{1}{2}$ fermions.

The same process that we have used for Dirac spinor could be applied to spin-1 bosons using $(\frac{1}{2}, \frac{1}{2})$ representation of Lorentz group. In this case, however the spin addition formula (47) says that we will get two possible $SO(3)$ representations: spin-0 and spin-1. The spin-0 representation is fictitious and cannot take part in physical processes. Its elimination is the basis of the Gauge Theory.

Representation theory has been very fruitful for particle physics. The non-negative energy unitary representations of Poincaré group (Lorentz group with translations) has been classified by Wigner [2], and give basis to and description of intrinsic angular momentum of massive (spin) and massless (polarization) particles.

ACKNOWLEDGMENTS

This paper would not be possible without excellent reference texts written by: Matthew D. Schwartz [1], Michael E. Peskin and Daniel V. Schroeder [3], and Steven Weinberg [4]. Curious reader with an interest in video material about Quantum Field Theory might find useful the series of lectures by Tobias Osborne [5], to whom we are greatly thankful as well. We would like to additionally thank the teaching staff of MITx 8.06 and our peers, and the user with nickname "*loose*" from the ##physics channel on Freenode IRC server for giving a review and reporting mistakes in this paper.

---

[1] M. D. Schwartz, *Quantum field theory and standard model.* Cambridge University Press, 2013. `https://amzn.com/1107034736`.

[2] E. Wigner, "On unitary representations of the inhomogeneous lorentz group," *Annals of Mathematics* **40** (1939) no. 1, 149–204. `http://www.jstor.org/stable/1968551`.

[3] M. E. Peskin and D. V. Schroeder, *An Introduction To Quantum Field Theory.* CRC Press, 1995. `https://amzn.com/0201503972`.

[4] S. Weinberg, *The Quantum Theory of Fields.* Cambridge University Press, 1995. `https://amzn.com/0521550017`.

[5] T. Osborne, "Quantum field theory," Oct, 2016. `https://youtu.be/T58H6ofI0pE`.

Coordinate-space wavefunctions for the simple harmonic oscillator via algebraic operator methods

James K. Freericks

(Dated: April 6, 2019)

The simple harmonic oscillator is solved in 8.04-06x via differential equations and via ladder operator methods. But then the traditional construction of the wavefunctions from the eigenstates involves an nth-order differential equation acting on the ground state; this arises from evaluation of $\langle x|\frac{(\hat{a}^\dagger)^n}{\sqrt{n!}}|0\rangle$ in the coordinate representation with $\hat{p} = -i\hbar\frac{d}{dx}$. The method is not efficient to calculate, nor is it illuminating (even if it leads to a so-called Rodrigues formula). In this paper, I will show how one can adapt the conventional ladder operator methods to directly construct the Hermite polynomial recurrence relation for the coordinate-space wavefunctions $\langle x|n\rangle = \psi_n(x)$. This methodology will introduce you to the power of the translation operator; technically, it employs both the Hadamard lemma and the Baker-Campbell-Hausdorff formula in the analysis (identities already worked out in 8.04-06x). Hints for this approach can be found in Arno Bohm's *Quantum Mechanics: Foundations and Applications*, but the strategy taken here is markedly different, emphasizing the use of the translation operator and illustrating how it can be employed more generally for the determination of wavefunctions without differential equations. The paper concludes with a brief sketch of how one can achieve similar results for the momentum-space wavefunctions and beyond to more general systems.

I. INTRODUCTION TO THE TRANSLATION OPERATOR AND EIGENSTATES OF $\hat{x}$ AND $\hat{p}$

In this paper, we describe how one can construct the wavefunctions of the simple harmonic oscillator from purely algebraic methods. While nearly every quantum text describes how to construct the energy eigenfunctions $|n\rangle$ from the ladder operators, almost none describe how to construct the coordinate and momentum-space wavefunctions via operator methods; in fact we have not found any that proceed as we do here, although Bohm hints at alternatives to the "standard" approach [1]. We begin by simply noting that wavefunctions are the overlap of the energy eigenfunctions $|n\rangle$ with the position $|x\rangle$ or momentum $|p\rangle$ eigenfunctions, or $\psi_n(x) = \langle x|n\rangle$ and $\phi_n(p) = \langle p|n\rangle$. So we must start by constructing those position and momentum eigenfunctions. Our strategy is to employ operator methods without resorting to specific representations of the operators, so we do not need to introduce the coordinate space representation of the momentum operator in terms of a derivative with respect to the coordinate. Instead, we follow the representation-independent operator-based approach initiated by Dirac in 1926 [2].

We start with the canonical commutation relation $[\hat{x}, \hat{p}] = \hat{x}\hat{p} - \hat{p}\hat{x} = i\hbar$, where hats are used to denote operators. For this paper, we simply state this as a postulate, but one can strongly motivate the canonical commutation relation from the facts that atoms have sharp spectral lines, the existence of stationary energy eigenstates, and the Planck-Einstein relation for energy and frequency [3]. Our goal is to use these operators to construct position eigenstates. We will assume that an eigenstate for the coordinate at the origin exists $|x{=}0\rangle$, which satisfies $\hat{x}|x{=}0\rangle = 0$, and use that state to construct all other position eigenstates. Note that we do not need to worry about the normalization of the state for anything that we do in this paper, so we do not discuss this issue further here (as it requires calculus to settle it properly).

To start working with the translation operator, we use the so-called Hadamard lemma (derived below), which allows us to evaluate the similarity transformation of the operator $\hat{x}$ as follows (with x_0 a real number):

$$\begin{aligned} e^{\frac{i}{\hbar}x_0\hat{p}}\hat{x}e^{-\frac{i}{\hbar}x_0\hat{p}} &= \hat{x} + \frac{i}{\hbar}x_0[\hat{p}, \hat{x}] - \frac{x_0^2}{2\hbar^2}[\hat{p}, [\hat{p}, \hat{x}]] + \cdots \\ &= \hat{x} + x_0. \end{aligned} \tag{1}$$

The final equality occurs because $[\hat{p}, \hat{x}] = -i\hbar$ is a number, not an operator, and subsequently it commutes with all additional multiple commutators of $\hat{p}$; this truncates the expression after the first commutator. Next, we multiply the left and right hand sides of Eq. (1) by $\exp(-ix_0\hat{p}/\hbar)$ from the left to yield

$$\hat{x}e^{-\frac{i}{\hbar}x_0\hat{p}} = e^{-\frac{i}{\hbar}x_0\hat{p}}(\hat{x} + x_0). \tag{2}$$

With this identity, we establish the eigenfunction $|x_0\rangle$, which satisfies $\hat{x}|x_0\rangle = x_0|x_0\rangle$ (here, x_0 is a number and a label for the Dirac ket):

$$|x_0\rangle = e^{-\frac{i}{\hbar}x_0\hat{p}}|x{=}0\rangle. \tag{3}$$

Operating $\hat{x}$ onto the state $|x_0\rangle$ yields

$$\hat{x}|x_0\rangle = \hat{x}e^{-\frac{i}{\hbar}x_0\hat{p}}|x{=}0\rangle = e^{-\frac{i}{\hbar}x_0\hat{p}}(\hat{x} + x_0)|x{=}0\rangle = x_0|x_0\rangle. \tag{4}$$

The last equality follows because $\hat{x}|x{=}0\rangle = 0$, numbers always commute with operators and the definition of $|x_0\rangle$. Hence, Eqs. (3) and (4) establish that $|x_0\rangle$ is the eigenstate of $\hat{x}$ with eigenvalue x_0.

Similarly, one can also derive that the momentum eigenstates satisfy

$$|p_0\rangle = e^{\frac{i}{\hbar}p_0\hat{x}}|p{=}0\rangle. \tag{5}$$

This result will be used in subsequent calculations.

II. ALGEBRAIC CONSTRUCTION OF THE ENERGY EIGENFUNCTIONS

We will be working with the simple harmonic oscillator, which is defined by the Hamiltonian with a quadratic potential

$$\hat{\mathcal{H}}=\frac{\hat{p}^2}{2m}+\frac{1}{2}m\omega_0^2\hat{x}^2. \tag{6}$$

Here m is the mass of the particle and ω_0 is the characteristic frequency of the harmonic oscillator. The operator method for the harmonic oscillator was fully covered in the 8.04-8.06 sequence. But let's revisit it anyway to understand a bit about the history of the method. It was first introduced in the 1930 edition of Dirac's monograph on quantum mechanics [4]. In that text, Dirac worked with dimensionless position and momentum operators and tried to factorize the Hamiltonian $(\hat{p}^2+\hat{q}^2)/2$ in terms of $\hat{p}\pm i\hat{x}$. The factorization $(\hat{p}+i\hat{x})(\hat{p}-i\hat{x})/2$ produces the Hamiltonian up to a constant shift. The operator approach has since been modified. The i factors are moved from the coordinate to the momentum, and we work with dimensionful coordinate and momentum operators. The dimensionless raising $\hat{a}^\dagger$ and lowering $\hat{a}$ operators are then defined to be

$$\hat{a}^\dagger=\sqrt{\frac{m\omega_0}{2\hbar}}\left(\hat{x}-i\frac{\hat{p}}{m\omega_0}\right),\quad \hat{a}=\sqrt{\frac{m\omega_0}{2\hbar}}\left(\hat{x}+i\frac{\hat{p}}{m\omega_0}\right). \tag{7}$$

One can immediately compute that

$$[\hat{a},\hat{a}^\dagger]=\frac{m\omega_0}{2\hbar}\frac{i}{m\omega_0}2[\hat{p},\hat{x}]=1 \tag{8}$$

or $[\hat{a},\hat{a}^\dagger]=1$ and

$$\hat{\mathcal{H}}=\hbar\omega_0\left(\hat{a}^\dagger\hat{a}+\frac{1}{2}\right). \tag{9}$$

Since $\hat{a}^\dagger\hat{a}$ is a positive semidefinite operator, because

$$\langle\psi|\hat{a}^\dagger\hat{a}|\psi\rangle=\|\hat{a}|\psi\rangle\|^2\geq 0, \tag{10}$$

we immediately learn that the ground state $|0\rangle$ of the simple harmonic oscillator satisfies

$$\hat{a}|0\rangle=0, \tag{11}$$

and the ground-state energy is $E_0=\hbar\omega_0/2$.

The commutator of the Hamiltonian with the raising operator is simple to compute, since

$$[\hat{\mathcal{H}},\hat{a}^\dagger]=\hbar\omega_0[\hat{a}^\dagger\hat{a},\hat{a}^\dagger]=\hbar\omega_0\hat{a}^\dagger[\hat{a},\hat{a}^\dagger]=\hbar\omega_0\hat{a}^\dagger. \tag{12}$$

This can then be generalized by induction to show that

$$\left[\hat{\mathcal{H}},\left(\hat{a}^\dagger\right)^n\right]=n\hbar\omega_0\left(\hat{a}^\dagger\right)^n. \tag{13}$$

Equation (12) is the base case, and then one simply assumes the result is true for $n-1$ and uses the product rule for the commutator to establish the general case. The commutation relation in Eq. (13) is next used to find the higher energy eigenstates. we define the nth excited energy eigenstate $|n\rangle$ to have energy E_n. Then we claim that

$$|n\rangle\propto\left(\hat{a}^\dagger\right)^n|0\rangle. \tag{14}$$

The proof that this is an eigenstate follows by direct computation:

$$\hat{\mathcal{H}}|n\rangle=\left[\hat{\mathcal{H}},\left(\hat{a}^\dagger\right)^n\right]|0\rangle+\left(\hat{a}^\dagger\right)^n\hat{\mathcal{H}}|0\rangle=\hbar\omega_0\left(n+\frac{1}{2}\right)|n\rangle. \tag{15}$$

So, we learn that $E_n=\hbar\omega_0(n+1/2)$ due to the commutator in Eq. (13) and the fact that $|0\rangle$ is an eigenstate of the Hamiltonian with energy $\hbar\omega_0/2$.

Finally, we need to normalize the eigenstate. If we assume the ground state is normalized $\langle 0|0\rangle=1$, then, using the fact that $\hat{a}|0\rangle=0$, we find that

$$\begin{aligned}\langle 0|\left(\hat{a}\right)^n\left(\hat{a}^\dagger\right)^n|0\rangle&=\langle 0|\left(\hat{a}\right)^{n-1}\left[\hat{a},\left(\hat{a}^\dagger\right)^n\right]|0\rangle\\&=n\langle 0|\left(\hat{a}\right)^{n-1}\left(\hat{a}^\dagger\right)^{n-1}|0\rangle\\&=n!\end{aligned} \tag{16}$$

so that we find

$$|n\rangle=\frac{\left(\hat{a}^\dagger\right)^n}{\sqrt{n!}}|0\rangle \tag{17}$$

is the normalized nth excited state with energy E_n. Note that we used the fact that $\left[\hat{a},\left(\hat{a}^\dagger\right)^n\right]=n\left(\hat{a}^\dagger\right)^{n-1}$ in the derivation of the normalization factor. This result for the commutator is easily established by induction, and was covered in 8.04-06, so will not be repeated here.

III. COORDINATE-SPACE WAVEFUNCTIONS

In this section, we will compute the wavefunction in coordinate space using purely algebraic methods. But first, we need to determine two critical operator identities—the Hadamard lemma and the Baker-Campbell-Hausdorff identity.

The Hadamard lemma is given by

$$e^{\hat{A}}\hat{B}e^{-\hat{A}}=\sum_{m=0}^{\infty}\frac{1}{m!}[\hat{A},[\hat{A},\cdots,[\hat{A},\hat{B}]\cdots]_m \tag{18}$$

where the m subscript on the commutators denotes that there are m nested commutators; this lemma is also called the Baker-Hausdorff lemma and the braiding relation. But as far as I can tell, it was first discovered by Campbell in 1897 (see Eq. 19 of Ref. [5]) and hence should be called the Campbell lemma. It is not clear at all where the Hadamard lemma name comes from. To prove the Hadamard lemma, we need to use induction, but first, to get a feel for the identity, we examine the first few terms in the expansion. To start, we expand the two exponentials in a power series, so that

$$e^{\hat{A}}\hat{B}e^{-\hat{A}}=\sum_{n=0}^{\infty}\frac{1}{n!}\left(\hat{A}\right)^{n}\hat{B}\sum_{n'=0}^{\infty}\frac{1}{n'!}(-1)^{n'}\left(\hat{A}\right)^{n'}. \quad (19)$$

Grouping the terms in the power series in terms of powers of the operator $\hat{A}$, we find

$$\begin{aligned}e^{\hat{A}}\hat{B}e^{-\hat{A}}&=\hat{B}+\hat{A}\hat{B}-\hat{B}\hat{A}\\&+\frac{1}{2}\left(\hat{A}^2\hat{B}-2\hat{A}\hat{B}\hat{A}+\hat{B}\hat{A}^2\right)+\cdots\\&=\hat{B}+[\hat{A},\hat{B}]+\frac{1}{2}[\hat{A},[\hat{A},\hat{B}]]+\cdots. \quad (20)\end{aligned}$$

We immediately see that the first few terms of the Hadamard lemma come from this reorganization of the terms in the expansion.

For the full proof, we need to use induction. Our goal is to show that the term with m $\hat{A}$ terms, satisfies

$$\begin{aligned}&\sum_{n=0}^{m}\frac{1}{(m-n)!n!}(-1)^n\left(\hat{A}\right)^{m-n}\hat{B}\left(\hat{A}\right)^{n}\\&=\frac{1}{m!}[\hat{A},[\hat{A},\cdots,[\hat{A},\hat{B}]\cdots]_m. \quad (21)\end{aligned}$$

The term on the left hand side comes from collecting all terms of order $\hat{A}^m$ from the power series in terms of the two exponentials and the right hand side is our goal. The base case, with $m=1$, is already established in Eq. (20). We assume it holds for $m-1$, which we rewrite in the following form, after multiplying both sides by $(m-1)!$,

$$\begin{aligned}&\sum_{n=0}^{m-1}\frac{(m-1)!}{(m-1-n)!n!}(-1)^n\left(\hat{A}\right)^{m-1-n}\hat{B}\left(\hat{A}\right)^{n}\\&=[\hat{A},[\hat{A},\cdots,[\hat{A},\hat{B}]\cdots]_{m-1}. \quad (22)\end{aligned}$$

Take the commutator of both sides with respect to $\hat{A}$ to yield

$$\begin{aligned}&\sum_{n=0}^{m-1}\frac{(m-1)!}{(m-1-n)!n!}(-1)^n\left[\hat{A},\left(\hat{A}\right)^{m-1-n}\hat{B}\left(\hat{A}\right)^{n}\right]\\&=[\hat{A},[\hat{A},\cdots,[\hat{A},\hat{B}]\cdots]_{m}. \quad (23)\end{aligned}$$

The left hand side becomes

$$\begin{aligned}&\sum_{n=0}^{m-1}\frac{(m-1)!}{(m-1-n)!n!}(-1)^n\left(\hat{A}\right)^{m-n}\hat{B}\left(\hat{A}\right)^{n} \quad (24)\\&+\sum_{n=0}^{m-1}\frac{(m-1)!}{(m-1-n)!n!}(-1)^{n+1}\left(\hat{A}\right)^{m-1-n}\hat{B}\left(\hat{A}\right)^{n+1}.\end{aligned}$$

Multiply the first term by $(m-n)/(m-n)=1$. Using the fact that 0!=1, we can then extend the first summation to $n=m$ on the upper limit (which contributes nothing because the numerator, proportional to $m-n$ vanishes when $n=m$). For the second term, we shift $n\rightarrow n-1$ and find

$$\begin{aligned}&\sum_{n=0}^{m}\frac{(m-1)!(m-n)}{(m-n)!n!}(-1)^n\left(\hat{A}\right)^{m-n}\hat{B}\left(\hat{A}\right)^{n} \quad (25)\\&+\sum_{n=1}^{m}\frac{(m-1)!}{(m-n)!(n-1)!}(-1)^n\left(\hat{A}\right)^{m-n}\hat{B}\left(\hat{A}\right)^{n}.\end{aligned}$$

Now we multiply the second term by $n/n=1$ and extend the lower limit to $n=0$ after rewriting the denominator as $n!$ (which adds zero, since $0!=1$ again). Adding the two terms together and combining the numerator into $m!$, then finally establishes Eq. (21). This completes the proof of the Hadamard lemma.

The Hadamard lemma can now be employed to establish additional identities. Any function $f(\hat{B})$ of an operator $\hat{B}$ that can be written as a power series in $\hat{B}$ satisfies

$$\begin{aligned}e^{\hat{A}}f(\hat{B})e^{-\hat{A}}&=e^{\hat{A}}\sum_{m=0}^{\infty}f_m\hat{B}^m e^{-\hat{A}}=\sum_{m=0}^{\infty}f_m\left(e^{\hat{A}}\hat{B}e^{-\hat{A}}\right)^m\\&=f(e^{\hat{A}}\hat{B}e^{-\hat{A}})\\&=f\left(\sum_{m=0}^{\infty}\frac{1}{m!}[\hat{A},[\hat{A},\cdots,[\hat{A},\hat{B}]\cdots]_m\right). \quad (26)\end{aligned}$$

This is an exact relation. Choosing $f(\hat{B})=\exp(\hat{B})$ then yields an important identity after some simple rearranging of terms:

$$e^{\hat{A}}e^{\hat{B}}=e^{\sum_{m=0}^{\infty}\frac{1}{m!}[\hat{A},[\hat{A},\cdots,[\hat{A},\hat{B}]\cdots]_m}e^{\hat{A}}. \quad (27)$$

This relation is often called a braiding relation. When $[\hat{A},\hat{B}]$ is a number and not an operator, then we have the re-ordering identity

$$e^{\hat{A}}e^{\hat{B}}=e^{\hat{B}}e^{\hat{A}}e^{[\hat{A},\hat{B}]}, \quad (28)$$

which includes a correction term when the exponential operators are re-ordered.

This last identity is not enough to allow us to carry out our calculation. We also need an identity that is "halfway" between the re-ordering identity, which rewrites the exponential of the sum of the operators in terms of the two exponential operators and a correction factor. This identity is an alternate form of the famous Baker-Campbell-Hausdorff (BCH) identity [6–8] (which is most aptly called the exponential identity). Unlike the Hadamard lemma and its application to exponential re-ordering, the BCH identity does not have any simple explicit formula for its result in the general case (although one can write the result in closed form [9, 10]). Fortunately for us, we need it only for the case where $[\hat{A},\hat{B}]$ is a number, which commutes with all other operators. In this case, the BCH formula is rather easy to derive through a differential equation (while it can be derived completely algebraically, the derivation is rather long and takes up too much space to present here). The differential equation approach is rather straightforward though and we present it next.

We assume $[\hat{A},[\hat{A},\hat{B}]]=[\hat{B},[\hat{A},\hat{B}]]=0$ in the following. Then we define the operator function $f(\lambda)$ by

$$f(\lambda)=e^{-\lambda\hat{A}}e^{\lambda(\hat{A}+\hat{B})}e^{-\lambda\hat{B}}. \tag{29}$$

Clearly, $f(\lambda{=}0)=\mathbb{I}$, and the derivative satisfies

$$\begin{aligned}\frac{df(\lambda)}{d\lambda}&=e^{-\lambda\hat{A}}(-\hat{A}+\hat{A}+\hat{B})e^{\lambda(\hat{A}+\hat{B})}e^{-\lambda\hat{B}}\\&-e^{-\lambda\hat{A}}e^{\lambda(\hat{A}+\hat{B})}\hat{B}e^{-\lambda\hat{B}}\end{aligned} \tag{30}$$

because $d\exp(\lambda\hat{A})/d\lambda=\hat{A}\exp(\lambda\hat{A})$ and $\hat{A}$ commutes with $\exp(\lambda\hat{A})$. Using the Hadamard lemma, we find that

$$e^{\lambda(\hat{A}+\hat{B})}\hat{B}=\left(\hat{B}+\lambda[\hat{A},\hat{B}]\right)e^{\lambda(\hat{A}+\hat{B})}. \tag{31}$$

Using this relation transforms Eq. (30) into

$$\frac{df(\lambda)}{d\lambda}=-\lambda[\hat{A},\hat{B}]f(\lambda) \tag{32}$$

because the commutator commutes with $\hat{A}$ and $\hat{B}$. This differential equation can be integrated immediately to yield

$$f(\lambda)=f(\lambda{=}0)e^{-\frac{1}{2}\lambda^2[\hat{A},\hat{B}]}. \tag{33}$$

Using the fact that $f(\lambda{=}0)=\mathbb{I}$ and setting $\lambda=1$, finally yields the Baker-Campbell-Hausdorff result when the commutator commutes with all other operators as

$$e^{\hat{A}}e^{\hat{B}}=e^{\hat{A}+\hat{B}+\frac{1}{2}[\hat{A},\hat{B}]} \tag{34}$$

and

$$e^{\hat{B}}e^{\hat{A}}=e^{\hat{A}+\hat{B}-\frac{1}{2}[\hat{A},\hat{B}]}. \tag{35}$$

The BCH proof is completely consistent with the braiding relation in Eq. (28), as can be seen with a little rearranging of the terms.

We now have all the technical tools needed to determine the coordinate-space wavefunction $\psi_n(x)=\langle x|n\rangle$. Using the position eigenstates and the energy eigenstates, we immediately find that

$$\psi_n(x)=\langle x|n\rangle=\frac{1}{\sqrt{n!}}\langle x{=}0|e^{\frac{i}{\hbar}x\hat{p}}\left(\hat{a}^\dagger\right)^n|n{=}0\rangle. \tag{36}$$

The operators $\hat{p}$ and $\hat{a}^\dagger$ can be easily identified by their hats.

The strategy to determine the wavefunction takes a few steps. First, we replace the momentum operator in the exponent of the translation operator by its expression in terms of the ladder operators

$$\hat{p}=-i\sqrt{\frac{m\hbar\omega_0}{2}}\left(\hat{a}-\hat{a}^\dagger\right). \tag{37}$$

The wavefunction becomes

$$\psi_n(x)=\frac{1}{\sqrt{n!}}\langle x{=}0|e^{\sqrt{\frac{m\omega_0}{2\hbar}}x(\hat{a}-\hat{a}^\dagger)}\left(\hat{a}^\dagger\right)^n|n{=}0\rangle. \tag{38}$$

Then we use the BCH relation in Eq. (34) with $\hat{A}\propto\hat{a}^\dagger$ and $\hat{B}\propto\hat{a}$ to factorize the translation operator into a factor involving the raising operator on the left and the lowering operator on the right. This is given by

$$\begin{aligned}\psi_n(x)&=\frac{1}{\sqrt{n!}}e^{-\frac{m\omega_0}{4\hbar}x^2}\\&\times\langle x{=}0|e^{-\sqrt{\frac{m\omega_0}{2\hbar}}x\hat{a}^\dagger}e^{\sqrt{\frac{m\omega_0}{2\hbar}}x\hat{a}}\left(\hat{a}^\dagger\right)^n|n{=}0\rangle.\end{aligned} \tag{39}$$

Third, we take the relation in Eq. (26) and multiply by $\exp(\hat{A})$ on the right to create the general functional braiding relation and apply it to the matrix element for the wavefunction with $f(\hat{B})=(\hat{a}^\dagger)^n$. This yields

$$\begin{aligned}\psi_n(x)&=\frac{1}{\sqrt{n!}}e^{-\frac{m\omega_0}{4\hbar}x^2}\\&\times\langle x{=}0|e^{-\sqrt{\frac{m\omega_0}{2\hbar}}x\hat{a}^\dagger}\left(\hat{a}^\dagger+\sqrt{\frac{m\omega_0}{2\hbar}}x\right)^n e^{\sqrt{\frac{m\omega_0}{2\hbar}}x\hat{a}}|n{=}0\rangle.\end{aligned} \tag{40}$$

The rightmost exponential factor gives 1 when it operates on the state because $\hat{a}|n{=}0\rangle=0$

$$\begin{aligned}\psi_n(x)&=\frac{1}{\sqrt{n!}}e^{-\frac{m\omega_0}{4\hbar}x^2}\\&\times\langle x{=}0|e^{-\sqrt{\frac{m\omega_0}{2\hbar}}x\hat{a}^\dagger}\left(\hat{a}^\dagger+\sqrt{\frac{m\omega_0}{2\hbar}}x\right)^n|n{=}0\rangle.\end{aligned} \tag{41}$$

Next, we introduce a new exponential factor with the opposite sign of the exponent multiplying the ground-state wavefunction, because it equals 1 when operating against the state:

$$\begin{aligned}\psi_n(x)&=\frac{1}{\sqrt{n!}}e^{-\frac{m\omega_0}{4\hbar}x^2}\\&\times\langle x{=}0|e^{-\sqrt{\frac{m\omega_0}{2\hbar}}x\hat{a}^\dagger}\left(\hat{a}^\dagger+\sqrt{\frac{m\omega_0}{2\hbar}}x\right)^n e^{-\sqrt{\frac{m\omega_0}{2\hbar}}x\hat{a}}|n{=}0\rangle.\end{aligned} \tag{42}$$

The general functional braiding relation is used again to bring the rightmost exponential factor to the left through the $\hat{a}^\dagger$ term raised to the nth power

$$\begin{aligned}\psi_n(x)&=\frac{1}{\sqrt{n!}}e^{-\frac{m\omega_0}{4\hbar}x^2}\\&\times\langle x{=}0|e^{-\sqrt{\frac{m\omega_0}{2\hbar}}x\hat{a}^\dagger}e^{-\sqrt{\frac{m\omega_0}{2\hbar}}x\hat{a}}\left(\hat{a}^\dagger+\sqrt{\frac{2m\omega_0}{\hbar}}x\right)^n|n{=}0\rangle.\end{aligned} \tag{43}$$

Now, we use the BCH relation again to combine the two exponentials into one which increases the Gaussian exponent by a factor of two

$$\begin{aligned}\psi_n(x)&=\frac{1}{\sqrt{n!}}e^{-\frac{m\omega_0}{2\hbar}x^2}\\&\times\langle x{=}0|e^{-\sqrt{\frac{m\omega_0}{2\hbar}}x(\hat{a}^\dagger+\hat{a})}\left(\hat{a}^\dagger+\sqrt{\frac{2m\omega_0}{\hbar}}x\right)^n|n{=}0\rangle.\end{aligned} \tag{44}$$

Finally, we use the fact that the sum of the raising and lowering operator is proportional to the position operator

$$\hat{x} = \sqrt{\frac{\hbar}{2m\omega_0}}\left(\hat{a} + \hat{a}^\dagger\right). \tag{45}$$

We replace the sum of the raising and lowering operator in the exponent and let it act on the state to the left, where it gives 1, because the position operator annihilates the state $\langle x{=}0|$. The wavefunction has now become

$$\psi_n(x) = \frac{1}{\sqrt{n!}} e^{-\frac{m\omega_0}{2\hbar}x^2} \langle x{=}0| \left(\hat{a}^\dagger + \sqrt{\frac{2m\omega_0}{\hbar}}x\right)^n |n{=}0\rangle. \tag{46}$$

We are almost done now. We have achieved a reduction of the problem into a Gaussian function multiplied by a matrix element which is an nth degree polynomial in x. All that is left is evaluating the polynomial. To do this, we first introduce a definition of the polynomial, which we will then show is a so-called Hermite polynomial H_n. We write the wavefunction as

$$\psi_n(x) = \frac{1}{\sqrt{n!2^n}} H_n\left(\sqrt{\frac{m\omega_0}{\hbar}}x\right) e^{-\frac{m\omega_0}{2\hbar}x^2} \langle x{=}0|n{=}0\rangle, \tag{47}$$

which defines the Hermite polynomial via

$$\begin{aligned} H_n\left(\sqrt{\frac{m\omega_0}{\hbar}}x\right) &= \frac{\sqrt{2^n}}{\langle x{=}0|n{=}0\rangle} \\ &\quad \times \langle x{=}0| \left(\hat{a}^\dagger + \sqrt{\frac{2m\omega_0}{\hbar}}x\right)^n |n{=}0\rangle. \end{aligned} \tag{48}$$

Note that the number $\langle x{=}0|n{=}0\rangle$ is the normalization constant for the ground-state wavefunction; we will discuss how to determine it below. This definition allows us to immediately determine the first two polynomials H_0 and H_1. Choosing $n = 0$ in Eq. (49) immediately yields $H_0 = 1$. Choosing $n = 1$, produces

$$\begin{aligned} H_1\left(\sqrt{\frac{m\omega_0}{\hbar}}x\right) &= 2\sqrt{\frac{m\omega_0}{\hbar}}x \\ &\quad + \frac{\sqrt{2}}{\langle x{=}0|n{=}0\rangle}\langle x{=}0|\hat{a}^\dagger|n{=}0\rangle. \end{aligned} \tag{49}$$

The second term vanishes for the following reason: we first note that $\hat{a}^\dagger|n{=}0\rangle = (\hat{a}^\dagger + \hat{a})|n{=}0\rangle$, because the lowering operator annihilates the ground state. Hence $\hat{a}^\dagger|n{=}0\rangle \propto \hat{x}|n{=}0\rangle$. But $\langle x{=}0|\hat{x} = 0$, so this state vanishes when it acts against the position eigenstate.

For the remainder of the Hermite polynomials, we work out a two-term recurrence relation. We focus on the nontrivial matrix element, and factorize the terms as follows:

$$\langle x{=}0| \left(\hat{a}^\dagger + \sqrt{\frac{2m\omega_0}{\hbar}}x\right)\left(\hat{a}^\dagger + \sqrt{\frac{2m\omega_0}{\hbar}}x\right)^{n-1} |n{=}0\rangle. \tag{50}$$

The constant term in the first factor can be removed from the matrix element and it multiplies the matrix element with $n{-}1$ operator factors (which is proportional to H_{n-1}). For the remaining term proportional to $\hat{a}^\dagger$, we replace the operator by $\hat{a}^\dagger \rightarrow \hat{a}^\dagger + \hat{a} - \hat{a}$. The term proportional to $\hat{a}^\dagger + \hat{a}$ is proportional to $\hat{x}$, and so it annihilates when it operates on the left against the $\langle x{=}0|$ state. The remaining $\hat{a}$ operator can be replaced by the commutator of the $n-1$ power of the $\hat{a}^\dagger$ term, because $\hat{a}|n{=}0\rangle = 0$. The remaining commutator is straightforward to evaluate via

$$\left[\hat{a}, \left(\hat{a}^\dagger + \sqrt{\frac{2m\omega_0}{\hbar}}x\right)^{n-1}\right] = (n{-}1)\left(\hat{a}^\dagger + \sqrt{\frac{2m\omega_0}{\hbar}}x\right)^{n-2}. \tag{51}$$

We can assemble all of these results to find the recurrence relation for the Hermite polynomials, which becomes

$$\begin{aligned} H_n\left(\sqrt{\frac{m\omega_0}{\hbar}}x\right) &= 2\sqrt{\frac{m\omega_0}{\hbar}}xH_{n-1}\left(\sqrt{\frac{m\omega_0}{\hbar}}x\right) \\ &\quad - 2(n-1)H_{n-2}\left(\sqrt{\frac{m\omega_0}{\hbar}}x\right). \end{aligned} \tag{52}$$

This recurrence relation, which is of the form $H_n(z) = 2zH_{n-1}(z) - 2(n-1)H_{n-2}(z)$, is the standard Hermite polynomial recurrence relation when $H_0(z) = 1$ and $H_1(z) = 2z$, as we have here.

We have now established that the simple-harmonic-oscillator wavefunction satisfies

$$\psi_n(x) = \frac{1}{\sqrt{n!2^n}} H_n\left(\sqrt{\frac{m\omega_0}{\hbar}}x\right) e^{-\frac{m\omega_0}{2\hbar}x^2} \langle x{=}0|n{=}0\rangle. \tag{53}$$

The last task in front of us is to find the normalization factor. This is computed for the ground state via

$$|\langle x{=}0|n{=}0\rangle|^2 \int_{-\infty}^{\infty} dx e^{-\frac{m\omega_0}{\hbar}x^2} = 1 \tag{54}$$

or

$$\langle x{=}0|n{=}0\rangle = \left(\frac{m\omega_0}{\pi\hbar}\right)^{\frac{1}{4}}. \tag{55}$$

This has finally produced the wavefunction for the simple harmonic oscillator using algebraic methods. Note that calculus is only needed for the last normalization step since the BCH formula can also be derived algebraically (not shown here).

In Table I, we list the first six Hermite polynomials as a function of the argument z. In Fig. 1, we plot the wavefunctions (left) and the probability distributions (right) for the lowest few eigenfunctions of the simple harmonic oscillator. The different curves are centered on their energies. These wavefunctions behave as we expect them to. The number of nodes starts from zero in the ground state and increases by one with each higher energy level. The wavefunctions oscillate in the allowed region, and exponentially decay in the forbidden region. The

n	$H_n(z)$
0	1
1	$2z$
2	$4z^2-2$
3	$8z^3-12z$
4	$16z^4-48z^2+12$
5	$32z^5-160z^3+120z$

Table I. First six Hermite polynomials.

ground state is an even function of x and the higher-energy states alternate from being odd and even as the energy is increased. Finally, the wavefunctions for higher-energy states have their probability largest near the turning points as expected as well.

IV. MOMENTUM-SPACE WAVEFUNCTIONS

In this short section, we will sketch how one can use similar methods to compute the wavefunctions in momentum space. To start, the momentum "boost" operator is given by $\exp(ip\hat{x}/\hbar)$ and the momentum eigenstates satisfy

$$|p\rangle = e^{\frac{i}{\hbar}p\hat{x}}|p{=}0\rangle. \tag{56}$$

The wavefunction satisfies $\phi_n(p) = (i)^n\langle p|n\rangle$; we added an additional global phase to ensure we reproduce the standard results—you will see why this is important below. The wavefunction can be expressed in terms of the operators as

$$\phi_n(p) = \frac{(i)^n}{\sqrt{n!}}\langle p{=}0|e^{-\frac{i}{\hbar}p\hat{x}}\left(\hat{a}^\dagger\right)^n|n{=}0\rangle. \tag{57}$$

The remainder of the calculations proceeds as before for the coordinate-space wavefunction. We start by replacing the $\hat{x}$ operator by the sum of raising and lowering operators; in this case, the coefficients of the raising and lowering operators are now purely imaginary. Then we use BCH to factorize the exponential into a raising operator on the left and lowering operator on the right. Then we use the braiding identity to move the exponential through the $(\hat{a}^\dagger)^n$ terms and let it operate on the ground state, where it produces 1. The shift term added to the raising operator is now purely imaginary. Next, we introduce a factor of 1 at the ground state, which is the same exponential operator of the lowering operator, but with the sign of the exponent changed. Then we use the braiding identity to bring it back to the left, BCH to place the operators in one exponential, and evaluate the momentum operator on the momentum eigenstate. At this stage, the wavefunction has become

$$\phi_n(p) = \frac{(i)^n}{\sqrt{n!}}e^{-\frac{p^2}{2\hbar\omega_0 m}}\langle p{=}0|\left(\hat{a}^\dagger - i\frac{\sqrt{2}p}{\sqrt{\hbar\omega_0 m}}\right)^n|n{=}0\rangle. \tag{58}$$

Note the additional factors of i and the replacement of $\sqrt{m\omega_0/\hbar}x$ by $p/\sqrt{\hbar\omega_0 m}$. The Hermite polynomial now needs to be defined via

$$\begin{aligned} H_n\left(\frac{p}{\sqrt{\hbar\omega_0 m}}\right) &= \frac{\sqrt{2^n}i^n}{\langle p{=}0|n{=}0\rangle} \\ &\quad\times\langle p{=}0|\left(\hat{a}^\dagger - i\frac{\sqrt{2}p}{\sqrt{\hbar\omega_0 m}}\right)^n|n{=}0\rangle \end{aligned} \tag{59}$$

Starting with $H_0 = 1$ and $H_1 = 2p/\sqrt{\hbar\omega_0 m}$, we find the same Hermite polynomials as in table I, but now with $z = p/\sqrt{\hbar\omega_0 m}$. The rest of the calculation is similar to the coordinate space calculation. The normalization factor is found by a simple integral. One can see that this procedure will lead to the momentum-space wavefunction, which finally satisfies

$$\phi_n(p) = \frac{1}{(\pi\hbar\omega_0 m)^{\frac{1}{4}}}\frac{1}{\sqrt{n!2^n}}H_n\left(\frac{p}{\sqrt{\hbar\omega_0 m}}\right)e^{-\frac{p^2}{2\hbar\omega_0 m}}. \tag{60}$$

Aside from some different constants, the coordinate-space and momentum-space wavefunctions have identical functional forms. This is expected from the outset, because the Hamiltonian is quadratic in both momentum *and* position. Hence, each wavefunction must be isomorphic.

V. CONCLUSIONS

We end this paper with a short discussion of where one can go further with this approach, First, any problem that can be solved analytically with differential equations can also be solved algebraically with operators. The approach is commonly called the Schrödinger factorization method, and was introduced by Schrödinger in the early 1940s [11, 12]. Most textbooks that present this methodology use it to compute the energy eigenvalues, but often employ the more standard approach of expressing the raising and lowering operators in terms of differential operators to create first-order differential equations to compute the wavefunctions (this strategy was discussed for the simple harmonic oscillator in the 8.04-06 series and appears in almost all textbooks). But, as you can see, the approach presented here, which employs the translation (or "boost") operators, is a novel technique to find the wavefunctions. The number of other problems this can be applied to is large (including at least the Ploschl-Teller potential, the Morse potential, and the radial problems for the spherical box, the harmonic oscillator and the Coulomb problem in three dimensions). The three-dimensional radial problems are a bit more complex, because the translation operator uses the radial momentum operator. A careful computation finds that the radial translation operator has extra terms in it that cause it to vanish as $r \to 0$, because one cannot translate the radial coordinate to go less than 0. Nevertheless, one can find wavefunctions in this algebraic fashion there as well. The development of these methods will be completed elsewhere.

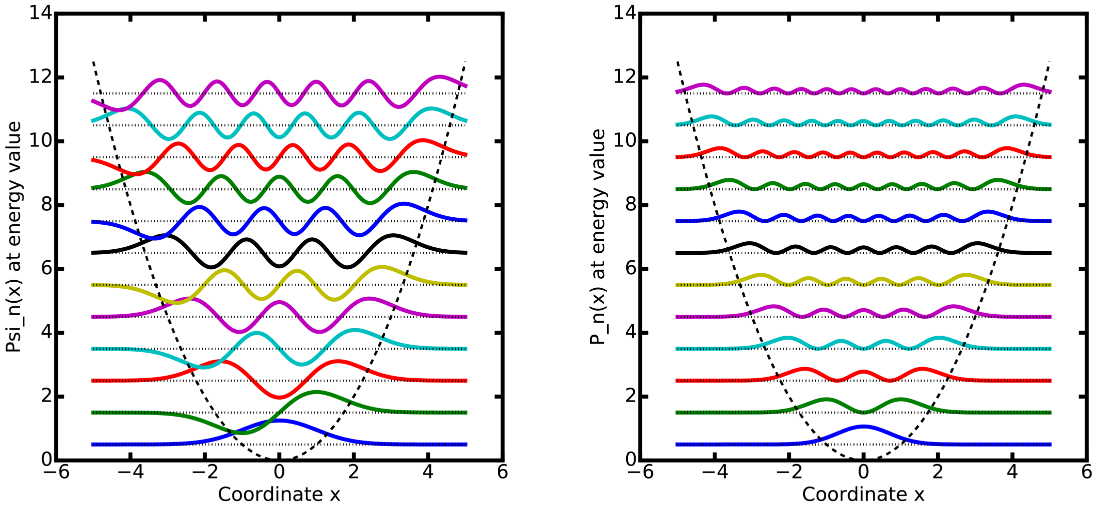

Figure 1. In the panel on the left, we plot the wavefunctions, while in the panel on the right, we plot the probability distributions for the simple harmonic oscillator. The results are each centered on their respective energy levels.

As far as I am aware, this approach to solving the Schrödinger equation and finding the wavefunction is a new approach. It does not appear to be in any textbook I have seen (if you have seen it somewhere, please let me know). Interestingly, many textbooks use the translation operator to compute the overlap between position and momentum eigenstates $\langle x|p\rangle$, but the extension to use similar methods to compute wavefunctions for bound-state problems seems to not have been developed elsewhere.

We also find it compelling that one can determine energy eigenvalues and energy eigenstates for many problems using just high school level algebra. This dispels the oft heard myth that one needs to know calculus, differential equations, and special functions to solve bound-state problems. One doesn't!

Stay tuned for more details in the future as these ideas get incorporated into a book that provides a radically different pedagogy for teaching quantum mechanics. It will be called *Quantum Mechanics without Calculus* [13]. While it cannot teach everything (most notable is the omission of scattering, perturbation theory and semiclassics), it does cover many topics at a much higher level than in conventional textbooks and eventually brings readers who master the material close to the point where they can contribute to current research problems.

[1] Arno Bohm, *Quantum Mechanics Foundations and Applications*, 3rd ed. (New York: Springer-Verlag, Inc., 1993)

[2] P. A. M. Dirac, "Elimination of the nodes in quantum mechanics," Proc. Roy. Soc. (London), Ser. A: Mathematical, Physical and Engineering Sciences **111**, 281–305 (1926).

[3] Herbert S. Green, *Matrix Mechanics* (Groningen, Netherlands: P. Noordhoff Ltd., 1965)

[4] P. A. M. Dirac, *The Principles of Quantum Mechanics* 1st ed. (Oxford, Oxford University Press, 1930).

[5] Rüdiger Achilles and Andrea Bonfiglioli, "The early proofs of the theorem of Campbell, Baker, Hausdorff, and Dynkin," Arch. Hist. Exact Sci. **66**, 295–358 (2012).

[6] H. F. Baker, "On the Exponential Theorem for a Simply Transitive Continuous Group, and the Calculation of the Finite Equations from the Constants of Structure," Proc. Lond. Math. Soc., **34,** 91–129 (1901); "On the Calculation of the Finite Equations of a Continuous Group," Proc. Lond. Math. Soc. **35,** 332–333 (1902).

[7] J. E. Campbell, "On a Law of Combination of Operators bearing on the Theory of Continuous Transformation Groups," Proc. Lond. Math. Soc., **28**, 381–390 (1896); "On a Law of Combination of Operators (Second Paper)*," Proc. Lond. Math. Soc., **29,** 14–32 (1897).

[8] F. Hausdorff, "Die symbolische Exponentialformel in der Gruppentheorie," Ber. Verh. Saechs Akad. Wiss. (Leipzig) **58** 19–48 (1906).

[9] E. B. Dynkin, "Calculation of the coefficients in the Campbell-Hausdorff formula," (Russian) Doklady Akademii Nauk SSSR **57**, 323–326 (1947).

[10] Ravinder R. Puri, *Non-relativistic quantum mechanics* (Cambridge, Cambridge University Press, 2017); the derivation of the BCH formula is in Chapter 2.8.

[11] E. Schrödinger "A Method of Determining Quantum-Mechanical Eigenvalues and Eigenfunctions," Proc. Royal Irish Acad. Section A: Math. and Phys. Sci. **46** 9–16 (1940/1941).

[12] E. Schrödinger "Further Studies on Solving Eigenvalue Problems by Factorization," Proc. Royal Irish Acad. Section A: Math. and Phys. Sci. **46,** 183–206 (1940/1941).

[13] James K. Freericks, *Quantum Mechanics without Calculus*, in preparation.

Decomposition of unitary matrix into quantum gates

Dmytro Fedoriaka

(Dated: June 19, 2019)

Algorithm is proposed to convert arbitrary unitary matrix to a sequence of X gates and fully controlled R_y, R_z and R_1 gates. This algorithm is used to generate Q# implementation for arbitrary unitary matrix. Some optimizations are considered and complexity of result is analyzed.

I. INTRODUCTION

In this paper I will solve a problem of implementing a unitary matrix with a sequence of quantum gates which can be expressed using standard library of Q# language.

Q# is a domain-specific programming language used for expressing quantum algorithms, developed by Microsoft [1]. Its standard library currently doesn't support explicitly specifying unitary operation by a matrix. Instead, programmer has to express it as a sequence of built-in quantum gates. However, while designing some quantum algorithms it may be necessary to implement a unitary operation which is given by a matrix and decomposition of this matrix into standard gates is not obvious (for example, [2, problem B2]).

In this paper I will describe algorithm which can be used to generate Q# code using only fully-controlled R_x, R_y and R_1 gates and single-qubit X gates. Length of this code (in terms of number of commands) will be $\mathcal{O}(4^n)$, where n is number of qubits.

I will start by giving some basic definitions. Then I will describe proposed algorithm (which is based on [3, 4]). Then I will analyze complexity of this algorithm. I will conclude with discussion of several related topics.

II. DEFINITIONS

Qubits. *Qubit* is a quantum system which can be in superposition of two basis states $|0\rangle$ and $|1\rangle$.

Register of n qubits is a quantum system which consists of n qubits and its state space is tensor product of state spaces of those qubits. Register's state space is span of 2^n basis states, each of which is tensor product of qubits' basis states (although not any register's state is a tensor product of qubits' states).

We denote states in qubit register of n qubits by binary string consisting of n bits. The leftmost bit in string corresponds to qubit 0, rightmost bit corresponds to qubit $n-1$. Also we denote state by an integer $i \in 0, \dots 2^n - 1$, represented by that binary string in little-endian style (i.e. leftmost bit is least significant). For example, if $n = 5$ then register has 32 basis states, and state 25 is

$$|25\rangle = |10011\rangle = |1\rangle \otimes |0\rangle \otimes |0\rangle \otimes |1\rangle \otimes |1\rangle \,. \tag{1}$$

If i is index of state, $i[j]$ is j-th bit of this index (i.e. j-th character in binary string representing i).

All notation is 0-indexed.

Quantum gate acting on one qubit is a unitary operator acting on state space of this qubit. Similarly, quantum gate acting on register of several qubits is a unitary operator acting on space which is tensor product of state spaces of those qubits.

Matrices. Complex-valued matrix $A \in \mathbb{C}^{n\times n}$ is called *unitary* if $U^\dagger = U^{-1}$. $\mathrm{U}(n)$ is set of all unitary matrices of size $n \times n$.

Matrix is called *special unitary*, if it is unitary and has determinant 1. $\mathrm{SU}(n)$ is set of all special unitary matrices of size $n \times n$.

Two-level unitary matrix is a unitary matrix obtained from identity matrix by changing a 2×2 principal submatrix.

Any quantum gate on register of n qubits, being an unitary operator, can be completely defined by unitary matrix $2^n \times 2^n$. Indexing of matrix elements follows the same pattern as indexing of register states, i.e. $U_{ij} = \langle i| U |j\rangle$, where $i, j \in [0, 2^n - 1]$.

Controlled gates. Let's consider a gate U acting on register t. Let's add a new qubit c to this register and define new gate CU as follows. If c is in state $|1\rangle$, this gate applies U on t, but if c is in state $|0\rangle$, this gate doesn't change the register's state:

$$\begin{cases} CU(|a\rangle \otimes |0\rangle) = |a\rangle \otimes |0\rangle \,, \\ CU(|a\rangle \otimes |1\rangle) = (U\,|a\rangle) \otimes |1\rangle \,. \end{cases} \tag{2}$$

Such gate is called *controlled*, qubits in t are called *target* qubits, and qubit c is called *control* qubit.

Example of a controlled gate is CNOT (controlled-X) gate:

$$CNOT = \begin{pmatrix} 1&0&0&0 \\ 0&1&0&0 \\ 0&0&0&1 \\ 0&0&1&0 \end{pmatrix}. \tag{3}$$

Similarly, let's define controlled gate with multiple control qubits. Gate CU acting on register $t_0, \dots, t_{T-1}, c_0, \dots, c_{C-1}$ is controlled by qubits $c_0, \dots, c_{C-1}$, if

$$CU(|a\rangle \otimes |b\rangle) = \begin{cases} (U\,|a\rangle) \otimes |b\rangle & \text{if } |b\rangle = |1\dots1\rangle \,, \\ |a\rangle \otimes |b\rangle & \text{otherwise,} \end{cases} \tag{4}$$

where $|a\rangle$ - basis state of target qubits $t_0, \dots t_{T-1}$, $|b\rangle$ - basis state of control qubits $c_0, \dots c_{C-1}$, $U \in \mathrm{U}(2^T)$. In other words, it applies U on target bits only if all control qubits are set to $|1\rangle$.

Matrix of a controlled gate has special form. It's an identity matrix $2^{C+T} \times 2^{C+T}$, where lower right submatrix $2^T \times 2^T$ is replaced by U. If $T = 1$, this matrix is two-level unitary.

We will denote I — unitary matrix; $X = \left(\begin{smallmatrix} 0 & 1 \\ 1 & 0 \end{smallmatrix}\right)$ — Pauli X matrix, also known as X gate or NOT gate.

Expression $a \oplus b$ means bitwise addition modulo 2 (also known as XOR), e.g. $25 \oplus 13 = 20$.

III. ALGORITHM

A. Two-level decomposition

First step is to decompose our unitary matrix $A \in \mathrm{U}(d)$ into product of two-level unitary matrices ($d = 2^n$). Following algorithm is based on algorithm in [4].

Let's make elements in first column equal to zeroes by multiplying matrix (from the right) by two-level unitary matrices. Assume that at current step elements $A_{0,i+1} \ldots A_{0,d-1}$ are already zeroes and we want to make element $A_{0,i}$ zero as well, without affecting already eliminated elements. This can be written as:

$$\left(\begin{smallmatrix} \ldots & a & b & 0 & \ldots & 0 \\ \ldots & \ldots & \ldots & \ldots & \ldots & \ldots \end{smallmatrix}\right) U = \left(\begin{smallmatrix} \ldots & c & 0 & 0 & \ldots & 0 \\ \ldots & \ldots & \ldots & \ldots & \ldots & \ldots \end{smallmatrix}\right). \tag{5}$$

Suppose $a \neq 0, b \neq 0$.

Matrix U can be chosen to be two-level unitary matrix acting on elements $(i, i+1)$ with non-trivial unitary 2×2 submatrix U', where

$$(a\ b)\ U' = (c\ 0). \tag{6}$$

Let's show that we can always find such special unitary matrix U' which satisfies condition (6), and makes c real positive number.

Any special unitary matrix U' can be written in form [3, §4.6]:

$$U' = \begin{pmatrix} \cos\theta e^{i\lambda} & \sin\theta e^{i\mu} \\ -\sin\theta e^{i\mu} & \cos\theta e^{-i\lambda} \end{pmatrix}, \tag{7}$$

where $\theta, \lambda, \mu \in \mathbb{R}$.

Substituting (7) in (6), we get:

$$\begin{cases} a\cos\theta e^{i\lambda} - b\sin\theta e^{i\mu} = c, \\ a\sin\theta e^{i\mu} + b\cos\theta e^{-i\lambda} = 0. \end{cases} \tag{8}$$

From second equation we get:

$$\tan\theta = -\frac{b}{a}\exp\left(-i(\lambda + \mu)\right). \tag{9}$$

Let's demand that $\tan\theta$ is real and positive. Then:

$$\theta = \arctan\left(\left|\frac{b}{a}\right|\right), \tag{10}$$

$$\arg\left(-\frac{b}{a} exp(-i(\lambda + \mu))\right) = \pi + \arg(b) - \arg(a) - \lambda - \mu = 0 \tag{11}$$

From (11) we can express μ:

$$\mu = \pi + \arg(b) - \arg(a) - \lambda. \tag{12}$$

Let's find λ. For this, let's express c from first equation in (8), using (9):

$$c = \cos\theta(ae^{i\lambda} - b\tan\theta e^{-i\mu}) = \cos\theta\left(ae^{i\lambda} + \frac{b^2 e^{-2i\mu}}{ae^{-i\mu}}\right) \tag{13}$$

Let $\lambda = -\arg a$. Then $ae^{i\lambda} = |a|e^{i\arg a}e^{-i\arg a} = |a|$. From (12) we get $\mu = \pi + \arg b$, therefore $be^{-i\mu} = |b|e^{i\arg b}e^{-i\pi}e^{-i\arg b} = -|b|$, so

$$c = \cos\theta \cdot \left(|a| + \frac{|b|^2}{|a|}\right). \tag{14}$$

We have c real and positive, exactly what we wanted, so matrix U' is given by formula (7) with

$$\theta = \arctan\left(\left|\frac{b}{a}\right|\right);\ \lambda = -\arg(a);\ \mu = \pi + \arg(b). \tag{15}$$

If $b = 0$, we can just skip this step, formally putting $U' = I$. If $a = 0$, we can just replace columns by taking $U' = X = \left(\begin{smallmatrix} 0 & 1 \\ 1 & 0 \end{smallmatrix}\right)$ and proceed.

After we finished eliminating first row, all elements in it except first will be zeroes and matrix still will be unitary. First element then must have magnitude 1 (because norm of row in unitary matrix must be 1). As our construction always makes c real and positive, it must have value 1. All other elements in first column must be zeroes, because norm of first column must be 1. So, we get $(d-1)$-level matrix, and we can apply the same algorithm to remaining $(d-1) \times (d-1)$ submatrix and repeat it until only 2×2 non-trivial submatrix is left in A, which will make A 2-level unitary matrix.

For example, for matrix 4×4 this process looks like this:

$$\begin{pmatrix} * & * & * & * \\ * & * & * & * \\ * & * & * & * \\ * & * & * & * \end{pmatrix} \to \begin{pmatrix} 1 & 0 & 0 & 0 \\ 0 & * & * & * \\ 0 & * & * & * \\ 0 & * & * & * \end{pmatrix} \to \begin{pmatrix} 1 & 0 & 0 & 0 \\ 0 & 1 & 0 & 0 \\ 0 & 0 & * & * \\ 0 & 0 & * & * \end{pmatrix} \tag{16}$$

Let's denote U_1, U_2, $\dots U_D$ — all matrices which we applied during this algorithm and U_f - final two-level matrix we got. Then the whole process can be written as

$$A \cdot U_1 \cdot U_2 \dots U_D = U_f, \tag{17}$$

from which follows

$$A = U_f \cdot U_D^\dagger \cdot U_{D-1}^\dagger \dots U_1^\dagger. \tag{18}$$

Equation (18) gives desired decomposition of A into 2-level unitary matrices. This decomposition has $\frac{d(d-1)}{2}$ matrices. Indeed, each matrix in decomposition (including U_f) corresponds to one eliminated element in upper triangular part of matrix A, and there are $\frac{d(d-1)}{2}$ such elements.

All matrices in decomposition are special unitary, with two exceptions. First, if we were swapping columns due to a being zero, we will have two-level X matrices. Second, if $\det(A) \neq 1$, matrix U_f will not be special unitary.

B. Gray codes

Now all two-level matrices in decomposition act on pair of states $(i, i+1)$. For our purposes we want them to act on pairs of states differing only in one bit, i.e. $(i, i \oplus 2^k)$.

Luckily, for any positive integer n exists such permutation of numbers $0, 1, \dots, 2^n - 1$, that any two neighboring numbers in it differ only in one bit. Such permutation is called binary-reflected Gray code [5], and is given by formula

$$\pi_i = i \oplus \lfloor i/2 \rfloor, \tag{19}$$

where $i = 0, 1, \dots, 2^n - 1$.

For example, Gray code for $n = 3$ is $(0, 1, 3, 2, 6, 7, 5, 4)$.

Let's consider matrix $P \in \mathrm{U}(2^n)$, such that $P_{ij} = \delta_{i,\pi_j}$. This is permutation matrix, i.e. its action on a vector is permuting elements of that vector with permutation π. Then expression $P^\dagger A' P$ simultaneously permutes rows and columns of matrix A' with permutation π. If A' was a two-level matrix acting on states $(i, i+1)$, then $A = P^\dagger A' P$ will be two-level matrix acting on states (π_i, π_{i+1}) — exactly what we need.

So, we need to apply two-level decomposition algorithm to matrix $A' = PAP^\dagger$ and get decomposition $A' = \prod_i A'_i$. Then $A = P^\dagger A' P = \prod_i (P^\dagger A'_i P)$. So, we have decomposition of A into two-level unitary matrices acting on states differing in one bit.

Similar technique is used in [6].

C. Fully controlled gates

Let's call gate a fully controlled (FC) gate acting on qubit i if this gate acts on qubit i and is controlled by all other qubits in the register. This gate will act on certain basis state only if all bits in index of this state (except maybe i-th) are set to one. For example, if $n = 5$, FC gate U acting on bit 1 applies matrix U to states $|10111\rangle$ and $|11111\rangle$.

By convention, FC gate acting on single qubit is just simple one-qubit gate without control qubits.

FC gate applies a two-level unitary matrix. But also any two-level unitary matrix (acting on states differing in one bit) can be implemented with a fully controlled gate and possibly some single-qubit X gates. Let's show how.

Let U be two-level unitary acting matrix on states $(i, i \oplus 2^r)$. Let J_0 — set of all indices j, such that j-th bit of i is zero, J_1 — set of all indices j, such that j-th bit of i is one (both sets don't include r). Then we need to apply this two-level unitary only to pair of such states, whose indices have zeroes on positions J_0, and ones on positions J_1. If $J_0 = \emptyset$, this is simply fully-controlled gate on qubit r.

But if there is some $j \in J_0$, then we have to just apply X on j-th qubit, then apply U and then apply X on j-th qubit again.

This will work because X acting on j-th qubit swaps state i with state $i \oplus 2^j$, so if U does something only with states i where $i[j] = 1$, then XUX does the same thing with states i where $i[j] = 0$.

So, to implement two-level unitary matrix we have to apply X gate to all qubits from J_0, then apply fully-controlled gate on qubit r and then again apply X gate to all qubits from J_0.

Let's consider an example. Let $n = 5$ and we want to apply two-level unitary matrix with non-trivial 2×2 submatrix U acting on states $|10100\rangle$ and $|10110\rangle$. Then $r = 3$, $J_0 = \{1, 4\}$ and $J_1 = \{0, 2\}$. So, we need to build the following circuit:

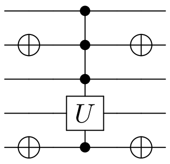

D. Implementing a single gate

At this point we have sequence of X gates and FC gates acting on single qubit, but each such gate is represented by arbitrary $U \in \mathrm{U}(2)$. We have to decompose U into product of matrices, which can be implemented by gates. In this paper I will consider how to decompose them into R_1, R_y and R_z gates, which are defined as:

$$R_1(\alpha) = \begin{pmatrix} 1 & 0 \\ 0 & e^{i\alpha} \end{pmatrix}, \tag{20}$$

$$R_y(\alpha) = \exp\left(\frac{i\alpha\sigma_y}{2}\right) = \begin{pmatrix} \cos(\alpha/2) & \sin(\alpha/2) \\ -\sin(\alpha/2) & \cos(\alpha/2) \end{pmatrix}, \tag{21}$$

$$R_z(\alpha) = \exp\left(\frac{i\alpha\sigma_z}{2}\right) = \begin{pmatrix} e^{i\alpha/2} & 0 \\ 0 & e^{-i\alpha/2} \end{pmatrix}. \tag{22}$$

First step is to make U special unitary matrix, if it's not such matrix already. Let $\phi = \arg\det U$ (recall that $|\det U| = 1$). Then $\det(R_1(-\phi)\cdot U) = e^{-i\phi}e^{i\phi} = 1$. So, takes place decomposition $U = R_1(\phi)U'$, where

$$U' = R_1(-\phi)U \tag{23}$$

and U' is special unitary.

Now all is left is to decompose special unitary matrix U' into gates. As U' is special unitary, it can be written in form [3, §4.6]:

$$U' = \begin{pmatrix} \cos\theta e^{i\lambda} & \sin\theta e^{i\mu} \\ -\sin\theta e^{i\mu} & \cos\theta e^{-i\lambda} \end{pmatrix}, \tag{24}$$

where

$$\theta = \arccos(|U'_{00}|), \lambda = \arg(U'_{00}), \mu = \arg(U'_{01}). \tag{25}$$

It can be directly checked that then

$$U' = R_z(\lambda+\mu)R_y(2\theta)R_z(\lambda-\mu). \tag{26}$$

So, action of single-qubit gate U can be implemented using four gates:

$$U = R_1(\phi)R_z(\lambda+\mu)R_y(2\theta)R_z(\lambda-\mu), \tag{27}$$

where $\phi = \arg\det U$ and other parameters are given by (25).

E. Optimizations

Combining all previous steps, we can build sequence of single-qubit X gates and FC gates R_1, R_y and R_z which implements given unitary matrix.

Each of $\mathcal{O}(4^n)$ FC gates is surrounded by $O(n)$ X-gates. It can happen that there are two X gates (after one FC gate and before next FC gate), which act on the same qubit. As $X^2 = I$, they both can be removed.

This will eliminate significant amount of X gates. When neighboring two-level matrices correspond to eliminating elements of the same row, they act on states (i_1, i_2) and (i_2, i_3), so mask J_0 for them can differ at most in two bits, so there will be not more than two X gates between almost all FC gates after optimization. There is only $\mathcal{O}(2^n)$ pairs of gates where this doesn't work and we can have up to n X gates (this happens when we proceed to next row in matrix). Overall, this guarantees that after optimization there will be $\mathcal{O}(n\cdot 2^n + 4^n) = \mathcal{O}(4^n)$ X gates, or $\mathcal{O}(1)$ X gates per one two-level matrix.

Another easy optimization to make is to remove all gates which are identity matrices, namely $R_1(2\pi k), R_y(4\pi k), R_z(4\pi k)$ for $k \in \mathbb{Z}$.

One more optimization is when we convert matrix to gates and matrix X occurs, don't apply usual procedure for not-special unitary matrix (which will result in decomposition $X = R_y(-\pi)R_1(\pi)$), but just use FC gate X instead. If we do that, we can guarantee that final circuit will contain at most one R_1 gate, and even this gate will be needed only if initial matrix was not special unitary.

F. Implementation

I implemented a Python program which uses described algorithm to transform arbitrary uniform matrix $U \in \mathrm{U}(2^n)$ into a Q# operation, which implements action of this matrix on array of n qubits. This program is available on GitHub [7].

This program performs all steps described above and then maps gates to standard Q# commands, namely `X, Controlled X, Controlled Ry, Controlled Rz, Controlled R1`.

IV. COMPLEXITY

One interesting question to consider is how many operations does it generally require to implement unitary matrix acting on n qubits.

Decomposition into two-level unitary matrices consisted of $\frac{2^n(2^n-1)}{2} = \mathcal{O}(4^n)$ matrices. Each two-level matrix was mapped to 3 or 4 fully-controlled gates and $\mathcal{O}(n)$ X gates, but after optimization we expect to have $\mathcal{O}(1)$ X gates per two-level unitary matrix. Thus we expect number of needed commands to be $\mathcal{O}(4^n)$.

Let's check it experimentally. I generated random matrices $U \in \mathrm{U}(2^n)$ for $n = 1\dots 9$, decomposed them using described algorithm, and calculated how many gates of each type appears in the decomposition $(\#(X), \#(R_y), \#(R_z), \#(R_1))$. Also I calculated total number of gates $G(n)$ and number of gates per matrix element, which is number of gates divided by 4^n. Results are shown in table I.

As we can see from the data, indeed $G(n) \sim 2.00 \cdot 4^n = \mathcal{O}(4^n)$.

Let's denote $G_{min}(n)$ — minimal number of gates (X, FC-$R_y(\alpha)$, FC-$R_z(\alpha)$, FC-$R_1(\alpha)$), needed to imple-

Table I. Number of gates in decomposition of random matrices

n	$\#(X)$	$\#(R_y)$	$\#(R_z)$	$\#(R_1)$	$G(n)$	$G(n)/4^n$
1	0	1	2	1	4	1.00
2	2	6	12	1	21	1.31
3	28	28	56	1	113	1.77
4	130	120	240	1	491	1.92
5	532	496	992	1	2021	1.97
6	2118	2016	4032	1	8167	1.99
7	8392	8128	16256	1	32777	2.00
8	33290	32640	65280	1	131211	2.00
9	132364	130816	261632	1	524813	2.00

ment arbitrary $2^n \times 2^n$ unitary matrix. We showed that $G_{min}(n) = \mathcal{O}(4^n)$.

Unitary matrix $2^n \times 2^n$ can be parametrized by 4^n independent real numbers [8, §IV.4]. So, to implement arbitrary matrix using gates parametrized by a real number, we will need at least 4^n such gates. So, we will have to use at least 4^n FC R_1, R_y and R_z gates, which gives us lower bound $G_{min}(n) = \Omega(4^n)$. Therefore, proposed algorithm gives asymptotically optimal result.

However, in some special cases matrix can be represented by much fewer number of gates, for example, if it was built as product of a few single-qubit gates and CNOT gates. Generally, proposed algorithm will not recognize special structure of the matrix and will still return $\Omega(4^n)$ gates.

V. DISCUSSION

A. Further decomposition

In this paper we consider fully controlled R_y, R_z and R_1 gates as primitives, because they are supported by Q# language. However, two-level matrix can be decomposed into sequence of simpler gates, namely R_y, R_z and R_1 gates acting on single qubit and CNOT (controlled-X) gate (acting on two qubits), and decomposition of a single two-level matrix will contain $\Theta(n^2)$ such gates. How to do that is shown in [3, §4.6].

B. Universality

Set of gates is *universal* if any quantum gate acting on any number of qubits can be implemented by combining gates from this set.

Universality is important property for quantum computers: if we have set of universal gates, we only need to be able to implement them on a particular quantum computer to be able to implement any irreversible computation on it. Possibility of implementing universal set of gates is one of DiVincenzo criteria [3, §11], meaning it is necessary requirement for any physical system to be a viable quantum computer.

This paper can be seen as a constructive proof that set of single-qubit X gate and fully-controlled gates $R_x(\alpha), R_y(\alpha), R_1(\alpha)$ with any number of control bits (including 0) and with any parameters is an universal set of gates.

However, this set can be reduced to just set of CNOT gate and single-qubit gates $R_y(\alpha), R_z(\alpha), R_1(\alpha)$ [3, §4.6]. Moreover, this set can be reduced to just one 2-qubit gate [9].

---

[1] "The Q# programming language." `https://docs.microsoft.com/en-gb/quantum/language`.

[2] M. Mykhailova and M. Roetteler, "Microsoft Q# coding contest - winter 2019 - main contest." `https://assets.codeforces.com/rounds/1116/contest-editorial.pdf`.

[3] M. Nakahara and T. Ohmi, *Quantum computing: from linear algebra to physical realizations.* CRC press, 2008.

[4] C.-K. Li, R. Roberts, and X. Yin, "Decomposition of unitary matrices and quantum gates," *International Journal of Quantum Information* **11** (2013) no. 01, 1350015.

[5] F. Gray, "Pulse code communication," Mar. 17, 1953. US Patent 2,632,058.

[6] J. J. Vartiainen, M. Möttönen, and M. M. Salomaa, "Efficient decomposition of quantum gates," *Physical review letters* **92** (2004) no. 17, 177902.

[7] `https://github.com/fedimser/quantum_decomp`.

[8] A. Zee, *Group theory in a nutshell for physicists.* Princeton University Press, 2016.

[9] D. E. Deutsch, A. Barenco, and A. Ekert, "Universality in quantum computation," *Proceedings of the Royal Society of London. Series A: Mathematical and Physical Sciences* **449** (1995) no. 1937, 669–677.

Dirac equation, spin and fine structure Hamiltonian

Fernando Chamizo

(Dated: May 27, 2019)

The Dirac equation is the starting point for relativistic quantum mechanics which evolved into the modern Quantum Field Theory. The purpose of this paper is to introduce it from a historical point of view and focus on two conspicuous applications. The first one is the explanation of the spin of the electron on a theoretical basis. The second is the derivation of the fine structure Hamiltonian that gives the relativistic corrections on the hydrogen atom.

I. HISTORICAL INTRODUCTION

Along the following sections we are going to give quite a number of historical references and comments but we want to devote this one entirely to the groundbreaking paper [1] in which Dirac introduced his new equation. After 80 years, it is noticeable how close this paper is to the modern reader. Definitively it is not only a fundamental contribution, it is also a very advisable reading.

The paper [1] has six sections and a general introduction that we label as 0. We describe here the contents with some comments avoiding deliberately formulas and technical points.

§0. Dirac notices firstly the discrepancy between the experiments and the quantum theory predictions for atoms. After mentioning the contribution of Pauli and Darwin to solve this problem, he indirectly suggests that they are artificial theories (with the funny sentence "The question remains as to why Nature should have chosen this particular model for the electron"). Finally he announces in an impersonal way a Hamiltonian in agreement with relativity and the experiments.

§1. *Previous Relativity Treatments.* This is a kind of technical continuation of the introduction. The Klein-Gordon equation (named here as Gordon-Klein) is considered as a tentative relativistic Schrödinger equation with two difficulties: Its limitation to define probabilities of dynamical variables and the existence of negative energies. The last paragraph contains an assertion between modest and prophetic: "we shall be concerned only with the removal of the first of these two difficulties. The resulting theory is therefore still only an approximation".

§2. *The Hamiltonian for No Field.* The content of this fundamental section is a derivation of the Dirac equation as a factorization of the Klein-Gordon equation in a way that could be found in any modern book except for slight changes in the notation. Something that sounds strange from the modern point of view is that Dirac seems to be prone to consider the needed extra dimensions (and even the matrices) as reflecting new "variables".

§3. *Proof of Invariance under a Lorentz Transformation.* Although the equation has been derived starting from a relativistic expression, it is not clear what Lorentz covariance means for it. The point to have in mind (that still puzzles students) is that the four coordinates of Ψ (the spinor wave function) are not the four coordinates of Minkowski space-time. In this section one can follow the steps of the proof but the underlying idea remains a little obscure. Paying a high price, the modern language of representations makes this point clearer [2, 4.2].

§4. *The Hamiltonian for an Arbitrary Field.* The equation for an electron in an electromagnetic field is displayed at the beginning and the rest of the section contains manipulations with $\boldsymbol{\sigma}$ that nowadays could be consider prolix.

§5. *The Angular Momentum Integrals for Motion in a Central Field.* This is an impressive and important part of the paper. In one sentence, the spin of the electron is deduced. Namely, it is proved is that $\boldsymbol{L}+\frac{\hbar}{2}\boldsymbol{\sigma}$ is a constant of motion under Dirac equation in a central field (and $\boldsymbol{L}$ is not). This is an honest theoretical physics answer for the philosophical question about the Nature in the introduction.

§6. *The Energy Levels for Motion in a Central Field.* The motivation here is to deduce that the correction for the hydrogen atom matches the theory of Pauli and Darwin. Dirac is sketchy in this section and some interesting implications appear in the second part of the paper [3]. Shortly after, Darwin published his study of the fine structure of the hydrogen atom [4].

Along this work we will tackle topics related to the sections in the paper by Dirac with the only important omission of the Lorentz covariance, which is more technical in nature. In connection with the last section, we derive the fine structure Hamiltonian which is one of the aftermaths of it.

II. SEVERAL FORMULATIONS

Let us start with some motivation following Dirac's steps. The idea to create a relativistic Schrödinger equation is to quantize the relation $E^2=p^2c^2+m^2c^4$ promoting E and p to be the corresponding operators. In this way it comes out the *Klein-Gordon equation* for the free particle (by a slip of the pen there is a wrong sign in [1])

$$-\hbar^2\partial_t^2\Psi=-\hbar^2c^2\nabla^2\Psi+m^2c^4\Psi. \tag{1}$$

This is a second order equation in time. It means that the wave function at a fixed time does not determine its evolution in later times. A deeper problem is that it lead to negative probabilities (see e.g. [5, §1.2]).

The Dirac equation is usually introduced, following the original [1, §5], as a "factorization" of Eq. (1). Let us examine a toy analogy. Consider the classical harmonic oscillator ruled by $\ddot{x}+\omega^2x=0$ and say that for some reason one wants to turn it into a first order linear equation $\alpha\dot{x}+\beta x=0$. The first reaction is to claim that this is blatantly impossible because we need the freedom to impose two initial conditions, one for position and another for velocity. The key point is that the dimension of the solution vector space can be increased keeping the order promoting x to be a vector and consequently the coefficients to matrices. In our example $\ddot{x}+\omega^2x=0$ is equivalent to the vector equation

$$\alpha\dot{X}+\beta X=O \quad \text{with} \quad \alpha=\mathbf{1}_{2\times 2},\ \beta=\begin{pmatrix}0 & -1\\ \omega^2 & 0\end{pmatrix}. \quad (2)$$

The matrix equation forces $X=(x,\dot{x})^t$ with x a solution of the scalar equation. This is the cheap and well-known mathematical trick of hiding higher order derivatives in coordinates. A calculation shows $(\alpha\frac{d}{dt}-\beta)(\alpha\frac{d}{dt}+\beta)=\frac{d^2}{dt^2}+\omega^2$ (Cayley-Hamilton theorem is working here) and we can say that we have factorized the original equation.

In the same way, we could write Eq. (1) as

$$\big(-i\hbar\partial_t+c\boldsymbol{\alpha}\cdot\boldsymbol{p}+\beta mc^2\big)\big(i\hbar\partial_t+c\boldsymbol{\alpha}\cdot\boldsymbol{p}+\beta mc^2\big)\Psi=0 \quad (3)$$

if we impose for $i,j\in\{1,2,3\}$, $i\neq j$,

$$\alpha_j^2=\beta^2=1, \quad \alpha_i\alpha_j+\alpha_j\alpha_i=0 \quad \text{and} \quad \alpha_j\beta+\beta\alpha_j=0. \quad (4)$$

Of course this cannot fulfilled with numbers, we need to move to the noncommutative realm of matrices. The first two relations for α_j are part of those for the Pauli matrices but the third spoils any choice of a 2×2 matrix β with $\beta^2=1$. Taking $\beta=1$ would work flipping the middle $+$ sign into $-$. In fact it can be proved [6, XX.7] that the smallest dimension to have a solution of Eq. (4) with Hermitian matrices is 4. Roughly speaking, flipping signs requires to increase the square roots of 1 doubling the dimension. A possible choice fulfilling Eq. (4) is

$$\alpha_j=\begin{pmatrix}O & \sigma_j\\ \sigma_j & O\end{pmatrix} \qquad \text{and} \qquad \beta=\begin{pmatrix}I & O\\ O & -I\end{pmatrix}, \quad (5)$$

written in blocks of 2×2 matrices. It is not the only choice but it can be proved that all possible choices are equivalent except for a change of basis [6, XX.III.10].

After the previous factorization, we infer the *Dirac equation* in its Hamiltonian form

$$i\hbar\partial_t\Psi=H\Psi \quad \text{with} \quad H=c\boldsymbol{\alpha}\cdot\boldsymbol{p}+\beta mc^2. \quad (6)$$

This is an evolution equation and then time plays a distinguished role (by the way, the conservation of the probability $\int\Psi^\dagger\Psi$ follows easily from it). With an eye to deal with Lorentz covariance, it is convenient to define

$$\gamma^j=\beta\alpha_j \quad \text{and} \quad \gamma^0=\beta. \quad (7)$$

With this notation the Dirac equation becomes

$$\big(i\hbar\gamma^\mu\partial_\mu-mc\big)\Psi=0 \quad (8)$$

where, as usual in relativity, it is assumed $\mu\in\{0,1,2,3,4\}$ and the summation convention. This is called the *covariant form* of the Dirac equation. In QFT (Quantum Field Theory) very often $\gamma^\mu\partial_\mu$ is abbreviated as $\not{\partial}$ and the equation acquires the minimalist form in natural units $(i\not{\partial}-m)\Psi=0$. The explicit form of the γ^μ corresponding to the choice Eq. (5) is the so-called *Dirac representation*

$$\gamma^0=\begin{pmatrix}I & O\\ O & -I\end{pmatrix}, \quad \gamma^j=\begin{pmatrix}0 & \sigma_j\\ -\sigma_j & 0\end{pmatrix}. \quad (9)$$

In some contexts it is convenient to define γ^0 differently, namely

$$\gamma^0=\begin{pmatrix}O & I\\ I & O\end{pmatrix}, \quad \gamma^j=\begin{pmatrix}0 & \sigma_j\\ -\sigma_j & 0\end{pmatrix}. \quad (10)$$

This is called the *Weyl representation.* It corresponds to a different choice of $\boldsymbol{\alpha}$ and β i.e., to switch the two couples of columns and to change the sign of the last couple of rows in Eq. (5).

The relations Eq. (4) translate into the suggestive compact formula

$$\gamma^\mu\gamma^\nu+\gamma^\nu\gamma^\mu=2\eta^{\mu\nu}\mathbf{1}_{4\times 4} \quad (11)$$

where $\eta^{\mu\nu}$ are the components of the Minkowski tensor. It turns out that under Lorentz transformations $\boldsymbol{\gamma}=(\gamma^0,\gamma^1,\gamma^2,\gamma^3)$ transforms as a vector and the Lorentz covariance of the Dirac equation means that there is a corresponding representation of the Lorentz group acting on Ψ.

Shortly we will examine some of the noteworthy achievements of the Dirac equation. Before going on, when one sees these 4×4 matrices a natural question shows up pointing an inconvenience. The physical meaning of the extra dimensions is unclear. The wave function was originally, as the name suggests, a function representing a wave, afterward it became a vector (a 2-spinor to be precise) to encode the two possibilities for the spin of the electron but we now have two more coordinates. The full answer is not easy and it is related to Dirac's self-criticism in [1, §1]. The equation contains information about two particles, the electron and the positron and they cannot be separated because they are excitations of the same quantum field [7, 37.4]. Then Ψ actually represents a field and the Dirac equation is a starting point of quantum field theory.

Nevertheless there is a symmetry between both particles, better expressed with Eq. (10), that implies that the new two extra components do not add degrees of freedom. Namely, when Eq. (10) is substituted in the Dirac equation $mc\Psi=i\hbar\gamma^\mu\partial_\mu\Psi$ we conclude that the first two components are determined by the two last components and vice-versa. As said in [2, §4.3], the four components are only necessary "to make room for the Dirac matrices" fulfilling Eq. (4). It motivates that in the applications we discuss, at some point we select one half of the 4-spinor Ψ.

III. THE SPIN OF THE ELECTRON

The spin and particularly the spin of the electron baffled the pioneers of quantum physics who saw that atomic spectroscopy in some aspects confirmed the theory and in some other did not. It is enlightening the last sentence in the seminal paper by Schrödinger [8] in which after noticing some contradictions with the experiments, he claims "The deficiency must be intimately connected with Uhlenbeck-Goudsmit's theory of the spinning electron. But in what way the electron spin has to be taken into account in the present theory is yet unknown". We address the reader to [9] to read from a master how the concept of spin evolved and how influential was.

A major advance was provided by Pauli (and also Darwin contributed) who according with the abstract of his famous paper [10] arrived at "a formulation of the quantum mechanics of the magnetic electron by the Schrödinger method of eigenfunctions". Pauli matrices appear there by the first time.

There is something slightly discomforting in the equation introduced by Pauli, in fact he was not satisfied with it. In some way, it is not fundamental, it is created having in mind that it has to reflect the expected magnetic moment. In this section we are going to see that the equation that Pauli got is a kind of nonrelativistic limit of the Dirac equation (created from first quantum relativistic principles) and the spin of the electron is embodied in the equation. Dirac considered it "an unexpected bonus".

To couple Eq. (6) to an electromagnetic field, the natural equation (minimal coupling) is

$$i\hbar\partial_t\Psi = \Big(c\boldsymbol{\alpha}\cdot\big(\boldsymbol{p}-\frac{e}{c}\boldsymbol{A}\big)+\beta mc^2+e\Phi\Big)\Psi \tag{12}$$

where, as usual, $\boldsymbol{A}$ is the vector potential and Φ is the scalar potential.

Recalling the form of β in Eq. (5) we note that we are adding the rest mass in the two first coordinates and subtracting it in the two latter coordinates. As we will promptly see, this causes that in the nonrelativistic setting the upper half Ψ_l of the spinor Ψ is "large" and the lower half Ψ_s is "small". Writing Eq. (12) in terms of Ψ_l and Ψ_s, we get

$$\begin{cases} i\hbar\partial_t\Psi_l = c\boldsymbol{\sigma}\cdot\big(\boldsymbol{p}-\frac{e}{c}\boldsymbol{A}\big)\Psi_s+mc^2\Psi_l+e\Phi\Psi_l,\\ i\hbar\partial_t\Psi_s = c\boldsymbol{\sigma}\cdot\big(\boldsymbol{p}-\frac{e}{c}\boldsymbol{A}\big)\Psi_l-mc^2\Psi_s+e\Phi\Psi_s.\end{cases} \tag{13}$$

If Ψ is an eigenstate with energy $\mathcal{E}$, in nonrelativistic situations, $\mathcal{E}$ should be close to the rest mass mc^2 and then the second equation can be approximated by $2mc\Psi_s = \boldsymbol{\sigma}\cdot(\boldsymbol{p}-\frac{e}{c}\boldsymbol{A})\Psi_l$ leading to v/c as the ratio of the size of Ψ_s to the size of Ψ_l, so the "small" part Ψ_s is actually small in this situation. When we substitute the approximate second equation into the first, we obtain

$$i\hbar\partial_t\Psi_l = \frac{1}{2m}\big(\boldsymbol{\sigma}\cdot(\boldsymbol{p}-\frac{e}{c}\boldsymbol{A})\big)^2\Psi_l+mc^2\Psi_l+e\Phi\Psi_l. \tag{14}$$

Recalling the well-known formula

$$(\boldsymbol{\sigma}\cdot\boldsymbol{u})(\boldsymbol{\sigma}\cdot\boldsymbol{v}) = \boldsymbol{u}\cdot\boldsymbol{v}+i\boldsymbol{\sigma}\cdot(\boldsymbol{u}\times\boldsymbol{v}), \tag{15}$$

which is also valid for operators, we have

$$i\hbar\partial_t\Psi_l = \frac{1}{2m}(S+P+mc^2)\Psi_l \tag{16}$$

where

$$S = \frac{1}{2m}(\boldsymbol{p}-\frac{e}{c}\boldsymbol{A})^2+e\Phi \tag{17}$$

gives the terms that would appear using the Schrödinger equation and

$$P = -i\frac{e}{c}\boldsymbol{\sigma}\cdot(\boldsymbol{p}\times\boldsymbol{A}+\boldsymbol{A}\times\boldsymbol{p}) \tag{18}$$

is a new extra (Pauli) term. Using the vector calculus formula for $\nabla\times(\varphi\boldsymbol{v})$ we have

$$(\boldsymbol{p}\times\boldsymbol{A}+\boldsymbol{A}\times\boldsymbol{p})\Psi_l = -i\hbar(\nabla\times\boldsymbol{A})\Psi_l = -i\hbar\boldsymbol{B}\Psi_l. \tag{19}$$

Finally, renaming Ψ_l as $\Psi e^{-imc^2t/\hbar}$ which corresponds to omit the contribution to the energy corresponding to the rest mass, we arrive to the *Pauli equation*

$$i\hbar\partial_t\Psi = \Big(\frac{1}{2m}\big(\boldsymbol{p}-\frac{e}{c}\boldsymbol{A}\big)^2+e\Phi-\frac{e\hbar}{2mc}\boldsymbol{\sigma}\cdot\boldsymbol{B}\Big)\Psi. \tag{20}$$

The term involving $\boldsymbol{\sigma}\cdot\boldsymbol{B}$ would not appear with Schrödinger's scalar wave function approach and shows an intrinsic coupling to the magnetic field with a gyromagnetic ratio e/m which doubles the one of a classic electron in a circular orbit. In other words, an electron behaves as a magnet with a strength that doubles the corresponding one to a classical spinning electron. This quantum property is, of course, the *spin*.

From the historical point of view, Eq. (20) was introduced by Pauli in [10] looking for something behaving as an angular moment to match the experiments. They suggested a new degree of freedom and motivate the introduction of vector wave functions with two coordinates. Ironically Kronig should be considered as the pioneer who introduced the spin but Pauli opposed to his idea and he did not publish it [9, §2], [11]. In a curious twist, later Kronig criticized the new view of the spin.

We have got Eq. (20) as a consequence of Dirac equation that is, so to speak, fundamental but a certain uneasy feeling persists because perhaps something is lost in the approximation and in principle the spin could be a nonrelativistic shadow of a more complex concept. Now, following [1, §5], we show another form to arrive to the spin without using any approximation.

Let us consider the Dirac equation in the form Eq. (6) for the free electron (Dirac also allows a central potential but it does not make any difference). A calculation proves

$$[H,L_z] = i\hbar c(\alpha_1p_2-\alpha_2p_1). \tag{21}$$

A similar calculation applies to the rest of the coordinates showing $[H, L] = -i\hbar c\boldsymbol{\alpha} \times \boldsymbol{p}$. It is then apparent that angular momentum is not conserved. This suggests that there is an internal spin of the electron compensating the missing angular momentum (this was taken by Pauli as starting point). Dirac just writes in his paper the formula for the corresponding operator S and checks $[H, L + S] = 0$. Here we give some insight about how to deduce or guess such term. We look for S_z Hermitian such that $[H, L_z + S_z] = 0$. When we impose that the coefficients of p_j and the independent term vanish we get the equations

$$-i\hbar\alpha_2 = [S_z, \alpha_1], \qquad i\hbar\alpha_1 = [S_z, \alpha_2] \tag{22}$$

and

$$[S_z, \alpha_3] = 0, \qquad [S_z, \beta] = 0 \tag{23}$$

The latter commutation formula implies that S_z is block diagonal and the former establishes a relation between both blocks. In this way we can write $S_z = \frac{1}{2}\hbar\,\mathrm{diag}(A, \sigma_3 A\sigma_3)$ with A a 2×2 Hermitian matrix. On the other hand, the equations Eq. (22) imply

$$2i\sigma_2 = A\sigma_1 + i\sigma_2 A\sigma_3, \quad -2i\sigma_1 = A\sigma_2 - \sigma_1 A\sigma_3. \tag{24}$$

In a more symmetric form, post-multiplying by σ_3,

$$2i\sigma_1 = \sigma_2 A - A\sigma_2, \quad 2i\sigma_2 = A\sigma_1 - \sigma_1 A. \tag{25}$$

We recognize immediately the commutation relations for Pauli matrices and the equations suggest $A = \sigma_3$ leading to $S_z = \frac{1}{2}\hbar\,\mathrm{diag}(\sigma_3, \sigma_3)$. In general the missing angular moment is $\frac{1}{2}\hbar\,\mathrm{diag}(\boldsymbol{\sigma}, \boldsymbol{\sigma})$. In other words, we are just duplicating the usual spin matrices to match the four coordinates of the 4-spinor.

A last comment is that although Eq. (25) suggests $A = \sigma_3$ it does not imply it, any diagonal matrix with $a_{11} - a_{22} = 2$ verifies it. One can avoid this ambiguity imposing that A^2 is a multiple of the identity. This proxy of $\sigma_j^2 = \mathrm{Id}$ comes from considering eigenstates of the angular moment, or some sort of symmetry. The resulting equality $S_x^2 + S_y^2 + S_z^2 = \frac{3}{4}\hbar^2$ proves that we are in the case of $\frac{1}{2}$-spin.

IV. THE FINE STRUCTURE HAMILTONIAN

We now focus on the case of the hydrogen atom model via Eq. (13) with $\Phi = -e/r$ and $\boldsymbol{A} = \boldsymbol{0}$ (no external magnetic field). To emphasize that the same arguments work for any central potential we write $V = e\Phi$ and we only assume $V = V(r)$.

For an eigenstate of energy $\mathcal{E}$, Eq. (13) acquires the time independent form

$$\begin{cases} \mathcal{E}\psi_l = c\boldsymbol{\sigma} \cdot \boldsymbol{p}\psi_s + mc^2\psi_l + V\psi_l, \\ \mathcal{E}\psi_s = c\boldsymbol{\sigma} \cdot \boldsymbol{p}\psi_l - mc^2\psi_s + V\psi_s. \end{cases} \tag{26}$$

Our target is to find a kind of relativistic correction of the Schrödinger equation. For comparison, it seems natural to separate the rest energy mc^2 and try to write Eq. (26) with some degree of approximation as

$$H\psi = E\psi \qquad \text{where} \quad E = \mathcal{E} - mc^2 \tag{27}$$

where ψ is a 2-spinor related in some way to ψ_l and ψ_s.

Recall that in Bohr model, as seen by Sommerfeld, the fine structure constant is the ratio of the electron velocity to c. Then the ratio of the relativistic kinetic energy to $\frac{1}{2m}p^2$ is 1 plus something comparable to α^2. Hence to keep the relativistic corrections we focus on a higher order in α^2. Namely, we do not distinguish between a factor 1 and a factor $1 + O(\alpha^4)$.

After these preliminary considerations, we are going to get a valid Eq. (27) following two approaches. The first one is taken from [12]. It is simpler but produces a nonstandard form of the result. The second approach (in which we follow mainly [13]) is more technical but suggests a general method that we do not explore here.

§1. *The fine structure Hamiltonian via a direct approach and perturbation theory.*

We proceed as before eliminating ψ_s but this time we do not use any nonrelativistic approximation. In this way we arrive to the exact equation

$$c^2\boldsymbol{\sigma} \cdot \boldsymbol{p}(2mc^2 + E - V)^{-1}\boldsymbol{\sigma} \cdot \boldsymbol{p}\psi_l + V\psi_l = E\psi_l. \tag{28}$$

If we parallel the procedure to derive Pauli equation we should consider $(2mc^2 + E - V)^{-1}$ as the constant $(2mc^2)^{-1}$ but then we would lose the relativistic correction. We instead note that $E - V$ is the kinetic energy, which is $O\big(mc^2\alpha^2\big)$ in the Sommerfeld model (see the comments above), and we infer

$$(2mc^2+E-V)^{-1} = \frac{1}{2mc^2}\Big(1-\frac{E-V}{2mc^2}\Big)+O\Big(\frac{\alpha^4}{mc^2}\Big). \tag{29}$$

Note that the simple identity $[\boldsymbol{p}, V] = -i\hbar\nabla V$ shows

$$\boldsymbol{\sigma}\cdot\boldsymbol{p}\Big(1-\frac{E-V}{2mc^2}\Big) = \Big(1-\frac{E-V}{2mc^2}\Big)\boldsymbol{\sigma}\cdot\boldsymbol{p}-\frac{i\hbar}{2mc^2}\boldsymbol{\sigma}\cdot\nabla V. \tag{30}$$

Let us approximate in the right hand side the kinetic energy $E - V$ by $\frac{1}{2m}\boldsymbol{p}^2$. Then we get substituting Eq. (29) and Eq. (30) in Eq. (28) our tentative form of the Hamiltonian

$$H = \frac{1}{2m}\Big(1-\frac{\boldsymbol{p}^2}{4m^2c^2}\Big)\boldsymbol{p}^2-\frac{i\hbar}{4m^2c^2}(\boldsymbol{\sigma}\cdot\nabla V)(\boldsymbol{\sigma}\cdot\boldsymbol{p})+V. \tag{31}$$

Appealing to the same heuristic argument as before, in the last approximation we are losing a factor $1 + O(\alpha^4)$ and we are under the allowed error.

The only remaining point is to simplify H to get a manageable expression and to identify the physical meaning of each term. The simplification repeats part of the strategy used in the Pauli equation: The application of Eq. (15) allows to write dot and cross products in terms of electromagnetic data that here are very simple because V is a central potential. Namely, V necessarily verifies $\nabla V = \frac{1}{r}\frac{dV}{dr}\boldsymbol{r}$ and Eq. (15) gives

$$(\boldsymbol{\sigma}\cdot\nabla V)(\boldsymbol{\sigma}\cdot\boldsymbol{p}) = \frac{dV}{dr}\frac{\boldsymbol{r}}{r}\cdot\boldsymbol{p} + i\boldsymbol{\sigma}\cdot\Big(\frac{dV}{dr}\frac{\boldsymbol{r}}{r}\times\boldsymbol{p}\Big) \quad (32)$$
$$= -i\hbar\frac{dV}{dr}\frac{\partial}{\partial r} + \frac{i}{r}\frac{dV}{dr}\boldsymbol{\sigma}\cdot\boldsymbol{L}$$

where we have used $\boldsymbol{r}\cdot\nabla = r\frac{\partial}{\partial r}$ and the definition of angular momentum. If we substitute this in Eq. (31) and put $\boldsymbol{S} = \frac{\hbar}{2}\boldsymbol{\sigma}$, we finally obtain the *fine structure Hamiltonian*

$$H = H_0 - \frac{\boldsymbol{p}^4}{8m^3c^2} - \frac{\hbar^2}{4m^2c^2}\frac{dV}{dr}\frac{\partial}{\partial r} + \frac{1}{2m^2c^2r}\frac{dV}{dr}\boldsymbol{S}\cdot\boldsymbol{L} \quad (33)$$

where

$$H_0 = \frac{\boldsymbol{p}^2}{2m} + V \quad (34)$$

is the part coming from the Schrödinger equation and the rest of the terms are the corrections. The first one is the natural relativistic correction of the energy linked to the approximation of the relativistic energy

$$\sqrt{p^2c^2 + m^2c^4} \approx mc^2 + \frac{p^2}{2m} - \frac{p^4}{8m^3c^2}. \quad (35)$$

The last term in Eq. (33) takes into account the coupling between the spin and the orbital angular momentum, it is the *spin-orbit term* and shows once again that the spin of the electron is embodied in the Dirac equation. Finally, the middle term is a little more mysterious. It is named the *Darwin term* and it can be interpreted as an effective smearing out of the potential due to the lack of localization of the electron (see [14] for more comments on this).

Actually Eq. (33) is the Hamiltonian as it appears in [12] but the form of the Darwin term seems to enter in contradiction with the rest of the texts we have checked ([5], [13], [15], [6], [14]). In them $-\frac{\hbar^2}{4m^2c^2}\frac{dV}{dr}\frac{\partial}{\partial r}$ is replaced by $\frac{\hbar^2}{8m^2c^2}\nabla^2 V$. The hint to solve this paradox came to us from a sentence in the old classic on atomic spectroscopy [16]. Note that these terms are of the lowest order. According to time independent perturbation theory they contribute to the energy as their expectations

$$-\frac{\hbar^2}{4m^2c^2}\langle\psi|\frac{dV}{dr}|\frac{\partial\psi}{\partial r}\rangle \quad \text{and} \quad \frac{\hbar^2}{8m^2c^2}\langle\psi|\nabla^2 V|\psi\rangle\,. \quad (36)$$

We are going to see that they coincide and then both terms give similar spectra to the limit of application of perturbation theory. We have for $\psi(\boldsymbol{r}) = R(r)Y(\theta,\varphi)$

$$2\langle\psi|\frac{dV}{dr}|\frac{\partial\psi}{\partial r}\rangle = \int_{S^2}\int_0^\infty \frac{dV}{dr}\frac{d(R^2)}{dr}|Y|^2 r^2\, dr d\Omega \quad (37)$$

and integrating by parts in the inner integral, this is

$$-\int_{S^2}\int_0^\infty \frac{d}{dr}\Big(r^2\frac{dV}{dr}\Big)R^2|Y|^2\, drd\Omega = \langle\psi|\nabla^2 V|\psi\rangle\,, \quad (38)$$

where we have employed $r^2\nabla^2 V = \frac{d}{dr}\Big(r^2\frac{dV}{dr}\Big)$ because V is radial.

§2. *The fine structure Hamiltonian via a Foldy-Wouthuysen transformation.*

Now we are going to show another approach that leads to the fine structure Hamiltonian in its standard form. To deduce the Pauli equation we showed that the equation Eq. (13) becomes decoupled in the nonrelativistic limit, getting Eq. (14). When we kept the relativistic terms, Eq. (28) was not entirely satisfactory because the left hand side that we would like to be the Hamiltonian depends itself on the energy. A clever idea introduced in [17] to deal with Eq. (13) keeping higher order terms is to introduce an artificial unitary change of basis U such that the system turns to be approximately decoupled. Roughly speaking it is like looking for a near to optimal choice of the small and large spinors. Recall that in our case $\boldsymbol{A} = \boldsymbol{0}$, $V = e\Phi$ (a central potential) and renaming, as before, the energy $\mathcal{E}$ in Eq. (26) as $E + mc^2$, we look for U such that

$$U\begin{pmatrix} V & c\boldsymbol{\sigma}\cdot\boldsymbol{p} \\ c\boldsymbol{\sigma}\cdot\boldsymbol{p} & V - 2mc^2\end{pmatrix}U^\dagger \approx \begin{pmatrix} H & O \\ O & H'\end{pmatrix}. \quad (39)$$

In honor to the authors of [17], U is called the *Foldy-Wouthuysen transformation.* In principle the method can be pushed to get any degree of approximation [18] [5] but the calculations become very complex (in an early published version of [18] the method is said to be "horrendous"). Here we only consider the first step that corresponds to

$$U = \begin{pmatrix} K & \frac{\boldsymbol{\sigma}\cdot\boldsymbol{p}}{2mc} \\ \frac{\boldsymbol{\sigma}\cdot\boldsymbol{p}}{2mc} & -K\end{pmatrix} \quad \text{with} \quad K = \sqrt{1 - \frac{\boldsymbol{p}^2}{4m^2c^2}}. \quad (40)$$

Note that U is unitary and Hermitian, $U = U^\dagger = U^{-1}$.

Before doing any calculation, let us examine the admissible degree of approximation in Eq. (39). We have that H is an approximation of $\frac{1}{2m}\boldsymbol{p}^2 + V$ then H' must be comparable to mc^2. If f is the size of the actual off-diagonal blocks in Eq. (39), the second couple of coordinates, our new small spinor, is suppressed by a factor $O(f/mc^2)$ with respect to the first. Then the off-diagonal upper block affects to H as $O(f^2/mc^2)$ and with f like $O(E\alpha)$ we get for H the admissible error $O(E\alpha^4)$ we want (recall that $E \sim \frac{1}{2}m(c\alpha)^2$ with Sommerfeld's heuristic).

Let us decompose the middle matrix in Eq. (39) as

$$M_V + M_p = \begin{pmatrix} V & O \\ O & V\end{pmatrix} + \begin{pmatrix} O & c\boldsymbol{\sigma}\cdot\boldsymbol{p} \\ c\boldsymbol{\sigma}\cdot\boldsymbol{p} & -2mc^2\end{pmatrix}. \quad (41)$$

When computing $UM_VU^\dagger$, it is clear that in the off-diagonal blocks V is multiplied by a factor $\boldsymbol{\sigma}\cdot\boldsymbol{p}/mc$ and this is absorbed by the admissible error $O(E\alpha)$. On the other hand, the first diagonal block coming form M_V is

$$H_V = KVK + \frac{1}{4m^2c^2}\boldsymbol{\sigma}\cdot\boldsymbol{p}V\boldsymbol{\sigma}\cdot\boldsymbol{p}. \quad (42)$$

In the same way, the off-diagonal blocks of $UM_pU^\dagger$ are third powers of $\boldsymbol{p}$ divided by m^2c and this is $O(E\alpha)$. The first diagonal block coming form M_p is

$$H_p = \frac{1}{m}K\boldsymbol{p}^2 - \frac{1}{2m}\boldsymbol{p}^2 \tag{43}$$

The Hamiltonian $H_p + H_V$ is consequently valid but it is too cumbersome to be useful. So we simplify it employing

$$K \approx 1 - \frac{\boldsymbol{p}^2}{8m^2c^2} \tag{44}$$

with the admissible error $O(\alpha^4)$. Hence

$$H_p \approx \frac{\boldsymbol{p}^2}{2m} - \frac{\boldsymbol{p}^4}{8m^3c^2}, \tag{45}$$

as expected from Eq. (35). For H_V we obtain, substituting Eq. (44),

$$H_V \approx V + \frac{1}{8m^2c^2}(2\boldsymbol{\sigma}\cdot\boldsymbol{p}V\boldsymbol{\sigma}\cdot\boldsymbol{p} - V\boldsymbol{p}^2 - \boldsymbol{p}^2V). \tag{46}$$

Note that $\boldsymbol{p}^2V = -\hbar^2\nabla^2V + 2(\boldsymbol{p}V)\cdot\boldsymbol{p} + V\boldsymbol{p}^2$. A calculation involving Eq. (15) shows that $\boldsymbol{\sigma}\cdot\boldsymbol{p}V\boldsymbol{\sigma}\cdot\boldsymbol{p} - (\boldsymbol{p}V)\cdot\boldsymbol{p} - V\boldsymbol{p}^2$ is

$$\hbar\boldsymbol{\sigma}\cdot(\nabla V\times\boldsymbol{p}) = \frac{\hbar}{r}\frac{dV}{dr}\boldsymbol{\sigma}\cdot(\boldsymbol{r}\times\boldsymbol{p}) = \frac{2}{r}\frac{dV}{dr}\boldsymbol{S}\cdot\boldsymbol{L}. \tag{47}$$

And we arrive to the fine structure Hamiltonian in its standard form

$$H = H_0 - \frac{\boldsymbol{p}^4}{8m^3c^2} + \frac{\hbar^2}{8m^2c^2}\nabla^2V + \frac{1}{2m^2c^2r}\frac{dV}{dr}\boldsymbol{S}\cdot\boldsymbol{L} \tag{48}$$

with H_0 as in Eq. (34).

V. DISCUSSION

The Dirac equation is a central topic in quantum mechanics and it opens the gate to QFT. It has many significant features from the theoretical and applied point of view. Some of these features treated in this paper are:

1. It allows to “factorize” the relativistic Schrödinger equation (a.k.a. Klein-Gordon equation) avoiding the unwanted properties of it that motivated that Schrödinger himself abandoned the relativistic approach and focused on the nonrelativistic version bearing his name.

2. It gives a theoretical basis for the existence of the spin of the electron. This is a major achievement because in the early times of quantum mechanics the spin was a source of misunderstandings (e.g. Stern-Gerlach experiment, anomalous Zeeman effect) and it had been introduced “by hand” to avoid the disagreement with the experiments.

3. When applied to the hydrogen atom, it produces a Hamiltonian that gives fine corrections on the energy levels that can be computed via perturbation theory and checked experimentally.

ACKNOWLEDGMENTS

I am deeply indebted to the staff of MITx: 8.06x. The explanations by Professor Zwiebach are crystal clear and I have received more attention from the kind and patient staff than in several non-massive classroom-based courses I have followed. I am sincerely very grateful to all of them.

---

[1] P. A. M. Dirac, “The quantum theory of the electron,” *Proceedings of the Royal Society of London. Series A, Containing Papers of a Mathematical and Physical Character* **117** (1928) no. 778, 610–624.

[2] G. B. Folland, *Quantum field theory*, vol. 149 of *Mathematical Surveys and Monographs*. American Mathematical Society, Providence, RI, 2008. A tourist guide for mathematicians.

[3] P. A. M. Dirac, “The quantum theory of the electron. Part II,” *Proceedings of the Royal Society of London. Series A, Containing Papers of a Mathematical and Physical Character* **118** (1928) no. 779, 351–361.

[4] C. G. Darwin, “The wave equations of the electron,” *Proceedings of the Royal Society of London. Series A, Containing Papers of a Mathematical and Physical Character* **118** (1928) no. 780, 654–680.

[5] J. D. Bjorken and S. D. Drell, *Relativistic quantum mechanics*. McGraw-Hill Book Co., New York-Toronto-London, 1964.

[6] A. Messiah, *Quantum Mechanics*. Dover Publications, 1999. Two volumes bound as one.

[7] T. Lancaster and S. J. Blundell, *Quantum field theory for the gifted amateur*. Oxford University Press, 2014.

[8] E. Schrödinger, “An undulatory theory of the mechanics of atoms and molecules,” *Phys. Rev.* **28** (1926) 1049–1070.

[9] S. Tomonaga, *The story of spin*. University of Chicago Press, Chicago, IL, 1997.

[10] W. Pauli, “Zur quantenmechanik des magnetischen elektrons,” *Z. Physik* **43** (1927) 601–623.

[11] E. D. Commins, “Electron spin and its history,” *Annual Review of Nuclear and Particle Science* **62** (2012) no. 1, 133–157.

[12] L. I. Schiff, *Quantum mechanics*. McGraw-Hill New York, 1968.

[13] F. Gross, *Relativistic quantum mechanics and field theory*. A Wiley-Interscience Publication. John Wiley & Sons, Inc., New York, 1999. Reprint of 1993 original.

[14] B. Zwiebach, *Lecture notes of the course 8.06x*. 2019.

[15] W. B. Berestetzki, E. M. Lifschitz, and L. P. Pitajewski, *Course of theoretical physics (“Landau-Lifšic”). Vol. IV*. Reverté, fourth ed., 1975. Relativistic quantum theory.

[16] E. Condon and G. Shortley, *The Theory of Atomic Spectra.* Cambridge University Press, 1951.

[17] L. L. Foldy and S. A. Wouthuysen, “On the Dirac theory of spin 1/2 particles and its non-relativistic limit,” *Phys. Rev.* **18** (1950) 29–36.

[18] F. J. Ynduráin, *Relativistic quantum mechanics and introduction to field theory.* Texts and Monographs in Physics. Springer-Verlag, Berlin, 1996.

Direct State Tomography using weak measurement, strong measurement and probe-controlled-system

Kieu Quang Tuan

June 19th, 2019

1 Introduction

Direct state measurement means that complex state can be measured directly via outcomes of pointers without any further complicated calculation of tomography. There is a efficient way towards direct state measurement, that is weak values. Since being introduced in [1], weak value is an interesting subject that physicists have been doing research about it. Let us begin with the definition of weak value

$$\langle \hat{A} \rangle = \frac{\langle \psi_f | \hat{A} | \psi_i \rangle}{\langle \psi_f | \psi_i \rangle} \tag{1}$$

where $\hat{A}$ is an operator, ψ_i and ψ_f are initial and final states, respectively.
When we choose $\hat{A} = |x\rangle\langle x|$, the weak value is

$$\langle |x\rangle\langle x| \rangle_W = \frac{\langle p_0 | x \rangle \langle x | \psi \rangle}{\langle p_0 | \psi \rangle} \sim \psi(x), \tag{2}$$

which is proportional to wave function in x basis.
From this idea, physicists have invented many methods to measure quantum state directly; and in this paper, I will present three of them: weak measurement, strong measurement and probe-controlled system.

2 Weak measurement

In 2011, J. S. Lundeen et al. [3] pointed out a new way to measure wave function in quantum mechanics which is called weak measurement based on weak value and weak interaction. In weak measurement, we have a system which weakly interacts with a device, this device is usually a qubit system. Due to weak coupling, the wave function after being measured is just slightly biased but not collapsed like in projective measurement. So in each time of measuring, we

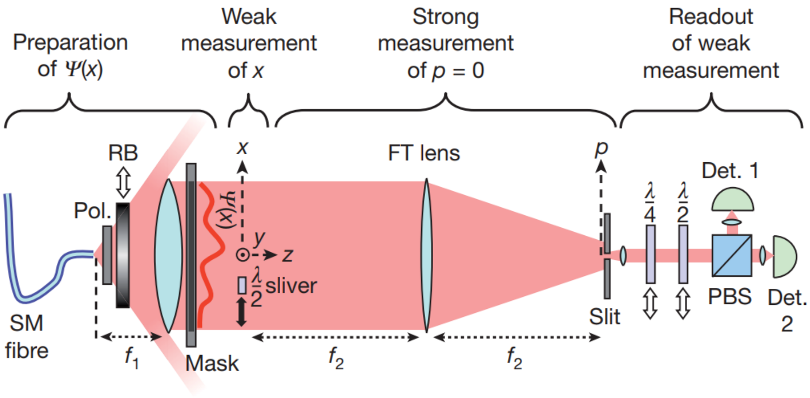

Figure 1: Weak measurement of the photon transverse wavefunction

extract a little bit information of the desired system; then, we have to do many times and use statistical average.

The first step of this method is preparation of identical photons having state $\Psi(x)$, then they will be weakly biased by a half-wave plate with a small angle α in x direction. The pointer here is the linear polarization angle of the photon; then, they did post-selection $p = 0$ by using a slit. Finally, the probability of polarization of photons is measured by detectors after passing through a polarizing beam-splitter [3]. A disadvantage here is that this method requires moving the half-wave plate throughout the x direction, so the calculation to reconstruct the wave function has to take into account time retardation; of course, it will be more difficult for higher dimension systems.

Here we do some calculation for this method. The initial state is chosen as $|\psi_i\rangle|0\rangle$, the unitary operator is $U(\theta) = e^{-i\theta\hat{A}\otimes\hat{\sigma}_y}$, where $\hat{A}\otimes\hat{\sigma}_y$ is the interaction Hamiltonian and θ is a small coupling constant.

The wave function after interaction is

$$\begin{aligned} e^{-i\theta\hat{A}\otimes\hat{\sigma}_y}|\psi_i\rangle|0\rangle &= [\hat{I} - i\theta\hat{A}\otimes\hat{\sigma}_y + O(\theta^2)]|\psi_i\rangle|0\rangle \\ &= |\psi_i\rangle|0\rangle + \theta\hat{A}|\psi_i\rangle|1\rangle + O(\theta^2) \end{aligned} \tag{3}$$

After being evolved, the system is projected onto $|\psi_f\rangle$ and the device is projected onto $|\pm\rangle[|\pm i\rangle]$ to get probabilities.

$$\begin{aligned}
P(\pm) &= |\langle\psi_f|\langle\pm|e^{-i\theta\hat{A}\otimes\hat{\sigma}_y}|\psi_i\rangle|0\rangle|^2 \\
&= |\langle\psi_f|\langle\pm(|\psi_i\rangle|0\rangle+\theta\hat{A}|\psi_i\rangle|1\rangle+O(\theta^2))|^2 \\
&= |\langle\psi_f|\psi_i\rangle\frac{1}{\sqrt{2}}\pm\theta\langle\psi_f|\hat{A}|\psi_i\rangle\frac{1}{\sqrt{2}}|^2+O(\theta^2) \\
&= \frac{1}{2}(\langle\psi_f|\psi_i\rangle\pm\theta\langle\psi_f|\hat{A}|\psi_i\rangle)(\langle\psi_i|\psi_f\rangle\pm\theta\langle\psi_i|\hat{A}|\psi_f\rangle)+O(\theta^2) \\
&= \frac{1}{2}(|\langle\psi_f|\psi_i\rangle|^2\pm\theta(\langle\psi_f|\hat{A}|\psi_i\rangle+\langle\psi_i|\hat{A}|\psi_f\rangle))O(\theta^2) \\
&= \frac{1}{2}(|\langle\psi_f|\psi_i\rangle|^2\pm\theta 2Re\langle\psi_i|\psi_f\rangle\langle\psi_f|\psi_i\rangle\frac{\langle\psi_f|\hat{A}|\psi_f\rangle}{\langle\psi_f|\psi_i\rangle}+O(\theta^2) \\
&= |\langle\psi_f|\psi_i\rangle|^2(\frac{1}{2}\pm\theta Re\langle\hat{A}\rangle_w)+O(\theta^2)
\end{aligned} \tag{4}$$

Similarly,

$$\begin{aligned}
P(\pm i) &= |\langle\psi_f|\langle\pm i|e^{-i\theta\hat{A}\otimes\hat{\sigma}_y}|\psi_i\rangle|0\rangle|^2 \\
&= |\langle\psi_f|\psi_i\rangle|^2(\frac{1}{2}\pm\theta Im\langle\hat{A}\rangle_w)+O(\theta^2)
\end{aligned} \tag{5}$$

Do some rearrangements, we get

$$P(+)+P(-)=|\langle\psi_f|\psi_i\rangle|^2 \tag{6}$$

$$P(+)-P(-)+i[P(+i)-P(-i)]=2\theta|\langle\psi_f|\psi_i\rangle|^2\langle\hat{A}\rangle_w+O(\theta^2) \tag{7}$$

Hence, if θ is known, $\langle\hat{A}\rangle_w$ can be calculated, and particularly, if we choose $\hat{A}=|x\rangle\langle x|$ the transverse wave function of photon in this case will be derived directly. Keep in mind the notation $P(+i)(P(-i))$ is the same as P_L (P_R).

3 Strong measurement

Instead of using weak interaction in section 2, here we use strong couple between the system and the device, and the result is indeed better than weak measurement. The word ‘strong’ can be understood that arbitrary strength measurement is used, the stronger the coupling is, the better the result come out, and the ideal case is that $\theta=\frac{\pi}{2}$.
Because of the similarity of these two methods, here I show the procedure for weak measurement again in the figure below, the strong one has difference at bigger angle θ.

I will do calculation for both pure states and mixed states.

- Pure states

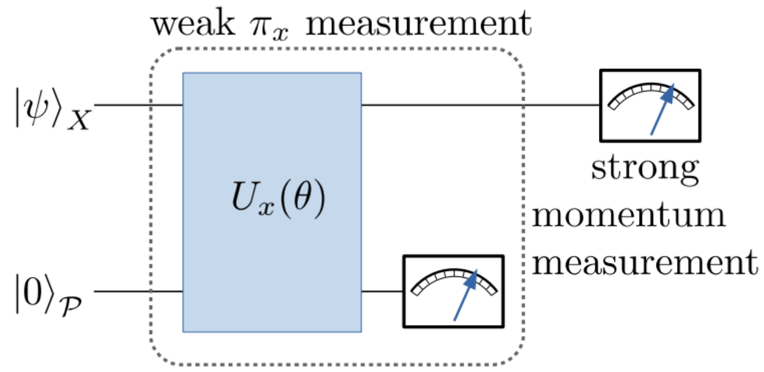

Figure 2: Scheme of weak measurement method

Let's begin with the unitary operator $U_x(\theta) = e^{-i\theta\pi_x\otimes\sigma_y}$, where π_x is x-projective operator , $\pi_x^n = \pi_x, \forall n \geqslant 1$ and σ_y is a Pauli operator.

$$\begin{aligned} U_x(\theta) &= \mathbb{I}_x \otimes \mathbb{I}_\pi + (-i\theta)(\pi_x \otimes \sigma_y) + \frac{(-i\theta)^2}{2!}(\pi_x \otimes \sigma_y)^2 + \frac{(-i\theta)^3}{3!}(\pi_x \otimes \sigma_y)^3 + ... \\ &= \mathbb{I}_x \otimes \mathbb{I}_\pi - i\theta\pi_x \otimes \sigma_y - \frac{\theta^2}{2!}\pi_x \otimes \mathbb{I}_\pi + i\frac{\theta^3}{3!}\pi_x \otimes \sigma_y + ... \\ &= \mathbb{I}_x \otimes \mathbb{I}_\pi - i(\theta - \frac{\theta^3}{3!} + \frac{\theta^5}{5!} - ...)\pi_x \otimes \sigma_y + (-\frac{\theta^2}{2!} + \frac{\theta^4}{4!} - ...)\pi_x \otimes \mathbb{I}_\pi \\ &= \mathbb{I}_x \otimes \mathbb{I}_\pi - isin\theta\pi_x \otimes \sigma_y + (cos\theta - 1)\pi_x \otimes \mathbb{I}_\pi \\ &= \mathbb{I}_x \otimes \mathbb{I}_\pi - \mid x\rangle\langle x \mid \otimes[(1 - cos\theta)\mathbb{I}_\pi + isin\theta\sigma_y] \end{aligned} \tag{8}$$

The pointer state after the momentum post-selection is

$$|\phi\rangle_{\mathcal{P}} = \langle p_0|U_x(\theta)|\Psi_{in}\rangle \tag{9}$$

Next I do the right part of above equation

$$\begin{aligned} U_x(\theta)|\Psi_{in}\rangle &= \{\mathbb{I}_x \otimes \mathbb{I}_\pi - |x\rangle\langle x| \otimes [(1 - cos\theta)\mathbb{I}_\pi + isin\theta\sigma_y]\}|\psi_X\rangle \otimes |H\rangle \\ &= |\psi\rangle_X \otimes |H\rangle - \psi_x|x\rangle \otimes [(1 - cos\theta)|H\rangle + isin\theta\sigma_y|H\rangle] \\ &= |\psi\rangle \otimes |H\rangle - \psi_x|x\rangle \otimes [(1 - cos\theta)|H\rangle + isin\theta|V\rangle)] \\ &= |\psi\rangle \otimes |H\rangle + \psi_x|x\rangle \otimes [(cos\theta - 1)|H\rangle + sin\theta|V\rangle] \\ &= |\psi\rangle_X \otimes |H\rangle + \psi_x|x\rangle \otimes |\chi\rangle \end{aligned} \tag{10}$$

where $|\chi\rangle = (cos\theta - 1)|H\rangle + sin\theta|V\rangle$ and $\tilde{\psi} = \sum_x \psi_x$. We can choose the phase of the wave function such that $\tilde{\psi} = |\tilde{\psi}|$. Then

$$\begin{aligned}|\phi\rangle_{\mathcal{P}} &= \langle p_0|U_x(\theta)|\Psi_{in}\rangle \\ &= \frac{1}{\sqrt{d}}(\sum_x \langle x|)|\psi_x\rangle \otimes |H\rangle + \frac{1}{\sqrt{d}}(\sum_x \langle x|)|\psi_x|x\rangle \otimes |\chi\rangle \\ &= \frac{1}{\sqrt{d}}(\sum_x \psi_x)|H\rangle + \frac{1}{\sqrt{d}}\psi_x|\chi\rangle \\ &= \frac{1}{\sqrt{d}}[\tilde{\psi}|H\rangle + \psi_x|\chi\rangle]\end{aligned} \tag{11}$$

From here, the probabilities can be derived, so I calculate the first case, the following cases are done similarly. Defining $\epsilon_\theta = 2sin^2\frac{\theta}{2}$.

$$\begin{aligned}&P_0^{(x)} = |\langle 0|\phi\rangle|^2 = |\langle H|\phi\rangle|^2 = |\frac{1}{\sqrt{d}}(\tilde{\psi} + \psi_x(cos\theta - 1))|^2 \\ &= \frac{1}{d}[\tilde{\psi}^2 + \tilde{\psi}(cos\theta - 1)2Re\psi_x + (cos\theta - 1)^2|\psi_x|^2] = \frac{1}{d}[\tilde{\psi}^2 - 2\epsilon_\theta\tilde{\psi}Re(\psi_x) + \epsilon_\theta^2|\psi_x|^2] \approx \frac{\tilde{\psi}^2}{d} \\ &P_1^{(x)} = \frac{1}{d}sin^2\theta|\psi_x|^2 \approx 0 \\ &P_+^{(x)} = \frac{1}{d}[\frac{\tilde{\psi}^2}{2} - (\epsilon_\theta - sin\theta)\tilde{\psi}Re(\psi_x) + (1 - sin\theta)\epsilon_\theta|\psi_x|^2] \approx \frac{\tilde{\psi}}{d}[\frac{\tilde{\psi}}{2} + \theta Re(\psi_x)] \\ &P_-^{(x)} = \frac{1}{d}[\frac{\tilde{\psi}^2}{2} - (\epsilon_\theta + sin\theta)\tilde{\psi}Re(\psi_x) + (1 + sin\theta)\epsilon_\theta|\psi_x|^2] \approx \frac{\tilde{\psi}}{d}[\frac{\tilde{\psi}}{2} - \theta Re(\psi_x)] \\ &P_L^{(x)} = \frac{1}{d}[\frac{\tilde{\psi}^2}{2} + sin\theta\tilde{\psi}Im(\psi_x) + \epsilon_\theta(|\psi_x|^2 - \tilde{\psi}Re(\psi_x))] \approx \frac{\tilde{\psi}}{d}[\frac{\tilde{\psi}}{2} + \theta Im(\psi_x)] \\ &P_R^{(x)} = \frac{1}{d}[\frac{\tilde{\psi}^2}{d} - sin\theta\tilde{\psi}Im(\psi_x) + \epsilon_\theta(|\psi_x|^2 - \tilde{\psi}re(\psi_x))] \approx \frac{\tilde{\psi}}{d}[\frac{\tilde{\psi}}{2} - \theta Im(\psi_x)]\end{aligned} \tag{12}$$

By algebraic rearrangement, we have what we are desiring: the real and imaginary of wave function.

$$\mathfrak{Re}(\psi_x) = \frac{d}{2\tilde{\psi}sin\theta}[P_+^{(x)} - P_-^{(x)} + 2tan(\frac{\theta}{2}P_1^x] \tag{13}$$

$$\mathfrak{Im}(\psi_x) = \frac{d}{2\tilde{\psi}sin\theta}[P_L^{(x)} - P_R^{(x)}] \tag{14}$$

When we choose $\theta = \pi/2$ for the strong case, we will have better results than weak measurement [4]; because the later uses weakly couple, so the extracted information will be dimmer, simply.

- Mixed states

This job is similar as the pure states, but because of the instructive purpose and dealing with mixed states in real experiments, I show it here.

We begin with the initial state of the system and the probe.

$$\rho \equiv \rho_X \otimes |0\rangle_{\mathcal{P}}\langle 0|, \rho_X = \sum_{x,y=1}^{n} \hat{\rho}_{x,y} |x\rangle\langle y| \tag{15}$$

The evolution operator $U_x(\theta) = e^{-i\theta|x\rangle\langle x|\otimes\sigma_y}$ and the final state $\rho'_x \equiv U_x(\theta)\rho U_x^\dagger(\theta)$. Then, the system is projected onto the momentum state $|p\rangle = \frac{1}{\sqrt{d}}\sum_{y=1}^{d} e^{\frac{2\pi iyp}{d}|y\rangle}$ (the reader can learn more about this Fourier transformation in Chapter 5 of [2]) to become

$$\rho^{\mathcal{P}}_{x,p} \equiv \langle p|\rho'_x|p\rangle = \begin{pmatrix} \rho_{00}(x,p) & \rho_{01}(x,p) \\ \rho_{10}(x,p) & \rho_{11}(x,p) \end{pmatrix} \tag{16}$$

Let's begin to verify it. First, we have

$$\begin{aligned}
U_x^\dagger(\theta)|p\rangle &= e^{i\theta|x\rangle\langle x|\otimes\sigma_y}[\frac{1}{\sqrt{d}}\sum_{y=1}^{d} e^{\frac{2\pi yp}{d}}|y\rangle \\
&= [\mathbb{I}\otimes\mathbb{I} + i\theta|x\rangle\langle x|\otimes\sigma_y + \frac{(i\theta)^2}{2!}|x\rangle\langle x|\otimes\mathbb{I} + \frac{(i\theta)^3}{3!}|x\rangle\langle x|\otimes\sigma_y + \ldots](\frac{1}{\sqrt{d}}\sum_{y=1}^{d} e^{\frac{2\pi iyp}{d}}|y\rangle) \\
&= |p\rangle\otimes\mathbb{I} + (i\theta)(\frac{1}{\sqrt{d}}e^{\frac{2\pi ixp}{d}}|x\rangle\otimes\sigma_y + \frac{(i\theta)^2}{2!}(\frac{1}{\sqrt{d}}e^{\frac{2\pi ixp}{d}}|x\rangle\otimes(\sigma_y)^2 \\
&+ \frac{(i\theta)^3}{3!}(\frac{1}{\sqrt{d}}e^{\frac{2\pi ixp}{d}}|x\rangle\otimes(\sigma_y)^3) + \ldots \\
&= |p\rangle\otimes\mathbb{I} + (\frac{1}{\sqrt{d}}e^{\frac{2\pi ixp}{d}}|x\rangle)\otimes(i\theta\sigma_y + \frac{(i\theta)^2}{2!}\sigma_y^2 + \frac{(i\theta)^3}{3!}\sigma_y^3 + \ldots \\
&= |p\rangle\otimes\mathbb{I} + (\frac{1}{\sqrt{d}}e^{\frac{2\pi ixp}{d}}|x\rangle)\otimes(e^{i\theta\sigma_y} - \mathbb{I})
\end{aligned} \tag{17}$$

Using Hermitian conjugate, we obtain

$$\langle p|U_x(\theta) = \langle p|\otimes\mathbb{I} + (\frac{1}{\sqrt{d}}e^{\frac{-2\pi ixp}{d}}\langle x|)\otimes(e^{-i\theta\sigma_y} - \mathbb{I}) \tag{18}$$

Combining them all

$$\begin{aligned}
\langle p|U_x(\theta)|\rho|U_x^\dagger(\theta)|p\rangle &= \langle p|\rho_X|p\rangle\otimes|0\rangle_{\mathcal{P}}\langle 0| \\
&+ \langle\ |\rho_X|\frac{1}{\sqrt{d}}e^{\frac{2\pi ixp}{d}}|x\rangle\otimes|0\rangle_{\mathcal{P}}\langle(e^{i\theta\sigma_y} - \mathbb{I}) \\
&+ \frac{1}{\sqrt{d}}e^{\frac{-2\pi ixp}{d}}\langle x|\rho_X|p\rangle\otimes(e^{-i\theta\sigma_y} - \mathbb{I})|0\rangle_{\mathcal{P}}\langle 0| \\
&+ \frac{1}{\sqrt{d}}e^{\frac{-2\pi ixp}{d}}\langle x|\rho_X|\frac{1}{\sqrt{d}}e^{\frac{2\pi ixp}{d}}|x\rangle\otimes(e^{-i\theta\sigma_y} - \mathbb{I})|0\rangle_{\mathcal{P}}\langle 0|(e^{i\theta\sigma_y} - \mathbb{I}) \\
&= A + B + C + D
\end{aligned} \tag{19}$$

Because of complication, I do calculation separately.
The second term in the RHS is

$$\begin{aligned} B &= \frac{1}{d}(\sum_{y=1}^{d} \rho_{y,x} e^{\frac{2\pi i(x-y)p}{d}}) \otimes [|0\rangle\langle 0| e^{i\theta\sigma_y} - |0\rangle\langle 0|] \\ &= \frac{1}{d}(\sum_{y=1}^{d} \rho_{y,x} e^{\frac{2\pi i(x-y)p}{d}}) \otimes [|0\rangle\langle 0|(cos\theta - 1) + |0\rangle\langle 1|sin\theta] \end{aligned} \tag{20}$$

The third term is the complex conjugate of the second one

$$C = \frac{1}{d}(\sum_{y=1}^{d} \rho_{x,y} e^{\frac{2\pi i(y-x)p}{d}}) \otimes [|0\rangle\langle 0|(cos\theta - 1) + |1\rangle\langle 0|sin\theta] \tag{21}$$

The fourth term is

$$\begin{aligned} &D = \frac{1}{d}\langle x|(\sum_{x,y} \rho_{x,y}|x\rangle\langle y|)|x\rangle \otimes [(cos\theta|0\rangle + sin\theta|1\rangle)(\langle 0|cos\theta + \langle 1|sin\theta) \\ &- (cos\theta|0\rangle + sin\theta|1\rangle)\langle 0| - |0\rangle(\langle 0|cos\theta + \langle 1|sin\theta) + |0\rangle\langle 0|] \\ &= \frac{1}{d}\rho_{x,x} \otimes [|0\rangle\langle 0|(cos^2\theta - 2cos\theta + 1) + |0\rangle\langle 1|(cos\theta sin\theta - sin\theta) \\ &+ |1\rangle\langle 0|(sin\theta cos\theta - sin\theta) + |1\rangle\langle 1|sin^2\theta] \\ &= \frac{1}{d}\rho_{x,x} \otimes [|0\rangle\langle 0|(1 - cos\theta)^2 + |0\rangle\langle 1|(cos\theta - 1)sin\theta + |1\rangle\langle 0|sin\theta(cos\theta - 1) + |1\rangle\langle 1|sin^2\theta] \end{aligned} \tag{22}$$

Combine the results, we gain these things

$$\begin{aligned} &\rho_{00}(x,p) = \frac{1}{d}[\sum_{x,y} \hat{\rho}_{x,y} e^{\frac{2\pi i(y-x)p}{d}} - 2sin^2\frac{\theta}{2}\sum_{y}(\hat{\rho}_{x,y} e^{\frac{2\pi i(y-x)p}{d}} + c.c) + 4sin^4\frac{\theta}{2}\hat{\rho}_{x,x}], \\ &\rho_{10}(x,p) = \frac{1}{d}sin\theta[\sum_{y} \hat{\rho}_{x,y} e^{\frac{2\pi i(y-x)p}{d}} - 2sin^2\frac{\theta}{2}\hat{\rho}_{x,x}], \\ &\rho_{01}(x,p) = \rho_{10}(x,p)^*, \\ &\rho_{11}(x,p) = \frac{1}{d}sin^2\theta\hat{\rho}_{x,x}. \end{aligned} \tag{23}$$

From above equations, we can derive that

$$\hat{\rho}_{x,y} \sim dtan\frac{\theta}{2}\delta_{x,y}\rho_{11}(x,p) + \sum_{p} e^{\frac{2\pi i(x-y)p}{d}}\rho_{10}(x,p) \tag{24}$$

For strong case ($\theta = \pi/2$)

$$\hat{\rho}_{x,y} \sim d\delta_{x,y}\rho_{11}(x,p) + \sum_{p} e^{\frac{2\pi i(x-y)p}{d}}\rho_{10}(x,p) \tag{25}$$

As you readers can see, to gain the final goal, we must have ρ_{11} and ρ_{10}. Actually, they are calculated through P_+, P_-, P_L, P_R , which are probabilities when the final state of probe in equation 16 is projected onto these polarization. By defining $P_i^{x,p} \equiv \langle i|\rho_{x,p}^{\mathcal{P}}|i\rangle$ and from equation 16, we can easily get that

$$\rho_{10}(x,p) = \frac{1}{2}[(P_+^{(x,p)} - P_-^{(x,p)} - i(P_L^{(x,p)} - P_R^{(x,p)}] \tag{26}$$

and

$$\rho_{11}(x,p) = P_1^{(x,p)} \tag{27}$$

After long and complicated calculation, we have proved that the either pure or mixed states of the system can be reconstructed directly by measuring the probabilities of the final state of the probe. It is indeed worth doing that.

4 Probe-controlled system

4.1 Fundamental concepts

We examine the combined system $\mathcal{H}_S \otimes \mathcal{H}_P$, where $\mathcal{H}_S$ is for the desired system and $\mathcal{H}_P$ is for the qubit probe. The Pauli operators are

$$\begin{aligned} \hat{\sigma}_x &= |0\rangle\langle 1| + |1\rangle\langle 0| = |+\rangle\langle +| - |-\rangle\langle -| \\ \hat{\sigma}_y &= -i|0\rangle\langle 1| + i|1\rangle\langle 0| = |+i\rangle\langle +i| - |-i\rangle\langle -i| \\ \hat{\sigma}_z &= |0\rangle\langle 0| - |1\rangle\langle 1| \end{aligned} \tag{28}$$

Here, I use notations $|\pm\rangle := (|0\rangle \pm |1\rangle)/\sqrt{2}$, $|\pm i\rangle := (|0\rangle \pm i|1\rangle)/\sqrt{2}$.
Let the total system undergo the probe-controlled system transformation $\hat{T}$:

$$\hat{T} := \hat{T}_0 \otimes |0\rangle\langle 0| + \hat{T}_1 \otimes |1\rangle\langle 1| \tag{29}$$

where $\hat{T}_0$ and $\hat{T}_1$ can be chosen later for desired purposes.

Next, we calculate the probabilities that the total system undergoes the transformation and then are projected onto $|\psi_f\rangle, |\pm\rangle[|\pm i\rangle]$ basis.

$$\begin{aligned} P(\pm) = \langle \Psi_i|\hat{T}^\dagger(|\psi_f\rangle\langle\psi_f| \otimes |\pm\rangle\langle\pm|)\hat{T}|\Psi_i\rangle = \frac{1}{4}(|\langle\psi_f|\hat{T}_0|\psi_i|^2 + |\langle\psi_f|\hat{T}_1|\psi_i\rangle|^2 \\ \pm 2Re\langle\psi_i|\hat{T}_0^\dagger|\psi_f\langle\rangle\psi_f|\hat{T}_1|\psi_i\rangle) \end{aligned} \tag{30}$$

$$\begin{aligned} P(\pm i) = \langle \Psi_i|\hat{T}^\dagger(|\psi_f\rangle\langle\psi_f| \otimes |\pm i\rangle\langle\pm i|)\hat{T}|\Psi_i\rangle = \frac{1}{4}(|\langle\psi_f|\hat{T}_0|\psi_i\rangle|^2 + |\langle\psi_f|\hat{T}_1|\psi_i|^2 \\ \pm 2Im\langle\psi_i|\hat{T}_0^\dagger|\psi_f\rangle\langle\psi_f|\hat{T}_1|\psi_i\rangle) \end{aligned} \tag{31}$$

Use clever arrangement, we have the following equation

$$P(+) - P(-) + i[P(+i) - P(-i)] = \langle\psi_i|\hat{T}_0^\dagger|\psi_f\rangle\langle\psi_f|\hat{T}_1|\psi_i\rangle \tag{32}$$

which quickly reminds us the weak value, and we can exploit it to rebuild the wanted wave function.

4.2 Transformation rules

From the result in the last part, we use a trick that is commonly used to calculate cross section in Quantum Field Theory.

$$\begin{aligned}\langle\psi_i|\hat{T}_0^\dagger|\psi_f\rangle\langle\psi_f|\hat{T}_1|\psi_i\rangle &= (\langle\psi_i|)_a(\hat{T}_0^\dagger)_{ab}(|\psi_f\rangle)_b(\langle\psi_f|)_c(\hat{T}_1)_{cd}(|\psi_i\rangle)_d \\ &= (|\psi_i\rangle)_d(\langle\psi_i|)_a(\hat{T}_0^\dagger)_{ab}(|\psi_f\rangle)_b(\langle\psi_f|)_c(\hat{T}_1)_{cd} \\ &= (|\psi_i\rangle\langle\psi_i|)_{da}(\hat{T}_0^\dagger)_{ab}(|\psi_f\rangle\langle\psi_f|)_{bc}(\hat{T}_1)_{cd} \\ &= tr(|\psi_i\rangle\langle\psi_i|\hat{T}_0^\dagger|\psi_f\rangle\langle\psi_f|\hat{T}_1)\end{aligned} \tag{33}$$

For the case of mixed states, the complex value is $tr(\hat{\rho}_i\hat{T}_0^\dagger\hat{\rho}_f\hat{T}_1)$. Since the cyclic permutation does not change the trace, we can figure transformation rules, which are extremely useful.

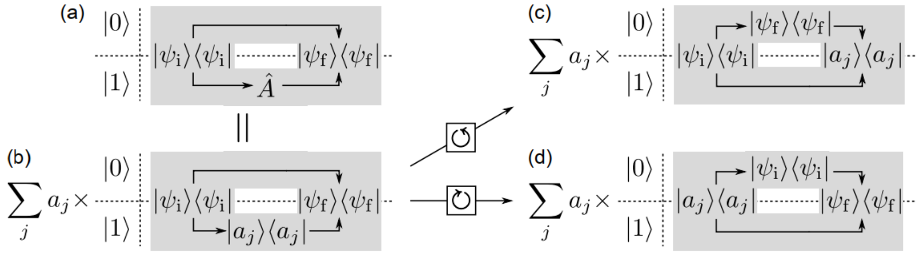

Figure 3: Transformation rules

In this picture, Fig. 2(a) and Fig. 2(b) is the same if $\hat{A}$ can be spectrally decomposed such as $\hat{A} = \sum_j a_j|a_j\rangle\langle a_j|$ and $\hat{A}$ presents a positive-operator valued measure (POVM), the reader can learn more in [2]. Fig. 2(c) and Fig. 2(d) are obtained by rotating Fig. 2(b) clockwise and counterclockwise, respectively. But the physical implication is indeed more meaningful than just mathematical stuff. For instance, instead the system is projected onto $|a_j\rangle$ in the probe mode $|1\rangle$ and then is projected onto $|\psi_f\rangle$ in the both probe mode in Fig. 2(b), the system is first projected onto $|\psi_f\rangle$ in the mode $|0\rangle$ and then is projected onto $|a_j\rangle$ in the both mode in Fig. 2(c). Thank to that, experimental devices can be arranged as well as possible.

4.3 Modified version for weak measurement

In Weak Measurement section, we see that there is $O(\theta^2)$ in the final result (equation 7). Now we modify this method by using probe-controlled framework. We choose the initial state $|\Psi_i\rangle = |\psi_i\rangle|+\rangle$ and the transformation operator $\hat{T} = \hat{I}\otimes|0\rangle\langle 0| + \theta\hat{A}\otimes|1\rangle\langle 1|$. Using equation 32 we have

$$\begin{aligned}P(+) - P(-) + i[P(+i) - P(-i)] &= \langle\psi_i|\psi_f\rangle\langle\psi_f|\theta\hat{A}|\psi_i\rangle \\ &= 2P(0)\theta\langle\hat{A}\rangle_w\end{aligned} \tag{34}$$

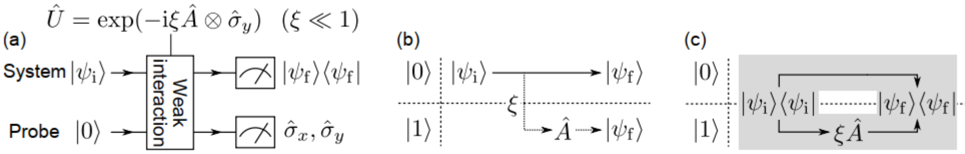

Figure 4: Modified weak measurement

where $P(0) = |\langle\psi_f|\psi_i\rangle|^2/2$ and $\{\hat{T}_0, \hat{T}_1\} = \{\hat{I}, \hat{\theta}\hat{A}\}$. Then we can choose $\hat{A} = |x\rangle\langle x|$ and measure the transverse wave function like section 2.
The idea is presented in Fig. 4(b), so we can think the weak interaction as a small extraction of the initial state $|\psi_i\rangle$ from mode $|0\rangle$ to mode $|1\rangle$.

4.4 Derivation of new method - Probe-controlled system

In section 2, I have introduced weak measurement, which is considered as the start of direct wave function using weak values. However, as you have seen, there are some cons of it consisting low precision and moving half-wave plate along x direction to measure the state.
And in section 4, a new framework and transformation rules are showed; in addition, a modified version of weak measurement is a promising way to upgrade the method of Lundeen et al.[3]. All of them created a new method for directly measuring wave function called probe-controlled system. In this figure, there are conventional weak measurement - Fig. 5(a,b) and probe-controlled system

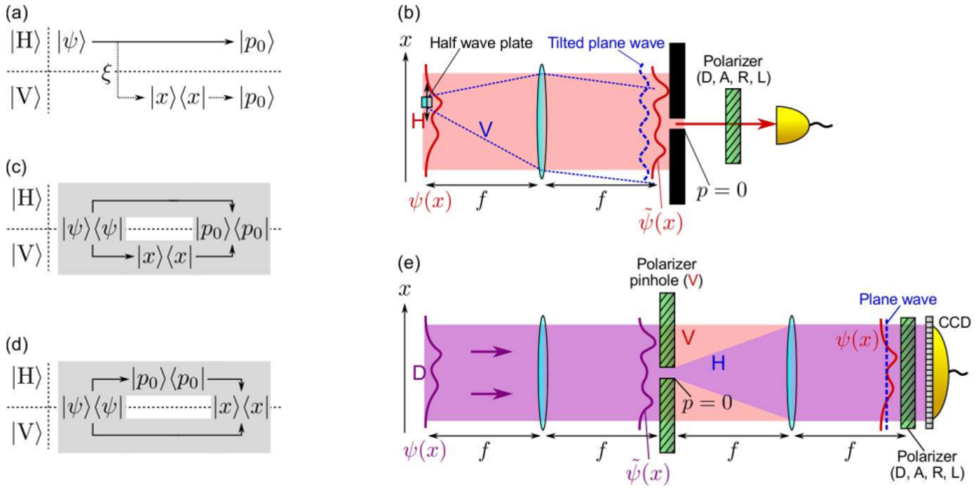

Figure 5: Derivation new method from weak measurement

are conventional weak measurement - Fig. 5(a,b) and probe-controlled system

- Fig. 5(d,e), the Fig. 5(c) is a halfway step. Here I concentrate on this new method.

First, we choose $\hat{A} = |x\rangle\langle x|$ to measure transverse wave function. Next, we set $\theta = 1$ which is the maximum value for highest precision as in Fig. 5(c). Then, we apply transformation rule for the clockwise case to transfer Fig. 5(c) to Fig. 5(d). In this scheme, the system is projected onto $|p_0\rangle$ in the mode $|H\rangle$ and then onto $|x\rangle$ in the both probe mode. The two modes $|H\rangle$ and $|V\rangle$ are the horizontal and vertical polarization of the photons, respectively.

As you can see in Fig. 5(e), in mode $|V\rangle$, the photons is let go through without any obstruction, but in mode $|H\rangle$, only photons have $p = 0$ can get through, which presents the projection onto $|p_0\rangle$ in Fig. 5(c). Finally, photon's polarization is measured in $\{|\pm\rangle\}$ (diagonal polarization and $\{|\pm i\rangle\}$ (circular polarization) thank to a device such as a charge-coupled device (CCD) camera.

From the framework in part 4.1, we have $\{\hat{T}_0, \hat{T}_1\} = \{|p_0\rangle\langle p_0|, \hat{I}\}$, so using formula 32 follows

$$P(+) - P(-) + i[P(+i) - P(-i)] = \langle\psi|p_0\rangle\langle p_0|x\rangle\langle x|\psi\rangle \sim \psi(x) \tag{35}$$

This thing means that the transverse wave function is directly measured in the optical scheme depicted in Fig. 5(e). Furthermore, this method has advantages concluding higher precision and scan-free arrangement than the conventional way in section 2. The mathematical derivation for probe-controlled system is similar to the thing displayed in section 3 for pure and mixed states, I think it will be an instructive exercise for whom it may concern.

5 Discussion

Direct state measurement is a quite new and interesting field to explore the quantum world, it is also a promising tool for quantum computation and quantum information. This paper has introduced three methods to attain that goal. All of them use probabilities of polarization of final states measured to reconstruct quantum wave function. Especially, probe-controlled system is a powerful and general way to upgrade and create other new methods for this purpose.

References

[1] Y. Aharonov, D. Z. Albert and L. Vaidman, Phys.Rev.Lett 1351, **60**(1988)

[2] Michael A. Nielsen and Isaac L. Chuang, Quantum Computation and Quantum Information (Cambridge University Press, 2010).

[3] J. S. Lundeen, B. Sutherland, A. Patel, C. Stewart, and C. Bamber, Nature 474, **188** (2011).

[4] G. Vallone and D. Dequal, Phys. Rev. Lett. **116**, 040502 (2016).; Denkmayr et al., Phys. Rev. Lett. **118**, 010402 (2017).

[5] K. Ogawa, O. Yasuhiko, H. Kobayashi, T. Nakanishi, and A. Tomita, New J. Phys. **21**, 043013 (2019).

Dynamical SU(n) Symmetry of the n-Dimensional Isotropic Harmonic Oscillator

Zhang Rundong

(Dated: June 20, 2019)

This paper briefly introduces the basic knowledge of Lie group, Lie algebra and representation theory. Using this knowledge, the SU(n) symmetry of the n-dimensional isotropic harmonic oscillator is demonstrated by utilizing ladder operators and generators of the symmetry group. This paper also introduces the connection between this symmetry and the counterpart in classical mechanics.

I. INTRODUCTION

If a quantum system has some symmetry, then the Hamiltonian of this system is invariant under certain operations. For example, for a system with a spherically symmetric potential energy function, the Hamiltonian of this system would remain unchanged under spatial rotation operations. Usually, for each spatial rotation operation, there is a unitary operator associated with it [1]. These unitary operators act on the Hilbert space and they commute with the Hamiltonian. In this situation, the eigenspace belonging to a certain energy level is invariant under the action of these operators, and the eigenstates pertaining to this energy level constitute the basis of representation of the symmetry group.

However, many systems with spherically symmetric potential energy functions actually have symmetry groups larger than that of spatial rotational symmetry, we then say these systems have dynamical symmetry. Two famous examples of dynamical symmetry would be the SO(4) symmetry of hydrogen atoms [2] and the SU(n) symmetry of n-dimensional isotropic harmonic oscillators [3]. For the dynamical symmetry group of a system, eigenstates belonging to a certain energy level constitute the basis of its irreducible representation. Thus, the degrees of degeneracy of a system are related to the dimensions of irreducible representations of its dynamical symmetry group [3].

In this paper we mainly introduce the SU(n) symmetry of the n-dimensional isotropic harmonic oscillator. The arrangement of this paper is as follows: we first introduce the basic knowledge of Lie group, Lie algebra and representation theory in the second section. Then in the third section we show the SU(n) symmetry of the n-dimensional isotropic harmonic oscillator through two ways. We will also point out the corresponding symmetry in classical mechanics. Finally there are the conclusions.

II. LIE GROUPS, LIE ALGEBRAS AND REPRESENTATION THEORY

A. Groups: Finite groups and Lie groups

A group $(G, \cdot)$ is a set G equipped with a binary operation "$\cdot$" that satisfies the following four axioms:

1. $\forall g_1, g_2 \in G$, $g_1 \cdot g_2 \in G$.
2. There is a unique element $e \in G$ satisfies $g \cdot e = e \cdot g = g$ for every $g \in G$, e is called the identity element of group G.
3. For every $g \in G$ there is a $g^{-1} \in G$ such that $g \cdot g^{-1} = g^{-1} \cdot g = e$. Here e is the identity element.
4. $\forall g_1, g_2, g_3 \in G$, $(g_1 \cdot g_2) \cdot g_3 = g_1 \cdot (g_2 \cdot g_3)$.

A typical example of group is the set of all unitary operators O that leave Hamiltonian H invariant under a unitary similarity transformation

$$O^\dagger H O = H. \tag{1}$$

Here, the binary operation of this group is the multiplication of two operators. We use $\mathscr{G}$ to denote this group.

A group can be classified as a finite group or an infinite group according to the number of its elements. A Lie group, or a continuous group, is an infinite group with a manifold structure. In layman's terms, a Lie group is a group whose group elements are continuously dependent on certain parameters θ_i. We can write the element g of a Lie group as $g\left(\theta_1, \theta_2, \cdots\right)$ and let $g\left(0, 0, \cdots\right) = e$. In this paper, we mainly focus on Lie groups.

Suppose there are two groups $(G_1, \cdot)$ and $(G_2, *)$, then we say that map $\sigma : G_1 \to G_2$ is a group homomorphism if it preserves group multiplications:

$$\sigma(g \cdot g') = \sigma(g) * \sigma(g'), \forall g, g' \in G_1. \tag{2}$$

A group homomorphism σ is said to be an isomorphism if σ is bijective.

In physics, the most important Lie groups would be the groups SO(n) and SU(n). They are all matrix groups, so the binary operation of these groups is the matrix multiplication. Where SO(n) is the group of all n-by-n orthogonal matrices whose determinants are 1. SU(n) group is the abbreviation for "n-order special unitary group", which is a group of all n-by-n unitary matrices with unit determinants.

B. Lie Algebras of SO(n) and SU(n)

In this section, we will discuss the matrix groups SO(n) and SU(n). One of their important features is that each of their elements can be generated in the following way

$$M = e^{iH}. \tag{3}$$

Where M is an element of $\mathrm{SO}(n)$ or $\mathrm{SU}(n)$, and H is a traceless Hermitian matrix. Moreover, H can be written as a real linear combination of the bases of some vector space $\mathcal{V}$ which is composed of specific matrices. We call the bases of space $\mathcal{V}$ the generators of the corresponding Lie group. In vector space $\mathcal{V}$, the operation "$[\cdot,\cdot]$", i.e. the commutator of two matrices is closed. The vector space $\mathcal{V}$ with the binary operation "$[\cdot,\cdot]$" is often called the Lie algebra of the corresponding Lie group. Now let's look for the generators and Lie algebras corresponding to $\mathrm{SO}(n)$ and $\mathrm{SU}(n)$.

We first consider the group $\mathrm{SO}(2)$. Notice that each element of $\mathrm{SO}(2)$ represents a rotation on a two-dimensional plane. To study rotations, one only has to study rotation through infinitesimal angles, since a rotation through finite angle can always be achieved by performing a series of infinitesimal rotations [4]. We notice that an infinitesimal rotation can be written as

$$R\left(\theta\right) \approx I + A. \tag{4}$$

Here A is a matrix of order θ, and θ is a small real parameter controlling the angle of this rotation. Matrix I is the identity matrix. When $\theta = 0, R = I$, there is no rotation at all. Then we impose the condition of orthogonality on $R\left(\theta\right)$

$$\begin{aligned} R^T R &\approx \left(I + A^T\right)\left(I + A\right) \\ &= I + \left(A^T + A\right) + A^T A = I. \end{aligned} \tag{5}$$

If we want the orthogonality condition to hold to first order in θ, then we have $A^T = -A$. Notice that there is only one independent 2-by-2 anti-symmetric matrix

$$\mathscr{T} = \begin{pmatrix} 0 & 1 \\ -1 & 0 \end{pmatrix}. \tag{6}$$

Thus, we know that $A = \theta\mathscr{T}$, and an infinitesimal rotation $R\left(\theta\right)$ must have the form

$$R(\theta) \approx I + \theta\mathscr{T}. \tag{7}$$

You may ask: what if I want to have a rotation through finite angle θ? Here is the answer:

$$\begin{aligned} R(\theta) &= \lim_{N\to\infty}\left[R\left(\frac{\theta}{N}\right)\right]^N \\ &= \lim_{N\to\infty}\left(I + \frac{\theta\mathscr{T}}{N}\right)^N = e^{\theta\mathscr{T}} = e^A. \end{aligned} \tag{8}$$

A brutal calculation of the matrix exponent gives

$$R\left(\theta\right) = e^{\theta\mathscr{T}} = \begin{pmatrix} \cos\theta & \sin\theta \\ -\sin\theta & \cos\theta \end{pmatrix}. \tag{9}$$

This is exactly the element of $\mathrm{SO}(2)$ group that we are familiar with. Matrix $\mathscr{T}$ is called the generator of $\mathrm{SO}(2)$. The way of obtaining a group element $R\left(\theta\right)$ from the generator $\mathscr{T}$ (as that in Eq. (8)) is called an exponential map.

We now move on to the group $\mathrm{SO}(n)$. It is obvious that Eq. (4) for infinitesimal rotations and Eq. (5) for the orthogonality condition still hold, so does the conclusion that A must be anti-symmetric. But this time there are more than one generators for $\mathrm{SO}(n)$, that is, there are more than one linearly independent n-by-n anti-symmetric matrices. Actually, all n-by-n real anti-symmetric matrices form a vector space over $\mathbb{R}$, and the number of linearly independent n-by-n anti-symmetric matrices is $n(n-1)/2$. We can label them as $\mathscr{T}_{(kl)}$, then A can be written as

$$A = \sum_{1\leqslant k<l\leqslant n} \theta_{(kl)}\mathscr{T}_{(kl)}. \tag{10}$$

Here we select anti-symmetric matrix $\mathscr{T}_{(kl)}$ to be [4]

$$\mathscr{T}_{(kl)ij} = \delta_{ik}\delta_{jl} - \delta_{il}\delta_{jk}. \tag{11}$$

We would like to remind readers that those indices in parentheses are used to mark matrices, and those indices outside parentheses are used to represent elements of matrices. One of the most important conclusions in the group theory of matrices is that any element of $\mathrm{SO}(n)$ can also be written as

$$R(\theta) = e^A = \exp\left(\sum_{1\leqslant k<l\leqslant n} \theta_{(kl)}\mathscr{T}_{(kl)}\right). \tag{12}$$

Here A is defined in Eq. (10). In physics, we usually define

$$J_{(kl)} = -i\mathscr{T}_{(kl)} \tag{13}$$

to be an Hermitian matrix. At this point, Eq. (12) can be written as

$$R(\theta) = \exp\left(i\sum_{1\leqslant k<l\leqslant n} \theta_{(kl)}J_{(kl)}\right) = e^{iH}. \tag{14}$$

Here $H = -iA$ is a traceless Hermitian matrix. It can be proved that $R(\theta)$ given by Eq. (12) has unit determinant. According to linear algebra, any Hermitian matrix H can be diagonalized by a unitary matrix W and we can write $H = W^\dagger\Lambda W$. Then

$$\begin{aligned} \det(R) &= \det\left(e^{iW^\dagger\Lambda W}\right) = \det\left(W^\dagger e^{i\Lambda}W\right) \\ &= \det\left(W^\dagger W\right)\det\left(e^{i\Lambda}\right) = \prod_{j=1}^{n} e^{i\lambda_j} \\ &= e^{i\sum_{j=1}^{n}\lambda_j} = e^{i\mathrm{tr}\Lambda} = e^{i\mathrm{tr}\left(W^\dagger\Lambda W\right)} = e^{i\mathrm{tr}H}. \end{aligned} \tag{15}$$

Here we used the cyclic identity of trace. Since H is traceless, Eq. (15) tells us that $\det(R) = 1$.

Since the commutator of two anti-symmetric matrices is still an anti-symmetric matrix, so it must can be expressed as a linear combination all generators, a tedious calculation shows that

$$\begin{aligned} \left[\mathscr{T}_{(kl)}, \mathscr{T}_{(pq)}\right] =& \delta_{kp}\mathscr{T}_{(ql)} + \delta_{lq}\mathscr{T}_{(pk)} \\ &+ \delta_{lp}\mathscr{T}_{(kq)} + \delta_{kq}\mathscr{T}_{(lp)}. \end{aligned} \tag{16}$$

This leads to commutators of matrices $J_{(kl)}$

$$\left[J_{(kl)}, J_{(pq)}\right] = i\left(\delta_{kp}J_{(lq)} + \delta_{lq}J_{(kp)} + \delta_{lp}J_{(qk)} + \delta_{kq}J_{(pl)}\right). \quad (17)$$

We conclude that any n-by-n special (unit determinant) orthogonal matrices can be generated by $n(n-1)/2$ anti-symmetric matrices $\mathscr{T}_{(kl)}$ through the way of Eq. (12). Moreover, these matrices $\mathscr{T}_{(kl)}$ form the basis of the real vector space of all n-by-n (real) anti-symmetric matrices, and there is a closed binary operation "$[\cdot,\cdot]$" in this vector space.

For SU(n), we can use the similar method to obtain its generators. We first write the n-by-n unitary matrix U near the identity I to be

$$U \approx I + iH. \quad (18)$$

Here H is a complex matrix with "very tiny" elements. By asking $U^\dagger U \approx (I - iH^\dagger)(I + iH) = I - i(H^\dagger - H) + H^\dagger H = I$ to hold to the leading order of H, we get $H^\dagger = H$. Thus, H has to an Hermitian matrix. Then, as the case in SO(n), a general unitary matrix U can be written as

$$U = e^{iH}. \quad (19)$$

We then have to impose the property "special" on H, in other word, we have to find the condition under which the determinant of U is 1. Notice that according to Eq. (15), we have $\det(U) = e^{i\mathrm{tr}H}$. This implies that H has to be traceless.

All n-by-n traceless Hermitian matrices form a real vector space with dimension $n^2 - 1$. To see this, we first let H to be purely imaginary. We write H as

$$H = -iA. \quad (20)$$

Here A is a real matrix. Then it easy to see that the Hermicity of H requires A to be an anti-symmetry matrix. Actually, in this case these traceless Hermitian matrices H are just matrices $J_{(kl)}$. We then let $H = S$ to be purely real, then Hermicity of H requires S to be a symmetry matrix. We define

$$S_{(kl)ij} = \delta_{ik}\delta_{jl} + \delta_{il}\delta_{jk} - \frac{2}{n}\delta_{kl}\delta_{ij}. \quad (21)$$

Matrices $S_{(kl)}$ in Eq. (21) are both symmetric and traceless, and matrices $S_{(kl)}$ with $k = l$ satisfy the identity

$$\sum_{k=1}^{n} S_{(kk)} = 0. \quad (22)$$

Since the commutator of two traceless Hermitian matrices is still a traceless Hermitian matrix, so it must can be expressed as a linear combination of all generators. Again, a tedious calculation shows that

$$\left[S_{(kl)}, S_{(pq)}\right] = i\left(\delta_{lp}J_{(kq)} + \delta_{lq}J_{(kp)} + \delta_{kp}J_{(lq)} + \delta_{kq}J_{(lp)}\right), \quad (23)$$

$$\left[J_{(kl)}, S_{(pq)}\right] = i\left(\delta_{kp}S_{(lq)} + \delta_{kq}S_{(lp)} - \delta_{lp}S_{(kq)} - \delta_{lq}S_{(kp)}\right). \quad (24)$$

There are $n(n-1)/2$ linearly independent matrices $J_{(kl)}$, and because of the existence of Eq. (22), there are $n(n+1)/2 - 1$ linearly independent matrices $S_{(kl)}$, put them together, we have $n^2 - 1$ generators. For SU(n) we have a parallel conclusion: any n-by-n special (unit determinant) unitary matrices can be generated by $n^2 - 1$ traceless Hermitian matrices $J_{(kl)}$ and $S_{(kl)}$ through the way of exponential map. These matrices $J_{(kl)}$ and $S_{(kl)}$ also form the basis of the real vector space of all n-by-n traceless Hermitian matrices, and there is also a closed binary operation "$[\cdot,\cdot]$" in this vector space.

For a general Lie group G, suppose it has N generators T_a that form the basis of some vector space $\mathcal{V}$. Usually the commutators (not necessarily the commutators of matrices now) between generators can be expressed as

$$[T_a, T_b] = i f_{abc} T_c, \quad (25)$$

with f_{abc} referred to as the structure constants. In the above formula we used Einstein's summation convention. The vector space $\mathcal{V}$ above, together with the map "$[\cdot,\cdot]$" from $\mathcal{V} \times \mathcal{V}$ to $\mathcal{V}$ is referred to as the Lie algebra of Lie group G.

C. Representation Theory

A linear representation σ of group G is a homomorphism from G to GL(V)[5]. Here, GL(V) is the group of all invertible linear transformations that act on vector space V. We assume that V is a vector space over $\mathbb{C}$. According to linear algebra, when a set of base vectors is selected in the vector space V, an isomorphism will form between GL(V) and GL$(n;\mathbb{C})$, where GL$(n;\mathbb{C})$ is the group of $n \times n$ invertible matrices with complex entries. So, in general, a linear representation of a group G can also be considered as a homomorphism from G to GL$(n;\mathbb{C})$.

In the context of quantum mechanics, the vector space V usually appears to the Hilbert space $\mathcal{H}$ of kets. Then, a representation σ of a group G is a map from G to the set of all invertible linear operators over $\mathcal{H}$ that preserves the group multiplication

$$\sigma(g_1 \cdot g_2) = \sigma(g_1)\sigma(g_2). \quad (26)$$

In the above formula, the group multiplication at the right side of the equal sign is the multiplication of linear operators.

If there is a non-trivial subspace W of V that is invariant under the action of all $\sigma(g), g \in G$, then we say representation σ of G is reducible, otherwise we say σ is irreducible. If group G has an irreducible representation over vector space V, we call the dimension $\mathcal{D}$ of V the dimension of irreducible representation.

One of the most important results in representation theory is that the dimensions $\mathcal{D}$ of irreducible representations of a given group are limited. In other words, a group cannot have an irreducible representation of arbitrary dimension.

In order to understand the degeneracy of the n-dimensional isotropic harmonic oscillator, we consider a $\mathrm{SU}(n)$ tensor $\boldsymbol{T}$ with m lower indices. When the basis of vector space V is transformed according to a matrix U in $\mathrm{SU}(n)$, the components of tensor $\boldsymbol{T}$ are transformed according to the following rule:

$$T'_{i_1 i_2 \cdots i_m} = U_{i_1 j_1} U_{i_2 j_2} \cdots U_{i_m j_m} T_{j_1 j_2 \cdots j_m}. \tag{27}$$

Here, we used Einstein's summation convention. It is obvious that the component $T'_{i_1 i_2 \cdots i_m}$ is a linear combination of the components $T_{j_1 j_2 \cdots j_m}$. Moreover, if all the components of tensor $\boldsymbol{T}$ are arranged into a vector, the correspondence between the transformation matrix $\mathscr{D}(U)$ of this vector and U is exactly a homomorphism [4], this means that $\mathscr{D}$ is a linear representation of $\mathrm{SU}(n)$. But for a general tensor $\boldsymbol{T}$, $\mathscr{D}$ is usually irreducible.

To see this, let's consider a $\mathrm{SO}(2)$ tensor $\boldsymbol{T}$ with two lower indices, and one of its components is T_{ij}. Loosely speaking, we can regard its components T_{ij} as abstract vectors marked with i and j. At this time, the components of $\boldsymbol{T}$ obeys the following transformation:

$$T'_{ij} = R(\theta)_{ik} R(\theta)_{jl} T_{kl}. \tag{28}$$

According to Eq. (9), we can know the transformation law of the vector composed of $\boldsymbol{T}$'s components is

$$\begin{pmatrix} T'_{11} \\ T'_{12} \\ T'_{21} \\ T'_{22} \end{pmatrix} = \mathscr{D}\left[R(\theta)\right] \begin{pmatrix} T_{11} \\ T_{12} \\ T_{21} \\ T_{22} \end{pmatrix}. \tag{29}$$

Where matrix $\mathscr{D}\left[R(\theta)\right]$ is

$$\begin{pmatrix} \cos^2\theta & \frac{1}{2}\sin 2\theta & \frac{1}{2}\sin 2\theta & \sin^2\theta \\ -\frac{1}{2}\sin 2\theta & \cos^2\theta & -\sin^2\theta & \frac{1}{2}\sin 2\theta \\ -\frac{1}{2}\sin 2\theta & -\sin^2\theta & \cos^2\theta & \frac{1}{2}\sin 2\theta \\ \sin^2\theta & -\frac{1}{2}\sin 2\theta & -\frac{1}{2}\sin 2\theta & \cos^2\theta \end{pmatrix}. \tag{30}$$

It can be proved that

$$\begin{aligned} \mathscr{D}\left[R(\theta_1)\right]\mathscr{D}\left[R(\theta_2)\right] &= \mathscr{D}\left[R(\theta_1+\theta_2)\right] \\ &= \mathscr{D}\left[R(\theta_1)R(\theta_2)\right]. \end{aligned} \tag{31}$$

This shows that $\mathscr{D}$ is indeed a group homomorphism from $\mathrm{SO}(2)$ to $\mathrm{GL}(4;\mathbb{C})$, and hence a representation of $\mathrm{SO}(2)$. However, this four-dimensional representation is reducible because the trace of $\boldsymbol{T}$ is invariant under transformations:

$$T'_{ii} = R_{ik}R_{il}T_{kl} = R^T{}_{ki}R_{il}T_{kl} = \delta_{kl}T_{kl} = T_{kk}. \tag{32}$$

This means that the one-dimensional subspace generated by $T_{ii} = T_{11} + T_{22}$ is invariant under the action of all $\mathscr{D}\left[R(\theta)\right]$.

For a general $\mathrm{SO}(n)$ or $\mathrm{SU}(n)$ tensor $\boldsymbol{T}$ with two lower indices, we know that

$$T_{ij} = \frac{1}{2}\left(T_{ij}+T_{ji}\right) + \frac{1}{2}\left(T_{ij}-T_{ji}\right) = S_{ij} + A_{ij}. \tag{33}$$

Here $S_{ij} = (T_{ij}+T_{ji})/2$ and $A_{ij} = (T_{ij}-T_{ji})/2$ are the symmetric and anti-symmetric parts of T_{ij}. The tensor $\boldsymbol{T}$ has $n(n+1)/2$ independent non-zero symmetric components and $n(n-1)/2$ independent non-zero antisymmetric components. It is easy to prove that they also obey the transformation law of tensors. Thus, the set of all components of $\boldsymbol{T}$ have some subsets that any component in one of these subsets only becomes a linear combination of other components in this subset during transformations.

It can be proved that if a $\mathrm{SU}(n)$ tensor $\boldsymbol{T}$ is completely symmetric about its m lower indices, then the transformation matrix of the vector formed by all $\boldsymbol{T}$'s independent components is irreducible [4], and the dimensional of this irreducible representation is

$$\mathcal{D}_m\left[\mathrm{SU}(n)\right] = \binom{m+n-1}{n-1}. \tag{34}$$

In fact, Eq. (34) represents the number of independent components of the tensor $\boldsymbol{T}$. It can be obtained by considering the problem of putting m indistinguishable balls in n boxes. While for $\mathrm{SO}(n)$, $\boldsymbol{T}$ not only has to be completely symmetric, but also has to to be traceless in respect to any two indices [4], i.e.

$$\delta_{i_1 i_2} T_{i_1 i_2 \cdots i_m} = 0. \tag{35}$$

Here we use the trace in respect to the indices i_1 and i_2, this is because $\boldsymbol{T}$ is completely symmetric. Equation (35) further reduces the number of non-zero independent components of $\boldsymbol{T}$ by $\mathcal{D}_{m-2}\left[\mathrm{SU}(n)\right]$. Then, the irreducible furnished by $\boldsymbol{T}$'s independent components has dimension

$$\begin{aligned} \mathcal{D}_m\left[\mathrm{SO}(n)\right] &= \binom{m+n-1}{n-1} - \binom{m-2+n-1}{n-1} \\ &= \frac{n+2m-2}{n-2}\binom{m+n-3}{m}. \end{aligned} \tag{36}$$

Finally, we point out the role of Lie algebra in constructing representations of a given group. Suppose we have a real linear map ϕ between Lie algebras of group G and $\mathrm{GL}(V)$ that also preserves the structure of Lie algebra

$$\phi([X,Y]) = [\phi(X), \phi(Y)]. \tag{37}$$

Then we can define a map σ from G to $GL(V)$ such that

$$\sigma(e^{iH}) = e^{i\phi(H)}, \tag{38}$$

for every $g = e^{iH}$ of Lie group G. Using B-C-H formula [5], one can verify that σ is a ("local") homomorphism, in other words, σ is a representation of G.

III. SU($\boldsymbol{N}$) SYMMETRY OF THE ISOTROPIC HARMONIC OSCILLATOR

A. Symmetry in Quantum Mechanics

In many cases, quantum mechanical systems exhibit some symmetry. The so-called symmetry is the invariance of the system's Hamiltonian under certain transformation operations. For example, for a system with spherical potential energy $V(r)$, the Hamiltonian of the system

$$H = \frac{\boldsymbol{p}^2}{2m} + V\left(r\right), \tag{39}$$

is invariant under the rotation transformation

$$\boldsymbol{r} \to \boldsymbol{r'} = \boldsymbol{R}^{-1}\boldsymbol{r}. \tag{40}$$

Here $\boldsymbol{R}$ is a special orthogonal matrix that depicts a rotation in coordinate space, and $\boldsymbol{r}$ is the position vector. Equation (40) is a symmetry operation of Hamiltonian (39). All these operations form a group, and we use $\mathcal{G}$ to represent it. For the Hamiltonian described in Eq. (39), the group $\mathcal{G}$ has subgroup SO(3).

On the other hand, transformations in quantum mechanics are usually associated with unitary operators. We donate the symmetry group $\mathscr{G}$ of Hamiltonian H to be the set of all unitary operators O that leave the Hamiltonian invariant under transformation

$$O^\dagger H O = H. \tag{41}$$

If $\left|\psi\right\rangle$ if an eigenstate of H with energy E_m, then for any $O \in \mathscr{G}$

$$HO\left|\psi\right\rangle = O(O^\dagger HO)\left|\psi\right\rangle = OH\left|\psi\right\rangle = E_m O\left|\psi\right\rangle. \tag{42}$$

This means $O\left|\psi\right\rangle$ is also an eigenstate of H with energy E_m, in other words, the eigenspace $\mathscr{E}_m$ belonging to the eigenvalue E_m is invariant under the action of O.

Generally speaking, group $\mathcal{G}$ and group $\mathscr{G}$ are isomorphic [1]. Since elements of $\mathscr{G}$ are linear operators, the isomorphism between $\mathcal{G}$ and $\mathscr{G}$ provides a representation of $\mathcal{G}$ over Hilbert space $\mathcal{H}$. This representation is usually irreducible when restricted to an eigenspace of the Hamiltonian H.

One of the main points in analyzing the symmetry of a given Hamiltonian H is that, when restricted to an eigenspace $\mathscr{E}_m$, the isomorphism between $\mathcal{G}$ and $\mathscr{G}$ is an irreducible representation of $\mathcal{G}$ over $\mathscr{E}_m$ [1]. Therefore, the dimension of the eigenspace $\mathscr{E}_m$ is also the dimension of an irreducible representation of $\mathcal{G}$.

B. Symmetry via Ladder Operators

Consider the Hamiltonian of the n-dimensional isotropic harmonic oscillator:

$$H = \sum_{i=1}^{n}\left(\frac{1}{2m}p_i^2 + \frac{1}{2}m\omega^2 x_i^2\right). \tag{43}$$

We define the j-th annihilation operator a_j to be [2]

$$a_j = \frac{1}{\sqrt{2\hbar m\omega}}\left(ip_j + m\omega x_j\right), \tag{44}$$

its Hermitian conjugate is the j-th creation operator

$$a_j^\dagger = \frac{1}{\sqrt{2\hbar m\omega}}\left(-ip_j + m\omega x_j\right). \tag{45}$$

Using the canonical commutation relations [2], we readily get

$$\left[a_k, a_l\right] = \left[a_k^\dagger, a_l^\dagger\right] = 0, \left[a_k, a_l^\dagger\right] = \delta_{kl}. \tag{46}$$

By using annihilation and creation operators, the Hamiltonian can be rewritten as

$$H = \hbar\omega\sum_{i=1}^{n}\left(a_i^\dagger a_i + \frac{1}{2}\right). \tag{47}$$

Then, one of the eigenstates belonging to the mth energy level

$$E_m = \left(m + \frac{n}{2}\right)\hbar\omega, \tag{48}$$

can be written as

$$\left|\psi\right\rangle = a_{i_1}^\dagger a_{i_2}^\dagger \cdots a_{i_m}^\dagger \left|0\right\rangle, \tag{49}$$

where $\left|0\right\rangle$ is the ground state, and values of $i_1, i_2, \cdots, i_m$ can range from 1 to n. It should be noted that since $a_{i_1}^\dagger, a_{i_2}^\dagger, \cdots, a_{i_m}^\dagger$ are mutually commutative, state $\left|\psi\right\rangle$ in Eq. (49) is completely symmetric with respect to indices $i_1, i_2, \cdots, i_m$.

We say the n-dimensional harmonic oscillator has a SU(n) symmetry, which means the Hamiltonian is invariant under the transformation

$$a_i \to a_i' = \sum_{j=1}^{n} U_{ij} a_j, \tag{50}$$

where U_{ij} is the matrix element of the special unitary matrix U that features the transformation. It's easy to verify that the Hamiltonian is invariant under this transformation, since the new Hamiltonian $\mathscr{H}$ is

$$\begin{aligned}
\mathscr{H} &= \hbar\omega\sum_{i=1}^{n}\left[\left(a_i'\right)^\dagger a_i' + \frac{1}{2}\right] \\
&= \hbar\omega\sum_{i=1}^{n}\left(\sum_{k=1}^{n}\sum_{l=1}^{n} U_{ki}^\dagger U_{il} a_k^\dagger a_l + \frac{1}{2}\right) \\
&= \hbar\omega\left(\sum_{k=1}^{n}\sum_{l=1}^{n}\delta_{kl} a_k^\dagger a_l + \frac{1}{2}\right) \\
&= \hbar\omega\left(\sum_{k=1}^{n} a_k^\dagger a_k + \frac{1}{2}\right) = H.
\end{aligned} \tag{51}$$

Transformation (50) also preserves the structure of commutators

$$\begin{aligned}
\left[a_k', a_l'\right] &= a_k' a_l' - a_l' a_k' \\
&= U_{ki} U_{lj}\left(a_i a_j - a_j a_i\right) = 0,
\end{aligned} \tag{52}$$

$$\left[\left(a_k'\right)^\dagger, \left(a_l'\right)^\dagger\right] = \left(a_k'\right)^\dagger \left(a_l'\right)^\dagger - \left(a_l'\right)^\dagger \left(a_k'\right)^\dagger = 0. \tag{53}$$

Here we used Einstein's summation convention. We also have

$$\begin{aligned}\left[a_k', \left(a_l'\right)^\dagger\right] &= U_{ki}U_{lj}^* a_i a_j^\dagger - U_{lj}^* U_{ki} a_j^\dagger a_i \\ &= U_{ki}U_{lj}^* \left(a_i a_j^\dagger - a_j^\dagger a_i\right) \\ &= U_{ki}U_{lj}^* \delta_{ij} = U_{ki}U_{il}^\dagger = \delta_{kl}.\end{aligned} \tag{54}$$

Under transformation described in Eq. (50), the eigenstate is transformed to:

$$\begin{aligned}\left|\psi'\right\rangle &= \left(a_{i_1}'\right)^\dagger \left(a_{i_2}'\right)^\dagger \cdots \left(a_{i_m}'\right)^\dagger \left|0\right\rangle \\ &= U_{i_1 j_1} U_{i_2 j_2} \cdots U_{i_m j_m} a_{j_1}^\dagger a_{j_2}^\dagger \cdots a_{j_m}^\dagger \left|0\right\rangle.\end{aligned} \tag{55}$$

Note that the eigenstate $|\psi\rangle$ transforms like a completely symmetric tensor with m lower indices, so Eq. (34) tells us that the degeneracy of E_m should be

$$d_m = \binom{m+n-1}{n-1}. \tag{56}$$

For $n = 3$ we have

$$d_m = \frac{1}{2}\left(m+1\right)\left(m+2\right), \tag{57}$$

which is far beyond what SO(n) implies in Eq. (36) when $n = 3$:

$$d_m = 2m + 1. \tag{58}$$

C. Symmetry via Generators

A clearer and more elegant way to construct the representation of SU(n) is by using Lie algebra. Note that we have found the Lie algebra of SU(n), if we find all generators of symmetry group $\mathscr{G}$ and the map ϕ satisfies Eq. (37) then Eq. (38) will automatically give us the desired representation.

We define [6]

$$J_{kl} = \frac{x_k p_l - x_k p_l}{\hbar} = i\left(a_k a_l^\dagger - a_k^\dagger a_l\right). \tag{59}$$

Then J_{kl} is anti-symmetric in respect to k, l, and define

$$\begin{aligned}S_{kl} &= \frac{2}{\hbar\omega}\left(\frac{1}{2m}p_k p_l + \frac{1}{2}m\omega^2 x_k x_l - \frac{1}{n}H\delta_{kl}\right) \\ &= a_k^\dagger a_l + a_k a_l^\dagger - \frac{2H}{n\hbar\omega}\delta_{kl}.\end{aligned} \tag{60}$$

Then S_{kl} is symmetric in respect to k, l, and we also have

$$\sum_{k=1}^{n} S_{kk} = 0. \tag{61}$$

There are $n(n-1)/2$ linear independent J_{kl} and $n(n+1)/2 - 1$ linear independent S_{kl}. Thus, the total number of linear independent J_{kl}s and S_{kl}s is $n^2 - 1$. It is easy to verify that all of them are conserved quantities, in other words, all of them commute with Hamiltonian H

$$\left[J_{kl}, H\right] = \left[S_{kl}, H\right] = 0. \tag{62}$$

Noether's theorem tells us that each generator of continuous symmetry corresponds to a conserved quantity. Therefore, it is natural to guess that each conserved quantity should also correspond to a generator of the symmetry group. A somewhat tedious calculation shows that the commutators of J_{kl}s and S_{kl}s are

$$\left[J_{kl}, J_{pq}\right] = i\left(\delta_{kp}J_{lq} + \delta_{lq}J_{kp} + \delta_{lp}J_{qk} + \delta_{kq}J_{pl}\right), \tag{63}$$

$$\left[S_{kl}, S_{pq}\right] = i\left(\delta_{lq}J_{kp} + \delta_{lp}J_{kq} + \delta_{kq}J_{lp} + \delta_{kp}J_{lq}\right), \tag{64}$$

$$\left[J_{kl}, S_{pq}\right] = i\left(\delta_{kq}S_{lp} + \delta_{kp}S_{lq} - \delta_{lq}S_{kp} - \delta_{lp}S_{kq}\right). \tag{65}$$

They have the form same as Eq. (17), (23) and (24). This means the symmetry group $\mathscr{G}$ of Hamiltonian H of the n-dimensional isotropic harmonic oscillator (generated by J_{kl}s and S_{kl}s) has the same structure constants as that of SU(n).

Let ϕ denotes the linear map that maps generators $J_{(kl)}$ and $S_{(kl)}$ of SU(n) to J_{kl} and S_{kl} of $\mathscr{G}$ respectively. Then, Eq. (37) holds and Eq. (38) gives the representation of SU(n).

IV. CONNECTION WITH CLASSICAL MECHANICS

In classical mechanics, if a mechanical quantity F does not explicitly contain time, then the necessary and sufficient condition for it to be a conserved quantity is that it commutes with the Hamiltonian H [7], that is

$$\left[F, H\right] = 0. \tag{66}$$

Here "$[\cdot,\cdot]$" is the Poisson bracket in classical mechanics. For two mechanical quantities φ and ψ, their Poisson bracket is

$$\left[\varphi, \psi\right] = \sum_{\alpha=1}^{s}\left(\frac{\partial\varphi}{\partial q_\alpha}\frac{\partial\psi}{\partial p_\alpha} - \frac{\partial\varphi}{\partial p_\alpha}\frac{\partial\psi}{\partial q_\alpha}\right). \tag{67}$$

Here q_α and p_α are generalized coordinates and canonical momentum, s is the degree of freedom of this system. If F is conserved quantity, then the infinitesimal canonical transformation [7] generated by F

$$Q_\alpha = q_\alpha + \varepsilon\frac{\partial F\left(q, p\right)}{\partial p_\alpha}, \tag{68}$$

$$P_\alpha = p_\alpha - \varepsilon\frac{\partial F\left(q, p\right)}{\partial q_\alpha}, \tag{69}$$

leaves the Hamiltonian H unchanged, since

$$\begin{aligned}\delta H &= \sum_{\alpha=1}^{s}\left(\frac{\partial H}{\partial q_\alpha}\delta q_\alpha + \frac{\partial H}{\partial p_\alpha}\delta p_\alpha\right)\\ &= \varepsilon\sum_{\alpha=1}^{s}\left(\frac{\partial H}{\partial q_\alpha}\frac{\partial F}{\partial p_\alpha} - \frac{\partial H}{\partial p_\alpha}\frac{\partial F}{\partial q_\alpha}\right)\\ &= \varepsilon\,[H,F] = 0. \end{aligned} \tag{70}$$

That is to say, F is a generator of the canonical transform group that keeps the Hamiltonian unchanged. By analogy, we can find that mechanical quantities defined as

$$J_{kl} = x_k p_l - x_l p_k, \tag{71}$$

$$S_{kl} = \frac{2}{\omega}\left(\frac{1}{2m}p_k p_l + \frac{1}{2}m\omega^2 x_k x_l - \frac{1}{n}H\delta_{kl}\right). \tag{72}$$

are all conserved in classical mechanics, that is, they all commute with the Hamiltonian H of the n-dimensional isotropic harmonic oscillator. And moreover, commutators (Poisson bracket) of them are closed:

$$[J_{kl}, J_{pq}] = J_{pl}\delta_{kq} + J_{qk}\delta_{lp} + J_{kp}\delta_{lq} + J_{lq}\delta_{kp}, \tag{73}$$

$$[S_{kl}, S_{pq}] = \delta_{lq}J_{kp} + \delta_{lp}J_{kq} + \delta_{kq}J_{lp} + \delta_{kp}J_{lq}, \tag{74}$$

$$[J_{kl}, S_{pq}] = \delta_{kq}S_{lp} + \delta_{kp}S_{lq} - \delta_{lq}S_{kp} - \delta_{lp}S_{kq}. \tag{75}$$

Equation (73), (74) and (75) will have the same form as Eq. (17), (23) and (24) if one further multiplies J_{kl} and S_{kl} in Eq. (71) and (72) by an imaginary unit "i". This means that the n-dimensional harmonic oscillator in classical mechanics also has the SU(n) symmetry [7].

Actually, if we define a similar quantity a_j in classical mechanics using Eq. (44), then the real and imaginary parts of the transformation (50) will give a canonical transformation of the generalized coordinates and the generalized momenta [8], and this canonical transformation keeps the Hamiltonian unchanged.

V. DISCUSSION

By using the basic knowledge of group theory, we demonstrated the the SU(n) symmetry of the n-dimensional isotropic harmonic oscillator through two different ways.

We first studied the SU(n) symmetry of the harmonic oscillator by using ladder operators. After defining the annihilation and creation operators, we can directly give the unitary transformation that keeps the Hamiltonian invariant. The annihilation operators then transform like n-dimensional vectors while eigenstates transform like completely symmetric tensors, whereby we give the degeneracy of the isotropic harmonic oscillator.

We then demonstrated the SU(n) symmetry of the n-dimensional isotropic harmonic oscillator using generators. We found the generators of those unitary transformations that keep the Hamiltonian unchanged, and they have exactly the same Lie algebra structure as that of the SU(n) group.

Finally, we point out that, in parallel with its quantum mechanics counterpart, the n-dimensional isotropic harmonic oscillator in classical mechanics possesses the same symmetry property. We also give the generators of infinitesimal canonical transformations.

In summary, the n-dimensional isotropic harmonic oscillator provides a good model for studying the dynamical symmetry.

ACKNOWLEDGMENTS

The author is very grateful to Dr. Jolyon Bloomfield for providing this topic and related references. At the same time, the author would like to thank teaching assistants Mark Weitzman and Jim Freericks for their help in learning group theory. The author also expresses his gratitude for the advice provided by Lyu Xinliang.

---

[1] A. W. Joshi, *Elements of group theory for physicists*. New Age International, 1997.

[2] J. J. Sakurai, J. Napolitano, *et al.*, *Modern quantum mechanics*. Pearson Harlow, 2014.

[3] G. A. Baker and Jr, "Degeneracy of the n-dimensional, isotropic, harmonic oscillator," *Phys Rev* **103** (1956) no. 103, 1119–1120.

[4] A. Zee, *Group theory in a nutshell for physicists*, vol. 17. Princeton University Press, 2016.

[5] B. Hall, *Lie groups, Lie algebras, and representations: an elementary introduction*, vol. 222. Springer, 2015.

[6] G. Maiella, "A general analysis of the dynamical symmetries of the n-dimensional harmonic oscillator," *Il Nuovo Cimento A (1971-1996)* **52** (1967) no. 4, 1004–1014.

[7] H. Goldstein, *Classical Mechanics*. Pearson Education India, 2002.

[8] P. Kramer, M. Moshinsky, and T. Seligman, "Complex extensions of canonical transformations and quantum mechanics," in *Group theory and its applications*, pp. 249–332. Elsevier, 1975.

Energy Levels of the Hydrogen Atom Via Sommerfeld's Old Quantum Theory and The Relativistic Dirac Equation

Mark Weitzman

(Dated: June 11, 2019)

The exact energy levels of the Hydrogen atom (up to fine structure but excluding hyperfine, Lamb, and finite nuclear size effects), can be obtained by solving the relativistic Dirac equation, via separation of variables, in a manner similar to Schrödinger's non-relativistic solution. These energy levels are given by a formula that is relatively complex involving nested square roots. In this paper we discuss and compare the remarkable calculation, almost a full decade before Dirac, by Sommerfeld, using the old quantum theory extended to take into account the relativistic velocity of the electron in its elliptic orbit, with Dirac's calculation using his celebrated wave equation. Sommerfeld's theory has no spin and no wave mechanics. Dirac's theory was the first relativistic wave mechanical equation which naturally incorporated spin 1/2. Yet the two theories are in exact agreement on the Hydrogen atom energy levels. We conclude with a very brief discussion of a resolution of this "Sommerfeld Puzzle" by Biedenharn [1], using the underlying symmetries of the problem.

I. INTRODUCTION

The calculations by Bohr, Sommerfeld, and Dirac of the energy levels of the Hydrogen atom and their remarkable agreement with experiment represents one of the high points of 20th century theoretical physics. Bohr's calculation using circular orbits and quantization of angular momentum was the first application of the developing quantum theory, pioneered by Planck, Einstein, and Debye to modeling atoms [3]. But Bohr's calculation was limited, in that they applied only to circular orbits, and single electron atoms.

In a series of papers in 1915-1916, and exposited in his influential book [2], Sommerfeld extended these calculations to elliptical orbits using what are now known as the Bohr-Wilson-Sommerfeld quantization conditions. This extension of the old quantum theory had some limited success in treating effects of electric and magnetic fields on atomic states[3]. But its greatest success was in the calculation of the fine structure of the hydrogen atom spectrum.

Using elliptical orbits, phase space quantization conditions, and classical mechanics extended to relativistic dynamics, Sommerfeld was able to arrive at an exact expression that completely agreed with experiment. This was a remarkable achievement for the old quantum theory, and led to the incorporation of some of the most advanced techniques of classical mechanics in the developing old quantum theory formalism. These techniques included Hamilton-Jacobi theory, action angle variables, and perturbation techniques from celestial mechanics [4].

Modern quantum mechanics began with Schrödinger's wave mechanics and Heisenberg's matrix mechanics formulations, which Dirac and others later showed to be equivalent. While both were successful at reproducing the Bohr energy levels, Schrödinger's attempts at a relativistic generalization (using what is now referred to as the Klein-Gordon equation) failed to agree with the fine structure spectrum [5].

Dirac [6] successfully tackled the problem by developing his famous relativistic spin 1/2 equation. The Dirac expression for the hydrogen fine structure energy levels agrees completely with Sommerfeld's expression developed a decade earlier. This agreement between two quite dissimilar theories, the first by Sommerfeld which has no wave mechanics and no spin, and the second by Dirac which is a relativistic wave equation that naturally incorporated spin is sometimes referred to as the "Sommerfeld Puzzle".

In section II we discuss Sommerfeld's derivation of the hydrogen atom energy levels including fine structure. In section III, we discuss the Dirac calculation using the separation of coupled differential equations. Finally in section IV we briefly discuss Biedenham's symmetry arguments and resolution of the "Sommerfeld puzzle".

II. SOMMERFELD'S CALCULATION

The Bohr model begins with the assumption of circular orbits, and the quantization condition $mvr = n\hbar$. Sommerfeld extended these quantization conditions to all canonical variables in the problem

$$\oint p_k \, dq_k = n_k h. \tag{1}$$

For the case of elliptical orbits in a plane (Sommerfeld also treated the case of three dimensional orbits) there are now two variables which need quantization r and ϕ, and the quantization conditions are

$$\oint_0^{2\pi} p_\phi d\phi = n_\phi h \quad \text{and} \quad \oint_{\text{orbit}} p_r dr = n_r h. \tag{2}$$

Sommerfeld's result for the energies (we opt to show the relativistic calculation below rather than the non-relativistic calculation), leads to the same values as the Bohr energy levels

$$E = -\frac{mc^2}{2}\frac{Z^2\alpha^2}{(n_r + n_\phi)^2}, \tag{3}$$

with the main difference being the added degeneracies in the energy levels, due to their being two integer quantum numbers. In a more exact relativistic calculation, these degeneracies will be broken, and will lead to the fine structure.

We choose to closely follow Biedenharn [1] in avoiding the Hamilton-Jacobi/action angle variables techniques [7], and instead proceed with a direct calculation of phase integrals using relativistic Kepler orbits. For an electron bound to a nucleus of positive charge Z, the Coulomb potential is $\Phi = \frac{Z|e|}{r}, \mathbf{A} = 0$ (our notation is $e < 0$), and the relativistic Hamiltonian can be obtained by the usual substitutions $E \to E - e\Phi, \mathbf{p} \to \mathbf{p} - e\mathbf{A}/c$ in the relativistic energy momentum relation

$$E^2 = \mathbf{p}^2c^2 + (mc^2)^2, \tag{4}$$

$$\left(H + \frac{Ze^2}{r}\right)^2 = \mathbf{p}^2c^2 + (mc^2)^2. \tag{5}$$

As in the classical Kepler problem we use radial and angular components of momentum with the corresponding relativistic expressions,

$$p_r = \frac{m\dot{r}}{\sqrt{1 - \frac{v^2}{c^2}}} = \gamma m\dot{r} \tag{6}$$

$$p_\phi = \frac{mr^2\dot{\phi}}{\sqrt{1 - \frac{v^2}{c^2}}} = \gamma mr^2\dot{\phi}. \tag{7}$$

Continuing to mimic the classical calculation we define $u = \frac{1}{r}$ and observe that $\frac{p_r}{p_\phi} = -\frac{du}{d\phi}$. Substituting into Eq. (5) leads to:

$$\left(\frac{H + Ze^2u}{mc^2}\right)^2 = 1 + \left(\frac{p_\phi}{mc}\right)^2 \left[\left(\frac{du}{d\phi}\right)^2 + u^2\right]. \tag{8}$$

Upon differentiating the above equation, one obtains an easily solvable linear differential equation for the orbit.

$$\frac{d^2u}{d\phi^2} + \Gamma^2 u = C\Gamma^2 \quad \text{where,} \tag{9}$$

$$1 - \frac{Z^2e^4}{c^2p_\phi^2} \equiv \Gamma^2 \quad \text{and} \tag{10}$$

$$\frac{Ze^2H}{p_\phi^2\Gamma^2c^2} \equiv C. \tag{11}$$

The solution can be verified as

$$\frac{1}{r} \equiv u = \frac{1}{a}\left(\frac{1 + \varepsilon\cos(\Gamma\phi)}{1 - \varepsilon^2}\right) \tag{12}$$

$$C = \frac{1}{a(1 - \varepsilon^2)}, \tag{13}$$

where we have chosen the constants to correspond to the standard parameters for an ellipse with semi-major axis a, and the eccentricity of the orbit ε.

Actually because $\Gamma\Phi$ is the parameter of the cosine function, our solution is not an ellipse but a rotating ellipse whose perihelion is precessing in the same direction as the orbit see Figure 1. The precession per orbit is $2\pi(\frac{1}{\Gamma} - 1)$, and if we substitute $Ze^2 \to GMm$, and use Kepler's 3rd law along with Eq. (10), we obtain a precession per orbit for a planet of

$$\frac{\pi GM}{c^2a(1 - \varepsilon^2)} \tag{14}$$

which is 1/6 of the well known general relativistic result. [8], [9].

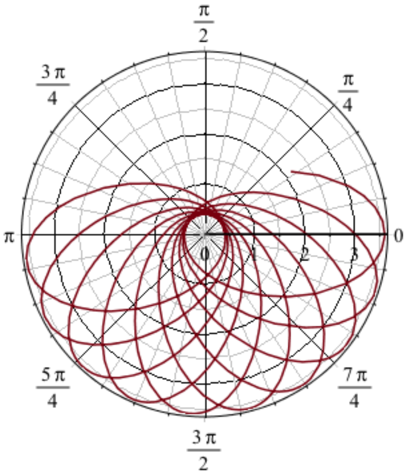

Figure 1. Precession of elliptical orbits

Thus the true periodic action angle variable is $\psi \equiv \Gamma\phi$. We now use the quantization conditions stated earlier Eq. (2) noting that whereas for p_ϕ, we integrate from $\phi = 0$ to $\phi = 2\pi$, for p_r we must integrate from $\psi = 0$ to $\psi = 2\pi$ in order for the radial variable to repeat (perihelion to perihelion):

$$\int_{\phi=0}^{\phi=2\pi} p_\phi d\phi = n_\phi h \tag{15}$$

$$\int_{\psi=0}^{\psi=2\pi} p_r dr = n_r h \tag{16}$$

Since, angular momentum is conserved for a central force potential, we immediately obtain from Eq. (15)

$$p_\phi = n_\phi \hbar \tag{17}$$

To solve the radial momentum integral, we earlier observed that $\frac{p_r}{p_\phi} = -\frac{du}{d\phi}$, which implies

$$p_r dr = p_\phi \left(\frac{1}{r}\frac{dr}{d\phi}\right)^2 d\phi = p_\phi \varepsilon^2 \Gamma \frac{\sin^2\psi}{(1 + \varepsilon\cos\psi)^2} d\psi, \tag{18}$$

using Eq. (9). Substituting into Eq. (16), we obtain the radial quantum condition.

$$\frac{1}{2\pi}\int_{\psi=0}^{\psi=2\pi} \frac{\varepsilon^2\sin^2\psi\, d\psi}{(1 + \varepsilon\cos\psi)^2} = \frac{n_r}{\Gamma n_\phi}. \tag{19}$$

The integral is elementary, and the LHS evaluates to $(1-\varepsilon^2)^{-\frac{1}{2}}-1$.This now gives us one of the orbit parameters ε in terms of the quantum numbers $n_{r,}, n_\phi$ (note that Γ is given by Eq. (10), and p_ϕ is given by Eq. (17)),

$$\varepsilon^2 = 1 - \frac{1}{\left(1+\frac{n_r}{\Gamma n_\phi}\right)^2}. \tag{20}$$

The second orbit parameter a, can be obtained from Eqs. (11), (13), and (17),

$$a = \frac{n_\phi^2 \Gamma^2 \hbar c}{Z\alpha H(1-\varepsilon^2)}. \tag{21}$$

Substituting the values of the orbit parameters a, ε into the orbit equation (12), and then into Eq. (8) leads after a couple of pages of unilluminating algebra [10], to Sommerfeld's celebrated equation (Note the corresponding equation (20) in Biedenharn's paper is missing a square on the bracketed term in the denominator)

$$H = mc^2 \left(1 + \frac{\alpha^2 Z^2}{\left[n_r + \sqrt{n_\phi^2 - \alpha^2 Z^2} \right]^2} \right)^{-\frac{1}{2}}. \tag{22}$$

III. THE DIRAC CALCULATION

Dirac developed his landmark equation [6] with the intention of finding a relativistic equation for the electron which overcame some of the difficulties of the relativistic Schrödinger/Klein-Gordon (KG) equation. One of the main difficulties concerned the lack of a positive definite conserved probability current. This problem was traced to the appearance of a second order time derivative in the KG equation, which follows from the relativistic energy momentum relation Eq. (4). In contrast a positive definite conserved probability current is readily obtained for the non-relativistic Schrdinger equation due to its being first order in the time derivative.

Dirac looked for an equation that was first order in the time derivative, and also first order in spatial derivatives, in order to treat time and space symmetrically as is required by relativity. The coefficients of the spatial and time derivatives could not be ordinary numbers as then the equation would not even be rotationally invariant, let alone Lorentz invariant. Thus Dirac tried a linear first order equation with matrices, and this led to tremendous success as it was found to naturally incorporate spin and antiparticles, and had the correct non-relativistic limit. Aditionally as first shown by Darwin it leads to the correct fine structure for Hydrogen [11].

Below we will show the Dirac equation including the incorporation of electromagnetic potentials, develop constants of the motion, and then separate the equation in a central potential. Finally we will solve the coupled differential equations for the exact energies in a Coulomb potential, and compare with Sommerfeld's equation. Discussions of the Dirac equation and its solutions in the Hydrogen atom are treated in the following well known texts: [5], [12], [13], and [14].

A. Dirac Equation in Electromagnetic Potentials

The Dirac equation in non-covariant Hamiltonian form is

$$i\hbar \frac{\partial \psi}{\partial t} = \left(c\boldsymbol{\alpha}\cdot\mathbf{p} + \beta mc^2 \right)\psi, \tag{23}$$

where ψ is a four-component object, known as a Dirac spinor, and $\boldsymbol{\alpha}, \beta$ are a set of four 4-dimensional matrices satisfying

$$\begin{aligned} \alpha_i^2 &= \beta^2 = 1 \\ \{\alpha_i, \alpha_j\} &\equiv \alpha_i\alpha_j + \alpha_j\alpha_i = 2\delta_{ij} \\ \{\alpha_i, \beta\} &\equiv \alpha_i\beta + \beta\alpha_i = 0 \end{aligned} \tag{24}$$

In the Dirac-Pauli energy representation they can be explicitly represented as

$$\alpha_i = \begin{pmatrix} 0 & \sigma_i \\ \sigma_i & 0 \end{pmatrix}, \quad \beta = \begin{pmatrix} 1 & 0 \\ 0 & -1 \end{pmatrix}, \tag{25}$$

where the σ_i are the standard Pauli matrices, and 1 is the two dimensional identity matrix. Following the previous classical prescription for introducing electromagnetic potentials (minimal coupling), and working with energy eigenstates, we obtain

$$(E - e\Phi)\psi = \left(c\boldsymbol{\alpha}\cdot\left(\mathbf{p} - \frac{e}{c}\mathbf{A}\right) + \beta mc^2 \right)\psi. \tag{26}$$

For a central potential $V = e\Phi$, and $\mathbf{A} = 0$,

$$H\psi = E\psi = \left(c\boldsymbol{\alpha}\cdot\mathbf{p} + \beta mc^2 + V \right)\psi. \tag{27}$$

B. Constants of the Motion

The Dirac equation incorporates spin 1/2 particles, so it is no surprise that the total angular momentum operator would involve orbital and spin angular momentum, and be conserved in a central potential. Thus we define the relativistic spin operator as $\boldsymbol{\Sigma}$ (basically just the diagonal 4 dimensional version of the Pauli matrices, and the total angular momentum operator (an operator like $\mathbf{L}$ not in matrix form is assumed to be multiplied by the four dimensional identity matrix) as

$$\boldsymbol{\Sigma} \equiv \begin{pmatrix} \boldsymbol{\sigma} & 0 \\ 0 & \boldsymbol{\sigma} \end{pmatrix} \tag{28}$$

$$\mathbf{J} = \mathbf{L} + \frac{\hbar}{2}\boldsymbol{\Sigma} \tag{29}$$

Using the usual commutation properties of angular momentum operators, $[L_i, S] = 0, [L_i, V_j] = i\hbar\epsilon_{ijk}V_k$, where $S, \mathbf{V}$ are respectively scalar and vector operators it is easy to show that $\mathbf{J}$ commutes with the Hamiltonian (although we sometimes use the explicit Dirac-Pauli representation, all of these properties can be established in a representation-free independent manner). Below we use Einstein summation convention for repeated indices.

$$\begin{aligned}[H, L_x] &= \left[c\boldsymbol{\alpha}\cdot\mathbf{p} + \beta mc^2 + V(r), L_x\right] \\ &= c[\alpha_i p_i, L_x] + [V(r), L_x] \\ &= -i\hbar c\alpha_y p_z + i\hbar c\alpha_z p_y \qquad (30) \\ [H, \Sigma_x] &= [c\alpha_i p_i + \beta mc^2 + V(r), \Sigma_x] \\ &= c[\alpha_i, \Sigma_x]p_i = -2ic\alpha_z p_y + 2ic\alpha_y p_z \qquad (31)\end{aligned}$$

From Eqs. (30) and (31) it follows that $[H, J_x] = 0$, and thus generalizing to all components, $\mathbf{J}$ is a constant of the motion.

The next constant of the motion physically involves whether the spin is parallel or antiparallel to the orbital angular momentum i.e. whether in the non-relativistic theory $j = l + 1/2$, or $j = l - 1/2$. The situation is a little more complicated relativistically and we define an operator $K = \beta(\mathbf{\Sigma}\cdot\mathbf{L}+\hbar)$. We will show that the operator K is conserved using an explicit representation of H, K

$$H = \begin{pmatrix} mc^2 + V(r) & c\boldsymbol{\sigma}\cdot\mathbf{p} \\ c\boldsymbol{\sigma}\cdot\mathbf{p} & -mc^2 + V(r)\end{pmatrix} \qquad (32)$$

$$K = \begin{pmatrix} \boldsymbol{\sigma}\cdot\mathbf{L} + \hbar & 0 \\ 0 & -(\boldsymbol{\sigma}\cdot\mathbf{L} + \hbar)\end{pmatrix}. \qquad (33)$$

In computing $[H, K]$, using $[L, V(r)] = 0$ (since V(r) is a scalar) we only have to verify

$$-c(\boldsymbol{\sigma}\cdot\mathbf{p})(\boldsymbol{\sigma}\cdot\mathbf{L} + \hbar) - c(\boldsymbol{\sigma}\cdot\mathbf{L} + \hbar)(\boldsymbol{\sigma}\cdot\mathbf{p}) = 0 \qquad (34)$$

which follows using the commutator for $[L_i, p_j]$, and the identity $(\boldsymbol{\sigma}\cdot\mathbf{p})(\boldsymbol{\sigma}\cdot\mathbf{L}) = i\boldsymbol{\sigma}\cdot\mathbf{p}\times\mathbf{L}$, since $\mathbf{p}\cdot\mathbf{L} = 0$. Using the same techniques it follows also that $[\mathbf{J}, K] = 0$.

Finally we have that in a central potential the operators $H, K, \mathbf{J}^2, \mathbf{J}$ all commute with each other, and we can use simultaneous eigenfunctions with corresponding eigenvalues that we will denote by $E, -\kappa\hbar, j(j+1)\hbar^2, j_z\hbar$.

C. Separation in Central Force Potential

We write $\psi = \begin{pmatrix}\psi_A \\ \psi_B\end{pmatrix}$, where ψ_A, ψ_B are each two-components spinors. In the non-relativistic approximation, the upper components ψ_A correspond to the usual Pauli two-component spinor for the electron, and the bottom two components ψ_B are smaller by a factor of v/c. In the Dirac-Pauli representation the K, and $\mathbf{\Sigma}$ operators are diagonal - this enables us to make use of the usual two-component Pauli formalism in constructing angular eigenfunctions of K, J^2, J_z.

The operator $\mathbf{L}^2$ when operating on the two-component spinors is equal to $\mathbf{J}^2 - \hbar\boldsymbol{\sigma}\cdot\mathbf{L} - \frac{3}{4}\hbar^2$, so any eigenfunction of $\mathbf{J}^2$ and K - see Eq. (33) - is also an eigenfunction of $\mathbf{L}^2$. Thus although the complete wave function ψ will not be an eigenfunction of $\mathbf{L}^2$ (since it does not commute with the Hamiltonian, and K operates differently on each of ψ_A, ψ_B), the separate pieces will be eigenfunctions of $\mathbf{L}^2$.

To get the relationship between j, κ, and l values for ψ_A, ψ_B, we make use of the following

$$K^2 = \mathbf{L}^2 + \hbar\mathbf{\Sigma}\cdot\mathbf{L} + \hbar^2 \qquad (35)$$

$$\mathbf{J}^2 = \mathbf{L}^2 + \hbar\mathbf{\Sigma}\cdot\mathbf{L} + \frac{3}{4}\hbar^2 \qquad (36)$$

$$K^2 = \mathbf{J}^2 + \hbar^2/4 \qquad (37)$$

This implies $\kappa^2\hbar^2 = j(j+1)\hbar^2 + \hbar^2/4 = (j+1/2)^2\hbar^2$ or

$$\kappa = \pm(j + 1/2). \qquad (38)$$

To get the corresponding relations for the values of l_A, l_B, we use Eq. (36), along with $(\boldsymbol{\sigma}\cdot\mathbf{L} + \hbar)\psi_A = -\kappa\hbar\psi_A$ in the two dimensional subspaces

$$\begin{aligned}\mathbf{L^2}\psi_A = l_A(l_A+1)\hbar^2\psi_A &= \left(\mathbf{J}^2 - \hbar\boldsymbol{\sigma}\cdot\mathbf{L} - \frac{3}{4}\hbar^2\right)\psi_A \\ &= \left(j(j+1)\hbar^2 + (\kappa+1)\hbar^2 - \frac{3}{4}\hbar^2\right)\psi_A \qquad (39)\end{aligned}$$

which implies $l_A(l_A+1) = j(j+1) + \kappa + \frac{1}{4}$. A similar analysis for ψ_B leads to $l_B(l_B+1) = j(j+1) - \kappa + \frac{1}{4}$. Table I (copied from p.124 of [14]) summarizes the relations among j, k, l_A, l_B.

Table I. Relations among κ, j, l_A, l_B

	l_A	l_B
$\kappa = j + 1/2$	$j + 1/2$	$j - 1/2$
$\kappa = -(j + 1/2)$	$j - 1/2$	$j + 1/2$

With these relations we can construct the full angular parts of the eigenfunction for ψ_A, ψ_B. The Pauli two-component theory (addition of angular momenta) [15],[13],[14], gives

$$\varphi^{+}_{j,j_3} = \begin{pmatrix}\sqrt{\frac{l+\frac{1}{2}+j_3}{2l+1}}\,Y_l^{j_3-\frac{1}{2}} \\ \sqrt{\frac{l+\frac{1}{2}-j_3}{2l+1}}\,Y_l^{j_3+1/2}\end{pmatrix}\left(j = l + \frac{1}{2}\right) \qquad (40)$$

$$\varphi^{-}_{j,j_3} = \begin{pmatrix}-\sqrt{\frac{l+\frac{1}{2}-j_3}{2l+1}}\,Y_l^{j_3-\frac{1}{2}} \\ \sqrt{\frac{l+\frac{1}{2}+j_3}{2l+1}}\,Y_l^{j_3+1/2}\end{pmatrix}\left(j = l - \frac{1}{2}\right) \qquad (41)$$

Notice the two φ's have opposite parity, since their l values differ by 1. When grouped together in a four component spinor, the spinor will be a parity eigenstate, since the parity operator in the Dirac theory is given by β, so the opposite signs from the l values will be canceled by the opposite signs from the β operator.

The wave function ψ can then be written as

$$\begin{pmatrix} \psi_A \\ \psi_B \end{pmatrix} = \begin{pmatrix} g(r)\varphi^A_{j,j_3} \\ if(r)\varphi^B_{j,j_3} \end{pmatrix} \tag{42}$$

where $\varphi^A = \varphi^+, \varphi^B = \varphi^-$ for $\kappa = -(j+1/2)$, and $\varphi^A = \varphi^-, \varphi^B = \varphi^+$ for $\kappa = (j+1/2)$. Additionally the radial wave functions depend on κ. The Dirac equation using the explicit form of the Hamiltonian operator Eq. (32) is then

$$\begin{aligned} c\boldsymbol{\sigma}\cdot\mathbf{p}\psi_B &= (E - V - mc^2)\psi_A \\ c\boldsymbol{\sigma}\cdot\mathbf{p}\psi_A &= (E - V + mc^2)\psi_B \end{aligned} \tag{43}$$

To make progress we use a trick (see [13],[14])and rewrite

$$\begin{aligned} \boldsymbol{\sigma}\cdot\mathbf{p} &= \frac{1}{r^2}(\boldsymbol{\sigma}\cdot\mathbf{x})(\boldsymbol{\sigma}\cdot\mathbf{x})(\boldsymbol{\sigma}\cdot\mathbf{p}) \\ &= \frac{(\boldsymbol{\sigma}\cdot\mathbf{x})}{r^2}\left(-i\hbar r\frac{\partial}{\partial r} + i\boldsymbol{\sigma}\cdot\mathbf{L}\right). \end{aligned} \tag{44}$$

We also use the fact that $\frac{\boldsymbol{\sigma}\cdot\mathbf{x}}{r}$ is a pseudo-scalar operator, and acting on φ^A, φ^B, gives $-\varphi^B, -\varphi^A$ respectively (with the phase conventions we are using in Eqs (40), (41). This is because under a pseudo-scalar operator $\mathbf{J}^2, J_z, \mathbf{L}^2$ won't change, but the parity will change. Additionally the operator applied twice is just the identity operator, so the phase change must be ±1. This action can also be painfully verified by using spherical harmonics identities.

Therefore using Eqs. (42),(44),

$$\begin{aligned} \boldsymbol{\sigma}\cdot\mathbf{p}\,\psi_B &= \frac{(\boldsymbol{\sigma}\cdot\mathbf{x})}{r^2}\left(-i\hbar r\frac{\partial}{\partial r} + i\boldsymbol{\sigma}\cdot\mathbf{L}\right) if(r)\varphi^B_{j,j_3} \\ &= i\frac{(\boldsymbol{\sigma}\cdot\mathbf{x})}{r^2}\left(-i\hbar r\frac{df}{dr} + i(\kappa-1)\hbar f\right)\varphi^B_{j,j_3} \qquad (45) \\ &= -\left(\hbar\frac{df}{dr} + \frac{(1-\kappa)\hbar}{r}f\right)\varphi^A_{j,j_3} \qquad (46) \end{aligned}$$

In exactly the same manner we also obtain

$$\boldsymbol{\sigma}\cdot\mathbf{p}\,\psi_A = \left(i\hbar\frac{dg}{dr} + i\frac{(1+\kappa)\hbar}{r}f\right)\varphi^B_{j,j_3}. \tag{47}$$

Now substituting in the Dirac Equation (43), the angular parts cancel and we obtain coupled differential equations for the radial wave functions $f(r), g(r)$

$$-c\hbar\frac{df}{dr} - \frac{(1-\kappa)\hbar c}{r}f = (E - V - mc^2)g \tag{48}$$

$$c\hbar\frac{dg}{dr} + \frac{(1+\kappa)\hbar c}{r}g = (E - V + mc^2)f. \tag{49}$$

D. Solving the Coupled Differential Equations

As in the non-relativistic radial equation we substitute $F(r) = rf(r), G(r) = rg(r)$ to obtain

$$\hbar c\left(\frac{dF}{dr} - \frac{\kappa}{r}F\right) = -(E - V - mc^2)G \tag{50}$$

$$\hbar c\left(\frac{dG}{dr} + \frac{\kappa}{r}G\right) = (E - V + mc^2)F \tag{51}$$

With $V = -\frac{Ze^2}{r}$, and the following substitutions

$$\begin{aligned} \alpha_1 &= \frac{mc^2 + E}{\hbar c}, & \alpha_2 &= \frac{mc^2 - E}{\hbar c} \\ \rho &= \sqrt{\alpha_1\alpha_2}\,r, & \gamma &= \frac{Ze^2}{\hbar c} = Z\alpha \end{aligned} \tag{52}$$

we will have dimensionless coupled DE's

$$\frac{dF}{d\rho} - \frac{\kappa}{\rho}F = \left(\sqrt{\frac{\alpha_2}{\alpha_1}} - \frac{\gamma}{\rho}\right)G \tag{53}$$

$$\frac{dG}{d\rho} + \frac{\kappa}{\rho}G = \left(\sqrt{\frac{\alpha_1}{\alpha_2}} + \frac{\gamma}{\rho}\right)F. \tag{54}$$

We attempt the usual power series solution, and try

$$F = e^{-\rho}\rho^s\sum_{m=0}^{\infty} a_m\rho^m, \quad G = e^{-\rho}\rho^s\sum_{m=0}^{\infty} b_m\rho^m \tag{55}$$

where $a_0 \neq 0$, and $b_0 \neq 0$ (From the coupled equations Eqs. (53),(54) we can see that s the smallest non-zero power of ρ must be the same for both F, G). Using the power series in Eqs (53), (54) leads to the following equations for the coefficients of the $\rho^s\rho^{q-1}$ for $q > 0$

$$(s + q - \kappa)a_q - a_{q-1} + \gamma b_q - \sqrt{\alpha_2/\alpha_1}\,b_{q-1} = 0 \tag{56}$$

$$(s + q + \kappa)b_q - b_{q-1} - \gamma a_q - \sqrt{\alpha_1/\alpha_2}\,a_{q-1} = 0 \tag{57}$$

For $q = 0$, the indicial equations are

$$(s - \kappa)a_0 + \gamma b_0 = 0 \tag{58}$$

$$-\gamma a_0 + (s + \kappa)b_0 = 0 \tag{59}$$

Since both a_0, b_0 are non-zero, the determinant of the above system must vanish, so

$$s = \pm\sqrt{\kappa^2 - \gamma^2} \tag{60}$$

Only the positive root is allowed as otherwise the wave function will diverge at the origin more rapidly than $\rho^{-\frac{1}{2}}$, and thus $|\psi|(\rho)|^2$ will also diverge.

We can obtain the asymptotic limit of the power series by first multiplying Eq. (56) by $\sqrt{\alpha_1}$ and subtracting Eq. (57) multiplied by $\sqrt{\alpha_2}$

$$\begin{aligned} &a_q\left(\sqrt{\alpha_1}(s + q - k) + \sqrt{\alpha_2}\gamma\right) \\ &= b_q\left(\sqrt{\alpha_2}(s + q + k) - \sqrt{\alpha_1}\gamma\right) \qquad (61) \\ &\to a_q = b_q\sqrt{\alpha_2/\alpha_1} \quad (q \to \infty) \qquad (62) \end{aligned}$$

Substituting this back in Eqs. (56), (57), and again taking the $q \to \infty$ limit, we find

$$\frac{a_q}{a_{q-1}} = \frac{2}{q}, \quad \frac{b_q}{b_{q-1}} = \frac{2}{q} \tag{63}$$

This implies that both the a, and b series asymptotically approach e^{ρ}, and the solutions F, G will diverge. To avoid this both power series must terminate, and we will assume that they terminate with the same integer power (the self-consistency of assuming this will be shown below). So we assume their exists an integer n' such that

$$a_{n'+1} = b_{n'+1} = 0, \quad a_{n'} \neq 0, \; b_{n'} \neq 0 \tag{64}$$

Putting $q = n' + 1$ in Eqs. (56),(57) leads to $a_{n'}/b_{n'} = -\sqrt{\alpha_2/\alpha_1}$ from both equations (this justifies our previous assumption). Comparing this ratio with that given by Eq. (61) and using Eq. (52) leads to

$$\gamma(\alpha_1 - \alpha_2) = \sqrt{\alpha_1\alpha_2}(2s + 2n') \tag{65}$$

$$(s + n')\sqrt{(mc^2)^2 - E^2} = E\gamma \tag{66}$$

A little manipulation, and remembering the value of κ Eq. (38) and s Eq. (60) we finally obtain

$$E = \frac{mc^2}{\sqrt{1 + \frac{\gamma^2}{(s+n')^2}}} \tag{67}$$

$$E = \frac{mc^2}{\sqrt{1 + \frac{Z^2\alpha^2}{\left[n' + \sqrt{(j+\frac{1}{2})^2 - Z^2\alpha^2}\right]^2}}} \tag{68}$$

which is identical to the Sommerfeld result Eq. (22) upon identifying the corresponding integers $n_r \leftrightarrow n'$, and $n_\phi \leftrightarrow j + \frac{1}{2}$. This is truly remarkable!

IV. BIEDENHARN'S ANALYSIS

In his paper on *The "Sommerfeld Puzzle" Revisited and Resolved* [1], Biedenharn uses very sophisticated symmetry arguments and calculations to explain the Sommerfeld and Dirac calculations. It would be almost impossible in this short paper to discuss the details of Biedenharn calculations and argument, and probably also well beyond the competancy of the author. Instead we will attempt to summarize some of the more interesting aspects of Biedenharn's conclusions.

One explanation of why the Sommerfeld and Dirac calculation's agree is that somehow offsetting errors in Sommerfeld's calculation cancel. Biedenharn quotes an explanation from the monograph of Yourgrau and Mandelstam [16], "...a valid theory of fine-structure must include both wave mechanics and spin. Sommerfeld's explanation was successful because the neglect of wave mechanics and the neglect of spin by chance cancel each other in the case of the hydrogen atom."

Biedenharn argues that this cannot be correct because Sommerfeld's calculation for the non-relativistic Kepler problem (see Eq. (3)) gives the same energy levels as the non-relativistic Schrödinger calculations, therefore "(nonrelativistic) wave mechanics *per se* makes no change in the answer." Indeed Biedenharn goes on to argue that the proper analog to Sommerfeld's non-relativistic calculation is not the non-relativistic Schrödinger theory, but the non-relativistic Schrödinger-Pauli theory of a spin-$\frac{1}{2}$ particle moving in a Coulomb potential. The spin in this case is an extra degree of freedom that is dynamically independent thus leading to the same energy levels.

The advantage of incorporating spin is two-fold. First it makes certain operators (including Hamiltonians) much easier to factorize as for example

$$\mathbf{L}^2 = (\boldsymbol{\sigma}\cdot\mathbf{L})(\boldsymbol{\sigma}\cdot\mathbf{L} + 1) \tag{69}$$

$$\mathbf{J}^2 = (\boldsymbol{\sigma}\cdot\mathbf{L} + 3/2)(\boldsymbol{\sigma}\cdot\mathbf{L} + 1/2). \tag{70}$$

Second it enables a symmetry for circular orbits to be duplicated and enforced between the classical and quantum calculations. Biedenharn shows that the analog of the of the classical eccentricity (which vanishes for circular orbits) for the non-relativistic quantum system without spin is

$$\varepsilon = \left[1 - \frac{l^2 + l + 1}{N^2}\right]^{1/2}. \tag{71}$$

This does not vanish for quantum mechanical circular orbits (node-less radial probability density) $l = N - 1$. But for the non-relativistic spin-$\frac{1}{2}$, the corresponding eccentricity operator

$$\varepsilon = (1 - \kappa^2/N^2)^{1/2} \tag{72}$$

does vanish for circular orbits.

Using these symmetries Biedenharn establishes the relationship between the Sommerfeld non-relativistic Kepler problem, and the Schrödinger-Pauli theory with a dynamically independent spin. He then goes on to establish that the transformation from the classical non-relativistic Kepler problem to the relativistic Kepler problem, (namely a transformation to a rotating reference frame), is mimicked by a similar transformation from the non-relativistic quantal Schrödinger-Pauli theory to the Dirac theory.

This transformation brings certain operators to diagonal form, and is given by

$$S = \exp\left[-\frac{i}{2}\boldsymbol{\alpha}\cdot\hat{\mathbf{r}}\tanh^{-1}(\alpha Z/\mathcal{H})\right] \tag{73}$$

and as Biedenharn explains S is a Lorentz boost with an operator-valued angle, which in the classical limit corresponds to a Lorentz transformation tangent to the orbit, and having velocity which exactly reproduces the Γ factor used in $\psi = \Gamma\phi$ for the precessing ellipse in Sommerfeld's calculation.

To summarize the logic in Biedenharn's puzzle resolution is that symmetries involving circular orbits/operators lead to the same energy levels for the non-relativistic Kepler problem, and the quantum Schrödinger-Pauli theory with dynamically independent spin. This equivalence is extended by similar transformations involving Lorentz boosts, to the classical relativistic Kepler problem and the Dirac theory. While this analysis is subtle and convulated at times it does seem to go a long way to explaining the equality of Eqs (22) and (68).

ACKNOWLEDGMENTS

The author wishes to thank Professor Barton Zwiebach, Professor Jolyon Bloomfield, and edX/MITx, for offering the 8.04x-8.06x sequence of superb online courses on quantum mechanics for which this paper was prepared.

---

[1] Biedenharn, L. C., *The 'Sommerfeld Puzzle' Revisited and Resolved*, Foundations of Physics, Vol 13, No. 1, (1983).
[2] Sommerfeld, A. (1919). *Atombau und Specktrallinten.* Braunschweig: Vieweg. The third edition was published in English as *Atomic Spectra and Spectral Lines, trans.* Brose, H. L., 1923 London: Methuen.
[3] Longair, M. *Quantum Concepts in Physics*, Cambridge University Press, Cambridge, UK (2013), p. 113. This is an excellent book on the history of quantum mechanics, and chapter 5 (along with subsequent chapters) covers in detail Sommerfeld's contributions.
[4] See for example chap. 9, Goldstein, H, *Classical Mechanics.* Reading, Mass.: Addison-Wesley (1950)
[5] See section 51, Schiff, L. I., *Quantum Mechanics Third Edition.* McGraw-Hill: New York (1968).
[6] Dirac, P. A. M., *The quantum theory of the electron.* Proceedings of the Royal Society of London, A117, 610-624, A118, 351-361 (1928).
[7] See Chap. 9, problem 11, p. 317 of [4].
[8] See Chap 6, problem 12, p. 214 of [4].
[9] Einstein, A., *Erklärung der Perihelbewegung des Merkur aus der allgemeinen Relativitätstheorie (Explanation of the perihelical motion of Mercury from the General Theory of Relativiry).* Ständiger Beobachter der Preussischen Akademie der Wissenschaften, Part 2 (Berlin), 831-839, (1915).
[10] For the author's handwritten calculations see: Algebra MITx 8.06x Applications of Quantum Mechanics, Discussion forum (2019).
[11] Darwin C. G., *The wave equations of the electron.* Proceedings.of the Royal Society of London, A118, 654-680, (1928).
[12] Dirac, P. A. M., *The Principles of Quantum Mechanics Fourth Edition.* Oxford University Press, Oxford (1958).
[13] Bjorken, J. D., Drell, S. D., *Relativistic Quantum Mechanics.* McGraw-Hill, Inc. New York (1964).
[14] Sakurai, J. J., *Advanced Quantum Mechanics.* Addison-Wesley, Reading, Mass. (1967).
[15] See General Addition of L and S Problem Set 15, Problem 1. MITx 8.05.3x Mastering Quantum Mechanics Part 3: Entanglement and Angular Momentum
[16] Yourgrau, W., Mandelstam, S., *Variational Principles in Dynamics and Quantum Theory 3rd ed..* W. B. Saunders Co, Philadelphia (1968)

Entanglement-assisted Quantum Error-correcting Code

Evan Ong

(Dated: June 18, 2019)

Intrinsically, the possible quantum errors on qubits can be modeled as n-fold tensor product of single qubit Pauli operators, generating a group . A quantum error-correcting code of length n can be succinctly constructed by choosing a stabilizer subgroup S of G_n, which constrained to be abelian. The resultant code is called a stabilizer code and as its name suggests, the code space is invariant under the action of those operators in its stablizer S. This paper is devoted to study on the usage of the pre-existing entanglements shared between the sender and receiver in removing the abelian constraint on S, thus arising to a more general and effective quantum error-correction scheme than the stabilizer formalism.

I. INTRODUCTION

One of the main applications of quantum mechanics is in the field of quantum computing. In a quantum computer, words are represented by n spin-1/2 states with some known Hamiltonian. Each spin-1/2 state is termed as a qubit, which can be expressed as a superposition of spin up $|\uparrow\rangle$ and spin down $|\downarrow\rangle$, that is, $a|\uparrow\rangle + b|\downarrow\rangle$ for some $a, b \in \mathbb{C}$. For convenience, we use $|0\rangle$ and $|1\rangle$ to denote $|\uparrow\rangle$ and $|\downarrow\rangle$ respectively. Writing $|0\rangle = \begin{pmatrix} 1 \\ 0 \end{pmatrix}$ and $|1\rangle = \begin{pmatrix} 0 \\ 1 \end{pmatrix}$ isomorphically, they form a basis for the two dimensional complex vector space $\mathbb{C}^2$.

While representing an n qubits state, the notion of tensor product is used to concatenate the qubits. An n-qubits state is written as a superposition of some n-tensor product of single qubit states, each in the form of $\bigotimes_{i=1}^{n} |a_i\rangle$ ($|a_1 a_2 \ldots a_n\rangle$ for brevity) for $a_i \in \mathbb{C}$. As a result, each n-qubits state is viewed isomorphically as an element in the 2^n dimensional complex vector space $\mathbb{C}^{2^n}$.

Quantum states are generally fragile as they could easily interact with the environment, results in the occurrence of decoherence during transmission. It is well known that classical error-correcting codes protects classical computers from bit errors[1], one of the ways is through repetition. However, for the quantum case, the famous "No Cloning Theorem"[2] seemed to suggest that quantum error correction is strictly infeasible.

Fortunately, the first systematic framework of constructing quantum error-correcting codes was introduced by Calderbank[3] in 1997, where the construction of quantum error-correcting codes are transformed to the problem of finding classical error-correcting codes over the finite field with four elements which are self-orthogonal[4]. The resultant codes are called stabilizer codes.

In Section 2, stabilizer codes are studied from the point of their stabilizers, using basic group theory. We provides some examples of renowned quantum error-correcting codes with good parameters. Section 3 is devoted to generalize the notion of stabilizer codes to entanglement-assisted quantum error-correcting codes. We show that with some pre-existing shared entanglements between the sender and receiver, the codes can comparitively achieve better parameters, thus better performance than the stabilizer codes[5-7].

II. QUANTUM ERROR CORRECTING CODE

As a starting point, the notion of group is introduced.

Definition 1 *Let G be a set and $\cdot$ be a binary operation. Then, $\langle G, \cdot \rangle$ is called a group if the following conditions hold:*

1. $a \cdot (b \cdot c) = (a \cdot b) \cdot c$ *for all* $a, b, c \in G$,
2. *There exists a unique* $e \in G$, *called the identity such that For every* $a \in G$, $a \cdot e = a = \cdot a$,
3. *For every* $a \in G$, *there exists a unique* $a^{-1} \in G$, *called its inverse, such that* $a^{-1} \cdot a = e = a \cdot a^{-1}$

In addition, if $a \cdot b = b \cdot a$ for all $a, b \in G$, then G is called an abelian group. The order of G is the total number of elements in G, denoted as $|G|$. For every element in $a \in G$, its order, denoted as $ord(a)$ is the smallest $k \in \mathbb{Z}^+$ such that $a^k = 1$. Let H be a subset of G which forms a group by inheriting the binary operation of G, then H is called a subgroup of G. For any subgroup H of G, its centralizer $Z(H)$ is the set of all elements in G that commute with every element in H, that is $Z(H) = \{g \in G | gh = hg, \forall h \in H\}$. Note that a centralizer is also a subgroup of G.

Consider a single qubit state $|\psi\rangle = \begin{pmatrix} a \\ b \end{pmatrix}$. Each possible error operator can be expressed as a 2×2 matrix over $\mathbb{C}$, that is, an element in $M_{2\times2}(\mathbb{C})$, the vector space of all 2×2 matrices over $\mathbb{C}$. Note that the set of all Pauli operators together with the identity matrix, $P = \{I = \begin{pmatrix} 1 & 0 \\ 0 & 1 \end{pmatrix}, X = \begin{pmatrix} 0 & 1 \\ 1 & 0 \end{pmatrix}, Z = \begin{pmatrix} 1 & 0 \\ 0 & -1 \end{pmatrix}, Y = \begin{pmatrix} 0 & -i \\ i & 0 \end{pmatrix}\}$ forms a basis for $M_{2\times2}(\mathbb{C})$. The set generated by the Pauli operators forms a multiplicative group G with $|G| = 2^4$.

Generalizing to n qubits state, each error operator are expressed as an n-fold tensor product of elements in P, thus with an overall phase of $\pm i$, forming the multiplicative group $G_n = \{i^j \bigotimes_{k=1}^{n} P_k | \forall j \in \{0,1,2,3\}, \forall P_k \in P\}$. The weight of an error $E \in G_n$, $wt(E)$ is the total numbers of its tensor component P_k which are non-identity. Note that $|G_n| = 2^{2n+2}$.

Also, it follows from the property of Pauli's operators that for every pair of elements $E_1, E_2 \in G_n$, either $[E_1, E_2] = 0$ or $\{E_1, E_2\} = 0$, where $[E_1, E_2]$ and $\{E_1, E_2\}$ denote the commutator and anti-commutator of E_1 and E_2 respectively. Moreover, every $E \in G_n$ is either of order 2 or 4, thus either $E^2 = 1$ or $E^2 = -1$. To correct an error E, we basically apply the error operator again to recover the original quantum state.

An encoding is a function that introduce redundant qubits into the original message space, resulting in a codespace with larger length. Mathematically, it is a linear transformation $f : \mathbb{C}^{2^k} \to \mathbb{C}^{2^n}$ for some $k, n \in \mathbb{Z}^+$ such that $n > k$. The resultant quantum error-correcting code is $C = Im(f)$, a k-dimensional subspace of $\mathbb{C}^{2^n}$. Each $|\psi\rangle \in C$ is said to a codeword and C is of length n and dimension k.

The decoding of a quantum error-correcting code is a process which determine the most likely codeword that might be sent, based on the received word. We introduce the concept of detectable error. An error operator $E \in G_n$ can be detected by a code C if the received codeword $E|\psi\rangle$ is always outside of $C(E|\psi\rangle$ is not a codeword in $C)$.

Definition 2 *Let C be a quantum error-correction code of length n. An error $E \in G_n$ is said to be detectable by C if for every codeword $|\psi\rangle \in C$, $E|\psi\rangle \notin C$.*

Example 3 *Consider the quantum error-correcting code C with an encoding function f defined as:*

$$f : |0\rangle \mapsto |000\rangle$$
$$f : |1\rangle \mapsto |111\rangle$$

Then, $f : a|0\rangle + b|1\rangle \mapsto a|000\rangle + b|111\rangle$ for every $a, b \in \mathbb{C}$. Every codeword in this code is in the form of $a|000\rangle + b|111\rangle$ for $a, b \in \mathbb{C}$. Unlike classical codes, it can be seen that a quantum code has infinitely many codewords. This code is of length three and dimension one and it is analogous to the classical repetition code of length three. This quantum error-correcting code can correct all single bit flip errors, for instance, if a bit flip error X_1 acts on the first qubit, the codeword $|\psi_1\rangle = a|000\rangle + b|111\rangle$ is changed to $|\psi_2\rangle = a|100\rangle + b|011\rangle$. In the decoding algorithm, the decoder always search for a smallest weight error acting on $|\psi_2\rangle$, transforming it to a codeword in C. As $wt(X_1) = 1$, the decoder applies X_1 and the error is successfully corrected $X_1|\psi_2\rangle = |\psi_1\rangle$.

On the other hand, suppose that the phase flip error Z_1 occurs when $|\psi_1\rangle = a|000\rangle + b|111\rangle$ is sent, then $Z_1|\psi_1\rangle = a|000\rangle - b|111\rangle = |\psi_2\rangle \in C$, thus the error operator Z_1 is not detectable. In fact, it can be easily seen that both Z_2 and Z_3 are not detectable by the code too.

An important parameter of C governing its error-correcting ability is the minimum distance d, that is the minimum weight of error operator that transforms a codeword to another codeword in C. Mathematically, $d = min\{wt(E) \mid E|\psi_1\rangle = |\psi_2\rangle, \forall|\psi_1\rangle, |\psi_2\rangle \in C, \forall E \in G_n\}$. Thus, the code illustrated in Example 3 has minimum distance 1. In general, a code with minimum distance d can correct all errors up to weight $\lceil \frac{d-1}{2} \rceil$.

We usually illustrate a quantum error correcting code by highlighting its three parameters as follows.

Definition 4 *A quantum error-correcting code of length n, dimension k and minimum distance d is called an $[[n, k, d]]$-code.*

III. STABILIZER QUANTUM ERROR-CORRECTING CODES

The construction of a stabilizer code of length n is started by choosing a stabilizer subgroup S of $\bar{G}_n$. The resultant code C is a subspace of $\mathbb{C}^{2^n}$, such that every state in C is invariant under every operation in S. In other words, C is the intersection of the eigenspace of each of the error operator in S with eigenvalue 1.

Definition 5 *Let C be a quantum error-correcting code of length n and S is a stabilizer subgroup of $\bar{G}_n$. Then, C is called a stabilizer code with stabilizer S if $C = \{|\psi\rangle \in \mathbb{C}^{2^n} \mid S_i|\psi\rangle = |\psi\rangle, \forall S_i \in S\}$.*

We now study the necessary conditions that a stabilizer subgroup must fulfill. First of all, if the error operator $-1 \bigotimes_{k=1}^{n} I_k \in S$, then by Definition 5, for $|\psi_1\rangle \in C$, we have $-1 \bigotimes_{k=1}^{n} I_k |\psi_1\rangle = |\psi_1\rangle$, that is:

$$-|\psi\rangle = |\psi\rangle \tag{1}$$

Note that there are no non-trivial n-qubits state $|\psi\rangle$ which satisfy (1), thus resulting the code to be trivial. Similarly, suppose that S is non-abelian, then there exists $E_1, E_2 \in S$ such that E_1 and E_2 does not commute. In our previous discussion, every pair of elements in G_n either commute or anti-commute, then $E_1E_2 = -E_2E_1$. Similarly, this results in:

$$E_1E_2|\psi\rangle = -E_2E_1|\psi\rangle$$
$$E_1|\psi\rangle = -E_2|\psi\rangle$$
$$|\psi\rangle = -|\psi\rangle$$

Hence, the stabilizer code C with stabilizer S is trivial unless S is abelian and $-1 \bigotimes_{k=1}^{n} I_k \notin S$

Proposition 6 *Let C be a non-trivial stabilizer code with stabilizer S. Then, S must be abelian and $-1 \bigotimes_{k=1}^{n} I_k \notin S$.*

Stabilizer codes are robust in practice. One of the reasons is that their dimension and minimum distance can be determined from the properties of its stabilizer S. Since $-1 \bigotimes_{k=1}^{n} I_k \notin S$, for every error operator $E \in S$, $ord(E) \neq 4$, otherwise $E^2 = -1 \bigotimes_{k=1}^{n} I_k \in S$. Hence, we have $ord(E) = 2$ or $E^2 = 1$. This special type of group which every non-trivial element in it has order 2 is called an elementary abelian 2-group. Every elementary abelian 2-group S with $|S| = 2^l$ has presentation in terms of l generators, that is, $S = \langle S_1, S_2, \ldots, S_l \rangle$. A stabilizer code with $|S| = 2^l$ has dimension $k = n - l$.

For the discussion of the minimum distance of a length n stabilizer code C, we need to go into the details on partitioning those errors in G_n which are correctable by C from those which are not correctable by C. First of all, note that $S \subseteq Z(S) \subseteq G_n$. Then, G_n can be partitioned into $G_n = S \cup (Z(S) - S) \cup (G_n - Z(S))$.

Firstly, for every $E \in S$, it can be easily seen from Definition 5 that E has no effect on the codespace C, thus those errors are correctable for C. Next, consider an operator $E \in Z(S) - S$. Note that since $E \in Z(S)$, then we have $ES = SE$. This implies that when E acts on a codeword $|\psi\rangle \in C$, then for every $S_1 \in S$, $S_1(E|\psi\rangle) = (S_1E)|\psi\rangle = (ES_2)|\psi\rangle = E(S_2|\psi\rangle) = E|\psi\rangle$ for some $S_2 \in S$. This implies that $E|\psi\rangle$ is another codeword in C such that $E|\psi\rangle \neq |\psi\rangle$. Therefore, E is not detectable, hence not correctable. For the third case, suppose that $E \in G_n - Z(S)$, then there exists $S_1 \in S$ such that E does not commute with, thus $ES_1 = -S_1E$. This results in $E|\psi\rangle = E(S_1|\psi\rangle) = (ES_1)|\psi\rangle = (-S_1E)|\psi\rangle = -S_1(E|\psi\rangle)$. Since $E|\psi\rangle = -S_1(E|\psi\rangle)$,$|\psi\rangle$ is not stabilize by $S_1 \in S$, thus $E|\psi\rangle$ is not a codeword in C. The error is detectable by C. Putting all these together, this leads to the following theorem.

Theorem 7 *Let C be a stabilizer code of length n with stabilizer S. Then, C can detect an error operator E if and only if $E \in S \cup (G_n - Z(S))$.*

Corollary 8 *Let C be an $[[n,k,d]]$-stabilizer code with stabilizer S consisting of l generators. Then, $k = n - l$ and $d = min\{wt(E) \mid \forall E \in Z(S) - S\}$.*

Example 9 *Let n=5. We let S be a stabilizer subgroup of G_n with representation $S = \langle S_1, S_2, S_3, S_4 \rangle$ where:*

$$\begin{gathered} S_1 = X \otimes Z \otimes Z \otimes X \otimes I \\ S_2 = I \otimes X \otimes Z \otimes Z \otimes X \\ S_3 = X \otimes I \otimes X \otimes Z \otimes Z \\ S_4 = Z \otimes X \otimes I \otimes X \otimes Z \end{gathered}$$

Then, we have $|S| = 2^4 = 16$. The length 5 stabilizer code thus have dimension $5 - 4 = 1$. Its encoding function $f : \mathbb{C}^2 \to \mathbb{C}^{2^5}$ maps:

$$\begin{aligned} f : |0\rangle \mapsto |0\rangle_c = {} & |00000\rangle + |10010\rangle + |01001\rangle + |10100\rangle + \\ & |01010\rangle + |00101\rangle - |11110\rangle - |01111\rangle - \\ & |10111\rangle - |11011\rangle - |11101\rangle - |01100\rangle - \\ & |00110\rangle - |00011\rangle - |10001\rangle - |11000\rangle \end{aligned}$$

$$\begin{aligned} f : |1\rangle \mapsto |1\rangle_c = {} & |11111\rangle + |01101\rangle + |10110\rangle + |01011\rangle + \\ & |10101\rangle + |11010\rangle - |00001\rangle - |10000\rangle - \\ & |01000\rangle - |00100\rangle - |00010\rangle - |10011\rangle - \\ & |11001\rangle - |11100\rangle - |01110\rangle - |00111\rangle \end{aligned}$$

For each of the $S_i \in S$, it can be verified that S_i is an error operator that has no effect on every codeword in the code as $S_i|0\rangle_c = |0\rangle_c$ and $S_i|1\rangle_c = |1\rangle_c$. Also, one of the minimum weight operators $E \in Z(S) - S$ is $E = X \otimes X \otimes X \otimes I \otimes I$ with $wt(E) = 3$. Note that $E|0\rangle_c = -|1\rangle_c \in C$. Hence, the error operator E is not detectable by C, that is C has minimum distance three. Thus, C is a $[[5,1,3]]$-stabilizer code, It can be verified that all error operators of weight 2 must be in $G_5(S)$, thus they are detectable by the stabilizer code. Indeed, researchers had shown that 5 is the smallest possible length for a stabilizer code with $k = 1$ and $d = 3$. More details on this code are illustrated in [8].

IV. ENTANGLEMENT-ASSISTED QUANTUM ERROR-CORRECTING CODE

In this section, we illustrate the main idea of constructing entanglement-assisted quantum error-correcting codes through an example of length four code.

Recall from Proposition 6 that, a necessary condition on stabilizer group S of a stabilizer code is being abelian. Now, we choose a non-abelian subgroup of G_4. Let S be a subgroup of G_4 such that $S = \langle S_1, S_2, S_3, S_4 \rangle$ where:

$$\begin{gathered} S_1 = Z \otimes X \otimes Z \otimes I \\ S_2 = Z \otimes Z \otimes I \otimes Z \\ S_3 = X \otimes Y \otimes X \otimes I \\ S_4 = X \otimes X \otimes I \otimes X \end{gathered}$$

Note that $|S| = 2^4 = 16$. As S_i and S_j are either commuting or anti-commuting pair for distinct $i, j \in \{1,2,3,4\}$, we enumerate their commutation relations as follows.

1. $[S_2, S_3] = 0$,
2. $\{S_1, S_j\}$=0 for all $j \in \{2,3,4\}$,
3. $\{S_4, S_j\}$=0 for all $j \in \{2,3\}$.

The following lemma on properties of S is needed in order to continue the discussion.

Lemma 10 *Let S be a subgroup of G_n with $|S| = 2^l$ for some $l \in \mathbb{Z}^+$. Then, there exists a set of l independent generators for S, that is $\{\bar{Z}_1, \bar{Z}_2, \ldots, \bar{Z}_m, \bar{X}_1, \bar{X}_2, \ldots, \bar{X}_{l-m}\}$ for some $l/2 \leq m \leq l$ such that the following conditions are satisfied:*

1. $[\bar{Z}_i, \bar{Z}_j] = [\bar{X}_i, \bar{X}_j] = 0$ *for all* i, j,
2. $[\bar{Z}_i, \bar{X}_j] = 0$ *for all* $i \neq j$,
3. $\{\bar{Z}_i, \bar{X}_i\} = 0$ *for all* i.

Note that we use the conventional symbols of $\bar{Z}_i$ and $\bar{X}_j$ as the commutation relations above are exactly the same as the commutation relations of Pauli operators Z_i and X_j. The subgroup $G_I = \langle \bar{Z}_{l-m+1}, \dots, \bar{Z}_l \rangle$ is called a isotropic subgroup of S and $G_S = \langle \bar{Z}_1, \dots, \bar{Z}_{l-m}, \bar{X}_1, \dots, \bar{X}_{l-m} \rangle$ is called a symplectic subgroup of S.

For our subgroup $S = \langle S_1, S_2, S_3, S_4 \rangle$, one of the choices for the set of generators is:

$$
\begin{aligned}
\bar{Z}_1 &= Z \otimes X \otimes Z \otimes I \\
\bar{X}_1 &= Z \otimes Z \otimes I \otimes Z \\
\bar{Z}_2 &= Y \otimes X \otimes X \otimes Z \\
\bar{Z}_3 &= Z \otimes Y \otimes Y \otimes X
\end{aligned}
$$

Here, we choose two generators of S, $\bar{Z}_2 = S_2 S_3$ and $\bar{Z}_3 = S_1 S_3 S_4$ to replace S_2 and S_3. In this case, our isotropic and symplectic subgroup of S are $V_I = \langle \bar{Z}_2, \bar{Z}_3 \rangle$ and $V_S = \langle \bar{Z}_1, \bar{X}_1 \rangle$ respectively. As $S = \langle S_1, S_2, S_3, S_4 \rangle = \langle \bar{Z}_1, \bar{X}_1, \bar{Z}_2, \bar{Z}_3 \rangle$, we can define a group automorphism of S, that is, $\phi : S \to S$ such that:

$$
\begin{aligned}
\phi &: S_1 \mapsto \bar{Z}_1 \\
\phi &: S_2 \mapsto \bar{Z}_2 \\
\phi &: S_3 \mapsto \bar{Z}_3 \\
\phi &: S_4 \mapsto \bar{X}_1
\end{aligned}
$$

Such automorphism turns out to be acquiring the following property.

Lemma 11 *Let S be a subgroup of G_n with two group presentations $S = \langle S_1, S_2, \dots, S_l \rangle = \langle V_1, V_2, \dots, V_l \rangle$ where $l = |S|$. Then, there exists an automorphism $\phi : S \to S$ such that $\phi : S_i \mapsto V_i = U^{-1} S_i U$ for some unitary $U \in G_n$.*

Back to our example, the goal now is to extend the non-commuting generators of S to a new set of commuting generators, which results in an abelian group. This can be done by appending a Pauli operator Z at the end of $\bar{Z}_1$ and a Pauli operator X at the end of $\bar{X}_1$, followed by an identity at the end of $\bar{Z}_2$ and $\bar{Z}_3$. Thus, we have:

$$
\begin{aligned}
\bar{Z}'_1 &= Z \otimes X \otimes Z \otimes I \otimes Z \\
\bar{X}'_1 &= Z \otimes Z \otimes I \otimes Z \otimes X \\
\bar{Z}'_2 &= Y \otimes X \otimes X \otimes Z \otimes I \\
\bar{Z}'_3 &= Z \otimes Y \otimes Y \otimes X \otimes I
\end{aligned}
$$

Here, let $B = \langle \bar{Z}'_1, \bar{X}'_1, \bar{Z}'_2, \bar{Z}'_3 \rangle$,$B_S = \langle \bar{Z}'_1, \bar{X}'_1 \rangle$ and $B_I = \langle \bar{Z}'_2, \bar{Z}'_3 \rangle$. As illustrated above, B is an abelian subgroup of G_5. Then, the codespace is defined similarly as for stabilizer codes, that is $C = \{ |\psi\rangle \in \mathbb{C}^{2^n} \mid S|\psi\rangle = |\psi\rangle, \forall S \in B \}$. As a result, we have:

$$
\begin{aligned}
f : |0\rangle \mapsto |0\rangle_c = |0_s 0000_r\rangle + |1_s 0001_r\rangle \\
f : |1\rangle \mapsto |1\rangle_c = |0_s 0010_r\rangle + |1_s 0011_r\rangle
\end{aligned}
$$

The first and the fifth qubit state is a maximally entangled state shared between the sender and the reciever, that is $\frac{1}{\sqrt{(2)}}(|0_s 0_r\rangle + |1_s 1_r\rangle)$. Because of the usage of entanglement in the code construction,the resultant code is called an entanglement-assisted quantum error-correcting code. We use the notation $[[n, k, d; c]]$ to denote an entanglement-assisted quantum error-correcting code of length n and minimum distance d that encodes k qubits(k dimensional code) with the help of c ebits(entanglement qubits). The number of ebits c needed for the encoding us the number of anti-commuting pairs of generators in V_S. Note that our example code constructed above is a $[[4, 1, 3; 1]]$-code.

We end this paper with some discussions on the error-detection condition of the entanglement-assisted quantum error correcting code. Firstly, the fifth qubit(the receiver's) is always assumed to be error-free. If an error $E_s \otimes I_r \in G_5$ anti-commutes with at least one of the operators in B, then by a similar argument as in the discussion of stabilizer codes, the error is detectable. This case will only happen when E_s anti-commutes with one of the operators in $S = \langle \bar{Z}_1, \bar{X}_1, \bar{Z}_2, \bar{Z}_3 \rangle$, that is to say that $E_s \in G_4 - Z(S)$ or equivalently $E_s \in G_5 - Z(B)$. On the other hand, if $E_s \otimes I_r \in B$ or equivalently $E_s \otimes I_r \in B_I$, then the error has no effect on the code. As a consequence, we have C can detect an error operator E if and only if $E \in B_I \cup (G_5 - Z(B))$. The last theorem gives a general description on the error-detecting capability of an entanglement-assisted quantum error correcting code.

Theorem 12 *Let C be an $[[n, k, d; c]]$-entanglement-assisted quantum error-correcting code with a stabilizer S extended to an abelian subgroup B. Then, C can detect an error operator E if and only if $E \in B_I \cup (G_{n+c} - Z(B))$.*

---

1 C.E. Shannon, A mathematical theory of communication, The Bell System Technical Journal, Vol.27 (1948): 379-423.

2 W.K.Wootters, W.H.Zurek, A single quantum cannot be cloned, Nature 299, (1982) 802-803

3 D. Gottesman, Stabilizer codes and quantum error correction, Ph.D. thesis, California Institute of Technology, Pasadena, CA (1997)

4 A. R. Calderbank, E. M. Rains, P. W. Shor, N. J. A. Sloane, Quantum error correction via codes over GF(4) , IEEE Trans. Inform. Theory 44 (1998), 1369-1387.

5 G. Bowen, Entanglement required in achieving entanglement-assisted channel capacities, Phys. Rev. A, vol. 66, no. 5 (2002)

6 T. A. Brun, I. Devetak, M.-H. Hsieh, Correcting quantum errors with entanglement, Science, vol. 314, no. 5798

(2006) pp. 436-439
7 C.-Y. Lai, T. A. Brun, M. M. Wilde, Duality in entanglement-assisted quantum error correction, IEEE Trans. Inf. Theory, vol. 59, no. 6 (2013) pp. 4020-4024.
8 R. Laflamme, C. Miquel, J.P.Paz, W.H.Zurck, Perfect quantum error correction code, Phys. Rev. Lett. 77, 198 (1996)

Feynman's Path Integral Approach to Quantum Mechanics

Joonghee Lee
from Seoul, South Korea

(Dated: June 18, 2019)

The path integral formulation provides an alternative description of the time evolution of quantum mechanical states, equivalent to the Schrödinger and Heisenberg formulations. In this paper, we will introduce Feynman's idea and try to justify it, appreciating what kind of new insights we can get from it. Despite its intuitive appeals, assigning a rigorous mathematical meaning to the Feynman path integral is quite subtle and elusive. We will also try to understand what's the nature of the difficulty.

I. INTRODUCTION

Feynman's path integral approach to quantum mechanics, which was first presented in [1], provides a way to describe time evolution of quantum mechanical states. It's a postulate about the time evolution, alternative and equivalent to the Schrödinger and Heisenberg approaches.

In this paper, we will introduce Feynman's idea in comparison with the Schrödinger picture and demonstrate their equivalence. As an overview, be noted that the Feynman formulation generalizes Lagrangian mechanics, especially the action principle, while the Schrödinger formulation is based on Hamiltonian mechanics. To follow this paper, no knowledge about Lagrangian or Hamiltonian mechanics is necessary, except for the principle of least action, about which enough explanation will be given at some appropriate place in the paper.

In the following section, we will first present the path integral formulation with a heuristic definition of the path integral. Then, we will attempt to justify the idea in various ways. Before concluding the paper, we will touch on the issue of the mathematical basis of what we've been discussing and try to see things from mathematical perspectives.

II. PATH INTEGRAL FORMULATION

Let's first recall how the Schrödinger picture describes time evolution. We restrict our interest to the simple case of a particle of mass m in $\mathbb{R}^d$ subject to a potential V that only depends on positions. Let *state vectors* be written as

$$|\Psi, t\rangle\,, \tag{1}$$

where t is the time parameter. Then, in this picture, the time evolution is represented by the *Schrödinger equation*

$$i\hbar\frac{\partial}{\partial t}\,|\Psi, t\rangle = \hat{H}\,|\Psi, t\rangle\,, \tag{2}$$

where the *Hamiltonian operator* $\hat{H}$ is given by

$$\hat{H} = \frac{\hat{\mathbf{p}}^2}{2m} + V(\hat{\mathbf{x}}). \tag{3}$$

In the position basis, Eq. (2) can be written as

$$i\hbar\frac{\partial}{\partial t}\Psi(\mathbf{x}, t) = \left(-\frac{\hbar^2}{2m}\nabla^2 + V(\mathbf{x})\right)\Psi(\mathbf{x}, t) \tag{4}$$

with $\nabla^2 \equiv \sum\limits_{i=1}^{d} \frac{\partial^2}{\partial x_i^2}$ and $\Psi(\mathbf{x}, t) = \langle \mathbf{x}\,|\Psi, t\rangle$.

Time evolution can also be presented in terms of unitary *time-evolution operators* $\mathcal{U}$ as

$$|\Psi, t\rangle = \mathcal{U}(t, t')\,|\Psi, t'\rangle \tag{5}$$

for times t' and t. The relationship between the Hamiltonian operator $\hat{H}$ and the time-evolution operator $\mathcal{U}$ is explicitly known. Actually, $\mathcal{U}$ depends only on the time difference $t - t'$ and is related to $\hat{H}$ as

$$\mathcal{U}(t - t') = \exp\left\{-\frac{i}{\hbar}\cdot(t - t')\,\hat{H}\right\}. \tag{6}$$

Now, let's see how time evolution is represented in Feynman's path integral formulation.[1] Define the *propagator* K to be

$$K(\mathbf{x}, t; \mathbf{x}', t') \equiv \langle \mathbf{x}|\,\mathcal{U}(t - t')\,|\mathbf{x}'\rangle\,, \quad t > t' \tag{7}$$

for $\mathbf{x}', \mathbf{x} \in \mathbb{R}^d$. Then, in the path integral formulation, time evolution of states is described by representing the propagator K as a sum – or an integral – of equal-weight contribution $\phi[\gamma]$ from each path γ, taken from the collection $\Gamma^{\mathbf{x},t}_{\mathbf{x}',t'}$ of all paths $\gamma\colon [t', t] \to \mathbb{R}^d$ with $\gamma(t') = \mathbf{x}'$ and $\gamma(t) = \mathbf{x}$, with some normalization factor C:

$$K(\mathbf{x}, t; \mathbf{x}', t') = C \cdot \sum_{\gamma\in\Gamma^{\mathbf{x},t}_{\mathbf{x}',t'}} \phi[\gamma]. \tag{8}$$

Here, the contribution $\phi[\gamma]$ of $\gamma \in \Gamma^{\mathbf{x},t}_{\mathbf{x}',t'}$ is given by

$$\phi[\gamma] \equiv \exp\left(\frac{i}{\hbar}\,\mathcal{S}[\gamma]\right), \tag{9}$$

---

[1] Straightforward adaptation from 2.2 and 2.4 of [2] and 8.1 of [3].

where $\mathcal{S}[\gamma]$ is the *action* of the path γ defined, from the classical *Lagrangian* $L(\mathbf{x}, \dot{\mathbf{x}})$ corresponding to H, as

$$\mathcal{S}[\gamma] \equiv \int_{t'}^{t} L(\gamma, \dot{\gamma})\, d\tau. \tag{10}$$

The normalization factor C would depend on the time interval $t - t'$ and be determined considering the system – that is, the Lagrangian – of the problem.

Simply inserting the formula (9) for the summand into Eq. (8), we can write the propagator as

$$K(\mathbf{x}, t; \mathbf{x}', t') = C \cdot \sum_{\gamma \in \Gamma^{\mathbf{x},t}_{\mathbf{x}',t'}} \exp\left(\frac{i}{\hbar}\, \mathcal{S}[\gamma]\right) \tag{11}$$

and this sum – or integral – over paths in $\Gamma^{\mathbf{x},t}_{\mathbf{x}',t'}$ is called the *Feynman path integral*. We adopt the notation

$$K(\mathbf{x}, t; \mathbf{x}', t') = \int\limits_{\gamma \in \Gamma^{\mathbf{x},t}_{\mathbf{x}',t'}} \exp\left(\frac{i}{\hbar}\, \mathcal{S}[\gamma]\right) \mathcal{D}[\gamma] \tag{12}$$

to express this. In this notation, the normalization factor C is absorbed into the "measure" $\mathcal{D}[\gamma]$.

Before concluding this section, note two things. First, we still didn't specify clearly what kind of paths should constitute the domain of integration $\Gamma^{\mathbf{x},t}_{\mathbf{x}',t'}$. Second, the summation on the right-hand side of Eq. (11) would be an uncountable sum since $\Gamma^{\mathbf{x},t}_{\mathbf{x}',t'}$ would more likely be an uncountable set, which means we need a careful definition of the sum – or the integral. We will come back to this issue in a later section.

III. PHYSICAL MEANING OF THE FORMULATION

The propagator $K(\mathbf{x}, t; \mathbf{x}', t')$ as defined in (7) represents the *probability amplitude* for a particle to travel from the position $\mathbf{x}'$ at time t' to the position $\mathbf{x}$ at time t. If, in Eq. (8), we can interpret each contribution $\phi[\gamma]$ as the probability amplitude associated to the path γ, what Feynman's path integral formulation roughly says is that the probability amplitude of a particle traveling from $\mathbf{x}'$ to $\mathbf{x}$ is the sum of probability amplitudes of all possible alternative paths between the two points, which should be properly normalized if its absolute square would be interpreted as probability. Note that this is a simple restatement of experimental facts we learned from Mach-Zehnder or Davisson-Germer.

Being probability amplitudes, it seems natural to set $\phi[\gamma] = \exp(i\, \alpha[\gamma])$ for some real $\alpha[\gamma]$. The choice $\alpha[\gamma] = \frac{1}{\hbar}\mathcal{S}[\gamma]$ would be justified from the classical limit of the path integral formulation as we will soon see below.

IV. JUSTIFYING THE FORMULATION

For simplicity, in the remainder of the paper, we focus on the case of the one-dimensional space $\mathbb{R}^1$. The Hamiltonian operator $\hat{H}$ would then become

$$\hat{H} = \frac{\hat{p}^2}{2m} + V(\hat{x}). \tag{13}$$

This time, let's write the corresponding classical Lagrangian L explicitly as

$$L(x, \dot{x}) = \frac{1}{2} m \dot{x}^2 - V(x). \tag{14}$$

and accordingly, the action $\mathcal{S}[\gamma]$ for $\gamma \in \Gamma^{x,t}_{x',t'}$ as

$$\begin{aligned} \mathcal{S}[\gamma] &\equiv \int_{t'}^{t} L(\gamma, \dot{\gamma}) d\tau \\ &= \int_{t'}^{t} \left\{ \frac{m}{2} (\dot{\gamma}(\tau))^2 - V(\gamma(\tau)) \right\} d\tau. \end{aligned} \tag{15}$$

Note that the results below can be easily modified for more general cases.

A. The Classical Limit

In classical mechanics, the *principle of least action* dictates that the system favors the path, out of all the possible paths, which minimizes the action. In other words, if there is a path $\widetilde{\gamma}$ which makes the inequality

$$\mathcal{S}[\widetilde{\gamma}] \leq \mathcal{S}[\gamma] \tag{16}$$

satisfied for any $\gamma \in \Gamma^{x,t}_{x',t'}$, then the system gets to follow $\widetilde{\gamma}$ from time t' to t. We call $\widetilde{\gamma}$ the *classical path*.

The classical path $\widetilde{\gamma}$ being an minimum point of $\mathcal{S}$, for a small change $\delta\gamma$ in $\widetilde{\gamma}$, the change in $\mathcal{S}$ should be zero to first order in $\delta\gamma$:

$$\mathcal{S}[\widetilde{\gamma} + \delta\gamma] - \mathcal{S}[\widetilde{\gamma}] = 0 + \mathcal{O}(\delta\gamma^2). \tag{17}$$

In this way, we can call the principle of least action the *principle of stationary action*. Here, $\delta\gamma$ should be chosen from $\Gamma^{0,t}_{0,t'}$ to satisfy $\delta\gamma(t') = 0$ and $\delta\gamma(t) = 0$, so that $\widetilde{\gamma} + \delta\gamma$ belongs to $\Gamma^{x,t}_{x',t'}$.

If $\widetilde{\gamma}$ is favored classically, in any reasonable quantum mechanical formulation, the same path should also be favored in its classical approximation – that is, in our case, when the magnitude of $\mathcal{S}$ is much larger compared to $\hbar$. But how can it be like this? Recall that in the path integral formulation of time evolution in (12), each path from $\Gamma^{x,t}_{x',t'}$ contributed with the same weight to the propagator.

Here, the *stationary phase principle* comes to our rescue.[2] In the integral expression in (12), due to the oscillatory nature of the integrand $\exp\left(\frac{i}{\hbar}\mathcal{S}[\gamma]\right)$, only such path at which the change $\frac{1}{\hbar}\delta\mathcal{S}[\gamma]$ of the phase to first order

---

[2] This is basically the explanation in 2.3 of [2] and 8.2 of [3].

in $\delta\gamma$ vanishes can provide meaningful contribution to the result of the integration. That means, the classical path $\widetilde{\gamma}$ should actually be favored in the integration. So. approximately, we always can insist

$$K(x,t;x',t') \approx C \cdot \exp\left(\frac{i}{\hbar}\,\mathcal{S}[\widetilde{\gamma}]\right) \tag{18}$$

for some normalization factor C depending on the time interval $t - t'$.

The case in which we can be the most dramatically convinced that this approximation should really hold is when the potential V is given as a quadratic function of positions, which includes the free particle and the harmonic oscillator:

$$V(x) = a + bx + cx^2 \tag{19}$$

for real coefficients a, b, and c, any of which can be zero.[3] With such quadratic potential, we get to have "exact equality" in the approximation (18).

To see this, let $\widetilde{\gamma}$ be the classical path of our system and note that for any $\gamma \in \Gamma^{x,t}_{x',t'}$ there exists appropriate $\epsilon \in \Gamma^{0,t}_{0,t'}$ satisfying

$$\gamma = \widetilde{\gamma} + \epsilon, \tag{20}$$

so that we have

$$\begin{aligned}
\mathcal{S}[\gamma] &= \mathcal{S}[\widetilde{\gamma}+\epsilon] && \text{(21a)}\\
&= \int_{t'}^{t} \left\{ \frac{m}{2}\left(\dot{\widetilde{\gamma}} + \dot{\epsilon}\right)^2 - V(\widetilde{\gamma}+\epsilon) \right\} d\tau && \text{(21b)}\\
&= \mathcal{S}[\widetilde{\gamma}] + \int_{t'}^{t} \left(\frac{m}{2}\,\dot{\epsilon}^2 - c\epsilon^2\right) d\tau, && \text{(21c)}
\end{aligned}$$

where we simply ignored all the terms of first order in ϵ and $\dot{\epsilon}$ because $\mathcal{S}[\widetilde{\gamma}+\epsilon] - \mathcal{S}[\widetilde{\gamma}]$ is zero to first order in those variables as we noted in (17). Now, the propagator integral becomes

$$\begin{aligned}
K(x,t;x',t') &= \int\limits_{\gamma \in \Gamma^{x,t}_{x',t'}} \exp\left(\frac{i}{\hbar}\,\mathcal{S}[\gamma]\right) \mathcal{D}[\gamma] && \text{(22a)}\\
&= \int\limits_{\epsilon \in \Gamma^{0,t}_{0,t'}} \exp\left(\frac{i}{\hbar}\,\mathcal{S}[\widetilde{\gamma}+\epsilon]\right) \mathcal{D}[\epsilon] && \text{(22b)}\\
&= C \cdot \exp\left(\frac{i}{\hbar}\,\mathcal{S}[\widetilde{\gamma}]\right), && \text{(22c)}
\end{aligned}$$

where the normalization factor C is given by

$$C = \int\limits_{\epsilon \in \Gamma^{0,t}_{0,t'}} \exp\left\{ \int_{t'}^{t} \frac{i}{\hbar}\left(\frac{m}{2}\,\dot{\epsilon}^2 - c\epsilon^2\right) d\tau \right\} \mathcal{D}[\epsilon]. \tag{23}$$

It is obvious that C depends on the time difference $t - t'$ and is independent of the end points x' and x of the propagator. Also, note that we assumed equivalence of "measures" $\mathcal{D}[\gamma]$ and $\mathcal{D}[\epsilon]$ when we arrive at Line (22b) from Line (22a).

B. Deriving Path Integral Formulation from Schrödinger Picture

Here, we will see how the Schrödinger formulation implies – or, at least, motivates – something that can be interpreted as the path integral formulation. For this purpose, we are to express the propagator

$$K(y,T;x,0) = \langle y|\, \mathcal{U}(T)\, |x\rangle \tag{24}$$

in a form which would remind us of the path integral formulation. We will derive the result solely within the Schrödinger picture.[4]

First, let's consider the simple case of free particle. Let $\hat{H}_0$ be the Hamiltonian operator for a free particle of mass m in one dimensional space:

$$\hat{H}_0 = \frac{\hat{p}^2}{2m} \tag{25}$$

and K_0 be the corresponding propagator. Then, within the Schrödinger picture, by considering the momentum basis $|p\rangle$, we can make the propagator K_0 look like the formula in (22c):

$$\begin{aligned}
&K_0(y,T;x,0) && \text{(26a)}\\
&= \left\langle y \middle| \exp\left(-\frac{iT}{\hbar}\,\hat{H}_0\right) \middle| x \right\rangle && \text{(26b)}\\
&= \int_{-\infty}^{\infty} \langle y\,|p\rangle \left\langle p \middle| \exp\left(-\frac{iT}{\hbar}\,\hat{H}_0\right) \middle| x \right\rangle dp && \text{(26c)}\\
&= \int_{-\infty}^{\infty} \langle y\,|p\rangle \cdot \exp\left(\frac{-iTp^2}{2m\hbar}\right) \cdot \langle p\,|x\rangle\, dp && \text{(26d)}\\
&= \int_{-\infty}^{\infty} \frac{e^{\frac{iyp}{\hbar}}}{(2\pi\hbar)^{\frac{1}{2}}} \cdot e^{-\frac{iTp^2}{2m\hbar}} \cdot \frac{e^{\frac{-ixp}{\hbar}}}{(2\pi\hbar)^{\frac{1}{2}}}\, dp && \text{(26e)}\\
&= \frac{1}{2\pi\hbar} \int_{-\infty}^{\infty} e^{\frac{i(y-x)p}{\hbar}}\, e^{-\frac{iTp^2}{2m\hbar}}\, dp && \text{(26f)}\\
&= \frac{1}{2\pi\hbar}\, e^{\frac{im(y-x)^2}{2\hbar T}} \int_{-\infty}^{\infty} e^{-\frac{iT}{2m\hbar}\left(p - \frac{m(y-x)}{T}\right)^2} dp && \text{(26g)}\\
&= \left(\frac{m}{2\pi i\hbar T}\right)^{\frac{1}{2}} \cdot \exp\left\{\frac{im}{2\hbar}\,\frac{(y-x)^2}{T}\right\}. && \text{(26h)}
\end{aligned}$$

By noting that the free-particle classical Lagrangian L_0 of this case is

$$L_0(x,\dot{x}) = \frac{1}{2}m\dot{x}^2 \tag{27}$$

---

[3] Taken and adapted from 3.5 of [2] and 8.6 of [3].

[4] Presenting arguments from 1.2 and 1.3 of Chapter 5 of [4] with some ideas taken from 21.1 of [3].

and that the classical path $\widetilde{\gamma}_0$ of a free particle should be a straight line:

$$\widetilde{\gamma}_0(t) = x + \frac{y-x}{T} \cdot t, \tag{28}$$

we conclude that

$$\begin{aligned} K_0(y,T;x,0) &= C \cdot \exp\left\{ \frac{im}{2\hbar} \frac{(y-x)^2}{T} \right\} && \text{(29a)} \\ &= C \cdot \exp\left(\frac{i}{\hbar} \int_0^T L_0(\widetilde{\gamma}_0, \dot{\widetilde{\gamma}}_0)\, d\tau \right) && \text{(29b)} \\ &= C \cdot \exp\left(\frac{i}{\hbar}\, \mathcal{S}_0[\widetilde{\gamma}_0] \right), && \text{(29c)} \end{aligned}$$

where $\mathcal{S}_0$ is the corresponding free-particle action and the normalization factor C is given by

$$C = \left(\frac{m}{2\pi i\hbar T} \right)^{\frac{1}{2}}. \tag{30}$$

Now, let's consider the case of a particle subject to a potential which is represented by the Hamiltonian in (13):

$$\hat{H} = \hat{H}_0 + V(\hat{x}). \tag{31}$$

Note that we cannot write

$$\begin{aligned} &\exp\left\{ -\frac{iT}{\hbar} \left(\hat{H}_0 + V(\hat{x}) \right) \right\} \\ &= \exp\left(-\frac{iT}{\hbar}\, \hat{H}_0 \right) \cdot \exp\left(-\frac{iT}{\hbar}\, V(\hat{x}) \right) && \text{(32)} \end{aligned}$$

because the operators $\hat{H}_0$ and $V(\hat{x})$ do not commute. Instead, according to the *Lie-Kato-Trotter product formula*,[5] what we can actually say is

$$\begin{aligned} &\exp\left\{ \frac{-iT}{\hbar} \left(\hat{H}_0 + V(\hat{x}) \right) \right\} \\ &= \lim_{n\to\infty} \left\{ \exp\left(-\frac{i}{\hbar}\frac{T}{n} \hat{H}_0 \right) \exp\left(-\frac{i}{\hbar}\frac{T}{n} V(\hat{x}) \right) \right\}^n. && \text{(33)} \end{aligned}$$

To make our equations look less messy, let's adopt the notation

$$A_n(p) = \exp\left(-\frac{i}{\hbar} \cdot \frac{T}{n} \hat{H}_0 \right) \tag{34}$$

$$B_n(x) = \exp\left(-\frac{i}{\hbar} \cdot \frac{T}{n} V(\hat{x}) \right). \tag{35}$$

Then, the propagator can be expressed as

$$\begin{aligned} &K(y,T;x,0) && \text{(36a)} \\ &= \left\langle y \middle| \exp\left\{ \frac{-iT}{\hbar} \left(\hat{H}_0 + V(\hat{x}) \right) \right\} \middle| x \right\rangle && \text{(36b)} \\ &= \lim_{n\to\infty} \langle x_n | \left(A_n \cdot B_n \right)^n | x_0 \rangle && \text{(36c)} \\ &= \lim_{n\to\infty} \int\limits_{\mathbb{R}^{n-1}} \left(\prod_{k=0}^{n-1} \langle x_{k+1} | A_n \cdot B_n | x_k \rangle \right) \prod_{k=1}^{n-1} dx_k, && \text{(36d)} \end{aligned}$$

where we first used Eq. (33) to arrive at Line (36c), then set

$$x_0 = x,\ x_n = y, \tag{37}$$

and inserted $n-1$ resolutions of the identity

$$\int_{-\infty}^{\infty} |x_k\rangle \langle x_k|\ dx_k \tag{38}$$

for $k = 1, 2, \cdots, n-1$ between each B_n and A_n in some appropriate order.

Note that, in Line (36d) above, the terms of the product inside of the integrand can be easily simplified:

$$\begin{aligned} &\langle x_{k+1} | A_n(p) \cdot B_n(x) | x_k \rangle && \text{(39a)} \\ &= \langle x_{k+1} | A_n(p) | x_{k-1} \rangle \cdot B_n(x_k) && \text{(39b)} \\ &= C' \cdot \exp\left\{ \frac{i}{\hbar} \cdot \frac{T}{n} \left(\frac{m}{2} \left(\frac{\Delta x_k}{T/n} \right)^2 - V(x_k) \right) \right\} && \text{(39c)} \\ &= C' \cdot \exp\left\{ \frac{i}{\hbar} \cdot \frac{T}{n} \left(\frac{m}{2} \dot{x_k}^2 - V(x_k) \right) \right\} && \text{(39d)} \\ &= C' \cdot \exp\left\{ \frac{i}{\hbar} \cdot \frac{T}{n}\, L(x_k, \dot{x_k}) \right\}, && \text{(39e)} \end{aligned}$$

where we used the free particle propagation formula in (26h) to arrive at Line (39c) from Line (39b) and set

$$\Delta x_k = x_{k+1} - x_k \tag{40}$$

$$\dot{x_k} = \frac{\Delta x_k}{T/n} \tag{41}$$

$$C' = \left(\frac{m}{2\pi i\hbar T/n} \right)^{\frac{1}{2}}. \tag{42}$$

For small enough $\frac{T}{n}$, if we are allowed to approximate

$$\frac{T}{n}\, L(x_k, \dot{x_k}) \approx \int_{t_k}^{t_{k+1}} L(x_k, \dot{x_k})\, d\tau \tag{43}$$

with $t_k = \frac{kT}{n}$, we can finally express the propagator in a more recognizable way as

$$\begin{aligned} &K(y,T;x,0) && \text{(44a)} \\ &= \lim_{n\to\infty} \int\limits_{\mathbb{R}^{n-1}} C'^n \exp\left(\frac{i}{\hbar} \sum_{k=0}^{n-1} \frac{T}{n}\, L(x_k, \dot{x_k}) \right) \prod_{k=1}^{n-1} dx_k && \text{(44b)} \\ &= \int \exp\left(\frac{i}{\hbar} \int_0^T L(x, \dot{x})\, d\tau \right) \mathcal{D}^*[x], && \text{(44c)} \end{aligned}$$

where we adopted an integration notation

$$\int \cdots \mathcal{D}^*[x] \equiv \lim_{n\to\infty} C' \int\limits_{\mathbb{R}^{n-1}} \cdots \prod_{k=1}^{n-1} \left(C' \cdot dx_k \right). \tag{45}$$

The path integral "expression" derived in this way is called the *configuration space path integral.* Now, we can see that the resulting form in Line (44c) of the propagator looks almost the same as the form of the Feynman path integral in (12).

---

[5] See, for example, Theorem 1.1 in Chapter 5 of [4].

V. MATHEMATICAL CONSIDERATIONS

We still didn't provide any concrete mathematical meaning to the Feynman path integral. To discuss how to do this is the purpose of this section.

To begin with, recall what were the requirements from Section II. For sure, we wanted the Feynman path integral to be some sort of "integral", where we evaluate the integrand for each point γ – which actually is a path – from the domain of integration $\Gamma^{x,t}_{x',t'}$ and accumulate evaluated values with respect to some "measure" $\mathcal{D}[\gamma]$ to get the result. Also, quite obviously, to evaluate the Lagrangian in the integrand, the domain of integration $\Gamma^{x,t}_{x',t'}$ – which is a collection of paths – should consist of differentiable paths, where some limited number of singular points can be allowed.

A. Definition via Configuration Space Path Integral Expression

Let's first try and see if we can provide a meaningful definition via the formula for the configuration space path integral in (44).

Considering the form of "measure" $\prod_{k=1}^{n-1} dx_k$ at the end of Line (44b), it seems to be suggested that the "measure" $\mathcal{D}^*[x]$ should be compatible with the usual *Euclidean volume*. Such measures are called *Lebesgue-type* measures and it's a well-known fact, from the measure theory, that an infinite dimensional Lebesgue measure cannot be constructed meaningfully. To get a glimpse of what has gone wrong here, note that an n-cube in $\mathbb{R}^n$ with edge length a has volume a^n. So, when n becomes infinity, the volume of a ∞-cube can be only one of three values: zero, one, infinity.

In conclusion, $\mathcal{D}^*[x]$ cannot be related to a Lebesgue measure, and in fact the formula in Line (44c) should be interpreted as a sequential limit, not as an integral in the sense of the measure-based integration theory.[6]

B. Schrödinger Equation as Parabolic PDE

What if we think purely mathematically? Note that we can write down the general solution of parabolic PDEs(partial differential equations), in case of real coefficients, as an integral over paths with respect to some measure, using what is called the *Feynman-Kac formula.*[7] Since the Schrödinger equation is just a parabolic PDE with complex coefficients, we might be able to utilize, in some way, the Feynman-Kac formula of the real case to represent the general solution of the Schrödinger equation. Then, we might be able to pick out the kernel part to write down the propagator in some appropriate form separately.

In fact, we can do so.[8] After a change of variable, replacing t by $-it$ in the Schrödinger equation, we obtain

$$\hbar \frac{\partial}{\partial t}\Psi(x,t) = \left(\frac{\hbar^2}{2m}\cdot\frac{\partial^2}{\partial x^2} - V(x)\right)\Psi(x,t), \qquad (46)$$

which is a real-coefficient parabolic PDE. Now, we can apply the Feynman-Kac formula and then change back into our original time variable. This surely will give a correct mathematical formula. But, the major problem with this approach is that almost all[9] the paths exploited in the Feynman-Kac formula are nowhere differentiable. Remember that we needed differentiable paths with which the Lagrangian can be computed. This approach might result in a meaningful formula, representing the propagator as an integral over paths with respect to a concrete measure, but at least it can never be used to realize Feynman's idea. As is pointed out in [4], in this representation, we can no longer see the action and the connection with classical mechanics is lost.

C. Highly Oscillatory Integral

As it turns out, providing a proper mathematical definition to the Feynman path integral is a bit beyond the scope of this paper in terms of required technical sophistication. But, at least, we can state what is the right direction to explore. The key is to recognize that the integrand of the Feynman path integral is highly oscillatory and lots of cancellation should occur in the process of integration. We noticed it when we applied the stationary phase principle in deriving the classical limit of the path integral formulation.

The conventional measure-based integration theory is not fit for handling such oscillatory integrals. It's quite obvious from its construction. So, let's briefly review how integrals are defined in that theory. Assume a measure μ on a set X is given. As the first step, the integral $\int_X g\, d\mu$ is defined only for non-negative functions $g : X \to [0,\infty)$ as some non-negative real number, which possibly can be infinite. Then, as the second step, for real-valued functions $f : X \to \mathbb{R}$, the integral $\int_X f\, d\mu$ is defined as

$$\int_X f\, d\mu \equiv \int_X f^+\, d\mu - \int_X f^-\, d\mu \qquad (47)$$

only when both $\int_X f^+\, d\mu$ and $\int_X f^-\, d\mu$ are well-defined as finite real numbers, where non-negative functions f^+

---

[6] As is mentioned in [5].

[7] See, for example, 4.4 of [6].

[8] See Chapter 6 of [4].

[9] By "almost all", we mean "with probability one" with respect to some probability measure.

and f^- are given by

$$f^+(x) \equiv \max\left(f(x), 0\right) \tag{48}$$

$$f^-(x) \equiv -\min\left(f(x), 0\right), \tag{49}$$

so that they satisfy

$$f = f^+ - f^-. \tag{50}$$

As the last step, for complex functions $h : X \to \mathbb{C}$, the integral $\int_X h \, d\mu$ is defined as

$$\int_X h \, d\mu \equiv \int_X \mathrm{Re}(h) \, d\mu + i \cdot \int_X \mathrm{Im}(h) \, d\mu \tag{51}$$

only when both $\int_X \mathrm{Re}(h) \, d\mu$ and $\int_X \mathrm{Im}(h) \, d\mu$ are well-defined as finite real numbers, where $\mathrm{Re}(z)$ and $\mathrm{Im}(z)$ are the real and imaginary parts, respectively, of complex number z. Now, at least, we can clearly see that under these definitions all possible oscillations and cancellations are simply ignored.

To handle strongly oscillating integrands, special mathematical devices are needed. Various approaches have been developed in this direction and we refer interested readers to [5].

VI. CONCLUSION

We began this paper by directly presenting Feynman's path integral formulation itself. Then, we tried to assign appropriate physical meaning to it. Our next step was to justify the formulation first by observing how its classical limit behaves and then by analyzing its relationship with the Schrödinger picture. Finally, we discussed how to provide concrete mathematical meaning to the formulation. It wasn't easy. We reviewed several options, but no satisfactory answer was found. We were able to point out the right direction to advance the discussion, and referred readers to a more advanced source for further information.

ACKNOWLEDGMENTS

This paper was written as the term paper of the edX MITx 8.06x class which started on 20th Feb 2019. I express my sincere gratitude to all who made this amazing class possible. I also would like to thank my editors for their thoughtful and invaluable suggestions.

[1] R. P. Feynman, "Space-time approach to non-relativistic quantum mechanics," *Rev. Mod. Phys.* **20** (Apr, 1948) 367–387.

[2] R. P. Feynman and A. R. Hibbs, *Quantum Mechanics and Path Integrals, Emended Ed.* Dover Publications, 2010.

[3] R. Shankar, *Principles of Quantum Mechanics, 2nd Ed.* Springer, 1994.

[4] L. A. Takhtajan, *Quantum Mechanics for Mathematicians.* American Mathematical Society, 2008.

[5] S. A. Albeverio, R. J. Hegh-Krohn, and S. Mazzucchi, *Mathematical Theory of Feynman Path Integrals: An Introduction, 2nd Ed.* Sprnger, 2008.

[6] I. Karatzas and S. E. Shreve, *Brownian Motion and Stochastic Calculus.* Springer, 1991.

The Forced Harmonic Oscillator

M. E. Lacy

(Dated: May 25, 2019)

The behavior of an oscillator subjected to a time-dependent force is of importance in many contexts. When the oscillations are those of a small massive system, such as a molecule, the force can often be approximated as being constant over the dimensions of the unforced motions (*dipole interaction*), and is described by adding the potential $\hat{x}f(t)$ to the Hamiltonian. In the case of radiation, the unforced oscillations are those of the modes of the free electromagnetic field, while the sources responsible for emission and absorption of radiation add the term $\mathbf{j}\cdot\mathbf{A}$ to the Hamiltonian of the free field. After Fourier analysis, the latter also add a term of the form $\hat{x}f(t)$ to each mode oscillator. The discussion that follows is therefore relevant to a wide range of phenomena.

I. INTRODUCTION

For many applications, especially in many body and field theory, it is desirable to consider the dynamical effects produced by the addition of a time-dependent interaction that is linear in $\hat{x}$ to the Hamiltonian of the harmonic oscillator:

$$\hat{H} = \frac{\hat{p}^2}{2m} + \frac{1}{2}m\omega^2\hat{x}^2 - \hat{x}X(t) \tag{1}$$

where $X(t)$ is a real-valued function of t. This perturbation corresponds to an external time-dependent force that does not depend on the coordinate x (*dipole interaction*). With no additional effort, we may generalize the Hamiltonian even further by introducing a velocity-dependent term:

$$\hat{H} = \frac{\hat{p}^2}{2m} + \frac{1}{2}m\omega^2\hat{x}^2 - \hat{x}X(t) - \hat{p}P(t) \tag{2}$$

where $P(t)$ is also a real function of t.

As in the case of the unforced harmonic oscillator, we introduce the following *non-Hermitian* operators

$$\hat{a} = \sqrt{\frac{m\omega}{2\hbar}}(\hat{x} + i\frac{\hat{p}}{m\omega}), \tag{3}$$

$$\hat{a}^\dagger = \sqrt{\frac{m\omega}{2\hbar}}(\hat{x} - i\frac{\hat{p}}{m\omega}), \tag{4}$$

which satisfy the commutation relation

$$[\hat{a}, \hat{a}^\dagger] = 1. \tag{5}$$

With the substitutions (3) and (4), the Hamiltonian (2) may be cast in the form

$$\begin{aligned}\hat{H} &= \hbar\omega\left(\hat{a}^\dagger\hat{a} + \frac{1}{2}\right) + f(t)\hat{a} + f^*(t)\hat{a}^\dagger && (6)\\ &= \hbar\omega\left(\hat{a}^\dagger(t)\hat{a}(t) + \frac{1}{2}\right) + f(t)\hat{a}(t) + f^*(t)\hat{a}^\dagger(t) && (7)\end{aligned}$$

in either the Schrödinger or Heisenberg picture, provided that we define the complex-valued function $f(t)$:

$$f(t) = -\sqrt{\frac{\hbar}{2m\omega}}X(t) + i\sqrt{\frac{\hbar m\omega}{2}}P(t). \tag{8}$$

II. DISCUSSION

In most applications, we are interested in the changes produced by the time-dependent forces in an initially unperturbed harmonic oscillator. It is therefore reasonable to assume that the disturbance $f(t) \neq 0$ acts only during the finite time interval $T_0 < t < T_1$ and that before T_0 and after T_1 the Hamiltonian is that of a free oscillator.

The time development of the forced harmonic oscillator can be solved in the interaction picture, in which time evolution is separated into two parts, one subject to a model, unperturbed Hamiltonian, and the other to an interaction, time-dependent Hamiltonian (for a full treatment of the interaction picture, see [1], §14, and also [2]).

A. The Forced Harmonic Oscillator Hamiltonian in the Interaction Picture

In the interaction picture, we regard the Hamiltonian of the forced harmonic oscillator as the sum, $\hat{H} = \hat{H}_0 + V(t)$, of an unperturbed Hamiltonian

$$\hat{H}_0 = \hbar\omega(\hat{a}^\dagger\hat{a} + \frac{1}{2}), \tag{9}$$

and an explicitly time-dependent "interaction" term,

$$V(t) = f(t)\hat{a} + f^*(t)\hat{a}^\dagger. \tag{10}$$

Time-dependent Hamiltonians require a more careful treatment than time-independent ones, because in the general case, the interaction operators at two different times do not commute.[3]

We choose the unperturbed Hamiltonian operator $\hat{H}_0$ as the model Hamiltonian to define the interaction picture. Note that if the model Hamiltonian is time-independent and thus conservative, the time-dependent unitary transformation $U_0(t)$ is

$$U_0(t) = \exp\left(-\frac{i}{\hbar}\hat{H}_0 t\right). \tag{11}$$

The transformed interaction operator is then

$$\tilde{V}(t) = U_0^\dagger(t) V U_0(t) \tag{12}$$
$$= e^{i\omega\hat{a}^\dagger\hat{a}t}(f(t)\hat{a} + f^*(t)\hat{a}^\dagger)e^{-i\omega\hat{a}^\dagger\hat{a}t}. \tag{13}$$

The interaction operator can be evaluated using the following commutator identity:

$$e^{\lambda A} B e^{-\lambda A} = e^{\lambda\gamma} B, \quad \text{if} \quad [A, B] = \gamma B, \quad [4] \tag{14}$$

since $[\hat{a}^\dagger\hat{a}, \hat{a}] = -\hat{a}$ and $[\hat{a}^\dagger\hat{a}, \hat{a}^\dagger] = \hat{a}^\dagger$. We thus obtain

$$\tilde{V}(t) = f(t)\hat{a}e^{-i\omega t} + f^*(t)\hat{a}^\dagger e^{i\omega t}. \tag{15}$$

The equation of motion for the instantaneous eigenstate in the interaction picture is then

$$i\hbar\frac{d}{dt}|\tilde{\Psi}(t)\rangle = \left(f(t)\hat{a}e^{-i\omega t} + f^*(t)\hat{a}^\dagger e^{i\omega t}\right)|\tilde{\Psi}(t)\rangle. \tag{16}$$

B. Time-Ordered Products

Likewise the instantaneous eigenstate, the time development operator $\tilde{U}(t_1, t_0)$ in the interaction picture, defined as

$$\tilde{U}(t_1, t_0) = U_0^\dagger(t_1) U(t_1, t_0) U_0(t_0), \tag{17}$$

also satisfies the equation of motion:

$$i\hbar\frac{d}{dt}\tilde{U}(t, t_0) = \tilde{V}(t)\tilde{U}(t, t_0). \tag{18}$$

Integration of Eq. (18) over the interval (t_0, t) and the use of the initial condition $\tilde{U}(t_0, t_0) = 1$ produce an integral equation for the time development operator:

$$\tilde{U}(t, t_0) = 1 - \frac{i}{\hbar}\int_{t_0}^{t} \tilde{V}(t')\tilde{U}(t', t_0)dt'. \tag{19}$$

A formal solution of Eq. (19) can be constructed by successive iteration:

$$\tilde{U}(t, t_0) = 1 - \frac{i}{\hbar}\int_{t_0}^{t} \tilde{V}(t')\, dt' + \left(-\frac{i}{\hbar}\right)^2 \int_{t_0}^{t} \tilde{V}(t')\, dt' \int_{t_0}^{t'} \tilde{V}(t'')\, dt'' + \dots . \tag{20}$$

It is sometimes convenient to write this series expansion in a more symmetric form by using the *time-ordered product* of operators. We define time ordering of two operators as

$$T[\tilde{V}(t')\tilde{V}(t'')] = \begin{cases} \tilde{V}(t')\tilde{V}(t'') & t'' \le t' \\ \tilde{V}(t'')\tilde{V}(t') & t' \le t''. \end{cases} \tag{21}$$

That is, time ordering orders timed factors from right to left, with the rightmost operator the earliest.

This convention can be generalized to products of any number of time-dependent operators

$$T[\tilde{V}(t_1')\tilde{V}(t_2')\dots\tilde{V}(t_n')] = \sum_p \theta(t_{p_1}' > t_{p_2}' > \dots > t_{p_n}') \tilde{V}(t_{p_1}')\tilde{V}(t_{p_2}')\dots\tilde{V}(t_{p_n}'), \tag{22}$$

where the sum is over all the permutations p, and $\theta(x)$ is the Heaviside step function.

With it we can prove that if $t > t_0$, the time development operator may be written in the form

$$\tilde{U}(t, t_0) = 1 + \sum_{n=1}^{\infty}\frac{1}{n!}\left(-\frac{i}{\hbar}\right)^n \int_{t_0}^{t}\int_{t_0}^{t}\dots \int_{t_0}^{t} dt_1' dt_2' \dots dt_n' T[\tilde{V}(t_1')\tilde{V}(t_2')\dots\tilde{V}(t_n')], \tag{23}$$

or formally and compactly as

$$\boxed{\tilde{U}(t, t_0) = T\exp\left(-\frac{i}{\hbar}\int_{t_0}^{t}\tilde{V}(t')\, dt'\right).} \tag{24}$$

C. Time-Ordered Product of the Forced Harmonic Oscillator Potential

If Eq. (24) is applied to the forced linear harmonic oscillator with the interaction potential (15), we obtain

$$\tilde{U}(t, t_0) = T\exp\left(-\frac{i}{\hbar}\int_{t_0}^{t}\left(f(t')\hat{a}e^{-i\omega t'} + f^*(t')\hat{a}^\dagger e^{i\omega t'}\right) dt'\right). \tag{25}$$

This is a compact expression for the time development operator, but because of the unwieldy time ordering operator T, it is not yet in a form convenient for calculating transition amplitudes.

In order to get the time development operator in a more manageable form, we can consider the case of the potential $V(t)$ having additional general properties. We will see that commutation of $\tilde{V}(t)$ at different times is too strong a condition for the forced harmonic oscillator problem; but commutation with the commutator, i.e. $\left[\tilde{V}(t), \left[\tilde{V}(t'), \tilde{V}(t'')\right]\right] = 0$ is exactly the property exhibited by the forced harmonic oscillator.

To begin, we use the group property of the time development operator

$$U(t_2, t_0) = U(t_2, t_1)U(t_1, t_0), \tag{26}$$

and write

$$\tilde{U}(t, t_0) = \lim_{N\to\infty} e^{V_N}e^{V_N - 1}e^{V_N - 2}\dots e^{V_2}e^{V_1} \tag{27}$$

where, by definition,

$$V_n = -\frac{i}{\hbar}\int_{t_0+(n-1)\epsilon}^{t_0+n\epsilon} \tilde{V}(t')\; dt' \quad \text{and} \quad N\epsilon = t - t_0. \tag{28}$$

Equation (27) is valid, even if the interaction operators do not commute at different times, because the time intervals of length ϵ are infinitesimally small and are not subject to internal time ordering.

Equation (27) can be further reduced if the commutators $\left[\tilde{V}(t'), \tilde{V}(t'')\right]$ are numbers for all t' and t''. This is indeed the case for the forced harmonic oscillator, since according to Eq. (15),

$$\begin{aligned}&\left[\tilde{V}(t'), \tilde{V}(t'')\right] = \\ &\qquad f(t')f^*(t'')e^{-i\omega(t'-t'')} - f^*(t')f(t'')e^{i\omega(t'-t'')},\end{aligned} \tag{29}$$

which is a complex number.

The Baker-Campbell-Hausdorff (BCH) relation, also known as the Hadamard lemma [4],

$$e^A e^B = e^{A+B+\frac{1}{2}[A,\ B]} \quad \text{if } [A,[A,\ B]] = 0, \tag{30}$$

can then be applied repeatedly to give

$$\tilde{U}(t,t_0) = \lim_{N\to\infty} \exp\left(\sum_{n=1}^{N}\left(V_n + \frac{1}{2}\left[V_n, \sum_{k=1}^{n} V_k\right]\right)\right) \tag{31}$$

or, if the limit $N\to\infty$ and $\epsilon\to 0$ is carried out,

$$\begin{aligned}\tilde{U}(t,t_0) = \exp\Bigg(&-\frac{i}{\hbar}\int_{t_0}^{t}\tilde{V}(t')\; dt' - \\ &\frac{1}{2\hbar^2}\int_{t_0}^{t} dt' \int_{t_0}^{t'} dt'' \left[\tilde{V}(t'),\ \tilde{V}(t'')\right]\Bigg).\end{aligned} \tag{32}$$

For the forced harmonic oscillator, inserting Eq. (15) and Eq. (29) into Eq. (32), we thus obtain the time development operator in the interaction picture in the desired form:

$$\tilde{U}(t,t_0) = e^{i\beta(t,t_0)} \exp\left(-\zeta^*(t,t_0)\hat{a} + \zeta(t,t_0)\hat{a}^\dagger\right), \tag{33}$$

where we have defined

$$\zeta(t,t_0) = -\frac{i}{\hbar}\int_{t_0}^{t} e^{i\omega t'} f^*(t')dt'. \tag{34}$$

This expression can be connected with the Fourier integral of the applied force:

$$g(\omega) = \int_{T_0}^{T_1} e^{-i\omega t'} f(t')\; dt' = \int_{-\infty}^{\infty} e^{-i\omega t'} f(t')\; dt', \tag{35}$$

that is,

$$g(\omega) = -i\hbar\zeta^*(T_1,T_0) = -i\hbar\zeta^*(+\infty,-\infty). \tag{36}$$

The real phase β in Eq. (33) manifests when eliminating the time ordering operator, and stands for:

$$\begin{aligned}&\beta(t,t_0) = \\ &\quad \frac{i}{2\hbar^2}\int_{t_0}^{t} dt' \int_{t_0}^{t'} dt'' \Big(f(t')f^*(t'')e^{-i\omega(t'-t'')} \\ &\qquad\qquad - f^*(t')f(t'')e^{i\omega(t'-t'')}\Big).\end{aligned} \tag{37}$$

D. Coherent States and the Forced Harmonic Oscillator

If the initial state at $t = t_0$ is a coherent state $|\alpha\rangle$ ([1] §10.7(10.110), and also [5]), the state at time t is

$$\begin{aligned}|\tilde{\Psi}(t)\rangle &= \tilde{U}(t,t_0)\,|\alpha\rangle & (38)\\ &= e^{i\beta(t,t_0)} e^{-\zeta^*(t,t_0)\hat{a}+\zeta(t,t_0)\hat{a}^\dagger} e^{\alpha\hat{a}^\dagger - \alpha^*\hat{a}}\,|0\rangle & (39)\\ &= e^{i\beta(t,t_0)} e^{-\zeta^*\hat{a}+\zeta\hat{a}^\dagger+\alpha\hat{a}^\dagger-\alpha^*\hat{a}+(\zeta\alpha^*-\zeta^*\alpha)/2}\,|0\rangle & (40)\\ &= e^{i\beta(t,t_0)} e^{(\zeta+\alpha)\hat{a}^\dagger-(\zeta^*+\alpha^*)\hat{a}+(\zeta\alpha^*-\zeta^*\alpha)/2}\,|0\rangle & (41)\\ &= e^{i\beta(t,t_0)} e^{(\zeta\alpha^*-\zeta^*\alpha)/2} e^{(\zeta+\alpha)\hat{a}^\dagger-(\zeta^*+\alpha^*)\hat{a}}\,|0\rangle & (42)\\ &= e^{i\gamma(t,t_0)}\,|\alpha+\zeta\rangle\,, & (43)\end{aligned}$$

where we applied the BCH relation (30) in the second to third line, collected terms on $\hat{a}^\dagger$ and $\hat{a}$, and moved the (commuting) one-half term in the exponential to the left; so that γ, like β, is a numerical phase.

We arrive at the intriguing and important conclusion that, under the influence of the (dipole) interaction $f(t)\hat{a} + f^*(t)\hat{a}^\dagger$, a coherent state remains coherent at all times, because the time development operator (33) is a displacement operator ([1] §10.98, and also [6] §4.2(c)(108)) for coherent states.

Thus, what we have discovered is the property that coherent states in the forced harmonic oscillator evolve into other coherent states (under spatially uniform forcing). The immediate consequence of this is that we now see how to physically create coherent states: reduce (e.g. by cooling) harmonic oscillators to their ground state, and then apply a (spatially uniform) force pulse.

As an aside, we know from classical mechanics ([7], §22) that a forced harmonic oscillator Hamiltonian produces oscillations displaced from their unforced motions. This similarity between classical and quantum mechanics can be taken as a starting point for building an Ansatz based on the displacement operator, in order to solve the forced harmonic oscillator by other methods (see [6], §4.2(c)).

E. Scattering Operator

Of particular interest is the limit of the operator $\tilde{U}(t,t_0)$ as $t_0\to-\infty$ and $t\to\infty$. This limiting time development operator is known as the S (or *scattering*) *operator* and is defined formally as

$$\boxed{S = \tilde{U}(+\infty, -\infty).} \tag{44}$$

For the forced harmonic oscillator with a finite duration interaction during the interval (T_0, T_1), the S operator is

$$\boxed{S = e^{i\beta} \exp\left(-\frac{i}{\hbar} g(\omega)\hat{a} - \frac{i}{\hbar} g^*(\omega)\hat{a}^\dagger\right),} \tag{45}$$

where we have denoted

$$\beta = \beta(+\infty, -\infty), \tag{46}$$

and $g(\omega)$, defined in Eq. (35) is the Fourier transform of the generalized force $f(t)$. Substituting the expression for $g(\omega)$ according to Eq. (36), we obtain

$$S = \\ e^{i\beta} \exp\left(-\frac{i}{\hbar} \int_{-\infty}^{+\infty} \left(f(t)\hat{a}e^{-i\omega t} + f^*(t)\hat{a}^\dagger e^{i\omega t}\right) dt\right). \tag{47}$$

If the oscillator is in the ground state before the start of the interaction, what is the probability that it will be found in the nth excited oscillatory energy eigenstate after the interaction?
The interaction produces the state $S\left|0\right\rangle$, which is a coherent state with eigenvalue $\alpha = -i/\hbar\; g^*(\omega)$. The transition probability of finding the oscillator in the nth energy eigenstate after the interaction is a Poisson distribution (see [1], §10.7(10.110), and also [5]):

$$\begin{aligned} \left|\left\langle n\right| S \left|0\right\rangle\right|^2 &= \left|\left\langle n \mid -i/\hbar\; g^*(\omega)\right\rangle\right|^2 = P_n(\alpha) && (48) \\ &= \frac{1}{n!}\left|\frac{g(\omega)}{\hbar}\right|^{2n} e^{-|g(\omega)|^2/\hbar^2} && (49) \\ &= \frac{\langle n\rangle^n}{n!} e^{-<n>}, && (50) \end{aligned}$$

a fact of great significance in radiation theory: These results can be interpreted in terms of a system of n quanta. The interaction term in the Hamiltonian is linear in $\hat{a}^\dagger$ and $\hat{a}$, and creates and annihilates quanta. The strength of the interaction determines the average number $\langle n\rangle$ of quanta present, and characterizes the Poisson distribution, which represents the probability that a dipole interaction pulse incident on the vacuum state of our system of quanta leaves after its passage a number of n quanta behind.

These features of the dynamics of the forced or driven linear harmonic oscillator can then help understand the creation and annihilation of photons. [1] §23

F. Time Evolution in the Schrödinger Picture

Finally, we use the results from the interaction picture to deduce the time development operator in the Schrödinger picture. From Eq. (17) we infer that

$$U(t_1, t_0) = e^{-(i/\hbar)\hat{H}_0 t_1} \tilde{U}(t_1, t_0) e^{(i/\hbar)\hat{H}_0 t_0}. \tag{51}$$

If we employ the oscillator Hamiltonian (9) for $\hat{H}_0$ and the time development operator (33) in the interaction picture, we obtain

$$\begin{aligned} U(t_1, t_0) = e^{i\beta(t_1,\ t_0)} \\ \exp\Big(- \zeta^*(t_1,\ t_0)\hat{a}\ e^{i\omega t_1} + \zeta(t_1,\ t_0)\hat{a}^\dagger\ e^{-i\omega t_1}\Big) \\ e^{-(i/\hbar)\hat{H}_0\ (t_1 - t_0)}. \end{aligned} \tag{52}$$

ACKNOWLEDGMENTS

Thanks to J. K. Freericks for suggesting to work on this problem.

---

[1] E. Merzbacher, *Quantum Mechanics.* John Wiley & Sons, 3rd ed., 1998.

[2] "See [8], Week 6, Lecture 11, The interaction picture and time evolution.".

[3] "See [9], Week 8, Lecture 13, Finding the unitary time-evolution operator, case of time-dependent Hamiltonians.".

[4] "See [10], Week 3, PS3, Proof of the Hadamard lemma.".

[5] "See [9], Week 8, Lecture 14, Poisson distribution in coherent states.".

[6] K. Gottfried, *Quantum Mechanics: Fundamentals.* Springer, 2nd ed., 2003.

[7] L. D. Landau, *Mechanics.* Butterworth Heinemann, 3rd ed., 2000.

[8] B. Zwiebach, "Applications of Quantum Mechanics." Course, 2019.

[9] B. Zwiebach, "Mastering Quantum Mechanics Part 2: Quantum Dynamics." Course, 2018.

[10] B. Zwiebach, "Mastering Quantum Mechanics Part 1: Wave Mechanics." Course, 2018.

Fractional statistics in two dimensions

Diwakar

(Dated: June 18, 2019)

In 3 dimensions, particles are grouped in two categories: bosons and fermions, depending on whether they follow Fermi-Dirac or Bose-Einstein statistics. But in 2 dimensions, there exists a continuous range of statistics between these two extremes and the particles that follow them are called "anyons". Bosons have integral spins and fermions have half integral spins, but 2-D anyons can have fractional spins. The main practical application of anyons and fractional statistics is in condensed matter systems where it has been used to explain fractional quantum hall effect. The paper will start by explaining how a 2D system called 'cyon' acts as anyon followed by calculation of partition functions and end with discussion of fractional quantum hall effect.

I. STATISTICS AND WAVEFUNCTIONS

Suppose we have two particles labeled as 1 and 2. The wavefunction associated to them is $\psi(1,2)$. Next we interchange the particles. In case of fermions, the new wavefunction will differ from old wavefunction by a minus sign while in case of bosons the new wavefunction will be same as old wavefunction.
If instead of interchanging particles, we rotate one particle around the other by an angle $\Delta\phi$ in plane, the wavefunction transformation can be written as

$$\psi(1,2) \rightarrow e^{i\nu\Delta\phi}\psi(1,2) \tag{1}$$

ν is called the statistics of the particles. It can be seen by taking $\Delta\phi = \pi$(which means we are interchanging particles) that for bosons, ν=0 and for fermions, ν=1. For anyons, ν can be arbitrary.

II. CYON ACTING AS AN ANYON

A cyon consists of an infinity long and thin solenoid with a charged particle inside it. Suppose the solenoid is oriented along the z direction and passing through origin. The magnetic field of the solenoid will be solely along z direction.

$$\vec{B} = B\hat{z} \tag{2}$$

The motion of the charged particle in the z direction is free because no Lorentz force will act in z direction. The motion in (x-y) plane is governed by the following Lagrangian:

$$L = \frac{1}{2}mv^2 + \frac{e}{c}\vec{v}\cdot\vec{A} \tag{3}$$

,where $\vec{v} = \dot{\vec{r}}$
and $\vec{r} = x\hat{x} + y\hat{y}$
and $\vec{A}$ is the vector potential for the magnetic field $\vec{B}$

We assume the following magnetic field created by solenoid:

$$\vec{B} = \Phi\delta^{(2)}(\vec{r})\hat{z} \tag{4}$$

We can see that:

$$\int dr^2\vec{B} = \Phi \tag{5}$$

Hence Φ is the flux of the magnetic field due to solenoid.
The vector potential for $\vec{B}$ is:

$$\vec{A}(\vec{r}) = \frac{\Phi}{2\pi}(\frac{-y\hat{x}}{r^2} + \frac{x\hat{y}}{r^2}) \tag{6}$$

Note that $r^2 = x^2 + y^2$. Everywhere in the discussion of cyon, r is only in (x-y) plane and the z direction is not included anywhere.

The canonical momentum is defined as

$$\vec{p} = \frac{\partial L}{\partial\dot{\vec{r}}} = \frac{\partial L}{\partial\vec{v}} = m\vec{v} + \frac{e\vec{A}}{c} \tag{7}$$

We can now calculate the Hamiltonian

$$H = \vec{p}\,\dot{\vec{r}} - L = \vec{p}\,\vec{v} - L = \frac{mv^2}{2} \tag{8}$$

It is the Hamiltonian for a free particle. But effect of magnetic field is there as it shows up in the relation between canonical momentum and kinetic momentum as seen in (7).

The Lagrangian (3) is rotationally invariant. The conserved quantity associated with this rotational symmetry is canonical angular momentum J_c

$$J_c = \vec{r}\times\vec{p}$$

Using expression of $\vec{p}$ from (7)

$$\vec{J_c} = \vec{r}\times m\vec{v} + \frac{e\vec{r}\times\vec{A}}{c} = \vec{J} + \frac{e\Phi}{2\pi c} \tag{9}$$

where $\vec{J}$ is the kinetic angular momentum.
It has been shown (Jackiw and Redlich, 1983) that eigenvalues of $\vec{J_c}$ are integral multiples of $\hbar$. Hence

$$\vec{J_c} = m\hbar \qquad m \in \mathbb{Z}$$

This gives us the following value for kinetic angular momentum

$$\vec{J} = \hbar(m - \frac{e\Phi}{hc}) \qquad m \in \mathbb{Z} \tag{10}$$

Hence in the presence of magnetic field, the values of kinetic angular momentum are shifted from the integal multiple of $\hbar$
Spin of a cyon is defined as

$$s = \frac{\vec{J}(m=0)}{\hbar} = \frac{-e\Phi}{hc} \tag{11}$$

In general, s is neither integer nor half-integer. So we expect cyon to behave like an anyon. To find the statistics of a cyon, we consider two cyons and their wavefunction is $\psi(1,2)$. Now imagine that the one cyon is rotated by 2π around each other. Particles in both the cyons would acquire a phase due to rotation in the magnetic field of the solenoid of the other cyon. The phase acquired by one particle on such rotation around closed loop $\boldsymbol{L}$ is given by Aharonov Bohm effect:

$$exp(\frac{-ie\Phi}{\hbar c})$$

This is the phase acquired when one cyon particle is rotated around another cyon solenoid enclosing flux Φ. But the second particle will also acquire similar phase since it will also seem to rotate around the first cyon. So, total phase acquired by two cyons are given complete rotation is twice of this

$$exp(\frac{-2ie\Phi}{\hbar c}) = exp(\frac{-2\pi 2ie\Phi}{hc})$$

Note that on the right hand side above, it is h instead of $\hbar$. Comparing this with equation (1) and noting that $\Delta\phi = 2\pi$, we get

$$\nu = \frac{-2e\Phi}{hc} \tag{12}$$

Comparing equation (12) with equation (11), we get the following relation between statistics and spin

$$\nu = 2s$$

Thus in general, a cyon is an anyon and the standard spin-statistics relation is satisfied.

III. STATISTICAL MECHANICS OF ANYONS

A. Partition function

Suppose a constant particle number system has energy levels: $E_1, E_2, ..., E_N$. Then the partition function of the system is defined as

$$\mathbb{Z} = \sum_{n=1}^{N} exp(-\beta E_i) \tag{13}$$

where $\frac{1}{\beta} = k_B T$, T is temperature of system
This is called canonical partition function. Here the number of particles in the system are fixed.

B. Calculating partition function for 2 particles

Calculating partition function for fermions and bosons is easier than for anyons. Here i have calculated partition function of bosons and fermions for single and 2 particle system.
The system we consider is a 2D harmonic oscillator in a plane. The energy levels for one particle in 2D oscillator is given by

$$E(n_1, j_1) = (n_1 + j_1 + 1)\hbar\omega \tag{14}$$

where $n_1, j_1 = 0, 1, 2, ...$

<u>CASE 1</u>: Single particle

Single particle partition function can be calculated as

$$\mathbb{Z}_1 = \sum_{n_1=0}^{\infty}\sum_{j_1=0}^{\infty} exp(-\beta E(n_1, j_1))$$

$$= \sum_{n_1=0}^{\infty}\sum_{j_1=0}^{\infty} exp(-\beta(n_1 + j_1 + 1)\hbar\omega)$$

$$= exp(-\beta\hbar\omega)\sum_{n_1=0}^{\infty} exp(-\beta n_1\hbar\omega)\sum_{j_1=0}^{\infty} exp(-\beta j_1\hbar\omega)$$

$$= exp(-\beta\hbar\omega)\Big(\sum_{n=0}^{\infty} exp(-\beta n\hbar\omega)\Big)^2$$

The infinite series is convergent and converges to

$$\frac{1}{1 - exp(-\beta\omega)}$$

Hence,

$$\mathbb{Z}_1 = \frac{exp(-\beta\omega)}{(1-exp(-\beta\omega))^2} = \frac{1}{4sinh^2(\frac{\beta\omega}{2})} \tag{15}$$

$\mathbb{Z}_1$ is same for bosons, fermions and anyons since there is no statistics to speak of in case of single particle.

CASE 2: Two particles

In case of two particles, energy is given by

$$E(n_1, j_1, n_2, j_2) = (n_1 + j_1 + n_2 + j_2 + 2)\hbar\omega \tag{16}$$

The 2 body partition function for bosons is given by

$$\mathbb{Z}_2^{bos} = \sum_{[n_1,j_1,n_2,j_2]} exp(E(n_1, j_1, n_2, j_2)) \tag{17}$$

The sum over all 4 integers is not independent of each other. The new state given by interchanging particles in a given state is not to be counted. For example the difference between states $(n_1 = 1, j_1 = 2; n_2 = 3, j_2 = 4)$ and $(n_1 = 3, j_1 = 4; n_2 = 1, j_2 = 2)$ is just interchange of particles 1 and 2. These two states have to be counted only once.
With a little manipulation, the 'restricted sum' could be converted into 'independent sum' by noting the following

$$\sum_{n_1,j_1=0}^{\infty}\sum_{n_2,j_2=0}^{\infty} + \sum_{n_1=n2=0,j_1=j_2=0}^{\infty} = 2\sum_{[n_1,j_1,n_2,j_2]} \tag{18}$$

Using this, we have

$$\mathbb{Z}_2^{bos} =$$

$$\tfrac{1}{2}[\textstyle\sum_{n_1,j_1=0}^{\infty}\sum_{n_2,j_2=0}^{\infty} exp(-\beta\hbar\omega(n_1+j_1+n_2+j_2+2))+$$

$$\textstyle\sum_{n,j=0}^{\infty} exp(-\beta\hbar\omega(2n + 2j + 2))]$$

$$= \frac{1}{2}[\frac{exp(-2\beta\hbar\omega)}{(1-exp(\beta\hbar\omega))^4} + \frac{exp(-2\beta\hbar\omega)}{(1-exp(2\beta\hbar\omega))^2}]$$

$$\mathbb{Z}_2^{bos} = \frac{cosh(\beta\hbar\omega)}{8sinh^2(\frac{\beta\hbar\omega}{2})sinh^2(\beta\hbar\omega)} \tag{19}$$

The fermionic 2 body partition function can also be calculated in a similar way

$$\mathbb{Z}_2^{fer} = \sum_{[n_1,j_1,n_2,j_2]} exp(E(n_1, j_1, n_2, j_2)) \tag{20}$$

Just like for bosons, the sum is restricted here also. The states obtained by interchanging of particles have to be counted just once. Additionally, due to Pauli's exclusion principle, both the particles cannot be in the same state.
Here also we convert the restricted sum to independent sum but the equation will get modified to include Pauli's exclusion principle.

$$\sum_{n_1,j_1=0}^{\infty}\sum_{n_2,j_2=0}^{\infty} - \sum_{n_1=n2=0,j_1=j_2=0}^{\infty} = 2\sum_{[n_1,j_1,n_2,j_2]} \tag{21}$$

Using this, we have

$$\mathbb{Z}_2^{fer} =$$

$$\tfrac{1}{2}[\textstyle\sum_{n_1,j_1=0}^{\infty}\sum_{n_2,j_2=0}^{\infty} exp(-\beta\hbar\omega(n_1+j_1+n_2+j_2+2))-$$

$$\textstyle\sum_{n,j=0}^{\infty} exp(-\beta\hbar\omega(2n + 2j + 2))]$$

$$= \frac{1}{2}[\frac{exp(-2\beta\hbar\omega)}{(1-exp(\beta\hbar\omega))^4} - \frac{exp(-2\beta\hbar\omega)}{(1-exp(2\beta\hbar\omega))^2}]$$

$$\mathbb{Z}_2^{fer} = \frac{1}{8sinh^2(\frac{\beta\hbar\omega}{2})sinh^2(\beta\hbar\omega)} \tag{22}$$

Calculations for higher N particles partition function is also possible in similar way but the equations (18) and (21) become more and more complicated as N becomes higher and higher.
However, this method cannot be used to calculate partition function of anyons. The partition function for anyons of any general statistics, ν has been derieved in "Lecture notes on anyons" by Alberto Lerda (Chapter 7, page 96-98). Here, i have directly written the formula for two particle anyon system

$$\mathbb{Z}_2(\nu, 0) = \frac{cosh((1-\nu)\beta\hbar\omega)}{8sinh^2(\frac{\beta\hbar\omega}{2})sinh^2(\beta\hbar\omega)} \tag{23}$$

Note that we recover eqn (19) for $\nu = 0$(bosons) and eqn (22) for $\nu = 1$(fermions)

IV. QUANTUM HALL EFFECT

Quantum Hall effect is observed in 2D system at very low temperatures (few degrees kelvin) and very high magnetic field (10 Tesla). Under these conditions, electrons in the system can move only in the layer perpendicular to the direction of magnetic field. In Quantum Hall Effect (QHE), the Hall conductance (σ_H) is given by

$$\sigma_H = \nu\frac{e^2}{h} \tag{24}$$

where ν can be an integer (Integer QHE) or a fraction (Fractional QHE)
The quantum number, ν is actually equal to a physical quantity called 'filling factor' which is defined as number of electrons per number of Landau levels available. In the presence of magnetic field, the energy spectrum of electrons split into Landau levels. For a finite sample of area A, the number of Landau levels is given by

$$\frac{A}{2\pi l_0^2} \tag{25}$$

l_0 is called magnetic length and is given by

$$l_0 = \sqrt{\frac{\hbar c}{eB}} \tag{26}$$

The filling factor thus becomes

$$\nu = \frac{N}{\frac{A}{2\pi l_0^2}} = \frac{N}{\frac{ABe}{hc}} = \frac{N}{\frac{\phi}{\phi_0}} \tag{27}$$

where N is number of electrons in the system, $\phi = BA$ is magnetic flux and $\phi_0 = \frac{hc}{e}$ is flux unit.

The proof that the quantum number, ν appearing in (24) is indeed the filling factor ν of (27) can be found in book Prange and Garvin, 1990.

If ν is integer (integer QHE), it means that all the Landau levels are filled. If ν is fraction (fractional QHE), it means that only a fraction of the Landau levels are filled.

When $\nu = \frac{1}{m}$ where m is odd integer, the ground state wavefunction is given by (Laughlin, 1983)

$$\psi_m = N_m \prod_{I<J} (z_i - z_j)^m exp(\frac{-\sum_I |z_I|^2}{4l_0^2}) \tag{28}$$

where z_I, z_J are coordinates of Ith and Jth electrons respectively and N_m is normalization constant.

We can produce excitations in this system by bringing about change in the number density of electrons, for example by changing flux at some point. These excitations can be of two types 'quasi-particles' and 'quasi-holes'. We want to prove that these excitations have fractional charge as well as fractional statistics. I have considered the case of only quasi-holes here.
For a system with filling factor $\nu = \frac{1}{m}$, the wavefunction with one quasi-hole at z_α can be written as

$$\psi_m^{z_\alpha} = N_{z_\alpha} \prod_I (z_I - z_\alpha)\psi_m \tag{29}$$

where ψ_m is ground state wavefunction of (28).

We want to see the charge and the statistics of the these quasi-hole excitations. We shall see that the charge of quasi-hole is $\frac{1}{m}$ of electronic charge,e. And the statistics is equal to the filling factor $\nu = \frac{1}{m}$. This will prove that quasi-hole excitations are anyons.
The charge of quasi-hole will be calculated by looking at the phase that the wavefunction acquires when the quasi-hole is moved adiabatically in a closed loop around a flux ϕ.
Since the motion of quasi-hole in a closed loop around flux ϕ is adiabatic, the phase acquired by the wavefunction is equal to

$$exp(-i\gamma) \tag{30}$$

where,

$$\gamma = -i \int_{t_0}^{t_1} \langle\psi(t)| \frac{d}{dt} |\psi(t)\rangle \, dt \tag{31}$$

Here t_0 and t_1 are respectively the times when the quasi-hole starts the loop and comes back to the initial point after completing the loop.
Eqn (30) is called Berry phase.
We can calculate γ by putting expression of wavefunction from eqn(29) into eqn(31). Note that wavefunction in eqn(29) will be treated as function of time because position of quasi-hole z_α is function of time as it is going around in a loop. The calculation is skipped here (check Lecture notes on anyons, Alberto Lerda, pg 115). The final result is equal to

$$\gamma = 2\pi N_e \tag{32}$$

where N_e is number of electrons inside the loop traversed by quasi-hole. According to Aharonov-Bohm effect, when a particle of charge q is moved around in loop encircling a flux of ϕ, the wavefunction picks up a phase

$$exp(\frac{-iq\phi}{\hbar c}) \tag{33}$$

Comparing this with the phase we have obtained

$$\frac{q\phi}{\hbar c} = 2\pi N_e \tag{34}$$

We can find the relation between ϕ and N_e using eqn(27)

$$\nu = \frac{1}{m} = N_e\frac{\phi_0}{\phi} \tag{35}$$

Using this in eqn (34), we get

$$q = \frac{e}{m} \tag{36}$$

proving that quasi-holes have fractional charges.
The other kind of excitation called quasi-particle also equal but opposite charge to quasi-hole.
The next task is to prove that quasi-holes have statistics of $\frac{1}{m}$ and are thus anyons.
For this we consider two quasi-holes at positions z_α and

z_β. The wavefunction will be the generalisation of eqn (29)

$$\psi_m^{z_\alpha z_\beta} = N_{z_\alpha z_\beta} \prod_I (z_I - z_\alpha)(z_I - z_\beta)\psi_m \tag{37}$$

Just like in the case of calculating charge, here also we will move z_α in a loop while keeping z_β fixed and calculate the Berry phase

$$\gamma = -i \int_{t_0}^{t_1} \left\langle \psi_m^{z_\alpha z_\beta}(t) \right| \frac{d}{dt} \left| \psi_m^{z_\alpha z_\beta}(t) \right\rangle dt \tag{38}$$

In the above integral z_α is a function of time while z_β is constant. If the loop followed by z_α does not include z_β, the result of the integral will be

$$\gamma = 2\pi N_e \tag{39}$$

where N_e is the number of electrons inside the loop just like we got in eqn (32). If z_β is contained inside the loop then the integral will be

$$\gamma = 2\pi(N_e - \frac{1}{m}) \tag{40}$$

which has a physical interpretation of a quasi-hole acting as $\frac{1}{m}$ fraction of an electron.

Comapring (40) and (39), we see that wavefunction picks an extra phase

$$exp(-i\Delta\gamma) = exp(i\frac{2\pi}{m}) \tag{41}$$

The moving of one quasi-hole around the other in closed loop corresponds to $\Delta\phi = 2\pi$ in eqn (1). Thus the statistics of two quasi-holes is given by

$$\nu = \frac{1}{m} \tag{42}$$

which is equal to the filling fraction.

When m=1, the two quasi-holes system is fermionic but for m=3,5,..., quasi-holes are anyons.

V. REFERENCES

- Lecture Notes in Physics, Anyons by Alberto Lerda
- Aharonov and Bohm 1959: Y.Aharonov and D.Bohm, Phys. Rev.115 (1959) 485
- Laughlin 1983: R.B. Laughlin, Phys. Rev. B23 (1983) 3383
- Prange and Garvin, 1990 The Quantum Hall Effect

Further explanations on Runge-Lenz vector

Rui Yin

The Kepler problem is about a two body system interactng by inverse square force, whose solution curve turns out to be a conic section. Classcially, Runge-Lenz vector is conserved for Kepler problem and has close relationship with the eccentricity of the ellipse orbit. Same analogy works for quantum mechanics. Moreover, a conserved quantity corresponds to a symmetry of the system. As a result, conservation of Runge-Lenz vector reveals some hidden symmetry in higher dimensions.

I. INTRODUCTION

The Kepler problem is a two-body system, in which the interaction force $\vec{f}(r)$ goes like $\frac{1}{r^2}$ or potential $V(r)$ goes like $\frac{1}{r}$ between them. The solution orbit can be circle, ellipse, parabola or hyperbola for different energy and initial conditions. Here we mainly focus on the case of ellipse where the target object is bounded with $E < 0$.

II. CLASSICAL DESCRIPTION OF RUNGE-LENZ VECTOR

A. Definition

Suppose the Hamiltonian of the system takes the form:

$$H = \frac{\vec{p}^2}{2m} - \frac{k}{r}$$

Then the corresponding Runge-Lenz vector is given by

$$\vec{R} = \frac{1}{mk}(\vec{p} \times \vec{L} - \frac{\vec{r}}{r})$$

B. Conservation and derivation

Since the interaction is a central force $\vec{f}(r)$ equal to $\frac{k}{r^2}$, the Hamiltonian H and angular momentum L are constants of motion. We can see that the Runge-Lenz vector is also a constant of motion by checking:

$$\begin{aligned} \frac{d}{dt}((\vec{p} \times \vec{L}) &= \frac{d\vec{p}}{dt} \times \vec{L} \\ &= \vec{f}(r) \times \vec{L} \\ &= f(r)\frac{\vec{r}}{r} \times (\vec{r} \times \vec{p}) \\ &= \frac{f(r)}{r}\vec{r} \times (\vec{r} \times m\dot{\vec{r}}) \\ &= \frac{mf(r)}{r}(\vec{r} \times \vec{r} \times \dot{\vec{r}}) \end{aligned} \tag{2.1}$$

Using the equality

$$\vec{a} \times \vec{b} \times \vec{c} = (\vec{a} \cdot \vec{c})\vec{b} - (\vec{a} \cdot \vec{b})\vec{c} \tag{2.2}$$

The above equation can be written as

$$\frac{d}{dt}((\vec{p} \times \vec{L}) = \frac{mf(r)}{r}((\vec{r} \cdot \dot{\vec{r}})\vec{r} - (\vec{r} \cdot \vec{r})\dot{\vec{r}}) \tag{2.3}$$

In order to get a constant of motion,we need to rewrite the right hand side as a total derivative. Notice that

$$\vec{r} \cdot \vec{r} = r^2 \tag{2.4}$$

$$\vec{r} \cdot \dot{\vec{r}} = \frac{1}{2}(\vec{r} \cdot \dot{\vec{r}} + \dot{\vec{r}} \cdot \vec{r}) = \frac{1}{2}\frac{d}{dt}\vec{r} \cdot \vec{r} = \frac{1}{2}\frac{dr^2}{dt} = r\dot{r} \tag{2.5}$$

We get

$$\begin{aligned} \frac{d}{dt}((\vec{p} \times \vec{L}) &= -\frac{mf(r)}{r}(r^2\dot{\vec{r}} - r\dot{r}\vec{r}) \\ &= -mf(r)r^2(\frac{\dot{\vec{r}}}{r} - \frac{\dot{r}\vec{r}}{r^2}) \\ &= -mf(r)r^2\frac{d}{dt}(\frac{\vec{r}}{r}) \end{aligned} \tag{2.6}$$

To get a new constant of motion, we need to make the coefficient $f(r)r^2$ unchange, which leads to the inverse square force or Coulomb potential. Thus, unlike energy and angular momentum, Runge-Lenz vector is a special constant of motion of the system under Coulomb potential. Besides,the second term in the parenthese of Runge-Lenz vector $(-\frac{\vec{r}}{r})$ contains the information of potential, which proves our point.

C. Geometric representation

First of all, what is the direction of Runge-Lenz vector? The below two pictures give the behavior under $\frac{1}{r}$ potential without and with little perturbation respectively. FIG.1 and FIG.2 shows that a small deviation from $\frac{1}{r}$ potential causes the rotation and shape change of the ellipse. Under little perturbation, it is reasonable to believe that Runge-Lenz vector has also changed for the reason that it is highly dependent on the $\frac{1}{r}$ potential. As a result, we tend to make a connection between the Runge-Lenz vector and some geometric features. Candidates are the direction of semi-major axis, eccentricity, envolope area of ellipse and so on. Actually, the direction of Runge-Lenz vector is along the semi-major axis, pointing to the perihelion, and the magnitude of Runge-Lenz vector is proportional to the eccentricity of the orbit. FIG.3 below can give intuition about these facts.

Next, we want to clarify some notations. See FIG.4 below. The sun stays at the focus on the semi-major axis. We denote the length of semi-major axis as a, length of

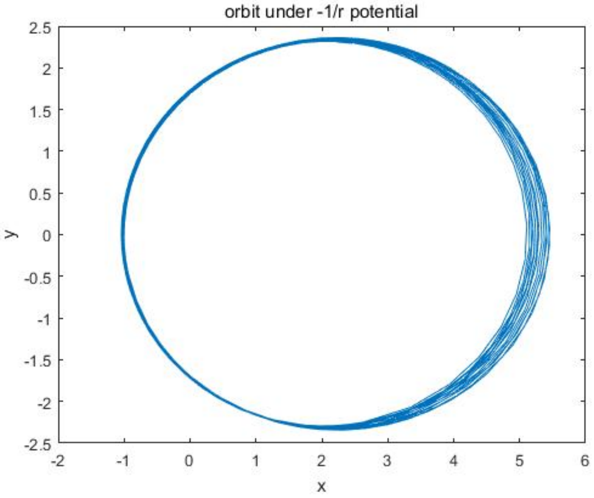

FIG. 1. Orbit without perturbation

perterbation.jpg

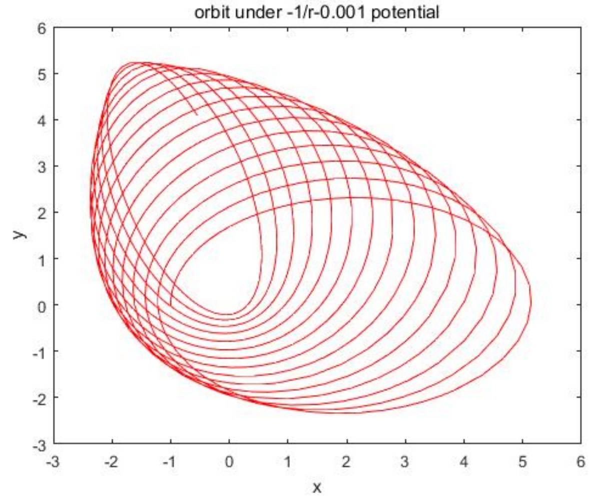

FIG. 2. Orbit with perturbation

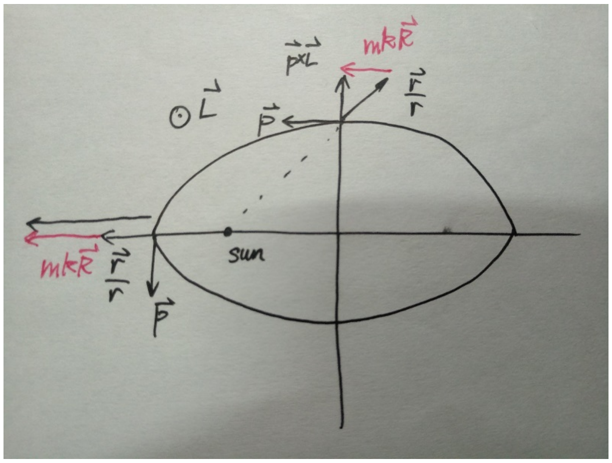

FIG. 3. Runge-Lenz vector demonstration

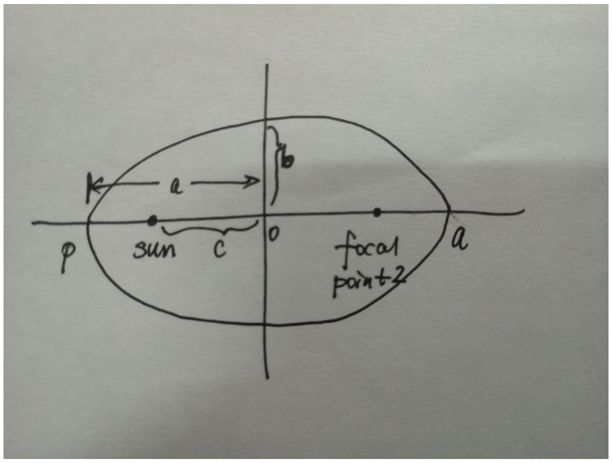

FIG. 4. Elliptical orbit

semi-minor as b, foci as c, eccentricity as $e = \frac{c}{a}$. Besides, the relation $a^2 = b^2+c^2$ holds. Also, we denote the vector from sun to perihelion p as $\vec{r_p}$, the vector from sun to aphelion a as $\vec{r_a}$. Finally, we want to show $\vec{R} = e\frac{\vec{r_p}}{r_p}$.

$$\begin{aligned}\vec{p}\times\vec{L} &= \vec{p}\times\vec{r}\times\vec{p}\\ &= (\vec{p}\cdot\vec{p})\vec{r} - (\vec{p}\cdot\vec{r})\vec{p}\end{aligned} \tag{2.7}$$

At the perihelion, $\vec{p}$ is perpendicular to $\vec{r}$, we get

$$(\vec{p}\times\vec{L})_p = p^2\vec{r_p} = \frac{L^2}{r_p^2}\vec{r_p} \tag{2.8}$$

We now need to find the expression for L^2 in terms of r_p. In spherical coordinates, the Hamiltonian can be written as

$$H = \frac{p_r^2}{2m} + \frac{L^2}{2mr^2} - \frac{k}{r}$$

where p_r represents the radial momentum of the mass point. At the perihelion and aphelion, $p_r = 0$, then

$$E = \frac{L^2}{2mr_a^2} - \frac{k}{r_a} \tag{2.9}$$

$$E = \frac{L^2}{2mr_p^2} - \frac{k}{r_p} \tag{2.10}$$

Eliminate the E term, we get

$$\frac{L^2}{2m}\left(\frac{1}{r_a} + \frac{1}{r_p}\right) = k \tag{2.11}$$

$$L^2 = 2mk\frac{r_a r_p}{r_a + r_p} \tag{2.12}$$

Plug in $r_a = a + c$ and $r_p = a - c$, we have

$$\begin{aligned}L^2 &= 2mk\frac{a^2-c^2}{2a}\\ &= mka\frac{a^2-c^2}{a^2}\\ &= mka(1-e^2)\end{aligned} \tag{2.13}$$

Similarly, eliminate L^2 term, we have

$$E = -\frac{k}{2a} \tag{2.14}$$

Plug back into Eq(2.8), yielding

$$\begin{aligned}(\vec{p}\times\vec{L})_p &= \frac{L^2}{r_p^2}\vec{r_p} \\ &= \frac{mka(1-e^2)}{(a-c)r_p}\vec{r_p} \\ &= \frac{mk(1-e^2)}{(1-e)r_p}\vec{r_p} \\ &= \frac{mk(1+e)}{r_p}\vec{r_p}\end{aligned} \tag{2.15}$$

Finally, we get

$$\frac{1}{mk}(\vec{p}\times\vec{L}) - \frac{\vec{r_p}}{r_p} = e\frac{\vec{r_p}}{r_p}$$

D. Other properties

We know that an mass point in 3D space has 6 degrees of freedom, 3 for position and 3 for momentum. Given the restriction of ellipse orbit, there is 5 degrees of freedom remains. On the other hand, there are 3 quantities conserved, i.e. energy E, angular momentum $\vec{L}$ and Runge-Lenz vector $\vec{R}$, 7 degrees of freedom totally. It shows that there are 2 dependent quantities or 2 unknown restrictions. Take the energy and angular momentum to be independent, there will be 2 dependent relations for Runge-Lenz vector in both direction and magnitude aspects. We will give the conclusion directly.

$$\vec{L}\cdot\vec{R} = 0 \tag{2.16}$$

$$R^2 = 1 + \frac{2EL^2}{mk^2} \tag{2.17}$$

Eq(2.16) makes sense for the reason that Runge-Lenz vector $\vec{R}$ lies in the plane of orbit while $\vec{L}$ is perpendicular to the plane. To get Eq(2.16) explicitly, on the left hand side, ignore the constant prefactor $\frac{1}{mk}$, we have

$$\begin{aligned}LHS &= \vec{L}\cdot(\vec{p}\times\vec{L} - \frac{\vec{r}}{r}) \\ &= \vec{L}\cdot(\vec{p}\times\vec{L}) - \frac{1}{r}\vec{L}\cdot\vec{r} \\ &= 0 - \frac{1}{r}(\vec{r}\times\vec{p})\cdot\vec{r} \\ &= 0\end{aligned} \tag{2.18}$$

Since $\vec{p}\times\vec{L}$ is perpendicular to $\vec{L}$ and same relation for $\vec{r}\times\vec{p}$ and r. Eq(2.17) is just expressed R^2 in terms of E and L^2 using Eq(2.13) and Eq(2.14).

III. QUANTUM VERSION OF RUNGE-LENZ VECTOR

A. Review

To meet the requirement of Hermitian operator, the quantum Runge-Lenz vector takes the form

$$\mathbf{R} = \frac{1}{2mk}(\mathbf{p}\times\mathbf{L} - \mathbf{L}\times\mathbf{p}) - \frac{\mathbf{r}}{r}$$

From 8.05, we know that

$$[\mathbf{R},\mathbf{H}] = 0 \tag{3.1}$$

$$\mathbf{R}\cdot\mathbf{L} = 0 \tag{3.2}$$

$$\mathbf{R}^2 = 1 + \frac{2\mathbf{H}}{mk^2}(\mathbf{L^2} + \hbar^2) \tag{3.3}$$

The above equations make good correspondence to classical ones, given $\hbar \approx 0$ in Eq(3.3) for common life.

The energy level of Hydrogen atom is given by $E_n = -\frac{e^2}{2a_0}\frac{1}{n^2}$, which is independent of quantum number l and m. Each level has degeneracy n^2. Compared with 3D harmonic oscillator with Hamiltonian $\mathbf{H} = \hbar\omega(\mathbf{N}_1 + \mathbf{N}_2 + \mathbf{N}_3 + \frac{3}{2})$, for the first excited state, 3D harmonic oscillator has degeneracy 3, while Hydrogen atom has 4. Hydrogen atom is more than 3D rotational symmetry, where Runge-Lenz vector may play a role.

From another point of view, Noether's theorem says that every conservation law corresponds to a symmetry of the system. We've heard that translation invariance corresponds to momentum conservation and rotation invariance corresponds to angular momentum conservation. Then comes the question: what kind of symmetry does Runge-Lenz vector conservation corresponds to?

B. Commutation relations

In the beginning, considering the commutation relation for $\mathbf{L}$,

$$[\mathbf{L}_i,\mathbf{L}_j] = i\hbar\epsilon_{ijk}\mathbf{L}_k$$

It is natural to think about the commutator $[\mathbf{R}_i,\mathbf{R}_j]$. Remember the equality $\mathbf{p}\times\mathbf{L} = -\mathbf{L}\times\mathbf{p} + 2i\hbar\mathbf{p}$, we rewrite $\mathbf{R}$ as

$$\mathbf{R} = \frac{1}{mk}(\mathbf{p}\times\mathbf{L} - i\hbar\mathbf{p}) - \frac{\mathbf{r}}{r}$$

With some calculation, we can show that

$$[\mathbf{R}_i,\mathbf{R}_j] = i\hbar\epsilon_{ijk}(\frac{-2\mathbf{H}}{mk^2})\mathbf{L}_k \tag{3.4}$$

$$[\mathbf{L}_i,\mathbf{R}_j] = i\hbar\epsilon_{ijk}\mathbf{R}_k \tag{3.5}$$

Eq(3.4)(3.5) means that Runge-Lenz vector is a vector under rotation and its commutation algebra isn't closed by itself alone. Contrary to the commutation behavior of **L**, **R** is somehow mixed with **L**. Suppose we are working in the energy eigenstate with energy , we can replace **H** with E in Eq(3.4). Set $\tilde{\mathbf{R}} = \sqrt{\frac{-mk^2}{2E}}\mathbf{R}$, we can rewrite Eq(3.4)(3.5) as

$$[\tilde{\mathbf{R}}_i, \tilde{\mathbf{R}}_j] = i\hbar\epsilon_{ijk}\mathbf{L}_k \tag{3.6}$$

$$[\mathbf{L}_i, \tilde{\mathbf{R}}_j] = i\hbar\epsilon_{ijk}\tilde{\mathbf{R}}_k \tag{3.7}$$

The rescaled Runge-Lenz vector $\tilde{\mathbf{R}}$, together with angular momentum **L** forms a closed commutation algebra, which in fact make a generalization from 3D rotation to 4D rotation.

We can also define two vector operators from **L** and $\tilde{\mathbf{R}}$

$$\mathbf{J}_1 = \frac{1}{2}(\mathbf{L} + \tilde{\mathbf{R}}) \tag{3.8}$$

$$\mathbf{J}_2 = \frac{1}{2}(\mathbf{L} - \tilde{\mathbf{R}}) \tag{3.9}$$

Then the commutation realtions simply becomes

$$[\mathbf{J}_{1i}, \mathbf{J}_{1j}] = i\epsilon_{ijk}\mathbf{J}_{1k} \tag{3.10}$$

$$[\mathbf{J}_{2i}, \mathbf{J}_{2j}] = i\epsilon_{ijk}\mathbf{J}_{2k} \tag{3.11}$$

$$[\mathbf{J}_1, \mathbf{J}_2] = 0 \tag{3.12}$$

The above relations mean that $\mathbf{J}_1$ and $\mathbf{J}_2$ are decoupled and constitute angular momentum algebra separately.

C. Group structure

We will first review our familiar structure of angular momentum. All 3D rotation transform O form a group, so-called SO(3), satisfying following two conditions:

$$O^T O = I, det(O) = 1 \tag{3.13}$$

The first orthogonal condition makes the inner product of vectors unchange, in other words, the distance between two points is invariant under rotation. For example, given a vector in 3D space $\vec{v}$, the length square is a constant, put in matrix form:

$$v^T v = c \tag{3.14}$$

After rotation, $v' = Ov$, and the length square becomes:

$$v'^T v' = (Ov)^T(Ov) = v^T O^T O v = c \tag{3.15}$$

which shows the unitary condition. The second determinant condition for O makes the right-hand coordinates unchange under 3D rotations. Take a close look at O near the neibhorhood of identity element. Then O can be expressed by $O = I + A\theta$, where we let θ to be a small change of angles and call A the generator of O. Similarly, $O^T = I + A^T\theta$. To achieve our orthogonal reqirement in Eq(3.13), we get

$$(I + A^T\theta)(I + A\theta) = I \tag{3.16}$$

$$I + A^T\theta + A\theta + A^T A\theta^2 = I \tag{3.17}$$

By ignoring the second order of θ, we get

$$A^T + A = 0 \tag{3.18}$$

which means the generator A can be represented by a anti-symmetric matrix. The exact expression for O is $O = e^{\theta A}$, as we encountered in course. Thus the determinant condition requires that

$$det(e^{\theta A}) = e^{\theta tr(A)} = 1 \tag{3.19}$$

$$tr(A) = 0 \tag{3.20}$$

There can be 3 basis for anti-symmetric and traceless matrices:

$$A_1 = \begin{bmatrix} 0 & 0 & 0 \\ 0 & 0 & -1 \\ 0 & 1 & 0 \end{bmatrix}, A_2 = \begin{bmatrix} 0 & 0 & 1 \\ 0 & 0 & 0 \\ -1 & 0 & 0 \end{bmatrix}, A_3 = \begin{bmatrix} 0 & -1 & 0 \\ 1 & 0 & 0 \\ 0 & 0 & 0 \end{bmatrix}$$

with commutation relations $[A_i, A_j] = -\epsilon_{ijk}A_k$.

By set $\mathbf{L}_i = -iA_i$, we get our familiar representation for angular momentum($\hbar = 1$).

$$\mathbf{L}_1 = i\begin{bmatrix} 0 & 0 & 0 \\ 0 & 0 & 1 \\ 0 & -1 & 0 \end{bmatrix}, \mathbf{L}_2 = i\begin{bmatrix} 0 & 0 & -1 \\ 0 & 0 & 0 \\ 1 & 0 & 0 \end{bmatrix}, \mathbf{L}_3 = i\begin{bmatrix} 0 & 1 & 0 \\ -1 & 0 & 0 \\ 0 & 0 & 0 \end{bmatrix}$$

where the anti-symmetric condition becomes the Hermitian condition for matrix and the commutation relations satisfy. The dimension of rotation group, or the numbers of basis, equals the numbers of entries at the right-up corner of matrix. For 3D case, it is 3 , and it is 6 for 4D rotation, which is exactly the sum of the numbers for angular momentum and Runge-Lenz vectors.

Now we add a fictitious axis w in front of x, y, z axis. Then the above 3D rotation basis, or angular momentum operators become:

$$\mathbf{L}_1 = i\begin{bmatrix} 0 & 0 & 0 & 0 \\ 0 & 0 & 0 & 0 \\ 0 & 0 & 0 & 1 \\ 0 & 0 & -1 & 0 \end{bmatrix}, \mathbf{L}_2 = i\begin{bmatrix} 0 & 0 & 0 & 0 \\ 0 & 0 & 0 & -1 \\ 0 & 0 & 0 & 0 \\ 0 & 1 & 0 & 0 \end{bmatrix}, \mathbf{L}_3 = i\begin{bmatrix} 0 & 0 & 0 & 0 \\ 0 & 0 & 1 & 0 \\ 0 & -1 & 0 & 0 \\ 0 & 0 & 0 & 0 \end{bmatrix}$$

Hence, bt fufilling the left entries at the right-up corner, the expressions for remaining 3 basis in 4D rotation matrices naturally come out as follows:

$$\tilde{\mathbf{R}}_1 = i\begin{bmatrix} 0 & 1 & 0 & 0 \\ -1 & 0 & 0 & 0 \\ 0 & 0 & 0 & 0 \\ 0 & 0 & 0 & 0 \end{bmatrix}, \tilde{\mathbf{R}}_2 = i\begin{bmatrix} 0 & 0 & -1 & 0 \\ 0 & 0 & 0 & 0 \\ 1 & 0 & 0 & 0 \\ 0 & 0 & 0 & 0 \end{bmatrix}, \tilde{\mathbf{R}}_3 = i\begin{bmatrix} 0 & 0 & 0 & 1 \\ 0 & 0 & 0 & 0 \\ 0 & 0 & 0 & 0 \\ -1 & 0 & 0 & 0 \end{bmatrix}$$

It is easy to check these matrices satisfy the relations in Eq(3.6)(3.7) Eq(3.10)(3.11)(3.12) told us that the 4D rotation group falls into 2 independent pieces of 3D rotations. It is actually a special feature for 4 dimension space.

Let us make a analogy for better understanding. The most common 4D vector we may get reach to can be 4-vector in spacetime expressed by $x^\mu(\mu = 0, 1, 2, 3)$, where t denoted by x^0. The invariance is called proper time τ, calculated by

$$(cd\tau)^2 = (cdt)^2 - (dx)^2 - (dy)^2 - (dz)^2 \tag{3.21}$$

where $d\tau$ is the small segment of proper time, and c is the velocity of light. Just like distance in 3D space, we can treat proper time as distance in spacetime. From passive perspective, the 4-vector x^μ in frame 1 can be represented by $x^{\mu\prime}$ in frame 2 with $x^{\mu\prime} = Tx^\mu$, where T is a 4D rotation transform. Then T can be decomposed into 2 kinds of transforms, one is the usual 3D rotation, the other is the boost, the translation between two inertial reference frames. The boost is an analogy for the rescaled Runge-Lenz vector $\tilde{\mathbf{R}}$.

IV. CONCLUSION

The central force without any orientation preference provides 3D rotation symmetry. Furthermore, for potential decreases precisely as $\frac{1}{r}$, there is more symmetry added to the system with Runge-Lenz vector conserved in correspondence. It turns out to be a 4D rotation symmetry which can be decomposed into two 3D rotation symmetry.

ACKNOWLEDGMENTS

Thanks for the effort of MIT course team so that I can have a chance to write my first paper. Limited by my knowledge, there is a loss of rigorous mathmatical explanation. I still have passions for physics even though I choose another major as well as another job for living. Hope to learn more math and physics courses in the near future!

Grassmann Algebra to Fermionic Coherent States

Andrew Lowry

(Dated: June 19, 2019)

The Grassmann algebra captures the defining properties of fermions. The anti-commutativity of Grassmann numbers corresponds to the state of a multi-fermion system being totally antisymmetric, while their nilpotency is classically equivalent to the Pauli exclusion principle. After reviewing the Fock spaces for bosons and fermions, we proceed to define the Grassmann algebra. Then we explore Grassmann analysis, aiming towards Gaussian integration on Grassmann algebras. We finally define fermion displacement operators (Weyl translations) for Grassmann variables and deduce some basic properties of the associated fermion coherent states.

I. INTRODUCTION

A. Fock Spaces

Following [1], let us consider a quantum system of an unspecified number of identical particles. Here, the quantum state of each particle is an element of the Hilbert space $\mathcal{H}$, so that the states of systems of N particles are in the Hilbert space $\mathcal{H}^{\otimes N} = \mathcal{H} \otimes \cdots \otimes \mathcal{H}$. If the number of particles is allowed to vary then the total Hilbert space is the Fock space:

$$\mathcal{F}(\mathcal{H}) := \bigoplus_{N=0}^{\infty} \mathcal{H}^{\otimes N}. \tag{1}$$

Let $\mathcal{S}_N$ denote the symmetric group of permutations from the set $\{1, 2, \ldots, N\}$ to itself, and let the group homomorphism $sgn : \mathcal{S}_N \to \{1, -1\}$ give the parity of a permutation. According to the symmetry postulate, a quantum system of N identical bosons is completely symmetric with respect to the group action of $\mathcal{S}_N$ on $\mathcal{H}^{\otimes N}$; while a quantum system of N identical fermions is completely antisymmetric with respect to the group action [2].

We can express this formally using the symmetrizer and antisymmetrizer:

$$\Pi_B(\psi_1 \otimes \cdots \otimes \psi_N) = \frac{1}{N!} \sum_{\pi \in \mathcal{S}_N} \psi_{\pi(1)} \otimes \cdots \otimes \psi_{\pi(N)} \tag{2}$$

$$\Pi_F(\psi_1 \otimes \cdots \otimes \psi_N) = \frac{1}{N!} \sum_{\pi \in \mathcal{S}_N} sgn(\pi) \psi_{\pi(1)} \otimes \cdots \otimes \psi_{\pi(N)} \tag{3}$$

where $\psi_1, \ldots \psi_N \in \mathcal{H}$. We can then define the Fock space for bosons as the subspace $\mathcal{F}_B(\mathcal{H}) := \Pi_B \mathcal{F}(\mathcal{H})$, and the Fock space for fermions as the subspace $\mathcal{F}_F(\mathcal{H}) := \Pi_F \mathcal{F}(\mathcal{H})$.

B. Creation and Annihilation Operators (CAP)

In $\mathcal{F}_B(\mathcal{H})$ we have the boson CAP satisfying the canonical commutation relations (CCR):

$$[\hat{a}_i, \hat{a}_j^\dagger] = \delta_{i,j},\ [\hat{a}_i, \hat{a}_j] = [\hat{a}_i^\dagger, \hat{a}_j^\dagger] = 0. \tag{4}$$

While in $\mathcal{F}_F(\mathcal{H})$ we have the fermion CAP satisfying the canonical anti-commutation relations (CAR):

$$\{\hat{c}_i, \hat{c}_j^\dagger\} = \delta_{i,j},\ \{\hat{c}_i, \hat{c}_j\} = \{\hat{c}_i^\dagger, \hat{c}_j^\dagger\} = 0. \tag{5}$$

II. GRASSMANN ALGEBRA

From the CAR (5) above, we derive the nilpotent relation, $(\hat{c}_i^\dagger)^2 = 0$; this demands the introduction of a new type of number, the Grassmann number. Nilpotency can be considered to be classically equivalent to the Pauli exclusion principle which characterizes fermions, and the Grassmann numbers provide a convenient mathematical tool for computations in supersymmetric models of nature [1].

The Grassmann algebra $\mathfrak{G}_n$ is an associative algebra, with unit 1, over a $\mathbb{C}$-linear space, with n generators $\{\theta_1, \ldots, \theta_n\}$ (called Grassmann numbers or g-numbers) that satisfy the anti-commutation relation

$$\theta_i \theta_j = -\theta_j \theta_i,\ \forall i, j = 1, \ldots, n. \tag{6}$$

This sign change, produced by changing the order of the product of g-numbers is the key difference between complex numbers (c-numbers) and g-numbers; as a consequence, the g-numbers exhibit nilpotency:

$$\theta_i^p = 0,\ \forall i, j = 1, \ldots, n \tag{7}$$

with $p \geq 2$.

A. Grassmann Functions

We form a basis of $\mathfrak{G}_n$ by collecting the sets of ${}_nC_k = \binom{n}{k}$ distinct monomials $\{\theta_{i_1}\theta_{i_2} \cdots \theta_{i_k} | i_1 < i_2 < \cdots < i_k\}$ of degree k, where $0 \leq k \leq n$ (any monomial of degree $> n$ is zero because of (7)), and hence its demension is $\sum_{k=0}^{n} {}_nC_k = 2^n$. A Grassmann function of n g-numbers is an element of $\mathfrak{G}_n$ and can be expressed as a linear combination of monomials, which requires a total of 2^n c-numbers:

$$f(\theta_1, \ldots, \theta_n) = \sum_{k=0}^{n} \sum_{i_1, \ldots, i_k} f^{(k)}_{i_1, \ldots, i_k} \theta_{i_1} \cdots \theta_{i_k} \tag{8}$$

where the $f^{(k)}_{i_1,\ldots,i_k}$ are completely antisymmetric tensors (permuting the indices in the paired monomial should introduce a sign change, which should be met by an accompanying sign change in the coefficient function; if two of the indices are equal then that term should be zero) with elements being c-numbers.

Following convenient notation from [1], we can introduce the n-dimensional multi-index $\varepsilon = (\varepsilon_1, \ldots, \varepsilon_n) \in \mathcal{E}[n] = \{0,1\}^n$, allowing us to write $\theta^\varepsilon = \theta_1^{\varepsilon_1} \cdots \theta_n^{\varepsilon_n}$. Elements of $\mathfrak{G}_n$ are thereby elements of a linear vector space (over a field $\mathbb{C}$ in this case) with basis $\{\theta^\varepsilon | \varepsilon \in \mathcal{E}[n]\}$. There exists a unique decomposition for every $f(\theta) \in \mathfrak{G}_n$ as:

$$f(\theta) := f(\theta_1, \ldots, \theta_n) = \sum_{\varepsilon \in \mathcal{E}[n]} f^{(|\varepsilon|)}_\varepsilon(\theta)\theta^\varepsilon \tag{9}$$

where $f^{(|\varepsilon|)}_\varepsilon(\theta)$ are c-numbers and $|\varepsilon| := \varepsilon_1 + \cdots + \varepsilon_n$ is the number of fermionic states occupied.

We then introduce the linear parity operator defined by $\mathcal{P}(\theta^\varepsilon) := (-1)^{|\varepsilon|}\theta^\varepsilon$. Because the monomials in the basis $\{\theta^\varepsilon | \varepsilon \in \mathcal{E}[n]\}$ can be separated by the parity operator, we have a direct sum decomposition $\mathfrak{G}_n = \mathfrak{G}_{n,E} \oplus \mathfrak{G}_{n,O}$, where the elements of $\mathfrak{G}_{n,E}$ are said to be *even* and elements of $\mathfrak{G}_{n,O}$ are said to be *odd*.

Elements in the subspace $\mathfrak{G}_{n,E}$ can be decomposed as in (8), but with the first summation only over even k (even monomials):

$$\begin{aligned} f_E(\theta) &= \sum_{k=0}^{\lfloor n/2 \rfloor} \sum_{i_1,\ldots,i_{2k}} f^{(2k)}_{i_1,\ldots,i_{2k}} \theta_{i_1} \cdots \theta_{i_{2k}} && (10) \\ &= \sum_{\substack{\varepsilon \in \mathcal{E}[n] \\ |\varepsilon|\ even}} f^{(|\varepsilon|)}_\varepsilon(\theta)\theta^\varepsilon; && (11) \end{aligned}$$

this subspace consists of eigenvectors of the parity operator with eigenvalue 1, i.e. $\mathcal{P}(f_E(\theta)) = f_E(\theta)$. Similarly, elements in the subspace $\mathfrak{G}_{n,O}$ can be decomposed as in (8), but with the first summation only over odd k (odd monomials):

$$\begin{aligned} f_O(\theta) &= \sum_{k=0}^{\lfloor n/2 \rfloor} \sum_{i_1,\ldots,i_{2k+1}} f^{(2k+1)}_{i_1,\ldots,i_{2k+1}} \theta_{i_1} \cdots \theta_{i_{2k+1}} && (12) \\ &= \sum_{\substack{\varepsilon \in \mathcal{E}[n] \\ |\varepsilon|\ odd}} f^{(|\varepsilon|)}_\varepsilon(\theta)\theta^\varepsilon; && (13) \end{aligned}$$

this subspace consists of eigenvectors of the parity operator with eigenvalue -1, i.e. $\mathcal{P}(f_O(\theta)) = -f_O(\theta)$.

The product of Grassmann monomials satisfies:

$$\theta^\varepsilon \theta^\zeta = (-1)^{|\varepsilon|\cdot|\zeta|}\theta^\zeta\theta^\varepsilon \tag{14}$$

for $\varepsilon, \zeta \in \mathcal{E}[n]$. Then by examining the product of Grassmann functions $f, h \in \mathfrak{G}_n$

$$\begin{aligned} f(\theta)h(\theta) &= \sum_{\varepsilon,\zeta \in \mathcal{E}[n]} f^{(|\varepsilon|)}_\varepsilon(\theta) h^{(|\zeta|)}_\zeta(\theta)\, \theta^\varepsilon\theta^\zeta && (15) \\ &= \sum_{\varepsilon,\zeta \in \mathcal{E}[n]} (-1)^{|\varepsilon|\cdot|\zeta|} h^{(|\zeta|)}_\zeta(\theta) f^{(|\varepsilon|)}_\varepsilon(\theta)\, \theta^\zeta\theta^\varepsilon, && (16) \end{aligned}$$

we can determine how even and odd Grassmann functions commute. From (14), we see that even elements commute with every element of the algebra, while odd elements commute with even elements but anti-commute with other odd elements; as such, only the odd elements of the Grassmann algebra are nilpotent. Thus, since even functions are only composed of even elements and odd functions are only composed of odd elements, $\forall f_E, h_E \in \mathfrak{G}_{n,E}$ and $\forall f_O, h_O \in \mathfrak{G}_{n,O}$ we have the following commutation relations:

$$\begin{aligned} [f_E, h_E] = [f_E, h_O] = [f_O, h_E] &= 0, && (17) \\ [f_O, h_O] &= 2f_O h_O. && (18) \end{aligned}$$

Therefore, the center of the algebra is $Z(\mathfrak{G}_n) = \mathfrak{G}_{n,O}$. Furthermore, for arbitrary $f, h \in \mathfrak{G}_n$, decomposed as $f = f_E + f_O$ and $h = h_E + h_O$, we obtain the commutation relations:

$$\begin{aligned} [f, g] &= [f_E, h_E] + [f_E, h_O] + [f_O, h_E] + [f_O, h_O] && (19) \\ &= [f_O, h_O] = 2f_O h_O. && (20) \end{aligned}$$

Thus:

$$\begin{aligned} [f, [f, h]] &= [f_E + f_O, 2f_O h_O] && (21) \\ &= 2f_O[f_O, h_O] = 4(f_O)^2 h_O = 0. && (22) \end{aligned}$$

Hence, the Grassmann functions themselves behave algebraically as Grassmann numbers [3].

This feature enables us to apply the Baker-Campbell-Hausdorff formula to the Grassmann functions:

$$e^f e^h = e^{f+h} e^{\frac{1}{2}[f,h]} = e^{f+h} e^{f_O h_O}. \tag{23}$$

As a result of (22), the exponential transformation law for the Grassmann functions $f, h \in \mathfrak{G}_n$ reduces to:

$$\begin{aligned} e^f\, h\, e^{-f} &= f + [f, h] + \frac{1}{2!}[f, [f, h]] + \ldots && (24) \\ &= f + [f, h]. && (25) \end{aligned}$$

B. Complex Conjugation

We can now introduce the notion of complex conjugation for Grassmann numbers by defining the antilinear map $^\star : \mathfrak{G}_n \to \mathfrak{G}_n$, which is an antiautomorphism and involution; hence it satisfies the following properties:

$$\begin{aligned} (\theta_i^\star)^\star &= \theta_i, && (26) \\ (c_i\theta_i + c_j\theta_j)^\star = \theta_i^\star c_i^\star + \theta_j^\star c_j^\star &= c_i^\star\theta_i^\star + c_j^\star\theta_j^\star, && (27) \\ (\theta_i\theta_j)^\star &= \theta_j^\star\theta_i^\star. && (28) \end{aligned}$$

$\forall \theta_i, \theta_j \in \mathfrak{G}_n$ and $\forall c_i, c_j \in \mathbb{C}$ (where the star operator is normal complex conjugation for the c-numbers). This antilinear mapping is reminiscent of the Hermitian adjoint in quantum mechanics.

We can also define the real and imaginary parts of for a g-number, in an analogous manner to that for c-numbers:

$$\theta_{\Re} := \frac{1}{2}(\theta + \theta^{\star}), \tag{29}$$

$$\theta_{\Im} := \frac{1}{2i}(\theta - \theta^{\star}), \tag{30}$$

such that $\theta_{\Re} = \theta_{\Re}^{\star}$ and $\theta_{\Im} = \theta_{\Im}^{\star}$ are self-adjoint like their complex number counterparts.

If we include the conjugates with original n g-numbers in the generator set, then we can compose 2^{2n} monomials of degree up to $2n$; elements of the Grassmann algebra can be decomposed as a generalization of (8).

III. GRASSMANN CALCULUS

A. Grassmann Differentiaion

As a result of the general anti-commutation relation (6), derivatives with respect to Grassmann variables can provide different results depending on their direction of action, left or right. The left and right derivatives of a Grassmann function can be defined via their actions on the basis $\{\theta^{\varepsilon} | \varepsilon \in \mathcal{E}[n]\}$ of $\mathfrak{G}_n$. For a basis element which includes the Grassmann variable being differentiated the process of differentiation is defined as follows: (a) in the case of left differentiation we move the differentiated variable to the leftmost position in the monomial utilizing the sign change from anti-commutativity (*sign rule*), while in the case of right differentiation we move the differentiated variable to the rightmost position in the monomial utilizing the sign rule; then (b) remove the differentiated variable from the monomial; finally, (c) the other Grassmann variables in the monomial are treated as constants after the sign rule is fully exploited ([3],[4]).

The left derivative of a general degree k monomial, $\theta_{i_1} \cdots \theta_{i_k} \in \mathfrak{G}_n$ is then

$$\frac{\overrightarrow{\partial}}{\partial \theta_i} \theta_{i_1} \cdots \theta_{i_k} = \sum_{j=1}^{k} (-1)^{j-1} \delta_{i i_j} \theta_{i_1} \cdots \widehat{\theta}_{i_j} \cdots \theta_{i_k}, \tag{31}$$

where $\widehat{\theta}_{i_j}$ indicates that this Grassmann number is removed from the monomial; the right derivative of the same monomial basis element is:

$$\theta_{i_1} \cdots \theta_{i_k} \frac{\overleftarrow{\partial}}{\partial \theta_i} = \sum_{j=1}^{k} (-1)^{k-j} \delta_{i i_j} \theta_{i_1} \cdots \widehat{\theta}_{i_j} \cdots \theta_{i_k}. \tag{32}$$

Higher-order derivatives are defined by successive application of the differential operators ordered by proximity to the Grassmann function being differentiated.

B. Grassmann Integration

Integrals over Grassmann numbers have no geometric significance (as in real or complex analysis) and must be formally defined ([5]). Firstly, we want to introduce the Grassmann differentials $\{d\theta_1, \dots, d\theta_n\}$, which are g-numbers in themselves, and thereby satisfy the anti-commutation relations

$$\{d\theta_i, d\theta_j\} = \{\theta_i, d\theta_j\} = 0 \tag{33}$$

$\forall i, j = 1, \dots, n$.

In analogy with the case for integration over reals of $\int_{-\infty}^{\infty} f(x)\, dx = \int_{-\infty}^{\infty} f(x+a)\, dx$, the integral in Grassmann variables is postulated to be translationally invariant under a shift by another Grassmann number η ([6]):

$$\int f(\theta)\, d\theta = \int f(\theta + \eta)\, d\theta. \tag{34}$$

With $f(\theta) = \theta$, this translational invariance yields

$$\int \eta\, d\theta = 0. \tag{35}$$

In general, for a set of g-numbers $\{\theta_1, \dots \theta_n\}$ we postulate that

$$\int \theta_i\, d\theta_j = \delta_{ij}, \tag{36}$$

$\forall i, j = 1, \dots, n$.

Multiple integrals are understood to be iterated integrals. For example, the multiple integral of a monomial basis element is:

$$\int \theta_{i_1} \cdots \theta_{i_k} \prod_{j=1}^{n} d\theta_j = \epsilon(i_1, \dots, i_k), \tag{37}$$

where the Levi-Civita symbol in n dimensions $\epsilon(i_1, \dots, i_k)$, is the parity of the permutation $(i_1\, i_2 \dots i_k)$ of $(1\, 2 \dots n)$, if it is a permutation, and is zero otherwise.

Consider a change of variables for a single Grassmann variable, given by

$$\theta = a\,\eta + \zeta \tag{38}$$

where $a \in \mathbb{C}$ and ζ is a constant Grassmann number ([7]). By (36), the Grassmann integral yields:

$$1 = \int \theta\, d\theta = \int (a\eta + \zeta)\, d\theta = \int a\eta\, d\theta \tag{39}$$

$$\implies d\theta = \frac{1}{a} d\eta. \tag{40}$$

Now consider two sets of generators, $\{\theta_1, \dots, \theta_n\}$ and $\{\eta_1, \dots, \eta_n\}$, related by the change of variables $\theta_i = \sum_{j=1}^{n} \mathsf{A}_{i,j} \eta_j$, for an anti-symmetric matrix $\mathsf{A} = -\mathsf{A}^{\top}$. The products of all the Grassmann differentials (the integration measure) transforms as:

$$\prod_{i=1}^{n} d\eta_i = \prod_{i=1}^{n} \sum_{j_i=1}^{n} \mathsf{A}_{i,j_i} d\theta_{j_i} \tag{41}$$

$$= \sum_{j_1,\dots,j_n} \mathsf{A}_{1,j_1} \cdots \mathsf{A}_{n,j_n} \epsilon(j_1, \dots, j_n) \prod_{k=1}^{n} d\theta_k \tag{42}$$

$$= \det(\mathsf{A}) \prod_{k=1}^{n} d\theta_k, \tag{43}$$

which is the opposite of the change of variables case for real or complex numbers.

C. Gaussian Integrals

In the case of the Grassmann algebra $\mathfrak{G}_{2n}$, with generators $\{\theta_1, \ldots, \theta_n, \theta_1^\star, \ldots, \theta_n^\star\} = \{\theta, \theta^\star\}$, with the complex structure as established in the section on complex conjugation for Grassmann numbers, $2n$-dimensional multiple integrals are naturally defined iteratively as:

$$\int f(\theta^\star, \theta)\, \mathcal{D}\theta^\star \mathcal{D}\theta := \int f(\theta^\star, \theta) \prod_{i=1}^{n} d\theta_i^\star d\theta_i. \tag{44}$$

Following [1] and [7], let $\mathsf{U} \in \mathsf{U}(n)$, and consider the change of variables $\theta = \mathsf{U}\eta$ and $\theta^\star = \eta^\star \mathsf{U}^\dagger$. By repeatedly exploiting the sign rule for Grassmann differentials (33), then applying (43), followed by another round of exploiting the sign rule for differentials (33), the $2n$-dimensional integration measure transforms as

$$\begin{aligned}
\mathcal{D}\eta^\star \mathcal{D}\eta &= \prod_{i=1}^{n} d\eta_i^\star d\eta_i && (45)\\
&= d\eta_1^\star d\eta_1 \cdots d\eta_n^\star d\eta_n && (46)\\
&= -d\eta_1^\star d\eta_2^\star d\eta_1 d\eta_2 d\eta_3^\star d\eta_3 \cdots d\eta_n^\star d\eta_n && (47)\\
&= \cdots = (-1)^{\sum_{k=1}^{n-1} k} \prod_{i=1}^{n} d\eta_i^\star \prod_{j=1}^{n} d\eta_j && (48)\\
&= (-1)^{\sum_{k=1}^{n-1} k}\, \overline{\det(\mathsf{U})}\, \det(\mathsf{U}) \prod_{i=1}^{n} d\theta_i^\star \prod_{j=1}^{n} d\theta_j && (49)\\
&= (-1)^{\sum_{k=1}^{n-1} k + n - 1} d\theta_1^\star d\theta_1 \prod_{i=2}^{n} d\theta_i^\star \prod_{j=2}^{n} d\theta_j && (50)\\
&= \cdots = (-1)^{2\sum_{k=1}^{n-1} k} \prod_{i=1}^{n} d\theta_i^\star d\theta_i && (51)\\
&= \mathcal{D}\theta^\star \mathcal{D}\theta && (52)
\end{aligned}$$

wherein we used $|\det(\mathsf{U})| = 1$. Then the integral (44) can be seen to be invariant under a unitary change of variables:

$$\int f(\theta^\star, \theta)\, \mathcal{D}\theta^\star \mathcal{D}\theta = \int f(\eta^\star \mathsf{U}^\dagger, \mathsf{U}\eta)\, \mathcal{D}\eta^\star \mathcal{D}\eta. \tag{53}$$

Again, let A be an $n \times n$ anti-symmetric matrix. Then $\exists\, \mathsf{U} \in \mathsf{U}(n)$ which diagonalizes A, such that $\mathsf{U}^\dagger \mathsf{A} \mathsf{U} = \mathsf{\Lambda} = \mathrm{diag}(\lambda_1, \ldots, \lambda_n)$. Using the change of variables $\theta = \mathsf{U}\eta$ and $\theta^\star = \eta^\star \mathsf{U}^\dagger$ the following Gaussian integral transforms as:

$$\begin{aligned}
\int e^{-\theta^\star \mathsf{A}\, \theta}\, \mathcal{D}\theta^\star \mathcal{D}\theta &= \int \exp(-\eta^\star \mathsf{U}^\dagger \mathsf{A} \mathsf{U}\, \eta)\, \mathcal{D}\eta^\star \mathcal{D}\eta && (54)\\
&= \int \exp(-\eta^\star \mathsf{\Lambda}\, \eta)\, \mathcal{D}\eta^\star \mathcal{D}\eta && (55)\\
&= \prod_{i=1}^{n} \int \exp(-\eta_i^\star \lambda_i \eta_i)\, d\eta_i^\star d\eta_i && (56)\\
&= \prod_{i=1}^{n} \int (1 - \eta_i^\star \lambda_i \eta_i)\, d\eta_i^\star d\eta_i && (57)\\
&= \prod_{i=1}^{n} \lambda_i \int \eta_i \eta_i^\star\, d\eta_i^\star d\eta_i && (58)\\
&= \prod_{i=1}^{n} \lambda_i = \det(\mathsf{\Lambda}) = \det(\mathsf{A}), && (59)
\end{aligned}$$

wherein we exploited the fact that the exponential of a Grassmann function is $e^{f(\theta)} = 1 + f(\theta)$.

Comparatively, following [8], suppose A is a real $n \times n$ symmetric matrix. Then $\exists\, \mathsf{O} \in \mathsf{O}(n)$ which diagonalizes A, such that $\mathsf{O}^\top \mathsf{A} \mathsf{O} = \mathsf{\Lambda} = \mathrm{diag}(\lambda_1, \ldots, \lambda_n)$. Applying the change of variables $x = \mathsf{O}y$, with corresponding Jacobian determinat $|\det(\mathsf{O})| = 1$, we can see that the following Gaussian integral transforms as:

$$\begin{aligned}
\int_{-\infty}^{\infty} e^{-\frac{1}{2}x^\top \mathsf{A} x} \mathcal{D}x &= \int_{-\infty}^{\infty} e^{-\frac{1}{2}y^\top \mathsf{O}^\top \mathsf{A} \mathsf{O} y} \mathcal{D}y && (60)\\
&= \int_{-\infty}^{\infty} e^{-\frac{1}{2}y^\top \mathsf{\Lambda} y} \mathcal{D}y && (61)\\
&= \prod_{i=1}^{n} \int_{-\infty}^{\infty} e^{-\frac{1}{2}\lambda_i y_i^2} dy_i && (62)\\
&= \prod_{i=1}^{n} \sqrt{\frac{2\pi}{\lambda_i}} = \sqrt{\frac{(2\pi)^n}{\det(\mathsf{A})}}, && (63)
\end{aligned}$$

which is distinctly different from (59).

IV. FERMIONIC COHERENT STATES

A. Grassmann vectors and operators

In analogy to bosons, Grassmann vectors can be defined in a fermionic Hilbert space as linear combinations of basis vectors with g-number coefficients; these Grassmann vectors are fermionic coherent states, which are a useful tool for analyzing quantum systems that may consist of an infinite number of particles. Similarly, we can form Grassmann operators on the fermionic Hilbert space by taking linear combinations of products of fermion CAPs with g-number coefficients ([7]).

To facilitate these constructions, we note that g-numbers commute with boson CAPs, anti-commute with fermion CAPs, and naturally commute with the vacuum state $|0\rangle$ ([3]):

$$[\theta, \hat{a}_i] = \left[\theta, \hat{a}_i^\dagger\right] = 0, \tag{64}$$

$$\{\theta, \hat{c}_i\} = \left\{\theta, \hat{c}_i^\dagger\right\} = 0, \tag{65}$$

$$[\theta, |0\rangle] = [\theta, \langle 0|] = 0. \tag{66}$$

From (65), we see that a product of an even number of fermion CAPs (even operators) commute with g-numbers, while a product of an odd number of fermion CAPs (odd operators) anticommute with g-numbers.

B. Fermion Displacement Operator

The Weyl translation defined on the Grassmann algebra $\mathfrak{G}_{2n}$, with generators $\{\theta, \theta^\star\}$ is the unitary fermion displacement operator:

$$\hat{D}_f(\theta, \theta^\star) := \exp\left(\sum_{i=1}^{n} \left(\hat{c}_i^\dagger \theta_i - \theta_i^\star \hat{c}_i\right)\right) \tag{67}$$

$$= \prod_{i=1}^{n} \exp\left(\hat{c}_i^\dagger \theta_i - \theta_i^\star \hat{c}_i\right), \tag{68}$$

wherein each mode is associated with a particular g-number.

We can further reduce this operator form by noting that the square of each exponent is:

$$\left(\hat{c}_i^\dagger \theta_i - \theta_i^\star \hat{c}_i\right)^2 = -\hat{c}_i^\dagger \theta_i \theta_i^\star \hat{c}_i - \theta_i^\star \hat{c}_i \hat{c}_i^\dagger \theta_i \tag{69}$$

$$= \left(\hat{c}_i^\dagger \hat{c}_i - \hat{c}_i \hat{c}_i^\dagger\right) \theta_i^\star \theta_i \tag{70}$$

$$= \left(2\hat{c}_i^\dagger \hat{c}_i - 1\right) \theta_i^\star \theta_i. \tag{71}$$

Then, by expanding each exponential, we can write the displacement operator as

$$\hat{D}_f(\theta, \theta^\star) = \prod_{i=1}^{n} \left(1 + \hat{c}_i^\dagger \theta_i - \theta_i^\star \hat{c}_i + \left(\hat{c}_i^\dagger \hat{c}_i - \frac{1}{2}\right) \theta_i^\star \theta_i\right); \tag{72}$$

here the last term in this expansion form shows that the fermion displacement operator contains monomials up to order 2^{2n}. The Hermitian adjoint of the displacement operator is also given by

$$\hat{D}_f(\theta, \theta^\star)^\dagger = \exp\left(\sum_{i=1}^{n} \left(\theta_i^\star \hat{c}_i - \hat{c}_i^\dagger \theta_i\right)\right) \tag{73}$$

$$= \hat{D}_f(-\theta, -\theta^\star). \tag{74}$$

For an additional set of Grassmann numbers $\{\eta, \eta^\star\}$, we compute the commutator of the exponents of the displacement operators corresponding to the two sets of generators using (5) and (6):

$$\sum_{i,j=1}^{n} \left[\theta_i^\star \hat{c}_i - \hat{c}_i^\dagger \theta_i, \eta_j^\star \hat{c}_j - \hat{c}_j^\dagger \eta_j\right] = \sum_{i=1}^{n} \left(\eta_i^\star \theta_i - \theta_i^\star \eta_i\right) \tag{75}$$

Then we can use (23) to write the product of two Weyl translations, $\hat{D}_f(\theta, \theta^\star)\hat{D}_f(\eta, \eta^\star)$, as

$$\hat{D}_f(\theta + \eta, \theta^\star + \eta^\star) \exp\left(\frac{1}{2}\sum_{i=1}^{n} \left(\eta_i^\star \theta_i - \theta_i^\star \eta_i\right)\right). \tag{76}$$

In addition, the Baker-Campbell-Hausdorff result in (23) can be used to write the displacement operator in the form

$$\hat{D}_f(\theta, \theta^\star) = e^{\sum_i \hat{c}_i^\dagger \theta_i} e^{-\sum_i \theta_i^\star \hat{c}_i} e^{-\frac{1}{2}\sum_i \theta_i^\star \theta_i}. \tag{77}$$

While the exponential transformation law (25) can be applied to the fermion CAPs to obtain the following transformations ([3]):

$$\hat{D}_f(\theta, \theta^\star)^\dagger \, \hat{c}_i \, \hat{D}_f(\theta, \theta^\star) = \hat{c}_i + \theta_i, \tag{78}$$

$$\hat{D}_f(\theta, \theta^\star)^\dagger \, \hat{c}_i^\dagger \, \hat{D}_f(\theta, \theta^\star) = \hat{c}_i^\dagger + \theta_i^\star. \tag{79}$$

Similar to how the bosonic coherent states are produced by applying the Glauber displacement operator to the vacuum state, the fermionic coherent state is the following Grassmann vector:

$$|\theta, \theta^\star\rangle = \hat{D}_f(\theta, \theta^\star) \, |0\rangle \tag{80}$$

$$= \prod_{i=1}^{n} \left(1 + \hat{c}_i^\dagger \theta_i - \theta_i^\star \hat{c}_i + \left(\hat{c}_i^\dagger \hat{c}_i - \frac{1}{2}\right) \theta_i^\star \theta_i\right) |0\rangle \, . \tag{81}$$

This fermion coherent state can also be written as the product of coherent states for each mode:

$$|\theta, \theta^\star\rangle = \prod_{i=1}^{n} |\theta_i, \theta_i^\star\rangle \tag{82}$$

$$= \prod_{i=1}^{n} \exp\left(\hat{c}_i^\dagger \theta_i - \theta_i^\star \hat{c}_i\right) |0_i\rangle \tag{83}$$

where $|0_i\rangle$ are the vacuum states for each mode.

Similarly to the boson case, the fermion coherent states are eigenstates of the fermion annihilation operator

$$\hat{c}_i \, |\theta, \theta^\star\rangle = \theta_i \, |\theta, \theta^\star\rangle \, , \tag{84}$$

except here the eigenvalues are g-numbers as opposed to c-numbers.

V. DISCUSSION

The direct sum decomposition of the Grassmann algebra, exhibited by $\mathfrak{G} = \mathfrak{G}_E \oplus \mathfrak{G}_O$, is the quintessential property of super vector spaces. $\mathfrak{G}$ is said to be a super-algebra, because the even and odd elements in this super vector space satisfy the containment relations:

$$\mathfrak{G}_E\mathfrak{G}_E \subset \mathfrak{G}_E, \; \mathfrak{G}_E\mathfrak{G}_O \subset \mathfrak{G}_O, \tag{85}$$

$$\mathfrak{G}_O\mathfrak{G}_E \subset \mathfrak{G}_O, \; \mathfrak{G}_O\mathfrak{G}_O \subset \mathfrak{G}_E. \tag{86}$$

Moreover, $\mathfrak{G}$ is said to be super-commutative because its homogeneous elements satisfy a graded version of commutativity ((14) as reiterated here):

$$\theta^{\varepsilon}\theta^{\zeta} = (-1)^{|\varepsilon|\cdot|\zeta|}\theta^{\zeta}\theta^{\varepsilon}. \tag{87}$$

In quantum physics, a theory is said to possess supersymmetry if it enjoys a global symmetry which associates to each boson a superpartnered fermion, and vice versa ([9]). As such, superalgebras are a necessary component of any supersymmetric physical model.

The fermionic coherent states are utilized extensively to compute fermionic path integrals. Specifically, the resolution of the identity

$$\mathbb{I} = \int \mathcal{D}\theta^{\star}\mathcal{D}\theta \left|\theta, \theta^{\star}\right\rangle \left\langle\theta, \theta^{\star}\right|, \tag{88}$$

can be inserted repeatedly between exponentials in the evolution operator kernel, in a manner similar to how the Feynman phase space path integrals are computed using the resolutions of the identity in phase space ([5]):

$$\mathbb{I} = \int_{-\infty}^{\infty} dx \left|x\right\rangle \left\langle x\right|, \tag{89}$$

$$\mathbb{I} = \int_{-\infty}^{\infty} \frac{dp}{2\pi\hbar} \left|p\right\rangle \left\langle p\right|. \tag{90}$$

Furthermore, there are many green's functions and generating functions found in many-body theory that are computed from partition functions of similar form to the Gaussian integral considered here in (59).

[1] M. Combescure and D. Robert, *Coherent States and Applications in Mathematical Physics.* Theoretical and Mathematical Physics. Springer Netherlands, 2012.

[2] Y. Nazarov and J. Danon, *Advanced Quantum Mechanics: A Practical Guide.* Advanced Quantum Mechanics: A Practical Guide. Cambridge University Press, 2013.

[3] B. Dalton, J. Jeffers, and S. Barnett, *Phase Space Methods for Degenerate Quantum Gases.* International series of monographs on physics. Oxford University Press, 2015.

[4] L. Prokhorov and S. Shabanov, *Hamiltonian Mechanics of Gauge Systems.* Cambridge Monographs on Mathematical Physics. Cambridge University Press, 2011.

[5] R. Shankar, *Quantum Field Theory and Condensed Matter: An Introduction.* Cambridge University Press, 2017.

[6] F. Wegner, *Supermathematics and its Applications in Statistical Physics: Grassmann Variables and the Method of Supersymmetry.* Lecture Notes in Physics. Springer Berlin Heidelberg, 2016.

[7] B. Baaquie, *Path Integrals and Hamiltonians: Principles and Methods.* Cambridge University Press, 2014.

[8] J. Zinn-Justin, *Path Integrals in Quantum Mechanics.* Oxford Graduate Texts. OUP Oxford, 2010.

[9] A. Rogers, *Supermanifolds: Theory and Applications.* World Scientific Publishing Company Pte Limited, 2007.

Harmonic oscillator by Path integral

NGUYEN Huu Nha

(Dated: June 18, 2019)

Harmonic oscillator is a very fundamental and important system in Quantum Mechanics. In this paper, I will consider this system by a non-conventional method, the Path Integral, which was invented by Feynman. The propagator of the harmonic oscillator calculated by Path Integral will then be used to derive the energies and the wavefunctions of the harmonic oscillator. Finally, the close relation between the Path Integral and Statistical Mechanics will be considered by deriving the partition function of a system of harmonic oscillators by the Path Integral method.

I. DEFINITION OF THE EVOLUTION OPERATOR AND THE PROPAGATOR

The main purpose of quantum mechanics is to solve the Schrödinger equation [1]:

$$i\hbar\frac{d}{dt}\,|\Psi(t)\rangle = \hat{H}\,|\Psi(t)\rangle \tag{1}$$

The time evolution operator is used to find the wave function at any later time if we know the wave function at previous time, it is defined by

$$|\Psi(t)\rangle = U(t,t_0)\,|\Psi(t_0)\rangle \tag{2}$$

Substituting the time-dependent wave function into the Schrödinger equation (1), we can find the operator equation for evolution operator:

$$\begin{aligned} i\hbar\frac{d}{dt}U(t,t_0)\,|\Psi(t_0)\rangle &= \hat{H}U(t,t_0)\,|\Psi(t_0) \\ i\hbar\frac{d}{dt}U(t,t_0) &= \hat{H}U(t,t_0) \end{aligned} \tag{3}$$

If the Hamiltonian of the system $\hat{H}$ does not depend on time, the solution of Eq.(3) is quite simple

$$U(t,t_0) = \exp\left\{-\frac{i}{\hbar}\hat{H}(t-t_0)\right\} \tag{4}$$

We often choose $t_0 = 0$, so the common formula for the evolution operator is:

$$U(t,0) = \exp\left(-\frac{i}{\hbar}\hat{H}t\right) \tag{5}$$

From now on, we only consider the time-independent Hamiltonian, so we use Eq. (5) in the whole paper. We also consider only one dimentional problems. The general case for three dimensions can be readily generalized.

By using the eigenstates $|\varphi_n\rangle$ and the eigenvalues E_n of the Hamiltonian $\hat{H}$ as the basis, we can expand the evolution operator in terms of $|\varphi_n\rangle$ by using the completeness relation $\sum_n |\varphi_n\rangle\langle\varphi_n| = \mathbf{1}$:

$$\begin{aligned} U(t,0) &= \exp\left(-\frac{i}{\hbar}\hat{H}t\right)\sum_n |\varphi_n\rangle\langle\varphi_n| \\ &= \sum_n \exp\left(-\frac{i}{\hbar}E_n t\right)\,|\varphi_n\rangle\langle\varphi_n| \end{aligned} \tag{6}$$

We can also write Eq.(2) in the configuration space by inserting the completeness relation $\int |x'\rangle\langle x'|\,dx' = 1$,

$$\begin{aligned} \langle x \mid \Psi(t)\rangle &= \int \langle x \mid U(t,0) \mid x'\rangle\langle x' \mid \Psi(0)\rangle\,dx' \\ \Psi(x,t) &= \int K(x,t;x',0)\,\Psi(x',0)dx' \end{aligned} \tag{7}$$

Here the matrix element of the evolution operator in the configuration space is called the propagator and is used to find the wave function at any time by the integral in Eq. (7)

$$\begin{aligned} K(x,t;x',0) &= \langle x \mid U(t,0) \mid x'\rangle \\ &= \langle x|\exp\left(-\frac{i}{\hbar}\hat{H}t\right)|x'\rangle \end{aligned} \tag{8}$$

We only use the propagator for $t > 0$, so we can put $K = 0$ for $t < 0$. The precise definition for K is:

$$\begin{aligned} K(x,t;x',0) &= \theta(t)\,\langle x \mid U(t,0) \mid x'\rangle \\ &= \theta(t)\,\langle x|\exp\left(-\frac{i}{\hbar}\hat{H}t\right)|x'\rangle \end{aligned} \tag{9}$$

Where $\theta(t)$ is the Heaviside function (or step function). Note that if $t \to 0^+$, we have

$$\lim_{t\to 0+} K(x,t;x',0) \ = \langle x \mid x'\rangle = \delta(x-x') \tag{10}$$

Expanding the propagator in terms the eigenstates of $\hat{H}$, we have:

$$\begin{aligned} &K(x,t;x',0) \\ &= \theta(t)\,\langle x|\exp\left(-\frac{i}{\hbar}\hat{H}t\right)\left(\sum_n |\varphi_n\rangle\langle\varphi_n|\right)|x'\rangle \\ &= \theta(t)\sum_n \exp\left(-\frac{i}{\hbar}E_n t\right)\varphi_n^*(x')\,\varphi_n(x) \end{aligned} \tag{11}$$

The equation for the propagator K can be found by taking the derivative of Eq. (9),

$$\begin{aligned} &i\hbar\frac{\partial}{\partial t}K(x,t,x',0) \\ &= i\hbar\,\langle x|\,U(t,0)\,|x'\rangle\,\frac{d}{dt}\theta(t) + i\hbar\theta(t)\,\langle x|\,\frac{d}{dt}U(t,0)\,|x'\rangle \\ &= i\hbar\,\langle x|\,U(t,0)\,|x'\rangle\,\delta(t) + \theta(t)\,\langle x|\,\hat{H}(\hat{x},\hat{p})U(t,0)\,|x'\rangle \\ &= i\hbar\delta(x-x')\delta(t) + \hat{H}\left(x,\frac{\hbar}{i}\frac{\partial}{\partial x}\right)K(x,t,x',0) \end{aligned}$$

$$\left[i\hbar\frac{\partial}{\partial t}-\hat{H}\right]K\left(x,t;x',0\right)=i\hbar\delta\left(t\right)\delta(x-x') \tag{12}$$

According to the Green method to solve differential equations, $K(x,t;x',0)$ is the retarded Green's function. Remember the condition for $t<0$

$$K\left(x,t;x',0\right)=0 \text{ if } t<0 \tag{13}$$

II. INTRODUCTION TO PATH INTEGRAL FORMALISM

Now we need to find the path integral form of the propagator to see a relationship with Lagrangian mechanics. In time-space coordinates, between two points $(x',0)$ and (x,t), we divide the time interval $[0,t]$ into N uniform segments of size $\varepsilon=\frac{t}{N}$:

$$t_0=0,\ t_n=n\varepsilon,\ t_N=t \tag{14}$$

and for each instant t_n, a position x_n in space:

$$x_0=x',\ x_N=x \tag{15}$$

We will use the case when $N\to\infty$, and as a consequence $\varepsilon\to 0$. Using the evolution operator product of two consecutive intervals, we have:

$$U\left(t_3,t_1\right)=U\left(t_3,t_2\right)U\left(t_2,t_1\right) \tag{16}$$

Similarly, the evolution operator can be expressed as the product of N terms

$$U\left(t,0\right)=U\left(t,t_{N-1}\right)U\left(t_{N-1},t_{N-2}\right)\dots U(t_2,t_1)U(t_1,0) \tag{17}$$

Inserting each unity $\int\left|x_n\right\rangle\left\langle x_n\right|dx_n=1$ between two evolution operators of Eq. (17) and using Eq. (9), we have:

$$\begin{aligned}&K\left(x,t;x',0\right)=\left\langle x\mid U\left(t,0\right)\mid x'\right\rangle\\&=\int dx_{N-1}\int dx_{N-2}\cdots\int dx_1 K\left(x,t;x_{N-1},t_{N-1}\right)\\&K\left(x_{N-1},t_{N-1};x_{N-2},t_{N-2}\right)\dots K(x_1,t_1;x',0)\end{aligned} \tag{18}$$

We always consider the case $t>0$, so we do not need to use the Heaviside function in the formula.

We can now calculate a propagator as an example:[2]

$$\begin{aligned}&K\left(x_n,t_n;x_{n-1},t_{n-1}\right)=\left\langle x_n\,\middle|\,\exp\left(-\frac{i\varepsilon}{\hbar}\hat{H}\right)\,\middle|\,x_{n-1}\right\rangle\\&=\left\langle x_n\,\middle|\,\exp\left(-\frac{i\varepsilon}{\hbar}\left(\frac{\hat{p}^2}{2m}+V\left(\hat{x}\right)\right)\right)\,\middle|\,x_{n-1}\right\rangle\\&\approx\left\langle x_n\,\middle|\,\exp\left(-\frac{i\varepsilon}{\hbar}\frac{\hat{p}^2}{2m}\right)\exp\left(-\frac{i\varepsilon}{\hbar}V\left(\hat{x}\right)\right)\,\middle|\,x_{n-1}\right\rangle\\&=\left\langle x_n\,\middle|\,\exp\left(-\frac{i\varepsilon}{\hbar}\frac{\hat{p}^2}{2m}\right)\,\middle|\,x_{n-1}\right\rangle\exp\left(-\frac{i\varepsilon}{\hbar}V\left(x_{n-1}\right)\right)\end{aligned} \tag{19}$$

where we have omitted the terms in higher orders of ε in the expansion $e^Ae^B=e^{(A+B)+1/2[A,B]+\cdots}$.

By inserting the unity of momentum states into the kinetic term, we have

$$\begin{aligned}&\left\langle x_n\,\middle|\,\exp\left(-\frac{i\varepsilon}{\hbar}\frac{\hat{p}^2}{2m}\right)\,\middle|\,x_{n-1}\right\rangle\\&=\left\langle x_n\,\middle|\,\exp\left(-\frac{i\varepsilon}{\hbar}\frac{\hat{p}^2}{2m}\right)\int_{-\infty}^{\infty}dp\left|p\right\rangle\left\langle p\right|\,\middle|\,x_{n-1}\right\rangle\\&=\int_{-\infty}^{\infty}\exp\left(-\frac{i\varepsilon}{\hbar}\frac{p^2}{2m}\right)\left\langle x_n\mid p\right\rangle\left\langle p\mid x_{n-1}\right\rangle dp\end{aligned} \tag{20}$$

Using the eigenstates of momentum in x-space:

$$\left\langle x\mid p\right\rangle=\frac{1}{\sqrt{2\pi\hbar}}e^{ipx/\hbar} \tag{21}$$

we have

$$\begin{aligned}&\left\langle x_n\,\middle|\,\exp\left(-\frac{i\varepsilon}{\hbar}\frac{\hat{p}^2}{2m}\right)\,\middle|\,x_{n-1}\right\rangle\\&=\frac{1}{2\pi\hbar}\int_{-\infty}^{\infty}\exp\left(-\frac{i\varepsilon}{\hbar}\frac{p^2}{2m}\right)e^{ipx_n/\hbar}\,e^{-ipx_{n-1}/\hbar}\,dp\\&=\frac{1}{2\pi\hbar}\int_{-\infty}^{\infty}\exp\left[-\frac{i\varepsilon}{2m\hbar}p^2+\frac{i}{\hbar}\left(x_n-x_{n-1}\right)p\right]dp\end{aligned} \tag{22}$$

Using the Gaussian integral: $\int_{-\infty}^{\infty}e^{-ax^2+bx}dx=\sqrt{\frac{\pi}{a}}e^{\frac{b^2}{4a}}$

$$\begin{aligned}&\left\langle x_n\,\middle|\,\exp\left(-\frac{i\varepsilon}{\hbar}\frac{\hat{p}^2}{2m}\right)\,\middle|\,x_{n-1}\right\rangle\\&=\left(\frac{m}{2\pi i\hbar\varepsilon}\right)^{1/2}\exp\left[\frac{im(x_n-x_{n-1})^2}{2\hbar\varepsilon}\right]\end{aligned} \tag{23}$$

We have the explicit formula for a propagator:

$$\begin{aligned}&K\left(x_n,t_n;x_{n-1},t_{n-1}\right)=\left(\frac{m}{2\pi i\hbar\varepsilon}\right)^{1/2}\\&\exp\left[\frac{im(x_n-x_{n-1})^2}{2\hbar\varepsilon}\right]\exp\left(-\frac{i\varepsilon}{\hbar}V\left(x_{n-1}\right)\right)\end{aligned} \tag{24}$$

Substituting this result into Eq. (18) we have the whole propagator:

$$\begin{aligned}K\left(x,t;x',0\right)=\left(\frac{m}{2\pi i\hbar\varepsilon}\right)^{1/2}\int\prod_{n=1}^{N-1}\left(\frac{m}{2\pi i\hbar\varepsilon}\right)^{1/2}dx_n\\\exp\sum_{n=1}^{N}\left[\frac{im(x_n-x_{n-1})^2}{2\hbar\varepsilon}-\frac{i\varepsilon}{\hbar}V\left(x_{n-1}\right)\right]\end{aligned} \tag{25}$$

The integrand can be written as follows

$$\begin{aligned}&\exp\sum_{n=1}^{N}\left[\frac{im(x_n-x_{n-1})^2}{2\hbar\varepsilon}-\frac{i\varepsilon}{\hbar}V\left(x_{n-1}\right)\right]\\&=\exp\left\{\frac{i}{\hbar}\sum_{n=1}^{N}\left[\frac{1}{2}m\left(\frac{x_n-x_{n-1}}{\varepsilon}\right)^2-V(x_{n-1})\right]\varepsilon\right\}\end{aligned} \tag{26}$$

If $N \to \infty$, then $\varepsilon \to 0$ and we can write the infinite sum as the integral

$$\begin{aligned}&\sum_{n=1}^{N}\left[\frac{1}{2}m\left(\frac{x_n - x_{n-1}}{\varepsilon}\right)^2 - V\left(x_{n-1}\right)\right]\varepsilon \\ &= \int_0^t \left(\frac{1}{2}mv^2 - V\left(x\right)\right)d\tau = \int_0^t L\left(x, \dot{x}\right)d\tau = S\end{aligned} \tag{27}$$

S is the action of Lagrangian mechanics and Eq. (26) is the discretized version of $e^{iS/\hbar}$, using the compact notation specific for path integral

$$\int \mathfrak{D}x = \lim_{N\to\infty}\left(\frac{m}{2\pi i\hbar\varepsilon}\right)^{1/2}\int\prod_{n=1}^{N-1}\left(\frac{m}{2\pi i\hbar\varepsilon}\right)^{1/2}dx_n \tag{28}$$

The propagator has the symbolized formula

$$\begin{aligned}K\left(x,t;x',0\right) &= \int \mathfrak{D}x e^{iS/\hbar} \\ &= \int_{x'}^{x}\mathfrak{D}[x\left(\tau\right)]\exp\left[\frac{i}{\hbar}\int_0^t L\left(x,\dot{x}\right)d\tau\right]\end{aligned} \tag{29}$$

III. THE PROPAGATOR OF HARMONIC OSCILLATOR BY PATH INTEGRAL

First we consider the potential which is a quadratic polynomial in x

$$V\left(x\right) = ax^2 + bx + c \tag{30}$$

For each path, we change to the coordinate y by using the classical path:

$$x\left(\tau\right) = x_{cl}\left(\tau\right) + y(\tau) \tag{31}$$

where x_{cl} is the solution of the Euler-Lagrange equation:

$$\frac{d}{d\tau}\frac{\partial L}{\partial \dot{x}} - \frac{\partial L}{\partial x} = 0 \tag{32}$$

All paths are fixed at two end points, so $y\left(0\right) = y\left(t\right) = 0$. At each intermediate time $\tau = t_n$

$$x_n = x\left(t_n\right) = x_{cl}\left(t_n\right) + y\left(t_n\right) = x_{cl}\left(t_n\right) + y_n \tag{33}$$

The classical path is fixed for each potential, so

$$dx_n = dy_n$$

and

$$\int_{x'}^{x}\mathfrak{D}[x\left(\tau\right)] = \int_0^0 \mathfrak{D}[y\left(\tau\right)] \tag{34}$$

and the propagator is:

$$K\left(x,t;x',0\right) = \int_0^0 \mathfrak{D}y(\tau)\exp\left\{\frac{i}{\hbar}S\left[x_{cl}\left(\tau\right) + y\left(\tau\right)\right]\right\} \tag{35}$$

Expand the action S about x_{cl}:

$$\begin{aligned}S\left[x_{cl}+y\right] &= \int_0^t L\left(x,\dot{x}\right)d\tau \\ &= \int_0^t \Bigg[L\left(x_{cl},\dot{x}_{cl}\right) + \left(\left.\frac{\partial L}{\partial x}\right|_{x_{cl}} y + \left.\frac{\partial L}{\partial \dot{x}}\right|_{x_{cl}}\dot{y}\right) \\ &+ \frac{1}{2}\left(\left.\frac{\partial^2 L}{\partial x^2}\right|_{x_{cl}} y^2 + 2\left.\frac{\partial^2 L}{\partial x \partial \dot{x}}\right|_{x_{cl}} y\dot{y} + \left.\frac{\partial^2 L}{\partial \dot{x}^2}\right|_{x_{cl}}\dot{y}^2\right)\Bigg]d\tau\end{aligned} \tag{36}$$

where

$$L = \frac{1}{2}m\dot{x}^2 - \left(ax^2 + bx + c\right) \tag{37}$$

The linear terms in y and $\dot{y}$ vanish by using integration by parts and the Euler equation for x_{cl}. The terms left are:

$$\begin{aligned}S\left[x_{cl}+y\right] &= \int_0^t \left[L\left(x_{cl},\dot{x}_{cl}\right) + \frac{1}{2}\left(-2ay^2 + m\dot{y}^2\right)\right]d\tau \\ &= \int_0^t L\left(x_{cl},\dot{x}_{cl}\right)d\tau + \int_0^t\left(\frac{1}{2}m\dot{y}^2 - ay^2\right)d\tau \\ &= S_{cl} + \int_0^t\left(\frac{1}{2}m\dot{y}^2 - ay^2\right)d\tau\end{aligned} \tag{38}$$

The propagator is then

$$\begin{aligned}&K\left(x,t;x',0\right) \\ &= \exp\left(\frac{iS_{cl}}{\hbar}\right)\int_0^0 \mathfrak{D}y(\tau)\exp\left\{\frac{i}{\hbar}\int_0^t\left(\frac{1}{2}m\dot{y}^2 - ay^2\right)d\tau\right\} \\ &= \exp\left(\frac{iS_{cl}}{\hbar}\right)A(a,t)\end{aligned} \tag{39}$$

where $A(a,t)$ is an unknown function of time t and the coefficient a of x^2 in the potential.

Now we apply the formalism for the free-particle propagator. The classical action can be found easily by solving the Euler-Lagrange equation:

$$L = \frac{1}{2}m\dot{x}^2 \to \frac{\partial L}{\partial \dot{x}} = m\dot{x} = \text{const} \to \dot{x}_{cl} = \text{const} \tag{40}$$

The classical path is a straight line passing through two end points $(x',0)$ and (x,t)

$$x_{cl}\left(\tau\right) = x' + \frac{x-x'}{t}\tau \to \dot{x}_{cl} = \frac{x-x'}{t}$$

$$S_{cl} = \int_0^t L\left(\dot{x}_{cl}\right)d\tau = \int_0^t \frac{1}{2}m\dot{x}_{cl}^2 d\tau = \frac{1}{2}m\frac{\left(x-x'\right)^2}{t} \tag{41}$$

$$K\left(x,t;x',0\right) = A\left(t\right)\exp\left[\frac{im(x-x')^2}{2\hbar t}\right] \tag{42}$$

To find $A(t)$, we use the limit (10) of the propagator and the gaussian representation of the delta function

$$\delta\left(x-x'\right)=\lim_{\Delta\to 0}\frac{1}{\left(\pi\Delta^2\right)^{\frac{1}{2}}}\exp\left[-\frac{\left(x-x'\right)^2}{\Delta^2}\right] \tag{43}$$

So $A(t)$ must be

$$A\left(t\right)=\left[\frac{m}{2\pi i\hbar t}\right]^{1/2} \tag{44}$$

The propagator for free particle is:

$$K_0\left(x,t;x',0\right)=\left[\frac{m}{2\pi i\hbar t}\right]^{1/2}\exp\left[\frac{im(x-x')^2}{2\hbar t}\right] \tag{45}$$

For the harmonic oscillator problem, the potential is

$$V=\frac{1}{2}m\omega^2x^2 \tag{46}$$

and the motion equation is

$$\begin{aligned}&\ddot{x}_{cl}+\omega^2x_{cl}=0\\ &\to\begin{cases}x_{cl}\left(\tau\right)=A\cos\left(\omega\tau\right)\ +B\sin\left(\omega\tau\right)\\ \dot{x}_{cl}\left(\tau\right)=-\omega A\sin\left(\omega\tau\right)\ +\omega B\cos\left(\omega\tau\right)\end{cases}\end{aligned} \tag{47}$$

The boundary conditions are

$$\begin{aligned}&\begin{cases}x_{cl}\left(0\right)=x'\\ x_{cl}\left(t\right)=x\end{cases}\to\begin{cases}A=x'\\ A\cos(\omega t)\ +B\sin(\omega t)\ =x\end{cases}\\ &\to\begin{cases}A=x'\\ B=\frac{x-x'\cos(\omega t)}{\sin(\omega t)}\end{cases}\end{aligned} \tag{48}$$

The classical action can be found by integration by parts as

$$\begin{aligned}S_{cl}&=\int_0^t\left(\frac{1}{2}m\dot{x}_{cl}^2-\frac{1}{2}m\omega^2x_{cl}^2\right)d\tau\\ &=\frac{1}{2}m\dot{x}_{cl}x_{cl}\Big|_0^t\\ &=\frac{m\omega}{2\sin\omega t}\left[\left(x^2+x'^2\right)\cos\omega t\ -2xx'\right]\end{aligned} \tag{49}$$

The propagator for the harmonic oscillator is:

$$\begin{aligned}&K_\omega\left(x,t;x',0\right)=\exp\left(\frac{iS_{cl}}{\hbar}\right)\ A\left(\omega,t\right)\\ &=A\left(\omega,t\right)\exp\left\{\frac{im\omega}{2\hbar\sin\omega t}\left[\left(x^2+x'^2\right)\cos\ \omega t\ \ -2xx'\right]\right\}\end{aligned} \tag{50}$$

where $A\left(\omega,t\right)$ is determined by

$$A\left(\omega,t\right)=\int_0^0\mathfrak{D}y(\tau)\exp\left\{\frac{i}{\hbar}\int_0^t\left(\frac{1}{2}m\dot{y}^2-ay^2\right)d\tau\right\} \tag{51}$$

We can find $A\left(\omega,t\right)$ by Fourier series as in Feynman's classics [3]. The exact formula is

$$A\left(\omega,t\right)=\left[\frac{m\omega}{2\pi i\hbar\sin\omega t}\right]^{1/2} \tag{52}$$

and the full propagator for harmonic oscillator is

$$\begin{aligned}&K_\omega\left(x,t;x',0\right)=\left[\frac{m\omega}{2\pi i\hbar\sin\omega t}\right]^{1/2}\\ &\exp\left\{\frac{im\omega}{2\hbar\sin\omega t}\left[\left(x^2+x'^2\right)\cos\omega t\ \ -2xx'\right]\right\}\end{aligned} \tag{53}$$

If we take the limit of $K_\omega\left(x,t;x',0\right)$ when ω approaches ∞, we must have the free particle propagator

$$\begin{aligned}&\lim_{\omega\to\infty}K_\omega\left(x,t;x',0\right)\\ &=\left[\frac{m}{2\pi i\hbar t}\right]^{1/2}\exp\left\{\frac{im}{2\hbar t}\left[\left(x^2+x'^2\right)-2xx'\right]\right\}\\ &=K_0\left(x,t;x',0\right)\end{aligned} \tag{54}$$

IV. DERIVATION OF THE QUANTIZED ENERGIES AND THE WAVEFUNCTIONS OF THE HARMONIC OSCILLATOR

From Eq. (11) we know that the propagator can be expanded in terms of the eigenvalues and eigenstates of the harmonic oscillator

$$K_\omega\left(x,t;x',0\right)=\sum_n\exp\left(-\frac{i}{\hbar}E_nt\right)\ \varphi_n^*\left(x'\right)\varphi_n(x) \tag{55}$$

Setting $x=x'=0$ in Eq. (53), we have

$$\begin{aligned}K_\omega\left(0,t;0,0\right)&=\left(\frac{m\omega}{2\pi i\hbar\sin\omega t}\right)^{\frac{1}{2}}\\ &=\sum_n\exp\left(-\frac{i}{\hbar}E_nt\right)\ \left|\varphi_n\left(0\right)\right|^2\end{aligned} \tag{56}$$

Because the harmonic potential is symmetric, the wave functions are odd and even alternatively and the odd wave functions at the origin are zero ($\left|\varphi_{\text{odd}}\left(0\right)\right|^2=0$). So if we expand this propagator in Taylor series of $e^{-i\omega t}$, we only get the even eigenvalues. Rewriting the closed form of $K_\omega\left(0,t;0,0\right)$ and expanding in Taylor series of $e^{-i\omega t}$ by using

$$\left(\frac{1}{x}-x\right)^{-\frac{1}{2}}=x^{1/2}+\frac{x^{5/2}}{2}+\frac{3x^{9/2}}{8}+\frac{5x^{13/2}}{16}+\frac{35x^{17/2}}{128}+\ldots$$

we get

$$\begin{aligned}&K_\omega\left(0,t;0,0\right)=\left(\frac{m\omega}{\pi\hbar}\right)^{1/2}\left(e^{i\omega t}-e^{-i\omega t}\right)^{-1/2}\\ &=\left(\frac{m\omega}{\pi\hbar}\right)^{\frac{1}{2}}\left[\left(e^{-i\omega t}\right)^{\frac{1}{2}}+\frac{1}{2}\left(e^{-i\omega t}\right)^{\frac{5}{2}}+\frac{3}{8}\left(e^{-i\omega t}\right)^{\frac{9}{2}}+\ldots\right]\\ &=\left(\frac{m\omega}{\pi\hbar}\right)^{\frac{1}{2}}\left[e^{-i\left(\frac{\hbar\omega}{2}\right)\frac{t}{\hbar}}+\frac{1}{2}e^{-i\left(\frac{5\hbar\omega}{2}\right)\frac{t}{\hbar}}+\frac{3}{8}e^{-i\left(\frac{9\hbar\omega}{2}\right)\frac{t}{\hbar}}+\ldots\right]\end{aligned} \tag{57}$$

We can see clearly that the exponentials correspond only to the even quantum numbers if the energy is written as:

$$E_n = \left(n + \frac{1}{2}\right)\hbar\omega \tag{58}$$

From the rhs of Eq. (57) we can know the values of squared modulus of the even wavefunctions at the origin in this series:

$$\begin{aligned}\sum_n \left|\varphi_n(0)\right|^2 e^{-iE_n t/\hbar} &= \left|\varphi_0(0)\right|^2 e^{-iE_0 t/\hbar} \\ &+ \left|\varphi_2(0)\right|^2 e^{-iE_2 t/\hbar} + \left|\varphi_4(0)\right|^2 e^{-iE_4 t/\hbar} + \dots\end{aligned} \tag{59}$$

We can also derive the eigenstates by setting $x = x'$ in Eq. (53), we have

$$\begin{aligned}&K_\omega(x,t;x,0) \\ &= \left(\frac{m\omega}{2\pi i\hbar\sin\omega t}\right)^{\frac{1}{2}} \exp\left\{\frac{im\omega}{\hbar\sin\omega t}\left(x^2\cos\omega t - x^2\right)\right\} \\ &= \sum_n \left|\varphi_n(x)\right|^2 e^{-iE_n t/\hbar}\end{aligned} \tag{60}$$

We see in this case that all the wavefunctions contribute to the series in the rhs.

Rewrite the lhs in function of $e^{-i\omega t}$, we have

$$\begin{aligned}\text{lhs} &= \left(\frac{m\omega}{2\pi i\hbar\sin\omega t}\right)^{\frac{1}{2}} \exp\left[\frac{im\omega x^2}{\hbar\sin\omega t}\left(\cos\omega t - 1\right)\right] \\ &= \left(\frac{m\omega}{\pi\hbar\left(e^{i\omega t} - e^{-i\omega t}\right)}\right)^{\frac{1}{2}} \exp\left[-\frac{m\omega x^2}{\hbar}\frac{\left(e^{i\omega t} + e^{-i\omega t} - 2\right)}{\left(e^{i\omega t} - e^{-i\omega t}\right)}\right]\end{aligned} \tag{61}$$

Using this Taylor series:

$$\begin{aligned}&\left(\frac{1}{x} - x\right)^{-1/2} \exp\left(\frac{a\left(\frac{1}{x} + x - 2\right)}{\frac{1}{x} - x}\right) \\ &\qquad = e^a x^{1/2} - 2(ae^a)x^{3/2} + \dots\end{aligned} \tag{62}$$

We can derive the eigenvalues and eigenstates of the harmonic oscillator:

$$\begin{aligned}&\left(\frac{m\omega}{\pi\hbar}\right)^{\frac{1}{2}}\left[e^{\frac{-m\omega x^2}{\hbar}} e^{-i\left(\frac{\hbar\omega}{2}\right)t/\hbar}\right. \\ &\left.+ \frac{2m\omega x^2}{\hbar} e^{\frac{-m\omega x^2}{\hbar}} e^{-i\left(\frac{3\hbar\omega}{2}\right)t/\hbar} + \dots\right] \\ &= \left|\varphi_0(x)\right|^2 e^{-iE_0 t/\hbar} + \left|\varphi_1(x)\right|^2 e^{-iE_1 t/\hbar} + \dots\end{aligned} \tag{63}$$

For example, we can have the explicit formulae for the first two levels:

$$\begin{aligned}E_0 &= \frac{\hbar\omega}{2}; \left|\varphi_0(x)\right|^2 = \left(\frac{m\omega}{\pi\hbar}\right)^{\frac{1}{2}} e^{-\frac{m\omega x^2}{\hbar}} \\ E_1 &= \frac{3\hbar\omega}{2}; \left|\varphi_1(x)\right|^2 = \left(\frac{m\omega}{\pi\hbar}\right)^{\frac{1}{2}} \frac{2m\omega x^2}{\hbar} e^{-\frac{m\omega x^2}{\hbar}}\end{aligned} \tag{64}$$

So the propagator is a kind of generating function for both the eigenvalues and the eigenstates.

V. AN EXAMPLE OF THE APPLICATION OF PATH INTEGRAL IN STATISTICAL MECHANICS

In statistical mechanics, we need to calculate the partition function defined as

$$Z = \sum_n e^{-\beta E_n} \tag{65}$$

where $\beta = 1/kT$, T is the temperature, k is Boltzmann constant, E_n is the eigenvalue of the nth eigenstate of the Hamiltonian. We can rewrite it as

$$Z = \sum_n \left\langle \varphi_n \mid e^{-\beta H} \mid \varphi_n \right\rangle = \mathrm{Tr}(e^{-\beta H}) \tag{66}$$

where we have used the eigenstates of Hamiltonian as the basis. We know that the trace is invariant under unitary transformation and we can use the position basis instead:

$$Z = \int_{-\infty}^{\infty} \left\langle x \mid e^{-\beta H} \mid x \right\rangle dx \tag{67}$$

By putting $t = -i\tau$ and $x = x'$ in Eq. (8)

$$K(x, -i\tau; x, 0) = \langle x| \exp\left(-\frac{1}{\hbar}\hat{H}\tau\right)|x\rangle \tag{68}$$

or $\tau = \beta\hbar$ to express Eq. (67) in terms of the propagator

$$Z = \int_{-\infty}^{\infty} K(x, t = -i\beta\hbar; x, 0)\, dx \tag{69}$$

From the propagator for the harmonic oscillator in Eq. (53) we can calculate the explicit formula for Z by the path integral method:

$$\begin{aligned}Z &= \int_{-\infty}^{\infty} K(x, -i\beta\hbar; x, 0)\, dx \\ &= \left(\frac{m\omega}{2\pi\hbar\sinh\omega\beta\hbar}\right)^{\frac{1}{2}} \\ &\int_{-\infty}^{\infty} \exp\left\{\frac{-m\omega}{\hbar\sinh\omega\beta\hbar}(\cosh\omega\beta\hbar - 1)x^2\right\} dx \\ &= \frac{1}{[2(\cosh\omega\beta\hbar - 1)]^{1/2}} = \frac{1}{2\sinh\frac{\omega\beta\hbar}{2}}\end{aligned} \tag{70}$$

We can compare this result with the one calculated directly by using Eq. (65) and the energies of the quantum harmonic oscillator $E_n = \left(n + \frac{1}{2}\right)\hbar\omega$

$$Z = \sum_{n=0}^{\infty} e^{-\beta\hbar\omega(n+1/2)} = \frac{e^{-\beta\hbar\omega/2}}{1 - e^{-\beta\hbar\omega}} = \frac{1}{2\sinh\frac{\omega\beta\hbar}{2}} \tag{71}$$

So we can calculate the partition function directly from the propagator even if we don't know the exact energies of the system.

ACKNOWLEDGMENTS

I would like to thank Professor Barton Zwiebach and his staff for three excellent series of lectures on Quantum mechanics on edx.org. I also would like to thank staff members and participants for the useful comments and suggestions to this paper.

[1] Cohen-Tannoudji, *Quantum mechanics.* Wiley, 1997.
[2] R. Shankar, *Principles of Quantum Mechanics.* Plenum, 1994.
[3] R. Feynman and A. Hibbs, *Quantum Mechanics and Path Integrals.* (amended by D. Styer), Dover, 2010.

Ideal Fermi Gas

Quoc Trung Ho
Theoretical Physics Department, National University in Ho Chi Minh City, Vietnam

In dealing with many-particle system, specifically when we are studying physical properties of metals where electrons play an important role, we will consider a simple model, in which all particle interactions are neglected. Despite the simplicity and a little "abuse" assumption of non-interacting system, however, the power of Ideal Fermi gas is to give us the first look into some general properties of metals, and also explain many experimental results that cannot be understood by using classical models. In this paper, after a short introduction to quantum gases which contains the general description of identical particles and second quantization formalism, we will investigate the Ideal Fermi Gas: the Fermi function, density of states, and related useful tools when dealing with non-interacting system. Finally, we will study about specific applications of the method by calculating the heat capacity and Pauli magnetic susceptibility of the electron gas in metals.

I. INTRODUCTION

In dealing with the system of many-particles, physicists have come up with a lot of ways to describe the physical properties of the system, especially its dynamics quantities. One of the most successful theories is the statistical formulation of mechanics, based on statistical methods, probability theory and the microscopic physical laws and telling us a lot of information about the thermodynamic behaviour of large systems. For example, from classical statistical mechanics, we can derive the Maxwell-Boltzmann distribution function:

$$f(E) = 2\left(\frac{E}{\pi}\right)^{1/2}\left(\frac{1}{k_BT}\right)^{3/2} e^{-\frac{E}{k_BT}} \tag{1}$$

which represents the distribution for the energy. The Maxwell-Boltzmann distribution gives us a very useful and accurate tool to calculate thermodynamics quantities at normal temperature and low density system, such as calculating the internal energy for ideal gas, or derive the equation of states $pV = \nu RT$. However, in the opposite conditions- low temperature and/or high enough densities, the quantum effects take place and lead us to a totally different picture, as we will see later with the model of ideal Fermi gas. Before we start, let us first consider the range of validity of classical gas: The partition function of a classical ideal gas is:

$$Z = \frac{Z_1^N}{N!}, \quad Z_1 = \frac{V}{\lambda_T^3} = V\left(\frac{2\pi m k_B T}{h^2}\right)^{3/2} \tag{2}$$

with the length scale $\lambda_T \equiv \frac{\hbar}{\sqrt{mk_BT}}$. We can also derive an approximation of the length scale in ideal gas by using the de Broglie wavelength: $\lambda_B \equiv \frac{h}{p}$. For classical ideal gas, the internal energy (which is also the total kinetics energy of all particles) is:

$$U = \left\langle \frac{\boldsymbol{p^2}}{2m} \right\rangle = \frac{3}{2}k_BT \Rightarrow p_{RMS} = \sqrt{3mk_BT}$$
$$\Rightarrow \lambda_T \approx \frac{h}{p_{RMS}} \approx \frac{h}{\sqrt{3mk_BT}} \tag{3}$$

It is reasonable that classical description of the system will fail if λ_T is much smaller than the typical spacing between particles. This means the validity of classical mechanics requires:

$$\lambda_T \ll \left(\frac{V}{N}\right)^3 \Rightarrow \frac{T}{n^{3/2}} \gg \frac{h^2}{mk_B} \tag{4}$$

with n is the number density of the particles. When this condition is violated, we have to replace the classical model by the one where quantum rules play the main roles.

Next, we will focus on the ideal quantum gases. Unlike the classical cases where each particles of our system has a specific trajectory that we can follow using Hamiltonian equation of motions; in subatomic world, the distinguishability no longer make sense, meaning interchange two arbitrary particles in our system will leave all of the physical descriptions invariant. If we have a wavefunction that describe N-particles state of the system, it is requires:

$$|\psi(\ldots x_i \ldots x_j \ldots)|^2 = |\psi(\ldots x_j \ldots x_i \ldots)|^2 \tag{5}$$

Swapping the two particles twice gives back the original states. This implies:

$$\psi(\ldots x_i \ldots x_j \ldots) = \pm\psi(\ldots x_j \ldots x_i \ldots) \tag{6}$$

As we see, there are two choices for the sign of the wavefunction. Each one is corresponding to a specific type of particles:

- **Bosons**:
  - Particles which have the symmetric wavefunction: $\psi(\ldots x_i \ldots x_j \ldots) = +\psi(\ldots x_j \ldots x_i \ldots)$
  - Bosons have integer spin (proved in quantum field theory, verified by experiments).
  - Corresponding statistics: Bose-Einstein distribution
- **Fermions**:

  - Particles which have the antisymmetric wavefunction: $\psi(\dots x_i \dots x_j \dots) = -\psi(\dots x_j \dots x_i \dots)$
  - Fermions have half-integer spin (proved in quantum field theory, verified by experiments).
  - Corresponding statistics: Fermi-Dirac distribution

These special symmetric properties of identical particles will lead us on our way to build a general form of wavefunction for the N-particle system, and finally the symmetry will be packed into the commutation relations of creation and annihilation operators in second-quantization formalism. From here to the rest of the paper, we will study a special case of quantum gas, which is ideal Fermi gas - a system of identical fermions where the interactions between those particles would be neglected.

II. THE FORMALISM OF SECOND QUANTIZATION

In quantum world, it is common to work with the system of identical particles; ones that have the same physical properties and are indistinguishable. To begin with, let us consider the one-particle Schrödinger equation, which is assumed to be solved:

$$\hat{H}^{(i)} |\lambda\rangle = \varepsilon_\lambda |\lambda\rangle \tag{7}$$

where λ is a complete set of quantum numbers, and the (i) superscript denotes the Hamiltonian for the ith particle. The **principle of indistinguishability** will then force the N-particle wavefunction to have the symmetry properties: Every interchange of two particles would left the wavefunction invariant up to a change in sign. These symmetrised N-particle wavefunction can be taken as:

$$\begin{aligned} |\boldsymbol{\lambda}\rangle^{(\pm)} &= \left|\lambda^{(1)}, \lambda^{(2)}, \dots, \lambda^{(N)}\right\rangle \\ &= \sum_{\mathcal{P}} \frac{(\pm 1)^{sgn(\mathcal{P})}}{\sqrt{N! \prod_\lambda (n_\lambda !)}} \mathcal{P}\left(\left|\lambda^{(1)}\right\rangle \otimes \dots \otimes \left|\lambda^{(N)}\right\rangle\right) \end{aligned} \tag{8}$$

with n_λ is the number of particles in state $|\lambda\rangle$, $\mathcal{P}$ denotes the permutation of N-tensor product state, and $sgn(\mathcal{P})$ is the sign of the permutation. From **spin-statistics theorem**, it is proved that:

$$\begin{cases} \textbf{Bosons} \rightarrow \text{interger spin} \rightarrow \text{symmetric states} \\ \textbf{Fermions} \rightarrow \text{half-integer spin} \rightarrow \text{antisymmetric states} \end{cases}$$

which has the form of wavefunction in (8) with "+" and "–" sign respectively. We define the **vacuum state** $|\mathbf{0}\rangle$ which contains no particles, and a set of **creation and annihilation** as follow:

$$\begin{cases} a_\lambda |\mathbf{0}\rangle = 0 \\ |\lambda_i\rangle = a^\dagger_{\lambda_i} |\mathbf{0}\rangle \\ |\lambda_i, \lambda_j\rangle = a^\dagger_{\lambda_i} a^\dagger_{\lambda_j} |\mathbf{0}\rangle, \dots \end{cases}$$

and we postulate the commutation relations between a and $a^\dagger$ as:

$$\left[a_{\lambda_i}, a^\dagger_{\lambda_j}\right]_\pm = \delta_{ij}, \quad \left[a_{\lambda_i}, a_{\lambda_j}\right]_\pm = \left[a^\dagger_{\lambda_i}, a^\dagger_{\lambda_j}\right]_\pm = 0 \tag{9}$$

where the plus sign is used for bosons, and the minus sign is for fermions. It is easy to see that all of the definitions and commutation relations of field operators a and $a^\dagger$ are similar to the harmonic oscillation case. It has similar interpretation: each excitation of energy will "create" one more particle at specific state, and we can reverse the process by using annihilation operator.

We define the number operator, which counts the number of particles in specific state λ:

$$\begin{aligned} n_\lambda |\boldsymbol{\lambda}\rangle = n_\lambda \left|\lambda^{(1)}, \dots, \lambda^{(N)}\right\rangle &= a^\dagger_\Lambda a_\lambda \frac{a^\dagger_{\lambda_1} \dots a^\dagger_{\lambda_N} |\mathbf{0}\rangle}{\sqrt{\prod_\lambda n_\lambda !}} \\ &= \sum_{i=1}^{N} \delta_{\lambda\lambda_i} \left|\lambda^{(1)}, \dots, \lambda^{(N)}\right\rangle \end{aligned} \tag{10}$$

We want to find the representation of the N-particles system in second quantization, which usually consist of one-particle part and two-particle part:

$$\hat{F}_N = \sum_{i=1}^{N} \hat{F}_1^{(1)} + \frac{1}{2} \sum_{i,j}^{i \neq j} F_2^{(i,j)} \tag{11}$$

First consider one-particle operator $\hat{F}_1$, which is diagonal in the basis $\{|\boldsymbol{\lambda}\rangle\}$, and by spectral theorem can be decomposed as: $\hat{F}_1 = \sum_\lambda f_\lambda |\lambda\rangle \langle\lambda|$. The matrix element of $\hat{F}_1$ in second quantization basis is:

$$\begin{aligned} \left\langle \boldsymbol{\lambda'} | \hat{F}_1 | \boldsymbol{\lambda} \right\rangle &= \left(\sum_{i=1}^{N} f_{\lambda_i}\right) \langle \boldsymbol{\lambda'} | \boldsymbol{\lambda} \rangle = \left(\sum_\lambda f_\lambda \delta_{\lambda\lambda_i}\right) \langle \boldsymbol{\lambda'} | \boldsymbol{\lambda} \rangle \\ &= \langle \boldsymbol{\lambda'} | \sum_\lambda f_\lambda n_\lambda | \boldsymbol{\lambda} \rangle \end{aligned} \tag{12}$$

Hence, in second quantization formalism: $F_1 = f_\lambda n_\lambda = f_\lambda a^\dagger_\lambda a_\lambda$. By transforming to general basis, we obtain the matrix representation of $\hat{F}_1$:

$$\begin{aligned} F_1 &= \sum_{\lambda\alpha\beta} \langle \alpha | \lambda \rangle f_\lambda a^\dagger_\alpha a_\beta \langle \lambda | \beta \rangle \\ &= \sum_{\alpha\beta} \langle \alpha | \hat{F}_1 | \beta \rangle a^\dagger_\alpha a_\beta \end{aligned} \tag{13}$$

Examples: The total spin operator In Schrödinger picture, the total spin operator is given by: $\mathbf{S} \equiv \frac{\hbar}{2} \boldsymbol{\sigma}$

In second quantization representation:

$$\hat{\mathbf{S}} = \sum_{\lambda\alpha\alpha'} \mathbf{S}_{\alpha\alpha'} \hat{a}^\dagger_{\lambda\alpha} \hat{a}_{\lambda\alpha'} \tag{14}$$

where $\alpha, \alpha' = \uparrow, \downarrow$ are the spin quantum number. Especially: $\hat{S}_z = \frac{1}{2}\sum_\lambda \left((S_z)_{\alpha\alpha'}\hat{a}^\dagger_{\lambda\alpha}\hat{a}_{\lambda\alpha'}\right) = \frac{\hbar}{2}\sum_\lambda(\hat{n}_{\lambda\uparrow}-\hat{n}_{\lambda\downarrow})$.

In a similar manner, we consider the 2-particles operator $\hat{F}_2$, which can be decomposed in its eigenbasis as: $\hat{F}_2 = \sum_{\lambda\lambda'} \langle\lambda| \langle\lambda'| f_{\lambda\lambda'} |\lambda\rangle |\lambda'\rangle$. We can think of the 2-particles operator as a combination of tensor products of two 1-particle operator, each can transform independently under the change of basis. This claim leads us to write down the second quantization representation of $\hat{F}_2$:

$$F_2 = f_{\lambda\lambda'} n_\lambda n_{\lambda'} \tag{15}$$

We continue to transform to a more general basis, in which F_2 takes the form:

$$F_2 = \sum_{\alpha\beta\mu\nu} \left(\hat{F}_2\right)^{\mu\nu}_{\alpha\beta} a^\dagger_\alpha a^\dagger_\beta a_\mu a_\nu,$$

$$\text{where } \left(\hat{F}_2\right)^{\mu\nu}_{\alpha\beta} = \langle\alpha| \langle\beta| \hat{F}_2 |\mu\rangle |\nu\rangle \tag{16}$$

III. IDEAL FERMI GAS & RELATED CONCEPTS

A. Density of states

Consider the fermions are contained in a box of the edge lengths L_x, L_y, L_z. Applying the boundary condition leads to the discretization of the wave vector $\boldsymbol{k}$:

$$k_{x,y,z} = \frac{(2\pi)^3}{L_x L_y L_z} n_{x,y,z}, \quad n_{x,y,z} \in \mathbb{Z}$$

$$\Rightarrow \Delta k = \Delta k_x \Delta k_y \Delta k_z = \frac{(2\pi)^3}{L_x L_y L_z} = \frac{(2\pi)^3}{V} \tag{17}$$

In the thermodynamic limit: $V \to \infty, N \to \infty, n \equiv V/N \to const$, the wave vectors are quasi-densely, which let us to replace the sum by an integral:

$$\sum_\lambda \cdots \to (2S+1)\frac{1}{\Delta k}\int d^3k \cdots \tag{18}$$

where the sum is defined over all eigenstates; since our Hamiltonian is spin-independent, we have to take into account the (2S + 1) spin-degenerate states with the same energy eigenvalue $\boldsymbol{k}$ but different m_s.

The density of states is defined as the number of states divided by the range of energy. More rigorously:

$$D(E)dE = \frac{2S+1}{\Delta k} \int\limits_{E \leq \varepsilon_{\boldsymbol{k}} \leq E+dE} d^3k \tag{19}$$

with $\varepsilon_{\boldsymbol{k}}$ is the one-particle energy. In non-interacting case, $\varepsilon_{\boldsymbol{k}}$ has the isotropic form: $\varepsilon_{\boldsymbol{k}} = \frac{\hbar^2 k^2}{2m} \Rightarrow k = \sqrt{\frac{2mE}{\hbar^2}}$. Together with the grid volume *Deltak*, we can rewrite $D(E)$ in the following form:

$$\begin{aligned} D(E) &= (2S+1)\frac{V}{(2\pi)^3}\frac{d}{dE}\int\limits_{\varepsilon_{\boldsymbol{k}} \leq E} d^3k \\ &= (2S+1)\frac{V}{(2\pi)^3}\frac{d}{dE}\frac{4\pi}{3}\left(\frac{2mE}{\hbar^2}\right)^{3/2} = \tau\sqrt{E} \\ \tau &= (2S+1)\frac{V}{4\pi^2}\left(\frac{2m}{\hbar^2}\right)^{3/2} \end{aligned} \tag{20}$$

We can further find a relation between coefficient τ and the number of fermions N: at 0K, all the fermions states lies inside the Fermi sphere:

$$\begin{aligned} N &= dE\int_{-\infty}^{\infty} D(E)f(E) = \int_0^{E_F} dE\tau\sqrt{E} = \frac{2}{3}\tau E_F^{3/2} \\ &\Rightarrow \tau = \frac{3N}{2E_F^{3/2}} \end{aligned} \tag{21}$$

B. Fermi function

The Fermi function provides the probability of occupancy of energy levels by Fermions - particles with half-integer spin particles, which obey the Pauli exclusion principle. The Fermi function is given by:

$$f(\varepsilon) = \frac{1}{e^{\frac{\varepsilon-\mu}{k_B T}} - 1} = \frac{1}{e^{\beta(\varepsilon-\mu)} - 1} \tag{22}$$

From the density of states which tells us about the density of the available energy states, and the Fermi function which gives the probability of occupation of fermions, the *density of the states which are occupied at the temperature T* is simply $D(E)f(E)$.
Let us consider the two limiting cases:

- Classical limit: $\varepsilon \geq k_B T \Rightarrow \beta(\varepsilon-\mu) \geq 1$: The fermions occupy the states with energy much higher than the sum of Fermi energy and the thermal kinetic energy. The Fermi function will tend to the Maxwell-Boltzmann distribution function:

  $$f(\varepsilon) \propto e^{-\beta(\varepsilon-\mu)} \tag{23}$$

- Degenerate Fermi gas: $\varepsilon \leq k_B T \Rightarrow \beta(\varepsilon-\mu) \leq 1$:

  $$f(\varepsilon) \propto \Theta\mu(T) - \varepsilon \approx \Theta(E_F - \varepsilon) \tag{24}$$

  where E_F is the Fermi energy, defined as the limitation: $E_F \equiv \lim_{T\to 0}\mu(T)$ In this degenerate case, the derivative of Fermi function is:

$$f'(\varepsilon) = \frac{-\beta e^{\beta(\varepsilon-\mu)}}{(e^{\beta(\varepsilon-\mu)}+1)^2} = \frac{-\beta/4}{\cosh\left(\frac{\beta}{2}(\varepsilon-\mu)\right)^2} \to \frac{-\beta}{4} \tag{25}$$

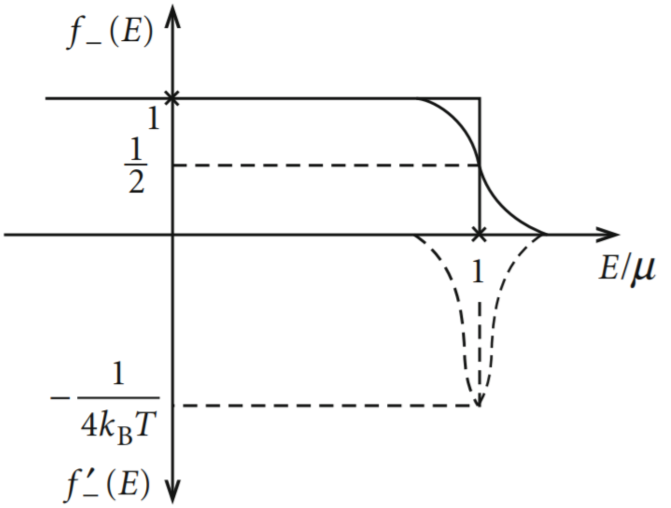

FIG. 1: The Fermi function and its derivative

At T = 0K, $f'(\varepsilon)$ is in the form of delta function $-\delta(\varepsilon - E_F)$. At finite temperature, the Fermi function is "smeared out" as in the Figure 1.

This is the case of our interest where there are many quantum behavior results that we cannot use the classical model to explain. At the end of this section, we will have some illustrations for the Fermi gas physical properties.

C. Sommerfeld expansion

Our task in this part is to find an approximation for the integral of the form:

$$I(T) = \int_{-\infty}^{+\infty} dE g(E) f(E) \tag{26}$$

which arises many times in dealing with Fermi gas. There are a few conditions applied to the function g(E) in this approximation:

$$\begin{cases} \lim\limits_{E\to-\infty} g(E) = 0 \\ \exists n \in \mathbb{R}^+ : \lim\limits_{E\to\infty} \frac{g(E)}{E^n} = 0 \\ g(E) \text{ is regular within the Fermi layer.} \end{cases} \tag{27}$$

Define: $p(E) = \int\limits_{-\infty}^{E} dx g(x) \to g(E) = \frac{dp(E)}{dE}$

As we shall see, the first two conditions ensure the vanishes of the function $p(E)f(E)$, and the last one is a necessary condition for $g(E)$ to be expanded in Taylor series around $E = \mu$. Applying integration by part, and noting that $f(E)$ disappears at upper bound, and $p(E)$ vanishes at lower bound, we have:

$$I(T) = -\int_{-\infty}^{\infty} dE p(E) \frac{\partial f(E)}{\partial E} \tag{28}$$

By inserting the Taylor expansion of $p(E)$ around μ, also note that since the derivative of Fermi function is an even function with respect to $E-\mu$, only the even powers in Taylor series would contribute to $I(T)$. After a short calculation, we derive:

$$I(T,\mu) = I_0(T,\mu) + \beta \sum_{n=1}^{\infty} \frac{1}{(2n)!} \left[\frac{d^{2n-1}g(E)}{dE^{(2n-1)}}\right]_{E=\mu} I_{2n}(T,\mu) \tag{29}$$

with:

$$I_0(T,\mu) = -p(\mu) \int_{-\infty}^{\infty} dE \frac{\partial f(E)}{\partial E} = p(\mu) = \int_{-\infty}^{\mu} dx g(x) \tag{30}$$

$$\begin{aligned} I_{2n}(T,\mu) &= \int_{-\infty}^{\infty} dE (E-\mu)^{2n} \frac{e^{\beta(E-\mu)}}{(e^{\beta(E-\mu)}+1)^2} \\ &= \frac{4n}{\beta^{(2n+1)}} \left(\int_0^{\infty} dy \frac{y^{2n+1}}{e^y+1}\right) && (31) \\ &= 2(1-2^{1-2n})\beta^{-(2n+1)}(2n)!\zeta(2n) && (32) \end{aligned}$$

In the above formula, $\zeta(x)$ is the **Riemann's zeta function**.The detailed calculation will be derived in Appendix. Substitute (30) and (32) into (29), we obtain the **Sommerfeld expansion**:

$$\begin{aligned} I(T,\mu) = &\int_{-\infty}^{\mu} dE g(E) \\ &+ 2\sum_{n=1}^{\infty} (1-2^{1-2n})\zeta(2n)(k_BT)^{2n} \left[\frac{d^{2n-1}g(E)}{dE^{2n-1}}\right]_{E=\mu} \end{aligned} \tag{33}$$

In the first-order approximation:

$$I(T,\mu) \approx \int_{-\infty}^{\mu} dE g(E) + \frac{\pi^2}{6}(k_BT)^2 g'(\mu) \tag{34}$$

IV. APPLICATIONS: HEAT CAPACITY & SPIN-PARAMAGNETISM

A. Electron gas heat capacity

We will now concentrate on the heat properties of a system of electrons in metal, which are considered as an ideal Fermi gas. In classical formalism, each electron has 3 degrees of freedom, and each degrees of freedom contain an amount of thermal energy k_BT. Suppose that our system has N electron, the internal energy due to the thermal motion of electrons, and the heat capacity followed is:

$$U(T) = \frac{3}{2}Nk_BT \Rightarrow C_V(T) = \frac{3}{2}Nk_B \tag{35}$$

From experimental results, we know that this result will hold at a high temperature. For a low temperature, it is observed that:

$$C_V(T) \propto T \qquad \text{and} \qquad \lim_{T\to 0} C_V(T) = 0 \tag{36}$$

Using the ideal Fermi gas model, we can give a quite good approximation for $C_V(T)$ at low temperature, where the quantum mechanics plays the main role. The internal energy of the electron gas is: $U(T) = \int_{-\infty}^{\infty} dEED(E)f(E)$ where:

$$D(E) = \begin{cases} \tau\sqrt{E}, & E \geq 0 \\ 0, & o.w \end{cases} \tag{37}$$

It is clear that D(E) satisfies the 3 conditions for using Sommerfeld expansion:

$$\begin{cases} \lim\limits_{E\to-\infty} D(E) = 0 \\ \lim\limits_{E\to\infty} \frac{D(E)}{E^n} = \lim\limits_{E\to\infty} \tau E^{1/2-n} = 0, \forall n > 1/2 \\ D(E) \text{ is smooth over the real domain} \end{cases} \tag{38}$$

Hence we can apply first-order Sommerfeld expansion (34) to obtain an approximate for internal energy:

$$\begin{aligned} U(T) &\approx \int_{-\infty}^{\mu} dED(E)E + \frac{\pi^2}{6}(k_BT)^2\left(ED(E)\right)'_{E=\mu} \\ &= \int_{0}^{\mu} dE\tau E^{3/2} + \frac{\pi^2}{6}(k_BT)^2\left(\mu\tau\frac{1}{2\sqrt{\mu}} + \tau\sqrt{\mu}\right) \\ &= \frac{2\tau}{5}\tau\mu^{5/2} + \frac{\pi^2}{4}(k_BT)^2\tau\mu^{1/2} \end{aligned} \tag{39}$$

The chemical potential is actually time-dependent; to find that relation, we apply the Sommerfeld expansion to the number of particles:

$$\begin{aligned} N &= \int_{-\infty}^{\infty} dED(E)f(E) \approx \int_{-\infty}^{\mu} dED(E) + \frac{\pi^2}{6}(k_BT)^2D'(\mu) \\ &= \frac{2}{3}\tau\mu^{3/2} + \frac{\pi^2}{12}(k_BT)^2\tau\mu^{-1/2} \\ &= N\left(\frac{\mu}{E_F}\right)^{3/2}\left[1 + \frac{\pi^2}{8}\left(\frac{k_BT}{\mu}\right)^2\right] \\ \Rightarrow 1 &\approx \left(\frac{\mu}{E_F}\right)^{3/2}\left[1 + \frac{\pi^2}{8}\left(\frac{k_BT}{\mu}\right)^2\right] \\ \Rightarrow \mu(T) &\approx \frac{E_F}{\left[1 + \frac{\pi^2}{8}\left(\frac{k_BT}{\mu}\right)^2\right]} \end{aligned}$$

Since we are considering degenerate case: $k_BT \ll E_F \leftrightarrow \frac{k_BT}{E_F} \ll 1$, the chemical potential can be approximate as:

$$\begin{aligned} \mu(T) &\approx E_F\left[1 - \frac{\pi^2}{12}\left(\frac{k_BT}{E_F}\right)^2\right] \\ \to \mu(T)^n &\approx E_F\left[1 - \frac{n\pi^2}{12}\left(\frac{k_BT}{E_F}\right)^2\right] \end{aligned} \tag{40}$$

Substitute the expression (40) into (39) and applying the approximation of the form $(1 + x^n) \approx 1 + nx$, we obtain:

$$U(T) \approx U(0)\left[1 + \frac{5\pi^2}{12}\left(\frac{k_BT}{E_F}\right)^2\right], \text{ where: } U(0) = \frac{2}{5}\tau E_F^{5/2} \tag{41}$$

Finally, taking the derivative of $U(T)$ with respect to T to obtain the heat capacity for system of N-electrons gas:

$$C_V(T) = \frac{\partial U(T)}{\partial T} = \frac{5\pi^2}{6}U(0)\left(\frac{k_B}{E_F}\right)^2 T \tag{42}$$

which agrees with our claim above: The heat capacity of electron gas is linearly dependent on the temperature, and tends to 0 when the temperature tends to 0K.

B. Spin-Paramagnetism

Magnetic susceptibility is a dimensionless proportionality constant that indicates the degree of magnetization of a material in response to an applied magnetic field. This quantity is defined as:

$$\chi = \frac{\partial M}{\partial H} \tag{43}$$

In most cases, this formula holds except in ferromagnetic crystals, the relationship between the magnetization M and the magnetic field strength H is not linear. Our task now is to compute the susceptibility of the electron gas with the simple Ideal Fermi Gas model.

The term paramagnetism refers to the magnetic state of an atom with one or more unpaired electrons interact with a magnetic field due to the electrons' magnetic dipole moments contributed by the electron spin. The interaction between N unpaired electrons with a constant magnetic field $\boldsymbol{B}_0 = B_0\boldsymbol{e}_z$ will contribute to the non-interacting Hamiltonian an amount of:

$$\delta\hat{H} = -\sum_{i=1}^{N}\boldsymbol{\mu}^{(i)}\boldsymbol{B}_0 = 2\frac{\mu_B}{\hbar}B_0\sum_{i=1}^{N}S_z^{(i)} \tag{44}$$

In second quantization, we can write $\delta\hat{H}$ with the help of (14). The total Hamiltonian is:

$$H^{(Fermi)} = \sum_{\boldsymbol{k},\alpha}(\varepsilon_{\boldsymbol{k}} + z_\alpha\mu_BB_0)a^\dagger_{\boldsymbol{k}\alpha}a_{\boldsymbol{k}\alpha} \tag{45}$$

where z_α is the eigenvalues of σ_z operator: $\sigma_\alpha\left|\alpha\right\rangle = z_\alpha\left|\alpha\right\rangle$, where $\alpha = (\uparrow,\downarrow) \Leftrightarrow z_\alpha = (+1,-1)$.

Our task now is to calculate the susceptibility of the electron gas:

$$\chi = \frac{1}{V}\left(\frac{\partial m}{\partial H}\right)_T = \left(\frac{\partial M}{\partial H}\right)_T \tag{46}$$

When the magnetic field is switched off, there are as many electrons with spin up as electrons with spin down due to statistically distribution, which implies: $D_{\uparrow} = D_{\downarrow} = \frac{1}{2}D(E)$. When the field is switched on:

$$\varepsilon_{\boldsymbol{k}} \longrightarrow \varepsilon_{\boldsymbol{k}} + z_\alpha \mu_B B_0 \tag{47}$$

$$D_\alpha(E) = \frac{1}{2}D(E) \longrightarrow \frac{1}{2}D(E - z_\alpha \mu_B B_0) \tag{48}$$

The electrons tend to fill the lower energy states first, which means they will choose to have spin point into opposite direction of the magnetic field. The spin-dependent electron numbers is:

$$\begin{aligned} N_\alpha &= \frac{1}{2}\int\limits_{z_\alpha \mu_B B_0}^{\infty} dE D(E - z_\alpha \mu_B B_0) f(E) \\ &= \frac{1}{2}\int_0^\infty dy D(y) f(y + z_\alpha \mu_B B_0) \\ &\approx \frac{1}{2}\int_0^\infty dy D(y)\left[f(y) + z_\alpha \mu_B B_0 \frac{\partial f}{\partial y}\right] \end{aligned} \tag{49}$$

Hence, the magnetization of electron gas is:

$$\begin{aligned} M &= \frac{\mu_B}{V}(N_\downarrow - N_\uparrow) \approx -\frac{\mu_B^2}{V}B_0 \int_{-\infty}^{\infty} dy D(y) \frac{\partial f}{\partial y} \\ &= -\frac{\mu_B^2}{V}B_0 \left[f(y)D(y)|_0^\infty + \int_0^\infty dy D'(y) f(y)\right] \\ &= -\frac{\mu_B^2}{V}B_0 \int_0^\infty dy D'(y) f(y) \end{aligned} \tag{50}$$

And the Pauli susceptibility:

$$\chi_p(T) = \left(\mu_0 \frac{\partial M}{\partial B_0}\right) = -\frac{\mu_0 \mu_B^2}{V}\int_0^\infty dy D'(y) f(y) \tag{51}$$

Now we can apply the Sommerfeld expansion:

$$\begin{aligned} \chi_p(T) &= \frac{\mu_0 \mu_B^2}{V}\left[\int_0^\mu dy D(y) + \frac{\pi^2}{6}(k_B T)^2 D''(\mu)\right] \\ &= \frac{\mu_0 \mu_B^2 \tau}{V}\left[\sqrt{\mu} - \frac{\pi^2}{24}(k_B T)^2 \mu^{-3/2}\right] \\ &\approx \frac{3N}{2V}\frac{\mu_0 \mu_B^2}{E_F}\left[1 - \frac{\pi^2}{12}\left(\frac{k_B T}{E_F}\right)^2\right] \end{aligned} \tag{52}$$

The susceptibility of the conduction electron does depend on the temperature, but at second order. An estimation for metal electrons at room temperature ($T_r \approx 300K$) is given below to illustrate how very weakly-dependence of χ_p:

$$\begin{cases} E_F \ 10eV \\ k_B T_r \approx 0.026eV \end{cases} \Rightarrow \frac{\pi^2}{12}\left(\frac{k_B T}{E_F}\right)^2 \approx 5.56 \times 10^{-6}, \tag{53}$$

which is much smaller than 1 as expected. Thus, the temperature-independent susceptibility is a very good approximation in many cases.

---

[1] Wolfgang Nolting. *Theoretical Physics 8: Statistical Physics*, Springer, 2017.

[2] Don Koks. *Microstates, Entropy and Quanta-An Introduction to Statistical Mechanics*, Springer, 2018.

[3] Ulrich Rssler. , *Solid State Theory: An Introduction*, Springer, 2009

[4] P.J.H. Denteneer. *Lecture notes with course Quantum Theory*, Fall 2008.

Instanton and Tunneling

Zu Yao Teoh

(Dated: June 19, 2019)

This paper explores tunneling phenomena using the instanton method, a method that has proved to be useful in quantum field theories. We examine the method using the standard example of tunneling through the bump of a double-well potential $V(x) \sim (x^2 - a^2)^2$, calculating the transmission amplitude, showing that the result agrees with that given by WKB.

I. INTRODUCTION

Tunneling is a hallmark of quantum theory. Many phenomena that could not be well-explained classically are elucidated with the advent of the tunneling concept. Even biological processes involve tunneling. For instance, smell receptors operate via quantum tunneling (cf. [1]).

Figure 1: When you are captivated by the smell of your favorite milk tea, tunneling is taking place in your smell receptor.

Tunneling is often introduced in a first course in quantum mechanics, beginning with the tunneling across a square barrier to the semiclassical WKB approximations for slowly varying potentials. The time-independent Schrödinger equation for a particle with mass m in a potential $V(x)$ is given by

$$\hat{H}\psi(x) = E\psi(x), \tag{1}$$

which in one-dimension, the Hamiltonian $\hat{H}$ is given by $\hat{H} = \frac{\hbar^2}{2m}\frac{\partial^2}{\partial x^2} + V(x)$. This equation is an eigenvalue problem. We want to solve for a complex function $\psi(x)$ and an energy E. The Hamiltonian is Hermitian, so the energy will always turn out real. In regions where $E - V(x) \geq 0$, the particle is said to be in a *classically allowed* region, whereas the region is said to be *classically forbidden* if it is a region where $E - V(x) < 0$. In a classically forbidden region, $\psi(x)$ assumes a decaying exponential $e^{-\beta x}$ with $\beta > 0$ a real number. The fact that $\psi(x)$ is nonvanishing in the classically forbidden region means that the particle has a nonvanishing probability to be in that region, a region where classical particles can never be found. More interestingly, $\psi(x)$ is nonvanishing across the barrier (the classically forbidden region). Thus, a quantum particle can find itself across a barrier from its place of origin–this is tunneling. A WKB computation has the *transmission coefficient* or *tunneling probability* coming out with an exponential suppression

$$\mathcal{T} \sim \exp\left(-2\int_a^b \kappa(x')\,dx'\right), \tag{2}$$

where $\kappa(x) = \frac{1}{\hbar}\sqrt{2m(V(x) - E)}$ and the interval (a, b) is the classically forbidden region.

In this paper, I seek to achieve two goals. Firstly, the method to be illustrated is a fruitful method in quantum field theory and this exposition offers a first glimpse into the method. Secondly, due to the nonintuitive (nonclassical) manner of tunneling, we seek to take a step back, adopt a different point of view of quantum mechanics that incorporates classical mechanics, and deduce tunneling. This different formulation is nothing more than Feynman's path integral approach to quantum mechanics.

Let me summarize the goal of this exposition explicitly. GOAL: To expound on an alternative method–the instanton method–to analyze tunneling and to obtain the tunneling probability and show that it is in *agreement* with that predicted by WKB.

II. PATH INTEGRAL, IMAGINARY TIME & EUCLIDEAN FORMALISM

Classical mechanics centers around Newton's Laws of Motion. The Principle of Least Action states that a particle of mass m under the influence of a potential $V(x)$ traverses a path $x(t)$ in such a way that the path integral

$$S = S(x) = \int_{t_1}^{t_2} (T - V)\,dt \tag{3}$$

is a minimum (a saddle point to be exact) among all possible paths. The function $L = T - V$ is known as the *Lagrangian* of the system and the integral S is known as the *action* of the system. Newton's equations of motion $F = m\ddot{x}$ can then be derived from a necessary condition for S to be an extremum, a well known condition from the calculus of variations collectively known as *Euler-Lagrange's equations*:

$$\frac{d}{dt}\left(\frac{\partial L}{\partial \dot{x}}\right) - \frac{\partial L}{\partial x} = 0. \tag{4}$$

The age-old mantra summarizes the principle most aptly: *a classical particle moves in such a way as to minimize the action.*

Classically, a particle moves from a point x_1 in space to another point x_2 in such a way that S attains a minimum. Quantum mechanically, one postulates that the particle has continuumly many equal chances to traverse from x_1 to x_2. Feynman's *path integral* approach then states that the probability amplitude for a particle known to be at x_1 at time t_1 to be found at x_2 at time t_2 is given by

$$\langle x_2; t_2 | e^{\frac{i(t_2-t_1)}{\hbar}\hat{H}} | x_1; t_1 \rangle = N \int_\Gamma e^{\frac{i}{\hbar}S(x)}\, Dx, \tag{5}$$

where $|x_1; t_1\rangle$ and $|x_2; t_2\rangle$ are position eigenstates (with time labels), N is an appropriate normalization constant, Γ is the class of paths connecting x_1 to x_2, and Dx is a measure the integral is performed with respect to. The amplitude Eq. 5 is often referred to as the *propagator* and we denote it by $U(x_2, t_2; x_1, t_1)$.

Although Eq. 5 is an integral over Γ, the amplitude is often said to be obtained by "summing" over all paths $x(t) \in \Gamma$. The summing or integral is a sophisticated matter, but in general the path integral Eq. 5 is dominated by the classical trajectories $x_{cl}(t)$ so that the amplitude can be approximated as

$$U(x_2, t_2; x_1, t_1) \approx N \sum_{x_{cl}} e^{\frac{i}{\hbar}S(x_{cl})}. \tag{6}$$

A heuristic reason as to why classical trajectories dominate has to do with destructive interference of the phase contributions $e^{\frac{i}{\hbar}S(x)}$ for $x(t) \in \Gamma$ as a whole. Only paths in small neighborhoods of classical trajectories $x_{cl}(t)$ contribute constructively. Chapter 8 of [2] gives an example: for a free particle of mass 1 g to travel 1 cm away from its point of origin in 1 second, the deviation of the action in a quadratic trajectory $x = t^2$ from the classical trajectory $x = t$ is roughly $1.6 \times 10^{26}\hbar$, whereas for an electron whose mass is roughly $10^{-27}g$, the deviation is $\hbar/6$. What this means is that a deviation of $x = t^2$ from the classical trajectory $x = t$ is enormous for a classical particle and, therefore, the alternate trajectory contributes almost nothing to the path integral. On the other hand, electrons indeed behave quantum mechanically. The same chapter and Chapter 21 of the text offer a detailed discussion; a proof that the path integral formulation is equivalent to the Schrödinger formulation of quantum mechanics can also be found in that same chapter.

Now, if the classical trajectory is of importance in the path integral approach, how then do we understand tunneling from classical mechanics? Tunneling occurs through a classically forbidden region, so there is no classical trajectory to dominate the integral. This is when we need to step into imaginary time τ: $t \mapsto -i\tau$. This process is formally known as *Wick rotation.* Wick rotating the propagator with the old Lagrangian $L = T - V$ and action $S(x(t))$ will present us with a new Lagrangian L_E called the *Euclidean* Lagrangian, one whose potential term $V_E(x)$ is the old potential $V(x)$ standing upside down $-V(x)$, as we will see.

To begin the analysis, the relation $t = -i\tau$ yields $dt = -i\, d\tau$. The Lagrangian L consists of the kinetic energy T that is a function of velocity, whereas the potential $V(x)$ is a function of position x. Thus, upon Wick rotation, the kinetic energy becomes

$$T = \frac{1}{2}m\left(\frac{dx}{dt}\right)^2 = \frac{1}{2}m\left(\frac{dx}{d\tau}\cdot\frac{d\tau}{dt}\right)^2 \tag{7}$$

$$= -\frac{1}{2}m\left(\frac{dx}{d\tau}\right)^2 = -T_E \tag{8}$$

while $V(x)$ remains unchanged, and writing $V_E(x) = -V(x)$, the Lagrangians L and L_E can now be seen to be related by

$$L = T - V = -T_E - V = -(T_E - V_E) \tag{9}$$

$$= -L_E. \tag{10}$$

As for the quantity $\frac{i}{\hbar}S$, Wick rotation yields

$$\frac{i}{\hbar}S_E = \frac{i}{\hbar}\int_{\tau_1}^{\tau_2} -L_E\,(-i\, d\tau) = -\frac{1}{\hbar}\int_{\tau_1}^{\tau_2} L_E\, d\tau. \tag{11}$$

All the Wick rotations culminate in the propagator in imaginary-time form:

$$U(x_2, \tau_2; x_1, \tau_1) = \int_\Theta e^{-\frac{1}{\hbar}S_E(x(\tau))}\, Dx, \tag{12}$$

where the class of paths to be integrated over is now replaced by a new class Θ corresponding to the Euclidean Lagrangian. The oscillatory nature of Eq. 5 has also now been replaced by a decaying exponential. Since the propagator gives the amplitude for a particle starting at x_1 in the system at time τ_1 to end up at x_2 at time τ_2, the decaying exponential of the imaginary time propagator suggests that we are now staring at *tunneling* phenomenon. Our next task is to elaborate on this surmise with the double-well as an example. The following observation adds insight:

In terms of energy representation, the propagator assumes the form

$$U(x_2; x_1) = \langle x_2|n\rangle \sum_n \exp\left(-\frac{T}{\hbar}\hat{H}\right)\langle n|x_1\rangle \tag{13}$$

$$= \sum_n \exp\left(-\frac{E_n T}{\hbar}\right)\langle x_2|n\rangle\langle n|x_1\rangle, \tag{14}$$

where we drop references to time and replace $\tau_2 - \tau_1$ by T. Here, $\hat{H}$ is the original time-independent Hamiltonian and the $E_n \in \mathbb{R}$ are its eigenvalues, both of which remain unchanged by Wick rotation. This expansion allows us to see that the dominant term in the sum is the one contributed by the ground state $E_n = E_0$, from which E_0 can be computed as

$$E_0 = \lim_{T\to\infty}\left(\frac{-\hbar \ln U(x_2; x_1)}{T}\right). \tag{15}$$

This is a method used in quantum chromodynamics (QCD) to calculate hadron masses (Section 2.1.2, [3]).

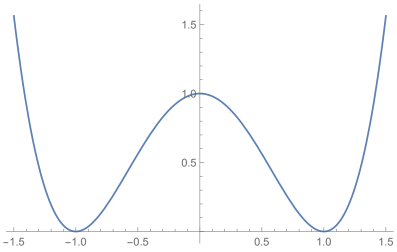

Figure 2: Example of a double-well potential. The wells sit at $x = \pm 1$ in this example $V(x) = (x^2 - 1)^2$.

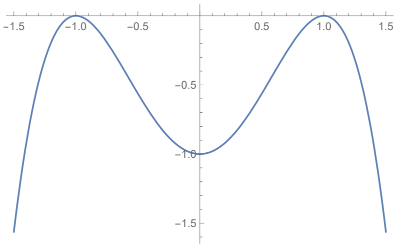

Figure 3: The double-well of Fig. 2 inverted. Now a double-hill with a valley in between.

III. DOUBLE-WELL POTENTIAL AND INSTANTON

A double-well potential is one which is given by

$$V(x) = A^2(x^2 - a^2)^2. \tag{16}$$

The potential has two wells whose bottoms touches the x-axis at $\pm a$ and a hump between them centered at the origin. We explicitly declare that $A > 0$.

Classically, if the system has energy below the top A^2a^4 of the hump, a particle that is confined in the left well will remain in the same well and there is no classical trajectory across the barrier in the region where $V(x)$ is greater than the total energy. However, the Euclidean Lagrangian now has $V(x)$ standing upside down.

Since classical trajectories play a significant role in approximating the propagator, let us now analyze the classical trajectories pertaining to L_E. Our intuition tells us that if we place the particle on the left of the hill with a summit at $x = -a$, it will roll down indefinitely and gain speed as it goes. Similar situation happens if we place it to the right of $x = a$. If we place the particle on either top and not give it any kinetic energy, it will remain on top forever. If we place it ϵ distance to the right of $x = -a$ or to the left of $x = a$, then it will roll down the slope into the valley and roll up the other slope within a finite amount of time T, going going back and forth between the two peaks, but as we take ϵ to 0, we are back in the former situation where we place the particle at $x = \pm a$ and the time it takes to roll down and up now becomes $T \to \infty$. Indeed, if we look at the conserved quantity $E = T_E + V_E$ of the system, the total energy, and setting $E = 0$, we obtain $\frac{1}{2}m(dx/d\tau)^2 = -V_E(x)$, keeping in mind that now the time variable is the imaginary time τ. Solving for $dx/d\tau$, we have

$$\frac{dx}{d\tau} = \pm\sqrt{\frac{2V(x)}{m}}, \tag{17}$$

which we separate variables and integrate to

$$\pm\sqrt{\frac{m}{2}}\int_{x_{cl}(\tau_1)}^{x_{cl}(\tau)} \frac{dx}{\sqrt{V(x)}} = \int_{\tau_1}^{\tau} d\tau' \tag{18}$$

$$\pm\sqrt{\frac{m}{2A^2}}\int_{x_{cl}(\tau_1)}^{x_{cl}(\tau)} \frac{dx}{x^2 - a^2} = \int_{\tau_1}^{\tau} d\tau' \tag{19}$$

$$\pm\sqrt{\frac{m}{2(aA)^2}}\Big[\arctan(x/a)\Big]_{x_{cl}(\tau_1)}^{x_{cl}(\tau)} = \tau - \tau_1 \tag{20}$$

and finally obtaining a classical trajectory

$$x_{cl}(\tau) = \pm a\tanh\left(\sqrt{\frac{2}{m}}aA\tau\right), \tag{21}$$

one which we set to satisfy $x_{cl}(0) = 0$. Such a solution to the Euclidean equation of motion is called an *instanton*. As a matter of choice, we call the solution with the positive sign an instanton and the one with a minus sign an *anti-instanton*, just to be more specific. This instanton corresponds to the discussion above, where we place a particle ϵ distance away to the right of $x = -a$ and taking $\epsilon \to 0$, reaching the bottom of the valley $x = 0$ at (imaginary) time $\tau = 0$, and then rolling up the other hill to $x = a$ as $\tau \to \infty$. The characteristic of an instanton is one where a transition from a position eigenstate such as $|-a\rangle$ to $|a\rangle$ takes almost an instant (as can be seen from the steep slope centered around the origin in Fig. 4) while it stays in the position eigenstates most of the time. In fact, in view of Eq. 15, these position eigenstates correspond to the ground states of the system, albeit degenerate.

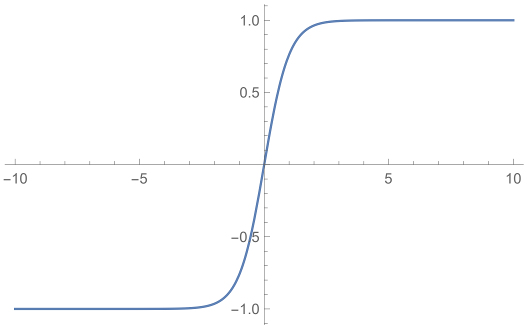

Figure 4: An instanton in the form of Eq. 21.

To recapitulate with rigor, from the very start, it was easy to identify the solutions $x_{cl}(\tau) = -a$ and $x_{cl}(\tau) = a$ as solutions to the Euclidean equation of motion for the double-well potential, but these constant solutions cannot contribute to the computation of the propagator $U(x_2,;x_1)$ of Eq. 5 with $x_1 = -a$ and $x_2 = a$. They certainly contribute to the computation of the propagator for $x_1 = x_2 = -a$ or $x_1 = x_2 = a$, which they indeed give a correct computation:

$$U(\pm a;\pm a) \approx \exp\left(-\frac{1}{\hbar} S_E(\pm a)\right) = \exp(0) = 1. \qquad (22)$$

The exponential has a vanishing argument because the action vanishes if the path is a point, which is the case here. Now, towards our goal, let us use the classical trajectory given by the instanton, which we now denote by x_I, to show that it produces a transition amplitude predicted by WKB. First, the action along the instanton computes as

$$\begin{aligned} S_I &= m \int_{\tau_1}^{\tau_2} \left(\frac{dx_I}{d\tau}\right)^2 d\tau = m \int_{-a}^{a} \frac{dx_I}{d\tau}\, dx_I && (23)\\ &= m \int_{-a}^{a} \sqrt{\frac{2V(x)}{m}}\, dx && (24)\\ &= \int_{-a}^{a} \sqrt{2mV(x)}\, dx, && (25) \end{aligned}$$

from which we have used Eq. 17 as we go from line 23 to the next. In case one wonders why we have kept the subscript I in the (dummy) variable of integration in line 23, it is to emphasize that the integral is done over the instanton. The limits of integration are also indications of such an integral (the limits indicate a propagation from $-a$ to a as opposed to the other two classical trajectories, where the particle remains put at either a or $-a$). We can now quickly see that the propagator approximates to

$$U(a;-a) \approx \exp\left(-\frac{1}{\hbar} \int_{-a}^{a} \sqrt{2mV(x)}\, dx\right) \qquad (26)$$

and, correspondingly, its square

$$\mathcal{T} \approx \exp\left(-\frac{2}{\hbar} \int_{-a}^{a} \sqrt{2mV(x)}\, dx\right) \qquad (27)$$

represents the transmission probability, which agrees *perfectly* with the WKB prediction Eq. 2! Note that the energy involved is vanishing for this agreement to hold. This is the reason why we did not immediately make a calculation after Eq. 5 to demonstrate this agreement. Had we attempted to do so, we would have ended up trying to integrate $\sqrt{2m(V(x)+E)}$, which would not jibe with the WKB prediction unless $E = 0$. In short, *the instanton solution, obtained from the consideration of a vanishing E, yielded a tunneling phenomenon whose tunneling or transmission probability agrees perfectly with that given by WKB.*

We need not stop at Eq. 25; we may go on to compute the actual transmission probability in terms of the parameters of the potential:

$$\begin{aligned} S_I &= \int_{-a}^{a} \sqrt{2mA^2(x^2-a^2)^2}\, dx && (28)\\ &= \sqrt{2m} \int_{-a}^{a} -A(x^2-a^2)\, dx && (29)\\ &= \frac{4Aa^3\sqrt{2m}}{3}. && (30) \end{aligned}$$

The negative sign in the integrand in line 29 warrants a quick mention. It is the result of taking a positive square-root of $2mV(x)$, for $x^2 - a^2$ dips below the x-axis in the region $x \in (-a, a)$. Thus, for a double-well potential $V(x) = A^2(x^2-a^2)^2$ with total energy $E = 0$, tunneling takes place through the barrier in the (classically forbidden) region $(-a, a)$ with a transmission probability

$$\mathcal{T} \approx \exp\left(-\frac{8Aa^3\sqrt{2m}}{3\hbar}\right). \qquad (31)$$

IV. DISCUSSION

We set out with a goal to derive the tunneling amplitude using a different method rather than the usual WKB approximation and to compare the two results. The method is called the instanton method and we illustrated it with the double-well cum double-hill potential, showing that both methods agree in perfect unison. The machinery behind the instanton method is Feynman's famous path integral and a formal analytic continuation from real time t to imaginary time $-i\tau$.

We should really go beyond computing the transmission amplitude and compute the splitting of the ground state of the system as a result of the tunneling, or we should even compute the exact transmission amplitude by performing the path integral of Eq. 12. To accomplish these tasks, a deeper analysis and discussion will have to be put in place, one including the definition of the measure Dx appearing in the path integrals Equations 5 and 12 for instance. Due to the enormous amount of knowledge that would involve, for now we will entrust the task to other texts and let ourselves be content with getting acquainted with the method of an instanton the way it is used to derive the tunneling amplitude. A mastery of the basic idea discussed here should prepare one well for those further analyses and pave a way to the mastery of the subject.

We now want to justify our seemingly long-winding road to the tunneling amplitude. Instanton has an important place in QCD, for instance. As the whole exposition is about, instanton is associated with tunneling phenomena, which abound in quantum theory. Once the basics of the instanton is understood in simpler particle mechanics, one can concentrate on the additional complications brought in by field theories. A good survey exposition on the subject is [3]. To quote an excerpt of that paper verbatim, "There are interesting relations and interactions between instantons and their topological cousins, the non-abelian monopoles and vortices. In several theories, probably including QCD, instantons are responsible for spontaneous chiral symmetry breaking. The role of instantons in deep inelastic scattering and other hard QCD processes has been examined, and also their impact on weak-interaction processes at RHIC, LHC and beyond. In inflationary cosmology and elsewhere relatives of instantons (sometimes called bounces) describe the 'decay of the false vacuum'." Thus, the uses and importance of instantons are many and unsurpassable. Instantons are not only instrumental to the advance of quantum field theory, it has also played a role in the advance of mathematical theories (cf. [4]).

We conclude with some references for further studies. They are S. Coleman's classical paper *The Uses of Instantons* [5], H. Forkel's *A Primer on Instantons in QCD* [3], which we have cited several times, and *Instantons in QCD* by T. Schäfer and E.V. Shuryak [6]. The primary reference for this paper is *Principles of Quantum Mechanics* by R. Shankar [2], in which the introduction to path integrals is given in Chapters 8 and 21, the latter which also contains an introduction to instantons.

ACKNOWLEDGMENTS

Many thanks to the initiative taken by Prof. Barton Zwiebach and Dr Jolyon Bloomfield to make the signature quantum mechanics course series at MIT available for the learning pleasure of an international audience. Many thanks also go to Mark Weitzman and Jim Freericks for their many help in my learning experience. I also thank my girlfriend Lai Yeng Kuan for her patience as I spend time learning the subject hard; the same goes to my cute kitties Alfred, Jr., Safety, Flory, and Berry (named after Sir Michael Berry). Finally, big thanks to my late father Chin Seng Teoh for his instilling in me a love for math and physics, and knowledge in general.

[1] T. M. (Editor), *Atom Tunneling Phenomena in Physics, Chemistry and Biology.* Springer, 2004.

[2] R. Shankar, *Principles of Quantum Mechanics, 2nd Ed.* Plenum Press, 1994.

[3] H. Forkel, "A primer on instantons in QCD, v2," *arXiv:hep-ph/0009136v2* (2002) .

[4] S. Donaldson, "Instantons and geometric invariant theory," *Commun. Math. Phys.* (1984) no. 93, 453–460.

[5] S. Coleman, "The uses of instantons," *Proc. of the 1977 School of Subnuclear Physics* (1977) .

[6] T. Schäfer and E. Shuryak, "Instantons in QCD, v3," *arXiv:hep-ph/9610451v3* (1998) .

Instantons in Quantum Mechanics

Omar Alsheikh

(Dated: June 19, 2019)

It is well known that in quantum mechanics, a particle can tunnel through a potential barrier even if its energy is lower than that of the barrier. The standard route to calculating the tunneling amplitude, and the most convenient, is the WKB procedure. However, there exists another means of analyzing the problem through Feynman's path integral formulation, where the classical action of the system is employed. By finding the Euclidean classical path followed by the particle and then slightly perturbing it, we can reproduce the results known from standard quantum mechanics. We reproduce the spectrum of the 1D harmonic oscillator using this method as a means of introducing it, and then we calculate the tunneling amplitude between the two wells of a quartic potential, where an interesting classical solution, the instanton, will show up. We finish with the consideration of periodic potentials.

Note: Throughout the paper, we put $\hbar = 1$. It can be retrieved anytime through dimensional analysis.

I. EUCLIDEAN FORMULATION

The Lagrangian functional $L(x, \dot{x})$ of a classical point particle of unit mass moving in one-dimension in a potential $V(x)$ is given by the simple formula

$$L(x, \dot{x}) = \frac{1}{2}\dot{x}^2 - V(x). \tag{1}$$

Traditionally, the transition to quantum mechanics involves finding the Hamiltonian $H(x, p)$ of the system, promoting the position x and the canonical momentum p to operators by imposing the canonical commutation relation $[x, p] = i$, and then solving the Schrödinger equation

$$i\frac{\partial}{\partial t}|\Psi(t)\rangle = H|\Psi(t)\rangle, \tag{2}$$

where $|\Psi(t)\rangle$ is an element of the Hilbert space and essentially contains all the information about the system. In particular, the inner product $\langle x|\Psi(t)\rangle \equiv \Psi(x, t)$, which is the familiar wavefunction in the position basis, determines the probability amplitude of finding the particle at the point x i.e. in the state $|x\rangle$ at time t.

However, Feynman showed us another way to do quantum mechanics, known as the path integral formulation [1]. Suppose the particle is sitting at the point x_i at initial time $-t_0/2$, and we want to calculate the probability of finding the particle at the point x_f at time $t_0/2$. The amplitude of such a process is equal to the quantity $\langle x_f|e^{-iHt_0}|x_i\rangle$. Classically, the particle will follow a certain path which minimizes the action S given by[1]

$$S = \int_{-t_0/2}^{t_0/2} \mathrm{d}t\, L(x, \dot{x}). \tag{3}$$

In quantum mechanics, all possible paths connecting the two points contribute to the amplitude of this process with the weight $e^{iS[x(t)]}$, where $S[x(t)]$ is the action corresponding to the path $x(t)$. This is contained in the equation

$$\langle x_f|e^{-iHt_0}|x_i\rangle = N\int [Dx]\, e^{iS[x(t)]}, \tag{4}$$

where N is a normalization factor and $[Dx]$ is the measure corresponding to the integration over all functions $x(t)$ with boundary conditions $x(-t_0/2) = x_i$ and $x(t_0/2) = x_f$.

Next, we expand the left-hand side in terms of energy eigenstates $|n\rangle$ such that $H|n\rangle = E_n|n\rangle$, $E_0 < E_1 < \dots$ and using the completeness relation $\sum_{\mathrm{all}\, n} |n\rangle\langle n| = 1$:

$$\begin{aligned}\langle x_f|e^{-iHt_0}|x_i\rangle &= \sum_n \langle x_f|e^{-iHt_0}|n\rangle\langle n|x_i\rangle \\ &= \sum_n e^{-iE_nt_0}\psi_n(x_f)\psi_n^*(x_i),\end{aligned} \tag{5}$$

where $\psi_n(x) \equiv \langle x|n\rangle$ is the energy eigenfunction. Now we analytically continue the time by making the transition $t \to -it$. This substitution is often called the Wick rotation, and we observe the following transformations:

$$L \to -\frac{1}{2}\dot{x}^2 - V(x) \equiv -L_E \tag{6}$$

$$S \to i\int \mathrm{d}t\, L_E \equiv iS_E \tag{7}$$

$$e^{-iE_nt_0} \to e^{-E_nt_0} \tag{8}$$

$$e^{iS} \to e^{-S_E}, \tag{9}$$

and (4) becomes

$$\sum_n e^{-E_nt_0}\psi_n(x_f)\psi_n^*(x_i) = N\int [Dx]\, e^{-S_E[x(t)]}. \tag{10}$$

---

[1] Strictly speaking, the action needs to be *stationary*. This includes a local maximum or a saddle point.

This is the Euclidean variant of theory, hence the 'E' in the subscripts.[2] From now on, we will omit the subscripts, having in mind that we are working with the Euclidean version. Notice the decaying exponential on the left-hand side; in the limit of large t_0, the leading term in the series becomes $e^{-E_0 t_0}\psi_0(x_f)\psi_0^*(x_i)$. Thus we see that the Wick rotation is not just a matter of mathematical manipulation, as it enabled us to determine the ground state configuration, which is almost always what we are looking for. We shall also see later that it provides very useful means of describing some phenomena in quantum mechanics.

To evaluate the right-hand side, we have to make sense of the measure $[Dx]$. Let $\bar{x}(t)$ be some function that satisfies the boundary conditions. An arbitrary function $x(t)$ satisfying the same boundary conditions can be written as

$$x(t) = \bar{x}(t) + \sum_n c_n x_n(t), \tag{11}$$

where the set $x_n(t)$ is a complete set of orthonormal functions that vanish at the boundaries:

$$\int_{-t_0/2}^{t_0/2} \mathrm{d}t\, x_n(t) x_m(t) = \delta_{nm}. \tag{12}$$

Therefore we can define the measure to be

$$[Dx] = \prod_n \frac{1}{\sqrt{2\pi}}\,\mathrm{d}c_n. \tag{13}$$

In the semiclassical approximation,[3] paths that differ only a little from the classical path contribute the most to the path integral, and so, assuming the semiclassical approximation works, we look at the variation of the action δS around its minimum $S_0 \equiv S[\bar{x}(t)]$, where $\bar{x}(t)$ is the classical path, or the 'stationary point' of the integral S, and satisfies the classical equation of motion[4]

$$\ddot{\bar{x}} = V'(\bar{x}) \tag{14}$$

with $V'(x) \equiv \mathrm{d}V(x)/\mathrm{d}x$. The first variational derivative of S is of course rendered zero by virtue of (14), so we look at the second variational derivative (remember that we are only interested in small deviations around the stationary point, so we ignore higher orders):

$$\begin{aligned}\delta S &= \int_{-t_0/2}^{t_0/2} \mathrm{d}t\left(\frac{1}{2}\delta\dot{x}^2 + \frac{1}{2}V''(\bar{x})\,\delta x^2\right)\\ &= \frac{1}{2}\delta x\,\delta\dot{x}\Big|_{-t_0/2}^{t_0/2} - \int_{-t_0/2}^{t_0/2}\mathrm{d}t\,\frac{1}{2}\delta x\,\delta\ddot{x}\\ &\qquad + \int_{-t_0/2}^{t_0/2}\mathrm{d}t\,\frac{1}{2}V''(\bar{x})\,\delta x^2\\ &= \int_{-t_0/2}^{t_0/2}\mathrm{d}t\,\delta x\,\frac{1}{2}\Big[-\frac{\mathrm{d}^2}{\mathrm{d}t^2} + V''(\bar{x})\Big]\delta x,\end{aligned} \tag{15}$$

where it is understood that the square bracket is an operator that acts on δx. We obtained the second line by integrating the first term in the first line by parts. The boundary term vanishes for δx and its derivatives. Now suppose we know the eigenfunctions and their corresponding eigenvalues of our differential operator:

$$\Big[-\frac{\mathrm{d}^2}{\mathrm{d}t^2} + V''(\bar{x})\Big]x_n = \varepsilon_n x_n, \tag{16}$$

then we can take this set as our complete set in the expansion (11) and (12),[5] and (15) becomes

$$\begin{aligned}\delta S &= \int_{-t_0/2}^{t_0/2}\mathrm{d}t\,\frac{1}{2}\sum_m c_m x_m\Big[-\frac{\mathrm{d}^2}{\mathrm{d}t^2} + V''(\bar{x})\Big]\sum_n c_n x_n\\ &= \sum_{m,n}\frac{1}{2}\varepsilon_n c_m c_n \int_{-t_0/2}^{t_0/2}\mathrm{d}t\, x_m x_n\\ &= \sum_n \frac{1}{2}\varepsilon_n c_n^2.\end{aligned} \tag{17}$$

Now we are all set to evaluate the path integral. Putting $S = S_0 + \delta S$,

$$\begin{aligned}\int [Dx]\, e^{-S[x(t)]} &= e^{-S_0}\prod_n \int_{-\infty}^{\infty}\frac{1}{\sqrt{2\pi}}\,\mathrm{d}c_n\, e^{-\varepsilon_n c_n^2/2}\\ &= e^{-S_0}\prod_n \varepsilon_n^{-1/2}\\ &\equiv e^{-S_0}\Big[\det\Big(-\frac{\mathrm{d}^2}{\mathrm{d}t^2} + V''(\bar{x})\Big)\Big]^{-1/2}.\end{aligned} \tag{18}$$

We see that the problem has reduced to evaluating the determinant of the operator (16). Formula (10) become

$$\begin{aligned}&\sum_n e^{-E_n t_0}\psi_n(x_f)\psi_n^*(x_i)\\ &\qquad = N e^{-S_0}\Big[\det\Big(-\frac{\mathrm{d}^2}{\mathrm{d}t^2} + V''(\bar{x})\Big)\Big]^{-1/2}.\end{aligned} \tag{19}$$

---

[2] Using the label 'Euclidean' might seem unmotivated and out of place. However, it makes perfect sense in relativistic theories, which we will not discuss in this work.

[3] Mathematicians call it the method of steepest descent.

[4] Remember that V goes to $-V$ in the Euclidean theory.

[5] This operator is similar to the Hamiltonian in Schrödinger mechanics i.e. it is Hermitian, and thus its eigenfunctions form a complete set.

Before we continue, it is worth noting several points:

1. We have assumed there is only one stationary point. If there is more than one, one has to sum the contributions of all of them. This will become important when we consider tunneling.

2. One might question the limits of the Gaussian integral in (18). After all, the set x_n is supposed to span *all* possible paths that satisfy the boundary conditions, and if we allow c_n to vary without bounds, δx will vary arbitrarily as well i.e. the 'smallness' of δx should constrain the length of the vector c_n. While this is partially true, what we are interested in is the integral itself, and the integral receives the most contribution around the center of the Gaussian ($c_n = 0$ in our case). Therefore, we can extend the limits of the integral to infinity at the cost of a minor numerical error.

3. In evaluating (18), we have assumed that the spectrum of the operator (16) is positive-definite. Otherwise, the integral would diverge. A simple argument eliminates the possibility of negative eigenvalues: ε_n signifies the response of S as we perturb $\bar{x}$ along the direction x_n in the function space. Since $S[\bar{x}]$ is a minimum of S, any perturbation will either increase the value of S or keep it unchanged.[6] The former corresponds to $\varepsilon_n > 0$ while the latter corresponds to $\varepsilon_n = 0$, which are called zero-frequency modes. We shall see later that the problem of these zero-frequency modes can be solved by integrating over what is called a collective coordinate.

II. THE HARMONIC OSCILLATOR

Most of what follows starting from this section can be found in [2–4].

We now study the case of a particle in a quadratic potential $V(x) = \omega^2 x^2/2$. Although this problem has been studied extensively using more conventional methods, we reproduce some of the well-known results as they will serve as an intermediate step when we analyze tunneling through a barrier in the next section. We have $V'' = \omega^2$ and the differential operator becomes

$$-\frac{\mathrm{d}^2}{\mathrm{d}t^2} + \omega^2. \tag{20}$$

This operator is similar to the Hamiltonian of a particle in a box of width a (and an energy shift ω^2):

$$H = -\frac{1}{2}\frac{\mathrm{d}^2}{\mathrm{d}x^2} + \omega^2, \qquad E_n = \frac{n^2\pi^2}{2a^2} + \omega^2, \quad n = 1, 2, 3, \ldots \tag{21}$$

and we immediately read off the eigenvalues of (20):

$$\varepsilon_n = \frac{n^2\pi^2}{t_0^2} + \omega^2, \qquad n = 1, 2, 3, \ldots. \tag{22}$$

The next step is to fix N. We do that by rewriting the infinite product in the determinant as

$$\begin{aligned} N\left(\prod_{n=1}^{\infty} \frac{n^2\pi^2}{t_0^2} + \omega^2\right)^{-1/2} \\ = \left[N\left(\prod_{n=1}^{\infty} \frac{n^2\pi^2}{t_0^2}\right)^{-1/2}\right]\left[\prod_{n=1}^{\infty}\left(1 + \frac{\omega^2 t_0^2}{n^2\pi^2}\right)\right]^{-1/2}. \end{aligned} \tag{23}$$

The first square bracket would be the determinant had we started with $V(x) = 0$ and must give the result for a (free) particle in a box of width t_0 with $E_n = p_n^2/2$ and p_n is the momentum. By taking $x_i = x_f = 0$, S_0 vanishes, and in the limit of large t_0, ε_n approaches a continuum, and we can use the plane wave solutions as our eigenstates.

$$\begin{aligned} N\left(\prod_{n=1}^{\infty} \frac{n^2\pi^2}{t_0^2}\right)^{-1/2} &= \langle 0|e^{-p^2 t_0/2}|0\rangle \\ &= \int_{-\infty}^{\infty} \frac{\mathrm{d}p}{2\pi}\, e^{-p^2 t_0/2} = \frac{1}{\sqrt{2\pi t_0}}. \end{aligned} \tag{24}$$

Our choice of x_i and x_f is not random; it is the only choice that gives finite S_0 to avoid any potential problems associated with the vanishing of the exponential term on the right-hand side of (19). The integral is obtained by considering the representation of the state $|0\rangle$ in the momentum space, which is easily found by taking the Fourier transform of $\langle x|0\rangle = \delta(x)$.

The final remaining step is to evaluate the second square bracket in (23). The product can be readily evaluated, we quote the final result here:

$$\prod_{n=1}^{\infty}\left(1 + \frac{\omega^2 t_0^2}{n^2\pi^2}\right) = \frac{1}{\omega t_0}\sinh(\omega t_0). \tag{25}$$

Piecing everything together we arrive at the final result:

$$\begin{aligned} \sum_n e^{-E_n t_0}|\psi_n(0)|^2 &= \frac{1}{\sqrt{2\pi t_0}}\left(\frac{1}{\omega t_0}\sinh(\omega t_0)\right)^{-1/2} \\ &= \sqrt{\frac{\omega}{\pi}}\,(2\sinh(\omega t_0))^{-1/2} \\ &= \sqrt{\frac{\omega}{\pi}}\, e^{-\omega t_0/2}\left(1 + \frac{1}{2}e^{-2\omega t_0} + \ldots\right), \end{aligned} \tag{26}$$

---

[6] This argument obviously fails if $\bar{x}$ was a maximum or a saddle point of S. Fortunately, in the majority of the cases S will indeed be minimized.

reproducing the spectrum of the harmonic oscillator. Namely, $E_0 = \omega/2$ with $|\psi_0(0)|^2 = \sqrt{\omega/\pi}$, $E_2 = 5\omega/2$ with $|\psi_2(0)|^2 = \frac{1}{2}\sqrt{\omega/\pi}$, etc. Notice that only terms with even n appear in the series, since $\psi_n(0) = 0$ for odd n. The results are exact, and this is due to the fact that all higher-order variational derivatives of S vanish for a quadratic potential, making (15) exact.

III. TUNNELING IN A QUARTIC POTENTIAL

Suppose we now place our particle in a double-well potential $V(x) = \lambda(x^2 - \eta^2)^2$. This potential has two minima at $x = \pm\eta$, with a frequency of oscillation $\omega^2 = 8\lambda\eta^2$ which may be found by looking at the quadratic term in the expansion of $V(x)$ around $x = \pm\eta$. The height of the barrier separating the two wells is $V(0) = \omega^4/64\lambda$. In the limit $\lambda \to 0$, the barrier is of infinite height and the ground state of the system is doubly degenerate; the particle oscillates near $x = -\eta$ or $x = \eta$. However, if λ is set to a small, albeit non-zero, value, the degeneracy is broken. If the particle was initially at $-\eta$, it can tunnel through the barrier and there is a non-zero probability that we find it at η at a later time. The true ground state is an even combination between the previously degenerate states, and an odd combination has a slightly higher energy. The difference between the two energy levels goes like $e^{-1/\lambda}$ i.e. it vanishes faster than any (positive) power of λ, and thus perturbation theory cannot be used in this problem.

In this section we will show how tunneling can be understood in the context of the Euclidean theory and we will reproduce the results of the WKB scheme.

A. The Instanton Solution

Like before, we look for stationary points of the classical action with the inverted potential. Two trivial solutions are $\bar{x}(t) = -\eta$ and $\bar{x}(t) = \eta$, corresponding to the particle sitting at the top of either humps, and the analysis is identical to what we did in the preceding section. There exists, however, another family of topologically nontrivial solutions with finite action that connect the points $-\eta$ and η.[7] Such solutions correspond to the particle sliding from one hump to the other. In the limit of large t_0, the total energy $E = \dot{\bar{x}}^2/2 - V(\bar{x})$ is zero (for the particle to take infinite time to slide from one hump to the other, it must start with ~ 0 kinetic energy). This equation can be readily integrated to find $\bar{x}(t)$:

$$\dot{\bar{x}} = -\frac{\omega}{2\eta}(\bar{x}^2 - \eta^2) \tag{27}$$

$$\int \mathrm{d}\bar{x}\,\frac{-1}{\bar{x}^2 - \eta^2} = \frac{\omega}{2\eta}\int \mathrm{d}t$$

$$\frac{1}{\eta}\tanh^{-1}\frac{\bar{x}}{\eta} = \frac{\omega}{2\eta}(t - t_c)$$

$$\bar{x}(t, t_c) = \eta \tanh\frac{\omega(t - t_c)}{2}, \tag{28}$$

where t_c is an integration constant and indicates the center of the solution.[8] The particle starts at $-\eta$ and slides to η. This solution is called the 'instanton'.[9] By substituting t with $-t$ (corresponding to the positive root in (27)), we get the 'anti-instanton' solution where the particle starts at η and ends up at $-\eta$. The action of the instanton (and anti-instanton) is

$$S_0 = \int_{-\infty}^{\infty} \mathrm{d}t\,\dot{\bar{x}}^2 = \int_{-\eta}^{\eta} \mathrm{d}\bar{x}\,\sqrt{2V(\bar{x})} = \frac{\omega^3}{12\lambda}, \tag{29}$$

and so we have evaluated the exponential term in (19). We stop to make a couple of comments:

1. The exponential e^{-S_0} is similar to the tunneling amplitude we get from the WKB method. This is in fact no coincidence, and holds generally for similar problems [5].
2. The action does not depend on t_c, and this is expected from the time translation symmetry of the original Lagrangian, that is the time origin can be chosen to be any value. This suggests that we have to take into account the contribution an infinite number of instantons (and anti-instantons), and this will be the subject of the following sections.

B. Zero-Frequency Mode

Our next task is to calculate the determinant. There is more than one approach to this problem. A particularly interesting and relatively quick one is developed by Coleman in his lectures [3]. However, many key points can be easily missed if the reader is not careful enough, so we resort to a more direct, yet more laborious, approach [2].

---

[7] They are topological in the sense that one cannot continuously *deform* a function in one topological class to another class while keeping the action finite.

[8] We emphasize the dependence of $\bar{x}$ on t_c as it will be relevant soon.

[9] The term 'instanton' was coined by 't Hooft. The reason is that instantons are very similar in structure to solitons, particle-like solutions of field theories, and thus the -on. They are also functions of time, hence the instant-. Another name used in the literature, invented by Polyakov, is 'pseudoparticle', since they are particle-like solutions in imaginary time.

We calculate the contribution of one instanton ($t_c = 0$ for simplicity). We have $V''(x) = 12\lambda x^2 - 4\lambda\eta^2$. Substituting with the explicit form of $\bar{x}(t)$ from (28) in (16) we get

$$\begin{aligned}-\ddot{x}_n + 8\lambda\eta^2\left(\frac{3}{2}\tanh^2\frac{\omega t}{2} - \frac{1}{2}\right)x_n \\ = -\ddot{x}_n + \omega^2\left(1 - \frac{3}{2}\operatorname{sech}^2\frac{\omega t}{2}\right)x_n = \varepsilon_n x_n. \quad (30)\end{aligned}$$

This equation is satisfied by the associated Legendre polynomials [6]. In the limit of large t_0, it admits (in the context of quantum mechanics) discrete bound states as well as a continuum of scattering states. First we will consider the discrete levels, which are given by

$$\varepsilon_n = \omega^2 - \frac{\omega^2}{16}(4 - 2n)^2, \qquad n = 0, 1 \qquad (31)$$

i.e. $\varepsilon_0 = 0$ and $\varepsilon_1 = 3\omega^2/4$. We now encounter a zero-frequency mode, and the integral over c_0 will make the functional integral (18) diverge. Fortunately, there is a pleasant trick to remedy this problem and will be the subject of this section.

The normalized eigenfunction for $\varepsilon_0 = 0$ is

$$x_0(t) = -\sqrt{\frac{3\omega}{8}}\operatorname{sech}^2\frac{\omega t}{2}, \qquad (32)$$

and it represents the direction in the function space along which S remains unchanged. One immediately suspects that this direction is related to the indifference of the system to the choice of t_c. To show this we consider a perturbation on S_0 by varying t_c (which is zero since S_0 does not depend on t_c):

$$\delta S_0 = \int_{-\infty}^{\infty} \mathrm{d}t\, 2\dot{\bar{x}}\,\frac{\mathrm{d}\dot{\bar{x}}}{\mathrm{d}t_c}\,\delta t_c = \int_{-\infty}^{\infty}\mathrm{d}t\, 2\dot{\bar{x}}\left(-\frac{\mathrm{d}\dot{\bar{x}}}{\mathrm{d}t}\right)\delta t_c.^{10} \qquad (33)$$

In the function space this variation takes the form

$$\delta S_0 = \int_{-\infty}^{\infty}\mathrm{d}t\, 2\dot{\bar{x}}\,\delta\dot{x} = \int_{-\infty}^{\infty}\mathrm{d}t\, 2\dot{\bar{x}}c_0\dot{x}_0. \qquad (34)$$

Comparing both forms we conclude that x_0 is proportional to $\dot{\bar{x}}$. We can fix the proportionality constant by normalizing x_0:

$$\int_{-\infty}^{\infty}\mathrm{d}t\, x_0^2 = 1 = A^2\int_{-\infty}^{\infty}\mathrm{d}t\,\dot{\bar{x}}^2 = A^2 S_0 \;\Rightarrow\; A = -\frac{1}{\sqrt{S_0}},$$

or

$$x_0(t) = -\frac{1}{\sqrt{S_0}}\,\dot{\bar{x}}(t). \qquad (35)$$

It is easy to check that (32) and (35) are indeed equivalent. Furthermore, the equivalence of the expressions (33) and (34) suggests that we can replace the integration over c_0 with an integration over t_c. In the literature, t_c is called a collective coordinate. To find how the two variables are related, consider how an infinitesimal change $\mathrm{d}c_0$ affects $\bar{x}$:

$$\mathrm{d}\bar{x} = x_0\,\mathrm{d}c_0.$$

Next, consider how changing t_c changes $\bar{x}$:

$$\mathrm{d}\bar{x} = \frac{\mathrm{d}\bar{x}}{\mathrm{d}t_c}\,\mathrm{d}t_c = -\dot{\bar{x}}\,\mathrm{d}t_c = \sqrt{S_0}\,x_0\,\mathrm{d}t_c.$$

From these two relations we arrive at

$$\mathrm{d}c_0 = \sqrt{S_0}\,\mathrm{d}t_c \qquad (36)$$

which not only solves the problem of the divergent integral, but also takes into account the contribution of instantons with different centers, which was what we commented on at the end of the previous section.[11] This result is actually quite general; for systems with multiple zero-frequency modes, we obtain a factor of $\sqrt{S_0}$ for each mode. We will perform the integral in due time.

C. Positive-Frequency Modes

When it comes to evaluating the rest of the determinant, it is often convenient to use the determinant of the harmonic oscillator as such:

$$\begin{aligned}&\left[\det\left(-\frac{\mathrm{d}^2}{\mathrm{d}t^2} + V''(\bar{x})\right)\right]^{-1/2} \\ &= \sqrt{\frac{S_0}{2\pi}}\left[\det\left(-\frac{\mathrm{d}^2}{\mathrm{d}t^2} + \omega^2\right)\right]^{-1/2} \times \\ &\left[\frac{\det'(-\mathrm{d}^2/\mathrm{d}t^2 + V''(\bar{x}))}{\omega^{-2}\det(-\mathrm{d}^2/\mathrm{d}t^2 + \omega^2)}\right]^{-1/2}\omega\,\mathrm{d}t_c, \qquad (37)\end{aligned}$$

where $\det'$ is the determinant without ε_0. The contribution of ε_1 is known, and we calculate the contribution of the continuum. The solutions to (30) have the asymptotic form

$$\begin{aligned} x_p^+(t) &\sim e^{ipt} && \text{as} \quad t \to \infty \\ x_p^+(t) &\sim e^{ipt + i\Lambda_p} && \text{as} \quad t \to -\infty, \qquad (38)\end{aligned}$$

where p is related to the continuous eigenvalue ε by $p = \sqrt{\varepsilon - \omega^2}$ and the phase $e^{i\Lambda_p}$ has the form

$$e^{i\Lambda_p} = \frac{1 + ip/\omega}{1 - ip/\omega}\,\frac{1 + 2ip/\omega}{1 - 2ip/\omega}. \qquad (39)$$

---

[10] Recall that $\bar{x} = \bar{x}(t - t_c)$, so we can exchange the derivative with respect to t_c with a time derivative at the cost of a minus sign.

[11] . The integral is still naively divergent, since t_c extends from $-t_0/2$ to $t_0/2$, which extends to infinity. What we really did is contextualize this divergence into a sensible limit ($t_0 \to \infty$) that we can deal with later.

A general solution $x_p(t)$ is a linear combination of $x_p^+(t)$ and $x_p^-(t) = x_p^+(-t)$. By using the boundary conditions $x_p(\pm t_0/2) = 0$, it is possible to evaluate the second bracket of (37):

$$\frac{\det'(-\mathrm{d}^2/\mathrm{d}t^2 + V''(\bar{x}))}{\omega^{-2}\det(-\mathrm{d}^2/\mathrm{d}t^2 + \omega^2)} = \frac{1}{9\omega^2}\,\varepsilon_1 = \frac{1}{12} \tag{40}$$

and we obtain the nice formula[12]

$$\begin{aligned}\langle\eta|e^{-Ht_0}|-\eta\rangle_1 &= \langle-\eta|e^{-Ht_0}|\eta\rangle_1 \\ &= Ne^{-S_0}\left[\det\left(-\frac{\mathrm{d}^2}{\mathrm{d}t^2} + V''(\bar{x})\right)\right]^{-1/2} \\ &= \left(\sqrt{\frac{\omega}{\pi}}\,e^{-\omega t_0/2}\right)\left(\sqrt{\frac{6S_0}{\pi}}\,e^{-S_0}\right)\omega\,\mathrm{d}t_c,\end{aligned} \tag{41}$$

where we have kept only the leading term in the harmonic oscillator expansion (26). The 1 in the subscript indicates that this is the contribution of one instanton (or anti-instanton).

D. Dilute Instanton Gas

The last element of the solution is noticing that the one-instanton solution is not the only classical path. A string of widely separated instantons and anti-instantons, corresponding to the particle going back and forth between the humps, constitutes a possible (approximate) classical path with finite S_0 as well. Exactly how widely seperated they have to be can be deduced from looking at the asymptotic (large t) behavior of the instanton. We know that at large t, $\bar{x}$ approaches η. Therefore, we can expand (28) about $\bar{x} = \eta$:

$$\dot{\bar{x}} \approx -\omega(\bar{x} - \eta)$$

or

$$\bar{x} - \eta \sim e^{-\omega t}. \tag{42}$$

Thus, instantons are well-localized in time, with a size of order $1/\omega$. This means that for successive instantons and anti-instanons to be sufficiently separated, their centers have to be seperated by an amount much larger than $1/\omega$.

We construct the solution by attaching n instantons and anti-instantons with centers t_i such that $-t_0/2 < t_1 < t_2 < \cdots < t_n < t_0/2$. This setup is called the dilute instanton gas; it is dilute in the sense that the instantons do not interact with each other.[13] We note that if it were not for the transitions near the centers, V'' would be ω^2 for all t, leaving us with the harmonic oscillator solution. Therefore, this n-particle setup will modify the harmonic oscillator solution. We read off the correction factor from (41):

$$\left(\sqrt{\frac{6S_0}{\pi}}\,e^{-S_0}\right)^n \prod_{i=1}^{n}\omega\,\mathrm{d}t_i \equiv \rho^n \prod_{i=1}^{n}\omega\,\mathrm{d}t_i, \tag{43}$$

where ρ is the instanton density. Now we finally evaluate the integral over the centers:

$$\begin{aligned}\sqrt{\frac{\omega}{\pi}}\,e^{-\omega t_0/2}\rho^n\omega^n \int_{-t_0/2}^{t_0/2}\mathrm{d}t_n \cdots \int_{-t_0/2}^{t_3}\mathrm{d}t_2 \int_{-t_0/2}^{t_2}\mathrm{d}t_1 \\ = \sqrt{\frac{\omega}{\pi}}\,e^{-\omega t_0/2}\,\frac{(\rho\omega t_0)^n}{n!}.\end{aligned} \tag{44}$$

The limits of the integrals mean that each center can be anywhere from $-t_0/2$ up to the consecutive center. The last remaining step is to sum over n. If the particle starts at $\pm\eta$ and ends up at $\mp\eta$, then only odd n contribute. Likewise, if it starts and finishes at the same point, only even n contribute.

$$\begin{aligned}\langle\pm\eta|e^{-Ht_0}|\pm\eta\rangle &= \sqrt{\frac{\omega}{\pi}}\,e^{-\omega t_0/2}\sum_{\text{even}\,n}\frac{(\rho\omega t_0)^n}{n!} \\ &= \sqrt{\frac{\omega}{\pi}}\,e^{-\omega t_0/2}\cosh(\rho\omega t_0) \\ &= \frac{1}{2}\sqrt{\frac{\omega}{\pi}}\left(e^{-\omega(1/2-\rho)t_0} + e^{-\omega(1/2+\rho)t_0}\right),\end{aligned} \tag{45}$$

$$\begin{aligned}\langle\pm\eta|e^{-Ht_0}|\mp\eta\rangle &= \sqrt{\frac{\omega}{\pi}}\,e^{-\omega t_0/2}\sum_{\text{odd}\,n}\frac{(\rho\omega t_0)^n}{n!} \\ &= \sqrt{\frac{\omega}{\pi}}\,e^{-\omega t_0/2}\sinh(\rho\omega t_0) \\ &= \frac{1}{2}\sqrt{\frac{\omega}{\pi}}\left(e^{-\omega(1/2-\rho)t_0} - e^{-\omega(1/2+\rho)t_0}\right).\end{aligned} \tag{46}$$

Both expressions lead to two closely-spaced energy levels

$$E_\pm = \frac{\omega}{2} \pm \rho\omega = \frac{\omega}{2} \pm \omega\sqrt{\frac{\omega^3}{2\pi\lambda}}\,e^{-\omega^3/12\lambda} \tag{47}$$

which are, of course, identical to the result obtained from the WKB method. Furthermore, if we look at the coefficients of the exponentials in (45) and (46) we find that

$$|\psi_\pm(\eta)|^2 = |\psi_\pm(-\eta)|^2 = \frac{1}{2}\sqrt{\frac{\omega}{\pi}},$$

$$\psi_\pm(\eta)\psi_\pm^*(-\eta) = \psi_\pm(-\eta)\psi_\pm^*(\eta) = \mp\frac{1}{2}\sqrt{\frac{\omega}{\pi}},$$

---

[12] The analysis for the anti-instanton is identical, since $V''(\bar{x}(t))$ is an even function in t.

[13] It is called this way because it is similar to the dilute gas approximation in statistical mechanics.

from which we deduce

$$\psi_\pm(\eta) = \mp\psi_\pm(-\eta) \tag{48}$$

i.e. the true ground state ψ_- is indeed the spatially even combination, and the first excited state ψ_+ is the odd combination, with the particle having equal probability to be at η or $-\eta$.

It is important to note that nowhere have we explicitly taken any measures to ensure that the instantons are sufficiently separated. However, this is already taken care of by the summations in (45) and (46). The series $\sum x^n/n!$ is dominated by the terms with $n \sim x$. In our case, we have $n \sim \rho\omega t_0$ or $n/t_0 \sim \rho\omega$ i.e. the number of instantons in a time interval is of order ρ. Therefore, by taking ρ to be small (by taking λ small), we are ensured that the gas is dilute enough.

IV. PERIODIC POTENTIALS

Suppose now that our potential has an infinite number of wells with minima at $x = 0, \pm1, \pm2$, etc. The analysis is the same as before up to the point where we sum over n. When we had only two humps, the particle was only allowed to swing back and forth which restricted us to a string of alternating instantons and anti-instantons. On the other hand, for a periodic potential with infinite humps, we lose this restriction; the particle can go back and forth, but it can also go forward skipping 20 humps then roll back 2 humps, then roll forward again *ad infinitum.*

Mathematically speaking, this is implemented by summing (44) over instantons and anti-instantons independently while constraining the difference between their numbers to be equal to the net change in the position of the particle. We have the equation

$$\langle m|e^{-Ht_0}|m'\rangle = \sqrt{\frac{\omega}{\pi}}e^{-\omega t_0/2}\times \sum_{n,n'=0}^{\infty} \frac{(\rho\omega t_0)^{n+n'}}{n!n'!}\,\delta_{(n-n')(m-m')}, \tag{49}$$

where n and n' are the numbers of instantons and anti-instantons, respectively, and m and m' are the final and initial positions of the particle, respectively. By using the identity for δ_{mn} as a contour integral

$$\delta_{mn} = \frac{1}{2\pi i}\oint_{|z|=1} \mathrm{d}z\, z^{m-n-1} = \frac{1}{2\pi}\int_0^{2\pi} \mathrm{d}\theta\, e^{i(m-n)\theta}, \tag{50}$$

(49) becomes two independent exponential series:

$$\begin{aligned}\langle m|e^{-Ht_0}|m'\rangle =&\sqrt{\frac{\omega}{\pi}}\,e^{-\omega t_0/2}\,\frac{1}{2\pi}\int_0^{2\pi}\mathrm{d}\theta\, e^{i(m'-m)\theta}\times\\ &\sum_{n=0}^{\infty}\frac{(\rho\omega t_0 e^{i\theta})^n}{n!}\sum_{n'=0}^{\infty}\frac{(\rho\omega t_0 e^{-i\theta})^{n'}}{n'!}\\ =&\sqrt{\frac{\omega}{\pi}}\,e^{-\omega t_0/2}\,\frac{1}{2\pi}\int_0^{2\pi}\mathrm{d}\theta\,\big[e^{i(m'-m)\theta}\times\\ &e^{\rho\omega t_0 e^{i\theta}}e^{\rho\omega t_0 e^{-i\theta}}\big]\\ =&\sqrt{\frac{\omega}{\pi}}\,e^{-\omega t_0/2}\,\frac{1}{2\pi}\int_0^{2\pi}\mathrm{d}\theta\, e^{i(m'-m)\theta}e^{2\rho\omega\cos\theta\, t_0},\end{aligned} \tag{51}$$

from which we deduce the energy levels (as a function of the continuous angle θ)

$$E(\theta) = \frac{\omega}{2} - 2\omega\sqrt{\frac{\omega^3}{2\pi\lambda}}\cos\theta\, e^{-\omega^3/12\lambda}, \tag{52}$$

and (invoking the completeness statement $\int_0^{2\pi}\mathrm{d}\theta\,|\theta\rangle\langle\theta| = 1$)

$$\langle\theta|m\rangle = \left(\frac{\omega}{\pi}\right)^{1/4}\frac{1}{\sqrt{2\pi}}\,e^{im\theta}. \tag{53}$$

These are, naturally, the results we obtain from Bloch's theorem, which is the traditional treatment for periodic potentials.

---

[1] R. Feynmanand A. Hibbs, *Quantum mechanics and path integrals*, International series in pure and applied physics (McGraw-Hill, 1965).

[2] A. I. Vainshtein, V. I. Zakharov, V. A. Novikov, and M. A. Shifman, ABC's of Instantons, Sov. Phys. Usp. **25**, 195 (1982), [,201(1981)].

[3] S. R. Coleman, The Uses of Instantons, *Instantons in gauge theories*, Subnucl. Ser. **15**, 805 (1979), [,382(1978)].

[4] R. Rajaraman, *Solitons and Instantons. An Introduction to Soltions and Instantons in Quantum Field Theory* (1982).

[5] L. Ryder, *Quantum Field Theory* (Academic Publishers, 1985).

[6] L. Landauand E. Lifshitz, *Quantum Mechanics: Non-Relativistic Theory*, Course of Theoretical Physics (Elsevier Science, 1981).

The integer quantum Hall effect

Le Huu Thong

(Dated: June 19, 2019)

The quantum Hall effect is one of the most important discoveries since the late 20th century. This paper provides explanation for the precise plateaux of resistivity observed in quantum Hal experiment, requiring just basic quantum mechanics of most undegraduates. After reviewing the classical Hall effect, we get on the quantum regime by considering Landau quantization of electron states in a magnetic field. The precisely quantized resistivity is then derived for an idealized sample. Finally, an account for impurities in real sample will explain fully the Hall experiment.

I. INTRODUCTION

In 1980, von Klitzing discovered the integer quantum Hall effect, which brought him a Nobel proze in 1985 [4].

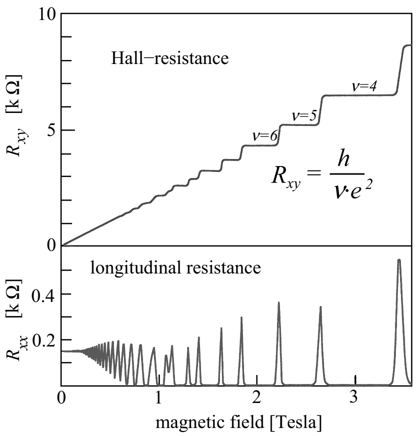

Figure 1: Hall resistance R_{xy} and longitudinal resistance R_{xx} in integer quantum Hall effect.

The integer quantum Hall effect is observed in two-dimensional electron gas, under low temperature and strong magnetic length. When the magnatic field is varied, the Hall resistivity exhibits quantized value

$$\rho_{xy} = \frac{1}{\nu}\frac{2\pi\hbar}{e^2}, \nu \in \mathbf{Z}$$

with abrupt transition between plateaux. Also, the plateaux ρ_{xy} is accompanied with zero values of longitudinal resistivity ρ_{xx}. And when ρ_{xy} jumps between plateaux, ρ_{xx} peaks up together. More interestingly, the values of ν are measured with extrodinary precision – 10^{-9}. This is an exemplar for a stable quantum regime, despite the inescapable impurities in experiment samples.

Classical Hall effect

To appreciate the striking quantum behavior, let us review the classical approximation. The Drude model equation of motion, which incorporates scattering effect in the parameter τ (relaxation time)

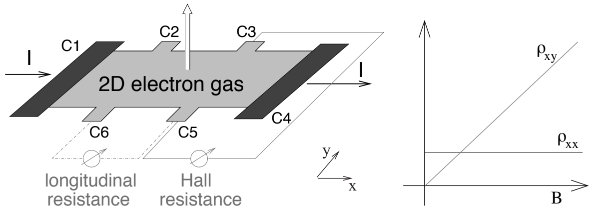

Figure 2: Left: the Hall experiment set-up: $R_{xx} = V_x/I_x$ (longitudinal) and $R_{xy} = V_y/I_x$ (Hall); Right: resistivities in classical Hall effect.

$$m\frac{d\mathbf{v}}{dt} = -e\mathbf{E} - e\mathbf{v}\times\mathbf{B} - \frac{m\mathbf{v}}{\tau}. \tag{1}$$

In equilibrium, we expect $\frac{d\mathbf{v}}{dt} = 0$, and then arrive at

$$\mathbf{v} + \frac{e\tau}{m}\mathbf{v}\times\mathbf{B} = -\frac{e\tau}{m}\mathbf{E}. \tag{2}$$

Since $\mathbf{J} = -ne\mathbf{v}$, the above expression show linear dependence of $\mathbf{J}$ on $\mathbf{E}$

$$\begin{pmatrix} 1 & \omega_B\tau \\ -\omega_B\tau & 1 \end{pmatrix}\mathbf{J} = \frac{ne^2\tau}{m}\mathbf{E}, \quad \omega_B \equiv \frac{eB}{m}. \tag{3}$$

Identifying the above with Ohm's law $\mathbf{J} = \sigma\mathbf{E}$ gives

$$\rho = \frac{m}{ne^2\tau}\begin{pmatrix} 1 & \omega_B\tau \\ -\omega_B\tau & 1 \end{pmatrix} \tag{4}$$

$$\sigma = \frac{ne^2\tau}{m(1+\omega_B^2\tau^2)}\begin{pmatrix} 1 & -\omega_B\tau \\ \omega_B\tau & 1 \end{pmatrix}. \tag{5}$$

Thus in the classical approximation

$$\rho_{xx} = \frac{m}{ne^2\tau} \quad \text{and} \quad \rho_{xy} = \frac{B}{ne}. \tag{6}$$

We see that there is linear dependence of the Hall resistance on magnetic strength but not the plateaux as in the quantum case. And the vanishing of longitudinal resistance, as in the quantum case, may be attributed to infinite scattering time, or rather, zero dissipation on electron motion.

II. LANDAU QUANTIZATION

For the triangular geometry of the experiment, as described in figure 2, the Landau gauge is particularly useful since it preserves the translational symmetry in the x direction

$$\mathbf{A} = -yB\hat{\mathbf{x}}. \tag{7}$$

Translational invariance in x direction gives us

$$\psi_k(x, y) = e^{ikx} f_k(y), \tag{8}$$

that is to say, our basic set of functions can be chosen to be x-momentum eigenfunctions, similar to 1D free particles.
Without electric field

$$H_0 = \frac{1}{2m}(\mathbf{p} + e\mathbf{A})^2 = \frac{1}{2m}p_y^2 + \frac{1}{2m}(p_x + eBy)^2 \tag{9}$$

$$= \frac{1}{2m}p_y^2 + \frac{1}{2}m\omega_B^2(y + kl_B^2)^2, \quad l_B^2 = \frac{\hbar}{eB} \tag{10}$$

Due to the resemblance to the second harmonic oscillator, we can easily obtain the Landau spectrum in magnetic field

$$E_n = \hbar\omega_B(n + \frac{1}{2}), \quad \omega_B \equiv \frac{eB}{m} \tag{11}$$

$$\psi_{n,k}(x, y) = e^{ikx}\varphi_n(y + kl_B^2) \tag{12}$$

where φ_n are the well-known SHO solutions.

For simplicity, we ignore the spins of electrons in this whole treatment. Although the Zeeman splitting $g\mu_B B = g\frac{e\hbar}{2m}$ is equal to Landau level at first glance, this does not happen in real materials. On the one hand, the mass determining ω_B is the effective mass of the electron in solid $\omega_B = \frac{eB}{m_{eff}}$. On the other hand, the effective g factor may depends on the band structure as well. As an example, Landau level is 70 times bigger than Zeeman splitting in $GaAs$.

Since the spectrum does not depend on the x degrees of freedom, there is degenacy in each Landau levels n in (11). Considering a finite sample with size L_x, L_y. Since the wave functions (19) are localized about $y = -kl_B^2$ while $0 < y < L_y$, we expect

$$-L_y/l_B^2 < k < 0; \quad k = \frac{2\pi m}{L_x}, m \in \mathbf{Z}, \tag{13}$$

where the quantized values of k are due to periodic boundary condition along the x axis. Therefore the degeneracy is calculated to be

$$\frac{2\pi N}{L_x} = L_y/l_B^2 \Rightarrow N = \frac{eBL_xL_y}{2\pi\hbar} = \frac{\Phi}{\Phi_0}, \; \Phi_0 \equiv \frac{2\pi\hbar}{e} \tag{14}$$

Having derived the Landau quantization, we now turn on an electric field in the y direction $\mathbf{E} = E\hat{\mathbf{y}}$ to have the new Hamiltonian

$$H = \frac{1}{2m}p_y^2 + \frac{1}{2}m\omega_B^2(y + kl_B^2)^2 + eEy \tag{15}$$

$$= \frac{1}{2m}p_y^2 + \frac{1}{2}m\omega_B^2(y + kl_B^2 + \frac{eE}{m\omega_B^2})^2 \tag{16}$$

$$+ eE\left(-kl_B^2 - \frac{eE}{m\omega_B^2}\right) + \frac{1}{2}\frac{(eE)^2}{m\omega_B^2} \tag{17}$$

It is then easy to obtain the new Landau levels.

$$E_{nk} = \hbar\omega_B(n + \frac{1}{2}) + eE(-kl_B^2 - \frac{eE}{m\omega_B^2}) + \frac{m}{2}\frac{E^2}{B^2}, \tag{18}$$

$$\psi_{n,k}(x, y) = e^{ikx}\varphi_n\left(y + kl_B^2 + \frac{eE}{m\omega_B^2}\right) \tag{19}$$

where the first term represents oscillation energy, second term the electric potential energy and last term kinetic energy. The potential term is there because the wavefunctions are now localized at $y = kl_B^2 + \frac{eE}{m\omega_B^2}$.

But what is moving to give out that kinetic term? Well, since E_{nk} depends on k, all the electrons, in all Landau levels, exhibit drift along the x axis with the same group velocity

$$v_x = \frac{1}{\hbar}\frac{\partial E_{nk}}{\partial k} = -\frac{eEl_B^2}{\hbar} = -\frac{E}{B}. \tag{20}$$

That is, we have proved a drift current along the x axis, which is in the direction of $\mathbf{E} \times \mathbf{B}$ and perpendicular to the electric field. The Hall resistivity is going to arrive!

When ν Landau levels are filled

We are now able to explain the nicely quantized values $\frac{1}{\nu}\frac{2\pi\hbar}{e^2}$ advertised in the Introduction. Intuitively, we may see a connection between the quantized Landau levels and quantized Hall resistivities.

From the degeneracy (14) of each Landau levels, we see that the stronger the $\mathbf{B}$ field, the more electrons each level can accommodate. It is worthwhile attempting to answer what will happen if B reaches values that make exactly ν Landau levels filled? In that case, the 2D electron density

$$n = \nu\frac{N}{L_xL_y} = \nu\frac{eB}{2\pi\hbar} \Leftrightarrow B = \frac{2\pi\hbar n}{\nu e}. \tag{21}$$

With the drift velocity just derived, we can calculate the transverse current, and then the expected Hall resistivity for these particular values of B.

$$J_x = -nev_x = ne\frac{E}{B}, \tag{22}$$

$$\Rightarrow \rho_{xy} = -\frac{E}{J_x} = \frac{B}{ne} = -\frac{2\pi\hbar}{\nu e^2} \tag{23}$$

Bravo! We have in part explained the quantized values observed in figure 1. In the next section, we will see that it is the macrosopic disorders in the sample that causes the quantized resistivities to exist within a wide range of B.

III. THE ROLE OF DISORDERS

Having explained the quantized values of resistivity, we still need to account for the plateaux of these values over a wide range of B. And also, how do the levels come out exact despite the inescapable impurities in real samples.

We will model both the electric field and inpurities by adding a potential V to the Hamiltonian (15), and impose contraints on it to give out the quantum Hall effect. The first one is that impurities is small compared to Landau levels splitting $V \ll \hbar\omega_B$. The second is that V does not change appreciably on the magnetic length scale $|\Delta V| \ll \dfrac{\hbar\omega_B}{l_B}$.

First, we will prove that electrons will drift along equipotentials of V. We remember that classically, a free electron under a magnetic field will move in circles with cyclotron frequency.

$$m\frac{d\mathbf{v}}{dt} = -e\mathbf{v}\times\mathbf{B} \tag{24}$$

$$\Rightarrow \begin{cases} x(t) = X - R\sin(\omega_B t + \phi) \\ x(t) = X + R\cos(\omega_B t + \phi) \end{cases}, \tag{25}$$

where X and Y are center of the orbit.
Motivated by the above classical analog, we introduce the center-of-orbit quantum operator

$$\begin{cases} X = x + \dfrac{v_y}{\omega_B} \\ Y = y - \dfrac{v_x}{\omega_B} \end{cases}. \tag{26}$$

We can straightforwardly prove the following result, which have been done this already in Problem 5.3: *General Aspects of Quantum Motion in a Magnetic Field* - MIT8.06x

$$[X, Y] = il_B^2 \tag{27}$$

$$\begin{cases} i\hbar\dot{X} = [X, H] = [X, H+V] = [X, V] \\ i\hbar\dot{Y} = [Y, H] = [Y, H+V] = [Y, V] \end{cases}. \tag{28}$$

$$\Rightarrow \begin{cases} i\hbar\dot{X} = [X, Y]\dfrac{\partial V}{\partial Y} = il_B^2\dfrac{\partial V}{\partial Y} \\ i\hbar\dot{Y} = [Y, X]\dfrac{\partial V}{\partial X} = il_B^2\dfrac{\partial V}{\partial X} \end{cases}. \tag{29}$$

It is seen from the above that the center-of-orbit of electrons will drift along the equipotentials of V. And due to the assumption that $|\Delta V| \ll \dfrac{\hbar\omega_B}{l_B}$, we don't have to care much about the cyclotron orbits of the electrons.

Although the impurities have broken translational symmetry, we can still develop our theory from derivation of Landau levels from section II.
Since the impurities is not too large $V \ll \hbar\omega_B$, it is intuitively clear that the density of states are now broaden around the old values $\hbar\omega_B(n + 1/2)$.

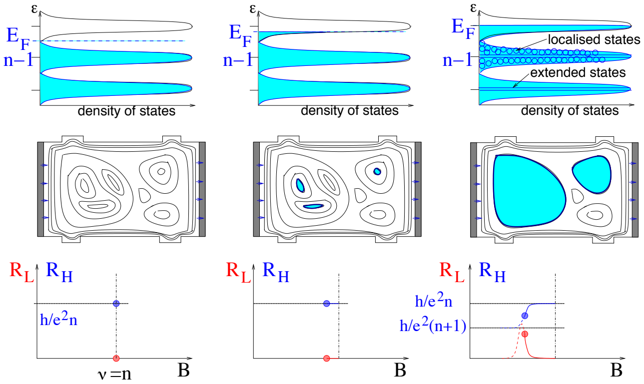

Figure 3: The quantum Hall resistivity corresponding to filling of Landau levels. First row: Density of state - Landau levels are broaden by impurities. Second rows: Potential V represented as landscape filled with electrons. Third rows: Corresponding measured resistivities

We have already considered the first column in figure 3, where exactly ν Landau levels are filled.

Now let us have a look at the shape of V in a particular sample in figure 3, which contains various peaks and troughs. In the second column, when B is decreased a little, each Landau levels can accomodate fewer electrons, so that a few electrons fill gradually fill up the next higher level. But these electrons now get unfortune by being trapped in the valleys of the potential landscape in the bulk of the sample and cannot contribute to the current across it. Therefore, the Hall resistivities remain on the plateau.

If the magnetic field B is lowered further, causing the next Landau levels be about half-filled, we see a transition of Hall resistivities between plateaux. That is because the valleys occupied by the electrons are now opened and linked together, letting the electrons to transit from localised states into extended states, thus contributing to the Hall resistivities again. As more electrons are involved, the resistance decreases and then reach the lower Hall plateau.

IV. DISCUSSION

We have seen that the precise quantized values of Hall resistivity has its origin from Landau level of electron under magnetic field

$$\rho_{xy} = \frac{2\pi\hbar}{\nu e^2}. \tag{30}$$

But for these values to be observed in experiments, in macroscopic sample, the diorders, while being random, have an important role. The main reason is that impurities create trap for the electrons inside the bulk of the material. And the trapped electrons cannot contribute to the current. Hence, when the magnetic field is varied around the proper values $B = \dfrac{2\pi\hbar n}{\nu e}$ in (23), the Hall resistivities happily stay on the plateau.
It is worth noting the significance of the Hall phenomenon. Usually, quantized values can be detected in microscopic level, such as the hydrogen spectral lines. But now we know that we ca bring the wonderful properties of the quantum world to macroscopic devices, open up a new horizon for awesome technology. In fact, in metrology, the integer quantum Hall effect is applied to give standard for resistance calibration, and the determination of fine-structure constant[4].

Acknowledgments

I would like to give thanks to the whole course team who give good advice and answers in the discussion forum of MIT8.06x. Furthermore, I appreciate my instructor Nguyen Huu Nha for introducing me to take on this wonderful course. And of course, I am so grateful that my finacial aid on edX was accepted so that I can earn my first MOOC certificate.

---

[1] M. O. Goerbig, *Quantum Hall Effects*, arXiv:0909.1998 [cond-mat.mes-hall].

[2] David Tong, *Lectures on the Quantum Hall Effect*, arXiv:1606.06687 [hep-th].
Note: although being pedagogical, the lectures may cause confusion between localized and extended states; geometry of the experiment is not presented, either.

[3] Steven M. Girvin, *The Quantum Hall Effect: Novel Excitations and Broken Symmetries*, arXiv:cond-mat/9907002 [cond-mat.mes-hall].

[4] J. Weis, *Quantum Hall Effect*, Encyclopedia of Condensed Matter Physics, 2005, Pages 22-29.

[5] Figure 2 is adapted from [4].
Figure 2 is adapted from [1].
Figure 3 is adapted from [1].

The integer quantum Hall effect

myq53

(Dated: June 15, 2019)

In 1879 Edwin Hall observed that a magnetic field B transverse to a plate, together with a current with density J flowing in one direction above the plate, induce an electric field E in a perpendicular direction in the plate. Classically, the resulting Hall conductance $\frac{J}{E}$ can be seen using the Lorentz Force Law to be a linear function of $\frac{1}{B}$. However in 1980 von Klitzing, Dorda, and Pepper discovered that in some settings the Hall conductance is exactly quantized in integer multiples of $\frac{e^2}{h}$. A year later, Robert Laughlin gave an elegant explanation of this by considering the effect of threading a quantum of flux through a ring. After setting up the needed background, we describe Laughlin's argument, showing how the adiabatic theorem implies that, as the flux is increased, one electron is transferred from the bottom of the ring to the top for each filled Landau level, and how this leads to the quantization of the conductance. We also describe a more topological argument due to Avron, Seiler, and Yaffe that adapts Laughlin's reasoning to a more general setting.

I. INTRODUCTION

An 1879 paper of Edwin Hall [2] reports on experiments in which a strip of gold leaf carrying a current was placed in a magnetic field passing perpendicular to the strip. This resulted in a potential difference between the two sides of the strip, perpendicular both to the current and to the electric field, and proportional to JB where J is the current density and B is the magnitude of the magnetic field. The fact that a magnetic field induces a potential difference perpendicular to the current in a two-dimensional conductor is now accordingly called the Hall effect.

Hall explained that his experiments were motivated by his (in retrospect well-founded) skepticism of an assertion by Maxwell that a current in a conductor subjected to a magnetic field will, in the steady state, "be found to be the same as if no magnetic force were in action." The Lorentz Force Law was not yet known in 1879, but once it was discovered it provided a simple explanation for the Hall effect: since $\mathbf{\hat{x}_1} \times \mathbf{\hat{x}_3} = -\mathbf{\hat{x}_2}$ a charge $-e$ with velocity $v\mathbf{\hat{x}_1}$ subjected to a magnetic field $B\mathbf{\hat{x}_3}$ experiences a force $\frac{evB}{c}\mathbf{\hat{x}_2}$; thus a current density $\vec{J} = J\mathbf{\hat{x}_1}$ (with $J > 0$) passing along a long thin strip will lead to a buildup of negative charge on the bottom (negative-x_2) edge of the strip and hence an electric field E in the negative x_2 direction that is proportional to JB. In particular the **Hall conductance**, namely the ratio $\sigma_{12} = \left|\frac{J}{E}\right|$, is proportional to $\frac{1}{B}$.[1]

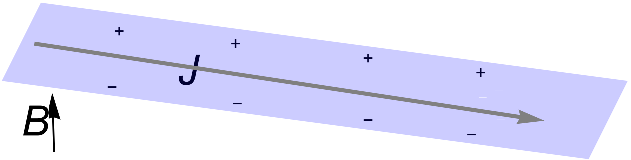

Figure 1. The Hall effect: a current flowing in the x_1 direction, in the presence of a magnetic field in the x_3 direction, leads to a potential difference in the x_2 direction.

About a century later, it was discovered [4] that, under certain conditions involving strong magnetic fields at low temperatures, the Hall conductance σ_{xy} takes only values of the form $\frac{e^2}{h}\nu$ where ν is an *integer*. When plotted as a function of the $\frac{1}{B}$, the conductance exhibits an increasing sequence of plateaus on each of which it remains constant to extremely high precision. Indeed this phenomenon is so robust that for some time it was used to obtain high-precision measurements of fundamental constants of nature; in 2018 the kilogram was redefined so as to make the quantum of Hall conductance $\frac{e^2}{h}$ take an exact value [3].

In this paper we explain two arguments that provide explanations for the quantization of the Hall conductance, at least in a modified setting where the strip is replaced by a ring or a torus (*i.e.*, periodic boundary conditions are imposed in the direction in which the current is flowing, or in both directions). The first argument, due to Laughlin [5], involves a thought experiment in which an additional magnetic flux is passed through the center of a ring. Laughlin's argument begins by considering a relatively simple special case that can be solved exactly, and extracts features from this special case—specifically, the statement that adiabatically increasing the flux from 0 to the special value $\Phi_0 = \frac{hc}{e}$ results in the transfer of an integer number of electrons from one edge of the ring to the other—that have good reason to persist in more realistic settings. The other argument that we discuss, based on [1], is somewhat more abstract in the sense that it does not involve describing explicit states or tracking the behavior of individual electrons, but rather explains the quantization of the Hall conductance in terms of Berry curvature. Correspondingly this argument is quite robust; in particular, unlike Laughlin's argument, it does not rely

---

[1] The reader will likely have noticed that this discussion is rather over-simplified: for instance we are neglecting the fact that the deflection given by the Lorentz force law means that the current is in fact not purely in the x direction. See [8, Section 1.2] for a more careful treatment.

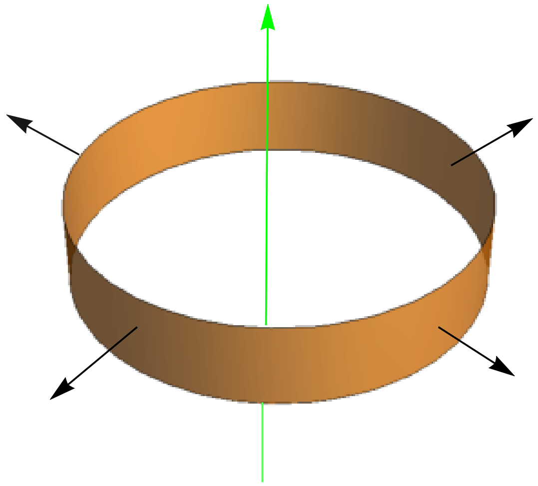

Figure 2. The setup of Laughlin's thought experiment for the Hall effect. The circumference of the ring is parametrized by x_1, and the height by x_2. The magnetic field producing the Hall effect is in black; Laughlin's hypothetical magnetic flux is represented by the green arrow. Note that the magnetic field producing this flux is not present at points on the ring, but does affect the vector potential there.

on disregarding interactions between electrons.

We now describe the organization of the paper. After setting up some notation and pointing out some very general features of the problem in Section II, in Section III we set up the problem and work out the energy levels for a single electron on a cylindrical ring in the presence of constant magnetic and electric fields and a flux passing through the center of the ring. In Section IV, following [5], we consider the effect of adiabatically varying the flux from 0 to the special value $\Phi_0 = \frac{hc}{e}$ (which returns the system to a gauge-equivalent version of itself). By relating the current J_x and the Hall electric field E to the effects of such a (hypothetical) variation, we manage to relate J_x and E to each other, and this relation demonstrates that the conductance σ_{xy} is indeed quantized in units of $\frac{e^2}{h}$. The problem solved in Sections III and IV is idealized; Section V gives a brief explanation of how Laughlin's reasoning persists in more realistic settings involving impure materials. Finally, Section VI explains the argument from [1] (which has antecedents in work such as [7]), which is based on properties of the Berry connection associated to varying two independent fluxes that thread through the respective circles given by two periodic coordinates.

II. GENERAL SETUP

Throughout the paper we will regard the system as consisting of a large number N of electrons having effective mass m^* and charge $-e$, on a two-dimensional surface parametrized by coordinates x_1, x_2 with $0 \leq x_j \leq L_j$. There will be a (constant-in-time) magnetic field orthogonal to the surface, given by a vector potential $(A_1(x_1, x_2), A_2(x_1, x_2))$ (so the magnetic field itself is $\partial_{x_1} A_2 - \partial_{x_2} A_1$).

We will always assume periodic boundary conditions for x_1, and in the last section will also assume them for x_2. Equivalently we are regarding x_1 (and possibly x_2) as varying over a circle rather than a line segment, and this will in fact be important for our arguments. While this might seem inconsistent with the setup of Figure 1, it should be noted that the current in the x_1 direction might be measured by a device that is attached to both the left and right ends of the rectangle, and if this device is regarded as part of the system then the geometry is cylindrical rather than rectangular. A similar remark applies to the measurement of the voltage (or electric field) in the x_2 direction.

The cylindrical geometry in which x_1 varies over the circle allows the possibility of passing a magnetic flux Φ_1 along the axis of the cylinder, as in Figure 2. While this contributes nothing to the magnetic field along the cylinder itself, it does make a contribution $\mathbf{A}_\Phi$ to the vector potential there: by Stokes' theorem, in order to produce flux Φ_1 through a disk with boundary C_1 running along the cylinder, we should have $\int_{C_1} \mathbf{A}_\Phi \cdot d\mathbf{r} = \Phi_1$. This (together with the fact that $\nabla \times \mathbf{A}_{\Phi_1} = \vec{0}$ along the ring) a uniquely specifies $\vec{A}_{\Phi_1}$ modulo addition of the gradient of a periodic-in-x function; the simplest choice is to take $\mathbf{A}_{\Phi_1} = \left(\frac{\Phi_1}{L_1}, 0\right)$. (Note that in our coordinates $d\mathbf{r} = (dx_1, 0)$.) Similarly if we are regarding x_2 as varying over a circle we can thread a flux Φ_2 through that circle, contributing an additional $\left(0, \frac{\Phi_2}{L_2}\right)$ to the vector potential. We will regard the fluxes Φ_1 and Φ_2 as parameters throughout the discussion; our arguments will consider the effect of varying these parameters adiabatically.

Write $\mathbf{x}^{(r)} = (x_1^{(r)}, x_2^{(r)})$ for the position of the rth electron. The operators $\hat{v}_j^{(r)}$ describing the jth component (for $j = 1, 2$) of the velocity of the rth electron will be

$$\hat{v}_{j,\Phi_j}^{(r)} = \frac{1}{m^*}\left(\frac{\hbar}{i}\frac{\partial}{\partial x_j^{(r)}} + \frac{e}{c}A_j(x_1^{(r)}, x_2^{(r)}) + \frac{e\Phi_j}{cL_j}\right) \tag{1}$$

and the Hamiltonian will be

$$\hat{H}(\Phi_1, \Phi_2) = \sum_{r=1}^{N} \frac{m^*}{2}\left((\hat{v}_{1,\Phi_1}^{(r)})^2 + (\hat{v}_{2,\Phi_2}^{(r)})^2\right) + V(\{\mathbf{x}^{(r)}\}_{r=1}^{N}) \tag{2}$$

for some potential energy function V. (The interpretation of $\hat{v}_{j,\Phi_j}^{(r)}$ as a velocity operator is justified by Ehrenfest's theorem and the fact that $[\hat{x}_j^{(r)}, \hat{H}(\Phi_1, \Phi_2)] = i\hbar \hat{v}^{(r)}_{j,\Phi_j}$.) The Hall effect relates the current density J_1 in the x_1 direction and an electric field in the x_2 direction. The electric field will be incorporated into the Hamiltonian, either through the choice of the potential function V (in Sections III and IV) or by taking the flux Φ_2 to be time-dependent (in Section VI). The x_1 component of the current density, meanwhile, is given as a quantum operator by

$$\hat{J}_1 = \frac{1}{L_1 L_2} \sum_{r=1}^{N} -e\hat{v}^{(r)}_{1,\Phi_1}. \tag{3}$$

It will be quite useful to relate this to the dependence of $\hat{H}$ on the flux parameter Φ_1, via the observation (cf. [5, Equation (1)])

$$\begin{aligned} \frac{\partial \hat{H}(\Phi_1, \Phi_2)}{\partial \Phi_1} &= m^* \sum_{r=1}^{N} \hat{v}^{(r)}_{1,\Phi_1} \frac{\partial \hat{v}^{(r)}_{1,\Phi_1}}{\partial \Phi_1} && (4) \\ &= \frac{e}{cL_1} \sum_{r=1}^{N} \hat{v}^{(r)}_{1,\Phi_1} && (5) \end{aligned}$$

and thus

$$\hat{J}_1 = -\frac{c}{L_2} \frac{\partial \hat{H}(\Phi_1, \Phi_2)}{\partial \Phi_1}. \tag{6}$$

III. LANDAU LEVELS IN THE PRESENCE OF AN ELECTRIC FIELD AND A THREADED FLUX

Our first step will be to analyze the case in which the potential V is given entirely by a constant electric field in the x_2 direction, contributing a term $eEx_2^{(r)}$ for each electron. (Note that we do not impose periodic boundary conditions in the x_2 variable in this section, and correspondingly the flux Φ_2 will always be zero.) We moreover take the magnetic field to be a constant B, and use Landau gauge $(A_1, A_2) = (-By, 0)$ for the vector potential. Thus the Hamiltonian decomposes as

$$\hat{H}(\Phi_1, 0) = \sum_{r=1}^{N} \hat{H}^{(r)}_{\Phi_1} \tag{7}$$

where each $\hat{H}^{(r)}_{\Phi_1}$ is given by the identical formula

$$\hat{H}^{(r)}_{\Phi} = \frac{1}{2m^*}\left(\left(\hat{p}_1 - \frac{eBx_2}{c} + \frac{e\Phi}{cL_1}\right)^2 + \hat{p}_2^2\right) + eEx_2. \tag{8}$$

(We suppress superscript (r)'s from the notation to reduce clutter.)

The energy states of $\hat{H}^{(r)}_{\Phi}$ exhibit a largely familiar pattern with Landau levels that we will now derive; the main difference from cases considered in class is that, when $E \neq 0$, the states within the same Landau level now have different energies, with the first component of the momentum contributing a linear term to the energy. Because $\hat{H}^{(r)}_{\Phi}$ commutes with $\hat{p}_1$, we can restrict attention to states that are eigenstates of $\hat{p}_1$ with eigenvalue $\hbar k$; such a state can be written as $\psi(x_1, x_2) = e^{ikx_1}\phi(x_2)$. Note that the fact that the variable x_1 is periodic with period L_1 means that the only allowed values of k are those with the property that $e^{ikL_1} = 1$, *i.e.* $k = 2\pi\ell/L_1$ for some $\ell \in \mathbf{Z}$.

A state $\psi(x_1, x_2) = e^{ikx_1}\phi(x_2)$ is an eigenstate of the Hamiltonian $\hat{H}_j$ if and only if ϕ is an eigenstate of the one-dimensional Hamiltonian

$$\begin{aligned} \hat{\mathcal{H}}_k &= \frac{1}{2m^*}\left(\left(\hbar k - \frac{eBx_2}{c} + \frac{e\Phi}{cL_1}\right)^2 + \hat{p}_2^2\right) + eEx_2 && (9) \\ &= \frac{\hat{p}_2^2}{2m^*} + \frac{m^*}{2}\left(\frac{eB}{m^*c}\right)^2\left(x_2 - \frac{\hbar kc}{eB} - \frac{\Phi}{BL_1}\right)^2 + eEx_2. && (10) \end{aligned}$$

Writing

$$\omega_c = \frac{eB}{m^*c}, \quad y(k) = \frac{\hbar k}{m^*\omega_c} + \frac{\Phi}{BL_1} - \frac{eE}{m^*\omega_c^2}, \tag{11}$$

we find

$$\begin{aligned} \hat{\mathcal{H}}_k &= \frac{\hat{p}_2^2}{2m^*} + \frac{m^*\omega_c^2}{2}\left(x_2^2 - 2\left(\frac{\hbar k}{m^*\omega_c} + \frac{\Phi}{BL_1} - \frac{eE}{m^*\omega_c^2}\right)x_2 \right. \\ &\qquad \left. + \left(\frac{\hbar k}{m^*\omega_c} + \frac{\Phi}{BL_1}\right)^2\right) && (12) \\ &= \frac{\hat{p}_2^2}{2m^*} + \frac{m^*\omega_c^2}{2}\left(x_2^2 - 2y(k)x_2 + \left(y(k) + \frac{eE}{m^*\omega_c^2}\right)^2\right) && (13) \\ &= \frac{\hat{p}_2^2}{2m^*} + \frac{m^*\omega_c^2}{2}\left((x_2 - y(k))^2 + \left(y(k) + \frac{eE}{m^*\omega_c^2}\right)^2 \right. \\ &\qquad \left. - y(k)^2\right) && (14) \\ &= \frac{\hat{p}_2^2}{2m^*} + \frac{m^*\omega_c^2}{2}(x_2 - y(k))^2 + eE\left(y(k) + \frac{eE}{2m^*\omega_c^2}\right). && (15) \end{aligned}$$

Thus we recognize in $\hat{\mathcal{H}}_k$ the Hamiltonian for a one-dimensional harmonic oscillator with frequency ω_c, but with its equilibrium position shifted to $x_2 = y(k)$ and its spectrum shifted uniformly upward by the constant (depending on k) $eE\left(y(k) + \frac{eE}{2m^*\omega_c^2}\right)$. The eigenvalues of the Hamiltonian $\hat{\mathcal{H}}_k$ (and hence, as k varies, the one-electron Hamiltonian $\hat{H}^{(r)}_{\Phi}$ for any r and Φ) are consequently, for any nonnegative integer n,

$$\mathcal{E}_{n,k} := \left(n + \frac{1}{2}\right)\hbar\omega_c + eE\left(y(k) + \frac{eE}{2m^*\omega_c^2}\right). \tag{16}$$

We regard the nth Landau level as consisting of states with the same value of n; since $y(k)$ depends on k we see that if $E \neq 0$ the Landau levels are not degenerate (so this is arguably an abuse of terminology). Given that $y(k)$ (which is a linear function of k with slope $\frac{\hbar}{m^*\omega_c} = \frac{\hbar c}{eB}$) is confined to an interval of length L_2 and that k is an integer multiple of $\frac{2\pi}{L_1}$, one finds that there are only (up to integer rounding) $\frac{eBL_1L_2}{hc}$ allowed values of k. Thus each Landau level consists of $\frac{eBL_1L_2}{hc}$ different states.

While the Landau levels are non-degenerate, we will assume throughout what follows that our parameters are chosen so that the variation of energy within a single Landau level is much smaller than the energy gap between successive Landau levels; since $y(k)$ varies through an interval of length L_2 this amounts to the statement that

$$eEL_2 \ll \hbar\omega_c = \frac{\hbar eB}{m^*c}. \tag{17}$$

In particular we are assuming that the magnetic field is large in comparison to the electric field.

IV. LAUGHLIN'S ADIABATIC FLUX THREADING ARGUMENT

We regard the magnetic flux Φ as an adiabatic parameter in our Hamiltonian $\hat{H}(\Phi, 0) = \sum_r \hat{H}_\Phi^{(r)}$. Note that the parameter $y(k)$ in (11) depends on Φ, and hence so do the energies $\mathcal{E}_{n,k}$ in (16). The adiabatic theorem implies that, as the flux Φ is varied slowly, if an electron is initially in a state with energy $\mathcal{E}_{n,k}$ it will (barring energy crossings, which we assume our parameters to forbid) continue to be in such a state throughout the variation. As this happens, its energy changes, at a rate

$$\frac{\partial \mathcal{E}_{n,k}}{\partial \Phi} = eE\frac{\partial y(k)}{\partial \Phi} = \frac{eE}{BL_x}. \tag{18}$$

Introducing the flux Φ amounts to adding the constant $(\Phi/L_1, 0)$ to the vector potential. If our conductor were a rectangle rather than a ring, this would be a symmetry of the whole system, corresponding to multiplication of the wave function by the phase $e^{\frac{ie\Phi}{L_1\hbar c}x_1}$. But since x_1 is periodic with period L_1 this phase is ill-defined unless $\frac{e\Phi}{\hbar c}$ is an integer multiple of 2π, *i.e.* unless Φ is a multiple of $\frac{hc}{e}$. The **quantum of flux** is defined to be

$$\Phi_0 = \frac{hc}{e}. \tag{19}$$

As we adiabatically vary Φ from 0 to Φ_0, the system passes through a family of inequivalent systems but finally returns to one equivalent to the original one; however the above discussion shows that the state of the system will have changed, with the expectation value $y(k)$ of the x_2 coordinate of each electron increasing by

$$\delta y = \frac{\Phi_0}{BL_1} = \frac{hc}{eBL_1}. \tag{20}$$

Recall that the momentum parameter k is quantized in integer multiples of $\frac{2\pi}{L_1}$. We find from (11) that

$$y\left(k + \frac{2\pi}{L_1}\right) - y(k) = \frac{2\pi\hbar/L_1}{m^*\frac{eB}{m^*c}} = \frac{hc}{eBL_1} = \delta y. \tag{21}$$

Writing $k_\ell = \frac{2\pi\ell}{L_1}$, this shows that adiabatically increasing Φ from 0 to Φ_0 has the effect of moving an electron from a state in Landau level n and $k = k_\ell$ to a state with Landau level n and $k = k_{\ell+1}$.

The discussion up to this point has focused on a single electron. Considering the electrons collectively, the exclusion principle dictates that each of them will reside in a different state. We assume that the system is in its ground state (as will be true with extremely high probability at low temperature, which is the context in which the quantum Hall effect is usually observed), in which case then N electrons will occupy the N lowest energies $\mathcal{E}_{n,k}$.[2] We also make the crucial assumption that each Landau level is either completely filled by electrons or is empty, *i.e.* that the Fermi energy lies between two successive Landau levels.

Under these assumptions, the foregoing analysis implies that as Φ increases from 0 to Φ_0, within each of the filled Landau levels the electron that is initially in the state with $\langle x_2 \rangle = y(k_\ell)$ moves to the state with $\langle x_2 \rangle = y(k_{\ell+1}) = y(k_\ell) + \delta y$. Having each of the electrons within a Landau level move up by one step is equivalent to having a single electron move from the lowest value of x_2 (namely 0, to very good approximation) to the highest value of x_2 (namely L_2). So if $\nu \in \mathbf{Z}$ is the number of filled Landau levels, the overall effect of increasing Φ from 0 to Φ_0 is to move ν electrons a distance L_2. This increases the energy of the system by

$$\Delta E = \nu eEL_2. \tag{22}$$

But the increase in the energy can be related to the current via (6). Using the Feynman-Hellmann theorem, we have (in the ground state)

$$\langle \hat{J}_1 \rangle = -\frac{c}{L_2}\frac{\partial}{\partial \Phi}\langle \hat{H}(\Phi, 0) \rangle. \tag{23}$$

Now $\frac{\partial}{\partial \Phi}\langle \frac{\hat{H}(\Phi,0)}{\partial \Phi} \rangle$ is the sum over the filled states of the derivatives of the $\mathcal{E}_{n,k}$ with respect to Φ, and these derivatives are independent of Φ. Hence integrating (23) from $\Phi = 0$ to $\Phi = \Phi_0$ and using (22) yields

$$\langle \hat{J}_1 \rangle \Phi_0 = -\frac{c}{L_2}\Delta E = -ec\nu E. \tag{24}$$

---

[2] We are ignoring spin, on the basis that the magnetic field would induce a Zeeman splitting between the spin-up and spin-down versions of the Landau levels, which would be enough for the same analysis to go through in the presence of spin. See [8, p. 19] for more on this.

Recalling that $\Phi_0 = \frac{hc}{e}$ we obtain the relation

$$\langle \hat{J}_1 \rangle = -\frac{e^2}{h} \nu E, \tag{25}$$

Thus the Hall conductivity in the ground state, $\sigma_{12} = \frac{\langle \hat{J}_1 \rangle}{E}$, is an integer multiple of $\frac{e^2}{h}$, with the integer being interpreted as the negative of the number of filled Landau levels.

V. IMPURITIES AND EDGE STATES

The above calculations were based on our ability to exactly analyze the specific Hamiltonian $\hat{H}_\Phi^{(r)}$ from (8). However a real-world quantum Hall system should be expected to involve a less symmetric Hamiltonian due to impurities in the material and other features; the experimental fact is that the quantization of the Hall conductance still holds with high precision in such a system. Let us briefly describe, following [5],[6],[8, Section 2.2.2], how Laughlin's argument is robust to such issues.

We continue here to assume that the electrons are non-interacting, so that it suffices to add an additional potential term $V_{\text{pert}}(x_1, x_2)$ to the one-particle Hamiltonian $\hat{H}_\Phi^{(r)}$. We assume that this perturbation vanishes near the edges of our ring (where x_2 is close to either 0 or L_2). Since the eigenstates $e^{ikx_1}\phi(x_2)$ with energy $\mathcal{E}_{n,k}$ that were found in the previous section have their x_2 coordinates localized near the value $y(k)$, in the case that $y(k)$ is close to 0 or L_2 (*i.e.* for k near 0 or near the maximal allowed value $\frac{eBL_2}{\hbar c}$) the eigenstate with energy $\mathcal{E}_{n,k}$ will survive the addition of the new potential V_{pert}. Thus the "edge states" representing electrons near the edges of the ring behave just as in the previous section, with the adiabatic variation of the flux from 0 to Φ_0 resulting in an electron in the nth Landau level moving from a state with $k = k_\ell$ to a state with $k = k_{\ell+1}$.

In the absence of additional information about the potential term V_{pert} we cannot expect to make precise statements about the electrons that are not near the edges of the ring. Because V_{pert} depends on x_1, not just on x_2, these electrons will almost certainly not have wavefunctions of the form $e^{ikx_1}\phi(x_2)$ as in the previous section. In many cases the wavefunctions will be *localized* in both the x_1 and x_2 directions; other states will continue to be *extended* in the sense that they are nonzero at x_1 values that go all the way around the ring. Localized and extended states behave differently under the adiabatic variation of Φ: if a state $\psi(x_1, x_2)$ is localized and thus vanishes for x_1 outside some interval of length less than L_1, then there is no problem in applying the gauge transformation $\psi(x_1, x_2) \mapsto e^{\frac{ie\Phi}{L_1 \hbar c} x_1}\psi(x_1, x_2)$ for *any* choice of the flux Φ, not just those Φ which are integer multiples of the quantum of flux Φ_0. Consequently under adiabatic variation of Φ an electron in a localized state $\psi(x, y)$ has its wave function simply multiplied by a phase, without changing its energy. On the other hand electrons in extended states can see their state change as a result of the change in Φ from 0 to Φ_0, as we have already seen.

Putting this together, at least if V_{pert} is small enough so that the previous Landau levels do not collide with each other under the perturbation, we obtain the following picture of what happens in each Landau level as a result of Laughlin's flux threading thought experiment. Some of the states in the Landau level will likely be localized, and as just discussed these will only be multiplied by a phase. Others will be extended, including the edge states that act just as in the previous section. Whatever happens to the extended states in general, electrons in the edge states must each move up one step, which just as in the previous section forces the net effect of the adiabatic variation to be to move an electron from the bottom of the strip to the top.

Thus just as in the unperturbed case increasing Φ from 0 to Φ_0 will result in the transfer of ν electrons upward by a distance L_2, where ν is the number of filled Landau levels. Since V_{pert} is assumed to vanish near the edges of the ring, so that the potential energy near the edges is still eEx_2, this again increases the energy of the system by νeEL_2. Since (6) again implies[3] that this change in energy is also equal to $-\frac{L_2}{c}\langle \hat{J}_1 \rangle \Phi_0 = -\frac{L_2 h}{e}\langle \hat{J}_1 \rangle$, the relation $\langle \hat{J}_1 \rangle = -\nu \frac{e^2}{h} E$ follows just as in the previous section.

In fact, as noted in [6, p. 868], Laughlin's flux threading argument is *more* compelling in the presence of impurities that cause V_{pert} to be nonzero than it is in the simpler case described in the previous section. One of the assumptions made therein was that the Fermi energy—in this context, the Nth-lowest energy in the spectrum of the one-particle Hamiltonian $\hat{H}_\Phi^{(r)}$—lies between two Landau levels, so that (at low temperature) all Landau levels are either completely filled or empty. This amounts to assuming that the number N of electrons is an integer multiple of the (large) number $\frac{eBL_1L_2}{hc}$ of states per Landau level, and there is no particular reason for this to be true, even approximately.

On the other hand in the perturbed case, where there are both localized states and extended states, since the localized states are unaffected by the variation in Φ our argument only depended on all of the *extended* states in the first ν Landau levels being occupied. If the perturbation is moderately large, the extended states will have energies relatively close to the original $\mathcal{E}_{n,k}$, while the energies of the localized states will typically spread somewhat further, as indicated in Figure 3. This makes it significantly more reasonable to suppose that the Fermi energy is in the required location—the Fermi energy just

---

[3] There is a slight additional assumption being made here, namely that $\langle \hat{J}_1 \rangle$ is independent of Φ (in the unperturbed case this could be seen by direct inspection of the exact solution). Without this assumption, what the argument here shows is that the average value of $\langle \hat{J}_1 \rangle$ over all possible fluxes is $-\nu \frac{e^2}{h} E$.

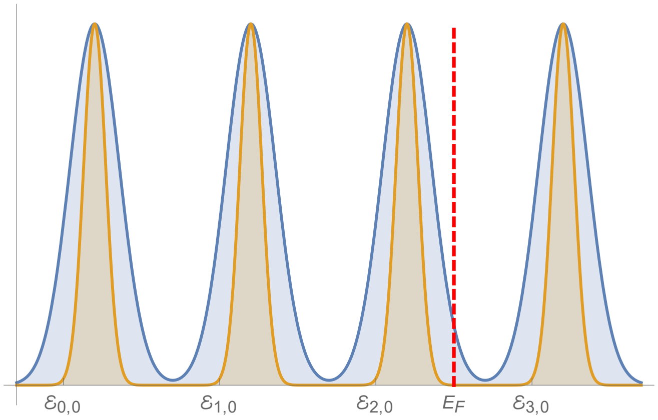

Figure 3. A possible density of states in the presence of a perturbation V_{pert}, with extended states shown in orange and localized states in blue. The flux-threading argument depends on the Fermi energy E_F lying between two successive orange regions.

needs to be in the gap between the energy regions occupied by extended states in successive Landau levels, but it can be equal to the energy of a localized state.

VI. THE QUANTUM HALL EFFECT AND THE BERRY PHASE

In this final section, which is based on [1], we give a somewhat different explanation for the quantization of the Hall conductance, exhibiting its connection to topology via the adiabatic theorem and Berry curvature. Unlike in the previous sections we will regard both coordinates x_1 and x_2 as periodic (so that our Hall conductor is topologically a torus). This allows for the possibility of introducing two independent fluxes Φ_1 and Φ_2, one threaded through the x_1 circle and the other through the x_2 circle. We consider rather general Hamiltonians having the basic form $\hat{H}(\Phi_1, \Phi_2)$ as in (2); in particular in contrast to the previous two sections the potential energy V is permitted to have terms involving interactions between the separate electrons. Because of the periodicity of both x_1 and x_2, for both $j = 1, 2$ multiplication by $e^{2\pi i \sum_r x_j^{(r)}/L_j}$ gives a gauge symmetry that identifies the version of the system with $\Phi_j = 0$ with the version of the system with $\Phi_j = \Phi_0 = \frac{hc}{e}$.

Another contrast to the previous two sections is that instead of incorporating the electric field $E\mathbf{\hat{x}_2}$ into the potential energy[4] we will incorporate it by making the flux Φ_2 time-dependent:

$$\Phi_2 = -EcL_2 t \tag{26}$$

so that the velocity operator in (1) is

$$\hat{v}_2^{(r)} = \frac{1}{m^*}\left(\frac{\hbar}{i}\frac{\partial}{\partial x_2^{(r)}} + \frac{e}{c}A_2(x_1^{(r)}, x_2^{(r)}) - eEt\right). \tag{27}$$

Thus our Hamiltonian $\hat{H}(\Phi_1, \Phi_2) = \hat{H}(\Phi_1, -EcL_2 t)$ is time-dependent. As before, E is assumed to be small and thus the time-dependence of our Hamiltonian will be small enough to justify appeal to the adiabatic theorem.

We will suppose there to be a non-degenerate normalized ground state $|0_{\Phi_1\Phi_2}\rangle$, depending smoothly on Φ_1 and on $\Phi_2 = -EcL_2 t$, for each of the time-independent Hamiltonians $\hat{H}(\Phi_1, \Phi_2)$. According to the adiabatic theorem, we can (and do) choose the phases for these ground states such that, to good approximation[5], as the second flux parameter Φ_2 varies with Φ_1 held fixed these states satisfy the time-dependent Schrödinger equation $i\hbar\frac{\partial}{\partial t}|0_{\Phi_1,-EcL_2t}\rangle = H(\Phi_1, -EcL_2 t)|0_{\Phi_1,-EcL_2t}\rangle$. Thus, under this approximation which we henceforth assume to be exact, we have by the chain rule

$$\hat{H}(\Phi_1, \Phi_2)|0_{\Phi_1\Phi_2}\rangle = -i\hbar c L_2 E \left|\frac{\partial 0_{\Phi_1\Phi_2}}{\partial \Phi_2}\right\rangle. \tag{28}$$

The current density appearing in the quantum Hall effect is the expectation value of $\hat{J}_1$ in this ground state. In view of (6) computing this current density is equivalent to computing the expectation value of $\frac{\partial \hat{H}(\Phi_1,\Phi_2)}{\partial \Phi_1}$. We find:

$$\begin{aligned}
&\left\langle 0_{\Phi_1\Phi_2}\left|\frac{\partial \hat{H}(\Phi_1,\Phi_2)}{\partial \Phi_1}\right|0_{\Phi_1\Phi_2}\right\rangle \\
&= \left\langle 0_{\Phi_1\Phi_2}\left|\frac{\partial}{\partial \Phi_1}\left(\hat{H}(\Phi_1,\Phi_2)|0_{\Phi_1\Phi_2}\rangle\right)\right.\right\rangle \\
&\qquad - \left\langle 0_{\Phi_1\Phi_2}\left|\hat{H}(\Phi_1,\Phi_2)\right|\frac{\partial 0_{\Phi_1\Phi_2}}{\partial \Phi_1}\right\rangle \qquad (29)\\
&= -i\hbar c L_2 E\left(\left\langle 0_{\Phi_1\Phi_2}\left|\frac{\partial}{\partial \Phi_1}\left(\frac{\partial 0_{\Phi_1\Phi_2}}{\partial \Phi_2}\right)\right.\right\rangle\right. \\
&\qquad \left. + \left\langle \frac{\partial 0_{\Phi_1\Phi_2}}{\partial \Phi_2}\middle|\frac{\partial 0_{\Phi_1\Phi_2}}{\partial \Phi_1}\right\rangle\right) \qquad (30)\\
&= -i\hbar c L_2 E\frac{\partial}{\partial \Phi_2}\left(\left\langle 0_{\Phi_1\Phi_2}\middle|\frac{\partial 0_{\Phi_1\Phi_2}}{\partial \Phi_1}\right\rangle\right). \qquad (31)
\end{aligned}$$

Here in (29) we have used the product rule (in the form $(\partial_{\Phi_1} A)x = \partial_{\Phi_1}(Ax) - A\partial_{\Phi_1} x$); in (30) we have twice used (28); and in (31) we have again used the product rule as well as equality of mixed partials.

So by (6) we obtain that the expectation value of the x_1-component of the current in the ground state is given

---

[4] Note that the usual potential term eEx_2 lacks the required periodicity, so could not be used in the present context.

[5] We are sweeping quite a bit under the rug with this phrase; much of the work done in [1] involves proving adiabatic-theorem-type estimates with sufficient precision as to justify the steps which appear below.

by

$$\langle \hat{J}_1 \rangle = \hbar c^2 E \frac{\partial}{\partial \Phi_2}\left(i \left\langle 0_{\Phi_1\Phi_2} \middle| \frac{\partial 0_{\Phi_1\Phi_2}}{\partial \Phi_1} \right\rangle \right). \tag{32}$$

In principle $\langle \hat{J}_1 \rangle$ depends on the fluxes Φ_1 and Φ_2; similarly to footnote 4 we will assume that it is (to good approximation) independent thereof, in which case $\langle \hat{J}_1 \rangle$ can be computed as the average, as Φ_1, Φ_2 both vary between 0 and $\Phi_0 = \frac{hc}{e}$, of the right-hand side of (32):

$$\langle \hat{J}_1 \rangle = \left(\frac{hc}{e}\right)^{-2} \hbar c^2 E \int_0^{hc/e} \int_0^{hc/e} \frac{\partial}{\partial \Phi_2}\left(i \left\langle 0_{\Phi_1\Phi_2} \middle| \frac{\partial 0_{\Phi_1\Phi_2}}{\partial \Phi_1} \right\rangle \right) d^2\Phi \tag{33}$$

$$= \left(\frac{1}{2\pi} \int_0^{\Phi_0} \int_0^{\Phi_0} \frac{\partial}{\partial \Phi_2}\left(i \left\langle 0_{\Phi_1\Phi_2} \middle| \frac{\partial 0_{\Phi_1\Phi_2}}{\partial \Phi_1} \right\rangle \right) d^2\Phi \right) \frac{e^2}{h} E. \tag{34}$$

Thus the statement that the Hall conductance is an integer multiple of $\frac{e^2}{h}$ amounts to the statement that the above double integral is an integer multiple of 2π.

To begin to understand why this is, we will first show that the integral is the negative of the integral of the Berry curvature associated with the family of ground states $|0_{\Phi_1\Phi_2}\rangle$. This curvature is $i\left(\frac{\partial \mathcal{A}_2}{\partial \Phi_1} - \frac{\partial \mathcal{A}_1}{\partial \Phi_2}\right)$ where the Berry connection is given by $\mathcal{A}_j = \left\langle 0_{\Phi_1\Phi_2} \middle| \frac{\partial 0_{\Phi_1\Phi_2}}{\partial \Phi_j} \right\rangle$.

The integrand in (34) is thus $i\frac{\partial \mathcal{A}_1}{\partial \Phi_2}$. But the integral of the other term $i\frac{\partial \mathcal{A}_2}{\partial \Phi_1}$ that appears in the Berry curvature vanishes due to our choice of phases for the $|0_{\Phi_1\Phi_2}\rangle$. Indeed, if the energy of the ground state $|0_{\Phi_1\Phi_2}\rangle$ is $\mathcal{E}_{\Phi_1\Phi_2}$, then (28) yields

$$\frac{\partial \mathcal{A}_2}{\partial \Phi_1} = \frac{i}{\hbar c L_2 E} \frac{\partial}{\partial \Phi_1} \mathcal{E}_{\Phi_1,\Phi_2}, \tag{35}$$

and, for any choice of Φ_2, integrating this from $\Phi_1 = 0$ to $\Phi_1 = \Phi_0$ yields a constant times $\mathcal{E}_{\Phi_0,\Phi_2} - \mathcal{E}_{0,\Phi_2}$ which is zero because of the gauge symmetry associated with increasing Φ_1 by an amount Φ_0.

So the integral in (34) is equal to $-\int_0^{\Phi_0}\int_0^{\Phi_0} i\left(\frac{\partial \mathcal{A}_2}{\partial \Phi_1} - \frac{\partial \mathcal{A}_1}{\partial \Phi_2}\right) d^2\Phi$. A concise, somewhat mathematically sophisticated, explanation for why this is 2π times an integer is that in view of the gauge symmetry the phases over which the integral is taken parametrize a torus with the ground states giving a complex line bundle over the torus, and the integral of the curvature of a connection on a complex line bundle over a closed surface is 2π times the first Chern number of the line bundle, which is always an integer. However one does not need to be acquainted with the language of the previous sentence to understand the integrality in this case. Green's theorem equates our double integral with the line integral $-i\oint_C \mathcal{A}\cdot d\mathbf{r}$ of the Berry connection over the perimeter C of the square. Now $e^{i\oint_C \mathcal{A}\cdot d\mathbf{r}}$ has the following geometric significance: it is the phase that the state $|0_{00}\rangle$ is multiplied by as a result of being adiabatically transported around the perimeter of the square $[0, \Phi_0] \times [0, \Phi_0]$. Since addition of Φ_0 either to Φ_1 or to Φ_2 is a gauge symmetry of the system, up to gauge transformations that we suppress from the notation the adiabatic transport along each of the four sides C_1, C_2, C_3, C_4 of the square will return $|0_{00}\rangle$ to a multiple of itself; let us write $e^{i\gamma_j}$ for the phase by which $|0_{00}\rangle$ is multiplied upon adiabatic transport along C_j, so $e^{i\oint_C \mathcal{A}\cdot d\mathbf{r}} = e^{i\gamma_1}e^{i\gamma_2}e^{i\gamma_3}e^{i\gamma_4}$. But again due to the gauge symmetry, the adiabatic transports along opposite edges of the square will be inverses to each other (since opposite edges represent the same curve but with opposite orientation). Thus $e^{i\gamma_1} = e^{-i\gamma_3}$ and $e^{i\gamma_2} = e^{-i\gamma_4}$, whence finally

$$e^{i\oint_C \mathcal{A}\cdot d\mathbf{r}} = 1. \tag{36}$$

Thus $\oint_C \mathcal{A}\cdot d\mathbf{r}$ is indeed an integer multiple of 2π, as therefore is the integral in (34). This confirms that the Hall conductivity is an integer multiple of $\frac{e^2}{h}$.

We have thus explained the quantization of the Hall conductance—at least averaged over all possible fluxes—on quite general grounds, relying on little more than the assumption that the ground state is non-degenerate for all choices of the fluxes. By contrast the *fractional* quantum Hall effect, which lies beyond the scope of this paper, arises in certain settings where the ground state is degenerate, see [8, Section 3.2.4].

---

[1] J. E. Avron, R. Seiler, and L. G. Yaffe. Comm. Math. Phys. **110**, 33 (1987).

[2] E. Hall, Amer. J. Math. **2**, 287 (1879).

[3] K. V. Klitzing, Phys. Rev. Lett. **122**, 200001 (2019).

[4] K. V. Klitzing, G. Dorda, and M. Pepper, Phys. Rev. Lett. **45**, 494 (1980).

[5] R. B. Laughlin, Phys. Rev. B **23**, 5632 (1981).

[6] R. B. Laughlin, Rev. Mod. Phys. **71**, 863 (1999).

[7] D. J. Thouless, M. Kohmoto, M. Nightingale, and M den Nijs. Phys. Rev. Lett. **49**, 405 (1982).

[8] D. Tong, arXiv:1606.06687.

Introduction to Density Matrix Formalism for Solving Spin-Spin Interactions in Nuclear Magnetic Resonance

Nilesh Goel

(Dated: June 19, 2019)

In physics, the spin-spin relaxation is the mechanism by which the transverse component of the magnetization vector exponentially decays towards its equilibrium value in nuclear magnetic resonance (NMR). In actual NMR experiments, we have a test tube with 10^{20} spins at room temperature and we cannot measure their individual spins. Instead, suppose that two nuclear spins get close to each other and interact briefly. This produces a time-dependent perturbation in the Hamiltonian of NMR, which leads to decrease in amplitudes of spin states. In this paper, we will first introduce the notation of density matrices and using them, we will study how we can solve the spin-spin interactions to get time evolution of the spin states.

I. INTRODUCTION

Quantum mechanics is a fundamental theory in physics describing nature of atomic and subatomic particles. As we apply various quantum mechanics theories, we see that they turn out to be perfectly correct for isolated systems and non-ensemble particles and spin states. For real-world implications, we have to apply different approximations.

Similarly, density matrix formalism is a practical tool used to deal with ensembles or statistical mixtures. It is just an alternate representation of of a quantum state, written with ket of the state multiplied on right by the bra of the state. Note that this is kind of similar to a projection operator. That's why density matrix is also known as density operator, but we shall follow the widely accepted terminology of density matrix, with variable $\hat{\rho}$ as its representation. We require this formalism because in real-world example, isolated spins do not exist and is in contact with its environment as well. This affects the states of the spins and as we will learn soon, reduced density matrices help us in getting measurement statistics of the system in interest without explicit calculations on the environment system.

In this paper, we will study Nuclear Magnetic Resonance and spin-spin interactions. But, even in a test tube, under effect of a magnetic field, there are atleast 10^{20} spins interacting with each other. The best method to deal with the whole system is to consider affect on a single spin state due to rest of the system taking them as an environment. For this, we will use density matrix formalism and try to find how a spin state in Nuclear Magnetic Resonance evolve in time due to spin-spin interactions.

II. THE CONCEPT OF DENSITY MATRICES[4]

Let us first see how we define density matrix/operator $\hat{\rho}$ for a pure quantum state vector $|\psi\rangle$. The density matrix is given by:

$$\hat{\rho} \equiv |\psi\rangle \langle\psi| . \tag{1}$$

This is simply the projection operator on the state $|\psi\rangle$. If we have basis states $|\psi_i\rangle$, and we have:

$$|\psi\rangle = \sum_i c_i |\psi_i\rangle . \tag{2}$$

Then, the corresponding density matrix can be written as:

$$\hat{\rho} = \sum_{i,j} c_i c_j^* |\psi_i\rangle \langle\psi_j| . \tag{3}$$

The terms here with $i \neq j$ of the equation above are referred as interference terms and represent quantum coherence between components of basis $|psi_i\rangle$. These terms are what bring "quantumness" in the system, and have no classical explanation. These terms are interference between different basis states $|\psi_i\rangle$.

We have successfully defined the new formalism for quantum state vectors, but we also need to assert the action of operators in this formalism as well, so that we can perform measurement on the system. For this, we will consider a Hermitian operator $\hat{O}$ and claim that:

$$\langle\hat{O}\rangle = Tr(\hat{\rho}\hat{O}). \tag{4}$$

where $Tr(A)$ represents the trace of matrix A.

Note that, expectation value is a number so it is equal to its own trace. Hence, we can prove the claim as follows:

$$\begin{aligned} \langle\hat{O}\rangle &= Tr(\langle\hat{O}\rangle) \\ &= Tr(\langle\psi| \hat{O} |\psi\rangle) \\ &= Tr(|\psi\rangle \langle\psi| \hat{O}). \qquad (5) \\ \Rightarrow \langle\hat{O}\rangle &= Tr(\hat{\rho}\hat{O}). \qquad (6) \end{aligned}$$

In eq. (5), we have used the cyclic property of trace to get the result.

If we choose $\hat{O} = \hat{I}$, we get the expected result:

$$\begin{aligned} Tr(\hat{\rho}) &= 1. \qquad (7) \\ \Rightarrow \langle\psi| |\psi\rangle &= 1. \qquad (8) \end{aligned}$$

Mixed States

Now, let us consider the case of mixed-state density matrices. A mixed quantum state is a statistical ensemble of pure quantum state and presents insufficient information about system's state i.e. the system can be in any one of the given pure states $|\psi_i\rangle$, but the observer can only relate classical(statistical) probabilities p_i to each of the states $|\psi_i\rangle$.

An example of this situation, a preparation device can be created which prepares either of $|\psi_1\rangle$ or $|\psi_2\rangle$. We perform a process in which we measure spin of an arbitrary unknown spin quantum state, using a Stern-Gerlach experiment, and if spin turns out to be up $|\psi_1\rangle$ is prepared and for down spin $|\psi_2\rangle$ is prepared. If the observer inquires only about states prepared by the device, she will therefore only know that either of $|\psi_1\rangle$ or $|\psi_2\rangle$. She won't know which state has been prepared and since, she does not know the process of preparation of state and hence, cannot predict any of the state. But, note that the origin of these states is purely classical and the probabilities of obtaining each state is completely deterministic (0.5 each). Hence, this set of pure states of $|\psi_1\rangle$ and $|\psi_2\rangle$ represents a classical ensemble, named such to convey that origin of probabilities is classical.

The example above is somewhat artificial, but this can be easily resonated into real-world examples as well. Let us consider our old pals Alice and Bob, each having a particle from entangled pair of particles, given by:

$$|\Psi\rangle = \frac{|+\rangle_A |-\rangle_B - |-\rangle_A |+\rangle_B}{\sqrt{2}}. \tag{9}$$

Now, consider that Alice and Bob do not know each other and have no way to contact each other, but if one of them performs a measurement, he/she can inform the other using a postal mail, but cannot inform him/her about their measurement outcome. Bob is very patient and decides to wait for a year before performing measurement on his state, but Alice is so curious, that she measures her state immediately. This process is known as partial measurement.

Bob receives mail from Alice informing him that she has measured her state, but there is no information about her measurement outcome. But, after this partial measurement what state is left with Bob? Compare this with the previous example. If Alice gets $|+\rangle$ as outcome, a hypothetical preparation device creates state $|\psi_1\rangle = |-\rangle$ for Bob, otherwise it creates state $|\psi_2\rangle = |+\rangle$ for him. Both cases now have purely deterministic probabilities creating a classical ensemble of $|+\rangle$ and $|-\rangle$ each with probability of 0.5. Hence, a classical ensemble has been created. This ensemble is known as mixed state.

Note that in principle, it is possible to backtrack each step of mixed state-preparation procedure and as clear in the last example, we can determine which pure state in the ensemble has been produced. Alice might send her measurement outcome as well, and without any measurement, Bob will realize what his pure measurement outcome is. The probabilities to each pure state in a mixed state simply expresses our decision to not inquire about finer details of the state preparation system or our inability to actually follow each step of state-preparation, so ignoring the preparation step, we actually get deterministic probabilities of each pure state and hence, we have a mixed state.

So, now let us see how we define density matrices for the cases of mixed states. We have to ensure that eq. (4) remains satisfied for the notation for mixed states as well. This is so as to ensure that measurement procedure in complete density matrix formalism is consistent. We claim that for a mixed state $|\psi\rangle$ with pure states $|\psi_i\rangle$ having probabilities of p_i, the density matrix is given by:

$$\hat{\rho} = \sum_i p_i |\psi_i\rangle \langle\psi_i| . \tag{10}$$

Putting this in eq. (4) we get:

$$\begin{aligned} Tr(\hat{\rho}\hat{O}) &= Tr(\sum_i p_i |\psi_i\rangle \langle\psi_i| \hat{O}) & (11)\\ &= \sum_i p_i Tr(|\psi_i\rangle \langle\psi_i| \hat{O}). & (12)\\ \Rightarrow Tr(\hat{\rho}\hat{O}) &= \sum_i p_i \langle\hat{O}\rangle_{|\psi_i\rangle} = \langle\hat{O}\rangle_{|\psi\rangle}. & (13) \end{aligned}$$

Hence, the action of operator can be defined in same way as that of pure state and we have successfully generalized the definition of a density matrix given by eq. (10). For only one pure state, with $p_i = 1$, eq. (10) reverts to eq. (1).

With new definition for density matrix, in the example of Alice and Bob, we can say that Bob has density matrix given by:

$$\begin{aligned} \hat{\rho} &= \frac{|+\rangle\langle+| + |-\rangle\langle-|}{2} & (14)\\ &= \frac{1}{2}\begin{pmatrix}1\\1\end{pmatrix}\begin{pmatrix}1 & 1\end{pmatrix} + \frac{1}{2}\begin{pmatrix}1\\-1\end{pmatrix}\begin{pmatrix}1 & -1\end{pmatrix} & \\ &= \frac{1}{2}\begin{pmatrix}1 & 1\\1 & 1\end{pmatrix} + \frac{1}{2}\begin{pmatrix}1 & -1\\-1 & 1\end{pmatrix} & \\ &= \frac{1}{2}\begin{pmatrix}1 & 0\\0 & 1\end{pmatrix} = \frac{E}{2}. & (15) \end{aligned}$$

where E is the identity matrix.

From now on, we will use $\hat{E}$ as the identity operator for the whole paper.

Now, in the next section, we will study about reduced density matrices.

III. REDUCED DENSITY MATRICES[4]

The motivation for the reduced density matrices arises from description of a system A quantum-correlated/entangled with another system B. The total combined system AB, in principle, might be completely known, but the observer can perform measurements on system A only, but not on B. This occurs when either the observer has access only to A or is interested only in measurements of system A. So, for example when considering interactions between many spin states, it is easier to consider the effect on the system of single spin (i.e. system A) due to other spins. We are interested in observing only that spin state, and hence, reduced density matrices come into play.

Note that since the observer has access to only system A, then everything about state of composite system must be derived only from measurements on A. The reduced density matrix does this job by extracting all measurement statistics of system A, and we claim that it can be defined as:

$$\hat{\rho}_A \equiv Tr_B \hat{\rho}. \tag{16}$$

Here $\hat{\rho}$ is the density matrix of the composite system AB and subscript "B" implies that the trace must be evaluated with respect to the orthonormal basis of Hilbert Space B only.

"Tr_B" is called partial trace over B, and is interpreted as tracing out degrees of freedom of the unobserved system B. Note that since system B cannot be observed, it becomes difficult to assign a quantum state where complete description of the composite system can be acknowledged. Because system B is in an environment of the system in interest, tracing over former's degrees of freedom results in a complete and exhaustive description of the system. Ignoring B, quantum state of system A might not accurately define the behaviour of system, and hence, by tracing over B, reduced density matrices are all we have to describe measurement statistics of the system.

Now, first let's try to verify our claim (16) and check whether this description does indeed help us comment about observations in system A only. For this first consider an entangled state in the composite system:

$$|\psi\rangle = \frac{1}{\sqrt{2}}(|a_1\rangle |b_1\rangle + |a_2\rangle |b_2\rangle). \tag{17}$$

where $|a_i\rangle$ and $|b_i\rangle$ may not be orthogonal but are normalized states of A and B, respectively. The density matrix for this state can be written as:

$$\hat{\rho} = \frac{1}{2}\sum_{i,j=1}^{2} |a_i\rangle \langle a_j| \otimes |b_i\rangle \langle b_j| \,. \tag{18}$$

Let $|\phi_k\rangle$ and $|\phi_l\rangle$ represent orthornormal bases of Hilbert spaces of A and B respectively. Since, we need to take measurements only in system A, we can define an operator $\hat{O}$ as:

$$\hat{O} = \hat{O}_A \otimes \hat{E}_B. \tag{19}$$

where $\hat{O}_A$ is an observable in space of A which gives us the required measurement and $\hat{E}_B$ is the identity operator in space of B.

What we need now is to evaluate the expectation value of $\hat{O}$ using eq. (4), hoping that we get a relation describing the system measurements in such a way that observation is only in space of A, we can get complete description of the whole system. Hence, using the definition of trace, we can write:

$$\begin{aligned}
\langle\hat{O}\rangle &= Tr(\hat{\rho}\hat{O}) \\
&= \sum_{k,l} \langle\phi_l| \langle\phi_k| \hat{\rho}(\hat{O}_A \otimes \hat{E}_B) |\phi_k\rangle |\phi_l\rangle && (20) \\
&= \sum_{k} \langle\phi_k| (\sum_{l} \langle\phi_l| \hat{\rho} |\phi_l\rangle)\hat{O}_A |\phi_k\rangle && (21) \\
&= \sum_{k} \langle\phi_k| (Tr_B\hat{\rho})\hat{O}_A |\phi_k\rangle \,. && (22) \\
\Rightarrow \langle\hat{O}\rangle &= Tr_A((Tr_B\hat{\rho})\hat{O}_A). && (23)
\end{aligned}$$

Now, notice in the eq. (23), the expectation value of $\hat{O}$ can be completely described in the space of A and this equation takes up the form of eq. (4) in terms of observable in Hilbert Space of A, such that the term $Tr_B\hat{\rho}$ represents a density matrix relating measurement statistic in whole system to measurement in space of A. This was exactly what we claimed in eq. (16) and hence, we have got a mathematical description of reduced density matrix.

Partial Trace

In eq. (16) we defined $Tr_B\hat{\rho}$ as partial trace of density matrix ρ over B. Let us now see how we can evaluate this for a system in two Hilbert spaces of two-dimensions each. For this, note that any density matrix in the four-dimensional composite system of AB of can be written in following form:

$$\hat{\rho} = \sum_{i,j,k,l} c_{ijkl} |i\rangle \langle j|_A \otimes |k\rangle \langle l|_B \,. \tag{24}$$

where $|i,j\rangle_A$ and $|k,l\rangle_B$ represent basis vectors of A and B, respectively.

Note that, in eq. (24), for partial trace with respect to degree of freedoms of B, we can simply apply trace to the part of the density matrix corresponding to space B. Hence, we get:

$$\begin{aligned}
Tr_B\hat{\rho} &= \sum_{i,j,k,l} c_{ijkl} |i\rangle \langle j|_A \otimes Tr(|k\rangle \langle l|)_B && (25) \\
& \sum_{i,j,k,l} c_{ijkl} |i\rangle \langle j|_A \otimes Tr(\langle l| |k\rangle)_B && (26) \\
& \sum_{i,j,k,l} c_{ijkl} |i\rangle \langle j|_A \times \delta_{kl}. && (27) \\
\Rightarrow Tr_B\hat{\rho} &= \sum_{i,j,k,k} c_{ijkk} |i\rangle \langle j|_A \,. && (28)
\end{aligned}$$

Thus, we can use eq. (28) to calculate partial trace. In terms of elements of the density matrix we can write:

$$\hat{\rho} = \begin{pmatrix} a_{11,11} & a_{11,12} & a_{12,11} & a_{12,12} \\ a_{11,21} & a_{11,22} & a_{12,21} & a_{12,22} \\ a_{21,11} & a_{21,12} & a_{22,11} & a_{22,12} \\ a_{21,21} & a_{21,22} & a_{22,21} & a_{22,22}. \end{pmatrix} \tag{29}$$

Now, using eq. (28), we can write the partial trace as:

$$\begin{aligned}
\hat{\rho}_A &= Tr_B\hat{\rho} \\
&= \begin{pmatrix} a_{11,11} + a_{11,22} & a_{12,11} + a_{12,22} \\ \\ a_{21,11} + a_{21,22} & a_{22,11} + a_{22,22} \end{pmatrix}. && (30)
\end{aligned}$$

This is thus a reduced density matrix in two-dimensional space of A.

IV. NUCLEAR MAGNETIC RESONANCE [1]

Let us now introduce the theory of Nuclear Magnetic Resonance. It is a phenomenon where spins are kept in a rotating magnetic field.

Here, we have spins in a time-dependent magnetic field given by:

$$\mathbf{B}(t) = B_0\mathbf{z} + B_1(\mathbf{x}cos\omega t - \mathbf{y}sin\omega t), B_0 >> B_1. \tag{31}$$

This results in spin Hamiltonian given by:

$$H_S(t) = -\gamma(B_0\hat{S}_z + B_1(cos\omega t\hat{S}_x - ysin\omega t\hat{S}_y)). \tag{32}$$

Solving this Hamiltonian(see Appendix A), we get time evolution of a state as follows:

$$\begin{aligned}
|\Psi, t\rangle &= e^{\frac{i\omega t\hat{S}_z}{\hbar}} e^{\frac{i\gamma(\mathbf{B}_R\cdot\mathbf{S})t}{\hbar}} |\Psi, 0\rangle \,. && (33) \\
with: &\qquad \mathbf{B}_R = B_1\mathbf{x} + B_0(1 - \frac{\omega}{\Omega})\mathbf{z}. && (34)
\end{aligned}$$

Here, we will consider a special case where:

$$\begin{aligned} \omega &= \Omega. & (35)\\ \Rightarrow \mathbf{B}_R &= B_1\mathbf{x}. & (36)\end{aligned}$$

In such case, in eq. (33), the rightmost exponential becomes responsible for spin precession about x-axis. This results in movement of spin towards y-axis with angular velocity $\omega_1 = \gamma B_1$. The effect of other exponential is rotating spin about z-axis with angular velocity $\omega = \Omega = \gamma B_0$, and since, $B_0 >> B_1$, rotation about z-axis will be much faster than rotation about x-axis. Hence, tip of the spin can be visualized as performing spiral on surface of a sphere.

What we now do, is time the rotating frequency magnetic to a time T, so as to get:

$$\omega_1 T = \frac{\pi}{2}. \qquad (37)$$

After time T, we will switch off the rotating field and only $B_0\mathbf{z}$ will remain switched on. The result of eq. (37) is that after time T, the state will point along y-axis (Initially, it pointed towards z-axis). Now, if we switch off the rotating field, only rotation about z-axis will occur, and the spin will effectively continue to rotate in $x - y$ plane only.

We will use this system of $\frac{\pi}{2}$ pulse in NMR to describe rest of our problem as in the next section, where we will also consider perturbations due to spin-spin interactions.

V. SPIN-SPIN INTERACTIONS

In real-life examples or even in laboratory experiments, it is impossible to isolate a single spin and put it in a magnetic field. So, it becomes imperative that we also consider how spin states will evolve in presence of other spins.

We will assume that spins interact only with external magnetic field and each other and there are no collisions with surroundings and no other interactions. First, we will consider only two spins.

Consider the following situation:

Let the spins that are present be named I and S. Initially, they are put in magnetic field aligned along z-axis i.e. $B_0\hat{\mathbf{z}}$ and are allowed to come to rest from t=$-\infty$ to t=0. Hence, at t=0, both the spins get aligned in z-direction. Then we will apply a $\frac{\pi}{2}$ pulse on the system, after which it will be turned off and only $B_0\hat{\mathbf{z}}$ field will exist for last period. Hence, spins will rotate about z-axis in $x - y$ plane. Now the interaction between the two spins is given by[2]:

$$\partial H = b\hbar \hat{S}_z \otimes \hat{I}_z. \qquad (38)$$

In the eq. (38), b is very very small. In general, $b << \mathbf{B}_R$, hence during the period of the $\frac{\pi}{2}$ pulse, this spin-spin interaction can be ignored and can be considered its effect after both spins reach $x - y$ plane.

Let us now consider the period after rotating field is turned off. Note that magnetic field along z-axis is still on. Hence, we have the Hamiltonian as:

$$\mathcal{H} = \hbar(\Omega_S \hat{S}_z \otimes \hat{E} + \hat{E} \otimes \Omega_I \hat{I}_z + b\hat{S}_z \otimes \hat{I}_z), \qquad (39)$$
$$where:\ \Omega_n = \gamma_n B_0; n = I, S.$$

Note that the Hamiltonian is time-independent, so taking the initial density operator to be $\hat{\rho}(0)$, we can write the time evolution as:

$$\begin{aligned} \hat{\rho}(t) &= e^{-i(\Omega_I \hat{I}_z + \Omega_S \hat{S}_z + b\hat{S}_z\hat{I}_z)t}\hat{\rho}(0)\\ &\times\ e^{i(\Omega_I \hat{I}_z + \Omega_S \hat{S}_z + b\hat{S}_z\hat{I}_z)t}. & (40)\end{aligned}$$

To solve eq. (40), we will simply follow the following steps[3]:

$$\begin{aligned} e^{it\Omega_S\hat{S}_z\otimes\hat{E}} &= \begin{pmatrix} e^{i\Omega_S t} & 0\\ 0 & e^{-i\Omega_S t}\end{pmatrix} \otimes \begin{pmatrix} 1 & 0\\ 0 & 1\end{pmatrix}\\ &= \begin{pmatrix} e^{i\Omega_S t} & 0 & 0 & 0\\ 0 & e^{i\Omega_S t} & 0 & 0\\ 0 & 0 & e^{-i\Omega_S t} & 0\\ 0 & 0 & 0 & e^{-i\Omega_S t}\end{pmatrix}. & (41)\end{aligned}$$

$$\begin{aligned} e^{it\hat{E}\otimes\Omega_I\hat{I}_z} &= \begin{pmatrix} 1 & 0\\ 0 & 1\end{pmatrix} \otimes \begin{pmatrix} e^{i\Omega_I t} & 0\\ 0 & e^{-i\Omega_I t}\end{pmatrix}\\ &= \begin{pmatrix} e^{i\Omega_I t} & 0 & 0 & 0\\ 0 & e^{-i\Omega_I t} & 0 & 0\\ 0 & 0 & e^{i\Omega_I t} & 0\\ 0 & 0 & 0 & e^{-i\Omega_I t}\end{pmatrix}. & (42)\end{aligned}$$

$$\begin{aligned} \hat{S}_z \otimes \hat{I}_z &= \begin{pmatrix} 1 & 0\\ 0 & -1\end{pmatrix} \otimes \begin{pmatrix} 1 & 0\\ 0 & -1\end{pmatrix}\\ &= \begin{pmatrix} 1 & 0 & 0 & 0\\ 0 & -1 & 0 & 0\\ 0 & 0 & -1 & 0\\ 0 & 0 & 0 & 1\end{pmatrix}. & (43)\\ \Rightarrow (\hat{S}_z\hat{I}_z)^{2n} &= \hat{E}. & (44)\end{aligned}$$

Now, expand the exponential $e^{ibt\hat{S}_z\hat{I}_z}$ and group together odd and even powers and apply eq. (44), to get:

$$\begin{aligned} e^{ibt\hat{S}_z\hat{I}_z} &= \hat{E}(1 - \frac{b^2t^2}{2!} + \frac{b^4t^4}{4!} + ...)\\ &\quad + i\hat{S}_z\hat{I}_z(bt - \frac{b^3t^3}{3!} + \frac{b^5t^5}{5!} + ...)\\ &= \hat{E}cos(bt) + i\hat{S}_z\hat{I}_z sin(bt). & (45)\end{aligned}$$

$$\Rightarrow e^{ibt\hat{S}_z\hat{I}_z} = \begin{pmatrix} e^{ibt} & 0 & 0 & 0\\ 0 & e^{-ibt} & 0 & 0\\ 0 & 0 & e^{-ibt} & 0\\ 0 & 0 & 0 & e^{ibt}\end{pmatrix}. \qquad (46)$$

Now, we will also need $\hat{\rho}(0)$ in eq. (40). Note that spin-spin interactions are ignored for rotating field period. Hence, a $\frac{\pi}{2}$ pulse will simply rotate spins from initially aligned towards z-axis to aligned towards y-axis. This can also be obtained by applying rotation operator on density operator of state aligned along z axis for $t = \frac{\pi}{2}$(see detailed calculation in Appendix B) and hence, we get:

$$\begin{aligned} \hat{\rho}(0) &= -\Omega_S \hat{S}_y \otimes \hat{E} - \Omega_I \hat{E}\hat{I}_y\\ &= \begin{pmatrix} 0 & i\Omega_I & i\Omega_S & 0\\ -i\Omega_I & 0 & 0 & i\Omega_S\\ -i\Omega_S & 0 & 0 & i\Omega_I\\ 0 & -i\Omega_S & -i\Omega_I & 0\end{pmatrix}. & (47)\end{aligned}$$

For flexibility in calculations, let term corresponding to spin state $\hat{S}_y$ be multiplied with a constant k. We can later put $k = 1$.

$$\begin{aligned}\hat{\rho}(0) &= -k\Omega_S\hat{S}_y \otimes \hat{E} - \Omega_I\hat{E}\hat{I}_y \\ &= \begin{pmatrix} 0 & i\Omega_I & ik\Omega_S & 0 \\ -i\Omega_I & 0 & 0 & ik\Omega_S \\ -ik\Omega_S & 0 & 0 & i\Omega_I \\ 0 & -ik\Omega_S & -i\Omega_I & 0 \end{pmatrix}. \end{aligned} \tag{48}$$

Now, use eq.'s (41), (42), (46) and (48) can be used to solve eq. (40), and we get final time evolved state as follows:

$$e^{i(\Omega_I\hat{I}_z+\Omega_S\hat{S}_z+b\hat{S}_z\hat{I}_z)t} = \begin{pmatrix} e^{i(\Omega_I+\Omega_S+b)t} & 0 & 0 & 0 \\ 0 & e^{i(-\Omega_I+\Omega_S-b)t} & 0 & 0 \\ 0 & 0 & e^{i(\Omega_I-\Omega_S-b)t} & 0 \\ 0 & 0 & 0 & e^{i(-\Omega_I-\Omega_S+b)t} \end{pmatrix}. \tag{49}$$

$$\Rightarrow \quad Evaluating:$$

$$\hat{\rho}(t) = \frac{i}{2}\begin{pmatrix} 0 & \Omega_I e^{-2i(\Omega_I+b)t} & k\Omega_S e^{-2i(\Omega_S+b)t} & 0 \\ -\Omega_I e^{2i(\Omega_I+b)t} & 0 & 0 & k\Omega_S e^{-2i(\Omega_S-b)t} \\ -k\Omega_S e^{2i(\Omega_S+b)t} & 0 & 0 & \Omega_I e^{-2i(\Omega_I-b)t} \\ 0 & -k\Omega_S e^{2i(\Omega_S-b)t} & -\Omega_I e^{2i(\Omega_I-b)t} & 0 \end{pmatrix} \tag{50}$$

Eq. (50) gives us four-dimensional density matrix for two spin state system. But in real world situations, NMR spectroscopy has spins of order of 10^{20}, resulting in density matrix of 10^{40} dimensions. To apply observables on the whole system and attempting to evaluate the whole system is not only tedious and meaningless, but also it becomes very difficult to track all spins together. But, if we take $\Omega_I = \Omega_S$ and notice that all the spins are identical and will behave more or less similar manner, we realize that observation on single spin can be more or less generalized to the whole system. That's where the reduced density matrices come into play. First, we consider only interactions between 2 spins out which we are attempting observation on single one. To get reduced density matrix in the space of spin S, we will apply eq. (30) on the density matrix of eq. (50). The reduced density matrix we get is:

$$\begin{aligned}\hat{\rho}(t) &= \\ i\Omega_S &\times \begin{pmatrix} 0 & ke^{-2i\Omega_S t}cos(2bt) \\ -ke^{2i\Omega_S t}cos(2bt) & 0 \end{pmatrix}. \end{aligned} \tag{51}$$

Also, remember that $\hat{\rho}(0)$ in spin system S was given by $-ik\Omega_S\hat{S}_y$.

$$\hat{\rho}(0) = -k\Omega_S \begin{pmatrix} 0 & -i \\ i & 0 \end{pmatrix}. \tag{52}$$

Now, note that we can write eq. (51) in another way, as follows:

$$\begin{aligned}\hat{\rho}(t) &= k\Omega_S cos(2bt) \begin{pmatrix} 0 & icos(2\Omega_S t) \\ -icos(2\Omega_S t) & 0 \end{pmatrix} \\ &+ k\Omega_S cos(2bt) \begin{pmatrix} 0 & sin(2\Omega_S t) \\ sin(2\Omega_S t) & 0 \end{pmatrix}. \end{aligned} \tag{53}$$

$$\begin{aligned}\Rightarrow \hat{\rho}(t) &= k\Omega_S cos(2bt) \times \\ &(-cos(2\Omega_S t)\hat{S}_y + sin(2\Omega_S t)\hat{S}_x). \end{aligned} \tag{54}$$

Observe the eq. (54), the term in the bracket clearly represents rotation of spin S in $x - y$ plane with $\hat{\rho}(t = 0) \; - \hat{S}_y$ as expected. This rotation of the spin is due to external magnetic field along z-axis. But, there is another factor in multiplication, namely $cos(2bt)$, which is just affecting the amplitude of rotating spin. This results in oscillation of amplitude of the spin with frequency $2b$. The maximum value this can take is 1. But, we know that smaller the frequency, greater will be spread of the cosine function horizontally(because wavelength is large), and since b is very very small, the spread of oscillation of amplitude of the spin is very large, so even one complete oscillation takes much more time than the duration of interest.

The $cos(2bt)$ term is influenced by spin-interaction and hence, is decreasing spin polarization of the spin S. But, note that spin state S is in influence of not only spin I, but is actually influenced by many other (about 10^{20}) spins as well. Here, k plays an important role. Since in both eq.'s (52) and (54), the constant k does not get affected and remains in product form throughout, we can simply perform procedure leading to eq. () on the final reduced density matrix using a third spin, then a fourth spin...and so on. The net result will be that phase factor(as in eq. (51)) simply implies spin-rotation and $cos(2bt)$ factor gets multiplied continuously, to give oscillation of spin amplitude in eq. (54) of the order $cos^n(2bt)$ for interactions with n spins, where n is very large.

Now, note that as power of $cos(2bt)$ is increased, the width of the function starts decreasing, and hence, for large values of n, the width becomes very small as compared to the wavelength of the function(because of small b, wavelength itself is very large). Hence, much before second oscillation of amplitude of the spin starts, its amplitude becomes negligible. This happens to all spins, and each spin loses its amplitude completely. Hence, spin-spin interactions will be lost and b will tend to zero. Thus, with time, strength of oscillation of amplitude due to b will decrease and instead of coming back up for second oscillation, the spin amplitudes remain negligible. This decay of amplitude is characterized by dephasing time T_2, used to signify the time taken for this decay to occur.

Since, we are talking about spin polarization in $x - y$ plane, which is the cause of transverse magnetization in a system, dephasing time is also referred to as time taken by a system to lose its transverse magnetization. The process of spin losing its polarization due to interactions between spins is known as spin-spin relaxation or T_2-relaxation. This process is very important in Magnetic Resonance Imaging. The human body is mostly composed of water molecules. MRI machine first creates a large magnetic field along axis of machine(call it z-axis). After sometime, when all water molecular spins can be safely assumed to be lying along axis of machine, a $\frac{pi}{2}$ pulse is applied to get spins to rotate in $x - y$ plane. These rotating dipoles create a magnetic field(due to transverse magnetization). This signal due to transverse magnetization, decays with time, dephasing time T_2. Since, greater the number of spins, greater the spin interactions, lesser will be dephasing time and hence, a weighted image of T_2 can help doctors to detect abnormal fluid accumulations.

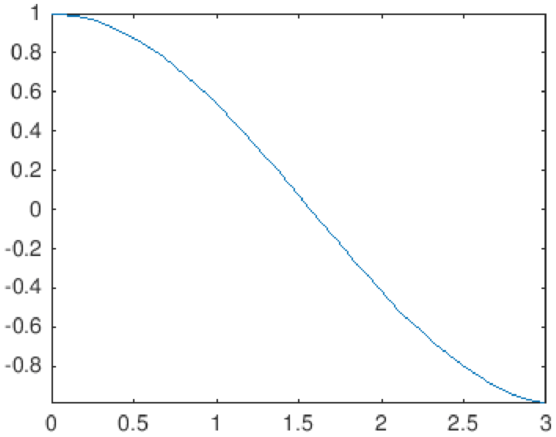

FIG. 1: $cos(x)$

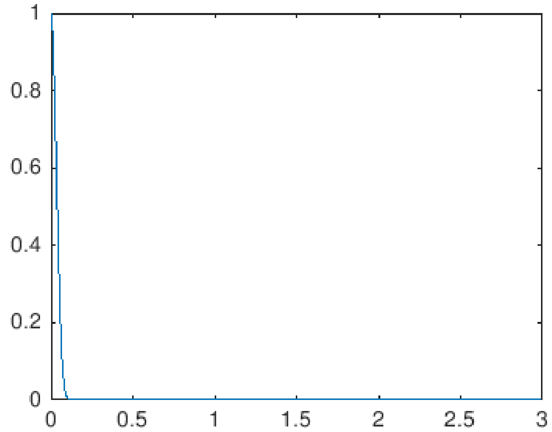

FIG. 2: $cos^{1000}(x)$
Note that in $cos^n x$, when n is increased, the width of the plot has decreased. For $n = 1000$, majority of the value of the function has been restricted inside 0.1, much less than whole range of π. For even greater n, the width will decrease even more.

VI. CONCLUSION

Henceforth, in this paper, we have introduced density matrix formalism and have discussed its special case, namely reduced density matrices. We then described time evolution of unperturbed Nuclear Magnetic Resonance, introduced Hamiltonian due to spin-spin interactions and using density matrix formalism solved the time evolution of a spin state.

In conclusion, we saw that, once the rotating magnetic field was switched off, while in absence of spin-spin interactions, the spins should have just kept on rotating about z-axis without any loss of amplitudes. But, due to interactions between the spins, they will start losing their amplitudes and transverse magnetization(which arises due to spin in $x-y$ plane) goes off to zero after a certain time known as dephasing time, T_2.

VII. APPENDIX

A. Solving Unperturbed NMR Hamiltonian[1]

Let us try to solve the Unperturbed NMR Hamiltonian. In Nuclear Magnetic Resonance, we have spins in a time-dependent magnetic field given by:

$$\mathbf{B}(t) = B_0\mathbf{z} + B_1(\mathbf{x}cos\omega t - \mathbf{y}sin\omega t), B_0 >> B_1. \tag{55}$$

This results in spin Hamiltonian given by:

$$H_S(t) = -\gamma(B_0\hat{S}_z + B_1(cos\omega t\hat{S}_x - ysin\omega t\hat{S}_y)). \tag{56}$$

Note that this is a non-trivial time evolution problem because Hamiltonian at different times does not commute. To simplify this problem, we consider a frame of reference rotating with angular velocity ω about the z axis. This is generated by unitary transformation $\mathcal{U}$ as follows:

$$\mathcal{U}(t) = exp(-\frac{i\omega t\hat{S}_z}{\hbar}). \tag{57}$$

This results in rotating frame Hamiltonian as given by:

$$H_{\mathcal{U}} = \omega\hat{S}_z. \tag{58}$$

And, we can define a state $|\psi_R, t\rangle$ in the new rotating frame as given by:

$$|\Psi_R, t\rangle = \mathcal{U}(t)\,|\Psi, t\rangle\,. \tag{59}$$

But, performing time evolution for $|\psi, t\rangle$ using the unitary operator $\mathcal{U}_S$ which is associated with H_S, we get:

$$|\Psi_R, t\rangle = \mathcal{U}(t)\mathcal{U}_S(t)\,|\Psi, 0\rangle\,. \tag{60}$$

Clearly then $\mathcal{U}(t)\mathcal{U}_S(t)$ is the net unitary operator for the rotating frame of reference which can be used to calculate the net Hamiltonian, remembering that the the Hamiltonian is given by $i\hbar(\partial_t\mathcal{U})\mathcal{U}^\dagger$. Therefore, we get:

$$\begin{aligned} H_R &= i\hbar\partial_t(\mathcal{U}\mathcal{U}_S)\mathcal{U}_S^\dagger\mathcal{U}^\dagger && (61)\\ &= i\hbar\partial_t(\mathcal{U})\mathcal{U}^\dagger + \mathcal{U}i\hbar\partial_t(\mathcal{U}_S)\mathcal{U}_S^\dagger\mathcal{U}^\dagger. && (62)\\ H_R &= H_{\mathcal{U}} + \mathcal{U}H_S\mathcal{U}^\dagger. && (63)\end{aligned}$$

This H_R turns out to be time-independent and after inserting H_S and U in eq. (63), we get:

$$\begin{aligned} H_R &= (-\gamma B_0 + \omega)\hat{S}_z \\ &- \gamma B_1 e^{-\frac{i\omega t\hat{S}_z}{\hbar}}(cos\omega t\hat{S}_x - sin\omega t\hat{S}_y)e^{\frac{i\omega t\hat{S}_z}{\hbar}}. && (64)\\ Let:& \\ H_R &= (-\gamma B_0 + \omega)\hat{S}_z - \gamma B_1\hat{M}(t). && (65)\end{aligned}$$

Finding $\hat{M}(t)$ from eq.'s (64) and (65) and calculating its time derivative, we get:

$$\begin{aligned}
\partial_t \hat{M} &= e^{-\frac{i\omega t\hat{S}_z}{\hbar}}\Big(-\frac{i\omega}{\hbar}[\hat{S}_z, cos\omega t\hat{S}_x - sin\omega t\hat{S}_y] \\
&\quad +(-\omega sin\omega t\hat{S}_x - \omega cos\omega t\hat{S}_y)\Big)e^{\frac{i\omega t\hat{S}_z}{\hbar}} \\
&= e^{-\frac{i\omega t\hat{S}_z}{\hbar}}(\omega cos\omega t\hat{S}_y + \omega sin\omega t\hat{S}_x \\
&\quad -\omega sin\omega t\hat{S}_x - \omega cos\omega t\hat{S}_y)e^{\frac{i\omega t\hat{S}_z}{\hbar}}. \qquad (66) \\
\Rightarrow \partial_t \hat{M} &= 0. \qquad (67)
\end{aligned}$$

Hence, we observe that $\hat{M}(t)$ is actually constant in time. So, to get its value at all times, we can simply put $\hat{M}(t=0)$, i.e. $\hat{S}_x$, in eq. (65), to get:

$$\begin{aligned}
H_R &= (-\gamma B_0 + \omega)\hat{S}_z - \gamma B_1 \hat{S}_x. \qquad (68) \\
H &= -\gamma[B_0(1-\frac{\omega}{\Omega})\hat{S}_z + B_1\hat{S}_x], \qquad (69) \\
where: &\quad \Omega = \gamma B_0, \qquad (70) \\
Hence: &\quad H_R = -\gamma \mathbf{B}_R \cdot \mathbf{S}, \qquad (71) \\
with: &\quad \mathbf{B}_R = B_1\mathbf{x} + B_0(1-\frac{\omega}{\Omega})\mathbf{z}. \qquad (72)
\end{aligned}$$

Note that H_R is time-independent Hamiltonian, so it is easy to write its unitary operator $\mathcal{U}_S(\sqcup)$, for time evolution of $|\Psi_R, t\rangle$ and then using eq.'s (57), (59) and (60), we can write full solution of state as:

$$|\Psi, t\rangle = e^{\frac{i\omega t\hat{S}_z}{\hbar}} e^{\frac{i\gamma(\mathbf{B}_R\cdot\mathbf{S})t}{\hbar}} |\Psi_R, 0\rangle\,. \qquad (73)$$

At $t = 0$, $|\Psi_R, 0\rangle = |\Psi, 0\rangle$.
And hence, finally we get:

$$|\Psi, t\rangle = e^{\frac{i\omega t\hat{S}_z}{\hbar}} e^{\frac{i\gamma(\mathbf{B}_R\cdot\mathbf{S})t}{\hbar}} |\Psi, 0\rangle\,. \qquad (74)$$

This is our final time-evolved state.

B. Action of Rotation Operator on $\mathbf{S}_z$[3]

Here, we will apply rotation operator(about x-axis) on density matrix notation of states aligned in z-direction. In single Hilbert Space, we have:

$$\hat{\mathbf{R}}_x(\theta) = \begin{pmatrix} cos(\theta/2) & -isin(\theta/2) \\ -isin(\theta/2) & cos(\theta/2) \end{pmatrix}. \qquad (75)$$

For $\theta = \frac{\pi}{2}$, we get:

$$\hat{\mathbf{R}}_x(\frac{\pi}{2}) = \frac{1}{\sqrt{2}}\begin{pmatrix} 1 & -i \\ -i & 1 \end{pmatrix}. \qquad (76)$$

For a density operator given by $\hat{S}_z$:

$$\hat{S}_z = \begin{pmatrix} 1 & 0 \\ 0 & -1 \end{pmatrix}. \qquad (77)$$

The rotation operator will act on spin state as follows:

$$\hat{\mathbf{R}}_x(\frac{\pi}{2})\hat{S}_z\hat{\mathbf{R}}_x^\dagger(\frac{\pi}{2}) = \frac{1}{2}\begin{pmatrix} 1 & -i \\ -i & 1 \end{pmatrix}\begin{pmatrix} 1 & 0 \\ 0 & -1 \end{pmatrix}\begin{pmatrix} 1 & i \\ i & 1 \end{pmatrix}. \qquad (78)$$

$$\Rightarrow \hat{\mathbf{R}}_x(\frac{\pi}{2})\hat{S}_z\hat{\mathbf{R}}_x^\dagger(\frac{\pi}{2}) = \begin{pmatrix} 0 & i \\ -i & 0 \end{pmatrix} = -\hat{S}_y. \qquad (79)$$

Hence, rotation about x-axis by $\frac{\pi}{2}$ of spin along z-axis, results in a spin pointing in negative-y axis.

Thus, initially, if rotating field is applied to $\hat{S}_z$ for a $\frac{\pi}{2}$ pulse, we get $-\hat{S}_y$, which we used in eq. (47).

[1] Refer MIT OCW 8.05, Quantum Physics-II, Fall 2013, Lecture Notes, Lec.#16 − 18, Part 6, Nuclear Magnetic Resonance, Pg 17

[2] Gonzalo Agustin Alvarez, *Decoherence of many-spin systems in NMR: From molecular characterization to an environmentally induced quantum dynamical phase transition*, 2007

[3] John Cavanagh, *Protein NMR Spectroscopy, Principles and Practice*, Second Edition, Elsevier, 2007

[4] Maximilian Schlosshauer, *Decoherence and Quantum-to-Classical Transition*, Springer, 2007

[5] Cohen-Tannoudji, C. Quantum Mechanics. Vol. 2. Wiley-VCH, 1991

Introduction to the Landauer-Büttiker formalism of quantum transport

Panteleimon Lapas

(Dated: June 19, 2019)

An introduction to the Landauer-Büttiker formalism of the steady state mesoscopic coherent (dissipationless) quantum transport is developed in this manuscript.

I. Introduction

During the last decades there have been a whole series of solid state phenomena, predominantly appearing in low-dimensional objects, which clearly pointed towards the need of treating the electric current carriers as waves propagating through a solid, instead of viewing them as particles subject to the laws of the Newtonian mechanics. Such an approach naturally then raises the issue of the conditions under which the wave nature of the current carriers can conclusively be manifested, where it turns out that in order to answer such questions, it is far more efficient to focus on factors that could suppress the wave nature (which is always there according to the wave-particle duality principle). Loosely speaking, that could be any event that could scramble or randomize the phase of the wavefunction of a carrier, thus annihilating the potentiality of any kind of interference effects which presuppose phase coherence, but let us be slightly more detailed on that. Systematic study has shown that there are two main factors that can suppress quantum mechanical effects in transport phenomena, the first one being any phase-breaking scattering processes, and the second one being the temperature [1]. Typical phase-breaking scattering processes are inelastic collisions where a carrier exchanges energy with a scatterer (which can change its internal state), or, elastic collisions where the states of the carrier and the scatterer are modified without necessarily any energy exchange at the same time (e.g. spin-dependent scattering from a magnetic impurity). As for the second factor, at any finite temperature T, due to thermal effects, there is an uncertainty in the energy of a carrier roughly of the order of k_BT (k_B denoting the Boltzmann constant), which in turn entails an uncertainty in the phase shift accumulated during the motion of the carrier, and if the latter exceeds the value of $\sim \pi$, then the carrier's phase is effectively uncertain and we do not expect to observe clear-cut interference effects. Therefore, as a rule of thumb it can be said that small device dimension (with respect to an average distance traversed from one phase breaking scattering event to another) which is expected to restrict the frequency of the phase-breaking scattering processes, in conjunction with low temperature, are conducive to the observation of quantum mechanical effects in transport phenomena, which are a defining feature of the so-called **mesoscopic carrier transport**.

The idea that the current through low-dimensional objects can be directly related to their scattering properties was first formulated as early as 1957 by Rolf Landauer, and was subsequently refined by Markus Büttiker (1986), leading to what is nowadays called the "scattering approach to quantum transport" (or else the so-called Landauer-Büttiker formalism) [2]. The Landauer-Büttiker formalism is a rather general formalism that can treat any kind of non-interacting transport (either truly non-interacting or effectively non-interacting, in the spirit of some mean field theory approach to the carriers), concomitant with any kind of interference effects. The key steps of the aforementioned formalism boil down to identifying the scattering states inside the leads (we come back to this concept in the following section), defining the so-called "scattering matrix" that connects the amplitudes of the aforementioned scattering states via a scattering region of interest, and connecting the properties of the aforementioned scattering states to the current flowing through the scattering region of interest. The rest of this work consists of a more detailed presentation of the steps delineated above, setting completely aside any complications related to the interactions of the current carriers with their surroundings (that could be other carriers as well).

II. Quantum junction model and identification of available transport channels

In this section, we are going to enter the territory of the very complex domain of out-of-equilibrium phenomena, and in order to reduce the complexity of the problem we immediately focus on steady state situations of "mesoscopic quantum transport". Saying so, it is now well understood that a good starting point for approaching the aforementioned effect, is the so-called quantum junction model, to be elaborated in the following.

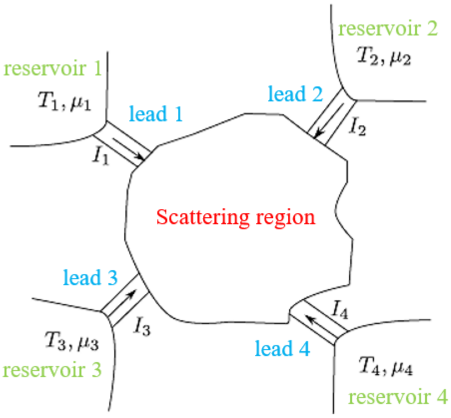

Figure 1. (Color online) Set-up consisting of four reservoirs with specified temperatures and chemical potentials, all connected to a scattering region in the center, via semi-infinite ideal leads. Picture borrowed (and modified) from Ref.[2].

To begin with, let us consider a number of non-magnetic reservoirs, connected to a central scattering region, via semi-infinite ideal leads, as depicted in Fig.1. The reservoirs act as very large, constant sources of carriers, always assumed in thermal equilibrium, as a result of which their state is sufficiently defined by specifying their chemical potential and their temperature (the reservoirs by definition can accommodate a whole lot of carrier states that form a wide continuum). It is further presumed that all the carriers that end up to some reservoir are completely thermalized via a series of inelastic scattering events happening there, and therefore, any phase information that was carried by them before entering that particular reservoir is completely lost within there. Of course, for this to happen, any carrier heading towards a particular reservoir should never suffer any kind of reflection during the transit from the lead to the reservoir at issue, and on top of that, spend a reasonable amount of time in the reservoir at issue before exiting it. Saying so, any carriers leaving a reservoir are supposed to have a completely randomized phase (and spin since we assumed non-magnetic reservoirs), and hopefully no memory of what was going on at previous times, as a result of which, their energy distribution can be adequately described by the Fermi distribution function $f(E, \mu_\alpha, T_\alpha)$, with μ_α, T_α denoting the chemical potential and the temperature of the α-th reservoir (from where the carrier emerged). Furthermore, the leads act as quantum waveguides for the carriers leaving the reservoirs and are further assumed to have a well-defined mode structure (we come back to this detail in a little while). On top of that, they are presumed semi-infinite and completely free of any kind of disorder, as a consequence of which, any carrier entering them shouldn't ever suffer any scattering (while traversing them) towards either the central scattering region or the reservoir to which the lead is connected. Finally, the central scattering region could be something as simple as one tunnel barrier or a bunch of random δ-function like elastic scatterers, or, as complex as an interacting non-equilibrium molecule. For simplicity, the scattering region will be viewed as a continuum medium, whose effect on the carriers traversing it, can adequately be described by some potential function $U(\mathbf{r})$ (disorder ascribed to random δ-function like elastic scatterers can directly be superposed onto the background continuous potential $U(\mathbf{r})$). Concluding this paragraph, it should be mentioned that the requirement of semi-infinite leads is necessary for two reasons: In the first place, the boundary of any reservoir is presumably far enough from the central scattering region, which is a highly non-equilibrium region (otherwise the assumptions about the carriers entering to or exiting from a reservoir might be in jeopardy). In the second place, if the reservoirs are sufficiently far from the scattering region, they are sufficiently far from each other as well, as a result of which there is no kind of interaction (directly via tunneling or indirectly via the scattering region) among them.

Next, we turn our attention to the identification of the so-called *available transport channels* (of a lead), and we attempt to illustrate the concept via the simplest possible example. As already stated, in an ideal semi-infinite lead (by definition) there are no sources of scattering, and to be more precise, we want to preclude any factor that could act as a source of scattering from one transport channel of a lead to another transport channel of that same lead (such an effect could for instance be triggered by the geometry of the lead, in the absence of any impurity-driven scattering processes). Therefore, all the available transport channels of a lead are assumed completely independent of each other (in the sense that if a carrier exiting a reservoir is fed to one of the transport channels of the accompanying lead, there is nothing within the lead to perturb the carrier), and only the interaction of a carrier with the central scattering region could kick it off its (lead-related) transport channel prior to approaching the scattering region. Lastly, the motion of any carrier within an ideal lead is for simplicity presumed effectively one-dimensional, along the lead's greatest dimension. Keeping all this in mind, a very simple (ideal) lead geometry that meets the aforementioned requirements, is the semi-infinite lead of constant cross-section and hard wall boundaries anywhere along its length. In such a case, the time-independent Schrödinger equation reads as

$$\begin{aligned}&\left[-\tfrac{\hbar^2}{2m}\left(\tfrac{\partial^2}{\partial x^2}+\tfrac{\partial^2}{\partial y^2}+\tfrac{\partial^2}{\partial z^2}\right)+U(x,y)\right]\Psi_E(x,y,z)\\&=E\Psi_E(x,y,z)\end{aligned} \tag{1}$$

where m is the effective mass of the carrier, and z the direction of its motion (i.e. the direction along the length of the lead). Using the ansatz that $\Psi_E(x,y,z)=\phi_n(x,y)e^{ik_n z}$, the previous equation reduces to

$$\left\{-\frac{\hbar^2}{2m}\left(\frac{\partial^2}{\partial x^2}+\frac{\partial^2}{\partial y^2}\right)+U(x,y)\right\}\phi_n(x,y)=E_n\phi_n(x,y) \tag{2}$$

where the discrete index n has been introduced in anticipation of discrete solutions in the transverse directions (i.e. the x and y directions) owing to the strong spatial confinement, and further, we've defined that

$$E=E_n+\frac{\hbar^2 k_n^2}{2m} \tag{3}$$

where E_n denotes the transverse energy, whereas, the second term is the kinetic energy along the direction of propagation (the parameter k_n could be discrete or quasicontinuous depending on how big is the length of the lead). As an example, for a rectangular hard wall potential with transverse sizes L_x and L_y, the transverse eigenenergies (also to be referred as " transverse modes" later on) would be

$$E_{n_x,n_y}=\frac{\hbar^2}{2m}\left[\left(\frac{\pi n_x}{L_x}\right)^2+\left(\frac{\pi n_y}{L_y}\right)^2\right],\ n_x,n_y=1,2,3,... \tag{4}$$

Going a bit further, Eq.(3) dictates that at a given energy E, the transverse modes that *can propagate* are only those with energy $E_n < E$, since otherwise the wavevector k_n turns imaginary leading to "evanescent" (non-propagating) modes within the lead [1]. Even so, not all the transverse modes that *can propagate* do necessarily contribute to the transport current through a set-up. It turns out that a transverse mode (of a lead) can contribute to the current only if its energy E_n is, additionally, lower than the Fermi energy E_F of the reservoir that feeds the carriers onto the lead at issue, but yet the contribution to the current depends on the thermal/statistical occupancy of each current-contributing mode. For example, at very low temperatures, the current-contributing modes of the α-th lead do essentially originate from transverse modes that energetically lie well below the Fermi energy of the α-th reservoir (due to the step-function like character of the statistical occupancy at very low temperatures). Saying so, any transverse modes that satisfy all of the aforementioned conditions constitute what is usually called *open transport channels*, with the rest of the modes belonging to the set of the *closed transport channels*. The open and the closed transport channels together constitute the so-called *available transport channels* of a lead. Concluding this section, for more complicated junction geometries, such as the *adiabatic junction geometry*, which uses the adiabatic approximation to solve the Schrödinger equation (typically separated into transverse and longitudinal contributions), the reader is referred to Ref.[3], section 7.3.

III. Scattering matrix and scattering states

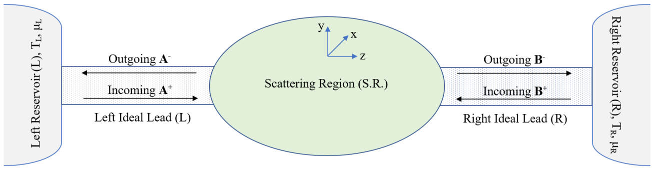

Figure 2. (Color online) Set-up consisting of two reservoirs with specified temperatures and chemical potentials (L and R), connected to a scattering region in the center, via semi-infinite ideal leads. Incoming and outgoing modes to/from the scattering region, on the left and the right side of it are represented collectively.

To begin with, let us consider the simpler set-up of Fig.2, the reservoirs and the leads of which have *all* those good properties elaborated in the previous section. If it is so, we can then set aside any evanescent modes within any lead to simplify the following analysis (we will come back to this point at the end of this section), and focus on the propagating modes of any lead only. On top of that, the scattering region (S.R.) is assumed to extend from $z = z_L$ to $z = z_R$ ($z_R > z_L$), it is presumed that no recombination or generation of current carriers can take place anywhere within the S.R., and further, it is found convenient to categorize the available transport channels on each side of the scattering region (S.R.) into channels incoming to the S.R. and channels outgoing from the S.R. (see Fig.2). It is further reminded that we focus on a transport regime in which quantum-mechanically coherent dissipationless (complete absence of inelastic scattering processes outside the reservoirs) transport over the whole S.R. (and the leads of course) is possible. Saying so, any (independent) available transport channels on the left and the right side of the S.R., entering or exiting the S.R., can quantum-mechanically be represented (based on the ansatz mentioned above Eq.(2), and also, without any inelastic scattering processes over the S.R. and the leads E is a good quantum number) as

$$\begin{aligned}
\psi^{+}_{LnE}(\mathbf{r}) &= \tfrac{A_{n+}}{\sqrt{2\pi\hbar v_{Ln}}}\phi_{Ln}(x,y)e^{+ik_n z}, \quad z < z_L \\
\psi^{-}_{LnE}(\mathbf{r}) &= \tfrac{A_{n-}}{\sqrt{2\pi\hbar v_{Ln}}}\phi_{Ln}(x,y)e^{-ik_n z}, \quad z < z_L \\
\psi^{+}_{RmE}(\mathbf{r}) &= \tfrac{B_{m+}}{\sqrt{2\pi\hbar v_{Rm}}}\phi_{Rm}(x,y)e^{-ik'_m z}, \quad z > z_R \\
\psi^{-}_{RmE}(\mathbf{r}) &= \tfrac{B_{m-}}{\sqrt{2\pi\hbar v_{Rm}}}\phi_{Rm}(x,y)e^{+ik'_m z}, \quad z > z_R
\end{aligned} \tag{5}$$

where n and m denote the different available transport channels, $A_{n\pm}$ and $B_{m\pm}$ are the wave amplitudes, $\phi_{Ln}(x,y)$ and $\phi_{Rm}(x,y)$ the transverse modes, $v_{Ln} = \hbar k_n/m_L$ and $v_{Rm} = \hbar k'_m/m_R$ the propagation speeds, m_L and m_R the effective carrier mass, $\hbar k_n = \sqrt{2m_L(E-E_n)}$ and $\hbar k'_m = \sqrt{2m_R(E-E_m)}$ the propagation wavevectors, and E_n and E_m the transverse eigenenergies, on the left and the right side of the S.R. respectively. Proceeding further, the so-called *scattering matrix* $\mathbf{S}$ by definition relates all *outgoing* (from the S.R.) modes with all *incoming* (to the S.R.) modes (remember that all the aforementioned modes are assumed to be propagating or current-contributing modes within the leads at this point) as below

$$\begin{pmatrix} A_{1-} \\ \vdots \\ A_{N_L-} \\ B_{1-} \\ \vdots \\ B_{N_R-} \end{pmatrix} = \underbrace{\begin{pmatrix} S_{11} & S_{12} & \cdots & S_{1N} \\ S_{21} & S_{22} & \cdots & S_{2N} \\ \vdots & \vdots & \cdots & \vdots \\ \vdots & \vdots & \cdots & \vdots \\ \vdots & \vdots & \cdots & \vdots \\ S_{N1} & S_{N2} & \cdots & S_{NN} \end{pmatrix}}_{\equiv \mathbf{S}(E)} \begin{pmatrix} A_{1+} \\ \vdots \\ A_{N_L+} \\ B_{1+} \\ \vdots \\ B_{N_R+} \end{pmatrix} \tag{6}$$

where N_L and N_R are the total available transport channels on the left and the right side of the S.R., $N = N_L + N_R$, and the energy dependence of the scattering matrix originates from the energy dependence of the wavevectors k_n and k'_m defined few lines above (we will see how this happens in a little while). The scattering matrix can be written more compactly in block form as below

$$\mathbf{S} = \begin{bmatrix} \mathbf{r}_{N_L\times N_L} & \mathbf{t'}_{N_L\times N_R} \\ \mathbf{t}_{N_R\times N_L} & \mathbf{r'}_{N_R\times N_R} \end{bmatrix}_{N\times N} \tag{7}$$

where the submatrix $\mathbf{r}_{N_L\times N_L}$ consists of the *reflection amplitudes* of the left-side incoming modes at the left boundary of the S.R., the submatrix $\mathbf{t}_{N_R\times N_L}$ consists of the *transmission amplitudes* of the left-side incoming modes towards the right lead ($z > z_R$), the submatrix $\mathbf{r'}_{N_R\times N_R}$ consists of the *reflection amplitudes* of the right-side incoming modes at the right boundary of the S.R., and finally, the submatrix $\mathbf{t'}_{N_L\times N_R}$ consists of the *transmission amplitudes* of the right-side incoming modes towards the left lead ($z < z_L$). For example, the matrix element t_{mn} of the transmission matrix $\mathbf{t}_{N_R\times N_L}$ represents the transmission amplitude from the left-side incoming mode n ($z < z_L$) to the right-side outgoing mode m ($z > z_R$), with the corresponding transmission probability being given by $\mathrm{T}_{mn}(E) = |t_{mn}(E)|^2$. Furthermore, we mention without proof (the reader is referred to Ref.[3], section 7.1.3 for the respective derivations) two very important properties of the scattering matrix $\mathbf{S}$: The first one is its unitarity, i.e. $\mathbf{S}^\dagger\mathbf{S} = \mathbf{S}\mathbf{S}^\dagger = \mathbf{1}$, which implies that the total probability of scattering from a given incoming state to one of the outgoing states (in our example back to the same or forward to the opposite lead) adds up to unity (with the reverse being also true, meaning that for any outgoing state, the total probability that it originated from the scattering of one of the incoming states adds up to unity as well). Notice that the unitarity property of the scattering matrix would be in trouble had we not assumed the complete absence of any carrier recombination or generation processes within the S.R.. The second one is related to the fact that under time-reversal symmetry (which in the simplest case is broken by the application of a magnetic field) the scattering matrix is additionally symmetric, i.e. $\mathbf{S} = \mathbf{S}^T$, with the superscript T denoting the transpose matrix, which implies that (under time reversal symmetry) the transmission probability from the left-side mode n to the right-side mode m, and, the transmission probability of the exact inverse process, do coincide (for a more detailed discussion on what happens under broken time reversal symmetry the reader is referred to Ref.[2], section 3.2.1). Lastly, it is noted that the (maybe at first sight weird) normalization of the wavefunctions appearing in Eqs.(5) has been chosen so as to preserve the unitarity of the scattering matrix $\mathbf{S}$.

Next we turn our attention to the definition of the so-called *scattering states*. For the left lead the scattering states are defined as

$$\Psi_{LnE}(\mathbf{r}) = \begin{cases} \frac{1}{\sqrt{2\pi\hbar v_{Ln}}}\phi_{Ln}(x,y)e^{ik_n z} + \\ + \sum\limits_{n'} \frac{r_{n'n}(E)}{\sqrt{2\pi\hbar v_{Ln'}}}\phi_{Ln'}(x,y)e^{-ik_{n'} z}, \ z < z_L \\ \sum\limits_{m} \frac{t_{mn}(E)}{\sqrt{2\pi\hbar v_{Rm}}}\phi_{Rm}(x,y)e^{ik'_m z}, \ z > z_R \end{cases} \tag{8}$$

whereas, for the right lead they are defined as

$$\Psi_{RmE}(\mathbf{r}) = \begin{cases} \frac{1}{\sqrt{2\pi\hbar v_{Rm}}}\phi_{Rm}(x,y)e^{-ik'_m z} + \\ + \sum\limits_{m'} \frac{r'_{m'm}(E)}{\sqrt{2\pi\hbar v_{Rm'}}}\phi_{Rm'}(x,y)e^{ik'_{m'} z}, \ z > z_R \\ \sum\limits_{n} \frac{t'_{nm}(E)}{\sqrt{2\pi\hbar v_{Ln}}}\phi_{Ln}(x,y)e^{-ik_n z}, \ z < z_L \end{cases} \tag{9}$$

where $r_{n'n}(E)$ is the scattering (reflection) amplitude from the left-side incoming state n to the left-side outgoing state n', $t_{mn}(E)$ the scattering (transmission) amplitude from the left-side incoming state n to the right-side outgoing state m and analogously for $r'_{m'm}(E)$ and $t'_{nm}(E)$. It is noted that the various propagation speeds as well as the various wavevectors also carry an energy dependence which is not shown explicitly for notational simplicity. Furthermore, the physical meaning of Eqs.(8) and (9) should be clear; according to Eq.(8) a left-side incoming state that interacts with the S.R. can end up either into modes of the left lead via reflection at $z = z_L$, or modes of the right lead via transmission through the S.R.. Similarly, a right-side incoming state that interacts with the S.R. can end up either into modes of the right lead via reflection at $z = z_R$, or modes of the left lead via transmission through the S.R. (those are all the possible decay channels for any incoming state to the S.R., from either side). It might seem that there are a whole lot of decay channels for any incoming state to the S.R., but in effect, its decay channels are singled out by the requirement that the energy E of the incoming state is conserved! Please notice that the scattering states defined above have the usual form we have recently seen in this course; they consist of an incoming state and outgoing states from the S.R., with the latter originating from reflection at or transmission through the boundary of the S.R.. The possible decay channels of an incoming state could possibly be viewed as 1-D counterparts of the partial waves of the scattering theory of phase shifts!

Concluding this section, we will attempt to sketch out the essential steps that are required for a realistic calculation of the scattering matrix, using as an example the set-up of Fig.2. The first step is to solve the time independent Schrödinger equation over the three regions of the quantum junction shown in Fig.2 (i.e. the left lead L, the S.R. and the right lead R), and find the available eigenstates and eigenenergies in each region. This will allow us to define the Hilbert space of each region and have a basis for it (the available transport channels). Knowledge of the eigenenergies is required if, for example, we are to distinguish between propagating and evanescent modes in any region. The second step is to solve a series of 1-D scattering problems using the basis of the scattering states (defined in the spirit of Eqs.(8) and (9)) as we move along the z-direction. For instance, the first scattering situation appears at the interface between the left lead L and the S.R., at $z = z_L$ (all interfaces should be treated as sources of scattering). Let us then focus on the scattering state $\Psi_{LnE}(\mathbf{r})$ of the left lead L, at energy E. In the region $z < z_L$ the scattering state has the same form as the upper term of Eq.(8), whereas, in the region $z > z_L$ it has the same form as the lower term of Eq.(8), except that the various quantities under the summation sign refer to the S.R. (not to the right lead!). The process of finding the various reflection and transmission amplitudes at this step is otherwise familiar; we employ the requirements of the continuity of the scattering states and their derivatives at $z = z_L$. This process might need to be repeated at several points within the S.R. (depending on the form of the potential function $U(\mathbf{r})$ - if it is spatially invariant or spatially inhomogeneous, if there are elastic point scatterers and so on) as well as the right interface at $z = z_R$, keeping in mind that a right-moving outgoing wave from one scattering subsection constitutes an incoming wave (incident from the left) to the next scattering subsection, until we end up to the outgoing wave implied by the lower term of Eq.(8) (at the right interface, $z = z_R$). This procedure should further be repeated for any left lead mode n and any energy E, and additionally, for any right lead scattering state $\Psi_{RmE}(\mathbf{r})$ that ends up to the left lead region, for all m and all energies E. All this might look like a highly cumbersome book-keeping, but, the scattering matrix formalism alleviates the situation significantly by collectively keeping track of every single component of a scattering state (incoming or outgoing) upon a scattering event, besides its capability to handle scattering in both directions along the z-axis at the same time (it kind of knows all incoming states from any direction, as well as all outgoing states towards any direction, along the z-axis). Concluding this paragraph, it should be underscored that in the aforementioned procedure, in general, one should take into consideration both propagating (current-contributing) and evanescent modes in any region, and the reason for this is that even though the evanescent modes do not contribute to the carrier current, their existence can affect (renormalize) the transmission amplitudes of the propagating modes, and therefore indirectly the carrier current. Saying so, the number of the evanescent modes that need to be taken into consideration in an actual calculation is chosen via the following rule of thumb: Suppose first that the scattering matrix is set up in such a way that the propagating modes are all collected within the same sub-block. We will have taken into consideration (in our analysis) a sufficient number of evanescent modes, only then, when the aforementioned sub-block turns out to be unitary or nearly unitary, since, if one incorporates in the scattering matrix both propagating and evanescent modes, then the unitarity property of the last is only restricted within the sub-block that contains all the propagating modes. In any other case, we need to take into consideration additional evanescent modes, and quite often it is the case that a number of evanescent modes much larger than that of the propagating modes is required in order to satisfy the aforementioned criterion [1].

IV. Two-terminal multi-channel Landauer formula

In this section, we turn our attention to the calculation of the carrier current across the simple set-up of Fig.2, assuming the existence of time reversal symmetry. To be more precise, we are not concerned about the spatial distribution of the carrier current within the S.R.. Our interest is on carrier currents flowing into or out of certain terminals, by applying specific voltages to those terminals (we give up on the term reservoir from now on and use the better suited term "terminal"). Saying so, the scattering states defined by Eqs.(8) and (9) are the appropriate tools for the following analysis, since they are connected with the leads, which keep control of what flows into or out of the terminals. To this end, we employ the following well-known formula (if the time reversal symmetry is broken due to some applied magnetic field, then the following formula should be modified accordingly as we've learned)

$$\mathbf{J} = q\frac{i\hbar}{2m}\left[\psi(\mathbf{r})\nabla\psi^*(\mathbf{r}) - \psi^*(\mathbf{r})\nabla\psi(\mathbf{r})\right] \tag{10}$$

for the current density carried by carriers of charge q and effective mass m, where only the z-component of it (i.e. the component across the whole set-up) is going to be of interest to us (therefore $\nabla(...) \to \frac{\partial}{\partial z}(...)$). The first step is to calculate the current due to a *single scattering state*, so let's choose the $\Psi_{LnE}(\mathbf{r})$ state first. The derivation is straight-forward to perform: (a) One can immediately plug Eq.(8) into Eq.(10), keeping in mind though that only the component of the scattering state $\Psi_{LnE}(\mathbf{r})$ that lies in the region $z > z_R$ can be perceived as a current that has crossed through the S.R., from one side of it to the other (the rest of the scattering state $\Psi_{LnE}(\mathbf{r})$ basically remains within the left lead and returns to the left reservoir where it participates in a series of inelastic scattering processes; so it is not something that is transmitted from one side of the S.R. to the other!). (b) Afterwards, we integrate the resulting expression over x and y, and the various contributions can be immediately simplified using the orthogonality property of the transverse modes $\int dxdy\ \phi^*_{\alpha\ell}(x,y)\phi_{\beta\ell'}(x,y) = \delta_{\alpha\beta}\delta_{\ell\ell'}$, where $\alpha = L, R$ and ℓ, ℓ' refer to the lead modes previously denoted as m, n. (c) The definitions of the propagation speeds $v_{Ln} = \hbar k_n/m_L$ and $v_{Rm} = \hbar k'_m/m_R$ can be used to simplify any remaining wavevector dependencies (that come out of the $\frac{\partial}{\partial z}$ operation). (d) $m = m_R$ should be used in the expression of Eq.(10). The final result is (be reminded that integration of the current density over a cross-section, for simplicity assumed uniform, i.e. over x and y, finally leads to a one-dimensional current along the z-direction)

$$I_{LnE} = \frac{q}{h}\sum_m |t_{mn}(E)|^2 = \frac{q}{h}\big(\mathbf{t}^\dagger(E)\mathbf{t}(E)\big)_{nn} \tag{11}$$

where we've used the definition that $[\mathbf{t}(E)]_{mn} = t_{mn}(E)$ (notice that the transmission probability matrix elements $[\mathbf{T}(E)]_{mn} = |t_{mn}(E)|^2 \neq [\mathbf{t}(E)]_{mn}$, although the two matrices have same dimensions). Following similar steps (for instance at step (d) we set $m = m_L$), for the $\Psi_{RmE}(\mathbf{r})$ scattering state we find

$$I_{RmE} = -\frac{q}{h}\sum_n |t'_{nm}(E)|^2 = -\frac{q}{h}\Big(\mathbf{t'}^\dagger(E)\mathbf{t}'(E)\Big)_{mm} \tag{12}$$

where we've used the definition that $[\mathbf{t}'(E)]_{nm} = t'_{nm}(E)$ (notice again that $[\mathbf{T}'(E)]_{nm} = |t'_{nm}(E)|^2 \neq [\mathbf{t}'(E)]_{nm}$, although the two matrices have same dimensions). Notice further that since different lead modes (transport channels) are completely independent of each other (according to the remarks preceding Eq.(1)) there is no interference among the transmission amplitudes of different lead modes, and therefore, in Eqs.(11) and (12) it makes sense to add the participating transmission probabilities (instead of the corresponding transmission amplitudes).

Going a bit further, the total current through the S.R. is obtained as follows

$$I_{q,s} = (2s+1)\sum_{\alpha\ell E} I_{\alpha\ell E} f_\alpha(E) \tag{13}$$

for carriers of charge q and spin quantum number s (to capture spin degeneracy as well), $f_\alpha(E)$ is the Fermi-Dirac distribution function of the α-th reservoir, and finally, $\alpha, \ell = L, n$ or R, m. It should be stressed however that in Eq.(13) one of the basic assumptions of this presentation was actually employed, according to which any carriers leaving a reservoir have an energy distribution that can be adequately described by the Fermi distribution function $f(E, \mu_\alpha, T_\alpha)$, with μ_α, T_α denoting the chemical potential and the temperature of the α-th reservoir from where the carrier emerged (based on the detailed reasoning given in Section II). After exiting a reservoir, a carrier's state is presumably some linear combination of scattering states of particular energy E (it is basically according to this quantum number that we can assign a Fermi-Dirac distribution function), representative of the lead that is connected to the reservoir whereby the carrier emerged, but each one of those scattering states actually extends over the whole set-up (having some component in every lead), which further implies that, once a scattering state (of the lead at issue) is occupied with some occupancy factor $f_\alpha(E)$, it is automatically "occupied" over all its components (in the sense that, once you know which scattering state has been chosen by an exiting carrier, you automatically know all its possible decay channels, both within the initial lead as well as all the other leads of your set-up). However, the issue is that we do not know so much about the state of an exiting carrier, and in order to make progress we recourse to the philosophy of the statistical mechanics, assigning to the scattering state $\Psi_{\alpha n E}(\mathbf{r})$ of the α-th lead an occupancy which is hopefully best represented by the (Fermi) distribution function $f_\alpha(E) = n_F(E - \mu_\alpha)$, which uses the chemical potential μ_α and the temperature T_α of the α-th reservoir (this is possibly the best we can do!). Finally, provided there are no inelastic scattering processes over the whole S.R. (which has also been assumed few lines before Eq.(5)), the aforementioned assigned occupancy of a particular scattering state is approximately valid over the whole spatial extent of that state (inelastic scattering events along the way could certainly wash out the assigned occupancy spoiling the effort we are doing here). Afterwards, from Eqs.(11)-(13), assuming for simplicity that $n = m$ (i.e. the same number of scattering states in the left and the right lead of our set-up), the total current injected from the left to the right lead is given by

$$\begin{aligned}
I_{q,s} &= (2s+1)\tfrac{q}{h}\sum_{\ell}\int_{-\infty}^{\infty} dE\left\{\left[(\mathbf{t}^\dagger(E)\mathbf{t}(E)\right]_{\ell\ell} n_F(E-\mu_L) - \left[\mathbf{t'}^\dagger(E)\mathbf{t'}(E)\right]_{\ell\ell} n_F(E-\mu_R)\right\} \Rightarrow \\
I_{q,s}(V_L,V_R) &= (2s+1)\tfrac{q}{h}\int_{-\infty}^{\infty} dE\; Tr\left[(\mathbf{t}^\dagger(E)\mathbf{t}(E)\right]\left\{n_F(E-\mu-qV_L) - n_F(E-\mu-qV_R)\right\}
\end{aligned} \tag{14}$$

where since the parameter E is regulated by the reservoirs we took into consideration all possible values of it and the occupancy factors themselves will take care of any 'inappropriate' E-values (or, the matrix elements of the appearing transmission matrices). In the second line, Tr denotes the trace, and further, the property that $Tr\left[\mathbf{t'}^\dagger(E)\mathbf{t'}(E)\right] = Tr\left[(\mathbf{t}^\dagger(E)\mathbf{t}(E)\right]$ was used, which in our case ($n = m$) can easily be proved using the unitarity of the scattering matrix, $\mathbf{S}^\dagger\mathbf{S} = \mathbf{S}\mathbf{S}^\dagger = \mathbf{1}$, in conjunction with the block form of the scattering matrix that is given by Eq.(7) (since we assumed that there exists time reversal symmetry, and further, given that only the propagating modes contribute to the current, there is no issue of validity about the last argument). Finally, the applied voltages on each reservoir/terminal V_α ($\alpha = L, R$) were introduced, as shifts from the equilibrium chemical potential μ of the whole set-up. Notice also that the occupancies of the scattering states (bequeathed by the appropriate reservoir in each case, according to the previous remarks) generally depend on the applied voltages, which loosely speaking, directly affect the states of the reservoirs, and as a result the energies of the exiting carriers, but, if they are too strong they can further affect the structure of the transmission/reflection amplitude matrices (for example, by causing an energy shift of the S.R. potential). Looking for a nicer formula in place of Eq.(14), we further restrict our analysis to low applied voltages (at any terminal), which allows us to Taylor-expand the current $I_{q,s}(V_L, V_R)$ in terms of qV_α around μ, to get

$$\begin{aligned}
&I_{q,s}(V_L,V_R) = (2s+1)\tfrac{q^2}{h}\times \\
&\int_{-\infty}^{\infty} dE\; Tr\left[(\mathbf{t}^\dagger(E)\mathbf{t}(E)\right]\left\{-\tfrac{\partial n_F(E-\mu)}{\partial E}\right\}(V_L - V_R)
\end{aligned} \tag{15}$$

whereby the proportionality between the total current $I_q(V_L, V_R)$ and the applied voltage difference $V_L - V_R$ yields the so-called "conductance"

$$\begin{aligned}
&G(\mu,T) = (2s+1)\tfrac{q^2}{h}\times \\
&\int_{-\infty}^{\infty} dE\; Tr\left[(\mathbf{t}^\dagger(E)\mathbf{t}(E)\right]\left\{-\tfrac{\partial n_F(E-\mu)}{\partial E}\right\}
\end{aligned} \tag{16}$$

the temperature and chemical dependence of which originates from the presence of the occupancy on the right hand side (RHS). As a last step, at nearly zero temperature, we can use the approximation that $-\frac{\partial n_F(E-\mu)}{\partial E} \approx \delta(E-\mu)$, to get an even simpler expression for the conductance (i.e. the calculation is restricted at the equilibrium chemical potential μ of the set-up)

$$G(\mu, T\to 0) = (2s+1)\frac{q^2}{h} Tr\left[(\mathbf{t}^\dagger(\mu)\mathbf{t}(\mu)\right] \tag{17}$$

Concluding this section, it is noted that the temperature dependence of the equilibrium chemical potential μ of the set-up for simplicity was neglected, and further, the low applied voltage limit is kind of a necessary assumption for our analysis, since in general higher applied voltages (or voltage differences) can significantly increase the complexity of the effect studied in this work, causing modifications to the potential of the S.R. and the eigenspectrum of the leads, affecting the charge distribution of the carriers over the whole quantum junction, and so on.

V. Multi-terminal Landauer-Büttiker formula

In the previous sections we focused on a set-up consisting of two leads (and reservoirs/terminals), the left and the right lead ($\alpha = L, R$), and going back to Eq.(13), we found (using Eqs.(11) and (12)) that the total current injected from the left lead L to the right lead R is given by

$$\begin{aligned}
&I_{q,s} = (2s+1)\tfrac{q}{h}\times \\
&\int_{-\infty}^{\infty} dE\left(\sum_{nm}|t_{mn}(E)|^2 f_L(E) - \sum_{mn}|t'_{nm}(E)|^2 f_R(E)\right)
\end{aligned} \tag{18}$$

where the first term on the RHS encompasses transmission processes starting in the lead L and ending in the lead R, and the second term encompasses transmission processes starting in the lead R and ending in the lead L (the sum over n in the first term and the sum over m in the second term correspond to the sum over α in Eq.(13) - all the scattering states of a given lead should be taken into consideration - whereas, the sum over m in the first term and the sum over n in the second term correspond to the sums appearing in Eqs.(11) and (12) respectively). Afterwards, we claim that the total current given by Eq.(18) is the total current in the left lead, decomposed into transmission processes from any left-lead mode n to any right-lead mode m, and inverse transmission processes (from any right-lead mode m to any left-lead mode n). Saying so, the advantage of defining the total current in a lead as above, is the direct generalization of the previous formalism to more complicated set-ups that might consist of more than two leads (additionally notice that since there are two separate summations over the left-lead and the right-lead modes, it is no longer required to assume that $n = m$, which was used for the transition from the first to the second line of Eq.(14)). Considering then a more general set-up that consists of more than two leads and terminals (with each lead connected to a particular terminal), based on the previous definition of the total current in a lead, the total current in lead α comes out by taking into account all the different transmission processes from the lead α towards any other lead α' of the set-up, as well as all the inverse transmission processes from all other leads α' towards the lead α, whose Fermi-Dirac distribution function is $f'_\alpha(E)$, chemical potential is μ'_α and temperature is T'_α. That is to say

$$I_\alpha^{q,s} = (2s+1)\frac{q}{h}\times \sum_{\alpha'\neq\alpha}\int_{-\infty}^{\infty} dE\,\left(\bar{\mathrm{T}}_{\alpha'\alpha}(E) f_\alpha(E) - \bar{\mathrm{T}}_{\alpha\alpha'}(E) f_{\alpha'}(E)\right) \qquad (19)$$

where we've used the following definitions (sort of collective transmission probabilities)

$$\bar{\mathrm{T}}_{\alpha'\alpha}(E) = \sum_{nn'}\left|t^{\alpha'\alpha}_{n'n}(E)\right|^2,\;\; \bar{\mathrm{T}}_{\alpha\alpha'}(E) = \sum_{n'n}\left|t^{\alpha\alpha'}_{nn'}(E)\right|^2 \qquad (20)$$

which encompass all the transmission processes (collectively denoted by n) starting in the lead α and ending in the different lead α' whose scattering states are collectively denoted as n' (leftmost definition), or, the other way round (rightmost definition).

As a final step, one could again assume low applied voltages over the whole set-up (such that any energy shifts, due to the applied voltages, from the equilibrium chemical potential of the whole set-up, are indeed small, and also small compared to the strength of the potential of the S.R.), express the occupancies as $f_\alpha(E) = n_F(E - \mu_\alpha) = n_F(E - \mu - qV_\alpha)$ (as previously), and Taylor-expand them (to lowest order) in terms of qV_α around μ, where μ denotes the equilibrium chemical potential of the whole set-up, whereas, V_α is the voltage applied to the α-th terminal. Doing so, with the help of the condition that $\sum_{\alpha'}\bar{\mathrm{T}}_{\alpha'\alpha}(E) - \sum_{\alpha'}\bar{\mathrm{T}}_{\alpha\alpha'}(E) = 0$ (where each sum separately actually adds up to the number of the transport channels/scattering states in the lead α, and those results actually originate from the unitarity of the scattering matrix in conjunction with the definitions of Eq.(20); for more details the reader is referred to Ref.[4], section 2.4, where the formalism of the scattering states is generalized to the multi-terminal case), it is finally found that

$$I_\alpha^{q,s} = \sum_{\alpha'\neq\alpha}\left(G_{\alpha'\alpha}(\mu,T)V_\alpha - G_{\alpha\alpha'}(\mu,T)V_{\alpha'}\right) \qquad (21)$$

where (in the spirit of Eq.(16)) we've used the following definition for the α-th conductance

$$G_{\alpha\alpha'}(\mu,T) = (2s+1)\frac{q^2}{h}\int_{-\infty}^{\infty} dE\,\left(-\frac{\partial n_F(E-\mu)}{\partial E}\right)\bar{\mathrm{T}}_{\alpha\alpha'}(E) \qquad (22)$$

and analogously for $G_{\alpha'\alpha}(\mu,T)$. It should be noted though that in equilibrium, other than a common chemical potential, a common temperature over the whole the set-up is additionally assumed, because we want to exclude any temperature-driven carrier transport from one region of the set-up to another. To put it differently, in equilibrium it is presumed that there is no kind of carrier transport whatsoever, i.e. $I^{q,s}_{\alpha,\,eq} = 0,\ \forall\ \alpha$. Applying the last condition to Eq.(21), we find (notice that in equilibrium it is not necessary that the applied voltages be zero, it is only required that all the applied voltage differences be zero, and therefore, in general it can be $V_\alpha = V_0 \neq 0,\ \forall\ \alpha$) that (and this is an example of a ”sum rule”)

$$\sum_{\alpha'} G_{\alpha'\alpha}(\mu,T) = \sum_{\alpha'} G_{\alpha\alpha'}(\mu,T) \qquad (23)$$

Finally, combining Eqs.(21) and (23) (the first term on the RHS of Eq.(21) is rewritten using Eq.(23)) we get

$$I_\alpha^{q,s} = \sum_{\alpha'} G_{\alpha\alpha'}(\mu,T)\left(V_\alpha - V_{\alpha'}\right) \qquad (24)$$

The above result which is valid in the limit of low applied voltages over a multi-terminal set-up concludes our presentation on the Landauer-Büttiker formalism of the steady state mesoscopic coherent transport. Please keep in mind that all this was just an introduction to the vast field of the physics of mesoscopic transport, and the interested reader can go deeper by consulting the provided references, and particularly Ref.[1], as well as Refs.[5]-[6] (whose author has offered related courses on edX as well).

---

[1] S. Bandyopadhyay, *Physics of nanostructured solid state devices.* Springer, 2012.

[2] T. T. Heikkilä, *”The physics of nanoelectronics”, Transport and fluctuation phenomena at low temperatures.* Oxford University Press, 2013.

[3] H. Bruus and K. Flensberg, *Many-body quantum theory in condensed matter systems.* Oxford University Press, 2009.

[4] D. A. Ryndyk, *”Theory of quantum transport at nanoscale”, An introduction.* Springer, 2016.

[5] S. Datta, *Lessons from Nanoelectronics; A New Perspective on Transport - Part A: Basic Concepts.* World Scientific, 2018.

[6] S. Datta, *Lessons from Nanoelectronics; A New Perspective on Transport - Part B: Quantum transport.* World Scientific, 2018.

Mapping Coulomb potential into 2D oscillator

Rvx Niltaans

(Dated: June 18, 2019)

We have shown before that the Hamiltonian of quantum motion in a magnetic field can be rewritten into a form resembling a harmonic oscillator Hamiltonian. In this paper, we will demonstrate how the 2D Coulomb potential is connected with 2D harmonic oscillator potential, and solve the problem of both the 2D and 3D hydrogen atom using this method.

I. Introduction

The hydrogen atom and the harmonic oscillator are simple but important quantum systems which can be solved analytically. Through the course, we have learned the structures and properties of these systems. In fact, there also exists a connection between harmonic oscillator and the Coulomb potential. Schwinger has shown in his book[1] this connection and turned the equations of one dynamical system into another one. To understand the symmetry of the hydrogen atom, it is possible rewrite the 2D oscillator potential into the form of a 3D Coulomb potential on a polar coordinate. As a analogy, the 2D Coulomb potential "toy model" [2] can also be rewritten into the form of a 2D oscillator potential on a parabolic coordinate. We will demonstrate both problems in this paper.

II. Review of Hydrogen atom

In this section, we will first review the solution of 3D hydrogen atom and demonstrate the solution of 2D hydrogen atom problem. The 3D hydrogen atom has the following Hamiltonian

$$H = \frac{\mathbf{p}^2}{2m} - \frac{e^2}{r} \tag{1}$$

Where $\mathbf{p}$ is the momentum operator, m is the mass of electron, and e the unit charge.

The energy levels are

$$E_{nl} = -\frac{e^2}{2a_0}\frac{1}{(n+l)^2},\, n \in \mathbb{N},\, l \in \mathbb{N}^* \tag{2}$$

This result can be obtained as follows. First, hypothise $E = -\frac{e^2}{2a_0}\frac{1}{\nu^2}$ where ν is an unknown parameter. This is plausible since $-\frac{e^2}{2a_0}$ are simply constants that give the correct units. Then, we introduce the Runge-Lenz vector

$$\mathbf{R} = \frac{1}{2m}\left(\mathbf{p} \times \mathbf{L} - \mathbf{L} \times \mathbf{p}\right) - e^2\frac{\mathbf{r}}{r}, \tag{3}$$

to reveal the hidden symmetries of this system, where $\mathbf{L}$ is the angular momentum operator. And we can prove that

$$[R_i, R_j] = -i\hbar\frac{2H}{me^2}\varepsilon_{ijk}L_k. \tag{4}$$

By using the familiar identity

$$\mathbf{L} \times \mathbf{u} + \mathbf{u} \times \mathbf{L} = 2i\hbar\mathbf{u}, \tag{5}$$

equation 4 also indicates that

$$\mathbf{R} \times \mathbf{R} = i\hbar\left(-\frac{2H}{me^4}\mathbf{L}\right). \tag{6}$$

We can also explicitly calculate the value of $\mathbf{R}^2$, which reads

$$\mathbf{R}^2 = 1 + \frac{2}{me^2}H\left(\mathbf{L}^2 + \hbar^2\right). \tag{7}$$

Since $\mathbf{R}$ is only consist of the sum of vector under rotations, (the cross product of vector under rotations is also a vector under rotation, such as $\mathbf{p}\times\mathbb{L}$), $\mathbf{R}$ itself is a vector under rotation. Thus

$$[L_i, R_j] = \epsilon_{ijk}R_k \tag{8}$$

.

From equations 4, 6, and 7, we can construct two abstract angular momentum

$$\begin{cases} \mathbf{J}_- = \frac{1}{2}\left(\mathbf{L} - \hbar\nu\mathbf{R}\right) \\ \mathbf{J}_+ = \frac{1}{2}\left(\mathbf{L} + \hbar\nu\mathbf{R}\right) \end{cases}. \tag{9}$$

We can also prove that $\mathbf{J}_+$ and $\mathbf{J}_-$ satisfy the properties of angular momenta

$$\begin{aligned} &\mathbf{J}_\pm \times \mathbf{J}_\pm = i\hbar\mathbf{J}_\pm \\ &[(\mathbf{J}_\pm)_i, (\mathbf{J}_\pm)_j] = 0 \\ &\mathbf{J}_+^2 = \mathbf{J}_-^2 = \hbar^2 j(j+1), j \in \frac{\mathbb{Z}}{2} \end{aligned} \tag{10}$$

Since

$$\mathbf{J}_+^2\mathbf{L}^2 + \hbar^2\nu^2\mathbf{R}^2 = \hbar^2(\nu^2+1) \tag{11}$$

Thus, by comparing equation 10 with 11, we can see that

$$\begin{aligned} &\nu = 2j+1 \in \frac{\mathbb{Z}}{2} \\ &E = -\frac{me^4}{2\hbar}\frac{1}{(2j+1)^2} \end{aligned} \tag{12}$$

Now, let's solve the 2D hydrogen atom with a similar method. For the 2D case, we can also hypothesise that $E = -\frac{e^2}{2a_0}\frac{1}{\nu^2}$. By defining a new angular momentum operator $\mathfrak{L} = L_3\mathbf{e}_3$. We are able to prove that vectors $\mathbf{u}$ on the x-y plane such as $\mathbf{x}$ and $\mathbf{p}$ satisfy the following relations.

$$[L_3, u_j] = i\hbar\epsilon_{jk}u_k \tag{13}$$

and $\mathfrak{L} \times \mathbf{u} + \mathbf{u} \times \mathfrak{L} = i\hbar\mathbf{u}$ which differs from the familiar identity equation 5 by a factor of 2. By defining the 2D Runge-Lenz vector as

$$\mathfrak{R} = \frac{1}{2m}\left(\mathbf{p} \times \mathfrak{L} - \mathfrak{L} \times \mathbf{p}\right) - e^2\frac{\mathbf{r}}{r} \tag{14}$$

We can see that

$$\begin{aligned} [\mathfrak{R}_i, r_j] =& -i\hbar\frac{4H_{2D}}{me^2}\varepsilon_{ij}\mathfrak{L} \\ \mathfrak{R} \times \mathfrak{R} =& i\hbar\left(-\frac{2H_{2D}}{me^4}\mathfrak{L}\right). \end{aligned} \tag{15}$$

This identities, are similar to the ones in the 3D case (compare equations 4 and 6). By using similar procedures, the value of $\mathfrak{R}^2$ can be obtained, which is

$$\mathfrak{R}^2 = 1 + \frac{2}{me^2}H_{2D}\left(\mathfrak{L}^2 + \frac{\hbar^2}{4}\right). \tag{16}$$

In this case, since $\mathfrak{L} + \hbar\nu\mathfrak{R}$ doesn't commute with $\mathfrak{L} - \hbar\nu\mathfrak{R}$, we can only define one abstract angular momentum $\mathfrak{J} = \mathfrak{L} + \hbar\nu\mathfrak{R}$, and we can obtain the result $j(j+1) = 4\nu^2 - 1$, which is similar compared with the 3D case (equation 12). However, we can't jump to the conclusion that $j \in \frac{\mathbb{N}}{2}$ as in ordinary abstract angular momenta. In this case since the z component of the Runge-Lenz vector $\mathfrak{R}_3 = L_3$, j in this case correspond to the azimuthal quantum number of L_3 and can only be integers. Thus ν can take the values $\frac{(2j+1)}{2}$, $j \in \mathbb{N}$, from which we can obtain the energy levels,

$$E_{2D} = -\frac{me^4}{2\hbar}\frac{1}{(j+\frac{1}{2})^2}, j \in \mathbb{N}. \tag{17}$$

In the following chapter, we will review the other quantum system—the 2D Harmonic Oscillator.

III. Review of 2D Harmonic Oscillator

The 2D Harmonic Oscillator has a potential of the form [3]

$$H = \frac{1}{2m}\left(p_x^2 + p_y^2\right) + \frac{m\omega}{2}\left(x^2 + y^2\right). \tag{18}$$

By constructing two sets of laddar operators

$$\begin{cases} a_{x/y} = \sqrt{\frac{m\omega}{2\hbar}}\left(x/y + \frac{ip_{x/y}}{m\omega}\right) \\ a_{x/y}^\dagger = \sqrt{\frac{m\omega}{2\hbar}}\left(x/y - \frac{ip_{x/y}}{m\omega}\right) \end{cases}, \tag{19}$$

where x/y indicates the subscripts or variables in the equation being x or y. The energy levels can be obtained[4],

$$E = \hbar\omega(n_x + n_y + 1),\ n_{x/y} \in \mathbb{N}. \tag{20}$$

After reviewing those systems, we will set up the connections between them in the following chapters.

IV. Introduction to the parabolic coordinate

To rewrite the hydrogen atom Hamiltonian in the form of a harmonic oscillator Hamiltonian, the Hamiltonian needs to be set up in the parabolic coordinate, which will be briefly introduced in this chapter.

The 2D parabolic coordinates, $x_{1'}$ and $x_{2\prime}$, is related to the Cartesian coordinate by the following formula:[5]

$$\begin{cases} x_1 = x_{1'}^2 - x_{2'}^2 \\ x_2 = 2x_{1'}x_{2'} \end{cases} . \tag{21}$$

And the length of a vector r can be written as $r = x_{\prime}^2 = x_{1'}^2 + x_{2'}^2$.

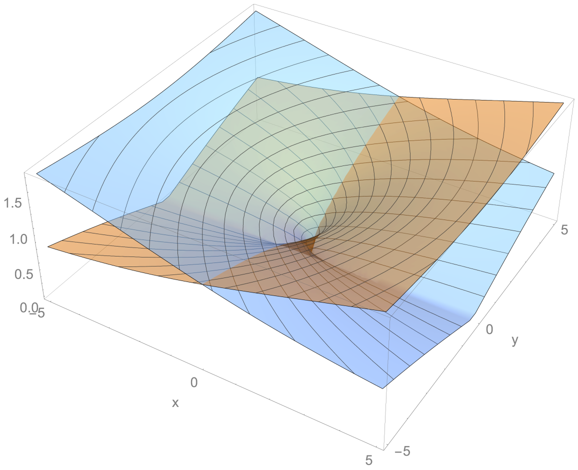

Fig. 1: Parabolic coordinate as contours

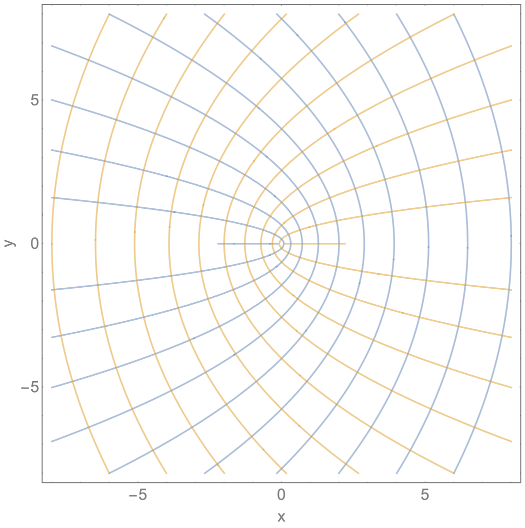

Fig. 2: Parabolic coordinate lines

Fig.1 shows that the parabolic coordinate can be viewed as a set of contours on the real and imaginary parts of the complex function $\omega(\mathfrak{z}) = \sqrt{\mathfrak{z}}$. The graph on the right shows the coordinate lines of $x_{1'}$ and $x_{2'}$, respectively. We can also get the transformation matrix elements $\beta^i_{j'}$ from Cartesian to parabolic coordinate and calculate the scale factors A_1, A_2 and A_3 (Einstein summation convention is used),

$$\beta^i_{j'} = \frac{\partial x_i}{\partial x_{j'}} = \begin{bmatrix} 2x_{1'} & -2x_{2'} \\ 2x_{2'} & 2x_{1'} \end{bmatrix} \tag{22}$$

$$\begin{aligned} g_{i'j'} &= \beta^{i'}_j \beta^{j'}_j \\ &= \begin{bmatrix} 4\left(x_{1'}^2 + x_{2'}^2\right) & 0 \\ 0 & 4\left(x_{1'}^2 + x_{2'}^2\right) \end{bmatrix} \end{aligned} \tag{23}$$

$$A_1 = A_2 = 2\sqrt{x_{1'}^2 + x_{2'}^2} = 2x_{\prime}. \tag{24}$$

From this, we can calculate the Laplacian for the sake of obtaining the Halmitonian operator in parabolic coordinate,

$$\begin{aligned}\nabla^2 &= \frac{1}{\Pi_i A_i}\frac{\partial^2}{\partial x_{i'}^2}\left(\frac{\Pi_i A_i}{A_j}\frac{\partial^2}{\partial x_{j'}^2}\right)\\ &= \frac{1}{4x_{\prime}^2}\left(\frac{\partial}{\partial x_{1'}}+\frac{\partial}{\partial x_{2'}}\right)\end{aligned} \tag{25}$$

V. Rewriting Two Dimensional Coulomb potential in oscillator form

We can start by transforming the Shrödinger equation for the 2D case into the parabolic coordinate using the identity 25[6]:

$$\begin{aligned} H\psi &= E\psi\\ \left(-\frac{\hbar^2}{8mx_{\prime}^2}\frac{\partial}{\partial x_{i'}}\frac{\partial}{\partial x_{i'}}-\frac{e^2}{x_{\prime}^2}\right)\psi &= E\psi\\ \left(-\frac{\hbar^2}{8m}\frac{\partial}{\partial x_{i'}}\frac{\partial}{\partial x_{i'}}-e^2\right)\psi &= x_{\prime}^2E\psi\end{aligned} \tag{26}$$

Here, we can see that the original potential energy term with e^2 becomes a constant term after both sides of the equation is multiplied by $x_{\prime}^2$, and the RHS become dependent of $x_{\prime}$. We can thus switch the position of these two terms and the equation will be come a familiar Shrödinger-like form.

$$\begin{aligned} \left(-\frac{\hbar^2}{8m}\frac{\partial}{\partial x_{i'}}\frac{\partial}{\partial x_{i'}}-x_{\prime}^2E\right)\psi &= e^2\psi\\ \left(-\frac{\hbar^2}{2(4m)}\frac{\partial}{\partial x_{i'}}\frac{\partial}{\partial x_{i'}}+\frac{1}{2}(4m)\sqrt{\frac{-E}{2m}}^2x_{\prime}^2\right)\psi &= e^2\psi\end{aligned} \tag{27}$$

We can recognize this as a Hamiltonian of a harmonic oscillator with $E' = e^2$, $m' = 4m$ and $\omega' = \sqrt{\frac{-E}{2m}}$. Thus it's energy levels should be

$$\begin{aligned} e^2 = E' &= \hbar\omega'\left(n_x+n_y+1\right)\\ &= \hbar\sqrt{\frac{-E}{2m}}\left(n_x+n_y+1\right).\end{aligned} \tag{28}$$

Where $n_x, n_y \in \mathbb{N}$ From which we can obtain the energy level of E:

$$E = \frac{-2\alpha e^2}{\hbar}\frac{2}{(n_x+n_y+1)^2}. \tag{29}$$

In the following diagrams, we can see the correspondence of the hydrogen atom states to the 2D oscillator states.

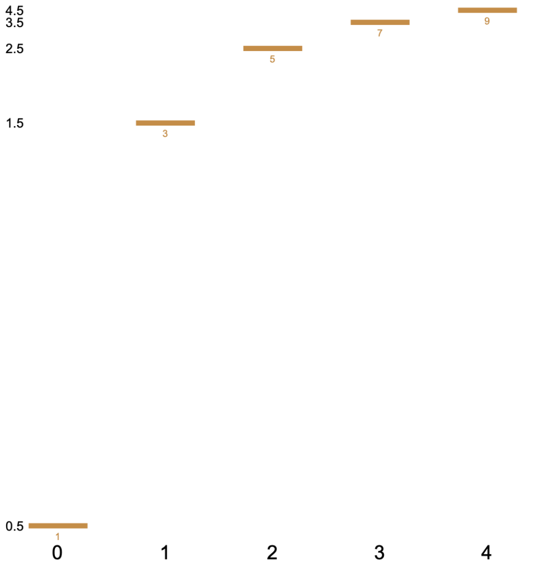

Fig. 3: Energy Eigenstates of the 2D hydrogen atom

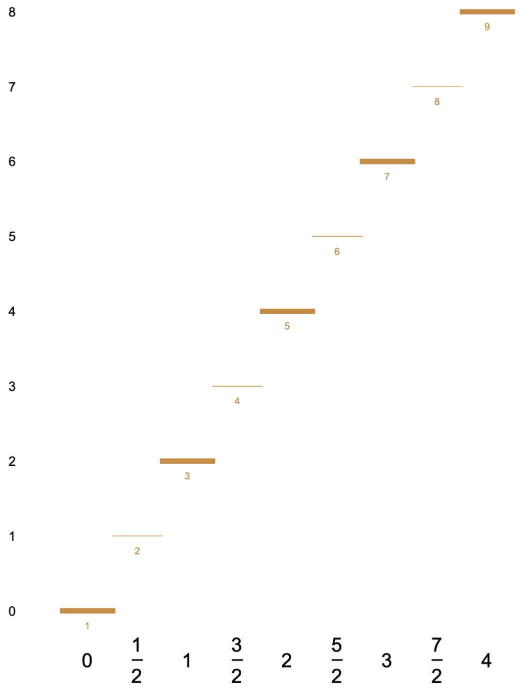

Fig. 4: Energy Eigenstates of the 2D oscillator

The brown horizontal bars represent the energy states. Fig.3 is the energy levels of the 2D hydrogen atom. The vertical ticks correspond to different values of l, which is the eigenvalue of the operator L_3 divided by $\hbar$; and the horizontal ticks denotes to the value of ν. Fig.4 is the energy levels of the 2D harmonic oscillator, the vertical ticks also correspond to l and the y axis correspond to $n_x + n_y$, where $n_x, n_y \in \mathbb{N}$ as in equation 29. The number below the horizontal indicate m degeneraces. We can see the connection of the two system by matching the $\nu = \frac{1}{2}$, $\frac{3}{2}$... states (the brown bars) on Fig.3 to the $n_x + n_y = 1$, 2, 3... states (the thick brown bars) on Fig.4. These states are respectively the same states obtained mathematically.

There is a more subtle reason for why the parabolic coordinate is used. As shown in section IV, since $\omega = \sqrt{\mathfrak{z}}$, we have $|\omega| = \sqrt{|\mathfrak{z}|}$. This give rise to the relationship $r = x_{\prime}^2$—the length of a vector in the parabolic coordinate is the squared length of a vector in the Cartesian coordinate.

In the parabolic coordinate, the Halmitonian gains a factor of $\frac{1}{x_{\prime}^2}$

$$H = -\frac{\hbar^2}{8mx_{\prime}^2}\frac{\partial}{\partial x_{i'}}\frac{\partial}{\partial x_{i'}} - \frac{e^2}{x_{\prime}^2}\psi. \tag{30}$$

By multiplying both sides of the Shrödinger equation by $x_{\prime}^2$, we can get the familiar oscillator-form equation.

VI. 2D oscillator in polar coordinates

In this section, the relation of the 2D oscillator and 3D hydrogen atom will be discussed. We will start from rewriting the 2D oscillator potential in a polar form. Suppose the harmonic oscillator has energy E', angular frequency ω' and mass m,[1] its Hamiltonian is

$$\begin{aligned} H &= -\frac{\hbar^2}{2m}\frac{\partial}{\partial x_i}\frac{\partial}{\partial x_i} + \frac{1}{2}m\omega'^2 x_i x_i \\ &= -\frac{\hbar^2}{2m}\left(\frac{1}{r}\frac{\partial}{\partial r}\left(r\frac{\partial}{\partial r}\right) + \frac{1}{r}\left(\frac{\partial^2}{\partial\theta^2}\right)\right) + \frac{1}{2}m\omega'^2 r^2 \end{aligned} \tag{31}$$

We will further simplify H by setting an ansatz. Since the Hamiltonian only contain $\frac{\partial^2}{\partial\theta^2}$, by assuming the solution is seperable, it is plausible that the ansatz should be of the form $\psi = e^{i\alpha\theta}\frac{1}{\sqrt{r}}R(r)$. By letting it act on ψ, the $\frac{\partial^2}{\partial\theta^2}$ will become α^2, thus H now reads,

$$H = -\tfrac{\hbar^2}{2m}\left(\tfrac{\partial^2}{\partial r^2} + \tfrac{1}{r}\tfrac{\partial}{\partial r} + \tfrac{\alpha^2}{r^2}\right) + \tfrac{1}{2}m\omega'^2 r^2 \tag{32}$$

Here, we will ues the identity

$$r^{-a}\frac{\partial^2}{\partial r^2}r^a = \left(\frac{\partial^2}{\partial r^2} + \frac{2a}{r}\frac{\partial}{\partial r} + \frac{a^2-a}{r}\right) \tag{33}$$

with $a = \frac{1}{2}$ to absorb the term with $\frac{\partial}{\partial r}$ to simplify the result.

$$
\begin{aligned}
&-\frac{\hbar^2}{2m}\left(\left(\frac{\partial^2}{\partial r^2}+\frac{1}{r}\frac{\partial}{\partial r}-\frac{\frac{1}{4}}{r^2}\right)-\frac{\alpha^2-\frac{1}{4}}{r^2}\right)+\frac{1}{2}m\omega^2r^2\\
=&-\frac{\hbar^2}{2m}\left(\frac{1}{\sqrt{r}}\frac{\partial^2}{\partial r^2}\sqrt{r}-\frac{\alpha^2-\frac{1}{4}}{r^2}\right)+\frac{1}{2}m\omega'^2r^2
\end{aligned}
\tag{34}
$$

Now, plug this Hamiltonian into the Shrödinger equation, we can get

$$
\begin{aligned}
H'\psi =& E'\psi\\
\left(-\frac{\hbar^2}{2m}\left(\frac{\partial^2}{\partial r^2}-\frac{\alpha^2-\frac{1}{4}}{r}+\frac{1}{2}m\omega'^2r^2\right)R\left(r\right)\right) =& E'\left(r\right).
\end{aligned}
\tag{35}
$$

Since we are trying to write this equation into the form of a radial equation of the hydrogen atom, we need the RHS to be $\sim \frac{1}{r}$ (the form of a Coulumb potential). We will change the variable r to r' by the following relation:

$$
r' = \frac{r^2}{2},
\tag{36}
$$

and we will get

$$
\begin{aligned}
&\left(-\frac{\hbar^2}{2m}\left(\frac{\mathrm{d}^2}{\mathrm{d}^2r'}+\frac{1}{2r'}\frac{\mathrm{d}}{\mathrm{d}r'}-\frac{\alpha^2-\frac{1}{4}}{r'^2}\right)+\frac{1}{2}m\omega'^2\right)\\
&R\left(r'\right)=\frac{E'}{r'}R\left(r'\right)
\end{aligned}
\tag{37}
$$

By using identity 33 again, we can absorb the terms $\frac{\partial}{\partial r'}$ and get

$$
\begin{aligned}
&\left(-\frac{\hbar^2}{2m}\left(\frac{1}{\sqrt[4]{r'}}\frac{\mathrm{d}^2}{\mathrm{d}^2r'}\sqrt[4]{r'}+\frac{1}{2r'}\frac{\mathrm{d}}{\mathrm{d}r'}-\frac{\alpha^2\frac{1}{16}}{r'^2}\right)-\frac{1}{2}m\omega'^2\right)\\
&R\left(r'\right)=E'R\left(r'\right).
\end{aligned}
\tag{38}
$$

To eliminate the $\sqrt[4]{r'}$, will then change $R\left(r\right)$ to $R'r' = \frac{1}{\sqrt[4]{r'}}R\left(r'\right)$ and get

$$
\left(-\frac{\hbar^2}{2m}\left(\frac{\mathrm{d}^2}{\mathrm{d}^2r'}-\frac{\alpha^2-\frac{1}{16}}{r'^2}\right)+\frac{1}{2}m\omega'^2\right)R\left(r'\right)=\frac{E'}{r'}R\left(r'\right).
\tag{39}
$$

Compare with the familiar hydrogen atom potential,

$$
\left(-\frac{\hbar^2}{2m}\left(\frac{\mathrm{d}^2}{\mathrm{d}^2r}-\frac{l(l+1)}{r^2}\right)-\frac{e^2}{r}\right)u\left(r\right)=\frac{E}{r}u\left(r\right),
\tag{40}
$$

where $u\left(r\right)$ is the radial part of the hydrogen eigenstates divided by r, $u\left(r\right) = \frac{f(r)}{r}$. We can see that the hydrogen atom equation has exactly the same form with the rewritten harmonic oscillator equations. $u\left(r\right)$ in equation 40 serves as $R'\left(r'\right)$ in equation 39; $\sqrt{\frac{-2E}{m}}$ is the new ω and e^2 functions as the new energy, $e^2 = \hbar\sqrt{\frac{-2E}{m}}\left(n+1\right), \in \mathbb{N}$, from which we get the familiar hydrogen atom energy levels

$$
E = -\frac{me^4}{2\hbar\left(n+1\right)^2},\ n \in \mathbb{N}.
\tag{41}
$$

In the following diagrams, we can again see the correspondence of the 2D oscillator states to the hydrogen atom states.

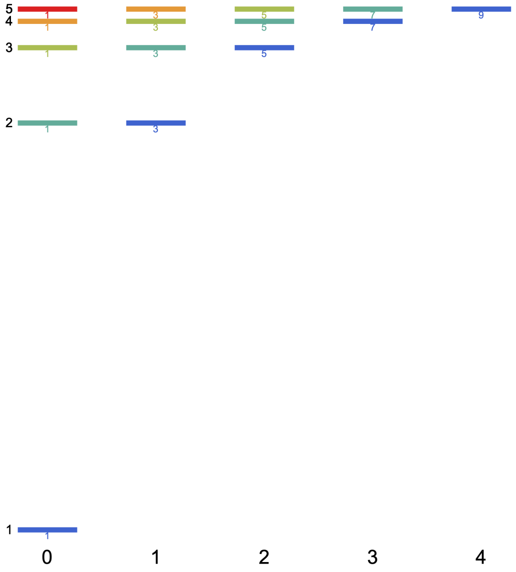

Fig. 5: Energy Eigenstates of the 3D hydrogen atom

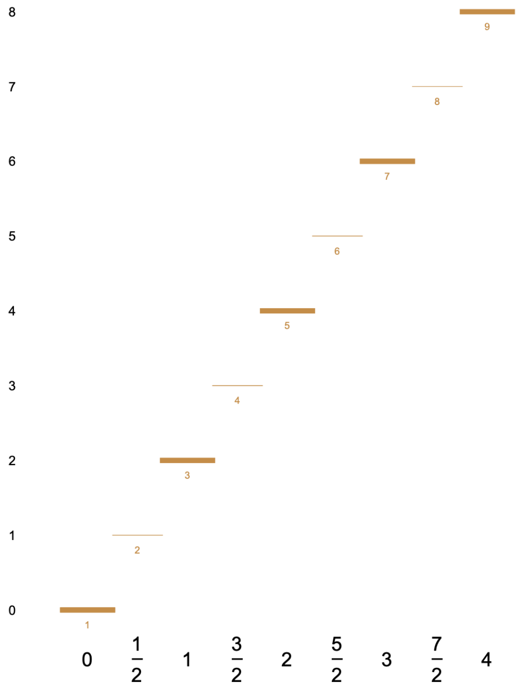

Fig. 6: Energy Eigenstates of the 2D oscillator

Fig.5 is the energy levels of the 3D hydrogen atom. The vertical ticks correspond to different values of l and the horizontal ticks denotes to the value of ν. Fig.6 is again the energy levels of the 2D harmonic oscillator which is already discussed in Section V. The number below the horizontal indicate m degeneraces. We can see the connection of the two system by matching the $\nu = \frac{1}{2}, \frac{3}{2}...$ states (the bars with the same color) on Fig.5 to the $n_x + n_y = 1, 2, 3...$ states (the thick brown bars) on Fig.6. One set of bars with the same color correspond to a set of oscillator states.

VII. Conclusion

These examples indicate that the hydrogen atom and harmonic oscillator are actually connected in their underlying mathematical structures. To dive further, this is related to the isomorphisms between SU (2), SO (3), and SO (4) groups. The methods in this paper also show that different physical phenomenon may be governed by the same mathematical laws and is able to transform between each other in different coordinates.

---

[1] Julian Schwinger. Quantum mechanics: symbolism of atomic measurements, 2003.

[2] B Zaslow and Melvin E Zandler. Two-dimensional analog to the hydrogen atom. *American Journal of Physics*, 35(12):1118–1119, 1967.

[3] Lev Davidovich Landau and Evgenii Mikhailovich Lifshitz. *Quantum mechanics: non-relativistic theory*, volume 3. Elsevier, 2013.

[4] Jun John Sakurai, Jim Napolitano, et al. *Modern quantum mechanics*. Pearson Harlow, 2014.

[5] Shi-Hai Dong and M Lozada-Cassou. An algebraic approach to the harmonic oscillator plus an inverse square potential in three dimensions. *The American Journal of Applied Sciences*, 2(1):376–382, 2005.

[6] Bo Fu, Fu-Lin Zhang, and Jing-Ling Chen. Connection between coulomb and harmonic oscillator potentials in relativistic quantum mechanics.

On the use of random matrices in physics

(Dated: June 16, 2019)

In systems with many interactions, for example the modeling of heavy nuclei, the explicit modelling of the system becomes practically impossible. Wigner took the bold step of assuming practically nothing about the Hamiltonian of the system and instead hypothesized properties like energy eigenvalue relative spacing of heavy nuclei could be modeled with the aid of random matrices. Remarkably the results show strong statistical correspondence to reality when appropriate distributions are chosen on the matrix entries. We will discuss some of the key results.

I. HISTORICAL BACKGROUND

As we have learned as our physics education has grown, most problems do not have closed form analytic solutions. To address systems that differ from exactly solvable systems one learns of perturbative methods to try to tackle changes to assumptions, where those changes are relatively small or alternatively one tries numerical methods to generate approximate results. When it came to studying complex systems with many interacting particles and forces, for example in studying the energy spectrum of large nuclei (a pressing issue in the nuclear age), the academic community was at somewhat of a loss. Neutron scattering experiments done by Fermi in the 30s revealed narrow resonances which indicated the energy eigenvalues were not independently distributed. In particular, elastic scattering of neutrons on heavy nuclei show sharp resonances with widths from 3 meV to 1 eV and such resonances cannot be due to the interaction of the neutron with a single nucleon. If one was to assume an independent particle model, with a nuclear radius of 5 femtometers and a potential well of several MeV, single particle states have energy spacings of several hundred keV, which is incompatible with the results seen[12]. In trying to interpret the results Bohr [1] argued that the resonance spacings were incompatible with an independent particle model and proposed a compound-nucleus model where the protons and neutrons were strongly interacting. Instead of trying to construct a dynamical theory of heavy nuclei, Wigner took Bohr's idea of the nucleus as a complex interacting system and focused on trying to model the statistics of energy spacings without using an explicit model of the system. Such an approach was highly innovative and ended up catalyzing a large pick up in research in random matrix theory. The approach taken by Wigner was to some extent a statistical mechanics approach to complex quantum mechanical phenomenon, but the spirit of the analysis is different. In particular in statistical mechanics the ensemble share the same Hamiltonian but have differing initial conditions, in random matrix theory one averages over all Hamiltonians of a particular symmetry type, properly normalized, and those results are used to understand the statistics of energy eigenvalue distributions. "What is here required is a new kind of statistical mechanics, in which we renounce exact knowledge not of the state of the system, but of the nature of the system itself. We picture a complex nucleus as a 'black box' in which a large number of particles are interacting according to unknown laws. The problem then is to define in a mathematically precise way an ensemble of systems in which all laws of interaction are equally probably." Dyson[2]

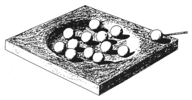

Figure 1. Bohr[1]

Random matrix theory itself had origins in the field of statistics and were introduced by Wishart in 1928. The field itself became far more active after Wigner's use of random matrices in physics and in the 50s and 60s many results on the mathematical foundations were derived by Wigner, Mehta and Gaudin and Dyson. The various classes of random matrices were cataloged by Dyson in a series of landmark papers as well as the philosophical foundation for their use in physics. From the 1960s to the 1980s, random matrix theories predictions were being tested against better nuclear reaction data from experimental physics with encouraging results. It was discovered that the distribution of eigenvalues of a random matrix, properly normalized, is often independent of the underlying distribution (known as universality) with only the weak condition of i.i.d required of the entries. Today the applications of random matrix theory in physics are wide and remarkable connections can be made between math and physics via the use of random matrices.

II. WIGNER SEMI-CIRCLE LAW

Wigner first attempted to model the heavy nucleii Hamiltonian via a random Schrodinger operator in which one treated the potential as having a stochastic component. $H = -\Delta + V(X,\omega)$ where $V(X,\omega)$ are independent identically distributed random variables (i.i.d). This model proved too challenging to solve and Wigner subsequently moved on to attempting to model heavy nuclei eigenvalue statistics with random matrices. As we know, a quantum mechanical system is described by an eigenvalue problem $H\psi_n = E_n\psi_n$ where H is a Hermitian operator and ψ_n is an eigenfunction with E_n

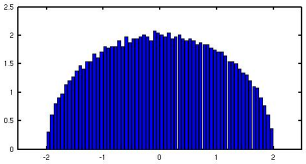

Figure 2. 3000x3000 RM

corresponding to the eigenvalue of the eigenfunction. For heavy nuclei there would be thousands of states and energy levels which are too complicated to model explicitly. By avoiding the problem of trying to find the actual operator and instead considering a family of random matrices and trying to see if there was a relationship between the random matrix averages and the heavy empirical nucleii results, Wigner stumbled onto fertile ground. The actual operator would be infinite dimensional so when considering random matrices one should study the behavior for large N and then take N→ ∞. Wigner noticed that random matrices had some scope to frame eigenvalue spacings and thus studied the distribution of real symmetric Gaussian ensembles.

Definition 1. The k'th moment of a distribution $F(x)$ is $\mu_k = \int_{-\infty}^{\infty} x^k dF$

In probability theory the first moment would represent the mean, the second moment represents the variance, the third the skew and the fourth the kurtosis. We saw the use of the moments of the wavefunction when computing the position expectation for example.

Wigner's SemiCircle Law Let X be a real symmetric matric of large order size N having independent identically distributed (i.i.d) random entries x_{ij} with 2nd moments equal to $\frac{R}{2}^2$ and such that the nth moments are bounded by given constants B_n, independent of i,j and N. Define S $= S_{\alpha\beta}(x, N)$ to be the number of eigenvalues of X that are in the interval $\left(\alpha N^(1/2), (\beta N^(1/2))\right)$for real $\alpha < \beta$. Then $\lim_{n\to\infty} \frac{E(S)}{N} = \frac{1}{2\pi m^2} \int_{\alpha}^{\beta} \sqrt{R^2 - x^2)} dx$

The Semi-circle law is effectively a central limit theorem for random matrices and the distribution to which the average spacing over all such random matrices converge to is the semi-circular distribution. Remarkably the underlying distribution of the entries is not particularly important for the convergence to occur. There are several ways one goes about proving this, Wigner proved it via comparing trace formulas for limits of the expected distribution of eigenvalues of matrices of increasing size to the moments of the semi-circular distribution. There are other measure theoretic approaches which were used later using the Stieltjes transform. We will give an overview of the methods used by Wigner [4] or for full details we recommend Tao [5].

The main argument used by Wigner when showing the convergence properties of the eigenvalue distribution of large random matrices was to look at the normalized moments of the average using the relationship between the trace of the matrix and the eigenvalues to compute the moments. In particular it was shown that E$\frac{1}{n}tr\left(\frac{1}{\sqrt{n}X_n}\right)^k = C_{\frac{k}{2}} + o_k(1)$ Where C$_k$ denote the Catalan numbers and X represents a real symmetric matrix as defined in Wigner's SemiCircle Law. The Catalan numbers show up in multiple combinatorial problems. For example the Catalan numbers represent the number of ways in which one can get n heads and n tails after flipping a coin 2n times where the number of heads flipped so far is always greater than or equal to the number of heads flipped by that same time. This represents a the number of paths a random walk could take that started and ended at 0 while never crossing the x-axis.

Definition 2 The **Catalan numbers** are a sequence of natural numbers that are defined as follows $C_n = \frac{1}{n+1}\binom{2n}{n}$

Definition 3 The standard **Semicircle** distribution is a probability distribution that has the form $f(x) = \frac{2}{\pi}\sqrt{1-x^2}$ for -1≤x≤1 and f(x) = 0 elsewhere.

As mentioned, the original proof that the limit of a real symmetric N x N random matrix eigenvalues, properly normalized, converged to the semi-circle distribution by showing the moments of the two distributions were the same. Below we discuss how to compute the moments for the semi-circle distribution

Let μ_{sc} be the probability distribution for the standard semicircle distribution. Let $m_k = \int_{-1}^{1} x^k \mu_{sc} dx$. As the semi-circle (semi ellipse actually) is symmetric all odd moments are 0. One can compute the even moments via trignometric substitution for x $= \sin\theta$. Note then that E$(X^{2n}) = \int_{-\pi/2}^{\pi/2} \frac{2}{\pi} \sin^{2n}\theta \cos^2\theta d\theta$ with such a substitution and this expectation can be computed via Mathematica to yield $\frac{1}{2}^{2n}\frac{1}{n+1}\binom{2n}{n}$. Thus the suitably normalized ensemble of Wigner type random matrices has the same moments for its distribution as the semi-circle distribution and has therefore the same distribution.

It is worth mentioning again that the semi-circle distribution does not represent the eigenvalue distribution of a heavy nucleii, which is unbounded. It represents that there exists a central limit theorem for a large class of random matrices which in turn have useful results for predicting local densities of eigenvalues for heavy nucleii.

III. WIGNER SURMISE

In studying the properties of random matrices and trying to apply the results to heavy nucleii spectrum Wigner was looking to understand whether local eigenvalue densities could be predicted. In particular one could ask the question of what the nearest neighbor distribution (the distribution of the distance to adjacent eigenvalue) would look like for the eigenvalues if one was to sort them in ascending order, this process is called *unfolding*. This lead to the bold conjecture known as Wigner Surmise which states that the probability of adjacent eigenvalue spacings

$$\mathrm{P(s)}\approx \frac{\pi s}{2} * e^{-\frac{\pi s^2}{4}} \ (1)$$

where s $= \frac{S}{D}$ where S a particular spacing and D is the average distance between neighboring intervals calculated from a particular interval unfolding.

To come to this conclusion it is suspected that what Wigner did was take a 2 x 2 matrix and worked out the eigenvalue distribution and by exploring the consequences of a 2 x 2 matrix eigenvalue gap distribution he inferred the relationship would hold to larger matrices and would model the empirical distribution of heavy nuclei. We will derive the distribution for the 2 x 2 below.

Definition 4. A Wigner matrix ensemble is an ensemble of Hermitian matrices $H = (H_{ij})$ where i,j range from 1 to n such that all upper triangular entries are iid complex random variables with mean zero and variance 1 and the diagonal entries are iid real variables with finite mean and variance.

One thing to note is if the spacing between eigenvalues was independent for any given nuclear spectrum then the distribution would be Poisson and of the form $\rho(s) = e^{-s}$ When considering the distributions of eigenvalues in random matrix theory one should remember the scale is always taken out by looking at the spacing of eigenvalues within any interval divided by the average spacing for all entries within that interval. This leads to a scale invariant way of framing the distribution and one does not have to worry about the parameter within the Poisson distribution for example as it is always rescaled to 1.

A subset of Wigner random matrices would be real symmetric matrices with iid entries also known as GOE (General Orthogonal Ensemble). We will explore a real symmetric 2 x 2 matrix.

Take a 2x2 matrix

$$\mathrm{H}=\begin{pmatrix} x_1 & x_3 \\ x_3 & x_2 \end{pmatrix} \ x_1, x_2 \sim \mathrm{N}(0,1) \text{ and } x_3 \sim \mathrm{N}\left(0, \tfrac{1}{2}\right) \ (2)$$

We can calculate the eigenvalues via from the roots of the characteristic equation using the approach from Livan, Novaes, Vivo [6]

$$\lambda^2 - \mathrm{Tr}(H)\,\lambda + \det(H) \ (3)$$

for the above matrix one gets

$$\lambda_{1,2} = (x_1 + x_2 \pm \sqrt{(x_1 - x_2)^2 + 4x_3^2}))/2 \ (4)$$

which leads to a spacing of s $= |\lambda_1 - \lambda_2| = \sqrt{(x_1 - x_2)^2 + 4x_3^2}$ the probability distribution of s can be calculated from the independence of the entries as a multivariate Gaussian, in particular

$$\rho(s) = \iiint_{-\infty}^{\infty} dx_1 dx_2 dx_3 \frac{1}{2\pi}\frac{1}{\sqrt{\pi}} e^{-\frac{1}{2}\left(x_1^2 + x_2^2 + 2x_3^2\right)} \delta\left(s - \sqrt{(x_1 - x_2)^2 + 4x_3^2}\right) \ (5)$$

via clever trignometric substitution

x$_1 - x_2 = r * \cos\theta$
$2 * x_3 = r * \sin\theta$
$x_1 + x_2 = \Psi$ (6)

One gets the Jacobian for x_1, x_2, x_3

$$\det\begin{pmatrix} \frac{\cos\theta}{2} & -\frac{r\cos\theta}{2} & \frac{1}{2} \\ -\frac{\cos\theta}{2} & \frac{r\sin\theta}{2} & \frac{1}{2} \\ \frac{sin\theta}{2} & \frac{r\cos\theta}{2} & 0 \end{pmatrix} = -\frac{r}{4} (7)$$

leading to

$$\rho(s) = \int_0^{\infty} dr\; r\delta(s - r) \int_0^{2\pi} d\theta \int_{-\infty}^{\infty} d\psi\; e^{\frac{-1}{2}\left(\left(\frac{r\cos\theta + \psi}{2}\right)^2 + \left(\frac{-r\cos\theta + \psi}{2}\right)^2 + \frac{r^2\sin^2\theta}{2}\right)} (8)$$

The particular choice of relative variance of the entries leads to very clean pdf, if one uses a GOE matrix the distribution come to

$$\rho(s) = \left(\frac{\pi * s}{2} * e^{\frac{-\pi s^2}{4}}\right) \ (9)$$

see Guhr [3] for the general form. Equation 7 is the Wigner surmise for the GOE. It is remarkable that from experimenting with such a simple random matrix and deriving a distribution for the expected distance for the only eigenvalue pair Wigner was able to hazard a remarkably accurate guess about the benefits of modelling heavy nuclei via large random matrices as well as the eigenvalue spacing distribution of those heavy nucleii. This remarkable realization led to a number of papers on the properties of GOE random matrices of large size and infinite dimension see Wigner [4]

It is very important to always keep in mind that the Wigner surmise represents an approximate distribution of the nearest neighbor of eigenvalues in the spectrum. It most certainly does not represent the distribution of eigenvalues for the system at large. Nonetheless for considering the local density properties of the eigenvalues of a complex system, the Wigner surmise is accurate in a statistical sense.

The Wigner Surmise is a close approximation to the nearest neighbor distribution for large random matrices but the exact form turned out to be different. The actual formula was deduced by Gaudin and Mehta [7] and has an asymptotic form. The Wigner surmise though is approximate within 5% where P(s) has non negligible density.

IV. SYMMETRY AND CLASSIFICATION IN RANDOM MATRICES

The notion of symmetry group is foundational when it comes to classification in quantum mechanics. In classical mechanics one is introduced to the symmetries of a physical system via conserved quantities and Noether's theorem. A symmetry classification for random matrix theory was described by Dyson[8] "that the most general matrix ensemble, defined with a symmetry group which may be completely arbitrary, reduces to a direct product of independent irreducible ensembles each of which belongs to one of one of the three types".

The general form of the **Wigner Surmise** is

P(s) = $C_\beta s^\beta e^{-a_\beta s^2}$ (10)

where the parameter $\beta \in \{1,2,4\}$ is determined by the particular symmetries of the system. In particular time reversal and spin rotation. P(s) represents a probability measure so the coefficients are taken to normalize the integral to 1. Each β refers to an ensemble type. $\beta = 1$ refers to GOE which was intuitively derived above (7) for the 2x2, all entries are real. $\beta = 2$ refers to the unitary ensemble GUE where the off diagonal entries are complex. $\beta = 4$ refers to the symplectic GSE where the off diagonal entries are quaternionic. See figure 3 for the differences relative to the Poisson distribution.

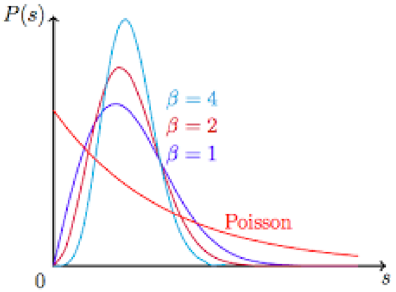

Figure 3. Cugliandolo [10]

The three symmetry classes are referred to as the orthogonal(real symmetric), unitary(complex Hermitian) and symplectic(quaternionic self-dual). These symmetry classes, associated with their particular Gaussian measure on the set of matrices which satisfy the appropriate symmetry, are referred to as the Gaussian ensembles. As mentioned above, Dyson, in a series of papers in the 60s [2] further solidified the foundation laid by Wigner and furthered the algebraic understanding of the methodologies with the landmark paper The Threefold Way [8]. The material for this is somewhat involved but Dyson realized that for the three associative division algebras $(\mathbb{R}, \mathbb{C}, \mathbb{H})$, each of these could be associated with a random matrix ensemble with the appropriate measure on it. Each ensemble with entries from a particular division algebra would have different physical symmetries associated with it. The original mathematical results come from Frobenius but Dyson recognized the physical significance for application in random matrices.

DefinitionThe GUE is the set of nxn Hermitian matrices with complex off diagonal entries with the Gaussian measure $\frac{1}{Z_{GUE(n)}} e^{-\frac{n}{2} trH^2}$.

The GUE is invariant under unitary conjugation but does not have time reversal symmetry.

DefinitionThe GOE is the set of nxn real symmetric matrices (subset of Hermitian) with Gaussian measure $\frac{1}{Z_{GOE(n)}} e^{-\frac{n}{4} trH^2}$

The GOE is invariant under orthogonal conjugation (rotation) and it models time reversal symmetry. Recall the time reversal properties stem from the ability to conjugate the time derivative in the Schrodinger equation. Real Hamiltonians allow for that but not necessarily complex Hermitian.

DefinitionThe GSE is the set of n x n quaternionic Hermitian matrices with the appropriate Gaussian measure on it. $\frac{1}{Z_{GUE(n)}} e^{-ntrH^2}$.

These matrices, which would be the least familiar to us at this point, model time reversal symmetry but not rotational symmetry. This corresponds to systems

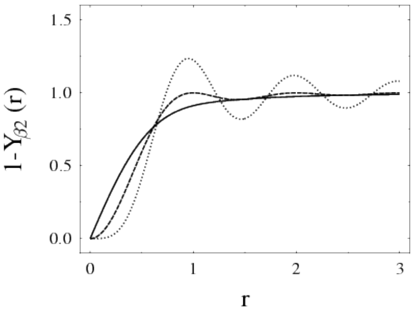

Figure 4. Guhr [3]

Table I. Dyson classification

β	Ensemble	Time Reversal	Rotational	H_{ij}
1	GOE	Yes	Yes	real
2	GUE	No	N/A	complex
4	GSE	Yes	No	real-quaternionic

with half integer spin. One can see the overview of the symmetry characteristics in Table 1.

These symmetry classes have differing nearest neighbor distributions which yield differing statistical observables, the distributions of which can be seen in figure 3. Another way of thinking about the difference is via the two-level correlation function with $r = \eta_1 - \eta_2$ which is of much practical use and relatively easy to compute from experimental data where η_n are the unfolded eigenvalues. The theoretical correlation functions show different eigenvalue repulsions for small r; the Poisson case would have $X_2(r) = 1$ which means no repulsion. One can see that as r increases the two-level correlation functions converge to the Poisson distribution (which just means independent). For the GOE there is repulsion that decreases monotonically, for the GUE there is repulsion with small oscillations around r = 1 and for the GSE there are monotonically decreasing oscillations at integer differences. This can be seen in figure 4 where the solid line represents the GOE, the wider dashed line the GUE and the dotted line the GSE, the scale is normalized so that r = 1 average nearest neighbor distance of the sample. Thus when thinking about symmetry classes in random matrix theory one looks at statistical observables to make inferences about the symmetries of the system.

V. PHYSICAL EXAMPLES

Figure 2 represents the nearest neighbor distribution of a collection of heavy nucleii. In particular it consists of 1407 resonance levels belonging to 30 sequences of 27 nucleii including Cd,Dm,Gd,Dy,Er,W,Th U. Of differing isotopes. As has been mentioned throughout, the spacing is normalized such that one is always dividing by the average distance computed from the element's sample. The result matches the GOE distribution very well and one can see that the Poisson distribution is not representative.

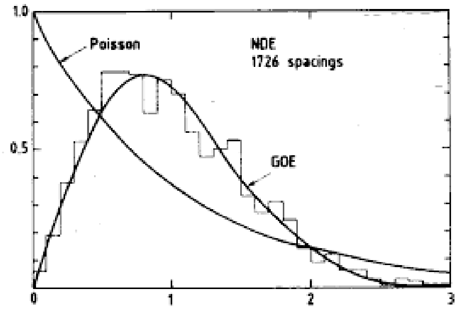

Figure 5. Guhr [3]

Remarkably one example of a quantum system which exhibits the properties of the GOE nearest neighbor distribution is a Hydrogen atom in a uniform magnetic field [9]. Chaos in quantum mechanics is at first an ambiguous concept. Chaotic motion is classically deterministic, but highly sensitive to initial conditions such that long term predictability is impossible in practice due to imprecision of the initial measurement. In quantum mechanics trajectories can only be defined approximately due to the uncertainty dependent on Planck's constant and as such the classical concept of chaos is inapplicable. Nonetheless for systems in which the classical system would be non-integrable, the quantum mechanical analogue can generate an energy spectrum which follows the nearest neighbor distributions generated by random matrics. The Hamiltonian of a hydrogen atom in a uniform magnetic field is accurately modeled by the following

$$H = \frac{p^2}{2m_e} - \frac{e^2}{r} + \omega l_z + \frac{1}{2}\omega^2(x^2 + x^2) \qquad (11)$$

where the direction of the field is in the z direction and omega is half the cyclotron frequency. One can define the dimensionless field strength parameter.

$$\gamma = \frac{\hbar\omega}{R} \qquad (12)$$

where R denotes the Rydberg energy. The classical dynamics of the hydrogen atom don't depend on the energy and field strength separately but rather together via the scaled energy $\epsilon = \frac{E}{\gamma^{\frac{2}{3}}}$. At ϵ = -∞ the hydrogen atom is effectively unperturbed and the classical motion is regular but around $\epsilon = -.35$ there is a sudden transition to chaotic motion. Such chaos occurs until $\epsilon = -.127268$. By studying the classical changes of behavior in phase space one can understand at what field strengths the behavior should change for the quantum energy spectrum.

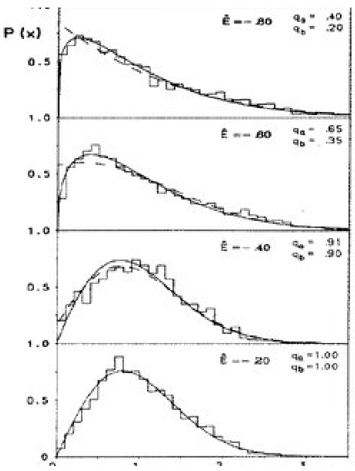

Figure 6. Friedrich Wintgen [9]

In fact one can understand the transitions by considering the classical system's Liapunov exponents which determine the properties of the dynamical systems manifolds[9]. This classical chaos leads to a transition of the statistical properties of the spectrum from Poisson to GOE.

In practice most real physical eigenvalue nearest neighbor distributions for complex or chaotic systems seem to overlap with the GOE distribution. The GOE can also model classical chaotic behaviour in systems like the Sinai billiard ball. In particular, when analyzing classically integrable systems, the eigenvalues of the spacings of the eigenvalues of the corresponding quantum system follow the Poisson distribution but if the system is non-integrable then the eigenvalues have the same pattern of eigenvalue nearest neighbor distributions that come from random matrices.

Random matrix theory is a field where the math developed before the full experimental evidence but it was conjectured that the GUE would be seen in classically chaotic systems where time symmetry was broken and this was seen experimentally in the mid 90 using a microwave cavity with thin ferrite strips next to the wall. Strong magnetic field applied to the ferrite breaks the time reversal symmetry and the eigenvalue nearest neighbor distributions change in line with the Wigner surmise [11].

VI. SUMMARY

By considering Random Matrices for the modeling of complex quantum phenomenon one takes both a practical as well as intellectual leap that proves useful and illuminating. One can gain insight into the nature of the symmetries of a particular system by looking at the statistics of its eigenvalues and one can also get an implicit understanding of how intractable a system might be to model by looking at its local spectrum. For the question of how many pieces of spectral data are required to construct the Hamiltonian, in the case of a GOE spectrum, the answer is all of them, implying the problem cannot be broken down. Thus both the nature of random matrices and the behavior of atomic spectra can be compared for productive benefit. What is remarkable is that we don't really know if quantum systems which have Hamiltonian's with Gaussian entries, yet if one takes the ensemble average of such systems and compare them to average nearest neighbor densities as in Figure 2, one gets the same results. This is because higher dimensional analogs of equation (4) all converge to the same correlation functions (once re-scaled) that lead to the nearest neighbor distribution of the GOE. This phenomenon we find empirically is referred to as *universality* and is of core importance in relating the mathematics of random matrices to the the physical eigenvalue spectrum. Random matrix theory is a remarkable field which crosses heavily between physics and mathematics. Results within physics have had influence within number theory though the reason for the connections remain unanswered. As a discipline it has a different philosophical background to classical wavefunction theories but it provides alternative ways to interpret physical results as well as offering alternative insights into the symmetries or lack thereof of complex systems.

[1] Bohr, Niels, Issue 137 (Nature, 1936)
[2] Dyson, Freeman, Statistical Theory of Energy Levels of Complex System. I (Journal of Mathematical Phyics V31, 1962)
[3] Guhr, Thomas and Müller–Groeling, Axel and Weidenmüller, Hans A, Random-matrix theories in quantum physics: common concepts, Physics Reports, 1998
[4] Wigner, Eugene P, Characteristic vectors of bordered matrices with infinite dimensions, The Collected Works of Eugene Paul Wigner, 1993
[5] Tao, Terence, Topics in random matrix theory, American Mathematical Soc., 2012
[6] Livan, Giacomo and Novaes, Marcel and Vivo, Pierpaolo, Introduction to random matrices: theory and practice, Springer, 2018
[7] Mehta, Madan Lal, Random matrices and the statistical theory of energy levels, Academic Press, 1967
[8] Dyson, Freeman J, The threefold way. Algebraic structure of symmetry groups and ensembles in quantum mechanics, Journal of Mathematical Physics, volume 3, 1962
[9] Friedrich, Harald and Wintgen, Hieter, The hydrogen atom in a uniform magnetic field—an example of chaos, Physics Reports, volume 183, 1989
[10] Cugliandolo, Laticia, Advanced Statistical Physics: Random Matrices, lecture notes, 2017
[11] So, Anlage, Ott, Oerter,Experiments with and without Time Reversal Symmetry: GUE and GOE Statistics,Physical Review Letters,volume 74, 1995

[12] Weidenmuller, H.A and Mitchell, G.E,Random Matrices and Chaos in Nuclear Physics,Reviews of Modern Physics,volume 81,2009

Oscillations of neutrinos as localized wave packets

Sergey Kotelnikov

(Dated: June 18, 2019)

Neutrino oscillation is well-known effect, which is often introduced in simple terms of plane waves. However, we need more realistic approach with neutrino as a localized particle in order to understand the prospects and limitations of neutrino experiments. Possible restrictions on neutrino-oscillation measurements are discussed.

I. INTRODUCTION

A. Neutrino generations

Since the discoveries of electron neutrino ν_e (Cowan & Reines in 1956), muon neutrino ν_μ (Lederman, Schwartz, Steinberger in 1962) and tau neutrino ν_τ (DONUT collaboration, Fermilab, 2000), they are considered as indispensable actors in most of weak interactions. These interactions are materialized by emission or absorption of heavy W (80 GeV) or Z (91 GeV) bosons, and therefore have very small probability, especially in a sub–GeV energy region. That is probably why all the neutrino types were first deduced theoretically from indirect observations, the very first being made by Pauli (1930) as n exotic workaround of the β–decay

$$n \rightarrow p + e^- + \tilde{\nu}_e \tag{1}$$

analysis problems. As soon as new analogues of electron, μ (1936) and τ (1970s) were found, within few years there came an idea of their associated neutrino types. As of now, three types (flavors) of neutrino together with their charged lepton counterparts constitute three pairs or generations of leptons. We distinguish these neutrinos primarily by their distinct charged-current interactions, as shown in Eq. (1) for the electron type. Another example of a charged-current interaction, this time for muon neutrino ν_μ, is the famous decay of a π-meson:

$$\pi^+ \rightarrow \mu^+ + \nu_\mu . \tag{2}$$

It is interesting to note, that neutrinos appear or disappear in pairs with the corresponding charged leptons, so that the so-called electron-, muon- or tau-lepton number is conserved. Later, in section II on the oscillation analysis , we shall describe these types of neutrino as *interaction eigenstates*, that is the neutrino eigenstates, which can be produced or detected through their specific weak interactions.

B. The Solar Problem

Due to the very small probability of neutrino interactions and before the era of high-energy particle accelerators, it was necessary to find available sources of neutrino of high intensity. Three of them were at hand: cosmic rays, nuclear power stations and the Sun. In 1938, Hans Bethe explained the mechanism of thermonuclear synthesis in the Sun, which happens to be the so-called proton-proton chain. Basically, this is a multi-step fusion of protons into ${}^4_2$He nuclei, γ-quanta and electron neutrinos ν_e. One of intermediate steps in the fusion chain has a special interest for us, because it generates ν_e with energies up to $14\,MeV$, which many detectors are sensitive to:

$${}^8_5\mathrm{B} \rightarrow {}^8_4\mathrm{Be} + e^+ + \nu_e \,. \tag{3}$$

The whole proton-proton chain happens to be an abundant source of electron neutrinos. A well-known aphorism by John Bahcall who did all calculation says that that 100 billion neutrinos pass through your thumbnail every second, or, in more standard units, 6.5×10^{10} neutrinos per second through every square centimeter on the Earth surface. And yet, when Ray Davis measured in 1968 the neutrino flux from the reaction

$$\nu_e + {}^{37}_{17}\mathrm{Cl} \rightarrow {}^{37}_{18}\mathrm{Ar} + e^- \tag{4}$$

he found it to be only 1/3 of the predicted value. In spite of many obstacles and difficulties of the experiment, it was not a problem of its accuracy. On the contrary, the precision was fantastic: Davis was able to extract every single radioactive Ar atom from 10^5 gallons of his tetrachloroethylene detector, that is from 2.35×10^{30} molecules. And the discrepancy found was too big to be explained by measurement errors anyway.

C. Oscillations

Interestingly, the idea of neutrino oscillations came much earlier by Pontecorvo, in 1958, and was motivated by analogy with oscillations of $K^0/\tilde{K}^0$ mesons. That time, it was only about $\nu \leftrightarrow \tilde{\nu}$ transitions. A particle mixture theory of neutrino assuming the existence of two kinds of neutrinos was proposed by Maki, Nakagawa and Sakata in 1962 [1]. However, it was the Solar Problem, which move this theory into full swing. In 1968 Pontecorvo tried to explain the deficit of electron neutrinos by their possible oscillation into another neutrino type. Finally, as if our progress really goes in a circle, it is interesting to note, that the Solar Problem was finally explained not by neutrino oscillations but rather by the Mikheyev-Smirnov-Wolfenstein (MSW) effect: the non-oscillatory effect of the surrounding matter onto the passing neutrino (see Smirnov [2]).

II. SIMPLE TWO-STATE MODEL

Let us consider an easy only two-neutrino model, for example, with ν_e and ν_χ neutrinos, where ν_e is an electron neutrino and ν_χ is of another type. This also happens to be rather practical for many experiments, where only one neutrino type is analyzed, while others are combined in a group. Let us denote the state of the system at time t as $|\nu(t)\rangle$, neutrino interaction eigenstates as $|\nu_\alpha\rangle$ where $\alpha = e, \chi$, and neutrino *mass eigenstates* as $|\nu_k\rangle$ where $k = 1, 2$ with $m_2 > m_1$. We introduce these latter states as a hypothesis to explain the oscillation effect. The mass states do not participate in any interaction, apart from the gravitation, so that we can deduce them only as a superposition of interaction states. The way to reveal them directly would be only through the gravitational force, which is almost negligible in particle experiments. However, they might be good candidates for sterile neutrinos, exotic particles some experiments are looking for.

Let the unitary operator for state transitions $U_{\alpha k}$ to be

$$U_{\alpha k} = \begin{pmatrix} \cos\theta & -\sin\theta \\ \sin\theta & \cos\theta \end{pmatrix}, \tag{5}$$

where θ is the mixing angle. Let the state at time 0 to be a pure electron neutrino: $|\nu(0)\rangle = |\nu_e\rangle$. We also consider that once a neutrino is created there are no interactions anymore, and our mass eigenstates propagate in time as free particles. Finally, we use units to satisfy $\hbar = c = 1$ and only one spacial coordinate x for simplicity. It turns out that at time 0 our pure electron state is already a mixture of mass eigenstates:

$$|\nu(0)\rangle = |\nu_e\rangle = U_{ek}\,|\nu_k\rangle\,, \tag{6}$$

where we use Einstein summation on repeated index k. Further on, the mass eigenstates propagate as free particles and get phase factors like any other stationary wave function:

$$|\nu(t)\rangle = U_{ek} \cdot e^{i(p_k x - E_k t)}\,|\nu_k\rangle\,. \tag{7}$$

As we know, a superposition of stationary functions is not a stationary function, where phase factors determine the time-dependence of its parameters and probabilities. Let's consider the amplitude of the $\nu_e \to \nu_\chi$ transition $A_{\chi\leftarrow e}$:

$$\begin{aligned} A_{\chi\leftarrow e} &= \langle \nu_\chi | \nu(t) \rangle \\ &= \langle U_{\chi j}\nu_j | U_{ek}\nu_k \rangle \cdot e^{i(p_k x - E_k t)} \\ &= U^*_{\chi j}\,\langle \nu_j | \nu_k \rangle\, U_{ek} \cdot e^{i(p_k x - E_k t)} \\ &= U_{\chi k} \cdot U_{ek} \cdot e^{i(p_k x - E_k t)} \end{aligned} \tag{8}$$

Now, from Eq. (5) follows $U_{\chi 1} \cdot U_{e1} = -U_{\chi 2} \cdot U_{e2} = \frac{1}{2}\sin 2\theta$. Then Eq. (8) turns into:

$$A_{\chi\leftarrow e} = \frac{1}{2}\sin 2\theta \cdot (e^{i(p_1 x - E_1 t)} - e^{i(p_2 x - E_2 t)}). \tag{9}$$

Now, we'll try to extract the time dependence. Let's write p_k and E_k as:

$$\begin{aligned} p_1 &= p - \Delta p & E_1 &= E - \Delta E \\ p_2 &= p + \Delta p & E_2 &= E + \Delta E. \end{aligned} \tag{10}$$

Substituting Eq. (10) into Eq. (9) we get:

$$\begin{aligned} A_{\chi\leftarrow e} &= \frac{1}{2}\sin 2\theta \cdot e^{i(p\cdot x - E\cdot t)} \\ &\quad \times (e^{-i(\Delta p\cdot x - \Delta E\cdot t)} - e^{i(\Delta p\cdot x - \Delta E\cdot t)}) \\ &= -i \cdot \sin 2\theta \cdot e^{i(p\cdot x - E\cdot t)} \cdot \sin(\Delta p \cdot x - \Delta E \cdot t). \end{aligned} \tag{11}$$

We get a general expression for the oscillation phase:

$$\Delta\phi_{osc} = \Delta p \cdot x - \Delta E \cdot t. \tag{12}$$

At this point many introductory texts select either Δp or ΔE equal to 0. The motivation, in spite of physically incorrectness, is due to simplicity and to getting surprisingly the right answer. For example, in Griffiths [3] we find $\Delta p = 0$ and for $m \ll E$ we get

$$E \approx p + \frac{1}{2}\frac{m^2}{p} \quad \Rightarrow \quad \Delta E = \Delta m^2/4E, \tag{13}$$

where $\Delta m^2 = m_2^2 - m_1^2$. Finally, the transition amplitude from Eq. (11) up to the common phase factor becomes:

$$A_{\chi\leftarrow e} \sim sin 2\theta \cdot \sin(\frac{\Delta m^2}{4E}t). \tag{14}$$

In other words, we get an oscillation phase in the assumption of $\Delta p = 0$:

$$\Delta\phi_{\Delta p=0} = \frac{\Delta m^2}{4E}t. \tag{15}$$

In terms of distance in SI units, this would give us an expression for the oscillation length, the distance, at which the conversion from one neutrino flavor to another is maximal, ℓ_{osc}:

$$\ell_{osc}[km] = 1.24 \times E[GeV]/\Delta m^2[eV^2]. \tag{16}$$

Figure 1 below illustrates how two mass eigenstates, ν_1 and ν_2 interfere at the beginning of ν_e creation, at a distance $\frac{1}{2}\ell_{osc}$ and at ℓ_{osc}. At the beginning, both waves are shifted by π, hence the ν_e. Then the phase difference tends to decrease to 0, thus forming ν_χ.

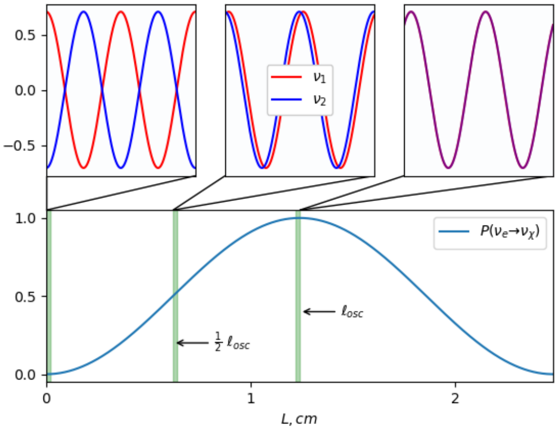

Figure 1. Interference of ν_1 and ν_2 at different distances (the three plots at the top). Below is the probability of conversion ν_e to ν_χ. The mixing angle θ is taken 45°, neutrino energy 10 keV, $\Delta m^2 = 1\ eV^2$

III. WAVE PACKET APPROACH

The condition $\Delta p = 0$ is, in fact, not convincing. It suggests that each of the neutrino mass eigenstates is an infinite plane wave, which contradicts the nature of neutrinos being created in one place, propagated, and detected elsewhere. However we still need a notion of interference in some space interval, where de Broglie waves of different neutrinos mix to produce the oscillation effect. A feasible solution would be to use the idea of wave packets to represent the neutrino states.

Let's consider each neutrino mass eigenstate as a wave packet with its mean momentum p_k, energy E_k and group velocity $v_{gk} = \frac{\partial E_k}{\partial p_k}$. Each has spatial and momentum uncertainties, σ_{xk} and σ_{pk}, related to each other like $\sigma_{xk} \sim 1/\sigma_{pk}$. For simplicity, we assume that these uncertainties do not depend on the neutrino type k. A very detailed treatment can be found in Akhmedov & Smirnov [4].

A. Oscillation conditions

The wave packet approach helps not only to represent the oscillation process in a more realistic way, it also helps to find out some conditions or restrictions under which the oscillations could be observed.

If we want to observe oscillations, that is the interference of the two mass eigenstates, their difference in energy and momentum must be smaller than the uncertainties of the corresponding wave packet parameters:

$$\Delta E \ll \sigma_E \qquad\qquad \Delta p \ll \sigma_p. \tag{17}$$

Conversely, if any of these two conditions is violated, the wave packet would serve, at least, potentially as a high-precision energy probe to distinguish between the mass eigenstates. One can also see this when Δp written as $\Delta p \sim \frac{\Delta m^2}{E}$, so that

$$\Delta p \ll \sigma_p \quad \Rightarrow \quad \Delta m^2 \ll E \cdot \sigma_p. \tag{18}$$

Taking into account $\sigma_x \sim 1/\sigma_p$ and ℓ_{osc} from Eq. (16), it may also be written as

$$\sigma_x \ll \ell_{osc}. \tag{19}$$

This is the so-called *localization condition* for neutrino production and detection [4]. It just says that both wave packets should be within the uncertainty range related to their mass difference.

The other is the *coherence condition*. It comes from the fact that two wave packets having different group velocities will go sooner or later apart, so that any interference between them becomes negligible. One can write a condition for coherence as

$$\Delta v_g/v_g \cdot L \ll \sigma_x, \tag{20}$$

where L is the distance traveled by neutrino in time L/v_g. After approximating Δv_g and v_g as:

$$\Delta v_g \sim \Delta m^2/E^2 \qquad\qquad v_g \sim p/E, \tag{21}$$

the coherent condition becomes

$$\frac{\Delta m^2}{Ep} \cdot L \ll \sigma_x, \tag{22}$$

which, in turn, using the oscillation length from Eq. (16) can be written as:

$$L \ll p \cdot \ell_{osc}\sigma_x, \tag{23}$$

where the right part is called the *coherence length* ℓ_{coh}. Finally, the condition takes form:

$$L \ll \ell_{coh}, \tag{24}$$

which puts a limit to the distance at which oscillations can be observed.

B. Oscillation formula again

The wave packet approach can also solve the puzzle why the simple plane wave model could get the right expression (14) for the oscillation transition amplitude. Let's take the correct formula for the oscillation phase $\Delta\phi_{osc}$ in Eq. (12) . This time, we present its ΔE as:

$$\Delta E \approx \frac{\partial E}{\partial p}\Delta p + \frac{1}{2}\frac{\partial E}{\partial m^2}\Delta m^2, \tag{25}$$

where in $\frac{\partial E}{\partial p}$ we recognize the averaged group velocity v_g of both wave packets. Our $\Delta\phi_{osc}$ then becomes

$$\Delta\phi_{osc} = (x - v_g t)\Delta p - \frac{\Delta m^2}{4E}t. \tag{26}$$

In the second term on the right we see $\Delta\phi_{\Delta p=0}$ from Eq. (15), which now describes the mixing of the point-like neutrinos, as if they we moving with $v_g = x/t$. The first term shows the phase correction, $\Delta\phi_{cor}$, due to the wave packet model. Now we need to understand how large this correction is. The $x - v_g t$ factor is determined by the wave packet $\sigma_x \sim 1/\sigma_p$, beyond this limit the wave packet is vanishing. This gives us under the conditions from Eq. (17)

$$\Delta\phi_{cor} = (x - v_g t)\cdot\Delta p \sim \sigma_x \Delta p \sim \Delta p/\sigma_p \ll 1. \tag{27}$$

Finally, we have for $\Delta\phi_{osc}$:

$$\Delta\phi_{osc} = \Delta\phi_{cor} - \Delta\phi_{\Delta p=0} \approx -\Delta\phi_{\Delta p=0}. \tag{28}$$

Thus, our previous formulas for the transition amplitude in Eq. (14) and the oscillation length in Eq. (16) remain valid in spite of arguable assumptions under which they were originally derived.

IV. DISCUSSION

The wave packet approach may be considered as an overkill: many neutrino oscillation characteristics can be derived from the plane wave model and quite precisely at that. However, it is only from wave packets that we can understand what actually happens and what conditions are necessary to fulfill to observe the effect of oscillations. Let's take two examples. It were experiments with β–decay from where the history of physics of neutrino started and since a long time they have been using as a tool to estimate the absolute value of the neutrino masses. These experiments are very delicate, require precise measurement and long time, but they are comparatively cheap and could be performed almost in any decent laboratory. Recently it was suggested to use a β–decay experiment to search for an exotic, if not hypothetical, heavy neutrino. In particular, it was suggested to find specific changes in the shape of the electron spectrum, which might be caused by oscillation $\nu_e \to \nu_\chi$ with the sterile neutrino mass of at least a few tens of keV.

Now, as we can see from the localization condition in Eqs. (17) – (19), the precision of our energy measurement must be at least by one order of magnitude higher than $1\,keV$. However, the resolution of the electron spectrum in β–decay experiment is of order of $1\,eV$. This gives us an upper limit on masses of hypothetical neutrino to be measured here. On the other hand, sterile neutrinos being so light would hardly produce any changes in the spectrum. The perspective of the such an experiment looks rather discouraging.

The same localization condition also puts restrictions on the size of the experimental setup. If the source of neutrinos is a container with radioactive particles, like tritium, and has a size of $\sim 1m$, the registration device, according to Eq. (19), must be over meters away to observe any oscillation effects.

Another example is related to the coherent condition in Eq. (24). Depending on the solar neutrino energy, their corresponding ℓ_{coh} varies from few hundreds of kilometers to several solar radii [2]. Therefore it is not oscillations that affect the neutrino flavor composition but rather other mechanisms (in this case it is due to the MSW effect).

Even more this applies to the case of supernova neutrinos. The distances they have to travel are beyond any possible coherent length. This leads to averaging over all three neutrino mass states, which would give us roughly 1/3 for each neutrino flavor.

One more interesting point mentioned in [4]. The coherence effect is not only restrictive but also ensures we have the same neutrino at distances close to its production and where the oscillation effect is still negligible. The absence of the coherence would mean averaging over all mass eigenstates, which would lead to non–conservation of the neutrino flavour almost immediately after its generation.

ACKNOWLEDGMENTS

This essay wouldn't have been written without encouragement, motivation and even requirement coming from

MIT 8.06x "Applications of Quantum Mechanics" course. It is difficult to overestimate the work done by its staff. They helped not only in understanding the material but also in creating an inspiring atmosphere of theoretical physics among the community of online students.

[1] Z. Maki, M. Nakagawa, and S. Sakata, "Remarks on the Unified Model of Elementary Particles," *Progress of Theoretical Physics* **28** (11, 1962) 870–880.
[2] A. Y. Smirnov, "Solar neutrinos: Oscillations or No-oscillations?," *arXiv e-prints* (Sep, 2016) arXiv:1609.02386, `arXiv:1609.02386 [hep-ph]`.
[3] D. J. Griffiths, *Introduction to Elementary Particles.* WILEY-VCH Verlag GmbH & Co. KGaA, 2008.
[4] E. K. Akhmedov and A. Y. Smirnov, "Paradoxes of neutrino oscillations," *Physics of Atomic Nuclei* **72** (Aug, 2009) 1363–1381, `arXiv:0905.1903 [hep-ph]`.

The partition function for ideal monatomic and diatomic gases

Rene A. Galvan

(Dated: June 14, 2019)

The partition function for systems in thermodynamic equilibrium is of fundamental importance, since classical thermodynamics can be constructed from it. We will use simple quantum models to find the energy levels of monatomic and diatomic molecules, and from these energies we will write the molecular partition function and then the partition function for monatomic and diatomic ideal gases. Finally we will obtain the equation of state of the ideal gases from the partition function, establishing a connection between microscopic phenomena governed by quantum mechanics and the macroscopic phenomena described by classical thermodynamics.

I. INTRODUCTION

"The volume of a given amount of gas is directly proportional to the number on moles of gas, directly proportional to the temperature and inversely proportional to the pressure." In this article we will obtain this law based on the principles of statistical mechanics. To do this, we will define the properties of a thermodynamic system based on the occupation of its energy states. In this way we will arrive at a fundamental relationship between the energy states and the probability that the system is in one of them in particular (Eq. 4). This relationship will allow us to define the partition function of a system. Then we will see that from this function the thermodynamic state functions of the system can be obtained. To obtain the partition function it will be necessary to know the energy states, so we will use quantum mechanics to find the so-called molecular partition function from simple models. Finally, we will use the partition function obtained to write the energy, the heat capacity and the equation of state for ideal monatomic and diatomic gases.

II. THE PARTITION FUNCTION AND THE THERMODYNAMIC STATE FUNCTIONS

A. Temperature

In classical thermodynamics, temperature is defined by zeroth law of thermodynamics [3]. In statistical mechanics, we will define the temperature in an analogous way. Consider two systems in contact with each other through a diathermic wall and both separated from the rest of the universe by means of an adiabatic wall. After a sufficiently long time, the systems will reach equilibrium, leaving each of them with fixed energies E_1 and E_2. System 1 will be in one of the $\Omega_1(E_1)$ possible *microstates* and system 2 will be in one of the $\Omega_2(E_2)$ possible microstates, therefore the complete system can be in one of a total of $\Omega_1(E_1)\Omega_2(E_2)$ microstates (a microstate is the detailed specification of a microscopic configuration of a state). From the principles of statistical mechanics it can be seen that the thermodynamic state (*macrostate*) that is associated with a greater number of microstates is the most probable macrostate (a macrostate is characterized by being determined by a finite number of variables, such as pressure, volume, number of particles, etc.). Then we try to maximize the product $\Omega_1(E_1)\Omega_2(E_2)$ for a certain division of energy. Mathematically it is expressed as

$$\frac{d}{dE_1}(\Omega_1(E_1)\Omega_2(E_2)) = 0 \tag{1}$$

From Eq. 1 it follows that

$$\frac{d\ln\Omega_1}{dE_1} = \frac{d\ln\Omega_2}{dE_2} \tag{2}$$

This relationship defines a common property that all systems have in thermal equilibrium with each other, known as *temperature* T:

$$\frac{1}{k_BT} = \frac{d\ln\Omega}{dE} \tag{3}$$

where k_B is the *Boltzmann constant* [4].

B. The Boltzmann factor and the partition function

Consider a *canonical ensemble* formed by a system in thermal contact with a huge reservoir at temperature T, isolated from the rest of the universe. Suppose that for each energy E_j of the system there is only one microstate. The system plus the reservoir have a fixed energy and the condition that *all microstates are equally likely* is met. Then the probability $p(j)$ that the system has the energy E_j is

$$p(j) = \frac{e^{-E_j/k_BT}}{\sum_i e^{-E_i/k_BT}} \tag{4}$$

where E_j is the energy of the microstate j and T is the temperature of the reservoir.

The probability distribution that defines is known as *canonical distribution* or *Boltzmann distribution.* The term e^{-E_j/k_BT} is known as the *Boltzmann factor* [4].

If the system has a fundamental state with some energy and excited states with energy that increase with the level number, then the ground state is the one that is more likely to be occupied and the excited states have decreasing probabilities, depending on the ratio between your energy and the energy k_BT [5].

The expression

$$Z = \sum_i e^{-E_i/k_BT} \tag{5}$$

is known as *partition function.* Its tremendous importance lies in the fact that, as we will see later, knowing the partition function of a system it is possible to express mathematically the thermodynamic functions of state. The key to knowing the partition function is to determine for each particular system (gas composed of diatomic molecules, for example) the available states and their corresponding energies. For this purpose, the tools provided by quantum mechanics must be used [1] [4].

C. Entropy

In a *microcanonical ensemble*, the systems that compose it have the same fixed energy. A macrostate can be associated with different microstates; assuming that within a microcanonical ensemble we have a particular macrostate with fixed energy and that Ω is the number of microstates associated with the macrostate, we define the entropy S of the system as [4]

$$S = k_B \ln \Omega \tag{6}$$

Now considering a system that has N different equally probable microstates, which can be divided into subsystems (macrostates) with n_i microstates in the i-th macrostate, and p_i is the probability of finding the system in macrostate i, the general definition of entropy is

$$S = -k_B \sum_i p_i \ln p_i \tag{7}$$

From this expression, we can deduce Eq. 6 and is entirely compatible with the classical definition of entropy [1] [4] [6].

D. Obtaining state functions

To obtain the state functions from the partition function we will initially calculate the internal energy U and the entropy S, and then the other variables, Helmholtz function F, pressure p, enthalpy H, Gibbs function G and heat capacity at constant volume C_V, from their relations to each other. The internal energy is calculated as the average of all the possible states of the system

$$U = \sum_i p_i E_i = \frac{\sum_i E_i e^{-\beta E_i}}{\sum_i e^{-\beta E_i}} \tag{8}$$

where we define

$$\beta = \frac{1}{k_BT} \tag{9}$$

Eq. 8 is equivalent to

$$U = -\frac{d \ln Z}{d\beta} \tag{10}$$

that is

$$U = k_BT^2 \frac{d \ln Z}{dT} \tag{11}$$

From Eq. 7 and Eq. 4 we get

$$S = \frac{U}{T} + k_B \ln Z \tag{12}$$

that is

$$S = k_B \ln Z + k_BT(\frac{\partial \ln Z}{\partial T})_V \tag{13}$$

Then from the relationships between thermodynamic variables [4]

$$F = U - TS = -k_BT \ln Z \tag{14}$$

$$p = -(\frac{\partial F}{\partial V})_T = k_BT(\frac{\partial \ln Z}{\partial V})_T \tag{15}$$

$$H = U + pV = k_BT \left[T(\frac{\partial \ln Z}{\partial T})_V + V(\frac{\partial \ln Z}{\partial V})_T \right] \tag{16}$$

$$G = F + pV = k_BT \left[-\ln Z + V(\frac{\partial \ln Z}{\partial V})_T \right] \tag{17}$$

$$C_V = (\frac{\partial U}{\partial T})_V = k_BT \left[2(\frac{\partial \ln Z}{\partial T})_V + V(\frac{\partial^2 \ln Z}{\partial T^2})_V \right] \tag{18}$$

III. THE PARTITION FUNCTION FROM MICROSCOPIC PROPERTIES

So far we have expressed the fundamental state variables of thermodynamics from the partition function. The challenge now is to calculate the partition function for the system we are studying. This article deals with ideal gases, so we will focus on the systems of particles (atoms or molecules) that are identical and do not interact with each other.

A. Partitioning function of a system of independent and distinguishable particles

Consider a system of N independent and distinguishable particles enclosed in a volume V. The total energy of the system, $E_{i_1,i_2\cdots i_N}$, will be

$$E_{i_1,i_2\cdots i_N} = E_{i_1}^{a_1} + E_{i_2}^{a_2} + \cdots + E_{i_N}^{a_N} \tag{19}$$

where $E_{i_j}^{a_j}$ is the energy of the particle a_j in the state i_j.

The partition function is

$$\begin{aligned} Z &= \sum_{i_1,i_2\cdots i_N} e^{-E_{i_1,i_2\cdots i_N}/k_BT} \\ &= \sum_{i_1,i_2\cdots i_N} e^{-(E_{i_1}^{a_1}+E_{i_2}^{a_2}+\cdots+E_{i_N}^{a_N})/k_BT} \end{aligned} \tag{20}$$

Because the particles are distinguishable and independent, the sums can be made on each index independently, then

$$\begin{aligned} Z = &\sum_{i_1} e^{-E_{i_1}^{a_1}/k_BT} \sum_{i_2} e^{-E_{i_2}^{a_2}/k_BT} \cdots \sum_{i_N} e^{-E_{i_N}^{a_N}/k_BT} \\ &= Z_{m,a_1} Z_{m,a_2} \cdots Z_{m,a_N} \end{aligned} \tag{21}$$

where the functions Z_m defined as

$$Z_m = \sum_i e^{-E_i/k_BT} \tag{22}$$

are called *molecular partition functions.*

When the energy states of all the particles (atoms or molecules) are the same, the partition function for a system of *independent and distinguishable* atoms or molecules is [1] [4] [5]

$$Z = (Z_M)^N \tag{23}$$

B. Partitioning function of a system of independent and indistinguishable particles

When the particles are independent and indistinguishable, the energy of the system is

$$E_{i_1,i_2\cdots i_N} = E_{i_1} + E_{i_2} + \cdots + E_{i_N} \tag{24}$$

In this case the partition function is

$$Z = \sum_{i_1,i_2\cdots i_N} e^{-E_{i_1,i_2\cdots i_N}/k_BT} = \sum_{(states)} e^{-E_{i_1,i_2\cdots i_N}/k_BT} \tag{25}$$

In this case the calculation is more complicated since it is much more difficult to determine the different states to perform the summation. Because the particles are indistinguishable, the total summation cannot be separated into a product of sums (one for each particle). If the particles are fermions then they can not occupy the same state simultaneously, then the elements of the same index must be eliminated from the summation. If the particles are bosons they can occupy the same state simultaneously. However, repeated configurations must be eliminated from the summation. In the special case in which the N particles (fermions or bosons) are always in different energy states, of the $N!$ possible permutations we must include only one in the summation. This condition is met when the number of available states is much greater than the number of particles in the system (Boltzmann statistics). In such case the partition function for a system of *independent and indistinguishable* atoms or molecules is [1] [4] [5]

$$Z = \frac{(Z_m)^N}{N!} \tag{26}$$

C. Ideal monatomic gas

The first step in finding the partition function of a monatomic ideal gas is to write the molecular partition function. In this case the total energy E will be

$$E = E^{trans} + E^{elec} \tag{27}$$

where E^{trans} is the energy due to the translation movement and E^{elec} is the energy corresponding to the electronic levels. Due to these contributions the molecular partition function Z_m will be:

$$Z_m = Z_m^{trans} Z_m^{elec} \tag{28}$$

For translational energy we propose a simple well model of infinite cubic potential of side a. Translational energy is

$$E^{trans} = \frac{h^2}{8ma^2}(n_x^2 + n_y^2 + n_z^2) \quad n_x, n_y, n_z = 1, 2, \cdots \tag{29}$$

where h is the Planck constant, m is the mass of the atom and (n_x, n_y, n_z) are the quantum numbers corresponding to each Cartesian axis of the well [2].

The translational contribution to the molecular partition function will be

$$Z_m^{trans} = \sum_{n_x=1}^{\infty} \sum_{n_y=1}^{\infty} \sum_{n_z=1}^{\infty} e^{\frac{1}{k_BT} \frac{h^2}{8ma^2}(n_x^2+n_y^2+n_z^2)} \tag{30}$$

Or, as the summations are independent

$$Z_m^{trans} = (\sum_{n=1}^{\infty} e^{\frac{1}{k_BT}\frac{h^2n^2}{8ma^2}})^3 \tag{31}$$

Each term of the sum is the area of a rectangle of base 1 and height $e^{\frac{1}{k_BT}\frac{h^2n^2}{8ma^2}}$ so the infinite sum can be approximated with an integral [5]

$$Z_m^{trans} = (\int_0^{\infty} e^{\frac{1}{k_BT}\frac{h^2n^2}{8ma^2}} dn)^3 \tag{32}$$

whose result is

$$Z_m^{trans} = (\frac{2\pi m k_B T}{h^2})^{\frac{3}{2}} V \tag{33}$$

where V is a^3 [1].

The electronic contribution to the molecular partition function is

$$Z_m^{elec} = \sum_{level\ i} g_i e^{\frac{1}{k_BT}E_i^e} \tag{34}$$

where g_i is the degeneracy and E_i^e is the energy of level i. The sum is not done on the states but on all the energy levels. You can choose the reference level of the electronic energy in such a way that $E_1^e = 0$, then

$$Z_m^{elec} = g_1 + g_2 e^{\frac{1}{k_BT}E_2^e} + \cdots \tag{35}$$

Finally, from Eq. 26 and 28 we get to the expression of the partition function for an ideal monoatomic gas [1]

$$Z = \frac{\left[(\frac{2\pi m k_B T}{h^2})^{\frac{3}{2}} V \cdot (g_1 + g_2 e^{\frac{1}{k_BT}E_2^e} + \cdots)\right]^N}{N!} \tag{36}$$

D. Ideal diatomic gas

The total energy of a diatomic molecule is

$$E = E^{trans} + E^{elec} + E^{vib} + E^{rot} \tag{37}$$

where to the translational E^{trans} and electronic E^{elec} energies defined for the monoatomic molecule, the internuclear vibrational energy E^{vib} and the rotation energy of the molecule E^{rot} are added. To each energy corresponds a molecular partition function Z_m^{trans}, Z_m^{elec}, Z_m^{vib} and Z_m^{rot} respectively. Using again the model of an infinite potential cubic well of side a, the translational contribution will be

$$Z_m^{trans} = (\frac{2\pi m k_B T}{h^2})^{\frac{3}{2}} V \tag{38}$$

where $m = m_1 + m_2$ is the mass of the molecule. The electronic contribution is written

$$Z_m^{elec} = g_1 e^{\frac{D_e}{k_BT}} + g_2 e^{\frac{1}{k_BT}E_2^e} \tag{39}$$

where $-D_e$ is the ground state energy and E_2^e is the energy of the first excited state. g_1 and g_2 are the degeneracies. $-D_e$ is the minimum internuclear potential energy when the atoms of the molecule are in their fundamental electronic state [1] [8].

The atomic nuclei vibrate with each other. The internuclear potential energy can be approximated with a Morse potential similar to the one shown in Fig. 1.

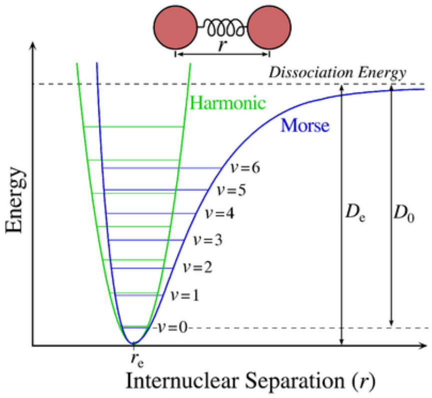

FIG. 1: Morse potential

For small amplitudes, molecular vibrations can be modeled as a quantum harmonic oscillator. In such a case, the vibrational energy E^{vib} will be [2]

$$E^{vib} = \hbar\omega(v + \frac{1}{2}) \quad v = 0, 1, 2\cdots \tag{40}$$

The vibrational contribution to the molecular partition function is

$$Z_m^{vib} = \sum_{v=0}^{\infty} e^{\frac{1}{k_BT}\hbar\omega(v+\frac{1}{2})} = e^{\frac{\hbar\omega}{2k_BT}} \sum_{v=0}^{\infty} (e^{\frac{\hbar\omega}{k_BT}})^v \tag{41}$$

Defining the vibrational temperature as

$$\Theta_{vib} = \frac{\hbar\omega}{k_B} \tag{42}$$

and solving the geometric series in Eq. 41 we get [1]

$$Z_m^{vib} = \frac{e^{-\Theta_{vib}/2T}}{1 - e^{-\Theta_{vib}/T}} \tag{43}$$

To calculate the rotation energy, we consider a simple model where atoms are point masses m_1 and m_2 located at fixed distances r_1 and r_2 from their center of mass .

The effect of vibration is neglected, therefore the distances are fixed and the model is known as a *rigid rotor*. The energy of the molecule is purely kinetic, therefore the Hamiltonian operator $\hat{H}$ will be

$$\hat{H} = \frac{\hbar^2}{2\mu}\nabla^2 \tag{44}$$

where μ is the *reduced mass* of the molecule. Expressing the Laplacian in spherical coordinates we arrive at an expression of the Schrödinger equation similar to that corresponding to the angular part of the hydrogen atom, from which the rotational energy E^{rot} is obtained as [2]

$$E_l^{rot} = \frac{\hbar^2}{2I} l(l+1) \quad l = 0, 1, 2, \cdots \tag{45}$$

where I is the *moment of inertia* of the molecule that is calculated by the expression

$$I = \mu r^2 \tag{46}$$

Analogous to the case of hydrogen, degeneracy is

$$g_l = 2l + 1 \tag{47}$$

Then the rotational contribution to the molecular partition function will be

$$Z_m^{rot} = \sum_{nivell} g_l e^{-\frac{1}{k_B T} E_l^{rot}} = \sum_{l=0}^{\infty} (2l+1) e^{\frac{\Theta_{rot}}{T} l(l+1)} \tag{48}$$

Approximating this sum by an integral we obtain

$$Z_m^{rot} = \int_0^{\infty} (2l+1) e^{\frac{\Theta_{rot}}{T} l(l+1)} dl \tag{49}$$

For this approximation to be valid, the integrand must encompass many values of l with significant contributions to the integral. The condition of validity then is

$$\frac{\Theta_{rot}}{T} \ll 1 \tag{50}$$

Calculating the integral we get to [1]

$$Z_m^{rot} = \frac{T}{\Theta_{rot}} \tag{51}$$

This equation is valid only for a heteronuclear diatomic molecule. For a homonuclear diatomic molecule, the rotation of the molecule by 180° takes the molecule to a configuration that can not be distinguished from the original configuration. This leads to an excessive count of the accessible states. To correct this, we divide the partition function by σ, which is called the *symmetry number*, which is equal to the different number of ways in which a molecule can be put into identical configurations by rotations [1] [5]. Therefore, the rotational contribution to the molecular partition function is written

$$Z_m^{rot} = \frac{T}{\sigma \Theta_{rot}} \tag{52}$$

where $\sigma = 1$ for a heteronuclear diatomic molecule and $\sigma = 2$ for a homonuclear diatomic molecule [1]. Multiplying the different contributions, the molecular partition function of a diatomic molecule will be

$$Z_m = (\frac{2\pi m k_B T}{h^2})^{\frac{3}{2}} V \cdot \frac{T}{\sigma \Theta_{rot}} \cdot \frac{e^{-\Theta_{vib}/2T}}{1 - e^{-\Theta_{vib}/T}} \cdot g_1 e^{\frac{D_e}{k_B T}} \tag{53}$$

Finally, the expression of the partition function for an ideal diatomic gas is [1]

$$Z = \frac{\left[(\frac{2\pi m k_B T}{h^2})^{\frac{3}{2}} V \cdot \frac{T}{\sigma \Theta_{rot}} \cdot \frac{e^{-\Theta_{vib}/2T}}{1 - e^{-\Theta_{vib}/T}} \cdot g_1 e^{\frac{D_e}{k_B T}} \right]^N}{N!} \tag{54}$$

E. Condition of validity of the Boltzmann distribution

For the equations of the ideal gas partition functions to be valid, it must be satisfied that the number of available states is much greater than the number of particles in the system. From the quantum point of view, each molecule of a gas is a wave packet whose spatial extent is characterized by the de Broglie wavelength λ_0

$$\lambda_0 = \frac{h}{p_0} \tag{55}$$

where p_0 is the average momentum of the molecule and h is the Planck constant [6].

The kinetic energy of an ideal monoatomic gas in equilibrium at temperature T is

$$\frac{p_0^2}{2m} = \frac{3}{2} k_B T \tag{56}$$

thereby

$$\lambda_0 = \sqrt{\frac{h^2}{3 m k_B T}} \tag{57}$$

We define a quantity of the same order of magnitude as λ_0 called *thermal wavelength* λ_{th}:

$$\lambda_{th} = \sqrt{\frac{h^2}{2\pi m k_B T}} \tag{58}$$

If the distance between molecules is less than λ_{th}, the wave packets will overlap and non-classical phenomena will occur. Hence the upper limit of the number density of particles for the classical regime is a particle in a volume λ_{th}^3 . Such a number density is represented by the symbol n_Q and is called *quantum concentration*:

$$n_Q = \frac{1}{\lambda_{th}^3} \tag{59}$$

Using these quantities Z_m^{trans} for ideal monoatomic or diatomic gases can be written

$$Z_m^{trans} = V n_Q = \frac{V}{\lambda_{th}^3} \tag{60}$$

Therefore, the smaller the numerical density n of the gas with respect to the quantum concentration n_Q, the greater the number of available states, consequently the condition of validity will be [4] [6] [7]

$$n = \frac{N}{V} \ll n_Q \tag{61}$$

IV. PROPERTIES OF IDEAL MONATOMIC AND DIATOMIC GASES

A. Molar heat capacity

To calculate the molar heat capacity $\bar{C}_V$ we make $N = N_A$, where $N_A = 6.022 \times 10^{23}\ mol^{-1}$ is the *Avogadro constant* and we use the *universal gas constant* $R = N_A k_B$. It is convenient to first calculate the molar energy $\bar{U}$ and then make use of the formula $\bar{C}_V = (\frac{d\bar{U}}{dT})_{N,V}$. For an ideal monatomic gas we combine Eq. 11 and 36. If we ignore the contributions of the excited electronic levels, we get

$$\bar{U} = \frac{3}{2} RT \tag{62}$$

$$\bar{C}_V = \frac{3}{2} R \quad \text{(ideal monatomic gas)} \tag{63}$$

For an ideal diatomic gas we combine Eq. 11 and 54 and obtain

$$\bar{U} = \frac{5}{2} RT + R\frac{\Theta_{vib}}{2} + R\frac{\Theta_{vib} e^{-\Theta_{vib}/T}}{1 - e^{-\Theta_{vib}/T}} - N_A D_e \tag{64}$$

It is interesting to note that if $T = 0$ the energy of the gas would be

$$\bar{U}(T = 0) = R\frac{\Theta_{vib}}{2} - N_A D_e = N_A(\frac{\hbar\omega}{2} - D_e) = -N_A D_0 \tag{65}$$

where

$$D_0 = D_e - \frac{\hbar\omega}{2} \tag{66}$$

is the *dissociation energy* of the molecule [7] [8]. It is noted that even at the absolute zero of temperature the molecule vibrates in its fundamental mode and the minimum energy necessary to separate the atoms (D_0) is smaller than the depth of the potential well (D_e).

From Eq. 64 we get [1]

$$\bar{C}_V = \frac{5}{2} R + R(\frac{\Theta_{vib}}{T})^2 \frac{e^{-\Theta_{vib}/T}}{(1 - e^{-\Theta_{vib}/T})^2} \quad \text{(ideal diatomic gas)} \tag{67}$$

B. The ideal gas law

The gas pressure is calculated from Eq. 15

$$p = k_B T (\frac{\partial \ln Z}{\partial V})_T \tag{68}$$

For ideal gases this equation can be written as

$$p = N k_B T (\frac{\partial \ln Z_m}{\partial V})_T \tag{69}$$

From Eq. 36 and 54 we see that for both monatomic and diatomic molecules the molecular partition function has the form

$$Z_m = f(T) V \tag{70}$$

Then

$$\ln Z_m = \ln f(T) + \ln V \tag{71}$$

From where you get

$$p = \frac{N k_B T}{V} \tag{72}$$

which is the equation of state for ideal gases [1] [4] [8].

V. CONCLUSION

The principles of statistical mechanics are simple. That characteristic makes them very general; they can be applied to any system of many particles. And as we saw briefly, it is possible to build classical thermodynamics from them. For this, a fundamental physical quantity is defined: the partition function. This function encapsulates all the information about the macroscopic (measurable) variables of the system. But statistical mechanics goes beyond classical thermodynamics because it allows us to give a more profound explanation of certain state functions (for example associating entropy with disorder or lack of information) and bridges the macroscopic and the microscopic by allowing us concretely calculate the partitioning function from the fundamental principles of quantum mechanics. We have seen an example of this when applying these concepts to the ideal monatomic and diatomic gases. Some expressions obtained, e.g. the heat capacity, are approximate; they can be improved by using more complex models (for example, considering the higher-order terms in the mathematical expansion of the Morse potential). But beyond the complexity of the models, the sophistication of the mathematical tools and the rigor that we apply in our analyzes, at the end of the journey it must be concluded that: *"The volume of a given amount of gas is directly proportional to the number on moles of gas, directly proportional to the temperature and inversely proportional to the pressure."*

VI. ACKNOWLEDGMENTS

The author thanks his son Leandro Galván for his revision of the text and for his help in editing it.

---

[1] D.A. McQuarrie and J.D. Simon, *Physical chemistry: a molecular approach* (University Science Books, 1997). Chapter 17, chapter 18 and several sections of chapter 20 contain information on the partition function, the ideal gases and the derivation of the thermodynamic state functions.

[2] Cohen-Tannoudji and Claude et. al. *Quantum Mechanics, Vol. 1* (Wiley, 1977). The complement H_1 deals with the one-dimensional potential wells, in particular the infinitely deep well. The complement G_{II} deals with the two-dimensional infinite well. Chapter V studies the one-dimensional harmonic oscillator and the complement L_V treats the harmonic oscillator in thermal equilibrium. The complement C_{VI} deals with the rotation of diatomic molecules and introduces the rigid rotator model. The complement F_{VII} studies the vibrational-rotational levels of diatomic molecules in greater depth.

[3] M.W. Zemansky and R.H. Dittman, *Heat and thermodynamics: an intermediate textbook, 7th ed.* (McGraw-Hill, 1997). This is a classic text of thermodynamics. It develops classical thermodynamics from its fundamental principles and establishes the relationships between the variables and a thermodynamic system.

[4] S.J. Blundell and K.M. Blundell, *Concepts in Thermal Physics, 2nd Ed.* (Oxford University Press, 2010). In chapter 4 the ensambles, the temperature and the Boltzmann factor are defined. In chapter 14, entropy is defined on statistical bases and its relation to probability. Chapter 20 deals with the partition function and chapter 21 on statistical mechanics and ideal gases.

[5] D.V. Schroeder, *An introduction to thermal physics* (Addison-Wesley, 2000). Chapter 6 deals with the Boltzmann statistics and in particular shows under what conditions a summation can be replaced by an integral in the calculation of partition functions. Appendix A shows a summary of quantum mechanics.

[6] K. Huang, *Introduction to Statistical Physics* (Taylor and Francis, 2001). This book contains in a concise and precise way the main definitions of thermodynamics and statistical mechanics. In chapter 8 the thermal wavelength is defined and the limit between the classical regime and the quantum regime is established.

[7] C. Kittel and H. Kroemer, *Thermal physics, 2nd Ed.* (W. H. Freeman and Company, 1980). Chapter 3 deals with the Boltzmann distribution; in this chapter quantum concentration is defined and at the end of it contains a summary with the most important results.

[8] P. Atkins and J. de Paula, Physical chemistry, 9th Ed. (W. H. Freeman and Company, 2010). Chapters 10 to 14 study the molecular structure. Chapters 15 and 16 apply statistical mechanics to the study of molecules and gases.

[9] A. Ault, *The Partition Function: If That's What It Is Why Don't They Say So!*, `https://people.cornellcollege.edu/aault/Chemistry/PartitionFunction1.pdf` (accesed June 12, 2019). Provides a physical interpretation of the partition function.

Path Integral and Applications

User: jjpanda

June 17, 2019

Abstract

The free-particle Schrödinger equation is structurally identical to the diffusion equation, which allows us to deduce the Green function or the propagator directly from the solution to the diffusion equation. Building on top of the free-particle propagator, we motivate Feynman's path integral formulation of quantum mechanics and derive the configuration space path integral for an arbitrary potential. To show one of the many uses of path integral, we take the example of the quantum harmonic oscillator (QHO) as an exactly solvable path integral problem and recover the energy levels E_n and the eigenfunction squared $|\phi_n(x)|^2$.

1 Schrödinger's Equation as a Complex Diffusion Process

Before we discuss path integral, let us take a detour and look at Schrödinger's equation from a different perspective. To start with, we discuss the diffusion equation[1]:

$$\frac{\partial p}{\partial t} = D\nabla^2 p \tag{1}$$

where D is some diffusion constant. The p term here can be thought of as describing the concentration or density of some molecules that evolve in time. One way to "derive" the diffusion equation (1) is by postulating a formula for the flux of the diffusion process: $-D\nabla p$ where D is some positive constant (This is Fick's Law). This makes sense, because the direction of $-D\nabla p$ always points from higher concentration to lower concentration, justifying the physical picture of the diffusion process. Next, one can then demand conservation of probability (concentration) so that

$$\frac{\partial p}{\partial t} + \nabla \cdot (\text{flux}) = 0$$

Plugging in the flux term $-D\nabla p$, one readily obtains equation (1).

The physical intuition of the diffusion equation should be clear after discussing the following example. If at $t = 0$, we put a small blob of molecules at $x = 0$ (let's do this in 1-dimension), then we would expect the concentration to approximate a delta function at $t = 0$: $p(x, t = 0) = \delta(x)$. As t increases, however, the concentration "spreads out" evenly along both sides of $x = 0$ due to diffusion. In fact, there is an analytical solution to this process for a delta source at $t = 0$ and $x = 0$:

$$p(x,t) = \frac{1}{\sqrt{4\pi Dt}} \exp\left\{-\frac{x^2}{4Dt}\right\} \tag{2}$$

From the above solution, we see that p is a normalized Gaussian distribution peaked at $x = 0$. The peak gets higher and higher as t gets closer and closer to 0, thereby approximating a delta source at $t = 0$. By translational invariance of the diffusion equation, if we put the delta source at $x = x'$ rather than at $x = 0$ initially, the solution can be readily written down from eqn (2):

$$p(x,t) = \frac{1}{\sqrt{4\pi Dt}} \exp\left\{-\frac{(x-x')^2}{4Dt}\right\} \tag{3}$$

In fact, the above eqn is precisely the Green function $G(x, x', t)$ for the diffusion equation[2], since we solved it for a delta source. Therefore, if we specify

---

[1] The discussion of the diffusion equation follows largely that of [1].

[2] More precisely speaking, the constraint here is that the initial condition is specified at $t = 0$, for otherwise the Green function will depend on the time difference $t - t'$.

an arbitrary source at $t = 0$, say $p(x, t = 0)$, then the full solution at t is

$$\begin{aligned} p(x,t) &= \int_{-\infty}^{+\infty} G(x,x',t)p(x',t=0)dx' \\ &= \int_{-\infty}^{+\infty} \frac{1}{\sqrt{4\pi Dt}} \exp\left\{-\frac{(x-x')^2}{4Dt}\right\} p(x',t=0)dx' \end{aligned} \tag{4}$$

The reason we spend so much time discussing the diffusion equation is that the free-particle Schrödinger equation can be thought of as a complex diffusion process. Indeed, from the free-particle Schrödinger equation:

$$\frac{\partial \Psi}{\partial t} = \frac{i\hbar}{2m}\nabla^2\Psi \tag{5}$$

one readily sees that the "complex diffusion constant" here equals $i\hbar/2m$, upon comparing with eqn (1). Therefore, solving the free-particle Schrödinger's equation is equivalent to solving the diffusion equation, which we have already done! To translate everything from diffusion to quantum mechanics, we can simply replace every D with $i\hbar/2m$ in all of the above equations. Hence, the Schrödinger Green function U, which is more commonly termed the *free-particle propagator*, takes the following form (using eqn (3)):

$$U(x,x',t,t') = \sqrt{\frac{m}{2\pi i\hbar(t-t')}} \exp\left\{im\frac{(x-x')^2}{2\hbar(t-t')}\right\} \tag{6}$$

2 Generalization to Path Integral

Before we define what path integral is, we mention that one of the many uses of path integral is that it helps us calculate the propagator[3] (an example is eqn (6)) for arbitrary potentials[4]. Indeed, the analogy with the diffusion equation fails when one adds a potential term to the Schrödinger equation, and eqn (6) will no longer be a valid propagator. In the following, we shall see how one can deduce the general property of the propagator by assuming an arbitrary potential. For the sake of computational ease, we restrict ourselves to the 1-dimensional case.

Formally, we are interested in the form of the position space wave function of $|\Psi(t)\rangle$, given the initial ket $|\Psi(t')\rangle$ at some time t'. We know that these two states are related by the time evolution operator (for any time-independent Hamiltonian H)

$$|\Psi(t)\rangle = \exp\left\{-\frac{i}{\hbar}H(t-t')\right\}|\Psi(t')\rangle$$

In general, the Hamiltonian H might have time dependence. To make any further progress in our calculation, we can assume that the difference in time

---

[3] The derivation of path integral follows largely that of [2] and [3].

[4] Having obtained the propagator, the Schrödinger equation is essentially solved, since we can write down the solution at all x and $t \geq t_0$ once we know the initial condition at $t = t_0$. This is why we care about the propagator

$\epsilon \equiv t - t'$ is so small that to first order in ϵ any Hamiltonian H (be it time-independent or not) will result in the following evolution operator:

$$|\Psi(t)\rangle = \exp\left\{-\frac{i}{\hbar}H\epsilon\right\}|\Psi(t')\rangle$$

The wave function $\langle x|\Psi(t)\rangle$ can then be obtained by inserting a complete set of position basis:

$$\langle x|\Psi(t)\rangle = \int_{-\infty}^{+\infty} \langle x|\exp\left\{-\frac{i}{\hbar}H\epsilon\right\}|x'\rangle\,\langle x'|\Psi(t')\rangle\,dx'$$

Defining the position space wave functions as $\Psi(x,t) = \langle x|\Psi(t)\rangle$, the above equation becomes

$$\Psi(x,t) = \int_{-\infty}^{+\infty} \langle x|\exp\left\{-\frac{i}{\hbar}H\epsilon\right\}|x'\rangle\,\Psi(x',t')dx'$$

Therefore, the infinitesimal propagator can be read directly from the above equation:

$$U(x,x',\epsilon) = \langle x|\exp\left\{-\frac{i}{\hbar}H\epsilon\right\}|x'\rangle \tag{7}$$

How do we calculate $U(x,x',\epsilon)$? In fact, we have already done half of the job. In the previous section, we calculated the free-particle propagator (see eqn (6)), which we copy here by making contact with the quantum-mechanical definition:

$$\langle x|\exp\left\{-\frac{i}{\hbar}\frac{p^2}{2m}\epsilon\right\}|x'\rangle = \sqrt{\frac{m}{2\pi i\hbar\epsilon}}\exp\left\{im\frac{(x-x')^2}{2\hbar\epsilon}\right\} \tag{8}$$

Since $H = \frac{p^2}{2m} + V(x)$, we've yet to calculate the contribution from $V(x)$. To do so, we note that

$$\exp\left\{-\frac{i}{\hbar}\epsilon H\right\} = \exp\left\{-\frac{i}{\hbar}\frac{p^2}{2m}\epsilon\right\}\exp\left\{-\frac{i}{\hbar}\epsilon V(x)\right\} + O(\epsilon^2)$$

where the higher order terms result from taking the commutator as in $e^{A+B} = e^A e^B e^{-1/2[A,B]} + ...$ Substituting this expression into (7), and noting that $|x\rangle$ is an eigenket of $V(x)$, we have, to first order in ϵ,

$$\begin{aligned}
U(x,x',\epsilon) &= \langle x|\exp\left\{-\frac{i}{\hbar}\frac{p^2}{2m}\epsilon\right\}\exp\left\{-\frac{i}{\hbar}\epsilon V(x)\right\}|x'\rangle \\
&= \exp\left\{-\frac{i}{\hbar}\epsilon V(x')\right\}\langle x|\exp\left\{-\frac{i}{\hbar}\frac{p^2}{2m}\epsilon\right\}|x'\rangle \\
&= \sqrt{\frac{m}{2\pi i\hbar\epsilon}}\exp\left\{im\frac{(x-x')^2}{2\hbar\epsilon} - \frac{i}{\hbar}\epsilon V(x')\right\} \qquad (9)
\end{aligned}$$

where, in the last step, we plugged in the free-particle propagator from equation (8). The infinitesimal propagator can be cast into a more illuminating form. Factoring out $i\epsilon/\hbar$ in the exponent, we obtain

$$\begin{aligned} U(x,x',\epsilon) &= \sqrt{\frac{m}{2\pi i\hbar\epsilon}}\exp\left\{\frac{i\epsilon}{\hbar}\left(m\frac{(x-x')^2}{2\epsilon^2}-V(x')\right)\right\} \\ &= \sqrt{\frac{m}{2\pi i\hbar\epsilon}}\exp\left\{\frac{i\epsilon}{\hbar}\left(\frac{mv^2}{2}-V(x')\right)\right\} \end{aligned} \tag{10}$$

where v is the local speed at x' defined as $v' = (x-x')/\epsilon$ in the small ϵ limit. The quantity in the parenthesis is nothing other than the local Lagrangian[5] at x', and hence

$$U(x,x',\epsilon) = \sqrt{\frac{m}{2\pi i\hbar\epsilon}}\exp\left\{\frac{i\epsilon}{\hbar}L(x')\right\} \tag{11}$$

Having computed the infinitesimal propagator, let us now consider a full-scale problem: we want to calculate

$$U(x,x',t) = \langle x|\exp\left\{-\frac{i}{\hbar}Ht\right\}|x'\rangle$$

where t and $x-x'$ are no long assumed infinitesimal. The strategy is as follows: we divide t into N infinitesimal time intervals such that $t = N\epsilon$ and take the limit $N\to\infty$ and $\epsilon\to 0$. This allows us to break the finite propagator $\exp\{-\frac{i}{\hbar}Ht\}$ into N infinitesimal propagators which we have already solved. Therefore,

$$U(x,x',t) = \langle x|\exp\left\{-\frac{i}{\hbar}H\epsilon\right\}\exp\left\{-\frac{i}{\hbar}H\epsilon\right\}\dots\exp\left\{-\frac{i}{\hbar}H\epsilon\right\}|x'\rangle$$

where we have N infinitesimal propagators sandwiched between the initial and the final state. To keep track of them, we relabel $x\to x_N$ and $x'\to x_0$, and insert N complete sets of basis between each infinitesimal propagator:

$$U = \int\dots\int dx_{N-1}\dots dx_1\,\langle x_N|\exp\left\{-\frac{i}{\hbar}H\epsilon\right\}|x_{N-1}\rangle\,\langle x_{N-1}|\exp\left\{-\frac{i}{\hbar}H\epsilon\right\}|x_{N-2}\rangle\dots\langle x_1|\exp\left\{-\frac{i}{\hbar}H\epsilon\right\}|x_0\rangle$$

Now, each of the N infinitesimal propagators can be read from eqn (9), and the final expression is

$$\begin{aligned} U(x_N,x_0,t) &= \left(\frac{m}{2\pi i\hbar\epsilon}\right)^{N/2}\int\dots\int dx_{N-1}\dots dx_1\exp\left\{\frac{i\epsilon}{\hbar}\sum_{i=1}^{N}\left(m\frac{(x_i-x_{i-1})^2}{2\epsilon^2}-V(x_{i-1})\right)\right\} \\ &= \left(\frac{m}{2\pi i\hbar\epsilon}\right)^{N/2}\int\dots\int dx_{N-1}\dots dx_1\exp\left\{\frac{i\epsilon}{\hbar}\sum_{i=1}^{N}L(x_{i-1})\right\} \end{aligned} \tag{12}$$

---

[5] Recall that the Lagrangian is defined as the kinetic energy minus the potential energy

where $L(x_{i-1})$ is the Lagrangian evaluated at x_{i-1}. In the continuum limit as $N \to \infty$ and $\epsilon \to 0$, we can define the integration measure

$$\int_{x_0}^{x_N} \mathcal{D}[x(t)] \equiv \lim_{N\to\infty} \left(\frac{m}{2\pi i\hbar\epsilon}\right)^{N/2} \int \dots \int dx_{N-1} \dots dx_1$$

and notice that the sum in eqn (13) is turned into an integral:

$$\lim_{N\to\infty} \exp\left\{\frac{i\epsilon}{\hbar} \sum_{i=1}^{N} L(x_{i-1})\right\} = \exp\left\{\frac{i\epsilon}{\hbar} S[x(t)]\right\}$$

where $S[x(t)]$ is the action $\int L dt$ of the path $x(t)$ that begins at x_0 and ends at x_N. Therefore, the propagator is (relabeling x_0 and x_N to some arbitrary points x' and x)

$$U(x, x', t) = \int_{x_0}^{x_N} \mathcal{D}[x(t)] \exp\left\{\frac{i\epsilon}{\hbar} S[x(t)]\right\} \tag{13}$$

Let us now discuss the physical significance behind this result. The above equation, if we put it in words, says that the propagator can be found by summing over a pure phase for each possible path (be it physical or not) the particle can take between x and x' as long as the path starts at x' at time $t = 0$ and ends at x at time t. If each possible path contributes equally (the phases are not weighted) to the result, then why do macroscopic objects always take the classical least-action path? The reason is that the exponent $S[x(t)]/\hbar$ for a microscopic object is so big that the oscillating phase leads to cancelations except for near the stationary path where $S[x(t)]$ is an extremum. This reasoning in turn provides microscopic origin of the least-action principle found in classical mechanics: particles always follow the least-action path because only near this path can we have constructive interference of phases. On the other hand, microscopic objects such as electrons have small $S[x(t)]/\hbar$ exponent that may not oscillate as much, so we should not expect to find them follow classical trajectories.

The above argument shows that the least action principle in classical mechanics emerges out of the path integral formulation. We now show that the Schrödinger equation also emerges out of the path integral formulation, thereby showing the equivalence between the path integral approach and the Schrödinger equation approach to quantum mechanics[6]. If we are given $\Psi(x, t')$ at some time t', the Schrödinger equation tells us what Ψ looks like in the next instant if we have the Hamiltonian. In the path integral formulation, this is done by using the propagator. Consider the infinitesimal propagator in eqn (9). Suppose we are given $\Psi(x', t')$, then at the next instant $t = t' + \epsilon$, the wave function is given as

$$\Psi(x, t) = \sqrt{\frac{m}{2\pi i\hbar\epsilon}} \int_{-\infty}^{+\infty} \exp\left\{im\frac{(x - x')^2}{2\hbar\epsilon} - \frac{i}{\hbar}\epsilon V(x')\right\} \Psi(x', t') dx' \tag{14}$$

---

[6] We've used the Schrödinger equation to derive the path integral formulation, so here all we need to do is to see if the reverse can happen as well.

For small ϵ, the first term in the exponent is large, and the integral will be nonvanishing only for stationary phase, where $x - x'$ is small. This suggests that we expand terms using $\Delta = x - x'$ and keep only terms to second order in Δ and first order in ϵ, since the first exponent $im(x-x')^2/(2\hbar\epsilon)$ suggests that $O(\Delta^2) \sim O(\epsilon)$ if we want to have a small phase. To proceed, we note that

$$\exp\left\{-\frac{i}{\hbar}\epsilon V(x')\right\} \approx 1 - \frac{i}{\hbar}\epsilon V(x)$$

$$\Psi(x',t') \approx \Psi(x,t') - \Delta\frac{\partial}{\partial x}\Psi(x,t') + \frac{\Delta^2}{2}\frac{\partial^2}{\partial x^2}\Psi(x,t')$$

Note that the first exponential has $V(x')$ changed into $V(x)$ after expanding. This is because ϵ multiplies $V(x')$, and so we can only keep the zeroth order term in the expansion of $V(x')$, which gives us $V(x)$. Plugging these into eqn (14) and discarding higher order terms (and a term odd in Δ which integrates out to 0), we have

$$\Psi(x,t) = \sqrt{\frac{m}{2\pi i\hbar\epsilon}}\int_{-\infty}^{+\infty}\exp\left\{im\frac{\Delta^2}{2\hbar\epsilon}\right\}\left(\Psi(x,t') + \frac{\Delta^2}{2}\frac{\partial^2}{\partial x^2}\Psi(x,t') - \frac{i}{\hbar}\epsilon V(x)\Psi(x,t')\right)d\Delta$$

Note that we have substituted $\Delta = x - x'$ into the above equation. The Gaussian integral is easily done, and the result is

$$\Psi(x,t) = \Psi(x,t') + \frac{i\epsilon\hbar}{2m}\frac{\partial^2}{\partial x^2}\Psi(x,t') - \frac{i\epsilon}{\hbar}V(x)\Psi(x,t')$$

Rearranging, we obtain

$$i\hbar\frac{\Psi(x,t) - \Psi(x',t)}{\epsilon} = -\frac{\hbar^2}{2m}\frac{\partial^2}{\partial x^2}\Psi(x,t') + V(x)\Psi(x,t')$$

which gives exactly the Schrödinger equation when $\epsilon \to 0$. This derivation shows that the path integral formulation is equivalent to the Schrödinger equation.

2.1 Momentum Space Path Integral

Recall that, when we derived the full propagator in eqn (12), we inserted N resolutions of identity in the position space $\int |x\rangle\langle x|\,dx$. We can also insert resolutions of identity in the momentum space $\int |p\rangle\langle p|\,dp$. For example, for a typical term of an infinitesimal propagator, we have (upon introducing both the position space resolution and the momentum space resolution)

$$\int \ldots dp \int dx \ldots |x_i\rangle\langle x_i| \exp\left\{-\frac{i}{\hbar}\epsilon\frac{p^2}{2m}\right\}|p_{i-1}\rangle\langle p_{i-1}|\exp\left\{-\frac{i}{\hbar}\epsilon V(x)\right\}|x_{i-1}\rangle\langle x_{i-1}|$$

and it is easy to see that

$$\langle x_i|\exp\left\{-\frac{i}{\hbar}\epsilon\frac{p^2}{2m}\right\}|p_{i-1}\rangle\langle p_{i-1}|\exp\left\{-\frac{i}{\hbar}\epsilon V(x)\right\}|x_{i-1}\rangle$$

reduces to

$$\frac{i\epsilon}{\hbar}\left[p_{i-1}\frac{dx_{i-1}}{dt}-(\frac{p_{i-1}^2}{2m}+V(x_{i-1}))\right]$$

in the continuum limit. But the quantity in the bracket is simply the familiar Lagrangian written as the Legendre transform of the Hamiltonian H.

$$L = p\dot{x} - H$$

Similar to what we did for the position space path integral, in this case we have

$$U(x,x',t) = \int \mathcal{D}_p\mathcal{D}_x \exp\left\{\frac{i}{\hbar}\int_0^t (p\dot{x}-H)dt\right\} \tag{15}$$

where $\mathcal{D}_p\mathcal{D}_x$ define the continuum limit of the measure of integration, similar to the one below eqn (12).

This section is brief, and it aims to show that there are other types of path integral in addition to the standard configuration space integral. In fact, [3] shows that there is more. There is also the coherent state path integral which uses other forms of resolutions of identity.

3 Applications of Path Integral

In this section, we consider a few applications of path integral. In addition to giving a closed-form solution of the propagator, path integral has *at least* the following uses:

- It can calculate the energy levels of a system without diagonalizing the Hamiltonian which is oftentimes hard[3][4].
- It can calculate the wave functions of a system without diagonalizing the Hamiltonian which is oftentimes hard[3][4].
- It can perform semi-classical calculations (the bridge to classical mechanics here is the action term in the amplitude $e^{iS/\hbar}$)[3].
- It can calculate the approximate Schödinger equation of a system (think Born-Oppenheimer)[3].
- It can explain many physical experiments (quantum interference due to gravity, diffraction, etc.)[2][4].

In this paper, we focus on the first application using the example of the quantum harmonic oscillator. The reason we focus on this application is that we will pick up useful computational techniques along the way. They will help us tackle future problems such as the motion of charged particles in magnetic field.

3.1 Quantum Harmonic Oscillator, the Path Integral Approach

In 8.05, and in most of the standard quantum mechanics books, the quantum harmonic oscillator (QHO) is solved using the operator method where we factor the Hamiltonian. In this section, we consider extracting the energy levels of the QHO using the path integral approach.

To make a general statement, the problem of QHO belongs to a broader class of problems whose Lagrangian is at most quadratic[2]:

$$L(x) = a + bx + cx^2 + d\dot{x} + e\dot{x}x + f\dot{x}^2$$

Feynman [4] showed that this class of problem is exactly solvable, in the sense that one can perform the path integral

$$U = \int \mathcal{D}[x(t)] \exp\left\{ \frac{i}{\hbar} S[x(t)] \right\}$$

and get the corresponding propagator U. The trick is to parameterize every possible path by the deviation $y(t)$ from the classical least-action path, denoted by $x_c(t)$, rather than directly using the path variable $x(t)$. This is encapsulated in the following equation

$$x(t) = x_c(t) + y(t) \tag{16}$$

Since the endpoints of all paths are fixed, we have $y(0) = y(t_1) = 0$ where 0 and t_1 denote the start and end time. This condition says that there is no deviation from the endpoints of the paths. Having this equation, we can then expand the action around the classical paths which follow the equation of motion. Then, using the quadratic Lagrangian we have above, we can compute the action

$$\begin{aligned} S[x(t)] &= S[x_c(t) + y(t)] \\ &= \int_0^{t_1} L(x_c(t) + y(t), \dot{x}_c(t) + \dot{y}(t)) dt \\ &= \int_0^{t_1} \left(L(x_c(t), \dot{x}_c(t)) + \frac{\partial L}{\partial x} y(t) + \frac{\partial L}{\partial \dot{x}} \dot{y}(t) + \frac{1}{2} \frac{\partial^2 L}{\partial x^2} y^2(t) + \frac{1}{2} \frac{\partial^2 L}{\partial \dot{x}^2} \dot{y}^2(t) + \frac{\partial^2 L}{\partial x \partial \dot{x}} y(t)\dot{y}(t) \right) dt \\ &= S_c[x(t)] + \int_0^{t_1} \left(cy^2(t) + f\dot{y}^2(t) + ey(t)\dot{y}(t) \right) dt \qquad (17) \end{aligned}$$

where $S_c[x(t)]$ is the classical least-action. Note that the terms linear in y and $\dot{y}$ cancel after integrating by parts and using the equation of motion. Since we changed the variable from $x(t)$ to $y(t)$, the integration measure and range

$$\int \mathcal{D}[x(t)]$$

should change accordingly to

$$\int_0^0 \mathcal{D}[y(t)]$$

The integration limits reflect the fact that there is no variation of the paths at the endpoints. Therefore, using eqn (17), the path integral for this quadratic class of problem can be written as

$$U = F(t_1)\exp\left\{\frac{i}{\hbar}S_c[x(t)]\right\} \tag{18}$$

where $F(t_1)$ depends only on the the final time:

$$F(t_1) = \int_0^0 \mathcal{D}[y(t)]\exp\left\{\frac{i}{\hbar}\int_0^{t_1}\left(cy^2(t) + f\dot{y}^2(t) + ey(t)\dot{y}(t)\right)dt\right\} \tag{19}$$

Let us now find F for the QHO. The Lagrangian is

$$L = \frac{1}{2}m\dot{x}^2 - \frac{1}{2}m\omega^2 x^2$$

suggesting that the only nonvanishing constants in our quadratic potential ansatz are $c = -\frac{m\omega^2}{2}$ and $f = \frac{m}{2}$. Plugging this into eqn (19), we obtain

$$F(t_1) = \int_0^0 \mathcal{D}[y(t)]\exp\left\{\frac{i}{\hbar}\int_0^{t_1}\left(\frac{-m\omega^2}{2}y^2(t) + \frac{m}{2}\dot{y}^2(t)\right)dt\right\} \tag{20}$$

Feynman [4] solved this by using a Fourier series, noting that $y(t)$ can be expanded into

$$\begin{aligned} y(t) &= \sum_{n=1} a_n \sin\frac{n\pi t}{t_1} \\ \dot{y}(t) &= \frac{\pi}{t_1}\sum_{n=1} n a_n \cos\frac{n\pi t}{t_1} \end{aligned}$$

This expansion makes sense, because the boundary condition $y(0) = y(t_1) = 0$ is satisfied. The integral in the exponent and be performed by using the orthogonality relation

$$\int_0^{t_1}\sin\frac{n\pi t}{t_1}\sin\frac{m\pi t}{t_1}dt = \int_0^{t_1}\cos\frac{n\pi t}{t_1}\cos\frac{m\pi t}{t_1}dt = \delta_{n,m}\frac{t_1}{2}$$

Thus,

$$\begin{aligned} \int_0^{t_1}\left(\frac{-m\omega^2}{2}y^2(t) + \frac{m}{2}\dot{y}^2(t)\right)dt &= -\frac{m\omega^2}{2}\sum_{mn}\int_0^{t_1} a_n a_m \sin\frac{n\pi t}{t_1}\sin\frac{m\pi t}{t_1}dt \\ &\quad + \frac{m\pi^2}{2t_1^2}\sum_{mn}\int_0^{t_1} mn a_n a_m \cos\frac{n\pi t}{t_1}\cos\frac{m\pi t}{t_1}dt \\ &= \frac{mt_1}{4}\sum_n \frac{\pi^2 n^2}{t_1^2}a_n^2 - \frac{mt_1\omega^2}{4}\sum_n a_n^2 \\ &= \frac{mt_1}{4}\sum_n\left(\frac{\pi^2 n^2}{t_1^2} - \omega^2\right)a_n^2 \end{aligned}$$

Having computed the exponent in eqn (20), let us now do the full integral. We note that the change of variable from y to a_n is linear, so the integration measure is related by a Jacobian factor J. We then have (note that, unlike y, each a_n runs from $-\infty$ to $+\infty$)

$$\int \mathcal{D}[y(t)] = \Big(\frac{m}{2\pi i\hbar\epsilon}\Big)^{N/2} \int \dots dy_1 \int dy_{N-1} \quad = J\Big(\frac{m}{2\pi i\hbar\epsilon}\Big)^{N/2} \int \dots da_1 \int da_{N-1}$$

Plugging this into (20), using our previous result for the exponent, we have

$$F(t_1) = J\Big(\frac{m}{2\pi i\hbar\epsilon}\Big)^{N/2} \int \dots da_1 \int da_{N-1} \exp\Bigg\{\frac{imt_1}{4\hbar}\sum_n \left(\frac{\pi^2 n^2}{t_1^2} - \omega^2\right) a_n^2\Bigg\}$$

Note that each integral is Gaussian. For each n we have

$$\begin{aligned}\Big(\frac{m}{2\pi i\hbar\epsilon}\Big)^{1/2} \int da_n \exp\Bigg\{\frac{imt_1}{4\hbar}\left(\frac{\pi^2 n^2}{t_1^2} - \omega^2\right) a_n^2\Bigg\} &= \Big(\frac{m}{2\pi i\hbar\epsilon}\Big)^{1/2}\left(\frac{4\pi i\hbar}{mt_1}\right)^{1/2}\left(\frac{\pi^2 n^2}{t_1^2} - \omega^2\right)^{-1/2} \\ &= \sqrt{\frac{2}{\epsilon t_1}}\left(\frac{\pi^2 n^2}{t_1^2} - \omega^2\right)^{-1/2}\end{aligned}$$

Hence, if we multiply all such factors from $n = 1$ onwards, we get

$$\begin{aligned}F(t_1) &= A\prod_{n=1}\left(\frac{\pi^2 n^2}{t_1^2} - \omega^2\right)^{-1/2} \\ &= B\prod_{n=1}\left(1 - \frac{\omega^2 t_1^2}{\pi^2 n^2}\right)^{-1/2} \\ &= B\left(\frac{\sin(\omega t_1)}{\omega t_1}\right)^{-1/2}\end{aligned}$$

where A and B are constants independent of ω. Note that the last step follows by using the famous identity[4]. One way to determine B is to set $\omega = 0$. This reduces to the case of the free-particle, which we have already solved. For the case of the free-particle, we know from eqn (6) that the prefactor is

$$\sqrt{\frac{m}{2\pi i\hbar t_1}}$$

Therefore, $B = \sqrt{\frac{m}{2\pi i\hbar t_1}}$, and for the QHO,

$$F(t_1) = \sqrt{\frac{m\omega}{2\pi i\hbar\sin(\omega t_1)}}$$

We have not obtained the full propagator yet. Plugging the above equation into eqn (18), we have

$$U = \sqrt{\frac{m\omega}{2\pi i\hbar\sin(\omega t_1)}}\exp\Bigg\{\frac{i}{\hbar}S_c[x(t)]\Bigg\}$$

The only task that remains is to determine the classical action for the harmonic oscillator. This is easy: we can simply solve for the trajectory and then integrate the Lagrangian. The answer is [3]

$$S_c[x(t)] = \frac{m\omega}{2\sin\omega t_1}\left[(x'^2 + x^2)\cos\omega t_1 - 2x'x\right]$$

for a path starting at x' and ending at x from $t = 0$ to $t = t_1$. Therefore, the full propagator for the QHO is

$$U(x', x, t_1) = \sqrt{\frac{m\omega}{2\pi i\hbar\sin(\omega t_1)}}\exp\left\{\frac{i}{\hbar}\frac{m\omega}{2\sin\omega t_1}\left[(x'^2 + x^2)\cos\omega t_1 - 2x'x\right]\right\} \tag{21}$$

To find the energy states, we claim that there is an intimate relationship between the propagator and the eigenfunctions of the Hamiltonian. Suppose the Hamiltonian has a discrete spectrum, then by the spectral theorem[5]

$$H = \sum_n E_n \left|n\right\rangle \left\langle n\right|$$

where $\left|n\right\rangle$ is the nth eigenstate with the corresponding energy E_n. Then the propagator $U(x', x)$ is simply

$$\begin{aligned} U(x', x, t_1) &= \left\langle x'\right| \exp\left\{-\frac{i}{\hbar}Ht_1\right\}\left|x\right\rangle \\ &= \sum_n \left\langle x'|n\right\rangle \left\langle n|x\right\rangle \exp\left\{-\frac{i}{\hbar}E_n t_1\right\} \\ &= \sum_n \phi_n(x')\phi_n^*(x)\exp\left\{-\frac{i}{\hbar}E_n t_1\right\} \end{aligned} \tag{22}$$

where the second step follows from inserting the spectral decomposition of H into the exponent.

To find the energy levels E_n of the QHO, let's now equate eqn (21) with eqn (22):

$$\sum_n \phi_n(x')\phi_n^*(x)\exp\left\{-\frac{i}{\hbar}E_n t_1\right\} = \sqrt{\frac{m\omega}{2\pi i\hbar\sin(\omega t_1)}}\exp\left\{\frac{i}{\hbar}\frac{m\omega}{2\sin\omega t_1}\left[(x'^2 + x^2)\cos\omega t_1 - 2x'x\right]\right\} \tag{23}$$

Setting $x' = x = 0$, the above equation becomes

$$\sum_n |\phi_n(0)|^2 \exp\left\{-\frac{i}{\hbar}E_n t_1\right\} = \sqrt{\frac{m\omega}{2\pi i\hbar\sin(\omega t_1)}} \tag{24}$$

On the left hand side, each term is a real number $|\phi_n(0)|^2$ multiplying a phase. To find E_n, let us thus expand the right hand side to have a similar form to the left hand side and match E_n with the corresponding quantity:

$$\begin{aligned}\sqrt{\frac{m\omega}{2\pi i\hbar\sin(\omega t_1)}} &= \sqrt{\frac{m\omega}{\pi\hbar(\exp\{i\omega t_1\}-\exp\{-i\omega t_1\})}} \\ &= \sqrt{\frac{m\omega}{\pi\hbar}}\exp\left\{-\frac{1}{2}i\omega t_1\right\}\left(1-\exp\{-2i\omega t_1\}\right)^{-1/2} \\ &= \sqrt{\frac{m\omega}{\pi\hbar}}\exp\left\{-\frac{1}{2}i\omega t_1\right\}\left(1+b_1\exp\{-2i\omega t_1\}+b_2\exp\{-4i\omega t_1\}+\ldots\right) \\ &= \sqrt{\frac{m\omega}{\pi\hbar}}\left(\exp\left\{-\frac{1}{2}i\omega t_1\right\}+b_1\exp\left\{-\frac{5}{2}i\omega t_1\right\}+b_2\exp\left\{-\frac{8}{2}i\omega t_1\right\}+\ldots\right)\end{aligned}$$

where the bs are real constants. Writing out the left hand side of eqn (24) and equating it with the above expansion, we have

$$|\phi_1(0)|^2\exp\left\{-\frac{i}{\hbar}E_1t_1\right\}+|\phi_2(0)|^2\exp\left\{-\frac{i}{\hbar}E_2t_1\right\}+\ldots=\sqrt{\frac{m\omega}{\pi\hbar}}\left(\exp\left\{-\frac{1}{2}i\omega t_1\right\}+b_1\exp\left\{-\frac{5}{2}i\omega t_1\right\}+\ldots\right) \tag{25}$$

We see that the energy levels are $\frac{1}{2}\hbar\omega$, $\frac{5}{2}\hbar\omega$, etc. The energy levels in between cannot be retrieved from the above expansion, since the corresponding $\phi_n(0)$ (for even n) vanishes due to parity consideration!

There is another way that can allow us to extract both the energy levels and the wave function (norm squared). Going back to eqn (23), we set $x'=x$. The equation then becomes

$$\sum_n|\phi_n(x)|^2\exp\left\{-\frac{i}{\hbar}E_nt_1\right\}=\sqrt{\frac{m\omega}{2\pi i\hbar\sin(\omega t_1)}}\exp\left\{\frac{i}{\hbar}\frac{m\omega}{\sin\omega t_1}\left[x^2\cos\omega t_1-x^2\right]\right\} \tag{26}$$

We again do the same trick and expand the right hand side in powers of $e^{-i\omega t_1}$. The prefactor expansion has already been done (see the right hand side of eqn (25)). We only need to expand the complex exponential, the second term of the above right hand side. This can be done by making the trigonometric functions into complex exponentials:

$$\begin{aligned}\exp\left\{\frac{i}{\hbar}\frac{m\omega}{\sin\omega t_1}\left[x^2\cos\omega t_1-x^2\right]\right\} &= \exp\left\{-i\frac{m\omega}{\hbar}x^2\tan\frac{\omega}{2}t_1\right\} \\ &= \exp\left\{-\frac{m\omega}{\hbar}x^2\frac{\exp\{i\frac{\omega}{2}t_1\}-\exp\{-i\frac{\omega}{2}t_1\}}{\exp\{i\frac{\omega}{2}t_1\}+\exp\{-i\frac{\omega}{2}t_1\}}\right\} \\ &= \exp\left\{-\frac{m\omega}{\hbar}x^2\frac{1-\exp\{-i\omega t_1\}}{1+\exp\{-i\omega t_1\}}\right\} \\ &= \exp\left\{-\frac{m\omega}{\hbar}x^2(1-\exp\{-i\omega t_1\})(1-\exp\{-i\omega t_1\}+\exp\{-2i\omega t_1\}+\ldots)\right\} \\ &= \exp\left\{-\frac{m\omega}{\hbar}x^2\right\}\exp\left\{2\frac{m\omega}{\hbar}x^2e^{-i\omega t_1}+\ldots\right\} \\ &= \exp\left\{-\frac{m\omega}{\hbar}x^2\right\}+2\frac{m\omega}{\hbar}x^2\exp\left\{-\frac{m\omega}{\hbar}x^2\right\}e^{-i\omega t_1}+\ldots\end{aligned}$$

Note that the dots indicate higher orders of $e^{-i\omega t_1}$. Multiplying the above result with our previous expansion of the prefactor using eqn (25), and setting the resulting sum equal to the left hand side of eqn (26), we obtain

$$\sum_n |\phi_n(x)|^2 \exp\left\{-\frac{i}{\hbar}E_n t_1\right\} = \sqrt{\frac{m\omega}{\pi\hbar}} \exp\left\{-\frac{m\omega}{\hbar}x^2\right\} \exp\left\{-\frac{1}{2}i\omega t_1\right\} + 2\sqrt{\frac{m\omega}{\pi\hbar}}\frac{m\omega}{\hbar}x^2 \exp\left\{-\frac{m\omega}{\hbar}x^2\right\} \exp\left\{-\frac{3}{2}i\omega t_1\right\} + \dots$$

Comparing the left hand side with the right hand side, we immediately see that

$$E_1 = \frac{1}{2}\hbar\omega$$
$$E_2 = \frac{3}{2}\hbar\omega$$

for the first 2 energy levels. The corresponding wave function squared is

$$|\phi_1(x)|^2 = \sqrt{\frac{m\omega}{\pi\hbar}} \exp\left\{-\frac{m\omega}{\hbar}x^2\right\}$$
$$|\phi_2(x)|^2 = 2\sqrt{\frac{m\omega}{\pi\hbar}}\frac{m\omega}{\hbar}x^2 \exp\left\{-\frac{m\omega}{\hbar}x^2\right\}$$

in exact agreement with what we obtained in 8.05 using the operator method.

Although we have only gotten to the second energy level, it is not hard to see that we can use this method to find every $|\phi_n(x)|^2$ and E_n by expanding the exponential to sufficiently large power and matching both sides of the equation.

4 Conclusion

In this paper, we looked at the path integral formulation of quantum mechanics, which we showed to be equivalent to the Schrödinger equation. The path integral formulation is not only as a powerful interpretation of quantum mechanics (all paths contribute equally to the probability amplitude); it can also be used as a powerful computational tool to solve problems that are otherwise hard to solve using conventional methods such as diagonalizing the Hamiltonian. Using the example of QHO, we saw that we could calculate all energy levels and the associated wave function squared by using the path integral formulation. This obviates the need to solve any differential equation and gets straight to the propagator.

In addition to QHO, other applications of path integral (perhaps more elegant) abound, but we cannot go through the list given the limited space here. We encourage interested reader to check out chapter 21 of [3] or even Feynman's original work [4].

References

[1] V. Balakrishnan. *Mathematical Physics with Applications, Problems and Solutions.* Ane Books, 2017.

[2] J. S. Townsend. *A Modern Approach to Quantum Mechanics, 2nd ed.* University Science Books, 2012.

[3] R. Shankar *Principles of Quantum Mechanics, 2nd ed.* Plenum Press, 2011.

[4] R. P. Feynman, A. R. Hibbs, and D. F. Styler. *Quantum Mechanics and Path Integrals: Emended Edition.* Dover Books on Physics, 2010.

[5] M. Nielsen, I. Chuang. *Quantum Computation and Quantum Information: 10th Anniversary Edition.* Cambridge University Press, 2011.

Periodic Potentials and Energy Band Structures

Benjamin Björnsson

(Dated: June 19, 2019)

Many materials form periodic structures at low enough temperatures. Although their structure may be very similar, their physical properties can be strikingly different. In particular, their electronic resistivity can vary by as much as 10^{32} ohm-cm for crystals at temperatures around 1K. In this article we show how these differences can be explained with the help of Bloch's theorem, and how the spectrum of the Bloch functions form a so called energy band structure. We use degenerate perturbation theory to show that the energy spectrum of a free particle split, at spacial points in the spectrum, for a simple harmonic perturbation. We also use numerical calculations to diagonalize the Hamiltonian in the first Brillouin zone. Finally, we connect the formation of the energy band structures with the Pauli exclusion principal to argue which crystals form conductors and which crystals form insulators.

I. INTRODUCTION

At low enough temperatures, many materials form crystal structures, with a characteristic periodic space dependence. Although crystal structures share their periodic nature, some properties are strikingly different. One of the most striking differences is that of electronic resistivity. For different crystals at temperatures around 1K, the electronic resistivity range from 10^{-10} to 10^{22} ohm-cm, for pure metals and good insulators, respectively [1].

We know that the Scrödinger equation describes in great detail systems like the hydrogen atom. It is interesting to ask if the electronic properties of a crystal can be explained from a quantum mechanical perspective. In particular, are the differences of conductors and insulators described by quantum mechanics?

In this article, we show that by solving the Schödinger equation for a periodic potential, the difference between conductors and insulators can be explained. The solutions are called Bloch functions, and these are the eigenstates of the full Hamiltonian. We will show that each of these wave-function can be connected to a unique choice of vector in the so called first Brillouin zone.

We use degenerate perturbation theory to show that the energy spectrum of a free particle split to first order for a simple periodic potential, giving rise to so called energy gaps. Using numerical calculations we calculate the exact energy spectrum (within a truncated basis) for the same periodic potential. We use Pauli's exclusion principal to argue which crystals form insulators and which crystals form conductors.

II. MATHEMATICAL FRAMEWORK OF A LATTICE

To describe the lattice of a crystal, we introduce the three-dimensional lattice translation vector

$$\mathbf{T} = u_1\mathbf{a}_1 + u_2\mathbf{a}_2 + u_3\mathbf{a}_3, \tag{1}$$

where the u_i's are integers and the $\mathbf{a}_i$'s are a set of primitive translation vectors. We construct the lattice by taking all combinations of the u_i's in Eq.(1). Figure 1 shows the $\mathbf{a}_1$-$\mathbf{a}_2$ plane of such a lattice. By construction, the lattice is invariant under lattice translation $\mathbf{T}$. Because of this invariance, it is natural to expect that some quantities are also invariant under lattice translation $\mathbf{T}$. We mean by this that for a function $f(\mathbf{r})$ we have that

$$f(\mathbf{r} + \mathbf{T}) = f(\mathbf{r}), \tag{2}$$

for any set of integers u_1, u_2 and u_3 in Eq.(1).

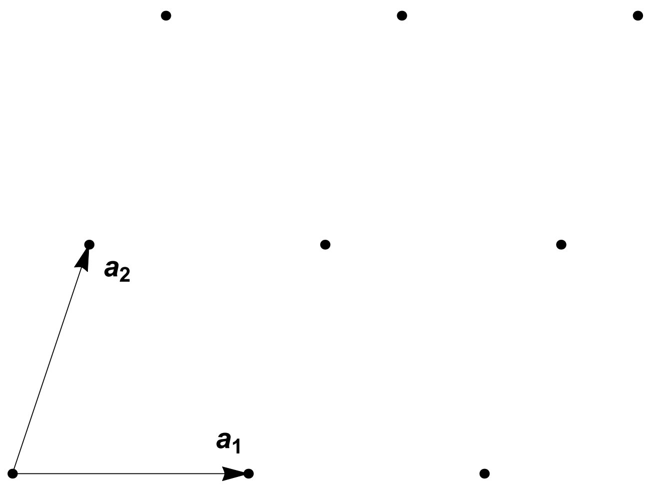

Figure 1. The $\mathbf{a}_1$-$\mathbf{a}_2$-plane of a three-dimensional lattice in ordinary space.

To analyse these function, we remind ourselves of the basic result of Fourier analysis for periodic functions. In one-dimension we have that any reasonable function can be expanded in a Fourier series

$$f(x) = \sum_n c_n e^{2\pi i n x/a}, \tag{3}$$

where n runs over all integers and a is the period. Consider now functions invariant under lattice translations $\mathbf{T}$. In analogy with Eq.(3), these functions can be expanded in a Fourier series [1]

$$f(\mathbf{r}) = \sum_{\mathbf{G}} C_{\mathbf{G}} e^{i\mathbf{G}\cdot\mathbf{r}}, \tag{4}$$

where the sum is over all reciprocal lattice vectors $\mathbf{G}$. The reciprocal lattice vector is given by [1]

$$\mathbf{G} = v_1\mathbf{b}_1 + v_2\mathbf{b}_2 + v_3\mathbf{b}_3, \tag{5}$$

where the v_i's are integers and the $\mathbf{b}_i$'s are primitive translation vectors of Fourier-space. Note how Eq.(5) is completely analogous to Eq.(1) and that as we take all possible combinations of the v_i's, we construct the reciprocal lattice of Fourier-space. The $\mathbf{b}_i$'s in Eq.(5) are related to the $\mathbf{a}_i$'s of Eq.(1) by the equation [1]

$$\mathbf{b}_i = 2\pi\epsilon_{ijk}\frac{\mathbf{a}_j \times \mathbf{a}_k}{\mathbf{a_1}\cdot\mathbf{a}_2\times\mathbf{a_3}}. \tag{6}$$

Note that for $i \neq j$, the $\mathbf{b}_i$'s are orthogonal to the $\mathbf{a}_j$'s since $\mathbf{a}_j \cdot \mathbf{a}_j \times \mathbf{a}_k = 0$. Combining this orthogonality condition with the cyclicity of the triple scalar product

$$\mathbf{a}_1\cdot(\mathbf{a}_2\times\mathbf{a}_3) = \mathbf{a}_3\cdot(\mathbf{a}_1\times\mathbf{a}_2) = \mathbf{a}_2\cdot(\mathbf{a}_3\times\mathbf{a}_1), \tag{7}$$

we find that

$$\mathbf{b}_i\cdot\mathbf{a}_j = 2\pi\delta_{ij}. \tag{8}$$

Using Eq.(8), we have that the dot product of the lattice translation vector $\mathbf{T}$ and the reciprocal lattice vector $\mathbf{G}$ is given by

$$\mathbf{G}\cdot\mathbf{T} = 2\pi(u_1v_1 + u_2v_2 + u_3v_3). \tag{9}$$

Note that the quantity inside the parenthesis is a sum of integers, which is itself an integer. Using this we have that

$$e^{i\mathbf{G}\cdot\mathbf{T}} = e^{2\pi i(u_1v_1+u_2v_2+u_3v_3)} = 1, \tag{10}$$

and we can now use Eq.(10) to confirm the periodicity of Eq.(4)

$$\begin{aligned} f(\mathbf{r}+\mathbf{T}) &= \sum_{\mathbf{G}} C_{\mathbf{G}} e^{i\mathbf{G}\cdot(\mathbf{r}+\mathbf{T})} \\ &= \sum_{\mathbf{G}} e^{i\mathbf{G}\cdot\mathbf{T}} C_{\mathbf{G}} e^{i\mathbf{G}\cdot\mathbf{r}} \\ &= \sum_{\mathbf{G}} C_{\mathbf{G}} e^{i\mathbf{G}\cdot\mathbf{r}} = f(\mathbf{r}). \end{aligned} \tag{11}$$

We have already mentioned that in analogy with the lattice translation vector $\mathbf{T}$, the set of vectors $\mathbf{G}$ form a lattice in Fourier space. See figure 2. Imagine now drawing lines from any lattice-point to the 26 nearest lattice-points ($3^3 = 27$ possible combinations of the $v_i = 0$ or $v_i = 1$, excluding the $v_i = 0$ for all i). We intersect each line at the middle by an orthogonal plane. See the red lines in figure 2. The red region in figure 2 is referred to as the Brillouin zone whereas the very special Brillouin zone centered at the origin is refereed to as the first Brillouin zone. We note that by construction the first Brillouin zone consists of all the points that are closest to the lattice-point $\mathbf{G} = 0$. By a translation $\mathbf{G}$, the points will consist of all the points closest to the point $\mathbf{G}$. It is therefore clear that any point $\mathbf{k}$ can be written as $\mathbf{k} = \mathbf{k}_0 + \mathbf{G}'$, where $\mathbf{k}_0$ is in the first Brillouin zone.

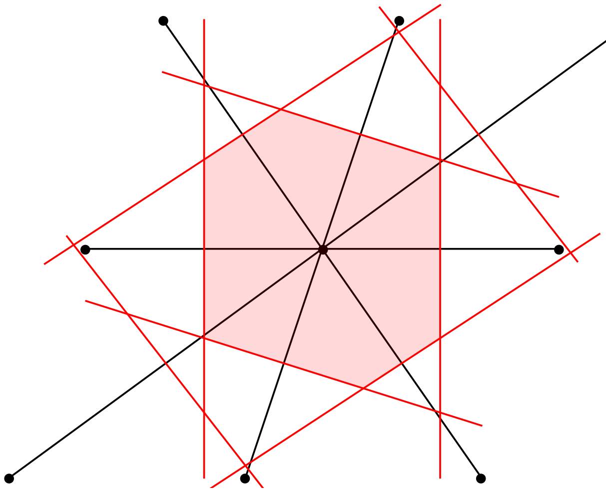

Figure 2. A plane in the lattice of Fourier-space. The red lines are orthogonal to the lines joining the lattice-points, intersecting these lines at the middle. The red region inside these lines is the Brillouin zone associated with the center lattice-point.

III. BLOCH FUNCTIONS AND ENERGY BAND STRUCTURES

In this section we begin by reviewing the main results for a free particle in three dimensions. We then give the result of Blochs theorem and show how the eigenstates to the periodic Schrödinger equation, the so called Bloch functions, are constructed from the free particle wave-functions. Using degenerate perturbation theory, we show that for the simplest periodic potentials the energy spectrum of a free particle split, thus creating energy gaps.

A. Free Particle

The free particle wave-function is given by

$$\psi_{\mathbf{k}}(\mathbf{r}) = \frac{1}{\sqrt{N}} e^{i\mathbf{k}\cdot\mathbf{r}}, \tag{12}$$

where $\mathbf{k}$ denotes the wave vector and $\frac{1}{\sqrt{N}}$ is a constant of normalization. These are eigenstates that form a complete set of basis vectors and their energies are given by

$$E_{\mathbf{k}} = \frac{\hbar^2 k^2}{2m}, \tag{13}$$

where $k = |\mathbf{k}|$, making states with equal magnitude of $\mathbf{k}$ degenerate.

The completeness of this basis allows for any function $\psi(\mathbf{r})$ to be expressed as a linear combination of these basis vectors. As we will see next, for a particle in a periodic potential the linear combination of these basis vectors are restricted to a very special form.

B. Bloch Functions

It was Felix Bloch who first found that for a particle in a periodic potential, the solutions of the time-independet Schödinger equation are of the form [1]

$$\psi_{\mathbf{k}}(\mathbf{r}) = u_{\mathbf{k}}(\mathbf{r})e^{i\mathbf{k}\cdot\mathbf{r}}, \tag{14}$$

where $u_{\mathbf{k}}(\mathbf{r})$ is periodic under lattice translations $\mathbf{T}$. Note that even though the $u_{\mathbf{k}}$ is periodic, Eq.(14) is not. The result of Eq.(14) could have been anticipated by arguing that the probability density for a stationary state must be periodic. This means that the wave-function must be periodic up to a possibly spatially varying phase, which is exactly the result stated in Eq.(14).

Using that $u_{\mathbf{k}}$ is periodic we can expand $u_{\mathbf{k}}$ as in Eq.(4) and Eq.(14) becomes

$$\begin{aligned}\psi_{\mathbf{k}}(\mathbf{r}) &= u_{\mathbf{k}}(\mathbf{r})e^{i\mathbf{k}\cdot\mathbf{r}}\\ &= \sum_{\mathbf{G}} C_{\mathbf{G}} e^{i(\mathbf{G}+\mathbf{k})\cdot\mathbf{r}},\end{aligned} \tag{15}$$

where we have brought the spatially dependent phase into the sum. We see that this is a sum over the free particle wave-function in Eq.(12), separated by reciprocal lattice vectors $\mathbf{G}$.

Now using that we can always write $\mathbf{k} = \mathbf{k}_0 + \mathbf{G}'$, where $\mathbf{k}_0$ is a vector in the first Brillouin zone, to write Eq.(15) as

$$\begin{aligned}\psi_{\mathbf{k}}(\mathbf{r}) &= u_{\mathbf{k}}(\mathbf{r})e^{i\mathbf{k}\cdot\mathbf{r}}\\ &= \sum_{\mathbf{G}} C_{\mathbf{G}} e^{i(\mathbf{G}+\mathbf{k})\cdot\mathbf{r}}\\ &= \sum_{\mathbf{G}} C_{\mathbf{G}} e^{i(\mathbf{G}+\mathbf{G}'+\mathbf{k}_0)\cdot\mathbf{r}}.\end{aligned} \tag{16}$$

By shifting the sum and remembering that the sum is over all reciprocal lattice vectors we have

$$\begin{aligned}&\sum_{\mathbf{G}} D_{\mathbf{G}} e^{i(\mathbf{G}+\mathbf{k}_0)\cdot\mathbf{r}}\\ &\quad= u_{\mathbf{k}_0}(\mathbf{r})e^{i\mathbf{k}_0\cdot\mathbf{r}},\end{aligned} \tag{17}$$

where the last step follows from using Eq.(15) and labeling the function $\mathbf{k}_0$ instead of $\mathbf{k}$ to emphasize that $u_{\mathbf{k}} \neq u_{\mathbf{k}_0}$ in general. Since Eq.(17) is of the same form as Eq.(14), we see that the $\mathbf{k}$ in the exponent can be restricted to the first Brillouin zone without loss of generality.

We can gain some intuition from focusing on a lattice in one-dimension. We have that in one-dimension Eq.(15) becomes

$$\begin{aligned}\psi_{k_0}(x) &= u_{k_0}(x)e^{ik_0x}\\ &= \sum_{n} C_g e^{(ng+k_0)x},\end{aligned} \tag{18}$$

where g is the magnitude of the shortest reciprocal lattice vector and k_0 is a point in the first Brillouin zone. This sum can be visualized as a sum over points, corresponding to free particle wave-functions in the graph of Eq.(13). See figure 3. These points are centered at k_0 and separated by a distance g. In figure 4 we have redrawn figure 3 with periodic conditions at $\pm\frac{1}{2}g$. Drawn in this way, instead of summing over points along the parabola, we are now summing over points on the vertical line at k_0. We note that the lines of the energy crossing at $k = 0$ and $k = \pm\frac{1}{2}g$. For these values, we have an infinite set of pairs of degenerate states. We know that in the language of perturbation theory, these degeneracies may split as a result of a perturbation. As we will see next, with a perturbation of a simple periodic potential, the lowest pair of degeneracies split to first order.

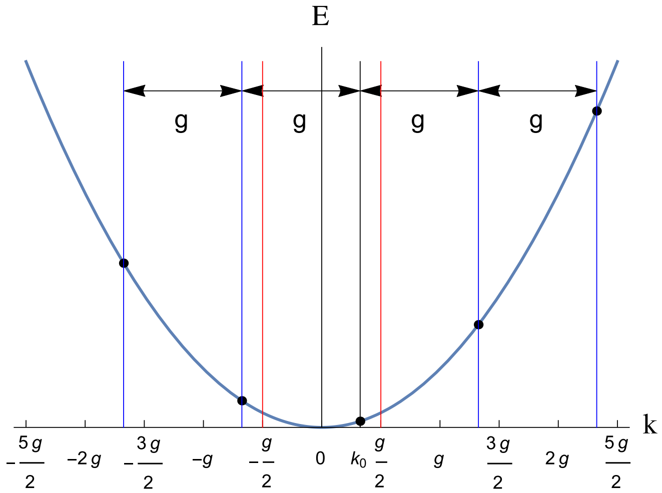

Figure 3. Energy as a function of k for a free particle in one-dimension. The points along the parabola are separated by the distance g and centered around k_0 in the first Brillouin zone.

C. Energy Band Gaps

One way to see how the energy spectrum of the free particle split is through the use of degenerate perturbation theory. Working in a one-dimensional lattice of periodicity a, and taking for simplicity the perturbation to be

$$\delta H(x) = V_0 \cos(gx), \tag{19}$$

where V_0 is a constant and $g = \frac{2\pi}{a}$ from Eq.(6). Note that this is the first harmonic (i.e the first non-constant

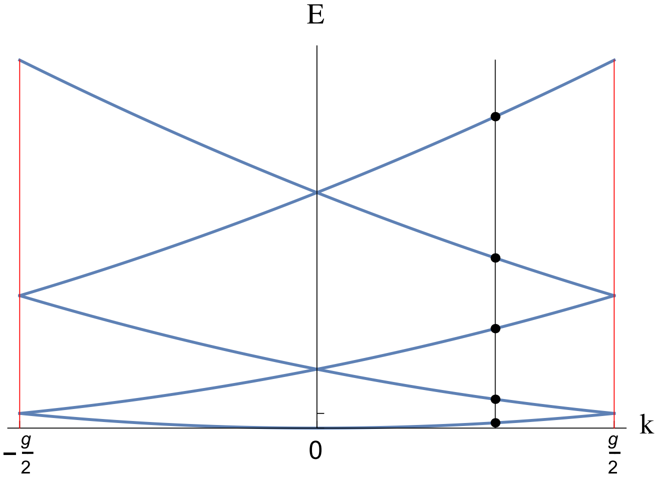

Figure 4. Energy as a function of k in one-dimension, redrawn with periodic conditions at $\pm\frac{1}{2}g$.

term) in the Fourier series compatible with the lattice periodicity. We focus on the two lowest degenerate states at the Brillouin zone boundary $k_0 = \frac{g}{2} = \frac{\pi}{a}$ where we have the two wave-functions

$$\begin{aligned}\psi_1(x) &= \frac{1}{\sqrt{a}} e^{i\frac{\pi x}{a}} \\ \psi_2(x) &= \frac{1}{\sqrt{a}} e^{-i\frac{\pi x}{a}}.\end{aligned} \tag{20}$$

These states couple to states of higher energy in general, but we know from perturbation theory that the coupling to higher states is suppressed by the large energy difference, making the exclusion of higher energy states acceptable.

We have by simple integration that

$$\delta H_{ij} = \int_0^L \psi_i(x)\delta H \psi_j(x)dx = (1-\delta_{ij})\frac{V_0}{2}, \tag{21}$$

and in matrix notation, δH becomes

$$\delta H = \frac{V_0}{2}\begin{bmatrix} 0 & 1 \\ 1 & 0 \end{bmatrix}. \tag{22}$$

In order to get the degenerate perturbation going, we need to find a good basis in which δH is diagonal. Diagonalizing Eq.(23) is easy and we have that

$$\delta H = \frac{V_0}{2}\begin{bmatrix} 1 & 0 \\ 0 & -1 \end{bmatrix}, \tag{23}$$

where the eigenstates have now become

$$\begin{aligned}\psi_+(x) &= \frac{1}{\sqrt{2}}(\psi_1(x)+\psi_2(x)) \\ \psi_-(x) &= \frac{1}{\sqrt{2}}(\psi_1(x)-\psi_2(x)).\end{aligned} \tag{24}$$

We can simply read the energy splitting from Eq.(23), yielding

$$\Delta E = E_+ - E_- = V_0, \tag{25}$$

where E_+ and E_- denotes the ψ_+ and ψ_- eigenvalues, respectively.

What we have calculated here is the splitting of the first energy bands for a particular choice of vector in the first Brillouin zone. In order to see how the rest of the spectrum deforms, we can discretize k-space and perform a numerical calculation, which is the subject of the next section.

IV. NUMERICAL EXAMPLE OF ENERGY BAND GAPS

We saw in Eq.(25) that for a periodic potential of the first harmonic, the lower degeneracies at the Brillouin zone boundary split to first order in perturbation theory. In a similar manner, for any other k_0, the different terms in the sum Eq.(18) will generally have terms that mix. We know from perturbation theory that the states of higher energy tend to push lower levels down. Similarly, the lower levels tend to push the higher levels up, leading to a continuous deformation of all energy levels. To see this, we turn to a numerical analysis for a particle in a periodic potential. We introduce a modulator $L = ma$, where m is an integer and a is the periodicity of the one-dimensional lattice. We impose on the wave-function periodic boundary conditions. The main consequence is that k-space is discretized, with m discrete points in the first Brillouin zone. See figure 5 for an illustration with $m = 20$. Note that in the limit as $m \to \infty$, the discrete points goes to the continuum and the effect of the modulator L disappears. For simplicity, we truncate the energies at the second degeneracy of the Brillouin zone boundary. This will not be a good approximation for the higher energy states. However, the lower energies will be more accurate and illustrate the main point. The truncation leads to a set of 3×3 matrices for each discrete point in the first Brillouin zone. For each k_0, we have the

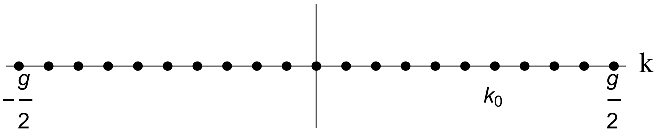

Figure 5. Discrete version of the first Brillouin zone for a one-dimensional reciprocal lattice.

three wave-functions

$$
\begin{aligned}
\psi_{k_0,1}(x) &= \frac{1}{\sqrt{L}} e^{ik_0 x} \\
\psi_{k_0,2}(x) &= \frac{1}{\sqrt{L}} e^{i(k_0-G)x} \\
\psi_{k_0,3}(x) &= \frac{1}{\sqrt{L}} e^{i(k_0+G)x}.
\end{aligned} \tag{26}
$$

We can now form the matrix elements of the Hamiltonian by sandwiching the Hamiltonian between the different states

$$H_{ij} = \int_0^L \psi_i(x) H(x) \psi_j(x) dx, \tag{27}$$

where $H(x)$ is the Hamiltonian. The Hamiltonian is of the form

$$H(x) = \frac{\hat{p}^2}{2m} + V(x), \tag{28}$$

where V(x) is the periodic potential with periodicity a. In order to compare the result with Eq.(25) we choose the potential $V(x)$ in analogy with Eq.(19)

$$V(x) = V_0 \cos{(gx)}, \tag{29}$$

where $V_0 = 10$ and g the magnitude of the shortest reciprocal lattice vector.

As we have noted earlier, the states will in general mix and so calculating the matrix elements in Eq.(27) will then lead to non-zero terms on the off-diagonal. By diagonalizing the resulting matrices we can obtain the energies of the full Hamiltonian. The eigenstates of the diagonalized Hamiltonian are linear combination of the three states in Eq.(26), exactly as expected from Eq.(18). For practical calculations, choosing $m = 200$, we have in figure 6 the result of the first three energy bands in the approximation where k-space is truncated after the third band. We can see in figure 6, that the splitting in energy at the Brillouin zone boundary is approximately $\Delta E = 10$, as predicted in Eq.(25) for $V_0 = 10$.

V. VALENCE ELECTRONS: METALS AND INSULATORS

We next want to fill the states with the available electrons. We therefore begin by counting the number of states. In order to count the number of states we again introduce the modulator variable $L = ma$. Using the periodic boundary conditions as we did for our numerical calculation, we have that k-space becomes discrete and the states are countably infinite. We have m k-points for each energy band inside the first Brillouin zone. See black dots in figure 6 for the case of $m = 10$. According to Pauli's exclusion principal, each band can be occupied by $2m$ states, where we have taken into account the electron spin. We focus for simplicity on the energy band structure of figure 6. We fill these bands by starting at the lowest energy and continuing up. Imagine now that for each point in the lattice, we have a set of p valence electrons. Consider p being an even number, we then have that the last energy band, also called the valence band, will be completely filled. In order to accomplish a change in the system, a finite energy will have to be supplied. We therefore have that for a weak electric field, no reorganization of the states is possible and the material is an insulator. In contrast, for p an odd number we have that the last energy band, now called a conduction band, will be only half-filled. No finite energy is needed to be supplied, and by applying a weak electric field we will have a system reorganization, thus changing the system configuration and the material is a conductor.

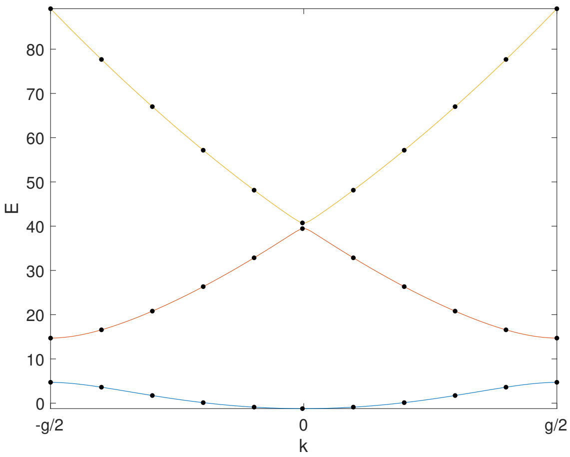

Figure 6. Numerical result in the approximation that k-space is truncated after the first three energy bands. Lines correspond to interpolations for $m = 200$ whereas dots correspond to $m = 10$.

VI. DISCUSSION

We have seen that in order to give a mathematical description of a crystal, we need a set of primitive translation vectors, forming the lattice translation vector **T**. For quantities invariant under lattice translations, we have used that these quantities can be expanded in a Fourier series. We stated the result of Bloch's theorem and saw that the Bloch functions are constructed by a restricted combination of the free particle wave-functions.

By using degenerate perturbation theory with a potential of the first harmonic, we calculated that the first set of degenerate states split to first order. We confirmed this splitting by means of a numerical example. In the approximation of a truncated k-space, we calculated the deformation of the first three energy bands for the same potential used in the perturbation. We noted in figure 6 that the states on the Brillouin zone boundary indeed split by V_0 as predicted by perturbation theory in Eq.(25).

We used the modulator L and periodic boundary conditions in order to calculate the number of states. By using Pauli's exclusion principal we were able to fill the states of the energy bands from lowest energy and up. We used the number of valence electrons together with the energy band structure to argue that crystals become insulators or conductors depending on whether their valence band is completely filled or not.

ACKNOWLEDGMENTS

I would like to thank my family for their endless support. A special thanks to my brother Kristofer for always encouraging me and for all our enlightening discussions. Finally, I would also like to show my greatest gratitude to MIT and the MITx team for your generosity in providing excellent education to all of us.

[1] C. Kittel, *Introduction to Solid State Physics.* Wiley, 2005.

The properties of the Deuteron

Diego Valdes

(Dated: June 18, 2019)

In this paper I will try to present a first approach to the main properties of the Deuteron nucleus in order to study the first features of the nuclear force, using concepts and models developed in undergraduated physics courses, like the Schrödinger equation in potential wells, central potentials in two body problem and scattering states.

I. INTRODUCTION

The deuteron is the isotope of Hydrogen formed by one proton and one neutron. It is the only stable atomic nucleus with two nucleons, as p-p or n-n possibilities are not.

Historically, that feature gave the Deuteron a key role in the first studies trying to understand the structure and properties of the strong nuclear force. Both experimental and theoretical data were obtained from experiments and models in order to perform a first characterization of the Deuteron properties.

In addition, the understanding of the properties of deuterium is very important due to the key role it plays in several fields of physics, being one of the most important the Big Bang theory.

Deuterium played a key role in the process of setting the ratios of the elements formed in the Big Bang. Thermodynamic arguments allow to calculate the fraction of protons and neutrons when the cosmic expansion cooled the Universe enough to form nuclei, being seven protons per neutron. The process to form helium nuclei from protons and neutrons requires the intermediate formation of deuterium. During much of the few minutes after the Big Bang in which nucleosynthesis could have happen, the temperature was high enough that the mean energy per particle was higher than the binding energy of deuterium, so that all the deuterium formed was destroyed. This is called the deuterium bottleneck. The bottleneck delayed the formation of helium until deuterium was available, at a temperature equivalent to 100 keV. Then, there was a burst of elements formation, from deuterium to helium, but shortly after the Universe became too cool and the nucleosynthesis stopped. At this point, the abundances of elements were almost fixed. The deuterium bottleneck together with the impossibility for stable combinations of helium with hydrogen or with itself (there are no stable nuclei with mass number of five or eight) leads to the practical absence of heavier nuclei than helium and the big abundance of hydrogen after the Big Bang. The measuring of the abundances of deuterium in the Universe at different scales, play a key role in the understanding of the creation of the Universe, the first, and in the creation of solar (star) systems and planets, the second. This measurements performed in comets indicate that the origin of the water of the Earth could be in comets and asteroids. Then, the study of all the properties of deuterium is fundamental for the interpretation of all these kind of measurements.

Deuterium also plays important roles both in nuclear fusion and fission reactions that are studied in our society, as well as in other applications like hydrogen NMR, where the spectrum of deuterium is clearly different from hydrogen one and deuterium solvents are then used often.

From a nowadays point of view, the deuteron offers us a system whose first properties can be obtained using relatively simple models, which gives us a first insight about the first steps given in the study of the strong nuclear force and a pedagogical tool to apply concepts and models studied in undergraduated quantum mechanics courses.

In this work, we will apply the said simple models to estimate some properties of the deuteron. In first place, in Section II we will try to characterize the strength of the potential between the proton and the neutron; in second place, in III we will describe the scattering cross section theory in order to, in IV, study the information that can be obtained from the scattering of neutrons on hydrogen, including the size of the nucleus, the range and the spin dependence of the nuclear force. Finally, we will enumerate the main conclusions obtained

II. STRUCTURE OF THE DEUTERON

The binding energy of the deuteron can be obtained experimentally with the thermal capture of neutrons by hydrogen

$$n + H^1 \longrightarrow H^2 + \gamma \tag{1}$$

Measuring the energy of the gamma rays emitted in the reaction gives a binding energy of 2.23 MeV, so we will begin our model assuming that energy like ground state energy for the deuteron.

We will treat the nucleus like a two body problem with a central potential. Then, following the typical treatment of this problem, like was developed in Lectures 20 and 21 in [1] or elsewhere, we will take the wave function in the “time-independent Schrödinger equation” like

$$\psi(\vec{r}) = R(r)Y_l^m$$

with a reduced mass

$$\mu = m_p/2$$

being m_p the mass of the proton and assuming the same mass for both nucleons. Then, we will consider the potential like a radial finite square well

$$V(r) = \begin{cases} -V_0 & r \leq r_0, V_0 > 0 \\ 0 & r > r_0 \end{cases}$$

The radial "time-independent Schrödinger equation" will be solved using that potential. We take $l = 0$ in the radial equation, since there is evidence that the ground state of deuteron is a 1s state, both from theoretical considerations related to general potential and experimental facts, measuring the magnetic moment of the deuteron, which is almost the algebraic sum of the moments of the proton and the neutron, with spins aligned (so it is a triplet state, although spin is not included in next calculations) and no orbital motion of one nucleon with respect to the other[2].

Then, with the usual change $u(r) = rR(r)$ we will finally solve the Schrödinger equation

$$-\frac{\hbar^2}{2\mu}\frac{d^2u}{dr^2} + V(r)u(r) = Eu(r) \tag{2}$$

The detailed solution of this problem can be found in the Problem Set 6 in [1] or elsewhere and take us to the next solution for the wavefunction:

$$u(r) = \begin{cases} N sin(kr) & r \leq r_0 \\ N\frac{sin(kr_0)}{e^{-\kappa r_0}}e^{-\kappa r} & r > r_0 \end{cases} \tag{3}$$

where

$$k^2 = \frac{2\mu(E + V_0)}{\hbar^2} \qquad \kappa^2 = -\frac{2\mu E}{\hbar^2} \tag{4}$$

The normalization constant N can be calculated as usual, solving

$$\begin{aligned} N^2\int_0^{r_0} \sin kr^2 dr + N^2 \sin kr_0{}^2 e^{2\kappa r_0}\int_{r_0}^{\infty} e^{-2\kappa r}dr = 1 \\ N^2\left(\frac{r_0}{2} - \frac{\sin 2kr_0}{4k}\right) + N^2\frac{\sin kr_0}{2\kappa} = 1 \\ N^2 = \frac{1}{\frac{R}{2} - \frac{\sin 2kr_0}{4k} + \frac{\sin kr_0{}^2}{2\kappa}} = \frac{2\kappa}{1 + kr_0} \end{aligned} \tag{5}$$

Using the continuity condition for the wave function and its derivative the energy selection equation is

$$\kappa r_0 = -kr_0 \cot(kr_0) \tag{6}$$

We can rewrite previous equation in a different way like

$$tan(kr_0) = -\left(\frac{V_0 + E}{|E|}\right)^{\frac{1}{2}} \tag{7}$$

Now, assuming that the potential will be much deeper than the ground state energy, we could consider $kr_0 \approx \frac{\pi}{2}$, that will take us to the next expression for the depth of the potential

$$V_0 = \left(\frac{\pi}{2}\right)^2 \frac{\hbar^2}{2\mu r_0^2} - E \tag{8}$$

From scattering experiments of neutrons on hydrogen that will be studied in the next section, we have an approximated value for the radius $r_0 \approx 2F$, that used in (8) gives us 27.8MeV for the depth of the potential. Checking the distance for which the exponential in (3) decreases in a 1/e factor we obtain $\frac{1}{\kappa} = 4.31F$, telling us that the two nucleons in the deuteron spend a large fraction of time at distances $r > r_0$.

A calculation of the root-mean-square radius using (3) with the parameters used here gives us 3.9F, a value quite close to the experimental value from scattering experiments, which is 4.2F.

A different but instructive approach comes from using another experimental parameter: the root mean square radius measured in scattering experiments (Chapter 3 in[3]).

The root mean square is defined as

$$R_{rms}^2 = \frac{\int_0^{\infty} r^2 R^2(r) r^2 dr}{\int_0^{\infty} R^2(r) r^2 dr} = \frac{\int_0^{\infty} u^2(r) r^2 dr}{\int_0^{\infty} u(r)^2 dr} \tag{9}$$

being the denominator the normalization of the function. Using (3) with the previous definition, we obtain

$$\begin{aligned} N^2\int_0^{r_0} r^2 \sin kr^2 dr + \\ + N^2 \sin kr_0{}^2 e^{2\kappa r_0}\int_{r_0}^{\infty} r^2 e^{-2\kappa r}dr = (4.2F)^2 \end{aligned} \tag{10}$$

where 4.2F is the experimental value measured for the deuteron root mean square radius. Solving these integrals, we finally get

$$\begin{aligned} N^2\frac{4(kR)^3 + 3\sin(2kR) - 6kR(kR\sin(2kR) + \cos 2kR)}{24k^3} \\ + N^2\frac{\sin^2(kR)(2\kappa R(\kappa R + 1) + 1)}{4\kappa^3} = (4.2F)^2 \end{aligned} \tag{11}$$

which, together with Eq.6, are a system of two equations with two unknowns, k and R, that will allow us to calculate the depth of the potential using the energy value of the bound state, $E_B = -2.3MeV$, and Eq.4. The system can be solved numerically. Using MATLAB, I obtained R=2.79F and then $V_0 = 21.53Mev$, which are similar values to those in the calculation above and in the literature [3, 4].

In Fig.1 we show the shape of the wave function of the bound state and the depth of the radial square well obtained. It is important to point out that the wave function needs to have its maximum before the end of the square well, so that the trigonometric part could match

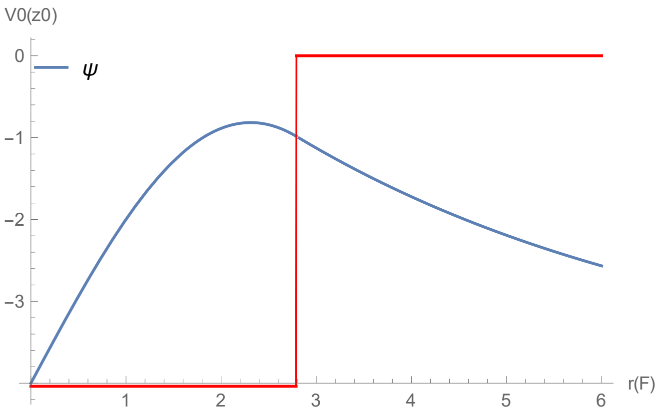

Figure 1. Square radial potential well for the deuteron and wave function of the bound state. The potential units are z_0, defined as $z_0^2 \equiv \frac{2*\mu R^2 V_0}{\hbar^2}$. The units of the wave function are not shown.

with the decreasing exponential part in the classically forbidden region.

These values obtained for the size and the potential of the nucleus give the first estimate of the range of the nuclear force, being a short range force, and of the strength of the force, bigger than the Coulomb force, as the Coulomb potential between two protons at the same distance is only 0.6 MeV. Finally, we will say that the deuteron is weakly bound, if we compare the depth of the potential with the binding energy.

III. SCATTERING THEORY

In order to go on with our analysis of the deuteron, we have to understand a bit the scattering quantum theory, to be able of obtaining information from scattering experiments of neutrons on hydrogen.

In first place, we have to define cross-section. The cross section σ measures the probability that a reaction or an interaction occurs. To focus already in our subject, imaging that neutrons are colliding on a sheet at a rate I [number of neutrons/second]. The sheet has a thickness Δx in cm and the neutrons collide on a surface A in cm^2 of the sheet. The density of the sheet is N [number of nuclei/cm^3]. Then, the number of nuclei exposed will be $NA\Delta x$, assuming no shadowing between nuclei. If we think in collisions neutron-nucleus, the collision (reaction) probability will be simply $P = N\Delta x\sigma$, the number of nuclei exposed per unit area by the probability σ. The cross section has then units of area.

In a more formal way, we can define the differential cross section $\sigma(\theta,\phi) \equiv \frac{d\sigma}{d\Omega} = \frac{I(\theta,\phi)}{I_0}$, the ratio of the scattered particle flux at the detector per unit solid angle and of the incident flux. The total scattering cross section is defined as the total number of particles scattered per unit time divided by the incident flux, and it would be calculated integrating the differential expression over the total solid angle.

When dealing with the scattering problem quantum mechanically, we first define the cross section $\sigma(\theta)$ in terms of the scattering amplitude $f(\theta)$ and then we calculate $f(\theta)$ solving the Schrödinger equation.

In the first step, the incident wave is taken like a plane wave

$$\Psi_{inc} = Ae^{i(\vec{k}\vec{r}-\omega t)}$$

, where A is a normalization constant and usually $\vec{k} = k\vec{z}$ is taken along the incident direction z-axis, with k defined with respect to the reduced mass and the relative energy of the particles colliding. For the scattering wave resulting from the interaction, we will write it like a outgoing spherical wave,

$$\Psi_{scat} = Af(\theta)\frac{e^{i(\vec{k}\vec{r}-\omega t)}}{r}$$

, where $f(\theta)$ denotes the amplitude of scattering in the direction of polar angle θ, having units of length. Now, using the quantum probability density current, it is obtained that

$$\sigma(\theta) = |f(\theta)|^2$$

Details of the calculation can be found in Lecture 7 in[5].

In fact, both the previous and the next step follow the same ideas developed for the scattering problem in one dimension worked in [1], so that advantage can be taken from the understanding of the 1D problem.

To calculate $f(\theta)$ we can solve the time independent Schrödinger equation for a two-body problem with a central potential, using the reduced mass μ, in a standard way:

$$\left(-\frac{\hbar^2}{2\mu}\nabla^2 + V(r)\right)\psi(\vec{r}) = E\psi(\vec{r}) \qquad (12)$$

We will focus this time in the scattering solutions instead in the bound-state solutions and we will write the sum of the incident and scattered wave as

$$\psi_k(\vec{r}) = e^{ikz} + f(\theta)\frac{e^{ikr}}{r}, r \gg r_0 \qquad (13)$$

where r_0 is the range of the force, potential is zero for $r > r_0$. The subscript k accounts for the fact that all the analysis is performed a fixed incoming energy $E = \frac{\hbar^2 k^2}{2\mu}$. Very far away from the potential, the wave equation is therefore that of a free particle, so we will try to match up (13) with the free particle solution.

Expressing the wave function like

$$\psi(\vec{r}) = R(r)P_l(cos(\theta))$$

and writing the potential using the angular momentum like we did in II, we get to the radial equation

$$\left(\frac{d^2}{dr^2} + k^2 - \frac{2\mu}{\hbar^2}V(r) - \frac{l(l+1)}{r^2}\right)u_l(r) = 0 \qquad (14)$$

Notice that we are ignoring this time the azimuthal component of the wavefunction, as only depends on r and θ, which not change the radial equation. Setting v(r)=0 we get a second-order differential equation whose general solutions are spherical Bessel functions:

$$u_l(r) = B_l r J_j(kr) + C_l r N_l(kr)$$

where B_l and C_l are integration constants and J_l and N_l are spherical Bessel and Neumann functions, respectively. Using the asymptotic expressions for J_l and N_l, Lecture 7[5], we get

$$u_l(r) = \frac{A_l}{k} sin\left(kr - \frac{l\pi}{2} + \delta_l\right), kr \gg 1 \tag{15}$$

where the integration constants were redefined, appearing a phase shift with a parallel meaning to that in 1D case. In a straightforward way, we get for the total wavefunction

$$\psi(r,\theta) = \sum_l \frac{A_l}{kr} sin\left(kr - \frac{l\pi}{2} + \delta_l\right) P_l(cos(\theta)), kr \gg 1 \tag{16}$$

Now, we will expand $f(\theta)$ in (13) in spherical harmonics like

$$f(\theta) = \sum_l f_l P_l(cos(\theta)) \tag{17}$$

and expanding as well the incident plane wave:

$$e^{ikz} = e^{ikrcos(\theta)} = \sum_l i^l (2l+1) J_l(kr) P_l(cos(\theta)) = \tag{18}$$

$$\sum_l i^l (2l+1) \frac{sin\left(kr - \frac{l\pi}{2}\right)}{kr} P_l(cos(\theta)), kr \gg 1 \tag{19}$$

Now, substituying (17) and (19) in (13), setting that equal to (16), writting all the sine functions as exponentials and assuming that the coefficients of each different exponential have to be the same, it is obtained

$$a_l = i^l (2l+1) e^{i\delta}$$

$$f_l = \frac{(-i)^l}{2ik}(a_l e^{i\delta} - i^l(2l+1))$$

so finally

$$f(\theta) = \frac{1}{k} \sum_l (2l+1) e^{i\delta} sin(\delta) P_l(cos(\theta)) \tag{20}$$

and

$$\sigma(\theta) = |f(\theta)|^2 = \frac{1}{k^2} \left| \sum_l (2l+1) e^{i\delta} sin(\delta) P_l(cos(\theta)) \right|^2$$

Finally, integrating in the solid angle and taking into account the orthogonality

$$\sigma = \frac{4\pi}{k^2} \sum_l (2l+1)^2 sin^2(\delta)$$

Since we are going to study scattering processes with slow neutrons, we are only interested in neutron cross sections in low energy case, $kr \ll 1$, just the leading term in the expansion, l=0, will be important, which is called the s-wave. In this approximation

$$\begin{aligned} \sigma(\theta) &= \frac{1}{k^2} sin^2(\delta_0(k)) \\ \sigma &= \frac{4\pi}{k^2} sin^2(\delta_0(k)) \end{aligned} \tag{21}$$

A useful parameter when working with slow neutrons is the so called scattering length. It is defined as

$$a = \lim_{k \to 0} (-f_0) \tag{22}$$

then, using (20), since f_0 has to be finite

$$a = \lim_{k \to 0} \left(- \frac{e^{i\delta_0} sin(\delta_0)}{k} \right) = -\frac{\delta_0}{k} \tag{23}$$

The cross section can be written

$$\sigma(k \longrightarrow 0) = 4\pi a^2$$

The meaning of the scattering length and its sign comes from the analysis of the scattered wave. The radial function, as it is done in the next section, depends on the $\sin(kr + \delta_0)$ (far away from the scatterer), being the scattering effect represented by δ_0 or by the scattering length through (23). If we take the limit with kr_0 small, low energy, the scattered wave can be written $u_0 \approx k(r - a)$; then the scattering length a is the distance at which the wave function linearly goes to zero from its value and slope at $r = r_0$. There are two possibilities of doing this depending on the value of kr_0. If $kr_0 > \frac{pi}{2}$, the wave function has passed the maximum and has negative slope, so the linear continuation gives a positive scattering length; if $kr_0 < \frac{pi}{2}$, the wave function has not get the maximum, so the slope is positive and the linear continuation gives negative scattering length. $a > 0$ means that the potential is such that there is a bound state, as the sine wave function inside the potential can match with the decreasing exponential for the bound state in the forbidden region. $a < 0$ means that only a virtual state is possible, as the sine function inside the potential cannot match with the decreasing exponential.

In Fig.2, we show the scattering length described before, applied to the case of the potential and wave function calculated in Section II. The extrapolation gives us a value for the scattering length of $a = 7.2F$.

IV. NEUTRON-PROTON SCATTERING

We are going to apply the concepts developed in the previous section to the scattering of very low energy neutrons in hydrogen.

In order to do this, we will have to calculate the phase shift in the s-wave approximation (21) or the scattering

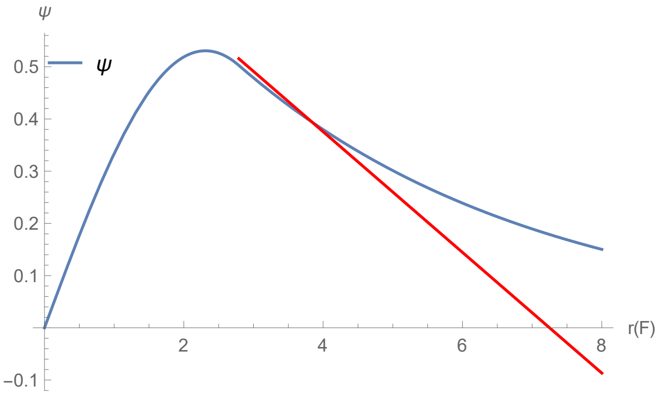

Figure 2. Approximated representation of the scattering length using the wave function and more data obtained in SectionII, and the linear extrapolation described at the end of Section III

length (23). We are going to consider the scattering-state solution for the radial equation of the same square radial potential used in II, which corresponds to a one dimension scattering states exactly like were studied in Lectures 16 to 19 in [1]. Following that structure, radial wavefunction for $E > 0$ will be

$$u(r) = \begin{cases} Bsin(k'r) & r \leq r_0 \\ Ce^{i\delta_0}sin(kr + \delta_0) & r > r_0 \end{cases} \tag{24}$$

where

$$k'^2 = \frac{2m(E + V_0)}{\hbar^2} \quad and \quad k^2 = \frac{2mE}{\hbar^2}$$

Applying continuity conditions at r_0 it is obtained

$$k' \cot(k'r_0) = k \cot(kr_0 + \delta_0) \tag{25}$$

which relates the incoming energy with the potential parameters. Considering we are dealing with very slow neutrons, we will do two approximations: 1)we neglect kr_0 compared to δ_0, $kr_0 \ll \delta_0$. 2) Since $KE \ll V_0$, we assume $k' \approx k$ and using (6) we can write

$$k \cot(\delta_0) \approx -\kappa \tag{26}$$

with κ given by (4). Then, using (26) in (21) and the identity $\sin^2(\theta) = 1/(1+\cot^2(\theta)$, we obtain that the cross section is

$$\sigma \approx \frac{4\pi}{k^2}\frac{1}{1+\cot^2(\delta_0)} = 4\pi\frac{\hbar^2}{2\mu}\frac{1}{T_0 + E_b} \tag{27}$$

where T_0 is the kinetic energy associated to the incident neutron and E_b the binding energy of the deuteron. Using again that $T_0 \ll E_b$, we obtain $\sigma \approx 2.34 \times 10^{-28}m^2 = 2.34 \times 10^{-24}cm^2 = 2.34b$ with b meaning $1barn = 10^{-24}cm^2$, a usual unit in scattering problems. This value is quite lower than the experimental value of the scattering cross section of hydrogen, which is 20.4 barns[2].

Wigner already suggested the explanation to this discrepancy in 1931. He noticed that in the scattering of neutrons with hydrogen, the particles could collide either with total spin 1, giving a triplet state, or with toal spin 0, a singlet state. Then, (21) and (27) have to be modified. The probability of colliding with a triplet state will be three times grater than doing with a singlet state, so we can write for the cross section (21)

$$\sigma(\theta) = \frac{1}{k^2}\left(\frac{1}{4}\sin^2(\delta_{0,singlet} + \frac{3}{4}\sin^2(\delta_{0,triplet})\right) \tag{28}$$

We have already said that the ground state of the deuteron is a triplet state with energy $E = -E_b$. If the singlet state is a virtual state of energy $E = E^*$, the (27) can be written as

$$\sigma \approx \frac{\pi\hbar^2}{2\mu}\left(\frac{3}{E_b} + \frac{1}{E^*}\right) \tag{29}$$

Taking $E^* \approx 70keV$, we obtain, using the previous equation, 20.4 barns for the cross section, a value which agrees with the experiment.

This was the first evidence of the nuclear force dependence in the spin, a new feature compared with coulomb interaction.

The approximations made in (25) to get (26) and (27) allow us to calculate the scattering length as defined in (23) but not the range of the force r_0, this information is lost by the said approximations. To understand how r_0 is obtained from the experiments, we come back to the scattering radial wavefunction (24) in the limit $r \longrightarrow \infty$; let be $\chi(r)$ the asymptotic form of the wavefunction in that limit, then $\chi(r) = N\sin(kr + \delta)$, we can build the object

$$\frac{1}{\chi(0)}\left[\frac{\partial\chi(r)}{\partial r}\right]_{r=0} = k\cot(\delta) \tag{30}$$

If now we do a Taylor expansion of that object about k=0, we obtain

$$k\cot(\delta) = -\frac{1}{a} + \frac{1}{2}r_{eff}k^2 + ... \tag{31}$$

defining the effective range in this way. We can consider this object in a different way. If we take again (20) with l=0, we have

$$f(\theta) = \frac{1}{k}e^{i\delta}\sin(\delta) = \frac{1}{k}\frac{\sin(\delta)}{\cos(\delta) - i\sin(\delta)} = \frac{1}{k\cot(\delta) - ik} \tag{32}$$

so if we understand $k\cot(\delta)$, we understand the scattering amplitude. Schwinger and others examined the properties of $k\cot(\delta)$, finding that for a finite range potential of range R, it has a power series expansion around k=0 that converges for $k < \frac{1}{R}$,

$$k\cot(\delta) = -\frac{1}{a} + \frac{1}{2}r_0k^2 + r_1 * k^4 + ...$$

The study of the measured cross section using previous expressions will give us the best estimations of the scattering length, range of the nuclear force and depth of the potential:

$$\begin{aligned} n-p\ triplet\ a_{triplet} = 5.42F\ r_{0,triplet} = 1.73F \\ V_{0,triplet} \approx 30MeV \\ n-p\quad singlet\quad a_{singlet} = -23.71F\quad r_{0,singlet} = 2.73F \\ V_{0,singlet} \approx 18MeV \end{aligned}$$

V. CONCLUSIONS

In this paper I have tried to characterize the main properties of the deuteron using relatively simple quantum mechanical tools. The goal was to give an insight of a very important system in different areas of physics, not introduced before in the context of our undergraduate quantum mechanics courses, using some models and tools developed in the said courses.

We have obtained a first estimation for the strength of the potential between the proton and the neutron using the scheme of the two body radially symmetric problem and solving the radial equation for a finite square well. Besides the strength of the potential, we could obtained a first estimation of the radius of the deuterium.

Next, we described briefly the scattering theory in order to be applied in the scattering of low energy neutrons on hydrogen. The experimental cross sections measured, combined with the first model, allowed us to refine the values for the strength and range (radius) of the potential. These values told us about the short range of the nuclear force and its big strength compared with electromagnetic forces.

Finally, it also showed the existence of two different total spin states of deuterium, and both have to be considered to match the theoretical and experimental results. These two states have different energies, rising up the dependence of the nuclear force with the spin.

ACKNOWLEDGMENTS

I would like to thank to all my colleagues at 8.06x who have read the dreft of this paper and/or have given comments and ideas to develop and to improve the contents of this paper.

I would also like to than to all the staff of the course for the same, and for all the effort in developing and managing a great course like this.

---

[1] B. Zwiebach, “8.04x quantum physics i. fall 2018. massachusetts institute of technology: Mitx.” `https://courses.edx.org/courses/course-v1:MITx+8.04.1x+3T2018/course/`, 2018. accessed: 2019-05-27.

[2] W. E. Meyerhof, *Elements of Nuclear Physics.* McGraw-Hill, New York, 1967.

[3] B. L. Cohen, *Concepts of Nuclear Physics.* McGraw-Hill, New York, 1971.

[4] E. Segre, *Nuclei and Particles.* W. A. Benjamin, New York, 1965.

[5] S. Yip, “22.101 applied nuclear physics. massachusetts institute of technology:mit opencourseware.” `https://ocw.mit.edu`,license: Creative commons by-nc-sa., 2006. accessed: 2019-05-27.

Quantizing the Damped Linear Harmonic Oscillator

Nilay A. Pradhan

(Dated: June 19, 2019)

The damped linear oscillator is one of most widely studied systems in classical mechanics, with manifestations in multiple branches of physics. The quantization of such a fundamental system would seem to be a simple extension of that of the textbook quantum harmonic oscillator, but that is not the case. This is primarily so because the Hamiltonian formulation, fundamental to canonical quantization, is ill-equipped to deal with classically dissipative systems. In this paper, we discuss an attempt to quantize this system using a generalized approach to Dirac's canonical procedure, and its shortcomings.

I. INTRODUCTION

The simple harmonic oscillator (SHO) is probably the simplest conservative system in mechanics and forms the backbone of almost every undergraduate curriculum in physics [1]. The extensive study of this system is well justified by their wide application to diverse physical phenomena. Similarly, the quantum analog of the SHO, the quantum (linear) harmonic oscillator (QHO), is also one of the most well-studied cases in quantum mechanics texts [2].

The next best-known and well understood system in classical physics, namely the Damped Linear Harmonic Oscillator (DHO), is also well-understood and is also a very well studied problem in mechanical and electronic systems. However, this is one of the simplest cases of a dissipative system, and as such, is not amenable to the Hamiltonian formulation of classical mechanics *by itself* because its dynamics are not reversible in time. Indeed, given the equation of motion for the DHO (taking the mass m to be unity, as we will continue to do in this report):

$$\ddot{x} + 2\gamma\dot{x} + \Omega^2 x \ = \ 0, \tag{1}$$

we see that the rate of change of energy is given by $\frac{dE}{dt} = -2\gamma\dot{x}^2$, which is indeed dissipative. Due to this, it does not lend itself to the usual Hilbert space formulation of quantum mechanics. This is because the Schrödinger equation defines a unitary time-evolution operator and hence the quantum dynamics is perfectly time-reversible in the Schrödinger picture [3] [4].

II. THE BATEMAN HAMILTONIAN

To address the problem that a dissipative system could not be discussed within the Hamiltonian framework on its own, Bateman [5] devised a unique way out for the classical disspative system of the DHO. In this formulation, the dissipative system is coupled to an *identical* mirror system that simultaneously gains the energy that the real physical system loses. This involves doubling the degrees of freedom, only half of which pertain to the actual physical system. The rest are thought to represent the reservoir degree(s) of freedom. We must reiterate that Bateman's work was in a purely classical context [5]. The Bateman Hamiltonian was subsequently quantized by Feshbach and Tikochinsky [6], and independently by Bopp [7]. We will follow here the logical flow of Dekker's 1981 review [4]. After quantizing the Bateman-Feshbach-Tikochinsky (BFT) system using canonical methods, we will explore its spectral features and its eigenstates, and subsequently understand its shortcomings. We will then compare this with an alternative treatment by Bopp [7]. We shall conclude with a note to the fact that the correct approach to this system is that of open quantum systems, though this investigation is beyond the scope of the report.

Let us consider the case of the 1D damped oscillator (given by x), and an identically weighted but *amplified* oscillator (related by $x \to \bar{x}$, $t \to -t$):

$$\ddot{x} + 2\gamma\dot{x} + \Omega^2 x \ = \ 0, \tag{2a}$$

$$\ddot{\bar{x}} - 2\gamma\dot{\bar{x}} + \Omega^2 \bar{x} \ = \ 0. \tag{2b}$$

Now, the two oscillators can be coupled into a Lagrangian $\mathcal{L}$ given by:

$$\mathcal{L} \ = \ \dot{x}\dot{\bar{x}} - \Omega^2 x\bar{x} + \gamma(x\dot{\bar{x}} - \dot{x}\bar{x}). \tag{3}$$

It can be easily verified that the Lagrangian in Eq.(3) does in fact, yield the equations of motion above. What is interesting is that those equations are completely decoupled, whereas the Lagrangian itself is coupled. This will have a strong bearing on the quantum treatment of this system. From this, we can get the generalized momenta for the x and $\bar{x}$variables.

$$\mathscr{p} \ = \ \frac{\partial \mathcal{L}}{\partial \bar{x}} \ = \ \dot{\bar{x}} - \gamma\bar{x}, \tag{4a}$$

$$\bar{\mathscr{p}} \ = \ \frac{\partial \mathcal{L}}{\partial x} \ = \ \dot{x} \ + \gamma x. \tag{4b}$$

Another very important fact is that the canonical momentum $\mathscr{p}$ for this system is *not* its kinetic momentum p, but is comprised of the dual variables and their derivatives. This fact will be crucial when we attempt to quantize the system and obtain its spectrum and the uncertainty relations.

The Hamiltonian is given by:

$$\mathcal{H} \ = \ \textstyle\sum_q \mathscr{p}_q \dot{q} - \mathcal{L} = \ \dot{x}\mathscr{p} + \dot{\bar{x}}\bar{\mathscr{p}} - \mathcal{L} \tag{5}$$

Substituting the values of the canonical momenta obtained in equations Eqs. (4a) and (4b), we get the expression for the Bateman Hamiltonian:

$$\mathcal{H} \ = \ \mathscr{p}\bar{\mathscr{p}} - \gamma(x\mathscr{p} - \bar{x}\bar{\mathscr{p}}) + \omega^2 x\bar{x} \tag{6}$$

where $\omega^2 = \Omega^2 - \gamma^2$ is the reduced frequency of the dual oscillator system. The beauty of the Bateman system is that as the physical oscillator (x) loses energy, it is simultaneously gained by its dual ($\bar{x}$), *together* forming a conservative system. From the Hamiltonian standpoint, there is no distinction between the actual and the dual system, but we must not lose sight of the fact that the dual system does not represent any physical degrees of freedom. It is just a mathematical construct.

From the Hamiltonian (6), it is easy to see that the Hamiltonian itself is a constant of motion. After all, the energy dissipated one part is instantly absorbed by the other, and gives the following equations of motion (note the absence of the kinetic momentum):

$$\dot{x} \ = \ \partial_{\mathscr{p}}\mathcal{H} \ , \qquad \dot{\mathscr{p}} \ = \ -\partial_x\mathcal{H} \ . \tag{7a}$$
$$\dot{\bar{x}} \ = \ \partial_{\bar{\mathscr{p}}}\mathcal{H} \ , \qquad \dot{\bar{\mathscr{p}}} \ = \ -\partial_{\bar{x}}\mathcal{H} \ . \tag{7b}$$

From the equations above, we can show the Hamiltonian itself is not equal to the total energy of the closed system, even when $\gamma \to 0$. As a result we have a fundamental hindrance to the quantization of the system, but this can be fixed by only admitting the solutions to Hamilton's equations where both the oscillators start from the same initial state (to balance the energy loss/gain rate). Even then, we see that the next obstacle to our canonical quantization comes in the form of calculating the non-vanishing Poisson brackets for the system, where we see that the only ones that survive are:

$$\{x, \mathscr{p}\} \ = \ 1 \ , \qquad \{\bar{x}, \bar{\mathscr{p}}\} \ = \ 1. \tag{8}$$

which leads to the commutators:

$$[x, \mathscr{p}] \ = \ i\hbar \ , \qquad [\bar{x}, \bar{\mathscr{p}}] \ = \ i\hbar. \tag{9}$$

It is now that we realize the main problem behind quantizing the Bateman system. We never see a non-zero commutator between x and the kinetic momentum p even in the limit of vanishing γ, where we should get back our familiar canonical commutation relation, i.e., $[x, p] = i\hbar$. This is a persistent issue with this description of the damped oscillator, but it is still instructive to pursue this approach, if only to see the flaws of the canonical formalism when applied to dissipative systems.

In order to proceed, we propose that the canonical variables $x, \mathscr{p}$, and $\bar{x}, \bar{\mathscr{p}}$ are operators in a linear space (Note: this is not a Hilbert space, as this is a dissipative system, so unitary time evolution may not always apply). We now define the following operators, following the treatment of the usual QHO, and from Feshbach and Tikochinsky [6]:

$$a = \frac{1}{\sqrt{2\hbar\omega}}(\mathscr{p} - i\omega x) \ , \ \bar{a} = \frac{1}{\sqrt{2\hbar\omega}}(\bar{\mathscr{p}} - i\omega\bar{x}) \tag{10a}$$
$$a^\dagger = \frac{1}{\sqrt{2\hbar\omega}}(\mathscr{p} + i\omega x) \ , \ \bar{a}^\dagger = \frac{1}{\sqrt{2\hbar\omega}}(\bar{\mathscr{p}} + i\omega\bar{x}) \tag{10b}$$

Here, $a^\dagger$ is the common Hermitian conjugate of a, and the bar is considered as a formal operation called mirror conjugation, whereby $\{x, \mathscr{p}\} \leftrightarrow \{\bar{x}, \bar{\mathscr{p}}\}$, and $\gamma \leftrightarrow -\gamma$. Evaluating the fundamental commutation relation yields

$$\begin{aligned}[a, a^\dagger] \ &= \ \frac{1}{2\hbar\omega}\left[(\mathscr{p} - i\omega x), (\mathscr{p} + i\omega x)\right] \\ &= \ \frac{1}{2\hbar\omega}\left([\mathscr{p}, \mathscr{p}] + i\omega[\mathscr{p}, x] + i\omega[x, \mathscr{p},] + \omega^2[x, x]\right) \\ &= \ \frac{1}{2\hbar\omega}\left(i\omega(-i\hbar) - i\omega(i\hbar)\right) \\ &= \ 1\end{aligned} \tag{11}$$

as we would expect from Eq. (9). A similar relation holds for $[\bar{a}, \bar{a}^\dagger]$. Now let us define the operators:

$$\mathscr{A} \ = \ \frac{a + \bar{a}}{\sqrt{2}} \ ; \qquad \mathscr{B} \ = \ \frac{a - \bar{a}}{\sqrt{2}} \tag{12}$$

Thus, we get the commutation relation $[\mathscr{A}, \mathscr{A}^\dagger] = [\mathscr{B}, \mathscr{B}^\dagger] = 1$, all others being zero. Furthermore, we have:

$$\begin{aligned}\mathscr{A}^\dagger\mathscr{A} &= \tfrac{1}{2}(\bar{a} + \bar{a}^\dagger)(a + a^\dagger) \\ &= \tfrac{1}{4\hbar\omega}\left((\mathscr{p} + \bar{\mathscr{p}}) + i\omega(x + \bar{x})\right) \\ &\quad \times \ \left((\mathscr{p} + \bar{\mathscr{p}}) - i\omega(x + \bar{x})\right) \\ &= \tfrac{1}{4\hbar\omega}((\mathscr{p}^2 + \bar{\mathscr{p}}^2 + 2\mathscr{p}\bar{\mathscr{p}}) \\ &\quad + \omega^2(x^2 + \bar{x}^2 + 2x\bar{x}) - 2\hbar\omega).\end{aligned} \tag{13}$$

Similarly, we have:

$$\begin{aligned}\mathscr{B}^\dagger\mathscr{B} &= \tfrac{1}{4\hbar\omega}((\mathscr{p}^2 + \bar{\mathscr{p}}^2 - 2\mathscr{p}\bar{\mathscr{p}}) \\ &\quad + \omega^2(x^2 + \bar{x}^2 - 2x\bar{x}) - 2\hbar\omega).\end{aligned} \tag{14}$$

Thus,

$$\hbar\omega(\mathscr{A}^\dagger\mathscr{A} - \mathscr{B}^\dagger\mathscr{B}) \ = \ \mathscr{p}\bar{\mathscr{p}} + \omega^2 x\bar{x}. \tag{15}$$

Continuing along the same lines, we have:

$$\begin{aligned}\mathscr{A}^\dagger\mathscr{B}^\dagger &= \tfrac{1}{4\hbar\omega}((\mathscr{p}^2 - \bar{\mathscr{p}}^2) - \omega^2(x^2 - \bar{x}^2) \\ &\quad + 2i\omega(x\mathscr{p} - \bar{x}\bar{\mathscr{p}})),\end{aligned} \tag{16a}$$
$$\begin{aligned}\mathscr{A}\mathscr{B} &= \tfrac{1}{4\hbar\omega}((\mathscr{p}^2 - \bar{\mathscr{p}}^2) - \omega^2(x^2 - \bar{x}^2) - \\ &\quad - 2i\omega(x\mathscr{p} - \bar{x}\bar{\mathscr{p}})).\end{aligned} \tag{16b}$$

and thus, upon subtracting the second identity from the first, and multiplying by $\hbar$, we get

$$i\hbar\gamma(\mathscr{A}^\dagger\mathscr{B}^\dagger - \mathscr{A}\mathscr{B}) = -\gamma(x\mathscr{p} - \bar{x}\bar{\mathscr{p}}). \tag{17}$$

From Eqs. (15) and (17) and comparing with Eq. (6), we can deduce the quantized version for the Bateman Hamiltonian:

$$\begin{aligned}\hat{\mathcal{H}} \ &= \ \hbar\omega(\mathscr{A}^\dagger\mathscr{A} - \mathscr{B}^\dagger\mathscr{B}) + i\hbar\gamma(\mathscr{A}^\dagger\mathscr{B}^\dagger - \mathscr{A}\mathscr{B}) \\ &= \ \hat{\mathcal{H}}_0 + \hat{\mathcal{H}}_1.\end{aligned} \tag{18}$$

From the above expression, we can see that the eigenvalues of $\hat{\mathcal{H}}_0$ are those of the ordinary Hilbert space of the two oscillators, i.e., those of $\mathscr{A}^\dagger\mathscr{A}$ and $\mathscr{B}^\dagger\mathscr{B}$. These can be quantified as $n_A, n_B = 0, 1, 2, \ldots$ and so the eigenvalues of $\hat{\mathcal{H}}_0$ are $\hbar\omega(n_A - n_B)$. Note that it is the *difference* of the dual oscillators that goes into this expression. Meanwhile even in the limit of $\gamma \to 0$, we get the usual number operator $N = n_A$ only if the dual oscillator is maintained in the ground state, i.e., $n_B = 0$, i.e. turned off by hand.

In order to explore the spectrum of $\hat{\mathcal{H}}$, we have to obtain an eigenbasis for both $\hat{\mathcal{H}}_0$ and $\hat{\mathcal{H}}_1$. Now, the naïve Fock basis eigenstates $|n_A, n_B\rangle$ are the eigenvectors of $\hat{\mathcal{H}}_0$ alone, though not of $\hat{\mathcal{H}}_1$. However, by using Eq. (11) and the other commutator identities, we see that $\hat{\mathcal{H}}_0$ and $\hat{\mathcal{H}}_1$ actually commute! So we can now arrive at a simultaneous eigenbasis of the two, which will yield the spectrum of the full Hamiltonian.

To be able to do this, we need to follow the dynamical the symmetry of the Bateman system, which is found to be $SU(1,1)$ [3]. Using the treatment in refs. [4] and [8] for the group algebra, we have the following operators:

$$\phi_0 = \tfrac{1}{2}(\mathscr{A}^\dagger\mathscr{A} - \mathscr{B}^\dagger\mathscr{B}) \tag{19a}$$

$$\phi_1 = \tfrac{1}{2}(\mathscr{A}^\dagger\mathscr{B}^\dagger + \mathscr{A}\mathscr{B}) \tag{19b}$$

$$\phi_2 = \tfrac{i}{2}(\mathscr{A}^\dagger\mathscr{B}^\dagger - \mathscr{A}\mathscr{B}) \tag{19c}$$

$$\phi_3 = \tfrac{1}{2}(\mathscr{A}^\dagger\mathscr{A} + \mathscr{B}^\dagger\mathscr{B}) \tag{19d}$$

It can be shown that ϕ_0 is, in fact, the Casimir operator for the group that commutes with the generators ϕ_i, where $i = (1, 2, 3)$, i.e., $[\phi_0, \phi_i] = 0$. In addition, the generators ϕ_i can be shown to define the characteristic $SU(1,1)$ algebra[1] [8]:

$$[\phi_1, \phi_2] = i\phi_3 \tag{20a}$$

$$[\phi_3, \phi_2] = i\phi_1 \tag{20b}$$

$$[\phi_1, \phi_3] = i\phi_2 \tag{20c}$$

Let us introduce the following quantities to characterize the eigenvalues of our operators:

$$j = \tfrac{1}{2}(n_A - n_B) \;\; ; \quad m = \tfrac{1}{2}(n_A + n_B)\,. \tag{21}$$

Now, we can see from Eq. (18) that $\mathcal{H}_0 = 2\hbar\omega\phi_0$ and $\mathcal{H}_1 = 2\hbar\gamma\phi_2$. Thus $\mathcal{H} = 2\hbar(\omega\phi_0 + \gamma\phi_2)$. Moreover, from Eqs. (19d) and (21), the eigenvalues of ϕ_3 are given by: $\frac{1}{2}(n_A + n_B + 1) = (m + \frac{1}{2})$. This means that if we can relate the eigenvalues and eigenstates of ϕ_2 to those of ϕ_3, we can obtain the spectrum of $\mathcal{H}$. This is true because the eigenvalues and eigenstates of ϕ_3 are now already known, and because ϕ_3 already commutes with ϕ_0.

To obtain such as basis, we consider the following identity via the Baker-Campbell-Hausdorff formula:

$$\begin{aligned} e^{\mu\phi_1}\phi_2 e^{-\mu\phi_1} &= \phi_2 + \mu[\phi_1, \phi_2] + \tfrac{1}{2!}[\phi_1, [\phi_1, \phi_2]] + \ldots \\ &= \phi_2 + \mu(i\phi_3) - \tfrac{1}{2!}\phi_2\mu^2 + \tfrac{(i)^3}{3!}\phi_3\mu^3 + \ldots \\ &= \phi_2 \cos\mu + i\phi_3 \sin\mu. \end{aligned} \tag{22}$$

If we choose μ so that $\cos\mu = 0$, i.e., $\mu = \pm\frac{\pi}{2}$, then we obtain the following relation:

$$e^{\pm\frac{\pi}{2}\phi_1}\phi_2 e^{\mp\frac{\pi}{2}\phi_1} = \pm i\phi_3. \tag{23}$$

Or, more usefully,

$$\phi_2 e^{\mp\frac{\pi}{2}\phi_1} = \pm i e^{\mp\frac{\pi}{2}\phi_1}\phi_3. \tag{24}$$

In order to proceed further, we need to work in a basis $|j, m\rangle$ where j and m are the good quantum numbers[2]. This is valid because j is an eigenvalue for ϕ_0, and m for ϕ_3. The arguments of the preceding sections require us to operate in a basis where both ϕ_0 and ϕ_3 are diagonal. Thus by choosing to operate on the eigenfunctions $|j, m\rangle$ of ϕ_3, we have,

$$\phi_2 e^{\mp\frac{\pi}{2}\phi_1}|j, m\rangle = \pm i(m + \tfrac{1}{2})e^{\mp\frac{\pi}{2}\phi_1}|j, m\rangle \tag{25}$$

Using the substitution $\Psi^{\pm}_{jm} = e^{\mp\frac{\pi}{2}\phi_1}|j, m\rangle$, we get the eigenvalue equation:

$$\phi_2\Psi^{\pm}_{jm} = \pm i(m + \tfrac{1}{2})\Psi^{\pm}_{jm} \tag{26}$$

Note that the Ψ's cannot be normalized in the usual way since they do not belong to the familiar Hilbert space, but they nevertheless function as simultaneous eigenstates for ϕ_0 and ϕ_2 since the two commute. The final step to obtaining the spectrum of $\mathcal{H}$ is to determine the values of m for a given value of j. This is done by following the same methods used for angular momentum. We define:

$$\phi_{\pm} = \phi_1 \mp \phi_3. \tag{27}$$

It is easy to see that:

$$[\phi_2, \phi_{\pm}] = \pm i\phi_{\pm}. \tag{28}$$

Thus the $\phi_{\pm}$ function as raising and lowering operators, just like the $J_{\pm}$ operators of angular momentum. Together with the $SU(1,1)$ Casimir identity $\phi_0^2 = \frac{1}{4} + \phi_3^2 - (\phi_1^2 + \phi_2^2)$, we can show that the highest/lowest value of m is given by $\pm|j|$. Since j increments by $\frac{1}{2}$ from the definition (Eq.(21)), we have $m = |j|, |j| + \frac{1}{2}, |j| + 1, \ldots$ so we can now think of writing the action of the Hamiltonian on the $\Psi^{\pm}_{jm}$ on the basis of Eqs. (21) and (26) as:

$$\begin{aligned} \mathcal{H}\Psi^{\pm}_{jm} &= 2\hbar\left(\omega\phi_0 + \gamma\phi_2\right)\Psi^{\pm}_{jm} \\ &= 2\hbar\left(\omega j \pm i\gamma(m + \tfrac{1}{2})\right)\Psi^{\pm}_{jm}. \end{aligned} \tag{29}$$

---

[1] Note the differences between these generators and those of the familiar $SU(2)$ Lie algebra of the Pauli spin matrices.

[2] We can readily go from $|j, m\rangle$ to $|n_A, n_B\rangle$ using Eq. (21).

Thus we now have the spectrum of the Bateman-Feshbach-Tikochinsky (BFT) oscillator given by:

$$H^{\pm}_{jm} \;=\; 2\hbar\omega j \;\pm\; i\hbar\gamma(2m+1);\; m = |j|, |j|+\frac{1}{2}, |j|+1, \ldots \tag{30}$$

with the eigenfunctions:

$$\begin{aligned}\Psi^{\pm}_{jm}(t) &= \exp[-\tfrac{iH^{\pm}_{jm}t}{\hbar}]\Psi^{\pm}_{jm} \\ &= e^{(-2i\omega jt \pm \gamma(2m+1)t \mp \frac{\pi}{2}\phi_1)}|j,m\rangle. \end{aligned}\tag{31}$$

Now, let us consider the special case $\gamma \to 0$, i.e., the quasi-free oscillator. In this case, we keep $n_B = 0$ and so $2j = 2m = n_A = n$. Then the spectrum is:

$$H^{\pm}_{n} = n\hbar\omega \pm i\gamma\hbar(n+1). \tag{32}$$

We should recognize this as a serious problem, since even in the limit of shutting down our virtual oscillator, we still have its term remaining in the spectrum. Since the mirror oscillator is only a mathematical construct to allow us the use of the Hamiltonian formalism, the only physical variable is x, for which we are missing the correct commutation relation ($[x, p] = i\hbar$). Nevertheless, we will persist for the moment with the Schrödinger-Hamilton formalism to obtain the dispersion relations for the BFT system, which will also bring into focus its principal flaw.

Let us now calculate the uncertainty relations for this system. Following the time-dependent Schrödinger equation, we have for an observable F:

$$i\hbar\frac{\partial\Psi}{\partial t} = H\Psi, \tag{33a}$$

$$\partial_t\langle F\rangle = -\frac{i}{\hbar}\,\langle[F,H]\rangle. \tag{33b}$$

Using the above equations and the expression Eq.(6) for the BFT Hamiltonian $\mathcal{H}$, we get the following relations:

$$\begin{aligned}\partial_t\langle x\rangle &= \frac{-i}{\hbar}\big\langle[x,\mathcal{H}]\big\rangle \\ &= \frac{-i}{\hbar}\big\langle[x, \not{p}\bar{\not{p}} - \gamma(x\not{p} - \bar{x}\bar{\not{p}}) + \omega^2 x\bar{x}]\big\rangle \\ &= \frac{-i}{\hbar}\big\langle[x,\not{p}]\bar{\not{p}} \;-\gamma x[x,\not{p}]\big\rangle \\ &= \langle\bar{\not{p}}\rangle - \gamma\langle x\rangle. \end{aligned}\tag{34a}$$

Similarly,

$$\partial_t\langle\bar{x}\rangle = \langle\not{p}\rangle - \gamma\langle\bar{x}\rangle, \tag{34b}$$

$$\partial_t\langle\not{p}\rangle = \gamma\langle\not{p}\rangle - \omega^2\langle\bar{x}\rangle, \tag{34c}$$

$$\partial_t\langle\bar{\not{p}}\rangle = \gamma\langle\not{p}\rangle - \omega^2\langle x\rangle. \tag{34d}$$

Using the time evolution relations for the second order operators, we have:

$$\partial_t\langle x^2\rangle = \frac{-i}{\hbar}\big\langle[x^2,\mathcal{H}]\big\rangle = -2\gamma\langle x^2\rangle + 2\langle x\bar{\not{p}}\rangle, \tag{35a}$$

$$\partial_t\langle\bar{\not{p}}^2\rangle = -2\gamma\langle\bar{\not{p}}^2\rangle - 2\omega^2\langle x\bar{\not{p}}\rangle, \tag{35b}$$

$$\partial_t\langle x\bar{\not{p}}\rangle = \langle\bar{\not{p}}^2\rangle - 2\gamma\langle x\bar{\not{p}}\rangle - \omega^2\langle x^2\rangle. \tag{35c}$$

To move ahead, we use the the definition of the variances:

$$\sigma_x^2 \equiv \sigma_{xx} = \langle x^2\rangle - \langle x\rangle^2, \tag{36a}$$

$$\sigma_{pp} = \langle p^2\rangle - \langle p\rangle^2, \tag{36b}$$

$$\sigma_{xp} = \langle xp\rangle - \langle x\rangle\langle p\rangle. \tag{36c}$$

Using these, we can obtain the rates of change in the variances as follows:

$$\begin{aligned}\partial_t\sigma_{xx} &= \partial_t\langle x^2\rangle - 2\langle x\rangle\partial_t\langle x\rangle \\ &= -2\gamma\langle x^2\rangle + 2\langle x\bar{\not{p}}\rangle - 2\langle x\rangle(\langle\bar{\not{p}}\rangle - \gamma\langle x\rangle) \\ &= 2\langle xp\rangle - 2\langle x\rangle\langle p\rangle \\ &= 2\sigma_{xp} \end{aligned}\tag{37a}$$

Similarly,

$$\partial_t\sigma_{pp} = -4\gamma\sigma_{pp} - 2\Omega^2\sigma_{xp} \tag{37b}$$

$$\partial_t\sigma_{xp} = \sigma_{pp} - 2\gamma\sigma_{xp} - \Omega^2\sigma_{xx} \tag{37c}$$

where we have used the expression Eq. (4b) for $\bar{\not{p}}$ in terms of p and the one for Ω^2. These equations can be solved using a computer algebra package. The resultant expressions are for the variances σ_{xx} and σ_{pp} are based on the assumptions that $\sigma_{xx}(0) = \hbar/2\Omega$ and $\dot{\sigma}_{xx}(0) = 0$:

$$\sigma_{xx}(t) = \frac{\hbar}{2\Omega}e^{-2\gamma t}\left[1 + \frac{\gamma}{\omega}\sin 2\omega t + 2\frac{\gamma^2}{\omega^2}\sin^2\omega t\right] \tag{38}$$

$$\sigma_{pp}(t) = \frac{\hbar\Omega}{2}e^{-2\gamma t}\left[1 - \frac{\gamma}{\omega}\sin 2\omega t + 2\frac{\gamma^2}{\omega^2}\sin^2\omega t\right] \tag{39}$$

Thus we see that:

$$\Delta x(t)\Delta p(t) = \sqrt{\sigma_{xx}(t)\sigma_{pp}(t)} \sim \mathcal{O}(e^{-2\gamma t}). \tag{40}$$

This the most fundamental flaw with the Feshbach-Tikochinsky picture, that the fundamental uncertainty product inevitably approaches zero, as long as $\gamma \neq 0$, now matter how small, and hence violates Heisenberg's uncertainty principle for the physical oscillator. This is the reason, this treatment cannot be the definitive answer to quantizing dissipative systems.

III. BOPP'S ALTERNATIVE TREATMENT OF THE BATEMAN SYSTEM

The Feshbach -Tikochinsky approach, however, is not the only path to the quantization of the Bateman system. Almost at the same time, Bopp [7] published another approach to this problem. In Bopp's method, a canonical transformation $\{x, \bar{x}, \not{p}, \bar{\not{p}} \leftrightarrow X, \bar{X}, P, \bar{P}\}$ is first applied to the Hamiltonian. We have the following ansatz:

$$\not{p} = \tfrac{1}{2}(P + \omega\bar{X} + i\bar{P} + i\omega X), \tag{41a}$$

$$\bar{\not{p}} = \tfrac{1}{2}(P + \omega\bar{X} - i\bar{P} - i\omega X), \tag{41b}$$

$$x = \tfrac{i}{2\omega}(P - \omega\bar{X} + i\bar{P} - i\omega X), \tag{41c}$$

$$\bar{x} = \tfrac{-i}{2\omega}(P - \omega\bar{X} - i\bar{P} + i\omega X). \tag{41d}$$

Substituting these equations into Eq. (6) yields a diagonal form in the new variables:

$$\mathcal{H}_B = \frac{1}{2}(1-\frac{i\gamma}{\omega})(P^2+\omega^2X^2)+\frac{1}{2}(1+\frac{i\gamma}{\omega})(\bar{P}^2+\omega^2\bar{X}^2). \tag{42}$$

Clearly Eq. (42) represents two oscillators, one being the physical reality (X, P) and the other is its dual $(\bar{X}, \bar{P})$(and which are manifestly uncoupled when $\gamma \to 0$). At this point we make a choice to introduce a change in variables:

$$a = \frac{1}{\sqrt{2\hbar\omega}}(P - i\omega X),\ \bar{a} = \frac{1}{\sqrt{2\hbar\omega}}(\bar{P} - i\omega\bar{X}), \tag{43a}$$

$$a^* = \frac{1}{\sqrt{2\hbar\omega}}(P + i\omega X),\ \bar{a}^* = \frac{1}{\sqrt{2\hbar\omega}}(\bar{P} + i\omega\bar{X}) \tag{43b}$$

Reversing these equations, we get:

$$P = \sqrt{\frac{\hbar\omega}{2}}(a + a^*),\ X = \sqrt{\frac{\hbar}{2\omega}}(a^* - a), \tag{44a}$$

$$\bar{P} = \sqrt{\frac{\hbar\omega}{2}}(\bar{a} + \bar{a}^*),\ \bar{X} = \sqrt{\frac{\hbar}{2\omega}}(\bar{a}^* - \bar{a}), \tag{44b}$$

Making this substitution in the expression for the Bopp Hamiltonian in Eq. (42), we get the expression,

$$\begin{aligned}\mathcal{H}_B &= \hbar\omega(a^*a + \bar{a}^*\bar{a}) - i\hbar\gamma(a^*a - \bar{a}^*\bar{a}) \\ &= (\hbar\omega - i\hbar\gamma)a^*a + (\hbar\omega + i\hbar\gamma)\bar{a}^*\bar{a}.\end{aligned} \tag{45}$$

and the Poisson brackets for this expression are given by:

$$\{a, a^*\} = i/\hbar, \quad \{\bar{a}, \bar{a}^*\} = i/\hbar. \tag{46}$$

We must now realize that in order to canonically quantize this system, the Poisson bracket is replaced by the commutator of the kind $\{a, a^*\} \to \frac{i}{\hbar}[a, a^\dagger]$. Thus we have:

$$[a, a^\dagger] = 1, \quad [\bar{a}, \bar{a}^\dagger] = 1. \tag{47}$$

But now that we are replacing the classical variables with their operator versions, we should replace:

$$a^*a \to \tfrac{1}{2}(a^\dagger a + aa^\dagger) = (a^\dagger a + \tfrac{1}{2}), \tag{48a}$$

$$\bar{a}^*\bar{a} \to \tfrac{1}{2}(\bar{a}^\dagger\bar{a} + \bar{a}\bar{a}^\dagger) = (\bar{a}^\dagger\bar{a} + \tfrac{1}{2}). \tag{48b}$$

Following this, the Hamiltonian assumes the form:

$$\begin{aligned}\mathcal{H}_B &= \left(\hbar\omega(a^\dagger a + \tfrac{1}{2}) - i\hbar\gamma a^\dagger a\right) \\ &\quad + \left(\hbar\omega(\bar{a}^\dagger\bar{a} + \tfrac{1}{2}) + i\hbar\gamma\bar{a}^\dagger\bar{a}\right), \\ &= \mathscr{H} + \mathscr{H}^*.\end{aligned} \tag{49}$$

The first observation is that we have now *separated* the Hamiltonian into two components: one for the physical oscillator and one for its dual, which we were not able to accomplish earlier. Recognizing that the physical oscillator is the only component of any significance, we shall now focus on this portion of the full Hamiltonian. This compromises the Hermiticity of the physical Hamiltonian, which is now given by

$$\mathscr{H} = \hbar(\omega - i\gamma)a^\dagger a + \tfrac{\hbar\omega}{2}. \tag{50}$$

which restores the known Hamiltonian when $\gamma \to 0$. However, we shall ignore this fact for the moment.s

The second thing we note is that although we have been using the Schrödinger formalism all along, it assumes the existence of a state space and vectors with conserved norm. This is not entirely true in the case of dissipative systems, where a non-Hermitian Hamiltonian implies a time varying norm. The correct approach then, is to adopt the language of density operators, but still making use of notions such as expectation values of operators i.e., $\langle F\rangle = \langle\ |F|\ \rangle/\langle\ |\ \rangle$. We shall therefore introduce a density operator $w = |\psi\rangle\langle\psi|$ where $|\psi\rangle$ are the state vectors on the space where $\mathscr{H}$ is defined. Following the time dependent Schrödinger equation, we have:

$$i\hbar\dot{w} = i\hbar(|\psi\rangle\langle\psi|) = \mathscr{H}w - w\mathscr{H}^\dagger. \tag{51}$$

If we now use w in the number representation, then we may state (using the resolution of the identity twice):

$$w = \sum_{n,m}|n\rangle\langle n|w|m\rangle\langle m| = \sum_{n,m}|n\rangle w_{nm}\langle m|. \tag{52}$$

Using the fact that $\mathscr{H}|n\rangle = n\hbar(\omega - i\gamma)|n\rangle$, and using Eq. (51), we get,

$$\dot{w}_{nm} = -i\omega(n-m)w_{nm} - \gamma(n+m)w_{nm}. \tag{53}$$

where we notice that a)$\{w_{nm}\}$ has a decaying trace, and b) the diagonal and off diagonal elements do not mix as they evolve. Thus $w_{nm}(t)$ can be written as

$$w_{nm}(t) = \rho_{nm}(0)e^{[-i\omega(n-m)-\gamma(n+m)]t}. \tag{54}$$

where,

$$\rho_{mn}(t) = w_{mn}(t)/\mathrm{Tr}(w(t)). \tag{55}$$

is the properly defined density matrix, ensuring that $\mathrm{Tr}(\rho(t)) = 1$, such that $\langle F\rangle = \mathrm{Tr}(\rho F)$. The only problem with this is that we are given w_{nm} and not ρ_{nm}. Thus ironically, the precise indication of the system's initial state, i.e., $\rho_{nm}(0)$ is required to move forward with the steady state solution.

This brings us to our final observation. Having begun with a classically dissipative system, we must pay due attention to the classical initial conditions in light of Ehrenfest's theorem. Stationary states certainly do not behave very classically, (we can readily see that $\langle P\rangle = 0$ since $\langle a\rangle = \langle a^\dagger\rangle = 0$), so we must choose states that show behavior closest to classical solutions to the equations of motion. These, of course, are the coherent states $|\alpha\rangle$, with the property that if a is the annihilation operator, then $a|\alpha\rangle = \alpha|\alpha\rangle$, where $\alpha \in \mathbb{C}$. We, also know from quantum mechanics texts that these states form an over-complete set with the following properties:

$$\frac{1}{\pi}\int |\alpha\rangle\langle\alpha|\; d^2\alpha = 1, \tag{56}$$

$$|\alpha\rangle = e^{-\frac{1}{2}|\alpha|^2}\sum_{n=0}^{\infty}\frac{\alpha^n}{\sqrt{n}}|n\rangle, \tag{57}$$

and,

$$|\langle\alpha|\beta\rangle| = \exp\left(-\tfrac{1}{2}|\alpha-\beta|^2\right). \tag{58}$$

where $d^2\alpha = d\Re(\alpha)\,d\Im(\alpha)$ and the integration is performed over the entire complex α-plane. Then, in analogy to Eq. (52), we may define a density operator ρ in the coherent state representation[3]:

$$\rho \;=\; \int P(\alpha)|\alpha\rangle\langle\alpha|\; d^2\alpha. \tag{59}$$

If at time $t=0$, the oscillator is prepared in a pure coherent state $|\alpha_0\rangle$, then we have $P(\alpha) = \delta(\alpha-\alpha_0)\delta(\alpha^*-\alpha_0^*)$ and so $\rho^{(0)}(0) = |\alpha_0\rangle\langle\alpha_0|$. Substituting into Eq. (57), we obtain as the matrix elements of $\rho(0)$:

$$\rho^{(0)}_{nm}(0) \;=\; \exp\left(-|\alpha_0|^2\right)\alpha_0^n\alpha_0^{*m}/\sqrt{n!\,m!}. \tag{60}$$

Now using the fact that $w_{nm}(0) = \rho_n m(0)$, and substituting into Eq. (54):

$$w_{nm}(t) = e^{-|\alpha_0|^2}\,\frac{\alpha_0^n\alpha_0^{*m}}{\sqrt{n!\,m!}}\,e^{\left(-i\omega(n-m)t-\gamma(n+m)t\right)}. \tag{61}$$

Now we take the trace:

$$\begin{aligned}\mathrm{Tr}(w(t)) \;&=\; \sum_{n,m} w_{nm}(t)\,\delta_{n,m}\\ &=\; \sum_{n} e^{-|\alpha_0|^2}\,\frac{|\alpha_0|^{2n}}{n!}\,e^{-2n\gamma t}\\ &=\; e^{-|\alpha_0|^2(1-\exp(-2\gamma t))}.\end{aligned} \tag{62}$$

And using the definition Eq. (55) of $\rho_{nm}(t)$, we have:

$$\rho^{(0)}_{mn}(t) = \frac{\alpha_0^n\alpha_0^{*m}}{\sqrt{n!\,m!}}\,e^{\left(-|\alpha_0|^2\exp(-2\gamma t)-i\omega(n-m)t-\gamma(n+m)t\right)}. \tag{63}$$

We can now substitute this equation in the general definition of ρ_{nm}:

$$\rho_{nm} \;=\; \int P(\alpha_0)\,\rho^{(0)}_{nm}(t)\,d^2\alpha_0 \tag{64}$$

We should state here that we have used rather specific initial conditions, namely the damped pure coherent state, but in this report we restrict ourselves to cases where Ehrenfest's quantum-classical correspondence is manifest for all γ (including $\gamma=0$) and any arbitrary $X(0)$ and $P(0)$. It is also possible to maintain the correspondence by averaging over α_0 in Eq. (63), but this aspect is beyond the scope of this report, as it brings into question the applicability of Schrödinger's equation to this problem. We are now in a position to calculate the expectation values of the operators:

$$\begin{aligned}\langle a\rangle \;&=\; \mathrm{Tr}(\rho a) = \sum_{n.m}\langle n|\rho|m\rangle\;\overbrace{\langle m|a|n\rangle}^{\sqrt{n}\,\delta_{m,n-1}}\\ &=\; \langle\alpha_0\rangle\; e^{-i\omega t-\gamma t}.\end{aligned} \tag{65}$$

Similarly,

$$\langle a^2\rangle \;=\; \langle\alpha_0^2\rangle\; e^{-2i\omega t-2\gamma t}, \quad \text{and,} \tag{66}$$

$$\sigma_{aa} \;=\; \langle a^2\rangle - \langle a\rangle^2 = \sigma_{aa}(0)\; e^{-2i\omega t-2\gamma t}, \tag{67a}$$

$$\sigma_{a^\dagger a^\dagger} \;=\; \sigma_{a^\dagger a^\dagger}(0)\; e^{2i\omega t-2\gamma t}, \tag{67b}$$

$$\sigma_{a^\dagger a} \;=\; \sigma_{a^\dagger a}(0)\; e^{-2\gamma t}, \tag{67c}$$

$$\sigma_{aa^\dagger} \;=\; \sigma_{aa^\dagger}(0)\; e^{-2\gamma t} + (1-e^{-2\gamma t}). \tag{67d}$$

Now using the definitions of X and P using Eqs.(44a), (44b) and the commutation relations, we get for the initial ground state uncertainty:

$$\sigma_{aa}(0) \;=\; \frac{\gamma(\gamma-i\omega)}{2\Omega},\; \sigma_{a^\dagger a^\dagger}(0) \;=\; \frac{\gamma(\gamma+i\omega)}{2\Omega}, \tag{68}$$

$$\sigma_{a^\dagger a}(0) \;=\; \Omega/2\omega - \tfrac{1}{2},\; \sigma_{aa^\dagger}(0) \;=\; \Omega/2\omega + \tfrac{1}{2}. \tag{69}$$

Furthermore from the definitions of a and $a^\dagger$, i.e., Eq. (44a),

$$\begin{aligned}\sigma_{XX} &= \frac{-\hbar}{2\omega}\left[\sigma_{aa} - (\sigma_{aa^\dagger}+\sigma_{a^\dagger a}) + \sigma_{a^\dagger a^\dagger}\right], \\ \sigma_{PP} &= \frac{-\hbar}{2\omega}[(\omega-i\gamma)^2\sigma_{aa}\\ &\quad -\Omega^2(\sigma_{aa^\dagger}+\sigma_{a^\dagger a}) + (\omega+i\gamma)^2\sigma_{a^\dagger a^\dagger}].\end{aligned} \tag{70}$$

This leads to our final expressions for the variances (or squared uncertainties):

$$\begin{aligned}\sigma_{XX}(t) &= \frac{\hbar}{2\Omega}e^{-2\gamma t}\left[1+\frac{\gamma}{\omega}\sin 2\omega t + 2\frac{\gamma^2}{\omega^2}\sin^2\omega t\right]\\ &\quad + \frac{\hbar}{2\omega}(1-e^{-2\gamma t}),\end{aligned} \tag{71}$$

$$\begin{aligned}\sigma_{PP}(t) &= \frac{\hbar\Omega}{2}e^{-2\gamma t}\left[1-\frac{\gamma}{\omega}\sin 2\omega t + 2\frac{\gamma^2}{\omega^2}\sin^2\omega t\right]\\ &\quad + \frac{\hbar\Omega^2}{2\omega}(1-e^{-2\gamma t}).\end{aligned} \tag{72}$$

---

[3] The $P(\alpha)$ is often called a *quasi*-probability distribution since it can in general take negative values.

Thus we have $\sigma_{XX} \cdot \sigma_{PP} \geqslant 0$ for all t and γ. Thus by imposing the correct commutator algebra, we have reinstated Heisenberg's principle. However, in the process of separating the physical system from its adjoint and working within Schrödinger's state vector formalism, we have glossed over a few subtleties.

IV. CONCLUSION

In this report, we have analyzed the simplest dissipative system, namely the damped linear harmonic oscillator, and attempted to quantize it analogously to its undamped version. A quasi-2D classical model was proposed as per Bateman, and later treated quantum mechanically by Feshbach and Tikochinsky. The dissipative physical oscillator was mirrored by a dual oscillator which allowed for mathematical dexterity and allowed the use of the Hamiltonian formalism by making the total system energy conserving. The naïve canonical quantization of the system yielded a vanishing commutator in the physical oscillator's dynamical variables, leading to a violation of Heisenberg's uncertainty principle. We cannot let this fact be obscured by a sophisticated treatment of the Hamiltonian and its spectrum.

As it turns out, the true solution to the dissipative oscillator problem lies in relaxing the requirement of a pure state vector framework and allowing mixed states represented by a density operator from the outset. The environment is treated as bath with infinite degrees of freedom. Furthermore, the phase space representation is done explicitly for the dual system, and the mirror variables are then eliminated by integrating over their classical phase space *before* quantizing the system. The resulting dynamical equations are identical with those from Bopp's treatment [4], but this is beyond the scope of the present report.

ACKNOWLEDGMENTS

Support of the MIT library system and its electronic and physical resources is gratefully acknowledged.

---

[1] D. Halliday, R. Resnick, and J. Walker, *Fundamentals of Physics, 9th ed.* John Wiley and Sons, Inc., 2003.

[2] D. J. Griffiths, *Introduction to Quantum Mechanics.* Cambridge University Press, 2018.

[3] D. Chruściński and J. Jurkowski, "Quantum damped oscillator i: dissipation and resonances," *arXiv:quant-ph/0506007* **1** (2005) .

[4] H. Dekker, "Classical and quantum mechanics of the damped harmonic oscillator," *Phys. Rep.* **80** (1981) no. 1, 1–112.

[5] H. Bateman, "On dissipative systems and related variational principles," *Phys. Rev.* **38** (1931) no. 4, 815.

[6] H. Feshbach and Y. Tikochinsky, "Quantization of the damped harmonic oscillator," in *A Fetschrift for I.I. Rabi*, vol. 38, pp. 44–53. Trans. New York Ac. Sc. ser 2, 1977.

[7] F. Bopp, "Quantisierung des gedämpften harmonischen oszillators," 1974. `http://publikationen.badw.de/de/003384331`.

[8] L. Biedernharn, J. Nuyts, and N. Straumann, "On the unitary representations of su(1,1) and su(2,1)," *Ann. Inst. Henri Poincaré* **3** (1965) no. 1, 13–39.

Quantum Nature of Classical Information

Vishal Johnson

(Dated: June 19, 2019)

Properties such as entanglement and superposition are generally considered distinctly quantum. This paper attempts to demonstrate situations in which classical information systems show such properties. The paper starts with a brief introduction to the qubit and some of its properties. A quantum mechanical description of classical information, using qubits, is then developed wherein parallels between classical information and quantum states is drawn. This description is used to demonstrate how some classical systems show quantum behaviour. Finally, the popular chinese whisper game is analysed using perturbation theory. The paper concludes with a discussion on the classical limit of quantum information.

At length and time scales that correspond to common human experience, intuition is guided by classical physics[1]. This is because classical physics successfully explains most of the phenomena experienced at these scales, albeit with some arbitrary underlying assumptions. This shall henceforth be referred to as the *classical domain.* On the other hand, at length and time scales corresponding to atoms and nuclei, quantum theory successfully explains most of the phenomena, with some arbitrary underlying assumptions nonetheless, and this shall be referred to as the *quantum domain.* Classical behaviour sometimes seems to violate the principles of quantum mechanics, the paper starts with an attempt to explain these differences. On the other hand, quite surprisingly, some classical behaviour still possess quantum mechanical nuances and this shall be discussed next. The perspective of information is adopted.

I. INTRODUCTION TO THE QUBIT

Common sense dictates ideal classical information systems to possess certain properties. A few of the obvious ones are listed below.

- Objectivity: Inspired by [1], objectivity is the property by which different measurements of the classical information yields consistent results[2]. Consistency could be over different observers or over different times.
- Fixed Basis: Measurements of classical information yield results that are distinct, are mutually exclusive and belong to fixed categories. There exists nothing between a and b; this property is related to discreteness given below.
- Discreteness: While this is a property that is neither unique to nor possessed by all classical systems, most encodings of classical information is inherently discrete. A discrete alphabet is used to encode the information.

Many quantum information systems are also discrete, in that the basis states form a countable set. But they differ from classical information systems in the other two aspects. Firstly, different observers may obtain different outcomes. This happens, for example, if the quantum state is a superposition state. In this case, each basis state only has a certain probability of being observed. It is not possible to predict the outcome a priori. Because of this, objectivity is lost. There cannot be a consensus on the basis state that the system is in[3]. There is another way in which these quantum states may be inconsistently measured; and that corresponds to a "rotation" of the measuring apparatus. The measurement could be done in a different basis and that would affect the result; this again is non-classical.

Consider the example of a one dimensional quantum harmonic oscillator[3, p. 283][4]. The hamiltonian of the oscillator is:

$$H = \frac{p^2}{2m} + \frac{1}{2}m\omega^2x^2, \text{ with solutions,} \tag{1a}$$

$$\psi_0(x), \psi_1(x), \psi_2(x)..., \text{ satisfying,} \tag{1b}$$

$$-\frac{\hbar^2}{2m}\frac{\mathrm{d}^2\psi_n(x)}{\mathrm{d}x^2} + \frac{1}{2}m\omega^2x^2\psi_n(x) = E_n\psi_n(x). \tag{1c}$$

The $\psi's$ form the energy eigenstates of the system. Choosing any two states of the system, $\psi_0(x)$ and $\psi_1(x)$

---

[1] Classical physics referring to newtonian mechanics, classical thermodynamics, classical electromagnetism and so on. In this paper, relativistic effects are ignored in both, the classical and quantum domains.

[2] This is not to say that the same results would be obtained each time. In case one measures the *classical position* of a particle, one might get a different position at different points in time. However, the positions would be consistent with the velocity of the particle. That is what is meant by consistent.

[3] In this case, it is assumed that the quantum information system is a machine that consistently produces arbitrarily many instances of a certain general *quantum* state. It is possible to probe the state using techniques such as weak measurement and then obtain the state as a superposition[2]. The point here is to see that the behaviour differs from that of classical information.

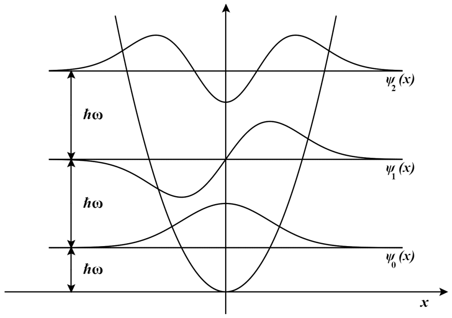

Figure 1. The Harmonic oscillator potential and wavefunctions.

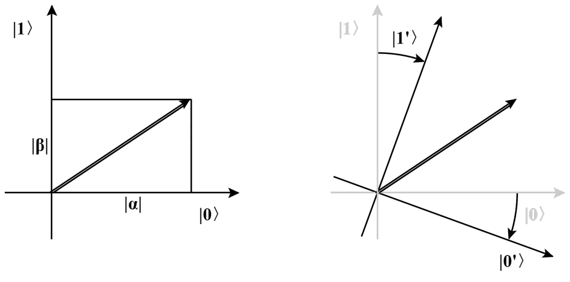

(a). Some basis.

(b). A rotated basis.

Figure 2. (a) Measurement in a basis. (b) Rotating the apparatus of measurement.

for convenience, and restricting the system to stay in these states, one gets a qubit. It is much more convenient to express these wavefunctions in the dirac notation and this shall be used henceforth. The states are thus,

$$\begin{aligned} |0\rangle &= \psi_0(x), \text{ and,} \\ |1\rangle &= \psi_1(x). \end{aligned} \tag{2}$$

These states differ from classical information basis states as they can be in a superposition state,

$$|\psi\rangle = \alpha\,|0\rangle + \beta\,|1\rangle\,. \tag{3}$$

If an observer were to measure the state $|\psi\rangle$, they obtain state $|0\rangle$ with a probability of $|\alpha|^2$ and state $|1\rangle$ with a probability of $|\beta|^2$. It is possible that two observers measure something different given the same quantum state and, thus, measurement is not consistent[4]. Finally, the states can be measured by "rotating" the apparatus and this introduces further subtleties, see figure 2.

II. A QUANTUM DESCRIPTION OF CLASSICAL INFORMATION

If quantum mechanics is the correct description of matter, classical behaviour should be obtained as a limit of the quantum. However, as classical behaviour differs significantly from the quantum it is not obvious how the limit is obtained. This section attempts to use qubits to build a classical state; ad-hoc conditions are imposed on the qubits in order for classical behaviour to emerge. It further explores these ideas in the purview of quantum decoherence and einselection [5].

Classical behaviour is characterised by highly consistent, highly repeatable measurement outcomes. An attempt is made to obtain these classical states from qubits. An arbitrary qubit is represented in a state such as,

$$|\psi\rangle = \alpha\,|0\rangle + \beta\,|1\rangle\,. \tag{4}$$

Here, $|0\rangle$ and $|1\rangle$ represent the basis states that the qubit is measured against. The basis states represent something physical such as the direction of magnetic field or the splitting of beams in an interferometer apparatus and are necessary while physically describing the qubit. As many quantum systems are infinite dimensional and also contain a large number of particles it would be impossibly cumbersome to describe them in the physical basis. In order to describe classical states it makes more sense to talk about a "logical" basis. The logical states encode whether or not the qubit is rotated in the correct direction with respect to obtaining the classical measurement outcomes[5].

This is best described using an example. Consider a tiny patch of paper in a book, on which is written 'a'. In this case the molecules of ink and the molecules of the paper form the physical part of the classical system. The letter 'a' is recognised by looking at those points in which the molecules of ink are absorbed and hence the positions of all the ink molecules, in the patch of paper, could be considered as the state space of the system. If one looks at a particular molecule of ink, only certain positions within the lattice of paper molecules would correspond to consistent representations of 'a'. Even though the Hilbert space is not two dimensional in this case, one could divide it into positions corresponding to consistent representations and those not. In this way, the state-space could be divided into,

$$|0_L\rangle \leftrightarrow \text{states(locations) corresponding to 'a'} \tag{5a}$$

$$\left|\overline{0}_L\right\rangle \leftrightarrow \text{states(locations) not corresponding to 'a'} \tag{5b}$$

---

[4] It is again emphasised that the quantum information system does not produce just one instance of the state but rather produces arbitrarily many instances. In this sense, the quantum information produces the *quantum states* consistently, but that does not imply that the measured results would be consistent.

[5] See, for example [3, p. 283] cited before. In this case the article goes on further do describe the logical states $|00_L\rangle$, $|01_L\rangle$, $|10_L\rangle$ and $|11_L\rangle$. These states are logical states in that they encode what values the qubit logically refer to, irrespective of their particular physical characteristics

Thus, each molecule of ink is in a state such as,

$$|\psi_L\rangle = \alpha\,|0_L\rangle + \beta\,|\bar{0}_L.\rangle \tag{6}$$

This discussion was for one instance of a representation of 'a'. In fact the logical state would remain unaltered if the entire text were shifted slightly to the left or to the right or if it were slightly expanded or contracted. Thus, there are many physical configurations that lead to a consistent logical state. This is one factor that adds to the resilience of classical states. In order to carry forward this discussion it is assumed that there exists the ideal 'a' whose physical state perfectly captures the essence of 'a'ness. The logical basis of the ideal 'a' is then used to describe any other instance. The $|0_L\rangle$ and $|\bar{0}_L\rangle$ refer to these basis states. Any instance of 'a' is not simply $|0_L\rangle^{\otimes N}$ but is a more complicated state, it would look like a mixed state with a certain probability distribution over states close to the ideal 'a'.

Before the 'a' is written, the molecules of paper and the molecules of ink are in a random, uncoordinated state. It is then written down and a coordinated 'a' state is formed; the interaction with the environment occurs when the state is being written. One could ask what caused the 'a' to exist in the first place, or why it it written the way it is. The 'a' written on a patch of paper is not a stand-alone system, its formation and existence is shared with every other 'a', and with several other interacting systems. There is a certain component of 'a'ness in any of its written instances. This is inevitably linked to the environment, it is in the writing of the 'a' that there is an interaction in the environment and where the component of 'a'ness gets infused in it. One could thus be write the state of the 'a' as,

$$\left|\psi_{'a'}\right\rangle = \left|\psi_{'a'}\right\rangle_P \otimes \left|\psi_{'a'}\right\rangle_L, \tag{7}$$

where the $|\psi_{'a'}\rangle_P$ corresponds to the physical part of the 'a', where the molecules are placed and so on, as discussed in a prededing paragraph, and the $|\psi_{'a'}\rangle_L$ corresponds to the logical part, that is guided by the interaction with the environment. The composite state $|\psi_{'a'}\rangle$ is intimately connected to both and the two subsystems are indispensable for the whole state. While the state of the $|\psi\rangle_P$ could be a mixed state; it is assumed that in the enlarged Hilbert space that it lives, $|\psi\rangle_{'a'}$ is indeed a pure state. The state $|\psi_{'a'}\rangle$ could thus be a superposition of many states of varying distance from the ideal 'a' state[6]. It is proposed that the composite state would look like a gaussian curve in the enlarged Hilbert space, figure 3. The motivation is that the errors tend to be normally distributed; a justification of this is provided in section IV.

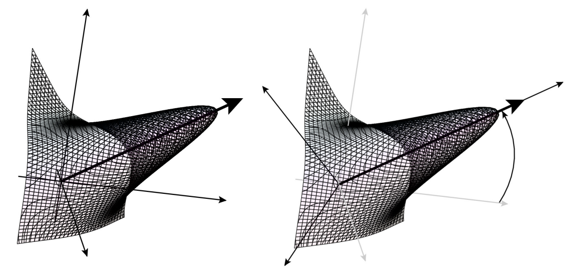
(a). "classical" state in a physical basis.
(b). Rotating the basis to measure the state.

Figure 3. (a) Physical states making up the basis. The *classical* state pointing somewhere in the state space. (b) Rotating the basis to point along the classical state.

The interaction with the environment stays on even after the 'a' is written;, the environment continues to influence the logical state of the system, this is discussed later. Not only does the environment guide the formation of the state but so also does it guide its measurement. Any observer wishing to *read* the 'a' is guided by the environment in doing so. In a sense, the axes of measurement are *rotated* to correspond to the logical basis, figure 3(b).

To be more specific about the interaction with the environment it is assumed that there exists an 'a' gas; the part of the environment that influences the 'a' systems. This 'a' gas has an existence extended over the earth in space and over centuries in time. It is a sort of memetic state that tries to keep repeating itself. There is competition between the different versions of the 'a' and there is a quantum darwinism that einselects the states more suitable to the environment[1]. If in no other way, the 'a' state at least influences the environment in adding itself to the 'a' gas; thus, not only does the environment influence the 'a' state but so also does the 'a' system influence the environment[7].

$$\begin{aligned}(|\phi\rangle_P \otimes |\phi'\rangle_L) \otimes \left|\psi_{'a'}\right\rangle_{env} \rightarrow \\ (\left|\psi_{'a'}\right\rangle_P \otimes \left|\psi_{'a'}\right\rangle_L) \otimes \left|\psi'_{'a'}\right\rangle_{env}.\end{aligned} \tag{9}$$

Here the $|\phi\rangle$ represent random, uncoordinated states. And $|.\rangle_{env}$ represents the 'a' gas of the environment. There is similarly, a 'b' gas and a 'c' gas so on. These gases are governed by grammar and morphology[6], much like the 'a' gas guides the physical state of a written instance. These form even larger states that interact with the letter gases, they are grammar states and word states; only certain strings of letters make sense and only certain combinations of words make sense. These states in turn guided by meaning states and beauty states and so on.

---

[6] The ideal 'a' state here includes the physical and logical parts.

[7] This could also explain the ability of classical states to be copied,

$$\left|\psi_{'a'}\right\rangle \otimes |\psi_u\rangle \otimes |\phi_e\rangle \rightarrow \left|\psi_{'a'}\right\rangle \otimes \left|\psi_{'a'}\right\rangle \otimes |\phi'_e\rangle \tag{8}$$

Here, $\left|\psi_{'a'}\right\rangle$ is the classical 'a' states, $|\psi_u\rangle$ is an uncoordinated random state and $|\phi\rangle$ are environment states. The environment enables copying.

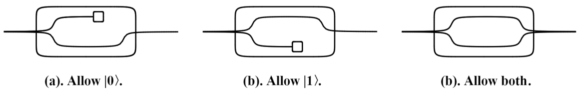

(a). Allow |0⟩.

(b). Allow |1⟩.

(b). Allow both.

Figure 4. Schematic Stern-Gerlach apparatus. (a) Apparatus turned to only allow $|0\rangle$ states (b) Apparatus turned to allow only $|1\rangle$ states (a) Apparatus turned to allow all states.

There is a hierarchy in which the higher states guide the lower states.

In order to continue the discussion to classical systems that show quantum effects it would be helpful to declare a few quantum states that will be used. For our discussion it is enough to stick to the morpheme level. A morpheme is the minimum unit of meaning[6, p. 40]; for the purpose of the paper it could be described as a state that conveys something definitive. Some examples of morphemes are $|motorola\rangle$, $|milk\rangle$ and $|breakfast\rangle$. These all have specific meanings and the state codifies the specific meaning that these morphemes carry. Some other examples could be $|count\rangle$ and $|key\rangle$. But these morphemes are under specified. *count* could have multiple meanings and so could *key*, that is they have the same physical state but different logical states. How does one decide what meaning to use? The meaning usually becomes clear through context. If one wrote, "The count of monte cristo", the text takes on that value of $|count\rangle$. If on the other hand one wrote, "I lost count of the cards", the text takes on a different $|count\rangle$ value. The surrounding words cause the collapse to a particular $|count\rangle$ state! This is one of the ways in which the environment continues to influence a written state once it is written.

One could be a lot more specific while writing down the states. The notation $|count\rangle_{''count''}$ is used in place of the previous $|''count''\rangle_P \otimes |count\rangle_L$[8]. It refers to the specific $|count\rangle$ state that a particular written instance, *"count"* takes on. Thus, $|\psi\rangle_{''count''}$ collapses to a particular $|count\rangle$ state when surrounded by extra information. If, for example,

$$|0\rangle \leftrightarrow \text{count of monte cristo} \tag{10a}$$

$$|1\rangle \leftrightarrow \text{count of cards,} \tag{10b}$$

then, $|0\rangle_{''count''}$ refers to "count" as in "count of monte cristo" and $|1\rangle_{''count''}$ refers to "count" as in "the count of cards". "count" here might refer not just to a written state but also a spoken state, a digital copy or any other physical representation[9].

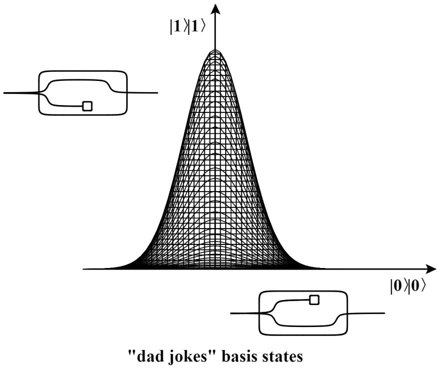

Figure 5. The states corresponding to "dad jokes" and the Stern Gerlach apparatus used to measure them.

It is interesting to look at the rotations guided by the higher order language states. In order to motivate this, it is assumed that the collapse of a state happens because of a Stern-Gerlach apparatus[7]. With respect to our example, the environment is acting as a Stern-Gerlach apparatus, guiding the axes as well as the specific value that the state collapses to. Figure 4 clarifies the issue.

III. QUANTUM BEHAVIOUR OF CLASSICAL INFORMATION SYSTEMS

It is hard to see quantum behaviour in the *classical states.* These states are *too classical* to behave quantumly. One must rather look at higher order language states such as grammar and meaning to get a clear picture of the quantum behaviour. This shall be demonstrated using an example.

Consider the phrase, "dad jokes". It could be interpreted in at least two different ways,

"dad jokes" - As in the noun "dad-jokes", the kinds of jokes dads tend to make. In this case "dad" is an adjective-noun and "jokes" is a noun. They are both half the noun "dad jokes". This could be denoted as state $|0\rangle$.

"dad jokes" - As in the noun - verb "dad jokes", the statement that dad makes jokes. In this case, "dad" is a noun and "jokes" is a verb. This could be denoted as state $|1\rangle$.

$|0\rangle$ and $|1\rangle$ are morpheme states. They are not exact quantum states but rather codify the *classical* states and guide their interpretation. They could be seen as the logical qubits for the *classical* states. Let the state space be restricted to the two morpheme states, see figure 5. In that case, the phrase "dad jokes" could correspondingly

---

[8] The single quotation marks used for 'a' were to make it stand out. Here the double quotation marks used for "count" represent a written instance of the system, in other words the physical part of the composite system.

[9] Observe how the morpheme states dictate the axes used to measure the "count" *classical* states. Higher order states like morphemes dictate the rotations of lower order *classical*, physical, states. The morpheme states are themselves dictated by even higher order language states such as spelling and grammar and meaning.

be in two different states,

$$|\psi\rangle_{''dad\ jokes''} = |0\rangle_{''dad''} \otimes |0\rangle_{''jokes''}\ , \text{ or,} \tag{11a}$$

$$|\psi\rangle_{''dad\ jokes''} = |1\rangle_{''dad''} \otimes |1\rangle_{''jokes''} \tag{11b}$$

When there is a source of ”dad jokes” phrases it is always assumed to be in one of the two morpheme states. The question is whether the state of such a phrase is a superposition state or a mixture state a prioi. It is clear that a state such as $|\psi\rangle_{''dad\ jokes'',P}$, the physical representation of the information such as an instantiation on a piece of paper, is a classical state and thus a measurement would not change its state. On the other hand it is not clear whether the morpheme states, that is the logical states behave classically or quantumly. Beginning with a classical assumption, it is proposed that the state is in a mixture state such as,

$$|\psi\rangle_{''dad\ jokes''} = \begin{cases} |0\rangle_{''dad''} \otimes |0\rangle_{''jokes''}\ , & \text{probability p} \\ |1\rangle_{''dad''} \otimes |1\rangle_{''jokes''}\ , & \text{probability 1-p.} \end{cases} \tag{12}$$

This means that the state is along the basis, it only takes on either $|0\rangle_{''dad''} \otimes |0\rangle_{''jokes''}$ or $|1\rangle_{''dad''} \otimes |1\rangle_{''jokes''}$. And thus, when the phrase is given some context, the meaning becomes immediately apparent.

When one says,

”I love telling dad jokes.”

the state collapses[10] to $|0\rangle_{''dad''} \otimes |0\rangle_{''jokes''}$. This could be interpreted as a restriction of the measurement space to only one of the alternatives, see figure 6. So far, so good. If however, one proceeds to read further and comes across,

”I love telling dad jokes. He especially likes knock knock jokes”,

one is forced to choose the other alternative, $|1\rangle_{''dad''} \otimes |1\rangle_{''jokes''}$. If the state was in a mixture state and was restricted to only one alternative, it does not make sense to change that alternative later. It does not even make sense from a classical information perspective because in that case it seems to violate the objectivity conditions[11]!

To make matters worse, the sentence could further read,

”I love telling dad jokes. He especially likes knock knock jokes, but Matt enjoys the occasional dad joke too.”.

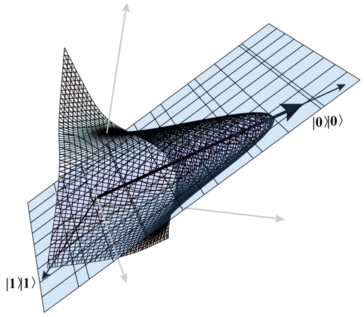

Figure 6. ”Collapse” of a classical state.

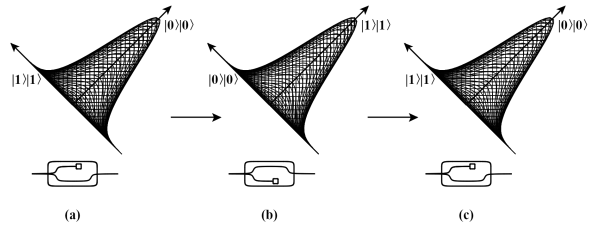

Figure 7. Rotation of the morpheme measurement axes to correspond to the classical state.

Now the state is back to being $|0\rangle_{''dad''} \otimes |0\rangle_{''jokes''}$! It must, thus, be that the morpheme state is in a superposition state of $|0\rangle_{''dad''} \otimes |0\rangle_{''jokes''}$ and $|1\rangle_{''dad''} \otimes |1\rangle_{''jokes''}$. A physical *classical* state, such as ”dad jokes” written on a piece of paper is unlikely to undergo such a change. This is because the states are too classical, they are very well designed. But even if the state was in a superposition such as $\alpha\,|0\rangle_{''dad''} \otimes |0\rangle_{''jokes''} + \beta\,|1\rangle_{''dad''} \otimes |1\rangle_{''jokes''}$, that does not answer the question. Once the state has settled to one of the basis states, it cannot turn into the other. If instead, one imagines the morpheme axes to turn to correspond to the *classical* state, it does not violate any of our requirements. The classical state remains unaffected by the rotation of the axes and the state can still be said to collapse to the required morpheme state. Thus, measurements in these systems correspond to rotations of the axes of measurement, see figures 6 and 7. Not only are classical states affected by morpheme states but so are morpheme state affected by classical states! Linear algebra saves the picture once again. All of this could be done with classical mechanics, what role does quantum mechanics play in this interaction?

One might wonder, could the morpheme ever be in a state such as $|0\rangle_{''dad''} \otimes |1\rangle_{''jokes''}$? Again, the environment does not allow that! It does not make sense to form a phrase out of a half noun and a verb! One could say that the axes cannot rotate in that direction, the environment prevents it. This is reminiscent of an entangled state[3, p. 95] $\alpha\,|0\rangle \otimes |0\rangle + \beta\,|1\rangle \otimes |1\rangle$. The state of any one of the morpheme fixes the state of the other.

Now consider, the set of statements,

”I love telling dad jokes!

---

[10] Of course as a classical state it must have always been in that state.

[11] One might say that the state was always in a consistent state and not fully revealed when the sentence was only partially read. Well, it might be that the page is torn off after that phrase and so somebody may not get to read the complete sentence. In that case they would be *stuck* with the incomplete, apparently wrong collapse of the state!

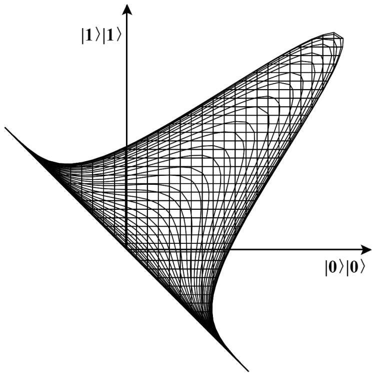

Figure 8. Rotation of the morpheme measurement axes by $\frac{\pi}{4}$

Figure 9. True or False?

He doesn't enjoy them so much though."

In what state is the "dad jokes" phrase now? Neither is it in the state $|0\rangle_{\text{"}dad\text{"}} \otimes |0\rangle_{\text{"}jokes\text{"}}$ nor is it in the state $|1\rangle_{\text{"}dad\text{"}} \otimes |1\rangle_{\text{"}jokes\text{"}}$. It seems to be in the state $\frac{1}{\sqrt{2}}|0\rangle_{\text{"}dad\text{"}} \otimes |0\rangle_{\text{"}jokes\text{"}} + \frac{1}{\sqrt{2}}|0\rangle_{\text{"}dad\text{"}} \otimes |0\rangle_{\text{"}jokes\text{"}}$! A superposition of morpheme states. The joke only makes sense if both morpheme meanings can simultaneously be realised. The axes have been turned by $\frac{\pi}{4}$! See figure 8.

Humour is one of the higher order language skills where such phenomena are observed. One should have no difficulty imagining such a superposition state for emotional states, philosophical quotes, moral questions and so on. In fact for some of these higher level states one could imagine a continuum between the states. For examples, the moral value of something can be imagined to be on a spectrum between good and bad. What's more these states evolve with time and are different in different places. So the morality wavefunction seems to have a variation over space and time. These states seem to be quite common!

What is surprising is that some of the more physical, lower order *classical states* also show such behaviour. The "Laurel-Yanny" debate is a recent example of something like that in the case of speech[8]. Again, one of the prerequisites is a closeness in physical space between the two states, that is, closeness of their classical states. In this case, it can be seen that the signals are close in frequency space[9]. See figure 9 for an example involving written text.

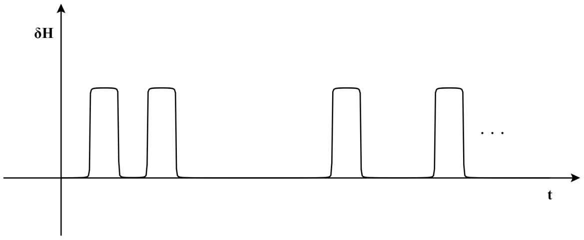

Figure 10. The perturbing hamiltonian has a constant amplitude and acts periodically over time.

IV. PERTURBATION THEORY

Consider again the 'a' state of section II. Before being written and after being written, the physical state $\left|\psi_{'a'}\right\rangle_P$ is only minimally affected by the environment; there may be changes to the logical state. It is while the 'a' is being written that the environment interacts with the state causing its einselection and this is the perturbation that causes the 'a' state to form. Consider once again the equation regarding environmental selection, equation 9; the hamiltonian driving this transition is a perturbation hamiltonian $\delta H(t)$ whose time dependence is such as to exist for only a small amount of time, wherein the 'a' is being written down, see figure 10.

Assume that the *ideal* 'a' state, $\left|\psi_{'a'}\right\rangle_P = |0_L\rangle^{\otimes N}$, is produced immediately after the hamiltonian acts, it then takes some amount of time before the state settles down; during this time the classical state *spreads* over the state space into a gaussian distribution, figure 3. The gaussian behaviour is seen by considering the states to spread in a random walk. A molecule in a state $|0_L\rangle$ would transition to a state $\left|\overline{0}_L\right\rangle$ with a probability p. As each molecule approximately has a certain fixed probability to change its state, the number of particles that possess the $\left|\overline{0}_L\right\rangle$ state would be binomially distributed with a mean Np and variance $Np(1-p)$. For sufficiently large N the normal distribution is approached. This idea is motivated from [10, p. 588].

In order to calculate the probability of transition one could look at the random walk of an ink particle. Assume that it is written on a patch of paper $1cm^2$. It takes about $1s$ for the ink to dry and the actual lines are about $0.5mm$ thick. The distance traversed by the molecule in a random walk has a mean 0 and a variance $R^2 = 2Dt$[7, 10], where D is the diffusion coefficient and t is the time of about a second. One gets $R \simeq 2.2 \times 10^{-5}m$ for a sucrose molecule[11, p.286]. In order for the molecule to change state from $|0_L\rangle$ to $\left|\overline{0}_L\right\rangle$ it would have to travel a distance of at least $0.5mm = 510^{-4}m$. The length required to travel is around 22.4 standard deviations. The probability of that occurring is about 10^{-111}! If the area of $1cm^2$ is broken into squares of $0.5mm$ one gets a grid of 400 segments. Assuming about a fifth of the space is occupied by the ink, one gets the number of possible states to be $\binom{400}{80}$ which is about 10^{85}. Even the immense number of states cannot out-power the extremely low probability of occurrence.

Consider a perturbing hamiltonian that has a transition amplitude of $\sqrt{p}$ leads to a probability p of changing state and E is its energy. This hamiltonian simply reassigns states with a different probability.

$$\delta H = E \begin{pmatrix} \sqrt{1-p} & \sqrt{p} \\ \sqrt{p} & \sqrt{1-p} \end{pmatrix} \tag{13}$$

Equation (5.3.35) of [12, Ch. 5] states that the probability of a transition to the continuum is given by equation,

$$P_{f \leftarrow i}(t) = \frac{2\pi}{\hbar} |\delta H_{fi}|^2 \rho(E_f) t. \tag{14}$$

In this case δH_{fi} is $E\sqrt{p}$, the transition amplitude. $\rho(E_f)$ is the density of states at the final energy and thus, $E\rho(E_f)$ equals the number of states, about 10^{85}. The probability of transition is,

$$P_{f \leftarrow i}(t) = \frac{2\pi}{\hbar} ENpt. \tag{15}$$

Substituting $\frac{3}{2}k_B T$ for the average energy, k_B being the boltzmann constant and T the temperature, it is seen that the probability of transition is about 10^{-12}, quite negligible.

V. DISCUSSION

The emergence of classical behaviour from the quantum has been discussed at great length[1, 5]. It is seen that classical behaviour is quite distinct from quantum behaviour and that the environment plays a major role in the transition from classical to quantum.

However, it is also seen that there is some residual quantumness in even these classical states. Viewing the environment as a hierarchy of systems that influence the ones below them, it can be seen how the classical behaviour is einselected to generate the immense objectivity in these states. There is a quantum darwinism that selects the states which are most suitable to the environment.

The ideas about perturbation theory is developed only approximately. It is critical to carry out the calculation in much more detail as the solutions are very sensitive to the input. All in all, this paper just touches upon the ideas that are developed here and does not go into much detail. There seems to be immense scope for further research into this topic.

ACKNOWLEDGMENTS

The author sincerely thanks Abhijit Sahu, Abhishek Vijayvergiya, Afreen Aliya, Akanksha Garg, Basil Zaman, Karthikeya Koushik, Nibha Gupta, Sai Mahadev, Samar Riaz, Srikar Raghavan, Sumeet Kshatriya and Vivek Singhal for their help with this paper. The author also thanks Jim Freericks and IllusoryAltruist for their highly useful insights on the development of the paper. The author is indebted to Shreyas Kolpe and Pradhan Sarathi for their detailed analyses of the paper. Finally, thanks to the 8.06 staff and community for the motivation to write the paper.

---

[1] W. H. Zurek, “Quantum darwinism,” *arXiv:0903.5082v1* (2009) .
[2] B. Tamir and E. Cohen, “Introduction to weak measurements and weak values,” *Quanta* **2** (2013) no. 1, 7–17. `http://quanta.ws/ojs/index.php/quanta/article/view/14`.
[3] M. A. Nielsen and I. L. Chuang, *Quantum Computation and Quantum Information.* Cambridge University Press, 2000.
[4] D. J. Griffiths, *Introduction to Quantum Mechanics (2nd Edition).* Pearson Prentice Hall, 2nd ed., 2004.
[5] W. H. Zurek, “Decoherence, einselection, and the quantum origins of the classical,” *arXiv:quant-ph/0105127v3* (2003) .
[6] V. Fromkin, R. Rodman, and N. M. Hyams, *An Introduction to Language, 9th Ed.* Wadsworth, Cengage Learning, 2011.
[7] R. P. Feynman, R. B. Leighton, and M. L. Sands, *The Feynman Lectures on Physics.* Reading, Mass: Addison-Wesley Pub. Co, 1963.
[8] M. Salam and D. Victor, “Yanny or laurel? how a sound clip divided america,”.
[9] J. Katz, J. Corum, and J. Huang, “We made a tool so you can hear both yanny and laurel,”.
[10] R. K. Pathria and P. D. Beale, *Statistical Mechanics.* Elsevier Ltd., 2011.
[11] P. Atkins and J. de Paula, *Physical Chemistry for the Life Sciences.* W. H. Freeman, 2011. `https://books.google.ae/books?id=WPwA3E0Xs0QC`.
[12] B. Zwiebach, “8.06 quantum physics iii. spring 2018.,”. `https://ocw.mit.edu`.

The Rotation Group in Non-Relativistic Quantum Mechanics

Su Kee Ng

(Dated: June 20, 2019)

In quantum mechanics, the angular momentum operator − which includes the orbital and spin angular momenta − is known as the generator of rotations that obeys certain fundamental commutation relations and it has discrete eigenvalues. It turns out that all proper rotations form a Lie group whose fundamental structure underlies the aforementioned angular momentum properties. This paper presents the three dimensional rotation group in matrix representation. The more intuitive representation by unit-determinant orthogonal 3×3 real matrices that form the SO(3) subgroup will first be studied, followed by the more complete representation using unit-determinant unitary 2×2 complex matrices that constitute the SU(2) subgroup. This paper will also discuss the parameter space and topological structure of these two subgroups and show that SO(3) is doubly covered by SU(2), which gives rise to the integer and half-integer quantum numbers.

I. GROUPS AND REPRESENTATION

A. A Brief Introduction to Group Theory

A *group* G is a set of elements $\{g_i \mid i \in \mathbb{Z}\}$ under a defined composition that satisfies the following axioms:

1. Closure: the composition product of any two group elements is also a group element: $g_i \circ g_j = g_k \in G$
2. Identity: there exists an identity element that takes each group element to itself: $\mathbb{1} \in G : \mathbb{1} \circ g_i = g_i \circ \mathbb{1} = g_i$
3. Associativity: $g_i \circ (g_j \circ g_k) = (g_i \circ g_j) \circ g_k = g_i \circ g_j \circ g_k$
4. Inverse: each group element has an inverse such that $g_i \circ g_i^{-1} = g_i^{-1} \circ g_i = \mathbb{1}$

The composition defined can be any abstract operation, including the common addition and multiplication. Any set of elements that satisfies the above conditions form a general group. We normally specify further properties to define the structure of the group of interest. For instance, a group whose elements are parametrised by continuous variables is a continuous group. Any subset of a group that satisfies the above four axioms forms a group by itself, and it is a *subgroup* of its parent group.

A group generally consists of abstract elements, and in many cases it is more convenient to represent them with a set of other objects facilitate the study of the characteristics of the group. A useful *representation* of a group must meet all fundamental conditions of the group, but they can have a different composition rule. Physicists often use groups and their representations to study the transformation properties of physical observables. We will focus on the common way of representing the rotation group using matrices.

B. Lie Groups and Lie Algebra

A Lie group $\mathcal{L}$ is a continuous group whose elements are analytic functions[1] and the group operations are smooth. This means that the composition of any two group elements must induce a differentiable map[4]. This allows us to study a group by examining its local structure near its identity element and find the *generators* of infinitesimal transformations and then write down the analytic function. In many cases, the analytic function can be derived by exponentiating the generators of the group, which we will see later in this presentation.

The generators of a Lie group by themselves form a set $\mathcal{G}$ of *Lie algebra* which is closed under the operation of the Lie bracket [,] that satisfies the following conditions:

1. Bilinearity

$$[a\mathcal{J}_k + b\mathcal{J}_l, \mathcal{J}_m] = a[\mathcal{J}_k, \mathcal{J}_m] + b[\mathcal{J}_l, \mathcal{J}_m], \tag{1}$$

$$[\mathcal{J}_k, a\mathcal{J}_l + b\mathcal{J}_m] = a[\mathcal{J}_k, \mathcal{J}_l] + b[\mathcal{J}_l, \mathcal{J}_m], \tag{2}$$

$$\text{for } a, b \in \mathbb{C}, \text{and } \forall \mathcal{J}_k, \mathcal{J}_k, \mathcal{J}_m \in \mathcal{G}$$

2. Antisymmetry

$$[\mathcal{J}_k, \mathcal{J}_l] = -[\mathcal{J}_l, \mathcal{J}_k] \ \forall \mathcal{J}_k, \mathcal{J}_l, \mathcal{J}_m \in \mathcal{G} \tag{3}$$

3. Jacobi identity

$$[\mathcal{J}_k, [\mathcal{J}_l, \mathcal{J}_m]] + [\mathcal{J}_m, [\mathcal{J}_k, \mathcal{J}_l]] + [\mathcal{J}_l, [\mathcal{J}_m, \mathcal{J}_k]] = 0, \tag{4}$$

$$\forall \mathcal{J}_k, \mathcal{J}_l, \mathcal{J}_m \in \mathcal{G}$$

The Lie bracket that happens to be the commutator $[\mathcal{J}_k, \mathcal{J}_l] = \mathcal{J}_k\mathcal{J}_l - \mathcal{J}_l\mathcal{J}_k$ for matrix groups, but it can be other operations such as the Poisson bracket as long as the above conditions are satisfied[4].

C. The Rotation Group

There are two equivalent ways of modelling rotations. We can either rotate the coordinate frame of reference or rotate the object of interest. Both operations will produce the same relative angular displacement. In this paper the former convention is used.

A rotation $\mathcal{R}$ is a linear transformation of coordinates $x_k \longmapsto x'_k = \mathcal{R}x'_k$ that preserves the origin O (homogeneous), the distance between two arbitrary points (orthogonal), as well as the orientation (handedness) of the coordinates (unit determinant).

The set of rotations in n-dimensional space fulfils all the fundamental axioms to form a group $\boldsymbol{\mathcal{R}}$. A rotation by an angle α followed by another rotation by an angle β is a rotation by an angle $\alpha+\beta$. A rotation of a vector by a multiple of 2π is the same as no rotation (i.e. its identity). Each rotation can be reversed by a rotation by the same amount in the opposite sense. $\boldsymbol{\mathcal{R}}$ is also a Lie group, so a finite rotation can be attained by a series of continuous infinitesimal rotations generated by elements that satisfy the Lie algebra. Rotations in n dimensions generally do not commute, except for $n \leq 2$. This can be verified physically.

In general, one should think of rotation in n-dimensional Euclidean space to occur on a plane instead of an axis. Of course, these mutually orthogonal planes need not be normal to a defined axis. In order to convince myself that a rotation about an axis is unique for the 3D manifold, I must prove that the number of mutually orthogonal planes is equal to the number of independent axes iff (if and only if) the dimension of the space is 3. This can be expressed mathematically as

$$nC2 = \frac{n(n-1)}{2} = n \implies n = 0, 3 \tag{5}$$

Due to the fact that there is a unique axis for a rotation in 3-dimensions, we can take it for granted and use this fact in our parametrisation.

Rotations in n-dimensional space can be represented by SU(n).

II. SPECIAL ORTHOGONAL GROUP SO(3)

It is instructive to look at the general SO(n) first and then come come back to SO(3) later. SO(n) stands for special orthogonal group in n dimensions. Special means unit determinant, and orthogonality means $R^TR = RR^T = 1$, where R^T denotes the transposition of R. So, SO(n) consists of $n \times n$ orthogonal matrices R with $\det R = +1$ and they satisfy the axioms of a group under multiplication:

1. The product of two orthogonal matrices is also an orthogonal matrix:
$$R_iR_j = R_k, \ \forall R_i, R_j, R_k \in \mathrm{SO}(n) \tag{6}$$
$$R_k^2 = R_kR_k^T = R_iR_j(R_iR_j)^T = R_iR_jR_j^TR_i^T = \mathbb{1} \tag{7}$$
2. Matrix multiplications are associative:
$$(R_iR_j)R_k = R_i(R_jR_k) = R_iR_jR_k \tag{8}$$
3. Identity matrix $\mathbb{1}_n$ has $\det \mathbb{1}_n = 1$ and belongs is an element of the set such that $\mathbb{1}R_i = R_i\mathbb{1} = R_i$.
4. All matrices with non-zero determinant are invertible. The inverse R_i^{-1} of R_i corresponds to rotations in the opposite sense and also belongs the set:
$$R_i^{-1}R_i = R_i1R_i^{-1} = \mathbb{1}_n \tag{9}$$

Unit determinant corresponds to *proper* rotations because any rotation can be done by a series of successional rotations with unit determinant. This preserves the orientation of the rotation. Matrices with determinant -1 corresponds to improper transformation as every second operation changes the sign of the determinant. They do not comprise a group as the the identity matrix $\mathbb{1}_n$ is not in the set.

A vector $\mathbf{x}$ rotated by a matrix R has its components x_i transforming like $x_i \longmapsto x_i' = R_{ij}x_j$, where R_{ij} corresponds to each matrix element of R. The Einstein's summation notation is used, so the repeated indices are summed over.

Orthogonality manifests naturally from distance preservation. The dot product $\mathbf{x}\cdot\mathbf{y} = x_iy_j$ of two vectors must be conserved[3]:

$$\begin{aligned} x_iy_i &= R_{ij}x_jR_{ik}y_k = R_{ji}R_{ik}x_jy_k \qquad (10)\\ &= (R^TR)_{jk}x_jy_k \qquad (11) \end{aligned}$$

With the manipulation of the dummy indices, we can also write $x_iy_i = x_jy_j = \delta_{jk}x_jy_k$ and compare it with Eq. (11). Therefore,

$$(R^TR)_{jk} = \delta_{jk} \tag{12}$$
$$R^TR = RR^T = \mathbb{1} \to R^T = R^{-1} \tag{13}$$

In the language of SO(n) representation, a rotation is a real, linear, homogeneous, orthogonal, and unit-determinant transformation that leaves the scalar product of two vectors invariant.

For the rotation in 3-dimensional Euclidean space, we represent a vector $\mathbf{r}$ by a 3×1 column matrix with components r_i. The rotation operator is then represented by a 3×3 SO(3) matrix $R(n,\psi)$ with elements R_{ij}. As mentioned in the previous section, three parameters are needed to model the rotations in 3 dimensions and we can exploit the coincidence that there is a unique axis for every rotation by specifying a unit vector $\mathbf{n}$ along an axis to provide the direction of the rotation and specify an angle θ by which the rotation occurs. The matrices $R(\mathbf{n_k},\theta)$ for the rotation along each of the Cartesian unit vectors $(\mathbf{n_1},\mathbf{n_2},\mathbf{n_3})$ can be constructed geometrically:

$$R(\mathbf{n_1},\theta) = \begin{pmatrix} 1 & 0 & 0 \\ 0 & \cos\theta & \sin\theta \\ 0 & -\sin\theta & \cos\theta \end{pmatrix} \tag{14}$$

$$R(\mathbf{n_2},\theta) = \begin{pmatrix} \cos\theta & 0 & -\sin\theta \\ 0 & 1 & 0 \\ \sin\theta & 0 & \cos\theta \end{pmatrix} \tag{15}$$

$$R(\mathbf{n_3},\theta) = \begin{pmatrix} \cos\theta & \sin\theta & 0 \\ -\sin\theta & \cos\theta & 0 \\ 0 & 0 & 1 \end{pmatrix} \tag{16}$$

It can be verified by construction that matrices (14), (15), and (16) are in fact orthogonal and unimodular.

A. Generators of Infinitesimal Rotations

We know that a rotation by θ about an axis is generated by a sequence of n infinitesimal rotations by $\delta\theta$ in the same direction, and we have already constructed three orthogonal matrices to represent rotations in 3-dimensions. Now, we want to find out the generators J of infinitesimal rotations by expressing the above rotation matrices in the form

$$R(\mathbf{n_k}, \delta\theta) = \mathbb{1}_3 - iJ_k\delta\theta,\ k = 1, 2, 3 \tag{17}$$

For an infinitesimally small angle $\delta\theta$, $\cos\delta\theta \simeq 1$, $\sin\delta\theta \simeq \delta\theta$. It follows that

$$J_1 = \begin{pmatrix} 0 & 0 & 0 \\ 0 & 0 & i \\ 0 & -i & 0 \end{pmatrix} \tag{18}$$

$$J_2 = \begin{pmatrix} 0 & 0 & -i \\ 0 & 0 & 0 \\ i & 0 & 0 \end{pmatrix} \tag{19}$$

$$J_3 = \begin{pmatrix} 0 & i & 0 \\ -i & 0 & 0 \\ 0 & 0 & 0 \end{pmatrix} \tag{20}$$

J_1, J_2, and J_3 are the generators of the SO(3) group. Note that in (17) the i factor is necessary to ensure that J_k is hermitian and the minus sign is for convention.

We can extend the above formulae to an arbitrary direction $\mathbf{n} = (n_1, n_2, n_3)$ in the 3-dimensional space. We know that finite rotations in different directions do not commute, but the their infinitesimal counterparts do commute up to first order. Hence,

$$\begin{aligned} R(\mathbf{n}, \delta\theta) &\simeq \prod_{k=1}^{3} (\mathbb{1}_3 - iJ_k n_k \delta\theta) \\ &\simeq \mathbb{1}_3 - i\delta\theta \sum_{k=1}^{3} J_k n_k \\ R(\mathbf{n}, \delta\theta) &= \mathbb{1}_3 - i(\mathbf{J}\cdot\mathbf{n})\delta\theta \end{aligned} \tag{21}$$

A finite rotation can then be formed by applying the infinitesimal rotations n times, thus

$$\mathbf{R}(\mathbf{n}, \theta) = [\mathbf{R}(\mathbf{n}, \delta\theta)]^n = [\mathbb{1}_3 - i(\mathbf{J}\cdot\mathbf{n})\delta\theta]^n \tag{22}$$

Since $\theta = n\delta\theta$, as $n \to \infty$ (22) becomes

$$\mathbf{R}(\mathbf{n}, \theta) = \lim_{n\to\infty} \left(\mathbb{1}_3 - i\frac{(\mathbf{J}\cdot\mathbf{n})\theta}{n} \right)^n = e^{-i(\mathbf{J}\cdot\mathbf{n})\theta} \tag{23}$$

Note that the repeated indices in the second equation are not summed over, and a summation symbol was shown intentionally in the last equation for clarity. $\mathbf{R}(\mathbf{n}, \theta)$ is so-called the rotation operator for SO(3) that transforms vectors and preserves scalars.

It can be shown directly that the generators constructed above satisfy the commutation relation

$$[J_k, J_l] = i\epsilon_{klm} J_m, \epsilon_{123} = +1 \tag{24}$$

This is the Lie algebra for rotation group in three dimensions. It should be noted that the generators defined above are dimensionless and the commutation relations are purely mathematical. The next step is to incorporate quantum mechanics to the results. We have learned from quantum mechanics that the generator of rotations is the angular momentum operator and the fundamental constant with the physical dimension of angular momentum is the Plank's constant $\hbar$. The quantum mechanical version for Eq. (23) and Eq. (24) can be attained by simply letting $J_k \to \frac{\hat{J}_k}{\hbar}$ for all indices. Therefore, Eq. (23) and Eq. (24) become

$$\hat{\mathbf{R}}(\mathbf{n}, \theta) = \exp\left(-i\frac{(\hat{\mathbf{J}}\cdot\mathbf{n})\theta}{\hbar} \right) \tag{25}$$

$$\left[\hat{J}_k, \hat{J}_l\right] = i\hbar\epsilon_{klm} \hat{J}_m, \epsilon_{123} = +1 \tag{26}$$

Equation (26) is so called the angular momentum algebra and is the defining property of angular momenta in quantum mechanics. Since the general angular momentum operator $\hat{\mathbf{J}} = (\hat{J}_1, \hat{J}_2, \hat{J}_3)$ the sum $\hat{\mathbf{J}} = \hat{\mathbf{L}} + \hat{\mathbf{S}}$ of the orbital $\hat{\mathbf{L}} = (\hat{L}_1, \hat{L}_2, \hat{L}_3)$ and spin $\hat{\mathbf{S}} = (\hat{S}_1, \hat{S}_2, \hat{S}_3)$ angular momenta, all components of $\hat{L}_k$ of $\hat{\mathbf{L}}$ and $\hat{S}_{kk}$ of $\hat{\mathbf{S}}$ must satisfy the the angular momentum algebra.

III. SPECIAL UNITARY GROUP SU(2)

SU(n) stands for special unitary group in n dimensions. It consists of a collection of $n \times n$ unitary matrices with complex entries and unit determinant that satisfy the fundamental axioms of a group. A general $n \times n$ matrix has n^2 complex entries and each of which is made up from two real numbers, so the total real parameters are $2n^2$. Unitarity (27) reduces the degrees of freedom by half and unit determinant adds one more constraint. The number real parameters required to specify an element of SU(n) is then $n^2 - 1$. Thus, an SU(2) element U, same of that of SO(3), needs 3 real parameters to specify. This is the first condition for SU(2) to be a representation of the rotations in 3-dimensions. Let us denote $U^\dagger$ as the conjugate transpose of U, then unitarity requires

$$UU^\dagger = U^\dagger U = \mathbb{1}_2 \tag{27}$$

A unitary 2×2 matrix with unit determinant can generally be written as

$$U = \begin{pmatrix} a & b \\ -b^* & a^* \end{pmatrix}, \text{ with } a, b \in \mathbb{C}, \tag{28}$$

$$\text{and } |a|^2 + |b|^2 = 1 \tag{29}$$

a and b are complex and can be expressed explicitly as

$$a = a_1 + ia_2,\ b = b_1 + ib_2,\ a_1, a_2, b_1, b_2 \in \mathbb{R} \tag{30}$$

The equation for unit determinant in (29) can be expanded to

$$|a_1|^2 + |a_2|^2 + |b_1|^2 + |b_2|^2 = 1 \tag{31}$$

This is the equation for the parameter space of SU(2) and it is topologically a unit 3-sphere (the 3-dimensional surface of a 4-dimensional sphere. Since the radius is fixed, we need only need 3 parameters to know the fourth, which is consistent with what we mentioned before.

Recall that any three objects that satisfy the commutation relation (26) are the generators of a group that represents rotations, and then we exponentiate them to get the rotation operator. So we can anticipate the SU(2) rotation matrix to be a 2×2 unitary exponential of Hermitian generators, given the fact that the complex exponential of a Hermitian matrix is unitary. So, the generators must be a 2×2 Hermitian matrix. Any arbitrary 2×2 Hermitian matrix can be constructed in terms of the identity matrix $\mathbb{1}_2$ and Pauli matrices. We will now review the Pauli matrices and their properties. The Pauli matrices are given by

$$\sigma_1 = \begin{pmatrix} 0 & 1 \\ 1 & 0 \end{pmatrix}, \sigma_2 = \begin{pmatrix} 0 & 1 \\ 1 & 0 \end{pmatrix}, \sigma_3 = \begin{pmatrix} 1 & 0 \\ 0 & -1 \end{pmatrix} \tag{32}$$

Pauli matrices have the following known properties:

1. Hermiticity and unitarity
$$\sigma_k^\dagger \sigma_k = \sigma_k^2 = \mathbb{1}_2 \implies \sigma_k = \sigma_k^\dagger = \sigma_k^{-1} \tag{33}$$
2. It follows from (33) that the eigenvalues can only be ± 1 with eigenvectors $\begin{pmatrix} 1 \\ 0 \end{pmatrix}$ and $\begin{pmatrix} 0 \\ 1 \end{pmatrix}$ respectively.
3. Zero trace $\mathrm{Tr}(\sigma_k) = 0$
4. Commutator of
$$\left[\frac{\sigma_k}{2}, \frac{\sigma_l}{2}\right] = i\epsilon_{klm}\frac{\sigma_m}{2}, \epsilon_{123} = 1 \tag{34}$$
5. Anticommutator of
$$\{\sigma_k, \sigma_l\} = \sigma_k\sigma_l + \sigma_l\sigma_k = 2\delta_{kl}\mathbb{1} \tag{35}$$
6. Rotational invariance[2]
$$\sigma'_k = \hat{R}(\mathbf{n}, \theta)\sigma_k = \sigma_k \tag{36}$$

It can be concluded by comparing Eq.(34) with Eq.(24) that the triplets $(\frac{\sigma_1}{2}, \frac{\sigma_2}{2}, \frac{\sigma_1}{2})$ are the generators of SU(2) in 2-dimensional representation. The spin angular momentum algebra in quantum mechanics can be obtained by letting $\hat{S}_k = \frac{\hbar}{2}\sigma_k$ and the commutator becomes

$$\left[\hat{S}_k, \hat{S}_l\right] = i\hbar\epsilon_{klm}\hat{S}_m \tag{37}$$

The rotation operator $\hat{\mathbf{U}}(\mathbf{n}, \theta)$ for the two dimensional representation of SU(2) is then simply the 2×2 analogue of Eq.(25):

$$\begin{aligned} \hat{\mathbf{U}}(\mathbf{n}, \theta) &= \exp\left(-i\frac{(\hat{\mathbf{S}} \cdot \mathbf{n})\theta}{\hbar}\right) \\ &= \exp\left(-i\frac{(\boldsymbol{\sigma} \cdot \mathbf{n})\theta}{2}\right), \boldsymbol{\sigma} = (\sigma_1, \sigma_2, \sigma_3) \end{aligned} \tag{38}$$

We have seen that a 3×3 matrix R in SO(3) rotates a 3-vector v, what does a 2×2 matrix in SU(2) transform? We now want to construct an equation that represents the same transformation using a 2×2 matrix, but a 2×2 matrix cannot act on a 3-dimensional column vector. The only meaningful objects that can be acted on by 2×2 matrices are 2×1 and 2×2 matrices, and they will be discussed in the later sections. Before doing that, it is important to understand the transformation properties of scalar and vector operators first.

IV. SCALAR AND VECTOR UNDER ROTATIONS

In this section, we will investigate the transformation of physical observables in the quantum mechanical domain under rotation, and study the properties scalar and vector operators under rotation.

When the state $|\psi\rangle$ of a quantum mechanical system is rotated, it has to remain normalised, and the rotation operator $\hat{U}$ must be unitary. Its transformation can then be written as $|\psi\rangle \to |\psi'\rangle = \hat{U}|\psi\rangle$. When the operator $\hat{Q}$ of a physical observable acts upon $|\psi\rangle$, it results in another ket $|\phi\rangle = \hat{Q}|\psi\rangle$ in the projective Hilbert space. We can look at how $\hat{Q}$ transform by rotating the whole system by $\hat{U}$:

$$\hat{U}\hat{Q}|\psi\rangle = \hat{U}\hat{Q}\mathbb{1}|\psi\rangle = \hat{U}\hat{Q}\hat{U}^\dagger\hat{U}|\psi\rangle = \hat{Q}'|\psi'\rangle \tag{39}$$

An identity operator has been inserted in between $\hat{U}$ and $|\psi\rangle$ in the second term in (39), followed the unitarity of $\hat{U}$ in the third term. The mapping between the transformed operator $\hat{Q}'$ and the original operator $\hat{Q}$ is therefore given by

$$\hat{Q}' = \hat{U}\hat{Q}\hat{U}^\dagger \tag{40}$$

Equation (40) applies to all physical observables. We can then take the infinitesimal transformation to relate an observable to angular momenta:

$$\begin{aligned} \hat{Q}'(\delta\theta) &= \hat{U}(\delta\theta)\hat{Q}\hat{U}^\dagger(\delta\theta) \\ &= (\mathbb{1} - i\frac{\delta\theta\hat{J}_k}{\hbar})\hat{Q}(\mathbb{1} + i\frac{\delta\theta\hat{J}_k}{\hbar}) \\ \hat{Q}'(\delta\theta) &= \hat{Q} - i\frac{\delta\theta}{\hbar}[\hat{J}_k, \hat{Q}] \end{aligned} \tag{41}$$

We now have all the equipments to study scalar and vector operators. An operator is a scalar S if remains invariant $S' = S$ under rotation. Applying this condition to Eq. (41) gives

$$[\hat{J}_k, S] = 0 \text{ or } [\hat{\mathbf{J}}, S] = 0 \tag{42}$$

A vector $\mathbf{V}$ is a quantity whose components V_k transform under rotations $\hat{R}$ exactly the same way as the position coordinates do[1], or mathematically

$$V_k = R_{kl} V_l \tag{43}$$

R_{kl} corresponds to all matrix elements of R. In quantum mechanics, a vector operator of an observable is a vector $\hat{\mathbf{V}}$ whose components $\{\hat{V}_k\}$ are valued by operators, and it transforms as per Eq.(40). However, its expectation value $\langle \hat{V}_k \rangle$ − which corresponds to an observable in classical systems − transform like a number-valued vector[2]. For a state that transforms under rotation $|\psi\rangle \longmapsto |\psi'\rangle$,

$$\langle \hat{V}_k \rangle \longmapsto \langle \hat{V}_k{}' \rangle = R_{kl} \langle \hat{V}_k \rangle \tag{44}$$

$$\langle \psi | \hat{V}_k{}' | \psi \rangle = \langle \psi | \hat{U}^\dagger \hat{V}_k \hat{U} | \psi \rangle = R_{kl} \langle \psi | \hat{V}_k | \psi \rangle$$

It follows that

$$\hat{U}^\dagger \hat{V}_k \hat{U} = R_{kl} \hat{V}_k \tag{45}$$

Taking the infinitesimal transformation, Eq.(45) becomes

$$\left(\mathbb{1} + i \frac{\hat{J}_l \delta\theta}{\hbar} \right) \hat{V}_k \left(\mathbb{1} - i \frac{\hat{J}_l \delta\theta}{\hbar} \right) = R_{kl} \hat{V}_k$$

$$\hat{J}_l + i \frac{\delta\theta}{\hbar} [\hat{J}_l, \hat{V}_k] = R(\hat{\mathbf{m}}, \delta\theta) \hat{V}_k \tag{46}$$

Note that $R_{kl}(\delta\theta) = R(\hat{\mathbf{n_m}}, \delta\theta)$ and the indices k, l, m permute cyclically. Each commutator for each pair of components of $\hat{\mathbf{V}}$ and of $\hat{\mathbf{J}}$ can be evaluated explicitly by applying Eq.(17), Eq.(18), Eq.(19), and Eq.(20) to Eq.(46). Equation (46) can then be simplified to

$$[\hat{J}_k, \hat{V}_l] = i\hbar \epsilon_{klm} \hat{V}_m \tag{47}$$

This is the defining property of vectors under rotations for operators. Since angular momenta − the generators of the rotation themselves − are vector operators, they also fulfil this algebra.

V. SPINORS

Spinors is an abstract element belong to a complex vector space that has certain transformation properties under certain operations like Lorentz boosts[9]. Spinors are more sophisticated than vectors as they are more sensitive to transformations than their vector counterpart. For the purpose of the studying the representation of SU(2), we only consider the spinors that live in a two-dimensional complex vector space. The most familiar example of spinors in non-relativistic quantum mechanics are the spin-$\frac{1}{2}$ states $|\pm\rangle$. The spinors corresponding to opposite physical directions are mutually orthogonal. This clearly shows that they differ from ordinary vectors. A spinor $\boldsymbol{\chi}$ associated with a vector $\mathbf{r}(r, \theta, \phi)$ a 2×1 matrix defined as[9]

$$\boldsymbol{\chi}(r, \theta, \phi, \alpha) = |\chi\rangle = \begin{pmatrix} \chi_1 \\ \chi_2 \end{pmatrix} \tag{48}$$

$$= \sqrt{r} e^{-i\alpha/2} \begin{pmatrix} \cos(\frac{\theta}{2}) e^{-i\frac{\phi}{2}} \\ \sin(\frac{\theta}{2}) e^{i\frac{\phi}{2}} \end{pmatrix} \tag{49}$$

We can then write a vector in terms of the components of the spinor as

$$\mathbf{r}(r, \theta, \phi) = \begin{pmatrix} x_1 \\ x_2 \\ x_3 \end{pmatrix} = \begin{pmatrix} \chi_1 \chi_2^* + \chi_1^* \chi_2 \\ i(\chi_1 \chi_2^* - \chi_1^* \chi_2) \\ |\chi_1|^2 - |\chi_2|^2 \end{pmatrix} \tag{50}$$

The magnitude χ of the spinor is the square root of the length r of the vector

$$r = |\chi_1|^2 + |\chi_2|^2 = \chi^2 \tag{51}$$

The mapping between a spinor $\boldsymbol{\chi}$ and a vector $\mathbf{r}$ is given by[9]

$$\mathbf{r} = \boldsymbol{\chi}^\dagger \boldsymbol{\sigma} \boldsymbol{\chi} = \langle \chi | \boldsymbol{\sigma} | \chi \rangle, \boldsymbol{\sigma} = (\sigma_1, \sigma_2, \sigma_3) \tag{52}$$

Note that in Eq.(49) that the spinor has an overall phase that the vector does not have. It can be seen in Eq.(52) that the phase will cancel with its conjugate when a spinor is mapped to a vector. This means that a spinor can change sign but it is still mapped to the same vector. It can be anticipated that a 2×1 spinor is transformed by the 2×2 spin rotation matrices given by Eq.(38) such that

$$|\chi'\rangle = \hat{\mathbf{U}}(\mathbf{n}, \theta) |\chi\rangle = \exp\left(-i \frac{(\boldsymbol{\sigma} \cdot \mathbf{n})\theta}{2} \right) |\chi\rangle \tag{53}$$

The corresponding transformed vector $\mathbf{r}'$ can then be expressed as

$$\mathbf{r}' = \langle \chi' | \boldsymbol{\sigma} | \chi' \rangle = \langle \chi | U^\dagger \boldsymbol{\sigma} U | \chi \rangle \tag{54}$$

The Hermiticity of the Pauli matrices has been applied. We want to work out explicitly how exactly the vector $\mathbf{r}$ is transformed given a transformed spinor $|\chi'\rangle$. It is more convenient to do this component by component. Applying Eq.(54) direction $\mathbf{k}$,

$$|\chi'; \mathbf{k}\rangle = U_k |\chi\rangle = e^{-i\frac{\theta}{2}\sigma_k} |\chi\rangle \tag{55}$$

The l component x_l of vector $\mathbf{r}$ can be determined by applying the hermiticity and rotational invariance of the

Pauli matrices (36), and Euler's formula for matrices to Eq.(54):

$$\begin{aligned} x'_l &= \langle \chi'; \mathbf{k}|\sigma_l|\chi'; \mathbf{k}\rangle = \langle \chi|U_k^\dagger \sigma_l U_k|\chi\rangle \\ &= \left\langle \chi \middle| e^{i\frac{\theta}{2}\sigma_k}\sigma_l e^{-i\frac{\theta}{2}\sigma_k} \middle| \chi \right\rangle \\ x'_l &= \cos\theta\langle\chi|\sigma_l|\chi\rangle - i\sin\theta\langle\chi|\sigma_l\sigma_k|\chi\rangle \end{aligned} \tag{56}$$

The next step is to evaluate x'_l for each l using the properties of Pauli matrices stated in Eq.(34) and Eq.(35) relations to (56). The result is $\mathbf{r}' = R_k\mathbf{r}$, where R_k are exactly the same as previously defined Eq.(14), Eq.(15), and Eq.(16). The result implies that rotating a spinor with half angle corresponds to rotating the vector by a full angle. In other words, a spinor needs two full rotations 4π to come back to its identity, and it changes sign after a full rotation 2π. This is manifestation of the double covering of SO(3) by SU(2) and explains spin-$\frac{1}{2}$.

Let us now look at the application of two dimensional representation of SU(2) with spinors tin quantum mechanics. Consider a normalised state in the projective Hilbert space, so $r = 1$. We also demand that the overall phase does not alter the physics of the system, so we set $\alpha = 0$. Therefore, a spin-$\frac{1}{2}$ state corresponding to an arbitrary physical direction $\mathbf{n}$ has the form

$$|\mathbf{n}\rangle = \begin{pmatrix} \cos(\frac{\theta}{2})e^{-i\frac{\phi}{2}} \\ \sin(\frac{\theta}{2})e^{i\frac{\phi}{2}} \end{pmatrix} \tag{57}$$

In particular, let us investigate this in a specific direction $\pm\mathbf{z}$ where $\theta = 0, \pi$. Note that ϕ is undefined along the poles, and the $\sin\frac{\theta}{2}$ and $\cos\frac{\theta}{2}$ are 0 and 1 alternatively for these two angles $\theta = 0, \pi$. So, the relative phase factor becomes a global phase in either cases. We an then set $\phi = 0$, thus

$$|\mathbf{z}; +\rangle = \begin{pmatrix} 1 \\ 0 \end{pmatrix} = |+\rangle \tag{58}$$

$$|\mathbf{z}; -\rangle = \begin{pmatrix} 0 \\ 1 \end{pmatrix} = |-\rangle \tag{59}$$

This is the spin states $\frac{1}{2}; +$ and $\frac{1}{2}; -$ that we are familiar with. We can then write

$$|\mathbf{n}\rangle = \cos\left(\frac{\theta}{2}\right)e^{-i\frac{\phi}{2}}|+\rangle + \sin\left(\frac{\theta}{2}\right)e^{i\frac{\phi}{2}}|-\rangle \tag{60}$$

VI. 2 × 2 MATRIX REPRESENTATION OF 3-VECTORS

We now want to construct a 2×2 matrix X that remains form-invariant under the transformation by an SU(2) matrix. The way to do that is to take a dot product of the vector $\mathbf{r} = (x_1, x_2, x_3)$ and the Pauli matrices $\boldsymbol{\sigma} = (\sigma_1, \sigma_2, \sigma_3)$:

$$X = \mathbf{r}\cdot\boldsymbol{\sigma} = x_k\sigma_k = \begin{pmatrix} x_3 & x_1 - ix_2 \\ x_1 + ix_2 & -x_3 \end{pmatrix} \tag{61}$$

The result is a Hermitian and traceless matrix that has determinant

$$\det X = -x_i x_i = -(x_1^2 + x_2^2 + x_3^2) = -x^2 \tag{62}$$

Since X is Hermitian, when it is acted on by an SU(2) matrix, it should transform like a Hermitian operator as per Eq.(40):

$$X \to X' = UXU^\dagger = \mathbf{r}'\cdot\boldsymbol{\sigma} = R\mathbf{r}\cdot\boldsymbol{\sigma}, \tag{63}$$
$$\text{where } U = \exp\left(-i\frac{(\sigma\cdot\mathbf{n})\theta}{2}\right)$$

Notice from Eq. (54) and Eq. (63) that the transformed X' remains unchanged if U changes sign. This does not happen in SO(3) because if the rotation operator changes sign, the transformed vector will change sign. This implies that two elements $SU(2)$ double cover an element of SO(3), and X can completely represent $\mathbf{r}$ but not vice versa.

VII. TOPOLOGICAL CONNECTION BETWEEN SU(2) AND SO(3)

The connection between SU(3) and SU(2) can be seen rather intuitively by comparing the topological properties of their parameter spaces. We need a little bit of terminology before getting started. A group A is isomorphic to a group B the group elements the two groups are in one-to-one correspondence. If all elements of a group is mapped to a portion of the elements of another group, the map is called homomorphism. Group A is said to cover group B if more elements of A are mapped to all elements in group B. A group is simply connected if an arbitrary loop in the space it spans can be continuously shrunk to a point. There is a theorem in topology that says every Lie group has a universal covering group which is simply connected[4]. At the end of this discussion, we will know that SU(2) is the universal covering group for SO(3).

Equation (31) tells us that the parameter space of SU(2) is a 3-sphere S^3, which is the 3-dimensional "surface" of a 4-dimensional unit hypersphere in the Euclidean space. Although it is a 4-dimensional object, it is rather easy to understand by the analogy of the two surface S^2 of a 3-dimensional sphere. If we trace a loop anywhere on the surface of a sphere, it can be continuously deformed to another loop and also shrunk to a point. So the parameter space of SU(2) is simply connected.

SO(3) has a more peculiar topology in a sense that its parameter space does not belong to the Euclidean 3-dimensional space. To begin with, we can verify physically that a rotation by π about an arbitrary axis is identified by a rotation by π in the opposite (negative) direction. Hence we only need π to bound the parameter space of SO(3).

Consider a solid sphere shown in the Figure 1(a). Strictly speaking, this picture does not fully represent the parameter space of SO(3), but we can get some motivation from it. We can represent the angular displacement corresponding to a rotation by the length of an arrow pointing outward from the origin O. Knowing the fact that a rotation by π is the same as a rotation by $-\pi$, the radius of the sphere to π is then bounded to π. In other words, each point at the outermost surface of the ball is identified with its antipodal point.

If we trace a loop anywhere inside the ball, it can always be continuously deformed to a point. If we trace a path from the origin O to point A, we can continue from its antipodal point $\bar{A}$ and come back to the origin. Once we complete this loop, we can no longer shrink the the path. This shows that SO(3) is not simply connected. However, we can shrink the path to a point if we trace another loop, from O through B, $\bar{B}$, and then come back to O. The trick is to move $A-\bar{A}$ and $B-\bar{B}$ until A meets with $\bar{B}$ and B meets with $\bar{A}$, as depicted in the picture in the middle. The loop can then be continuously shrunk to a point, as shown in the picture to the right. Therefore, SO(3) is doubly-connected. It is doubly covered by SU(2). Locally, these two groups are identical (they have the same Lie algebra), but globally they are very different (they have different parameter spaces). This topological structure underlies spin-$\frac{1}{2}$ and the integer and half-odd-integer quantum numbers that puzzle a lot of us.

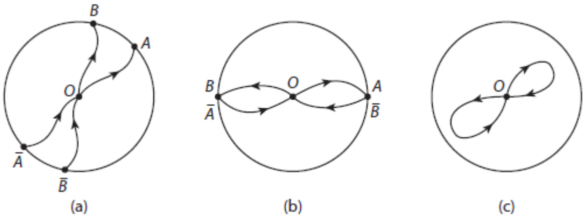

Figure 1. SO(3) is doubly connected

---

[1] V. Balakrishnan, *A Miscellany of Mathematical Physics.* Indian Academy of Sciences, 2018.

[2] J. Sakurai and J. Napolitano, *Modern Quantum Mechanics.* Cambridge University Press, 2017. `https://books.google.com.au/books?id=010yDwAAQBAJ`.

[3] S. Weinberg, *Lectures on Quantum Mechanics.* Cambridge University Press, 2 ed., 2015.

[4] J. Schwichtenberg, *Physics from Symmetry.* Undergraduate Lecture Notes in Physics. Springer International Publishing, 2 ed., 2018.

[5] A. Zee, *Group Theory in a Nutshell for Physicists.* Princeton University Press, 2016.

[6] V. Balakrishnan, "IIT NPTEL Quantum Physics Lectures 24-25," 2009. `https://nptel.ac.in/courses/122106034/24`.

[7] V. Balakrishnan, "IIT NPTEL Selected Topics on Mathematical Physics Lectures 34-36," 2014. `https://nptel.ac.in/courses/115106086/34`.

[8] V. Balakrishnan, "IIT NPTEL Classical Physics Lectures 32-34," 2009. `https://nptel.ac.in/courses/122106027/32`.

[9] A. M. Steane, "An introduction to spinors," *arXiv e-prints* (Dec, 2013) arXiv:1312.3824, `arXiv:1312.3824 [math-ph]`.

Rotations, Wigner D-Matrices and the Wigner-Eckart Theorem

Purvaash P U

(Dated: June 18, 2019)

Many operators in quantum mechanics consist of a large number of elements. Wigner-Eckart Theorem reduces the load of computation of these elements by exploiting the symmetry of the system. In a way, this theorem talks about rotational symmetry and conservation of angular momentum. This paper would deal with the rotation symmetry and how the theorem exploits it to calculate the matrix elements.

I. INTRODUCTION

Quantum Mechanics is filled with operators, and sometimes of large dimensions. Computing them is sometimes challenging and can be simplified using the Wigner-Eckart Theorem. To understand this theorem, the action od rotations are to be studied.

II. ROTATIONS IN 3-D EUCLIDEAN SPACE

In a 3-d Euclidean space (and using a right handed system) the rotation operator R maps points $(\mathbf{r}')$ to $(\mathbf{r})$, i.e. $R : \mathbb{R}^3 \to \mathbb{R}^3$. What R possibly could be, can be decoded from its properties. Firstly, $R\mathbf{0} = \mathbf{0}$, i.e. the origin is mapped to itself. $|R\mathbf{r}|^2 = |r|^2$, i.e., the length(and hence angles) is invariant under rotation. This implies that a parallelogram after rotation remains congruent to itself before the rotation was applied. As vector addition can be expressed in terms of a parallelogram this implies, $R(\mathbf{r}_1 + \mathbf{r}_2) = R\mathbf{r}_1 + R\mathbf{r}_2$. Also straight lines remain straight under rotation, i.e.,$R(a\mathbf{r}) = aR\mathbf{r}$.

These properties ascertain that R is a linear operator. Hence R is invertible and has an inverse R^{-1}. Moreover, there are two types of rotations. If only one coordinate system is used and the vector is rotated, i.e., $\mathbf{r}' = R\mathbf{r}$ where $\mathbf{r}$ is the old point and $\mathbf{r}'$ is the point after rotation. Such an interpretation is called the active point of view. The other point of view is the passive viewpoint, where the coordinate axis is rotated, while the point remains the same. Almost most of the rotations used in this paper are viewed in the active point of view.

Consider a vector $\mathbf{B}$ and let it be rotated by R. From the properties, $|R\mathbf{B}|^2 = |B|^2 \to B^T R^T R B = B^T B$, where we represent vectors as column vectors and its dual as rows. Since this holds for arbitrary $\mathbf{B}$, $R^T R = I \to R^T = R^{-1}$. Hence R are orthogonal matrices. Also the set of all rotation matrices R for a group as they follow the axioms of a group and are called O(3), 3 indicates dimensionality. Moreover, from the finite dimensionality we have $RR^T = R^T R = I$. Hence $(det(R))^2 = 1 \to det(R) = \pm 1$. $\det(R) = +1$ are proper rotations and $\det(\mathrm{R}) = -1$ are improper rotations. Now a special group SO(3), (S - for special) can be constructed which is the set of all rotation matrices with determinant 1. Unfortunately the other set of matrices with determinant -1 do not form a group as the lack the identity in their set. Also $SO(3) \subset O(3)$.

R can be parameterized either by axis-angle or by using Euler angles. Any rotation can be parameterized by an axis of rotation ($\hat{\mathbf{n}}$, a unit vector) and an angle of rotation (θ), and R is denoted as $R(\hat{\mathbf{n}}, \theta)$. Geometrically it easy to understand that rotation about the same axis commute which implies,

$$R\left(\hat{\mathbf{n}}, \theta_1\right) R\left(\hat{\mathbf{n}}, \theta_2\right) = R\left(\hat{\mathbf{n}}, \theta_2\right) R\left(\hat{\mathbf{n}}, \theta_1\right) = R\left(\hat{\mathbf{n}}, \theta_1 + \theta_2\right) \tag{1}$$

Consider an infinitesimal near identity rotation, R can be expressed as, $R = 1 + \epsilon A$, where A is an anti symmetric matrix which will be shortly shown and ϵ is an infinitesimal angle. Since $R = 1 + \epsilon A$, its inverse would rotate in the opposite direction to bring the point to the same position. Hence $R^{-1} = R^T = 1 - \epsilon A^T$. From eq. (1),$RR^T = I = (1 + \epsilon A)(1 - \epsilon A)$ On neglecting $\theta(\epsilon^2)$ square terms fives,

$$A + A^T = 0 \tag{2}$$

The anti-symmetric matrix A can be parameterized as follows,

$$A = \begin{pmatrix} 0 & -a_3 & a_2 \\ a_3 & 0 & -a_1 \\ -a_2 & a_1 & 0 \end{pmatrix} = \sum_{i=1}^{3} a_i j_i \tag{3}$$

,where $(j_i)_{jk} = -\epsilon_{ijk}$ and hence 3×3 matrices. These j matrices have the following properties, $[(\mathbf{a}.\mathbf{j})\mathbf{u}]_i = (\mathbf{a}.\mathbf{j})_{ij} u_j = a_k (j_k)_{ij} u_j = -a_k \epsilon_{kij} = (\mathbf{a} \times \mathbf{u})_i$

$$[(\mathbf{a}.\mathbf{j})\mathbf{u}] = (\mathbf{a} \times \mathbf{u}) \tag{4}$$

Similarly it can be shown,

$$[j_i, j_j] = \epsilon_{ijk} j_k \to [\mathbf{a}.\mathbf{j}, \mathbf{b}.\mathbf{j}] = (\mathbf{a} \times \mathbf{b}).\mathbf{j} \tag{5}$$

In general $[R_1, R_2] \neq 0$, i.e. rotations don't commute. But they do if they are about the same axis. Hence R for finite rotations can be obtained as,

$$R = \lim_{N \to \infty} \left(I + \frac{\theta}{N} (\hat{\mathbf{n}}.\mathbf{j}) \right)^N$$

, where $\epsilon = \dfrac{\theta}{N}$. This gives the expression from the well known formula in limits (can also be extended to matrices),

$$R(\hat{\mathbf{n}}, \theta) = e^{\theta(\hat{\mathbf{n}}.\mathbf{j})} \tag{6}$$

Another property of R in proper rotations is,

$$R(\mathbf{a} \times \mathbf{u}) = (R\mathbf{a}) \times (R\mathbf{u}) \tag{7}$$

From eq. (4) both sides can be re-written as,

$$R(\mathbf{a}.\mathbf{j})\mathbf{u} = [(R\mathbf{a}).\mathbf{j}]R\mathbf{u}$$

Let $\mathbf{u} = R^{-1}\mathbf{v}$. Therefore,

$$R(\mathbf{a}.\mathbf{j})R^{-1} = [(R\mathbf{a}).\mathbf{j}]$$

With few substitutions, this can be written in a convenient form. Let $\mathbf{a} = \theta\hat{\mathbf{n}}$ and $R = R_0$.

$$R_0(\theta\hat{\mathbf{n}}.\mathbf{j})R_0^{-1} = \theta(R_0\hat{\mathbf{n}}).\mathbf{j}$$

On exponentiating both sides and by mere expansion, it is easy to find,

$$R_0 R(\hat{\mathbf{n}}, \theta) R_0^T = R\left(R_0\hat{\mathbf{n}}, \theta\right) \tag{8}$$

Another elegant way of parameterizing rotations are using Euler angles. When R acts on $\hat{\mathbf{z}}$ it gives $\widehat{\mathbf{z}'}$, i.e. $R\hat{\mathbf{z}} = \widehat{\mathbf{z}'}$. Consider another rotation operator $R_1 = R(\hat{\mathbf{z}}, \alpha)R(\hat{\mathbf{y}}, \beta)$ which also satisfies $R_1\hat{\mathbf{z}} = \hat{\mathbf{z}}'$ At max R and R_1 can differ another rotation about the $\widehat{\mathbf{z}'}$, i.e. $R = R\left(\hat{\mathbf{z}}', \gamma\right) R_1 = R\left(\hat{\mathbf{z}}', \gamma\right) R(\hat{\mathbf{z}}, \alpha)R(\hat{\mathbf{y}}, \beta)$. It would be practical to represent all the rotations with respect to the same axis.

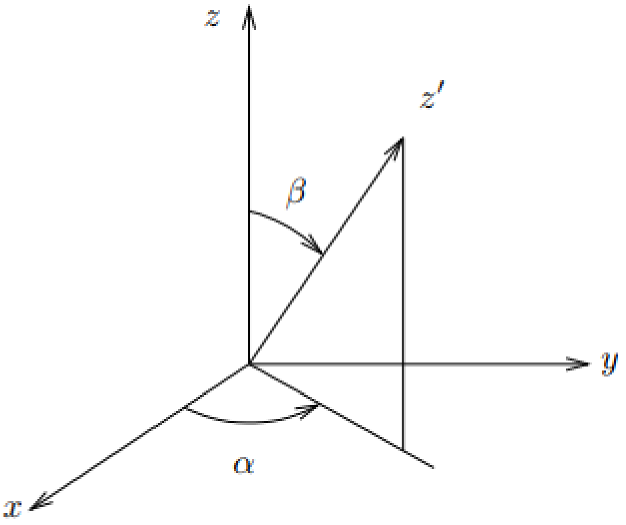

Figure 1. The two angles α and β which determine z' after rotation

$$R(\alpha, \beta, \gamma) = R_1 R1^{-1} R(\hat{\mathbf{z}}\prime, \gamma) R_1$$

From eq. (8) $R_1^{-1}R(\widehat{\mathbf{z}'}, \gamma)R_1 = R(R^{-1}\widehat{\mathbf{z}'}, \gamma) = R(\hat{\mathbf{z}}, \gamma)$

$$R(\alpha, \beta, \gamma) = R(\hat{\mathbf{z}}, \alpha)R(\hat{\mathbf{y}}, \beta)R(\hat{\mathbf{z}}, \gamma) \tag{9}$$

This is the zyz convention of Euler angle representation of rotation.

III. ROTATION IN QUANTUM MECHANICS

A quantum state can be represented with a state vector $|\psi\rangle$ and the state vector can be rotated. The state vector is an element of Hilbert space $\mathcal{H}$. The rotation of such states can be parameterized by R, i.e. $R \mapsto U(R)$, where $det(R) = 1$. Similarly U(R) has to satisfy few properties. Firstly U(R) is unitary, i.e. $U(R)^{-1} = U^\dagger(R)$, as a particle cannot be lost by rotation and $R = I$, no rotation, implies $U(R) = I$. $U(R)$ reproduces the multiplication law as in $\mathbb{R}^3$, i.e. $U\left(R_1\right)U\left(R_2\right) = U\left(R_1R_2\right)$. This implies $U\left(R^{-1}\right) = U^\dagger(R)$. To obtain a concise form of U, it is Taylor expanded.

$$U(\boldsymbol{\theta}) = 1 + \sum_k \left.\frac{\partial U(\boldsymbol{\theta})}{\partial\theta_k}\right|_{\boldsymbol{\theta}=0} \theta_k \tag{10}$$

, where ($\boldsymbol{\theta} = \theta\hat{\mathbf{n}}$, $U(\boldsymbol{\theta}) := U(R)$ and $I = U(0)$. Defining $J_k = i\hbar \left.\frac{\partial U(\boldsymbol{\theta})}{\partial\theta_k}\right|_{\boldsymbol{\theta}=0}$, the generators of rotation. Finite rotation can be obtained by taking products of it to yield.

$$U(\hat{\mathbf{n}}, \theta) = \exp\left(-\frac{i}{\hbar}\theta\hat{\mathbf{n}}.\mathbf{J}\right) \tag{11}$$

As $UU^\dagger$ it can be seen that as expected, $J_k = J_k^\dagger$. Also similar expression like in classical rotations once could also obtain the following expressions.

$$\left[\hat{\mathbf{n}}_1.\mathbf{J}, \hat{\mathbf{n}}_2.\mathbf{J}\right] = i\hbar\left(\hat{\mathbf{n}}_1 \times \hat{\mathbf{n}}_2\right).\mathbf{J} \tag{12}$$

Which imply, $[J_i, J_j] = i\hbar\epsilon_{ijk}J_k$

IV. ROTATION OF QUANTUM STATES AND WIGNER D-MATRIX

When the system under study has angular momentum encoded in its dynamics either via orbital or spin, it is represented in the Standard Angular Momentum Basis, denoted by $|\gamma jm\rangle$, where j, m are angular momentum quantum numbers. The necessity of introducing of γ as one of the quantum numbers, is to resolve any degeneracy if it exist, i.e.γ represents the quantum numbers or eigenvalues of the other operators in the Complete set of Commuting Observables. While few angular momentum operators (J's) are diagonal in m, all of them including $J_\pm, J_x$ etc are diagonal in γ and m. Hence rotations will be diagonal in γ, j. Thus the rotation operator between two Standard Angular momentum Basis define the D matrices as,

$$\left\langle\gamma jm\left|U(\hat{\mathbf{n}}, \theta)\right|\gamma' j' m'\right\rangle = \delta_{\gamma\gamma'}\delta_{jj'}D^j_{mm'}(\hat{\mathbf{n}}, \theta) \tag{13}$$

These matrices are called as Wigner D-matrices (D - Drehung, rotation in German). These D-matrices are the unitary matrix representation of $U(R)$ and follow

$$\left(D^j_{mm'}(R)\right)^{-1} = \left(D^{j*}_{mm'}(R)\right)^T = \left(D^{j*}_{m'm}(R)\right) \tag{14}$$

In Euler angle form, $U(\hat{\mathbf{n}},\theta) = U(\alpha,\beta,\gamma) = U(\hat{\mathbf{z}},\alpha)U(\hat{\mathbf{y}},\beta)U(\hat{\mathbf{z}},\gamma)$. Now introducing the resolution of Identity twice and as the operators are diagonal in J, the expression $\langle jm|U(\alpha,\beta,\gamma)|jm'\rangle$ reduces to,

$$\sum_{m_1m_2} \langle jm|U(\hat{\mathbf{z}},\alpha)|jm_1\rangle \langle jm_1|U(\hat{\mathbf{y}},\beta)|jm_2\rangle \langle jm_2|U(\hat{\mathbf{z}},\gamma)|jm'\rangle$$

Defining $d^j_{mm'}(\beta) = \langle jm|U(\hat{\mathbf{y}},\beta)|jm'\rangle$, which is called the reduced rotation matrix. The two matrices are related as,

$$D^j_{mm'}(\alpha,\beta,\gamma) = e^{-i(m\alpha - m'\gamma)}d^j_{mm'}(\beta) \tag{15}$$

V. SPHERICAL HARMONICS AND WIGNER *D*-MATRICES

The spherical harmonic $Y_{lm}(\theta,\phi)$ are defined with respect the z-axis. Sometimes calculations are easier if they were defined on some other axis, i.e. a rotated version of Y_{lm}. Since the spherical harmonics for a completed basis for the functions on a unit sphere one can represent the rotated spherical harmonics in terms of the spherical harmonics. The spherical harmonics are defined as,

$$Y_{lm}(\hat{\mathbf{r}}) = \langle\hat{\mathbf{r}}|lm\rangle = \langle\theta,\phi|lm\rangle \tag{16}$$

Our expectation of the rotation operator on the $|\mathbf{x}\rangle$ of the wavefunction, where $\mathbf{x}$ are the non-denumerable basis, is

$$U(R)|\mathbf{x}\rangle = |R\mathbf{x}\rangle \tag{17}$$

which is very similar to the translation operation on such states,$T(\mathbf{a})|\mathbf{x}\rangle = |\mathbf{x}+\mathbf{a}\rangle$. The state $|\psi\rangle$ in these basis are,

$$|\psi\rangle = \int d^3\mathbf{x}|\mathbf{x}\rangle\langle\mathbf{x}|\psi\rangle = \int d^3\mathbf{x}|\mathbf{x}\rangle\psi(\mathbf{x}) \tag{18}$$

Letting $U(R)$ act on eq. (18) and defining, $|\psi'\rangle = U(R)|\psi\rangle$

$$|\psi'\rangle = \int d^3\mathbf{x}|R\mathbf{x}\rangle\psi(\mathbf{x})$$

Making a change of variables $\mathbf{x}\to R\mathbf{x}$, the Jacobian of the transformation makes $d^3\mathbf{x}'\to(\det R)d^3\mathbf{x} = d^3\mathbf{x}$, as $\det R = 1$.This yields,

$$\psi'(\mathbf{x}) = (U(R)\psi)(\mathbf{x}) = \psi\left(R^{-1}\mathbf{x}\right) \tag{19}$$

, which is again similar to translations, $(T(\mathbf{a})\psi)(\mathbf{x}) = \psi(\mathbf{x}-\mathbf{a})$. With this the rotation of Y_{lm} can be obtained. The rotated Y_{lm} is given by,

$$\left(U(R)Y_{lm}\right)(\hat{\mathbf{r}}) = \langle\hat{\mathbf{r}}|U(R)|lm\rangle$$

From eq. (19) and inserting the resolution of the identity (and sinice the rotation operator is diagonal in 'l'),

$$Y_{lm}\left(R^{-1}\hat{\mathbf{r}}\right) = \sum_{m'}\langle\hat{\mathbf{r}}|lm'\rangle\langle lm'|U(R)|lm\rangle$$

Hence, from eq. (13) and eq. (16),

$$\left(U(R)Y_{lm}\right)(\hat{\mathbf{r}}) = Y_{lm}\left(R^{-1}\hat{\mathbf{r}}\right) = \sum_{m'}Y_{lm'}(\hat{\mathbf{r}})D^l_{m'm}(R) \tag{20}$$

Equation (20) relates Y_{lm} at a point as a linear combination of others. Another useful expression can be extracted from eq. (20). Any point $\hat{\mathbf{r}}$ can be obtained by rotating the z-axis by suitable rotation parameterized by the polar angles as Euler angles of rotation, i.e.,

$$R(\phi,\theta,0)\hat{\mathbf{z}} = \hat{\mathbf{r}} \tag{21}$$

Letting $\hat{\mathbf{r}} = \hat{\mathbf{z}}$,

$$Y_{lm}\left(R^{-1}\hat{\mathbf{z}}\right) = \sum_{m'}Y_{lm'}(\hat{\mathbf{z}})D^l_{m'm}(R)$$

Let $R^{-1}\to R$

$$Y_{lm}\left(R\hat{\mathbf{z}}\right) = \sum_{m'}Y_{lm'}(\hat{\mathbf{z}})D^l_{m'm}(R^{-1})$$

From eq. (21)

$$Y_{lm}\left(\hat{\mathbf{r}}\right) = \sum_{m'}Y_{lm'}(\hat{\mathbf{z}})D^l_{m'm}(R) \tag{22}$$

Since the the spherical harmonics in terms of the associated Legendre polynomials with normalization are given by,

$$Y_{lm}(\theta,\phi) = (-1)^m\sqrt{\frac{2l+1}{4\pi}\frac{(l-m)!}{(l+m)!}}e^{im\phi}P_{lm}(\cos\theta); m\geq 0 \tag{23}$$

$$Y_{l,-m}(\theta,\phi) = (-1)^m Y_{lm}(\theta,\phi)^* \tag{24}$$

and since $P_{lm}(cos\theta)$ vanish for $\theta = 0$ (+ve z-axis) unless $m = 0$. This yields,

$$Y_{lm}(\hat{\mathbf{z}}) = \sqrt{\frac{2l+1}{4\pi}}\delta_{m0} \tag{25}$$

Hence from eq. (22) and eq. (25),

$$Y_{lm}(\theta,\phi) = \sqrt{\frac{2l+1}{4\pi}}D^{l*}_{m0}(\phi,\theta,0) \tag{26}$$

Other helpful relations between Y_{lm} and the Wigner D-matrices can be obtained while consider tensor product between two angular momentum spaces. Consider the rotation of the reducible state $U\left|j_1j_2m_1m_2\right\rangle = \left(U_1\left|j_1m_1\right\rangle\right)\left(U_2\left|j_2m_2\right\rangle\right)$, where $U_1 = e^{\left(\frac{-i}{\hbar}\theta\hat{\mathbf{n}}.J_1\right)}$, $U_2 = e^{\left(\frac{-i}{\hbar}\theta\hat{\mathbf{n}}.J_2\right)}$, $U := U_1\otimes U_2$. To the left hand side introducing the resolutions of the identity in the respective space yields for example, $U_1|j_1m_1\rangle = \sum_{m_1'}|j_1m_1'\rangle D^{j_1}_{m_1'm_1}$. Similarly introducing the identity on the right side using the standard basis gives the Clebsch Gordan coefficient and the D matrix as,

$$U|j_1j_2m_1m_2\rangle = \sum_{jmm'} |jm'\rangle\, D^j_{m'm}\, \langle jm|j_1j_2m_1m_2\rangle$$

Acting with $\langle j_1j_2m_1'm_2'|$ on both sides yields,

$$D^{j_1}_{m_1m_1'}\, D^{j_2}_{m_2m_2'} = \sum_{jmm'} \langle j_1j_2m_1m_2|jm\rangle\, D^j_{mm'}\, \langle jm'|j_1j_2m_1'm_2'\rangle \tag{27}$$

Setting $j_1 = l_1, j_2 = l_2, j = l, m_1' = m_2' = 0 \to m_1' + m_2' = m' = 0$(for other combinations the Clebsch-Gordan coefficients are 0) in eq. (27) and taking complex conjugate gives along with eq. (26),

$$\begin{aligned} Y_{l_1m_1}(\theta,\phi)Y_{l_2m_2}(\theta,\phi) = &\sum_{lm} \sqrt{\frac{(2l_1+1)\,(2l_2+1)}{4\pi(2l+1)}} \\ &\times Y_{lm}(\theta,\phi)\,\langle l0|l_1l_200\rangle\,\langle l_1l_2m_1|lm\rangle \end{aligned} \tag{28}$$

Equation (28) is called the three-Y_{lm} formula. Multiplying both sides by $Y^*_{l_3m_3}$ and integrating over solid angle yields from orthogonality of the spherical harmonics,

$$\begin{aligned} \int d\Omega Y^*_{l_3m_3} Y_{l_1m_1} Y_{l_2m_2} = &\sqrt{\frac{(2l_1+1)\,(2l_2+1)}{4\pi\,(2l_3+1)}} \\ &\langle l_3m_3|l_1l_2m_1m_2\rangle\,\langle l_1l_200|l_30\rangle \end{aligned} \tag{29}$$

VI. WIGNER-ECKART THEOREM

The Wigner-Eckart Theorem is widely used to calculate possible transitions which help in determining selection rules in transitions. As state vectors transform under rotations so do Operators. This can be understood as follows. Operators can be represented in matrix form under certain basis which helps in understanding the properties of the operator. Rotation yields another set of basis and a similarity transformation is performed in it to obtain its equivalent representation in the new basis. Hence it is worthwhile to study the behaviour of operators under rotation. Let $|\psi\rangle$ be a state and $|\psi'\rangle = U(R)|\psi\rangle$ be the rotated state. Let $\mathcal{O}$ be an operator and $\mathcal{O}'$ the rotated operator. By demanding the expectation values of the rotated states with the rotated operator to be equal to initial states with original operator, $\langle\psi'|\mathcal{O}'|\psi'\rangle = \langle\psi|\mathcal{O}|\psi\rangle \to \langle\psi|U^\dagger(R)\mathcal{O}'U(R)|\psi\rangle = \langle\psi|\mathcal{O}|\psi\rangle$, which is true for any $|\psi\rangle$,

$$\mathcal{O}' = U(R)\mathcal{O}U^\dagger(R) \tag{30}$$

, which can be considered as the definition of a rotated operators. Based on the behaviour under rotations operators can be classified as follows

1. Scalar Operator: An operator invariant under rotation, i.e. $U(R)KU^\dagger(R) = K$. Letting U to be infinitesimal rotation yields $[J_i, K] = 0; i = 1, 2, 3.$
2. Vector Operator: A collection of three operators cannot be called a Vector operator. It has to satisfy transformation properties as in classical mechanics (say contravariant or covariant vectors). Demanding the expectation value of a vector operator to behave as vector of numbers under rotation, i.e. $\langle\psi'|\mathbf{V}|\psi'\rangle = R\langle\psi|\mathbf{V}|\psi\rangle$. Again considering infintesimal rotation yields, $[J_i, V_j] = i\hbar\epsilon_{ijk}V_k$
3. Tenor Operator : Similarly a Tensor operator of rank 2 transforms as, $U(R)T_{ij}U^\dagger(R) = \sum_{kl} T_{kl}R_{ki}R_{lj}$

A. Spherical Basis

There exists another equivalent way of representing vectors in 3-d Euclidean space which are called spherical basis which dramatically simplifies problems in many scenarios. Let the old Cartesian basis be from now denoted as, $\hat{\mathbf{c}}_1 = \hat{\mathbf{x}}; \quad \hat{\mathbf{c}}_2 = \hat{\mathbf{y}}; \quad \hat{\mathbf{c}}_3 = \hat{\mathbf{z}}$, and the spherical basis are,

$$\hat{\mathbf{e}}_1 = -\frac{\hat{\mathbf{x}} + i\hat{\mathbf{y}}}{\sqrt{2}}; \quad \hat{\mathbf{e}}_0 = \hat{\mathbf{z}}; \quad \hat{\mathbf{e}}_{-1} = \frac{\hat{\mathbf{x}} - i\hat{\mathbf{y}}}{\sqrt{2}} \tag{31}$$

The inner product between the basis of the vector and it covectors is summarized by, $\hat{\mathbf{e}}_q.\hat{\mathbf{e}}^*_{q'} = \delta_{qq'}$. The components of vector $\mathbf{V}$ are, $V_q = \hat{\mathbf{e}}_q.\mathbf{V}$. Hence the vector in spherical basis is,

$$\mathbf{V} = \sum_q \hat{\mathbf{e}}^*_q V_q \tag{32}$$

Identity is given by the outer product of the basis with its dual and summed, i.e. $I = \sum_q \hat{\mathbf{e}}^*_q\hat{\mathbf{e}}_q$ From the table of Y_{lm} it can be observed,

$$rY_{1\pm1}(\theta,\phi) = \mp r\sqrt{\frac{3}{8\pi}}\sin\theta e^{\pm i\phi} = \mp\sqrt{\frac{3}{4\pi}}\left(\frac{x \pm iy}{\sqrt{2}}\right) \tag{33}$$

$$rY_{10}(\theta,\phi) = r\sqrt{\frac{3}{4\pi}}\cos\theta = \sqrt{\frac{3}{4\pi}}(z) \tag{34}$$

The right hand comprises of the spherical components x_q of the position vector $\mathbf{x}$. These expressions come in handy while calculating matrices elements of say dipole operator which sis $\mathbf{d} = -e\mathbf{x}$. Calculating these elements are easier in spherical basis than Cartesian with the help of the three-Y_{lm} formula. The expression $\langle nlm|\mathbf{x}|n'l'm'\rangle$ is calculated separately for each x_q as,

$$\begin{aligned} \langle nlm\,|x_q|\,n'l'm'\rangle = &\int_0^\infty r^2 dr R^*_{nl}(r) r R_{n'l'}(r) \\ &\times \sqrt{\frac{4\pi}{3}}\int d\Omega Y^*_{lm}(\theta,\phi)Y_{1q}(\theta,\phi)Y_{l'm'}(\theta,\phi) \end{aligned} \tag{35}$$

The radial integral is simplified using Clebsh-Gordan coefficients and eq. (28). So it easy to see that transitions which do not satisfy $m' = m + q$ do no occur under dipole approximation.

Moving from $\mathcal{H} \rightarrow \mathbb{R}^3$, the rotation operators become $U(R) \rightarrow R$, as orthogonal matrices are also unitary. Previously the generators J were extracted from $U(R)$. For infinitesimal rotation it was give, $U(\hat{\mathbf{n}}, \theta) = 1 - i\theta\hat{\mathbf{n}}.\mathbf{J}$, where $\frac{1}{\hbar}$ is absorbed by J making it now dimensionless. This $U(R)$ consisting of dimensionless generator on comparison with $R(\hat{\mathbf{n}}, \theta) = 1 + \theta\hat{\mathbf{n}}.\mathbf{j}$ for infinitesimal can define,

$$\mathbf{J} = i\mathbf{j} \tag{36}$$

Initially j_i's were antisymmetric. Hence ij_i are Hermitian. Also on squaring it can be found, $\sum_{i=1}^{3} j_i^2 = j^2 = 2I_{3\times3}$. Hence all vectors of normal space are eigenvectors with eigenvalues 2. Since $\hbar$ was absorbed in the definition it can be written as $j^2\mathbf{x} = 2\mathbf{x} =$ j(j+1), were j = 1. Therefore we can construct an irreducible space with j = 1 in the normal 3-d space. From the set of $\{j_i\}$ we can also construct the j_+, j_- operators and the spherical basis follow properties very similar to standard angular momentum basis like,i.e. $j_3\hat{\mathbf{e}}_q = q\hat{\mathbf{e}}_q; q = 0, \pm1$ and similarly for $j\pm$ (without $\hbar$). Also as extension of eq. (13),

$$\left(\hat{\mathbf{e}}_{q'}^*, R\hat{\mathbf{e}}_q\right) = D_{q'q}^1(R) \tag{37}$$

B. Reducible and Irreducible Operators

The space of operator themselves form a vector space and can be classified into orthogonal subspace. The scalar operator spans a 1-d space of operators. Hence a irreducible space of dimension one. From the definition of a vector operator it can be shown that, $U(R)V_iU^\dagger(R) = \sum_j V_jR_{ji}$, i.e. rotating a vector of operator gives a linear sum of the components its components where each component itself is operator. Such vector of operators constitute a irreducible space of dimensionality = 3. A tensor of operator of rank 2, T as outer product of 2 vector operators, $\mathbf{V}, \mathbf{W}$, $T_{ij} = V_iW_j$. Even though V, W are separately irreducible their product is reducible analogous to the product $|j_1m_1\langle, ||j_2m_2\langle$. It is easy to verify that the trace T_{ii} is a space of dim = 1. The antisymmetric operator constructed from T, $T_{[ij]} = \frac{1}{2}(T_{ij} - T_{ji})$ constitute a space of dim = 3. The remaining part of T is its symmetric part without its trace which is $\frac{1}{2}(T_{ij} + T_{ji}) - \frac{1}{3}\delta_{ij}Tr(T)$.An important thing to be notes is that the dimension of the space was divided into $9 = 1 + 3 + 5$ which strikes the similarity between $1 \otimes 1 = 0 \oplus 1 \oplus 2$ in standard angular momentum basis.

In general while taking product of two tenors operator, their ranks play role analogous to l(only integers) and the can be broken down to irreducible subspace in the spherical basis such that under rotations,

$$UT_q^kU^\dagger = \sum_{q'} T_{q'}^k D_{q'q}^k(U) \tag{38}$$

, where k is analogous to j and q is analogous to m. Hence the tensor operator T^k has $2k + 1$ components T_q^k. This is similar to $U|\gamma jm\rangle = \sum_{m'} |\gamma jm'\rangle \, D_{m'm}^j$. A scalar operator $K = T_0^0$ under rotation in this notation $U(R)T_0^0U^\dagger(R) = T_0^0D_{00}^0(R) = T_0^0$ satisfies its properties. Similarly a vector operator (V) can be written as $T_1^1 := V_q = \hat{\mathbf{e}}_q.\mathbf{V}$ under rotation rotation $U(R)V_qU(R)^\dagger = \hat{\mathbf{e}}_q.\left(R^{-1}\mathbf{V}\right) = (R\hat{\mathbf{e}}_q) \cdot \mathbf{V} = \sum_{q'} V_{q'}D_{q'q}^1(R)$, (eq. (37). Also it is easy to show another analogy between these irreducible operators spaces and $|jm\rangle$ from the expression and definition of D matrices. $[J_z, T_q^k] = \hbar qT_q^k$, $[J_\pm, T_q^k = \left[J_\pm, T_q^k\right] = \hbar\sqrt{(k \mp q)(k \pm q + 1)}T_{q\pm1}^k] =$ etc.. Other similar commutator relations to resemble the action of the action of J on $|jm\rangle$. Also the tensor product of two spaces with standard angular momentum basis $|j_1m_1\rangle \otimes j_2m_2\rangle$ are standard angular momentum basis of the tensored space. The irreducible space of this new space is obtained with the help of Clebsch-Gordan coefficients. Similarly in the case of construction of a tensor operator from to two tensor operators X and Y can be decomposed into irreducible space of operators as,

$$X_{q_1}^{k_1}Y_{q_2}^{k_2} = \sum_{kq} T_q^k \, \langle kq|k_1k_2q_1q_2\rangle \tag{39}$$

The Wigner-Eckart Theorem states that the matrix element of irreducible operator between two standard angular momentum basis can be simplified into a product of reduced matrix element and Clebsch-Gordan coefficients. The magnetic quantum number's dependence is taken care by the Clebsch-Gordan coefficients.

$$\left\langle \gamma'j'm' \left| T_q^k \right| \gamma jm \right\rangle = \left\langle \gamma'j' \left\| T^k \right\| \gamma j \right\rangle \langle j'm'|jkmq\rangle \tag{40}$$

The Clebsh-Gordan coefficients take care of the magnetic quantum number. The other quantum number's dependence are taken care by the reduced matrix element. To prove this theorem let us consider the action of T_q^k on a state $|\gamma jm\rangle$. Let a rotation operator U act on it.

$$U\left(T_q^k|\gamma jm\rangle\right) = UT_q^kU^\dagger U|\gamma jm\rangle \tag{41}$$

From eq. (38) and eq. (13)

$$\sum_{q'm'} T_{q'}^k D_{qq'}^k D_{mm'}^k |\gamma jm\rangle \tag{42}$$

Hence the state $T_q^k|\gamma jm\rangle$ has the representation of $k \otimes j$ space of angular momentum. Therefore $T_q^k|\gamma jm\rangle$, transforms like a state vector in $k \otimes j$ space. There are many ways to prove the Wigner-Eckart theorem. But proving them using the commutation relation as is Rose is one elegant way. Since $[J_z, T_q^k] = \hbar qT_q^k$ and other analogous commutators similar to their action on kets hold, the matrix elements of the commutator with J_z yield,

$$(m' - m - M)\,\langle j'm'|T_q^k|jm\rangle = 0 \tag{43}$$

Hence, $\langle j'm'|T_q^k|jm\rangle = 0$ unless $m' = q + m$. Similarly using the commutator $[J_\pm, T_q^k]$,

$$\langle j'm'|J_\pm T_q^k|jm\rangle - \langle j'm'|T_q^kJ_\pm|jm\rangle = \hbar\Gamma_\pm(k, q)\langle j'm'|T_{q\pm1}^k|jm\rangle \tag{44}$$

, where $\Gamma_{\pm}(k,q) = \sqrt{(k\mp q)(k\pm q+1)} \equiv \sqrt{j(j+1)-m(m\pm 1)}$.

$$\begin{aligned}\Gamma_{\mp}(j',m')\langle j'm'|T^k_q|jm\rangle - \Gamma_{\pm}(j,m)\langle j'm'|T^k_q|jm\rangle \\ = \Gamma_{\mp}(k,q)\langle j'm'|T^k_{q\pm1}|jm\rangle\end{aligned} \tag{45}$$

The three terms in the above equation have 3 matrix elements and each term according to eq. (43) give the same result, i.e. $,m' = q+m\pm 1$. To understand eq. (45) better consider the tensor product of 2 spaces,$k\otimes j$. The standard angular momentum basis are given by,

$$|j'm'\rangle = \sum_{mq} |jkmq\rangle(\langle jkmq|j'm'\rangle) \tag{46}$$

, where the term in parenthesis are the Clebsch Gordan coefficients, denoted hereafter as in rose as $C\,(jkj';mkm')$. The term in the parenthesis are 0, unless, $m' = m+q$ and $j'\epsilon\{j+q, j+q-1, ..., |j-q|\}$. Using the raising and lowering operators on both sides, $J'_{\mp} = J_{\mp} + L_{\mp}$,

$$\begin{aligned}\Gamma_{\mp}(j',m')|j'm'\mp 1\rangle = & \textstyle\sum_{mq} \begin{array}{l}\Gamma_{\mp}(j,m)|jk(m\mp 1)q\rangle \\ (\langle jkmq|j'm'\rangle)\end{array} \\ + & \textstyle\sum_{mq} \begin{array}{l}\Gamma_{\mp}(k,q)|jkmq\rangle \\ (\langle jkm(q\mp 1)|j'm'\rangle)\end{array}\end{aligned} \tag{47}$$

Replacing left hand side by eq. (46) and replacing the dummy summation indices in the right hand side as and replacing $m\mp 1$ with μ and q with λ in the first term and m with μ and $q\mp 1$ with λ in the other term gives,

$$\begin{aligned}\sum_{\mu\lambda}\Gamma_{\mp}(j',m')|jk\mu\lambda\rangle(\langle jk\mu\lambda|j'm'\rangle) = \\ \sum_{\mu\lambda}\Gamma_{\pm}(j,\mu)|jk(\mu)\lambda\rangle(\langle jk\mu\lambda|j'm'\rangle) \\ +\sum_{\mu\lambda}\Gamma_{\pm}(k,\lambda)|jk\mu\lambda\rangle(\langle jk\mu\lambda|j'm'\rangle)\end{aligned} \tag{48}$$

Equating coefficients of $\mu = m$ and $\lambda = q$, and moving the first term in the right to left hand side,

$$\begin{aligned}\Gamma_{\mp}(j',m')|jk\mu\lambda\rangle(\langle jk\mu\lambda|j'm'\rangle) - \\ \Gamma_{\pm}(j,\mu)|jk(\mu)\lambda\rangle(\langle jk\mu\lambda|j'm'\rangle) \\ = \Gamma_{\pm}(k,\lambda)|jk\mu\lambda\rangle(\langle jk\mu\lambda|j'm'\rangle)\end{aligned} \tag{49}$$

The above equation is very similar to eq. (45), where each individual term vanishes unless, $,m' = q+m\pm 1$. This extracts the magnetic quantum numbers' dependence as Clebsch Gordan coefficients. This implies that eq. (40) and the center idea is that the matrix elements are zero unless $m' = m+q$ and $j'\epsilon\{j+q, j+q-1, ..., |j-q|\}$.

C. Projection theorem

While studying Time independent perturbation in weak-field Zeeman Effect, to remove the magnetic quantum numbers' dependence between matrix elements, the projection lemma was used. This can be proved using the Wigner Eckart Theorem. The matrix element of a vector operator $\mathbf{V}$ is given by,

$$\left\langle \gamma' jm' \left| V^1_q \right| \gamma jm\right\rangle = \frac{\langle\gamma' jm'|\mathbf{J}.\mathbf{V}|\gamma jm\rangle}{\hbar^2 j(j+1)}\left\langle \gamma jm' \left| J_q\right| \gamma jm\right\rangle \tag{50}$$

In spherical basis, $\mathbf{J}\cdot\mathbf{V} = J_0V_0 - \frac{1}{2}(J_+V_- + J_-V_+)$. Consider,

$$\begin{aligned}\left\langle \gamma' jm\right| \mathbf{J}.\mathbf{V}\left|\gamma jm\right\rangle &= m\hbar\left\langle \gamma' jm\left|V_0\right|\gamma jm\right\rangle \\ &-\frac{\hbar}{2}\sqrt{j(j+1)-m(m-1)}\left\langle\gamma j(m-1)\left|V_-\right|\gamma jm\right\rangle \\ &-\frac{\hbar}{2}\sqrt{j(j+1)-m(m+1)}\left\langle\gamma j(m+1)\left|V_+\right|\gamma jm\right\rangle \\ &= c_j\left\langle\alpha', j\|\mathbf{V}\|\alpha j\right\rangle\end{aligned} \tag{51}$$

Where in the last line the Wigner Eckart theorem was used. The coefficient to the reduced matrix element should have been c_{jm}. But since $\mathbf{J}.\mathbf{V}$ is a scalar operator it would not have any m dependence. Replacing $\mathbf{V}$ by $\mathbf{J}$, it could be written as,

$$\left\langle\gamma' jm\left|\mathbf{J}^2\right|\gamma jm\right\rangle = c_j\left\langle\gamma' j\|\mathbf{J}\|\gamma j\right\rangle \tag{52}$$

These two equation can be written as,

$$\frac{\left\langle\gamma' jm'\left|V_q\right|\gamma jm\right\rangle}{\left\langle\gamma jm'\left|J_q\right|\gamma jm\right\rangle} = \frac{\langle\gamma' j\|\mathbf{V}\|\gamma j\rangle}{\langle\gamma j\|\mathbf{J}\|\gamma j\rangle} \tag{53}$$

or equivalently from eq. (51) and eq. (52) as ,

$$\frac{\left\langle\gamma' jm'\left|V_q\right|\gamma jm\right\rangle}{\left\langle\gamma jm'\left|J_q\right|\gamma jm\right\rangle} = \frac{\langle\gamma' jm|\mathbf{J}.\mathbf{V}|\gamma jm\rangle}{\langle\gamma jm|\mathbf{J}.\mathbf{J}|\gamma jm\rangle} \tag{54}$$

This can be re-written as,

$$\left\langle \gamma' jm' \left| V^1_q \right| \gamma jm\right\rangle = \frac{\langle\gamma' jm'|\mathbf{J}.\mathbf{V}|\gamma jm\rangle}{\hbar^2 j(j+1)}\left\langle \gamma jm' \left| J_q\right| \gamma jm\right\rangle \tag{55}$$

D. Transitions under dipole approximation

Let $|n'l'm'\rangle$ and $|nlm\rangle$ be two possible states. To see whether a transition can occur between these states under dipole approximation the Wigner Eckart Theorem can be used. The dipole operator is $\mathbf{d} = q\mathbf{r}$. $\mathbf{r}$ is tensor operator of rank 1. Its matrix element are easier to calculate if the operator is expanded in spherical basis, i.e. $r_q = \hat{\mathbf{e_q}}.\mathbf{r}$. Hence it ultimately reduces to calculate the matrix elements of r_q, i.e. $\langle n'l'm'|r_q|nlm\rangle$. The r_q's can be expressend in terms of spherical harmonics as in eq. (33) and eq. (34). Hence it boild down to the calculation of,

$$\int_0^\infty r^2 dr R*_{n'l'}(r)R_{nl}(r)\sqrt{\frac{4\pi}{3}}\int d\Omega Y*_{l'm'}Y_{1q}Y_{lm} \tag{56}$$

From eq. (29) this is greatly simplified as computation of the integral over angular variable is not necessary. Hence the reduced matrix element in eq. (56) is,

$$\begin{aligned}\langle n'l'||r^1||nl\rangle = \langle l100|l'0\rangle \sqrt{\frac{(2(1)+1)\,(2l+1)}{4\pi\,(2l'+1)}} \\ \int R^*_{m'l'}(r) r R_{nl}(r) r^2 dr\end{aligned} \tag{57}$$

As previously stated, the product of two irreducible tensor can be decomposed into irreducible tensor operators. This follows from the logic that $T^k_q|\gamma jm\rangle$, under rotations transform like tensor product of the angular momentum space $j \otimes k$, $|jm\rangle \otimes |kq\rangle$. The product of two irreducible operators $X^{k_1}_{q_1} Y^{k_2}_{q_2}$ transform under rotation exactly as the tensor product $|k_1q_1\rangle \otimes |k_2q_2\rangle$. Such a product can be written as combination of irreducible tensor operators $X^{k_1}_{q_1} Y^{k_2}_{q_2} = \sum_{kq} T^k_q \langle kq|k_1k_2q_1q_2\rangle$ where $k\epsilon\{|k_1-k_2|, \ldots, k_1+k_2\}$, or alternatively,

$$T^k_q = \sum_{q_1q_2} X^{k_1}_{q_1} Y^{k_2}_{q_2} \langle k_1k_2q_1q_2|kq\rangle \tag{58}$$

Rotation of such an operator yields,

$$UT^k_qU^\dagger = \sum_{q_1q_2} UX^{k_1}_{q_1}U^\dagger UY^{k_2}_{q_2}U^\dagger \langle k_1k_2q_1q_2|kq\rangle$$

From eq. (38)

$$UT^k_qU^\dagger = \sum_{q_1q_2}\sum_{q'_1q;_2} X^{k_1}_{q'_1} Y^{k_2}_{q'_2} D^{k_1}_{q'_1q_1}(U) D^{k_2}_{q'_2q_2}(U) \langle k_1k_2q_1q_2|kq\rangle \tag{59}$$

The product of two Wigner-d Matrices according to eq. (27) can be written as,

$$\begin{aligned}D^{k_1}_{q^1_1q_1}(U) D^{k_2}_{q'_2q_2}(U) = \sum_{KQQ'} \langle k_1k_2q'_1q'_2|KQ'\rangle D^K_{Q'Q}(U) \\ \langle KQ|k_1k_2q_1q_2\rangle\end{aligned} \tag{60}$$

While substituting eq. (60) in eq. (59), the term $\sum_{q_1q_2} \langle KQ|k_1k_2q_1q_2\rangle \langle k_1k_2q_1q_2|kq\rangle$ reduces to $\delta_{Kk}\delta_{Qq}$ as $\sum_{q'_1q'_2} |k_1k_2q_1q_2\rangle \langle k_1k_2q_1q_2|$ is a resolution of the identity. So the right hand side reduces to $\sum_{KQQ'} T^K_{Q'} D^K_{Q'Q} \delta_{Kk}\delta_{Qq} \rightarrow \sum_{Q'}\sum_{KQQ'} T^K_{Q'} D^K_{Q'q}$ and the right hand side $UT^k_qU^\dagger \rightarrow \sum_{q'} T^k_{q'} D^k_{q'q}(U)$. As Q', q' are just dummy summing indices both expressions are equivalent. Hence T^k_q is a irreducible tensor operator.

Example: The product of two vector operators $\mathbf{V}, \mathbf{W}$ (rank 1) can be decomposed by using the Clebsch-Gordan Coefficients as, $T^k_q = \sum_{q_1q_2} V_{q_1} W_{q_2} \langle 11q_1q_2|kq\rangle$,

$$\begin{aligned}T^{(2)}_{+2} &= \mathbf{V}_{+1}\mathbf{W}_{\pm1} \\ T^{(2)}_{\pm1} &= \frac{1}{\sqrt{2}} (\mathbf{V}_{\pm1}\mathbf{W}_0 + \mathbf{V}_0\mathbf{W}_{\pm1}) \\ T^{(2)}_0 &= \frac{1}{\sqrt{6}} (\mathbf{V}_{+1}\mathbf{W}_{-1} + \mathbf{V}_{-1}\mathbf{W}_{+1} + 2\mathbf{V}_0\mathbf{W}_0) \\ T^1_1 &= \sqrt{\frac{1}{2}} (\mathbf{V}_1\mathbf{W}_0 - \mathbf{V}_0\mathbf{W}_1)\end{aligned} \tag{61}$$

Similarly other elements can be found using the Clebsch-Gordan coefficients.

VII. DISCUSSION

The methods illustrated here are heavily used in atomic, optical, molecular Physics and also in Nuclear physics. These methods come in very handy and simplify many calculations and give deeper physical insights, in this case conservation of angular momentum, polarization of photons as in dipole transition.

ACKNOWLEDGMENTS

In writing this draft of this term paper, the book by M.E. Rose [1], Elementary theory of Angular momentum, Dover Publication was instrumental. Other usefull books were [2] [3] [4] [5]. The lecture notes of Robert Littlejohn [6] were the most elucidate notes and were of tremendous help. Few examples were taken from Prof. David Rubin's lecture notes [7]. Utmost thanks to edX and MITx for offering one of the best online certified courses to aspiring Physicist and making world class education available to everyone. This course was all possible because of the efforts of Prof. Barton Zwiebach, Prof. Joylon Bloomfield and their colossal efforts. In addition thanks to TA Mark Weitzman for clearing technical doubts and for offering guidance and TA Jim Freericks, whose suggestions were of great help in moulding this paper.

---

[1] M. E. Rose. *Elementary theory of angular momentum.* Dover Publications, 1995.

[2] V. Devanathan. *Angular Momentum Techniques in Quantum Mechanics.* Springer, 2002.

[3] D. A. Varshalovich et al. *Quantum Theory Of Angular Momemtum.* World Scientific, 1988.

[4] A. R. Edmonds. *Angular momentum in quantum physics.* Princeton University Press, 1996.

[5] J. D. Louck L. C. Biedenharn. *Angular momentum in quantum physics.* Addison-Wesley Publishing Company, 1981.

[6] Robert Littlejohn. Physics 221ab quantum mechanics, 2019. URL `http://bohr.physics.berkeley.edu/classes/221/1819/221.html`.

[7] David Rubin. Physics 6572 - fall 2011, 2011. URL `https://www.classe.cornell.edu/~dlr/teaching/p6572/`.

The Schrödinger Equation on a Branching One-Dimensional Network

Michael Garry

(Dated: June 19, 2019)

This paper explores solutions of the Schrödinger equation on a branching network of one-dimensional line intervals. The intervals can be finite or infinite. Examples of branching networks in the macroscopic world are river deltas and blood circulation systems. The linear wave equation is used to study wave propagation through such networks, and the solution methods can be applied directly to the Schrödinger equation on branching networks. A system of complex linear equations is generated for each problem. Solutions are straightforward, even for large networks. Applications include periodic potentials and some multi-dimensional problems.

I. A SOLUTION METHOD FOR THE 1-D SCHRÖDINGER EQUATION

In the first part of this paper I will describe a general approach for solving the one-dimensional Schrödinger equation that will be useful for branching networks. The time-independent Schrödinger equation on the real line for a particle with mass m is

$$\psi''(x) + [E - V(x)] \cdot \psi(x) = 0 \tag{1}$$

where Plank's constant $\hbar$, the length scale a, and the energy scale $\hbar^2/2ma^2$ are each set to unity. Let's consider 1-D potentials $V(x)$ composed of a finite number of linear segments, steps, and delta functions. The junctions between segments occur at the points

$$X_0 < X_1 < \cdots < X_n \tag{2}$$

where the endpoints X_0 and X_n can be finite or infinite. Figure 1 shows a simple example.

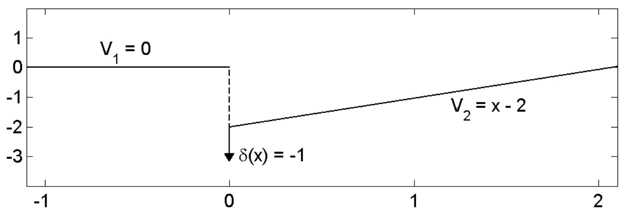

Figure 1. Potential with $n = 2$ lines. $V = 0$ from $X_0 = -\infty$ to $X_1 = 0$ where there is a step down and a delta function, followed by a a ramp extending to $X_2 = +\infty$.

There are a total of n line segments, each with a linear potential and known length $L_k, k = 1, \ldots, n$. Define the coordinate x_k on each line by $x_k = x - X_{k-1}$, so that x_k runs from 0 to L_k. The potential on line k is

$$V_k(x_k) = c_k \cdot x_k + v_k, \tag{3}$$

where $v_k = V(X_{k-1})$ and c_k is the slope. There is one exception to this prescription: If line #1 extends to $-\infty$, then we set $x_1 = x - X_1$, so that $x_1 \in (-\infty, 0]$ and $v_1 = V(X_1)$. We now have n Schrödinger equations for the n wave functions $\psi_k(x_k)$.

$$\psi_k''(x_k) + [E - V_k(x_k)] \cdot \psi_k(x_k) = 0 \tag{4}$$

The general solution on each line has the form

$$\psi_k(x_k) = a_k \cdot f_k(x_k) + b_k \cdot g_k(x_k). \tag{5}$$

where a_k and b_k are complex constants and the functions f_k and g_k are independent solutions. When $c_k = 0$ we set

$$f_k(x_k) = \exp\left(ix_k\sqrt{E - v_k}\right) \tag{6a}$$

$$g_k(x_k) = \exp\left(-ix_k\sqrt{E - v_k}\right). \tag{6b}$$

Note that $\sqrt{E - v_k}$ may be real or imaginary. If $c_k \neq 0$, then f_k and g_k are Airy functions (Zwiebach [1, Ch. 3]).

$$f_k(x_k) = \mathrm{Ai}\left(\frac{c_k \cdot x_k + v_k - E}{|c_k|^{2/3}}\right) \tag{7a}$$

$$g_k(x_k) = \mathrm{Bi}\left(\frac{c_k \cdot x_k + v_k - E}{|c_k|^{2/3}}\right) \tag{7b}$$

The coefficients a_k and b_k are determined by the conditions at the endpoints of the lines. At the interior junctions $X_k, k = 1, \ldots, n-1$ the wave functions and their derivatives must satisfy

$$\psi_k(0) - \psi_{k-1}(L_{k-1}) = 0 \tag{8a}$$

$$\psi_k'(0) - \psi_{k-1}'(L_{k-1}) = Q_k \cdot \psi_k(0) \tag{8b}$$

where Q_k is the strength of the delta function at X_k. The first equation states that $\psi(x)$ must be continuous at X_k, and the second results from integrating the Schrödinger equation across the junction. See Zwiebach [2, Ch. 11]) for the derivation.

The system (8) is a set of $2n-2$ linear equations in the $2n$ complex unknowns a_k, b_k. Two more equations are determined by the boundary conditions at X_0 and X_n. For large n most of the matrix entries of the equation are zero. Standard methods for solving such sparse linear systems are described in Saad [3] and implemented in numerical software packages such as Matlab [4].

As a concrete example, the linear equations for the potential in Figure 1 are

$$\begin{bmatrix} 1 & 0 & 0 & 0 \\ -1 & -1 & \alpha_{23} & \alpha_{24} \\ \sqrt{E} & -\sqrt{E} & \alpha_{33} & \alpha_{34} \\ 0 & 0 & 0 & 1 \end{bmatrix} \cdot \begin{bmatrix} a_1 \\ b_1 \\ a_2 \\ b_2 \end{bmatrix} = \begin{bmatrix} 0 \\ 0 \\ 0 \\ 0 \end{bmatrix} \tag{9}$$

where

$$\alpha_{23} = \mathrm{Ai}(-2-E) \tag{10a}$$
$$\alpha_{24} = \mathrm{Bi}(-2-E) \tag{10b}$$
$$\alpha_{33} = \mathrm{Ai}'(-2-E) + \mathrm{Ai}(-2-E) \tag{10c}$$
$$\alpha_{34} = \mathrm{Bi}'(-2-E) + \mathrm{Bi}(-2-E) \tag{10d}$$

The first row of Eq. (9) sets a_1 to zero because when $E < 0$ in Eq. (5) we must have $\psi_1(x_1) \to 0$ as $x_1 \to -\infty$. Similarly, the last row of Eq. (9) sets b_2 to zero because $\psi_2(x_2)$ must also go to zero as $x_2 \to +\infty$. The matrix coefficients in the second and third rows are from Eq. (8).

For there to be a nonzero solution of Eq. (9), the matrix must be singular. At least one of its singular values must therefore be zero. (See Horn [5] for background on singular value decomposition.) Figure 2 shows a plot of the two smallest singular values vs energy. The only bound state solution occurs for $E = -0.987402$. Moreover, since the second smallest singular value is not zero at E, we know that the solution is nondegenerate. Locating the zeros of the smallest singular $\sigma_1(E)$ is a convenient method for finding a valid solution of Eq. (4) and its associated energy. Also, the number of singular values which are zero at that energy indicates the level of degeneracy of that solution.

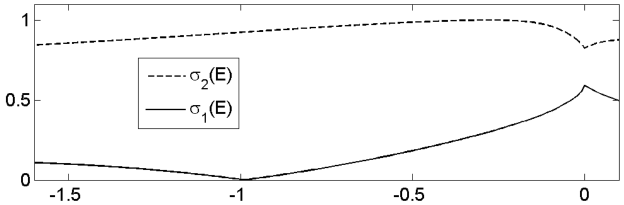

Figure 2. The two smallest singular values of the matrix in Eq. (9) as functions of energy E.

II. PERIODIC POTENTIALS

The solution method above can be applied to *periodic* potentials by considering X_0 and X_n to be the same point. A 1-D potential V is periodic if

$$V(x+L) = V(x) \tag{11}$$

for all x and a fixed L. Perhaps the simplest example of a periodic potential is $V_1 = 0$ on a single line connected at both ends to the point X_1. This line can be viewed as a circle, so we set the length $L_1 = 2\pi$. The singular values for this problem are plotted in Figure 3. They show that there are solutions for $E_n = n^2$, $n = 1, 2, \ldots$, and that there are two solutions for each value of n. This type of degeneracy is typical for periodic potentials since waves can travel in either direction around the loop.

The periodic double well potential $V_{dw}(x)$ in Figure 4 has period 2π, and Figure 5 shows that there are solutions for $E = -10$, -2.777, -0.236, 0, 0.450, 2.443, 3.577, 7.432, 8.824,... Not surprisingly, as $E \to \infty$ the energy levels for V_{dw} converge to a sequence of closely spaced pairs that approach the n^2 levels of the circle in Figure 3.

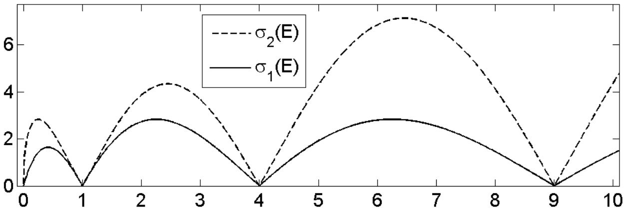

Figure 3. The singular values for the potential $V_1 = 0$ on a loop of length $L_1 = 2\pi$.

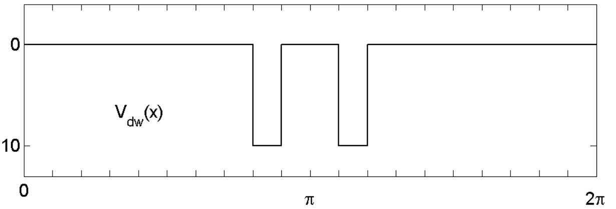

Figure 4. Double well potential with period 2π

.

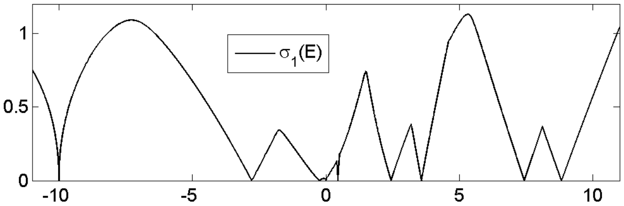

Figure 5. Smallest singular value $\sigma_1(E)$ of V_{dw}.

An interesting phenomenon emerges for periodic potentials that have sub-periods. Let's construct a new potential V_{25dw} from V_{dw} by taking $V_{25dw}(x)$ to be 25 periods of V_{dw}, so that $V_{25dw}(x)$ has period 50π. Even though $V_{25dw}(x)$ has a sub-period of 2π, in general the complex-valued wave function $\psi(x)$ will not. This is a consequence of Bloch's Theorem, which states that solutions of the Schrödinger equation (1) with the periodic potential in Eq. (11) will satisfy

$$\psi(x+L) = \exp(ikx) \cdot \psi(x) \tag{12}$$

where k is a real constant (Griffiths [6, Ch. 5]).

The singular values in Figure 6 show that the positive energy levels for V_{25dw} occur in dense bands separated by gaps where there are no solutions. In this problem there is also a small band of negative energies near $E = -0.3$. Energy bands often occur for periodic potentials which have small sub-periods. Such potentials are used to model the structure of crystals.

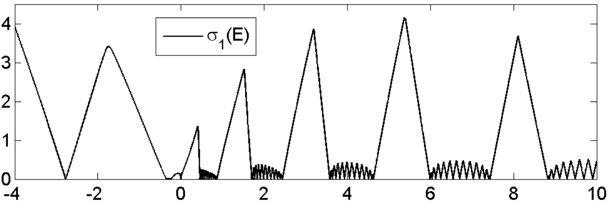

Figure 6. Energy levels for $V_{25dw}(x)$ occur in dense bands.

Even though this example does not have a particularly large number of lines ($25 \cdot 4 = 100$), it does indicate that the solution method is scalable for large problems. It can resolve the closely spaced energies in each band.

III. BRANCHING NETWORKS

The 1-D solution method can be extended to find wave functions on *branching networks* in which junctions may connect more than two line segments. Figure 7 shows three infinite lines meeting at branch point J. The arrows indicate the direction of increasing x_k along each line.

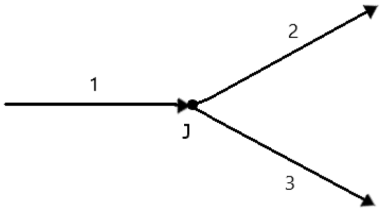

Figure 7. Three lines which meet at a junction.

The wave functions at a branch point must satisfy Kirchhoff boundary conditions so that (a) the ψ_k are continuous at the junction and (b) the sum of the outgoing rates of change of the ψ_k equals the strength of the delta function source at the branch point. This is a generalization of Eq. (8) above. As before, the number of equations at a junction equals the number of line segments which meet there. For example, the equations at junction J in Figure 7 are

$$\psi_2(0) - \psi_1(L_1) = 0 \tag{13a}$$

$$\psi_3(0) - \psi_1(L_1) = 0 \tag{13b}$$

$$\psi_3'(0) + \psi_2'(0) - \psi_1'(L_1) = Q_J \cdot \psi_1(L_1) \tag{13c}$$

The signs of the derivatives in Eq. (13c) are determined by the direction of the arrows in Figure 7. The system of equations for a branch point with any number of lines can be written by following this example.

Wave propagation through a branch point depends on the energy level and the potentials in the lines. For example, if we set $V_1 = 0$ and $V_2 = V_3 = 1$ in Figure 7, then we see in Figure 8 that transmission through a branch differs from transmission through a simple 1-D potential step from $V_1 = 0$ to $V_2 = 1$. The transmission coefficient through a unit step on the real line increases to 1 monotonically with energy. However, transmission through the branch point rises rapidly to 1 and then *decreases* asymptotically to $T = 8/9$. The branching junction becomes transparent at finite energy, much like resonant transmission across a 1-D square well (Zwiebach [2, Ch. 14]).

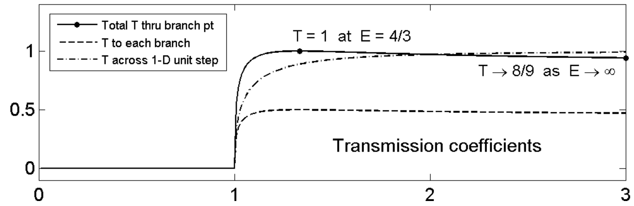

Figure 8. Comparison of transmission through a branch point and a 1-D unit step.

Now let's change line #3 in Figure 7 so that $L_3 = \pi$ and $\psi_3(L_3) = 0$. We also set $V_1 = V_2 = V_3 = 0$. As Figure 9 shows, the finite length of line #3 suppresses wave transmission from line #1 to line #2 when $E_n = n^2$. If line #3 were not present, transmission T_{12} would be 1 for all energies, but line #3 resonates at E_n and absorbs the incoming wave from line #1.

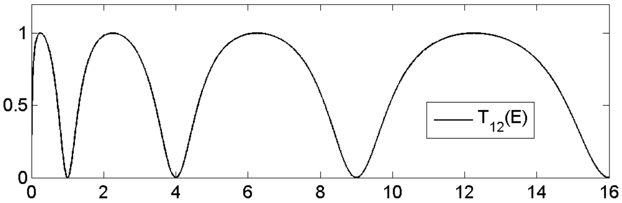

Figure 9. Resonance in a branch of finite length.

The same phenomenon occurs in macroscopic branching networks. Resonant elements are often used for noise suppression in acoustics (Kinsler [7]). Engine mufflers are a good example.

Resonance also occurs when there is a loop in the network. Lines #2 and #3 in Figure 10 are parallel paths between lines #1 and #4, and they also form a loop. For $V = 0$ on all four lines and $L_2 = L_3 = \pi$ the transmission coefficient peaks at the resonant energies $E_n = n^2$. However, wave transmission is sensitive to the line lengths. Varying L_2 and L_3 while maintaining $L_2 + L_3 = 2\pi$ produces large changes in transmission. The network is transparent at $E_n = n^2$ when L_2 and L_3 are exactly π, but T_{14} jumps to zero when the loop is not perfectly symmetrical.

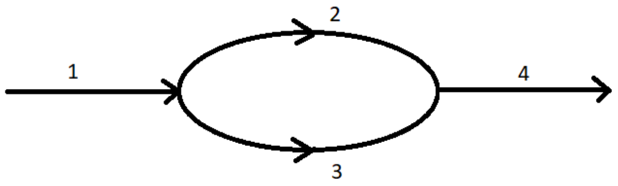

Figure 10. Simple network with a loop.

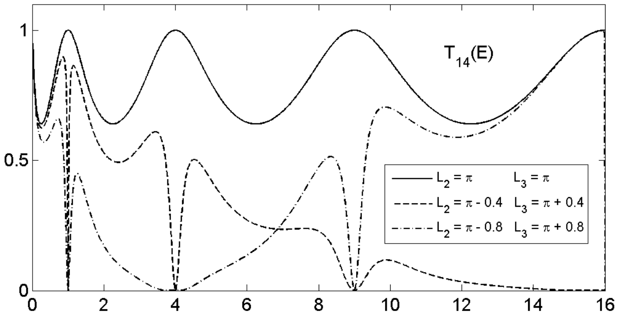

Figure 11. Transmission coefficient T_{14} for Figure 10.

IV. SOME APPLICATIONS

Branching 1-D networks are referred to as *graphs* by mathematicians, and this term is often used in the physics literature. A survey by Kuchment [8] discusses applications of quantum graphs, including quantum wires, photonic crystals, conjugated molecules in chemistry, and quantum chaos. A few other simple applications are described below.

A. Mach-Zehnder interferometer

The Mach-Zehnder interferometer described in Zwiebach [2, Ch. 2] can be modeled as a 1-D branching network. A small change to the solver is needed to obtain the correct phase shifts at the beam splitters and the mirrors. The length of both the reference beam and the sample beam between the splitters is set to π. Figure 12 shows that there is no transmission to detector #2 when there is no test sample. A phase shift of 0.001π in the sample beam produces the result in Figure 13. The interferometer is sensitive to small changes in phase.

B. Nonlinear potentials

The potentials under consideration here are finite combinations of linear segments, steps, and delta functions. The solution method is exact for these potentials, up to numerical accuracy of the computation. By using interpolation or other numerical approximation methods, these functions can often be adapted to describe nonlinear potentials.

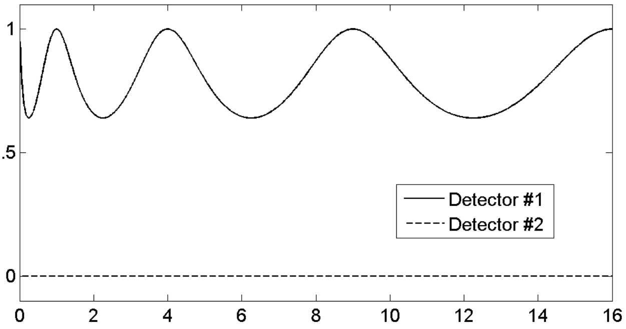

Figure 12. Transmission in the Mach-Zehnder interferometer with no sample.

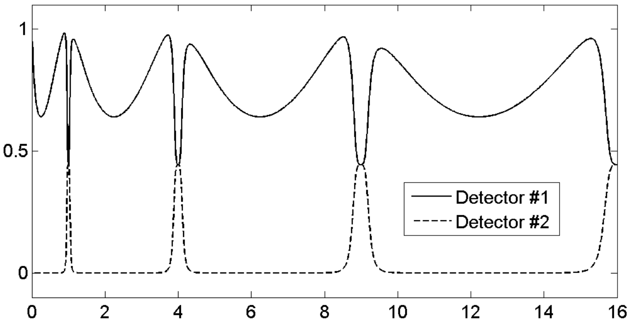

Figure 13. Transmission when there is a small phase shift due to the sample.

Also note that the solution method can be applied to any independent general solutions f_k and g_k in Eq. (5). For example, the WKB approximations described in Zwiebach [1, Ch. 3] can be used for lines with nonlinear potentials that vary slowly. The leading order WKB solutions are

$$f_k(x_k) = Q_k^{-1/4}(x_k) \cdot \exp\left[i \int_0^{x_k} ds \sqrt{Q(s)}\right] \qquad (14a)$$

$$g_k(x_k) = Q_k^{-1/4}(x_k) \cdot \exp\left[-i \int_0^{x_k} ds \sqrt{Q(s)}\right] \qquad (14b)$$

where $Q_k(x_k) = E - v_k(x_k)$. As discussed in [1], care must be taken near the turning points given by $Q_k(x_k) = 0$.

C. 2-D and 3-D problems

Methods for solving 1-D branching systems can be applied to some problems in which the network is embedded in two or three dimensions. The multidimensional Schrödinger equation is

$$\nabla^2\psi + [E - V(\vec{x})] \cdot \psi = 0. \qquad (15)$$

If the potential can be expressed as a sum such that

$$V(x, y, z) = V_x(x) + V_y(y) + V_z(z) \tag{16}$$

then using separation of variables we can solve three 1-D problems to obtain the solution of Eq. (15) as

$$\psi(x, y, z) = \psi_x(x) \cdot \psi_y(y) \cdot \psi_z(z). \tag{17}$$

where the energy levels are

$$E = E_x + E_y + E_z \tag{18}$$

A simple 2-D example is

$$V(x, y) = |x| + |y| \tag{19}$$

The 1-D eigenvalues are

$$E_x = E_y = 1.019, 2.338, 3.248, 4.088, \ldots, \tag{20}$$

so the energy levels for the 2-D solution are

$$E = 2.038, 3.357, 4.267, 4.676, 5.107, 5.586, \ldots \tag{21}$$

Most of the energy values correspond to two degenerate solutions, but some are nondegenerate, *e.g.*, 2.038 and 4.676.

The solution method can also be adapted to solve multidimensional problems using separation of variables in other coordinate systems. For example, following the development in Zwiebach [1, Ch. 8] for scattering problems in spherical coordinates, the radial Schrödinger equation

$$\psi_k''(r_k) + \left[E - \frac{l(l+1)}{r_k^2}\right] \cdot \psi_k(r_k) = 0 \tag{22}$$

has independent solutions

$$f_k(r_k) = j_l(r_k\sqrt{E}) \tag{23a}$$

$$g_k(r_k) = n_l(r_k\sqrt{E}) \tag{23b}$$

where j_l and n_l are the spherical Bessel functions.

D. Linear wave equation

Lastly, we note that the solution method can be applied to macroscopic networks as well. The exponentials of the form in Eq. (6) are also amplitudes of solutions of the linear wave equation

$$\frac{\partial^2 \phi}{\partial t^2} = c^2 \nabla^2 \phi. \tag{24}$$

We can solve problems involving fluid flow, electrical circuits, vibrations, optics, and other phenomena governed by equation (24).

[1] Barton Zwiebach. *Course Notes for MIT 8.06x.* Massachusetts Institute of Technology, 2019.

[2] Barton Zwiebach. *Course Notes for MIT 8.04x.* Massachusetts Institute of Technology, 2018.

[3] Y. Saad. *Iterative Methods for Sparse Linear Equations.* PWS Publishing Company, 1996.

[4] *Matlab.* The Mathworks, Inc. `https://www.mathworks.com`

[5] R. A. Horn, C. R. Johnson. *Matrix Analysis.* Cambridge University Press, 2013.

[6] D. J. Griffiths. *Introduction to Quantum Mechanics.* Prentice-Hall, 1995.

[7] L. E. Kinsler, *et.al. Fundamentals of Acoustics.* Johns Wiley, 2000.

[8] P. Kuchment. *Graph models for waves in thin structures.* Waves in Random Media 12(2002), no. 4, R1-R24.

Single-particle interpretation of Dirac equation and its limitations

Tomasz Szymański

(Dated: June 18, 2019)

Dirac's original idea was to give a relativistic quantum mechanical description of an electron (or, more generally, a single spin-$\frac{1}{2}$ particle). However, it was noticed very soon that its interpretation encounters serious problems stemming from negative energy solutions. We show that a single particle interpretation can be performed to some extent if we agree that only even operators can be regarded as observables. Still, the validity range of the one-particle interpretation is restricted. We determine its limits and show that beyond them one encounters interpretational difficulties and contradictions such as Zitterbewegung ("shaky movement") that can be solved satisfactorily only on the ground of quantum field theory.

I. A BRIEF INTRODUCTION TO DIRAC EQUATION.

A. Klein-Gordon equation.

Energy-momentum relation known from classical mechanics

$$E = \frac{p^2}{2m} \tag{1}$$

together with quantum mechanical rule of replacing classical quantities with operators

$$E \to i\hbar\frac{\partial}{\partial t}, \vec{p} \to -i\hbar\vec{\nabla} \tag{2}$$

leads to nonrelativistic equation for free particles

$$i\hbar\frac{\partial}{\partial t}\psi\left(\vec{x},t\right) = -\frac{\hbar^2}{2m}\nabla^2\psi\left(\vec{x},t\right) \tag{3}$$

known as Schrödinger equation. This equation, however, is not Lorentz covariant - due to different orders of spatial and temporal derivatives it changes its structure passing from one inertial system to another.

In 1926 Schrödinger suggested considering relativistic energy-momentum relation

$$\frac{E^2}{c^2} - \vec{p}\cdot\vec{p} = m^2c^2 \tag{4}$$

Using the usual correspondence rule for operators (2) he obtained the following

$$-\hbar^2\frac{\partial^2}{\partial t^2}\psi = (-\hbar^2c^2\nabla^2 + m^2c^4)\psi \tag{5}$$

This is known as the free Klein - Gordon equation. Its solutions are of the form

$$\psi = e^{-\frac{i}{\hbar}(Et-\vec{p}\cdot\vec{x})} \tag{6}$$

Insertion of (6) into (5) leads to the condition

$$E = \pm c\sqrt{m^2c^2 + p^2} \tag{7}$$

As we can see, along with positive energy solutions there are negative energy solutions. It was considered as a serious interpretational problem. Moreover, problems with probabilistic interpretation were noted. To see what the point is, let's try to construct the continuity equation connected with (5). Multiplying (5) by $\psi^\star$ from the left and subtracting the complex conjugate we get:

$$\hbar^2\left(\psi^\star\frac{\partial^2\psi}{\partial t^2} - \psi\frac{\partial^2\psi^\star}{\partial t^2}\right) = \hbar^2c^2\left(\psi^\star\nabla^2\psi - \psi\nabla^2\psi^\star\right) \tag{8}$$

$$\frac{1}{c^2}\frac{\partial}{\partial t}\left(\psi^\star\frac{\partial\psi}{\partial t} - \psi\frac{\partial\psi^\star}{\partial t}\right) = \vec{\nabla}\cdot\left(\psi^\star\vec{\nabla}\psi - \psi\vec{\nabla}\psi^\star\right) \tag{9}$$

Inspired by analogous considerations concerning Schrödinger equation, we may try to define probability density

$$\rho = \frac{i\hbar}{2mc^2}\left(\psi^\star\frac{\partial\psi}{\partial t} - \psi\frac{\partial\psi^\star}{\partial t}\right) \tag{10}$$

and probability current

$$\vec{j} = -\frac{i\hbar}{2m}\left(\psi^\star\vec{\nabla}\psi - \psi\vec{\nabla}\psi^\star\right) \tag{11}$$

We can see that

$$\frac{\partial\rho}{\partial t} + \vec{\nabla}\cdot\vec{j} = 0 \tag{12}$$

The problem is, such defined ρ doesn't guarantee it is positive definite. Presence of the second time derivative indicates that the initial values of ψ and $\frac{\partial\psi}{\partial t}$ can be chosen independently and thus at later times ρ may be either positive or negative. At first [1], this difficulty seemed to be insurmountable and because of that, Klein - Gordon equation was regarded to be physically absurd.

An equation with positive definite probability density was found by Dirac.

---

[1] It is worth noting however, that $e\rho$ can be interpreted as charge density and $e\vec{j}$ as charge current density. Together with negative energy solutions it indicates the existence of particles and antiparticles in the theory.

B. Formulation of the free Dirac equation.

Dirac wanted to avoid problems with probabilistic interpretation so he decided to look for an equation of first order in time. The requirement of Lorentz-covariance suggests treating temporal and spatial coordinates equally so he wanted spatial derivatives to be of first order too. Moreover, solutions of the new equation must fulfill the requirements of relativistic energy-momentum relation.

In order to achieve his goal, Dirac proposed a new ansatz for a Hamiltonian in equation (3):

$$H = c\vec{\alpha}\cdot\vec{p} + \beta mc^2 \tag{13}$$

with additional condition

$$H^2 = c^2\vec{p}\cdot\vec{p} + m^2c^4 \tag{14}$$

which is in fact equivalent to (5). From condition (14) we can easily see that α_i and β cannot be numbers since there are no terms mixing them. We also see they must commute with p_i for (14) to hold. It is reasonable to suspect they are square matrices. To find out what exactly they are we write our equation

$$i\hbar\frac{\partial\psi}{\partial t} = \left(c\vec{\alpha}\cdot\vec{p} + \beta mc^2\right)\psi \tag{15}$$

and iterate it [2].

$$\begin{aligned}-\hbar^2\frac{\partial^2}{\partial t^2}\psi =& i\hbar\frac{\partial}{\partial t}\left(\frac{\hbar c}{i}\alpha_i\partial_i\psi + \beta mc^2\psi\right)\\ =& \frac{\hbar c}{i}\alpha_j\partial_j\left(\frac{\hbar c}{i}\alpha_i\partial_i\psi + \beta mc^2\psi\right)\\ &+ \beta mc^2\left(\frac{\hbar c}{i}\alpha_i\partial_i\psi + \beta mc^2\psi\right)\\ =& -\hbar^2c^2\alpha_j\partial_j\alpha_i\partial_i\psi + \frac{\hbar mc^3}{i}\left(\alpha_i\beta + \beta\alpha_i\right)\partial_i\psi\\ &+ \beta^2m^2c^4\psi\\ =& -\frac{1}{2}\hbar^2c^2\left(\alpha_i\alpha_j + \alpha_j\alpha_i\right)\psi\\ &+ \frac{\hbar mc^3}{i}\left(\alpha_i\beta + \beta\alpha_i\right)\partial_i\psi + \beta^2m^2c^4\psi\end{aligned} \tag{16}$$

We clearly see that the (14) can be satisfied only if α_i and β matrices obey the algebra

$$\{\alpha_i, \alpha_j\} = \delta_{ij} \quad , \quad \{\alpha_i, \beta\} = 0 \quad , \quad \alpha_i^2 = \beta^2 = 1 \tag{17}$$

We also note that Hermiticity of H imposes Hermiticity of α_i and β matrices. From this it follows that their eigenvalues are real. Moreover $\alpha_i^2 = \beta^2 = 1$, so the eigenvalues can only be equal to ±1.

Further we have

$$\begin{aligned}\mathrm{tr}\left(\alpha_i\right) &= \mathrm{tr}\left(\beta^2\alpha_i\right) = \mathrm{tr}\left(\beta\alpha_i\beta\right) &(18)\\ &= \mathrm{tr}\left(-\alpha_i\beta^2\right) = -\mathrm{tr}\left(\alpha_i\right) &(19)\end{aligned}$$

and similarly $\mathrm{tr}\beta = -\mathrm{tr}\beta$. Hence

$$\mathrm{tr}\alpha_i = \mathrm{tr}\beta = 0 \tag{20}$$

The trace of a matrix is equal to the sum of its eigenvalues so the dimension N of all α and β must be even. $N = 2$ is impossible because there are only three anticommuting matrices of such size - Pauli matrices σ_i. Thus, the smallest dimension for which (17) holds is $N = 4$. One possible representation of the algebra (17) is the Dirac representation

$$\alpha_i = \begin{pmatrix} 0 & \sigma_i \\ \sigma_i & 0 \end{pmatrix} \qquad \beta = \begin{pmatrix} 1 & 0 \\ 0 & -1 \end{pmatrix} \tag{21}$$

We see that equation (15) turns out to be a fourdimensional matrix equation and the wave function ψ turns out to be a fourdimensional vector - bispinor:

$$\psi = \begin{pmatrix} \psi_1 \\ \psi_2 \\ \psi_3 \\ \psi_4 \end{pmatrix} \tag{22}$$

Next we construct continuity equation. For that we multiply (15) from the left by $\psi^\dagger = (\psi_1^\star, \psi_2^\star, \psi_3^\star, \psi_4^\star)$:

$$i\hbar\psi^\dagger\frac{\partial\psi}{\partial t}\psi = \frac{\hbar c}{i}\psi^\dagger\alpha_i\partial_i\psi + mc^2\psi^\dagger\beta\psi \tag{23}$$

Now we form the Hermitean conjugate of (15) and multiply it from the right by ψ:

$$-i\hbar\frac{\partial\psi^\dagger}{\partial t}\psi = -\frac{\hbar c}{i}\partial_i\psi^\dagger\alpha_i\psi + mc^2\psi^\dagger\beta\psi \tag{24}$$

Substraction yields

$$i\hbar\frac{\partial}{\partial t}\left(\psi^\dagger\psi\right) = \frac{\hbar c}{i}\partial_i\left(\psi^\dagger\alpha_i\psi\right) + \tag{25}$$

or

$$\frac{\partial\rho}{\partial t} + \vec{\nabla}\cdot\vec{j} = 0 \tag{26}$$

where

$$\rho = \psi^\dagger\psi \;, \quad \vec{j} = -c\psi^\dagger\vec{\alpha}\psi \tag{27}$$

We clearly see ρ is positive definite and therefore it can be accepted as a probability density and, correspondingly, $\vec{j}$ can be accepted as probability current density.

Having shown that the probabilistic interpretation of the Dirac equation is possible we now turn to find its solutions. Our ansatz is

$$\psi\left(x,t\right) = \begin{pmatrix} \phi_0 \\ \chi_0 \end{pmatrix} \mathrm{e}^{\frac{i}{\hbar}\left(\vec{p}\cdot\vec{x} - Et\right)} = \begin{pmatrix} \phi_0 \\ \chi_0 \end{pmatrix} \mathrm{e}^{-\frac{i}{\hbar}Et} \tag{28}$$

---

[2] We adopt Einstein summation convention

where ϕ_0, χ_0 are twodimensional constant spinors. Inserting this into (15) yields

$$E\begin{pmatrix}\phi_0\\ \chi_0\end{pmatrix} = c\begin{pmatrix}0 & \vec{\sigma}\\ \vec{\sigma} & 0\end{pmatrix}\cdot\vec{p}\begin{pmatrix}\phi_0\\ \chi_0\end{pmatrix} + mc^2\begin{pmatrix}1 & 0\\ 0 & -1\end{pmatrix}\cdot\vec{p}\begin{pmatrix}\phi_0\\ \chi_0\end{pmatrix} \tag{29}$$

where $\vec{p}$ are eigenvalues of the momentum operator. We get a linear homogeneous system of equations for ϕ_0 and χ_0:

$$\begin{cases}\left(E - mc^2\right)\phi_0 - c\vec{\sigma}\cdot\vec{p}\chi_0 = 0\\ -c\vec{\sigma}\cdot\vec{p}\phi_0 + \left(E + mc^2\right)\chi_0 = 0\end{cases} \tag{30}$$

It has non-trivial solutions only if

$$\begin{vmatrix}\left(E - mc^2\right) & -c\vec{\sigma}\cdot\vec{p}\\ c\vec{\sigma}\cdot\vec{p} & \left(E + mc^2\right)\end{vmatrix} = 0 \tag{31}$$

This equation is equivalent to [3]

$$E^2 = m^2c^4 + c^2p^2 \tag{32}$$

We've obtained the relativistic energy-momentum relation! This yields

$$E^+ = +c\sqrt{p^2 + m^2c^2} \quad E^- = -c\sqrt{p^2 + m^2c^2} \tag{33}$$

We see that we have to deal with two types of solutions corresponding to positive and negative energies. We find them by plugging E^+ and E^- into (30) to obtain:

$$\chi_0 = \frac{c\vec{\sigma}\cdot\vec{p}}{E^\pm + mc^2}\phi_0 \tag{34}$$

and finally [4]:

$$\psi^\pm(x,t) = \begin{pmatrix}\phi_0\\ \frac{c\vec{\sigma}\cdot\vec{p}}{E^\pm + mc^2}\phi_0\end{pmatrix}\mathrm{e}^{\frac{i}{\hbar}\left(\vec{p}\cdot\vec{x} - E^\pm t\right)} \tag{35}$$

For simplicity we will call ψ^+ a positive solution and ψ^- a negative solution.

II. SINGLE-PARTICLE INTERPRETATION OF THE DIRAC THEORY.

A. Even and odd operators.

We have seen that the Dirac equation has two kinds of solutions. A consistent one-particle theory however can only use states with a specified sign of energy. In order to try to construct such theory we introduce [Gre97], [Wac11] the sign operator $\hat{\Lambda}$ [5]:

$$\hat{\Lambda} = \frac{H}{\sqrt{H^2}} = \frac{c\vec{\alpha}\cdot\vec{p} + mc^2\beta}{c\sqrt{p^2 + m^2c^2}} \tag{36}$$

Of course

$$\Lambda\psi^+ = \frac{+|E|}{|E|}\psi^+ = \psi^+, \quad \Lambda\psi^- = \frac{-|E|}{|E|}\psi^- = \psi^- \tag{37}$$

Let us also define the energy projection operators $\hat{\Lambda}_\pm$ for later use

$$\hat{\Lambda}_\pm = \frac{1}{2}(1 \pm \hat{\Lambda}) \tag{38}$$

It is clear that

$$\begin{aligned}\Lambda^+\psi^+ &= \psi^+ && (39)\\ \Lambda^-\psi^+ &= 0 && (40)\\ \Lambda^+\psi^- &= 0 && (41)\\ \Lambda^-\psi^- &= \psi^- && (42)\end{aligned}$$

We will now convince ourselves that not every relativistic operator is physically sensible in one-particle theory. To see this let's invoke the Heisenberg picture. The Heisenberg operators are defined by

$$\hat{\mathcal{O}}(t) = \mathrm{e}^{\frac{i}{\hbar}Ht}\hat{\mathcal{O}}\mathrm{e}^{-\frac{i}{\hbar}Ht} \tag{43}$$

which yields the equation of motion [6]:

$$\frac{d\hat{\mathcal{O}}}{dt} = \frac{1}{i\hbar}[\hat{\mathcal{O}}, \hat{H}] \tag{44}$$

Now let's analyze the case of the "velocity operator" [7].

$$\begin{aligned}\vec{v} = \frac{d\vec{x}}{dt} &= \frac{1}{i\hbar}[\vec{x}, c\vec{\alpha}\cdot\vec{p} + mc^2\beta] && (45)\\ &= \frac{c}{i\hbar}[\vec{x}, \vec{\alpha}\cdot\vec{p}] + \frac{mc^2}{i\hbar}[\vec{x}, \beta] && (46)\\ &= \frac{c}{i\hbar}[x_ie_i, x_jp_j] && (47)\\ &= \frac{c}{i\hbar}\left([x_i, \alpha_j]p_je_i + \alpha_j[x_i, p_j]e_i\right) && (48)\\ &= \frac{c}{i\hbar}\alpha_j\left(i\hbar\right)e_i\delta_{ij} && (49)\\ &= c\alpha_je_j = c\vec{\alpha} && (50)\end{aligned}$$

---

[3] We use here $\left(\vec{\sigma}\cdot\vec{A}\right)\left(\vec{\sigma}\cdot\vec{B}\right) = \vec{A}\cdot\vec{B} + i\vec{\sigma}\cdot\left(\vec{A}\times\vec{B}\right)$.

[4] Unnormalized.

[5] An alternative way of introducing even and odd operators involves Feshbach-Villars transformation which is presented in [KF58]. [Wac11] contains an especially clear presentation of this technique.

[6] Given $\frac{\partial\hat{\mathcal{O}}}{\partial t}$

[7] e_i are cartesian unit basis vectors

Noting that the eigenvalues of $\vec{\alpha}$ are ± 1, we get $|\vec{v}| = c$! It is obviously not physical. We also want to calculate $\frac{d\vec{\alpha}}{dt}$. In order to obtain this result first we need to compute:

$$[\alpha_i, \alpha_j p_j] = [\alpha_i, \alpha_j]p_j + \alpha_j[\alpha_i, p_j] = [\alpha_i, \alpha_j]p_j \tag{51}$$
$$= 2\delta_{ij}p_j - 2\alpha_j\alpha_i p_j = 2p_i - 2\alpha_j\alpha_i p_j \tag{52}$$

Using this we have

$$\frac{d\vec{\alpha}}{dt} = \frac{1}{i\hbar}[\vec{\alpha}, c\vec{\alpha}\cdot\vec{p} + mc^2\beta] \tag{53}$$
$$= \frac{1}{i\hbar}[\alpha_i e_i, c\alpha_j p_j + mc^2\beta] \tag{54}$$
$$= \frac{1}{i\hbar}(c[\alpha_i, \alpha_i p_j]e_i + mc^2[\alpha_i, \beta]e_i) \tag{55}$$
$$= \frac{2}{i\hbar}(cp_i e_i - c\alpha_j\alpha_i p_j e_i - mc^2\beta\alpha_i e_i) \tag{56}$$
$$= \frac{1}{i\hbar}(2c\vec{p} - 2(c\vec{\alpha}\cdot\vec{p} + mc^2\beta)\vec{\alpha}) \tag{57}$$
$$= \frac{2}{i\hbar}(c\vec{p} - H\vec{\alpha}) \tag{58}$$

This result means that, for free particles, $\vec{v} = c\vec{\alpha}$ is not constant! It seems to be unphysical too. Finally, $[\alpha_i, \alpha_{j\neq i}] \neq 0$ implies that different components of $\vec{v}$ cannot be measured simultaneously! All these results seem to be absurd.

The problem stems from the fact that $\vec{\alpha}$ turns positive solutions of the Dirac equation into negative (and vice versa). We call such operators "odd". It turns out that the only acceptable operators in the single-particle theory are "even" operators, i.e. operators that do not mix positive and negative states.

We formalize this as follows. Every operator $\hat{\mathcal{O}}$ can be split into an atom an even $[\hat{\mathcal{O}}]$ and odd $\{\hat{\mathcal{O}}\}$ part:

$$\hat{\mathcal{O}} = [\hat{\mathcal{O}}] + \{\hat{\mathcal{O}}\} \tag{59}$$

Let's write

$$\hat{\mathcal{O}}\psi^+ = [\hat{\mathcal{O}}]\psi^+ + \{\hat{\mathcal{O}}\}\psi^+ \tag{60}$$

Using (36) we get

$$\hat{\Lambda}\hat{\mathcal{O}}\hat{\Lambda}\psi^+ = \hat{\Lambda}\hat{\mathcal{O}}\psi^+ \tag{61}$$
$$= \hat{\Lambda}[\hat{\mathcal{O}}]\psi^+ + \hat{\Lambda}\{\hat{\mathcal{O}}\}\psi^+ \tag{62}$$
$$= [\hat{\mathcal{O}}]\psi^+ - \{\hat{\mathcal{O}}\}\psi^+ \tag{63}$$

By addition and subtraction of (60) and (61) we obtain

$$[\hat{\mathcal{O}}] = \frac{1}{2}(\hat{\mathcal{O}} + \hat{\Lambda}\hat{\mathcal{O}}\hat{\Lambda}) \tag{64}$$
$$\{\hat{\mathcal{O}}\} = \frac{1}{2}(\hat{\mathcal{O}} - \hat{\Lambda}\hat{\mathcal{O}}\hat{\Lambda}) \tag{65}$$

B. One-particle operator for velocity.

We can now find the true velocity operator $[\vec{v}] = c[\vec{\alpha}]$. According to (64) we first need

$$\Lambda\alpha_i\Lambda = \frac{H}{\sqrt{H}}\alpha_i\frac{H}{\sqrt{H}} \tag{66}$$

In order to compute the above we notice

$$\{H, \alpha_i\} = \{c\alpha_j p_j + \beta mc^2, \alpha_i\} \tag{67}$$
$$= c\{\alpha_j, \alpha_i\}p_j + \{\alpha_i, \beta\}mc^2 \tag{68}$$
$$= c(2\delta_{ij})p_j = 2cp_i \tag{69}$$

Hence

$$\Lambda\alpha_i\Lambda = \frac{H}{\sqrt{H}}\frac{2cp_i - H\alpha_i}{\sqrt{H^2}} \tag{70}$$
$$= -\alpha_i + 2cp_i\frac{\Lambda}{\sqrt{H^2}} \tag{71}$$

We also need

$$[H, \vec{p}] = [c(\vec{\alpha}\cdot\vec{p} + \beta mc^2, \vec{p}] \tag{72}$$
$$= c[(\alpha_i p_i, p_j e_j] \tag{73}$$
$$= c([p_i, p_j]e_j + [\alpha_i, p_j]p_i e_j \tag{74}$$
$$= 0 \tag{75}$$

Using this we obtain

$$[v_i] = c[\alpha_i] = \frac{c}{2}\left(\alpha_i + (-\alpha_i) + 2cp_i\frac{\Lambda}{\sqrt{H^2}}\right) \tag{76}$$
$$= \frac{c^2 p_i\Lambda}{\sqrt{H^2}} \tag{77}$$

Finally

$$[\vec{v}] = \frac{c^2\vec{p}\Lambda}{\sqrt{H^2}} \tag{78}$$

Accordingly

$$[\vec{v}]\psi^{\pm} = \frac{c^2\vec{p}\Lambda}{\sqrt{H^2}}\psi^{\pm} = \frac{c^2\vec{p}}{E^{\pm}}\psi^{\pm} \tag{79}$$
$$= \pm\frac{c^2\vec{p}}{|E|}\psi^{\pm} \tag{80}$$

The result still seems to be paradoxical for negative solutions - in this case the velocity is directed against the momentum - the particles with negative energy behave as if they had a negative mass. [8]

C. Zitterbewegung.

We will discuss the *Zitterbewegung* phenomenon using the Heisenberg picture [9]. Let's consider again (45) and (53):

$$\frac{d\vec{x}}{dt} = c\vec{\alpha} \qquad \frac{d\vec{\alpha}}{dt} = \frac{2}{i\hbar}(c\vec{p} - H\vec{\alpha}) \tag{81}$$

---

[8] It can be explained on the basis of Feynman-Stückelberg interpretation of negative solutions. One can find very clear presentation of this in [Wac11].

[9] An analysis of this phenomenon using Schrödinger picture can be found in [Sch08].

We have already shown that $[H, \vec{p}] = 0$ (meaning $\vec{p} = const$) so we can safely try to integrate the second equation and insert the result to the first. We proceed with the integration [Gre97], [Sch08], [Sid]:

$$-i\hbar\frac{d\vec{\alpha}}{dt} = 2H(\vec{\alpha} - cH^{-1}\vec{p}) \tag{82}$$

Let's introduce

$$\vec{\eta} = \vec{\alpha} - cH^{-1}\vec{p} \tag{83}$$

Then

$$-i\hbar\frac{d\vec{\eta}}{dt} = 2H\vec{\eta} \tag{84}$$

$$\vec{\eta}(t) = e^{\frac{2i}{\hbar}Ht}\vec{\eta}(0) \tag{85}$$

$$\vec{\alpha}(t) - cH^{-1}\vec{p} = e^{\frac{2i}{\hbar}Ht}\left(\vec{\alpha} - cH^{-1}\vec{p}\right) \tag{86}$$

And finally

$$\vec{\alpha}(t) = cH^{-1}\vec{p} + e^{\frac{2i}{\hbar}Ht}\left(\vec{\alpha} - cH^{-1}\vec{p}\right) \tag{87}$$

In order to obtain $\vec{x}(t)$ we have to integrate (87):

$$\vec{x}(t) = c^2H^{-1}\vec{p}t + \frac{\hbar c}{2i}H^{-1}e^{\frac{2i}{\hbar}Ht}\left(\vec{\alpha}(0) - cH^{-1}\vec{p}\right) + \vec{x_0} \tag{88}$$

Since

$$\vec{x}(0) = \frac{\hbar c}{2i}H^{-1}\left(\vec{\alpha}(0) - cH^{-1}\vec{p}\right) + \vec{x_0} \tag{89}$$

We finally obtain [10]

$$\vec{x}(t) = \vec{x}(0) + c^2H^{-1}\vec{p}t \tag{90}$$

$$+\frac{\hbar c}{2i}H^{-1}\left(e^{\frac{2i}{\hbar}Ht} - 1\right)\left(\vec{\alpha} - cH^{-1}\vec{p}\right) \tag{91}$$

As we can see, apart from a term linear in time, (90) contains an oscillating term. This term represents the *Zitterbewegung* - a "shaky" movement around the classical trajectory. We'll show that the *Zitterbewegung* vanishes only if we consider wave packets consisting exclusively of either positive or negative energy states.

Let us use the energy projection operators (38) to convince ourselves that:

$$\Lambda_\pm H^{-1}\left(e^{\frac{2i}{\hbar}Ht} - 1\right)\left(\vec{\alpha} - cH^{-1}\vec{p}\right)\Lambda_\pm = 0 \tag{92}$$

Since $[H, \Lambda_\pm] = 0$, it is enough to show

$$\Lambda_\pm\left(\vec{\alpha} - cH^{-1}\vec{p}\right)\Lambda_\pm = 0 \tag{93}$$

Using previously computed commutator [11]

$$[H, \vec{\alpha}] = 2c\vec{p} - 2\vec{\alpha}H \tag{94}$$

we have

$$[\Lambda_\pm, \vec{\alpha}] = \frac{1}{2}[(1 \pm \Lambda), \vec{\alpha}] = \pm\frac{1}{2|E|}[H, \vec{\alpha}] \tag{95}$$

$$= \pm\frac{c\vec{p}}{|E|} \mp \vec{\alpha}\frac{H}{|E|} \tag{96}$$

Hence

$$\Lambda_\pm\vec{\alpha} = \vec{\alpha}\Lambda_\pm \pm \frac{c\vec{p}}{|E|} \mp \vec{\alpha}\frac{H}{|E|} \tag{97}$$

and

$$\Lambda_\pm\left(\vec{\alpha} - cH^{-1}\vec{p}\right)\Lambda_\pm = \left(\vec{\alpha} \pm \frac{c\vec{p}}{|E|} \mp \vec{\alpha}\frac{H}{|E|} - \frac{c\vec{p}}{H}\right)\Lambda_\pm \tag{98}$$

$$= 0 \tag{99}$$

This means that the $\vec{\alpha} - cH^{-1}\vec{p}$ operator has non-zero matrix elements only between states of identical momentum and opposite energies. Hence, the *Zitterbewegung* must occur if there are both positive and negative states in the wave packet.

The positive states alone do not constitute a complete set of solutions of the Dirac equation. In fact, even when at $t = 0$ wavefunction is a superposition of positive energy states only, negative energy contributions start to enter the wave packet as soon as an interaction with some external field comes along. Therefore, the "shaky movement", stemming from the interference between positive and negative components, seems to be an inevitable feature of the relativistic quantum mechanics.

We can now try to estimate the amplitude and the frequency of the oscillatory movement. First, let's assume the velocity v is small as compared to c[12]. Then the term

$$|cH^{-1}\vec{p}| = c\frac{\gamma mv}{m\gamma c^2} = \frac{v}{c}, \tag{100}$$

where $\gamma = (1 - \frac{v^2}{c^2})^{-\frac{1}{2}}$, can be ignored and the amplitude can be estimated to be

$$A_z \sim \frac{\hbar c}{2mc^2} = \frac{\hbar}{2mc} \tag{101}$$

which is half the Compton wavelength. As for the frequency:

$$\omega_z = \frac{2mc^2}{\hbar} \tag{102}$$

For an electron we get:

$$A_z = 3.9 \times 10^{-11}cm \tag{103}$$

$$\omega_z = 1.55 * 10^{-21}Hz \tag{104}$$

---

[10] Noting that $\vec{\alpha}(0) = \vec{\alpha}$.

[11] In (53).

[12] A reasonable assumption for a single-particle theory - see the next section

It is worth noting [Zal18] that

$$\omega_z^{-1} = 6.4 \cdot 10^{-22} s \tag{105}$$

This is equal to the lifetime of energy fluctuation allowing creation and annihilation of virtual electron-positron pair

$$\Delta t \sim \frac{\hbar}{2mc^2} \tag{106}$$

suggesting that the *Zitterbewegung* is somehow connected to the enforced single-particle interpretation of the Dirac equation.

We can also see that one should imagine a relativistic electron not as a point particle but rather as a fuzzy "cloud" whose trajectory is a kind of a "tube" whose radius is of the order of the Compton wavelength. One important consequence of this fuzziness is the existence of the Darwin term in the Hamiltonian of the electron in electrostatic central potential [Wac11], [Sch08], [Zal18].

D. Validity range of the single-particle interpretation.

The estimated value of the amplitude of the electron's "trembling motion" suggests that when the particle is localized in length scale smaller than its Compton wavelength, the contribution of the negative energy components to its wavefunction is significant. Hence, complete decoupling starts to be problematic if the particle is confined to a region of size

$$\Delta x < \frac{\hbar}{mc} \tag{107}$$

From Heisenberg's uncertainty relation we get

$$\Delta p > \frac{\hbar}{\Delta x} = mc \tag{108}$$

Then the particle's energy uncertainty

$$\Delta E \sim c\Delta p = mc^2 \tag{109}$$

permits pair creation. As a consequence, single-particle theory no longer makes any sense and must be replaced by a many-particle theory.

Let us also note that when (107), then

$$\Delta t \sim \frac{\Delta x}{c} < \frac{\hbar}{mc^2} \tag{110}$$

When we consider processes at this time scale, the energy uncertainty:

$$\Delta E \sim \frac{\hbar}{\Delta t} = mc^2 \tag{111}$$

Hence, for a one-particle theory to make sense, the time scale under consideration must be

$$t > \frac{\hbar}{mc^2} \tag{112}$$

To give a meaningful description of processes involving time scales shorter than (112) one cannot confine himself to a one-particle regime anymore but instead he/she has to utilize methods of quantum field theory.

[Gre97] Walter Greiner. *Relativistic Quantum Mechanics - Wave Equations.* Springer, 2nd. edition, 1997.

[KF58] F. Villars K. Feschbach. Elementary relativistic wave mechanics of spin 0 and spin-1/2 particles. *Rev. Mod. Phys.*, 30(1):24–45, January 1958.

[Sch08] Franz Schwabl. *Advanced Quantum Mechanics.* Springer, 4th edition, 2008.

[Sid] Burra G. Sidharth. Revisiting zitterbewegung. `https://arxiv.org/pdf/0806.0985v1.pdf`.

[Wac11] Armin Wachter. *Relativistic Quantum Mechanics.* Springer, 2011.

[Zal18] Kacper Zalewski. Wykady z relatywistycznej mechniki kwantowej. `http://th.if.uj.edu.pl/~zalewski/not-rmq.pdf`, October 2018. in Polish.

Spin-spin interactions in Nuclear Magnetic Resonance

Apollonious

(Dated: June 18, 2019)

Introductory treatments of Nuclear Magnetic Resonance (NMR) consider the dynamics of a single spin–1/2 interacting with the magnetic field. In that setting, the NMR spectrum consists of a single resonant frequency and the dynamics is described by unitary evolution. However, in NMR experiments spin interactions play a major role in both determining the shape of the NMR spectra and the relaxation dynamics of the spin ensemble. The main interactions to consider are (a) those of the single spins with the local magnetic field induced by electronic currents, (b) direct dipolar spin-spin interactions and (c) indirect spin-spin coupling. After discussing the mechanisms for those interactions, the spin-pair Hamiltonian will be analysed with the main aim of predicting the frequencies and relative intensities of the spectral lines.

I. INTRODUCTION

Nuclear Magnetic Resonance relies on the paramagnetic properties of the atomic nucleus, whereby the intrinsic magnetic moment of nucleons interacts with external magnetic fields. By an appropriate combination of static and time-varying fields, transitions between nuclear spin states can be achieved whose time evolution and spectra give important information about the molecular environment, as is done in Nuclear Magnetic Resonance Spectroscopy (NMRS) [1]. NMR has also widespread use within medicine in Magnetic Resonance Imaging (MRI), where gradient static fields induce spatially localised resonant frequencies that allow detailed 3D imaging information of biological tissue from the measurement of the relaxation of the magnetisation [2]. NMR was first introduced in 1938 by Isidor Rabi [3], when it was originally applied to molecular beams as an extension of the Stern-Gerlach experiment, and was later further developed by Felix Bloch and and Edward Mills to be applied in liquids and solids [4, 5].

Although the overall behaviour of the the nuclear spins in NMR is determined by the interaction between the nuclear magnetic moment and the external fields, much of the relevant information about molecular structure in NMRS and the nature of the biological tissue in MRI depend on pair interactions between nuclear spins, and interactions between spins and the molecular electronic currents. The main aim of this paper is to present a brief overview of the effects of those interactions on the spectral lines produced by the allowed transitions between coupled spin states in NMR. While the basis of the approach that will be presented is valid for nuclei of any spin value, for reasons of space the scope of the more detailed analysis will be limited to the case of spin-1/2. The generalisation to higher spin systems follows a similar formalism, which is developed in the cited literature. The main sources consulted were [6–8], and references to specific chapters will be given where appropriate [1].

The outline of the paper is as follows. First, an overview is presented of the NMR dynamics deriving from a single-spin Hamiltonian. That is followed by a brief discussion of the main internal magnetic interactions, and how they can be incorporated into a spin-pair Hamiltonian. The spin-pair energy levels and eigenstates are obtained for the experimentally relevant case of isotropic liquids. Furthermore, the allowed transitions and relative intensity of spectral lines of the fine structure spin-pair interactions are also briefly discussed.

II. OVERVIEW OF NMR

The Hamiltonian of an isolated charged particle with non-zero spin is as follows:

$$\hat{H} = -\gamma \mathbf{B} \cdot \hat{\mathbf{S}}\,, \tag{1}$$

where $\gamma = \frac{qg}{2m}$, with q being the nuclear charge, m the nuclear mass, and g the nuclear gyromagnetic ratio.

In NMR, the magnetic field $\mathbf{B}$, normally consists of a static component along the z direction and a rotating radio-frequency part on the x, y plane. Thus, the total magnetic field can be written as $\mathbf{B} = B_0 \mathbf{z} + B_{xy} \mathbf{n}(t)$, with $\mathbf{n}(t) = \cos(\omega t)\mathbf{i} - \sin(\omega t)\mathbf{j}$.

By expanding the dot product in eq. (1) and writing the spin-1/2 operators in terms of the Pauli matrices, the Hamiltonian can be written as,

$$\hat{H} = -\frac{\hbar}{2}\omega_0 \sigma_z + \frac{\hbar}{2}\Omega\left(\sigma_+ e^{i\omega t} + \sigma_- e^{-i\omega t}\right)\,, \tag{2}$$

where $\omega_0 = -\gamma B_0$ is the Larmor frequency, and $\Omega = -\gamma B_{xy}$ is the Rabi frequency of transitions between spin up and spin down states. Writing the Hamiltonian in terms the ladder operators emphasises the role of the transversal time-dependent perturbation in inducing transitions. We note that in NMR, the transverse perturbation is only on during brief pulses, while the much stronger longitudinal field along z is continuously on.

The Hamiltonian can be written in the frame of the rotating field by the transformation $\tilde{H} = U^{\dagger}(t)\hat{H}U(t)$

---

[1] The original notation used in the different sources has been adapted for consistency of presentation

where

$$U(t) = e^{i\frac{\omega}{2}t\sigma_z} \,. \tag{3}$$

This transformation to the rotating frame leads to the following time independent Hamiltonian:

$$\tilde{H} = -\frac{\hbar}{2}(\omega_0 - \omega)\sigma_z + \frac{\hbar}{2}\Omega\left(\sigma_+ + \sigma_-\right) \,. \tag{4}$$

For $\omega_0 - \omega = 0$ the rotating frame frequency matches that of free precession and the transformation to the rotating frame coincides with the interaction picture representation. It is apparent that in exact resonance, the interaction with the rotating field purely induces transitions between the up and down states. When only near-resonance is achieved, the dynamics is a combination of precession around the z-axis and transversal transitions.

III. SPIN INTERACTIONS

In the case of spin-1/2 particles, the major interactions effects to be considered are the following: (a) chemical shifts; (b) direct dipole-dipole interactions; and (c) indirect spin-spin interactions, also called J-coupling interactions. In considering general interactions, electric effects can have an indirect influence on the dynamics of magnetic nuclear moments through the indirect interactions with the electronic clouds. Therefore, terms in the electric multipole expansion of the nucleus may play a role in the full interaction Hamiltonian. However, it can be shown that for spin-1/2 nuclei, all electric moments above zeroth order are zero ([9], Chapter 8). For higher spin, the electric quadrupolar moment of the nucleus becomes important.

It is convenient to split the full Hamiltonian as follows:

$$\hat{H} = \hat{H}_0 + \hat{H}_{\mathrm{RF}} + \hat{H}_{\mathrm{C}} + \hat{H}_{\mathrm{D}} + \hat{H}_{\mathrm{J}} \,, \tag{5}$$

where the contributions of the static field, the radio-frequency rotating field, the chemical shifts, J-coupling, and dipolar interactions, are separated. In the following each of the internal interactions terms will be introduced.

A. Chemical shifts

Identical nuclear spins in different electronic environments will interact with slightly different local magnetic fields. While the external magnetic field is spatially homogeneous at a macroscopic level, at the scale of the nucleus it will vary depending on the state of the local electronic currents. This local inhomogeneity is taken into account by the chemical shifts. The consequence of the local spatial fluctuations of the field is that the Larmor frequency of two protons in different parts of a molecule may be slightly different. This is an important effect that makes NMR useful to probe molecular structure. In general, the field at a local site within a molecule, $\mathbf{B}_l = \mathbf{B}_0 + \mathbf{B}_{\mathrm{ind}}$, with $\mathbf{B}_{\mathrm{ind}} = \boldsymbol{\delta} \cdot \mathbf{B}_0$, where $\boldsymbol{\delta}$ is the chemical shift tensor ([9], Chapter 9). In the case of isotropic liquids where molecular motion is averaged and as a good approximation in other situations, it is common to consider only an effective chemical shift scalar value modifying the local field, thus, $\mathbf{B}_l = \mathbf{B}_0(1+\delta)$. This change in the local field at the spin site, leads to a modified Larmor frequency $\omega_0' = \omega_0(1+\delta)$.

B. Dipolar interactions

As each spin acts as an elementary magnetic dipole moment, spin pairs interact through the following dipole-dipole Hamiltonian.

$$\hat{H}_D = \frac{\gamma_1\gamma_2}{r_{12}^3}\left(\hat{\mathbf{S}}_1 \cdot \hat{\mathbf{S}}_2 - 3\frac{(\hat{\mathbf{S}}_1 \cdot \mathbf{r}_{12})(\hat{\mathbf{S}}_2 \cdot \mathbf{r}_{12})}{r_{12}^2}\right) \,. \tag{6}$$

It is possible to write the full dipolar contribution to the Hamiltonian as $\hat{H}_D = b_{12}\mathbf{S_1}\hat{\mathbf{D}}_{12}\mathbf{S_2}$, where $b_{12} = \frac{\gamma_1\gamma_2}{r_{12}^3}$,and $\hat{\mathbf{D}}_{12} = \mathbb{1} - 3\hat{\mathbf{r}}_{12}\hat{\mathbf{r}}_{12}^T$ is a tensor operator. The dipolar Hamiltonian can be expanded into six terms representing different qualitative components of the dipolar interaction,

$$\hat{H}_D = \frac{\gamma_1\gamma_2}{r_{12}^3}\left(\hat{A} + \hat{B} + \hat{C} + \hat{D} + \hat{E} + \hat{F}\right) \,, \tag{7}$$

with he following meaning for the individual terms:

$$\begin{aligned}
\hat{A} =& \hat{S}_{1z}\hat{S}_{2z}(3\cos^2(\theta) - 1)\\
\hat{B} =& -\frac{1}{4}(\hat{S}_{1+}\hat{S}_{2-} + \hat{S}_{1-}\hat{S}_{2+})(1 - 3\cos^2(\theta))\\
\hat{C} =& -\frac{3}{2}\cos(\theta)\sin(\theta)(\hat{S}_{1z}\hat{S}_{2-} + \hat{S}_{1-}\hat{S}_{2z})e^{i\phi}\\
\hat{D} =& C^*\\
\hat{E} =& -\frac{3}{4}\sin^2(\theta)\hat{S}_{1+}\hat{S}_{2+}e^{-2i\phi}\\
\hat{F} =& E^* \,.
\end{aligned} \tag{8}$$

In writing the expressions in eq. (8) the raising and lowering spin operators make it easier to interpret the effect of each term. Since $\hat{H}_0$ and $\hat{H}_D$ do not commute, the resulting Hamiltonian operator will in general have all non-zero matrix elements. However, a significant simplification of the Hamiltonian is possible due to the presence of the high magnetic field along the z component, in which case the *secular approximation* can be applied. This approximation consists in truncating the expansion of the dipolar Hamiltonian in the basis of the unperturbed part, $\hat{H}_0$ (for a more detailed discussion see [7] and [8]). In order to illustrate the approximation, let us consider a situation not restricted to spin–1/2. In the secular approximation, the dipolar Hamiltonian is written as follows:

$$\hat{H}_D^{(s)} = \sum_n \langle n|\hat{H}_D|n\rangle\, |n\rangle\langle n| + {\sum_{m\neq n}}' \langle m|\hat{H}_D|n\rangle\, |m\rangle\langle n| \ . \tag{9}$$

The primed summation contains only elements that connect degenerate or near degenerate states in $\hat{H}_0$. More precisely, the elements of $\hat{H}_D$ for which $(\hat{H}_D)_{mn} \ll |E_m - E_n|$, where E_n represents the $n-th$ eigenvalue of $\hat{H}_0$, are omitted from the approximated Hamiltonian. In this approximation, the dipolar Hamiltonian has a block diagonal structure, retaining all the diagonal elements and those in blocks along the diagonal corresponding to degenerate or near degenerate subspaces of H_0. By considering the terms $\hat{A}$–$\hat{F}$ above, the only ones fulfilling the criterion of the secular approximation are the terms $\hat{A}$ and $\hat{B}$ (See [7], Chaper IV, and [9], Appendix A.6). Thus,

$$\hat{H}_D^{(s)} = \frac{\gamma_1\gamma_2}{r_{12}^3}\left(\hat{A} + \hat{B}\right) . \tag{10}$$

The term $\hat{A}$ contributes only to the diagonal of $\hat{H}_D^{(s)}$, while $\hat{B}$ represents a transition term within the degenerate subspace of $\hat{H}_0$. For instance, in the case of the spin-1/2 in the uncoupled basis, $\hat{B}$ represents transition between the states $|+-\rangle$ and $|-+\rangle$. The resulting approximated dipolar Hamiltonian can be written as,

$$\hat{H}_D^{(s)} = d_{12}(3\hat{S}_{1z}\hat{S}_{2z} - \hat{\mathbf{S}}_1 \cdot \hat{\mathbf{S}}_2) , \tag{11}$$

where $d_{12} = \frac{b_{12}}{2}\left(3\cos^2\theta - 1\right)$, and the angle θ is measured between the direction of the static field and the relative position vector of the two nuclei. Therefore, the effective contribution of the dipolar term will depend on the resulting average of d_{12} over the possible values of θ. In particular, the resulting contribution of the dipolar Hamiltonian, will be significant for crystalline solids where there is a consistent orientation of the nuclear pairs with respect to the external fields, and will be zero in the case of isotropic liquids due to the averaging effect of molecular mobility. The latter result is easy to obtain by calculating the angular average of d_{12},

$$\overline{d_{12}} = \frac{b_{12}}{2}\int \left(3\cos^2\theta - 1\right) d\Omega = 0. \tag{12}$$

However, even in the case of isotropic liquids, the dipolar contribution to the Hamiltonian is relevant in the relaxation of the spin dynamics and line broadening [10].

C. J-couplings

Although direct dipolar interactions are stronger, they are not responsible for the fine structure of the NMR spectrum in liquids, as discussed above. Indirect spin-spin interactions, or J-couplings are still significant in isotropic liquids and are responsible for the main features of their NMR spectra. Two nuclear spins in the same molecule can interact via the effects their magnetic moments induce on the electronic clouds. Normally, indirect spin-spin coupling is stronger for spins that are separated by a small number of chemical bonds. Therefore, the effects of this indirect coupling in the NMR spectra contributes important information about chemical bonding in molecules. The most general form to represent this interaction is as

$$\hat{H}_{\mathrm{J}} = \hat{\mathbf{S}}_1 \cdot \mathbf{J}_{12} \cdot \hat{\mathbf{S}}_2 , \tag{13}$$

where $\mathbf{J}_{12}$ is the J-coupling tensor. In the case of spatial homogeneity, as in isotropic liquids, the average of the J-coupling interaction over all possible orientations, simplifies the contribution to the Hamiltonian, leading to $\hat{H}_{\mathrm{J}} = J_{12}\hat{\mathbf{S}}_1 \cdot \hat{\mathbf{S}}_2$ [9], where $J_{12} = 1/3(J_{12,xx} + J_{12,yy} + J_{12,zz})$ is the average of the diagonal of the J-coupling tensor.

IV. SPIN-SPIN INTERACTION HAMILTONIAN

When only the effects of the chemical shifts are incorporated into the time independent Hamiltonian, it takes the form,

$$\hat{H}^0 = -\gamma B_0(1+\delta_1)S_{1z} - \gamma B_0(1+\delta_2)S_{2z} , \tag{14}$$

where we also assumed the homonuclear case for which $\gamma_1 = \gamma_2$, as in the case of two interacting protons.

It is straightforward to estimate the energies considering the product basis of the isolated spin system: $|++\rangle$,$|+-\rangle$,$|-+\rangle$,$|--\rangle$. Using $\Delta = \delta_1 - \delta_2$, $\omega_1 = \omega_0(1+\delta_1)$, and $\omega_2 = \omega_0(1+\delta_2)$, the energies of the uncoupled spin system are as follows:

$$\begin{aligned} E_1 &= -\frac{\hbar}{2}\omega_1 - \frac{\hbar}{2}\omega_2 \\ E_2 &= -\frac{\hbar}{2}\omega_0\Delta \\ E_3 &= \frac{\hbar}{2}\omega_0\Delta \\ E_4 &= \frac{\hbar}{2}\omega_1 + \frac{\hbar}{2}\omega_2 \, . \end{aligned} \tag{15}$$

Since the chemical shifts differ normally by a small amount, the two states $|+-\rangle$,$|-+\rangle$, are almost degenerate.

The almost degeneracy of the states $|+-\rangle$ and $|-+\rangle$ of the uncoupled system is lifted when the interaction terms are considered. Within the secular approximation and considering isotropic chemical shifts and J-couplings, the Hamiltonian in the absence of the transversal radiofrequency field takes the following form:

$$\begin{aligned}\hat{H}^{(s)} =& -\gamma B_0(1+\delta_1)\hat{S}_{1z} - \gamma B_0(1+\delta_2)\hat{S}_{2z} + \\ &+ J_{12}\hat{\mathbf{S}}_1\cdot\hat{\mathbf{S}}_2 + d_{12}(3\hat{S}_{1z}\hat{S}_{2z} - \hat{\mathbf{S}}_1\cdot\hat{\mathbf{S}}_2)\,,\end{aligned} \tag{16}$$

where we have now included the J-coupling and dipolar interaction.

To cast the Hamiltonian into a more amenable form, the product operators $\hat{\mathbf{S}}_1\cdot\hat{\mathbf{S}}_2$ can be written in terms of raising and lowering operators by noting that $\hat{\mathbf{S}}_1\cdot\hat{\mathbf{S}}_2 = \hat{S}_{1z}\hat{S}_{2z} + \frac{1}{2}\left(\hat{S}_{1+}\hat{S}_{2-} + \hat{S}_{1-}\hat{S}_{2+}\right)$. With this, the full spin-pair Hamiltonian can be written as follows:

$$\begin{aligned}\hat{H}^{(s)} =& \omega_1\hat{S}_{1z} + \omega_2\hat{S}_{2z} + (J_{12}+2d_{12})\hat{S}_{z1}\hat{S}_{z2} + \\ &+ \frac{1}{2}(J_{12}-d_{12})\left(\hat{S}_{1+}\hat{S}_{2-} + \hat{S}_{1-}\hat{S}_{2+}\right)\,.\end{aligned} \tag{17}$$

It is straightforward to compute the matrix elements of the Hamiltonian in the uncoupled basis, which results in the following matrix:

$$\hat{H}^{(s)} = \frac{\hbar}{2}\begin{pmatrix} \omega_1+\omega_2+\omega_{12}^A & 0 & 0 & 0 \\ 0 & \omega_1-\omega_2-\omega_{12}^A & \omega_{12}^B & 0 \\ 0 & \omega_{12}^B & -\omega_1+\omega_2-\omega_{12}^A & 0 \\ 0 & 0 & 0 & -\omega_1-\omega_2+\omega_{12}^A \end{pmatrix}, \tag{18}$$

where frequencies from the spin-pair terms are as follows:

$$\begin{aligned}\omega_{12}^A =& \frac{1}{2}(J_{12}+2d_{12})\hbar \\ \omega_{12}^B =& (J_{12}-d_{12})\hbar\,.\end{aligned} \tag{19}$$

A. Magnetically equivalent spins

It is interesting to study the relevant case in which the two spins are magnetically equivalent. That means that both have the same chemical shift and thereby the same Larmor frequency. In this case, $\omega_1 = \omega_2 \equiv \omega_0$. The interaction Hamiltonian takes the following form:

$$\hat{H}^{(s)} = \frac{\hbar}{2}\begin{pmatrix} 2\omega_0+\omega_{12}^A & 0 & 0 & 0 \\ 0 & -\omega_{12}^A & \omega_{12}^B & 0 \\ 0 & \omega_{12}^B & -\omega_{12}^A & 0 \\ 0 & 0 & 0 & -2\omega_0-\omega_{12}^A \end{pmatrix}. \tag{20}$$

Given the symmetry of the matrix elements, it is apparent that the matrix will be diagonal in the triplet-singlet coupled basis of two spins 1/2. Therefore, for magnetically equivalent spins we have the following eigenstates:

$$\begin{aligned}|1,1\rangle =& |{+}{+}\rangle \\ |1,0\rangle =& \frac{|{+}{-}\rangle + |{-}{+}\rangle}{\sqrt{2}} \\ |0,0\rangle =& \frac{|{+}{-}\rangle - |{-}{+}\rangle}{\sqrt{2}} \\ |1,-1\rangle =& |{-}{-}\rangle\;.\end{aligned} \tag{21}$$

In this basis, the Hamiltonian matrix is diagonal with the following values for the energy of the states,

$$\begin{aligned}E_1 =& \hbar\omega_0 + \frac{\hbar^2}{4}(J_{12}+2d_{12}) \\ E_2 =& \frac{\hbar^2}{4}(J_{12}-d_{12}) \\ E_3 =& -\frac{3\hbar^2}{4}J_{12} \\ E_4 =& -\hbar\omega_0 + \frac{\hbar^2}{4}(J_{12}+2d_{12})\,.\end{aligned} \tag{22}$$

B. Spectral fine structure in isotropic liquids

In the following we will consider the experimentally relevant situation of an isotropic liquid in which the the two spins have similar chemical shifts. That means that $\Delta \ll 1$, and $d_{12} = 0$, thus leaving the indirect spin-spin coupling and the only spin interaction term in the Hamiltonian.

In this case the Hamiltonian matrix assumes the following form:

$$\hat{H}^{(s)} = \frac{\hbar}{2}\begin{pmatrix} 2\omega_0+\frac{\hbar J}{2} & 0 & 0 & 0 \\ 0 & \omega_0\Delta-\frac{\hbar J}{2} & \hbar J & 0 \\ 0 & \hbar J & -\omega_0\Delta-\frac{\hbar J}{2} & 0 \\ 0 & 0 & 0 & -2\omega_0+\frac{\hbar J}{2} \end{pmatrix}, \tag{23}$$

where we dropped the subscript in the J-coupling constant to simplify the notation.

The energies are,

$$\begin{aligned} E_1 =& \hbar\omega_0 + \frac{\hbar^2 J}{4} \\ E_2 =& -\frac{\hbar^2}{4}J + \frac{\hbar}{2}\sqrt{(\omega\Delta)^2 + (\hbar J)^2} \\ E_3 =& -\frac{\hbar^2}{4}J - \frac{\hbar}{2}\sqrt{(\omega\Delta)^2 + (\hbar J)^2} \\ E_4 =& -\hbar\omega_0 + \frac{\hbar^2}{4}J\,. \end{aligned} \tag{24}$$

The energy levels normalised by the parameter $\hbar\sqrt{\omega_0^2 + (\hbar J)^2}$ as a function of $(\omega_0\Delta)/(\hbar J)$, where $\Delta = 10^{-6}$, showing how the relative shifts in energy change as the relationship between the chemical shifts difference and the spin-spin coupling changes.

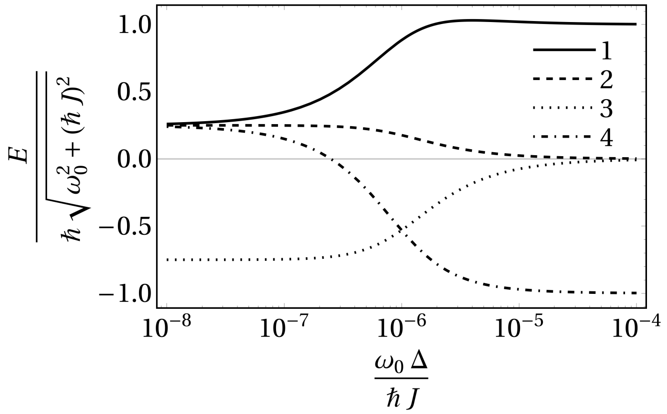

Figure 1. The normalised energies of the spin interaction Hamiltonian in eq. 23 as a function of $\omega_0\Delta/(J\hbar)$, for a chemical shift difference $\Delta = 10^{-6}$. In the limit of very strong J-coupling interaction there are three degenerate levels. The degeneracy splits as soon as the the J-coupling interaction becomes weaker in relation to $\omega_0\Delta$. For a ratio $\omega_0\Delta/(J\hbar)$ of 10^{-4} the levels have already their assymptoptic values.

Given the symmetry of the Hamiltonian matrix, it is clear that the eigenstates will have the following form:

$$\begin{aligned} |\phi_1\rangle =& |{+}{+}\rangle \\ |\phi_2\rangle =& \alpha\,|{+}{-}\rangle + \beta\,|{-}{+}\rangle \\ |\phi_3\rangle =& \beta\,|{+}{-}\rangle - \alpha\,|{-}{+}\rangle \\ |\phi_4\rangle =& |{-}{-}\rangle\ , \end{aligned} \tag{25}$$

where α and β can be found by acting with the Hamiltonian on the either of $|\phi_1\rangle$ or $|\phi_2\rangle$ and using the normalisation condition of the states. The result is,

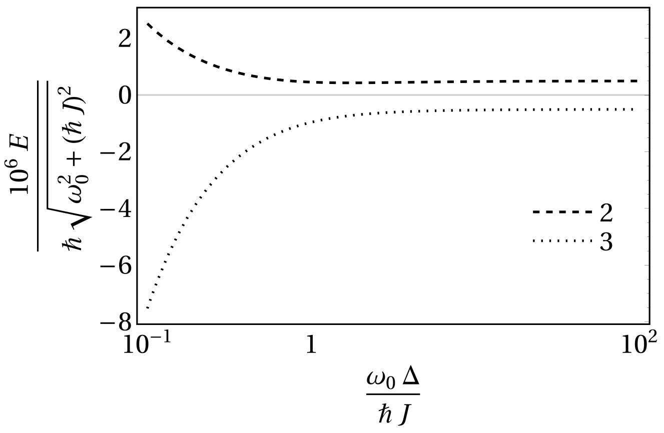

Figure 2. Asymptotic normalised energies (scaled by 10^6) of the spin interaction Hamiltonian in eq. (23) as a function of $\omega_0\Delta/(J\hbar)$ for the levels 2 and 3 (see Figure 1), also using $\Delta = 10^{-6}$. For very weak J-coupling interaction the two levels have an asymptotic split of the normalised energy equal to Δ.

$$\begin{aligned} \alpha =& \left[1 + \left(\frac{\omega_0\Delta}{\hbar J} - \sqrt{1 + \left(\frac{\omega_0\Delta}{\hbar J}\right)^2}\right)^2\right]^{-\frac{1}{2}} \\ \beta =& \left[1 + \left(\frac{\omega_0\Delta}{\hbar J} - \sqrt{1 + \left(\frac{\omega_0\Delta}{\hbar J}\right)^2}\right)^{-2}\right]^{-\frac{1}{2}} . \end{aligned} \tag{26}$$

With these results it is possible now to estimate the allowed transition between the spin-pair states for different situations of experimental interest determined by the relative value between the chemical shift term, $\omega_0\Delta$, and the strength of the J-coupling interaction, $\hbar J$.

C. Allowed transitions and spectral lines

In order to predict the spectrum we first need to determine which are the allowed transitions between the eigenstates of the Hamiltonian. The problem can be analysed perturbatively. In experimental conditions the transverse magnetic field is much weaker than the longitudinal field $\mathbf{B}$. In that situation it is possible to approach the problem with time-dependent perturbation theory. In particular, we can consider that the transverse magnetic field is a perturbation of the time-independent Hamiltonian.

The transversal RF field can be written as

$$\mathbf{B}_{xy}(t) = B_{xy}\mathbf{n}(t)\,, \tag{27}$$

with $\mathbf{n}(t) = \cos(\omega' t)\mathbf{i} - \sin(\omega t)\mathbf{j}$. The following analysis is simpler if we consider the equivalent situation of an oscillating electric field with linear polarisation on the x, y plane, such as $\mathbf{B}_{xy}(t) = \mathbf{B}_{xy}\cos(\omega t)$. This polarised field can be constructed by summing two counter rotating fields as described by eq. (27), with angular frequencies of opposing sign.

The total Hamiltonian is then the sum of the time independent part and the time-dependent perturbation from the oscillating field,

$$\hat{H}(t) = \hat{H} + \delta\hat{H}(t)\,, \tag{28}$$

where $\delta\hat{H}(t) = -\hat{\mathbf{M}}\cdot\mathbf{B}_{xy}(t)$, and $\hat{\mathbf{M}} = \gamma(1+\delta_1)\hat{\mathbf{S}}_1 + \gamma(1+\delta_2)\hat{\mathbf{S}}_2$ is the magnetic moment operator corresponding to the two spins.

Within first-order time-dependent perturbation theory, the transition probability between states m and n is proportional to $|\langle n|\hat{\mathbf{M}}|m\rangle\cdot\mathbf{B}_{xy}|^2$. In order to compute the allowed transitions and the relative intensities of the spectral lines, it is convenient to write the magnetic moment operator,$\hat{\mathbf{M}}$, in term of raising and lowering operators. It is straightforward to verify that

$$\begin{aligned}\hat{\mathbf{M}} =& \frac{\tilde{\gamma}_1}{2}\left[\hat{S}_{1+}(\mathbf{i}-i\mathbf{j}) + \hat{S}_{1-}(\mathbf{i}+i\mathbf{j})\right] + \\ & \frac{\tilde{\gamma}_2}{2}\left[\hat{S}_{2+}(\mathbf{i}-i\mathbf{j}) + \hat{S}_{2-}(\mathbf{i}+i\mathbf{j})\right]\,,\end{aligned} \tag{29}$$

where $\tilde{\gamma}_i = \gamma(1+\delta_i)$. Without any loss of generality, the direction of polarisation of the oscillating transversal field can be taken along x. In that case, the matrix elements of the magnetic moment operator in the coupled basis given by eq. (25) take the form given in Table I.

	$\vert\phi_1\rangle$	$\vert\phi_2\rangle$	$\vert\phi_3\rangle$	$\vert\phi_4\rangle$
$\langle\phi_1\vert$	—	$\alpha\tilde{\gamma}_2+\beta\tilde{\gamma}_1$	$\alpha\tilde{\gamma}_1-\beta\tilde{\gamma}_2$	0
$\langle\phi_2\vert$	$\alpha\tilde{\gamma}_2+\beta\tilde{\gamma}_1$	—	0	$\alpha\tilde{\gamma}_1+\beta\tilde{\gamma}_2$
$\langle\phi_3\vert$	$\alpha\tilde{\gamma}_1-\beta\tilde{\gamma}_2$	0	—	$\alpha\tilde{\gamma}_2-\beta\tilde{\gamma}_1$
$\langle\phi_4\vert$	0	$\alpha\tilde{\gamma}_1+\beta\tilde{\gamma}_2$	$\alpha\tilde{\gamma}_2-\beta\tilde{\gamma}_1$	—

Table I. Matrix elements of the magnetic moment operator

Within first-order time-dependent perturbation theory, a transition between states m and n is forbidden if the corresponding matrix element of the perturbation is zero. It can be seen that such is the case of all the anti-diagonal elements in Table I. In particular, the transitions $|\phi_1\rangle \leftrightarrow |\phi_4\rangle$ and $|\phi_2\rangle \leftrightarrow |\phi_3\rangle$ are forbidden within first-order perturbation theory. We can now calculate the frequencies of the spectral lines for the allowed transitions:

$$\begin{aligned}\omega_2 =& \frac{E_1-E_3}{\hbar} = \omega_0 + (C + \frac{1}{2}\hbar J)\\ \omega_2' =& \frac{E_2-E_4}{\hbar} = \omega_0 + (C - \frac{1}{2}\hbar J)\\ \omega_1' =& \frac{E_1-E_2}{\hbar} = \omega_0 - (C - \frac{1}{2}\hbar J)\\ \omega_1 =& \frac{E_3-E_4}{\hbar} = \omega_0 - (C + \frac{1}{2}\hbar J)\,,\end{aligned} \tag{30}$$

where

$$C = \frac{1}{2}\sqrt{(\omega\Delta)^2 + (\hbar J)^2}\,. \tag{31}$$

As mentioned above, the shape of the spectrum will be determined by the relationships between $\omega\Delta$ and $\hbar J$. Figure 3 shows diagrammatically the different characteristic forms of the spectra. When $J = 0$ there are two lines separated by $\omega_0\Delta$ (panel (a)). This is the typical case of two nuclei without any coupling between them. When there is small spin coupling ($\hbar J \ll \omega_0\Delta$), each line splits into a doublet (panel (b)) with a separation given by $\hbar J$. When the spin coupling strength is similar to the chemical shift difference (panel (c)) the difference in the lines intensities of the duplets becomes apparent. For coupling interactions much stronger than the effect of the chemical shifts, there are two intense lines centred at ω_0, with a separation of approximate $(\omega_0^2\Delta^2)/(2\hbar J)^2$, and two much weaker lines each at a separation $\hbar J$ from its nearest stronger component. Finally, when $\Delta = 0$, the two stronger lines coalesce into a singlet, while the other weaker two lines become negligible and are displaced towards $\pm\infty$.

It is useful to relate the above analysis to the standard NMR nomenclature for systems of two magnetically non-equivalent spins. Cases represented in panels (a) and (b) of Figure 3, characterised by weak coupling, are denoted as AX systems. Systems represented in panels (c) and (d) with strong coupling relative to the chemical shift difference, are referred as AB. Case (d) shows the spectrum of a magnetically equivalent system, which is denoted as A_2–notice that this single-line spectrum corresponds to transitions between the triple-degenerate level upper level shown at the rightmost limit in Figure 1.

We end the section with a brief discussion on the calculation of the relative spectral-line intensities, which can be estimated from the modulus squared of the matrix elements in Table I. In order to simplify the analysis we assume that $\tilde{\gamma}_1 \sim \tilde{\gamma}_2$, which represents a pair of spins with very small chemical shift differences. This situation is both experimentally relevant and simpler to discuss. In that case, the intensities are equal to $(\alpha+\beta)^2$ for the inner lines and to $(\alpha-\beta)^2$ for the outer lines. For the case of $\omega_0\Delta \sim \hbar J$—which corresponds to panel (c) in Figure 3—the ratio between the intensities of the inner and outer lines is $\left(\sqrt{2}+1\right)/\left(\sqrt{2}-1\right)$. The limiting relative intensities for the cases shown in the other panels of Figure 3 can easily be checked in a similar manner. For instance, in panel (e), for $\omega_0\Delta = 0$, it is found that $\alpha = \beta = 1/\sqrt{2}$, resulting in a relative line intesity of 2.

V. DISCUSSION

Much of the value of NMR to provide information about molecular structure depends on the relevant interactions among nuclear spins, and between nuclear spins and the electronic clouds. Due to space constraints, the scope of

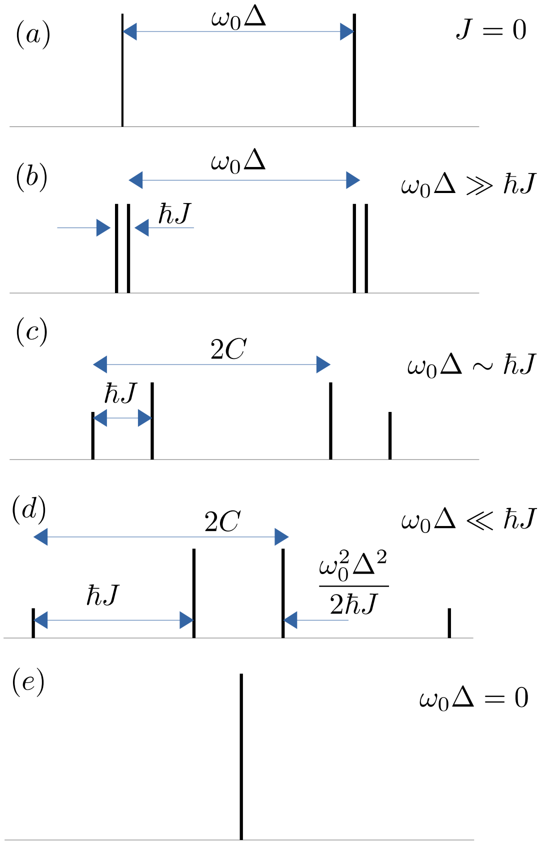

Figure 3. Spectral lines of the two-spin NMR Hamiltonian for different relationships between the chemical shift difference and spin-spin coupling interaction. The different panels show the spectrum under the typical conditions found in experiments. (a) A duplet resulting from an uncoupled spin. (b) Very weak coupling, where each line splits resulting in a quartet. (c) The chemical shift difference is comparable to the coupling strength. (d) Very strong coupling. (e) Magnetically equivalent spins.

this paper has been narrowly focused on the main consequences of spin-spin interactions in the NMR spectra. We left out the vast topic of relaxation in NMR, the analysis of systems with spin higher than 1/2, and systems where there are more than two interacting spins. The reader is directed to the cited literature in order to sample those topics. However, by studying the paradigmatic case of two spin–1/2 nuclei in a range of parameters that is relevant for real systems, we presented a study of the main consequences of spin-spin interactions in the NMR spectra. In particular, we found that the main parameter controlling the qualitative and quantitative structure of the spectrum is the ratio between an effective interaction between the nuclear spins and the local differences in the magnetic field—parametrised by the differences in chemical shifts—and the strength of the spin-spin coupling. The main result is depicted diagrammatically in Figure 3, which links the structure of the spectrum to the key quantities encoding the parameters of the interactions in the system.

There are some immediate possible extensions to this work. The more detailed analysis was focused on isotropic liquids for which there is no effective contribution from dipolar interactions. However, in solid state NMR the dipolar interactions do not necessarily cancel. Thus, a similar study could be done using the Hamiltonian shown in eq. 18, and analyse the resulting spectra incorporating the strength of the dipolar interaction. Another avenue of analysis that directly follows from here is the the study of the temporal dynamics of the interacting systems–more suitably done within the density matrix representation–including pulses sequences and echoes in interacting spin systems.

ACKNOWLEDGMENTS

First of all I would like to thank the superb team in charge of 8.06x at EDX. I have enjoyed enormously 8.06x, and a large part of that has been thanks to how well the course has been organised and supported. I also want to thank Carolina, my wife, whose admirable patience has been essential.

[1] J. Keeler, *Understanding NMR spectroscopy.* John Wiley & Sons, 2011.

[2] M. A. Brown and R. C. Semelka, *MRI: basic principles and applications.* John Wiley & Sons, 2011.

[3] I. I. Rabi, J. R. Zacharias, S. Millman, and P. Kusch, "A new method of measuring nuclear magnetic moment," *Physical Review* **53** (1938) no. 4, 318.

[4] F. B. W. H. M. Packard, "The nuclear induction experiment," *Physical Review* **70** (1946) .

[5] E. M. Purcell, H. C. Torrey, and R. V. Pound, "Resonance absorption by nuclear magnetic moments in a solid," *Physical review* **69** (1946) no. 1-2, 37.

[6] C. P. Poole and H. A. Farach, *The theory of magnetic resonance.* Wiley, 1972.

[7] A. Abragam and A. Abragam, *The principles of nuclear magnetism.* No. 32. Oxford university press, 1961.

[8] C. P. Slichter, *Principles of magnetic resonance*, vol. 1. Springer Science & Business Media, 2013.

[9] M. H. Levitt, *Spin dynamics: basics of nuclear magnetic resonance.* John Wiley & Sons, 2001.

[10] J. Kowalewski and L. Maler, *Nuclear spin relaxation in liquids: theory, experiments, and applications.* CRC press, 2017.

Spontaneous Emission Enhancement of Quantum Dots using Plasmonic Nanostructures

Saipavan Vengaladas

(Dated: June 19, 2019)

Quantum Dots (QD) are artificial atoms which can be modeled as a particle-in-the-box problem after some refinements .In this project, I would discuss how enhancement or quenching the emission or radiation decay rates of QDs can be tailored by engineering the environment using LDOS(Local Density of States) formalism, Purcell enhancement.Plasmonic nanostructures are taken to be Purcell environment in this project and quantum dot is modeled as a dipole emitter and Purcell enhancement is calculated by doing Electromagnetic simulations i.e., solving Maxwell equations with dipole emitter and surrounding medium.

I. INTRODUCTION TO QUANTUM DOTS

In the early days the use of colloidally dispersed pigment particles for producing colorful effects has been known.In 1980s experiments were done with semiconductor nanocrystals with application towards solar energy conversion and photocatalysis [1]. It was found as the size of the semiconductor nanocrystals is modified, strikingly different colors were observed,known as Quantum confinement effect.Exciton (Bound state of an electron-hole pair)in QDs are described by Hydrogen-like Hamiltonian

$$\hat{H} = -\frac{\hbar^2}{2m_h}\nabla_h^2 - \frac{\hbar^2}{2m_e}\nabla_e^2 - \frac{e^2}{\epsilon|r_e - r_h|} \quad (1)$$

where m_e and m_h are the mass of electron(e) and hole(h) respectively.As size of the nano crystal becomes small to the limit of the Bohr radius,the states of the exciton shift to higher energy as according to Heisenberg uncertainity principle as position gets defined well, momentum increases.In the limit of small particles the strongly screened Coloumbic attraction can be neglected (the last term in Eq.1).Both the electron and hole can be together treated as a particle-in-the-box problem model,leading to increase in different spectral energies as the size of the box (radius of QD) is made smaller given by

$$E_{confinement} = \frac{\hbar^2\pi^2}{2a^2}\left(\frac{1}{m_e} + \frac{1}{m_h}\right) \quad (2)$$

Where a is the radius of the QD.

However any other Quantum Emitter can be considered to increase the spontaneous emission rate but in this project QDs are considered.

II. SPONTANEOUS EMISSION & PURCELL ENHANCEMENT

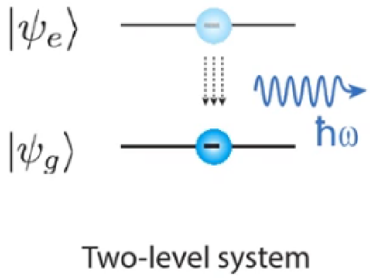

Figure 1. Showing spontaneous emission in a two-level system.Image courtesy:[2]

Spontaneous emission is the process by which excited electrons comes to ground state emitting photon while losing energy.Before Purcell seminal work the spontaneous emission was considered to be intrinsic property,but Purcell proved that it depends on electromagnetic environment [3].The spontaneous emission is a result of Heisenberg uncertainity principle,there is a always uncertainity in knowing the momentum and position of the particle analogously the lowest energy state is a non zero energy state.As harmonic oscillator applied to electromagnetic fields,considering each electromagnetic mode as harmonic oscillator the lowest energy as derived in class $\hbar\omega/2$. Taking time averaged energy of an electromagnetic wave, we get $\frac{Energy}{V} = \epsilon_0 n \mathcal{E}^2$, equating energy to minimum non zero energy $\hbar\omega/2$ .We get zero-point electric field as

$$\mathcal{E} = \sqrt{\frac{\hbar\omega}{2\epsilon_0 n^2 V}} \quad (3)$$

where ϵ_0 is the permittivity of the free space, n is the refractive index of the medium and V is the volume of electromagnetic mode.

This zero-point electric field interacts with every electron as a pertubation [4].Fermi's Golden rule taught in lectures can be deployed here to find the 2-level transition rate with this zero-point electric field as a pertubation.The transition rate W_{mn} from an initial state m to final state n given by

$$W_{if} = \frac{2\pi}{\hbar}\langle m|H'|n\rangle^2 \frac{dN}{dE} \tag{4}$$

where H' is the perturbation, interaction between electron and photon in the dipole approximation given by

$$H' = -q\mathbf{r}.\mathbf{E} \tag{5}$$

where $\mathbf{r}$ is the position vector of electron of charge q and $\mathbf{E}$ is the Electric field. $\frac{dN}{dE}$ is is the photonic density of states i.e the number available photon states per energy level.For free space, one may assume a box with length L in which photon lives as standing wave, requiring $sin(kL) = 0$, where k is the electromagnetic wave vector $k = p\frac{2\pi}{L}$ here p is an integer.Now we can approximate the number of modes in k-space as sphere in k space divided by the spacing between each mode,considering only positive 'k's and multiply by 2 to account for both polarizations

$$N(k) = \frac{\frac{4}{3}\pi k^3 * 2 * \frac{1}{8}}{\left(\frac{\pi}{L}\right)^3} \tag{6}$$

Writing interms of E

$$N(E) = \frac{\frac{1}{3}n^3E^3V}{\pi^2\hbar^3c^3} \tag{7}$$

Taking derivative w.r.t E to get photon density of states

$$\frac{dN}{dE} = \frac{n^3\omega^2V}{\hbar c^3\pi^2} \tag{8}$$

Involving second quantization to find the matrix element we get electric field as

$$\boldsymbol{E} = i\sqrt{\frac{\hbar\omega}{2\epsilon V}}\left(\boldsymbol{a}^\dagger e^{-i\boldsymbol{k}\cdot\boldsymbol{r}-i\omega t} + \boldsymbol{a}e^{i\boldsymbol{k}\cdot\boldsymbol{r}-i\omega t})\hat{e}\right) \tag{9}$$

$\hat{e}$ represents polarization. Where $\boldsymbol{a}^\dagger$ and $\boldsymbol{a}$ are raising and lowering operators for photon states.

$$|\langle\boldsymbol{r}\cdot\boldsymbol{E}\rangle|^2 = |\langle\boldsymbol{a}^\dagger + \boldsymbol{a}\rangle|^2\frac{\hbar\omega}{2n^2\epsilon V} \tag{10}$$

The dot product between the vectors yields a cosine and when averaged over solid angle gives 1/3. This is also equivalent to averaging over polarizations. If we consider the case that state m has 1 photon and state n has none, the spontaneous emission rate from Fermi's golden rule is then[4]

$$\frac{1}{\tau_{sp}} = \frac{2\pi}{3\hbar}|\langle 1, m|q\boldsymbol{x}(\boldsymbol{a}^\dagger + \boldsymbol{a})|0, n\rangle|^2\frac{\hbar\omega}{2n^2\epsilon V}\frac{n^3\omega^2V}{\hbar c^3\pi^2} \tag{11}$$

On operating with raising and lowering operators we have

$$\frac{1}{\tau_{sp}} = \frac{n\omega^3}{3\pi c^3\epsilon_0\hbar}|qx|^2 \tag{12}$$

The above is the spontaneous emission rate for a weak coupling regime in an homogenous environment.

A. Purcell effect

Now instead of free space, if the emission rate is considered in a cavity allowing single mode, calculated by Purcell in 1946 [3],again we bring Fermi's Golden rule for which only a single available photon in the finite energy interval $\hbar\Delta\omega$

Normalizing density of states we have

$$\int_0^\infty \frac{dN}{dE}dE = 1 \tag{13}$$

Assuming Lorentzian shape we get

$$\frac{dN}{dE} = \frac{2}{\pi\hbar\Delta\omega}\frac{\hbar\Delta\omega^2}{4\hbar(\omega-\omega_c)^2 + \hbar\Delta\omega^2} \tag{14}$$

where ω_c is the resonant frequency of the cavity

$$\frac{dN}{dE} = \frac{2}{\pi\hbar\Delta\omega} \tag{15}$$

$$\frac{1}{\tau_{sp}} = \frac{2\pi}{\hbar}|\langle m|q\boldsymbol{x}\boldsymbol{E}|n\rangle|^2\frac{2}{\pi\hbar\Delta\omega} \tag{16}$$

From the second quantization

$$\boldsymbol{E_{max}}^2 = \frac{\hbar\omega}{2\epsilon V} \tag{17}$$

The spontaneous emission rate in the cavity is now

$$\frac{1}{\tau_{sp}} = \frac{2}{\hbar\epsilon}|qx|^2\frac{Q}{V} \tag{18}$$

where $Q = \frac{\omega}{\Delta\omega}$, Quality factor

$$\text{Purcell Factor (PF)} = \frac{\text{Spontaneous emission rate in free space}}{\text{Spontaneous emission rate in cavity}}$$

$$PF = \frac{3}{4\pi^2}\frac{Q\left(\frac{\lambda}{n}\right)^3}{V} \tag{19}$$

But a higher quality factor would trap the photons inside the cavity.So if to increase the emission rate Quality factor should be judiciously chosen.

III. PLASMONIC NANOSTRUCTURES

For any quantum emitter the emission rate depends upon the dipole moment of the transition as derived Eq. (12) .Rewriting interms of dipole moment d

$$\gamma = \frac{1}{\tau} = \frac{k^3|\boldsymbol{d}|^2}{3\pi\epsilon\hbar} \tag{20}$$

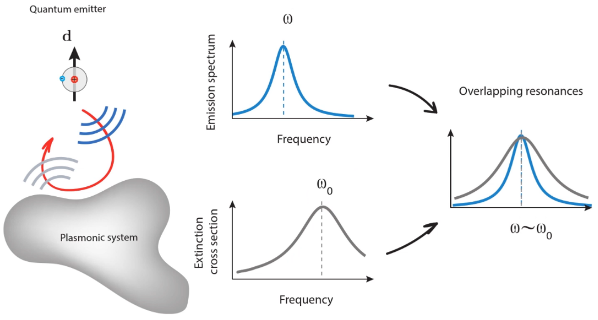

Figure 2. Plasmonic environment to modify the spontaneous emission. Image courtesy:[2]

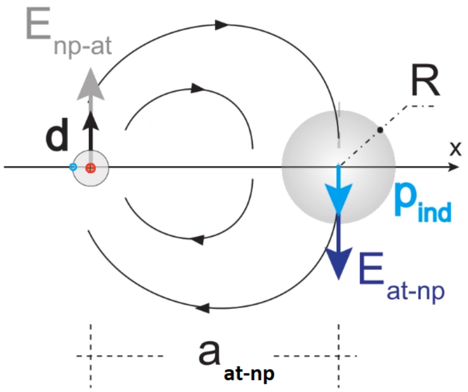

Figure 3. Coupling of Quantum emitter to nanoparticle,illustrating the self action.Image courtesy: [2]

Now we may consider plasmonic environment as shown in Figure 2, may be gold nanoparticle or optical antenna as the medium which changes dipole moment of the transition.Considering the emission spectra of the quantum emitter has resonance at frequency ω and if the plasmonic system has resonance at ω_0 i.e., the extinction crossection is high at ω_0 as shown in Fig 2. If the resonant frequency of the plasmonic system $\omega_0 \simeq \omega$ then emission rate can be increased. Taking the plasmonic system to a gold nanoparticle and a dipole quantum emitter as shown in Figure 3 i.e.,Emitter coupled to nanoparticle.

The atom generates field E_{at} due to emission,which inturn induces dipole moment p_{ind}, defined by the polarizability of the nanoparticle

$$p_{ind} = \alpha(\omega)E_{at-np} \tag{21}$$

where E_{at-np} is Electric field on the nanoparticle due to Quantum emitter, in our case QD where

$$E_{at-np} = g_T d \tag{22}$$

where d is the dipole moment of the QD. The coupling constant $g_T = \frac{-1}{4\pi\epsilon_0 a_{at-np}{}^3}$ where a_{at-np} is the distance between nanoparticle and Quantum emitter as shown.

Now nanoparticle with induced dipole moment which inturn generates a field back in the position of QD as shown in Figure 3, making back action or self action.So this additional field due to plasmonic system enhances the emission rate or quenches as per design and need.So QD can emit less or more because of this self action principle.

IV. EM SIMULATION & RESULTS

Enhancement rate is found by solving Maxwells equation with plasmonic environment i.e., gold nanopaticle coupled with QD,modeled as dipole emitter.We may solve them in any open source EM solvers like MEEP etc.

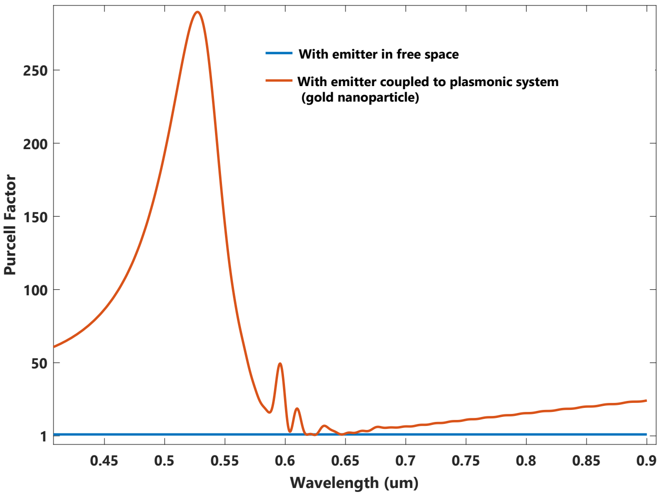

Figure 4. Plot showing the Purcell factor for geometry (see Figure 3)

The above graphs show Purcell enhancement in free space and QD coupled with a nanoparticle of diameter 60nm with $a_{at-np} = 35nm$ taking the dipole emitter's (modeled QD)emission wavelength to be varying from $400 - 900nm$

V. DISCUSSION

Using the formalism of Density of States one may design the suitable environment to modify the emission.Applications would be increasing the emission rate of single photons.Analogously this theory is employed in radiative decay engineering of metamaterials.

ACKNOWLEDGMENTS

I thank Prof.Zwiebach for his excellent lectures throught the course and the TA community for their insightful comments and I acknowledge Edx 8.04x ,8.05x and 8.06x

[1] L. Novotnry, *Principles of Nano-Optics.* Cambridge Publishers, 2016.

[2] ITMO, *Plasmonics: From Fundamentals to Modern Applications.* ITMOx,Edx, 2019.

[3] E.M.Purcell, *Spontaneous emission probabilities at Radio frequencies.* Phys. Rev. 69, 681, 1946.

[4] N. Kumar, *PhD thesis :Spontaneous Emission Rate Enhancement Using Optical Antennas.* UC Berkeley, 2013.

Study of Morse Potential : Exact Solution and Perturbation Technique

Arpon Paul

(Dated: June 19, 2019)

The interatomic interaction which causes vibration in a diatomic molecule can be modeled by the Morse Potential. In the vicinity of its equilibrium point, Morse potential can be regarded as perturbed harmonic oscillator potential. Morse potential models the molecular vibration in a better way than the harmonic oscillator potential because it allows bond dissociation, and the energy levels are not equally spaced. In this paper, the exact solution of Morse Potential will be obtained by analytic method. And then again, time-independent perturbation theory will be used to obtain the energy eigenvalue and energy eigenstates of Morse potential, and compared with the exact result.

I. INTRODUCTION

Any system in the vicinity of its equilibrium point can be modeled by harmonic oscillator potential. That is why Quantum Harmonic Oscillator is widely studied to model vibrations in molecules.

The harmonic oscillation nicely describes molecular vibration, but has some limitations. As the energy gap between successive energy levels in the harmonic oscillator is constant, all transitions occur at the same frequency. However experimentally many lines are found in vibrational specturm. The other limitation is harmonic oscillator has no upper limit of allowed energy level; that means the vibrational energy can be increased to infinity without breaking the bond.

These issues can be solved by the Morse potential, named after physicist Philip M. Morse. In this paper, we first apply some change of variables, and make an analogy with the 2D Harmonic Oscillator. Thus we determine the exact solution to the Morse Potential. And then the critical value of Morse Potential for bond formation is obtained.

In the limiting case, Morse potential becomes the Harmonic potential. So the problem is solved using Perturbation technique also. The higher order terms of Morse Potential is taken into account. So the theory for 2nd order perturbed Hamiltonain is derived in the paper as well.

II. MORSE POTENTIAL AND ITS EXACT SOLUTION

Morse Potential is given as [1]:

$$V(x) = D(e^{-\frac{2x}{a}} - 2e^{-\frac{x}{a}}) \tag{1}$$

As $x \to \infty$, $V(x) \to 0$. So there will be unbounded states for $E > 0$. And this allows bond breaking of molecules.

Now the Hamiltonian for Morse Potential is:

$$H = \frac{p^2}{2\mu} + D(e^{-\frac{2x}{a}} - 2e^{-\frac{x}{a}}) \tag{2}$$

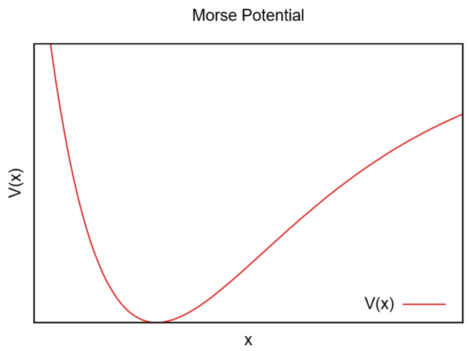

Figure 1. Morse Potential as a function of position

So, the Schrodinger's equation is:

$$-\frac{\hbar^2}{2\mu}\frac{d^2\psi}{dx^2} + D(e^{-\frac{2x}{a}} - 2e^{-\frac{x}{a}})\psi = E\psi \tag{3}$$

We introduce the following quantities to make the computation simpler:

$$\epsilon \equiv \frac{8\mu E a^2}{\hbar^2}, \tag{4}$$

$$\kappa^2 \equiv \frac{8\mu D a^2}{\hbar^2}, \tag{5}$$

$$r \equiv \sqrt{\kappa} e^{-\frac{x}{2a}} \tag{6}$$

After this substitution, we obtain the following,

$$\frac{d^2\psi}{dr^2} + \frac{1}{r}\frac{d\psi}{dr} - \frac{(-\epsilon)}{r^2}\psi + (2\kappa - r^2)\psi = 0 \tag{7}$$

And now we compare this with the radial equation for 2D Harmonic Oscillator[2]:

$$\frac{d^2\psi}{dr^2} + \frac{1}{r}\frac{d\psi}{dr} - \frac{m^2}{r^2}\psi + (2(n+1) - r^2)\psi = 0 \tag{8}$$

where, m is the quantum number related to L_z, and n is the energy quantum number of the 2D Harmonic Potential. And, here, $n = 0, 1, 2, 3...$; $m = n, n-2, n-4...$, i.e, $m = n - 2N$ for $N = 0, 1, 2...$

We can match the following terms:

$$m^2 \Leftrightarrow -\epsilon, \quad n+1 \Leftrightarrow \kappa$$

Using the relation $m = n - 2N$, we obtain:

$$E_n = -D\left(1 - \frac{\hbar}{a\sqrt{2\mu D}}(n + \frac{1}{2})\right)^2 \tag{9}$$

where $n = 0, 1, 2, 3...$

And Eigenfunctions (Similar to the case of 2D H.O.)

$$\psi_n(x) = N(n) r^{\kappa - 2n - 1} e^{-r^2/2} L_n^{(\kappa - 2n - 1)}(r^2) \tag{10}$$

where $N(n) = \left[\frac{(\kappa-2n-1)\Gamma(n+1)}{\Gamma(\kappa-n)}\right]^{1/2}$

And $L_n^{(k)}$ is the associated Laguerre Polynomial.

r and κ are defined as before.

III. BOUND AND UNBOUND STATES

We have already seen: $m \Leftrightarrow \sqrt{-\epsilon}$

And the value of m is a non-negative integer. Therefore, we must have :

$$1 - \frac{\hbar}{a\sqrt{2\mu D}}(n + \frac{1}{2}) \geq 0 \tag{11}$$

So, $E_n \leq E_{n+1}$

In case we have $E_n \geq E_{n+1}$, the E_{n+1} state is not a bound state. So the maximum value of E for bound state is 0. This agrees with classical results also.

We can find out a critical value for the constant D so that there exists at least one bound state. To find out the critical value D_c, we set $n = 0$:

$$1 - \frac{\hbar}{2a\sqrt{2\mu D_c}} = 0 \tag{12}$$

$$D_c = \frac{\hbar^2}{8\mu a^2} \tag{13}$$

So, if $D \leq D_c$, molecular bond formation will not be possible.

IV. PERTURBATION THEORY FOR TAYLOR SERIES EXPANSION OF HAMILTONIAN

Let the Hamiltonian can be expressed as a Taylor series expansion

$$H(\lambda) = H^{(0)} + \lambda H^{(1)} + \lambda^2 H^{(2)} + \lambda^3 H^{(3)} + ... \tag{14}$$

And the eigenvalue equation for this Hamiltonain

$$\begin{aligned}&\left(H^{(0)} + \lambda H^{(1)} + \lambda^2 H^{(2)} + ...\right)\left(|n^{(0)}\rangle + \lambda |n^{(1)}\rangle + ...\right)\\ &= \left(E_n^{(0)} + \lambda E_n^{(1)} + \lambda^2 E_n^{(2)} + ...\right)\left(|n^{(0)}\rangle + \lambda |n^{(1)}\rangle + ...\right)\end{aligned} \tag{15}$$

Now equating the coefficients of different powers of λ :

$$\lambda^0 : H^{(0)}|n^0\rangle = E_n^{(0)}|n^{(0)}\rangle \tag{16}$$

$$\lambda^1 : H^{(0)}|n^{(1)}\rangle + H^{(1)}|n^{(0)}\rangle = E_n^{(0)}|n^{(1)}\rangle + E_n^{(1)}|n^{(0)}\rangle \tag{17}$$

$$\begin{aligned}\lambda^2 : &H^{(0)}|n^{(2)}\rangle + H^{(1)}|n^{(1)}\rangle + H^{(2)}|n^{(0)}\rangle\\ &= E_n^{(0)}|n^{(2)}\rangle + E_n^{(1)}|n^{(1)}\rangle + E_n^{(2)}|n^{(0)}\rangle\end{aligned} \tag{18}$$

Multiplying equation (17) by $\langle m^{(0)}|$:

$$E_n^{(1)} = H_{nn}^{(1)} \tag{19}$$

$$|n^{(1)}\rangle = \sum_{m \neq n} \frac{H_{mn}^{(1)}}{E_n^{(0)} - E_m^{(0)}} |m^{(0)}\rangle \tag{20}$$

Here we assumed $|n^{(1)}\rangle, |n^{(2)}\rangle$... etc have no component along $|n^{(0)}\rangle$

Similarly, from equation (18)

$$E_n^{(2)} = H_{nn}^{(2)} + \langle n^{(0)}|H^{(1)}|n^{(1)}\rangle \tag{21}$$

$$= H_{nn}^{(2)} + \sum_{m \neq n} \frac{|H_{mn}^{(1)}|^2}{E_n^{(0)} - E_m^{(0)}} \tag{22}$$

$$\langle m^{(0)}|n^{(2)}\rangle = \frac{1}{E_n^{(0)} - E_m^{(0)}} \cdot \left(H_{mn}^{(2)} + \langle m^{(0)}|H^{(1)}|n^{(1)}\rangle - E_n^{(1)}\langle m^{(0)}|n^{(1)}\rangle\right) \tag{23}$$

V. SERIES EXPANSION OF MORSE POTENTIAL

$$V(x) = D(e^{-\frac{2x}{a}} - 2e^{-\frac{x}{a}}) \tag{24}$$

$$= D\left(1 - \frac{2x}{a} + \frac{1}{2} \cdot \frac{4x^2}{a^2} - \frac{1}{6} \cdot \frac{8x^3}{a^3} + \frac{1}{24} \cdot \frac{16x^4}{a^4} + ...\right) \tag{25}$$

$$- 2D\left(1 - \frac{x}{a} + \frac{1}{2} \cdot \frac{x^2}{a^2} - \frac{1}{6} \cdot \frac{x^3}{a^3} + \frac{1}{24} \cdot \frac{x^4}{a^4} + ...\right) \tag{26}$$

$$= -D + \frac{Dx^2}{a^2} - \frac{Dx^3}{a^3} + \frac{7Dx^4}{12a^4} + ... \tag{27}$$

$$= -D + \frac{Dx^2}{a^2} - \lambda \cdot \frac{Dx^3}{a} + \lambda^2 \cdot \frac{7Dx^4}{12} + ... \tag{28}$$

where $\lambda = \frac{1}{a^2}$

So the full Hamiltonian

$$H(\lambda) = \frac{p^2}{2\mu} + \frac{Dx^2}{a^2} - D - \lambda \cdot \frac{Dx^3}{a} + \lambda^2 \cdot \frac{7Dx^4}{12} + ... \tag{29}$$

Thus we get

$$H^{(1)} = -\frac{Dx^3}{a} \tag{30}$$

$$H^{(2)} = \frac{7Dx^4}{12} \tag{31}$$

VI. ENERGY EIGENVALUES AND EIGENSTATES

Comparing with the Harmonic Oscillator potential:

$$H = \frac{p^2}{2\mu} + \frac{1}{2}\mu\omega^2 x^2 \tag{32}$$

we obtain,

$$\omega = \sqrt{\frac{2D}{\mu a^2}} \tag{33}$$

Energy eigenvalues to the zeroth order

$$E_n^{(0)} = \hbar\omega\left(n + \frac{1}{2}\right) - D \tag{34}$$

We define the ladder operators

$$a = \sqrt{\frac{\mu\omega}{2\hbar}}\left(x + \frac{i}{\mu\omega}\right) \tag{35}$$

$$a^\dagger = \sqrt{\frac{\mu\omega}{2\hbar}}\left(x - \frac{i}{\mu\omega}\right) \tag{36}$$

And position operator in terms of ladder operators:

$$x = \sqrt{\frac{\hbar}{2\mu\omega}}(a^\dagger + a) \tag{37}$$

$$= x_0(a^\dagger + a) \tag{38}$$

where $x_0 = \sqrt{\frac{\hbar}{2\mu\omega}}$

Now

$$\langle n^{(0)}|x^3|n^{(0)}\rangle = x_0^3\langle n^{(0)}|(a^\dagger + a)^3|n^{(0)}\rangle \tag{39}$$

$$= 0 \tag{40}$$

So $E_n^{(1)} = 0$ And

$$\langle m^{(0)}|x^3|n^{(0)}\rangle \tag{41}$$

$$= x_0^3\langle m^{(0)}|(a^\dagger + a)^3|n^{(0)}\rangle \tag{42}$$

$$\begin{aligned}
&= x_0^3\big(\sqrt{n(n-1)(n-2)}\delta_{m,n-3} \\
&+ \sqrt{(n+1)(n+2)(n+3)}\delta_{m,n+2} \\
&+ \left((n+2)\sqrt{n+1} + (n+1)\sqrt{n+2} + n\sqrt{n+1}\right)\delta_{m,n+1} \\
&+ \left((n+1)\sqrt{n} + n\sqrt{n} + n\sqrt{n-1}\right)\delta_{m,n-1}\big)
\end{aligned} \tag{43}$$

Now

$$|n^{(1)}\rangle = \sum_{m\neq n}\frac{H_{mn}^{(1)}}{E_n^{(0)} - E_m^{(0)}}|m^{(0)}\rangle \tag{44}$$

$$\begin{aligned}
&= -\frac{Dx_0^3}{\hbar\omega a}\big(\frac{1}{3}\sqrt{n(n-1)(n-2)}|n-3^{(0)}\rangle \\
&- \frac{1}{2}\sqrt{(n+1)(n+2)(n+3)}|n+2^{(0)}\rangle \\
&- ((n+2)\sqrt{n+1} + (n+1)\sqrt{n+2} \\
&\qquad + n\sqrt{n+1})|n+1^{(0)}\rangle \\
&+ \left((n+1)\sqrt{n} + n\sqrt{n} + n\sqrt{n-1}\right)|n-1^{(0)}\rangle\big)
\end{aligned} \tag{45}$$

$$\langle n^{(0)}|x^4|n^{(0)}\rangle = x_0^4\langle n^{(0)}|(a^\dagger + a)^4|n^{(0)}\rangle \tag{46}$$

$$= x_0^4(5n^2 + 7n + 3) \tag{47}$$

$$E_n^{(2)} = H_{nn}^{(2)} + \sum_{m\neq n}\frac{|H_{mn}^{(1)}|^2}{E_n^{(0)} - E_m^{(0)}} \tag{48}$$

$$\begin{aligned}
&= \frac{7Dx_0^4}{12}\cdot(5n^2 + 7n + 3) \\
&+ \frac{D^2x_0^6}{a^2\hbar\omega}\Big[\frac{1}{3}n(n-1)(n-2) - \frac{1}{2}(n+1)(n+2)(n+3) \\
&- \left((n+2)\sqrt{n+1} + (n+1)\sqrt{n+2} + n\sqrt{n+1}\right)^2 \\
&+ \left((n+1)\sqrt{n} + n\sqrt{n} + n\sqrt{n-1}\right)^2\Big]
\end{aligned} \tag{49}$$

$$\begin{aligned}
&= \frac{\hbar^2a^2}{32\mu}\Big[\frac{7}{3}(5n^2 + 7n + 3) + \frac{1}{3}n(n-1)(n-2) \\
&- \frac{1}{2}(n+1)(n+2)(n+3) \\
&- \left((n+2)\sqrt{n+1} + (n+1)\sqrt{n+2} + n\sqrt{n+1}\right)^2 \\
&+ \left((n+1)\sqrt{n} + n\sqrt{n} + n\sqrt{n-1}\right)^2\Big]
\end{aligned} \tag{50}$$

Finally, upto second order

$$\begin{aligned}
E_n &= -D + \hbar\sqrt{\frac{2D}{\mu a^2}}\left(n + \frac{1}{2}\right) + \frac{\hbar^2}{32\mu a^2}\Big[\frac{7}{3}(5n^2 + 7n + 3) \\
&+ \frac{1}{3}n(n-1)(n-2) \\
&- \frac{1}{2}(n+1)(n+2)(n+3) \\
&- \left((n+2)\sqrt{n+1} + (n+1)\sqrt{n+2} + n\sqrt{n+1}\right)^2 \\
&+ \left((n+1)\sqrt{n} + n\sqrt{n} + n\sqrt{n-1}\right)^2\Big]
\end{aligned} \tag{51}$$

VII. DISCUSSION

In this article, we first changed the variable and made an analogy with the problem of 2D Harmonic Oscillator, and thus the exact solution is found. Then we solved the same problem using perturbation technique. The results agree upto first order term.

[1] A. Lucas, "The morse potential." `https://web.stanford.edu/~ajlucas/The%20Morse%20Potential.pdf`, March 2019.

[2] W. Pauli, *Wave Mechanics: Volume 5 of Pauli Lectures on Physics*. Dover Publications, 2000.

[3] "Wikipedia." `https://en.wikipedia.org/wiki/Morse_potential`, March 2019.

[4] M. S. J. P. Dahl, "The morse oscillator in position space, momentum space, and phase space," *Journal of Chemical Physics*, 1988.

[5] H. Taseli, "Exact solutions for vibrational levels of the morse potential," *J. Phys. A: Math. Gen. 31*, 1998.

[6] J. L. L.-B. M. Berrondo, A. Palma, "Matrix elements for the morse potential using ladder operators," *International Journal of Quantum Chemistry*, 1987.

Thermal Radiation from Quantum Transitions

David E. Brahm, Ph.D., CFA

(Dated: June 19, 2019)

Hot matter radiates, and in many cases the radiation approaches a blackbody distribution. How do we explain this using quantum mechanics? How do we reconcile the continuous spectrum seen in real life with the sharp spectral lines of discrete electron transitions that quantum theory predicts?

I. INTRODUCTION

Hot matter radiates. Examples include the sun, fire[1], an incandescent tungsten bulb filament, and a kiln. If we observe the visible radiation with a spectrometer (Fig. 1), in some cases, *e.g.* a sodium vapor streetlamp, we see distinct spectral lines which correspond to known atomic transitions. But often we see a continuous spectrum that roughly matches a Planck (or "blackbody") distribution characterized by a temperature T, whose mean energy density $U(\omega)$ is given by:

$$U(\omega)\mathrm{d}\omega = \frac{\hbar\omega^3}{\pi^2 c^3}\frac{\mathrm{d}\omega}{e^{\hbar\omega/(k_B T)}-1}. \tag{1}$$

Planck showed[2] that this was the expected result for a photon gas in thermal equilibrium with its environment. But how do the photons achieve thermal equilibrium, when 1) photons do not self-interact, and 2) they only interact with atoms which have discrete electron energy levels?

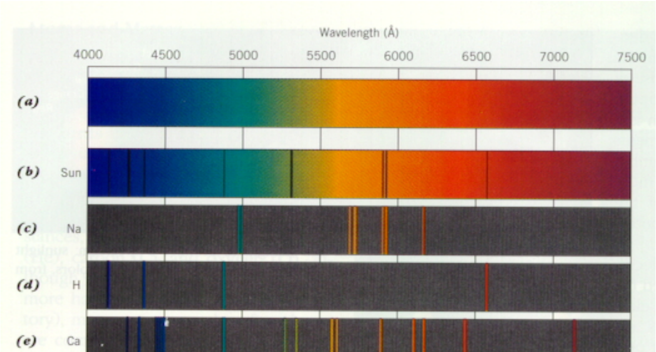

Figure 1. Emission Spectra

For numerical calculations, we will use $T = 5800\,\mathrm{K}$ for a typical temperature of interest, as that is roughly the effective temperature at the (optical) surface of the sun. With the Boltzmann constant $k_B = 8.62\times10^{-5}\,\mathrm{eV/K}$, we then have $1/\beta = k_B T = 0.5\,\mathrm{eV}$ to a good approximation. The distribution (1) peaks at about $\omega_{max} = 2.8\,k_B T/\hbar$ (Wien's displacement law[3]), where a photon's energy is $E_\gamma = 1.4\,\mathrm{eV}$, a wavelength of $885\,\mathrm{nm}$ (near-infrared). The peak in wavelength-space is closer to $500\,\mathrm{nm}$, (not coincidentally) right in the middle of the visible light spectrum. So for numerical calculations, we will take for round numbers:

$$k_B T \approx 0.5\,\mathrm{eV}, \qquad E_\gamma \approx 2\,\mathrm{eV} \tag{2}$$

II. PHOTON SELF-INTERACTIONS

Consider a cool gas in a warm box. Gas molecules in contact with the box gain energy from the walls; then those hotter, faster molecules collide with other gas molecules. These collisions (heat conduction) re-distribute energy throughout the bulk, until thermal equilibrium is reached.

Can photons in a box equilibrate the way gas molecules do? To first approximation they cannot, because (at tree level) **photons do not self-interact**. Equivalently: photons carry no electrical charge; $U(1)_{EM}$ is an Abelian gauge symmetry; there are no γ^3 or γ^4 terms in the Lagrangian; electric and magnetic fields add linearly. Note that no γ^3 terms can arise from loop diagrams either, due to Furry's Theorem[4].

However, at 1-loop the Feynman diagram Fig. 2 (and others related by exchange) results in a photon-photon cross-section (for energies well below the electron mass m)[5–7]:

$$\frac{\mathrm{d}\sigma}{\mathrm{d}\Omega} = \frac{139\alpha^4}{(180\pi)^2}\frac{\omega^6}{m^8}(3+\cos^2\theta)^2 \tag{3}$$

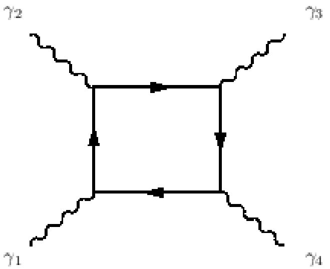

Figure 2. Photon-Photon Scattering at 1-Loop

The mean free path λ for a photon of energy E_γ in a thermal bath at inverse temperature β is derived in [5] as:

$$\lambda \approx 5.9 \times \frac{m^8\beta^6}{\alpha^4 E_\gamma^3} \tag{4}$$

One could have roughly estimated this result just from the 4 electron propagators which give rise to 8 powers of m/E_γ, and 4 vertices which give 4 powers of $1/\alpha$. Can this photon-photon cross-section cause a photon bath to equilibrate? Using $E_\gamma \approx 2\,\mathrm{eV}$ and $1/beta = k_BT \approx 0.5\,\mathrm{eV}$ as suggested in eq. (2), we get $\lambda \approx 10^{51}\,\mathrm{m}$, which is 25 orders of magnitude larger than the universe.

So our original conclusion is correct: photons do not thermalize in the bulk, because they are effectively non-self-interacting.

Note this is distinct from the phenomenon of radiative heating; different parts of the box can (and do) thermalize by exchanging photons. In a closed box that has reached thermal equilibrium, photons are absorbed and emitted by the walls at the same rate. But the photon bath itself can only have the thermal properties imparted to it by the walls.

III. LINE BROADENING

A. Einstein's A and B Coefficients

Let's review Einstein's argument about the rates of absorption B_a, stimulated emission B_e, and spontaneous emission A[3]. In a 2-state system with energy separation $\hbar\omega = E_b - E_a$, the Boltzmann ratio of their populations is $N_b/N_a = e^{-\hbar\omega/(k_BT)}$, and both populations are static $\dot{N}_a = \dot{N}_b = 0$. Then

$$\dot{N}_b = B_a U(\omega) N_a - B_e U(\omega) N_b - A N_b = 0 \tag{5}$$

leads to the requirement $B_e = B_a$ (the "principle of detailed balance"[8]), and

$$\frac{A}{B_e} = \frac{\hbar\omega^3}{\pi^2 c^3} \tag{6}$$

which provides a great way to find A when the calculation of B_e is easier (using harmonic perturbation theory). The ratio of contributions of spontaneous to stimulated emission is:

$$\frac{A}{B_e U(\omega)} = e^{\hbar\omega/(k_BT)} - 1 \tag{7}$$

When we consider photons near the peak of a thermal bath, with $\hbar\omega/(k_BT) \approx 4$ (2.8 – 5.0 depending on exactly how you define the "peak"), spontaneous emission actually provides the majority of the photons, and the mean population of a given mode $\langle n\rangle < 1$. So around the peak of the spectrum, the existence of the bath and the surrounding cavity is secondary; an isolated hot object (*e.g.* a glowing iron rod) emits approximately blackbody radiation just from spontaneous emission. This is sometimes called the "bad cavity limit".

B. The Optical Bloch Equations

Einstein's analysis treated the 2-state system classically (though statistically), with populations N_a and N_b. The true quantum state of any single 2-state atom is $\Psi = C_a\Psi_a + C_b\Psi_b$, and its statistical properties are described by the **density matrix**

$$\rho = \Psi\Psi^\dagger = \begin{pmatrix} |C_a|^2 = N_a/N & C_aC_b^* \\ C_a^*C_b & |C_b|^2 = N_b/N \end{pmatrix} \tag{8}$$

The **optical Bloch equations**[3] generalize eq. (5) above for a density matrix with non-zero off-diagonal elements, and are used to calculate line broadening. They are called "optical Bloch equations" by analogy to Felix Bloch's equations for a 2-state spin system in a magnetic field (see the discussion of Nuclear Magnetic Resonance in 8.05x chapter 10[9]). After applying the "rotating-wave approximation" (ignoring high-frequency terms and keeping only $(\omega_0 - \omega)$ terms), these are, analogous to Zwiebach's 8.06x eq. (5.3.57)[10][3]:

$$\frac{\mathrm{d}\rho_{22}}{\mathrm{d}t} = -\frac{\mathrm{d}\rho_{11}}{\mathrm{d}t} = \frac{\delta H'_{fi}}{i\hbar}\left[e^{i(\omega_0-\omega)t}\rho_{12} - e^{-i(\omega_0-\omega)t}\rho_{21}\right] \tag{9}$$

$$\frac{\mathrm{d}\rho_{12}}{\mathrm{d}t} = \frac{\mathrm{d}\rho_{21}^*}{\mathrm{d}t} = \frac{-\delta H'_{fi}}{i\hbar} e^{i(\omega_0-\omega)t}(\rho_{11} - \rho_{22}) \tag{10}$$

We will not show detailed derivations here, as the results for various kinds of line broadening can be motivated by simpler dimensional arguments, but the new physics (*vs* Einstein's approach) lies in the evolution of the atom's quantum phase, the off-diagonal term ρ_{12}.

C. Radiative and Power Broadening

Lines are (unavoidably!) broadened by the finite lifetime of the initial state (**radiative broadening**, also called lifetime broadening), and are also broadened when the light source (or surrounding bath) is very intense (**power broadening**). Both effects can be calculated[3] using the optical Bloch equations, but turn out to be very small and mostly irrelevant for visible-spectrum thermal radiation.

D. Doppler Broadening

Can the smooth blackbody spectrum arise from sharp lines that are blurred out due to Doppler broadening? That is, the molecules of the box are themselves moving with kinetic energy of order k_BT, so the frequency of their emitted light is Doppler shifted in the rest frame of the box. A sharp line of angular frequency ω gets blurred into a Gaussian of relative width[11]

$$\frac{\sigma_\omega}{\omega} = \sqrt{\frac{k_BT}{Mc^2}} \tag{11}$$

where M is the mass of the atom or molecule. If we again take $k_BT = 0.5\,\mathrm{eV}$, and consider sodium atoms with $Mc^2 = 21 \times 10^9\,\mathrm{eV}$, we see the lines are broadened by 5×10^{-6}, or about 0.003 nm, a fairly small effect, not even enough to overlap the two sodium D-lines. So again, under ordinary circumstances, Doppler broadening does not do much to smooth the spectrum.

On the other hand, if free electrons with $m_ec^2 = 5.11 \times 10^5\,\mathrm{eV}$ are the moving sources, the relative broadening is about 1 part in 100.

E. Collision (Pressure) Broadening

When an atom or molecule collides with another, its state is momentarily disrupted, and even when its energy levels are unchanged (elastic collision), their phase changes. Effectively this interrupts an emission process and broadens the line, causing a width $\sigma_\omega = 1/\tau_0$, where τ_0 is the mean time between collisions[3]. In a more rigorous derivation, the collision effect adds a new term to the second equation in eq. (10).

We note that collision broadening produces a Lorentz profile (not a Gaussian)[12]:

$$\phi(\omega) = \frac{\Gamma}{(\omega - \omega_0)^2 + \Gamma^2} \tag{12}$$

$$\Gamma = \gamma + 2\nu_{\mathrm{col}} \tag{13}$$

where ν_{col} is the collision frequency, and γ is the natural line width. This is notable mainly because a Lorentz distribution diminishes much more slowly than a Gaussian far away from the peak, and so sometimes Doppler broadening dominates close to the peak but collision broadening dominates further away.

Though it is just a heuristic, we like this picture from Rybicki & Lightman[12]: A sine wave, interrupted by random phase shifts, Fourier transforms into the Lorentz distribution of eq. (12).

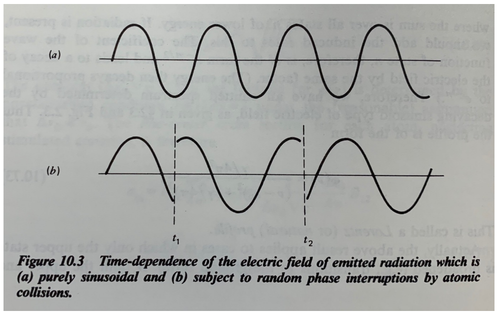

Figure 3. Light Output When the Phase is Frequently Interrupted

$\frac{1}{\tau_0}$ is (molecular velocity) / (mean free path), where the numerator is calculated from thermodynamics $v = \sqrt{3k_BT/M}$, and the inverse of (mean free path) is just cross-sectional area πd^2 times number density n. Here d is the effective size of the molecule. For an ideal gas, $n = P/(k_BT)$. Putting these together,

$$\frac{\sigma_\omega}{\omega} = \frac{1}{\omega\tau_0} \approx \pi d^2 \frac{\lambda}{2\pi} \frac{P}{k_BT} \sqrt{\frac{3k_BT}{Mc^2}}. \tag{14}$$

Again thinking of a sodium gas at 6000 K and 1 atmosphere pressure ($P = 10^5\,\mathrm{Pa}$), we plug in $d = 0.3\,\mathrm{nm}$, $\lambda = 589\,\mathrm{nm}$ (the sodium D lines), $k_B = 1.38 \times 10^{-23} J/K$, and $3k_BT/(Mc^2) = 3(0.5)/(21 \times 10^9)$. We find a collision time τ_0 of about 10^{-11} s, and a fractional line broadening of 3×10^{-5}. Note this is a bit larger than the Doppler broadening we derived above, though still too small to solve our puzzle yet. Loudon[3] says, "elastic . . . collisions . . . [have] the dominant line-broadening effect for a wide range of physical conditions."

Now we have something to work with. The same sodium gas at 10^4 atmospheres would have $\sigma_\omega/\omega \approx 1$, smearing its lines out entirely. That's an extreme pressure for a gas, but remember it's really the number density $n = P/(k_BT) \approx 10^{28}/\mathrm{m}^3$ that matters, and the number density of solid (metallic) sodium is several times that:

$$n = \frac{10^6 g}{\mathrm{m}^3} \cdot \frac{6.02 \times 10^{23}}{23\,\mathrm{g}} \approx 3 \times 10^{28}/\mathrm{m}^3. \tag{15}$$

Our analysis is woefully inadequate to describe the emergent properties of metals, crystals, and other solids, but we have shown that the density of solids alone should allow for the complete smearing (or redistribution) of atomic spectral lines.

IV. SOURCES OF RADIATION

We have concluded that a "blackbody" (or similarly a "gray body" which has emissivity less than one but produces a similar spectrum) can be either a gas at very high pressure (10^4 atm), or a liquid or solid. Armed with that idea, let us now review some sources of visible-range light.

Atomic transitions in a gas produce sharp emission lines, such as the sodium D-lines at approximately 590 nm (yellow), which arise from electrons dropping from 3p to 3s orbitals. Fine splitting of 3p into $3p_{3/2}$ and $3p_{1/2}$ explains why there are two lines about 0.6 nm apart. Low-pressure sodium vapor streetlamps, with their distinctive yellow glow, produce these lines by sending an electric arc through sodium vapor. Doppler and collision broadening effects are small. There are also "high-pressure sodium" lamps which show some pressure-broadening, and also introduce xenon and mercury to diversify the spectrum.

Mercury-vapor lamps work similarly, with sharp lines at 579 nm (orange), 546 nm (green), 436 nm (blue), and also ultraviolet lines 254 nm and 185 nm; see row (f) of Fig. 1. The net effect is much more bluish than sodium lamps, and you can always distinguish these two older kinds of streetlamps.

A **fluorescent lamp** is (usually) a low-pressure mercury vapor lamp coated with phosphor, which absorbs the UV and emits a broader spectrum of visible (mostly reddish) light. This process of absorption at one frequency and spontaneous emission at a lower frequency is called *fluorescence*[3]. A spectrograph of a fluorescent lamp shows a continuous spectrum superimposed on the distinct lines, see Fig. 4.

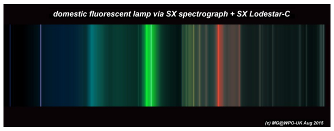

Figure 4. Spectrograph of a Fluorescent Lamp

Vibrational modes of molecules also produce distinct lines, but they usually lie in the infrared. For example, water's vibrational modes produce (or absorb) light around 3000 nm and 6000 nm. (Contrary to popular belief, this is **not** what microwave ovens couple to.) Rotational modes and intermolecular vibrations produce even longer wavelengths, in the far-infrared or microwave. While these contribute to the overall spectrum, they are generally not the source of visible-wavelength photons.

A **candle flame** seems to violate our conclusion, as it is a hot gas at 1 atm that shows both sharp lines and a smooth Planck-distributed background. The gases are mainly CO_2 and H_2O, because wax consists of hydrocarbons. The blue base of the flame emits the characteristic lines of CO_2 and H_2O. But the yellow top consists largely of hot soot particles (solid carbon and unburnt hydrocarbons), and that produces the smooth background.

In a **crystal**, light can couple to phonons (lattice vibrations) and to excitons (electron-hole pairs). With near-continuous energy levels, these can provide a broadly distributed light spectrum, *i.e.* crystals can be blackbodies (or gray bodies). A proper study is beyond the scope of this paper, but these emergent phenomena provide a more accurate picture than the extreme collision-broadening analysis done above.

In a solid **metal**, electrons inhabit conduction bands that traverse multiple atoms. Transitions between the closely-spaced conduction bands can provide a source of blackbody photons. These interactions can be modeled as photon-plasmon interactions, again beyond the scope of this paper but an important branch of quantum optics. A hot metal, such as a glowing iron rod or a tungsten filament, emits a continous Planck-like spectrum.

In a **plasma**, electrons are not bound to atoms, due to either high temperature or an external electric voltage (or both). The electrons inhabit a continuum of energy levels, so the spectrum is broad. A glowing plasma can produce a good blackbody spectrum. Most of the sun's interior is a hot plasma.

We end (as we began) with the sun. Very high-energy light is produced by nuclear fusion at its core. It thermalizes with the hot plasma, which shields the Earth from the most dangerous gamma radiation. The **solar photosphere** is a layer several hundred kilometers thick near the surface, consisting primarily of hydrogen gas (and some helium) at about 5800 K and 0.1 atm, and the surface of last scattering lies here. We have argued that this low-pressure gas produces sharp spectral lines, and indeed these are seen as *absorption* (dark) lines on top of the broad spectrum that comes from further below. The mechanism by which the broad spectrum reproduces a Planck distribution (with $T \approx 5800\,\mathrm{K}$) is still not clear to us – is hotter light from below somehow "cooled down" by absorption, or is there something in the photosphere that plays the role of "soot" in a flame? Above the photosphere, there is a thin but hot **chromosphere** (you can see it during an eclipse), which has a red hue from the 656 nm $n = 3 \to n = 2$ Balmer line of hydrogen.

V. DISCUSSION

From Reif[8] p.373: "Photons are continuously absorbed and re-emitted by the walls; it is, of course, by virtue of these mechanisms that the radiation inside the container depends on the temperature of the walls. But, as usual, it is not at all necessary to investigate the exact mechanisms which bring about the thermal equilibrium, since the general probability arguments of statistical mechanics suffice to describe the equilibrium situation."

We have shown, however, that photons cannot thermalize themselves in the bulk of a cavity, so for a photon of angular frequency ω to exist in the container, it must have been created by a particular process in the walls with energy gap $\hbar\omega$. Some materials have a continuum of levels available, so when heated they produce a blackbody spectrum; even when they are not perfect absorbers or emitters, they are called **gray bodies**. Other materials have only a few electron energy levels, and can only produce sharp line spectra. It is impossible to contain a photon bath in thermal equilibrium using a material that does not absorb/emit the full spectrum.

---

[1] T. C. Rains, *Flame Emission and Atomic Absorption Spectrometry: Elements and matrices*. M. Dekker, 1975.

[2] M. Planck, *The Theory of Heat Radiation*. P. Blakiston's Son & Co, 1914.

[3] R. Loudon, *The Quantum Theory of Light*. Oxford University Press, 2000.

[4] W. H. Furry, "A symmetry theorem in the positron theory," *Phys. Rev.* **51** (1937) 125.

[5] Y. Liang and A. Czarnecki, "Photonphoton scattering: a tutorial," *Canadian Journal of Physics* **90** (2012) no. 1, 11–16.

[6] H. H. Euler and B. Kockel, "Uber die streuung von licht

an licht nach der diracschen theorie," *Naturwissenschaften* **23** (1935) 246–247.

[7] H. H. Euler, "Uber die streuung von licht an licht nach der diracschen theorie," *Ann. Phys.* **418** (1936) no. 5, 398–448.

[8] F. Reif, *Fundamentals of Statistical and Thermal Physics.* McGraw-Hill, 1965.

[9] B. Zwiebach, "8.05x chapter 10: Two state systems,".

[10] B. Zwiebach, "8.06x chapter 5: Time dependent perturbation theory,".

[11] Wikipedia, "Doppler broadening." `https://en.wikipedia.org/wiki/Doppler_broadening`.

[12] G. B. Rybicki and A. P. Lightman, *Radiative Processes in Astrophysics.* John Wiley & Sons, 1991.

Tutorial Introduction to Dirac Particles and Flux Quantization in Low Dimension Spaces

David R Wolf
gmail: faradaywebermaxwell
(Dated: June 14, 2019)

Solutions for a Dirac particle in low dimension spaces are developed, extending the material presented in the MIT 8.06x course from the Schrodinger equation to the Dirac equation. The quantization of the magnetic field is discussed and contrasted with the method presented in 8.06x. Paper written for the course MIT 8.06x.

I. INTRODUCTION

Solving the Dirac equation for a particle residing on a low dimension compact space provides the opportunity to observe the interplay between the relativity and quantum mechanics in an uncomplicated setting.

The approach provides a nonstandard [1] tutorial for students becoming familiar with the Dirac equation. The presentation is not burdensome in terms of rigor, and is at the level required for learning the material the first time.

II. DIRAC EQUATION

It is useful to see the Dirac equation in various forms. Some of the often-seen forms of the Dirac equation, and the reasonably self-explanatory transformations between them are [2]

$$\begin{aligned}(\gamma^\mu p_\mu - m)\psi &= 0\\ (\gamma^\mu g_{\mu\nu} p^\nu - m)\psi &= 0\\ (\gamma^0 p^0 - \gamma^1 p^1 - \gamma^2 p^2 - \gamma^3 p^3 - m)\psi &= 0\\ (i\hbar[\gamma^0\partial_0 + \gamma^1\partial_1 + \gamma^2\partial_2 + \gamma^3\partial_3] - m)\psi &= 0\\ (i\gamma^0\partial_0 + i\gamma^1\partial_1 + i\gamma^2\partial_2 + i\gamma^3\partial_3 - m)\psi &= 0\\ (i\gamma^\mu\partial_\mu - m)\psi &= 0,\end{aligned}$$

In the above the Dirac matrices γ^μ, defined next, were used, the substitutions

$$p^0 = i\hbar\partial_t = i\hbar\partial_0, \quad p^i = -i\hbar\partial_i, i = 1,2,3$$

were made, the metric

$$g_{\mu\nu} = \begin{bmatrix}1 & 0 & 0 & 0\\ 0 & -1 & 0 & 0\\ 0 & 0 & -1 & 0\\ 0 & 0 & 0 & -1\end{bmatrix}$$

was used, and in the last two lines $\hbar$ was set to one. Note, in spite of the suggestive contraction notation the gamma matrices are fixed, do not form a four vector, and do not change under lorentz transformations. Regardless, this suggestive form is the usual one taken when demonstrating that by properly transforming the wavefunction the Dirac equation is 'covariant', or form invariant.

A. Pauli Matrices

The Pauli matrices σ_μ, $\mu = 0,1,2,3$ are

$$\sigma_0 = \begin{bmatrix}1 & 0\\ 0 & 1\end{bmatrix}, \sigma_1 = \begin{bmatrix}0 & 1\\ 1 & 0\end{bmatrix}, \sigma_2 = \begin{bmatrix}0 & -i\\ i & 0\end{bmatrix}, \sigma_3 = \begin{bmatrix}1 & 0\\ 0 & -1\end{bmatrix}$$

B. Dirac Matrices

In what is termed "the standard representation" [3] the Dirac matrices γ_μ, $\mu = 0,1,2,3$ are given in terms of Pauli matrices. First, define the α matrices of size 4×4 through

$$\alpha_0 = \begin{bmatrix}\sigma_0 & 0\\ 0 & \sigma_0\end{bmatrix}, \alpha_i = \begin{bmatrix}0 & \sigma_i\\ \sigma_i & 0\end{bmatrix}, i = 1,2,3,$$

and define the β matrix of size 4×4 as

$$\beta = \begin{bmatrix}\sigma_0 & 0\\ 0 & -\sigma_0\end{bmatrix}$$

With these the Dirac matrices are defined as

$$\gamma_\mu = \beta\alpha_\mu$$

giving

$$\gamma_0 = \beta = \begin{bmatrix}\sigma_0 & 0\\ 0 & -\sigma_0\end{bmatrix}, \gamma_i = \begin{bmatrix}0 & \sigma_i\\ -\sigma_i & 0\end{bmatrix}, i = 1,2,3,$$

in the standard representation, or explicitly

$$\gamma_0 = \begin{bmatrix}1 & 0 & 0 & 0\\ 0 & 1 & 0 & 0\\ 0 & 0 & -1 & 0\\ 0 & 0 & 0 & -1\end{bmatrix}, \quad \gamma_1 = \begin{bmatrix}0 & 0 & 0 & 1\\ 0 & 0 & 1 & 0\\ 0 & -1 & 0 & 0\\ -1 & 0 & 0 & 0\end{bmatrix},$$

$$\gamma_2 = \begin{bmatrix}0 & 0 & 0 & -i\\ 0 & 0 & i & 0\\ 0 & i & 0 & 0\\ -i & 0 & 0 & 0\end{bmatrix}, \quad \gamma_3 = \begin{bmatrix}0 & 0 & 1 & 0\\ 0 & 0 & 0 & -1\\ -1 & 0 & 0 & 0\\ 0 & 1 & 0 & 0\end{bmatrix}$$

III. SOLUTIONS TO THE DIRAC EQUATION

In the following sections several solutions to the Dirac equation in low dimension compact spaces are derived.

IV. PARTICLE ON A 1D TORUS - NO EM FIELD

For this example the geometry of the underlying one-dimensional space is the x-axis, where $x \sim x + L$ is taken to identify points to a segment of the axis of length L. With the solution represented as

$$\psi = \begin{bmatrix} u_1 \\ u_2 \\ u_3 \\ u_4 \end{bmatrix} e^{-i(Et-px)/\hbar}$$

the Dirac equation becomes the four equations

$$\begin{bmatrix} E-m & 0 & 0 & -p \\ 0 & E-m & -p & 0 \\ 0 & p & -E-m & 0 \\ p & 0 & 0 & -E-m \end{bmatrix} \begin{bmatrix} u_1 \\ u_2 \\ u_3 \\ u_4 \end{bmatrix} = \begin{bmatrix} 0 \\ 0 \\ 0 \\ 0 \end{bmatrix}$$

with the constraint $pL/(2\pi\hbar) = n \in \mathbb{Z}$ arising from the toroidal geometry. The form of the matrix implies there are two decoupled subspaces. The equation that holds in each of the subspaces $(1,4)$ and $(2,3)$ is

$$\begin{bmatrix} E-m & -p \\ p & -E-m \end{bmatrix} \begin{bmatrix} u_a \\ u_b \end{bmatrix} = \begin{bmatrix} 0 \\ 0 \end{bmatrix}$$

which may be written as a 2×2 matrix equation, using Pauli matrices, in a form similar to the 4×4 Dirac equation, as

$$(i\hbar\beta\sigma_0\partial_0 + i\hbar\beta\sigma_1\partial_1 - m)\psi = 0$$

where here $\beta = \sigma_3$, and

$$\psi = \begin{bmatrix} u_a \\ u_b \end{bmatrix} e^{-i(Et-px)/\hbar}.$$

For nontrivial solutions to exist the determinant of the matrix must be zero, a condition which leads to the invariant mass-squared relationship $E^2 = p^2 + m^2$. Due to the single-valuedness constraint on the wave function, the quantized energy is

$$E^2 = n^2\left(\frac{2\pi\hbar}{L}\right)^2 + m^2, \quad n \in \mathbb{Z}.$$

The matrix equation gives, in each subspace, two equations in two variables. Because the matrix is degenerate the two equations must represent the same constraint. The invariant mass relationship can be used to transform the first-row constraint equation

$$u_a = \frac{p}{E-m}u_b,$$

to the second-row constraint equation and back, as seen in

$$\begin{aligned} u_a &= \frac{E+m}{p}u_b = \frac{(E+m)(E-m)}{p(E-m)}u_b \\ &= \frac{p^2}{p(E-m)}u_b = \frac{p}{(E-m)}u_b, \end{aligned}$$

where (a,b) is either $(1,4)$ or $(2,3)$. Notice that in the nonrelativistic limit, when $p << E \sim m$, we have $u_a >> u_b$.

V. DIRAC PARTICLE ON A RING - NO FIELD

Here the particle is confined to a ring of radius ρ, parameterized by the angle ϕ. The gradient operator in cylindrical coordinates restricted to variation only in angle is $(1/\rho)\partial_\phi$ so that the operator $\gamma^\mu\partial_\mu = \gamma^0\partial_0 + \vec{\gamma}\cdot\vec{\nabla}$ becomes

$$\gamma^\mu\partial_\mu = \gamma^0\partial_0 + \vec{\gamma}\cdot\hat{\phi}\ \partial_\phi = \gamma^0\partial_0 + \gamma^\phi\rho^{-1}\partial_\phi$$

where

$$\gamma^\phi = -sin(\phi)\gamma^1 + cos(\phi)\gamma^2 = i\begin{bmatrix} 0 & 0 & 0 & -e^{-i\phi} \\ 0 & 0 & e^{i\phi} & 0 \\ 0 & e^{-i\phi} & 0 & 0 \\ -e^{i\phi} & 0 & 0 & 0 \end{bmatrix}$$

The striking property here is the angle dependence of the matrix, so that the components of the wave function must now have differing wavenumbers. Represent the solution as

$$\psi = \begin{bmatrix} u_1\, e^{ip_1\rho\phi/\hbar} \\ u_2\, e^{-ip_2\rho\phi/\hbar} \\ u_3\, e^{ip_3\rho\phi/\hbar} \\ u_4\, e^{-ip_4\rho\phi/\hbar} \end{bmatrix} e^{-iEt/\hbar} = \psi_p e^{-iEt/\hbar},$$

where $2\pi\rho$ is the circumference of the ring. Notice the choice of minus signs is without loss of generality and is made so that some formal similarities to the torroidal solution are clear later. The Dirac equation for a particle on a ring becomes the four equations

$$\begin{bmatrix} E-m & 0 & 0 & -e^{-i\phi}p_4 \\ 0 & E-m & -e^{i\phi}p_3 & 0 \\ 0 & e^{-i\phi}p_2 & -E-m & 0 \\ e^{i\phi}p_1 & 0 & 0 & -E-m \end{bmatrix} \psi_p = \begin{bmatrix} 0 \\ 0 \\ 0 \\ 0 \end{bmatrix}$$

Imposing single-valuedness forces the $n_i \equiv p_i\rho/\hbar$ to be integers. Here too there are the two two-dimensional subspaces, $(1,4)$ and $(2,3)$, each yielding an equation of the form

$$\begin{bmatrix} E-m & -e^{-i\phi}p_b \\ e^{i\phi}p_a & -E-m \end{bmatrix} \begin{bmatrix} u_a \\ u_b \end{bmatrix} = \begin{bmatrix} 0 \\ 0 \end{bmatrix}$$

where (a,b) are the indices in the corresponding subspace. To go from one subspace to the other substitute $\phi \to -\phi$. Again the determinant condition for nontrivial solutions provides a relationship between energy, momentum, and mass. However now the relationship is the more interesting

$$E^2 = p_a p_b + m^2.$$

Defining $E^2 - m^2 = p^2$ gives the somewhat curious $p^2 = p_a p_b$, which we interpret later. Due to the single-valuedness constraint, the quantized energy is

$$E^2 = n_a n_b \frac{\hbar^2}{\rho^2} + m^2, \quad n_a, n_b \in \mathbb{Z}.$$

The first row constraint equation

$$(E - m) u_a e^{i p_a \rho \phi / \hbar} - u_b p_b e^{-i(p_b \rho/\hbar + 1)\phi} = 0$$

must have the same angle dependence in each term, which imposes a relationship between the momenta, giving

$$n_a + n_b + 1 = 0.$$

The two components slip in and out of phase during one revolution around the the ring, illustrated here:

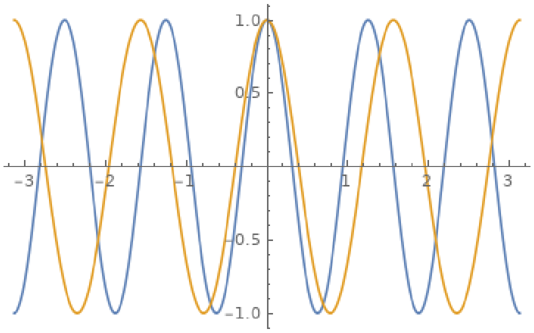

Dividing out the exponential factor yields

$$u_a = \frac{p_b}{E - m} u_b,$$

which is the same relationship between the components we found for the torus, but not for the same solution because the phases of the components now differ. The second-row of the matrix and the mass-energy identity produce the result

$$\begin{aligned} u_a &= \frac{E + m}{p_a} u_b = \frac{(E+m)(E-m)}{p_a(E-m)} u_b \\ &= \frac{p_a p_b}{p_a(E-m)} u_b = \frac{p_b}{(E-m)} u_b, \end{aligned}$$

which is the same constraint as the first row equation. Before proceeding be sure to see how the above results hold in both subspaces by repeating the steps after substituting $\phi \to -\phi$.

VI. FLUX QUANTIZATION AND GAUGE TRANSFORMATIONS

We prepare for deriving solutions for a Dirac particle in a non-zero electromagnetic field by reviewing gauge transformations. In the process we discuss the relationship between the approach to flux quantization found in 8.06x and the usual approach to flux quantization.

A. A Note on Gauge Transformations

Suppose we take ψ_0 as the solution to the Dirac equation in the special case when $\vec{A} = \vec{0}$. It would be useful if there were a simple transformation of the solution in this special case that creates the solution with $\vec{A} \neq \vec{0}$. Under minimal coupling the change to nonzero field amounts to changing the operator $i\partial$ to $i\partial + \frac{q}{\hbar c} A$ in the Dirac equation, so to the end of finding a solution to the second case given a solution to first, consider the wavefunction

$$\psi = e^{\frac{iq}{\hbar c}\Lambda} \psi_0$$

and observe the effect of operating on it with the minimally coupled momentum operator. We find

$$\begin{aligned} (i\partial + \frac{q}{\hbar c} A)\psi &= (i\partial + \frac{q}{\hbar c} A) e^{\frac{iq}{\hbar c}\Lambda} \psi_0 \\ &= i\partial (e^{\frac{iq}{\hbar c}\Lambda} \psi_0) + \frac{q}{\hbar c} A e^{\frac{iq}{\hbar c}\Lambda} \psi_0 \\ &= i(e^{\frac{iq}{\hbar c}\Lambda} \frac{iq}{\hbar c} (\partial \Lambda) \psi_0 + e^{\frac{iq}{\hbar c}\Lambda} (\partial \psi_0)) + \frac{q}{\hbar c} A e^{\frac{iq}{\hbar c}\Lambda} \psi_0 \\ &= -\frac{q}{\hbar c} e^{\frac{iq}{\hbar c}\Lambda} (\partial \Lambda) \psi_0 + i e^{\frac{iq}{\hbar c}\Lambda} (\partial \psi_0) + \frac{q}{\hbar c} A e^{\frac{iq}{\hbar c}\Lambda} \psi_0 \end{aligned}$$

With the alluring choice for Λ

$$\partial \Lambda = A$$

the result simplifies further, to

$$(i\partial + \frac{q}{\hbar c} A)\psi = e^{\frac{iq}{\hbar c}\Lambda} (i\partial \psi_0),$$

demonstrating ψ is a solution when $\vec{A} \neq \vec{0}$.

A limited class of solutions can be found in this manner, specifically those attained by adding $\nabla \Lambda$ to the zero vector potential. Vector potentials representing magnetic fields do not qualify, since $B = \nabla \times A$ and $A = \nabla \Lambda$ implies $B = \nabla \times \nabla \Lambda = 0$ (the curl of a gradient is always zero).

B. Gauging Away Part of the Vector Potential

Conversely, begin with nonzero field and solve for the wave function. Adding the gradient of any function $\Lambda(\vec{x})$ to the vector potential produces the same magnetic field. From the previous subsection the solution is the old solution multiplied by the phase factor $e^{\frac{iq}{\hbar c}\Lambda}$. Can $\vec{A}$ be reduced to one nonzero component?

Consider the vector potential

$$\vec{A} = (\frac{-B_0 y}{2}, \frac{B_0 x}{2}, 0) \qquad (1)$$

giving

$$\vec{B} = \nabla \times A = B_0 \hat{z}$$

Notice magnetic flux has units of magnetic field times units of area, and the units of the gauge function are the units of flux. The gauge function.

$$\Lambda(x,y) = \frac{B_0 xy}{2}$$

has gradient

$$\nabla\Lambda = (\frac{B_0 y}{2}, \frac{B_0 x}{2}, 0)$$

and produces the new vector potential

$$\vec{A} = (0, B_0 x, 0), \tag{2}$$

having all but one of its components zero. Before moving on verify the same magnetic field is produced.

In the context of a torus there is another interesting effect: magnetic flux is quantized, addressed in the next section.

C. Flux Quantization - Lecture Method

Here the context is a 2d toroidal space (edge-joined rectangular patch) with a magnetic field. Solutions must be periodic in both dimensions. For the moment assume we are generating solutions using gauge transformations, as described in the previous section. The gauge function we chose earlier,

$$\Lambda(x,y) = \frac{B_0 xy}{2}$$

does not produce gauge transformations periodic in both coordinates. The class of gauge transformations is more limited in a periodic space than in a Cartesian space. What to do? Try again! As an example, choose the gauge function

$$\Lambda(x,y) = B_G(L_x y + x L_y),$$

where the gauge magnetic field B_G is a 'gauge' magnetic field we hope to relate to the magnetic field on the torus. Most importantly, the gauge transformed solution will be torus-periodic in both coordinates when

$$\frac{q}{\hbar c} B_G L_x L_y = 2\pi n, \;\; n \in \mathbb{Z}.$$

or when

$$\Phi = B_G L_x L_y = n \frac{2\pi\hbar c}{q} = n\Phi_0$$

where Φ is the magnetic flux through the surface and $\Phi_0 = \frac{2\pi\hbar c}{q} = \frac{hc}{q}$ is the flux quantum.

This is a promising result. At this point we have determined that B_G is quantized. However, please notice two facts. First, so far there is no relationship between B_G and B_0, and second to finagle this result the vector potential is, quite simply, not single valued on the torus because a uniform nonzero magnetic field was claimed to exist. Specifically, to make sense of the vector potential producing the same magnetic field at the left and right boundaries of the rectangular patch we must have a foliated space to support the vector potential. (Strictly, in the 8.06x lecture notes the notion of 'overlapping patches of vector potential' is introduced. It soon becomes clear what is done here is without loss of generality). The foliations wrap around the torus ad-infinitum. Physically this is an untenable situation and we should worry something is terribly incorrect. But, again for the moment, let's push on anyway.

To address the vector potential having multiple values the 8.06x lecture imposed the condition

$$\vec{A}(x + n_x L_x, y + n_y L_y) = \vec{A}(x,y) + \nabla\Lambda, \;\; n_x, n_y \in \mathbb{Z}$$

for some gauge function Λ, i.e. after gauge transformation the vector potential takes on its value at an overlaying point in the foliation. Using the vector potential of eq. 2 and an $(n_x, 0)$ shift of the rectangle yields

$$\vec{A}(x + n_x L_x, y) = (0, B_0(x + n_x L_y), 0)$$
$$\vec{A}(x,y) + \nabla\Lambda = (0, B_0 x + B_G L_x, 0),$$

where to achieve a match we took the gauge function

$$\Lambda(x,y) = B_G L_x y.$$

As all components must be equal we determine

$$B_0 = B_G/n$$

for some $n \in \mathbb{Z}$. The same result holds for a shift $(0, n_y)$.

Two conditions in the preceding derivation have no rationale, without which the argument given in lecture falls apart. The first is a gauge transformation must shift the vector potential directly through the foliation, whereas all shifts appear physically reasonable. The second is the choice of the specific integer $n = 1$.

Further, if the vector potential is taken as in eq. 1 then $B_0 = 2B_G/n$ holds. If the same $n = 1$ is used, a different field quantum for the patch is found, an impossible result. If the different $n = 2$ is used to achieve the same flux quantum on the patch then a rationale must be given, but none appears.

Because other shifts and other vector potentials lead to other and different relationships between B_G and B_0 we must conclude the condition that the vector potential shifts directly through the foliation does not uniquely quantize flux. We are forced to conclude the approach taken in lecture does not work.

D. Flux Quantization, A Second Approach

Now take a different approach [4] [5] to the case considered in the previous section. First, consider a region of surface having a nonzero magnetic field. The flux through the surface is

$$\Phi = \int \vec{B} \cdot d\vec{A},$$

while the magnetic field may be written in terms of the vector potential as

$$B = \nabla \times \vec{A}$$

Using Stokes' theorem we find

$$\Phi = \int \nabla \times \vec{A} = \int \vec{A} \cdot d\vec{L},$$

giving the flux in terms of the boundary integral of the vector potential. Now, consider a circular region of radius a of nonzero constant magnetic field in the z direction with vector potential given in the nonzero region by the form we found before. We write this 'inner' ($\rho < a$) vector potential in cylindrical coordinates as

$$\begin{aligned}\vec{A}_{in} &= (\frac{-B_0 y}{2}, \frac{B_0 x}{2}, 0)\\ &= \frac{B_0}{2}\rho\ \hat{\phi}, \ \ \rho < a\end{aligned}$$

On the other hand, outside the magnetic field region ($\rho > a$), taking the outer vector potential to be a constant magnitude vector along the $\hat{\phi}$ direction and using Stokes theorem shows that

$$\Phi = \int \vec{B} \cdot d\vec{A} = \int \vec{A} \cdot d\vec{L} = A_\phi 2\pi\rho,$$

which immediately yields the vector potential outside the magnetic field region as

$$\vec{A}_{out} = \frac{B_0 a^2}{2\rho}\ \hat{\phi}, \ \ \rho > a.$$

Now recall, in section VI A we discovered that we were unable to write the inner vector potential as the gradient of a gauge function because that vector potential would result in a zero magnetic field. However, for the outer vector potential the story is different and we find

$$\vec{A}_{out} = \nabla\Lambda.$$

where the gauge function is

$$\Lambda = \frac{B_0 a^2}{2}\phi$$

Inverting gives us

$$\Delta\Lambda = \int_{\vec{x}_0}^{\vec{x}} \vec{A} \cdot d\vec{L}$$

in which the path of integration remains within the field-free region, where the vector potential is correctly given in terms of the gradient of the gauge function. We already discovered that when the solution ψ_0 for the zero vector potential case is available then

$$\psi(x) = exp\left(\frac{iq}{\hbar c}\Lambda\right)\ \psi_0(x)$$

is the solution when the vector potential is both nonzero and the gradient of a gauge function (which, again, happens in the zero magnetic field region only). Thus

$$\psi(\vec{x}) = exp\left(\frac{iq}{\hbar c}\int_{\vec{x}_0}^{\vec{x}} \vec{A} \cdot d\vec{L}\right)\ \psi_0(\vec{x})$$

is the solution in the zero magnetic field region, with the additional constraint that the path of integration is fully within the zero magnetic field region. The two forms differ only by a phase (attributable to the starting point of the integration).

With this we can now address flux quantization. Suppose the path is taken to completely enclose a bounded region containing a non-zero magnetic field. Single-valuedness implies $\psi(x_0) = \psi_0(x_0)$, requiring the phase factor to be one, and yields the quantization condition

$$\frac{q}{\hbar c}\oint \vec{A} \cdot d\vec{L} = \frac{q}{\hbar c}\Phi = 2\pi n$$

with the quantized flux

$$\Phi = 2\pi\frac{\hbar c}{q}n = \frac{hc}{q}n = \Phi_0 n$$

Notice, again, for this quantization condition to hold we imposed having a single valued wave function and having a path surrounding but fully outside the nonzero magnetic field region.

In the 8.06x lecture the field was taken nonzero eveywhere, uniform on and perpendicular to the toroidal patch, and there was no zero magnetic field region. Thus, the derivation above can not be used to fix the lecture. We already concluded the analysis in the lecture did not work. Now, the above derivation of flux quantization also provides no support for the lecture.

VII. CHARGED PARTICLE ON A 1D TORUS WITH NONZERO VECTOR POTENTIAL

With the experience of the zero-field solutions behind us, consider a one dimensional torus of length L_x on which the particle of mass m and charge q moves. The magnetic field is coupled to the momentum of the particle through the minimal coupling $\vec{p'} = \vec{p} - \frac{q}{c}\vec{A}$. In the Dirac equation, restrict the motion to the (x) direction, giving us

$$\begin{gathered}\left(\gamma^0 p^0 - \gamma^1(p^1 - \frac{q}{c}A_1) - m\right)\psi = 0\\ \left(i\hbar\gamma^0\partial_0 + \gamma^1(i\hbar\partial_1 + \frac{q}{c}A_1) - m\right)\psi = 0.\end{gathered}$$

Taking the trial solution

$$\psi_p = \begin{bmatrix}\psi_1\\ \psi_2\\ \psi_3\\ \psi_4\end{bmatrix} e^{-Et/\hbar}$$

again produces decoupled subspaces $(1,4)$ and $(2,3)$, and in each subspace we find the constraint equations have the form

$$\begin{bmatrix} E-m & (i\hbar\partial + \frac{q}{c}A) \\ -(i\hbar\partial + \frac{q}{c}A) & -(E+m)\end{bmatrix}\begin{bmatrix}\psi_a\\ \psi_b\end{bmatrix} = \begin{bmatrix}0\\ 0\end{bmatrix},$$

where the subscript has been dropped because there is one space coordinate. Notice the component wavefunctions and their derivatives are periodic in the length of the torus L_x and consider the terms that arise when the first-row contraint is taken:

$$(E-m)\psi_a + i\hbar\partial\psi_b + \frac{q}{c}A\psi_b = 0.$$

The fact the wavefunction is single valued means both wavefunction components are periodic on the 1d torus. This leads to a constraint on the vector potential. To see this take

$$\begin{bmatrix}\psi_a\\ \psi_b\end{bmatrix} = \begin{bmatrix}ae^{i\alpha x}\\ be^{i\beta x}\end{bmatrix},$$

and substitute in the first row constraint equation to find

$$A = \frac{\hbar c}{q}\beta - (E-m)\frac{a}{b}\frac{c}{q}e^{i(\alpha-\beta)x}.$$

Similarly, substituting in the second row constraint equation yields

$$A = \frac{\hbar c}{q}\alpha - (E+m)\frac{b}{a}\frac{c}{q}e^{-i(\alpha-\beta)x},$$

from which we observe, along with the constraint of single valuedness, that the only solution is a constant and real vector potential through

$$\alpha = \beta = \frac{2\pi n}{L_x},\ \ n \in \mathbb{Z},\ \ \frac{b^2}{a^2} = \frac{E-m}{E+m}.$$

Defining $p^2 = E^2 - m^2$ as we have done before, explicitly writing the vector potential, and solving for the quantized energy gives

$$A = \frac{hc}{q}\frac{n}{L_x} - \frac{pc}{q} = \Phi_0\frac{n}{L_x} - \frac{pc}{q},\ \ n \in \mathbb{Z}$$
$$E^2 = (\frac{h}{L_x}n - \frac{q}{c}A)^2 + m^2,\ \ n \in \mathbb{Z}$$

Taking another approach, solving the second row constraint equation for ψ_b provides

$$\psi_b = -\frac{1}{E+m}(i\hbar\partial + \frac{q}{c}A)\psi_a,$$

and substituting for ψ_b in the first constraint equation yields the quadratic constraint equation

$$\big[p^2 - (i\hbar\partial + \frac{q}{c}A)^2\big]\psi_a = 0.$$

Going the other way yields the same equation for ψ_b: both components satisfy the same quadratic constraint equation. As expected, the solutions for the energy and vector potential using the quadratic constraint equation are the same as those already found. An intermediate step yields

$$\big[p^2 - \big((\hbar\gamma - \frac{q}{c}A)^2 + i\hbar\frac{q}{c}\partial A\big)\big]\psi = 0$$

where we argue that if the vector potential is real then it must be a constant, affirming our earlier result (because the value in square brackets is just a number and the gradient of the vector potential appears in the only imaginary term in that number).

We might, at severe risk to the physics (recall, here we are considering a 1d torus, not a 1d ring, and a 1d torus can not ‘enclose’ a magnetic field), also impose our previous result, that the flux bounded by a wave function that is well defined in a zero magnetic field region is quantized, i.e.

$$A_\phi = \frac{hc}{q}\frac{n'}{L_x},\ \ n' \in \mathbb{Z}$$

to find the energy is quantized in a way that perhaps surprisingly makes the fact there is an external field irrelevant to the spectrum

$$E^2 = \left(\frac{h}{L_x}(n-n')\right)^2 + m^2,\ \ n, n' \in \mathbb{Z}$$

Having now studied the Dirac particle in a 1d toroidal space we will next address the Dirac particle in a 2d toroidal space.

VIII. CHARGED PARTICLE ON A 2D TORUS WITH NONZERO VECTOR POTENTIAL

With the experience of the 1d solutions behind us, consider a two dimensional torus of width L_x and height L_y on which the particle of mass m and charge q resides. The magnetic field is coupled to the momentum of the particle through the minimal coupling $\vec{p'} = \vec{p} - \frac{q}{c}\vec{A}$. In the Dirac equation, restrict motion to the (x,y) plane, giving us

$$\Big(\big[i\hbar\gamma^0\partial_0 + \gamma^1(i\hbar\partial_1 + \frac{q}{c}A_1) + \gamma^2(i\hbar\partial_2 + \frac{q}{c}A_2)\big] - m\Big)\psi = 0,$$

Taking the form of the solution as

$$\psi = \begin{bmatrix}u_1\, e^{i(p_{1x}x+p_{1y}y)/\hbar}\\ u_2\, e^{i(p_{2x}x+p_{2y}y)/\hbar}\\ u_3\, e^{i(p_{3x}x+p_{3y}y)/\hbar}\\ u_4\, e^{i(p_{4x}x+p_{4y}y)/\hbar}\end{bmatrix} e^{-iEt/\hbar} = \psi_p e^{-iEt/\hbar},$$

and substituting in the Dirac equation gives

$$\begin{bmatrix} E-m & -(p_b-\frac{q}{c}A)^* \\ p_a-\frac{q}{c}A & -(E+m) \end{bmatrix} \begin{bmatrix} u_a \\ u_b \end{bmatrix} = \begin{bmatrix} 0 \\ 0 \end{bmatrix}$$

in the $(a,b)=(1,4)$ subspace, and a similar system in the $(2,3)$ subspace, where $p_s=p_{sx}+ip_{sy}$, $s=a,b$, and $A=A_1+iA_2$. The toroidal constraint in 2d implies $p_{ax}=p_{bx}=p_x=hn_x/L_x, n_x\in\mathbb{Z}$ and $p_{ay}=p_{by}=p_y=hn_y/L_y, n_y\in\mathbb{Z}$, so that each term has the same harmonic dependence in both x and y. Together these imply $p_a=p_b$, which we take to be $p=p_x+ip_y$.

As before, the determinant constraint for non-trivial solutions produces the energy-mass-momentum relationship. Here we find, after substituting and simplifying, the energy is quantized in terms of two integers as

$$\begin{aligned} E^2 &= (p-\frac{q}{c}A)(p-\frac{q}{c}A)^*+m^2 \\ &= (p_x-\frac{q}{c}A_x)^2+(p_y-\frac{q}{c}A_y)^2+m^2 \\ &= (\frac{h}{L_x}n_x-\frac{q}{c}A_x)^2+(\frac{h}{L_y}n_y-\frac{q}{c}A_y)^2+m^2 \end{aligned}$$

where $n_x, n_y\in\mathbb{Z}$, and we took $A_x=A_1$ and $A_y=A_2$.

IX. SUMMARY

In this paper we derived these solutions for a Dirac particle in low dimension compact spaces:

- Particle on a 1d torus - no field
- Particle on a ring - no field
- Charge on a 1d torus - nonzero magnetic field
- Charge on a 2d torus - nonzero magnetic field

and addressed the quantization of the magnetic field that occurs when quantum states enclose a region of magnetic field, comparing the method here to the method presented in 8.06x. Two results are

- The quantization method in 8.06x does not work.
- Dirac particles on the 1d torus and ring differ, unlike the Schrodinger equation case.

ACKNOWLEDGMENTS

Thank you to my family, who made space in our lives to make this work a success, and to my 8.06x friends and cohort who gleefully share their blessings with all.

This work was enhanced through the support of the US Bureau of Reality Entanglement Dispersal (BREAD), the US Bureau of Time Travel Reversal (BUTTER), and the US Department of Trans-Optimal String Theory (TOAST).

X. BIBLIOGRAPHY

---

[1] Ravi Shankar, *Principles of Quantum Mechanics*, Springer, 2008.
[2] F. Mandl and G. Shaw, *Quantum Field Theory*, John Wiley and Sons, 1986.
[3] Hans A. Bethe and Roman W. Jakciw, *Advanced Quantum Mechanics*, Benjamin-Cummings, 1986.
[4] Lewis H. Ryder, *Quantum Field Theory*, Cambridge University Press, 1985.
[5] Junichiro J. Sakurai, *Quantum Field Theory*, Addison Wesley, 1987.

Two sites coherence and visibility

Abanoub Mikhail

(Dated: June 19, 2019)

Wave-particle duality and the superposition of quantum mechanical states furnish quantum mechanics with unique features which distinguishes it from classical mechanics and give it the apparently counter-intuition interpretation. The two principles are responsible for the observation of the interference effects of quantum particles such as electrons, atoms and molecules. Visibility is a measure of the wave nature and can be though of as a "normalized" coherence quantifier. Reduction in the visibility arises from dephasing (decoherence): a process in which the relative phases get partially or totally destroyed leading to domination of the particle nature. We calculate the coherence and visibility of an ensemble of a single electron and two electrons on two sites using the density matrix formulation.

I. INTRODUCTION

The superposition principle is a fundamental concept in physics. It applies to all kinds of waves: mechanical and electromagnetic in classical mechanics as well as De Broglie waves in quantum mechanics. The superposition principle states that if a quantum system can be found in a state $\psi_1(t)$ [1] and also in a state $\psi_2(t)$, then it can be found in any linear combination of them [2] $\psi(t) = \psi_1(t) + \psi_2(t)$[3].

In the position representation, When one evaluates the probability density $|\psi(t)|^2$, in adition to the separate probabilities of the two waves $|\psi_1(t)|^2$ and $|\psi_2(t)|^2$, there are cross terms $\psi_1^*(t)\psi_2(t) + \psi_2^*(t)\psi_1(t)$ which is called the interference terms as they are responsible for the observation of the interference effects [4].

When light from the sun passes through a hole, we do not see diffraction pattern and when it passes through two slits, there is also no interference pattern. That is because sun light is **incoherent** [5]. Therefore, incoherent sunlight behaves as particles. Once it has been made coherent, diffraction and interference patterns reappear. Thus, coherence is a manifestation of the wave nature. The same is true for quantum particles. In a **coherent superposition**, the interference effects can be observed due to the existence of interference terms while the interference terms vanish –or average out to zero– in **incoherent superposition** [2]. For example, consider the state

$$\psi(t) = \psi_1(t) + \psi_2(t) \tag{1}$$

the probability distribution is given by

$$\begin{aligned} |\psi|^2 &= |\psi_1|^2 + |\psi_2|^2 + \psi_1^*\psi + \psi_2^*\psi_1 \\ &= |\psi_1|^2 + |\psi_2|^2 + 2|\psi_1\psi_2|\cos(\alpha_{12}) \end{aligned} \tag{2}$$

where the last equality follows from writing ψ_1 and ψ_2 in the phasor form as $\psi_1 = |\psi_1|\exp(i\alpha_1)$, $\psi_2 = |\psi_2|\exp(i\alpha_2)$ and the relative phase is defined by $\alpha_{12} = \alpha_1 - \alpha_2$. A relative phase difference of $\frac{\pi}{2}$ completely destroys the interference term. That is referred to as destructive interference [6]. The superposition is called incoherent in this case. A maximally coherent superposition occurs when $\alpha_{12} = 0$.

Conventionally, visibility is a measure of the contrast of the interference pattern. For interference experiments with light such as the n-path experiments , the fringe visibility is defined locally as

$$\mathrm{V} = \frac{I_{max} - I_{min}}{I_{max} + I_{min}} \tag{3}$$

I_{max} is the maximum intensity of light and I_{min} is the minimum light intensity. Classically, Light intensity is proportional to the square of the electric field amplitude.

If the experimentalist have complete knowledge about the path that the quanton take, the interference pattern gets destroyed. That implies that the quantum particles behaved as classical particles in accordance with Bohr's principle of complementarity. For a two beam interferometer, a useful measure of the particle properties is the predictability P which is defined as $P = |\rho_{11} - \rho_{22}|$ where ρ_{ii} for $i = 1, 2$ are the diagonal elements of the density matrix. A wave-particle duality relation was introduced as [3]

$$P^2 + V^2 \leq 1 \tag{4}$$

The predictability was extended to n-path interferometer in Ref. [3].

This paper is organized as following: a quantifier of coherence is introduced in section II. Visibility, as a measure of the wave nature, is defined and linked to a coherence quantifier. In section III, the reader is introduced to the process of dephasing in which the relative phase shift is randomized followed by partial or total destruction of the interference pattern, hence, a reduction of

---

[1] Variables such as position and spin are included implicitly

[2] we have absorbed all constants into $\psi_1(t)$ and $\psi_2(t)$

[3] The extension to more than two states is straightforward

[4] In the interference experiments such as double slits experiment, the interference pattern is defined as the response of the fixed detectors as a function of phases [1]

[5] its constituent photons do not maintain constant relative phase and it has different frequencies as well.

[6] A relative phase difference of $\frac{\pi}{2}$ implies orthogonality between $\psi_1(t)$ and $\psi_2(t)$

the visibility and the transition of the system from the quantum like to the classical like behavior. Readers who find it helpful to study coherence and visibility in the framework of double and multipath interferometers, may find this preprint useful [4]. Starting from section IV, we apply the concepts and techniques developed in previous sections to Hubbard model of single and two electrons on two sites.

II. THEORETICAL BASIS

A. The density matrix

Although the state vector contains the maximal information about the system, in many situations, the system is not isolated and full information about it is not known. This loss of information is the reason behind the introduction of the density matrix in place of the state vector. Pure states refer to states in an ensemble that is prepared in the same Eigenstate or in the same superposition of Eigenstates. Mixed states refers to states in an ensemble in different superposition of Eigenstates –in a statistical mixture of pure states.Therefore, the quantum mechanical ensemble is characterized by the statistical operator (also called the density matrix operator) ρ defined by

$$\rho = \sum_k P_m \left|\psi_m\right\rangle \left\langle\psi_m\right| \tag{5}$$

where P_m is the probability to find the system in the pure state $|\psi_i\rangle$. In terms of of a complete orthonormal basis $|i\rangle$, the pure state is $|\psi_m\rangle = \sum_i c_i^m |i\rangle$ and the density matrix becomes

$$\rho = \sum_{i,j} \left(\sum_m P_m c_i^{(m)} (c_j^{(m)})^* \right) |i\rangle \langle j| \tag{6}$$

It follows that the density matrix elements are given by

$$\rho_{ij} = \sum_m P_m c_i^{(m)} (c_j^{(m)})^* \tag{7}$$

The diagonal elements give the probability of finding the system in one of the basis states $|i\rangle$, therefore, adding up these probabilities must be one. Meanwhile, the off-diagonal elements are a measure of the coherence between different states of the system –see the next section.Tr(ρ^2) can be used to test whether a given density matrix describes a pure or a mixed state as it is equal to one for pure states and less than one for mixed states. For more details on the density matrix and its applications, the reader is directed to the book by Karl Blum [5].

B. Quantifying quantum coherence

A rigorous and reliable quantifier of coherence was proposed in Ref. [6] by Baumgratz et al. In this approach, for a fixed basis $|i\rangle_{i=1,\ldots,n}$ of n-dimensional Hilbert space $\mathtt{H}$, all density matrices which are diagonal in this basis are called incoherent. This set of quantum states is labeled by $I \subset \mathtt{H}$. Therefore, all density operators $\rho^I \in I$ take the form $\rho^I = \sum_{i=1}^n \rho_i^I |i\rangle \langle i|$. A maximally coherent state is given by $|\psi_n\rangle = \frac{1}{\sqrt{n}} \sum_{i=1}^n |i\rangle$ and the coherence of this state is used as a unit of coherence.

Any coherence measure C should satisfies the following properties [6]: (1) it must vanishes on the set of incoherent states $C(\rho^I) = 0$ (2) Monotonicity under under incoherent completely positive and trace preserving maps (3) Nonincreasing under mixing of quantum states (convexity). The l_1 norm of the density matrix satisfies the previous conditions and is chosen as a suitable measure of coherence. Hence the coherence becomes

$$C(\rho) = \sum_{i \neq j} |\rho_{ij}| \tag{8}$$

C. Dephasing (Decoherence)

As pointed out in [7], the complementary principle prevents a perfect knowledge of conjugate pairs of physical quantities simultaneously. Wave particle duality is one of such pairs. The partial or total destruction of the interference terms yield a reduction in the visibility. This process of loss of the coherence is called decoherence or dephasing – the existence of coherence lies in the observation of interference effects [8]. In the double slit interference experiment, any attempt of the experimentalist to measure any property of the interfering quantons leads to weakening followed by partial or total destruction of the interference pattern. That is the interference pattern is visible –hence the wave-like nature dominates– when we do not know exactly the path that the quantons take and when there is no leakage of information about the them to the environment, an observer or any measuring instrument.

The study of dephasing can be proceed by realizing the changes that the system leaves on the environment or by considering the randomization of the system relative phase [9] due to the existence of the environment. In the latter description, the path that a particle takes becomes uncertain. A paper by Yakir Aharonov and his colleagues illustrates this point and they proved the equivalence of both approaches [9]. Their argument starts as follow: assume a left wave packet $|r(x,t)\rangle$ and a right wave packet $|r(x,t)\rangle$ crossing a ring in two opposite directions. Their interference is examined after they travel one-half of the ring in two opposite direction. The right wave packet can interact with the environment while the left wave packet cannot. The interaction Hamiltonian is assumed to have the following form

$$H_{int} = V(x, \eta) \tag{9}$$

where x is the particle space coordinate and η is the environment coordinates. The initial wave function is

$[|l(x)\rangle + |r(x)\rangle] \otimes |\chi(\eta)\rangle$. After time $t = \tau$, the wave function becomes

$$|\psi(\tau)\rangle = |l(\tau)\rangle \otimes |\chi(\eta)\rangle + |r(\tau)\rangle \otimes \exp\left(\frac{-i}{\hbar}\int_0^\tau V(x_r(t),\eta)\,dt\right)|\chi(\eta)\rangle \tag{10}$$

The interference term is given by
$2\mathrm{Re}[l^*(x,\tau)r(x,\tau)$
$\times \langle\chi(\eta)|\exp\left(\frac{-i}{\hbar}\int_0^\tau V(x_r(t),\eta)\,dt\right)|\chi(\eta)\rangle]$

Thus the effect of the environment on the particle is encoded in the factor $D(\phi,\eta) = \langle\chi(\eta)|\,e^{i\phi(\eta)}\,|\chi(\eta)\rangle$ where $\phi(\eta) \equiv \exp\left(\frac{-i}{\hbar}\int_0^\tau V(x_r(t),\eta)\,dt\right)$ is the phase shift. The first interpretation of the authors is based on the previous equation: quantum interference is lost when the two interfering waves shift the environment into two orthogonal states.

In the second interpretation,

$$\begin{aligned} D(\phi,\eta) &= \int |\chi(\eta)|^2 \exp\left(\phi(\eta)\right) d\eta \\ &= \int d\phi |\chi(\eta)|^2 \exp\left(\phi(\eta)\right) \frac{d\eta}{d\phi} \\ &= \int P(\phi) \exp\left(\phi(\eta)\right) d\phi \end{aligned} \tag{11}$$

where $P(\phi) \equiv |\chi(\eta)|^2 \frac{d\eta}{d\phi}$ is the distribution function. Since Equation is nothing but the stochastic average of the relative phase shift i.e, $\langle e^{i\phi}\rangle_\phi = \int P(\phi)\exp\left(\phi(\eta)\right) d\phi$. In this approach, ϕ is not well-defined. Rather it becomes a statistical variable described by the distribution function $P(\phi)$ [9]. If the factor $\langle e^{i\phi}\rangle_\phi$ vanishes when averaged over all the environment degrees of freedom, the interference terms become zero and the system behaves classically.

There are also other dephasing-inducing processes such as scattering and excitation. Dephasing can be thought of a result of: a. Stochastic classical process b. Interaction of the system with a bath in a random initial state c. Quantum randomness, see Ref. [1] for further detail.

D. Defining and linking visibility to coherence

Apparently the factor $\langle e^{i\phi}\rangle_\phi$ describes the modifications to the interference term due to the existence of the environment. Hence, the absolute value of this factor can be used more or less as a measure of the visibility [1]. If one insists on using the extrema of the interference terms, then, we should replace the concept of light intensity by the squared modulus of the probability amplitude and rewrite the visibility as

$$V = \frac{|\psi^C|^2 - |\psi^I|^2}{|\psi^C|^2 + |\psi^I|^2} \tag{12}$$

If ψ^C is maximally coherent states, constructive interference is possible –the two states are in phase. Meanwhile, an incoherent state ψ^I exhibits no interference $|\psi^I|^2 = |\psi_1|^2 + |\psi_2|^2$ because the two states are $\frac{\pi}{2}$ out of phase –pure particle behavior. It follows that the visibility is given by

$$\mathrm{V}(t) = \frac{|\psi_1(t)\psi_2(t)|}{|\psi_1(t)|^2 + |\psi_2(t)|^2 + |\psi_1(t)\psi_2(t)|} \tag{13}$$

Even if the basis states are orthonormal, one may think of other situations where interference is natural to the problem. For example, Suppose a two state system in the initial state

$$|\psi_i(t)\rangle = a_1(t)\,|1\rangle + a_2(t)\,|2\rangle \tag{14}$$

and the final state of the system is

$$|\psi_f(t)\rangle = b_1(t)\,|1\rangle + b_2(2)\,|2\rangle \tag{15}$$

The transition amplitude from the initial to the final is given by

$$|\langle\psi_f(t)|\psi_i(t)\rangle|^2 = |a_1|^2|b_1|^2 + |a_2|^2|b_2|^2 + 2\,\mathrm{Re}(a_1^* a_2 b_1 b_2^*) \tag{16}$$

In the phasor form $a_i(t) = |a_i(t)|e^{\alpha_i(t)}$ and $b_i(t) = |b_i(t)|e^{\beta_i(t)}$ for $i = 1, 2$ where the relative phase is defined by $\alpha_{12} = \alpha_1(t) - \alpha_2(t)$ and $\beta_{12} = \beta_1(t) - \beta_2(t)$, the interference term is

$$2\,\mathrm{Re}(a_1^* a_2 b_1 b_2^*) = 2|a_1 b_1 a_2 b_2|\cos\left(\alpha_{12} - \beta_{12}\right) \tag{17}$$

it is reduced by a factor of $\cos\left(\alpha_{12} - \beta_{12}\right)$. Again, the interference term completely vanishes when $\alpha_{12} - \beta_{12} = \frac{\pi}{2}$. It follows from equation (12) that the visibility for this system is

$$V(t) = \frac{|a_1 b_1 a_2 b_2|}{|a_1|^2|b_1|^2 + |a_2|^2|b_2|^2 + |a_1 b_1 a_2 b_2|} \tag{18}$$

Finally we extent the definition of visibility to the case of mixed states. In a paper by Stephan Dˆurr, the author proposed criteria for the visibility to be a good measure of the wave properties [3]:
(1) It should be possible to give a definition of V that is based only on the interference pattern without explicitly referring to the matrix elements of ρ
(2) V should vary continuously as a function of the matrix elements of ρ.
(3) If the system shows no interference V should reach its global minimum
(4) If ρ represent a pure state and all the states are equally populated, V should reach its global maximum.
(5) V considered as a function in the parameter space $(\rho_{11}, \rho_{12}, ..., \rho_{nn})$ should have only global extrema, no local ones.
(6) V should be independent of our choice of the coordinate system.

Notice that conditions (3) and (4) are analogous to the conditions imposed on the coherence quantifier. A straight forward extension of Equation (12) to mixed states yields

$$V(\rho) = \frac{|\rho^C| - |\rho^I|}{|\rho^C| + \rho^I|} \tag{19}$$

$$= \frac{0.5 \sum_{i=j} |\rho_{ij}(t)|}{\sum_{i=1} \rho_{ii}(t) + 0.5 \sum_{ij} |\rho_{ij}(t)|} \tag{20}$$

where ρ^C is a coherent state. When the density matrix $\rho^C = \rho^I$, $V(\rho)$ is zero and it approaches unity as the sum of the off-diagonal elements gets very large. All the conditions satisfied by the coherence quantifier are also satisfied $V(\rho)$. In this sense, Equation (19) is nothing but a normalized coherence measure.

III. APPLICATIONS

A. The visibility of two and four path interferometers

Now the visibility is defined a measure of the wave properties where its zero was assigned to a point of pure particle behavior. The visibility was scaled in Ref. [10] as

$$V_C(\rho) = \frac{1}{n-1} \sum_{i \neq j} \rho_{ij} \tag{21}$$

where n is the dimensionality of the Hilbert space. In the extreme limits, V_C is 0 for incoherent states and 1 for maximally coherent states. Meanwhile, V and V_C do agree for incoherent states and V approaches V_C in the limit of very large $C(\rho)$, the do not have to coincides in between. V can be used to compare the wave properties domination in different experiments. For example, we are expecting that the wave properties will become more and more dominant as the number of slits increase i.e, the the interference fringes become more bright and sharp. That is because as the number of slits increases, the interference terms becomes very large and so does the coherence; hence, V approaches unity.

To illustrates this point, let us assume two path interferometer and four path interferometer where the quantons are prepared in maximally coherent states in both experiments. If there is no path-detection or decoherence involved, the density matrices can be written respectively as

$$\rho = \frac{1}{2} \begin{bmatrix} 1 & 1 \\ 1 & 1 \end{bmatrix} \tag{22}$$

$$\rho = \frac{1}{4} \begin{bmatrix} 1 & 1 & 1 & 1 \\ 1 & 1 & 1 & 1 \\ 1 & 1 & 1 & 1 \\ 1 & 1 & 1 & 1 \end{bmatrix} \tag{23}$$

while V_C is 1 for both experiments, V is $\frac{1}{3}$ and $\frac{3}{4}$, respectively i.e, increases with coherence.

B. Hubbard Model

We have used the interference experiments to illustrate most of the concepts, but the formulas we have derived does not assume a particular system.

1. The Hamiltonian

Despite its simplicity, Hubbard Model [11] captures the essential physics of electrons in atoms, molecules and solids [12]. The model has been applied to the theory of magnetism , Mott metal-insulator transition [13–15] and high temperature superconductors. In solids, electrons interact with each other via screened Coulomb potential. When the site (the atom) is vacant or has a single electron, the electron-electron interaction energy is zero. When it is paired with opposite spin electrons, the interaction energy is assigned the parameter U [16]. That is electrons are correlated with each other in the same site but weakly correlated in different sites [11]. By hopping between site i and site j, electrons save kinetic energy T_{ij} [16]. Taking the interaction of electrons with nuclei into account, the Hamiltonian under the previous assumptions is

$$\hat{H} = -\sum_{i \neq j \sigma} T_{ij} c^{\dagger}_{i\sigma} c_{j\sigma} + \sum_{i\sigma} \epsilon_i n_{i\sigma} + U \sum_i n_{i\uparrow} n_{i\downarrow} \tag{24}$$

where $c^{\dagger}_{i\sigma}$ creates an electron at position i with spin σ (either ↑ or ↓) and $c_{j\sigma}$ destroys a σ-spinned electron at position j. The sums over i and j are understood to be over different sites ($i \neq j$) and no spin flopping processes are allowed. ϵ_i is the one-electron energy in site i. The operators $n_{i\uparrow}$ and $n_{i\downarrow}$ count the number of up-electrons and the number of down-electrons, respectively. Note that the hats have been dropped from all operators for clarity. The model in this form successfully accounts for localization of electrons in molecules and their delocalization in metals [17]. The extent of delocalization, wave property, is quantified by the visibility.

2. One electron on two sites

Assume an electron on two sites. Let $|1\rangle$ and $|2\rangle$ represent spatially-localized electron states at sites 1 and 2, respectively. If the electron adapts pure particle behavior, its state is either $|1\rangle$ or $|2\rangle$. However, quantum mechanics allows the electron to be in any linear superposition of $|1\rangle$ and $|2\rangle$. Since the two sites are indistinguishable, the wave-like behavior, hence interference, is possible [7].

The general state of an electron on two sites can be written in the following form

$$\begin{aligned}|\psi(t)\rangle &= \phi_1(t)\,|\uparrow;0\rangle + \phi_2(t)\,|0;\uparrow\rangle \\ &= \phi_1(t)\,|1\rangle + \phi_2(t)\,|2\rangle \end{aligned} \tag{25}$$

where the states: $|1\rangle = |\uparrow;0\rangle$ and $|2\rangle = |0;\uparrow\rangle$.

The general solution is a linear superposition of the Eigenvectors v_1 and v_2 that have Eigenvalues $E_1 = \epsilon - T$ and $E_2 = \epsilon + T$, respectively.

$$|\psi(t)\rangle = c_1\exp(-iE_1t/\hbar)v_1 + c_2\exp(-iE_1t/\hbar)v_2 \tag{26}$$

In case of an ensemble of such systems. The density matrix fully describes the system and all the observables can be calculated from it.

$$\begin{aligned}\rho(t) &= \rho_{11}(t)\,|1\rangle\langle 1| + \rho_{22}(t)\,|2\rangle\langle 2| \\ &+ \rho_{12}(t)\,|1\rangle\langle 2| + \rho_{21}(t)\,|2\rangle\langle 1| \end{aligned} \tag{27}$$

where ρ_{ij} for $i = 1,2$ and $j = 1,2$ are the matrix elements. Its equation of motion is

$$\frac{d\rho(t)}{dt} = \frac{-i}{\hbar}(\hat{H}\hat{\rho} - \hat{\rho}\hat{H}) \tag{28}$$

It follows that

$$\begin{aligned}\rho_{11}(t) = \frac{1}{2}[&\rho_{11}(0) + \rho_{22}(0) \\ &+ (\rho_{11}(0) - \rho_{22}(0))\cos(\omega_{12}t/\hbar) \\ &- i(\rho_{12}(0) - \rho_{21}(0))\sin(\omega_{12}t/\hbar)]\end{aligned} \tag{29}$$

$$\begin{aligned}\rho_{12}(t) = \frac{1}{2}[&\rho_{12}(0) + \rho_{21}(0) \\ &+ (\rho_{12}(0) - \rho_{21}(0))\cos(\omega_{12}t/\hbar)] \\ &i(\rho_{11}(0) - \rho_{22}(0))\sin(\omega_{12}t/\hbar)]\end{aligned} \tag{30}$$

$$\rho_{21}(t) = \rho_{12}^{\dagger}(t) \tag{31}$$

$$\begin{aligned}\rho_{22}(t) = \frac{1}{2}[&\rho_{11}(0) + \rho_{22}(0) \\ &+ (\rho_{22}(0) - \rho_{11}(0))\cos(\omega_{12}t/\hbar) \\ &+ i(\rho_{12}(0) - \rho_{21}(0))\sin(\omega_{12}t/\hbar)]\end{aligned} \tag{32}$$

where $\omega_{12} = (E_2 - E_1)/\hbar = (2T)/\hbar$. The visibility and coherence can be calculated by substitution of the previous equation in equation (3.17) and equation (3.4), respectively. We may define the site predictability, a measure of the particle nature, analogously to the path predictability as $P = |\rho_{11} - \rho_{22}| = |(\rho_{12}(0) - \rho_{21}(0))\sin(\omega_{12}t)\,|$. That is the site predictability is zero when the system is initially in a maximally coherent states i.e, $\rho_{12}(0) = \rho_{21}(0)$.

Figure (1) illustrates the variation of the site predictability and visibility as a function of $\omega_{12}t$. V and P are complementary in nature. If one peaks, the second is zero.

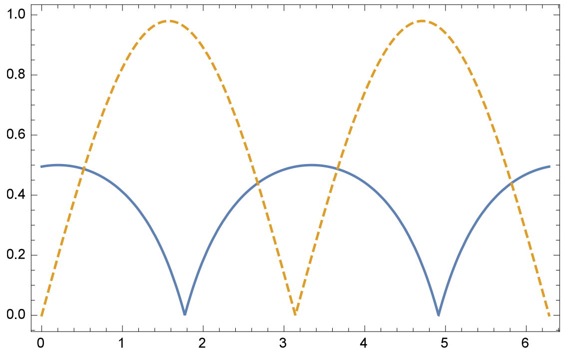

Figure 1. Visibility (solid) and site predictability (dashed) calculated using equation (19) for a single electron on two sites. Figure generated using $c_1 = \sqrt{\frac{60}{100}}\mathrm{i}$ and $c_2 = -\sqrt{\frac{40}{100}}$

3. *Two electron on two sites*

The general quantum state for two electrons on two sites can be written in the following form

$$\begin{aligned}|\psi(t)\rangle &= \phi_1(t)\,|\uparrow\downarrow;0\rangle + \phi_2(t)\,|\uparrow;\downarrow\rangle \\ &+ \phi_3(t)\,|\downarrow;\uparrow\rangle + \phi_4(t)\,|0;\uparrow\downarrow\rangle\end{aligned} \tag{33}$$

where $|\uparrow\downarrow;0\rangle$, $|\uparrow;\downarrow\rangle$, $|\downarrow;\uparrow\rangle$ and $|0;\uparrow\downarrow\rangle$ are the basis states and $\phi_1(t)$ to $\phi_4(t)$ are time dependent coefficients in the Schroedinger's picture. The general solution is

$$\begin{aligned}|\psi(t)\rangle &= c_1\exp(-iE_1t/\hbar)v_1 + c_2\exp(-iE_2t/\hbar)v_2 \\ &+ c_3\exp(-iE_3t/\hbar)v_3 + c_4\exp(-iE_4t/\hbar)v_4\end{aligned} \tag{34}$$

where E_1 to E_4 and v_1 to v_4 are the energy Eigenstates and Eigenvectors, respectively. The density matrix for this system is 4×4. Now we solve the equation of motion under the following approximations
case I: T=0, the off-diagonal elements evolves as

$$\rho_{12}(t) = \rho_{12}(0)\exp(-iUt/\hbar) \tag{35}$$
$$\rho_{13}(t) = \rho_{13}(0)\exp(-iUt/\hbar) \tag{36}$$
$$\rho_{14}(t) = \rho_{14}(0)\exp(iUt/\hbar) \tag{37}$$
$$\rho_{23}(t) = \rho_{23}(0) \tag{38}$$
$$\rho_{24}(t) = \rho_{24}(0)\exp(iUt/\hbar) \tag{39}$$
$$\rho_{34}(t) = \rho_{12}(0)\exp(iUt/\hbar) \tag{40}$$

In this approximation, the visibility is a constant function since the absolute values of the density matrix elements do not evolve with time.
Case II: U=0, the off-diagonal elements evolves as

$$\begin{aligned}\rho_{12}(t) = \frac{1}{16}[&2A_{12} + 2B_{12}e^{-i\omega_{12}t} + 2C_{12}e^{i\omega_{12}t} \\ &+ D_{12}e^{-2i\omega_{12}t} + 2E_{12}e^{2i\omega_{12}t}]\end{aligned} \tag{41}$$

$$\begin{aligned}\rho_{13}(t) = \frac{1}{16}[&2A_{13} + 2B_{12}e^{i\omega_{12}t} + C_{13}e^{-2i\omega_{12}t} \\ &+ 2D_{13}e^{3i\omega_{12}t} + E_{13}e^{4i\omega_{12}t}]\end{aligned} \tag{42}$$

$$\rho_{14}(t) = \frac{1}{16}[2A_{14} + 2B_{14}e^{-i\omega_{12}t} + 2C_{14}e^{i\omega_{12}t} + D_{14}e^{-2i\omega_{12}t} + E_{14}e^{2i\omega_{12}t}] \tag{43}$$

$$\rho_{23}(t) = \frac{1}{8}[A_{23} + B_{23}e^{-i\omega_{12}t} + C_{23}e^{i\omega_{12}t} + D_{23}e^{2i\omega_{12}t}] \tag{44}$$

$$\rho_{24}(t) = \frac{1}{16}[A_{24} + B_{24}e^{-i\omega_{12}t} + C_{24}e^{i\omega_{12}t} + D_{24}e^{2i\omega_{12}t} + E_{24}e^{3i\omega_{12}t} + F_{24}e^{4i\omega_{12}t}] \tag{45}$$

$$\rho_{34}(t) = \frac{1}{16}[2A_{34} + 2B_{34}e^{-i\omega_{12}t} + 2C_{34}e^{i\omega_{12}t} + D_{34}e^{-2i\omega_{12}t} + E_{34}e^{2i\omega_{12}t}] \tag{46}$$

where the time independent constants $A_{kl}, B_{kl}, C_{kl}, D_{kl}, E_{kl}$ and F_{kl} for $k \neq l$ can be determined from the the initial conditions.

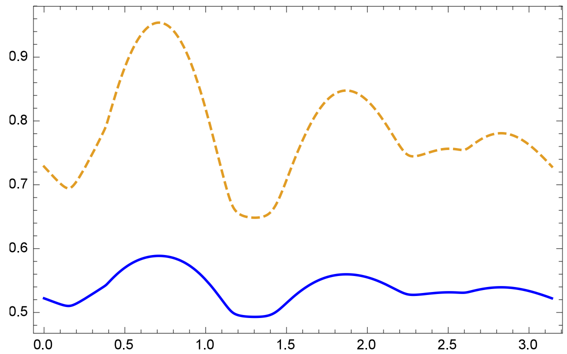

Figure 2. The vertical axis represents V (solid) and V_C (dashed) and the horizontal axis is $\omega_{12}t$ for an ensemble of two electrons on two sites.The Figure was generated using $c_1 = \frac{1}{4} + \frac{1}{4}i$, $c_2 = \frac{1}{4} + \frac{\sqrt{3}}{4}i$, $c_3 = -\frac{1}{4}$ and $c_4 = \frac{2}{2} - \frac{\sqrt{5}}{4}i$

Figure (2) shows that V_C and V follow the same pattern, but they are shifted with respect to one another. Both of them are independent of the single particle energy ϵ_i

IV. DISCUSSION

We introduced visibility as a measure of the wave nature. In doing so, the visibility was defined in terms of the extrema of the density matrix in the general case. The minimum density matrix is for incoherent states and the maximum is for maximally coherent states. This definition is an extension of equation (12). This equation was motivated by setting the minimum probability $|\psi|^2_{min}$ to $|\psi_1|^2 + |\psi_2|^2$ which is corresponding to a relative phase difference of $\frac{\pi}{2}$. However, one could argue that a phase difference of π would yield a smaller probability $|\psi_1|^2 + |\psi_2|^2 - 2|\psi_1\psi_2|$, but if no interference of quantum particles is observed, the square modulus of the resulting wave amplitude is the sum of the square modulus of the constituting components which justifies our choice [2] . Nonetheless, this choice has set limitation to the maximum visibility for a single particle interference namely one-half, see figure 1. Despite of that it indeed confines the values of visibility in the range $[0, 1]$ for multiparticle interference which the alternative choice fails to satisfies, see figure 2.

The relation between visibility and a coherence quantifier was presented. We discussed the difference between V_C which is scaled with $n-1$ and V which is scaled with the sum of ρ^C and ρ^I. The latter can be used to compare the degree of coherence for different systems. Site predictability, for two dimensional space, was defined exactly as the path predictability. For higher dimension, n-path predictability needs to be tested for its applicability to different systems.

ACKNOWLEDGMENTS

I would like to thank the staff and my colleagues in the online course "Applications of Quantum Mechanics" 8.06X at https://www.edx.org/course/applications-of-quantum-mechanics for reading and commenting on this paper.

---

[1] F. Marquardt and A. Puttmann, "Introduction to dissipation and decoherence in quantum systems." Sept., 2008.

[2] G. Auletta, *Foundation and Interpretation of Quantum Mechanics*. World Scientific Publishing Co.Pte.Ltd, revised edition 2001 ed., 2001.

[3] S. Dürr, "Quantitative wave-particle duality in multibeam interferometers,"*Phys. Rev. A* **64** (Sep, 2001) 042113. `https://link.aps.org/doi/10.1103/PhysRevA.64.042113`.

[4] T. Qureshi, "Coherence, interference and visibility." 2019.

[5] K. Blum, *Density Matrix Theory and Applications*. Springer Series on Atomic, Optical, and Plasma Physics. Springer Heidelberg Dordrecht London New York, 2012. `https://www.springer.com/gp/book/9783642205606#reviews`.

[6] T. Baumgratz, M. Cramer, and M. B. Plenio, "Quantifying coherence,"*Phys. Rev. Lett.* **113** (Sep, 2014) 140401. `https://link.aps.org/doi/10.1103/`

`PhysRevLett.113.140401`.

[7] E. Buks, R. Schuster, M. Heiblum, D. Mahalu, and V. Umansky, “Dephasing due to’ which path’ detector,” *Physica* **B249** (1998) 295, `arXiv:quant-ph/9709022 [quant-ph]`.

[8] G. D. M. Biswas Tanmoy and W. Andreas, “Interferometric visibility and decoherenc,”*Proc. R. Soc. A* (July, 2017) . `https://royalsocietypublishing.org/doi/10.1098/rspa.2017.0170`.

[9] A. Stern, Y. Aharonov, and Y. Imry, “Phase uncertainty and loss of interference: A general picture,”*Phys. Rev. A* **41** (Apr, 1990) 3436–3448. `https://link.aps.org/doi/10.1103/PhysRevA.41.3436`.

[10] M. N. Bera, T. Qureshi, M. A. Siddiqui, and A. K. Pati, “Duality of quantum coherence and path distinguishability,”*Phys. Rev. A* **92** (Jul, 2015) 012118. `https://link.aps.org/doi/10.1103/PhysRevA.92.012118`.

[11] J. Hubbard, “Electron correlations in narrow energy bands,” *Proc. R. Soc. Lond. A* **276** (1963) no. 1365, 238–257.

[12] W. Schmidt and M. Schreiber, “Exact and approximate solutions of the peierls–hubbard model,” *The Journal of chemical physics* **86** (1987) no. 2, 953–962.

[13] N. F. MOTT, “Metal-insulator transition,”*Rev. Mod. Phys.* **40** (Oct, 1968) 677–683. `https://link.aps.org/doi/10.1103/RevModPhys.40.677`.

[14] N. Mott, *Metal-insulator transitions.* CRC Press, 1990.

[15] S. Raghu, X.-L. Qi, C. Honerkamp, and S.-C. Zhang, “Topological mott insulators,” *Physical review letters* **100** (2008) no. 15, 156401.

[16] T. Lancaster and S. J. Blundell, *Quantum field theory for the gifted amateur.* Oxford University Press, Oxford, 2014.

[17] B. Alvarez-Fernández and J. Blanco, “The hubbard model for the hydrogen molecule,” *European journal of physics* **23** (2001) no. 1, 11.

The ultra-relativistic Bose gas and the spectrum of blackbody radiation

J. F. Pérez-Barragán
Posgrado en Ciencias Físicas, Universidad Nacional Autónoma de México, Circuito de la Investigación Científica, Ciudad Universitaria, 04510 Mexico City, Mexico

(Dated: June 19, 2019)

The basic formalism of the grand-canonical ensemble was reviewed so that the statistical description of an ideal gas made of photons could be deduced. The obtained results were compared with the empirical Stefan-Boltzmann law and used to deduce Planck's radiation law. This radiation law was also obtained from a historical point of view by making a review of the approach originally used by Planck in 1900, the one that led him to his proposal of the energy quanta.

I. INTRODUCTION

A blackbody is defined as a body which absorbs within itself the whole of the incident radiation [1]. Therefore, a blackbody is an ideal absorber of incident radiation. The spectrum of the radiation emitted by a blackbody is described by Planck's law [2, 3]:

$$u(\nu, T) = \frac{8\pi h}{c^3} \frac{\nu^3}{\exp(h\nu/k_B T) - 1}. \tag{1}$$

This radiation law is one of the most known results in the history of physics due to its deduction required heuristic hypothesis that eventually led to the development of quantum mechanics.

Nowadays Planck's radiation law is usually obtained by applying the general results of quantum statistical mechanics. For this purpose, the blackbody's radiation is viewed as a gas of photons in thermodynamic equilibrium with a cavity [4, 5]. On the other hand, Planck's original approach to obtain equation (1) is rarely discussed in textbooks despite its historical importance. The reason for this is that it was originally based on purely thermodynamic and electromagnetic arguments, and a mathematical interpolation that Planck himself called "a lucky guess" [1, 2]. While, its first theory consisted in a statistical procedure based in ad hoc arguments [3, 6]. In this paper, both approaches will be reviewed and compared in order to notice their physical equivalence.

II. GENERAL FORMALISM OF THE GRAND-CANONICAL ENSEMBLE

The main purpose of statistical mechanics is to connect the laws of mechanics, either classical or quantum, with the thermodynamic behavior of a macroscopic system by adding some uncertainty about the state in which it is. In order to do that, statistical mechanics defines the concept of statistical ensemble as the probability distribution of all the accessible states of the system in its phase-space [5]. There are many types of ensembles depending on the type of system wanted to be described.

The grand-canonical ensemble is the ensemble used to study open systems [4]. An open system is a kind of system in which heat and particles can be exchanged with the surroundings. These systems can be thought as to be in thermal and chemical equilibrium with a reservoir with given temperature and chemical potential, so that the systems no longer have neither a defined temperature nor a fixed number of particles, since energy and particles are continually exchanged with the reservoir [4]. In that sense, the grand-canonical ensemble is the one that is characterized by having states of varying energy and varying number of particles.

For a quantum system the statistical ensemble is defined by its density operator, which is also known as density matrix. This can be easily understood if one thinks that the phase-space distribution is a classical observable [4]. For an open system fixed at a chemical potential μ and absolute temperature T, the grand-canonical density operator $\hat{\rho}$ is given by

$$\hat{\rho} = \frac{\exp\{-\beta(\hat{H} - \mu\hat{N})\}}{\mathrm{Tr}\ (\exp\{-\beta(\hat{H} - \mu\hat{N})\})}, \tag{2}$$

where $\hat{H}$ is the Hamiltonian of the system, $\hat{N}$ is the particle number operator, and the quantity β is defined as $(k_B T)^{-1}$, being k_B the Boltzmann's constant [4]. The denominator in equation (2), known as the grand-canonical partition function $\mathcal{Z}(T, V, \mu)$, is needed to assure the normalization of the density operator, $\langle\hat{\rho}\rangle = 1$. From Boltzmann's equation it follows that entropy S is proportional to the ensemble average of the logarithm of the phase-space density,

$$S = -k_B \langle \ln \hat{\rho} \rangle, \tag{3}$$

in which the ensemble average of an operator $\hat{A}$ is defined as $\langle\hat{A}\rangle = \mathrm{Tr}\ (\hat{\rho}\hat{A})$ [4]. This implies that the entropy of the system is equal to

$$S = k_B \beta \langle\hat{H}\rangle - k_B \beta\mu\langle\hat{N}\rangle + k_B \ln \mathcal{Z}, \tag{4}$$

where it has been used that the density operator is an idempotent operator and that it is normalized [4]. If one identifies the mean energy $\langle\hat{H}\rangle$ with the thermodynamic energy U, and correspondingly, the mean number of particles $\langle\hat{N}\rangle$ with the thermodynamic particle number N, then the equation (4) becomes in

$$TS = U - \mu N + k_B T \ln \mathcal{Z}, \tag{5}$$

from which immediately follows that

$$\Phi \equiv U - TS - \mu N = -pV = -k_B T \ln \mathcal{Z}, \tag{6}$$

where Euler's relation has been used. The function $\Phi(T, V, \mu)$ is a thermodynamic potential, since all the thermodynamic quantities can be obtained from it, known as grand-canonical potential [4]. From equation (6) the following relations can be obtained:

$$S = -\frac{\partial \Phi}{\partial T}; \quad p = -\frac{\partial \Phi}{\partial V}; \quad N = -\frac{\partial \Phi}{\partial \mu}. \tag{7}$$

These relations show that the grand-canonical potential has been coded, through the grand-canonical partition function, with all the information about the thermodynamic properties of the system.

III. IDEAL QUANTUM SYSTEMS

A system composed of N identical noninteracting quantum particles is described by a Hamiltonian operator of the form

$$\hat{H}(\mathbf{r}_1, ..., \mathbf{r}_N, \mathbf{p}_1, ..., \mathbf{p}_N) = \sum_{i=1}^{N} \hat{h}(\mathbf{r}_i, \mathbf{p}_i), \tag{8}$$

where the Hamiltonian operator $\hat{h}(\mathbf{r}_i, \mathbf{p}_i)$ for one particle satisfies the following eigenvalue problem:

$$\hat{h}|k\rangle = \epsilon_k |k\rangle, \tag{9}$$

being $|k\rangle$ and ϵ_k the k-th one-particle state and energy [4, 5]. The state vector of the whole system can be constructed from the one-particle states $|k\rangle$, which are supposed to be normalized, by its direct product,

$$|\Psi\rangle = |k_1, ..., k_N\rangle = \prod_{i=1}^{N} |k_i\rangle. \tag{10}$$

Equation (10) means that the first particle is in the quantum state k_1, the second particle is in the state k_2, etc. In the same way, the system's Hilbert space is the direct sum of the one-particle spaces [4]. On the other hand, the energy associated with this wave function is

$$E = \sum_{i=1}^{N} \epsilon_i. \tag{11}$$

The Hamiltonian expressed in equation (8) commutes with the permutation operator, and thus eigenvectors with a well defined symmetry under an exchange of two arbitrary particle numbers can be constructed [4]. This is important because it is empirically known that the symmetry of the state vector is determined by the type of particle that it describes, meaning that in nature there are only two types of particles: fermions for symmetric vectors and bosons for antisymmetric vectors. [4, 5].

A state vector with a fully defined symmetry is completely characterized if the occupied one-particle states are known [4]. If the one-particle state $|k\rangle$ is enumerated by the index k, it is sufficient to know the occupation numbers $\{n_1, n_2, ...\}$ of each one-particle state to determine the N-particle state. For bosons, such as photons, each occupation number can assume all the integer values between 0 and N, as long as they fullfill that

$$\sum_{k=1}^{\infty} n_k = N. \tag{12}$$

In the same way, the energy eigenvalue of the whole system can be rewritten in terms of occupation numbers as

$$E = \sum_{k=1}^{\infty} n_k \epsilon_k. \tag{13}$$

The difference between equations (11) and (13) lies in that the second equation's index runs over one-particle states, rather than over single particles. Analogously, the states $|k_1, ..., k_N\rangle$ can be characterized by the occupation numbers as $|n_1, n_2, ...\rangle$.

In this new language, the grand-canonical partition function for a bosonic system is given by

$$\mathcal{Z} = \sum_{\{n_k\}} \exp\left(-\beta \sum_{k=1}^{\infty} n_k(\epsilon_k - \mu)\right), \tag{14}$$

where $\{n_k\}$ denotes the given set of occupation numbers [4]. From that, we immediately obtain that the grand-canonical partition function for a system made of noninteracting bosons is equal to

$$\begin{aligned} \mathcal{Z} &= \sum_{n_1, n_2, ... = 0}^{\infty} (e^{-\beta(\epsilon_1 - \mu)})^{n_1} (e^{-\beta(\epsilon_2 - \mu)})^{n_2} \cdots \\ &= \prod_{k=1}^{\infty} \sum_{n_k=0}^{\infty} (\exp\{-\beta(\epsilon_k - \mu)\})^{n_k} \\ &= \prod_{k=1}^{\infty} \frac{1}{1 - z\exp(-\beta\epsilon_k)}, \end{aligned} \tag{15}$$

being the quantity z, defined as $\exp(\beta\mu)$, the fugacity of the system.

From equations (6) and (15); and the third relation expressed in equation (7), the average particle number can be obtained, being it equal to

$$N = \sum_{k=1}^{\infty} \frac{1}{z^{-1}\exp(\beta\epsilon_k) - 1}. \tag{16}$$

Following equations (12), (13) and (16), we immediately get to the system's mean energy,

$$U = \sum_{k=1}^{\infty} \frac{\epsilon_k}{z^{-1}\exp(\beta\epsilon_k) - 1}. \tag{17}$$

IV. PHOTON GAS AND PLANCK'S RADIATION LAW

The photon is the elementary bosonic particle that carries the electromagnetic interaction. This elementary particle is characterized by having an invariant mass equal to zero and by always moving at the speed of light in vacuum, this is, for being an ultra-relativistic particle [4]. Those properties imply that all photon's one-particle energy comes from its momentum:

$$\epsilon_k = c|\mathbf{p}| = \hbar c|\mathbf{k}|. \tag{18}$$

In a photon gas fixed at thermal energies the photon-photon interaction is small enough to be negligible [4], which means that this kind of system under those circumstances can be considered as an ideal noninteracting system. Additionally, we usually think that the gas of photons is at equilibrium with a cavity, whose walls are considered to be a huge collection of harmonic oscillators. This implies that the wall's oscillators absorb and emit photons continuously, meaning that the number of photons in the gas fluctuates. All this arguments allow us to use the results of the previous section to describe a gas of photons inside a cavity.

From quantum mechanics, it is well known that having a free particle inside a box of volume $V = L^3$, with periodic boundary conditions, implies that its wave vector is quantized in the following way:

$$\mathbf{k} = \frac{2\pi}{L}(n_x, n_y, n_z), \tag{19}$$

where n_x, n_y and n_z are integer numbers. From equation (19) we immediately obtain that the minimum distance between two successive states in the k-space is equal to $\Delta k_i = (2\pi/L)\Delta n_i$, being $i = x, y, z$. Nevertheless, by taking the limit where the volume of the box is infinite, we note that the states come closer together due to its separation is inversely proportional to L. This means that, in this limit an infinitesimal cell of volume $(2\pi/L)^3$ corresponds to a single state of the system. The distribution of states is illustrated in figure 1.

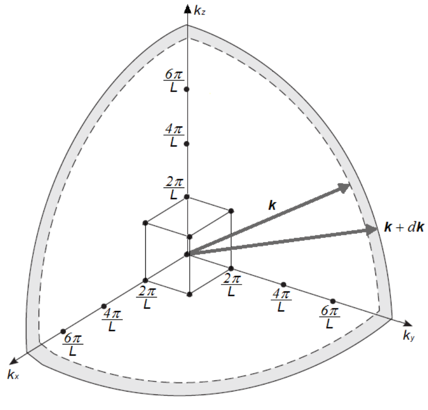

Figure 1. Distribution of states in k-space.

For this reason, if $V \to \infty$, the total number of states can be approximated as the integral over the k-space divided by the one-state volume. A numerical factor g_s must be included in this definition due to the degeneracy of spin, which in the case of photons is equal to 2 [4]. Because of this, and equation (18), from which it follows that ϵ_k depends only in the magnitude of $\mathbf{k}$, we obtain that the total number of states is

$$\Sigma \approx \frac{g_s V}{8\pi^3}\int d^3k = \frac{8\pi V}{h^3c^3}\int_0^\infty \epsilon^2 d\epsilon. \tag{20}$$

From equation (20) it immediately follows that the one-particle density of states is equal to

$$g(\epsilon) = \frac{d\Sigma}{d\epsilon} = \frac{8\pi V}{h^3c^3}\epsilon^2. \tag{21}$$

This deduction is relevant because it shows that the sums expressed in equations (16) and (17) can be approximated, in the large volume limit, as integrals if they are multiplied by the one-particle density of states [4, 5].

Additionally, the photon gas requires another consideration with respect to its chemical potential. Due to the massless character of photons, it is possible to create arbitrarily many of them having $\epsilon = 0$ without energy cost. This means that in the state $\epsilon = 0$ there may be, in principle, an infinite number of photons. Thus, the chemical potential, which is defined as the energy needed to change the particle number, must be equal to zero [4, 5]. By applying all these considerations to equation (17), the mean energy of the gas photons turns into

$$U = \frac{8\pi V}{h^3c^3}\int_0^\infty \frac{\epsilon^3 d\epsilon}{\exp(\beta\epsilon) - 1}. \tag{22}$$

The integral in equation (22) can be easily solved in terms of the gamma function and the Riemann zeta function. After that, it is immediate to obtain that the density of energy contained in the photon gas is equal to

$$\mathcal{U} \equiv \frac{U}{V} = \frac{8\pi^5 {k_B}^4}{15h^3c^3}T^4. \tag{23}$$

Since the photons in the gas are isotropically distributed and unpolarizated, the radiated energy density is proportional to the total power radiated per unit surface area, being the constant of proportionality equal to $(4/c)$ [6]. This means that equation (23) can be expressed as

$$\mathcal{U} = \frac{4\sigma}{c}T^4, \tag{24}$$

where σ is the Stefan-Boltzmann constant. The numerical value obtained from the found expression for this constant is in total agreement with the value empirically obtained by Stefan in 1879 [4].

Finally, the system's spectrum can be obtained if equation (22) is expressed in terms of the frequency of the photon by taking $\epsilon = h\nu$,

$$\mathcal{U} = \frac{8\pi h}{c^3}\int_0^\infty \frac{\nu^3 d\nu}{\exp(\beta h\nu) - 1}. \tag{25}$$

From equation (25) we immediately get by inspection to the radiation law associated with the photon gas model, which turns out to be equal to the form of Planck's law expressed in equation (1).

V. HISTORICAL APPROACH TO PLANCK'S RADIATION LAW

The development of blackbody's radiation law formally began in 1859 when Kirchhoff discovered, based on a great volume of diverse experimental data, the lack of dependence between the emitted light and the specific nature, size and shape of the emitter body [7]. Kirchhoff proved that, in situations of thermodynamic equilibrium, the radiation law depends only on the wavelength of the incident radiation and on the blackbody's temperature. The next important step was made by Stefan in 1879. He empirically found that the total power radiated per unit surface area of a blackbody across all wavelengths grows like the fourth power of its absolute temperature [7]. By that time, the light was already widely accepted to be electromagnetic radiation, and hence it was thought that the missing distribution law should be able to be obtained from purely thermodynamic and electromagnetic arguments. In that sense, Boltzmann was able to theoretically deduce Stefan's law in 1884, by studying the phenomenon of radiation pressure from the perspective of thermodynamics [7].

In 1894, Wien published his studies on the reflection of radiation within a perfectly reflecting sphere that contracts adiabatically [1]. He concluded that this process implies a redistribution with respect to the radiation's frequency in accordance with the Doppler effect, and that the radiation law must satisfy that

$$u(\nu, T) = \nu^3 F(\nu/T). \tag{26}$$

The function F was an unknown function of ν/T, which was thought to have a fundamental role in physics in view of the universal character of the blackbody's radiation. From equation (26), which was called Wien's displacement law, Wien was able to obtain that the wavelength with the maximum power emission is inversely proportional to the blackbody's absolute temperature [6], which turned out to fit perfectly with the experimental data. Two years later, Wien assumed that the wavelength of the radiation emitted by any blackbody's molecule and its correspondent intensity were functions of the molecule's velocity [1], so that, by combining its law with Maxwell's velocity distribution he obtained that the radiation law should be of the form

$$u(\nu, T) = A\nu^3 \exp(-B\nu/T), \tag{27}$$

where A and B are constants. The equation (27), known as Wien's distribution law, was thought to be confirmed by Paschen's experimental data in the high frequencies region, but Rubens and Kurlbaum showed in 1900 that Wien's law failed at the infrared region [6].

At the end of the 19th century, Planck had become one of the most outstanding specialists in thermodynamics in the Friedrich-Wilhelm University of Berlin. In those years, Planck believed in the apparent success of Wien's law. However, he thought that Wien's approach was not well founded, so he started working on what he called "the thermodynamic approach" of the blackbody's problem [1]. As Kirchhoff's successor, Planck knew that the radiation distribution at equilibrium is independent of the nature of the radiators [1], so he started his studies with the simplest possible assumption, that the radiators are linear harmonic oscillators of frequency ν. He established, from the electromagnetic theory, that the oscillator's dipole moment $f(t)$ satisfies the equation

$$\frac{d^2 f}{dt^2} + 2\sigma\nu\frac{df}{dt} + 4\pi^2\nu^2 f = \frac{3c^3\sigma}{4\pi^2\nu^2}Z(t), \tag{28}$$

where σ is the logarithmic decrement of the vibration amplitudes due to radiation and $Z(t)$ is the intensity of the component of the electric field in the direction of the resonator [8]. Planck solved equation (28), obtaining $f(t)$ as a Fourier series, from which he arrived to a relation between the density of the field energy and the mean energy associated with the oscillators [8],

$$u_\nu = \frac{8\pi\nu^2}{c^3}\mathcal{E}_\nu. \tag{29}$$

At this point, Planck introduced Wien's law into his results, so from equations (27) and (29) he obtained that the oscillator's average energy has the following form

$$\mathcal{E} = C\nu\exp(-B\nu/T), \tag{30}$$

or equivalently, that

$$\frac{1}{T} = -\frac{\ln(\mathcal{E}/C\nu)}{B\nu}. \tag{31}$$

Planck knew from thermodynamics that the relation $1/T = \partial S/\partial\mathcal{E}$ is satisfied when the system reaches the thermodynamic equilibrium [2], so he obtained that, in such situations, Wien's law unequivocally leads to

$$\frac{\partial^2 S}{\partial\mathcal{E}^2} = -\frac{1}{B\nu\mathcal{E}}. \tag{32}$$

Nevertheless, when Planck knew from Kurlbaum that the radiation law must be proportional to the temperature at very low frequencies on October 1900, he obtained, by using the same approach as before, that for low frequencies the second derivative of entropy with respect to energy should be equal to

$$\frac{\partial^2 S}{\partial\mathcal{E}^2} = -\frac{\text{const}}{\mathcal{E}^2} \tag{33}$$

[2]. Planck wanted to preserve both asymptotic behaviors, so he made a mathematical interpolation of both results that took him to propose that

$$\frac{\partial^2 S}{\partial\mathcal{E}^2} = -\frac{a}{\mathcal{E}(\mathcal{E}+b)}, \tag{34}$$

which, in fact, reduces for small values of U to equation (32) and hence to Wien's law, and for large values of U to equation (33) [2]. From this proposal, Planck arrived to

$$\mathcal{E}_\nu = \frac{b}{\exp(b/aT) - 1}. \tag{35}$$

To find the dependence of $\mathcal{E}_\nu$ on ν, Planck supposed, based on equations (26) and (29) [1], that $\mathcal{E} = \nu\phi(\nu/T)$, being ϕ an arbitrary function. This led him to obtain that the mean energy of an oscillator is

$$\mathcal{E}(\nu, T) = \frac{\mathcal{A}\nu}{\exp(\mathcal{B}\nu/T) - 1}. \tag{36}$$

Finally, Planck obtained from equation (29) that the radiation law is

$$u(\nu, T) = \frac{\mathcal{C}\nu^3}{\exp(\mathcal{B}\nu/T) - 1}, \tag{37}$$

where $\mathcal{B}$ and $\mathcal{C}$ are constants that must be adjusted to the experimental data [1, 2].

Rubens checked, through the night following the Academy session, Planck's formula against his experimental data, and found that both were in total agreement. After that, Planck's result was considered to be correct, but also to be an empirical formula since its basic assumption, the one expressed in equation (34), had no rigorous theoretical justification [1]. The behavior of Planck's law is compared with the asymptotic cases found by Wien, for the ultraviolet region, and by Kurlbaum, for the infrared region, in the figure 2.

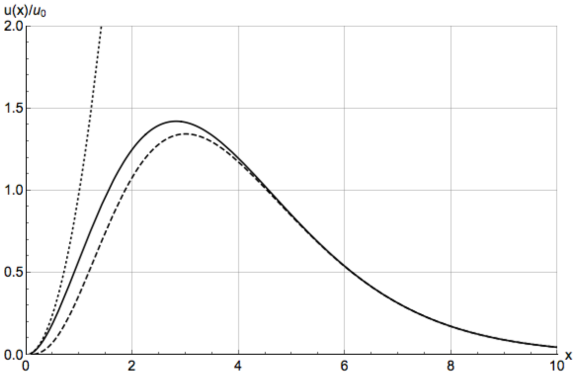

Figure 2. Planck's radiation law, solid curve, and its limit cases: Wien's law, dashed curve, and Kurlbaum's experimental result also known as Rayleigh-Jeans law, dotted curve, plotted as functions of $x = h\nu/k_BT$. The energy densities per unit frequency have been divided by $u_0 = 8\pi k_B^3T^3/h^2c^3$ in order to obtain dimensionless quantities.

In order to justify his "*eine glücklich erratene interpolationsformel*", Planck ultimately had to abandon his thermodynamic approach and turn to Boltzmann's probabilistic conception [1, 3], in which the entropy of a system is given by Boltzmann's equation

$$S_N = k_B \ln W, \tag{38}$$

where W is the number of distributions compatible with the energy of the system. In that sense, to obtain S_N Planck assumed that the system's total energy $\mathcal{E}_N$ consists of an integral number P of energy elements ϵ, so that $\mathcal{E}_N = P\epsilon$ [1, 3]. Then, he proceeded to calculate the number of possible ways of distributing P energy elements among N oscillators, obtaining that

$$W = \frac{(N+P-1)!}{(N-1)!P!} \approx \frac{(N+P)^{N+P}}{N^N P^P}, \tag{39}$$

where Stirling's formula has been used to obtain the last equality. Then he obtained from Boltzmann's equation, equation (38), that the system's entropy is

$$S_N = k_B N \left[\left(1 + \frac{\mathcal{E}}{\epsilon}\right)\ln\left(1 + \frac{\mathcal{E}}{\epsilon}\right) - \frac{\mathcal{E}}{\epsilon}\ln\left(\frac{\mathcal{E}}{\epsilon}\right)\right]. \tag{40}$$

From equation (40) it follows that the entropy of a single oscillator $S = S_N/N$ satisfies equation (34). Because of this fact, Planck felt sure about that his new approach, in which the energy is considered discrete, was the correct one [1]. After that, Planck obtained from Wien's displacement law and equation (29) that the entropy S can be written as

$$S = \varphi(\mathcal{E}/\nu), \tag{41}$$

where φ is an unknown function. By comparing the two expressions for the entropy of a single oscillator, Planck concluded that the energy element ϵ must be proportional to the frequency ν [3], thus:

$$\epsilon = h\nu, \tag{42}$$

and consequently:

$$S = k_B \left[\left(1 + \frac{\mathcal{E}}{h\nu}\right)\ln\left(1 + \frac{\mathcal{E}}{h\nu}\right) - \frac{\mathcal{E}}{h\nu}\ln\left(\frac{\mathcal{E}}{h\nu}\right)\right], \tag{43}$$

where h is a universal constant.

Planck substituted equation (42) in (40) and used again the thermodynamic relation between the temperature and the second derivative of the entropy with respect to the energy to obtain that the mean energy of the oscillator is given by

$$\mathcal{E}(\nu, T) = \frac{h\nu}{\exp(h\nu/k_BT) - 1}. \tag{44}$$

This result led him to obtain, from equation (29), his radiation law once again.

From his theory, Planck could theoretically derive Stefan's law and Wien's displacement law from equation (1), by integrating it over all the frequencies and by maximizing it, respectively. On the other hand, he was able to obtain, by using Kurlbaum's experimental data, the numerical values of the ratios k_B^4/h^3 and h/k, from which he could compute the numerical values of k_B and h [3]. Finally, Planck presented his results and his universal constant h at a meeting of the German Physical Society on December 14, 1900, a date which is currently know as the birthday of quantum mechanics [1].

VI. DISCUSSION

As we noticed at the beginning of this paper, the modern treatment of blackbody's radiation was merely a systematic application of the general results of quantum statistical mechanics. This treatment consisted in applying the fundamental properties of photons, such as their massless and bosonic character, to the general results statistically obtained for an ideal quantum system. In that way, we were able to obtain Planck's radiation law from equation (22) by expressing it in terms of the photon's frequency, by using the quantum energy-frequency relation, and by computing the energy density associated with a infinitesimal bandwidth $d\nu$ centered in ν.

On the other hand, we saw in the last section that the historical development of the blackbody's radiation law was anything but simple. The studies made by Kirchhoff, Boltzmann and Wien showed that a purely classical treatment of the system, which is composed of the radiation and the cavity, lead in all the cases to the Rayleigh-Jeans law and its ultraviolet catastrophe, as Rayleigh later proved in 1905. Planck was able to obtain equation (1) in October 1900 only because he obtained correctly equation (29) from a theory based in the fundamental principles of thermodynamics and the Maxwell's equations; and because he made a clever interpolation between Wien's law and Kurlbaum's experimental data. Even more, we noticed that in his first theory, Planck assumed unproved physical arguments, such as the one that establishes that $\mathcal{E}_N = Nh\nu$, in order to obtain an expression for the entropy of the oscillator which was fully compatible with equation (34). This implied that his first theory could not be considered as fundamental.

We should note that Planck never mentioned in his early writings that the assumption for $\mathcal{E}_N$ has a fundamental character within its theory. At that time, Planck was not sure whether the introduction of h was merely a mathematical device needed to obtain equation (1) or whether it expressed an innovation of profound physical significance [1]. Planck's first theory of blackbody's radiation turned out to be the statistical treatment of the oscillators in the wall of a cavity, which are capable of absorbing and emitting radiation in a discrete way. This statistical approach differs from Boltzmann's probabilistic method in so far as Planck associated the quantity W with the S_N at the equilibrium state without maximizing it. Planck's work, and a few more that came later, proved that in order to describe all the observed phenomena, a new kind of physics had to be considered. This new physical science began with Planck's postulate of energy quanta, and quickly showed its departure from the principles of classical physics.

Finally, we noted that both approaches led to the same result. This is because both analysis consider the fact of energy quantization. On the one hand, the modern analysis has the notion of energy quanta within itself since it has been constructed by using the quantum-mechanical description of photons; on the other hand, the analysis made by Planck was developed from a classical point of view, by describing the radiation within the cavity with Maxwell's equations, but included the assumption that the wall's oscillators absorb and emit radiation in a discrete way. As Einstein noted in 1905, Planck's theory was not consistent due to this assumption, but correctly led him to equation (1) because in situations of thermodynamic equilibrium the wall‘s oscillators and the radiation shares the distribution of energy.

Acknowledgments

The author thanks Brenda Nequiz for the conversations about the blackbody's radiation problem and for the final revision of this work, without which it would not have been possible. The author also thanks Jim Freericks for the comments and suggestions made.

[1] M. Jammer. *The Conceptual Development of Quantum Mechanics.* Mc-Graw Hill Book Company, 1966.

[2] M. Planck. "Über eine Verbesserung der Wien'schen Spectralgleichung" (in German). *Verhandlungen der Deutschen Physikalischen Gesellschaft*, **2**:202–204, 1900.

[3] M. Planck. "Über das Gesetz der Energieverteilung im Normalspektrum" (in German). *Annalen der Physik*, **309**:553–563, 1901.

[4] W. Greiner; L. Neise and H. Stöcker. *Thermodynamics and Statistical Mechanics.* Springer, 1995.

[5] L. García-Colín Scherer. *Introducción a la Física Estadística.* El Colegio Nacional, 2005.

[6] L. García-Colín Scherer. *La Naturaleza Estadística de la Teoría de los Cuantos.* El Colegio Nacional, 2004.

[7] J. Mehra and H. Rechenberg. *The Historical Development of Quantum Theory: Volume 1.* Springer-Verlag, 1982.

[8] M. Planck. "Über irreversible Strahlungsvorgänge" (in German). *Annalen der Physik*, **306**:69–122, 1900.

The van der Waals force/interaction of two hydrogen atom in the excited states

Vo Hoang Huy
Department of Theoretical Physics, University of Science - HCM City

June 19, 2019

1 Abstract

We assume that two atoms in the van der Waals range where two electrons is not overlap is the most important condition. We choose the Rydberg states for the general of the two hydrogen atoms in excited states interaction. The states of two atoms in this paper we will choose are same the each other that make a pair state for our system. The dipole - dipole interaction is described and fomulated that approximate with $1/R^3$. We will see the van der Waals interaction between two hydrogen atoms in the excited states by the perturbation approach. The factor $1/R^6$ appear when we expand perturbation of the V_{dd} - the potential energy of two hydrogen atoms. The van der Waals constant C_6 increases with the n^{11} that is calculated exactly by the numerical method. In the end, we discuss about some result of Rydberg atoms interaction that valuable experimental side like 'frozen Rydberg gas' , and about the quantum information process.

2 Introduction

We know that it always exist the van der Waals interaction(the van der Waals force) between two atoms if they are in the corresponding distance. We usually use the route that we image two atoms connect with each other by a string and two vibrate make the string vibrate like a harmonic oscillator with the that make it so easy to understand, but my route is different from that way. It is true that we have one hydrogen atom is likely a dipole consist of one positive charge is the nucleus and one negative charge is the electron, so in my view I think we should start from the potential energy of dipole - dipole interaction. The excited states of the hydrogen atom in this paper is the Rydberg state in general, so we still can use the for the interaction of two hydrogen atoms $(2S - 1S)$ pair that make alot of interesting problems which I will not show in this paper, so please forgive me because that things. The Stark effect is include of this paper. It is simple to see that the two hydrogen atoms, which we see, are neutralize in the average time, but it is not neutralize if we evaluate in a interval of time shorter. In addition, when the distance between them is large enough or we have also call that is the van der Waals range the electron clouds do not overlap each other. Since that it is strongly believed that it is useful when we use the dipole - dipole to describe two hydrogen atoms. In this paper we will approach by the perturbation theory that we just study so that understanding content maybe easier than another route. Also, the van der Waals constant need a numerical calculations, so maybe the route of the numerator is not included in this paper.

3 Rydberg States - Rydberg Atoms

3.1 Rydberg States

As we known, we have in the ordinary atomic states can described in term of electron configuration, telling how many electrons are to be assigned to a series of atomic orbitals, of decreasing ionization potential in the order written. Any one (or more) of the occupied atomic orbitals can be excited. In ordinary Rydberg states one electron is excited to a relatively large n (e.g. $ns, n = 4, 5, 6...$). Rydberg states are appropriated with the Rydberg formula for energy

$$E = E_\infty - \frac{hRy}{(n-\delta)^2} \tag{1}$$

which Ry is the Rydberg constant, and δ is the quantum defect.

3.2 Two features of Rydberg physics make a general approach attractive

First, when the external fields are small enough or vanish, each Rydberg multiplets is labeled by the value n and the spliting inside each multiplet is small compared to the splitting between them If we have a dynamical system which describes the internal structure of an individual n multiplet has two degrees of freedom. For large n, the set n^2 quantum levels is sufficiently large to be well studied by classical analysis.

Second, the isolated hydrogen has a large dynamical symmetry: that of the orthogonal group $O(4)$ and time reversal. That is exact symmetry fr the quantum mechanical study, in the non-relativistic approximation, of an electron in the static Coulomb potential of a point-like nucleus; then the energy of bound states depends only on the principal quantum number n, that exceptional energy degeneracy between the states of different orbital mementa of value l. The $O(4)$ dynamical symmetry is only an initial approximation for Rydberg states, which becomes exact at the asymtotic limit $n \to \infty$ when there are no external fields.

3.3 Some properties

We have Rydberg atoms are in states with a principal quantum number $n \gg 1$. This corresponds classically to a very large electron orbit, and the effect of the effect of the nucleus and remaining electrons (the ionic core) is essentially that of an elementary positive point charge: thus it is approciated with hydrogen atom. Rydberg states: the electric dipole matrix element between two neighboring states scales as n^2, while the energy spacing between adjacent Rydberg levels, which scales as n^{-3}. This gives the Rydberg atoms a long lifetime $\tau \sim n^3$ that is explained by the Heisenberg uncertainty principle with energy. In addition, a very strong sensitivity to electric fields: the polarizability scales as n^7. Thus, two nearby Rydberg atoms undergo very strong dipole - dipole interactions that make we choose the Rydberg states for this paper.

4 The dipole - dipole potential energy of two hydrogen atoms

As I just write above the dipole - dipole case is actually describe accurately two hydrogen atoms in any states. We just have a assumption here like the large distance of two atoms that make two electrons not overlap, that make the distrance larger than the displacemant vector of dipole alot of times.

4.1 Illustration

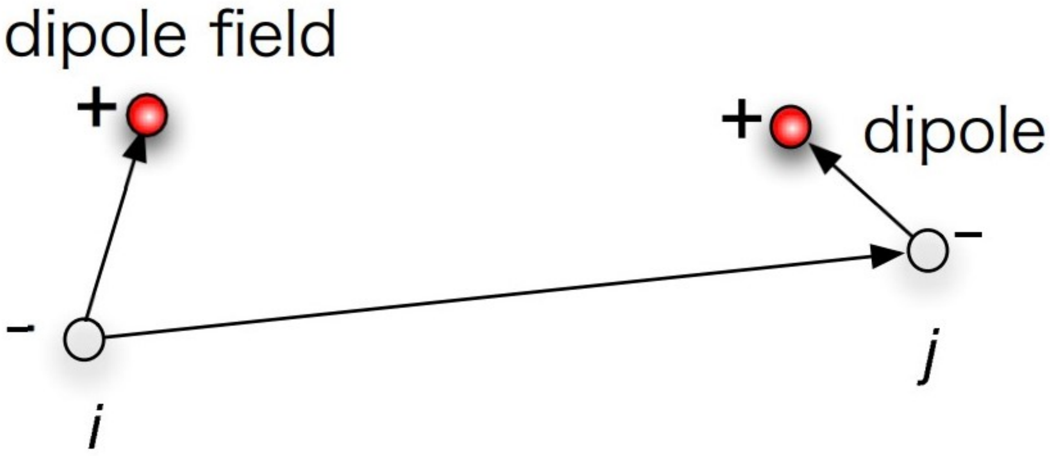

Figure 1: Dipole-Dipole

4.2 Form the equation - Demontration

We have some notations

$$\mathbf{p}_j \equiv \rho_j e \mathbf{d}_j$$
$$\mathbf{r}_j - \mathbf{r}_i \equiv \mathbf{r}_{ji}$$
$$|\mathbf{r}_{ji}| = r_{ji}$$

The $\mathbf{p}_j$ is the electric dipole operator of atom j We assume $r_{ji} \gg d_i, d_j$. We have the approximation of Taylor series expand of

$$(1+x)^{-\frac{1}{2}} \approx 1 - \frac{1}{2}x + \frac{3}{8}x^2 \tag{2}$$

We have the potential energy is derived in the form

$$
\begin{aligned}
V_{dd} &= \frac{(-\rho_i)(-\rho_j)e^2}{4\pi\epsilon_0}\frac{1}{|\mathbf{r}_j - \mathbf{r}_i|} + \frac{(-\rho_i)\rho_j e^2}{4\pi\epsilon_0}\frac{1}{|\mathbf{r}_j + \mathbf{d}_j - \mathbf{r}_i|} + \frac{\rho_i(-\rho_j)e^2}{4\pi\epsilon_0}\frac{1}{|\mathbf{r}_j - \mathbf{r}_i - \mathbf{d}_i|} \\
&+ \frac{(\rho_i)(\rho_j)e^2}{4\pi\epsilon_0}\frac{1}{|\mathbf{r}_j + \mathbf{d}_j - \mathbf{r}_i - \mathbf{d}_i|} \\
&= \frac{\rho_i\rho_j e^2}{4\pi\epsilon_0}\Big(\frac{1}{r_{ji}} - \frac{1}{\sqrt{r_{ji}^2 + 2\mathbf{r}_{ji}\cdot\mathbf{d}_j + \mathbf{d}_j^2}} + \frac{1}{\sqrt{r_{ji}^2 - 2\mathbf{r}_{ji}\cdot\mathbf{d}_i + \mathbf{d}_i^2}} \\
&+ \frac{1}{\sqrt{r_{ji}^2 - 2\mathbf{r}_{ji}\cdot\mathbf{d}_i + 2\mathbf{r}_{ji}\cdot\mathbf{d}_j + \mathbf{d}_i^2\mathbf{d}_j^2 - 2\mathbf{d}_i\cdot\mathbf{d}_j}}\Big) \\
&= \frac{\rho_i\rho_j e^2}{4\pi\epsilon_0 r_{ji}}\Big(1 - \frac{1}{[1 + (2\mathbf{r}_{ji}\cdot\mathbf{d}_j)/r_{ji}^2 + \mathbf{d}_j^2/r_{ji}^2]^{1/2}} + \frac{1}{[1 - (2\mathbf{r}_{ji}\cdot\mathbf{d}_i)/r_{ji}^2 + \mathbf{d}_i^2/r_{ji}^2]^{1/2}} \\
&+ \frac{1}{[1 - (2\mathbf{r}_{ji}\cdot\mathbf{d}_i)/r_{ji}^2 + (2\mathbf{r}_{ji}\cdot\mathbf{d}_j)/r_{ji}^2 + \mathbf{d}_i^2/r_{ji}^2\mathbf{d}_j^2/r_{ji}^2 - (2\mathbf{d}_i\cdot\mathbf{d}_j)/r_{ji}^2]^{1/2}}\Big) \\
&= \frac{\rho_i\rho_j e^2}{4\pi\epsilon_0 r_{ji}}\Big[1 - 1 + \frac{1}{2}\frac{2\mathbf{r}_{ji}\cdot\mathbf{d}_j}{r_{ji}^2} + \frac{1}{2}\frac{\mathbf{d}_j^2}{r_{ji}^2} - \frac{3}{8}\Big((2\mathbf{r}_{ji}\cdot\mathbf{d}_j)/r_{ji}^2 + \mathbf{d}_j^2/r_{ji}^2\Big)^2 \\
&- 1 + \frac{1}{2}\frac{-2\mathbf{r}_{ji}\cdot\mathbf{d}_i}{r_{ji}^2} + \frac{1}{2}\frac{\mathbf{d}_i^2}{r_{ji}^2} - \frac{3}{8}\Big((2\mathbf{r}_{ji}\cdot\mathbf{d}_i)/r_{ji}^2 + \mathbf{d}_i^2/r_{ji}^2\Big)^2 \\
&+ 1 - \frac{1}{2}\frac{-2\mathbf{r}_{ji}\cdot\mathbf{d}_i}{r_{ji}^2} - \frac{1}{2}\frac{2\mathbf{r}_{ji}\cdot\mathbf{d}_j}{r_{ji}^2} - \frac{1}{2}\frac{\mathbf{d}_i^2}{r_{ji}^2} - \frac{1}{2}\frac{\mathbf{d}_j^2}{r_{ji}^2} + \frac{1}{2}\frac{2\mathbf{d}_i\cdot\mathbf{d}_j}{r_{ji}^2} \\
&+ \frac{3}{8}\Big(\frac{-2\mathbf{r}_{ji}\cdot\mathbf{d}_i}{r_{ji}^2} + \frac{2\mathbf{r}_{ji}\cdot\mathbf{d}_j}{r_{ji}^2} + \frac{\mathbf{d}_i^2}{r_{ji}^2} + \frac{\mathbf{d}_j^2}{r_{ji}^2} - \frac{2\mathbf{d}_i\cdot\mathbf{d}_j}{r_{ji}^2}\Big)^2\Big] \\
&= \frac{\rho_i\rho_j e^2}{4\pi\epsilon_0 r_{ji}}\Big[\frac{\mathbf{d}_i\cdot\mathbf{d}_j}{r_{ji}^2} - 3\frac{(\mathbf{r}_{ji}\cdot\mathbf{d}_i)(\mathbf{r}_{ji}\cdot\mathbf{d}_j)}{r_{ji}^4}\Big] \\
V_{dd} &= \frac{1}{4\pi\epsilon_0 r_{ij}^3}\Big[\mathbf{p}_i\cdot\mathbf{p}_j - 3\frac{(\mathbf{p}_i\cdot\mathbf{r}_{ij})(\mathbf{p}_j\cdot\mathbf{r}_{ij})}{r_{ji}^2}\Big]
\end{aligned}
$$

Thus, we have the equation for the potential energy of dipole - dipole interaction

5 The van der Waals interaction

From the equation for the potential energy of dipole - dipole interaction, we use the perturbation theory to find the potential energy correction, and we will see if it have a factor that scale with $\frac{1}{r_{ij}^6}$. We did that with the assume that we choose the non-degeneracy excited states and states of two atoms are prepaired in the same state so the pair state which is defined $|\alpha\beta\rangle \equiv |\alpha\rangle \otimes |\beta\rangle$ have the form $|\alpha\alpha\rangle$. Thus we will use the non - degenegrate perturbation theory.

5.1 First-order in the perturbation theory

In the first - order we have the energy shift in form

$$\Delta E_{\alpha\alpha}^{(1)} = \langle\alpha\alpha|\, V_{dd}\, |\alpha\alpha\rangle = \big\langle V_{dd}\big\rangle_{\alpha\alpha} \tag{3}$$

However, this result is vanish due to the $\mathbf{p}$ is the odd-parity operator and the atomic state $|\alpha\rangle = |n, l, m, s\rangle$ is the eigenstate of the atom that have definite parity. Thus, there is no energy shift if we just expand the perturbation to the first-order. Explaning $|\alpha\rangle = \psi_\alpha(r)$

$$\begin{aligned}\Delta E^{(1)}_{\alpha\alpha} &= \langle\alpha\alpha| V_{dd} |\alpha\alpha\rangle \\ &= \int d\mathbf{r}_i \int d\mathbf{r}_j (\psi_\alpha(\mathbf{r}_i) \otimes \psi_\alpha(\mathbf{r}_j))^* V_{dd}(\psi_\alpha(\mathbf{r}_i) \otimes \psi_\alpha(\mathbf{r}_j)) \\ &= 0\end{aligned}$$

5.2 Second-order in the perturbation theory

The second - order, we have the energy shift in form

$$\Delta E^{(2)}_{\alpha\alpha} = \sum_{\beta,\gamma,\ldots} \frac{\left| \langle\alpha\alpha| V_{dd} |\beta\gamma\rangle \right|^2}{E_{\alpha\alpha} - E_{\beta\gamma}} \equiv \frac{C_6}{r^6_{ij}} \approx \frac{1}{r^6_{ij}} \tag{4}$$

In here, we sum extends all states that are dipole - coupled to $|\alpha\rangle$. The second-order in V_{dd} scale with $\frac{1}{r^6_{ij}}$ because $V_{dd} \approx \frac{1}{r^3_{ij}}$ so the absolute have the second power give the result that we simply see that it is the van der Waals interaction of two hydrogen atom in excited states. The result of $\Delta E^{(2)}_{\alpha\alpha}$ is proportional to dipole-moment to the fourth power, it scale as n^8, the denominator scales as $1/n^3$. Thus the coefficient C_6 increases with n as n^{11} when $n \to \infty$. The power-11 law of the asymptotic n-dependence for the numerical values.

6 Discussion

With van der Waals interactions and some other interactions that we will not show in this paper, two Rydberg atoms interact with each other that show some results interesting. Due to the availability of laser-cooled samples in which the atomic motion is negligible on relevant experimental timescales, thus realizing a ‘ frozen Rydberg gas’ . And the most interesting thing is some theoretical proposal suggesting the use of the Rydberg blockade for quantum infomation processing that will make the technology about quantum infomation have evolution-step.

7 Conclusion

Thus, we derived the van der Waals interaction of two excited hydrogen atoms. We introduced about the our system two hydrogen atom in excited states that we chosen as Rydberg states - a pair state. We explained about Rydberg state - Rydberg atoms, two physical features to make that interesting with us. We also explained about properties of Rydberg states that showed why we choose these states to describe the dipole-dipole interaction (the lifetime long ,the very strong sensitive about the external field - electric field) We explained why we modeled our interaction with the dipole-dipole interaction, and we calculated the formula for this potential of that dipole-dipole We see that it is easy to see that from the dipole-dipole potential energy by the perturbation approach, we obtain the van der Waals factor by the second order of non-degeneracy perturbation theory The van der Waals coefficent, which we obtained, is different from normal case. It is exactly calculated by the numerial method, but we see that it is proportional with n^{11}. In addition, we discuss some extending results like 'frozen Rydberg gas' and the new possibility contribution in the quantum information process that I think very interesting from the Rydberg states interact with each other or we can say two atoms hydrogen in excited stated interact with each other.

References

[1] J. Phys. B: At. Mol. Opt. Phys. 49 (2016) 152001

[2] Eur. Phys. J. D (2018) 72: 28

[3] Phys.Rev.A 95 (2017) 022704

[4] Physics Reports 341 (2001) 173-264

What Is a Single Photon and How to Detect It?

Xinliang(Bruce) Lyu
(Dated: June 14, 2019)

The notion of a photon was first proposed by Einstein in 1905, his year of miracles, in an attempt to explain the photoelectric effects. The subsequent experiment conducted by Compton demonstrated that the photon also carries momentum, which gave a strong evidence of the existence of a single photon. However, the satisfactory description incorporating both wave and particle nature of light didn't appear until the advent of quantum mechanics. In this paper, we will use the quantum mechanical description of light to explore the question: what is a single photon? We start by reviewing the quantization of a single mode of electromagnetic field and the photon state introduced in 8.05x. We will move on to extend our discussion to the quantization of a general electromagnetic field. One-photon multimode state is then introduced, which is the state analogous to an isolated corpuscle of light traveling in spacetime with speed of light. To answer the question that where the photon is, the principle of photodetectors is introduced. The detection probability of a photon at a given spacetime point is derived. We conclude with a phenomenon unique to a single photon: it can not be detected at different places at the same time!

I. INTRODUCTION

Before the 20th century, light was described successfully by Maxwell's equations and was thought to be electromagnetic waves. In 1905, Einstein treated light as photons to explain photoelectric effect successfully, while Maxwell's theory of light had difficult to explain such phenomenon. It was not clear why light sometimes behaves like waves but sometimes behaves like particles. The unified theory of light is the quantum version of Maxwell's theory, also known as quantum electrodynamics. The notion of a single photon is best understood under the framework of quantum electrodynamics.

The particle nature of light is usually demonstrated using light with extremely low intensity. In double slits experiments, in order to rule out the possibility that interaction among photons causes the interference pattern, light source with extremely low intensity has been used and it is said that photons appear on the screen one by one. Feynman explained the particle nature of light in his lecture [1], arguing that the light always comes as lump when we detect it. However, it should be emphasized that these arguments are inappropriate. Low intensity only indicates the average of photon number is much smaller than one, but not necessarily means there is only one photon in spacetime. In addition, the discrete clicks we hear in the detector can be well explained by the quantum nature of the detector alone, while the quantization of light is not indispensable.

This paper focuses on giving a unified description of a single photon. In section II, we start with the wave description of light, Maxwell's equations, and then construct its quantum version. In section III, we will see the notion of photons comes looking for us when we try to find the eigenstates of Hamiltonian of the electromagnetic field. Single-photon multimode state is introduced, which is the quantum state of light analogous to an isolated photon in spacetime. Finally, in section IV, the principle of photodetectors is introduced, and we calculate the detection probability of a single photon at a given spacetime point. A phenomenon unique to a single photon that makes it different from classical state of light is that the double detection probability at different places at the same time is zero.

II. QUANTIZATION OF THE ELECTROMAGNETIC FIELD

In chapter 9 of 8.05x, photon states are introduced, where we examined a single mode of the electromagnetic field in a rectangular cavity with frequency ω and wavenumber $k = \omega/c$, with c the speed of light in vacuum. We learned that the Hamiltonian of a single mode electromagnetic field resembles that of a one-dimensional harmonic oscillator with electric field acting like position variable and magnetic field acting like momentum variable (which is which is more of a convention). After promoting both dynamic variables to operators and imposing the canonical commutation relation, we construct the quantum theory of a single mode of the electromagnetic field. The classical electric and magnetic fields both become field operators.

We extend our discussion to an electromagnetic field with many modes. Since we have seen this topic in class using a specific example of the electromagnetic field in a rectangular cavity, we will make our discussion more general here. We will find that, due to the orthogonality between different modes, the extended version Hamiltonian is just the sum of different single mode Hamiltonians. Various vector identities used in this section can be found in Jackson's book [2] or be conveniently proved using index notation to write everything in its component form and applying the identity about Levi-Civita symbol $\epsilon_{ijk}\epsilon_{imn} = \delta_{jm}\delta_{kn} - \delta_{jn}\delta_{km}$. The discussion here follows Ballentine [3] and Aspect [4] closely.

The energy of the electromagnetic field is

$$E_{\text{EM}} = (8\pi)^{-1} \int d^3x \left(\mathbf{E}^2(\mathbf{x}, t) + \mathbf{B}^2(\mathbf{x}, t) \right). \qquad (1)$$

Notice Gaussian unit is used in this paper. We will see in the end of this section that Eq. (1) can be put into a nicer form that is convenient for us to postulate its quantum version. In vacuum, with no electric charge, $\mathbf{E}$ and $\mathbf{B}$ satisfies source-free Maxwell's equations

$$\nabla \cdot \mathbf{E} = 0, \tag{2}$$

$$\nabla \cdot \mathbf{B} = 0, \tag{3}$$

$$\nabla \times \mathbf{E} = -\frac{1}{c}\frac{\partial \mathbf{B}}{\partial t}, \tag{4}$$

$$\nabla \times \mathbf{B} = \frac{1}{c}\frac{\partial \mathbf{E}}{\partial t}, \tag{5}$$

which are called Gauss's law, no magnetic monopole, Faraday's law and Ampère's law respectively. We can eliminate $\mathbf{B}$ in Maxwell's equations to get one second order differential equation for $\mathbf{E}$: take the time derivative of Ampère's law Eq. (5), use Faraday's law Eq. (4) to eliminate $\mathbf{B}$, apply the vector identity $\nabla \times (\nabla \times \mathbf{a}) = \nabla(\nabla \cdot \mathbf{a}) - \nabla^2 \mathbf{a}$, and use Gauss's law Eq. (2) to have

$$\frac{1}{c}\frac{\partial^2 \mathbf{E}}{\partial t^2} = \nabla \times \left(\frac{\partial \mathbf{B}}{\partial t}\right) = -c\nabla \times (\nabla \times \mathbf{E}) = c\nabla^2 \mathbf{E}. \tag{6}$$

Apply our familiar separation of variable technique to write $\mathbf{E}(\mathbf{x}, t) = 2\sqrt{\pi}\omega q(t)\mathbf{u}(\mathbf{x})$, where the strange prefactor $2\sqrt{\pi}\omega$ is put there to make the final expression of energy looks nicer. Plug this ansatz into Eq. (6) and make some rearrangements

$$\nabla^2 \mathbf{u}(\mathbf{x}) = \left(\frac{1}{c^2}\frac{d^2 q(t)}{dt^2}\frac{1}{q(t)}\right)\mathbf{u}(\mathbf{x}). \tag{7}$$

It can be seen that $(d^2q/dt^2)(1/q)$ should be a constant, and we let it to be $-\omega^2$, or otherwise $\mathbf{u}(\mathbf{x})$ would have time dependence. Then Eq. (7) gives

$$\frac{d^2 q}{dt^2} = -\omega^2 q, \tag{8}$$

$$\nabla^2 \mathbf{u}(\mathbf{x}) = -\left(\frac{\omega}{c}\right)^2 \mathbf{u}(\mathbf{x}). \tag{9}$$

The spatial part Eq. (9) has a similar structure to the time-independent Schrödinger equation. After applying some boundary conditions, we will get a complete set of eigenfunctions $\mathbf{u}_m(\mathbf{x})$ and eigenvalues ω_m labeled by integer m. For each mode with eigenvalue ω_m, Eq. (8) can be solved for $q_m(t)$. $\mathbf{u}_m(\mathbf{x})$ is sometimes called mode function and can be chosen to satisfy the orthonormality condition

$$\int d^3x \mathbf{u}_{m'}(\mathbf{x}) \cdot \mathbf{u}_m(\mathbf{x}) = \delta_{m'm}. \tag{10}$$

A general solution is the linear combination of solutions with different m

$$\mathbf{E}(\mathbf{x}, t) = \sum_m 2\sqrt{\pi}\omega_m q_m(t)\mathbf{u}_m(\mathbf{x}), \tag{11}$$

and $\mathbf{B}$ can be obtained by plugging Eq. (11) into Faraday's law Eq. (4)

$$\mathbf{B}(\mathbf{x}, t) = \sum_m 2\sqrt{\pi}\frac{c}{\omega_m}p_m(t)\nabla \times \mathbf{u}_m(\mathbf{x}), \tag{12}$$

with $dp_m/dt = -\omega_m^2 q_m$. The curl of mode functions also has orthogonality property that the integral $\int d^3x(\nabla \times \mathbf{u}_{m'}(\mathbf{x})) \cdot (\nabla \times \mathbf{u}_m(\mathbf{x}))$ vanishes if $m' \neq m$. To show this, apply another vector identity $\nabla \cdot (\mathbf{a} \times \mathbf{b}) = \mathbf{b} \cdot (\nabla \times \mathbf{a}) - \mathbf{a} \cdot (\nabla \times \mathbf{b})$ with $\mathbf{a} = \mathbf{u}_{m'}(\mathbf{x})$ and $\mathbf{b} = \nabla \times \mathbf{u}_m(\mathbf{x})$

$$\begin{aligned}\nabla \cdot [\mathbf{u}_{m'}(\mathbf{x}) \times (\nabla \times \mathbf{u}_m(\mathbf{x}))] &= (\nabla \times \mathbf{u}_{m'}(\mathbf{x})) \cdot (\nabla \times \mathbf{u}_m(\mathbf{x})) \\ &- \mathbf{u}_{m'}(\mathbf{x}) \cdot (\nabla \times (\nabla \times \mathbf{u}_m(\mathbf{x}))). \end{aligned} \tag{13}$$

The second term in Eq. (13) can be simplified using the same trick in Eq. (6) as we eliminate $\mathbf{B}$ in Maxwell's equations

$$\begin{aligned}\mathbf{u}_{m'}(\mathbf{x}) \cdot (\nabla \times (\nabla \times \mathbf{u}_m(\mathbf{x}))) &= -\mathbf{u}_{m'}(\mathbf{x}) \cdot \nabla^2 \mathbf{u}_m(\mathbf{x}) \\ &= \left(\frac{\omega_m}{c}\right)^2 \mathbf{u}_{m'}(\mathbf{x}) \cdot \mathbf{u}_m(\mathbf{x}),\end{aligned} \tag{14}$$

where in the last step, we use the differential equation for $\mathbf{u}$ in Eq. (9). Integrate Eq. (13) over the space to have

$$\begin{aligned}&\int d^3x(\nabla \times \mathbf{u}_{m'}(\mathbf{x})) \cdot (\nabla \times \mathbf{u}_m(\mathbf{x})) \\ &= \left(\frac{\omega_m}{c}\right)^2 \delta_{m'm} + \int d^3x \nabla \cdot [\mathbf{u}_{m'}(\mathbf{x}) \times (\nabla \times \mathbf{u}_m(\mathbf{x}))] \\ &= \left(\frac{\omega_m}{c}\right)^2 \delta_{m'm}.\end{aligned} \tag{15}$$

The volume integral in second line of Eq. (15) can be shown to vanish by converting it to surface integral on the boundary and use the fact that $\mathbf{u}_{m'}(\mathbf{x})$ is perpendicular to the conducting surface. We are now ready to calcualte the energy of electromagnetic field. Let us plug $\mathbf{E}$ in Eq. (11) and $\mathbf{B}$ in Eq. (12) into the energy of electromagnetic field in Eq. (1)

$$\begin{aligned}E_{\mathrm{EM}} &= \frac{1}{2}\sum_{m',m}\int d^3x \big[\omega_{m'}\omega_m q_{m'}(t)q_m(t)\mathbf{u}_{m'}(\mathbf{x}) \cdot \mathbf{u}_m(\mathbf{x}) \\ &+ \frac{c}{\omega_{m'}}\frac{c}{\omega_m}p_{m'}(t)p_m(t)(\nabla \times \mathbf{u}_{m'}(\mathbf{x})) \cdot (\nabla \times \mathbf{u}_m(\mathbf{x}))\big] \\ &= \frac{1}{2}\sum_m \left[\omega_m^2 q_m^2(t) + p_m^2(t)\right],\end{aligned} \tag{16}$$

where we use the orthonormality condition for $\mathbf{u}_m$ in Eq. (10) and the orthogonality condition for $\nabla \times \mathbf{u}_m$ in Eq. (15) in the last step.

Equation (16) is our desired result. Compared with what we learned in 8.05x, where the energy of a single mode of the electromagnetic field is $E = 1/2\left(p^2(t) + \omega^2 q^2(t)\right)$, we notice the energy of multimode electromagnetic field is simply the sum of the energy of different modes. Let us go quantum! The procedure is similar to what we did in class. The only difference is that we have a summation symbol here. We postulate a Hamiltonian by promoting dynamic variables p_m and q_m to operators

$$\hat{H}_{\rm EM} = \frac{1}{2}\sum_m \left(\hat{p}_m^2 + \omega_m^2 \hat{q}_m^2\right), \tag{17}$$

where $\hat{p}_m$ and $\hat{q}_m$ are the promoted Schrödinger operators and they satisfy the canonical commutation relation $[\hat{q}_{m'}, \hat{p}_m] = i\hbar\delta_{m'm}$. The Hamiltonian is the same as a system of independent harmonic oscillators. As usual, we can define annihilation and creation operators associated with m-th mode, $\hat{a}_m$ and $\hat{a}_m^\dagger$, as

$$\hat{a}_m = \frac{1}{\sqrt{2\hbar\omega_m}}(\omega_m \hat{q}_m + i\hat{p}_m), \tag{18}$$

$$\hat{a}_m^\dagger = \frac{1}{\sqrt{2\hbar\omega_m}}(\omega_m \hat{q}_m - i\hat{p}_m). \tag{19}$$

It can be shown immediately that the commutation relation in terms of $\hat{a}_m$ and $\hat{a}_m^\dagger$ is

$$[\hat{a}_{m'}, \hat{a}_m^\dagger] = \delta_{m'm}, \tag{20}$$

and the Hamiltonian can be written using creation and annihilation operators

$$\begin{aligned}\hat{H}_{\rm EM} &= \sum_m \hbar\omega_m \left(\hat{a}_m^\dagger \hat{a}_m + \frac{1}{2}\right) \\ &= \sum_m \hbar\omega_m \left(\hat{N}_m + \frac{1}{2}\right),\end{aligned} \tag{21}$$

where the number operator is defined as usual, $\hat{N}_m = \hat{a}_m^\dagger \hat{a}_m$. The electric field $\mathbf{E}$ becomes a field operator after we promote p_m and q_m to operators

$$\begin{aligned}\hat{\mathbf{E}}(\mathbf{x}) &= \sum_m 2\sqrt{\pi}\omega_m \hat{q}_m \mathbf{u}_m(\mathbf{x}) \\ &= \sum_m \sqrt{2\pi\hbar\omega_m}(\hat{a}_m + \hat{a}_m^\dagger)\mathbf{u}_m(\mathbf{x}).\end{aligned} \tag{22}$$

It should be emphasized that the $\mathbf{x}$ in Eq. (22) is a label to indicate which operator we are talking about. It should not be confused as position operators $\hat{\mathbf{x}}$, which is a dynamic variable of a particle, or an observable.

III. NOTION OF A SINGLE PHOTON

Now we have the Hamiltonian of electromagnetic field in hand, it is time to find its spectrum. It is an easy task for us since the Hamiltonian is the same as a collection of independent harmonic oscillators. The ground state $|0\rangle$ is the state that is killed by all annihilation operators $\hat{a}_m$

$$\hat{a}_m |0\rangle = 0, \forall m. \tag{23}$$

The ground state is labeled by number 0 because it is eigenstate for all number operators $\hat{N}_m = \hat{a}_m^\dagger \hat{a}_m$ with eigenvalue 0, $\hat{N}_m |0\rangle = \hat{a}_m^\dagger \hat{a}_m |0\rangle = 0, \forall m$. If we define total number operator

$$\hat{N} = \sum_m \hat{N}_m, \tag{24}$$

then the state $|0\rangle$ is also its eignestate with eigenvalue 0. For this reason, the ground state is also known as vacuum, because it represents a world with nothing in it. A general energy eigenstate is built by acting creation operators repeatedly on vacuum and is labeled by various eigenvalues of $\hat{N}_m$

$$|n_1, n_2, ..., n_m, ...\rangle = (\hat{a}_1^\dagger)^{n_1}(\hat{a}_2^\dagger)^{n_2}...(\hat{a}_m^\dagger)^{n_m}... |0\rangle, \tag{25}$$

where the order of creation operators in right-hand side is not important since they all commute. The state in Eq. (25) is interpreted to have $n_1, n_2, ..., n_m, ...$ photons with frequency $\omega_1, \omega_2, ..., \omega_m, ...$ respectively.

A. One-photon Multimode State

Now it is natural to introduce the state that is analogous to an isolated corpuscle of light. What properties of the state do we expect if it represents a single photon propagating in spacetime at the speed of light? A single photon can have any frequency it likes but one thing we know for sure is that the total photon number should be one in such a state. Can we construct eigenstates of total number operator $\hat{N}$ with eigenvalue 1? The answer is yes and it is not hard. The state $\hat{a}_m^\dagger |0\rangle$ represents one photon with frequency ω_m, and it is an eigenstate of $\hat{N}$ with eigenvalue 1. The linear combination of such states with all possible m values will also be eigenstates of $\hat{N}$ with eigenvalue 1. Let us define

$$|1\rangle = \sum_m c_m \hat{a}_m^\dagger |0\rangle, \tag{26}$$

with c_m some coefficients. The state with the form given in Eq. (26) is called *one-photon multimode state*. We can check that

$$\hat{N}|1\rangle = \sum_m c_m \hat{N}\hat{a}_m^\dagger |0\rangle = \sum_m c_m \hat{a}_m^\dagger |0\rangle = |1\rangle. \tag{27}$$

To make the state well-normalized, the coefficients should satisfy $\sum_m |c_m|^2 = 1$. Since the number operator $\hat{N}_m$ commutes with the Hamiltonian $\hat{H}_{\rm EM}$, the total number operator $\hat{N}$ commutes with $\hat{H}_{\rm EM}$ too, and the total photon number is a conserved quantity. If the initial state of electromagnetic field is a one-photon multimode state of the form in Eq. (26) with some known coefficients, the time-evolved state $|1(t)\rangle$ will still be a one-photon multimode state. It looks we are on the right track.

B. Where is Our Photon?

Next, let us explore whether it is possible to recover the classical picture of a single photon flying in spacetime with speed of light. The first guess is that we can calculate the expectation value of the electric field operator. Consider a single photon that is localized at some region at a given time t, our hope is that the expectation value of the electric field operator in this region should be larger. However, this is not true, as will be shown below. In order to calculate the expectation value of the electric field operator at time t, we choose to use Heisenberg's picture here. The Heisenberg operator version of $\hat{\mathbf{E}}(\mathbf{x})$ in Eq. (22) can be obtained by replacing creation and annihilation operators on the right-hand side with their Heisenberg operator version

$$\begin{aligned}\hat{\mathbf{E}}(\mathbf{x},t) &= \sum_m 2\sqrt{\pi}\omega_m \hat{q}_m(t)\mathbf{u}_m(\mathbf{x}) \\ &= \sum_m \sqrt{2\pi\hbar\omega_m}\left(\hat{a}_m(t)+\hat{a}_m^\dagger(t)\right)\mathbf{u}_m(\mathbf{x}), \quad (28)\end{aligned}$$

where we add the time dependence to indicate Heisenberg operator. We have calculated $\hat{a}_m(t)$ and $\hat{a}_m^\dagger(t)$ several times in class. As a review, we repeat the calculation here. There is no explicit time dependence in $\hat{H}_{\mathrm{EM}}$ so the time evolution operator is $\hat{U}(t) = \exp(-it\hat{H}_{\mathrm{EM}}/\hbar)$. By definition, Heisenberg operator version of annihilation operator $\hat{a}_m$ is $\hat{a}_m(t) = \exp(it\hat{H}_{\mathrm{EM}}/\hbar)\hat{a}_m\exp(-it\hat{H}_{\mathrm{EM}}/\hbar) = \exp(i\omega_m t\hat{N}_m)\hat{a}_m\exp(-i\omega_m t\hat{N}_m)$. In the second step, we use the fact that all terms with subscript not equal to m in $\hat{H}_{\mathrm{EM}}$ commute through $\hat{a}_m$.We then take the time derivative to get a differential equation $\dot{\hat{a}}_m(t) = i\omega_m\exp(i\omega_m t\hat{N}_m)[\hat{N}_m,\hat{a}_m]\exp(-i\omega_m t\hat{N}_m) = -i\omega_m\hat{a}_m(t)$. The initial condition is $\hat{a}_m(t=0)=\hat{a}_m$ so we have $\hat{a}_m(t) = \exp(-i\omega_m t)\hat{a}_m$. Take the hermitian conjugate to get $\hat{a}_m^\dagger(t) = \exp(i\omega_m t)\hat{a}_m^\dagger$. Plug this results into Heisenberg operator $\hat{\mathbf{E}}(\mathbf{x},t)$ in Eq. (28),

$$\begin{aligned}\hat{\mathbf{E}}(\mathbf{x},t) &= \sum_m \sqrt{2\pi\hbar\omega_m}\left(\hat{a}_m e^{-i\omega_m t}+\hat{a}_m^\dagger e^{i\omega_m t}\right)\mathbf{u}_m(\mathbf{x}) \\ &= \hat{\mathbf{E}}^+(\mathbf{x},t)+\hat{\mathbf{E}}^-(\mathbf{x},t), \quad (29)\end{aligned}$$

where in the second step we break the electric field operator into positive and negative parts with the definitions

$$\hat{\mathbf{E}}^+(\mathbf{x},t) = \sum_m \sqrt{2\pi\hbar\omega_m}\hat{a}_m e^{-i\omega_m t}\mathbf{u}_m(\mathbf{x}), \quad (30)$$

$$\hat{\mathbf{E}}^-(\mathbf{x},t) = \sum_m \sqrt{2\pi\hbar\omega_m}\hat{a}_m^\dagger e^{i\omega_m t}\mathbf{u}_m(\mathbf{x}). \quad (31)$$

The reason for this decomposition will become clear in the next section where we discuss detection of photons. For now just remember there are two parts in the electric field operator, positive part containing all annihilation operators and negative part containing all creation operators. The expectation value of the electric field operator is

$$\begin{aligned}\langle 1|\hat{\mathbf{E}}(\mathbf{x},t)|1\rangle = \sum_{m,k,l}\sqrt{2\pi\hbar\omega_m}\big(c_l^* c_k\langle 0|\hat{a}_l\hat{a}_m\hat{a}_k^\dagger|0\rangle e^{-i\omega_m t} \\ + c_l^* c_k\langle 0|\hat{a}_l\hat{a}_m^\dagger\hat{a}_k^\dagger|0\rangle e^{i\omega_m t}\big)\mathbf{u}_m(\mathbf{x}) = 0. \quad (32)\end{aligned}$$

To see why it vanishes, let us look closely at the factor $\langle 0|\hat{a}_l\hat{a}_m\hat{a}_k^\dagger|0\rangle$. There is one creation operator but two annihilation operators, so by no means can we have $\hat{a}_l\hat{a}_m\hat{a}_k^\dagger|0\rangle \propto |0\rangle$, as a result $\langle 0|\hat{a}_l\hat{a}_m\hat{a}_k^\dagger|0\rangle = 0$. Same reason works for the other factor with two creation operators but only one annihilation operator. Nothing interesting happens if we only look at the expectation value of the electric field operator. They average to zero in one-photon multimode state $|1\rangle$.

However, what about the mean square of the electric field operator, $\langle 1|\hat{\mathbf{E}}(\mathbf{x},t)\cdot\hat{\mathbf{E}}(\mathbf{x},t)|1\rangle$? We know the mean square of the electric field is proportional to the intensity of light in classical electromagnetic theory so it is reasonable to expect this quantity peaks in the region where the single photon is localized. Let us calculate! The square of $\hat{\mathbf{E}}(\mathbf{x},t)$ is

$$\begin{aligned}\hat{\mathbf{E}}(\mathbf{x},t)\cdot\hat{\mathbf{E}}(\mathbf{x},t) = \hat{\mathbf{E}}^+(\mathbf{x},t)\cdot\hat{\mathbf{E}}^+(\mathbf{x},t)+\hat{\mathbf{E}}^-(\mathbf{x},t)\cdot\hat{\mathbf{E}}^-(\mathbf{x},t) \\ +\hat{\mathbf{E}}^-(\mathbf{x},t)\cdot\hat{\mathbf{E}}^+(\mathbf{x},t)+\hat{\mathbf{E}}^+(\mathbf{x},t)\cdot\hat{\mathbf{E}}^-(\mathbf{x},t). \quad (33)\end{aligned}$$

We calculate term by term. Moments of first two terms vanish: $\langle 1|\hat{\mathbf{E}}^+(\mathbf{x},t)\cdot\hat{\mathbf{E}}^+(\mathbf{x},t)|1\rangle = \langle 1|\hat{\mathbf{E}}^-(\mathbf{x},t)\cdot\hat{\mathbf{E}}^-(\mathbf{x},t)|1\rangle = 0$ because the number of creation operators is not equal to that of annihilation operators between the vacuum $\langle 0|\ldots|0\rangle$. For the third term in Eq. (33)

$$\begin{aligned}\hat{\mathbf{E}}^-(\mathbf{x},t)\cdot\hat{\mathbf{E}}^+(\mathbf{x},t) = \sum_{m,n}2\pi\hbar\sqrt{\omega_m\omega_n} \\ \times(\mathbf{u}_m\cdot\mathbf{u}_n)\hat{a}_m^\dagger\hat{a}_n e^{i(\omega_m-\omega_n)t}, \quad (34)\end{aligned}$$

while we have

$$\begin{aligned}\langle 1|\hat{a}_m^\dagger\hat{a}_n|1\rangle &= \sum_{k,l}c_k^* c_l\langle 0|\hat{a}_k\hat{a}_m^\dagger\hat{a}_n\hat{a}_l^\dagger|0\rangle \\ &= \sum_{k,l}c_k^* c_l\langle 0|[\hat{a}_k,\hat{a}_m^\dagger][\hat{a}_n,\hat{a}_l^\dagger]|0\rangle \\ &= \sum_{k,l}c_k^* c_l\delta_{km}\delta_{nl}\langle 0|0\rangle = c_m^* c_n. \quad (35)\end{aligned}$$

The moment of the third term in Eq. (33) is thus

$$\begin{aligned}\langle 1|\hat{\mathbf{E}}^-(\mathbf{x},t)\cdot\hat{\mathbf{E}}^+(\mathbf{x},t)|1\rangle = \sum_{m,n}2\pi\hbar\sqrt{\omega_m\omega_n} \\ \times(\mathbf{u}_m\cdot\mathbf{u}_n)c_m^* c_n e^{i(\omega_m-\omega_n)t}. \quad (36)\end{aligned}$$

The last term in Eq. (33) can be calculated in the same manner. We state the result here

$$\begin{aligned}\langle 1|\hat{\mathbf{E}}^+(\mathbf{x},t)\cdot\hat{\mathbf{E}}^-(\mathbf{x},t)|1\rangle = \sum_{m,n}2\pi\hbar\sqrt{\omega_m\omega_n} \\ \times(\mathbf{u}_m\cdot\mathbf{u}_n)c_n^* c_m e^{i(\omega_n-\omega_m)t}+\sum_m 2\pi\hbar\omega_m\mathbf{u}_m^2. \quad (37)\end{aligned}$$

Combine the results in Eq. (36) and Eq. (37) to get the mean square of the electric field operator

$$\begin{aligned}\langle 1|\hat{\mathbf{E}}(\mathbf{x},t)\cdot\hat{\mathbf{E}}(\mathbf{x},t)|1\rangle = \sum_m 2\pi\hbar\omega_m\mathbf{u}_m^2+\sum_{m,n}2\pi\hbar\sqrt{\omega_m\omega_n} \\ \times(\mathbf{u}_m\cdot\mathbf{u}_n)2\Re(c_m^* c_n e^{i(\omega_m-\omega_n)t}), \quad (38)\end{aligned}$$

where $\Re(z)$ means real part of a complex number z. The first term in Eq. (38) does not have c_m dependence or time dependence but only depends on the spectrum of the configuration. The second term can describe the disturbance propagating in spacetime. The peak of the distribution in space at time t is the region where the single photon is localized. We will give our statement here a physical picture in the next section, where we will find the moment of $\hat{\mathbf{E}}^-(\mathbf{x},t) \cdot \hat{\mathbf{E}}^+(\mathbf{x},t)$ in Eq. (36) will affect detection rate of a photodetector placed at position $\mathbf{x}$ at time t.

Still, we want to answer the question: where is the photon, more precisely. Is it possible to define a position operator $\hat{\mathbf{X}}$ similar to what we have in non-relativistic quantum mechanics for a single particle, so the eigenstate of this position operator $|\mathbf{x}\rangle$ represents a photon at position $\mathbf{x}$? Sidney Coleman argued in one of his quantum field theory lectures [5] that although such position operator can be well-defined, it will lead to unphysical results like traveling faster than the speed of light in vacuum. He argued further that the underlying physical reason is that once you try to localize a single particle to a small enough region, the uncertainty in its momentum will become so large that pair production will occur. As a result, we do not know whether we still have a single particle. The field operators are the right tool to use since they deal with this relativity causality automatically. In classical electrodynamics, the information of the existence of a charged particle in vacuum will travel at speed of light outwards in form of electromagnetic radiation. Outside the wavefront, the field is zero. In order to get an answer to the question: where is the photon, we should rephrase the question and ask "what is the probability to detect the photon at spacetime point $(\mathbf{x},t)$?", which is a more appropriate question in quantum mechanics. This leads us to our discussion on photon detection.

IV. DETECTION OF A SINGLE PHOTON

We claimed in previous section that the mean square of the electric field operator in Eq. (38) can be thought as intensity of the light, and the peak of this quantity in space is the region where the single photon localized. In this section, we will develop this idea and go deeper. First, let us think what the intensity of the light means when we have a single photon. Classically, when the intensity of light is larger, it means the light is brighter. When the brighter light hits on the retina in our eyes, more excited our optic nerve will be, which means the detection rate of our eye becomes larger. If we have a single photon, intensity of the light at spacetime point $(\mathbf{x},t)$ is naturally related to the probability of detecting the photon at position $\mathbf{x}$ and time t.

We have apparatus called photodetector to detect photons through its interaction with light. When light shines on such apparatus, the photons will kick a bounded electron in the atom out into its continuous spectrum. The signal of an outgoing electron is amplified, and then we can hear a click. We have encountered such process in 8.06x when we talked about ionization and light-atom interaction in chapter 5 and 6, where we focused on quantization of atom and treated the electric field as a classical object. The effect of electric field with amplitude E_0 enters the transition rate as a factor E_0^2. Similar results will be found here when we treat the electric field as a quantum mechanical object. The discussion in this section follows Ballentine [3], Aspect [4] and Cohen-Tannoudji [6] closely.

A. Principle of Photodetectors

The Hamiltonian of an atom-light system $\hat{H}$ has three pieces: atom contribution $\hat{H}_{\text{at}}$, electromagnetic field contribution $\hat{H}_{\text{EM}}$ and interaction of atom and field contribution $\delta\hat{H}$

$$\hat{H} = \hat{H}_{\text{at}} + \hat{H}_{\text{EM}} + \delta\hat{H} = \hat{H}_0 + \delta\hat{H}, \tag{39}$$

where we denote the sum of atom and electromagnetic field Hamiltonian as $\hat{H}_0$ to indicate we treat them as unperturbed Hamiltonian while we will treat the interaction Hamiltonian $\delta\hat{H}$ as perturbation and time dependent perturbation theory will be applied. $\hat{H}_{\text{EM}}$ has been solved in the previous section, and we assume the atom Hamiltonian has been solved too, so the eigenstate of $\hat{H}_0$ is tensor product of atom and electromagnetic field eigenstate. Let us put the detector at position $\mathbf{x}$, and consider the electric dipole interaction

$$\delta\hat{H} = -\hat{\mathbf{d}} \cdot \hat{\mathbf{E}}(\mathbf{x}), \tag{40}$$

where $\hat{\mathbf{d}}$ is the electric dipole operator of the atom, which is proportional to its position operator, and $\hat{\mathbf{E}}(\mathbf{x})$ is the electric field operator in Eq. (22). If there is no interaction term, atom and light live in different Hilbert space and mind their own business, nothing interesting happens. With the $\delta\hat{H}$ term, two systems talk to each other, and the ground state atom will be kicked to excited state accompanied by photon annihilation (We have seen this in 8.06x problem sets [7]). The calculation in this section will be more complicated than previous sections but the purpose is clear: *we want to calculate the probability we hear a click in our photodetector*. This corresponds to the transition probability where the atom stays in ground state $|g\rangle$ with the electromagnetic field in state $|\psi_i\rangle$ at time $t=0$, and after some time t the atom goes to excited state $|e\rangle$ while the electromagnetic field ends in state $|\psi_f\rangle$. The initial and final state of the system is

$$|i\rangle = |g\rangle \otimes |\psi_i\rangle\,, \tag{41}$$
$$|f\rangle = |e\rangle \otimes |\psi_f\rangle\,. \tag{42}$$

Go to the interaction picture where $\delta\hat{H}(t) = \exp(i\hat{H}_0 t/\hbar)\delta\hat{H}\exp(-i\hat{H}_0 t/\hbar)$. The time evolution operator will factorize into atom and field two parts, each acting on its corresponding operator in $\delta \hat{H}$

$$\delta \hat{H}(t) = -e^{i\hat{H}_{\text{at}}t/\hbar}\hat{\mathbf{d}}e^{-i\hat{H}_{\text{at}}t/\hbar} \cdot \hat{\mathbf{E}}(\mathbf{x}, t), \tag{43}$$

with $\hat{\mathbf{E}}(\mathbf{x}, t)$ the Heisenberg operator version of electromagnetic field operator in Eq. (29). According to first order time dependent perturbation theory [8], the transition amplitude of the event $|i\rangle \to |f\rangle$ at time t is

$$\begin{aligned}\frac{1}{i\hbar}\int_0^t dt' \langle f|\, \delta\hat{H}(t')\, |i\rangle &= -\frac{1}{i\hbar}\int_0^t dt' \langle \psi_f|\, \hat{\mathbf{E}}(\mathbf{x}, t')\, |\psi_i\rangle \\ &\cdot \langle e|\, e^{i\hat{H}_{\text{at}}t'/\hbar}\hat{\mathbf{d}}e^{-i\hat{H}_{\text{at}}t'/\hbar}\, |g\rangle \\ &= -\frac{1}{i\hbar}\int_0^t dt' e^{i\omega_{eg}t'} \langle e|\, \hat{\mathbf{d}}\, |g\rangle \cdot \langle \psi_f|\, \hat{\mathbf{E}}(\mathbf{x}, t')\, |\psi_i\rangle\,, \end{aligned} \tag{44}$$

with $\omega_{eg} = (E_e - E_g)/\hbar$, where E_e, E_g are energy of state $|e\rangle\,, |g\rangle$ respectively. Recall $\hat{\mathbf{E}}(\mathbf{x}, t')$ can be break into positive and negative parts defined in Eq. (30) and Eq. (31), one with its terms proportional to $\hat{a}_m \exp(-i\omega_m t')$, the other $\hat{a}_m^\dagger \exp(i\omega_m t')$. Since ω_m and ω_{eg} are both positive, only terms proportional to $\exp(i(\omega_{eg} - \omega_m)t')$ with $\omega_{eg} - \omega_m \approx 0$ will contribute much to the integral(remember the stationary phase argument), while terms associated with negative parts are all proportional to $\exp(i(\omega_{eg} + \omega_m)t')$, oscillating fast in the integral. As a result, it is reasonable to keep only the positive part of the electric field operator when calculating the transition amplitude, so we have

$$\begin{aligned}&\frac{1}{i\hbar}\int_0^t dt' \langle f|\, \delta\hat{H}(t')\, |i\rangle \\ &= -\frac{1}{i\hbar}\int_0^t dt' e^{i\omega_{eg}t'} \langle e|\, \hat{\mathbf{d}}\, |g\rangle \cdot \langle \psi_f|\, \hat{\mathbf{E}}^+(\mathbf{x}, t')\, |\psi_i\rangle\,. \end{aligned} \tag{45}$$

The modulus squared of the transition amplitude in Eq. (45) is the transition probability at time t

$$\begin{aligned}P_{e,f\leftarrow g,i}(t) &= \left(\frac{1}{\hbar}\right)^2 \sum_{\mu,\nu}\int_0^t dt' \int_0^t dt'' e^{i\omega_{eg}(t'-t'')} \\ &\times \langle g|\, \hat{d}_\nu\, |e\rangle \langle e|\, \hat{d}_\mu\, |g\rangle \langle \psi_i|\, \hat{E}_\nu^-(\mathbf{x}, t'')\, |\psi_f\rangle \langle \psi_f|\, \hat{E}_\mu^+(\mathbf{x}, t')\, |\psi_i\rangle\,, \end{aligned} \tag{46}$$

where we express the inner product of two vectors in its component form. For detectors that do not distinguish final state, we can sum over both atom excited state e and field final state f

$$\begin{aligned}P_{g,i}(t) &= \sum_{e,f} P_{e,f\leftarrow g,i}(t) \\ &= \left(\frac{1}{\hbar}\right)^2 \sum_{\mu,\nu,e}\int_0^t dt' \int_0^t dt'' e^{i\omega_{eg}(t'-t'')} \\ &\times \langle g|\, \hat{d}_\nu\, |e\rangle \langle e|\, \hat{d}_\mu\, |g\rangle \langle \psi_i|\, \hat{E}_\nu^-(\mathbf{x}, t'')\hat{E}_\mu^+(\mathbf{x}, t')\, |\psi_i\rangle\,, \end{aligned} \tag{47}$$

where we use the complete relation: $\sum_f |\psi_f\rangle \langle \psi_f| = \mathbb{1}$. One more approximation is to replace sum over e with integral, $\sum_e = \int d\omega_e n(\omega_e)$, where $n(\omega_e)$ is the usual density of state. To make the expression less messy, let us make a few more definitions. Group everything associated with electric field operators as

$$G_{\nu\mu}(\mathbf{x}, t''; \mathbf{x}, t') = \langle \psi_i|\, \hat{E}_\nu^-(\mathbf{x}, t'')\hat{E}_\mu^+(\mathbf{x}, t')\, |\psi_i\rangle\,, \tag{48}$$

which is called correlation function. Group everything about the atom along with the overall constant as

$$\begin{aligned}s_{\nu\mu}(t' - t'') &= \hbar^{-2}\int d\omega_e n(\omega_e) \langle g|\, \hat{d}_\nu\, |e\rangle \langle e|\, \hat{d}_\mu\, |g\rangle\, e^{i\omega_{eg}(t'-t'')} \\ &= \int d\omega_e s_{\nu\mu}(\omega_e) e^{i\omega_{eg}(t'-t'')}, \end{aligned} \tag{49}$$

where $s_{\nu\mu}(\omega_e) = \hbar^{-2}n(\omega_e) \langle g|\, \hat{d}_\nu\, |e\rangle \langle e|\, \hat{d}_\mu\, |g\rangle$ is called the frequency response function and $s_{\nu\mu}(t' - t'')$ sensitivity function. The transition probability in Eq. (47) can be expressed as

$$\begin{aligned}P_{g,i}(t) &= \sum_{\mu,\nu}\int_0^t dt' \int d\omega_e s_{\nu\mu}(\omega_e) \\ &\times \int_0^t dt'' e^{i\omega_{eg}(t'-t'')} G_{\nu\mu}(\mathbf{x}, t''; \mathbf{x}, t'). \end{aligned} \tag{50}$$

The integral in second line of Eq. (50) becomes negligible if $\omega_{eg} = \omega_e - \omega_g \gg 1$ since the integrand oscillates too fast, so $s_{\nu\mu}(\omega_e)$ only contributes in some narrow band. Let $s_{\nu\mu}(\omega_e) = s_{\nu\mu}$ in this narrow band and pull it out from the integral. Notice $\int d\omega_e e^{i\omega_{eg}(t'-t'')} = \delta(t' - t'')$ (We can extend the lower limit to minus infinity because its contribution in the original integral is negligible.), so the final result is

$$P_{g,i}(t) = \sum_{\mu,\nu}\int_0^t dt' s_{\nu\mu} G_{\nu\mu}(\mathbf{x}, t'; \mathbf{x}, t'). \tag{51}$$

The detection rate is

$$\begin{aligned}R(t) = \frac{dP_{g,i}(t)}{dt} &= \sum_{\mu,\nu} s_{\nu\mu} G_{\nu\mu}(\mathbf{x}, t; \mathbf{x}, t) \\ &= \sum_{\mu,\nu} s_{\nu\mu} \langle \psi_i|\, \hat{E}_\nu^-(\mathbf{x}, t)\hat{E}_\mu^+(\mathbf{x}, t)\, |\psi_i\rangle\,. \end{aligned} \tag{52}$$

Notice further that $s_{\nu\mu}$ involves the moment of atom position operators because $\hat{d}_\nu \hat{d}_\mu \propto \hat{x}_\nu \hat{x}_\mu$, so for isotropic detectors, we may have $s_{\nu\mu} = s\delta_{\nu\mu}$ for some constant number s. For such detectors, the detection rate is

$$R(t) = s \langle \psi_i|\, \hat{\mathbf{E}}^-(\mathbf{x}, t) \cdot \hat{\mathbf{E}}^+(\mathbf{x}, t)\, |\psi_i\rangle\,. \tag{53}$$

As promised before, the effect of electric field enters the detection rate of photoelectric detector as $\langle \psi_i|\, \hat{\mathbf{E}}^-(\mathbf{x}, t) \cdot \hat{\mathbf{E}}^+(\mathbf{x}, t)\, |\psi_i\rangle$.

B. No Double Detection

What is the detection rate for a detector placed at position $\mathbf{x}$ at time t if we have initial field state as one-photon multimode state $|\psi_i\rangle = |1\rangle$? We actually have calculated the moment $\langle 1|\, \hat{\mathbf{E}}^{-}(\mathbf{x},t)\cdot\hat{\mathbf{E}}^{+}(\mathbf{x},t)\,|1\rangle$ in Eq. (36), copy the result and plug it in Eq. (53)

$$R(\mathbf{x},t) = s\sum_{m,n} 2\pi\hbar\sqrt{\omega_m\omega_n}(\mathbf{u}_m\cdot\mathbf{u}_n)c_m^* c_n e^{i(\omega_m-\omega_n)t}. \tag{54}$$

In the single-photon multimode state, $R(\mathbf{x},t)$ can be interpreted as the probability of finding the photon at position $\mathbf{x}$ at time t and it is analogous to the modulus squared of the wavefunction of a particle we learned in quantum mechanics. However, nothing in principle can distinguish $|1\rangle$ from a classical field with the electric field amplitude specified by right choice of $c_m, \mathbf{u}_m$ and ω_m so that the detection rate is identical to what we have in Eq. (54).

What if we put two detectors at two different places and try to detect light at different positions $\mathbf{x}_1, \mathbf{x}_2$ at the same time? Classical, the probability of hearing two clicks at the same time is the product of rate $R(\mathbf{x}_1,t)R(\mathbf{x}_2,t)$. However, if we are in state $|1\rangle$, the probability to detect the photon at different places at the same time should be 0. We just have *one* photon in spacetime! Let us now demonstrate this. There are two detectors, so the interaction Hamiltonian in Eq. (39) should be

$$\delta\hat{H}_2 = -\hat{\mathbf{d}}_1\cdot\hat{\mathbf{E}}(\mathbf{x}_1) - \hat{\mathbf{d}}_2\cdot\hat{\mathbf{E}}(\mathbf{x}_2). \tag{55}$$

In the interaction picture

$$\begin{aligned}\delta\hat{H}_2(t) = &-e^{i\hat{H}_{\mathrm{at1}}t/\hbar}\hat{\mathbf{d}}_1 e^{-i\hat{H}_{\mathrm{at1}}t/\hbar}\cdot\hat{\mathbf{E}}(\mathbf{x}_1,t)\\ &- e^{i\hat{H}_{\mathrm{at2}}t/\hbar}\hat{\mathbf{d}}_2 e^{-i\hat{H}_{\mathrm{at2}}t/\hbar}\cdot\hat{\mathbf{E}}(\mathbf{x}_2,t),\end{aligned} \tag{56}$$

where $\hat{H}_{\mathrm{at1}}, \hat{H}_{\mathrm{at2}}$ are Hamiltonian of atom at position $\mathbf{x}_1, \mathbf{x}_2$ respectively. The initial and final state is

$$|i\rangle = |g_1\rangle\otimes|g_2\rangle\otimes|\psi_i\rangle\,, \tag{57}$$

$$|f\rangle = |e_1\rangle\otimes|e_2\rangle\otimes|\psi_f\rangle\,. \tag{58}$$

Since $\langle f|\,\delta\hat{H}_2(t)\,|i\rangle = 0$, first order correction vanishes. We must calculate the second order correction. It will not be surprising to you that the second order correction result for the transition rate is

$$\begin{aligned}&R(\mathbf{x}_1,t;\mathbf{x}_2,t) = s^2\\ &\times\sum_{l,m}\langle\psi_i|\,\hat{E}_l^-(\mathbf{x}_1,t)\hat{E}_m^-(\mathbf{x}_2,t)\hat{E}_m^+(\mathbf{x}_2,t)\hat{E}_l^+(\mathbf{x}_1,t)\,|\psi_i\rangle\,.\end{aligned} \tag{59}$$

The detailed derivation can be found in Cohen-Tannoudji's book [6]. Let $|\psi_i\rangle = |1\rangle$, the detection rate of a single photon at two different places at the same time indeed vanishes

$$\begin{aligned}&R(\mathbf{x}_1,t;\mathbf{x}_2,t) = s^2\\ &\times\sum_{l,m}\langle 1|\,\hat{E}_l^-(\mathbf{x}_1,t)\hat{E}_m^-(\mathbf{x}_2,t)\hat{E}_m^+(\mathbf{x}_2,t)\hat{E}_l^+(\mathbf{x}_1,t)\,|1\rangle\,.\\ &= 0,\end{aligned} \tag{60}$$

since $|1\rangle$ can not survive two consecutive annihilation operators. This unique property of single-photon multimode state was shown experimentally in 1986 by Grangier, Roger and Aspect [9].

ACKNOWLEDGMENTS

The author is grateful to Professor Jim Freericks and Mark Weitzman for providing this interesting topic and offering suggestions about several nice references. The author also wishes to thank Professor Barton Zwiebach, Professor Jolyon Bloomfield and edX for offering excellent 8.04x - 8.06x series courses on quantum mechanics for which the paper was prepared.

[1] "QED: Photons, Corpuscles of Light." `https://youtu.be/eLQ2atfqk2c`. See the clip from 36:32 to 39:40, where Richard Feynman describes why light is particles.

[2] J. D. Jackson, *Classical Electrodynamics*. Wiley, 1998.

[3] L. E. Ballentine, *Quantum Mechanics: a Modern Development*. World Scientific Publishing Company, 1998.

[4] G. Grynberg, A. Aspect, C. Fabre, and C. Cohen-Tannoudji, *Introduction to Quantum Optics: From the Semi-classical Approach to Quantized Light*. Cambridge University Press, 2010.

[5] B. G. ge Chen, D. Derbes, D. Griffiths, B. Hill, R. Sohn, and Y.-S. Ting, *Lectures of Sidney Coleman on Quantum Field Theory*. World Scientific, 2018.

[6] C. Cohen-Tannoudji, J. Dupont-Roc, and G. Grynberg, *Atom-Photon Interactions: Basic Processes and Applications*. Wiley, 1998.

[7] "MITx: 8.06x, Applications of Quantum Mechanics.". See solutions for part b of problem 6-2 in edX.

[8] B. Zwiebach, "Lecture notes for 8.06x: Chatper 5." see Eq. (5.2.12), Eq. (5.2.16) and Eq. (5.2.17).

[9] P. Grangier, G. Roger, and A. Aspect, "Experimental evidence for a photon anticorrelation effect on a beam splitter: a new light on single-photon interferences," *EPL (Europhysics Letters)* **1** (1986) no. 4, 173.

Wiener integral and Feynman-Kac formula

Abstract

The Wiener integral is the integral with respect to the Wiener measure on the classical Wiener space of parameterized continuous paths and it is related to the Brownian motion. It is mathematically well-defined. I will define the conditional Wiener measure, then I will state and prove the Feynman-Kac formula. The last step permits to illustrate a relation between the Feynman path integral and the Wiener functional integral. The results will be used to study a special case of a particle in a box.

Introduction

Starting with the double slit experiment, we observe an interference between the two possible paths of electrons from a source to a target screen. The idea of path integral formulation of Quantum Mechanics is to multiply the idea of double slit experiment by adding more screens and drill extra holes to generalize the double slit experiment by the superposition principle. This procedure is explained in Feynman's classical book. This leads to studying the propagator $\boldsymbol{K}(\vec{q}\,',t;\vec{q},0)$, that is, the integral kernel of the time evolution operator $U(t)=e^{-\frac{i}{\hbar}Ht}$.

Wiener integral is obtained by replacing the physical time t with the Euclidean time $-it$ which leads to the integral kernel of the $e^{-\frac{1}{\hbar}Ht},t>0$ semigroup (the imaginary-time semigroup of operators). If one could use path integrals to understand $e^{-\frac{1}{\hbar}Ht}$, then one is able to go back to the real time by analytic continuation over *t*.

Wiener measure and Wiener integral

Constructively, the probability space to define the Wiener measure is $\boldsymbol{C}=C^0([0,\infty),\mathbb{R}^n,0)$, the space of continuous paths in $\mathbb{R}^n$ starting at the origin, parameterized by $t\in[0,\infty)$.

It is convenient to to work in a compact topological space. This is so because of tacitly accepting, e.g., Riesz-Markov theorem and taking for granted the uniqueness of measures' extensions; thus, I'll consider $\hat{\mathbb{R}^n}=\mathbb{R}^n\cup\{\infty\}\simeq S^n$ instead of $\mathbb{R}^n$. Define

$$\Omega=\prod_{t=0}^{\infty}(\hat{\mathbb{R}^n})_t$$

This space is compact with the product topology.

Consider all partitions $\vec{t_m}=\{0\le t_1\le t_2\le\ldots\le t_m\}$ and all continuous functions $F:\prod_{i=1}^{m}(\mathbb{R}^n)_i\to\mathbb{R}$, and define $\phi:\Omega\to\mathbb{R}$ by

$$\phi(\gamma)=F(\gamma(t_1),\ldots,\gamma(t_m))\forall\gamma\in\Omega\ .$$

Let $\boldsymbol{C_{fin}}(\Omega)$ the subspace of $\boldsymbol{C}(\Omega)=C^0(\Omega,\mathbb{R})$ spanned by all such functions ϕ, defined by all partitions $\vec{t_m}$ and continuous functions F. On $\boldsymbol{C_{fin}}(\Omega)$ define the following linear functional

$$l(\phi)=\int_{\mathbb{R}^n}\dots\int_{\mathbb{R}^n} F(\vec{q}_1,\dots,\vec{q}_m)P(\vec{q}_m,\vec{q}_{m-1};t_m-t_{m-1})\dots P(\vec{q}_1,\vec{0}_{\mathbb{R}^n};t_1)\,d^n\vec{q}_1\dots d^n\vec{q}_m$$,

where

$$P(\vec{q}\,',\vec{q};t)=(4\pi Dt)^{-\frac{n}{2}}e^{-\frac{(\vec{q}\,'-\vec{q})^2}{4\mathrm{Dt}}}$$ with diffusion coefficient $D>0$.

The semigroup property (Chapman–Kolmogorov equation) implies that the functional *l* is well-defined; also $l(\phi)\geq 0\;\forall\phi\geq 0$, $l(1)=1$ (those *1:s* are constant functions) and *l* is bounded:

$$|l(\phi)|\leq\|\phi\|_\infty=\sup_{\gamma\in\Omega}|\phi(\gamma)|$$.

The space $\boldsymbol{C}_{\boldsymbol{fin}}(\Omega)$ separates points in Ω , $1\in\boldsymbol{C}_{\boldsymbol{fin}}(\Omega)$, so by Stone's theorem $\overline{\boldsymbol{C}_{\boldsymbol{fin}}(\Omega)}=\boldsymbol{C}(\Omega)$. The functional *l* has a unique extension to a continuous positive linear functional on $\boldsymbol{C}_{\boldsymbol{fin}}(\Omega)$ with norm *1*, and by the Riesz-Markoff theorem, there exists a <u>unique</u> regular Borel measure μ_W on Ω with $\mu_W(\Omega)=1$ such that

$$l(\phi)=\int_\Omega \phi\, d\mu_W$$

(is here where the compactification helps quite a bit).
μ_W is the Wiener measure and the integral is Wiener integral.

The support of the Wiener measure is the set of continuous paths, $\mu_W(\boldsymbol{C})=1.$

The Wiener integral can be constructed purely formal: by Kolmogorov extension theorem and semigroup property, one needs to specify a family $\{\nu_{t_1,\dots,t_m}\}$ of probability measures satisfying the said conditions. Fix $\vec{x}\in\mathbb{R}^n$ and define $P(\vec{x},\vec{y};t)=(4\pi Dt)^{-\frac{n}{2}}e^{-\frac{(\vec{x}-\vec{y})^2}{4\mathrm{Dt}}}$ for $\vec{y}\in\mathbb{R}^n, t>0$.
For $\vec{t}_m=\{0\leq t_1\leq t_2\leq\dots\leq t_m\}$ define

$$\nu_{t_1,\dots,t_m}(F_1 x\dots x F_m)=\int_{F_1}\dots\int_{F_m} P(\vec{x}_m,\vec{x}_{m-1};t_m-t_{m-1})\dots P(\vec{x}_1,\vec{0}_{\mathbb{R}^n};t_1)\,d^n\vec{x}_1\dots d^n\vec{x}_m$$

where $F_1,\dots,F_m$ are Borel sets in $\mathbb{R}^n$. Extend this definition to all finite sequences of $t_i's$ by Kolmogorov extension theorem, i.e., there exists a probability space $(\Omega,\boldsymbol{F},P^x)$ and a stochastic process (the Brownian motion) $\{B_t\}_{t\geq 0}$ such that

$$P^x(B_{t_1}\in F_1,\dots,B_{t_m}\in F_m)=\int_{F_1}\dots\int_{F_m} P(\vec{x}_m,\vec{x}_{m-1};t_m-t_{m-1})\dots P(\vec{x}_1,\vec{0}_{\mathbb{R}^n};t_1)\,d^n\vec{x}_1\dots d^n\vec{x}_m$$.

(Kolmogorov extension theorem guarantees this relation between stochastic processes of continuous time and well-suited collections of finite dimensional probability measures).

NB: The probability space $(\Omega,\boldsymbol{F},P^x)$ and a stochastic process $\{B_t\}_{t\geq 0}$ are not uniquely determined.

The construction extends to the $\sigma-\mathrm{algebra}$ generated by the cylindrical subsets of Ω :
In the case $n=1$ (for illustration), define, for every partition $\vec{t}_m=\{0\leq t_1\leq t_2\leq\dots\leq t_m\}$, intervals $(a_1,b_1),\dots,(a_m,b_m)$ and cylindrical set $\boldsymbol{C_t}=\{\gamma\in\Omega: a_1<\gamma(t_1)<b_1,\dots,a_m<\gamma(t_m)<b_m\}$, the measure

$$\mu(\boldsymbol{C_T})=\int_{a_1}^{b_1}\ldots\int_{a_m}^{b_m}P(q_m,q_{m-1};t_m-t_{m-1})\ldots P(q_{1,}0;t_1)\,dq_1\ldots dq_m$$
.

However, the set ***C*** of continuous paths starting at a fixed point turns out to be non-measurable in Ω , i.e.,

$$\mu_*(\boldsymbol{C})=0,\mu^*(\boldsymbol{C})=1$$,

the inner and outer measures of a set $E\subset\Omega$:

$$\mu_*(E)=\sup\{\mu(A),A\subset E\}$$
$$\mu^*(E)=\inf\{\mu(A),E\subset A\}$$,

$E\subset\Omega$ being measurable wrt $\mu\Leftrightarrow\mu_*(E)=\mu^*(E)$. The argumentation is outside of this limited scope, but one should think on the situation $\mathbb{Q}\subset\mathbb{R}$ with the rationals dense but of zero measure in reals. The situation can be fixed by starting with continuous paths, obtain the measure and extend it to the entire space, to obtain the same Wiener measure μ_W .
One could define the Wiener measure starting with cylindrical sets which is more intuitive.

The following result is useful for representing the integral kernel of the one-parameter semigroup $e^{-\frac{1}{\hbar}Ht},t>0$ by a Wiener integral.

Proposition 1: Let the real-valued function $V\in C(\mathbb{R}^n)$ be bounded below. Then for every $t\geq 0$ the function $F:C\rightarrow\mathbb{R},\boldsymbol{C}=C^0([0,\infty),\mathbb{R}^n,0)$ defined by

$$F_t(\gamma)=e^{-\int_0^t V(\gamma(\tau))}d\tau$$,

is integrable wrt the Wiener measure and

$$\int_{\boldsymbol{C}}F_t\,d\mu_W=\lim_{N\rightarrow\infty}\int_{\mathbb{R}^n}\ldots\int_{\mathbb{R}^n}\exp\Big(-\sum_{k=1}^{N}V(\vec{q}_k)\Delta t\Big)P(\vec{q}_N,\vec{q}_{N-1};\Delta t)\ldots P(\vec{q}_{1,}\vec{0};\Delta t)\,d^n\vec{q}_1\ldots d^n\vec{q}_N,\Delta t=\frac{t}{N}.$$

Proof:

For $\gamma\in\boldsymbol{C}$, $\int_0^t V(\gamma(\tau))\,d\tau=\lim_{N\rightarrow\infty}\sum_{k=1}^{N}V(\gamma(t_k))\Delta t$ where $t_k=k\Delta t$. By definition every function $\sum_{k=1}^{N}V(\gamma(t_k))\Delta t$ is Wiener-integrable on ***C***. Thus, F_t is measurable as a limit of a sequence of measurable function, point-wise. F_t being bounded is Wiener-integrable on ***C***, so by dominated convergence theorem $\int_{\boldsymbol{C}}F_t\,d\mu_W=\lim_{N\rightarrow\infty}\int_{\boldsymbol{C}}\exp\Big(-\sum_{k=1}^{N}V(\gamma(t_k))\Delta t\Big)d\mu_W(\gamma)$, which is the desired result via the definition of Wiener measure.
QED

Conditional Wiener measure

Define $\Omega_{\vec{q},\vec{q}\,'}=\{\gamma\in\prod_{t\le\tau\le t'}(\widehat{\mathbb{R}^n})_\tau:\gamma(t)=\vec{q},\gamma(t')=\vec{q}\,'\}$, the set of all parameterized paths in $(\widehat{\mathbb{R}^n})$ starting in $\vec{q}\in\mathbb{R}^n$ at *t* and ending at $\vec{q}\,'\in\mathbb{R}^n$ at *t'*. The corresponding subspace of continuous paths and the Wiener measure are denoted accordingly, $\boldsymbol{C}_{\vec{q},\vec{q}\,'}$ and $\mu_{\vec{q},\vec{q}\,'}$.

On $\boldsymbol{C_{fin}}(\Omega_{\vec{q},\vec{q}\,'})$ define the following linear functional

$l_{\vec{q},\vec{q}\,'}(\phi)=\int_{\mathbb{R}^n}\dots\int_{\mathbb{R}^n}F(\vec{q}_1,\dots,\vec{q}_m)P(\vec{q}\,',\vec{q}_m;t'-t_m)\dots P(\vec{q}_1,\vec{q};t_1-t)d^n\vec{q}_1\dots d^n\vec{q}_m$, where $\phi\in\boldsymbol{C_{fin}}(\Omega)$,

$t\le t_1\le t_2\le\dots\le t_m\le t'$ and $\phi(\gamma)=F(\gamma(t_1),\dots,\gamma(t_m))\forall\,\gamma\in\Omega$.

Then $l_{\vec{q},\vec{q}\,'}(\phi)=\int_{\Omega_{\vec{q},\vec{q}\,'}}\phi\,d\mu_{\vec{q},\vec{q}\,'}$.

The support of the conditional Wiener measure is the set of continuous paths, $\mu_{\vec{q},\vec{q}\,'}(\boldsymbol{C}_{\vec{q},\vec{q}\,'})=1$ and $\mu_{\vec{q},\vec{q}\,'}(\boldsymbol{C}_{\vec{q},\vec{q}\,'})=P(\vec{q},\vec{q}\,';t'-t)$

Feynman-Kac formula

The Schrödinger operator on $L^2(\mathbb{R}^n,d^n\vec{q})$ with continuous, real-valued, bounded from below potential $V(\vec{q})$ is

$$H=H_0+V=\frac{\hat{p}^2}{2\mathrm{m}}+V(\hat{q})$$

Then $L_\hbar(\vec{q}\,',t';\vec{q},t)=\int_{C_{\vec{q},\vec{q}'}}\exp(-\frac{1}{\hbar}\int_t^{t'}V(\gamma(\tau))d\tau)d\mu_{\vec{q},\vec{q}\,'}(\gamma)$. $L_\hbar(\vec{q}\,',t';\vec{q},t)$ is the integral kernel of the $T=e^{-\frac{t'-t}{\hbar}H}$, i.e., $T\psi(\vec{q}\,',t')=\int_{\mathbb{R}^n}L_\hbar(\vec{q}\,',t';\vec{q},t)\psi(\vec{q},t)d\vec{q}$ (in $L^2(\mathbb{R}^n,d^n\vec{q})$).

Proof: Using Lie-Kato-Trotter for the opreator $e^{\frac{-1}{\hbar}TH}$.

F-K formula can be introduced purely formal, as a generalization of Kolmogorov's backward equation, see reference 4.

Note: The intuitive point of F-K formula is that the Wiener measure can deal with the H_0 term, while F-K formula deals with the *V* term.

Relating Wiener and Feynman integrals

The operator $T=e^{-\frac{1}{\hbar}Ht},t>0$ is obtained from $U(t)=e^{-\frac{i}{\hbar}Ht}$ by analytic continuation $t\to-it$.
Heuristically, the conditional Wiener measure could be stated as

$$\boldsymbol{D}\boldsymbol{q}_W = e^{-\frac{m}{2\hbar}\int_t^{t'} \dot{\boldsymbol{q}}(\tau)^2 d\tau}\boldsymbol{D}_\hbar \boldsymbol{q}, \boldsymbol{D}_\hbar \boldsymbol{q} = \lim_{N\to\infty}\left(\frac{m}{2\pi\hbar\Delta t}\right)^{\frac{N}{2}}\prod_{k=1}^{N-1} d^n \boldsymbol{q}_k, \Delta t = \frac{t}{N}.$$

This $\boldsymbol{D}_\hbar \boldsymbol{q}$ cannot represent a measure (but the Wiener measure to fulfill this heuristic) since, at least, the infinite product is divergent, while the trajectories $\gamma = \boldsymbol{q}(\tau)$ aren't differentiable, the $\int_t^{t'} \dot{\boldsymbol{q}}(\tau)^2 d\tau$ is divergent. However, the negative sign at the exponential damps the divergences, so the analogy with the Wiener measure holds good. Going $\hbar \to i\hbar$ the exponential doesn't have any damping effect in $\boldsymbol{D}_{i\hbar}\boldsymbol{q}$ (has modulus *1* for differentiable trajectories, no meaning for non- differentiable ones). In the Feynman path integral case, the propagator of a quantum particle can be represented as

$$K_\hbar = \int_{\boldsymbol{q}(t)}^{\boldsymbol{q}(t')} e^{\frac{i}{\hbar}S(\gamma)}\boldsymbol{D}_{i\hbar}\boldsymbol{q}, S(\gamma) = \int_t^{t'} L(\boldsymbol{q}, \dot{\boldsymbol{q}})d\tau, \gamma = \boldsymbol{q}(t) \text{ and } L(\boldsymbol{q}, \dot{\boldsymbol{q}}) = \frac{1}{2\text{m}}\dot{\boldsymbol{q}}^2 - V(\boldsymbol{q})$$

being the Lagrangian.

Rewriting the Wiener integral by means of F-K formula as

$$L_\hbar(\boldsymbol{q}, t; \boldsymbol{q}', t') = \int_{\boldsymbol{q}(t)}^{\boldsymbol{q}(t')} e^{-\frac{1}{\hbar}E(\boldsymbol{q}, \dot{\boldsymbol{q}})d\tau}\boldsymbol{D}_\hbar \boldsymbol{q} \text{ where } E(\boldsymbol{q}, \dot{\boldsymbol{q}}) = \frac{1}{2\text{m}}\dot{\boldsymbol{q}}^2 + V(\boldsymbol{q})$$

which is similar with the $H_\hbar$ but, since the integral is not explicit of the action functional the connection quantum-classic is lost.

Note: The point here is the similitude of $\boldsymbol{D}_\hbar \boldsymbol{q}$ and $\boldsymbol{D}_{i\hbar}\boldsymbol{q}$ “measures”.

The relation between Feynman path integral and Wiener functional integral is obtained by analytic continuation: in the conditions of F-K formula, with a real-valued potential $V(\boldsymbol{q}) \in C(\mathbb{R}^n)$ bounded from below the kernel $L_\hbar$ (defined for $\hbar > 0$) and the propagator $K_\hbar$ have the following relation for the upper half-plane $\Re\hbar > 0$:

$$K_\hbar(\boldsymbol{q}, t; \boldsymbol{q}', t') = \lim_{\epsilon\to 0^+} L_{i\hbar+\epsilon}(\boldsymbol{q}, t; \boldsymbol{q}', t')$$

Applications

Particle in a box.

I take a more general approach and show the claimed going to imaginary-time and back to the real time. This is still a rather toy example and does not fully illustrate the power of the Wiener measure (but keeping in mind that the potential types that the Wiener measure can be used to rigorously compute is restricted). I've chose this example because the corresponding Feynman path integral calculation a simple mechanical translation.

Let

$$H = H_0 + V = \frac{\hat{p}^2}{2\text{m}} + V(\hat{q}) = -D^2 + u(t), D = \frac{d}{dt}$$

, where $u \in C^1([0, T])$ with Dirichlet boundary conditions.

The Gaussian integration formula for $\mathbb{R}^n$ is

$$\int_{\mathbb{R}^n} \exp\left(-\frac{1}{2}(Aq,q)\right) d^n\vec{q} = \sqrt{\frac{(2\pi)^n}{det\,A}} \quad ,$$

A being a positive defined, symmetric *nxn* real matrix.

Proposition 2: For $u(t) \geq 0$,

$$\sqrt{\frac{m}{\pi\hbar\,det\,A}} = \int_{C_{0,0}} e^{\left(-\frac{m}{2\hbar}\int_0^T u(t)\,y^2(t)\,dt\right)} d\mu_{0,0}(y)$$

Proof:

Using Proposition 1 and the Gaussian integration formula one obtains

$$\int_{C_{0,0}} e^{\left(-\frac{m}{2\hbar}\int_0^T u(t)\,y^2(t)\,dt\right)} d\mu_{0,0}(y) =$$

$$\lim_{n\to\infty} \left(\frac{m}{2\pi\hbar\Delta t}\right)^{\frac{n}{2}} \int_{\mathbb{R}^{n-1}} \exp\left(-\frac{m}{2\hbar\Delta t}\sum_{k=0}^{n-1}\left(\Delta t^2 u(t_k)\,{y_k}^2 + (y_{k+1}-y_k)^2\right)\right)\prod_{k=1}^{n-1} d\,y_k =$$

$$\lim_{n\to\infty}\sqrt{\frac{m}{2\pi\hbar\Delta t\,det\,A_{n-1}}}$$

Here $y_0 = y_n = 0, t_k = k\Delta t, \Delta T = \frac{T}{n}$ and

$$A_{n-1} = \begin{pmatrix} a_1 & -1 & 0 & \dots & 0 & 0 \\ -1 & a_2 & -1 & \dots & 0 & 0 \\ 0 & -1 & a_3 & \dots & 0 & 0 \\ \vdots & \vdots & \vdots & \vdots & \vdots & \vdots \\ 0 & 0 & 0 & \dots & a_{n-2} & -1 \\ 0 & 0 & 0 & \dots & -1 & a_{n-1} \end{pmatrix} ,$$

where $a_k = 2 + u(t_k)\Delta t^{2,} k = 1,\dots,n-1$. Let $y_k^{(n)}$ be the principal minor of order *(k-1)* times Δt of the matrix A_{n-1} , e.g., $y_n^{(n)} = \Delta t\,det\,A_{n-1}$. The sequence $y_k^{(n)}$ satisfies $y_2^{(n)} = 2\Delta t + O((\Delta t)^3), y_3^{(n)} = 3\Delta t + O((\Delta t)^3)$. Expanding $y_{k+1}^{(n)}$ wrt the last row the following recurrence relation is obtained:

$$y_{k+1}^{(n)} + y_{k-1}^{(n)} - 2y_k^{(n)} = u(t_k)\Delta t^2 y_k^{(n)}, k \geq 3 \quad .$$

Then $\lim_{n\to\infty} u(t_k) = u(t), \lim_{n\to\infty} t_k = t$ so $\lim_{k,n\to\infty} y_k^{(n)} = y(t)$, *y(t)* solution to

$$-y'' + u(t) = 0$$

with initial conditions $y(0) = \lim_{n\to\infty} y_2^{(n)} = 0, y'(0) = \lim_{n\to\infty}\frac{y_3^{(n)} - y_2^{(n)}}{\Delta t} = 1$.

We finally obtain $\lim_{n\to\infty}\Delta t\,det\,A_{n-1} = \lim_{n\to\infty} y_n^{(n)} = y(T) = \frac{1}{2}det\,A$

QED

One should compare this last result with the Feynman Gaussian path integral:

$\int\limits_{\left\{ \substack{y(t)=0 \\ y(0)=0} \right\}} e^{\left(\frac{im}{2\hbar}\int_0^T y'(t)-y^2(t)u(t)dt\right)} D\,y=\sqrt{\frac{m}{\pi i\hbar\, det\, A}}$, where $A=-D^2-u(t)$, a positive defined operator.

References:

1. Albeverio, Sergio A. et al., "Mathematical Theory of Feynman Path Integrals", Springer, 2008.
2. Feynman, R.P. and Hibbs, A.R., "Quantum Mechanics and Path Integrals", Dover, 2010.
3. Glimm, James and Jaffe, Arthur, "Quantum Physics A Functional Integral Point of View", Springer, 1987.
4. Kiyosi Itô, Henry P. McKean Jr. (auth.) K. “Diffusion processes and their sample paths”, Second printing, corrected, Die Grundlehren der mathematischen Wissenschaften, Band 125, Springer-Verlag, Berlin, 1974.

The Zeeman Effect in the $n = 3$ level of Hydrogen

edx username: Gleeson

(Dated: June 19, 2019)

The splitting of the spectral lines in Hydrogen due to an externally applied magnetic field (the Zeeman effect) can be calculated to first order using the tools of perturbation theory. This is often described in the strong and weak field limits. We will review these regimes briefly, and make some comments about their range of validity. We will then describe the more general intermediate field case and demonstrate how the answer reduces to the strong and weak field approximations in the appropriate limits. We focus on the $n = 3$ level throughout.

I. INTRODUCTION

We have as our starting point the Hydrogen atom Hamiltonian, including the fine structure,

$$H = \frac{p^2}{2m} - \frac{e^2}{r} + \delta H_{fs}, \tag{1}$$

where δH_{fs} is the fine-structure correction. As usual, r is the position of the electron relative to the proton, p is the momentum of the electron relative to the proton, and e is the elementary charge. m should really be the reduced mass of the electron and proton, but we will approximate this as just the mass of the electron.

We have previously seen how the natural basis for this Hamiltonian is the so-called "coupled" basis. We have calculated a formula for the first order corrections that δH_{fs} causes (8.06x notes chapter 2),

$$\delta E^{(1)}_{fs}(n, j) = -\alpha^4 \frac{mc^2}{2} \frac{1}{n^4} \left(\frac{n}{j + \frac{1}{2}} - \frac{3}{4} \right). \tag{2}$$

We now imagine switching on an external magnetic field, $\vec{B_{ext}}$. This requires us to augment our Hamiltonian (1) with an additional term, $-\vec{\mu} \cdot \vec{B_{ext}}$, which we will call δH_z:

$$\delta H_z = -\vec{\mu} \cdot \vec{B_{ext}}. \tag{3}$$

$\vec{\mu}$, the magnetic moment of the electron, as we know, has two contributions. One from orbital angular momentum of the electron, and one from the fact the electron has intrinsic spin:

$$\vec{\mu} = -\frac{\mu_B}{\hbar}(\vec{L} + 2\vec{S}), \tag{4}$$

where $\mu_B = \frac{e\hbar}{2mc}$ is the Bohr magneton.

If we choose our z axis to be the direction of the external B field, this reduces δH_z to

$$\delta H_z = \frac{\mu_B B_{ext}}{\hbar}(L_z + 2S_z). \tag{5}$$

Our task is now to analyse the Hamiltonian

$$H = \frac{p^2}{2m} - \frac{e^2}{r} + \delta H_{fs} + \delta H_z. \tag{6}$$

Specifically, we are interested in the first-order corrections to the $n = 3$ level energies.

From equation (2), we can see the fine-structure corrections are of order $\sim \frac{mc^2\alpha^4}{n^3}$, where $\alpha = \frac{e^2}{\hbar c} \sim \frac{1}{137}$ is the fine-structure constant. Whereas, from equation (5), we can see that the Zeeman corrections are of order $\sim \mu_B B_{ext}$. We will define a dimensionless number,

$$\gamma = \frac{\mu_B B_{ext} n^3}{mc^2\alpha^4} = \frac{\mu_B B_{ext} 3^3}{mc^2\alpha^4}, \tag{7}$$

the ratio of these two quantities, which will represent the strength of the external magnetic field relative to the fine structure energy scale. Most subsequent calculations will be in terms of this parameter.

We quote for reference the fine structure corrections, obtained from (2), that we will need later:

$$\delta E^{(1)}_{fs}(3, \tfrac{5}{2}) = \frac{mc^2\alpha^4}{3^3}\left(-\frac{1}{24}\right) \tag{8}$$

$$\delta E^{(1)}_{fs}(3, \tfrac{3}{2}) = \frac{mc^2\alpha^4}{3^3}\left(-\frac{1}{8}\right) \tag{9}$$

$$\delta E^{(1)}_{fs}(3, \tfrac{1}{2}) = \frac{mc^2\alpha^4}{3^3}\left(-\frac{3}{8}\right) \tag{10}$$

We leave the 3^3 factored out as we will typically be expressing energies in units of $\frac{mc^2\alpha^4}{3^3}$.

We have gone through the strong and weak field regimes before. We will review them now briefly, and make some comments about their range of validity, before proceeding to a discussion of the intermediate case.

II. WEAK FIELD ($\gamma \ll 1$)

Recall that when $\gamma \ll 1$ we can consider our known Hamiltonian, $H^{(0)}$, to be $\frac{p^2}{2m} - \frac{e^2}{r} + \delta H_{fs}$. And we consider δH_z to be our perturbation, δH, upon this. We work with the coupled basis and just quote the result here (8.06x notes chapter 2):

$$E_n \sim -\frac{1}{2}mc^2\alpha^2\frac{1}{n^2} + \delta E_{fs}(n,j) + \mu_B B g_J(l) m_j, \quad (11)$$

where $g_J(l)$ is the lande factor, $1 + \frac{j(j+1)-l(l+1)+\frac{3}{4}}{2j(j+1)}$.

An upper bound on this formula's validity comes directly from the $\gamma \ll 1$ requirement:

$$\gamma = \frac{\mu_B B_{ext} 3^3}{mc^2\alpha^4} \ll 1 \quad (12)$$

$$B_{ext} \ll \frac{mc^2\alpha^4}{3^3\mu_B} \quad (13)$$

$$\sim 1 \text{ Tesla}, \quad (14)$$

providing us with an upper bound on the field strength.

Even if we respect this upper bound, we have some cause to be concerned about the validity of approximation (11), as technically we only have computed the spectrum of this "known" Hamiltonian to first order. More precise fine structure corrections are given by an expression of the form:

$$\delta E^{(1)}_{fs} + \delta E^{(2)}_{fs} + ..., \quad (15)$$

where $\delta E^{(1)}_{fs}$ is the first order correction quoted in equation (2) above. $\delta E^{(2)}_{fs}$ is the second order correction, and the dots represent still higher order corrections. For us to be able to neglect $\delta E^{(2)}_{fs}$ and higher order terms, we need to ensure they are negligible compared to the Zeeman corrections. This means that for our established weak field approximation, (11), to be valid, we should require that

$$\delta E^{(2)}_{fs} \ll \mu_B B_{ext}. \quad (16)$$

We will make a back-of-the-envelope approximation of what lower bound on the field strength that translates into. We know the first order fine structure correction, $\delta E^{(1)}_{fs} \sim \frac{mc^2\alpha^4}{3^3}$. And, very roughly, this differs from the zeroth order energy by a factor of α^2. We can then argue that the second order fine structure correction is likely to differ from the first order correction also by a factor of $\sim \alpha^2$. So

$$\delta E^{(2)}_{fs} \sim \delta E^{(1)}_{fs} \cdot \alpha^2 \quad (17)$$

$$\sim \frac{mc^2\alpha^4}{3^3} \cdot \alpha^2 \quad (18)$$

$$= \frac{mc^2\alpha^6}{3^3}. \quad (19)$$

Which allows us to conclude that our weak field formula, equation (11), is valid when

$$\mu_B B_{ext} \gg \frac{mc^2\alpha^6}{3^3} \quad (20)$$

$$B_{ext} \gg \frac{mc^2\alpha^6}{3^3\mu_B} \quad (21)$$

$$\sim 5 \cdot 10^{-5} \text{ Tesla}. \quad (22)$$

This is perhaps a surprising result, as one may have naively thought (as I did) that the weak field approximation formula (11) would work for arbitrarily small values of the field. The point is that it doesn't make sense to calculate a small perturbation if we've already neglected significantly larger terms.

Putting this lower bound (22) together with the upper bound calculated in (14), we have can conclude that our weak field formula (11) is appropriate when, roughly,

$$\sim 5 \cdot 10^{-5} \text{ Tesla} \ll B_{ext} \ll\sim 1 \text{ Tesla}. \quad (23)$$

III. STRONG FIELD ($\gamma \gg 1$)

When $\gamma \gg 1$, we can consider our known Hamiltonian to be $H^{(0)} = \frac{p^2}{2m} - \frac{e^2}{r} + \delta H_z$. And we consider δH_{fs} to be a perturbation upon this. We work in the coupled basis and again just quote the result (see 8.06x Problem set 3):

$$E_n \sim -\frac{1}{2}mc^2\frac{1}{n^2} + \mu_B B(m_l + 2m_s) \quad (24)$$
$$+ \frac{\alpha^4 mc^2}{2n^3}\left(\frac{3}{4n} - \left[\frac{l(l+1) - m_l m_s}{l(l+\frac{1}{2})(l+1)}\right]\right),$$

where in the $l = 0$ case, the term in square parentheses must be set equal to 1.

A couple of questions may come to mind regarding this strong field approximation: Is there an upper bound on how strong the field can be for the approximation to be valid? And, before we get to that point, are there field strengths beyond which we can neglect fine structure? We make some brief back-of-the-envelope comments on these issues now.

For us to be confident in this approximation we need $\gamma \gg 1$, that is we need $\mu_B B \gg \frac{mc^2\alpha^4}{3^3}$. However, we also need to ensure that $\mu_B B$ remains small compared to the zeroth order energies $E^{(0)}_3 \sim \frac{mc^2\alpha^2}{3^2}$. In other words, we want that B_{ext} is large enough so that the Zeeman effect is large compared to the fine structure effects. But not so large that we can no longer think of the Zeeman effect as a small "perturbation".

So this strong field approximation (24) is likely good for roughly

$$\sim \frac{mc^2\alpha^4}{3^3\mu_B} \ll B_{ext} \ll\sim \frac{mc^2\alpha^2}{3^2\mu_B} \quad (25)$$

$$\sim 1 \text{ Tesla} \ll B_{ext} \ll\sim 50,000 \text{ Tesla} \quad (26)$$

Towards the lower end of this range, say very roughly $10 - 100$ Tesla, our strong field approximation should be quite good. We certainly cannot neglect the fine structure in this case.

As we move towards the higher end of this range we could neglect the fine structure entirely.

It is difficult to get magnetic fields of strengths over ~ 100 Tesla in labs (reference 8.06x forum). So, unless we have a neutron star in our lab, we don't need to worry about the $\mu_B B_{ext}$ getting too strong compared to the zeroth order energies. That is, we are extremely unlikely to encounter a field strong enough so that the strong field formula isn't valid.

IV. INTERMEDIATE FIELD ($\gamma \sim 1$)

Having recalled some of our previous work, we now begin a more general study of our full Hamiltonian (equation (6) above, repeated here for convenience),

$$H = \frac{p^2}{2m} - \frac{e^2}{r} + \delta H_{fs} + \delta H_z.$$

We consider δH_{fs} and δH_z on a more equal footing and allow for the possibility they are of comparable magnitude.

The Hamiltonian takes the form $H^{(0)} + \delta H$, where $H^{(0)}$ is our known Hamiltonian, the familiar gross structure of Hydrogen,

$$H^{(0)} = \frac{p^2}{2m} - \frac{e^2}{r}, \tag{27}$$

and our perturbation is the sum of two terms:

$$\delta H = \delta H_{fs} + \delta H_z. \tag{28}$$

Our goal is to focus on the degenerate $n = 3$ subspace of $H^{(0)}$, with its $2 \cdot 3^2 = 18$-fold degeneracy, and calculate the first order corrections to their zeroth order energy. Recall the $n = 3$ energy to zeroth order is

$$E_3^{(0)} = -\frac{1}{2} mc^2 \alpha^2 \frac{1}{3^2}. \tag{29}$$

We must work with a basis of eigenstates for our known Hamiltonian. As mentioned, this is an 18-dimensional subspace. Therefore we have 18 basis vectors. Then, to get the first order energy corrections, we must in principle calculate an 18x18 matrix, $\langle m|\delta H|n\rangle$, and compute its eigenvalues. These are the desired energy corrections. We will see that the matrix, although not diagonal is quite sparse, so it is nothing to be afraid of.

The two basis choices we have at our disposal are the uncoupled $|n = 3, l, m_l, m_s\rangle$, and the coupled $|n = 3, l, j, m_j\rangle$. We choose the coupled basis (we will also from now on drop the $n = 3$ label). It will mean that the δH_{fs} part of δH is diagonal, but that δH_z won't be. (We could have chosen the uncoupled basis, in which case, the δH_z part would have been diagonal and the δH_{fs} part wouldn't).

$\|1\rangle = \|2, \frac{5}{2}, \frac{5}{2}\rangle$	$\|7\rangle = \|2, \frac{5}{2}, \frac{3}{2}\rangle$	$\|13\rangle = \|2, \frac{5}{2}, \frac{1}{2}\rangle$
$\|2\rangle = \|2, \frac{5}{2}, -\frac{5}{2}\rangle$	$\|8\rangle = \|2, \frac{3}{2}, \frac{3}{2}\rangle$	$\|14\rangle = \|2, \frac{3}{2}, \frac{1}{2}\rangle$
$\|3\rangle = \|2, \frac{3}{2}, \frac{3}{2}\rangle$	$\|9\rangle = \|2, \frac{5}{2}, -\frac{3}{2}\rangle$	$\|15\rangle = \|1, \frac{3}{2}, \frac{1}{2}\rangle$
$\|4\rangle = \|1, \frac{3}{2}, -\frac{3}{2}\rangle$	$\|10\rangle = \|2, \frac{3}{2}, -\frac{3}{2}\rangle$	$\|16\rangle = \|1, \frac{1}{2}, \frac{1}{2}\rangle$
$\|5\rangle = \|0, \frac{1}{2}, \frac{1}{2}\rangle$	$\|11\rangle = \|2, \frac{5}{2}, -\frac{1}{2}\rangle$	$\|17\rangle = \|1, \frac{3}{2}, -\frac{1}{2}\rangle$
$\|6\rangle = \|0, \frac{1}{2}, -\frac{1}{2}\rangle$	$\|12\rangle = \|2, \frac{3}{2}, -\frac{1}{2}\rangle$	$\|18\rangle = \|1, \frac{1}{2}, -\frac{1}{2}\rangle$

Table I. Coupled basis states, $|l, j, m_j\rangle$ for $n = 3$ level of Hydrogen

We now need to populate our 18x18 matrix. In general this means calculating $\langle ljm_j|\delta H|l'j'm_j'\rangle$ for each pair of basis states. However, we can notice that L^2 and J_z (two of our commuting observables) both commute with δH. This allows us to conclude that the matrix elements corresponding to states with different values of l or m_j must be 0. Recall, for example,

$$\begin{aligned} 0 &= [J_z, \delta H] && (30) \\ &= \langle l, j, m_j|[J_z, \delta H]|l', j', m_j'\rangle && (31) \\ &= \hbar(m_j - m_j')\langle l, j, m_j|\delta H|l', j', m_j'\rangle, && (32) \end{aligned}$$

and so if $m_j \neq m_j'$, then the matrix element must be 0.

Observing our list of basis states in Table I above, and scanning their l and m_j eigenvalues, we see that the first six states have unique pairs of these values. These are then followed by six pairs of states which share l and m_j eigenvalues. What this means for our matrix is that it will begin with 6 terms down the main diagonal, followed by six 2x2 submatrices (corresponding to the indicated pairs). So the matrix is "almost" diagonal as promised.

We must now actually calculate these entries.

$$\begin{aligned} \langle m|\delta H|n\rangle &= \langle m|\delta H_{fs} + \delta H_z|n\rangle && (33) \\ &= \langle m|\delta H_{fs}|n\rangle + \langle m|\delta H_z|n\rangle && (34) \end{aligned}$$

As mentioned before, we know δH_{fs} is diagonal in our basis. So we merely refer to our formula for the fine-structure corrections (equation (2)) above and plug in the values for our basis states These results were quoted in equations (8) through (10). This gives the δH_{fs} contribution to the δH matrix.

Now we need to evaluate $\langle m|\delta H_z|n\rangle$ for the first six terms on the main diagonal, and as mentioned, for six 2x2 submatrices down the rest of the diagonal. We will work out the "7-8" submatrix as a representative example. The procedure is to refer to a table of Clebsch-Gordon coefficients and express the coupled basis in terms of the uncoupled basis, $|m_l m_s\rangle$. Thus making the evaluation of these matrix elements straight forward.

$$|7\rangle = |2, \tfrac{5}{2}, \tfrac{3}{2}\rangle = \sqrt{(\frac{1}{5})}|2, -\tfrac{1}{2}\rangle + \sqrt{(\frac{4}{5})}|1, \tfrac{1}{2}\rangle \quad (35)$$

$$|8\rangle = |2, \tfrac{3}{2}, \tfrac{3}{2}\rangle = \sqrt{(\frac{4}{5})}|2, -\tfrac{1}{2}\rangle - \sqrt{(\frac{1}{5})}|1, \tfrac{1}{2}\rangle \quad (36)$$

$$\delta H_z|7\rangle = \mu_B B_{ext}[\sqrt{(\frac{1}{5})}|2, -\tfrac{1}{2}\rangle + 2\sqrt{(\frac{4}{5})}|1, \tfrac{1}{2}\rangle] \quad (37)$$

$$\delta H_z|8\rangle = \mu_B B_{ext}[\sqrt{(\frac{4}{5})}|2, -\tfrac{1}{2}\rangle - 2\sqrt{(\frac{1}{5})}|1, \tfrac{1}{2}\rangle] \quad (38)$$

$$\langle 7|\delta H_z|7\rangle = \mu_B B_{ext}\frac{9}{5} = (\frac{mc^2\alpha^4}{3^3})\gamma\frac{9}{5} \quad (39)$$

$$\langle 8|\delta H_z|8\rangle = \mu_B B_{ext}\frac{6}{5} = (\frac{mc^2\alpha^4}{3^3})\gamma\frac{6}{5} \quad (40)$$

$$\langle 7|\delta H_z|8\rangle = \langle 8|\delta H_z|7\rangle = -\mu_B B_{ext}\frac{2}{5} = -(\frac{mc^2\alpha^4}{3^3})\gamma\frac{2}{5} \quad (41)$$

By the same process with slightly different numbers, we have our completed matrix,

$$M = \frac{mc^2\alpha^4}{3^3}\begin{pmatrix} A & & & & & & \\ & B & & & & & \\ & & C & & & & \\ & & & D & & & \\ & & & & E & & \\ & & & & & F & \\ & & & & & & G \end{pmatrix}. \quad (42)$$

Where A is a 6x6 diagonal matrix,

$$\begin{pmatrix} -\frac{1}{24}+3\gamma & 0 & 0 & 0 & 0 & 0 \\ 0 & -\frac{1}{24}-3\gamma & 0 & 0 & 0 & 0 \\ 0 & 0 & -\frac{1}{8}+2\gamma & 0 & 0 & 0 \\ 0 & 0 & 0 & -\frac{1}{8}-2\gamma & 0 & 0 \\ 0 & 0 & 0 & 0 & -\frac{3}{8}+\gamma & 0 \\ 0 & 0 & 0 & 0 & 0 & -\frac{3}{8}-\gamma \end{pmatrix}. \quad (43)$$

And B through G are the six 2x2 matrices:

$$B = \begin{pmatrix} -\frac{1}{24}+\frac{9}{5}\gamma & -\frac{2}{5}\gamma \\ -\frac{2}{5}\gamma & -\frac{1}{8}+\frac{6}{5}\gamma \end{pmatrix}, \quad (44)$$

$$C = \begin{pmatrix} -\frac{1}{24}-\frac{9}{5}\gamma & -\frac{2}{5}\gamma \\ -\frac{2}{5}\gamma & -\frac{1}{8}-\frac{6}{5}\gamma \end{pmatrix}, \quad (45)$$

$$D = \begin{pmatrix} -\frac{1}{24}-\frac{3}{5}\gamma & -\frac{\sqrt{6}}{5}\gamma \\ -\frac{\sqrt{6}}{5}\gamma & -\frac{1}{8}-\frac{2}{5}\gamma \end{pmatrix}, \quad (46)$$

$$E = \begin{pmatrix} -\frac{1}{24}+\frac{3}{5}\gamma & -\frac{\sqrt{6}}{5}\gamma \\ -\frac{\sqrt{6}}{5}\gamma & -\frac{1}{8}+\frac{2}{5}\gamma \end{pmatrix}, \quad (47)$$

$$F = \begin{pmatrix} -\frac{1}{8}+\frac{2}{3}\gamma & -\frac{\sqrt{2}}{3}\gamma \\ -\frac{\sqrt{2}}{3}\gamma & -\frac{3}{8}+\frac{1}{3}\gamma \end{pmatrix}, \quad (48)$$

$$G = \begin{pmatrix} -\frac{1}{8}-\frac{2}{3}\gamma & -\frac{\sqrt{2}}{3}\gamma \\ -\frac{\sqrt{2}}{3}\gamma & -\frac{3}{8}-\frac{1}{3}\gamma \end{pmatrix}. \quad (49)$$

As mentioned before, the 18 eigenvalues are our sought after energy corrections. The first 6 eigenvalues are sitting conveniently on the diagonal and can be read off. The remaining 12 are obtained by calculating the eigenvalues of each of the six 2x2 submatrices. At this point we resort to a computer. Finally we have our energy corrections. These are listed down the middle column of table II below.

Weak	Intermediate	Strong
$-\frac{1}{24}+3\gamma$	$-\frac{1}{24}+3\gamma$	$-\frac{1}{24}+3\gamma$
$-\frac{1}{24}-3\gamma$	$-\frac{1}{24}-3\gamma$	$-\frac{1}{24}-3\gamma$
$-\frac{1}{8}+2\gamma$	$-\frac{1}{8}+2\gamma$	$-\frac{1}{8}+2\gamma$
$-\frac{1}{8}-2\gamma$	$-\frac{1}{8}-2\gamma$	$-\frac{1}{8}-2\gamma$
$-\frac{3}{8}+\gamma$	$-\frac{3}{8}+\gamma$	$-\frac{3}{8}+\gamma$
$-\frac{3}{8}-\gamma$	$-\frac{3}{8}-\gamma$	$-\frac{3}{8}-\gamma$
$-\frac{1}{24}+\frac{9}{5}\gamma$	$-\frac{1}{12}+\frac{3\gamma}{2}+\frac{\sqrt{5}}{120}\sqrt{720\gamma^2+72\gamma+5}$	$-\frac{7}{120}+2\gamma$
$-\frac{1}{8}+\frac{6}{5}\gamma$	$-\frac{1}{12}+\frac{3\gamma}{2}-\frac{\sqrt{5}}{120}\sqrt{720\gamma^2+72\gamma+5}$	$-\frac{13}{120}+\gamma$
$-\frac{1}{24}-\frac{9}{5}\gamma$	$-\frac{1}{12}-\frac{3\gamma}{2}+\frac{\sqrt{5}}{120}\sqrt{720\gamma^2-72\gamma+5}$	$-\frac{13}{120}-\gamma$
$-\frac{1}{8}-\frac{6}{5}\gamma$	$-\frac{1}{12}-\frac{3\gamma}{2}-\frac{\sqrt{5}}{120}\sqrt{720\gamma^2-72\gamma+5}$	$-\frac{7}{120}-2\gamma$
$-\frac{1}{24}-\frac{3}{5}\gamma$	$-\frac{1}{12}-\frac{\gamma}{2}+\frac{\sqrt{5}}{120}\sqrt{720\gamma^2-24\gamma+5}$	$-\frac{11}{120}$
$-\frac{1}{8}-\frac{2}{5}\gamma$	$-\frac{1}{12}-\frac{\gamma}{2}-\frac{\sqrt{5}}{120}\sqrt{720\gamma^2-24\gamma+5}$	$-\frac{3}{40}-\gamma$
$-\frac{1}{24}+\frac{3}{5}\gamma$	$-\frac{1}{12}+\frac{\gamma}{2}+\frac{\sqrt{5}}{120}\sqrt{720\gamma^2+24\gamma+5}$	$-\frac{3}{40}+\gamma$
$-\frac{1}{8}+\frac{2}{5}\gamma$	$-\frac{1}{12}+\frac{\gamma}{2}-\frac{\sqrt{5}}{120}\sqrt{720\gamma^2+24\gamma+5}$	$-\frac{11}{120}$
$-\frac{1}{8}+\frac{2}{3}\gamma$	$-\frac{1}{4}+\frac{\gamma}{2}+\frac{\sqrt{3}}{24}\sqrt{48\gamma^2+8\gamma+3}$	$-\frac{5}{24}+\gamma$
$-\frac{3}{8}+\frac{1}{3}\gamma$	$-\frac{1}{4}+\frac{\gamma}{2}-\frac{\sqrt{3}}{24}\sqrt{48\gamma^2+8\gamma+3}$	$-\frac{7}{24}$
$-\frac{1}{8}-\frac{2}{3}\gamma$	$-\frac{1}{4}-\frac{\gamma}{2}+\frac{\sqrt{3}}{24}\sqrt{48\gamma^2-8\gamma+3}$	$-\frac{7}{24}$
$-\frac{3}{8}-\frac{1}{3}\gamma$	$-\frac{1}{4}-\frac{\gamma}{2}-\frac{\sqrt{3}}{24}\sqrt{48\gamma^2-8\gamma+3}$	$\frac{5}{24}-\gamma$

Table II. Table of Energy corrections, expressed in units of $\frac{mc^2\alpha^4}{3^3}$.

V. LIMITS

We now wish to confirm that as we take the limit of these intermediate field corrections as $\gamma \to 0$ they match up with the weak field energy corrections obtained from formula (11) above. And similarly, as $\frac{1}{\gamma} \to 0$ they match up with the strong field corrections obtained from formula (24) above .

Consider for example, from the above Table II, the seventh intermediate energy correction

$$E_7 = -\frac{1}{12} + \frac{3}{2}\gamma + \frac{\sqrt{5}}{120}\sqrt{720\gamma^2 + 72\gamma + 5}. \tag{50}$$

As $\gamma \to 0$, we have

$$E_7 \sim -\frac{1}{12} + \frac{3}{2}\gamma + \frac{\sqrt{5}\sqrt{5}}{120}(1 + \frac{36}{5}\gamma) \tag{51}$$

$$\sim -\frac{1}{24} + \frac{9}{5}\gamma \tag{52}$$

And as $\frac{1}{\gamma} \to 0$ we have

$$E_7 \sim \gamma(-\frac{1}{12}\frac{1}{\gamma} + \frac{3}{2} + \frac{\sqrt{5}\sqrt{720}}{120}(1 + \frac{72}{2 \cdot 720}\frac{1}{\gamma}) \tag{53}$$

$$\sim -\frac{7}{120} + 2\gamma \tag{54}$$

The other calculations are essentially the same.

Table II above is arranged so that from top to bottom, the intermediate energy corrections correspond to our six matrix A eigenvalues followed by the six pairs of eigenvalues for matrices B-G. The weak and strong field columns come from the weak and strong field formulae (11) and (24) above. The weak and field columns are arranged so as to match up with their appropriate intermediate field eigenvalue.

VI. SKETCHES

We can now sketch some diagrams of the first order energy corrections as functions of γ.

Figures 1, 2, and 3 below show the corrections (middle column of table II) plotted for small, intermediate, and large-ish ranges of γ respectively.

In figure 1 we can see that for $\gamma = 0$, corresponding to zero external field, we just have the three fine structure corrections as expected (equations (8), (9), and (10) above). As we increase γ slightly, the energy corrections fan out in a linear manner closely given by our weak field approximations (left hand column of table II).

If we zoom out and look at more intermediate values of γ in figure 2, we see the corrections evolve in a non-trivial manner.

And if we zoom out further and look at the corrections for larger values of γ in figure 3, we see they converge back towards the large field approximations (right hand column of table II).

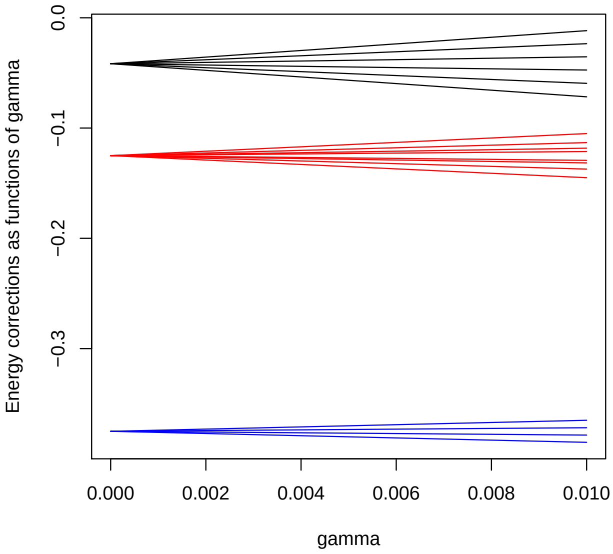

Figure 1. First order corrections as functions of γ, in units of $\frac{mc^2\alpha^4}{3^3}$. Plotted for low values of γ.

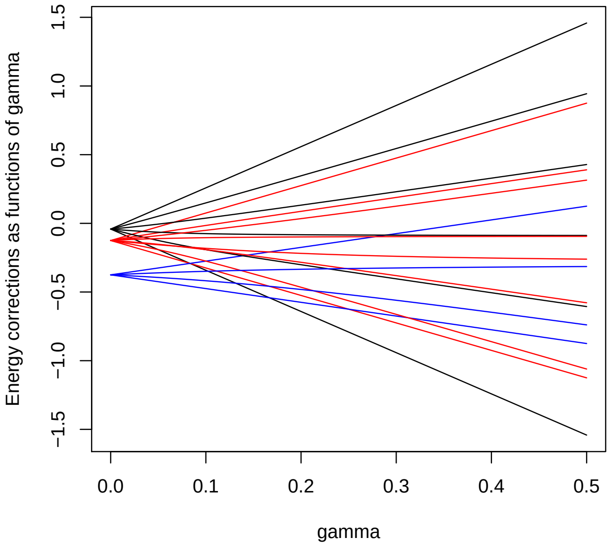

Figure 2. First order corrections as functions of γ, in units of $\frac{mc^2\alpha^4}{3^3}$. Plotted up to intermediate values of γ.

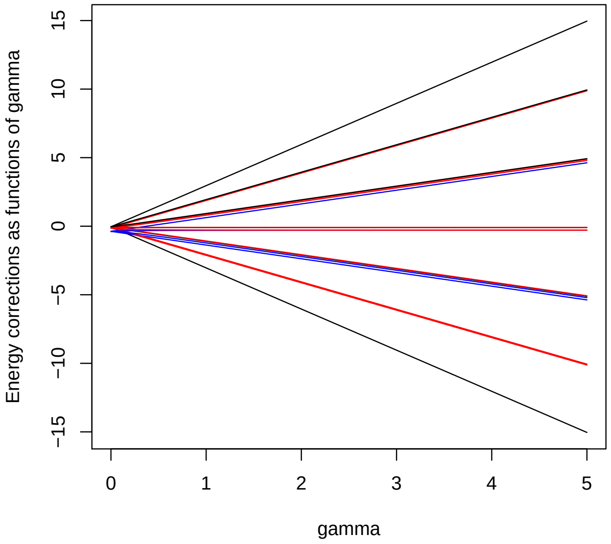

Figure 3. First order corrections as functions of γ, in units of $\frac{mc^2\alpha^4}{3^3}$. Plotted up to large-ish values of γ.

VII. CONCLUSION

We have thus calculated the first order corrections to energies of the $n = 3$ level of Hydrogen in the presence of an external magnetic field. We have commented on the validity of different approximations, and have demonstrated how these corrections change as the strength of the field is varied.

ACKNOWLEDGEMENTS

I'd like to thank the staff, TAs, and fellow students of 8.06x who answered my questions on the forum and reviewed my initial draft. Thanks as well to anyone who reads this final version. If there are errors or confusing points, please let me know.

I'd especially like to thank Jim and Jolyon who answered numerous questions. Jim also made a suggestion as to how to expand the paper, although I unfortunately didn't manage to do this before the deadline.

Finally, I'd also like to thank Ozzy the dog who kept watch while I typed and provided valuable insights at key moments.

REFERENCES

Griffiths, D. J., *Introduction to Quantum Mechanics*, 2nd edition, 2004. Textbook and solution manual. (paper topic is problem 6.26)

Sakurai, J. J., *Modern Quantum Mechanics.* Revised edition, 1993.

Tong, D., *Applications of Quantum Mechanics*, Online notes.

Binney J., Skinner, D., *The Physics of Quantum Mechanics.* 2013.

Littlejohn, R., *Physics 221A: The Zeeman Effect in Hydrogen and Alkali Atoms*, Online notes.